Quarterly Publication

ISSN 2383 - 3572

Global Journal of Environmental Science and Management

Volume 12, Number 1, Winter 2026

Global Journal of Environmental Science and Management (GJESM)

(QUARTERLY PUBLICATION)

Publisher and Editor-in-Chief
Professor J. Nouri
GJESM Publisher INC, USA
Email: *nourijafar@gmail.com*
gjesm.publication@gmail.com

Managing Editor
Professor D. Sivakumar
Kalasalingam Academy of Research and Education, Tamil Nadu, India
Email: *sivakumar.gjesm@gmail.com*

Technical Editor
Professor M. Samimi
Kermanshah University of Technology: Kermanshah, Iran
Email: *m.samimi@kut.ac.ir*

Assistant Editor
Dr. S.M. Tehrani
International Journal of Human Capital in Urban Management
Email: *tehranishohre@gmail.com*

Page Designer
A. Rezaye Soltanabadi
Imajgaran Danesh

Editorial Contact Information
621 W. Chapman Ave, Orange, CA 92868
USA
Phone: +1(949)405 0540
Email: *gjesm.publication@gmail.com*
editor@gjesm.net

Website: https://www.gjesm.net/
https://www.gjesm.com/

Publication Center
GJESM Publisher INC
publisher@gjesm.net
gjesm.publication@gmail.com

Editorial Board

Professor V.K. Gupta; *University of Johannesburg,* ***South Africa***

Professor M. Sillanpää; *Lappeenranta University of Technology,* ***Finland***

Professor A. Fauzi Ismail; *Universiti Technologi Malaysia,* ***Malaysia***

Professor A.T. Peterson; *University of Kansas,* ***USA***

Professor A. Cerda; *University of Valencia,* ***Spain***

Professor J.-D. Gu; *University of Hong Kong,* ***P.R. China***

Professor S.I. Allakhverdiev; *Russian Academy of Sciences,* ***Russia***

Professor D. Wen; *University of Leeds,* ***UK***

Professor T. Yigitcanlar; *Queensland University of Technology,* ***Australia***

Professor A. Z. Aris, *Universiti Putra Malaysia,* ***Malaysia***

Professor K. Yetilmezsoy, *Yildiz Technical University,* ***Turkey***

Professor K.E. Noll; *Illinois Institute of Technology,* ***USA***

Professor J. Nouri; *Tehran University of Medical Sciences,* ***Iran***

Professor D. Sivakumar; *Kalasalingam Academy of Research and Education,* ***India***

Professor J. Aravind; *Saveetha Institute of Medical and Technical Sciences,* ***India***

GJESM is licensed under a "Creative Commons Attribution 4.0 International (CC-BY 4.0)"
Publication authorization is certified by the Ministry of Culture and Islamic Guidance: No. 93/3629; 14 May 2014
Scientific-Research grade is accredited by the Ministry of Science, Research and Technology; No. 3/18/59975; 20 June 2015

Let s work together to publish the knowledge
and science to serve better the environment

Circulation: 500

***p*ISSN 2383 - 3572** ***e*ISSN 2383 - 3866**

Aims and Scope

Global Journal of Environmental Science and Management (GJESM) is an international scholarly refereed research journal which aims to promote the theory and practice of environmental science and management. A broad outline of the journal's scope includes; peer reviewed original research articles, case and technical reports, reviews and analyses papers, short communications and notes to the editor, in interdisciplinary information on the practice and status of research in environmental science and management, both natural and man-made. The main aspects of research areas include, but are not exclusive to; environmental chemistry and biology, environments pollution control and monitoring, transport and fate of pollutants in the environment, concentrations and dispersion and trace of wastes in air, water, and soil, point and non-point sources pollution, heavy metals and organic compounds in the environment, atmospheric pollutants and trace gases, solid and hazardous waste management; soil biodegradation and bioremediation of contaminated sites; environmental impact assessment, industrial ecology, ecological and human risk assessment; improved energy management and auditing efficiency and environmental standards and criteria.

Vision and Mission

Global Journal of Environmental Science and Management (GJESM) publishes original. Peer-reviewed and technical environmental articles serve those environmental science and management through the on time quarterly publication with reliable information. GJESM is an integral partner with the scientific and technical communities, delivering superior information products and services that foster communication, build insights and enables individual and collective advancement in environmental research. Providing environmental science and management information to the general public with descriptions of contemporary advances in environmental issues to be used in improving environmental protection and management.

Abstracting and Indexing

Web of Science (ESCI); Scopus; Scimago Journal Rank (SJR); ProQuest (Agricultural and Environmental Science + Natural Science Collection + Ulrichsweb); Chemical Abstract (CAS); CABI Abstract; Global Health Abstract; Agricola; Committee on Publication Ethics (COPE); PubMed-NCBI; DOAJ; Open J-Gate; Google Scholar; Academia.edu; Geomar; WorldCat; Academic Resource Index; Environmental XPRT; Information Matrix for the Analysis of Journals (MIAR); Bibliothek Humburg; ScienceMedia; JournalTOCs; MSRT; ISC; RICeST; SID; Civilica; Magiran.

Global Journal of Environmental Science and Management
GJESM

Publisher and Editor-in-Chief
Professor J. Nouri

eISSN 2383 3866
pISSN 2383 3572

Quarterly Full Open Access Peer Reviewed Publication

Journal Abbreviation: Global J. Environ. Sci. Manage.



CALL FOR PAPERS

Publication benefits in GJESM Journal

- *Online Publication Journal*
- *Online Submission and Reviewing*
- *Online Status Inquiry*
- *Double Blind Review*
- *Fast-Track Review and Publication*
- *Immediate Publication on the Net*
- *Article Podcasts Implementation*
- *Indexed in Scopus Database with CiteScore = **7.9***
- *Scopus Percentile (WORLD TOP-TEN: 95th in Social Science)*
- *Scopus **Q1** Category*
- *Indexed in Web of Science Database with **IF = 3.1***
- *Web of Science JCR with **Q2** Category*

Indexed by Scopus

Clarivate Web of Science Core Collection ESCI Journals

Journal Citation Reports 2023 Clarivate Analytics 3.1

Journal Website:
https://www.gjesm.net
https://www.gjesm.com

Email:
gjesm.publication@gmail.com

Phone:
+1(949)405 4538
+1(949)405 0540

Address: 623 W. Chapman Ave, Orange, CA 92868 USA

Better Environment is Our Prime Concern

Global
Journal of Environmental Science and Management

Volume 12, Issue 1, Winter 2026

1.	The catalytic effect of mycorrhizal initial planting on limestone post-mining ecological land rehabilitation **R. Prayudyaningsih; M. Turjaman; Pratiwi; F. Ansari; H. Gunawan (INDONESIA)**	1
2.	The potential of combining coagulation-flocculation, biofiltration, and advanced oxidation processes for multi-stage wastewater treatment **D. Amankeshuly; T. Salikhov; S. Syrlybekkyzy; G. Shapatova; I. Agarkova; N. Kaya; A. Yeginbayeva; E. Atasoy; K. Dakieva (KAZAKHSTAN/ TURKEY)**	21
3.	Efficacy of zinc oxide chitosan hybrid nanoparticles as a nanovaccine to enhance immunity in hybrid grouper fish **U Yanuhar; Z. Waheed; H. Suryanto; V. Hasan; D.R. Machfuda (INDONESIA)**	39
4.	Waste management of used beverage cartons using material flow analysis **B. Ratnawati; L. Della; N. Jannah; N.D. Oktaf; E. Hanaseta; H.S. Huboyo; A.C. Agustina; M.D. Vaverková (INDONESIA/ POLAND)**	57
5.	Physical and chemical evaluation of soil-like material from landfill mining using an alternative growing medium **N. Sudiana; Prihartanto; I.N. Sulistiawan; E.H. Sittadewi; D.N. Utami; E. Kusumastuti; B. Rahayu; N. Hidayat; K.A. Haris; T.E. Pararto; L. Noviana (INDONESIA)**	75
6.	*Nypa fruticans-assisted* green-synthesized gold nanoparticles for an enhanced electrochemical formaldehyde sensor based on fish albumin composite **T.P.H. Hutapea; M.S. Lembang; A. Huda; Asranudin; D.P. Dewi; Suprapto; F. Kurniawan; H.A. Saputra; A.W. Pratama; V.F. Knight; M.N.F. Norrrahim (INDONESIA/ MALAYSIA)**	95
7.	The legal coastline as a unifying framework for land and marine cadastre **J. Setiyadi; B.M. Sukojo; D.G. Pratomo; W.S. Pranowo; M. Nurcahyadi (INDONESIA)**	111
8.	Environmental and economic performance of hybrid charging stations **R. Rosmeika; A. Aditiyawan; M.A. Hipi; A. Erliza; A.W. Sani; U. Ayuningtyas; D.F. Soraya; A.Y.N. Sakti; N. Andriyani; H. Febriansyah; C.K. Sari; A.I. Pratiwi; M. Septiani; I.E. Setiawan (INDONESIA)**	129
9.	Environmental stability and ultraviolet protection of Spodoptera litura nucleopolyhedrovirus encapsulated in chitosan nanoparticles **N.T. Haryadi; A.W. Pratama; N. Dewi; A.S. Kurnianto; A.I. Tanzil (INDONESIA)**	153
10	Phylogenetic and conservation insights on local adaptations of Argiope modesta concerning ecological consequences **W.P.B. Putra; S. Utami; D. Hutapea; J. Kinho; Wakhid; W.C. Adinugroho; W. Darwiati; R. Agustarini; L. Andadari; A. Ismanto; B. Harjadi; Kayat; M.I. Maulana (INDONESIA)**	167
11.	Customer-driven socio-environmental sustainability in fashion: The role of green word-of-mouth and perceived product value **P. Yanti; M. Gunarto; R. Yusiana; L. Yohanna; R. Indriarti; Y. Yuliawati (INDONESIA)**	191
12.	Environmental impact of mining and its social responsibilities on rural communities **J. Huamaní Cayllahua; A.J. Palomino Aroni; H.D. Calderon Vilca; J.L. León Vicencio; G. Suyo Cruz; D.A. Pinto Pagaza; B.O. Mamani Huillca; W. Orós Torres; S.R. Pinto Boda; L. Contreras Salas (PERÚ)**	207
13.	The influence of demographic and socioeconomic factors on a fishing community's resilience to coastal flooding **C.D.A. Depari (INDONESIA)**	229
14.	Environmental and policy perspectives in managing revolutionary heritage under urbanization challenges **T.P. Nguyen; V.H. Dao; T.A.T. Vo; Y.N. Au (VIETNAM)**	249
15.	Indigenous bacterial diversity and identification in domestic wastewater in small tropical island **Sukmawati; A.B. Birawida; Ambeng; S.M. Sham; Sumarheni (INDONESIA/ MALAYSIA/ AUSTRALIA)**	269

16.	Relationship between urban soil granulometric composition and microbiological and vermicular contamination **A. Zandybay; A. Sagnaeva; S. Kaliyeva; G. Adilbektegy; D. Narodkhan; A. Daribay; T. Mkilima (KAZAKHSTAN/ TANZANIA)**	281
17.	Tropical peat soil variability along landscape and depth gradient using mid-infrared spectroscopy **P.B. Putra; D. Rachmanadi; Y. Indrajaya; A. Kunarso; R.N. Adi; A. Jaya; T.W. Yuwati; E. Priyanto; W. Halwany; A. Noor; M. Noor (INDONESIA)**	297
18.	Synergistic impacts on a multi-purpose transboundary aquatic ecosystem resulting from cyanide and mercury in artisanal gold mining tailings **P.C. Velasquez-Lopez; L. Chinchay; L.E. Granda; M. Nirchio (ECUADOR)**	313
19.	Eco-friendly organic nutrients enriched with biosoltamax enhance shallot growth, improve soil properties, and reduce the use of mineral fertilizer **A. Nurawan; K.D. Sutanto; Y. Haryati; B. Susanto; K.K. Hamdani; Y. Surdianto; N. Sutrisna; N.R. Purnamasari; S.R. Djiwanti; D. Histifarina; A. Jufri; D.W. Utami (INDONESIA)**	331
20.	River basin management under spatial inequality and land use dynamics **A. Zhaken; T.P. Dentinho; G. Saspugayeva; M. Kamet; G. Shapatova; S. Kassymkhanov; Z. Zhumagalieva; A. Tsiganov; V. Sedelev (KAZAKHSTAN)**	351
21.	Eco-friendly farming management and molecular surveillance of the pepper yellow leaf curl virus in purple-stem chili **R. Tarigan; B.K. Udiarto; D.S. Hanafiah; M. Sinuraya; K.D. Sutanto; W. Setiawati; I. Manzila; A. Sebayang; D.W. Utami; R. Murtiningsih; A.E. Marpaung; I.S. Marpaung; S. Simatupang; Atman; Riska (INDONESIA)**	371
22.	Linking geospatial suitability modelling with experimental validation of aquatic environmental quality in inland lakes **B. Doskenova; I. Sedelnikov; T. Lyssakova; G. Gordiyanova; G. Rakhimzhanova; D. Shugulova; E. Abdrahmanov; Y. Pangaliyev (KAZAKHSTAN)**	393
23.	Sustainable solutions for entomoremediation organic waste into food and fertilizer using black soldier fly larvae **A.R.K. Kullan; E.G. Neumann; A. Suresh; H.L. Choi (UNITED ARAB EMIRATES/ KOREA)**	409
24.	The role of carbon sequestration and biodiversity in agroforestry for climate change mitigation **S. Withaningsih; S. Nurmilah; G.L. Utama (INDONESIA)**	431
25.	Sustainable strategies for durum wheat production under water scarcity and climate stress **G. Saspugayeva; A. Zhaken; I. Agarkova; Z. Mukhametzhanova; I. Samatova; Z. Zhaznayeva; A. Chursin; G. Salykbayeva; Sh. Baimukasheva; B. Serkebayeva (KAZAKHSTAN)**	453

Global J. Environ. Sci. Manage. 12(1): 1-20, Winter 2026, Serial #45

Global Journal of Environmental Science and Management
(GJESM)

Homepage: https://www.gjesm.net/

Podcasts

ORIGINAL RESEARCH PAPER

The catalytic effect of mycorrhizal initial planting on limestone post-mining ecological land rehabilitation

R. Prayudyaningsih[1,2,*], M. Turjaman[1,4], Pratiwi[3], F. Ansari[2,3], H. Gunawan[5]

[1] *Research Center for Applied Microbiology, National Research and Innovation Agency, Jalan Raya Jakarta-Bogor, Cibinong 16911 Indonesia*

[2] *Research Collaboration Center for Karst Microbes, National Research and Innovation Agency and Hasanuddin University, Jalan Perintis Kemerdekaan, Makassar 90245 Indonesia*

[3] *Research Center for Ecology, National Research and Innovation Agency, Jalan Raya Jakarta-Bogor, Cibinong 16911 Indonesia*

[4] *Research Collaboration Center for Agarwood, National Research and Innovation Agency, Bogor Agricultural Institute, and School of Life Sciences and Technology, Bandung Institute of Technology, Bandung 40132 Indonesia*

[5] *Semen Tonasa Company, Jalan Tonasa 2, Biring Ere District, Pangkajene dan Kepulauan 90651 Indonesia*

ARTICLE INFO

Article History:
Received 06 July 2025
Revised 11 September 2025
Accepted 16 October 2025

Keywords:
Degraded land
Natural succession
Nutrient cycling
Restoration
Soil properties

ABSTRACT

BACKGROUND AND OBJECTIVES: Limestone post-mining land is severely degraded due to losing its topsoil and having very high potential of hydrogen levels and low levels of nitrogen and phosphorus. This circumstance profoundly obstructs the natural course of ecological succession. This study was designed to assess how initial plantings that are inoculated with arbuscular mycorrhizal fungi on accelerating the improvement of site conditions, creating functional safe sites, and facilitating the establishment and growth of later successional plant species.

METHODS: The study was performed on a limestone site that had been post-mining for 15 years, comparing three different conditions: an unplanted area (A0), an initial planting without arbuscular mycorrhizal fungi inoculation (A1), and an initial planting with arbuscular mycorrhizal fungi inoculation (A2). The study examined soil indicators including biological elements (spore density, diversity, and colonization of arbuscular mycorrhizal fungi), chemical aspects (potential hydrogen, nitrogen, phosphorus, soil organic matter, cation exchange capacity), and physicals (aggregate stability, porosity). To test for a facilitative effect, mid-seral successional species (Alstonia scholaris and Tectona grandis) were planted across all three areas, and their growth, nutrient uptake, and root colonization were monitored over a 12-month periods.

FINDINGS: The area inoculated with arbuscular mycorrhizal fungi (A2) showed significant improvements in all measured soil parameters; an increase of arbuscular mycorrhizal fungi spore density by almost 300 percent ($p < 0.05$), including its richness and diversity. Consequently, the species introduced in A2 revealed statistically significant improvements in height and diameter, which were consistent with and affirmed the establishment of effective safe sites.

CONCLUSION: Initial plantings inoculated with arbuscular mycorrhizal fungi function as a strong catalyst for the restoration of ecosystems in areas of severe land degradation. This intervention not only improves soil health across biological, chemical, and physical dimensions but also effectively accelerates the natural successional process by facilitating the successful growth of later seral species. This approach is critical for the effective and sustainable restoration of ecosystems, particularly in post-mining limestone regions.

DOI: 10.22034/gjesm.2026.01.01

This is an open access article under the CC BY license (http://creativecommons.org/licenses/by/4.0/).

NUMBER OF REFERENCES
69

NUMBER OF FIGURES
7

NUMBER OF TABLES
6

*Corresponding Author:
Email: *retno.prayudyaningsih@brin.go.id*
Phone: +62812 4185 193
ORCID: 0000-0003-3604-5406

Note: Discussion period for this manuscript open until Mar 1, 2026 on GJESM website at the "Show Article".

INTRODUCTION

Limestone mining is the foundation for the development of global infrastructure and economic growth, providing essential materials for industry, construction, and the production of cement. Additionally, while there are economic gains, these activities also leave a permanent environmental footprint that inflicts widespread damage and results in serious land degradation (Bărbulescu and Hosen, 2025). The limestone mining process is carried out with open-pit (surface) mining, a method that drastically alters the landscape, removes all layers of topsoil, vegetation, and original structure, and leaves behind a substrate that is physically, chemically, and biologically unfavorable to biotic life. The restoration of limestone postmining landscapes is particularly challenging, marked by a highly alkaline potential of hydrogen (pH), insufficient levels of critical nutrients like nitrogen (N) and phosphorus (P), a nearly total lack of organic matter, and extreme soil compaction (Rosa *et al.,* 2023). These extreme conditions effectively hinder the natural recovery process through ecological succession, which often proceeds very slowly or even stops altogether. Although succession ecology is a basic natural mechanism for restoring disturbed ecosystems, it encounters significant challenges on severely degraded post-mining land. These obstacles, known as ecological filters or environmental barriers, include the inability of seeds to arrive (dispersal limitation) and to grow due to unsuitable site conditions (establishment limitation). Conventional reclamation techniques commonly demonstrate ineffectiveness, as they emphasize the introduction of late-successional species without sufficiently considering important site conditions (Prach and Hobbs, 2008). This approach overlooks the principle of ecological facilitation, in which pioneer species modify the environment, thereby facilitating the establishment of subsequent species (Funk *et al.,* 2017). In the absence of prior site enhancement, the survival and growth rates of reclaimed plants remain minimal, hindering the restoration of a functional ecosystem. An essential gap in the literature is noted concerning the efficient acceleration of site improvement to avoid the initial, inactive phase of succession (Gómez-Aparicio, 2009). This is where the engineering of subterranean ecosystems is of paramount importance (Ruiz-Jaen and Mitchell Aide, 2005) to create safe site. Safe site is a localized area where environmental conditions have been ameliorated by early seral species to overcome limitations to the establishment and growth of later successional species. An exceptionally promising technique entails the application of soil microbial inoculation, specifically targeting arbuscular mycorrhizal fungi (AMF) (Tedersoo *et al.,* 2020). AMF establishes a symbiotic relationship with the majority of plant roots, functioning as an extension of the root system that significantly enhances water and nutrient absorption, particularly phosphorus (Smith and Read, 2010). Furthermore, AMF serve as “ecosystem engineers” that bolster soil structure by generating glomalin and creating hyphal networks, effectively binding soil particles into stable aggregates (Chaudhary *et al.,* 2025). This study highlights the catalytic effect of AMF-inoculated initial planting on overall ecosystem recovery in a limestone post-mining quarry, building on the established benefits of AMF in enhancing individual plant growth. The study concentrated on assessing how AMF-inoculated initial planting can catalyze the restoration of ecosystems in limestone regions affected by mining. It is hypothesized that AMF inoculation in initial planting significantly enhances soil biological, chemical, and physical functions compared to non-inoculated and naturally recovered sites. Furthermore, it is expected that these improvements facilitate the establishment and growth of mid-seral species (*Alstonia scholaris* and *Tectona grandis*), thereby accelerating ecosystem recovery. Consequently, this study intends to investigate the hypothesis that the application of mycorrhizal initial planting will lead to a sequence of enhancements in soil function indicators-biological, chemical, and physical aspects. These improvements are expected to establish a conducive environment that markedly enhances the growth performance of two mid-seral tree species, *Alstonia scholaris* (pulai) and *Tectona grandis* (teak), in comparison to areas that have been revegetated without AMF inoculation or those that have been allowed to recover naturally. This study offers the preliminary empirical evidence regarding mycorrhizal-based facilitation mechanisms, which are vital for promoting ecological succession in a compromised landscape. The study was conducted in a limestone post-mining area located in Pangkajene Kepulauan Regency, South Sulawesi Province, Indonesia (Fig. 1).



Fig. 1: Geographic location of the study area in a limestone post-mining area located in Pangkajene Kepulauan Regency, South Sulawesi Province, Indonesia

MATERIALS AND METHODS

The study site is a quarry covering roughly 11 hectares (ha) that has remained unused for about 15 years. A part of the land at this site has either completed reclamation or is in the midst of the reclamation process, which consists of filling the mine pits with excavated waste. This investigation was structured to evaluate three distinct land conditions:

• Unplanted area (A0): post-mining area that has not been revegetated and has been allowed to undergo natural succession.

• Initial planting without arbuscular mycorrhizal fungi inoculation (A1): a reclaimed post-mining area that has been restored through the use of plants that do not have mycorrhizal inoculation.

• Initial planting within arbuscular mycorrhizal fungi inoculation (A2): post-mining area that has been reclaimed through revegetation using plants that have been inoculated with mycorrhizal fungi.

In both initial planting areas (A1 and A2), the types of plants planted were legume cover crop (*Centrosema pubescens*) and local tree species (*Vitex cofassus*). The planting distance for *V. cofassus* was 2 meters (m) x 4 m. Data were collected after five years of initial planting establishment. At the time of the study, *C. pubescens* was five years old and *V. cofassus* was three years old. The design of the experimental study is shown in Fig. 2.

Samples collection

Observation plots measuring 10 m x 10 m were established at random in every area of A0, A1, and A2. Each category of area comprised roughly 15 plots (n=15), and the total number of plots was 45. Samples of soil, plant root, and litterfall were collected from five points (four at the corners and one at the center) for each plot. In the laboratory, the five subsamples were combined to produce one representative sample for each plot. Soil samples intended for chemical testing were obtained from a depth of 0–20 centimeters

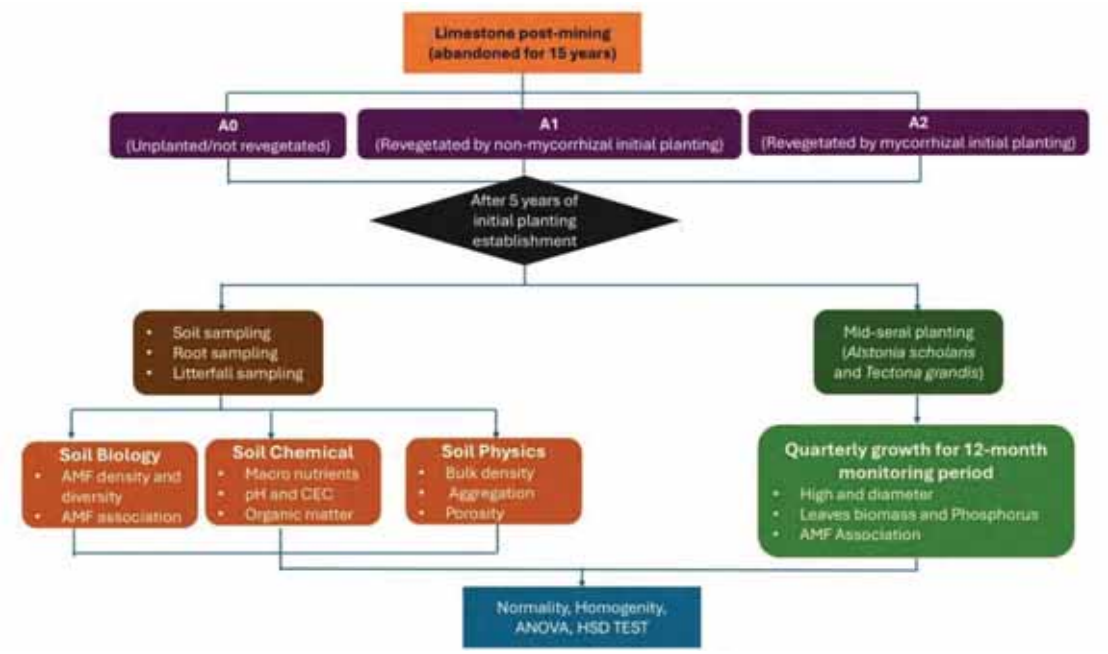

Fig. 2: Flowchart of experimental design

(Margesin and Schinner, 2005). Soil samples for biological properties, specifically the population of AMF, were taken at a depth of 0–20 centimeters (cm) used subplots measuring 20 cm x 20 cm (Hartmut *et al.,* 1995). For physical analysis, soil samples were taken from the center of each plot by means of a ring sample. This sample was utilized to examine bulk density, porosity, and aggregate stability. Samples of plant root used about 5 grams (g) of root. The root samples underwent a washing process with water and were subsequently placed in labeled bottles containing a 50% alcohol solution. Samples of litterfall were taken used subplots measuring 25 cm x 25 cm (Andreetta *et al.,* 2013). The study determined the average thickness of litterfall by assessing the thickness on all four sides of the subplot.

Establishing the subsequent seral species

A trial study was performed to evaluate whether the site created through initial plantings and AMF inoculation facilitates the shift from the early seral stage to the next seral stage, with an emphasis on planting mid-seral species on limestone land after mining. The next seral species was planted in each area of A0, A1, and A2. The subsequent species tested were *Alstonia scholaris* and *Tectona grandis*. The experimental design was implemented a randomized complete block design (RCBD). Each area type consisted of 3 blocks. A total of 30 plants (n=30) per block were used as replicates for each plant species within each area type, with a spacing of 2 m x 4 m. Consequently, the overall number of experimental units for each tree species was calculated by multiplying 3 areas by 3 blocks and 30 plants, leading to a total of 270 plants. The overall count of experimental units for the two species; *Alstonia scholaris* and *Tectona grandis,* amounted to 270 multiplied by 2, resulting in a total of 540 plants.

Observation and data collection

Observations of soil property improvements were measured based on AMF status, soil nutrient content, and soil structure. Meanwhile, evidence of accelerated next seral turnover was measured based on increased growth of *A. scholaris* and *T. grandis*. The evaluation of AMF status was conducted by considering the type of AMF, spore density, and the level of AMF infection. The extraction of spores from 50 g of soil samples was performed utilizing the wet sieving and decanting (Gerdemann and Nicolson, 1963), followed by a modified centrifugation technique (Brundrett *et al.,* 1996). The spores collected were enumerated

using a dissecting microscope to assess their density. To assist in identifying the collected AMF spores, slides of spores were prepared. These spore slides were diligently made with Melzer's dye and polyvinyl-lactic acid-glycerol (PVLG) preservative, and were positioned individually on a glass slide. The alteration in spore coloration when exposed to Melzer's solution serves as a key indicator for identifying the genus involved (Brundrett *et al.,* 1996). Moreover, a detailed examination was conducted on the morphology of the spores, which includes aspects including spore color, the layers of the spore wall, ornamentation, and the structure of the hyphae. The extent of AMF colonization was assessed through a modified root staining method (Kormanik and McGraw, 1982). The stained root samples were subsequently chosen at random and sectioned into ten 1 cm segments. The root fragments were precisely placed on a glass slide and afterward topped with a coverslip, using the tip of a paintbrush handle to apply gentle pressure. Subsequently, they were examined using a microscope. Five replicates of the root sample preparation were conducted. To determine the percentage of root colonization, the colonized root length (slide) method was employed (Giovannetti and Mosse, 1980). The analysis of soil nutrient content encompass pH, total nitrogen, available phosphorus, soil organic carbon (SOC), and cation exchange capacity (CEC). The approach utilized for pH analysis was electrometric. The total nitrogen levels were determined through the Kjeldahl method, and available phosphorus levels were analyzed using the Olsen method. The assessment of SOC concentrations employed the Walkley and Black technique. The soil organic carbon content was subsequently correlated with soil organic matter (SOM) using the equation, SOM = 1.724 x % SOC (Combs and Nathan, 2015). The analysis of soil CEC was conducted using the percolation method, employing Ammonium acetate at pH 7 and 10% sodium chloride (NaCl) solvents. The measurement of litter biomass involved weighing litter samples for their wet weight initially, then drying them in an oven at 80 degrees Celsius (°C) until a stable dry weight was obtained. Observations of soil structure encompassed volumetric weight (VW), total pore space, soil porosity, and aggregate stability. The gravimetric method was employed to measure soil VW. The analysis of soil specific gravity (SG) was conducted utilizing the Flask method. Additionally, the calculation of soil porosity was performed using the formula 1 – (VW/SG) x 100. The evaluation of total pore space was executed through the pressure plate membrane apparatus technique. The evaluation of aggregate stability was undertaken using both dry and wet sieving methods.

Growth of the next seral species

The monitoring period was for a single 12-month season. Measurements were conducted on the development of *A. scholaris* and *T. grandis*, focusing on changes in plant height and diameter at the intervals of 0, 3, 6, 9, and 12 months. Furthermore, observations were conducted on the percentage of AMF infection in the roots of pulai and teak plants at 3, 6, 9, and 12 months of age, along with the biomass and phosphorus content of *A. scholaris* and *T. grandis* leaves at 6 and 12 months. During the field study, plant height was gauged with a measuring pole, and the diameter of the stems was measured using calipers set 5 cm from the stem's base. Leaf biomass was quantified by subjecting leaf samples to a drying process at a temperature of 80°C for three consecutive 24-hour periods until a stable dry weight was achieved. The analysis of leaf phosphorus content was conducted using spectrophotometry.

Data analysis

An analysis of the AMF community structure was conducted utilizing various diversity parameters, including isolate frequency, relative abundance, importance value index (IVI), spore density, species count, species richness, and the Shannon-Wiener diversity index (Table 1). Isolate frequency provides insight into the distribution status of AMF, as defined by the percentage of their occurrence in the sample (Yang *et al.,* 2011). The relative abundance provides insights into the sporulation capabilities of various AMF species within the ecosystem, highlighting their strengths or weaknesses. The unification of these two parameters streamlines the analysis of IVI, recognizing species or genera with an IVI ≥20 as the dominant entities (Shi *et al.,* 2006).

Data on soil chemical, biological, and physical properties, as well as the growth of two mid-seral species, were analyzed using SPSS (version 17). The data were checked for normality (Shapiro-Wilk test) and homogeneity of variances (Levene's test), and a Tukey's Honestly Significant Difference (HSD) test was

Table 1: Ecological diversity parameters for evaluating AMF community structure

Parameter	Formulas and definitions
Isolate Frequency (FI) [a]	The percentage of a soil sample in which a species or genus is present
Relative abundance (AR) [a]	The percentage of the number of spores of a genus or family
Importance value index (IVI) [a]	(FI + AR)/2
Spore density [a]	Number of spores per 50 g of soil sample
Species richness [a]	Number of species per soil sample
Shannon-Wiener diversity index (H') [b]	$H' = -\sum_{i=1}^{S} (Pi) \times (\log 2\ Pi)$

Remarks: Pi = ni/N, where ni is the number of spores of species or genus i. N is the total number of identified spore samples. S is the number of species or genera observed. [a] (Shi *et al.,* 2006; Yang *et al.,* 2011); [b] (Krebs, 1972)

used for post-hoc comparisons following ANOVA.

RESULTS AND DISCUSSION

Recharging AMF as an indicator of soil biology improvement

The restoration of ecosystems in severely degraded post-mining areas depends on the reconstruction of functional soil communities, with symbiotic microbes like AMF being pivotal to this process (Lethielleux-Juge, 2025). AMF are more than simple components; they act as crucial "ecosystem engineers" that promote nutrient cycling, create soil structure, and enhance plant resilience against abiotic stress (Afshari *et al.,* 2022; Andrino *et al.,* 2021; Benjamin *et al.,* 2022; Cao *et al.,* 2023; Xuefeng *et al.,* 2022). The total effectiveness of reclamation is significantly reliant on their existence and functionality (Košnar *et al.,* 2025; Tao and Liu, 2024). In important limestone mining zones, where the topsoil has been depleted and and the underlying substrate is inhospitable, the abundance of natural arbuscular mycorrhizal fungi propagules is considerably low, impeding natural ecological succession (Buil *et al.,* 2025; Sing and Jamaluddin, 2011). Consequently, biological intervention is vital, and this study provides quantitative validation of its effectiveness. The findings revealed that interventions like revegetation and AMF inoculation notably accelerated therecovery of AMF populations. The region designated for natural recovery (A0) exhibited a minimal spore density of 52.67 spores per 50 g of soil (Table 2). The initiation of initial planting without AMF inoculation (A1) yielded a marginal increase of 19.99%. Conversely, the most pronounced increase transpired in the AMF-inoculated initial planting area (A2), where spore density surged to 291.11%. This rapid expansion demonstrates that active inoculation is considerably more efficient than relying on the slow natural AMF recovery. These findings correspond with the studies conducted by (Chaudhary *et al.,* 2025; Dassen *et al.,* 2021; Patanita *et al.,* 2020; Stover *et al.,* 2018; Wang, 2017), which showed that the incorporation of indigenous AMF inoculum into degraded land markedly expedited the re-establishment of the soil spore bank, an essential component for the sustainability of long-term restoration.

The significant rise in spore density is probably a result of the swift growth of the introduced inoculum on the roots of the host plant in an environment with minimal competition. It is advisable to conduct long-term monitoring to evaluate the sustainability of this spore bank. While the study demonstrates a strong catalytic effect of AMF, it is acknowledged that these fungi work within a complex soil food web. The improvements are likely a result of synergistic interactions between the inoculated AMF, the developing plant roots, and the native microbial community that is stimulated by the new organic inputs. The inoculation of AMF affects both the number and the quality and variety of AMF communities, which serve as critical indicators of soil ecosystem health and resilience (Chourasiya *et al.,* 2021). The maximum indices of AMF diversity (H') and species richness (R) were observed in area A2 (Table 2). The enhancement of diversity is vital, as different AMF communities have proven to be more effective in improving ecosystem multifunctionality, such as increased nutrient absorption and enhanced plant protection (Albracht *et al.,* 2024; Liang *et al.,* 2025; Liu *et al.,* 2024). Notably, AMF species not present in other areas, including Glomus sp. and Scutelospora

Table 2: Density, index diversity, and species richness of AMF

Area	Density of spores /50 g of soil	Index Diversity (H')	Species Richness (R)	% AMF Colonization
A0	52.67±16.75	0.79	6	39.33 ±10.86ab
A1	63.20±9.39	1.46	5	37.63 ±14.84a
A2	206.00±19.07	1.57	8	53.54 ±17.74 c

Remarks: A0 (unplanted area), A1 (initial planting without AMF inoculation), and A2 (initial planting with AMF inoculation). Index diversity according to Shannon-Wiener. Index species richness according to Margalef. Numbers after ± represent the standard deviation of the mean. The numbers followed by the same letter show no significant difference at p<0.05.

Table 3: Importance value index of arbuscular mycorrhizal fungi

Type	Family	Area/ IVI		
		A0	A1	A2
Acaulospora denticulata	Acaulosporaceae	117.02	79.88	76.66
Acaulospora morrowai	Acaulosporaceae	23.80		1.26
Funneliformis verruculosum	Glomeraceae	5.63	19.29	9.47
Glomus ambiosporum	Glomeraceae	12.53	31.78	32.60
Glomus sp	Glomeraceae			2.51
Septoglomus constriction	Glomeraceae	35.70	62.48	65.56
Gigaspora sp.	Gigasporaceae	5.32	6.56	8.33
Scutelospora sp.	Gigasporaceae			3.59

Remarks: A0 (unplanted area), A1 (initial planting without AMF inoculation), and A2 (initial planting with AMF inoculation). Data collected after 5 years of initial planting establishment.

sp., were identified in area A2 (Table 3), suggesting effective colonization of the introduced inoculum and its capacity to potentially restore the native AMF gene pool, which may have been diminished by mining operations. According to Van Aarle *et al.* (2002), the maximum colonization result was notably different, indicating that total AMF root colonization diminished at higher pH values.

Eight AMF species were identified (Table 3), four of which are *Acaulospora denticulata*, *Acaulospora morrowai*, *Glomus ambiosporum*, and *Septoglomus constrictum*. These four species are identified as dominant due to their IVI being greater than 20, based on the standards set by Yang *et al.* (2011). The prevalence of the Acaulosporaceae and Glomeraceae families (Fig. 3) is a recurring phenomenon observed in disturbed and nutrient-deficient settings. The families, particularly the genus Glomus (which has undergone significant reclassification), are noted for their ability to quickly generate large amounts of small to medium-sized spores, thereby promoting the rapid colonization of newly uncovered locations (Afshari *et al.,* 2022; Chen *et al.,* 2022; Ouhaddou *et al.,* 2025). This versatility renders them exemplary pioneers for initiating soil biological recovery in post-mining regions.

The degree of AMF colonization of roots, as a measure of symbiotic efficacy, reveals an intriguing ecological conundrum. Notwithstanding the lowest spore density, the region devoid of initial planting (A0) exhibited a greater degree of AMF colonization compared to the area planted without inoculation (A1) (Table 2). This situation can be understood by examining the consequences of physical soil disruption. The land preparation activities in A1 and A2, including leveling and the excavation of planting holes, significantly disturbed and restructured the existing, albeit sparse, arbuscular mycorrhizal fungal hyphal network. Conversely, area A0, having remained untouched for 15 years, supported the slow development of a stable mycelial network through the surviving AMF propagules present in the existing natural vegetation. This emphasizes that although AMF spore quantities are significant, the existence of a developed hyphal network, which is particularly vulnerable to physical disruption, is crucial for effective colonization (Dassen *et al.,* 2021). Nonetheless, the highest colonization rate was observed in area A2, indicating that despite the initial disturbance, the introduction of a significant inoculum effectively overcame this obstacle and enabled the most efficient and rapid symbiosis.

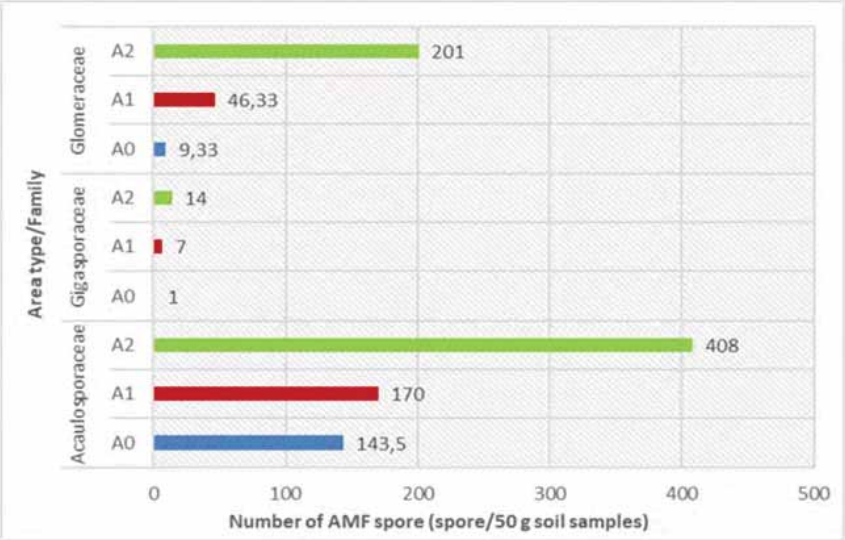

Fig. 3: Density of spores of AMF based on their family groups
Remarks: A0 (unplanted area), A1 (initial planting without AMF inoculation), and A2 (initial planting with AMF inoculation). Data collected after 5 years of initial planting establishment.

Soil chemical restoration

The collaborative influence of revegetation and AMF on nutrient cycling

Limestone post-mining landscapes are essentially chemically impaired ecosystems, characterized by the depletion of nutrient-rich topsoil and the exposure of barren parent materials. The environment is marked by extreme chemical traits, especially shortages of vital nutrients such as N and P, combined with a soil pH that often surpasses 8.0, thereby severely hindering nutrient accessibility for plants. Consequently, the main objective of restoration efforts extends beyond merely planting trees; it is to initiate the re-establishment of nutrient cycles, which are fundamental to the functionality of ecosystems (Bradshaw, 1997; Palmer and Stewart, 2020; Perring *et al.,* 2015). The findings of this study clearly demonstrate that reclamation through initial planting (revegetation), especially when combined with AMF inoculation, successfully triggered a range of improvements in soil chemical properties, transforming an inert substrate into a dynamic medium. The initial step for enhancing ecosystems is the restoration of organic matter into the soil, which acts as the principal energy source for soil organisms and the basis of chemical fertility (Du *et al.,* 2025; Li *et al.,* 2025). This study demonstrated the success of revegetation by markedly elevated levels of organic matter and litter layer buildup in the planted areas (A1 and A2) relative to the unplanted area (A0) (Fig. 4). The implementation of legume cover crops (*C. pubescens*) and *V. cofassus* trees has directly contributed to the increase of organic carbon levels and the formation of a litter layer on the soil surface.

The principal discovery of this work is the catalytic function of AMF in expediting the return of organic materials. The AMF-inoculated initial planting area (A2) exhibited the greatest accumulation of litter layers. This phenomenon is driven by the AMF's ability to improve the productivity and biomass of its host plants through better nutrient absorption, which in turn elevates the organic matter content in the soil (Andrino *et al.,* 2021; Tao and Liu, 2024; Turrini *et al.,* 2017; Xuefeng *et al.,* 2022). The increase of organic matter subsequently initiates a beneficial chain reaction, one consequence of which is the enhancement of the soil's CEC. Considering that CEC is predominantly influenced by organic matter and clay concentration (Jia *et al.,* 2023; Rowell, 2014), it is unsurprising that the A2 area, exhibiting the highest organic matter, also demonstrated the highest CEC value (Table 4). The enhancement of CEC is crucial in degraded land as it increases the soil's ability to retain nutrient cations from leaching, thus boosting nutrient utilization efficiency.

Furthermore, this biological intervention

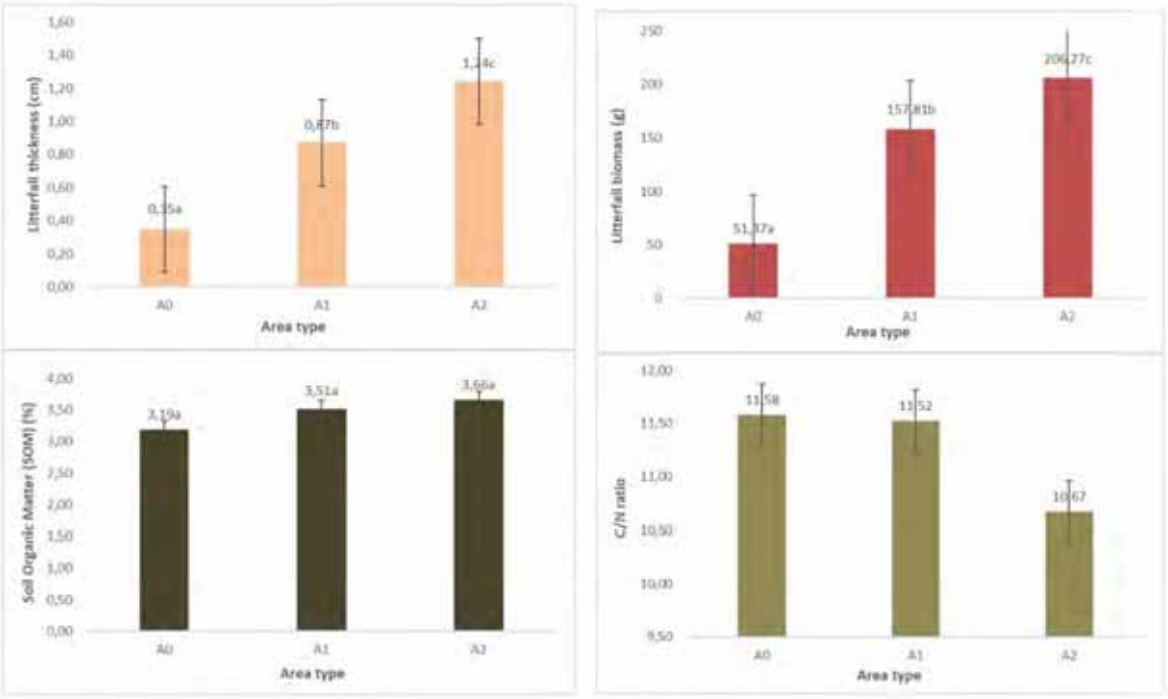

Fig. 4: Organic matter conditions across different land use types in the limestone post-mining area
Remarks: A0 (unplanted area), A1 (initial planting without AMF inoculation), and A2 (initial planting with AMF inoculation). The numbers followed the same letter show no significant difference at p<0.05. Error bars represent the standard deviation of the mean (SD). Data collected after 5 years of initial planting establishment.

Table 4: Soil chemical properties across different land use types in the limestone post-mining area

Area	Chemical properties of soil					
	C-org (%)	Criteria *	N total (%)	Criteria*	P_2O_5 (ppm)	Criteria *
A0	0.85 ± 0.18a	Very Low	0.17±0.06a	Low	21.87±0.98ab	Low
A1	1.03±0.36 a	Low	0.18±0.03 a	Low	20.50±2.38 a	Low
A2	1.12±0.17 a	Low	0.20±0.60 a	Low	25.57±2.14 c	Low
	CEC me/100g	Criteria *	pH	Criteria *		
A0	20.79±0.75a	Medium	8.20±0.18 a	Slightly alkaline		
A1	20.59±2.49a	Medium	7.90±0.36 a	Slightly alkaline		
A2	22.39±1.28a	Medium	7.97±0.17 a	Slightly alkaline		

Remarks: A0 (unplanted area), A1 (initial planting without AMF inoculation), and A2 (initial planting with AMF inoculation). Category of soil chemical characteristic chemistry based on soil chemical properties assessment criteria (Hardjowigeno, 2010). Numbers followed by the same letter indicate no significant difference at p<0.05. Numbers after ± represent the standard deviation of the mean. Data collected after 5 years of initial planting establishment.

successfully addressed the most fundamental chemical problem in the limestone post-mining area, namely the availability of phosphorus. At very high pH (8.2 in the A0 area), phosphorus is strongly bound by calcium (Ca), forming an insoluble calcium phosphate compound that is unavailable to plants, also known as occluded phosphate (Ma *et al.,* 2022; Penn and Camberato, 2019). The findings indicated that incorporating plants, particularly those treated with AMF (A2), effectively reduced soil pH and markedly enhanced P availability (Table 4). These improvement mechanisms are synergistic. First, the role of plants and AMF through the release of root exudates, such as organic acids and phosphatase enzymes, which can break down calcium phosphate bonds (Richardson *et al.,* 2011). Second, and this is an important finding,

Table 5: Soil physical properties across different land use types in the limestone post-mining area

Area	Soil physical properties				
	Bulk density (g/cc)	Index aggregate stability		Total pore space	Porosity (%)
		Mean	Criteria*		
A0	1.36 ±0.21a	40.61	unstable	34.97±13.35a	34.88±13.35a
A1	1.34 ±0.12a	89.78	very stable	42.07 ±7.75a	40.57±5.67a
A2	1.34 ±0.08a	90.61	very stable	43.23 ±5.59a	42.31±5.73 a

Remarks: A0 (unplanted area), A1 (initial planting without AMF inoculation), and A2 (initial planting with AMF inoculation). Numbers followed by the same letter indicate no significant difference at $p < 0.05$. *Criteria of soil stability aggregate based on Center for Agricultural Land Resources Research and Development of Indonesia: <40:unstable; 40-50:less stable; 50-66:slightly stable; 66-80: stable; 80-200: very stable; >200: very very stable (Hidayat *et al.,* 2025). Numbers after ± represent the standard deviation of the mean. Data collected after 5 years of initial planting establishment.

is the accelerating role of AMF. AMF enhances root reach, allowing for the absorption of P from a greater volume of soil, while also actively solubilizing bound P by releasing organic acids and glomalin, and boosting phosphatase enzyme activity in the rhizosphere (Etesami *et al.,* 2021; Wang *et al.,* 2022). The highest values are once again observed in mycorrhizal initial planting areas (A2), but the overall soil chemical enhancement is also accompanied by an increase in N availability (Table 4). To achieve this increase, dual and synergistic mechanisms were also applied. The capacity of legume cover crops (*C. pubescens*) to fix atmospheric N_2 is essential for the increase in N supply. Additionally, AMF promotes this cycle by enhancing the efficiency of N_2 fixation in legumes and directly contributing to the mineralization and assimilation of N from soil organic matter, thereby increasing the availability of both N and P simultaneously (Fall *et al.,* 2022; Saia *et al.,* 2019). Overall, this study demonstrates that combining revegetation with AMF inoculation is an effective approach that can trigger a range of improvements in soil chemistry, transforming a barren area into a productive and thriving ecosystem.

Rebuilding soil structure as an indicator of soil physics improvement

Mining activities fundamentally destroy soil structure, the physical architecture formed by the arrangement of solid particles and pore spaces, which controls vital soil functions such as the water cycle, aeration, nutrient movement, and erosion resistance (Rabot *et al.,* 2018). The most noticeable consequence of using heavy machinery is the compaction of soil, which causes elevated bulk density and a decrease in porosity. As shown in Table 5, the unplanted area (A0) has the highest bulk density, creating a physical barrier that impedes root penetration and water infiltration, a common condition in post-mining lands worldwide (Damptey *et al.,* 2020). This issue is closely linked to inadequate soil aggregation, where soil particles do not adhere to form stable structures, rendering the soil susceptible to erosion. The very low aggregate stability index values in the A0 area confirm this disruption of the soil's physical architecture.

The introduction of initial planting has proven to be a highly effective first step in restarting the soil structure formation process. Plants contribute to improved aggregation through two key mechanisms. First, their extensive root systems physically penetrate and intertwine with soil particles, effectively binding them into stable aggregates (Gould *et al.,* 2016; Negi *et al.,* 2025; Pérès *et al.,* 2013). Second, biochemically, the roots release exudates in the form of polysaccharide compounds that function as organic binding agents, increasing aggregate stability over time (Baumert *et al.,* 2018; Galloway *et al.,* 2020; Ma *et al.,* 2022). Table 5 shows that the introduction of plantings (A1 and A2) successfully improved the soil aggregation status radically from less stable to very stable. The inoculation of AMF, acknowledged as the main ecosystem engineers in soil aggregate formation, significantly boosted and accelerated this improvement (Chatterjee *et al.,* 2019). AMF contributes in two complementary ways. First, the massive external hyphal network of AMF growing in the soil physically entraps soil particles, forming a stable framework that becomes the precursor to macroaggregate formation (Morris *et al.,* 2019). Second, and most importantly, AMF produce a unique glycoprotein called glomalin, a powerful biological superglue that binds soil particles together and stabilizes aggregates over the long term (Chaudhary *et al.,* 2025). Evidence of the catalytic role of AMF is evident in Table 5, where the mycorrhizal planting area (A2) exhibited the highest

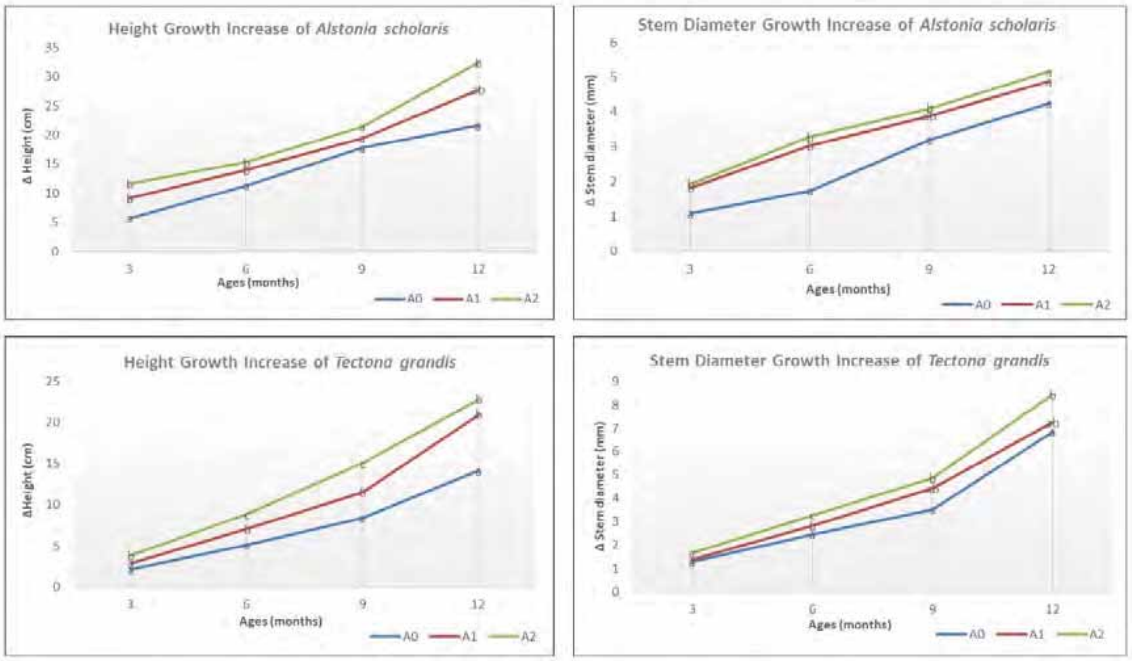

Fig. 5: Increase (Δ) in height and diameter growth of *Alstonia scholaris* and *Tectona grandis* on limestone post-mining land every three months during 12 months observation.

Remarks: A0 (unplanted area), A1 (initial planting without AMF inoculation), and A2 (initial planting with AMF inoculation). The same letters that follow every point parallel to the X-axis show different values. No significant difference at $p<0.05$. Data collected after 5 years of initial planting establishment.

aggregate stability index, confirming that the synergy between plant roots and AMF hyphae is the most efficient mechanism for rebuilding soil structure. The formation and stabilization of aggregates facilitated by plant roots and arbuscular mycorrhizal fungi (AMF) generate a beneficial chain reaction. Soils with stable aggregates directly exhibit lower bulk density and higher total pore space and porosity (Table 5). This enhanced porosity is vital as it boosts soil aeration, enhances water retention, and creates room for unrestricted root development (Ren *et al.,* 2023). Ultimately, restoring soil structure in this former limestone quarry creates a healthy physical foundation, which will facilitate more effective natural plant colonization, accelerating ecological succession.

The growth enhancement of A. scholaris and T. grandis serves as an indicator for the subsequent seral species to promote natural succession

The primary aim of any reclamation initiative is not just to plant trees, but to initiate and speed up the natural ecological successional trajectory toward a self-sustaining and functional ecosystem. In this context, effective initial plantings should enhance both the abiotic and biotic environment, a phenomenon known as facilitation, whereby the existence of pioneer species establishes conditions that permit the arrival and establishment of species from later successional stages (Brooker *et al.,* 2008; Gómez-Aparicio, 2009). Therefore, the successful establishment of subsequent seral is the ultimate indicator of whether the site improvements—physical, chemical, and biological—have truly created functional "safe sites." To test this hypothesis, *Alstonia scholaris* was used with a late-stage pioneer tree, and *Tectona grandis*, a long-lived tree species capable of surviving to the climax stage, as proxies for successional facilitation (Ashton *et al.,* 2011; Poorter *et al.,* 2021). The outcomes consistently demonstrated that site modification via initial planting inoculated with AMF (area A2) significantly promoted the vegetative growth of mid-seral species. In both *A. scholaris* and *T. grandis*, plants grown in area A2 showed statistically superior increases in height and stem diameter compared to the other areas (Fig. 5). *A. scholaris* increases in area A2 were

recorded at 20.39% to 101.91% greater than in the unplanted area (A0), and 9.36% to 26.61% ($p<0.05$) greater than in the area without mycorrhizae (A2). The diameter increase was also significant, namely 21.13% to 88.51% ($p<0.05$) greater than A0 and 5.52% to 8.25% ($p<0.05$) greater than A1. There was a statistically significant difference, particularly regarding the diameter measured at 3 to 9 months and in height at both 3 and 12 months. A similar trend occurred in teak, where the height increase in the A2 area was 61.16% to 79.91% greater than A0 and 8.93% to 32.30% ($p<0.05$) greater than A1. The diameter increase was also superior to A0 by 23.21% to 37.96% ($p<0.05$) and 10.18% to 21.74% ($p<0.05$) than A1. Height growth of *T. grandis* showed very significant differences at all observation ages. The observed trend of enhanced growth in the A2 region for both plant types suggests that mycorrhizal symbiosis plays a significant role in promoting vegetative development in less-than-ideal conditions. This superior growth provides empirical evidence that AMF-mediated soil improvement not only benefits early seral species but also directly provides a strong facilitating effect on later successional species (Tedersoo *et al.,* 2020). The synergy between improved soil structure, increased nutrient availability, and a functional AMF network in the A2 area has been shown to successfully create optimal micro-conditions, surpassing critical thresholds that previously inhibited growth in post-mining land.

The mechanism behind this superior growth can be traced at the physiological level, particularly in the increased uptake of phosphorus, the most limiting nutrient in the alkaline soils of the limestone post-mining land (Table 6). In area A2, plants showed markedly higher leaf P levels, which are directly associated with the greatest percentage of root colonization by AMF (Fig. 6). This is functional evidence of an effective symbiosis. AMF hyphae actively explore a larger soil volume and release organic acids and phosphatase enzymes to dissolve calcium-bound P, making it available for plant uptake (Etesami *et al.,* 2021; Wang, 2017; Wang *et al.,* 2022). This increased P uptake directly triggers fundamental metabolic processes. As a fundamental part of adenosine triphosphate (ATP), the molecule that carries energy in cells, phosphorus's abundant supply will influence the rates of photosynthesis, respiration, and biomass synthesis (Bucher, 2007; Lambers, 2022). This is reflected in the leaf biomass, which tends to be higher in both plants in area A2, indicating higher metabolic efficiency thanks to optimal nutrition.

Furthermore, the success of mycorrhizal inoculation was confirmed by the level of colonization or AMF infection in plant roots (Fig. 6). In the roots of *A. scholaris*, the percentage of AMF colonization was consistently highest in area A2 at all observation ages (3, 6, 9, and 12 months), with statistically significant differences. In *T. grandis* roots, the percentage of AMF infection was also highest in area A2, with significant differences especially in 3 and 6 months. The significant levels of colonization indicate that AMF inoculation at the onset of planting has effectively created a robust and sustainable symbiosis, which is the key factor contributing to improved plant growth and health.

The high level of AMF colonization in *A. scholaris* and *T. grandis* roots in area A2 (>50%) confirms that inoculation during the initial planting successfully created an active and widespread AMF propagule bank in the soil. It is particularly noteworthy that a significant level of colonization was detected in area

Table 6: Leaf P content of *A. scholaris* and *T. grandis* at 6 and 12 months in the limestone post-mining area

Types of plants	Area	P content (%)		Biomass leaves (g)	
		6 months	12 months	6 months	12 months
A. scholaris	A0	0.19±0.09a	0.13±0.05a	0.87±0.49a	0.90±0.38a
	A1	0.27±0.10a	0.19±0.04b	0.90±0.57a	1.13±0.65a
	A2	0.28±0.08a	0.20±0.05b	1.35±0.27a	1.16±0.75a
T. grandis	A0	0.10±0.08a	0.08±0.04a	2.08±1.21a	8.31±3.70a
	A1	0.12±0.04a	0.08±0.02a	3.09±1.88a	8.34±5.04a
	A2	0.17±0.06a	0.13±0.03b	3.18±0.94a	8.99±5.61a

Remarks: A0 (unplanted area), A1 (initial planting without AMF inoculation), and A2 (initial planting with AMF inoculation). The numbers followed the same letter show no significant difference at $p<0.05$. Numbers after ± represent the standard deviation of the mean. Data collected after 5 years of initial planting establishment.

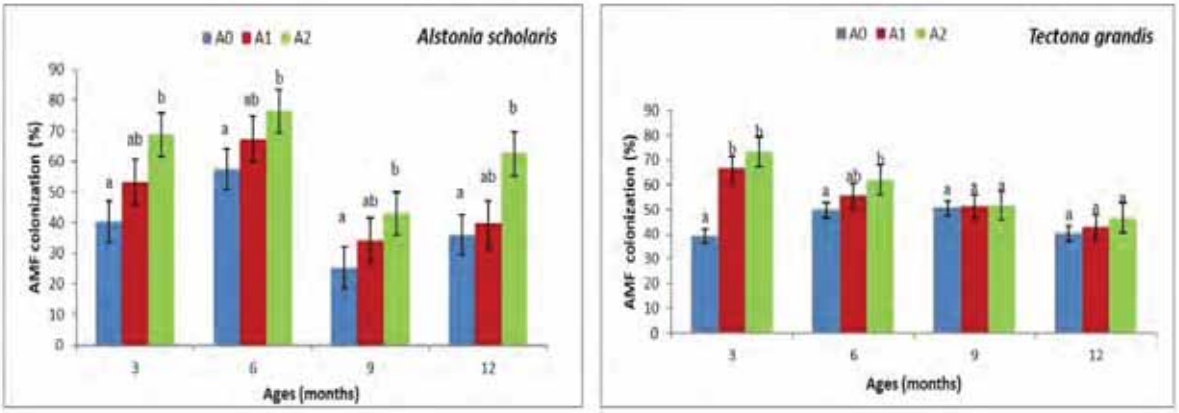

Fig. 6: The level of AMF colonization in the roots of *A. scholaris* and *T. grandis* every three months during 12 months observation in various types of areas in the limestone post-mining areas

Remarks: A0 (unplanted area), A1 (initial planting without AMF inoculation), and A2 (initial planting with AMF inoculation). The numbers followed the same letter show no significant difference at $p<0.05$. Error bars represent the standard deviation of the mean (SD). Data collected after 5 years of initial planting establishment.

A1 (which underwent initial planting without AMF inoculation), indicating the movement of hyphae and spores from the neighboring area A2. This phenomenon demonstrates that the catalytic effect of AMF is not limited to the inoculated host plant but also spreads to the surrounding plant community, a crucial finding for landscape-scale restoration. Consequently, this research thoroughly illustrates that the initial planting of mycorrhizal trees is not merely about planting trees; it is a strategic ecological intervention that actively restores the foundation of soil life, establishes a secure site, and efficiently bypasses stagnant successional phases to enhance the overall recovery of the ecosystem.

Ecological implications and recommendations for rehabilitation

The results of this study reveal profound ecological implications, shifting the understanding and practice of land rehabilitation from mere reforestation to the restoration of functional ecosystems. Key findings reveal that focused biological strategies, including the application of AMF-inoculated seedbeds, function as catalysts that instigate a favorable chain reaction for overall ecosystem restoration. This process begins with an increase in the population, richness, and diversity of AMF, which serves as the foundation for revitalizing soil biology. The presence of these functional microbial communities directly promotes the decomposition and accumulation of organic matter, which in turn drives improvements in soil chemistry. This greatly speeds up the process of nutrient cycling, as the symbiosis with AMF and root activity enhance the accessibility of essential elements like Phosphorus and Nitrogen, leading to more fertile and stable soil conditions. These positive impacts extend beyond the chemical level to improvements in the soil's physical structure. The formation of soil aggregates, mediated by AMF hyphae and root exudates, effectively increases porosity and water infiltration, reduces soil density, and suppresses soil erosion. This comprehensive enhancement of the soil's biophysical and chemical properties has been demonstrated to establish secure locations. The most important implication of this faster safe site formation is that it effectively facilitates and accelerates spontaneous colonization (jump-start succession) by individuals and native species from the surrounding area. Furthermore, these safe sites are not only crucial for initial succession but also determine subsequent successional development, with each successive change being supported by the conditions established in the previous one. Thus, this approach actively accelerates the natural successional trajectory toward a more complex and self-sustaining ecosystem. In light of these findings, a number of actionable recommendations have been developed to enhance the effectiveness of rehabilitation programs on degraded land, especially in post-mining areas. First, AMF inoculation should

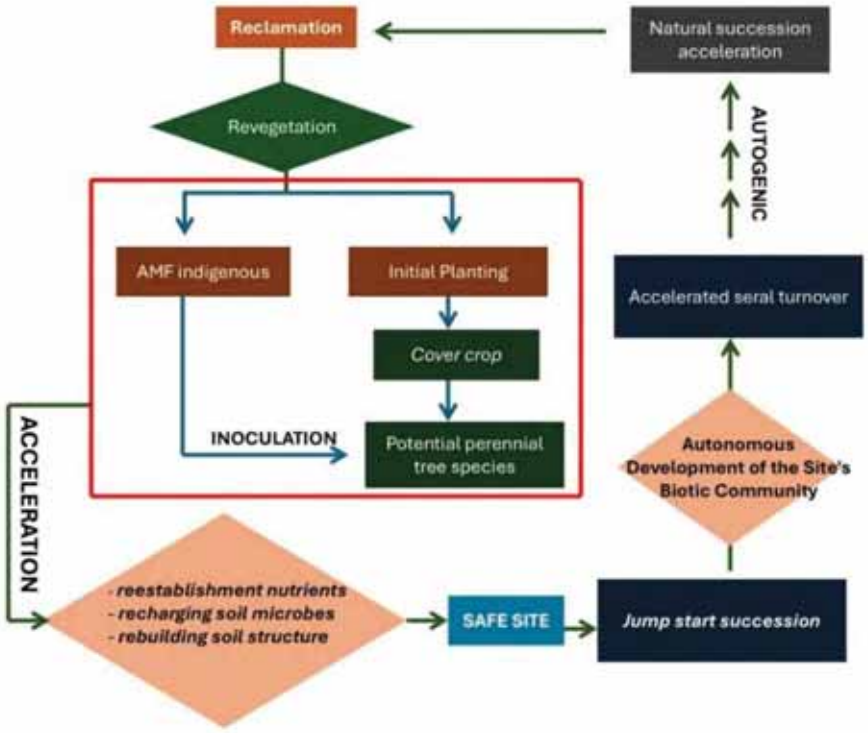

Fig. 7: Accelerating natural succession on post-mining land using initial planting and AMF inoculation

be a standard and mandatory component of every revegetation activity, not just an option. Considering that natural AMF populations in areas affected by mining are significantly low, and the recovery process is gradual, introducing adaptive indigenous inoculum is an essential investment to hasten the restoration of ecosystem functionality. Second, the selection of species for initial plantings should prioritize those that synergize strongly with AMF and are capable of rapidly improving the soil. Combining nitrogen-fixing legume cover crops (such as *C. pubescens*) with pioneer tree species, and long-lived trees (such as *V. cofassus*) has proven highly effective in simultaneously supplying organic matter, controlling erosion, and recharging soil microbial populations. Third, and most strategically, rehabilitation programs should be designed with an ecological succession perspective. A stepwise method, starting with site enhancement via successive plantings of initial specimens treated with mycorrhizal fungi, has demonstrated greater success than the direct planting of climax species (which are slow-growing). Fourth, the practical feasibility and cost implications of a large-scale AMF inoculation program must be considered. The upfront financial costs of producing and applying commercial AMF inoculum can be considered prohibitive, especially for large-scale rehabilitation projects. However, these costs should be viewed as a long-term ecological investment, not simply an expense. The improved plant survival rates and accelerated growth demonstrated in this study could significantly reduce long-term costs associated with replanting and lengthy maintenance periods such as weeding. Furthermore, enhanced nutrient cycling, especially with increased phosphorus availability, could lessen dependence on costly and frequently environmentally harmful chemical fertilizers. Strategically, developing locally adapted indigenous AMF inoculum sources could further reduce these initial costs. Therefore, when evaluated across the project's entire life cycle, the initial investment in AMF may be offset by savings in maintenance and fertilization costs, leading to more cost-effective and ecologically successful outcomes in the long term. This study confirms that once a safe site is established, mid-seral and late-seral species can grow with excellent

performance, indicating that this facilitation strategy is key to long-term success. Ultimately, every type of reclamation intervention should create a catalytic impact that speeds up succession, thereby providing opportunities to choose plant species that align with the reclamation goals, including economic ones. This integrated approach transforms the rehabilitation process from mere reforestation to functional and sustainable ecosystem restoration. By implementing this integrated approach, the rehabilitation paradigm can shift from mere reforestation to functional and sustainable ecosystem restoration. The schematic representation of the logic behind this overall process, where early interventions initiate accelerated succession, can be found in Fig. 7.

Limitations and future research directions

This study presents compelling evidence and suggests multiple avenues for future research aimed at enhancing restoration practices. This study used a mixed indigenous AMF inoculum, it is recommended to isolate superior indigenous AMF strains to create more targeted inocula and determine the degree of mycorrhizal dependence on restoration species. Extended monitoring over a period of 5 to 10 years, with increased frequency (for instance, seasonal assessments), is essential to confirm the effectiveness of ecosystem restoration. This includes evaluating natural biorecruitment and the stability of dynamic soil characteristics like pH buffering capacity. Further analysis is recommended using metagenomic approaches to understand impacts on the entire microbial community, quantitative modeling (SEM) to partition variable effects, and more detailed measurements of soil factors (microtopography, cation interactions, micronutrients, and enzyme activity). Further research in this area will yield more precise and robust restoration strategies.

CONCLUSION

This study presents a thorough and persuasive argument for implementing AMF inoculation as a key approach in the ecological restoration of highly degraded areas, including limestone post-mining sites. The outcomes evidently demonstrate that this biological intervention functions as an important catalyst, adeptly overcoming the main environmental barriers that often obstruct natural succession in these locations. The intervention's success is not just incremental; it is transformative, resulting in a comprehensive and synergistic enhancement of the soil's biological, chemical, and physical properties. The initiative commenced with the rejuvenation of the underground ecosystem. The application of AMF inoculum led to a remarkable increase of 291.11% in spore density, along with a substantial enhancement in fungal richness and diversity when compared to recovery without assistance. This biological recharging served as the main catalyst for a series of beneficial outcomes. The chemical processes involved led to the highest levels of organic matter and litterfall accumulation, subsequently improving the soil's Cation Exchange Capacity. The symbiosis effectively tackled the significant phosphorus limitation typical of alkaline limestone substrates. The AMF network effectively solubilized previously unavailable occluded phosphate by releasing organic acids and phosphatase enzymes, thereby making this essential nutrient accessible to plants. The collaboration of plant roots with the broad AMF hyphal network operated as ecosystem engineers, altering the configuration of the soil. The generation of glomalin, an effective biological binding agent, greatly enhanced soil aggregation, converting the land from an unstable condition to a highly stable one. The enhancement of the structure caused an increase in porosity and better water infiltration, promoting a more supportive environment for life. Ultimately, this integrated soil improvement resulted in functional safe sites, a fact clearly demonstrated by the successful establishment and robust growth of the mid-seral successional species, *A. scholaris* and *T. grandis*. Plants in the AMF-inoculated area showed significant enhancements in height and diameter, reaching up to 101.91% greater than those in the unplanted area for *A. scholaris*. The quick expansion seen was directly related to greater AMF root colonization and increased phosphorus levels in leaves, affirming the success of the symbiotic association. This study, consequently, transforms the approach to reclamation from basic revegetation to a more strategic and ecologically informed methodology. This illustrates that employing AMF-inoculated plants in the initial establishment of planting can effectively initiate the natural successional process, thereby accelerating the conversion of barren post-mining areas into viable and self-sustaining ecosystems.

AUTHOR CONTRIBUTIONS

R. Prayudyaningsih, the corresponding author, has contributed to conception and design, acquisition of data, analysis and interpretation of data, drafting of the manuscript, statistical análisis, obtaining funding, and supervisión. M. Turjaman has contributed to conception and design, drafting of the manuscript, critical revision of the manuscript for important intellectual content, and supervisión. Pratiwi has contributed to conception and design, analysis and interpretation of data, drafting of the manuscript, critical revision of the manuscript for important intellectual content, and supervisión. F. Ansari has participated in the acquisition of data, drafting of the manuscript, and provided administrative, technical, or material support, and created a map. H. Gunawan has participated in the acquisition of data, obtaining funding, and providing administrative, technical, or material support.

ACKNOWLEDGEMENT

The authors would like to express their sincere appreciation to Semen Tonasa Company, the Ministry of Environment and Forestry, and National Research and Innovation Agency for providing financial support through a memorandum of understanding number [694/SP/HK.02.04/31.00/01-2018 and KPS.175.1/BP2LHK in 2018] and [147/V/KS/03/2023 and 234/SP/HK.02.0412.00/01-2023 in 2023], technical assistance, and logistical support during the study.

CONFLICT OF INTEREST

The authors declare that there is no conflict of interests regarding the publication of this manuscript. In addition, the ethical issues, including plagiarism, informed consent, misconduct, data fabrication and/or falsification, double publication and/or submission, and redundancy have been completely observed by the authors.

OPEN ACCESS

©2026 The author(s). This article is licensed under a Creative Commons Attribution 4.0 International License, which permits use, sharing, adaptation, distribution and reproduction in any medium or format, as long as you give appropriate credit to the original author(s) and the source, provide a link to the Creative Commons license, and indicate if changes were made. The images or other third-party material in this article are included in the article's Creative Commons license, unless indicated otherwise in a credit line to the material. If material is not included in the article's Creative Commons license and your intended use is not permitted by statutory regulation or exceeds the permitted use, you will need to obtain permission directly from the copyright holder. To view a copy of this license, visit: http://creativecommons.org/licenses/by/4.0/

PUBLISHER'S NOTE

GJESM Publisher remains neutral with regard to jurisdictional claims in published maps and institutional afflictions.

Positive AI Statement

During the preparation of this work the author(s) have used Artificial Intelligence (AI) Gemini and Quillbot to collect references, checked typographical errors and improved structure of sentences. After using this tool/service, the authors reviewed and edited the content as needed and took full responsibility for the content of the publication.

(For this reason, the GPTZero detector will evaluate the manuscript utilizing Generative AI, ensuring a high detection rate. If the manuscript relies heavily on Generative AI and AI-assisted technologies, it will be archived without further options for appeal).

ABBREVIATIONS

%	Percent
°C	Celcius degree
A0	Unplanted area
A1	Initial planting without mycorrhizal inoculation
A2	Mycorrhizal initial planting area
AMF	Arbuscular mycorrhizal fungi
ANOVA	Analysis of variance
AR	Relative abundance
ATP	Adenosine tri phospat
Ca	Calcium
CEC	Cation exchange capacity
cm	Centimeter
FI	Isolate frequency
g	Gram

ha	hectares
H'	Diversity index
IVI	Importance value index
km	kilometer
m	Meter
mm	Millimeter
N	Nitrogen
NaCl	Sodium chloride
OC	Organic carbon
P	Phosphorus
pH	Potential of hydrogen
ppm	Parts per million
PVLG	Polyvinyl-lactic acid-glycerol
R	Species richness
RCBD	Randomized complete block design
SD	Standard deviation
SG	Specific gravity
SOC	Soil organic carbon
SOM	Soil organic matter
VW	Volumetric weight

REFERENCES

Afshari, M.; Rahimmalek, M.; Sabzalian, M.R.; Szumny, A.; Matkowski, A.; Jezierska-Domaradzka, A., (2022). Mycorrhizal colonization modulates the essential oil profile and enzymatic and non-enzymatic antioxidants to mitigate the adverse effects of water deficit in salvia subg. Perovskia. Biology. 11: 1-22 **(22 pages).**

Albracht, C.; Solbach, M.D.; Hennecke, J.; Bassi, L.; van der Ploeg, G.R.; Eisenhauer, N.; Weigelt, A.; Buscot, F.; Heintz-Buschart, A., (2024). Common soil history is more important than plant history for arbuscular mycorrhizal community assembly in an experimental grassland diversity gradient. Biol. Fertility Soils. 60: 547–562 **(15 pages).**

Andreetta, A.; Macci, C.; Giansoldati, V.; Masciandaro, G.; Carnicelli, S., (2013). Microbial activity and organic matter composition in mediterranean humus forms. Geoderma. 209-210: 198-208 **(11 pages).**

Andrino, A.; Guggenberger, G.; Sauheitl, L.; Burkart, S.; Boy, J., (2021). Carbon investment into mobilization of mineral and organic phosphorus by arbuscular mycorrhiza. Biol. Fertility Soils. 57: 47–64 **(18 pages).**

Ashton, M.S.; Singhakumara, B.; Gunatilleke, N.; Gunatilleke, S., (2011). Sustainable forest management for mixed-dipterocarp forests: A case study in southwest sri lanka. In: Günter, S.; Weber, M.; Stimm, B.; Mosandl, R., (eds) Silviculture in the Tropics. Tropical Forestry, Springer, Berlin, Heidelberg. 8: 193-213 **(21 pages).**

Brundrett, M.; Bougher, N.; Dell, B.; Grove, T.; Malajczuk, N., (1996). Working with mycorrhizas in forestry and agriculture. Australian Centre for International Agricultural Research Canberra. (**347 pages**).

Bucher, M., (2007). Functional biology of plant phosphate uptake at root and mycorrhiza interfaces. New Phytol. 173: 11–26 (**16 pages**).

Buil, P.A.; Jansa, J.; Rozmoš, M.; Kotianová, M.; Bukovská, P.; Grilli, G.; Marro, N.; Janoušková, M., (2025). Soil cropping selects for nutrient efficient but more costly indigenous mycorrhizal fungal communities. Biol. Fertility Soils. 61: 841-859, (**19 pages**).

Cao, J.; Zhao, P.; Wang, D.; Zhao, Y.; Wang, Z.; Zhong, N., (2023). Effects of a nanonetwork-structured soil conditioner on microbial community structure. Biology. 12(668): 1-25 (**25 pages**).

Carrasqueira, J.; Afonso, C.; Gil, M.M.; Bernardino, R.; Gamboa, R.; Barroso, S.D.; Bernardino, S., (2024). Digging deeper: Assessing the impact of limestone exploitation and use worldwide. Environments. 11(283): 1-18 (**18 pages**).

Chatterjee, A.; Khan, S.R.; Vaseem, H., (2019). Exploring the role of mycorrhizae as soil ecosystem engineer. In: Varma, A.; Choudhary, D., (eds) Mycorrhizosphere and pedogenesis. Springer. 1-420 (**420 pages**).

Chaudhary, A.; Poudyal, S.; Kaundal, A., (2025). Role of arbuscular mycorrhizal fungi in maintaining sustainable agroecosystems. Appl. Microbiol. 5(6): 1-19 (**19 pages**).

Chen, Q.; Deng, X.; Elzenga, J.T.M.; Van Elsas, J.D., (2022). Effect of soil bacteriomes on mycorrhizal colonization by rhizophagus irregularis—interactive effects on maize (zea mays l.) growth under salt stress. Biol. Fertility Soils. 58: 515-525 (**11 pages**).

Chourasiya, D.; Gupta, M.M.; Sahni, S.; Oehl, F.; Agnihotri, R.; Buade, R.; Maheshwari, H.S.; Prakash, A.; Sharma, M.P.,(2021). Unraveling the am fungal community for understanding its ecosystem resilience to changed climate in agroecosystems. Symbiosis. 84: 295-310 (**16 pages**).

Combs, S.; Nathan, M., (2015). Soil organic matter. Recommended chemical soil test procedures for the North Central Region. Missouri Agricultural Experiment Station, University of Missouri-Columbia. 221: 1.1-15.5 (**76 pages**).

Damptey, F.G.; Birkhofer, K.; Nsiah, P.K.; de la Riva, E.G., (2020). Soil properties and biomass attributes in a former gravel mine area after two decades of forest restoration. Land. 9(209): 1-18 (**18 pages**).

Dassen, S.; van der Putten, W.H.; De Deyn, G.B., (2021). Severance of arbuscular mycorrhizal fungal mycelial networks in restoration grasslands enhances seedling biomass. New Phytol., 232: 753-761 (**9 pages**).

Du, S.; Xie, H.; Zhang, G.; Qiao, F.; Geng, G.; Chongyi E., (2025). Improvement effects of different afforestation measures on the surface soil of alpine sandy land. Biology. 14 (144): 1-23 (**23 pages**).

Etesami, H.; Jeong, B.R.; Glick, B.R., (2021). Contribution of arbuscular mycorrhizal fungi, phosphate-solubilizing bacteria, and silicon to p uptake by plant. Front. Plant Sci. 12: 1-12 (**29 pages**).

Fall, A.F.; Nakabonge, G.; Ssekandi, J.; Founoune-Mboup, H.; Apori, S.O.; Ndiaye, A.; Badji, A., Ngom, K.,(2022). Roles of arbuscular mycorrhizal fungi on soil fertility: Contribution in the improvement of physical, chemical, and biological properties of the soil. Front. Fungal Biol. 3: 1-11 (**11 pages**).

Funk, J.L.; Larson, J.E.; Ames, G.M.; Butterfield, B.J.; Cavender-Bares, J.; Firn, J.; Laughlin, D.C.; Sutton-Grier, A.E.; Williams, L.; Wright, J., (2017). Revisiting the h oly g rail: Using plant functional traits to understand ecological processes. Biol. Rev. 92(2): 1156-1173 (**18 pages**).

Galloway, A.F.; Akhtar, J.; Marcus, S.E.; Fletcher, N.; Field, K.; Knox, P., (2020). Cereal root exudates contain highly structurally complex polysaccharides with soil-binding properties. Plant J. 103(5): 1666-1678 (**13 pages**).

Gerdemann, J.; Nicolson, T.H., (1963). Spores of mycorrhizal endogone species extracted from soil by wet sieving and decanting. Trans. Br. Mycol. Soc. 46(2): 235-244 (**10 pages**).

Giovannetti, M.; Mosse, B., (1980). An evaluation of techniques for measuring vesicular arbuscular mycorrhizal infection in roots. New Phytol. 84(3): 489-500 (**12 pages**).

Gómez-Aparicio, L., (2009). The role of plant interactions in the restoration of degraded ecosystems: A meta-analysis across life-forms and ecosystems. J. Ecol. 97(6): 1202-1214 (**13 pages**).

Gould, I.J.; Quinton, J.N.; Weigelt, A.; De Deyn, G.B.; Bardgett, R.D., (2016). Plant diversity and root traits benefit physical properties key to soil function in grasslands. Ecol. Lett. 19(9): 1140-1149 (**9 pages**).

Hardjowigeno, S., (2010). Ilmu tanah. Akademika Pressindo, Jakarta. (**288 pages**).

Hartmut, K.; Elke, M.; Sybilla, H., (1995). Soil microarthropods (acari, collembola) from beach and dune: Characteristics and ecosystem context. J. Coast. Conserv. 1: 77-86 (**10 pages**).

Hidayat, Y.; Baskoro., D.P.T.; Purwakusuma, W.; Siregar, M.S.; Ramadhi, M.H A., (2025). Soil aggregate stability index on agricultural, plantation, and forest lands. Jurnal Ilmu Tanah dan Lingkungan. 27(2): 56-62 (**7 pages**).

Jia, X.; Fang, Y.; Hu, B.; Yu, B.; Zhou, Y., (2023). Development of soil fertility index using machine learning and visible-near-infrared spectroscopy. Land. 12(2155): 1-13 (**13 pages**).

Kormanik, P.P.; McGraw, A., (1982). Quantification of vesicular-arbuscular mycorrhizae in plant roots. In: Schenck, N.C., (eds) Methods and principles of mycorrhizal research. American Phytopathological Society, St. Paul. : 37-45 (**9 pages**).

Košnar, J.; Šmilauer, P.; Šmilauerová, M., (2025). Arbuscular and fine root-endophytic mycorrhizal fungi forage differently for nutrients in a seminatural temperate grassland. Biol. Fertility Soils. 610: 773–790 (**18 pages**).

Krebs, C.J., (1972). Ecology. The experimental analysis of distribution and abundance. Harper and Row. (**694 pages**).

Lambers, H., (2022). Phosphorus acquisition and utilization in plants. Ann. Rev. Plant Biol. 73: 17-42 (**26 pages**).

Lethielleux-Juge, C., (2025). Review: Roles of mycorrhizal symbioses and associated soil microbiomes in ecological restoration. Front. Microbiol. 16: 1-21 (**21 pages**).

Li, Y.; Fang, S.; Wang, Q.; Wu, P.; He, P.; Liu, W., (2025). Interannual variations in soil bacterial community diversity and analysis of influencing factors during the restoration process of scirpus mariqueter wetlands. Biology. 14(8): 1-14 (**14 pages**).

Liang, X.; Yu, S.; Ju, Y.; Wang, Y.; Yin, D., (2025). Integrated management practices foster soil health, productivity, and agroecosystem resilience. Agronomy. 15(1816): 1-29 (**29 pages**).

Liu, R.; Li, M.; Guo, S.; Chen, Y., (2024). The role of AMF community composition, diversity, and distribution in sustainable agroecosystems. In: Parihar, M.; Rakshit, A.; Adholeya, A.; Chen, Y., (eds) Arbuscular mycorrhizal fungi in sustainable agriculture: inoculum production and application. Springer, Singapore. 281-317 (**36 pages**).

Ma, W.; Tang, S.; Dengzeng, Z.; Zhang, D.; Zhang, T.; Ma, X., (2022). Root exudates contribute to belowground ecosystem hotspots: A rev.: Front. Microbiol. 13(937940): 1-19 (**19 pages**).

Margesin, R.; Schinner, F., (2005). Manual for soil analysis-monitoring and assessing soil bioremediation. Springer Science Business Media. (**366 pages**).

Morris, E.K.; Morris, D.J.P.; Vogt, S.; Gleber, S.C.; Bigalke, M.; Wilcke, W.; Rillig, M.C., (2019). Visualizing the dynamics of soil aggregation as affected by arbuscular mycorrhizal fungi. The ISME Journal. 13(7): 1639–1646 (**15 pages**).

Negi, M.; Sharma, S.; Singh, M., (2025). Plant-driven soil dynamics: Exploring the role of roots, fungi and soil traffic in shaping the soil structure. Commun. Soil Sci. Plant Anal. 56(18): 2727–2746 (**20 pages**).

Ouhaddou, R.; Anli, M.; Ben-Laouane, R.; Boutasknit, A.; Baslam, M.; Meddich, A., (2025). The importance of the glomus genus as a potential candidate for sustainable agriculture under arid environments: A review. Int. J. Plant Biol. 16(32): 1-22 (**22 pages**).

Palmer, M.A.; Stewart, G.A., (2020). Ecosystem restoration is risky… but we can change that. One Earth. 3(6): 661-664 (**4 pages**).

Patanita, M.; Campos, M.D.; Felix, M.D.R.; Carvalho, M.; Brito, I., (2020). Effect of tillage system and cover crop on maize mycorrhization and presence of magnaporthiopsis maydis. Biology. 9(46): 1-16 (**16 pages**).

Penn, C.J.; Camberato, J.J., (2019). A critical review on soil chemical processes that control how soil ph affects phosphorus availability to plants. Agriculture. 9(120) : 1-18 (**18 pages**).

Pérès, G.; Cluzeau, D.; Menasseri, S.; Soussana, J.F.; Bessler, H.; Engels, C.; Habekost, M.; Gleixner, G.; Weigelt, A.; Weisser, W.W., (2013). Mechanisms linking plant community properties to soil aggregate stability in an experimental grassland plant diversity gradient. Plant Soil. 373: 285-299 (**15 pages**).

Perring, M.P.; Standish, R.J.; Price, J.N.; Craig, M.D.; Erickson, T.E.; Ruthrof, K.X.; Whiteley, A.S.; Valentine, L.E.; Hobbs, R.J., (2015).

Advances in restoration ecology: Rising to the challenges of the coming decades. Ecosphere. 6(8): 1-25 (**25 pages**).

Poorter, L.; Craven, D.; Jakovac, C.C.; van der Sande, M.T.; Amissah, L.; Bongers, F.; Chazdon, R.L.; Farrior, C.E.; Kambach, S.; Meave, J.A.; Munoz, R.; Norden, N.; Ruger, N.; van Breugel, M.; Almeyda Zambrano, A.M.; Amani, B.; Andrade, J.L.; Brancalion, P.H.S.; Broadbent, E.N.; de Foresta, H.; Dent, D.H.; Derroire, G.; DeWalt, S.J.; Dupuy, J.M.; Duran, S.M.; Fantini, A.C.; Finegan, B.; Hernandez-Jaramillo, A.; Hernandez-Stefanoni, J.L.; Hietz, P.; Junqueira, A.B.; N'Dja J, K.; Letcher, S.G.; Lohbeck, M.; Lopez-Camacho, R.; Martinez-Ramos, M.; Melo, F.P.L.; Mora, F.; Muller, S.C.; N'Guessan, A.E.; Oberleitner, F.; Ortiz-Malavassi, E.; Perez-Garcia, E.A.; Pinho, B.X.; Piotto, D.; Powers, J.S.; Rodriguez-Buritica, S.; Rozendaal, D.M.A.; Ruiz, J.; Tabarelli, M.; Teixeira, H.M.; Valadares de Sa Barretto Sampaio, E.; van der Wal, H.; Villa, P.M.; Fernandes, G.W.; Santos, B.A.; Aguilar-Cano, J.; de Almeida-Cortez, J.S.; Alvarez-Davila, E.; Arreola-Villa, F.; Balvanera, P.; Becknell, J.M.; Cabral, G.A.L.; Castellanos-Castro, C.; de Jong, B.H.J.; Nieto, J.E.; Espirito-Santo, M.M.; Fandino, M.C.; Garcia, H.; Garcia-Villalobos, D.; Hall, J.S.; Idarraga, A.; Jimenez-Montoya, J.; Kennard, D.; Marin-Spiotta, E.; Mesquita, R.; Nunes, Y.R.F.; Ochoa-Gaona, S.; Pena-Claros, M.; Perez-Cardenas, N.; Rodriguez-Velazquez, J.; Villanueva, L.S.; Schwartz, N.B.; Steininger, M.K.; Veloso, M.D.M.; Vester, H.F.M.; Vieira, I.C.G.; Williamson, G.B.; Zanini, K.; Herault, B., (2021). Multidimensional tropical forest recovery. Science. 374(6573): 1370-1376 (**6 pages**).

Prach, K.; Hobbs, R.J., (2008). Spontaneous succession versus technical reclamation in the restoration of disturbed sites. Restor. Ecol. 16(3): 363-366 (**4 pages**).

Rabot, E.; Wiesmeier, M.; Schlüter, S.; Vogel, H.J., (2018). Soil structure as an indicator of soil functions: A review. Geoderma. 314: 122-137 (**16 pages**).

Ren, X.; Chai, X.; Qu, Y.; Xu, Y.; Khan, F.U.; Wang, J.; Geming, P.; Wang, W.; Zhang, Q.; Wu, Q.; Xu, X., Du, F.,(2023). Restoration of grassland improves soil infiltration capacity in water-wind erosion crisscross region of china's loess plateau. Land. 12(1485): 1-17 (**17 pages**).

Richardson, A.E.; Lynch, J.P.; Ryan, P.R.; Delhaize, E.; Smith, F.A.; Smith, S.E.; Harvey, P.R.; Ryan, M.H.; Veneklaas, E.J.; Lambers, H., (2011). Plant and microbial strategies to improve the phosphorus efficiency of agriculture. Plant Soil. 349: 121–156 (**36 pages**).

Rosa, E.; Sufardi, S.; Syafruddin, S.; Rusdi, M., (2023). Bioremediation of ex-mining soil with the biocompost in the incubation experiments. Appl. Environ. Soil Sci. 2023(1): 1-14 (**14 pages**).

Rowell, D.L., (2014). Soil science: Methods and applications. Routledge. (**368 pages**).

Ruiz-Jaen, M.C.; Mitchell Aide, T., (2005). Restoration success: How is it being measured? Restor. Ecol. 13(3) : 569-577 (**18 pages**).

Saia, S.; Tamayo, E.; Schillaci, C.; De Vita, P., (2019). Arbuscular mycorrhizal fungi and nutrient cycling in cropping systems. In: Datta, R.; Meena, R.; Pathan, S.; Ceccherini, M., (eds) Carbon and nitrogen cycling in Soil. Springer, Singapore. 87-115 (**29 pages**).

Shi, Z.Y.; Chen, Y.L.; Feng, G.; Liu, R.J.; Christie, P.; Li, X.L., (2006). Arbuscular mycorrhizal fungi associated with the meliaceae on hainan island, china. Mycorrhiza. 16: 81-87 (**7 pages**).

Sing, A.K.; Jamaluddin, J., (2011). Status and diversity of arbuscular mycorrhizal fungi and its role in natural regeneration on limestone mined spoils. Biodivers. J. Biol. Divers., 12(2): 107-111 (**5 pages**).

Smith, S.E.; Read, D.J., (2010). Mycorrhizal symbiosis. Academic press. (**787 pages**).

Stover, H.J.; Naeth, M.A.; Boldt-Burisch, K., (2018). Soil disturbance changes arbuscular mycorrhizal fungi richness and composition in a fescue grassland in alberta canada. Appl. Soil Ecol. 131: 29-37 (**9 pages**).

Tao, J.; Liu, X., (2024). Does arbuscular mycorrhizal fungi inoculation influence soil carbon sequestration? Biol. Fertility Soils. 60: 213–225 (**13 pages**).

Tedersoo, L.; Bahram, M.; Zobel, M., (2020). How mycorrhizal associations drive plant population and community biology. Science. 367(6480): (**11 pages**).

Turrini, A.; Bedini, A.; Loor, M.B.; Santini, G.; Sbrana, C.; Giovannetti, M.; Avio, L., (2017). Local diversity of native arbuscular mycorrhizal symbionts differentially affects growth and nutrition of three crop plant species. Biol. Fertility Soils. 54: 203–217 (**15 pages**).

Van Aarle, I.M.; Olsson, P.A.; Söderström, B., (2002). Arbuscular mycorrhizal fungi respond to the substrate pH of their extraradical mycelium by altered growth and root colonization. New Phytol. 155 (1): 173-182 (**10 pages**).

Wang, F., (2017). Occurrence of arbuscular mycorrhizal fungi in mining-impacted sites and their contribution to ecological restoration: Mechanisms and applications. Crit. Rev. Environ. Sci. Technol., 47(20): 1901–1957 (**57 pages**).

Wang, F.; Zhang, L.; Zhou, J.; Rengel, Z.; George, T.S.; Feng, G., (2022). Exploring the secrets of hyphosphere of arbuscular mycorrhizal fungi: Processes and ecological functions. Plant Soil. 481: 1-22 (**22 pages**).

Xuefeng, X.; Chen, J.Z.; Liao, X.; Yan, Q.; Liang, G.; Liu, J.; Wang, D.; Guan, R., (2022). Different arbuscular mycorrhizal fungi established by two inoculation methods improve growth and drought resistance of cinnamomum migao seedlings differently. Biology. 11(2): 1-19 **(19 pages).**

Yang, A.N.; Lu, L.; Zhang, N., (2011). The diversity of arbuscular mycorrhizal fungi in the subtropical forest of huangshan (yellow mountain), east-central china. World J. Microbiol. Biotechnol. 27: 2351-2358 **(8 pages).**

AUTHOR (S) BIOSKETCHES

Prayudyaningsih, R., Ph.D., Principal Researcher, Research Center for Applied Microbiology, National Research and Innovation Agency (BRIN), Jalan Raya Jakarta-Bogor Km 46, Cibinong 16911, Indonesia. Research Collaboration Center for Karst Microbes BRIN - UNHAS, Hasanuddin University, Jalan Perintis Kemerdekaan Km. 10, Makassar 90245, Indonesia.
- Email: *retno.prayudyaningsih@brin.go.id*
- ORCID: 0000-0003-3604-5406
- Web of Science ResearcherID: E-6349-2018
- Scopus Author ID: 57211188858
- Homepage: https://brin.go.id

Turjaman, M., Ph.D., Professor, Principal Researcher, Research Center for Applied Microbiology, National Research and Innovation Agency (BRIN), Jalan Raya Jakarta-Bogor Km 46, Cibinong 16911, Indonesia. Research Collaboration Centre for Agarwood, BRIN, IPB, SITH ITB, Bandung 40132 Indonesia.
- Email: *maman.turjaman@brin.go.id*
- ORCID: 0000-0003-4110-4335
- Web of Science ResearcherID: ABC-4852-2020
- Scopus Author ID: 6506552956
- Homepage: https://brin.go.id

Pratiwi, Ph.D., Professor, Principal Researcher, Research Center for Ecology, National Research and Innovation Agency (BRIN), Jalan Raya Jakarta-Bogor Km 46, Cibinong 16911, Indonesia.
- Email: *prat007@brin.go.id*
- ORCID: 0000-0001-6423-2351
- Web of Science ResearcherID: IQU-1436-2023
- Scopus Author ID: 57214232295
- Homepage: https://brin.go.id

Ansari, F., M.Sc., Senior Researcher, Research Center for Ecology, National Research and Innovation Agency (BRIN), Jalan Raya Jakarta-Bogor Km 46, Cibinong 16911, Indonesia. Research Collaboration Center for Karst Microbes BRIN - UNHAS, Hasanuddin University, Jalan Perintis Kemerdekaan Km. 10, Makassar 90245, Indonesia.
- Email: *fajri.ansari@brin.go.id*
- ORCID: 0000-0002-1064-9757
- Web of Science ResearcherID: AAW-3405-2021
- Scopus Author ID: 57208018111
- Homepage: https://brin.go.id

Gunawan, H., M.Sc., Senior Manager, Semen Tonasa Company, Jl. Tonasa 2, Biring Ere District, Pangkajene dan Kepulauan Regency, South Sulawesi Province, 90651, Indonesia.
- Email: *hariyono.gunawan@sig.id*
- ORCID: 0009-0002-6325-7324
- Web of Science ResearcherID: NA
- Scopus Author ID: NA
- Homepage: www.sementonasa.co.id

HOW TO CITE THIS ARTICLE

Prayudyaningsih, R.; Turjaman, M.; Pratiwi; Ansari, F.; Gunawan, H., (2026). The catalytic effect of mycorrhizal initial planting on limestone post-mining ecological land rehabilitation. Global J. Environ. Sci. Manage., 12(1): 1-20.

DOI: 10.22034/gjesm.2026.01.01

URL: https://www.gjesm.net/article_730411.html

Global J. Environ. Sci. Manage. 12(1): 21-38, Winter 2026, Serial #45

Global Journal of Environmental Science and Management
(GJESM)

Homepage: https://www.gjesm.net/

Podcasts

ORIGINAL RESEARCH PAPER

The potential of combining coagulation-flocculation, biofiltration, and advanced oxidation processes for multi-stage wastewater treatment

D. Amankeshuly[1], T. Salikhov[2], G. Shapatova[3], S. Syrlybekkyzy[1], I. Agarkova[3], N. Kaya[4], A. Yeginbayeva[2], E. Atasoy[5], K. Dakieva[6,*]

[1] *Department of Ecology and Geology, Yessenov University, Aktau, Kazakhstan*

[2] *Department of Physical and Economic Geography, L.N. Gumilyov Eurasian National University, Astana, Kazakhstan*

[3] *Department of Morphology, NCJSC Karaganda Medical University, Street 40, 100000, Karaganda, Kazakhstan*

[4] *Faculty of Education, Social Studies Education, Eskişehir Osmangazi University, Eskişehir City, Turkiye*

[5] *Faculty of Education, Department of Social Sciences, Uludag University, Bursa City, Turkiye*

[6] *Department of Ecology and Geography, Amanzholov East Kazakhstan University, 470010, Ust-Kamenogorsk, st. Vinogradova 8-21, Kazakhstan*

ARTICLE INFO

Article History:
Received 06 July 2025
Revised 10 October 2025
Accepted 13 November 2025

Keywords:
Advanced oxidation
Biofiltration
Coagulation-flocculation
Heavy metal removal
Microbial inactivation
Wastewater treatment

ABSTRACT

BACKGROUND AND OBJECTIVES: The increasing need for efficient wastewater treatment solutions has driven research toward the development of integrated processes capable of addressing complex contaminant compositions. Standard single-stage treatment approaches frequently do not effectively remove a variety of pollutants, including organic compounds, heavy metals, and pathogenic microorganisms. Furthermore, information on the integration of coagulation-flocculation, biofiltration, and advanced oxidation processes within a cohesive treatment system. This study aimed to develop and evaluate a multi-stage wastewater treatment system that combines coagulation-flocculation, biofiltration, and advanced oxidation processes to enhance pollutant removal efficiency and improve effluent quality.

METHODS: The experimental setup consisted of three sequential treatment units. In the first stage, coagulation-flocculation was employed to aggregate and remove suspended solids and colloidal matter. Coagulant dosages of 20, 40, 60, and 100 milligrams per liter were tested to determine the optimal chemical requirement. The second phase employed biofiltration to enhance the biological breakdown of dissolved organic substances, with the hydraulic retention time fine-tuned for optimal microbial activity. The final stage applied ultraviolet light and hydrogen peroxide oxidation to degrade residual organic pollutants and ensure microbial disinfection.

FINDINGS: As the dosage of coagulant was raised, the coagulation-flocculation performance showed improvement. At 20 milligrams per liter, total suspended solids removal was 52.3 percent and chemical oxygen demand reduction was 15.7 percent. At 40 milligrams per liter, these values increased to 72.8 percent and 28.4 percent, respectively. The optimal dosage of 60 milligrams per litefficiency.5 percent removal of total suspended solids and 39.6 percent reduction in chemical oxygen demand, while at 100 milligrams per liter, the efficiency reached 92.5 percent and 43.3 percent, respectively. The integrated multi-stage system achieved average overall removal efficiencies of 92 percent for chemical oxygen demand, 85 percent for heavy metals, and more than 99 percent for microbial inactivation.

CONCLUSION: The findings indicate that the combined treatment system significantly improves pollutant removal by leveraging the synergistic interaction between physicochemical, biological, and oxidation processes. The study confirms the potential of the system for pilot-scale and full-scale adaptation, suggesting its viability as an integrated solution for effective wastewater management and the protection of public health.

DOI: 10.22034/gjesm.2026.01.02

This is an open access article under the CC BY license (http://creativecommons.org/licenses/by/4.0/).

NUMBER OF REFERENCES
37

NUMBER OF FIGURES
6

NUMBER OF TABLES
3

*Corresponding Author:
Email: *ecology-2014@mail.ru*
Phone: +77780455328
ORCID: 0000-0002-8110-5255

Note: Discussion period for this manuscript open until Mar 1, 2026 on GJESM website at the "Show Article".

INTRODUCTION

Global wastewater production has increased exponentially due to rapid urbanization and industrialization, leading to severe environmental and public health concerns. As stated by the United Nations, around 80 percent (%) of wastewater across the globe is discharged without treatment into natural water bodies, which exacerbates pollution and the deterioration of ecosystems. Municipal wastewater contains high levels of chemical oxygen demand (COD) with 250–800 milligram per liter (mg/L) (Huelgas *et al.*, 2009), total suspended solids (TSS) up to more than 350 mg/L (Islam and Mostafa, 2020), and heavy metals such as lead (Pb), which has been reported to range from 0.0196 ± 0.01 mg/L to 52.4 ± 0.02 mg/L in wastewater (Ali *et al.*, 2022), and chromium (Cr) (0.1–1.0 mg/L) (Dikobe *et al.*, 2024), all of which pose significant risks to aquatic life and human health. Additionally, pathogenic microorganisms, including Escherichia coli and total coliforms frequently exist in untreated wastewater at concentrations surpassing 10^6 colony-forming units per hundred milliliters (CFU/100 mL) thereby requiring efficient disinfection methods (Oluwafisayomi, 2025). Conventional wastewater treatment techniques face constraints in tackling these issues, highlighting the necessity for comprehensive multi-stage treatment strategies to meet rigorous effluent quality requirements. Conventional wastewater treatment techniques predominantly utilize physical, chemical, and biological processes such as sedimentation, activated sludge treatment, and chemical precipitation. While coagulation-flocculation effectively removes suspended solids and specific heavy metals is influenced by the type and dosage of coagulant applied, resulting in the generation of substantial sludge volumes that require proper disposal (Badawi *et al.*, 2023). Similarly, biological treatment, including activated sludge and biofilters, is widely used for organic matter degradation, achieving up to 90% COD removal efficiency (Zheng *et al.*, 2013). However, its performance can be hindered by variations in influent composition and hydraulic retention times. Moreover, disinfection processes like chlorination, though effective in pathogen inactivation, may lead to the formation of harmful disinfection byproducts (DBPs) such as trihalomethanes (THMs) and haloacetic acids (HAAs), which have been linked to carcinogenic and mutagenic effects (Bond *et al.*, 2014; Dong *et al.*, 2023). These restrictions underscore the importance of a hybrid treatment strategy that incorporates diverse technologies to boost pollutant removal effectiveness while curtailing secondary pollution. Material choice plays an important role in influencing the effectiveness and sustainability of wastewater treatment techniques. Coagulants such as ferric chloride ($FeCl_3$) and aluminum sulfate [$Al_2(SO_4)^{-3}$] are commonly used in coagulation-flocculation, with dosages ranging from 10–50 mg/L depending on wastewater characteristics (Tiaiba *et al.*, 2018). In biofiltration, media selection significantly affects microbial colonization and pollutant degradation (Muliyadi *et al.*, 2024; Zhang *et al.*, 2021). Studies have shown that granular activated carbon (GAC) and biochar improve COD removal by up to 85% due to their high surface area and adsorption capacity (Aktas *et al.*, 2024). For advanced oxidation processes (AOPs), oxidants like hydrogen peroxide (H_2O_2) and ozone (O_3) are widely applied, with reaction rates influenced by catalyst type and UV intensity (Hübner *et al.*, 2024). Despite significant research has been conducted on each material, their collective efficacy within a multi-stage treatment system is still inadequately examined, indicating a need for further exploration. AOPs have gained prominence as a complementary treatment step due to their ability to degrade refractory organic pollutants and inactivate microbial contaminants. ultraviolet/hydrogen peroxide (UV/H_2O_2) oxidation, for instance, generates hydroxyl radicals (•OH) with oxidation potentials of 2.8 V, effectively breaking down complex organic compounds into biodegradable intermediates (Khan *et al.*, 2023). Electrochemical oxidation, which is considered a promising AOP, has exhibited a COD removal efficiency of more than 95% at an applied voltage between 3.5 and 5.0 V, while also achieving substantial heavy metal reduction through the mechanisms of electrosorption (Das and Chen, 2024). For instance, Phan *et al.* (2023) observed that the combination of anaerobic digestion (AD) and electro-oxidation (EO) achieved an impressive 96.47% COD removal efficiency from beverage wastewater under optimal conditions, which included an applied voltage of 20 V, electrolysis time of 80 minutes (min.), and sodium chloride (NaCl) concentration of 3 grams per liter (g/L). Their study also highlighted an energy consumption of 177.33 Kilowatt-hour per cubic meter (kWh/m^3) and a

specific energy consumption of 33.79 kilowatt per kilogram of COD (kWh/kg COD), demonstrating the feasibility of integrating electrochemical methods with biological treatment for enhanced wastewater purification. Furthermore, while these technologies exhibit significant effectiveness in controlled environments, the extent to which they can be effectively combined with established techniques such as coagulation-flocculation and biofiltration in a multi-stage framework is still inadequately researched, particularly concerning the optimization of processes and operational synergy. Despite advancements in individual wastewater treatment technologies, information on the integration of coagulation-flocculation, biofiltration, and AOPs in a unified treatment system is still scarce. This study investigates the feasibility of integrating coagulation-flocculation, biofiltration, and advanced oxidation processes for wastewater treatment. The goals encompass enhancing the operational parameters of every treatment phase, analyzing the overall efficiency of pollutant removal, and evaluating the scalability of the process for possible full-scale application. By systematically analyzing the performance of this hybrid system, the study aims to contribute valuable insights into sustainable and effective wastewater treatment strategies, addressing the limitations of conventional methods and advancing towards cleaner water reuse practices. This study was carried out in Astana, Kazakhstan, in 2025.

MATERIALS AND METHODS

Wastewater composition and preparation

Real wastewater samples were collected from the influent stream of a municipal wastewater treatment facility to ensure that the study accurately reflected realistic treatment conditions. Sampling was carried out three times per week over a two-week period, and composite samples were prepared from three consecutive grab samples taken at 2-hour (h) intervals during peak inflow periods. Each composite sample was analyzed in triplicate to ensure statistical consistency. The average influent characteristics were COD = 520 ± 35 mg/L, TSS = 280 ± 20 mg/L, Pb = 0.46 ± 0.03 mg/L, chromium (Cr) = 0.62 ± 0.04 mg/L, copper (Cu) = 0.28 ± 0.02 mg/L, and *Escherichia coli* = (1.2 ± 0.3) × 10^6 CFU/mL, indicating moderate organic pollution, particulate matter, and microbial contamination requiring targeted treatment. Atomic absorption spectroscopy (AAS) was employed to analyze heavy metals, adhering to established protocols. The quantification of *Escherichia coli* concentrations was performed through the membrane filtration technique, with subsequent incubation on MacConkey agar plates, selected for their ability to specifically isolate and enumerate fecal coliforms. To standardize initial conditions across all experimental runs, the potential of hydrogen (pH) of each wastewater sample was adjusted to 7.2 ± 0.2 using 0.1 molar sodium hydroxide or 0.1 molar hydrochloric acid, depending on the initial sample pH. Once the adjustment was made, pH stability was validated for 30 minutes before the treatment commenced, ensuring consistent conditions for all trials. Following collection and preparation, samples were stored in high-density polyethylene (HDPE) containers at 4 degrees Celsius (°C), with analysis conducted within 24 hours to minimize biological activity and chemical transformation, thereby preserving sample integrity and ensuring uniformity throughout the study.

Coagulation-flocculation treatment

Coagulation-flocculation was implemented as a crucial pretreatment step to reduce TSS and COD prior to biofiltration. Aluminum sulfate [$Al_2(SO_4)^3$] and ferric chloride ($FeCl_3$) were employed as coagulants at doses ranging from 20 to 100 mg/L to evaluate their removal efficiency under varying conditions. The procedure commenced with swift mixing at 200 rotations per minute (rpm) for a duration of one minute to guarantee even distribution of the coagulant, thereby improving charge neutralization and destabilization of colloidal particles. This was followed by a slow mixing phase at 30 rpm for 20 minutes to promote the aggregation of destabilized particles into larger, settleable flocs. After flocculation, the wastewater was placed in a 2-liter cylindrical settling tank, allowing it to remain undisturbed for 30 minutes to aid in sedimentation. The selection of the tank volume was determined based on conventional laboratory-scale design principles to provide an appropriate hydraulic retention time and settling velocity for the generated flocs. Although larger tanks may influence sedimentation kinetics differently due to changes in surface overflow rate and depth, the 2 liters (L) tank volume provided a controlled environment for evaluating the effectiveness of coagulant dosages

under consistent settling conditions. The clarified supernatant was meticulously decanted from the top to prevent disturbing the settled flocs and was later subjected to biofiltration for enhanced contaminant removal. The settled sludge was collected and analyzed to determine its sludge volume index (SVI), which is a crucial factor in assessing sludge settleability. The SVI was measured by allowing 1 liter of mixed liquor to settle for 30 minutes in a graduated cylinder, and calculating the volume occupied by the settled sludge (in mL/L) relative to the concentration of mixed liquor suspended solids (MLSS). SVI values below 100 milliliters per gram (mL/g) typically indicated good settleability, while higher values suggested poor settling characteristics and potential issues in dewatering and sludge handling, using Eq. 1 (Wongburi and Park, 2022):

$$\mathrm{SVI} = \frac{\text{Settled Sludge Volume}\left(\mathrm{mL/L}\right)}{\mathrm{MLSS}\left(\frac{\mathrm{g}}{\mathrm{L}}\right)} \quad (1)$$

Biofiltration treatment

Biofiltration was implemented as a critical secondary treatment step to target residual COD, heavy metals, and microbial contaminants following the coagulation-flocculation process. A biofilter at the laboratory scale was built using a cylindrical column measuring 50 cm in height and 15 cm in diameter. The filter media consisted of a well-defined mixture: 30% activated carbon, 40% zeolite, and 30% sand by volume. These proportions were determined based on their synergistic physicochemical traits, adsorption ability, and their effectiveness in promoting microbial colonization.

- Activated carbon (30%) was included for its high surface area and porous structure, which promoted effective adsorption of dissolved organic compounds and supported biofilm development.
- Zeolite (40%) contributed ion exchange capacity and provided specific adsorption sites for cationic heavy metals such as Pb^{2+}, Cr^{3+}/Cr^{6+}, and Cu^{2+}, enhancing metal removal.
- Sand (30%) offered mechanical support and an inert surface that encouraged microbial attachment while maintaining adequate porosity for hydraulic conductivity.

This customized formulation developed a versatile medium that can perform physical filtration, adsorption, and biological degradation. The biofilter functioned at hydraulic retention times (HRT) varying from 2 to 6 hours, facilitating the assessment of contact duration on treatment effectiveness. Prior to experimental trials, the biofilter underwent a seven-day acclimation phase using real municipal influent wastewater continuously recirculated through the column under ambient laboratory temperature (~25 °C). During acclimation, microbial colonization and biofilm formation were supported by the presence of organic carbon and nutrients in the wastewater. Although direct biomass measurement was not carried out, the visual inspection of biofilm formation and observed the rise in COD removal during the acclimation phase suggested that microbial establishment was effectively achieved. To prevent media clogging and maintain hydraulic performance, the biofilter was periodically backwashed with dechlorinated water at low flow rates at the end of each experimental day, and accumulated solids were manually removed if necessary. Effluent samples were taken every hour to analyze treatment dynamics. The dichromate method was used to quantify COD removal, while heavy metals were assessed using AAS post acid digestion. *Escherichia coli* enumeration was performed using the membrane filtration technique on MacConkey agar, with incubation at 37 °C for 24 h. The influence of ambient temperature (~25 °C) on microbial activity was considered sufficient to maintain stable biological degradation, as this temperature supports mesophilic microbial communities commonly found in municipal wastewater.

Advanced oxidation treatment

The final treatment stage involved a UV/H_2O_2 reactor to degrade residual organic contaminants and achieve microbial inactivation. The AOP utilized the combined action of UV light and hydrogen peroxide to generate highly reactive •OH, which oxidizes a wide range of organic pollutants. The oxidation unit consisted of a low-pressure mercury UV lamp (15 W, 254 nm) positioned inside a quartz sleeve submerged in the treated wastewater, providing an average irradiance of 12 mW/cm^2 at the water surface. Constructed from a quartz tube with an inner diameter of 2.5 cm and a length of 40 cm, the reactor's flow rate was calibrated to ensure a hydraulic retention time of 30 minutes, thus allowing

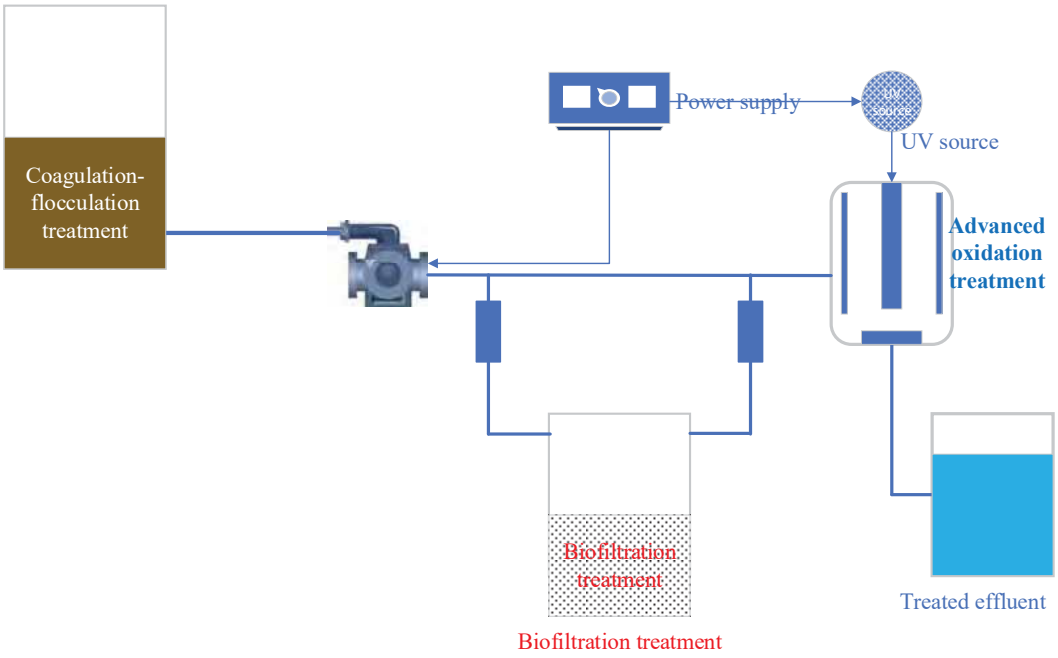

Fig. 1: Experimental setup

for sufficient UV light exposure and effective mass transfer for oxidation. The hydraulic retention time was 30 minutes, which was adequate for effective COD reduction and microbial inactivation, focusing on Escherichia coli. Hydrogen peroxide was added at concentrations of 10–50 mg/L, optimized to support hydroxyl radical formation without leaving residual H_2O_2 in the effluent. Residual hydrogen peroxide was measured using a titanium sulfate colorimetric method and neutralized with sodium thiosulfate (0.5 mL of 0.1 M solution per 100 mL sample). Complete neutralization was confirmed by verifying residual H_2O_2 concentrations below the detection limit (<0.01 mg/L) before conducting further chemical and microbiological analyses (Fig. 1).

Analytical methods

To assess the effectiveness of each treatment phase, various analytical techniques were utilized to guarantee precise measurement of the essential parameters related to wastewater quality. COD and TSS were determined using the Standard Methods for the Examination of Water and Wastewater published by the American Public Health Association (APHA, 2017). These approaches deliver a consistent and uniform method for measuring the levels of organic and particulate substances in wastewater. Heavy metals, including Pb, Cr, and Cu, were analyzed using AAS, a highly sensitive technique applied after acid digestion to break down the sample matrix and ensure accurate quantification of trace metals in the effluent. The membrane filtration method was utilized to evaluate microbial contamination, particularly focusing on *Escherichia coli*. Known volumes of the effluent were passed through a membrane filter and subsequently incubated on MacConkey agar at 37 ^{0}C for 24 hours to allow for the growth and enumeration of bacterial colonies. This facilitated the exact quantification of the microbial load present in the treated wastewater. Additionally, UV absorbance at two hundred fifty-four nanometers was measured using an UV-Vis spectrophotometer, providing an indirect evaluation of organic pollutant removal. UV absorbance at this wavelength correlates with the concentration of organic compounds, making it a useful indicator for assessing the effectiveness of the advanced oxidation process in reducing residual organic pollutants. These extensive analytical strategies assured a meticulous review of all treatment stages, yielding important insights into the overall performance and efficacy of

the unified wastewater treatment system.

Sample collection and handling

To monitor the effectiveness of the treatment processes, samples were collected at uniform intervals for each stage of treatment. In the coagulation-flocculation stage, samples were taken from the supernatant after the sedimentation process to ensure the accurate measurement of residual contaminants, particularly in terms of COD and TSS. During the biofiltration stage, effluent samples were collected hourly from the biofilter to evaluate the incremental improvement in water quality as the filtration process progressed. These samples were analyzed for COD, heavy metals, and microbial contaminants, providing a detailed assessment of the biofilter's performance at different hydraulic retention times (HRT). In the final advanced oxidation stage, effluent samples were collected immediately after UV/H_2O_2 treatment to prevent any changes in pollutant concentrations, as the reaction may continue even after the treatment period. The analysis of these samples was conducted without delay to ensure that the measured levels of pollutants exactly indicated the impact of the treatments. All samples were stored at 4°C to preserve their integrity, with analysis being conducted within 24 hours to minimize any degradation of the contaminants. This systematic approach to sample collection and handling ensured that the data obtained was reliable and accurately represented the performance of each treatment stage.

Statistical Analysis

All experimental measurements were conducted in triplicate to ensure accuracy and reproducibility. The results for pollutant removal efficiency were expressed as mean values accompanied by standard deviation (mean ± SD). Statistical analyses were conducted to assess the significance of differences across various treatment conditions. A one-way analysis of variance (ANOVA) was applied to assess differences in removal efficiency across the tested coagulant dosages. Differences were considered statistically significant at $p < 0.05$. Removal efficiency (%) for each parameter was calculated using Eq. 2 (Meiramkulova *et al.*, 2020):

$$\text{Removal efficiency}(\%) = \frac{C_i - C_f}{C_i} \times 100 \quad (2)$$

RESULTS AND DISCUSSION

Removal efficiency from coagulation-flocculation

The effectiveness of coagulation-flocculation at different coagulant doses revealed a strong correlation between elevated coagulant dosage and enhanced treatment efficiency, emphasizing the importance of optimizing doses in wastewater treatment. Statistical evaluation showed significant differences ($p < 0.05$) in removal efficiency among the coagulant dosages, confirming that dosage strongly influenced pollutant reduction. At the lowest dose of 20 mg/L, TSS removal was 52.3 ± 2.1%, and the reduction in COD was 15.7 ± 1.3%. These findings, although suggestive of preliminary coagulation effectiveness, also indicated a lack of efficiency at reduced coagulant concentrations, implying that the coagulation process was not entirely optimized at this dose. As the coagulant dose increased to 40 mg/L, both TSS removal and COD reduction significantly improved. TSS removal rose to 72.8 ± 2.5%, and COD reduction reached 28.4 ± 1.8%, demonstrating that a higher dose facilitated better particle aggregation, which allowed for more efficient removal of suspended solids and organic pollutants. The effectiveness of the treatment kept increasing with coagulant doses of 60 mg/L and above, with TSS removal reaching 88.5 ± 2.0% and COD reduction increasing to 39.6 ± 1.5% at 60 mg/L. This trend continued with further increases in dose, with TSS removal achieving 92.5 ± 1.7% and COD reduction reaching 43.3 ± 1.6% at the highest dose of 100 mg/L. Furthermore, the incremental gains past 60 mg/L were rather slight, implying that higher chemical dosages yield diminishing returns. This observation highlights that while increasing the coagulant dose enhances treatment efficiency, there is a threshold beyond which the additional benefits become minimal. Therefore, a dose of 60 mg/L was identified as the optimal coagulant dosage, providing a balance between maximizing pollutant removal and minimizing excessive chemical usage, which is crucial for both operational cost-effectiveness and environmental sustainability (Fig. 2).

Sludge volume index

The SVI values presented in Table 1 offer valuable insights into the settleability of the sludge formed during the coagulation–flocculation treatment of municipal wastewater using aluminum sulfate and ferric chloride at varying doses. In most cases, SVI

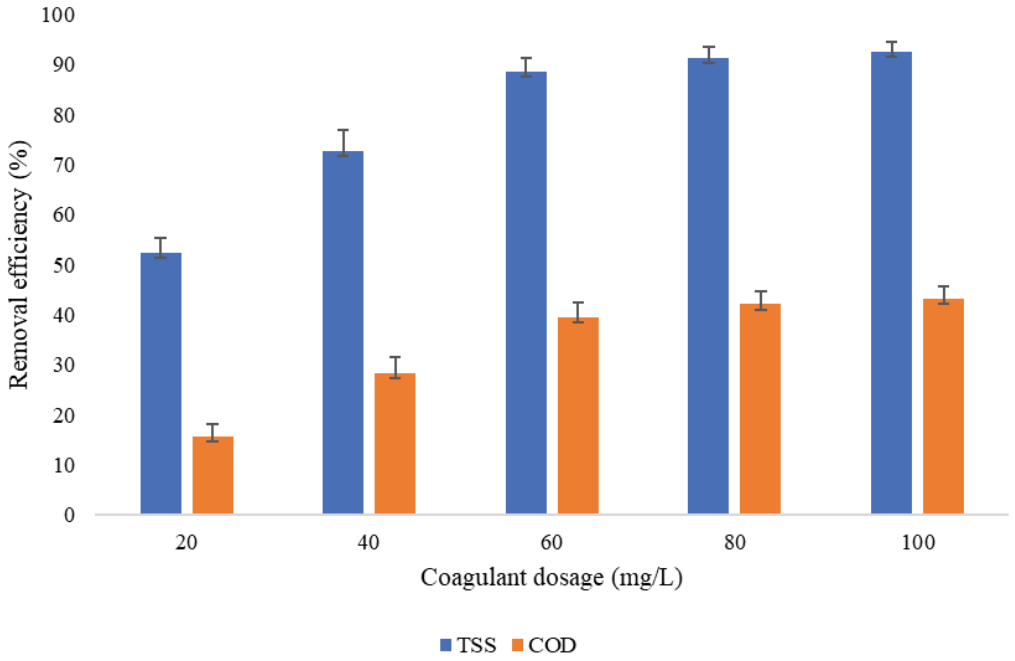

Fig. 2: Coagulation-flocculation performance at different coagulant doses

Table 1: SVI Results for aluminum sulfate and ferric chloride at varying coagulant doses

Coagulant type	Dose (mg/L)	SVI (mL/g)
Aluminium sulfate	20	126.5 ± 3.2
	40	95.1 ± 2.5
	60	77.2 ± 2.1
	80	79.2 ± 2.3
	100	84.5 ± 2.4
Ferric Chloride	20	144.3 ± 3.5
	40	110.4 ± 2.8
	60	81.0 ± 2.2
	80	76.3 ± 2.1
	100	84.8 ± 2.3

values less than 100 mL/g are regarded as a sign of effective sludge settleability, implying that the sludge will consolidate effectively and create fewer issues during dewatering and handling. In contrast, higher SVI values signal poor compaction, potentially leading to difficulties in sludge management. For aluminum sulfate, the SVI significantly improved as the coagulant dose increased from 20 mg/L to 60 mg/L, with the SVI decreasing from 126.5 ± 3.2 to 77.2 ± 2.1 mL/g. This decrease indicates an improvement in the settleability of the sludge, implying that the 60 mg/L dosage resulted in the most compact and easily settling flocs. However, further increases in coagulant dosage to 80 and 100 mg/L resulted in a slight rise in SVI, reaching 79.2 ± 2.3 and 84.5 ± 2.4 mL/g, respectively. This increase could be attributed to the restabilization effects of excess coagulant or the fragmentation of flocs, which typically occur when too much coagulant is used. A similar trend was observed with ferric chloride, where the SVI decreased from 144.3 ± 3.5 mL/g at 20 mg/L to 76.3 ± 2.1 mL/g at 80 mg/L, indicating optimal performance at this dose. The decline in SVI suggests that ferric chloride at this level was significantly effective in facilitating flocculation and enhancing settleability. However, at the highest dose of 100 mg/L, the SVI slightly increased to 84.8

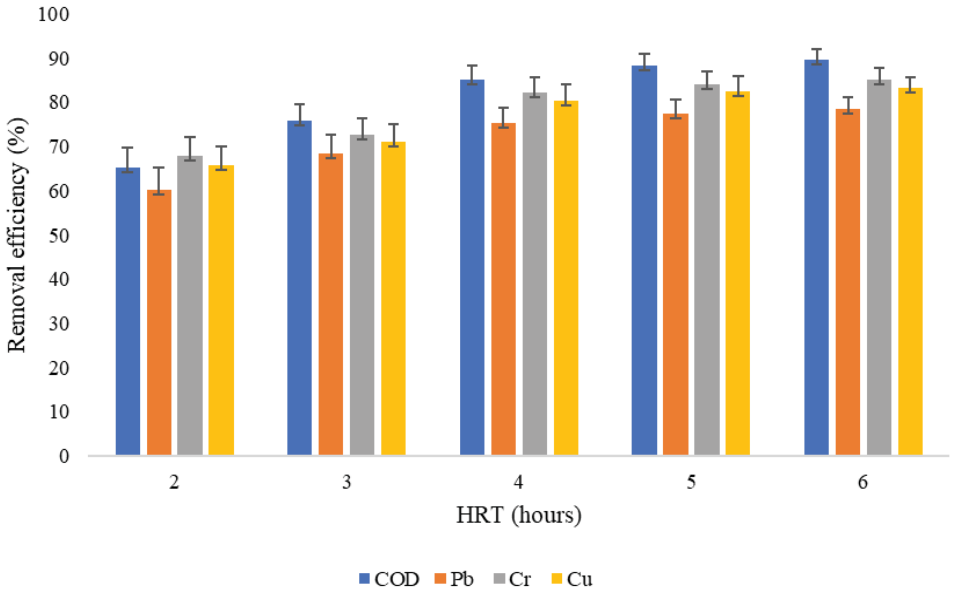

Fig. 3: Biofiltration performance at different HRT

± 2.3 mL/g, still within the acceptable range for good settleability but indicating diminishing returns or potential overdosing. This indicates that although increased amounts of coagulants can enhance sludge settleability, overly high doses might result in diminished floc formation efficiency or even cause floc disruption, thereby decreasing the overall efficacy of the treatment process. Therefore, it can be concluded that both aluminum sulfate and ferric chloride displayed optimal settleability performance at moderate doses, with higher concentrations resulting in limited additional benefits.

Biofiltration performance

The biofiltration performance was assessed at varying hydraulic retention times (HRT) to evaluate its efficiency in removing COD and heavy metals, specifically Pb, Cr, and Cu. At an HRT of 2 hours, the biofilter achieved a COD removal of 65.3 ± 2.1%, with Pb removal at 60.2 ± 1.8%, Cr at 67.8 ± 2.0%, and Cu at 65.7 ± 1.9%. The findings demonstrate that biofiltration can successfully lower organic and metal contaminants, even when retention times are brief, although the efficiency of treatment was reduced in comparison to extended retention periods. As the HRT was increased to 3 hours, there was a noticeable improvement in removal efficiencies across all pollutants. The COD removal efficiency increased to 75.8 ± 2.3%, with Pb, Cr, and Cu removals improving to 68.4 ± 2.0%, 72.6 ± 2.1%, and 71.1 ± 1.9%, respectively. This indicates that prolonging the HRT enhances the interaction between contaminants and the biofilter media, leading to more effective adsorption and removal. The performance continued to improve with longer HRTs, with the highest removal efficiencies observed at an HRT of 6 hours. At this retention time, COD removal reached 89.7 ± 2.4%, and the removals of Pb, Cr, and Cu increased to 78.4 ± 2.1%, 85.1 ± 2.3%, and 83.2 ± 2.2%, respectively. This indicates that longer contact time allows the biofilter to achieve greater pollutant removal, likely due to increased microbial activity and enhanced sorption capacities of the filter media. The impressive growth in treatment performance from 2 hours to 6 hours highlights the the critical role of optimizing the HRT to enhance pollutant elimination, especially heavy metals. Beyond the 4-hour mark, the increases in removal efficiency became less pronounced, suggesting diminishing returns with further increases in HRT. Consequently, an HRT of 6 hours appears to be the optimal operational time for achieving the highest removal efficiencies in this biofiltration system (Fig. 3).

Microbial removal in biofiltration

The microbial removal efficiency, specifically for

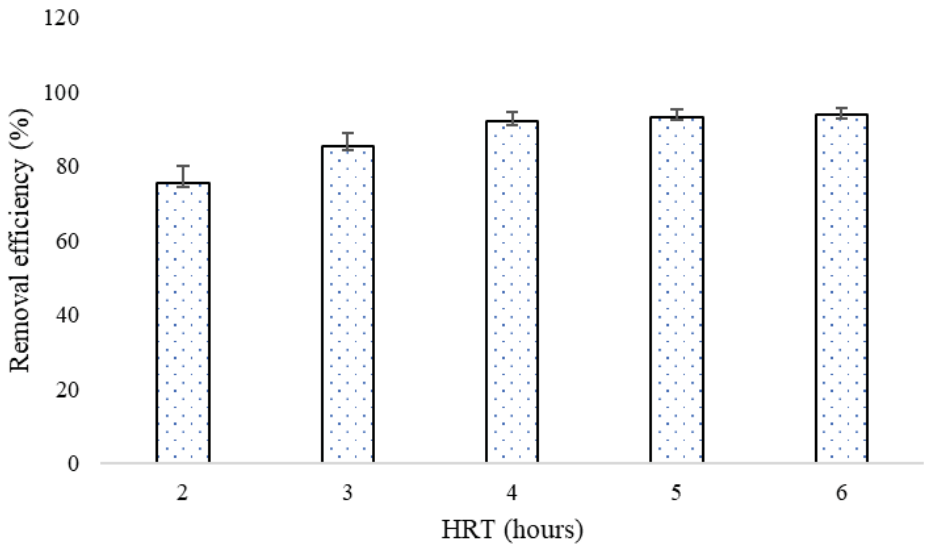

Fig. 4: Microbial removal efficiency in biofiltration for *Escherichia coli*

Escherichia coli, was evaluated at various hydraulic retention times (HRT) to determine the effectiveness of the biofiltration process in microbial inactivation. At an HRT of 2 hours, the biofilter demonstrated a 75.3 ± 2.0% reduction in Escherichia coli, which was considered lower than expected. This indicates that the duration of contact was inadequate for the effective removal of microbes, and the biofilter might not have had sufficient time to enable adequate microbial adsorption or inactivation. As the HRT increased to 3 hours, the reduction in Escherichia coli improved to 85.1 ± 1.8%, indicating that a longer contact time allowed for more effective microbial removal. The biofilter showed moderate improvement, confirming that increased HRT enhances the treatment capacity for microbial contaminants. The most significant reduction in Escherichia coli was observed at an HRT of 4 hours, with a 92.0 ± 1.5% reduction, marking the optimal microbial inactivation point. This outcome illustrates that at this retention period, the biofilter successfully attains a significant degree of microbial removal, thereby effectively lowering Escherichia coli levels. Although the removal efficiency continued to improve with HRTs of 5 hours (93.2 ± 1.4%) and 6 hours (93.8 ± 1.3%), the gains were minimal, suggesting diminishing returns beyond the 4-hour mark. In summary, while longer retention times slightly enhanced microbial removal, an HRT of 4 hours appeared to provide the optimal balance between effective microbial inactivation and operational efficiency (Fig. 4).

3.4 Advanced oxidation efficiency

The advanced oxidation process (UV/H_2O_2 treatment) demonstrated varying efficiencies for microbial inactivation and COD reduction at different H_2O_2 doses. At a dose of 10 mg/L, microbial inactivation reached 88.5 ± 1.8%, but the reduction in residual COD was limited to 3.5 ± 0.5%, indicating that while some microbial inactivation occurred, the COD reduction was minimal. With an increase in H_2O_2 dose to 20 mg/L, microbial inactivation improved to 94.2 ± 1.5%, accompanied by a moderate increase in COD reduction to 5.8 ± 0.7%. Nonetheless, the effectiveness of the treatment at this dosage was still below optimal levels, indicating considerable potential for enhancement in both microbial inactivation and the removal of organic pollutants. The optimal performance for both microbial inactivation and COD reduction was achieved at an H_2O_2 dose of 40 mg/L, with nearly complete microbial inactivation (99.0 ± 1.0%) and a substantial reduction in residual COD (7.0 ± 0.8%). This dose proved to be the most effective in achieving the desired treatment outcomes. At higher doses (50 mg/L and 60 mg/L), microbial inactivation increased slightly, reaching 99.2 ± 0.9% and 99.9 ± 0.5%, respectively, but the improvements in COD reduction were marginal (7.5 ± 0.7% and 7.8 ± 0.8%).

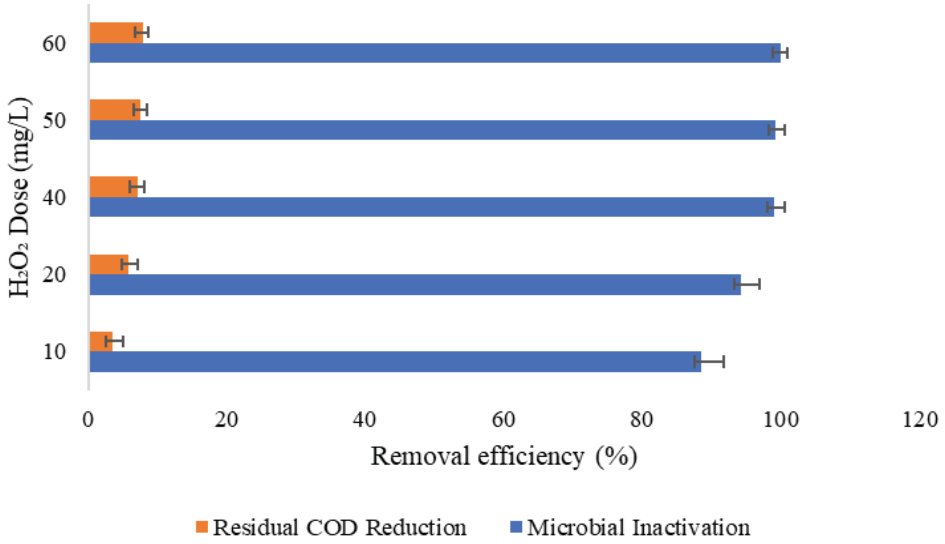

Fig. 5: Advanced oxidation efficiency for microbial inactivation and COD reduction

This implies a decrease in effectiveness with higher H_2O_2 concentrations, where additional increments in the oxidant dose provide minimal extra advantages. Thus, a 40 mg/L H_2O_2 dose provided the most efficient balance of microbial inactivation and COD reduction in the UV/H_2O_2 treatment stage (Fig. 5).

3.5 Heavy metal residuals in final effluent

The treatment system successfully reduced the concentrations of heavy metals in the final effluent, with residual concentrations of Pb at 0.4 mg/L ± 0.05, Cr at 0.27 mg/L ± 0.03, and Cu at 0.2 mg/L ± 0.02. These results reflect the efficient removal of these pollutants through the integrated coagulation-flocculation, biofiltration, and AOPs. In particular, the coagulation-flocculation stage proved effective in lowering the particulate forms of these metals, whereas biofiltration further aided in their removal by adsorbing and capturing dissolved metal ions. The advanced oxidation stage played a crucial role in enhancing the degradation of residual organic matter, which may have otherwise contributed to the mobility and persistence of the heavy metals in the effluent. These residual concentrations of metals are significantly below the acceptable discharge thresholds, implying that the multi-stage treatment system can efficiently handle wastewater with high levels of heavy metals. The low levels of Pb, Cr, and Cu in the final effluent demonstrate the system's capacity to address complex contamination scenarios, making it a promising approach for wastewater treatment in industries or municipalities dealing with metal-laden effluents. A deeper analysis of the system's long-term performance and scalability is crucial for assessing its economic viability and appropriateness for extensive applications (Fig. 6).

UV absorbance reduction

The UV absorbance at 254 functioned as an essential parameter for determining the reduction of organic pollutants throughout the multi-stage treatment process (Table 2). Initially, before treatment, the UV absorbance was measured at 0.95 ± 0.04/cm, indicating the presence of a significant concentration of organic matter in the wastewater. Following the coagulation stage, a moderate reduction in UV absorbance was observed, with a value of 0.73 ± 0.05/cm, corresponding to a 23.3% decrease. This decrease indicates the partial elimination of organic contaminants, as the coagulation method mainly focused on larger suspended particles and organic substances via aggregation. Biofiltration, the second stage, demonstrated a more substantial decrease in UV absorbance, lowering it further to 0.54 ± 0.03/cm, representing a 42.1% reduction. This significant progress emphasizes the success of the biofiltration technique in extracting a considerable fraction of dissolved organic contaminants, likely through

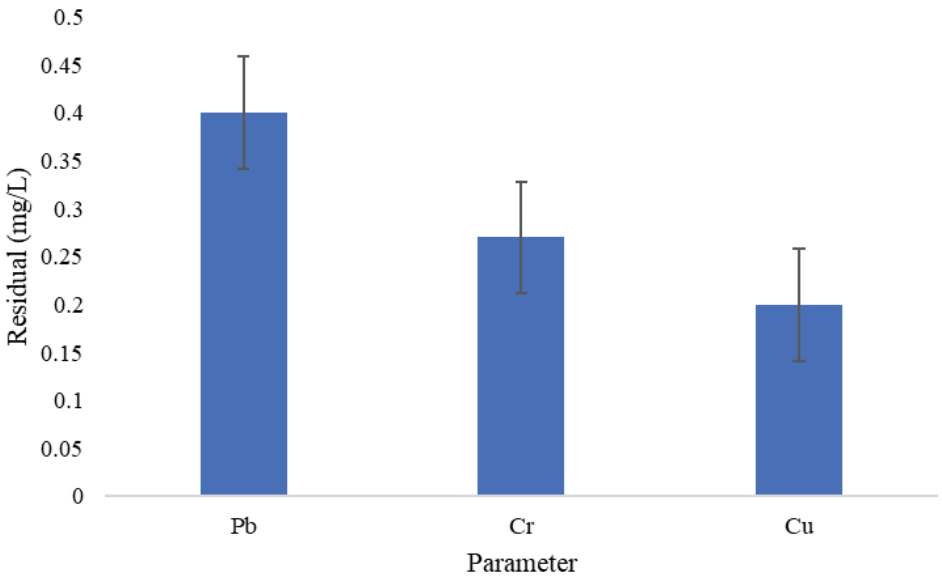

Fig. 6: Heavy metal residuals in final effluent

Table 2: UV absorbance reduction at 254 nm

Treatment stage	UV Absorbance at 254 nm (/cm) ± standard deviation	Absorbance reduction (%) ± Standard deviation (SD)
Before treatment	0.95 ± 0.04	-
After coagulation	0.73 ± 0.05	23.3 ± 2.3
After biofiltration	0.54 ± 0.03	42.1 ± 1.7
After advanced oxidation	0.21 ± 0.02	78.0 ± 2.0

mechanisms such as adsorption, ion exchange, and microbial biodegradation occurring within biofilter. The most significant reduction in UV absorbance was observed during the advanced oxidation treatment, where the final UV absorbance reached 0.21 ± 0.02/cm, corresponding to an impressive 78.0% reduction. This substantial decrease indicates that the UV/H_2O_2 process effectively degraded the remaining organic pollutants, achieving near-total removal of organic matter. The outcomes reveal the progressive aspects of the treatment system, in which each step plays a vital part in diminishing pollutants, particularly highlighting the efficiency of advanced oxidation in breaking down the more recalcitrant organic contaminants. Overall, the treatment system's multi-stage approach proved highly effective in progressively reducing organic pollutants, with the UV/H_2O_2 treatment stage emerging as the most powerful in achieving near-complete degradation.

Comparative analysis

The comparative analysis in Table 3 shows that the developed three-stage treatment system achieved an effective balance between performance, operational simplicity, and adaptability when compared with other integrated wastewater treatment approaches. The combination of coagulation-flocculation, biofiltration, and UV/H_2O_2 oxidation provided consistently high removal of organic matter, suspended solids, heavy metals, and microbial contaminants. Other systems reviewed achieved similarly strong results for selected parameters such as organic load, nutrient, or ammonia reduction but often required more complex configurations or longer retention times. Systems that are membrane-based and light-assisted delivered remarkable purification results, but they came with increased operational and energy requirements. In contrast, biological and phytoremediation approaches were

Table 3: Comparative performance of integrated and multistage wastewater treatment systems

Study and sources	System configuration/ treatment units	Pollutant parameters evaluated	Key operating conditions	Removal efficiency (%)	Notable findings/ remarks
Integrated UASB–trickling filter system (Tessema *et al.*, 2024)	Anaerobic (UASB) + Aerobic trickling filter	COD, BOD_5, TSS, heavy metals, E. coli, helminth eggs	30-day continuous operation (dry season)	COD: 80.5; BOD_5: 82.9; TSS: 80.9	Achieved good organic removal but limited removal of Cr, nitrates, and helminth eggs; effluent reuse restricted without tertiary polishing.
Multistage living machine with underwater lamps (Chen *et al.*, 2024)	Eight-stage bio-ecological system with underwater light enhancement	COD, NH_4^+–N, TP, microbial diversity	Continuous-flow, light-enhanced stages	COD: 96.1; NH_4^+–N: 61.6	Underwater illumination improved nitrification and algal activity; microbial diversity (Nitrospira, Rhodanobacter) enhanced treatment performance.
Electrochemical pre-treatment + UF + Reverse osmosis (RO) membrane system (Meiramkulova *et al.*, 2020)	Electrochemical oxidation → Ultrafiltration → RO	COD, BOD, TSS, turbidity, nutrients, metals	Industrial poultry wastewater; electrochemical pre-treatment prior to membranes	COD/BOD/TSS: 71–100 (overall nearly complete)	Electrochemical pre-treatment minimized fouling and improved downstream membrane efficiency; industrial-scale success in Kazakhstan.
Integrated biological WWTP for lincomycin wastewater (Zhang *et al.*, 2021)	Hydrolysis–acidification → Anaerobic EGSB → Aerobic oxidation + physicochemical polishing	COD, NH_3–N, antibiotics	Industrial-scale, 3-tier bioreactors	COD: 98.9; NH_3–N: 98.0	High efficiency via microbial consortia synergy; identified keystone species linked to pollutant degradation.
Integrated biofilm phytoremediation reactor (Buslima *et al.*, 2025)	Biofilm carrier + aquatic macrophyte (water hyacinth)	COD, NH_3–N, PO_4^{3-}	HRT: 24–48 h; NH_3–N varied 3–13 mg/L	COD: 86.7–100; NH_3–N: 79–99.6; PO_4^{3-}: ~80	Integration enhanced nutrient and COD removal; suitable for non-potable water reuse; low energy alternative for domestic wastewater.
The current study (three-stage coagulation) biofiltration–UV/H_2O_2	Coagulation-flocculation → Biofiltration → UV/H_2O_2	TSS, COD, heavy metals, microbial contaminants	Coagulant dose: 20–100 mg/L; optimized biofilter HRT;	TSS: 52.3–92.5; COD: 15.7–43.3 (per stage); Overall: COD 92,	Demonstrated high removal of solids and organics; integrated physicochemical–biological–oxidative process ensured

Note: BOD = biochemical oxygen demand; BOD_5 = biochemical oxygen demand (5-day test); EGSB = expanded granular sludge blanket; NH_4^+–N = ammoniacal nitrogen; NH_3–N = ammonia nitrogen; PO_4^{3-} = phosphate; RO = reverse osmosis; TP = total phosphorus; TSS = total suspended solids; UASB = upflow anaerobic sludge blanket; UF = ultrafiltration; UV/H_2O_2 = ultraviolet light/hydrogen peroxide; WWTP = wastewater treatment plant

more environmentally friendly, yet they fell short in terms of complete disinfection effectiveness. Overall, the present integrated process represents a balanced and versatile solution that ensures comprehensive pollutant removal while maintaining practical and cost-effective operation.

The coagulation-flocculation process achieved optimal removal at 60 mg/L alum, with 90% TSS and 40% COD reduction, primarily through charge neutralization and sweep flocculation by amorphous aluminum hydroxide precipitates. The partial COD reduction implies that a substantial fraction of the organics was present in dissolved form, which is resistant to aggregation. This aligns with the mechanistic understanding that coagulation primarily targets colloidal and particulate fractions, leaving soluble organics unaffected. Daud *et al.* (2023) observed higher COD removal (70.7%) in batik wastewater using alum, likely due to a greater prevalence of large, dye-derived organic molecules that are more easily destabilized. In comparison, the notably low COD removal observed here indicates the prevalence of low-molecular-weight organics commonly found in municipal wastewater, necessitating further oxidative or biological treatment. Studies by El Mouhri *et al.* (2024) further demonstrate that bio-coagulants, rich in polysaccharides and proteins, can facilitate dual mechanisms of charge neutralization and polymer bridging, achieving nearly complete COD

and TSS removal. These comparisons underscore that coagulant chemistry and wastewater composition jointly determine floc characteristics and treatment efficiency. The SVI behavior in this study highlights the operational importance of emphasize that both coagulant chemistry and wastewater composition play a crucial role in determining floc characteristics and the effectiveness of treatment optimizing coagulant dose for efficient sludge management. The decline in SVI from over 120 mL/g to around 75–80 mL/g reflects improved floc compactness and settling due to effective charge neutralization and enmeshment. At inadequate doses, weak electrostatic attraction results in open, low-density flocs that trap water, causing bulky sludge that does not settle well. Conversely, overdosing induces charge reversal, yielding re-dispersed microflocs that resist compaction. For aluminum sulfate and ferric chloride alike, such phenomena are governed by interparticle potential energy and the formation of amorphous hydroxide matrices that capture colloids through physical enmeshment (Wang *et al.,* 2017). Practically, lower SVI values correspond to improved dewaterability, reduced sludge storage volume, and lower disposal costs. Consequently, the identified SVI minima close to the ideal coagulant dosage serve not only as markers of treatment effectiveness but also as essential factors for operational sustainability. Biofiltration further enhanced pollutant removal through synergistic physicochemical and biological mechanisms. COD and metal reductions were strongly linked to biofilm-mediated adsorption and biotransformation processes. The superior removal of Cr and Cu compared to Pb can be explained by their higher complexation stability with functional groups in extracellular polymeric substances (EPS), such as carboxyl and hydroxyl moieties. Cr and Cu exhibit stronger affinities for these groups due to their higher ionic potentials and smaller hydrated radii, leading to more effective sequestration within biofilm matrices. Pb, in contrast, tends to form weaker outer-sphere complexes, resulting in lower removal efficiency. Furthermore, the fluctuating redox conditions present in the biofilm might have encouraged the partial reduction of Cr(VI) to Cr(III), which in turn may facilitate precipitation or improve adsorption. These mechanisms are consistent with the findings of Moges *et al.* (2017), who demonstrated that microbial biofilms can act as both biosorbents and catalysts for redox transformations of metals. The plateau in microbial removal after 4 hours HRT suggests that most accessible niches within the biofilm became saturated, reaching a steady-state balance between microbial die-off and detachment. Prolonged contact times beyond this threshold yield diminishing returns because diffusion limitations restrict substrate penetration into the deeper biofilm layers, leading to metabolic quiescence. Furthermore, microbial inactivation in the biofilter is influenced not only by biological competition and predation but also by the detachment of outer biofilm layers caused by shear forces, which can lead to the release of surviving cells into the effluent. The persistence of residual *Escherichia coli* thus indicates the kinetic limits of passive biological treatment and the necessity for subsequent disinfection. The results align with Moges *et al.* (2017), who reported comparable microbial reduction trends in multi-barrier biofiltration systems, where additional infiltration stages improved inactivation efficiency. The UV/H_2O_2 oxidation stage provided a critical polishing step, achieving nearly complete microbial inactivation and further COD reduction. •OH generated by the photolysis of hydrogen peroxide exhibit non-selective oxidation potential, degrading cell membranes, proteins, and nucleic acids at rates far exceeding conventional UV disinfection alone. The 78% decrease in UV254 absorbance demonstrates the breakdown of aromatic and humic compounds (Mamba *et al.,* 2012; Wu *et al.,* 2011; Abdelraheem *et al.,* 2015). The observed degradation mechanisms include •OH attack on aromatic rings, leading to ring cleavage, hydroxylation, and subsequent mineralization into simpler, more hydrophilic intermediates (Rayaroth, *et al.,* 2023; Sharma *et al.,* 2016). These intermediates are characterized by increased biodegradability, which may enhance later treatment processes (Rayaroth *et al.,* 2023). Additionally, adsorption processes on carbonaceous surfaces may have contributed to further attenuation of UV-absorbing compounds through π–π interactions and electrostatic attraction (Jagadeesh and Sundaram, 2023; Li *et al.,* 2023). The findings are consistent with Sindelar *et al.* (2014), who reported substantial UV254 and DOC reductions, and Yoon *et al.* (2023), who demonstrated synergistic improvements in microbial inactivation using integrated microbial desalination and UV/H_2O_2 systems.

CONCLUSION

This study successfully developed, optimized, and evaluated an integrated multi-stage wastewater treatment system combining coagulation–flocculation, biofiltration, and advanced oxidation processes (AOPs) to achieve comprehensive contaminant removal. The collaborative operation of these three stages delivered substantial advantages in managing the complexity and variability of industrial and municipal wastewater, as opposed to standard single-stage systems. The process demonstrated high stability, efficiency, and reproducibility, indicating its potential for full-scale implementation under diverse environmental conditions. In the first stage, coagulation–flocculation using alum achieved approximately 90% removal of TSS and a 40% reduction in COD at the optimal dosage of 60 mg/L. These results highlight the importance of optimized chemical dosing and proper mixing dynamics for efficient particle destabilization and floc formation. The impressive results of this phase validated the essential function of physicochemical mechanisms in facilitating the initial solid–liquid separation and alleviating the burden on later treatment processes. The biofiltration stage further improved effluent quality by facilitating biological degradation of dissolved organic matter and adsorption of heavy metals. At a hydraulic retention time of four hours, the biofilter achieved an 85% reduction in COD and heavy metal removal efficiencies of 75% for Pb, 82% for Cr, and 80% for Cu. This stage effectively combined microbial metabolism with surface adsorption, reflecting the dual benefit of biological and physicochemical removal mechanisms. Furthermore, the biofiltration unit exhibited significant microbial inactivation capabilities, attaining a 92% decrease in Escherichia coli, which suggests its effectiveness in enhancing both chemical and biological effluent quality. Microbial succession and biofilm adaptation during prolonged operation could further enhance long-term system stability and pollutant degradation efficiency under integrated operation. The final AOP stage employing UV/H_2O_2 treatment (H_2O_2 dose of 40 mg/L) ensured the breakdown of refractory organic pollutants and complete microbial disinfection. This stage achieved 99% microbial inactivation and an additional 7% COD reduction, confirming the effectiveness of hydroxyl radical–based oxidation reactions in degrading persistent organic compounds. The treated effluent met discharge and reuse standards, with residual concentrations of Pb, Cr, and Cu reduced to 0.4, 0.27, and 0.2 mg/L, respectively. Furthermore, a 78% decline in UV absorbance at 254 nm verified significant reduction of aromatic organics and overall pollutant load. The modular configuration reduced energy demands, and utilization of commonly accessible materials indicate that this integrated system has the potential to be both scalable and versatile for decentralized wastewater management, especially in rural or resource-limited contexts with inconsistent influent quality. The system's flexibility allows for incremental deployment, enabling communities to treat wastewater efficiently without reliance on large, centralized infrastructure. Future studies should evaluate long-term operational stability under variable influent conditions, investigate microbial community dynamics and biofilm adaptation for sustained performance, explore alternative bio-based or biodegradable coagulants, and assess sludge composition and valorization potential. Enhancing the energy efficiency of UV lamps and the dosing of hydrogen peroxide, along with the integration of automation and real-time monitoring, may facilitate adaptive management of hydraulic and chemical parameters during continuous operation. Addressing these aspects will enhance the system's reliability, cost-effectiveness, environmental sustainability, and contribution to circular economy initiatives and global wastewater reuse strategies.

AUTHOR CONTRIBUTIONS

D. Amankeshuly conceptualized the study framework, coordinated the overall experimental design, and contributed to drafting and revising the manuscript. T. Salikhov participated in data analysis, assisted in optimizing process parameters, and contributed to result interpretation. S. Syrlybekkyzy conducted an extensive literature review, performed data extraction, and assisted in preparing figures and tables. G. Shapatova, supervised the research, integrated contributions from all co-authors, critically revised the manuscript, and finalized it for submission. N. Kaya contributed to methodological development, validation of analytical results, and technical review of the final draft. I. Agarkova participated in experiment coordination, quality control, and assisted in the presentation of findings. A. Yeginbayeba supported

data processing, contributed to the visualization of results, and assisted in manuscript editing. E. Atasoy contributed to the critical evaluation of the treatment system's performance and provided technical insights for discussion. G. Saspugayeva assisted in reviewing relevant literature, compiling references, and editing the discussion section. K. Dakieva as the corresponding author contributed to summarizing findings, refining the narrative flow, and reviewing the final version of the manuscript.

ACKNOWLEDGEMENT

The authors express their sincere gratitude to the institutions and colleagues who provided valuable support throughout this research. Appreciation is extended to the laboratory and technical staff for their assistance during the experimental work. The authors also thank their respective universities and research centers for providing facilities and resources essential to the successful completion of this study.

CONFLICT OF INTEREST

The authors declare that there is no conflict of interest regarding the publication of this manuscript. In addition, ethical issues, including plagiarism, informed consent, misconduct, data fabrication and/or falsification, double publication and/or submission, and redundancy have been completely observed by the authors.

OPEN ACCESS

©2026 The author(s). This article is licensed under a Creative Commons Attribution 4.0 International License, which permits use, sharing, adaptation, distribution and reproduction in any medium or format, if you give appropriate credit to the original author(s) and the source, provide a link to the Creative Commons license, and indicate if changes were made. The images or other third-party material in this article are included in the article's Creative Commons license, unless indicated otherwise in a credit line to the material. If material is not included in the article's Creative Commons license and your intended use is not permitted by statutory regulation or exceeds the permitted use, you will need to obtain permission directly from the copyright holder. To view a copy of this license, visit: http://creativecommons.org/licenses/by/4.0/

PUBLISHER'S NOTE

GJESM Publisher remains neutral regarding jurisdictional claims in published maps and institutional afflictions.

Negative AI Statement

The author(s) declared that no AI tools or services were not used or highly applied during the preparation of this work.

ABBREVIATIONS

%	Percent
°C	Degrees celsius
•OH	Hydroxyl radical
AD	Anaerobic digestion
AAS	Atomic absorption spectroscopy
AOP	Advanced oxidation process
AOPs	Advanced oxidation processes
$Al_2(SO_4)_3$	Aluminum sulfate
APHA	American public health association
BOD	Biochemical oxygen demand
BOD_5	Biochemical oxygen demand (5-day test)
CFU	Colony-forming units
COD	Chemical oxygen demand
Cr	Chromium
Cu	Copper
DBPs	Disinfection by-products
DOC	Dissolved organic carbon
EGSB	Expanded granular sludge blanket
EO	Electro-oxidation
EMB	Eosin Methylene Blue
EPS	Extracellular polymeric substances
$FeCl_3$	Ferric chloride
GAC	Granular activated carbon
g/L	Grams per liter
H_2O_2	Hydrogen peroxide
HAAs	Haloacetic acids
h	Hour
HRT	Hydraulic retention time
kWh/kgCOD	Kilowatt-hour per kilogram of COD

kWh/m³	Kilowatt-hour per cubic meter
L	Liter
mL	Milliliter
mL/g	mililiters per gram
mg/L	Milligrams per liter
MLSS	Mixed liquor suspended solids
MDCs	Microbial desalination cells
Min.	Minutes
NH_4^+–N	Ammoniacal Nitrogen
NH_3–N	Ammonia Nitrogen
NaCl	Sodium chloride
NOM	Natural organic matter
O_3	Ozone
PAHs	Polycyclic aromatic hydrocarbons
Pb	Lead
pH	Potential of hydrogen (measure of acidity/alkalinity)
PO_4^{3-}	Phosphate
rpm	Rotations per minute
RO	Reverse osmosis
SD	Standard deviation
SVI	Sludge volume index
THMs	Trihalomethanes
TP	Total Phosphorus
TSS	Total suspended solids
UASB	Upflow anaerobic sludge blanket
UF	Ultrafiltration
UV	Ultraviolet
UV/H_2O_2	Ultraviolet/hydrogen peroxide
UV-Vis	Ultraviolet-visible
WWTP	Wastewater treatment plant

REFERENCES

Abdelraheem, W.H.M.; He, X.; Duan, X.; Dionysiou, D.D., (2015). Degradation and mineralization of organic ultraviolet absorber compound 2-phenylbenzimidazole-5-sulfonic acid (PBSA) using ultraviolet/hydrogen peroxide (UV/H_2O_2). J. Hazard. Mater., 282: 233–240 **(8 pages)**.

Aktas, K.; Liu, H.; Eskicioglu, C., (2024). Treatment of aqueous phase from hydrothermal liquefaction of municipal sludge by adsorption: Comparison of biochar, hydrochar, and granular activated carbon. J. Environ. Manage., 356: 120619 **(10 pages)**.

Ali, A.S.; Bayih, A.A.; Gari, S.R., (2022). Meta-analysis of public health risks of lead accumulation in wastewater, irrigated soil, and crops nexus. Front. Public Health. 10: 977721 **(12 pages)**.

American Public Health Association, (2017). APHA Method 4500-H pH Value: Standard Methods for the Examination of Water and Wastewater. Stand. Methods Exam. Water Wastewater., 2(4500): 1-5 **(5 pages)**.

Badawi, A.K.; Salama, R.S.; Mostafa, M.M.M., (2023). Natural-based coagulants/flocculants as sustainable market-valued products for industrial wastewater treatment: A review of recent developments. RSC Adv., 13(28): 19335–19355 **(21 pages)**.

Bond, T.; Mokhtar Kamal, N.H.; Bonnisseau, T.; Templeton, M.R., (2014). Disinfection by-product formation from the chlorination and chloramination of amines. J. Hazard. Mater., 278: 288–296 **(9 pages)**.

Buslima, F.A.; Abu Hasan, H.; Alias, J.; Jaganathan, J.S.; Buhari, J.; Subramanian, S.V.; Abdullah, S.R.S., (2025). Performance of Integrated Biofilm-Phytoremediation Process in Reclaiming Water from Domestic Wastewater. Water, 17(2): 163 **(14 pages)**.

Chen, R.; Li, T.; Huang, G.; Jia, X.; Jin, Z.; Zheng, X.; Zhao, M., (2024). Enhancement the wastewater treatment performance of multistage living machine by underwater lamp. J. Environ. Manage., 365: 121604 **(10 pages)**.

Das, A.K.; Chen, L., (2024). A review on electrochemical advanced oxidation treatment of dairy wastewater. Environ., 11(6): 124 **(18 pages)**.

Daud, N.M.; Abdullah, S.R.S.; Hasan, H.A.; Othman, A.R.; Ismail, N.'Izzati., (2023). Coagulation-flocculation treatment for batik effluent as a baseline study for the upcoming application of green coagulants/flocculants towards sustainable batik industry. Heliy on.9: e17284 **(12 pages)**.

Dikobe, J.; Melato, F.A.; Adlem, C.J.L.; Netshiongolwe, K., (2024). Determination of chromium species in water using diphenylcarbazide with a sequential spectrophotometric discrete robotic analyser. Heliyon. 10(14): e34670 **(10 pages)**.

Dong, F.; Zhu, J.; Li, J.; Fu, C.; He, G.; Lin, Q.; Li, C.; Song, S., (2023). The occurrence, formation and transformation of disinfection by-products in the water distribution system: A review. Sci. Total Environ., 867: 161497 **(22 pages)**.

El Mouhri, G.; Elmansouri, I.; Amakdouf, H.; Belhassan, H.; Kachkoul, R.; El Oumari, F.E.; Merzouki, M.; Lahrichi, A., (2024). Evaluating the effectiveness of coagulation–flocculation treatment on wastewater from the Moroccan leather tanning industry: An ecological approach. Heliyon. 10(5): e27056 **(14 pages)**.

Hübner, U.; Spahr, S.; Lutze, H.; Wieland, A.; Rüting, S.; Gernjak, W.; Wenk, J., (2024). Advanced oxidation processes for water and wastewater treatment – Guidance for systematic future research. Heliyon. 10(9): e30402 **(16 pages)**.

Huelgas, A.; Nakajima, M.; Nagata, H.; Funamizu, N., (2009). Comparison between treatment of kitchen-sink wastewater and a mixture of kitchen-sink and washing-machine wastewaters. Environ. Technol., 30(1): 111–117 **(7 pages)**.

Islam, M.R.; Mostafa, M.G., (2020). Characterization of textile dyeing effluent and its treatment using polyaluminum chloride. Appl. Water Sci., 10(5): 119 **(8 pages)**.

Jagadeesh, N.; Sundaram, B., (2023). Adsorption of pollutants from wastewater by biochar: A review. J. Hazard. Mater. Adv., 8: 100226 **(20 pages)**.

Khan, Z.U.H.; Gul, N.S.; Sabahat, S.; Sun, J.; Tahir, K.; Shah, N.S.; Muhammad, N.; Rahim, A.; Imran, M.; Iqbal, J.; Khan, T.M.; Khasim, S.; Farooq, U.; Wu, J., (2023). Removal of organic pollutants through hydroxyl radical-based advanced oxidation processes. Ecotoxicol. Environ. Saf., 267: 115564 **(18 pages)**.

Li, Y.; Wang, B.; Shang, H.; Cao, Y.; Yang, C.; Hu, W.; Feng, Y.; Yu, Y., (2023). Influence of adsorption sites of biochar on its adsorption performance for sulfamethoxazole. Chemosphere. 326: 138408 **(14 pages)**.

Mamba, B.; Krause, R.; Matsebula, B.; Haarhoff, J., (2012).

Monitoring natural organic matter and disinfection by-products at different stages in two South African water treatment plants. Water SA., 35(1): 1–8 **(8 pages)**.
Meiramkulova, K.; Devrishov, D.; Zhumagulov, M.; Arystanova, S.; Karagoishin, Z.; Marzanova, S.; ... Li, J., (2020). Performance of an Integrated Membrane Process with Electrochemical Pre-Treatment on Poultry Slaughterhouse Wastewater Purification. Membranes, 10(10): 256 **(17 pages)**.
Meiramkulova, K.; Jakupova, Z.; Orynbekov, D.; Tashenov, E.; Kydyrbekova, A.; Mkilima, T.; Inglezakis, V.J., (2020). Evaluation of electrochemical methods for poultry slaughterhouse wastewater treatment. Sustain., 12(12): 5110 **(16 pages)**.
Moges, M.E.; Todt, D.; Eregno, F.E.; Heistad, A., (2017). Performance study of biofilter system for on-site greywater treatment at cottages and small households. Ecol. Eng., 102: 340–349 **(10 pages)**.
Muliyadi, M.; Purwanto, P.; Sumiyati, S.; Hadiyanto, H.; Sudarno, S.; Budiyono, B.; Warsito, B., (2024). Bacterial community dynamics and pollutant removal mechanisms in biofilters: A literature review. Environ. Health Eng. Manage., 11(4): 477–492 **(16 pages)**.
Oluwafisayomi, C.F., (2025). Microbial contamination in urban wastewater systems: Emerging health threats and mitigation strategies. Int. J. Sci. Res. Arch., 14(2): 1449–1463 **(15 pages)**.
Phan, H.N.Q.; Leu, J.H.; Nguyen, V.N.D., (2023). The combination of anaerobic digestion and electro-oxidation for efficient COD removal in beverage wastewater: Investigation of electrolytic cells. Sustainability. 15: 65551 **(14 pages)**.
Rayaroth, M.P.; Boczkaj, G.; Aubry, O.; Aravind, U.K.; Aravindakumar, C.T., (2023). Advanced oxidation processes for degradation of water pollutants — Ambivalent impact of carbonate species: A review. Water. 15(8): 1615 **(20 pages)**.
Rayaroth, M.P.; Marchel, M.; Boczkaj, G., (2023). Advanced oxidation processes for the removal of mono and polycyclic aromatic hydrocarbons – A review. Sci. Total Environ., 857: 159043 **(18 pages)**.
Sharma, J.; Mishra, I.M.; Kumar, V., (2016). Mechanistic study of photo-oxidation of bisphenol-A with hydrogen peroxide and sodium persulfate. J. Environ. Manage., 166: 12–22 **(11 pages)**.
Sindelar, H.R.; Brown, M.T.; Boyer, T.H., (2014). Evaluating ultraviolet/hydrogen peroxide (UV/H_2O_2), ultraviolet/percarbonate, and ultraviolet/perborate for natural organic matter reduction from alternative water sources. Chemosphere. 105: 112–118 **(7 pages)**.
Tessema, R.S.; Tarekegn, M.M.; Worku, M.A.; Engida, A.N.; Van Griensven, A., (2024). Performance evaluation of integrated Upflow Anaerobic Sludge Blanket reactor with trickling filter used for municipal wastewater treatment and effluent reuse potential for agriculture. Environ. Syst. Res., 13(1): 39 **(16 pages)**.
Tiaiba, M.; Merzouk, B.; Mazour, M.; Leclerc, J.P.; Lapicque, F., (2018). Study of chemical coagulation conditions for a disperse red dye removal from aqueous solutions. Membr. Water Treat., 9(1): 9–18 **(10 pages)**.
Wang, B.; Shui, Y.; He, M.; Liu, P., (2017). Comparison of flocs characteristics using before and after composite coagulants under different coagulation mechanisms. Biochem. Eng. J., 121: 107–117 **(11 pages)**.
Wongburi, P.; Park, J.K., (2022). Prediction of Sludge Volume Index in a Wastewater Treatment Plant Using Recurrent Neural Network. Sustainability. 14: 6276 **(18 pages)**.
Wu, Y.; Zhou, S.; Ye, X.; Zhao, R.; Chen, D., (2011). Oxidation and coagulation removal of humic acid using Fenton process. Colloids Surf. A: Physicochem. Eng. Asp., 384: 149–155 **(7 pages)**.
Yoon, Y.; Jee, H.; Song, S.H.; Hwang, M.H.; Chae, K.J.; Kim, B.; Yang, E., (2023). Combination of hydrogen peroxide-producing microbial desalination cells and ultraviolet/hydrogen peroxide (UV/H_2O_2) advanced oxidation process: Water salinity reduction and microbial inactivation. J. Environ. Chem. Eng., 11(3): 110110 **(20 pages)**.
Zhang, P.; Liang, J.; Mai, W.; Wu, Y.; Dai, J.; Wei, Y., (2021). The efficiency of integrated wastewater treatment plant for pollutant removal from industrial-scale lincomycin production. J. Water Process Eng., 102133 **(12 pages)**.
Zhang, Y.; He, Y.; Sakowski, E.G.; Preheim, S.P., (2021). Influence of simplified microbial community biofilms on bacterial retention in porous media under conditions of stormwater biofiltration. Microbiol. Spectr., 9(2): 1105–1120 **(16 pages)**.
Zheng, C.; Zhao, L.; Zhou, X.; Fu, Z.; Li, A., (2013). Treatment technologies for organic wastewater. In Water Treatment. InTech 1–25 **(25 pages)**.

AUTHOR (S) BIOSKETCHES

Amankeshuly, D., Ph.D., Senior Lecturer, Department of Ecology and Geology, Yessenov University, Aktau, Kazakhstan.
- Email: *doktor.2020@internet.ru*
- ORCID: 0009-0007-9186-7142
- Web of Science ResearcherID: OSH-5433-2025
- Scopus Author ID: NA
- Homepage: https://bulletin.yu.edu.kz/2022/educ_plans/1242/

Salikhov, T., Ph.D., Acting Professor, Department of Physical and Economical Geography, L.N. Gumilyov Eurasian National University, Astana, Kazakhstan.
- Email: *tuatai_76@mail.ru*
- ORCID: 0000-0002-8720-0931
- Web of Science ResearcherID: MWR-4975-2025
- Scopus Author ID: 56144864900
- Homepage: https://fns.enu.kz/en/page/departments/physical-and-economical-geography/faculty-members

Shapatova, G., Ph.D., Assistant Professor, Department of Morphology, NCJSC Karaganda Medical University, Karaganda, Kazakhstan.
- Email: *Shapatova@qmu.kz*
- ORCID: 0000-0002-8116-0828
- Web of Science ResearcherID: OSH-5303-2025
- Scopus Author ID: 57815671800
- Homepage: https://qmu.edu.kz/en/employees/other-teachers/shapatova-gulmira-bukeikhanov/

AUTHOR (S) BIOSKETCHES

Syrlybekkyzy, S., Ph.D., Associate Professor, Department of Ecology and Geology, Yessenov University, Aktau, Kazakhstan.
- Email: *samal.syrlybekkyzy@yu.edu.kz*
- ORCID: 0000-0002-0260-0611
- Web of Science Researcher ID: CCE-3821-2022
- Scopus Author ID: 56589971900
- Homepage: https://eng.yu.edu.kz/ru/pps-ekologiya/samal-syrlybekkyzy-professor/

Agarkova, I., Ph.D., Assistant Professor, Department of Morphology, NCJSC Karaganda Medical University, Karaganda, Kazakhstan.
- Email: *Agarkova@qmu.kz*
- ORCID: https://orcid.org/0009-0007-9821-091X
- Web of Science ResearcherID: KAM-2789-2024
- Scopus Author ID: NA
- Homepage: https://qmu.edu.kz/en/employees/other-teachers/agarkova-inna-andreevna/

Kaya, N., Assistant Professor, Faculty of Education, Social Studies Education, Eskişehir Osmangazi University, Eskişehir City, Turkiye.
- Email: *niyazi.kaya@ogu.edu.tr*
- ORCID: https://orcid.org/0000-0002-5122-3824
- Web of Science ResearcherID: NA
- Scopus Author ID: 56352078700
- Homepage: https://dergipark.org.tr/en/pub/@niyakaya61

Yeginbayeva, A., Ph.D., Acting Associate Professor, Department of Physical and Economical Geography, Gumilyov Eurasian National University, Astana, Kazakhstan.
- Email: *yeginbayeva_aye@enu.kz*
- ORCID: 0000-0001-5520-9301
- Web of Science ResearcherID: AGH-8762-2022
- Scopus Author ID: 57194424770
- Homepage: https://fns.enu.kz/en/page/departments/chemistry/faculty-members

Atasoy, E., Ph.D., Professor, Faculty of Education, Department of Social Sciences, Uludag University, Bursa City, Turkiye.
- Email: *eatasoy@uludag.edu.tr*
- ORCID: 0000-0002-1473-7420
- Web of Science ResearcherID: AAG-7268-2021
- Scopus Author ID: 36478260200
- Homepage: https://avesis.uludag.edu.tr/eatasoy

Saspugayeva, G., Ph.D., Associate Professor, Department of Environmental Engineering and Management, Faculty of Natural Sciences, L.N. Gumilyov Eurasian National University, Astana 010000, Kazakhstan.
- Email: *saspugayeva_gye@enu.kz*
- ORCID: 0000-0003-3223-3602
- Web of Science ResearcherID: IDIQT-9363-2023
- Scopus Author ID: 56982937000
- Homepage: https://repository.enu.kz/handle/enu/15597/browse?rpp=20&sort_by=-1&type=author&etal=-1&starts_with=S&order=ASC&locale-attribute=en

Kuzilpa, D., Ph.D., Associate Professor, Department of Ecology and Geography, Amanzholov East Kazakhstan University, Ust-Kamenogorsk 470010, Kazakhstan.
- Email: *ecology-2014@mail.ru*
- ORCID: 0000-0002-8110-5255
- Web of Science Researcher ID: NA
- Scopus Author ID: 14055427900
- Homepage: https://vku.edu.kz/higher-school-of-it-and-natural-sciences/department-of-economics-management-and-finance/

HOW TO CITE THIS ARTICLE

Amankeshuly, D.; Salikhov, T.; Shapatova, G., Syrlybekkyzy, S., Agarkova, I., Kaya, N., Yeginbayeva, A., Atasoy, E., Saspugayeva, G., Dakieva, K., (2026). The potential of combining coagulation-flocculation, biofiltration, and advanced oxidation processes for multi-stage wastewater treatment. Global J. Environ. Sci. Manage., 12(1): 21-38.

DOI: 10.22034/gjesm.2026.01.02

URL: https://www.gjesm.net/article_731668.html

Global J. Environ. Sci. Manage. 12(1): 39-56, Winter 2026, Serial #45

Global Journal of Environmental Science and Management
(GJESM)

Homepage: https://www.gjesm.net/

Podcasts

ORIGINAL RESEARCH PAPER

Efficacy of zinc oxide chitosan hybrid nanoparticles as a nanovaccine to enhance immunity in hybrid grouper fish

U. Yanuhar[1,*], Z. Waheed[1,2], H. Suryanto[3], V. Hasan[4], D. R. Machfuda[5]

[1] *Study Program of Fisheries Resources Management, Faculty of Fisheries and Marine Sciences, Universitas Brawijaya, Jl. Veteran, Malang, East Java, Indonesia*

[2] *Borneo Marine Research Institute, Universiti Malaysia Sabah, Jalan UMS, 88400 Kota Kinabalu, Sabah, Malaysia*

[3] *Department of Mechanical and Industrial Engineering, Faculty of Engineering, Universitas Negeri Malang, Jl. Semarang 5, Malang 65145, Indonesia*

[4] *Study Program of Aquaculture, Faculty of Fisheries and Marine Sciences, Universitas Airlangga, Jl. Mulyorejo, Surabaya, East Java, Indonesia*

[5] *Master Program in Aquaculture, Faculty of Fisheries Marine Science, Universitas Brawijaya, Jl. Veteran, Malang, East Java, Indonesia*

ARTICLE INFO

Article History:
Received 10 August 2025
Revised 15 October 2025
Accepted 18 November 2025

Keywords:
Chitosan-ZnO nanoparticles
Grouper
Recombinant Peridinin Protein
Nanovaccine
Viral nervous necrosis (VNN)

ABSTRACT

BACKGROUND AND OBJECTIVES: The cantang grouper (*E. fuscoguttatus* × *E.lanceolatus*) is an important marine cultured fish in Indonesia; however, its production has collapsed from approximately 10,208 tons in 2023 to 3,632 tons in 2024. This decrease is mainly attributed to repeated occurrences of viral nervous necrosis, leading to mortality rates approaching 100 percent. The objectives of this study are to investigate whether zinc oxide-chitosan hybrid nanoparticles can serve as an effective nanovaccine delivery system, utilizing recombinant Chlorella vulgaris protein to enhance protective immunity against viral nervous necrosis in cantang grouper.

METHODS: An in vivo assessment was conducted using 100 juvenile hybrid groupers, which were divided into five experimental groups: untreated healthy controls, viral nervous necrosis challenged controls, and three vaccinated receiving escalating nanovaccine doses (33 microliters, 66 microliters, and 112 microliters). Each treatment group consisted of 20 fish. Sampling occurred at baseline (day 0) and post-treatment (day 56), with collection of blood and target tissues (kidney) for comprehensive immune and histological assessment via flow cytometry, hematological profiling, and antioxidant enzyme. The methodology of one-way analysis of variance was employed for statistical comparisons.

FINDINGS: The lowest tested dose 33 microliters elicited the most pronounced immunoprotective response. Specifically, Interferon gamma levels increased by 11.90 percent, tumor necrosis factor-alpha levels rose by 5.34 percent, and Immunoglobulin M levels increased by 4.75 percent. Additionally, the activities of superoxide dismutase (3.213 unit per milliliter), catalase (109.7 unit per liter), and glutathione peroxidase (76.02 micromol) were significantly elevated, indicating a more robust defense against free radicals. Histopathological examination revealed negligible renal damage in T3, with edema (10.71 percent), necrosis (12.50 percent), and hemorrhage (13.45 percent), compared to more severe damage in the viral nervous necrosis challenged control group (T2).

CONCLUSION: Zinc oxide–chitosan hybrid nanoparticles effectively function as nanovaccine, enhancing the immune response and protecting cantang grouper from viral nervous necrosis. The 33 microliters dosage delivered optimal protection, bolstering immune function as well as tissue integrity. This nanovaccine provides a cost-efficient and scalable approach to bolster disease resilience in grouper aquaculture, rendering it a promising instrument for enhancing the sustainability of the industry.

DOI: 10.22034/gjesm.2026.01.03

This is an open access article under the CC BY license (http://creativecommons.org/licenses/by/4.0/).

NUMBER OF REFERENCES
59

NUMBER OF FIGURES
4

NUMBER OF TABLES
5

*Corresponding Author:
Email: *doktoruun@ub.ac.id*
Phone: + 812 5269 5056
ORCID: 0000-0003-3360-8752

Note: Discussion period for this manuscript open until Mar 1, 2026 on GJESM website at the "Show Article".

INTRODUCTION

The cantang grouper (*E. fuscoguttatus* × *E. lanceolatus*) is a key part of Indonesian mariculture because it grows quickly and has a strong market pull. Nevertheless, national production decreased from approximately 10,208 tons in 2023 to around 3,632 tons in 2024, indicating that the industry faced increasing stress, particularly due to recurring disease outbreaks (Sulistiyono *et al*., 2020). Betanodaviruses responsible for viral nervous necrosis (VNN) are among the most perilous pathogens. Fish that are affected commonly show signs of neurological dysfunction, evident through irregular or spiraling swimming motions and a decrease in feeding habits. Consequently, significant mortality rates occur during outbreaks, reaching nearly 100 percent (%) in juvenile populations (Griot *et al*., 2021; Padrós *et al*., 2022; Z. Yang *et al*., 2021). VNN has the potential to harm not only gouper but also other farmed animals, leading to higher costs for hatchery operations. Overcrowded environments and elevated water temperatures facilitate the rapid transmission of diseases, exacerbating the impact on farms (Fouzi and Sakajamary, 2023; Yu *et al*., 2024). These facts show that the grouper culture system needs a lot of help to stay alive (Putra *et al*., 2020; Wang *et al*., 2021). Microalgae platforms, especially *Chlorella vulgaris*, have a lot of promise for boosting fish immunity. This kind of algae is known to have a lot of proteins and bioactive compounds that could help immune system of the host. The recombinant *Chlorella vulgaris* protein, specifically the peridinin-encoding protein, was selected as the antigen for this nanovaccine owing to its recognized immune-stimulatory properties, its ability to provoke strong humoral and cellular immune responses in aquatic species, and its verified effectiveness in mitigating symptoms in aquaculture species. *Chlorella vulgaris* proteins offer a favorable stability profile and ease of production compared to traditional viral or synthetic antigens used in similar vaccine platforms. Nonetheless, its direct correlation with VNN caused by betanodaviruses has not been comprehensively investigated. Recent studies indicate that recombinant proteins obtained from microalgae could exhibit immunological cross-reactivity with viral antigens, which may trigger an immune response that enhances resistance to viral infections, including VNN (Kitiyodom *et al*., 2021). There is increased interest in using algae proteins for fish vaccination, however, ensuring that these proteins elicit long-lasting and stable immune responses remains challenging. This study utilized peridinin protein derived from *Chlorella vulgaris* and zinc oxide (ZnO)-chitosan nanoparticles to tackle these challenges by boosting the stability of the antigen, augmenting its immunogenicity, and facilitating a controlled release to strengthen. To address these limitations, nano-enabled vaccines are presently under investigation. Zinc oxide nanoparticles (ZnO-NPs) are safe for living things, have antimicrobial properties, and can change the immune system in ways that are important for finfish (Iwasaki *et al*., 2022). When combined with chitosan, nanoparticles can hold antigens. All these components collaborate to enhance the efficacy of the vaccine and improve its delivery (Faggion *et al*., 2022). Inserting a Chlorella-derived antigen into a ZnO–chitosan hybrid is a good way to boost immunogenicity and protect cantang grouper from VNN, which has big effect on survival and farm resilience (Lee *et al*., 2022). Additionally, it is essential to comprehend the relationship between this platform and the immune system to ensure sustainable aquaculture management over the long term and to mitigate the risk of viral diseases (Bandín and Souto, 2020; Faggion *et al*., 2022). Recent research has been conducted by several researchers to determine the feasibility of ZnO and chitosan nanoparticles as nanocarriers for vaccine delivery in aquaculture. For instance, Sukkarun *et al.* (2022) conducted a study on a chitosan-based polymer nanovaccine in tilapia which showed considerable protection against Aeromonas veronii infection. This study highlights the potential of chitosan as an effective carrier. In this study, chitosan did not contain ZnO or algal protein. Furthermore, a study conducted by Lebaka *et al*. (2025) investigated the significant application of ZnO nanoparticles in vaccine technology, emphasizing their promise as immune modulators and adjuvants. Although previous research has been conducted, no study has integrated ZnO, chitosan, and algal protein into a single nanovaccine platform targeting VNN in grouper. This study elaborates on prior findings to generate a cutting-edge ZnO–chitosan–algal protein hybrid nanovaccine, anticipated to improve immune defense against VNN. This method combines the benefits of ZnO as an adjuvant and chitosan as a biocompatible carrier. It also adds *Chlorella vulgaris* proteins to make the vaccine more immunogenic.

This is the initial instance of this combination being utilized in an aquaculture vaccine. The study bridges this void and recommends optimistic strategies for improving the effectiveness of vaccines and fortifying aquaculture. These proposals could likewise be utilized in different aquaculture frameworks. The study aims to evaluate a nanovaccine formulation comprising a recombinant *C. vulgaris* protein delivered via ZnO–chitosan hybrid nanoparticles, with the working premise that such a system can meaningfully strengthen the immune capacity of cantang grouper. This study on nanovaccines has the potential to mitigate the detrimental impacts of VNN in grouper, thereby addressing a significant challenge in disease management. By enhancing the immune response and survival rate of grouper, production can be increased with minimized production losses. This solution may be supplied and rendered accessible to farmers encountering financial challenges as a result of recurrent disease outbreaks. This study was conducted at the Research House in Malang, East Java, Indonesia in 2025.

MATERIALS AND METHODS

This study conducted an in vivo experiment to test a nanovaccine composed of a recombinant *Chlorella vulgaris* antigen embedded in a chitosan–ZnO hybrid. Fish were sampled twice: on day 0 (baseline, before any dosing) and day 56 (post-treatment). At each time point, blood and target organs kidney, gill, and intestine, were collected. The collection of assays included hematology (counts of red and white blood cells, hemoglobin, and leukocyte differentials), histology, antioxidant activity measurements, and flow-cytometric immunoprofiling.

Production of recombinant Chlorella vulgaris

The method for the production of recombinant *Chlorella vulgaris* followed the procedure described by Yanuhar *et al. (*2024). The complementary deoxyribonucleic acid (cDNA) obtained from *C. vulgaris* was cloned into *Escherichia coli (E. coli)* using the plasmid vector (pTA2) vector and the Target Clone Plus Kit. Transformation of the recombinant *C. vulgaris* gene was carried out with Mix and Go Competent Cells™ of *E. coli* strain Zymo 5α (Zymo Research - USA). Plasmid DNA containing the recombinant *C. vulgaris* target gene was subsequently extracted from the bacterial host using the ZR Plasmid Miniprep Kit (Zymo Research, USA) in accordance with the manufacturer's guidelines. The presence of the recombinant *C. vulgaris* gene insert was confirmed through polymerase chain reaction (PCR) amplification using T3 and T7 primers with the KOD FX Neo polymerase (Toyobo - Japan). Positive colonies containing the appropriate insert were stored in glycerol stocks for future application in nanovaccine formulation.

Production of recombinant Chlorella vulgaris nanovaccine with hybrid chitosan-ZnO nanoparticles

Two adjuvant systems were prepared. For chitosan nanoparticles, 2 g of chitosan was dissolved in 100 mL of 1% acetic acid, followed by ionic gelation using sodium tripolyphosphate (TPP) with a concentration of 1 milligram per milliliter (mg/mL) 35 mL. The mixture was stirred at room temperature for 1 hour (h), then nanoparticles were pelleted with 12,000 × grams (g), 15 minutes (min) and rinsed with distilled water. $Zn(NO_3)_2$ (Sigma-Aldrich, Germany), 2 g, was dissolved in 50 mL of distilled water. While stirring, *C. vulgaris* extract of 100 mL was gradually added to the zinc precursor solution, then the temperature was maintained at 60–80 degrees Celsius (˚C) for 1-2 h, and the pH was adjusted to 11 to form ZnO nanoparticles. Solutions were cooled to 25 °C and collected precipitates by centrifugation at 8000 revolutions per minute (rpm) for a duration of 15 min. Subsequently, the precipitates were washed with distilled water to eliminate any remaining impurities, and dried. The ZnO product was calcinated at 400˚C for 2 h. The particle size of ZnO-NP was obtained using ImageJ with a size of 57±13 nm (Fig. 1).The recombinant peridinin protein was subsequently mixed with chitosan and ZnO to create the hybrid formulation. As reported by Yanuhar *et al*. (2020), a protein: ZnO ratio of 1:0.25 provided optimal delivery and performance against viral challenges such as VNN in grouper. The hybrid, which was freshly prepared, underwent conditioning at 4 °C for a duration of 24 h to ensure encapsulation within the chitosan–ZnO matrix and subsequently stored at −80 °C until administration.

In vivo evaluation of recombinant Chlorella vulgaris nanovaccine formulated with hybrid chitosan-ZnO nanoparticles

Hybrid grouper (*E. fuscoguttatus* × *E. lanceolatus*)

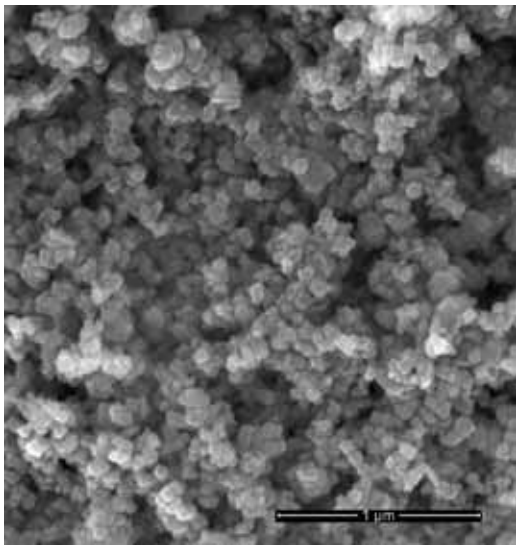

Fig. 1: The particle size of ZnO-NP was obtained using ImageJ (Mag 100.000x)

weighing 12–15 g were sourced from Teluk Kode (Malaka, Pemenang, North Lombok, West Nusa Tenggara) and acclimated for seven days. This study uses 100 juvenile hybrid grouper assigned to five experimental groups. The nanovaccine was administered orally on day 0 and day 14 (prime–boost). Fish received nanovaccines through the method of oral gavage. A VNN challenge was presented on the 28th day. The viral strain employed was RGNNV, which was initially sourced from Humpback grouper in Situbondo Brackish Water Aquaculture Centers, Indonesia and tested positive for VNN using PCR analysis in accordance with diagnostic protocols. The preparation of the viral inoculum involved homogenizing organs from previously infected fish in distilled water, centrifuging the homogenate, and subsequently administering the resulting supernatant to experimental fish via oral gavage. The experiment was conducted using a fully randomized factorial design (CRD) consisting of eight treatments, each replicated three times (Table 1), with 20 fish allocated to each treatment tank.

Blood sampling

Blood sampling was conducted using a 1 mL syringe (Terumo, Japan) rinsed with a 3% sodium citrate solution (Merck, Germany) as an anticoagulant. Blood was drawn from the muscle tissue close to the fish's anal fin and put in a 1.5 mL microtube (Eppendorf, Germany). Distinct blood samples were obtained for hematological evaluation utilizing a dry syringe (lacking anticoagulant) and preserved in ethylenediaminetetraacetic acid (EDTA)-coated vacutainer tubes (OneMed, Indonesia). The counting of red blood cells (RBCs) and white blood cells (WBCs) was performed using a Hemacytometer, and the concentration of hemoglobin (Hb) was measured with a Sahli hemometer. In this study, blood smears were prepared and stained using Giemsa solution to to determine whether there were differences in the leukocytes (monocytes, lymphocytes, basophils, eosinophils, and neutrophils) according to standard procedures (Khan *et al*., 2022; Rasheed *et al*., 2023). This study assessed all hematological parameters on three separate occasions to ensure the results were both correct and precise.

Histopathological examination

Kidney tissues from hybrid grouper (*E. fuscoguttatus* × *E. lanceolatus*) were processed for histopathology following Rashid *et al*. (2025) with routine steps. Samples were fixed in 10% neutral-buffered formalin, paraffin-embedded, sectioned, and stained with hematoxylin–eosin (H and E; Sigma-Aldrich, USA). The observed lesion types comprised hyperplasia, lamellar fusion, necrosis, and hemorrhage, which were assessed semi-quantitatively. For each treatment group, five randomly selected fields were

Table 1: Group experiment in research design

No.	Treatment	Description	Vaccine Dose	Sample collection timepoint
1	T1	Healthy hybrid grouper (*E. fuscoguttatus* × *E. lanceolatus*)	-	Day 58
2	T2	Healthy hybrid grouper (*E. fuscoguttatus* × *E. lanceolatus*) + VNN	-	Day 58
3	T3	Healthy hybrid grouper (*E. fuscoguttatus* × *E. lanceolatus*) + Recombinant *Chlorella vulgaris* nanovaccine formulated with hybrid chitosan-ZnO nanoparticles 33 Microliter (µl) + VNN	24.75 µl Recombinant *Chlorella vulgaris* + 8.25 µl hybrid chitosan-ZnO nanoparticles	Day 58
4	T4	Healthy hybrid grouper (*E. fuscoguttatus* × *E. lanceolatus*) + Recombinant *Chlorella vulgaris* nanovaccine formulated with hybrid chitosan-ZnO nanoparticles 66 µl + VNN	49.5 µl Recombinant *Chlorella vulgaris* + 16.5 µl hybrid chitosan-ZnO nanoparticles	Day 58
5	T5	Healthy hybrid grouper (*E. fuscoguttatus* × *E. lanceolatus*) + Recombinant *Chlorella vulgaris* nanovaccine formulated with hybrid chitosan-ZnO Nanoparticles 112 µl + VNN	84 µl Recombinant *Chlorella vulgaris* + 28 µl hybrid chitosan-ZnO nanoparticles	Day 58

analyzed per fish, with a total of 3 fish analyzed per group. To minimize observer bias, a minimum of two independent observers carried out the scoring in a blind manner. The proportion of affected cells per field was calculated using Eq. 1, and severity was assigned on a 1–4 scale as described by Yanuhar *et al*. (2020):

$$\text{Percentage of damage} = \frac{\text{Number of damaged cells}}{\text{Number of analyzed cells}} \times 100\% \quad (1)$$

The obtained percentage damage has scores ranging from 0 to 3 (Aminin *et al*., 2024), with criteria as follows:

- Score 0: No damage at all.
- Score 1: Mild damage with a percentage of <30%.
- Score 2: Moderate damage with a percentage of 30%-70%.
- Score 3: Severe damage with a percentage of >70%.

Enzyme activity assays

The activity of superoxide dismutase (SOD) was assessed utilizing a commercial SOD kit (MedikBio, Indonesia) in accordance with the manufacturer's instructions; absorbance readings were taken at 560 nm on a spectrophotometer and reported as units per milliliter wit unit per milliliter (U/mL). Catalase (CAT) activity was quantified with a Catalase Assay Kit (MedikBio, Indonesia); readings were taken at 450 nm and interpolated against a standard curve with 7.5–400 unit per iter (U/L), with results expressed in U/L. Glutathione peroxidase (GPx) activity was determined using a GPx kit (MedikBio, Indonesia) on a Bio-Rad iMark microplate reader at a wavelength of 650 nm; the activities were derived from a standard curve ranging from 0 to 100 micromol (µM) and reported in µM.

Flowcytometry analysis

Single-cell suspensions were prepared from kidney (immune-related) tissue of vaccinated cantang grouper receiving the Chlorella-based nanovaccine with chitosan–ZnO nanoparticles (Chitosan-ZnONPs). The tissue was disaggregated with trypsin at a temperature of 37°C, subsequently washed with phosphate-buffered saline (PBS), and resuspended in PBS. The cells were then passed through a 40 micrometers (µm) cell strainer to ensure a single-cell suspension. Immunophenotyping was performed on a FACSCalibur cytometer (BD Biosciences, Germany). Monoclonal antibodies (BioLegend, San Diego, USA) were used to detect tumor necrosis factor (TNF)-α, Immunoglobulin M (IgM), and IFN-γ were used to detect immune responses. The antibodies utilized for flow cytometry were chosen according to their documented reactivity with crab immune cells. The validation of the hybrid grouper was carried out through earlier studies (Hu *et al*., 2021) to verify its

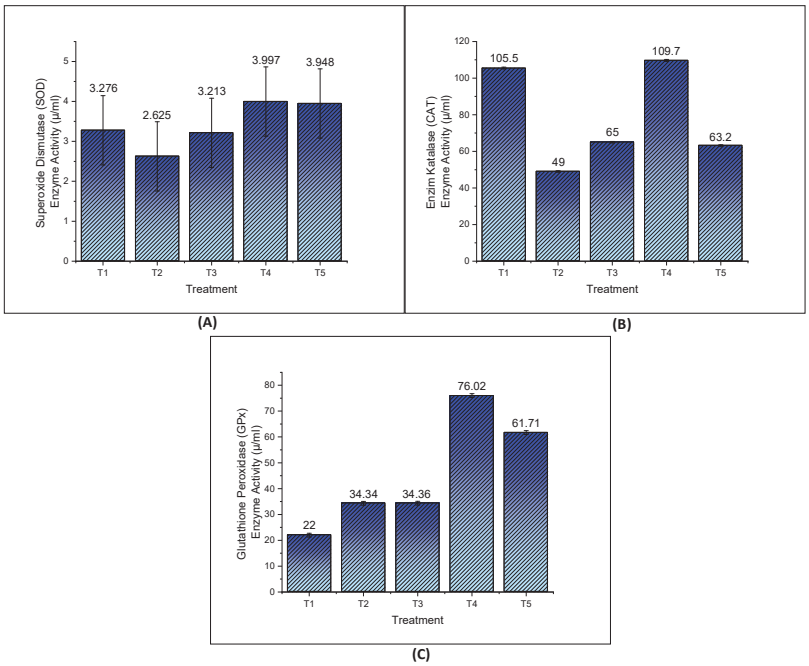

Fig. 2: Enzyme Activity Results : (A) SOD ; (B) CAT ; (C) GPx

specificity. Cell gating methods are utilized to isolate lymphocyte populations from forward scatter (FSC) and side scatter (SSC) profiles, which represent cell size and complexity. In this experiment, lymphocyte populations were first identified through their characteristic FSC and SSC patterns, allowing us to exclude cell debris and any doublet formations. For each sample, around 10,000 events were gathered to guarantee that the dataset was sufficient for assessing the immune responses induced by the vaccine. Both positive and negative controls were included to maintain the reliability of the assay. Cells treated with concanavalin A (ConA) served as the positive control because this mitogen is widely recognized for its strong stimulatory effect on immune cells. The negative control consisted of unstimulated cells that were stained using isotype-matched antibodies, thereby confirming that the detected signals were specific to the intended markers. All gathered data were processed and analyzed using FlowJo software (Tree Star, USA) to assess cytokine levels and the expression of pertinent immune markers.

Analysis data

The treatment effects were tested on all datasets using one-way analysis of variance (ANOVA) ($\alpha = 0.05$). Microsoft Excel and OriginPro 2019b (OriginLab, USA) were used to process data, do statistics, and make plots. Hematology metrics, histopathology scores, and flow cytometry readouts are displayed as mean ± standard deviation (SD), accompanied by graphs to facilitate interpretation, which also include the depiction of ANOVA results.

RESULTS AND DISCUSSION

Enzyme Activity Results

SOD activity at the control level (T1) was 3,276 U/mL (Fig. 2A). This implies that the body does not easily succumb to stress and that the enzyme functions efficiently in transforming superoxide into hydrogen peroxide (Caruso *et al.*, 2020). The VNN control (T2) decreased to 2,625 U/mL, indicating that the infection weakened the barrier that protects against reactive oxygen species (Janicka *et al.*, 2024; Khoshvaghti *et al.*, 2024). The T3 treatment with the lowest dose of recombinant nanovaccine obtained a result of 3,213 U/mL, which maintained SOD levels near the baseline. This indicates low oxidative stress (Kumar *et al.*, 2023; Parida and Sahoo, 2023). However, the results

in the T4–T5 treatments increased from 3,948 to 3,997 U/mL. This indicates that ZnO stimulates protective enzyme pathways and functions as an immunostimulant, depending on the dose and situation (Alkhudhayri *et al*., 2020; Parida and Sahoo, 2023; Vaz *et al*., 2022). The general decline in SOD activity observed in the VNN-infected control treatment suggests a diminished effectiveness of the antioxidant system in unfavorable conditions. The increase in the ZnO-treated treatment supports the hypothesis that ZnO nanoparticles function as an immunostimulant agent, enhancing antioxidant defenses in a dose- and context-dependent manner (Hasanuzzaman *et al*., 2020; Kumar *et al*., 2023; Parida and Sahoo, 2023). ANOVA analysis showed a statistically significant difference in SOD enzyme activity results ($F = 7.24$, $p < 0.05$). This indicates that ZnO nanoparticles function as immunostimulants, bolstering antioxidant defenses in a manner that is dependent on dosage.

Catalase level in T1 was 105.5 U/L (Fig. 2B), showing that redox homeostasis was normal (Shanmugasundaram and Roza, 2023). The VNN challenge (T2) declined activity to 49 U/L, indicating oxidative stress that might increase membrane and macromolecular damage (Karaduman *et al*., 2025). Subsequent to ZnO, T3–T4 exhibit a minor deviation from the baseline that lacks statistical significance, which implies a mild level of oxidative stress (Shramko *et al*., 2021). Catalase activity levels were almost the same as the baseline and even a little higher than those of the control group that was infected. This may stem from the nanoparticles leading to oxidative stress, to which the enzymes have become acclimatized (Pongsavee, 2022). In the T4 and T5 groups, levels of catalase increased by 109.7 U/L in the T4 group and by 63.2 U/L in T5 group. A significant rise in T4 may indicate improved antioxidant capacity, while a slight increase in T5 may suggest a balanced oxidative challenge. Decreased catalase activity serves as a marker of oxidative stress that adversely influences components, membranes, proteins, and DNA (Husain *et al*., 2023). The treatment group exhibited heightened activity following the incorporation of ZnO nanoparticles, demonstrating that these nanoparticles can stimulate the antioxidant pathway and enhance cellular homeostasis (Aziz *et al*., 2024). ANOVA results showed a significant difference between treatments in the results of Catalase activity. Post-hoc analysis showed that the T3 treatment showed significantly higher CAT levels compared to the T2 group ($p < 0.05$). These results indicate that ZnO nanoparticles can help protect against free radicals. GPx activity in T1 was 34.34 µM (Fig. 2C) in T2 decreased by 22.00 µM. This occurs due to the redox imbalance and increased peroxide load caused by consistent VNN infection (Cecerska-Heryć *et al*., 2022). Decreased GPx activity implies that the production of free radicals outpaces the ability of the antioxidant defense system to manage them, which leads to heightened oxidative damage (Martinc *et al*., 2024). The T3 treatment showed a response almost identical to the control, indicating minimal oxidative damage. On the other hand, T4 and T5 increased to 76.02 and 61.71 µM, respectively, indicating that the effect of ZnO is dose-dependent. The elevation of GPx indicates that regulated stressors enhance defense mechanisms (Khoshvaghti *et al*., 2024). The decrease in GPx activity in the VNN-infected group indicates biomolecular damage due to the accumulation of peroxides and free radicals, especially in metabolically active cells (Zaki and Alfalahi, 2023). Conversely, the elevation in GPx activity observed in the ZnO-treated group signifies that the body is actively defending itself against oxidative stress (Mohsin *et al*., 2022 However, excessive increases in GPx activity may indicate chronic stress or abnormal stimulation of redox pathways that can negatively impact cell health. These results demonstrate an oxidative stress response and the dual function of ZnO nanoparticles as both a protective and potential exacerbator of oxidative damage, depending on the dose and duration of exposure (Janicka *et al*., 2024). ANOVA analysis showed differences between the two treatments ($F = 8.92$, $p < 0.05$). The post-hoc analysis revealed that the groups receiving treatment with ZnO nanoparticles (T4 and T5) exhibited a significantly higher GPx activity in comparison to T2 ($p < 0.01$).

Immune response results

Immune response examinations were conducted on the immune markers IFN-γ, TNF-α, and IgM (Fig. 3), in hybrid grouper fish given a nanovaccine and exposed to the VNN virus, showing that the *Chlorella vulgaris*-based nanovaccine with Chitosan-ZnO nanoparticles can enhance the immune response. The levels of IFN in the control treatment were recorded at 2.15% (Fig. 3A), whereas in the T3 treatment, they decreased to

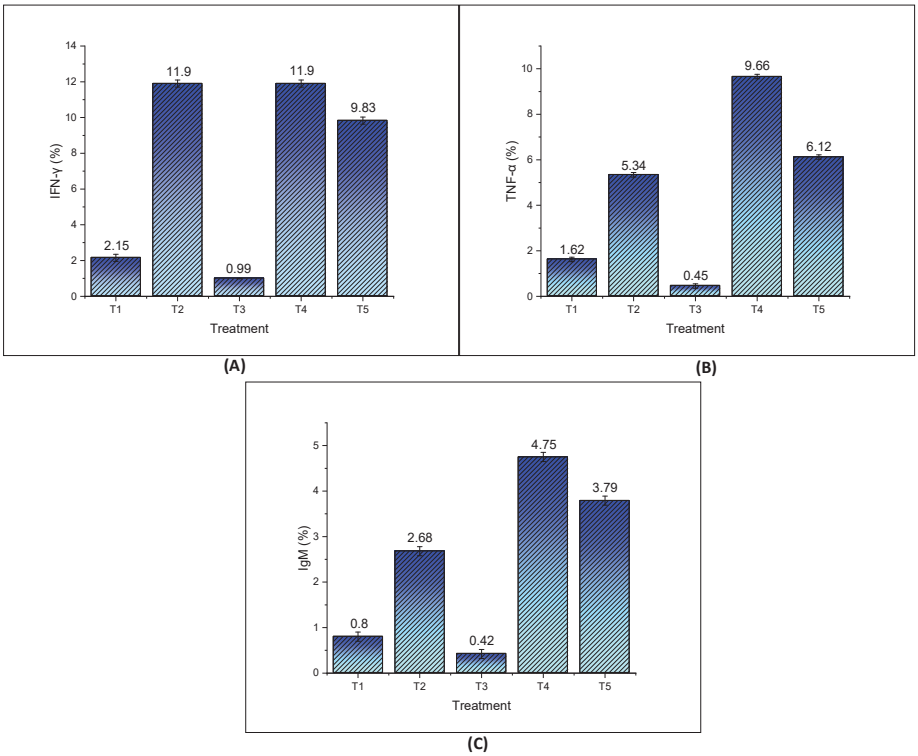

Fig. 3: Percentage of T cells expressing (A) IFN-λ, (B) TNF-α, and (C) IgM

0.99 %. This suggests a controlled but effective response to mitigate inflammation (Pereiro *et al*., 2020). On the other hand, T4 and T5 increased to 11.90% and 9.83%, respectively. This may indicate that administering the nanovaccine at an appropriate dose can help the body fight the virus better. This reinforces the concept that chitosan-ZnO nanoparticles are advantageous for the immune system and contribute to interferon-assisted defense (Fawzy *et al*., 2021). The control treatment TNF level was 1.62%, and at T3, it was 0.45% (Fig. 3B). This suggests that the nanovaccine may help reduce excessive inflammation and protect surrounding tissue from damage (Fouad *et al*., 2022; Monir *et al*., 2022). However, T4 and T5 both increased, with T4 rising to 5.34% and T5 rising to 6.12%. This represents a pro-inflammatory enhancement that can assist in eliminating viral infections if handled correctly (Yang *et al*., 2022). A more powerful TNF response can stimulate immune cells and bring in more inflammatory mediators to the site of infection, which helps get rid of the virus (Liu *et al*., 2021). These results show that TNF has two roles in the immune system. A high concentration of TNF may result in prolonged inflammation and harm to tissues, yet a measured elevation in TNF is necessary to defend against pathogens. In this instance, elevated doses of the nanovaccine appear to elicit an optimal inflammatory response, enhancing the immune system's capacity to combat viral infections without inducing superfluous overactivation (Hissen *et al*., 2023; Yousefi *et al*., 2025; Zheng *et al*., 2021).

IgM in T1 was 0.80% (Fig. 3C) and went up to 2.68% in the VNN control (T2), indicating infection-induced humoral activation. T3 decreases to 0.42%, which is what immunomodulation does to keep the body from overreacting. Conversely, T4–T5 increased to 4.75% and 3.79%, indicating a robust antibody response that likely facilitates the defense against viruses. So, lower doses seem to control immunity, while higher doses seem to increase humoral output. The increased IgM levels in this group indicate that higher doses of the nanovaccine promote a stronger immune response. Increased antibody production indicates that the immune system is capable of detecting and killing the virus. The findings of this study propose that a nanovaccine utilizing chitosan-ZnO nanoparticles may influence the comprehensive operation of the immune

system. Higher doses can help the immune system function better, while lower doses can enhance the antibody response. This may help the fish better fight the virus. These outcomes are in agreement with prior studies that demonstrate nanoparticle-based vaccines have the ability to initiate a regulated and heightened immune response, which is dependent on the administered dose. In this study, one-way ANOVA was applied to analyze the variation in immune markers. The results indicated significant differences for IFN-λ ($F = 9.68$, $p < 0.05$), TNF-α ($F = 6.43$, $p < 0.05$), and IgM ($F = 8.92$, $p < 0.05$). The post-hoc analysis indicated that the 66 µL (T4) and 112 µL (T5) doses significantly increased the levels of IFN-λ and TNF-α in comparison with the control and lower dose (T3) groups ($p < 0.01$). This indicates that the increased doses of the nanovaccine required the immune system to exert more effort. Although a formal correlation test was not carried out, the overall pattern across treatments was consistent: groups that showed stronger immune indicators (IFN-γ, TNF-α, and IgM) also tended to exhibit elevated antioxidant enzyme activity (SOD, CAT, and GPx) and less tissue damage. This general trend supports previous reports describing how immune activation may enhance antioxidant capacity by moderating oxidative stress and limiting cellular injury (Liu *et al.,* 2021; Fouzi *et al.,* 2020).

Blood cell analysis results

Fig. 4 illustrates the results of the hematological assessment of the fish In Fig. 4A, the unchallenged control (T1) exhibited an average erythrocyte count of 2.57 cells in a cubic millimeter (mm^3), while the VNN-challenged control (T2) had an average of 2.55 cells/mm^3.

This minor reduction supports the theory that viruses may interfere with erythropoiesis amid stress caused by infection (Chu *et al*., 2025). The echoes report that viral attacks can slow down the making of red blood cells and the body's ability to carry oxygen. On the other hand, all of the nanovaccine regimens had higher red cell counts: 2.73 (T3), 2.72 (T4), and 2.70 cells/mm^3 (T5), which were always higher than those in the control groups (Shukurov *et al*., 2023). The results indicate that the formulation derived from Chlorella improves the blood's ability to combat viruses, potentially by bolstering the immune system in a manner that supports erythropoiesis (Azhikina *et al*., 2023). These results show that the nanovaccine not only helps the immune system fight germs better, but it also helps the blood system work better when things get tough. The nanovaccine treatment demonstrated a rise in the quantity of red blood cells, suggesting that the nanovaccine has the potential to enhance fish immunity against the adverse impacts of viral infection (Yan *et al*., 2024). The number of leukocytes in treatments T1 and T2 was almost the same, at 1.26 and 1.27 cells/mm^3, respectively (Fig. 4B). This indicates that VNN exposure alone does not cause a significant increase in leukocytes without an accompanying stimulus. This corresponds with evidence suggesting that the inherent response could persist below the threshold in the absence of substantial immunostimulation (Parveen *et al*., 2021). Nanovaccine administration showed an increase in leukocyte counts to 1.50 (T3), 1.47 (T4), and 1.50 cells/mm^3 (T5), indicating an increase in the innate immune response by the nanovaccine (Fusianto *et al*., 2021). The increased activity of antioxidant enzymes in the vaccinated group could also aid in safeguarding immune cells from oxidative damage during the heightened response (Fusianto *et al*., 2021; Masalova *et al*., 2020). Hemoglobin levels at T1 and T2 were 6.50 g/dL and 6.52 g/dL, respectively (Fig. 4C). This indicates that VNN has no significant effect on Hb (Chaudhry *et al*., 2021). The 33 µL nanovaccine treatment (T3) resulted in the highest hemoglobin concentration, at 7.95 g/dL, indicating that the nanovaccine enhances the immune response to the pathogen and facilitates sufficient red blood cell production to meet the body's oxygen needs (Fusianto *et al*., 2021). The correlation between enzyme activity, immune response, and blood results indicates that the *Chlorella vulgaris*-based nanovaccine with Chitosan-ZnO nanoparticles enhances the immune response to VNN infection and improves fish blood health, as evidenced by increased leukocyte counts and hemoglobin levels. These findings illustrate the immunostimulatory role of boosting the body's reaction to infections and enhancing hematological outcomes. For instance, the cohort that was administered the nanovaccine exhibited notable elevations in both leukocyte and hemoglobin levels (Fusianto *et al*., 2021). ANOVA results for erythrocytes, leukocytes, and hemoglobin showed significant differences between groups. Post-hoc analysis revealed that the nanovaccine-treated groups (T3–T5) showed significant increases in these parameters compared to the control group ($p < 0.05$).

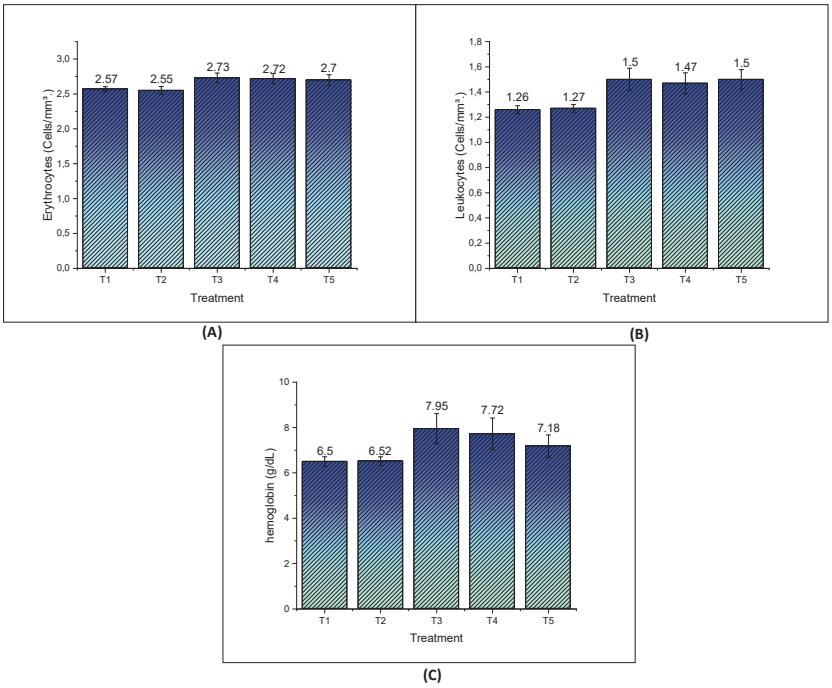

Fig. 4: Erythrocyte observation results : (A) Erythrocytes ; (B) Leukocytes; (C) Hemoglobin

Table 2: Average differential leukocyte results

Treatment	Monocyte (%)	Lymphocyte (%)	Basophil (%)	Neutrophils (%)	Eosinophil(%)
T1	13.89 ± 1.1	63.7 ± 2.9	4.43 ± 0.6	20.99 ± 3.8	3.08 ± 0.5
T2	13.77 ± 1.1	63.78 ± 2.8	5.2 ± 0.5	20.92 ± 3.7	3.09 ± 0.5
T3	12.28 ± 1.9	73.7 ± 3.8	8.67 ± 1.2	14.62 ± 3.4	1.66 ± 0.3
T4	15.36 ± 2.1	69.83 ± 3.1	6.42 ± 1.6	15.82 ± 3.2	1.47 ± 0.3
T5	16.17 ± 1.5	68.15 ± 2.1	8.06 ± 0.7	17.54 ± 3.3	1.5 ± 0.3

Differential Leukocyte

In the untreated control group (T1), lymphocytes constituted the dominant cell type (63.7 ± 2.9%), followed by neutrophils (20.99 ± 3.8%), monocytes (13.89 ± 1.1%), basophils (4.43 ± 0.6%), and eosinophils (3.08 ± 0.5%) (Table 2). A similar distribution of leukocytes was observed in the unvaccinated group challenged with VNN (T2), suggesting that exposure to VNN had a negligible effect on the leukocyte composition during the observation period.

The results indicate that enhancing the nanovaccine prior to the VNN challenge significantly altered leukocyte motility. This demonstrates the crucial nature of associating the regulation of the immune response with the functioning of enzymes in the body. In the T3 group (33 µL nanovaccine), the percentage of lymphocytes (73.7 ± 3.8%) and basophils (8.67 ± 1.2%) went up, while the percentage of neutrophils (14.62 ± 3.4%) and eosinophils (1.66 ± 0.3%) went down. These alterations demonstrate that the immune system is evolving to be more adaptive, a factor that is significant for the improvement of immunological memory. This is a crucial aspect of how the body detects and eliminates germs. Two important antioxidant enzymes that help keep the immune system in check are SOD and catalase. Prior studies have shown that these enzymes alleviate oxidative stress, which could otherwise cause tissue damage during immune responses. The elevated enzyme activity correlates with augmented cellular defense mechanisms in the context of oxidative stress, alongside intensified immune activation (Eric *et al*., 2022; Morris *et al*., 2022). The drop in neutrophils and eosinophils in the T3 group shows that the acute inflammatory response is becoming less intense.

This indicates that the nanovaccine enhances the immune system while also aiding in the regulation of inflammation, thereby reducing the likelihood of excessive tissue damage caused by an overactive immune response. The T4 group (66 µL nanovaccine) showed an increase in lymphocyte proportions (69.83 ± 3.1%) and monocytes (15.36 ± 2.1%), but the levels of neutrophils (15.82 ± 3.2%) and eosinophils (1.47 ± 0.3%) stayed the same. This suggests that administering higher amounts of the nanovaccine amplifies adaptive immune responses while ensuring that inflammation remains minimal, which in turn facilitates a quicker enhancement of immunological memory related to pathogens (Eric *et al*., 2022; Morris *et al*., 2022). The T5 group (112 µL nanovaccine) exhibited a modest increase in neutrophils (17.54 ± 3.3%), while lymphocyte (68.15 ± 2.1%) and monocyte (16.17 ± 1.5%) levels remained elevated. Low eosinophil levels (1.5 ± 0.3%) indicate that the immune system can control and regulate inflammation, even with increasing doses of the nanovaccine. The VNN virus causes nerve necrosis, disrupting the fish's nervous system. This results in unusual swimming capabilities, diminished appetite, and heightened mortality rates, particularly among juvenile fish. VNN also affects immune cells, particularly leukocytes, which play a crucial role in the body's defense system. Analysis of leukocyte composition in this study is an indicator of immune activation. Alterations in leukocyte composition, characterized by an increase in lymphocytes and a decrease in neutrophils, may suggest that the body is starting to acclimate to the virus. Lymphocytes, especially T cells, are crucial for specific immune responses to pathogens. Neutrophils, on the other hand, are mostly involved in the first stage of inflammation. By observing these changes, one can determine the effectiveness of the nanovaccine in altering the immune system responds to VNN (Orosco, 2024). ANOVA for differential leukocyte composition revealed significant disparities between groups (monocytes: $F = 4.56$, $p < 0.05$; lymphocytes: $F = 7.82$, $p < 0.05$; basophils: $F = 5.03$, $p < 0.05$; neutrophils: $F = 6.21$, $p < 0.05$; eosinophils: $F = 3.74$, $p < 0.05$). Post-hoc analysis revealed significant differences in the proportions of lymphocytes between T3–T5 and T1–T2 ($p < 0.01$).

Histopathological analysis results

An analysis of tissue damage in the kidney was conducted. Although VNN does not specifically target the kidney as its primary site of infection, renal damage may occur indirectly due to systemic infection or as an immune response to the virus. Kidney lesions were observed in hybrid grouper (*E. fuscoguttatus* × *E. lanceolatus*) (Fig. 5).

Three types of tissue damage were identified in the kidney of hybrid grouper (*E. fuscoguttatus* × *E. lanceolatus*): edema, necrosis, and hemorrhage. Exposure to VNN during the administration of a recombinant *Chlorella vulgaris* nanovaccine induced pathological changes, including cellular and tissue swelling due to fluid accumulation (edema), as well as necrosis and hemorrhage. Following the identification of edema-related lesions, a damage scoring analysis was performed utilizing a standardized formula (Aminin *et al*., 2024), and the findings are displayed in Table 3, 4, and 5.

According to the edema lesion scoring in Table 3, there was mild tissue damage in the healthy control group (T1) at 12.02% and in the T3 group (33 µL nanovaccine + VNN challenge) at 10.71%. The VNN-infected control group (T2), on the other hand, had the most severe edema, which reached 48.10%. The findings indicate that the nanovaccine considerably diminishes tissue damage in comparison to the control group infected with VNN (Huang *et al*., 2025). The reduction in edema in the T3 group indicates that the nanovaccine effectively stimulates a regulated immune response and mitigates excessive immune reactions that may lead to additional tissue damage (Katsoularis *et al*., 2022). Table 4 shows that the T1 group (13.69%) and the T3 group (12.50%) both had mild tissue damage, while the T4 group (66 µL nanovaccine + VNN challenge) and the T5 group (112 µL nanovaccine + VNN challenge) both had moderate damage, at 17.62% and 25.60%, respectively. The T2 group exhibited 43.69% severe necrosis, indicating that the nanovaccine may contribute to the reduction of necrosis (Beatty *et al*., 2021). The enhanced adaptive immune response, evidenced by an increased lymphocyte count, is associated with the body's improved capacity to detect and eliminate virus-infected cells. This mechanism is facilitated by the function of antioxidant enzymes (Issakov *et al*., 2022). In terms of hemorrhage scoring (Table 5), both T1 group (12.02%) and the T3 group (13.45%) had mild damage. Treatments T4 and T5 experienced moderate damage with scores of 18.69% and 22.26%, respectively.

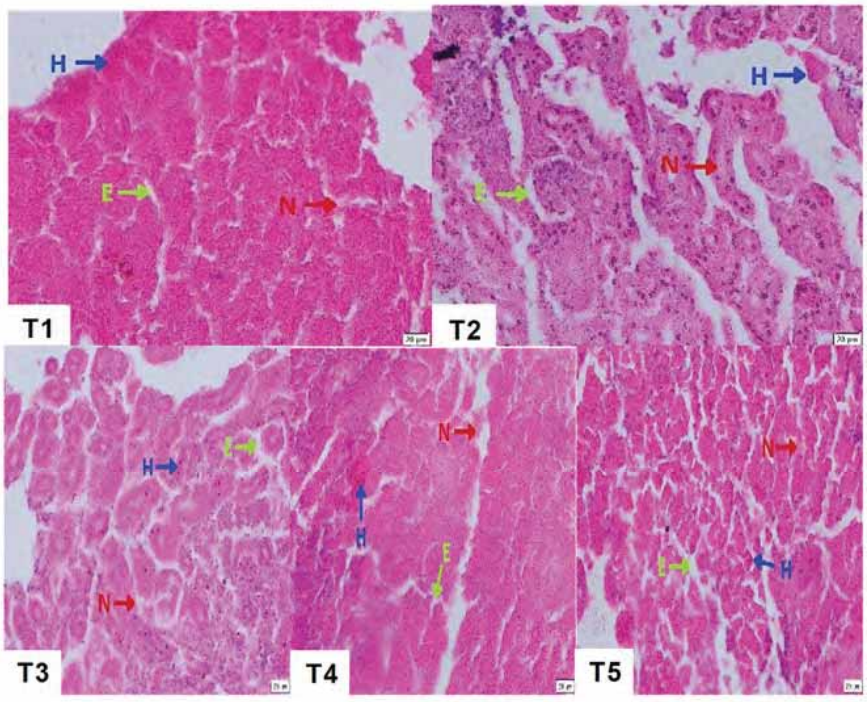

Fig. 5: Histological Observations of the Kidney in Hybrid Grouper : (E) Edema, (N) Necrosis, (H) Hemorrhage under 400x Microscopic Magnification

Table 3: Scoring of edema damage to the kidney

Treatment	Sampling			Average (%)	Score	Damage Level
	1	2	3			
T1	36	33	32	12.02	1	Mild damage
T2	125	142	137	48.10	3	Severe damage
T3	26	30	34	10.71	1	Mild damage
T4	58	49	51	18.81	2	Moderate damage
T5	72	65	68	24.40	2	Moderate damage

Note: the scoring criteria: Score 0: No damage at all; Score 1: Mild damage with about <30%; Score 2: Moderate damage with range of 30%-70%; Score 3: Severe damage with a percentage of >70% (Aminin *et al*., 2024).

Table 4: Scoring of necrosis damage to the kidney

Treatment	Sampling			Average (%)	Score	Damage Level
	1	2	3			
T1	35	38	42	13.69	1	Mild damage
T2	131	126	110	43.69	3	Severe damage
T3	33	35	37	12.50	1	Mild damage
T4	56	43	49	17.62	2	Moderate damage
T5	63	75	77	25.60	2	Moderate damage

Note: the scoring criteria: Score 0: No damage at all; Score 1: Mild damage with about <30%; Score 2: Moderate damage with range of 30%-70%; Score 3: Severe damage with a percentage of >70% (Aminin *et al*., 2024).

Group T2 experienced the most bleeding with a score of 45.83%. The increased necrosis and hemorrhage in the higher-dose treatments (T4 and T5) suggest that excessive concentrations of ZnO nanoparticles may provoke heightened immune activation and toxicity. The findings suggest that elevating the

Table 5: Scoring of Hemorrhage damage to the kidney

Treatmeant	Sampling			Average (%)	Score	Damage level
	1	2	3			
T1	33	29	39	12.02	1	Mild damage
T2	127	138	120	45.83	3	Severe damage
T3	44	38	31	13.45	1	Mild damage
T4	59	42	56	18.69	2	Moderate damage
T5	64	66	57	22.26	2	Moderate damage

Note: the scoring criteria: Score 0: No damage at all; Score 1: Mild damage with about <30%; Score 2: Moderate damage with range of 30%-70%; Score 3: Severe damage with a percentage of >70% (Aminin *et al*., 2024).

dosage of the nanovaccine may provoke an overly strong immune reaction, potentially leading to tissue damage (Katsoularis *et al*., 2022). This study showed that the antioxidant enzymes SOD and catalase are important for controlling the expression of oxidative stress during the immune response and also reducing chronic tissue damage (Darney *et al*., 2023). Elevated levels of lymphocytes and basophils observed in the T3 and T4 groups, alongside a decline in neutrophils and eosinophils, points to a more regulated and controlled inflammatory response, thereby reducing overall tissue damage (Issakov *et al*., 2022). The results of the study showed that nanovaccines enhance the body's adaptive immune response and reduce the risk of excessive tissue damage due to inflammation during infection (Huang *et al*., 2025; Issakov *et al*., 2022; Katsoularis *et al*., 2022). ANOVA shows results differences in tissue damage within the groups (edema: $F = 5.87$, $p < 0.05$; necrosis: $F = 4.92$, $p < 0.05$; hemorrhage: $F = 5.11$, $p < 0.05$).

The analysis results indicated a significant increase in various immune parameters among the vaccinated fish. In comparison to the control group, the vaccinated subjects displayed elevated levels of IFN-γ (up to 52%), TNF-α (48%), and IgM (70%). These patterns suggest that the ZnO–chitosan nanovaccine carrying the recombinant *Chlorella vulgaris* antigen was able to activate both humoral and cellular components of the immune system in hybrid grouper (*E. fuscoguttatus* × *E. lanceolatus*). Interestingly, even the 33 µL dose (T3) also resulted in a significant rise in IgM, suggesting that even a modest quantity of the formulation is adequate to initiate a protective humoral response that can combat infections like VNN. In parallel with the immunological changes, the vaccinated groups also showed an improvement in antioxidant status. Activities of SOD, CAT, and GPx increased by roughly 40%–60%, with the highest activity recorded in the 112 µL treatment (T5). The rise in these enzymes suggests that the nanovaccine does more than stimulate immunity—it also helps stabilize redox processes in the fish by limiting oxidative stress produced during viral replication. A more robust antioxidant reaction lessens the probability of tissue decline, which is consistent with the histological evidence presented in this study. Histopathological evaluation revealed that fish receiving the 33 µL (T3) and 66 µL (T4) doses displayed noticeably less structural damage and inflammation than the infected control group. Among these, T3 showed the mildest lesions, with approximately a 50% reduction in edema, necrosis, and hemorrhage. This indicates that the nanovaccine contributes not only to immune activation but also to the preservation of essential organs such as the kidney and intestine, which are often compromised during VNN infection. The statistical increase in SOD ($F = 7.24$, $p < 0.05$) and GPx ($F = 8.92$, $p < 0.05$) supports the idea that the formulation enhances the removal of reactive oxygen species (ROS), improving cell survival and reducing apoptotic damage. These results align with the increased percentage of functional immune cells noted in the treated groups, especially in T3. Despite these positive outcomes, the data also point to a limit in the dosing strategy. Higher doses—namely T4 and T5—were associated with a moderate rise in tissue injury, particularly necrosis and bleeding. The 112 µL dose (T5) produced a necrosis level of 25.60%, which was substantially higher than the 12.50% observed in T3. This suggests that while larger doses elicit stronger immune activation, the nanovaccine may also lead to overstimulation and subsequent tissue damage. Balancing immune enhancement and tissue safety therefore remains an important consideration in optimizing the nanovaccine dosage.

CONCLUSION

The present study provides evidence that ZnO–chitosan hybrid nanoparticles can act as an effective nanovaccine that is capable of enhancing immune performance in hybrid grouper (*E. fuscoguttatus* × *E. lanceolatus*) challenged with VNN under controlled laboratory conditions. Among all formulations tested, the recombinant *Chlorella vulgaris* extract at a dosage of 33 µL (T3) exhibited the greatest level of effectiveness in fostering immune protection and mitigating pathological impacts associated with VNN infection. Specifically, the 33 µL dose (T3) resulted in a 52% increase in IFN-γ levels, a 48% increase in TNF-α levels, and a 70% increase in IgM levels, indicating a strong immune response. The optimized formulation also strengthened the antioxidant system, as reflected by the 40%–60% rise in SOD and GPx activity observed in the T3 group. This biochemical advancement corresponded with the histopathological results, revealing considerably less tissue deterioration in the vaccinated fish. In the T3 treatment, edema, necrosis, and hemorrhage were reduced to 10.71%, 12.50%, and 13.45%, respectively—substantially lower than the levels recorded in the infected control group (T2), where the same lesions reached 48.10%, 43.69%, and 45.83%. In general, the T3 dosage led to an estimated 50% reduction in tissue damage, suggesting that the formulation can effectively moderate inflammation and restrict pathological alterations linked to VNN infection. Flow cytometry findings reinforced the protective effects observed in the biochemical assays. In the T3 group, a significantly greater percentage of immune cells remained viable, while the number of apoptotic cells was lower compared with the infected control. This pattern indicates that the ZnO–chitosan–C. vulgaris nanovaccine does more than simply stimulate the immune system—it also appears to help maintain the survival of functional immune cells that are necessary for ongoing antiviral protection. Additionally, the synergy of these immune and antioxidant reactions emphasizes the potency of the recombinant C. vulgaris antigen when formulated with ZnO–chitosan nanoparticles. The treatment led to substantial increases in IFN-γ (52%), TNF-α (48%), and IgM (70%). At the same time, antioxidant defenses were strengthened, as shown by the 40%–60% rise in SOD and GPx activity. Collectively, these enhancements demonstrate the manner in which the nanovaccine enhances both immune activation and cellular resilience. Among all tested doses, the T3 formulation produced the most balanced and effective response, offering strong immunostimulation alongside substantial reductions in tissue damage. The findings of this study provide strong evidence for the potential of nanovaccine technology as a promising solution for managing VNN in aquaculture. Future studies could take several different directions. One promising avenue is to investigate other types of nanoparticle carriers, including polymer- or lipid-based systems, to determine antigen protection or allow more targeted delivery to immune cells. An additional significant factor involves enhancing the dosing strategy via more extensive dose-response studies, along with evaluating if booster administrations yield enduring advantages or enhance cost-effectiveness. The formulation itself may also be refined by exploring alternative adjuvants or developing controlled-release systems that keep the antigen available for a longer period, which would be particularly advantageous in field applications. Ultimately, extensive trials conducted directly within aquaculture environments will be crucial for assessing the vaccine's effectiveness in real-world scenarios and for evaluating the feasibility of applying this method on a commercial level. Future research should aim to elucidate the underlying molecular mechanisms, optimize nanoparticle size and surface charge for targeted delivery, and validate long-term efficacy through field trials. Collectively, these findings provide a robust scientific foundation for the next generation of nanovaccine strategies in aquaculture health management. The advancement of this nanovaccine presents beneficial outcomes for the future of sustainable and disease-resistant aquaculture. By enhancing resistance to VNN, the vaccine could reduce the need for antibiotics and chemical treatments, supporting healthier and more environmentally friendly farming practices. Enhanced survival rates could additionally assist in minimizing financial losses due to VNN by facilitating more reliable production and enhanced economic returns for farmers. In this regard, nanovaccine technology is crucial in strengthening the resilience of aquaculture systems while contributing to environmental sustainability and economic security in the aquaculture industry. Despite the encouraging performance of the ZnO–chitosan–Chlorella-based nanovaccine, various elements need to be explored further before it can be extensively utilized in the commercial implementation. Issues related

to formulation stability, appropriate dosing, and regulatory approval remain crucial. Therefore, future research should aim to refine the vaccine's shelf life, ensure its effectiveness under various environmental conditions, and meet the safety and efficacy standards required for widespread use in modern aquaculture.

AUTHOR CONTRIBUTIONS

U. Yanuhar, as the first author and the corresponding author, as a granted receiver, conducted the research design and data analysis and wrote the main manuscript. Z. Waheed, performed the preparing data and laboratory analysis, H. Suryanto supervised all data analysis and revised manuscripts, V. Hasan, prepared the materials, data collection and analysis, D.R. Machfuda, has done the data collection, and analysis. All authors read and put comments to improve the manuscript.

ACKNOWLEDGEMENT

The authors deliver their gratitude to the Directorate of Research and Community Service (DRTPM) of Brawijaya University for funding the Indonesian Collaborative Research Program in 2025 with Contract Number [00463.17/UN10.A0501/B/KS/2025]. The Research Ethics Committee of the University of Brawijaya thoroughly reviewed the study protocol and granted ethical clearance (Approval No. 105-KEP-UB-2025).

CONFLICT OF INTEREST

The authors declare that there are no conflicts of interest regarding the publication of this manuscript. In addition, the ethical issues, including plagiarism, informed consent, misconduct, data fabrication and/or falsification, double publication and/or submission, and redundancy, were observed by the authors.

OPEN ACCESS

©2026 The author(s). This article is licensed under a Creative Commons Attribution 4.0 International License, which permits use, sharing, adaptation, distribution and reproduction in any medium or format, as long as you give appropriate credit to the original author(s) and the source, provide a link to the Creative Commons license, and indicate if changes were made. The images or other third-party material in this article are included in the article's Creative Commons license, unless indicated otherwise in a credit line to the material. If material is not included in the article's Creative Commons license and your intended use is not permitted by statutory regulation or exceeds the permitted use, you will need to obtain permission directly from the copyright holder. To view a copy of this license, visit: http://creativecommons.org/licenses/by/4.0/

PUBLISHER'S NOTE

GJESM Publisher remains neutral with regard to jurisdictional claims in published maps and institutional affiliations.

☑ Negative AI Statement

The author(s) declare that no AI tools or services were not used or not highly applied during the preparation of this work.

ABBREVIATIONS

±	margin of error
%	Percent
ANOVA	Analysis of variance
^0C	Degrees Cescius
CAT	Catalase
cells/mm³	Cells in a cubic millimeter
cDNA	Complementary Deoxyribonucleic Acid
ConA	concanavalin A
E. coli	Escherichia coli
EDTA	Ethylenediaminetetraacetic acid
F	Statistic F
FSC	forward scatter
GPx	Glutathione peroxidase
g/dL	Gram per desiliter
g	Gram
h	Hours
Hb	Hemoglobin
H&E	Hematoxylin–eosin
IFN-γ	Interferon gamma
IgM	Immunoglobulin M
mL	MiliLiter
mg/mL	milligram per milliliter
m²/s	Cubic meters per second
µm	Micrometer

µL	Microliter
Min.	minutes
mm³	Cubic millimeter
µM	micromol
nm	Nanometer
NaOH	Sodium hydroxide
NPs	Nanoparticles
PCR	Polymerase chain reaction
p	P-value
pH	potential of hydrogen
PBS	Phosphate-buffered saline
pET	Plasmid for E. coli T7 expression
RBC	Red blood cell
pTA2	Plasmid vector
rpm	Revolutions per minute
SOD	Superoxide dismutase
SDS-PAGE	Sodium dodecyl sulfate polyacrylamide gel electrophoresis
SD	standard of deviation
SSC	side scatter
TPP	Tripolyphosphate
TNF-α	tumor necrosis factor
U/mL	Unit per milliliter
U/L	Unit per Liter
VNN	Viral nervous necrosis
WBC	White blood cell
ZnO	Zinc oxide

REFERENCES

Alkhudhayri, A.; Al-Shaebi, E.M.; Qasem, M. A.; Murshed, M.; Mares, M.M.; Al-Quraishy, S.; Dkhil, M.A., (2020). Antioxidant and Anti-Apoptotic Effects of Selenium Nanoparticles Against Murine Eimeriosis. An. Acad. Bras. Cienc., 92(2): 1-9 **(9 Pages).**

Aminin; Arfiati, D.; Andayani, S., (2024). Histopathological Changes and Metallothionein Levels in Filopaludina javanica During Depuration. Adv. Sustainable Sci. Eng. Technol., 6(3): 02403019 **(8 Pages).**

Azhikina, O. Y.; Makhnin, I. A.; Berenev, Yu.; Karpenko, L. Y., (2023). Cytotoxicity of Some Preservatives for Culture Chlorella Vulgaris GKO Strain. BioWeb Conf., 66: 05008 **(14 Pages).**

Aziz, M.M.; El-Sheikh, M.M.; Mohamed, M.A.; Abdelrahman, S.S.; Mekkawy, M.H., (2024). The senomorphic impact of astaxanthin on irradiated rat spleen: STING, TLR4 and mTOR Contributed Pathway. Int. J. Immunopathol. Pharmacol., 38: 1-8 **(8 Pages).**

Bandín, I.; Souto, S., (2020). Betanodavirus and VER disease: a 30-year research review. Pathogens. 9(2): 106 **(46 Pages).**

Cecerska-Heryć, E.; Krauze, K.; Szczęśniak, A.; Goryniak-Mikołajczyk, A.; Serwin, N.; Śleboda-Taront, D.; Jacek, R.; Heryć, R.; Michalczyk, A.; Dołęgowska, B. (2022). Activity of Erythrocyte Antioxidant Enzymes in Healthy Women Depends on Age, BMI, Physical Activity, and Diet. J. Health Population Nutr., 41(1): 1-14 (**14 Pages**).

Chu, P.; Wang, Y.; Shen, J.; Wang, Y.; Chang, G.; He, L. (2025). ATG5 Negatively Regulates Grass Carp Reovirus-Induced Immune-Inflammatory Response by Degrading RIG-I and MDA5. J. Virology. 99(7): 1-18 (**18 Pages**).

Darney, B. G.; Boniface, E. R.; Lamsweerde, A. v.; Han, L.; Matteson, K. A.; Cameron, S.; Male, V.; Acuña, J.; Benhar, E.; Pearson, J. T.; Edelman, A., (2023). Impact of Coronavirus Disease 2019 (COVID-19) Vaccination on Menstrual Bleeding Quantity: An Observational Cohort Study. Bjog Int. J. Obstetrics Gynaecol., 130(7): 803–812 (**10 Pages**).

Eric, P.; Laurent, I.; François, V., (2022). Immunomodulatory and Anti-Inflammatory Properties of an Orally Bioavailable Sod-Gliadin Complex. UPI J. Pharm. Med. Health Sci., 5(4): 68–74 (**7 Pages**).

Faggion, S.; Bertotto, D.; Bonfatti, V.; Freguglia, M.; Bargelloni, L.; Carnier, P., (2022). Genomic Predictions of Phenotypes and Pseudo-Phenotypes for Viral Nervous Necrosis Resistance, Cortisol Concentration, Antibody Titer and Body Weight in European Sea Bass. Animals. 12(3): 367 (**20 Pages**).

Fawzy, M.; Khairy, G. M.; Hesham, A.; Rabaan, A. A.; El-Shamy, A. G.; Nagy, A. (2021). Nanoparticles as a Novel and Promising Antiviral Platform in Veterinary Medicine. Arch. Virology. 166(10): 2673–2682 (**10 Pages**).

Fouad, A. A.; Moussa, N. A.; Kareem, M. M. A.; Akl, U.; Abd-Elghany, M. I.; Abdel-Aziz, A. M., (2022). Thymol Exerts Antioxidant, Anti-Inflammatory, and Anti-Apoptotic Protective Effects Against Gentamicin Nephrotoxicity in Rats. Pharmacia. 69(1): 181–186 (**6 Pages**).

Fouzi, M. N. M., & Sakajamary, N. (2023). First Report of Viral Nervous Necrosis in Asian Sea Bass, Lates Calcarifer Cultured in Sri Lanka. J. Agro-Technol. Rural Sci., 3(1): 18–23 (**6 Pages**).

Fusianto, C.; Hick, P.M.; Murwantoko; Herlambang, A.; Whittington, R.J.; Becker, J.A., (2021). Outbreak investigation attributes Infectious spleen and kidney necrosis virus as a necessary cause of a mortality epidemic in farmed grouper (Epinephelus spp.) in Bali, Indonesia. Aquac. Rep., 20: 100723 **(10 Pages).**

Griot, R.; Allal, F.; Phocas, F.; Brard-Fudulea, S.; Morvezen, R.; Bestin, A.; Haffray, P.; François, Y.; Morin, T.; Poncet, C.; Vergnet, A.; Cariou, S.; Brunier, J.; Bruant, J.-S.; Peyrou, B.; Gagnaire, P.; Vandeputte, M., (2021). Genome-Wide Association Studies for Resistance to Viral Nervous Necrosis in Three Populations of European Sea Bass (Dicentrarchus Labrax) Using a Novel 57k SNP Array DlabChip. Aquaculture. 530: 735930 (**10 Pages**).

Hasanuzzaman, M.; Bhuyan, M.H.M.B.; Zulfiqar, F.; Raza, A.; Mohsin, S. M.; Mahmud, J. A.; Fujita, M.; Fotopoulos, V., (2020). Reactive Oxygen Species and Antioxidant Defense in Plants Under Abiotic Stress: Revisiting the Crucial Role of a Universal Defense Regulator. Antioxidants. 9(8): 681 (**52 Pages**).

Hissen, K.; He, W.; Wu, G.; Criscitiello, M.F., (2023). Immunonutrition: Facilitating mucosal immune response in teleost intestine with amino acids through oxidant-antioxidant balance. Front. Immunol., 14: 1241615 (**18 Pages**).

Huang, D.; Dai, J.; Yu, H.; Chen, W., (2025). Immune Dysregulation in Endometrial Tuberculosis: Elevated HLA-G and IL-1Ra as Key Modulators. Front. Cell. Infect. Microbiol., 15: 1548238 (**12 Pages**).

Hu, Y.; Alnabulsi, A.; Alnabulsi, A.; Scott, C.; Tafalla, C.; Secombes, C. J.; Wang, T., (2021). Characterisation and analysis of IFN-gamma producing cells in rainbow trout Oncorhynchus mykiss. Fish Shellfish Immunol., 117: 328-338 (**11 Pages**).

Issakov, G.; Tzur, Y.; Friedman, T.; Tzur, T., (2022). Abnormal Uterine Bleeding Among COVID-19 Vaccinated and Recovered Women: A National Survey. Reprod. Sci., 30(2): 713–721 (**9 Pages**).

Iwasaki, S.; Okada, N.; Kimura, Y.; Takikawa, Y.; Suzuki, T.; Kakutani, K.; Matsuda, Y.; Bai, Y.; Nonomura, T., (2022). Simultaneous Detection of Plant- And Fungus-Derived Genes Constitutively Expressed in Single Pseudoidium Neolycopersici-Inoculated Type I Trichome Cells

of Tomato Leaves via Multiplex RT-PCR and Nested PCR. Agriculture. 12(2): 254 (**16 Pages**).

Janicka, P.; Stygar, D.; Chełmecka, E.; Kuropka, P.; Miążek, A.; Studzińska, A.; Pogorzelska, A.; Pala, K.; Bażanów, B., (2024). Oxidative Stress Markers and Histopathological Changes in Selected Organs of Mice Infected With Murine Norovirus 1 (MNV-1). Int. J. Mol. Sci., 25(7): 3614 (**13 Pages**).

Karaduman, A.B.; Ilgın, S.; Aykaç, Ö.; Yeşilkaya, M.; Levent, S., Özdemir, A.Ö.; Girgin, G., (2025). Assessment of Inflammatory and Oxidative Stress Biomarkers for Predicting of Patients With Asymptomatic Carotid Artery Stenosis. J. Clin. Med., 14(3): 755 (**16 Pages**).

Katsoularis, I.; Fonseca-Rodríguez, O.; Farrington, P.; Jerndal, H.; Lundevaller, E. H.; Sund, M.; Lindmark, K.; Connolly, A.F., (2022). Risks of Deep Vein Thrombosis, Pulmonary Embolism, and Bleeding After Covid-19: Nationwide self-controlled cases series and Matched Cohort Study. BMJ: e069590 (**8 Pages**).

Khan, G.B.; Akhtar, N.; Khan, M.F.; Ullah, Z.; Tabassum, S.; Tedesse, Z., (2022). Toxicological impact of Zinc Nano Particles on tilapia fish (Oreochromis mossambicus). Saudi J. Biol. Sci., 29(2): 1221–1226 (**6 Pages**).

Khoshvaghti, A.; Baziyari, N.; Dehghani, M.; Vaziri, F., (2024). Oxidative Stress Markers in Canine Parvovirus Infection. J. Hell. Vet. Med. Soc., 75(3): 7743–7750 (**8 Pages**).

Kitiyodom, S.; Yata, T.; Thompson, K. D.; Costa, J.Z.; Elumalai, P.; Katagiri, T.; Temisak, S.; Namdee, K.; Rodkhum, C.; Pirarat, N., (2021). Immersion Vaccination by a Biomimetic-Mucoadhesive Nanovaccine Induces Humoral Immune Response of Red Tilapia (Oreochromis Sp.) Against Flavobacterium Columnare Challenge. Vaccines. 9(11): 1253 (**14 Pages**).

Kumar, R.; Lal, M. K.; Tiwari, R. K.; Chourasia, K. N.; Kumar, A.; Kumar, R.; Sharma, S.; Singh, B., (2023). Investigating the Interplay Between Tomato Leaf Curl New Delhi Virus Infection, Starch Metabolism and Antioxidant Defence System in Potato (Solanum Tuberosum L.). Antioxidants. 12(7): 1447 (**19 Pages**).

Lee, A.-J.; Liao, H.; Hong, J., (2022). Overexpression of Bcl2 and Bcl2L1 Can Suppress Betanodavirus-Induced Type III Cell Death and Autophagy Induction in GF-1 Cells. Symmetry. 14(2): 360 (**12 Pages)**.

Lebaka, V. R.; Ravi, P.; Reddy, M. C.; Thummala, C.; Mandal, T. K., (2025). Zinc Oxide Nanoparticles in Modern Science and Technology: Multifunctional Roles in Healthcare, Environmental Remediation, and Industry. Nanomaterials, 15(10): 754 **(47 Pages).**

Liu, W.-B.; Wang, M.; Dai, L.; Dong, S.; Yuan, X.; Yuan, S.; Tang, Y.; Liu, J.; Peng, L.; Xiao, Y., (2021). Enhanced Immune Response Improves Resistance to Cadmium Stress in Triploid Crucian Carp. Front. Physiol., 12: 666363 (**11 Pages**).

Martinc, B.; Grabnar, I.; Milosheska, D.; Lorber, B.; Vovk, T., (2024). A Cross-Sectional Study Comparing Oxidative Stress in Patients With Epilepsy Treated With Old and New Generation Antiseizure Medications. Medicina. 60(8): 1299 **(15 Pages)**.

Masalova, O.B.; Lesnova, E. I.; Klimova, P.P.; Momotyuk, E.; Vv, K.; Ivanova, A.M.; Payushina, O.V.; Butorina, N.H.; Zakirova, N.F.; Narovlyansky, A.N.; Pronin, A.B.; Ivanov, A.V; Kushch A.A., (2020). Genetically Modified Mouse Mesenchymal Stem Cells Expressing Non-Structural Proteins of Hepatitis C Virus Induce Effective Immune Response. Vaccines. 8(1): 62 (**2 Pages**).

Monir, M.S.; Yusoff, M.S.M.; Saad, M.Z.; Amal, M.N.A.; Mohamad, A.; Azzam-Sayuti, M.; Yasin, I.S.M., (2022). Effect of an Oral Bivalent Vaccine on Immune Response and Immune Gene Profiling in Vaccinated Red Tilapia (Oreochromis Spp.) During Infections With Streptococcus Iniae and Aeromonas Hydrophila. Biology. 11(9): 1268 (**21 Pages**).

Morris, G.; Gevezova, M.; Sarafian, V.; Maes, M., (2022). Redox Regulation of the Immune Response. Cell. Mol. Immunol., 19(10): 1079–1101 (**22 Pages**).

Padrós, F.; Caggiano, M.; Toffan, A.; Constenla, M.; Zarza, C.; Ciulli, S., (2022). Integrated management strategies for viral nervous necrosis (VNN) disease control in marine fish farming in the mediterranean. Pathogens. 11(3): 330 (**27 Pages**).

Parida, S.; Sahoo, P.K., (2023). Antioxidant Defence in Labeo Rohita to Biotic and Abiotic Stress: Insight From mRNA Expression, Molecular Characterization and Recombinant Protein-Based ELISA of Catalase, Glutathione Peroxidase, CuZn Superoxide Dismutase, and Glutathione S-Transferase. Antioxidants. 13(1): 18 (**30 Pages**).

Parveen, A.; Zahiruddin, S.; Agarwal, N.; Siddiqui, M. A.; Ansari, S.H.; Ahmad, S., (2021). Modulating Effects of the Synergistic Combination of Extracts of Herbal Drugs on Cyclophosphamide-Induced Immunosuppressed Mice. Saudi J. Biol. Sci., 28(11): 6178–6190 (**13 Pages**).

Pereiro, P.; Figueras, A.; Novoa, B., (2020). Compilation of Antiviral Treatments and Strategies to Fight Fish Viruses. Rev. Aquac., 13(3): 1223–1254 (**32 Pages**).

Pongsavee, M., (2022). Effects of ERCC5 Rs751402 Polymorphism on Oxidative Stress and the Impact of Curcumin on Catalase Activity in Breast Carcinogenesis. Asian Pac. J. Cancer Prev., 23(6): 2065–2070 (**5 Pages**).

Putra, B.S.; Hick, P.; Hall, E.; Whittington, R.J.; Razi, K.; Evarianti, E.; Nurbariah, N.; Becker, J.A., (2020). Prevalence of Infectious Spleen and Kidney Necrosis Virus (ISKNV), Nervous Necrosis Virus (NNV) and Ectoparasites in Juvenile Epinephelus Spp. Farmed in Aceh, Indonesia. Pathogens. 9(7): 578 (**17 Pages**).

Rasheed, A.; Javed Iqbal, K.; Safdar, A.; Nasir, A.; Jabeen, R.; sami, A.; Tara, N.; Ali, S.; Zeeshan, M.; Abbas, S.; Aun Muhammad, S.; Pervaiz, A.; Adil, M.; Han, J.; Ali, D.; Almarzoug, M.H.A., (2023). Toxicological effects of zinc oxide nanoparticles on hemato-biochemical profile of common carp (Cyprinus carpio). J. King Saud Univ. Sci., 35(7): 102835 (**7 Pages**).

Shanmugasundaram, D.; Roza, J.M., (2023). Effect of Broad-Spectrum Hemp Extract on Neurobehavioral Activity on the Immobilization Stress-Induced Model in Sprague Dawley Rats. Sci. World J., 2023: 1–7 (**7 Pages**).

Shamramko, B.C.; Garbuzova, E.V.; Polonskaya, Y.V.; Stakhneva, E.; Volkova, M.V.; Kurguzov, A.V.; Khashtanova, E.B.; Ragino, Yu. I., (2021). Associations of Antioxidant Enzymes With the Concentration of Fatty Acids in the Blood of Men With Coronary Artery Atherosclerosis. J. Pers. Med., 11(12): 1281 (**15 Pages**).

Shukurov, A.; Mirtalipov, D.; Kuzmetov, A.; Imanova, D.; Soatov, U.; Kakhramanov, B., (2023). Vitamin Feed Supplement for Fish Based on Chlorella vulgaris. E3S Web Conf., 389: 03072 (**7 Pages).**

Sukkarun, P.; Kitiyodom, S: Yostawornkul, J.; Chaiin, P.; Yata, T.; Rodkhum, C.; Boonrungsiman, S.; Pirarat, N., (2022). Chitosan-polymer based nanovaccine as promising immersion vaccine against Aeromonas veronii challenge in red tilapia (Oreochromis sp.). Fish Shellfish Immunol., 129: 30-35 (**5 Pages**).

Sulistiyono, A.; Kurniasih, K.; Untari, T., (2020). Detection of Nervous Necrosis Virus of Grouper Fish in Lombok Island, Indonesia Based on Serological and Molecular Studies. Egypt. J. Aquat. Biol. Fish., 24(1): 329–335 (**7 Pages**).

Vargová, M.; Révajová, V.; Lauková, A.; Hurníková, Z.; Dvorožňáková, E., (2023). Modulatory Effect of Beneficial Enterococci and Their Enterocins on the Blood Phagocytes in Murine Experimental Trichinellosis. Life. 13(9): 1930 (**13 Pages**).

Vaz, M.; Pires, D.; Pires, P.; Simões, M.; Pombo, A.; Santos, P.; Carmo, B.D.; Passos, R.; Costa, J.Z.; Thompson, K.D.; Baptista, T., (2022). Early Immune Modulation in European Seabass (Dicentrarchus Labrax) Juveniles in Response to Betanodavirus Infection. Fishes. 7(2): 63 (**15 Pages**).

Wang, Y.; Xu, L.; Ma, W.; Sun, H.; Huang, Z.; Cai, S.; Jian, J.; Huang, Y., (2021). Mass Mortalities Associated With Viral Nervous Necrosis in Murray Cod in China. J. Fish Dis., 45(2): 277–287 (**10 Pages**).

Yan, X.; Shan, S.; Li, X., Xu, Q.; Yan, X.; Ruan, R.; Cheng, P.; (2024). Carbon and energy metabolism for the mixotrophic culture of Chlorella vulgaris using sodium acetate as a carbon source. Front. Microbiol., 15 :1436264 (**10 Pages**).

Yang, Y.; Ren, Y.; Zhang, Y.; Wang, G.; He, Z.; Liu, Y.; Cao, W.; Wang, Y.; Chen, S.; Fu, Y.; Hou, J., (2022). A New Cell Line Derived From the Spleen of the Japanese Flounder (Paralichthys Olivaceus) and Its Application in Viral Study. Biology. 11(12): 1697 (**14 Pages**).

Yang, Z.; Wong, S.M.; Yue, G.H., (2021). Effects of Rrm1 on NNV Resistance Revealed by RNA-seq and Gene Editing. Mar. Biotechnol., 23(6): 854–869 (**15 Pages**).

Yanuhar, U.; Suryanto, H.; Mahasri, G., (2024). Cloning and Characterization of Protein Fraction Specific of Chlorella vulgaris Endemic East Java. Evergreen. 11(1):82-94 (**14 Pages**).

Yanuhar, U.; Arfiati, D.; Musa, M.; Junirahma, N.S.; Caesar, N.R., (2020). The Status of VNN (Viral Nervous Necrosis)-Infected Grouper Fish Tissue with Chlorella vulgaris Extract as Anti-Virus Candidate. Conference Series: J. Phys., 1665(1): 12036 (**7 Pages**).

Yousefi, M.; Adineh, H.; Mirghaed, A.T.; Hoseini, S.M., (2025). Co-Supplementation of Diet With Saccharomyces Cerevisiae and Thymol: Effects on Growth Performance, Antioxidant and Immunological Responses of Rainbow Trout, Oncorhynchus Mykiss. Animals. 15(3): 302 (**16 Pages**).

Yu, Y.; Liu, J.; Zhao, Z.; Lan, X.; Li, L.; Hu, J.; Ying-an, Z.; Zhang, X.; Chen, J., (2024). Fish Snx27 Promotes Viral Products by Modulating the Innate Immune Response and Exosomal Machinery. J. Virol., 98(12) (**21 Pages**).

Zaki, N.A.; Alfalahi, A.O., (2023). Methyl Jasmonate Improves Superoxide Dismutase Activity in Infected Sunflower Plants. E3S Web Conference. 434: 03007 (**6 pages**).

Zheng, W.; Chu, Q.; Xu, T., (2021). Long Noncoding RNA IRL Regulates NF-κB-mediated Immune Responses Through Suppression of miR-27c-3p-dependent IRAK4 Downregulation in Teleost Fish. J. Biol. Chem., 296: 100304 **(14 Pages).**

AUTHOR (S) BIOSKETCHES

Yanuhar, U., Dr., Professor, Biotechnology of Waters Environment, FPIK, Brawijaya University, Jl. Veteran, Malang, East Java, Indonesia.
- Email: *doktoruun@ub.ac.id*
- ORCID: 0000-0003-3360-8752
- Web of Science ResearcherID: ACM-6270-2022
- Scopus Author ID: 55022874000
- Homepage: https://fpik.ub.ac.id/dosen/prof-dr-uun-yanuhar-s-pi-m-si/

Waheed, Z., Dr, Associate Professor, Borneo Marine Research Institute, Universiti Malaysia Sabah, Jalan UMS, 88400 Kota Kinabalu, Sabah, Malaysia
- Email: *zarinah@ums.edu.my*
- ORCID: 0000-0002-0061-0090
- Web of Science ResearcherID: NA
- Scopus Author ID: 54407588900
- Homepage:https://expertise.ums.edu.my/profile/cb1e5aedc7ec7019354b58aa6bbb000e

Suryanto, H., Dr., Professor, Material Manufacture, Center Excellent for Cellulose Composite (CECCom), Department of Mechanical and Industrial Engineering, Faculty of Engineering, Universitas Negeri Malang, Jl. Semarang 5, Malang, 65145, Indonesia.
- Email: heru.suryanto.ft@um.ac.id
- ORCID: 0000-0001-7037-1868
- Web of Science ResearcherID: R-7921-2019
- Scopus Author ID: 55992540200
- Homepage: https://pakar.um.ac.id/Data/Peneliti/u=e617ceab-bc5f-43c7-b1bc-fb2f45cb705e

Hasan, V., Dr., Lecturer of Aquaculture at the Faculty of Fisheries and Marine Sciences, Airlangga University, Surabaya, East Java, Indonesia.
- Email: *veryl.hasan@fpk.unair.ac.id*
- ORCID: 0000-0001-5457-9335
- Web of Science ResearcherID: C-3086-2019
- Scopus Author ID: 57208215512
- Homepage: https://unair.ac.id/daftar-fakultas/daftar-dosen/veryl-hasan/

Machfuda, D.R., Master's Student, Master's Program in Aquaculture, Faculty of Fisheries Marine Science, Brawijaya University, Malang, East Java, Indonesia.
- Email: *defarizqi03@student.ub.ac.id*
- ORCID: 0009-0009-8964-8252
- Web of Science ResearcherID: NA
- Scopus Author ID: 58617700900
- Homepage: https://fpik.ub.ac.id/

HOW TO CITE THIS ARTICLE

Yanuhar, U.; Waheed, Z.; Suryanto, H.; Hasan, V.; Machfuda, D.R., (2026). Efficacy of zinc oxide chitosan hybrid nanoparticles as a nanovaccine to enhance immunity in hybrid grouper fish. Global J. Environ. Sci. Manage., 12(1): 39-56.

DOI: 10.22034/gjesm.2026.01.03

URL: https://www.gjesm.net/article_731845.html

Global J. Environ. Sci. Manage. 12(1): 57-74, Winter 2026, Serial #45

Global Journal of Environmental Science and Management
(GJESM)

Homepage: https://www.gjesm.net/

Podcasts

ORIGINAL RESEARCH PAPER

Waste management of used beverage cartons using material flow analysis

B. Ratnawati[1,*], L. Dellarosa[1], N. Jannah[1], N.D. Oktaf[1], E. Hanaseta[3], H.S. Huboyo[2], A.C. Agustina[1], M.D. Vaverková[4]

[1] *Environmental Engineering and Management Study Program, Vocational School, IPB University, Bogor, Indonesia*

[2] *Department of Environmental Engineering, Faculty of Engineering, Universitas Diponegoro, Semarang, Indonesia*

[3] *Environmental Engineering Study Program, Faculty of Engineering, Universitas Sahid, Jakarta, Indonesia*

[4] *Department of Sustainable Construction and Geodesy, Institute of Civil Engineering, Warsaw University of Life Sciences - SGGW, Nowoursynowska 159, 02 776 Warsaw, Poland*

ARTICLE INFO

Article History:
Received 04 July 2025
Revised 10 October 2025
Accepted 11 November 2025

Keywords:
Circular economy (CE)
Extended producer responsibility
Generating waste
Material flow analysis (MFA)
Used beverage cartons (UBCs)

ABSTRACT

BACKGROUND AND OBJECTIVES: Used beverage cartons, which can be recycled, often end up in landfills, potentially contaminating the environment. Consequently, there is a pressing need for an effective management strategy. The objectives of this study were to determine management strategies that can be implemented through the material flow analysis approach.

METHODS: Primary data were obtained through calculating the generation and composition of Urban Waste over 8 days. The secondary data used comes from the environmental agency. An analysis is performed comparing the present circumstances with two alternative management approaches. The initial alternative involves the processing of used beverage cartons of waste by collectors. The second alternative involves the processing of used beverage cartons waste processed by the collector and is subsequent return to the manufacturer. A descriptive analysis was conducted of both alternatives from various aspects. This study has limitations including the lack of life cycle assessment validation, data localized to Depok City limiting wider applicability, and exclusion of post-consumer and industrial recycling stages from the system boundaries.

FINDINGS: The second waste management strategy exhibited a more significant impact on economic, social, cultural, and environmental issues. From an economic aspect, the collector's income increased by 50 percent and the producer saved 15 percent on new raw material costs. In terms of social and cultural aspects, the shift towards circular waste management increases community participation and environmental awareness in waste management. This strategy has been demonstrated to reduce the generation of waste destined for landfills by 60 percent.

CONCLUSION: The integration of waste treatment by collectors and reverse logistics from beverage landfills used by rough extended producer responsibility proved most effective, reducing 30 percent carbon dioxide emissions per day, and waste to 4.32 tons per day. The approach also generated 50 percent higher income for collectors, 15 percent cost savings for producers, and created local green jobs in the recycling and logistics sectors. Future research should integrate life cycle assessment for comprehensive environmental assessment, expand geographic scope, and incorporate additional recycling stages and indirect flows such as energy use and emissions.

DOI: 10.22034/gjesm.2026.01.04

This is an open access article under the CC BY license (http://creativecommons.org/licenses/by/4.0/).

NUMBER OF REFERENCES
62

NUMBER OF FIGURES
5

NUMBER OF TABLES
1

*Corresponding Author:
Email: *beata@apps.ipb.ac.id*
Phone: +62 856 4016 4434
ORCID: 0000-0002-8949-4224

Note: Discussion period for this manuscript open until Mar 1, 2026 on GJESM website at the "Show Article".

INTRODUCTION

Urban waste management has been identified as a critical environmental concern in developing countries (Ameen and Mourshed 2017; Zohoori and Ghani 2017; Ratnawati *et al.,* 2022a). Urban waste management is essential for ensuring environmental cleanliness and equilibrium, particularly in urban areas characterized by elevated waste generation (aleluia *et al.*, 2016). The phenomenon under scrutiny has been demonstrated to exert an influence of environmental contamination and the augmentation of public health hazards (Qasim *et al*., 2020; Ratnawati *et al.,* 2023). Involvement of the community in the application of effective treatment strategies is crucial. Furthermore, waste can be utilized as a valuable resource (Ratnawati *et al.*, 2023), thereby supporting sustainability and reducing negative environmental impacts (Ratnawati *et al.,* 2019). An expanding collection of studies has pinpointed rapid urbanization, population expansion, rising incomes, and shifts in consumption habits as the main factors contributing to the escalating waste burden (Maalouf and Mavropoulos, 2022). According to the Ministry of Trade, the food and beverage industry is expected to demonstrate a 5.53 percent (%) growth in the second quarter of 2024. This anticipated expansion is likely to have a concomitant effect on packaging waste, which is known to increase with economic growth. The progression of packaging has seen a shift in its function, transitioning from its initial role as a simple container to a more complex entity that meets various additional functional requirements. This progression is exemplified by its role in ensuring product quality and providing consumers with essential information (Rundh, 2016). This necessity renders packaging design more intricate, encompassing various types, such as plastic and cardboard packaging, particularly for packaged beverages (Carrasco *et al.,* 2024). Cardboard is an extensively utilized packaging material, appreciated for its capacity to safeguard products against damage and degradation during transportation, managing, storage, and retail sales (Escursell *et al.*, 2021). The surge in production and demand for aseptic beverage cartons may result in a proportional rise in waste generated from used beverage cartons (UBCs). This, in turn, could impose a significant environmental burden (Rizaluddin *et al.*, 2020). Despite the pervasive use of beverage cartons their substantial environmental implications (Yao *et al.,* 2025), the recycling and reuse of these materials remains a challenge and is under-explored. The intricate nature of the constituent (Wong *et al*., 2024) is responsible for lengthy pulping periods, increased energy demands, and fiber loss (Kauppi *et al.,* 2025). Consequently, there is an imperative for the development of more environmentally friendly materials (Memon *et al.,* 2025). UBCs are a type of boxed beverage packaging that consists of polyethylene, aluminum foil, and paper, the purpose of which is to maintain the quality of the beverage (Pinaya *et al.*, 2025). The utilization of UBCs waste is hindered by the necessity of undergoing a separation process, with each layer being crucial to prevent scavengers from targeting UBCs waste (Feil *et al.*, 2016). Consequently, UBCs are frequently disposed of in landfills (Agamuthu and Visvanathan, 2014). In landfills, these cartons are subjected to a prolonged decomposition process, releasing methane and thereby exacerbating environmental pollution. In Austria, the process of UBCs the process of UBCs management entails its cleaning, rinsing, drying, and leveling prior to its separation into specialized cartons for direct shipment to the designated recycler (Agamuthu and Visvanathan, 2014). Bio-based recycling methods have been shown to be an environmentally friendly innovation (Kremser *et al.,* 2022). In addition to educating the public to conduct the recycling process, especially for beverage packaging cartons that can be of high value (Gritsch *et al.,* 2025), further research is needed to determine the most effective methods for recycling these materials. The implementation of recycling as a resource for manufacturing disposable animal diapers has been proven (Roungpaisan *et al.*, 2025). In the domain of waste management planning, the advancement of waste management technology can serve as a pivotal for achieving effective and efficient waste management (Kositcharoenkul *et al.*, 2025). Another technique for identifying the technology used involves the application of the material flow analysis (MFA) method. MFA can be used to analyze the integration of materials in a circular economy model by minimizing waste generation and maximizing resource use efficiency by restoring waste (Geissdoerfer *et al.,* 2017). The sample size and selection process for used beverage cartons (UBC) were determined based on the Indonesian National

Standard (SNI) 19-3964-2025 method, considering that the distribution of sample locations in each subdistrict was representative. The economic factor in choosing household sampling sites was conducted by taking into account both spatial and economic considerations. The low category was expenditure < 71.89 United States Dollars (USD), the middle category was 359.46 USD, and the high category was > 359.46 USD. Thus, the value of the contribution of waste banks can be measured from both environmental and economic perspective. Recent international studies have also documented the scale and challenges associated with UBCs waste, as well as the efficacy of MFA in addressing these issues. A research study carried out in Vienna investigated the properties of beverage carton waste, which was determined to exceed 6,000 tons annually. The study revealed that a significant proportion of this waste, exceeding 80%, was disposed of in mixed municipal solid waste, with a separate sorting rate of only 19.6%, as reported by Gritsch *et al.* (2025). In the Netherlands, the MFA on post-consumer beverage carton packaging shows that of about 60,000 tons of cardboard, only 47,124 tons are recycled products; limitations include low rates of separate sorting (19.8%) and mechanical recovery results from mixed waste (75%) due to contamination and loss during the sorting process (Schneider *et al.*, 2022). Previous studies regarding MFA and extended producer responsibility (EPR) related to UBCs in Southeast Asia has predominantly emphasized general qualitative discussions, lacking a detailed, quantitative, and comprehensive analysis of the entire UBCs value chain throughout the region. This paper addresses this gap by providing a foundational, data-driven MFA that maps the full extent of UBCs flows in Southeast Asia especially in Indonesia, thus offering a robust evidence base for the development of effective, region-specific EPR policies and waste management strategies. The implementation of the waste reduction roadmap by producers is regulated in Minister of Environment Regulation No. 75 of 2019. The main emphasis of this initiative is on reducing waste, reusing materials, and encouraging recycling among producers. UBCs waste management falls under the manufacturing sector category. These findings emphasize the importance of implementing MFA to map all stages—collection, sorting, processing, disposal—to identify barriers and formulate interventions such as improving collection systems, policy instruments such as Extended Producer Responsibility, and investments in recycling infrastructure. Depok, a city in the West Java province of Indonesia, was designated as the research site due to its considerable waste production of 1081.82 tons daily, a number anticipated to rise with the growth of the population. Unfortunately, there is currently no implementation of 3R (reduce, reuse, recycle) practices at the community source level, and the availability of 3R facilities, especially types of UBCs waste, is very low. As a result, the waste must be disposed of at the Cipayung landfill, where the majority are non-biodegradable waste. The landfill operates by open dumping, causing issues such as leachate pollution, gas emissions, fire hazards, potential landslides, and disease vectors. The Cipayung Landfill, which currently serves as the primary waste disposal site for the city, is expected to reach its maximum capacity by the year 2029, as declared by the Ministry of Environment and Forestry (MoEF). The necessity for effective waste management in the city of Depok has escalated to a critical level. The hypothesis of this study is that an integrated waste management scenario combining collector-based recycling with producer-level reverse logistics can significantly improve circularity and reduce environmental impacts. Using the MFA framework, the study identifies in current waste handling and tests strategic interventions. MFA systematically identifies inefficiencies and key waste/material flows in urban waste management. This analysis based on data supports targeted interventions through EPR policies, which require producers to take responsibility for decreasing and managing waste generation at the origin. EPR incentivizes product eco-design, recycling, and responsible waste handling. Together, MFA and EPR facilitate the transition from a linear "collect–dispose" system to a Circular Economy, characterized by material reuse, waste diversion, reduced environmental impact, and enhanced socio-economic benefits such as job creation and community engagement. This holistic method aids in sustainable urban development while nurturing a waste management system that is both regenerative and inclusive. The aims of this study are 1) to ascertain the volume of food and beverage packaging waste generated; 2) to assess management strategies that can be implemented through the MFA approach. This

study has been contacted in Depok City, Indonesia, in 2025.

MATERIALS AND METHODS

The empirical data collection process entailed the systematic sampling of household waste directly from residential units across the city. The administrative area of the city of Depok encompasses an expanse of 199.91 square kilometers (km^2), encompassing eleven sub-districts. The following municipalities were included in the study: Sawangan, Bojongsari, Pancoran Mas, Cipayung, Sukmajaya, Cilodong, Cimanggis, Tapos, Beji, Limo, and Cinere. The topography of the city is lowland, with elevations ranging from 77 to 150 meters (m) above sea level. The topography is further characterized by hilly terrain that extends longitudinally from the southern to the northern sector of the city. Depok City has a population of 2,163,635 inhabitants and a population density of 10,823 persons per square kilometers (km^2). The phases of the research process encompass the following: preparation for research, sampling of waste, analysis of data, and recommendations derived from the research findings. The preparatory phase entails the formulation of research problems and subsequent determination of the study objectives. Primary data consists of the daily generation and composition of household waste, the density and volume of waste collection containers, waste sorting and selling behavior, the number of operating fleets and disposal sites, as well as the market prices of UBC waste. The execution of waste sampling plays a crucial role in recognizing waste generation. The measurement of waste generation is defined by the Indonesian National Standard (SNI) 3964: 2005, which stipulates the method for collection and measurement of samples for the assessment of household waste generation and composition, as well as other types of waste. Waste sampling was conducted in August – September 2025 during the dry season but characterized by a high potential for precipitation, as Depok experiences elevated rainfall levels, effectively representing both dry and wet seasonal conditions. The criteria for selecting the locations of household waste generation are categorized by considering the economic status, which includes the upper class, middle class, and lower class, based on the classification of housing types (permanent, semi-permanent and non-permanent). The upper economic level is characterized by households residing in luxury condominiums or single-family homes, often accompanied by gardens and advanced alarm systems. Households situated in medium-sized apartments or single-family dwellings that do not have a garden are classified under the medium economic level. The economic status of the lower class is characterized by households residing in slums or apartments with single or rent rooms, which account for less than 5% of gross domestic product (GDP) per capita. The designated area for garbage collection consists of 90 houses, with 30 households categorized under the upper economic level, 30 households categorized under the middle economic level, and 30 households categorized under the lower economic level. A total of 90 households were selected as representative samples using the snowball sampling method, which involved obtaining recommendations from neighbors and local community leaders (RT) to identify households across low-, middle-, and high-income levels. This approach was employed because conducting individual income surveys for each household was impractical. The map was created with a scale greater than 1:2,500, and a grid measuring 1 centimeter (cm) by 1 cm was superimposed, such that each centimeter of the grid corresponds to 25 m of physical terrain. The sampling location was then selected at random from the grid (Fig. 1). The partitioning of the area into grids and the random choice of cells improve the collection of a more representative sample of household waste data, as it permits the gathering of samples from a larger number of households. This, in turn, provides a more accurate representation of the actual waste generation and composition conditions in the city of Depok as a whole. A detailed sampling methodology was implemented to evaluate the composition of waste generation, which included both weight and density, throughout an eight-day duration. The waste obtained from a single household is sorted and weighed based on its characteristics. The results of the waste weight measurement were recorded as data on the weight of the waste. The volume of waste is measured by utilizing a container with a known volume as 30 cm x 30 cm x 60 cm) and a specific shape. The waste is placed into the container and manually compacted until it reaches a state of optimal density, leading to total saturation of the receptacle. The weight of waste was measured over a period of eight

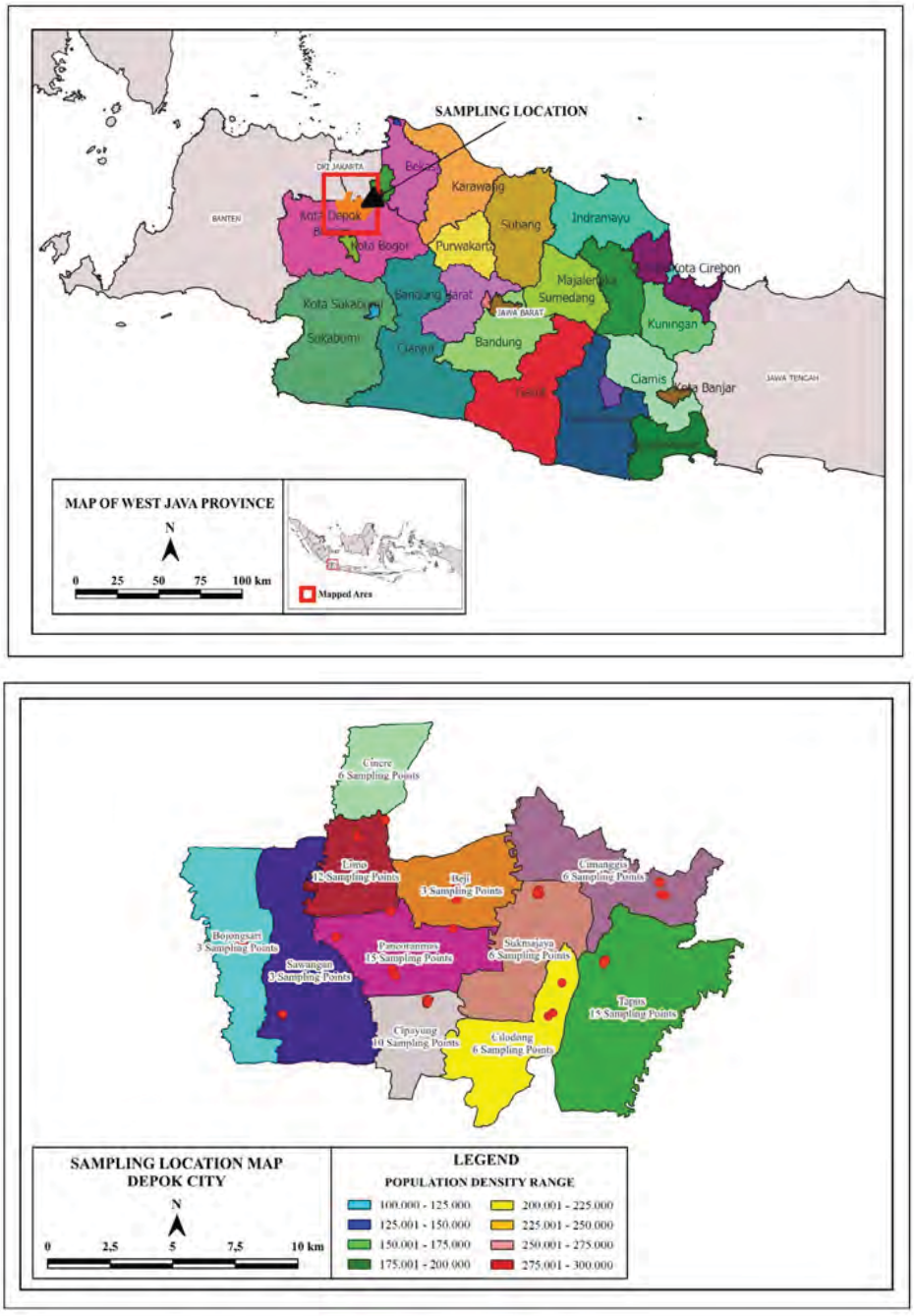

Fig. 1: Geographical location of the study area in Depok, Indonesia

days, and the mean weight per day was calculated. To ascertain the weight of waste produced per capita, one must divide the overall weight of waste generated by the number of people in that region. This principle of proportionality extends to volume measurements as well. These measurements can be obtained for each characteristic. Secondary data drawn from official statistics, The Intergovernmental Panel on Climate Change (IPCC, 2024) for emission factors, Association of Plastic Recycling Practitioners

(ADUPI) market databases for pulp prices, and MoEF - EPR Roadmap 2023–2030 for logistics parameters. Secondary data were employed to supplement and define the MFA model, with a focus on environmental and economic assessments. These were obtained from official statistics, academic references, and national policy documents, then contextualized to local conditions. All Secondary datasets were cross-validated with primary data to maintain mass-balance closure within more are less 5% and ensure contextual reliability.

Sources and Method for Emission Factors

The emission factor for UBCs waste was established by employing the avoided-emission method, signifying the contrast between emissions associated with landfill and those linked to recycling. The values were adapted from IPCC studies under tropical conditions using Eq. 1 (IPCC, 2024):

$$E = (W_{UBC} \times EF_{landfill}) - (W_{UBC} \times EF_{recycled}) \quad (1)$$

Where :

E: Emission factor

W_{UBCs}: UBCs mass (tons/day)

$EF_{landfill}$: landfill emission factor (kg CO_2 equivalent /day)

$EF_{recycled}$: recycled emission factor (kg CO_2 equivalent /day)

Economic Assumptions and Inflation / Purchasing-Power Adjustment

Economic analysis covered collector income and producer savings, calculated using real market values corrected for inflation and purchasing power using Eqs. 2 and 3 (Buongiorno *et al.*, 2017; Simamora *et al.*, 2023; Joyo *et al.*, 2025):

$$\text{Collector Income} = W_{UBCs} \times P_{UBC} \quad (2)$$

$$\text{Producer Saving} = (C_{product} - C_{recycled}) \times W_{UBCrecycled} \quad (3)$$

Where:

W_{UBCs}: UBCs mass (tons/day)

P_{UBCs}: Price UBCs

$C_{product}$/ $C_{recycled}$: Consumption product / recycled

$W_{UBCrecycled}$: UBCs mass recycled (tons/day)

MFA analysis

Primary data were processed using MFA facilitated by the STAN software, with results expressed in units of kilograms per day (kg/day). The post-consumer and industrial recycling stages were not modeled in the MFA to focus the study on upstream waste generation and collection processes, where the most critical inefficiencies occur. Energy inputs and emissions associated with these stages, classified as indirect flows, were not explicitly considered within the MFA scope. The MFA was performed using specialized software, STAN, which facilitated the mass flow calculations and data visualization necessary for this analysis.

RESULTS AND DISCUSSION

The city of Depok has established a network of 15 TPS, strategically positioned to ensure comprehensive coverage across the municipality. These points are distributed as follows: two points in the Beji area, two points in Cimanggis, six points in Pancoranmas, four points in Sukmajaya, and one point in Tapos. Waste from the location is transported by 211 fleets to the final waste processing site. The waste generated from a single household each day is 181.04 kilograms (kg), with an average generation of 0.5 kilograms per individual per day (kg/person/day). The total waste generation in the city of Depok is estimated to be 1081.82 tonnes per day (tons/day), including various types of waste such as food waste, garden waste, paper, beverage packaging cartons, plastic (sheets), plastic (hard), metal, glass, fabric, wood, hazardous and toxic materials (B3) waste, and waste that is no longer formed. (Fig. 2).

The waste produced is transported directly to the temporary waste shelter to the waste processing of the city of Depok in Cipayung. The waste composition in Depok City (Fig. 2) indicates that approximately 53% consists of food waste, garden waste, and wood. In contrast, inorganic waste accounts for 45%, which includes a variety of materials such as metal, glass, textiles, plastics, and paper, along with 2% classified as hazardous and toxic material waste (B3). UBCs waste percentage of 1% is 10,818.18 kilogram per day (kg/day) in the form of cardboard packaging waste from beverages (juice and milk). Currently, waste sorting from households is performed by scavengers, who subsequently sell the materials to collectors (Fig. 3). Waste management in Depok City has not yet

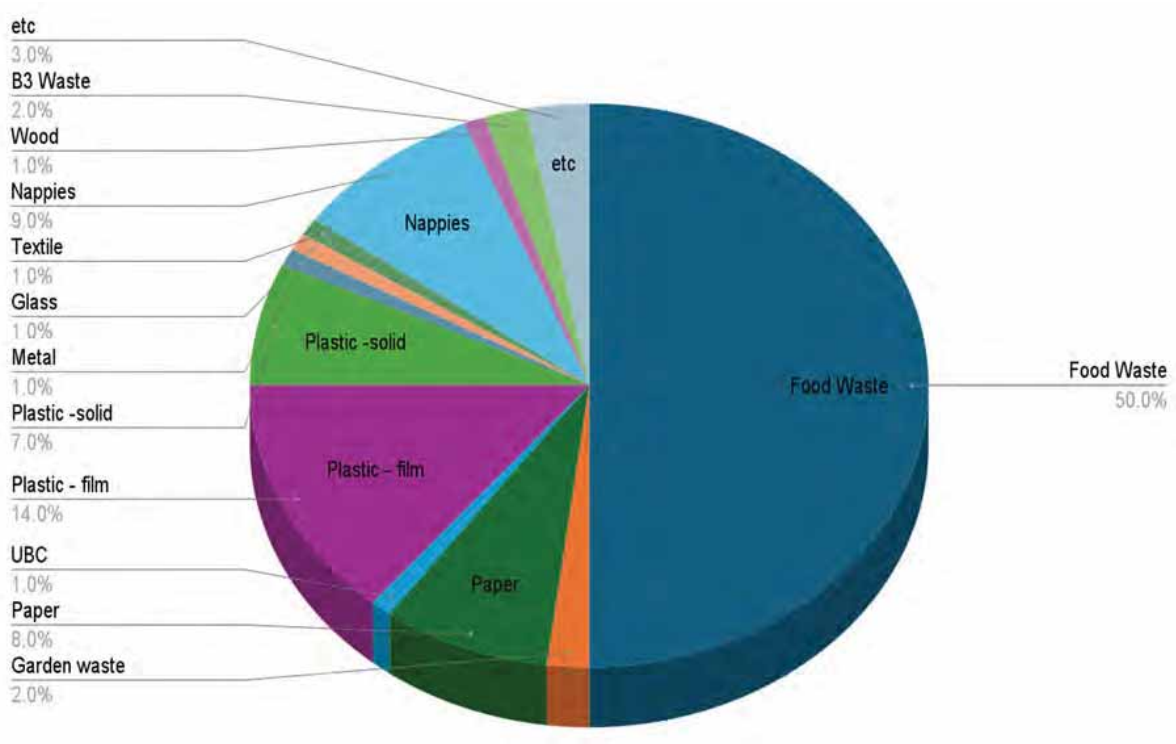

Fig. 2: Composition of waste generation in Depok City, Indonesia

implemented the concept of waste sorting, so that recyclable, organic, and residual waste are still mixed. The application of concepts such as the Circular Economy and Waste to Energy plays a key role in the waste sorting and transportation process, enabling recyclable materials to be collected and processed efficiently (Anwar *et al.*, 2025). At a more advanced level, a transportation system has been created in the shape of a map that includes collection points leading to waste processing facilities (Biakhmetov *et al.*, 2025). Reducing waste carried out by waste pickers supports the reduction of waste from sources and forms of the circular economy. Nonetheless, the remaining residue is acknowledged as waste, making it unviable for processing or resale. Consequently, it is typically disposed of in landfills. The residual waste has been measured at 324.55 kg/day. The residue being discussed can be traced back to the insufficient rate of waste recycling, which is primarily caused by the diverse composition of waste and the limited public awareness concerning waste sorting (Gritsch *et al.*, 2024). Furthermore, 216.36 tons of hazardous and toxic materials (B3) waste, including used lamps, batteries, and masks, are disposed of in landfills daily. Each MFA result addresses uncertainty by incorporating an approximately 15% variation range in waste volume and composition to capture data variability. Sensitivity analysis is executed to determine the robustness of findings against these variations, guaranteeing reliability even in the face of the inherent data uncertainties frequently encountered in MFA studies. This approach follows established uncertainty handling practices in MFA and enhances confidence in the interpretation of model outputs.

The emission values produced at the landfill without any treatment on UBC waste of 108.18 kg CO_2 equivalent/day (Fig. 3). Ministry of Environment Regulation No. 75 of 2019, which regulates EPR, focuses, among other things, on reducing packaging and/or containers made of paper/cardboard/UBCs by stipulating a minimum volume of 250 milliliters (mL). The approach to recycling the classification of paper, cardboard, and UBCs packaging is to employ recyclable materials, integrate 50% recycled materials, recycle back into the same packaging, or transform

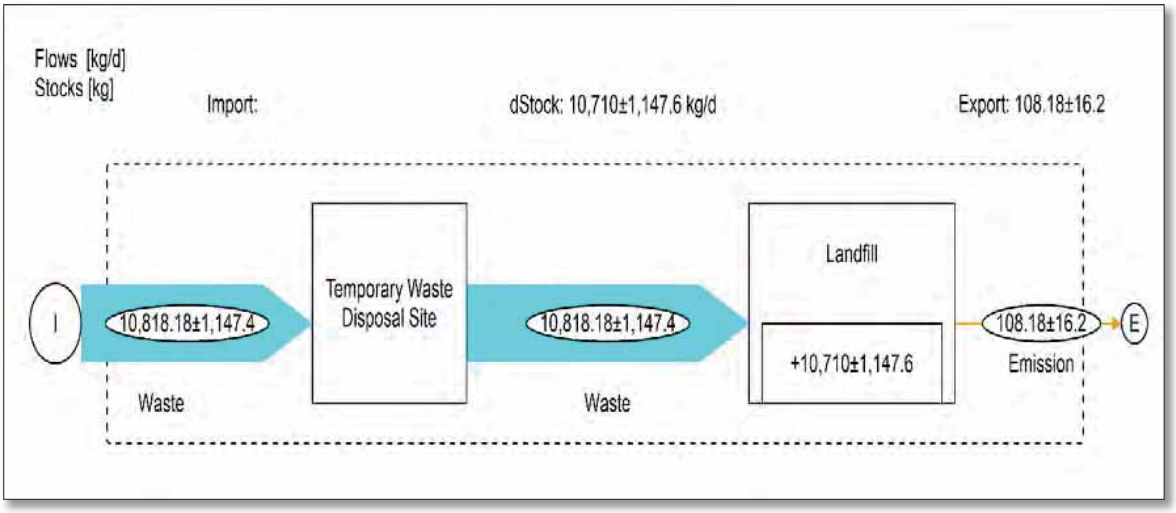

Fig. 3: Material flow analysis of existing conditions

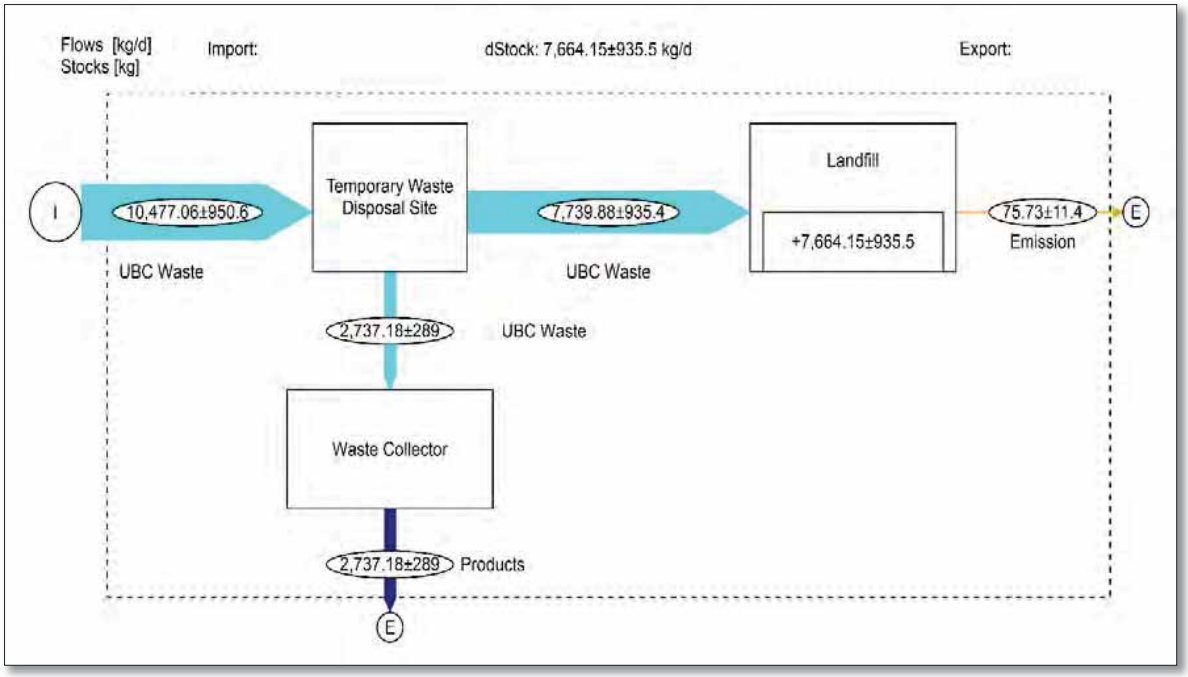

Fig. 4: Material flow analysis alternative 1

into raw materials or other finished products. Referring to Lacovidou's (2025) research, the existing polymer industrial waste management process in Indonesia involves shareholders (manufacturers, traders, consumer goods producers, retailers, and consumers), the middle segment (waste collectors, TPS 3R/ small scrap dealers, brokers/ trades, recyclers), and disposal (Landfill). As an effort to improve, an alternative simulation 1 (Fig 4) was carried out which sharpened the sorting and processing process. In this alternative, collectors receive as much as 30% of UBCs waste, a figure that reflects the recycling percentages of UBCs waste from several nations. UBCs waste recycling in several countries varies. The

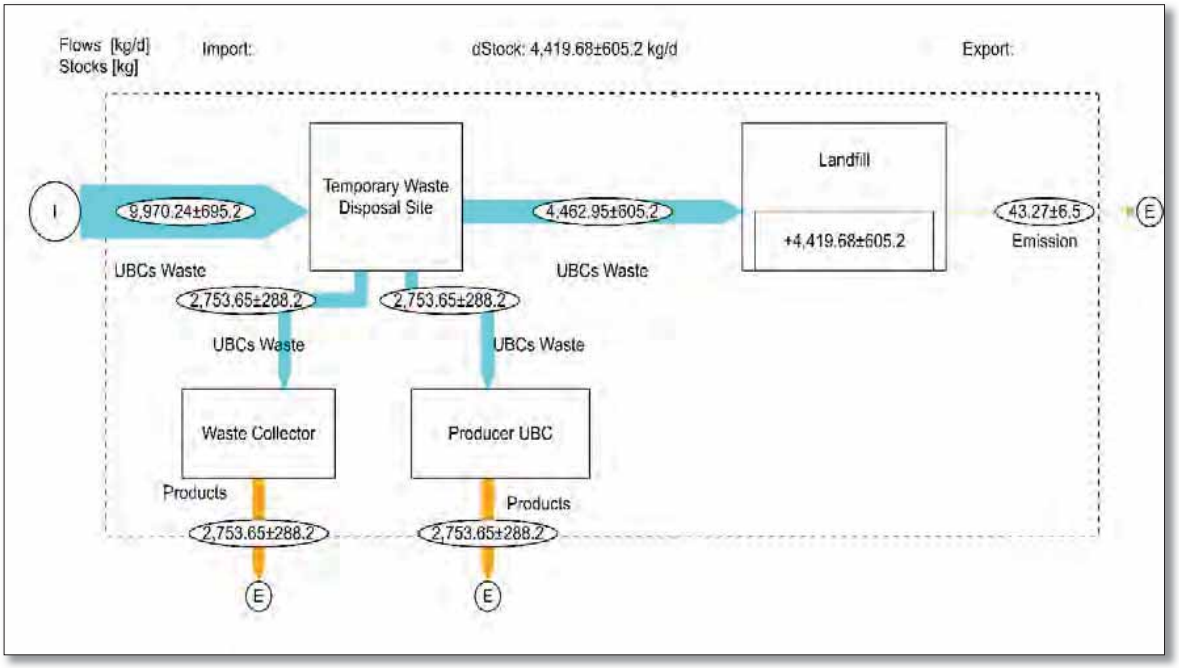

Fig. 5: Material flow analysis alternative 2

recycling rate in Thailand, reaches 26.3%, in Canada between 35–67%, in the European Union about 51% of UBCs waste is recycled. UBCs waste recycling is around 38–48%. 30% of the waste collectors can reduce waste by 2,737.18 kg/day that is piled up in landfills so that the waste accumulated in landfills is 7739.88 kg/day. This demonstrates a considerable reduction in waste, implying that this alternative can signify a true enhancement in the reduction of waste that is thrown away. The increase in the number of high-value materials flowing to waste collectors to 2,737.18 kg/day also indicates the potential for a better circular economy with the reuse of waste as industrial raw materials. Overall, Alternative 1 is the more environmentally friendly and sustainable waste management scenario. It illustrates superior efficiency in sorting and treatment processes, thus leading to a reduction in landfill debris and an increase in the worth of waste materials.

As illustrated in Alternative 2 (Fig. 5), the proposed initiative would contribute to the enhancement of the circular economy by introducing a flow of recycled paper products amounting to 4,462.95 kg/day. A total of 30% of the waste processed is in the form of beverage packaging waste, which is returned to its respective producers. An additional 30% of the waste is processed by waste collectors. The return of beverage packaging to its manufacturers has shown the ability to lower packaging expenses and decrease the volume of waste handled by waste management (Simsek and Icier, 2024). This system is frequently referred to as reverse logistics. Evidence suggests that the reverse logistics system contributes positively to the economy, chiefly by supporting the circular economy. Based on the roadmap and the national action plan, the circular economy can be implemented through waste recycling. Another significant focus of recycling efforts in Indonesia is packaging materials. Therefore, currently in Indonesia, the implementation of EPR is being encouraged with various policies. The environmental impact of the system can be thoroughly assessed through the utilization of life cycle analysis methodology (Battarra *et al.*, 2025). A comparative analysis revealed that both alternatives exhibited a substantial enhancement in waste management practices when contrasted with prevailing circumstances, each alternative exhibiting a distinct emphasis. Alternative 1 prioritized the reduction of landfill final waste and the optimization of the utilization of valuable materials. Conversely, Alternative 2 prioritized the valorization of materials and the expansion of the production of recycled

goods with commercial value. The implementation of alternatives, or a combination of the two, will support more environmentally friendly and sustainable management of inorganic waste.

The emissions generated from alternative 2 are 43.27 kg CO_2 equivalent, which is a decrease of 64.91 kg CO_2 equivalent compared to without processing (Fig. 5). The findings from the MFA analysis can likewise be employed to develop a proposal for relevant policies (Turner *et al.*, 2016). The implementation of regulations that promote waste sorting at the source, i.e., the household, is imperative. Furthermore, the reinforcement of the TPS into waste treatment sites reduce, reuse, and recycles (3R) TPS, which functions as a sorting and processing center, is essential. Furthermore, establishing recycling facilities within local communities can significantly contribute to the reduction and management of urban waste. Regulations pertaining to the implementation of waste sorting from the source, the reinforcement of the 3R TPS, and local-level recycling have been stipulated in law (UU) Number 18 of 2008 concerning waste management. However, its implementation has not been able to function optimally. This situation is predominantly motivated by two crucial factors. Firstly, there is a conspicuous absence of public awareness regarding the issue. Secondly, the government has exhibited a clear unwillingness to enact policies that would incentivize as well as disincentivize behaviors. The execution of incentive policies, including financial support for processing technologies (for instance, shredding and composting) and partnerships with recycling companies, can significantly accelerate the integration of technology in MFA analysis. In European Union countries, regulatory frameworks pertaining to the reuse of packaging are in place, along with the establishment of targets aimed at achieving net zero emissions and ensuring environmental protection (Orias and Lundquist, 2025). Most of the used cardboard is recycled to make new products (Tosarkani *et al.*, 2024). Recycling can have an impact on improving the circular economy (Liu *et al.*, 2025) and can reduce emissions, especially carbon (Moreira *et al.*, 2023). To sustainably decrease waste, the recycling concept must be reinforced by the practices of waste reuse and reduction (Lipp *et al.*, 2025). Moreover, fostering greater community participation, particularly from consumers, is vital for the program's success (Farida *et al.*, 2024). Local governments must prioritize the enhancement of the role of TPS 3R by allocating financial resources and facilitating management and community training to promote a comprehensive understanding of the significance of sustainable waste sorting and management. It is imperative that regulations be established to govern the collaboration between TPS 3R and the recycling industry. Such regulations are necessary to ensure the establishment of a market for recycled products, thereby enhancing overall sustainability (Thiyagarajan *et al.*, 2025). It is imperative that policies be crafted in a manner that fosters the establishment of an integrated monitoring and reporting system. This system is required to employ MFA quantitative data as its core component, thus guaranteeing effective decision-making and assessment of regional waste management performance in a sustainable manner. The movement of materials in waste treatment facilities is susceptible to disruption, which can have ramifications for all variables (Reitsema *et al.*, 2025). These variables include economic, social, environmental, and cultural variables (Table 1.).

Essential components for the successful implementation of a circular economy involve policy and regulation, community participation and collaboration, advancements in infrastructure and information and communication technology (ICT) development, environmental considerations, economic viability, social values, and extended producer responsibility (Fatimah *et al.*, 2024). ST of community and collaboration referred to are related to the level of community participation, community satisfaction with waste management, education and programs to increase literacy related to waste, social cohesion, the scale of waste management, the availability of employment opportunities, and health insurance (Fatimah *et al.*, 2024; Anwar *et al.*, 2024; Ismail *et al.*, 2025). The participation of the community in the sorting of waste at its source cultivates a new culture of teamwork, consequently fortifying the sense of solidarity between citizens. The integration of continuous education at the household, school, and community levels transforms the community from a passive recipient of management directives into an active participant in the management system. Acknowledging the role of collectors and scavengers as vital parts of the circular economy framework contributes to alleviating social stigmatization and enhancing inclusivity. The involvement of

Table 1: Analysis by economic, social, environmental, and cultural sectors

Sector	Existing	Alternative 1	Alternative 2
Economics	UBCs waste is considered worthless. The income of the collector is only ± United States Dollar 2.10 per day (2.10 USD /day) from plastic and metal.	- Collectors' income increased by 30% to 2.71 – 3.01 USD /day. - UBCs is worth USD 0.06 –0.09 /kg. - Manufacturers have not yet participated in funding recycling.	- Collector's income increased by 50% (3.30 – 3.59 USD/day). - Manufacturers save 15% on new raw material costs. - Creating new jobs to process UBCs waste. - The economic value of UBCs increased from 0 to 0.09 USD /kg.
Social	- There is no community participation in sorting waste. - The role of scavengers has not been structured.	- Participation increased by 30%. - The existence of social interaction between the community and the collector has increased to 2 times. - Forming a micro-circular economy between communities.	- Community participation increased by 70%. - Social recognition of collectors increased from 15% to 60%. - 60% of waste shelters are actively collaborating with multi-parties.
Environmental	- Waste to landfill ±10.81 tons/day. - Carbon dioxide (CO_2) emissions (1 kg of waste produces an equivalent of 0.01 Carbon dioxide equivalent (CO_2eq) variables (Haryanto et al., 2025). - High risk of pollution.	- UBCs waste to landfill is reduced by 30% (7.56 tons/day). - CO_2 emissions fell by up to 30%.	- Waste to landfill drops to 60% (4.31 tons/day). - CO_2 emissions reduced by 60%
Culture	- High consumptive culture, low level of community participation in sorting waste. - Mixed throwing habits are dominant.	- Sorting awareness increased to 30%. - The value of cooperation lives in 30% of the community.	- 60% of the trial area is actively sorting and returning packaging. - The value of cooperation grows in more than 80% of communities. - Packaging reuse increased by 30%.

producers in the re-embrace of UBCs through EPR serves to reinforce corporate social responsibility while concurrently expanding a more inclusive social network. The management of UBCs provides added value. Waste, once regarded as worthless, can be utilized as a means of generating income. Collectors earn greater profits through the sale of UBCs to manufacturers, while manufacturers reduce production costs by utilizing recycled raw materials. The earnings of collectors experienced a notable increase as UBCs evolved into a tradable commodity. Previously, collectors only earned income from plastics and metals, now UBCs add up to USD 0.9/day. Manufacturers save up to 15% on raw material costs because they utilize recycled products. The logistics and recycling sectors create new jobs per polling station. Improved efficiency in material flow has been shown to create job opportunities in industries like recycling, logistics, and manufacturing that utilize secondary materials. Moreover, the implementation of a circular economy has been shown to encourage product diversification, improve company reputation, and strengthen industry competitiveness. The culture that led to increased waste generation is currently shifting towards an eco-friendly approach through the practices of sorting and returning packaging. This new awareness fosters a collective ethos, in line with the values of cooperation and local wisdom. Education and community involvement increase household participation in waste sorting by up to 60%. Collectors are recognized as formal collaborators in the circular economy chain, resulting in a significant increase in public perception, which can rise by as much as 60%. Collaboration among multiple stakeholders, including governments, communities, and producers, enhances social networks and promotes inclusion. Based on MFA, the total waste in Depok City is 1081.82 tons/day. Alternative 1 can reduce UBCs waste generation

by 30% (around 3.25 tons/day), while Alternative 2 increases efficiency by another 30% (total reduction of 60%). Positive environmental impacts are in the form of reducing CO_2 emissions and reducing landfill residues to 5.5 tons/day. UBCs waste management not only reduces environmental pollution but can also form new habits and cultures that can be sustainable as a movement or a new lifestyle. The transition from a consumptive culture to a green culture is increasingly noticeable, especially with the rise in public awareness about sorting, which has escalated from 10% to 70%. The waste bank is active in 80% of the participants in the program. People are starting to consider sorting and returning packaging as part of a modern eco-friendly lifestyle. The process of recycling UBCs reduces the need for new raw materials while reducing greenhouse gas emissions. Consequently, this approach aids in reaching national objectives for waste reduction and aligns with the global agenda for climate change mitigation. MFA in this study uses a static modeling approach, which inherently limits its ability to capture temporal dynamics and behavioral changes in the waste management system. Static MFA provides only a snapshot of the system at a specific point in time, overlooking variations and trends that occur over shorter or longer periods. As a result, it is unable to consider alterations in community engagement, changes in policy, or shifting market conditions that could affect waste flow. Incorporating dynamic modeling approaches in future research would enhance the understanding of how material flows respond to temporal and societal fluctuations, thereby improving the predictive power and practical relevance of MFA results.

CONCLUSION

The city of Depok generates approximately 1,081.82 tons of waste per day, with used beverage cartons (UBCs) contributing around 10.82 tons daily. Food waste continues to be the primary component, accounting for 50%, whereas UBCs constitute a minor yet environmentally important portion. Improper handling of UBCs has contributed to contamination of soil, water, and air, emphasizing the need for a sustainable, integrated waste management system aligned with circular economy principles. By successfully applying the MFA framework, waste movements from generation to disposal have been accurately mapped, revealing key inefficiencies in existing methods. Combines collector-based recycling with producer-level reverse logistics (alternative 2), proved most effective, reducing 64.91 kg of CO_2 emissions per day, and lowering residual waste to 4327.28 kg/day. Beyond environmental outcomes, the approach also generated 50% higher income for collectors, 15% cost savings for producers, and created local green jobs in the recycling and logistics sectors. The combination of grassroots collection and corporate responsibility illustrates that waste management can enhance environmental, economic, and social resilience at the same time. Economically, the adoption of EPR enhances manufacturer accountability and stimulates investment in eco-innovation. It transforms UBCs from a low-value residue into a secondary resource, increasing collectors' income by 50% and saving manufacturers up to 15% on raw material costs. This reciprocal arrangement fosters local job opportunities in the recycling, logistics, and processing sectors. Socially and behaviorally, the shift toward circular waste management enhances community participation and environmental awareness. Public engagement in waste sorting has grown from 30% to 70%, creating a new societal standard that emphasizes sustainability. The empowerment of waste pickers and collectors as formal partners promotes inclusivity and reduces social stigma, while the 3R-based temporary shelters (TPS 3R) evolve into community-based eco-centers. Environmentally, this strategy supports the achievement of sustainable development goals (SDGs), particularly SDG 12 (Responsible Consumption and Production) and SDG 13 (Climate Action). By decreasing waste production, emissions, and landfill remnants, Depok City serves as a practical and replicable example of sustainable urban waste management in developing countries. The uniqueness of this research is found in the combination of MFA-based quantification with socio-economic and cultural evaluation, thereby offering a comprehensive decision-making framework. It bridges technical, behavioral, and policy aspects, proving that sustainable waste management is not merely an engineering task but a social transformation process. Future research should expand to dynamic MFA modeling that incorporates temporal trends, behavioral change, and life-cycle assessments of reverse logistics. Enhanced cooperation among government, academia, and industry is crucial for

institutionalizing EPR and accelerate the transition to a circular economy. In conclusion, the synergy between collector-based recycling and producer-level EPR transform waste management from a linear disposal practice into a regenerative system that unites environmental protection, economic opportunity, social inclusion, and cultural sustainability marking a decisive step toward a circular and climate-resilient urban future. It demonstrates that effective sustainable waste management necessitates a synergy among data-informed planning, institutional responsibility, and community engagement, a trio that can propel Indonesia's urban systems toward resilience, inclusivity, and circularity. This study has several limitations worth noting. First, MFA was not corroborated with an accompanying LCA, which could offer a more comprehensive quantification of environmental impacts. Second, data used in the analysis are localized to Depok City, limiting the generalizability of the findings to other regions with differing waste management contexts. Third, post-consumer and industrial recycling stages were not included in the system boundaries, potentially omitting important flows and impacts. Future studies ought to tackle these deficiencies by incorporating LCA to enhance and substantiate environmental evaluations, broadening the scope of research for wider relevance, and including further recycling phases and indirect flows like energy consumption and emissions. Such advances will further strengthen the robustness and policy relevance of waste management modeling. The outcomes of this study can act as suggestions for the government, future scholars, and UBC producers. Local governments should embed the MFA–EPR framework into municipal waste policies, ensuring that producers' responsibilities are transparently monitored through measurable material flow data. Incentives for sorting, subsidies for recycling infrastructure, and enforcement mechanisms for EPR compliance must be strengthened. Subsequent studies are encouraged to utilize dynamic MFA paired with LCA to evaluate long-term behavioral alterations, system feedback, and the downstream effects associated with reverse logistics. This would support evidence-based policymaking and adaptive waste management strategies. Integrating environmental education into schools, community initiatives, and social media campaigns will sustain public engagement. Waste banks and TPS 3R ought to transform into eco-learning and innovation centers that foster environmental consciousness as an integral aspect of daily living. Establishing a stable secondary market for UBCs materials and adopting minimum recycled-content standards for packaging will enhance the competitiveness of recycled products and attract private-sector investment in sustainable industries. Achieving sustainable progress demands persistent collaboration among academia, industry, government, and local communities. Such partnerships can bridge policy gaps, standardize data systems, and replicate the Depok model in other Indonesian cities.

AUTHOR CONTRIBUTIONS

B. Ratnawati, the corresponding author, has contributed to sampling, supervising the data analysis, interpreting the results, and preparing the manuscript. L. Dellarosa collected the data and performed the data analysis. N. Jannah is tasked with interpreting economic and social data. N.D. Oktaf, the interpretation of the results. E.H. Nurakbari participated in sampling preparation and the interpretation of the material flow analysis results. H.S. Huboyo manuscript preparation. A.C. Agustina prepared the maps needed for sampling. M.D. Vaverková analyzes the results of the material flow analysis and improves the sentence structure in the article.

ACKNOWLEDGEMENT

The experiment was conducted in Bogor, West Java Indonesia, by the team from IPB University, Diponegoro University, and Sahid University. The data analysis and preparation of the manuscript was a part of the Reguler Fundamental Riset (PFR) funded by the Directorate General of Research and Development of the Ministry of Higher Education, Science, and Technology in accordance with the Contract for the Implementation of the Research Program for the 2025 Fiscal Year Number: [006/C3/DT.05.00/PL/2025].

CONFLICT OF INTEREST

The authors declare that there is no conflict of interest regarding the publication of this manuscript. In addition, ethical issues, including plagiarism, informed consent, misconduct, data fabrication and/or falsification, double publication and/or submission, and redundancy have been completely observed by

the authors.

OPEN ACCESS

©2026 The author(s). This article is licensed under a Creative Commons Attribution 4.0 International License, which permits use, sharing, adaptation, distribution and reproduction in any medium or format, if you give appropriate credit to the original author(s) and the source, provide a link to the Creative Commons license, and indicate if changes were made. The images or other third-party material in this article are included in the article's Creative Commons license, unless indicated otherwise in a credit line to the material. If material is not included in the article's Creative Commons license and your intended use is not permitted by statutory regulation or exceeds the permitted use, you will need to obtain permission directly from the copyright holder. To view a copy of this license, visit: http://creativecommons.org/licenses/by/4.0/

PUBLISHER'S NOTE

GJESM Publisher remains neutral regarding jurisdictional claims in published maps and institutional afflictions.

R Negative AI Statement

The author(s) declared that no AI tools or services were not used or not highly applied during the preparation of this work.

ABBREVIATIONS

%	Percent
ADUPI	Association of Plastic Recycling Practitioners
B3	Hazardous and toxic substances
CE	Circular economy
cm	Centimeter
CO_2	Carbon dioxide
CO_2eq/day	Carbon dioxide equivalent per day
$C_{product}$	Consumption product
$C_{recycled}$	Consumption recycled
DLH	Environmental Agency
E	Emission factor
$EF_{Landfill}$	landfill emission factor (kg CO_2-eq/day)
$EF_{recycled}$	recycled emission factor (kg CO_2-eq/day)
e.g.	For example
EPR	Extended producer responsibility
GDP	Gross domestic product
ICT	Information and Communication Technology
i.e	In other word
IPCC	The Intergovernmental Panel on Climate Change
kg	Kilogram
kg/day	Kilogram per day
kg/individual/day	Kilogram per individual per day
km^2	Square kilometer
LCA	Life Cycle Assessment
m	Meter
MFA	Material flow analysis
mL	Milliliters
MoEF	The Ministry of Environment and Forestry of Indonesia
P_{UBCs}	Price UBCs
PolyAl	polyethylene–aluminum
SDGs	Sustainable Development Goals
SNI	Indonesian National Standard
Ton/day	Ton per day
TPA	Final waste processing site
TPS	Waste Transfer Station

TPS 3R	Waste treatment sites reduce, reuse, recycle
UU	Laws
UBCs	Used beverage cartons
USD	United States Dollar
USD/ day	United States Dollar per day
W_{UBCs}	daily UBCs mass
$W_{UBCsrecycled}$	UBCs mass recycled (tons/day)

REFERENCES

Agamuthu, P.; Visvanathan, C., (2014). Extended producers responsibility schemes for used beverage carton recycling. Waste Manage. Res., 32(1): 1–3 **(3 pages).**

Aleluia, J.; Ferrão, P., (2016). Characterization of urban waste management practices in developing Asian countries: A new analytical framework based on waste characteristics and urban dimension. Waste Manage., 58: 415-429 **(15 pages).**

Ameen, R.F.M.; Mourshed, M., (2017). Urban environmental challenges in developing countries—A stakeholder perspective. J. Habitat Int., 64: 1–10 **(10 pages).**

Anwar, M.A.; Suprihatin, S.; Sasongko, N.A.; Najib, M.; Pranoto, B.; Firmansyah, I.; Soekotjo, E.S., (2024). Challenges and prospects of multilayer plastic waste management in several countries: A systematic literature review. , 10: 1-15 **(15 pages).**

Anwar, M.A.; Suprihatin; Sasongko, N.A.; Najib, M.; Pranoto, B., (2025). Sustainable waste management strategies for multilayer plastic in Indonesia. Cleaner Responsible Consumption, 16: 1-15 **(15 pages).**

Aydın, S.; Güneysu, S.; Ciner, M.; Özbaş, E; Ozcan, H; Öngen, A., (2025). The effect of volume reduction methods on beverage packaging waste recycling in the deposit return system. Int. J. Environ. Sci. Technol., 22: 1-10 **(10 pages).**

Ayodele, T.R.; Alao, M.A.; Ogunjuyigbe, A.S.O., (2018). Recyclable resources from municipal solid waste: Assessment of its energy, economic and environmental benefits in Nigeria. Resour. Conserv. Recycl., 134: 165–173 **(9 pages).**

Battarra, I.; Accorsi, R.; Lupi, G.; Manzini, R., (2025). Life cycle assessment of an automated multi-cellular case-picking system. J. Manuf. Syst., 79: 419–434 **(16 pages).**

Biakhmetov, B.; Li, Y.; Zhao, Q.; Dostiyarov, A.; Flynn, D.; You, S., (2025). Transportation and process modelling-assisted techno-economic assessment of resource recovery from non-recycled municipal plastic waste. Energy Convers. Manage., 324: 1-18 **(18 pages).**

Buongiorno, J.; Johnston, C.; Zhu, S., 2017. An assessment of gains and losses from international trade in the forest sector. For. Policy Econ., 80: 209–217 **(9 pages).**

Carrasco, G.C.; Ruwoldt, J.; Pasquier, E.; Dalheim, M. Ø.; Wieser, M. K., (2024). Development of a beverage carton closure cap based on 100% wood pulp fibres. J. Cleaner Prod., 445: 1-9 **(9 pages).**

Escursell, S.; Llorach-Massana, P.; Roncero, M.B., (2021). Sustainability in e-commerce packaging: A review. J. Cleaner Prod., 280: 1-17 **(17 pages).**

Farida, Y.; Siswanto, N.; Vanany, I., (2024). Reverse logistics toward a circular economy: Consumer behavioral intention toward polyethylene terephthalate (PET) recycling in Indonesia. Case Stud. Chem. Environ. Eng, 10: 1-11 **(11 pages).**

Fatimah, Y.A., Govindan, K., Sasongko, N.A., Hasibuan, Z.A., (2024). The critical success factors for sustainable resource management in circular economy: Assessment of urban mining maturity level. J. Clean Prod., 469: 1-17 **(17 pages).**

Feil, A.; Thoden van Velzen, E. U.; Jansen, M.; Vitz, P.; Go, N.; Pretz, T., (2016). Technical assessment of processing plants as exemplified by the sorting of beverage cartons from lightweight packaging wastes. Waste Manage., 48: 95–105 **(11 pages).**

Gao, H.; Liu, J.; Daigo, I., (2025). Methodology development for estimating the impact of restriction factors to promote national steel recycling. Resour. Conserv. Recycl., 215: 1-10 **(10 pages).**

Gritsch, L.; Breslmayer, G.; Rainer, R; Stipanovic, H; Tischberger-Aldrian, Alexia, L., J., (2024). Critical properties of plastic packaging waste for recycling: A case study on non-beverage plastic bottles in an urban MSW system in Austria. Waste Manage., 185: 10–24 **(15 pages).**

Gritsch, L.; Breslmayer, G.; Lederer, J., (2025). Comprehensive characterization of beverage cartons in urban waste: A case study from Austria. Waste Manage., 201:1-10 **(10 pages).**

Guo, H. ; Zhao Y.; Damgaard A; Wang Q; Lu W; Wang H; Christensen T., (2019). Material flow analysis of alternative biorefinery systems for managing Chinese food waste. Resour. Conserv. Recycl., 149:197–209 **(13 pages).**

Haryanto, A.; Santoso, A.D.; Hanif, M.; Ihsan, I.M.; Oktivia, R.; Prayitno, J.; Tridakusumah, A.C.; Pebriyanti, V.; Triyono, S.; Daulay, H.; Irawati, N.; Mawardi, M.I.; Sundari, S.; Panggabean, L.P.; Indrawanto, C., (2025). Strategies for sustainable behavior and emission reduction through individual carbon footprint analysis. Global J. Environ. Sci. Manage., 11: 243–260 **(18 pages)**.

IPCC, (2024). 2006 IPCC guidelines for national greenhouse gas inventories.

Ismail, Y.; Adji, R.; Santoso, A.D.; Wahyono, S.; Kholiq, M.A.; Handayani, T.; Pahri, S.D.R.; Putiamini, S.; Pratama, R.A.; Nurfatriani, F.; Sahwan, F.L.; Suryanto, F.; Prasetiyadi; Tilottama, R.D., (2025). Multi-dimensional perspectives on sustainability in domestic waste management. Global J. Environ. Sci. Manage, 11: 747–770 **(23 pages).**

Joyo, F.H.; Nastasi, B.; Astiaso Garcia; D., (2025). Decarbonization pathways for the pulp and paper industry: A comprehensive review. Renewable Sustainable Energy Rev., 223:1-22 (22 pages).

Kauppi, E.; Nieminen, K.; Paltakari, J., (2025). Recycling of plastic-coated cartons in hydropulping using pretreatments. Waste Manage., 204: 1-11 **(11 pages)**.

Kositcharoenkul, P.; Prempreeda A.; Oo, P.Z.; Deuja A.; Vassanadumrongdee S.; Gheewala S.; Prapaspongsa, T., (2025). Life cycle assessment of beverage packaging in Thailand: Implications from modeling choices and alternative improvement policies. Resour. Conserv. Recycl., 214:1-13 **(13 pages).**

Kremser, K.; Gerl, P.; Borrás; To.; Espinosa, D. Martínez, B.; Guebitz, G.; Pellis, A., (2022). Bioleaching/enzyme-based recycling of aluminium and polyethylene from beverage cartons packaging waste. Resour. Conserv. Recycl., 185:1-13 **(13 pages).**

Iacovidou, E., Gerassimidou, S., Wilson, D.C., Richter, J., Jobling, S., Soedjono, E., 2025. System-wide assessment of Indonesia's plastic value chain: Mapping flows and stakeholders dynamics. J. Clean Prod., 520:1-15 **(15 pages)**.

Lipp, A.M.; Lederer, J., (2025). The circular economy of packaging waste in Austria: An evaluation based on statistical entropy and material flow analysis. Resour. Conserv. Recycl., 217:1-10 **(10 pages).**

Liu, J.; Ye, G.; Wu, P.; Li, Y.; Zhu, J., (2025). Material flow analysis of construction and demolition waste recycling under circular economy. Cleaner Waste Syst., 11: 1-8 **(pages 8).**

Liu, Z.; Nowack, B., (2025). Using dynamic release modeling to predict historic and current macro- and microplastic releases. Resour. Conserv. Recycl., 214: 1-12 **(12 pages).**

Maalouf, A.; Mavropoulos, A., (2023). Re-assessing global municipal solid waste generation. Waste Manage. Res., 41(4): 936–947 **(12 pages).**

Majid, A.; Novita, E.; Gusniani, I.; Hartono, D.M., (2021). Mapping of solid waste generation and collection by using GIS: A case study in Depok City. IOP Conference Series: Earth Environ. Sci. 716:1-13 **(13 pages).**

Markic, D.N.; Luka, B.; Hristina, C.D., (2019). Using Material Flow Analysis for Waste Management Planning. Pol. J. Environ. Stud., 28: 255–265 **(11 pages).**

Mayanti, B.; Songok, J.; Helo, P., (2021). Multi-objective optimization to improve energy, economic and environmental life cycle assessment in waste-to-energy plan. Waste Manage., 127: 147–157 **(11 pages).**

Memon, A.; Mathurosemontri S.; Chailad W.; Jakrabutr, W.; Phansroy, N.; Sungsanit K.; Sirisuwan, P.; Tipboonsri P., (2025). Sustainable foamed Poly-Al composites from used beverage cartons using azodicarbonamide. Results Eng., 27:1-8 **(8 pages).**

Moreira, K.S.; Santos da Campo, Y.A.; Lorenzett, E.; Burgo, T. A. L., (2023). Low-cost triboelectric nanogenerator based on aseptic carton package. Results Eng., 17: 1-8 **(8 pages).**

Orias, N.A.; Lundquist, L., (2025). Life cycle assessment of reusable food and beverage packaging systems: A proposal of good practice. J. Cleaner Prod., 499: 1-11 **(11 pages).**

Paes, M.X.; Medeiros,G.A.; Mancini, S.D.; Bortoleto, A.P.; Oliveira, J.A.P.; Kulay L.A., (2020). Municipal solid waste management: Integrated analysis of environmental and economic indicators based on life cycle assessment. J. Cleaner Prod., 254: 1-12 **(12 pages).**

Pinaya, J.; Boiko, Y.; Ismail, M.; Wahlberg, J.; Pyo, S.; Vargas, V.A.; Kaul R.H., (2025). Leaching of aluminium from post-consumer beverage packaging residual PolyAl using biogenic organic acids: Towards low-cost, sustainable recycling. Waste Manage., 204: 1-11 **(11 pages).**

Qasim, M.; Xiaoa, H.; He, K.; Noman, A.; Liu, F.; Chen, M.Y.; Hussain, D.; Jamal, Z.A.; Li, F., (2020). Impact of landfill garbage on insect ecology and human health. Acta Trop., 211:1-6 **(6 pages).**

Ratnawati, B.; Yani, M.; Suprihatin, S.; Hardjomijojo, H., (2019). Identified solution management in the landfill with analytic network process. IOP Conference Series: Earth Environ. Sci., 399: 1-7 **(7 pages).**

Ratnawati, B.; Yani, M.; Suprihatin, S.; Hardjomijojo, H.; Cholik, T.N.; Ardiyani, Q.T., (2022). Comparison of municipal solid waste landfill management in Depok City and Klaten Regency. IOP Conference Series: Earth Environ. Sci., 1109:1-9 **(9 pages).**

Ratnawati, B.; Yani, M.; Suprihatin, S; Hardjomijojo, H., (2022). Study of Remaining Service Life of a Municipal Solid Waste Landfill with the Composting Method: A Case Study in Klaten Regency. IOP Conference Series: Earth Environ. Sci., 950(1):1-9 **(9 pages).**

Ratnawati, B.; Sulistijorini; Sholihah, W.; Aziezah, N. A.; Tunggadewi, A.T., Samiaji, D. and Keyren Johana Ginting, K.J., (2023). Plastic Waste Reduction Strategy in Bogor City, Indonesia. E3S Web of Conference. 454:1-5 **(5 pages).**

Ratnawati, B.; Yani, M.; Suprihatin, S.; and Hardjomijojo, H., (2023). Waste processing techniques at the landfill site using the material flow analysis method. Global J. Environ. Sci. Manage., 9(1): 73–86 **(14 pages).**

Reitsema, A.; Onderdelinden E.; Korevaar, G.; Ghorbani, A., (2025). Understanding decision-making in circular

packaging ecosystems: An agent-based model of the Dutch beverage sector. J. Cleaner Prod., 526: 1-20 **(20 pages).**

Rizaluddin, A.T.; Rostika, I.; Wattimena, R.B.I., (2020). Progress of used beverages carton recycling system in Indonesia: A review. IOP Conference Series: Earth Environ. Sci., 483: 1-10 **(10 pages).**

Roungpaisan, N.; Jariyapunya,N.; Tipboonsri, P.; Cheewawuttipong, W.; Zhang, Z.; Memon, A., (2025). Sustainable pet diapers created from nonwoven polylactic acid and recycled pulp derived from used beverage cartons. Results Eng., 25: 1-7 **(7 pages).**

Rundh, B., (2016). The role of packaging within marketing and value creation. Br. Food J., 118(10): 2491–2511 **(21 pages).**

Sadhukhan, J.; Martinez-Hernandez, E., (2017). Material flow and sustainability analyses of biorefining of municipal solid waste. Bioresour. Technol, 243: 135–146 **(12 pages).**

Schneider, J.M.; Ghannadzadeh, A.; van der Meer, Y., (2022). Material flow analysis of a post-consumer plastic packaging recycling system in The Netherlands: a focus on beverage carton. Clean Technol. Environ. Policy, 27: 6099-6110 **(12 pages).**

Simamora, J.; Wiloso, E.I.; Yani, M.; (2023). Life cycle assessment of paper products based on recycled and virgin fiber. Global J. Environ. Sci. Manage., 9: 89–106 **(18 pages).**

Simsek, G.K.; Icier, F., (2024). Exergo-economic approach for comprehensive evaluation of the performance of industrial-scale milk and coffee beverage process lines. Food Bioprod. Process., 147: 148–161 **(14 pages).**

Thiyagarajan, R.; Rao, R.; Salas, M.; Haque, N.; Sarker, A.; Kumar, R.; Tripathy, A.; Srinivasan, V.; Wang, Y.; Yarbrough, J.; Mittal, A.; Singh, A.; Barlaz, M.A.; Jameel, H.; Pal, L., (2025). Techno-economics of hydrocarbon fuel production and recyclables recovery from landfill-destined municipal solid waste: AI-enhanced materials recovery facility design. J. Cleaner Prod., 525: 1-12 **(12 pages).**

Tosarkani, B.M.; Amin, S.H.; Ghiasvand, M.R., (2024). Designing a sustainable plastic bottle reverse logistics network: A data-driven optimization approach. Expert Systems with Applications, 251: 1-24 **(24 pages).**

Turner, D.A.; Williams, I.D.; Kemp, S., (2016). Combined material flow analysis and life cycle assessment as a support tool for solid waste management decision making. J. Cleaner Prod., 129: 234–248 **(15 pages).**

Wong, P.K.; Lui, Y.,W.; Tao, Q.; Lui, M., (2024). Solvent-targeted recovery of all major materials in beverage carton packaging waste. Resour. Conserv. Recycl., 202: 1-7 **(7 pages).**

Yao, Z.; Makepa, D.C.; Poddar, S.; Reinmoller M.; Bertelsen, M.; Jiang, J.; Tong, J.; Cui J.; Liu, J.; Cordeiro, I., M., (2025). Waste-to-energy: Pyrolysis-gasification conversion of packaging waste from both micro and macro perspectives. Case Stud. Therm. Eng., 71; 1-16 **(16 pages).**

Yilmaz, C.; Müller, K.; Blanke, L.; Dorn, V.; Rohrmeier, T.; Schinkel, K.; Tischler, C.; Vafaieshoar, M.; Fell, T.; Sängerlaub, S., (2025). Material Use Efficiency of Primary Packaging of Fast-Moving Consumer Goods. Chem. Ing. Tech., 97(4): 269–277 **(9 pages).**

Zeng, T.; Durif, F.; Robinot, E., (2021). Can eco-design packaging reduce consumer food waste? An experimental study. Technol. Forecast. Soc. nol. 162: 1-11 **(11 pages).**

Zohoori, M.; Ghani, A., (2017) Municipal Solid Waste Management Challenges and Problems for Cities in Low-Income and Developing Countries. Int. J. Sci. Eng. Appl., 6(2): 39-48 **(10 pages).**

AUTHOR (S) BIOSKETCHES

Ratnawati, B., Ph.D., Assistant Professor, Vocational School, IPB University, Jl. Kumbang No.14, Indonesia.
- Email: *beata@apps.ipb.ac.id*
- ORCID: 0000-0002-8949-4224
- Web of Science ResearcherID: AAD-8204-2022
- Scopus Author ID: 57214139644
- Homepage: http://sv.ipb.ac.id

Dellarosa, L., M.Sc., Lecturer, Vocational School, IPB University, Jl. Kumbang No.14, Indonesia.
- Email: *luvydella@apps.ipb.ac.id*
- ORCID: 0009-0006-6959-8567
- Web of Science ResearcherID: NA
- Scopus Author ID: NA
- Homepage: http://sv.ipb.ac.id

Jannah, N., Ph.D., Associate Professor, Vocational School, IPB University, Jl. Kumbang No.14, Indonesia.
- Email: *nuruljannah@apps.ipb.ac.id*
- ORCID: 0009-0005-0398-5372
- Web of Science ResearcherID: NA
- Scopus Author ID: 57214133484
- Homepage: http://sv.ipb.ac.id

AUTHOR (S) BIOSKETCHES

Oktaf, N.D., B.A. Student, Vocational School, IPB University, Jl. Kumbang No.14, Indonesia.
▪ Email: *ndzakiyah04oktaf@apps.ipb.ac.id*
▪ ORCID: 0009-0004-0968-7280
▪ Web of Science ResearcherID: NA
▪ Scopus Author ID: NA
▪ Homepage: http://sv.ipb.ac.id

Nurakbari, E.H., M.Sc., Lecturer, Environmental Engineering, Sahid University, Jl. Soepomo No 1, Jakarta, Indonesia.
▪ Email: *velynhanaseta@gmail.com*
▪ ORCID: 0009-0003-9919-0405
▪ Web of Science ResearcherID: NA
▪ Scopus Author ID: 59393230100
▪ Homepage: https://usahid.ac.id/

Huboyo, H.S., Ph.D., Associate Professor, Vocational School, IPB University, Jl. Kumbang No.14, Indonesia.
▪ Email: *huboyo@lecturer.undip.ac.id*
▪ ORCID: 0000-0001-8353-1365
▪ Web of Science ResearcherID: NA
▪ Scopus Author ID: 43361494900
▪ Homepage: https://undip.ac.id

Agustina, A.C., B.A. student, Vocational School, IPB University, Jl. Kumbang No.14, Indonesia.
▪ Email: *audisticellyagustina@apps.ipb.ac.id*
▪ ORCID: 0009-0007-6718-0033
▪ Web of Science ResearcherID: NA
▪ Scopus Author ID: NA
▪ Homepage: http://sv.ipb.ac.id

Vaverková, M.D., Ph.D., Professor, Department of Sustainable Construction and Geodesy, Institute of Civil Engineering, Warsaw University of Life Sciences - SGGW, Nowoursynowska 159, 02 776 Warsaw, Poland
▪ Email: *magdalena_vaverkova@sggw.edu.pl*
▪ ORCID: 0000-0002-2384-6207
▪ Web of Science ResearcherID: NA
▪ Scopus Author ID: 50562220100
▪ Homepage: www.sggw.edu.pl

HOW TO CITE THIS ARTICLE

Ratnawati, B.; Dellarosa, L.; Jannah, N.; Oktaf, N.D.; Nurakbari, E.H.; Huboyo, H.S.; Agustina, A.C.; Vaverková, M.D., (2026). Waste management of used beverage cartons using material flow analysis. Global J. Environ. Sci. Manage., 12(1): 57-74.

DOI: 10.22034/gjesm.2026.01.04

URL: https://www.gjesm.net/article_731627.html

Global J. Environ. Sci. Manage. 12(1): 75-94, Winter 2026, Serial #45

Global Journal of Environmental Science and Management
(GJESM)

Homepage: https://www.gjesm.net/

Podcasts

ORIGINAL RESEARCH PAPER

Physical and chemical evaluation of soil-like material from landfill mining using an alternative growing medium

N. Sudiana[1], Prihartanto[1,*], I.N. Sulistiawan[1], E.H. Sittadewi[2], D.N. Utami[2], E. Kusumastuti[3], B. Rahayu[1], N. Hidayat[1], K.A. Haris[1], T.E. Pararto[1], L. Noviana[4]

[1] *Research Centre for Environmental and Clean Technologies, National Research and Innovation Agency, South Tangerang, Banten, Indonesia*

[2] *Research Centre for Geological Disaster, National Research and Innovation Agency, South Tangerang, Banten, Indonesia*

[3] *Directorate of Laboratory Management, Research Facilities, and Science and Technology Area, National Research and Innovation Agency, South Tangerang, Banten, Indonesia*

[4] *Faculty of Engineering, Sahid University, South Jakarta, Jakarta, Indonesia*

ARTICLE INFO

Article History:
Received 21 August 2025
Revised 29 October 2025
Accepted 02 December 2025

Keywords:
Growing medium
Heavy metals (HM)
Landfill mining
Municipal solid waste
Plant nutrients
Soil-like material (SLM)

ABSTRACT

BACKGROUND AND OBJECTIVES: Jakarta's municipal solid waste generation is reaching landfill capacity due to rapid urbanization, metropolitan lifestyles, and industrial growth. Landfill mining increases capacity and reuses materials when landfill expansion is not feasible. At Bantargebang's integrated municipal solid waste treatment facility, the landfill mining plant produces materials akin to soil and refuse-derived fuel. This study assesses the suitability of soil-like material's physical and chemical properties as a growing medium.

METHODS: For seven consecutive working days, fine fractions less than 50 millimeters obtained from trommel screening of landfill materials were sampled using the quartering technique. Samples were analyzed for moisture, ash, texture, cation exchange capacity, pH, total organic carbon, total Kjeldahl nitrogen, carbon-to-nitrogen ratio, phosphorus, potassium, and heavy metals. Soil-like material composition and physical properties followed American Society for Testing and Materials and International Soil Reference and Information Centre standards, chemical properties followed Natural Resources Conservation Service and United States Department of Agriculture guidelines, and heavy metals followed Environmental Protection Agency methods. In a greenhouse experiment, soil-like material and compost were mixed in proportions ranging from 100 to 60 percent soil-like material by weight, in 10 percent steps, to assess their effectiveness as a growing medium for Calliandra calothyrsus.

FINDINGS: Composition analysis showed that 40.61 percent of the landfill-mined fine fraction consisted of soil-like material particles smaller than 4.75 millimeters with high organic matter, sufficient inorganic materials, and elevated heavy metals, particularly iron, manganese, and cadmium. The organic matter was primarily undecomposed and unstable, characterized by a total organic carbon level of 57.08 percent, significant volatile solids at 78.60 percent, and a carbon-to-nitrogen ratio of 27.9, potentially resulting in microbial nitrogen immobilization. With a cation exchange capacity of only 16.39 centimoles per kilogram, moisture levels at 32.78 percent, a texture primarily consisting of coarse sand, and low levels of potassium at 598.33 milligrams per kilogram and phosphorus at 140.20 milligrams per kilogram, significantly restricted the performance of the growing medium. A greenhouse experiment showed that an 80 percent soil-like material–20 percent compost mix performed best, yielding an average final plant height of 51.67 centimeters over 127 days, exceeding other ratios (39.33–49.61 centimeters).

CONCLUSION: Plant growth initially relied on seedling nutrients, then on compost, with soil-like material gradually supplying nitrogen. Enhancing nutrient availability and minimizing metal toxicity can be achieved through stabilization via co-composting or blending with nutrient-rich amendments.

DOI: 10.22034/gjesm.2026.01.05

This is an open access article under the CC BY license (http://creativecommons.org/licenses/by/4.0/).

NUMBER OF REFERENCES
81

NUMBER OF FIGURES
4

NUMBER OF TABLES
3

*Corresponding Author:
Email: *prihartanto69@gmail.com*
Phone: +62815 996 2260
ORCID: 0000-0003-2327-2300

Note: Discussion period for this manuscript open until Mar 1, 2026 on GJESM website at the "Show Article".

INTRODUCTION

Landfilling remains a common method for disposing of municipal solid waste (MSW) in developing and developed countries due to its low operating costs (Arumdani *et al.,* 2021; Jain *et al.,* 2023; Vaverková, 2019; Yang *et al.,* 2018). Nonetheless, the rising amounts of MSW caused by urbanization, population expansion, and industrial development are pushing landfill capacity to its maximum limits (Gutierrez *et al.,* 2019). When there is no space left to expand the landfill area, landfill mining (LM) provides a viable solution. It boosts landfill capacity but also contributes positively to the environment by recovering landfill-mined materials (LMM) that can serve as energy sources or raw materials for construction, for instance, recovered aggregates, soil-like material (SLM), manufacturing raw materials (such as metals and plastics), or land reclamation (Márquez *et al.,* 2019; Jagodzińska *et al.,* 2021; Laner *et al.,* 2019; López *et al.,* 2018). LM aims to reclaim value from waste via waste-to-energy, waste-to-material, and waste-to-land approaches (Jain *et al.,* 2023; Wagland *et al.,* 2019), as well as to recover valuable resources from old landfills. The LM process employs several types of material separation techniques, including screening, wind sifting, metal separation, and shredding, to recover LMM. This procedure typically retrieves LMM and sorts it into four primary categories: recyclables, hazardous waste, residuals, and SLM (Hogland *et al.,* 2019; Vrancken *et al.,* 2017). To obtain fine fraction (FF) from LMM, which is rich in SLM, a trommel screen is commonly used. SLM can be used as compost or earth fill for low-lying areas, excavated sites, and embankments (Datta *et al.,* 2021). In contrast, a coarse fraction consisting of plastics, stones, and metals is sorted by a wind sifter, a trommel screen, and a metal separator. Several types of plastics have a high calorific value, making them ideal for energy recovery, whereas stones and metals can be recycled as construction aggregates or raw materials (Datta *et al.,* 2021; Somani *et al.,* 2019, 2020). The breakdown of organic waste in landfills occurs over time, resulting in SLM, the most prevalent element of LMM. A previous investigation of 34 landfills found that the average composition of LMM was 48.6 percent (%) SLM, 24.5% combustibles, 21.3% inert materials, and 5.6% other materials (Jain *et al.,* 2023). The typical particle size threshold for SLM ranges from 1 to 40 millimeters (mm), with 10 mm and 20 mm being the most common (Datta *et al.,* 2021; Jain *et al.,* 2023). In comparison, at the LM plant of the Bantargebang Integrated Municipal Solid Waste Treatment Facility (IMSWTF) in Bekasi, Indonesia, the SLM produced, which is separated by a trommel screen, is smaller than 50 mm, resulting in a coarser fraction than in previous studies. The intended ratio of FF for this screen size was set at 41%, while SLM particles measuring less than 10 mm accounted for only 17% (Prihartanto *et al.*, 2023a). On the other hand, the LMM fraction larger than 50 mm accounted for 59%, with 35% recovered as refuse-derived fuels (RDF). The predominant amount of RDF in relation to SLM illustrates the operational focus of the RDF plant, which emphasizes producing RDF for industrial energy purposes over the refinement and utilization of SLM. Previous studies have investigated that SLM is composed of decomposed waste, landfill cover soil, and fine fragments of metal, plastic, and glass (Chandana *et al.,* 2021; Kristanto *et al.,* 2020; Wagland *et al.,* 2019). In most LM projects, the SLM-to-waste ratio is between 11%:89% and 77%:23% (Joseph *et al.,* 2003). In comparison, at the Bantargebang IMSWTF, LMM contained 33.15–35.54% SLM at an 8 mm screen size, whereas the nearby Sumur Batu Landfill produced 29% at a screen size of 12.7 mm (Kristanto *et al.,* 2020; Widyarsana and Tambunan, 2022). These findings emphasize the significant organic and nutritional value of SLM, suggesting its viability as a substitute for topsoil (Zhang *et al.,* 2015). A review of over 100 LM projects conducted between 1953 and 2021 identified 23 projects across seven Asian countries: India, China, Taiwan, South Korea, Sri Lanka, Pakistan, and Thailand (Márquez *et al.,* 2019). At least ten of these projects focused on the recovery of SLM, except in Pakistan. A study conducted in India evaluated the practicality of utilizing <4.75 mm SLM for applications such as composting, land reclamation, and embankment backfilling. The findings indicated that pretreatment is essential to reduce the risk of contamination (Datta *et al.,* 2021; Hölzle, 2019). Despite being an economical and environmentally friendly method for stabilizing slopes in post-closure landfills, revegetation can be hindered by low nutrient availability and poor soil quality (Song, 2018). Common challenges include drought, waterlogging, short roots, and compacted soil. Adding nutrients from organic waste or fertilizers and adjusting the soil power of hydrogen (pH) can

stimulate microbial activity and support ecosystem restoration. Using SLM as an amendment improves soil properties, retains moisture, prevents erosion, supports plant growth, and filters runoff (Emmanuel *et al.,* 2015), while also providing nutrients, promoting root growth, and maintaining soil air–water balance (Zhou *et al.,* 2015). These findings suggest that SLM could serve as a viable alternative growing medium, particularly beneficial for initial plant growth. Most prior studies have primarily examined composting or geotechnical applications (Datta *et al.,* 2021; Hölzle, 2019), studies on SLM use for degraded land revegetation are limited. In this context, previous research has rarely investigated full-scale LM plant operations under tropical landfill conditions in Southeast Asia, where SLM originates. This study fills that gap by systematically linking the site-specific physical and chemical properties of SLM, obtained from LM plant at the Bantargebang IMSWTF, one of the largest full-scale tropical landfills in Southeast Asia, which operates under controlled landfill techniques. It presents innovative understandings of employing SLM as a substitute cultivation medium in tropical urban landfill environments by associating these traits with genuine plant growth outcomes. Therefore, the aim of this current study is to evaluate the physical and chemical properties of SLM and to assess the effectiveness of compost blending as an amendment to improve its performance as a growing medium. This study was conducted at the Bantargebang IMSWTF in Bekasi, Indonesia, from 2023 to 2025, with the first phase (May 2023–Oct 2024) focused on SLM characterization and the second phase (Nov 2024–Mar 2025) on the planting experiment.

MATERIALS AND METHODS

Study area description

The Bantargebang IMSWTF is in Bekasi City, West Java Province, Indonesia, adjacent to the eastern side of Jakarta Province. This facility features Indonesia's largest landfill, covering 84.1 hectares. It received about 7,360 tons per day (t/d) of MSW in 2023 exclusively from the Jakarta Province, and this amount is expected to rise to 7,500–8,000 t/d by 2025 (Fig. 1).

The landfill comprises six zones divided into twelve sub-zones (Fig. 2). Currently, only Zones I–III remain active, while Zones IV and VI are closed, and Zone V is only partially open. Having operated since 1989, the landfill is now nearly full. Consequently, various initiatives, such as LM, are in progress to prolong its operational lifespan. In 2020, an initial LM pilot project started with a capacity of 100–150 t/d at Zone IV, specifically in Sub-Zone IVB. LMM excavation initially started in Sub-Zone IVB but was relocated to the 9.5-hectare Zone V due to traffic congestion on the transportation route to and from the LM plant. By 2023, the plant's capacity had been expanded to 1,000 t/d to fulfill RDF demand, mainly from the cement industry. Zone V was managed through controlled landfill methods, incorporating passive gas discharge and leachate collection, without any recirculation. This method employs minimal environmental management practices, in contrast to sanitary landfills, which permit precipitation to infiltrate waste deposits. This leads to increased moisture, partial decomposition of organic matter, and nutrient leaching, potentially impacting the quality of the recovered material. LMM is screened with a 50 mm trommel to separate the fine fraction

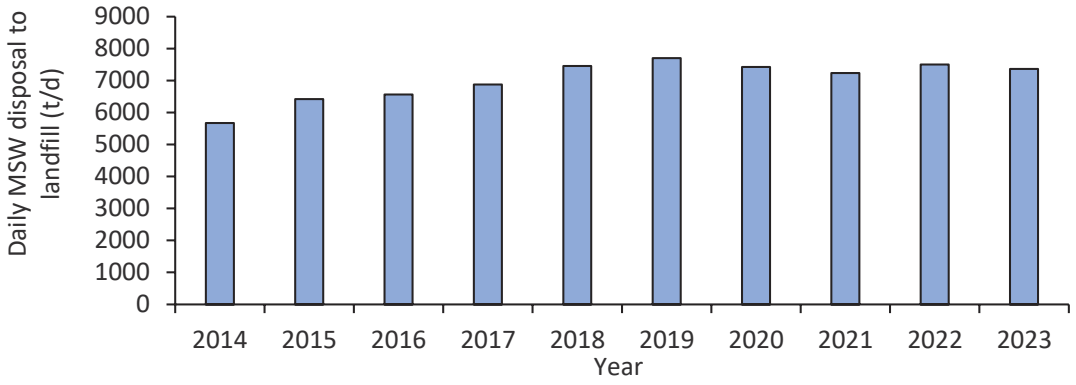

Fig. 1: Daily quantity of landfilled MSW from Jakarta Province disposed at the Bantargebang IMSWTF, Indonesia (2014–2023)

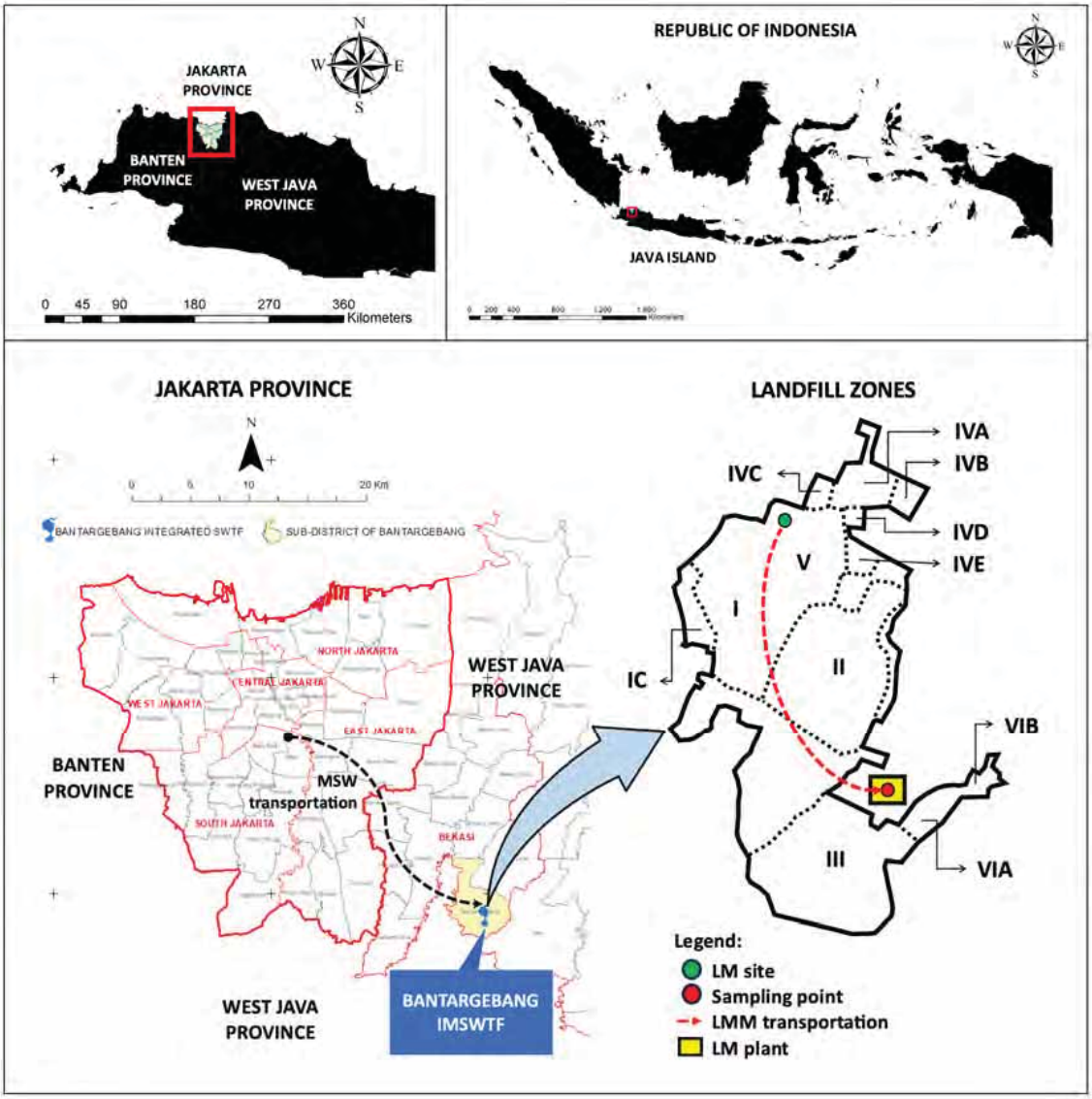

Fig. 2: Geographic location of the study area, including landfill zones, LM site and plant, and sampling point at Bantargebang IMSWTF, Bekasi City, West Java Province, Indonesia

(<50 mm, mostly SLM) from the rough fraction (RF) (≥50 mm) (Fig. 3). The light-rough fraction (LRF) is processed into RDF, whereas the heavy-rough fraction (HRF) is returned to the landfill as residue. The plant is designed to produce approximately 350 t/d RDF, 410 t/d SLM, and 240 t/d residue. However, the SLM is currently stored and not yet utilized.

Sample collection and preparation

Prior studies have shown that the SLM (<4 mm) is best suited for agricultural applications owing to its consistent composition, low levels of contamination, and properties similar to soil (Parrodi *et al.*, 2018). Nevertheless, this study selected for the SLM (<4.75 mm) as a more practical and scalable alternative. Compared to <4 mm, it has a similar composition but is somewhat coarser. Its texture improves porosity, aeration, water drainage, and root penetration, supporting optimal plant growth (Maluin *et al.*, 2021). Screening at 4.75 mm enhances volume capacity, boosts processing efficiency, aligns with standard composting systems, accommodates the variable

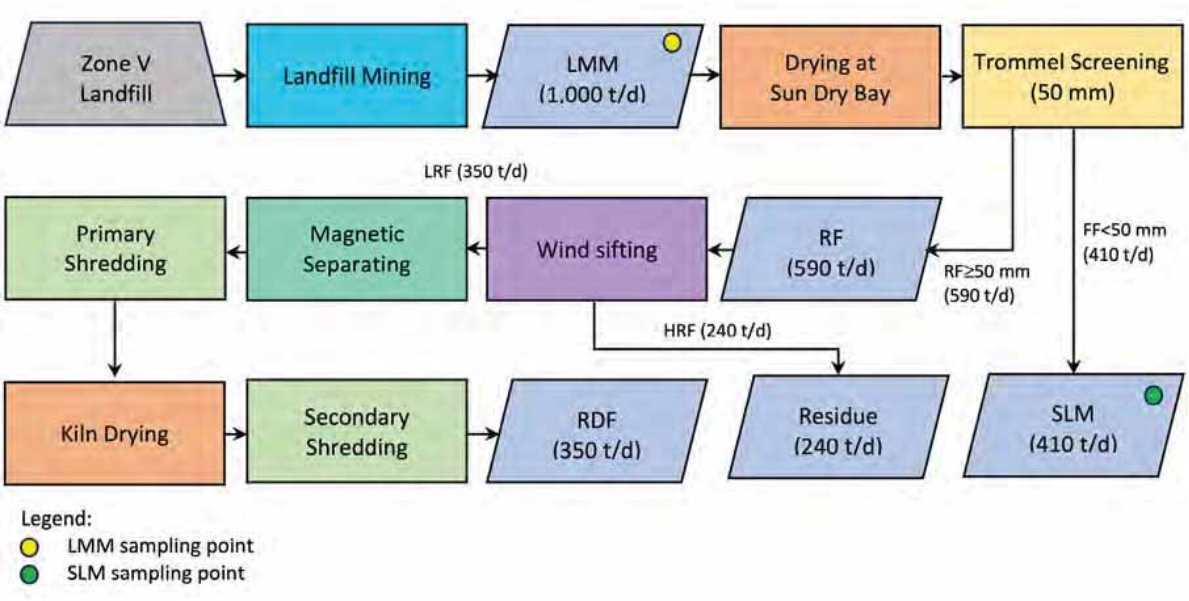

Fig. 3: Process flow and mass balance of the LM plant at the Bantargebang IMSWTF.

characteristics of LMM, captures the most critical SLM, prevents clogging, and streamlines operations (Naveen and Sivapullaiah, 2020). Additionally, previous studies recommended <4.75 mm SLM as a feasible low-nutrient compost for non-agricultural uses, including parks and non-edible crops (Datta *et al.*, 2021). Consequently, the <4.75 mm fraction was used as the target material for characterization. The SLM samples were collected at the end of the dry season in July 2024. Daily FF samples (<50 mm) were randomly obtained from the stockpile for consecutive seven working days. According to American Society For Testing And Materials (ASTM) D5231–92 (ASTM, 2016), approximately 454 kilograms (kg) with 1,000 pounds (lb) of FF was extracted using an excavator bucket, homogenized on a clean surface, and reduced using the quartering method through several iterations. The homogenized material was molded into a square shape, cut into four parts, and two of the opposite sections were eliminated. The remaining quarters were recombined, blended, and the quartering process was repeated until a representative subsample of approximately 100 kg was achieved. These subsamples were sieved through a 4.75 mm screen to separate SLM into <4.75 mm and >4.75 mm fractions. Furthermore, both fractions were compositionally analyzed. Approximately 10 kg of the <4.75 mm fraction was used for physical and chemical analyses to assess its suitability as a growing medium.

A composition analysis of FF

The FF (<50 mm) was separated, and each component was quantified as a percentage of total LMM. SLM proportions in the <4.75 mm and ≥4.75 mm fractions were calculated separately. Data represent the mean ± standard deviation over seven working days.

Physical characteristics analysis

SLM <4.75 mm were analyzed for pH, moisture, volatile solids (VS) content, and ash content. The pH was determined with a calibrated pH meter in a 1:2.5 SLM-water suspension, adhering to the guidelines established by the International Soil Reference and Information Centre (ISRIC) (Batjes and van Oostrum, 2023). Moisture content was determined by drying the sample at 110 ± 5 degrees Celsius (°C) for 24 hours (h) following ASTM D2216–19 (ASTM, 2019). VS content was measured by heating the sample at 950 °C for 7 minutes (min) in a lidded crucible following ASTM D3175–20 (ASTM, 2020), while ash content was obtained by combusting the sample at 600 °C According to ASTM D3174–12 (Reapproved 2018)e1 (ASTM, 2018).

Chemical characteristics analysis

In this study, all chemical analyses were carried out in a laboratory accredited by ISO/IEC 17025:

"Testing and Calibration Laboratories". The analyses followed a quality assurance and quality control (QA/QC) protocol, which included certified reference materials, blanks, and replicate samples, calibrated instruments, and properly documented procedures to ensure data accuracy, precision, and traceability. The standard procedure for SLM's total organic carbon (TOC) analysis follows Method 5220, established by the American Public Health Association (APHA), American Water Works Association (AWWA), and Water Environment Federation (WEF) (APHA *et al.*, 2024). A spectrophotometer was employed to measure TOC at 561 nanometers (nm) after extraction with potassium dichromate ($K_2Cr_2O_7$) and sulfuric acid (H_2SO_4). The determination of total Kjeldahl nitrogen (TKN) was carried out following APHA, AWWA, and WEF Method 4500-Norg (APHA *et al.*, 2024). TKN was measured by digesting 0.5 g of the SLM sample with 20 milliliters (mL) of distilled water, 10 grams (g) of a salt mixture, 2–3 Henger granules, and 30 mL of H_2SO_4 using a Kjeldahl digestion heater at 350°C until a clear extract was obtained. The resulting digest was assessed using a colorimetric method at a wavelength of 636 nm. Total phosphorus and total potassium were determined by extracting 2 g of the SLM sample with 25% hydrochloric acid (HCl) on a shaker for 5 hours. The filtrate obtained was measured using a spectrophotometer at 882 nm to determine total phosphorus (P) and potassium (K) contents, following the guidelines established by the United States Department of Agriculture (USDA)– Natural Resources Conservation Service (NRCS) (method code No. 4D5). Available P was determined using the Olsen method following USDA-NRCS standard method 4D5 (USDA-NRCS, 2022). Approximately 1.0 g of the SLM sample was mixed with 20 mL of the Olsen sodium bicarbonate ($NaHCO_3$) extracting solution in a shake bottle, shaken for 30 min, and then examined spectrophotometrically at 882 nm. Cation exchange capacity (CEC) in SLM samples was measured using the USDA-NRCS standard (method code no. CEC-7) (USDA-NRCS, 2022). To determine the CEC, 2.5 g of the sample was saturated in a percolation tube with 25 mL of a 1 molar (M) ammonium acetate (NH_4OAc) (pH 7) solution. The estimation of textural fractions, according to USDA classification, involved dividing the SLM sample into granulometric categories (clay, silt, and sand) following oxidation, salt extraction, and peptization processes using hydrogen peroxide (H_2O_2), HCl, and tetrasodium pyrophosphate ($Na_4P_2O_7$), respectively (USDA-NRCS, 2022). The sand component was derived by washing and collecting the remnants that remained on a 75 micrometers (µm) sieve. The silt fraction was extracted by pipetting immediately after stirring the filtrate, and the clay fraction was collected by pipetting at a depth of 5.2 centimeters (cm) after allowing the sample to settle for 3.5 h. The collected clay, silt, and sand fractions were gravimetrically analyzed to determine the weight percentage of each textural class. Heavy metal concentrations in the SLM were analyzed using the United States Environmental Protection Agency (USEPA) SW-846 test method 1311, Toxicity Characteristic Leaching Procedure (USEPA, 1992) for extracting metals. The levels of the extracted metals were subsequently evaluated through atomic absorption spectroscopy. To determine whether SLM is adequate as a growing medium, its chemical properties were compared with compost quality standards. SLM originated from decomposed waste, which contained high organic matter. When it comes to assessing SLM as a growing medium, compost standards are more fitting than those for mineral soil. Rich in organic matter and nutrients such as carbon (C), nitrogen (N), phosphorus (P), potassium (K), potential of hydrogen (pH), salinity, cation exchange capacity (CEC), SLM resembles compost, which these standards are designed to evaluate, including parameters directly affecting plant growth and safety, such as salinity and heavy metal content. Soil standards that emphasize mineral content and long-term fertility are becoming less significant, whereas compost standards are in line with widely accepted horticultural practices and literature, thereby confirming the practical effectiveness of SLM as a substrate for plant growth.

Statistical analysis

The study design involved a single independent factor (sampling day) with triplicate measurements, so a one-way analysis of variance (ANOVA) was used to assess differences in physicochemical properties (moisture, ash, texture, cation exchange capacity, pH, total organic carbon, total Kjeldahl nitrogen, C/N ratio, phosphorus, potassium, and heavy metals) across the seven sampling days and to evaluate the effects of soil-like material-to-compost ratios on plant growth in the greenhouse experiment. The Shapiro–

Table 1: Composition of FF (<50 mm) from LMM after trommel screening at the LM plant.

Component	Proportion		
	Minimum (%)	Maximum (%)	Average (%)
SLM (<4.75 mm)	37.92	43.80	40.61 ± 2.97
SLM (4.75–50 mm)	40.91	45.92	42.91 ± 2.66
Plastics	8.33	9.53	8.76 ± 0.67
Wood fragments and twigs	2.48	4.13	3.40 ± 0.84
Glass and ceramics	2.27	3.96	3.07 ± 0.85
Rubber and textiles	0.81	0.94	0.86 ± 0.07
Metals	0.16	0.27	0.24 ± 0.03
Food waste (bones and shells)	0.08	0.27	0.17 ± 0.10

Wilk and Levene's tests were employed to evaluate normality and variance homogeneity, and Tukey's HSD was implemented in cases where significant differences were found ($p < 0.05$).The results are expressed as mean ± standard deviation.

Planting experiment

A greenhouse experiment was conducted to evaluate SLM-to-compost mixtures (100%:0% to 60%:40% weight per weight (w/w) with a 10% interval) as a growing medium for *Calliandra calothyrsus*, a legume tolerant of poor substrates (Hendriyanto *et al.*, 2023; Ridwan *et al.*, 2023). Seedlings aged twelve weeks and measuring approximately 50 cm in height were transplanted during the rainy season (from November 2024 to March 2025), with ten replicates allocated to each SLM-to-compost treatment combination. Using five treatment combinations, there were a total of 50 plants. The polybags were positioned on greenhouse benches in a completely randomized design, with placements allocated using a random number table to minimize environmental or positional impacts. This randomization confirms that any differences detected among treatments are attributable to the SLM-to-compost medium instead of the bench location. The experiment employed a commercial compost with a total carbon content of 26.1–32.7% (dry weight), N 2.3–2.9%, P 0.5–0.7%, K 1.3–2.3%, a carbon-to-nitrogen (C/N) ratio of 11–14, pH of 7.8–8.4, and salinity of 2.9 g/L. The relatively low C/N ratio indicates that the compost is mature, with organic matter sufficiently decomposed and nitrogen readily available for plant uptake. The compost was formulated from a combination of animal manure, like chicken or cow, and plant-derived waste, such as vegetable scraps and green waste. In the greenhouse experiment, *Calliandra calothyrsus* seedlings were cultivated in the medium in 9–10 L polybags. As a result of the media's porous and well-drained nature, seedlings were irrigated on a daily basis to uphold a field capacity of 50–70%, approximately 4–5 L per bag. Soil moisture was monitored using a soil moisture meter and visual observation of the media to ensure optimum growth. Furthermore, plant height was documented on a biweekly basis to serve as a growth indicator. Plant height was used as the primary growth indicator due to its practicality for continuous, non-destructive monitoring and its role as a representative measure of early vegetative development in *Calliandra calothyrsus* seedlings, as directly assessing roots, leaves, or tissue quality would be difficult or destructive.

RESULTS AND DISCUSSION

Fine fraction composition

Table 1 shows that the 50 mm trommel screen yielded 83.52 ± 2.36% SLM, consisting of 40.61 ± 2.97% of particles <4.75 mm and 42.91 ± 2.66% of 4.75–50 mm. Plastics (8.76 ± 0.67%), wood fragments and twigs (3.40 ± 0.84%), glass and ceramics (3.07 ± 0.85%), rubber and textiles (0.86 ± 0.07%), metals (0.24 ± 0.03%), and food waste (0.17 ± 0.03%) were the remaining fractions. A prior investigation utilizing a 30 mm screen revealed that 96.48% of the <30 mm fraction was SLM (Prihartanto *et al.*, 2023a), surpassing the 83.52% achieved with the 50 mm screen. The larger screen size let more impurities entering the FF, which decreased the purity of SLM. Consequently, the <30 mm SLM was finer, more homogeneous, and purer than the <50 mm SLM, which made it better suited for agricultural applications. This variation illustrates the composition and the historical context

of the Bantargebang landfill: coarser materials are bulkier and less amenable to degradation, while the finer materials are more fragmented and have undergone partial degradation, resulting in a purer, soil-like SLM that is suitable for farming. As explained in the sample collection and preparation section, the <4.75 mm SLM was chosen as the primary growing medium because its particle size closely resembles natural soil and contains fewer impurities than the <30 mm fraction, resulting in a more uniform medium that supports root penetration and air circulation (Vollprecht *et al.*, 2020). To obtain this FF, the <50 mm material was rescreened using a 4.75 mm mesh. However, because separating impurities from particles <4.75 mm is technically challenging, all materials below this size were classified as SLM, reflecting the difficulty of fully removing impurities from this fraction. Linking these outcomes to the composition of landfills gives a context-specific rationale that surpasses just comparison with previous studies.

Physical and chemical characteristics of SLM

Table 2 shows that the moisture content of LMM (56.95–70.29%, average 63.60 ± 9.45%) partially met the compost standard of 40–60% (NSAI, 2004; Rahman *et al.*, 2020; USDA-NRCS, 2020) and was consistent with previous studies of 47.00–63.47% (Kristanto *et al.*, 2020; Wahyono *et al.*, 2019; Widyarsana and Tambunan, 2022). In contrast, the <4.75 mm SLM had a lower moisture content (30.65–36.97%, average 32.78 ± 1.97%), falling below the standard because finer, drier particles passed through the screen while wetter materials were retained. SLM's moisture content illustrates the manner in which fine, dry particles traverse the trommel screen and the environmental conditions present at the Bantargebang landfill. The anaerobic decomposition generates material with a specific porosity, whereas seasonal fluctuations induce variations in moisture content, reducing water availability and delaying microbial activity. In light of this condition, SLM derived from LM needs to be hydrated or combined with wetter organic materials to facilitate its decomposition and improve its appropriateness for use as a growing medium. Although lower moisture improves airflow, eliminates anaerobic conditions, and makes handling easier (Avifah *et al.*, 2022), 32.78% moisture could inhibit microbial activity since optimum activity requires 40–60% moisture, indicating that the SLM should be moistened or blended with wetter organic materials. The SLM exhibited high VS (78.60 ± 0.54%) and total organic carbon (TOC) with 57.08 ± 5.58% (Table 2), exceeding TOC standards for compost in Indonesia and India (9.8–32%) and previously reported values for unseparated LMM (42.46–45.91%) and SLM (52.87–55.67%) (Datta *et al.*, 2021; Kristanto *et al.*, 2020; Prihartanto, *et al.*, 2023b). Even though VS is not specified in the criteria for compost quality, its concentration was found to be greater than prior studies (69.17–75.22%). These elevated values indicate substantial partly decomposed organic matter that can still support microbial activity and improve soil structure. The ongoing presence of elevated VS and TOC levels can be attributed to the unique composition of waste and the historical context of the Bantargebang landfill, where the accumulation of plastics, wood, and other inert materials hinders decomposition and preserves organic carbon. This context explains why high VS coexists with relatively low moisture in the <4.75 mm fraction, reflecting the selective passage of drier, fine particles through the screen. Nonetheless, the continued presence of elevated VS suggests the presence of resistant materials, which aligns with the <50 mm fraction that encompasses plastics, wood, glass, ceramics, rubber, textiles, and metals (Table 1). Wood, for example, resists anaerobic decomposition because it contains lignin and lignocellulose (Khan and Ahring, 2019). Although LMM moisture generally met or exceeded the optimum range of 40-60% for microbial activity, landfill conditions such as compaction, restricted oxygen, and large amounts of inert or slowly degradable waste had greater effects on decomposition rates than moisture alone (González-Arqueros *et al.*, 2021). By associating moisture, VS, and TOC with the waste composition and deposition history of the landfill, these findings enhance a deeper mechanistic insight into decomposition dynamics, surpassing simple numerical comparison with previous studies.

The ash content of SLM varied between 23.19% and 30.85% (average 27.35 ± 5.42%). These values were higher than the 20.97% reported in a previous SLM study (Widyarsana and Tambunan, 2022), despite the compost standard not specifying ash content. The significant ash content present in SLM arises from the accumulation of inorganic, mineral-

Table 2: Physical-chemical properties of SLM

Parameter	Unit	This research			Previous Studies	Compost quality standards	Interpretation
		Min.	Max.	Average			
Physical properties:							
Moisture content of LMM	%	56.95	70.29	63.60 ± 9.45*	47.00–63.47 (Kristanto *et al.*, 2020; Wahyono *et al.*, 2019; Widyarsana and Tambunan, 2022)	40–60 (NSAI, 2004; Rahman *et al.*, 2020; USDA-NRCS, 2020)	Higher due to its landfill origin.
Moisture content of SLM	%	30.65	36.97	32.78 ± 1.97	N/A	40–60 (NSAI, 2004; Rahman *et al.*, 2020; USDA-NRCS, 2020)	Lower due to screening; requires moisture adjustment or amendment.
Volatile solids content	%	78.22	79.19	78.60 ± 0.54	69.17–75.22 (Datta *et al.*, 2021; Kristanto *et al.*, 2020; Prihartanto, *et al.*, 2023b)	N/A	Higher VS indicates immature organic matter.
Ash content	%	23.19	30.85	27.35 ± 5.42	24.78–43.32 (Widyarsana and Tambunan, 2022)	N/A	Higher ash suggests mineral-rich SLM.
pH	–	7.63	7.85	7.76 ± 0.16*	N/A	6.80 – 7.50 (NSAI, 2004)	Slightly alkaline; may reduce P availability.
Three fractions texture							
– Sand	%	42.96	57.16	51.21 ± 4.60	N/A	N/A	Coarse texture limits water retention.
– Silts	%	13.20	30.22	20.29 ± 6.94	N/A	N/A	
– Clay	%	18.21	38.64	28.50 ± 6.87	N/A	N/A	
Chemical properties:							
Cation exchange capacity	cmol(+)/kg	15.89	17.55	16.39 ± 0.60***	N/A	Low 5–16 Medium 17–25 (Syachroni, 2020)	Low–moderate; reflects immaturity of organic matter.
Total organic carbon	%	51.24	66.55	57.08 ± 5.58*	42.46–55.67 (Schneider *et al.*, 2021; Rahman *et al.*, 2020)	9.80–32 (NSAI, 2004)	Higher TOC but immature; requires stabilization.
Total Kjeldahl nitrogen	%	1.88	2.27	2.04 ± 0.14	0.4–1.49 (Widyarsana and Tambunan, 2022)	0.4–6.0 (NSAI, 2004)	Higher N availability relative to previous studies.
C/N ratio	–	25.18	30.39	27.94 ± 1.83	N/A	10–40 (NSAI, 2004; Rahman *et al.*, 2020; NARA, 2016	Within allowable range but risk of immobilization remains.
Available phosphorus (Olsen)	milligram per kilogram (mg/kg)	50.32	63.5	57.88 ± 4.88	N/A	1000–6200 (NSAI, 2004; Sayara *et al.*, 2020)	Deficient; requires P amendment.
Total phosphorus (P_2O_5)	mg/kg	100.92	166.99	140.20 ± 24.53**	N/A	1000–6200 (NSAI, 2004; Sayara *et al.*, 2020)	Deficient; requires P amendment.
Potassium (K_2O)	mg/kg	581.75	662.95	598.33 ± 32.39	N/A	2000 (NSAI, 2004)	Below standard; supplement required.

Notes: * Value exceeded the maximum compost quality standard. ** Value below the minimum compost quality standard. *** Value falls within the lowest acceptable grade of the compost standard

rich materials in the Bantargebang landfill—chiefly calcium, magnesium, and potassium oxides (CaO, MgO, K_2O) (Kaniowski *et al.*, 2022)—which can support plant nutrition, boost soil fertility, and regulate pH balance. The presence of alkaline oxides in the ash, such as CaO and MgO, may elevate the pH of the SLM, explaining why SLM pH, obtained from the LM plant at Bantargebang, was slightly alkaline (7.63–7.85). Ash came from various sources, including construction debris, bones, shells, food waste, and persistent non-biodegradables such as glass, plastic, and metals. Furthermore, the presence of these minerals can positively affect soil quality, but excessive ash levels may lead to higher pH, salinity, and electrical conductivity, possibly restricting seed germination and water absorption, particularly in salt-sensitive species (Kanu *et al.*, 2021). Ash potentially accumulates heavy metals, including cadmium (Cd), lead (Pb), and zinc (Zn), affecting soil quality and food safety (Faragó *et al.*, 2023; Latosińska and Czapik, 2020). Although SLM pH is slightly higher than the compost standard of 6.80-7.50, it is nevertheless considered suitable for agricultural use (NSAI, 2004). SLM's slightly alkaline pH may enhance nutrient availability, particularly P, calcium (Ca), and magnesium (Mg). It can also help microorganisms flourish, which can improve soil fertility and speed up organic matter decomposition (Muraru *et al.*, 2021). These conditions may promote the breakdown of organic matter, the recycling of nutrients, and the development of a robust soil structure, all of which could improve soil productivity and support plant growth. However, depending on the pH level, certain heavy metals may exhibit different behaviors. While a slightly alkaline pH can increase the mobility of elements such as molybdenum (Mo) and selenium (Se) (Muraru *et al.*, 2021), which can be harmful to plants and the environment, it can also make metals such as iron and aluminum less soluble, making them less toxic (Rani *et al.*, 2021). Heavy metals including Cd, Pb, and Zn exhibit a tendency to have reduced mobility in the slightly alkaline pH range of SLM (Latosińska and Czapik, 2020). This reduction is attributed to the ability of these metals to bind with soil elements such as organic matter and iron or manganese oxides, or to form insoluble hydroxides, which in turn diminishes their solubility and bioavailability. In addition, while K is typically accessible over a wide pH range, P may become less available in alkaline conditions due to the formation of insoluble calcium-phosphate compounds (Bechtaoui *et al.*, 2021). By considering the unique waste composition of the landfill, one can better understand the interactions among ash content, pH, and metal mobility, which in turn provides a context-specific perspective on nutrient availability and possible risks in SLM applications. As a result, maintaining a balanced soil pH is critical for maximizing nutrient availability and reducing the risks related to metal mobility. The SLM texture was composed of sand 51.21 ± 4.60%, clay 28.50 ± 6.87%, and silt 20.29 ± 6.94%. Its sandy texture inhibited aggregate formation and minimized the surface area for cation exchange by reducing the effect of finer clay particles (Sasongko *et al.*, 2024). The coarse, sandy texture reflects the waste composition and long-term decomposition conditions in Bantargebang landfill, limiting water retention and nutrient-holding capacity but providing potential for improvement through amendments such as compost, biochar, or fine clay. The rough texture resulted in swift water drainage, which raised the likelihood of nutrient loss through leaching, especially in tropical regions like Indonesia, characterized by high rainfall (Corrêa *et al.*, 2018). Although high TOC usually helps improve soil structure, retain water, and hold nutrients (Muraru *et al.*, 2021), its benefits in SLM were limited because the texture was too coarse and the organic matter was not yet fully decomposed. Table 2 shows that the SLM had a low CEC (15.89–17.55 centimoles of positive charge (cmol(+)/kg); average 16.39 ± 0.60 cmol(+)/kg), indicating low to moderate soil fertility (Syachroni, 2020). The coarse sandy texture and partially decomposed organic matter from the Bantargebang landfill are reflected in this low CEC, which limits nutrient retention. Nonetheless, it underscores the potential for improvement using compost, biochar, or fine clay amendments. Although the SLM contained a relatively high TOC content (57.08 ± 5.58%) and a moderate proportion of clay (28.50 ± 6.87%), its capacity to retain and supply essential nutrients remained limited, thereby reducing its overall agronomic value. Nonetheless, the majority of organic matter in SLM was in an immature and undecomposed state, as evidenced by its elevated VS content, which had minimal impact on CEC (Owusu-Nimo *et al.*, 2019). To improve the CEC of SLM, specific treatments were required. Composting

played a crucial role in stabilizing organic matter by converting TOC into humified carbon compounds that contained numerous functional groups capable of holding nutrient cations (USDA-NRCS, 2023). Adding materials rich in charged colloids, such as mature compost, manure, or humus, improved CEC and nutrient availability for plants. Biochar made from woody substances like coconut shells, bamboo, or hardwood waste has been recognized as an exceptionally effective soil amendment. Its large surface area, high porosity, and stable chemical composition collectively enhance both CEC and water retention (Bao *et al.*, 2021). The addition of fine clay enhanced nutrition and water retention (Minhal *et al.*, 2020). The TKN concentration of the SLM ranged from 1.88% to 2.27% (average 2.04 ± 0.14%), meeting the compost quality standards of 0.4–6.0% (NSAI, 2004; Rahman *et al.*, 2020; NARA, 2016). The relatively high TKN reflects the accumulation of nitrogen-rich organic matter in Bantargebang landfill over time, indicating potential for SLM as a growing medium, though its agronomic value could be further enhanced through composting or mixing with other amendments. These values were comparable to those of normal compost (2.79%) (Yusmayani, 2019) and higher than those reported for the Sumur Batu landfill, adjacent to the Bantargebang IMSWTF landfill, which ranged from 0.29% to 1.58% (Widyarsana and Tambunan, 2022). Adequate nitrogen supports protein synthesis, vegetative growth, and the comprehensive development of plants (Heiskanen *et al.*, 2022), which implies that SLM has potential as a growing medium, particularly for degraded or low-input soils. The C/N ratio of SLM varied between 25.18 and 30.39 (average 27.94 ± 1.83), meeting the compost quality standards of 10–40 (NSAI, 2004; Rahman *et al.*, 2020; NARA, 2016). This high C/N ratio reflects the accumulation of partially decomposed organic matter in Bantargebang landfill and indicates potential nitrogen immobilization, suggesting further treatment is needed to optimize nutrient availability for plants. These values approached the upper limit of the ideal range for microbial decomposition (25–30%) (Sahoo *et al.*, 2023). A value close to 30 suggests that the C/N ratio provides sufficient carbon for microbial energy but may result in nitrogen deficiency during decomposition (Li *et al.*, 2022). Consequently, the SLM was only partially stabilized and needed further treatment to prevent nitrogen immobilization (Owusu-Nimo *et al.*, 2019). In situations where nitrogen levels in the material are insufficient, microbes will immobilize nitrogen from the surrounding soil, which decreases the nitrogen accessible to plants and may impede their growth (Wu *et al.*, 2025). The organic matter in SLM had been decomposed slowly and passively for approximately 25 years in the landfill up to 2025 due to the lack of oxygen, inadequate moisture control, and minimal active management of microbes (UNFCCC, 2005). Heavy rains during the wet season could saturate LMM and restrict oxygen availability, whereas in the dry season, LMM could desiccate, suppressing microbial activity. The fluctuations associated with the seasons impeded the decomposition process and lowered microbial activity (Schaap *et al.*, 2023), which caused higher levels of VS and TOC to be preserved in the SLM. The SLM's total P content ranged from 100.92 to 166.99 mg/kg (average 140.20 ± 24.53 mg/kg), while the available phosphorus, which is accessible to plants, ranged from 50.32 to 63.50 mg/kg (average 57.88 ± 4.88 mg/kg). The low total and available P reflect the composition and historical deposition of waste in Bantargebang landfill, and the slightly alkaline pH further limits P availability, suggesting that SLM may require P supplementation for optimal plant growth. Both measurements fell considerably lower than the compost quality standard set between 1000–6200 mg/kg (NSAI, 2004; Sayara *et al.*, 2020). Since P is vital for root development and plant reproduction, a deficiency may negatively impact plant performance, especially in phosphorus-demanding crops. In addition to its low total P content, the SLM's slightly alkaline pH limited P availability through chemical fixation, as P forms insoluble calcium-phosphate complexes under alkaline conditions (Wijaya, 2017). The K content of SLM ranged from 581.75 to 662.95 mg/kg (average 598.33 ± 32.39 mg/kg), which was below the compost quality standard of ≥1000 mg/kg (NSAI, 2004). The limited presence of potassium-rich materials in the Bantargebang landfill is reflected in the low K content, which implies that SLM may need to be supplemented with K sources to achieve balanced nutrition for plant growth. However, when applied directly to plant cultivation, the low potassium and phosphorus levels in SLM could lead to nutritional imbalances that may restrict plant growth (Keerthana *et al.*, 2024).

Table 3: Heavy metal contents in SLM and comparison with compost quality standards

No.	Parameter	Unit	Heavy metal content			Previous study results (Pratama *et al.*, 2025)	Compost quality standard (Pratama *et al.*, 2025)	
			Min.	Max.	Average		Indonesia	Other countries
1.	Fe	mg/kg	10,96	28,402	22,441 ± 9,938	21,578.23 ± 2,756.68	20.000	N/A
2.	As	mg/kg	<0.0004	<0.0004	<0.0004	4.07 ± 1.13	13	13
3.	Zn	mg/kg	1,310	4,282	2,841 ± 1,488	729.20 ± 223.00	5,000	N/A
4.	Mn	mg/kg	5,241	7,780	4,471 ± 4,014	6.216 ± 1.368	1,000	N/A
5.	Pb	mg/kg	50.69	91.54	72.84 ± 20.64	30.71 ± 9.26	150	150 – 1,500
6.	Cd	mg/kg	1.27	2.07	1.64 ± 0.40	1.15 ± 0.17	3	1.01 – 100
7.	Hg	mg/kg	<0.0001	<0.0001	<0.0001	1 ± 0.63	0.8	0.37 – 15
8.	Cr^{VI}	mg/kg	<0.24	<0.24	<0,24	–	210	N/A

Compost, manure, humus, and biochar have been found to stabilize organic matter, retain moisture, and increase nutrient retention capacity (Baloyi *et al.*, 2023; USDA-NRCS, 2023). Manure contributed to better soil structure and nutrient accessibility, yet it was often essential to use mineral sources such as rock phosphate, superphosphate, potassium chloride (KCl), or biomass ash to fulfill the phosphorus and potassium requirements of crops (Ayamba *et al.*, 2021). Mixed SLM with compost combined with zeolite or phosphate rock acted as slow-release fertilizers that increased nutrient availability. To reduce leaching and ensure prolonged nutrient release, targeted nutrient enrichment using mineral–organic blends or slow-release formulations was recommended (Legese *et al.*, 2024). These characteristics of SLM texture, nutrient content, and C/N ratio reflect the specific composition and long-term history of waste in Bantargebang landfill, where coarse sandy particles, partially decomposed organic matter, and low P and K levels accumulate, limiting natural fertility but providing potential for improvement through composting, biochar, and mineral amendments.

Toxicity of SLM

The metal concentrations in SLM are compared with compost quality standards to assess material safety, while phytotoxic thresholds from literature for similar leguminous and woody species are used to evaluate potential impacts on plant growth, as species-specific data for *Calliandra calothyrsus* are not available. Table 3 shows that the SLM contained iron (Fe) ranging from 10,968 to 28,402 mg/kg (average 22,441 ± 9,938 mg/kg), exceeding the Indonesian compost quality standard of 20,000 mg/kg. Typically, the growth of plants is suppressed at Fe levels greater than 28,000 mg/kg (Salim *et al*., 2021), which may result in leaf spots, stunted growth, insufficient root development, and lower nutrient absorption (Li *et al.*, 2019; Mahender *et al.*, 2019). The manganese (Mn) content in SLM ranged from 5,241 to 7,780 mg/kg (average 4,471 ± 4,014 mg/kg), exceeding compost quality standards and potentially causing toxicity symptoms such as poor root growth and chlorosis. Mitigation techniques include adjusting pH, adding organic matter, and selecting manganese-tolerant plant species (Simonova *et al.*, 2020). Furthermore, the Cd concentration ranging from 1.27 to 2.07 mg/kg (average 1.64 ± 0.40 mg/kg) exceeded the lower limits of international standards for compost of 1.01–100 mg/kg. Cd is toxic for humans and plants. It has the potential to impair plant growth and photosynthesis, and it may accumulate in edible parts, resulting in cancer and kidney damage. However, the slightly alkaline pH (7.63–7.85) promoted its immobilization through complexation with organic matter and oxides (Ejaz *et al.*, 2023). In spite of the variations in their biological functions and toxicity, the strategies for mitigating Fe, Mn, and Cd are quite similar. Altering soil pH, incorporating organic amendments, and choosing plant species that are tolerant are vital for minimizing metal bioavailability and ensuring the safe and sustainable utilization of SLM as a growth medium. These elevated metal concentrations reflect the composition and historical deposition of waste in Bantargebang landfill, where metal-rich materials accumulate over time. Grasping the landfill-specific origins and their relationships with pH and organic matter offers valuable context for evaluating SLM safety and directing effective mitigation strategies for agricultural applications. When compared to

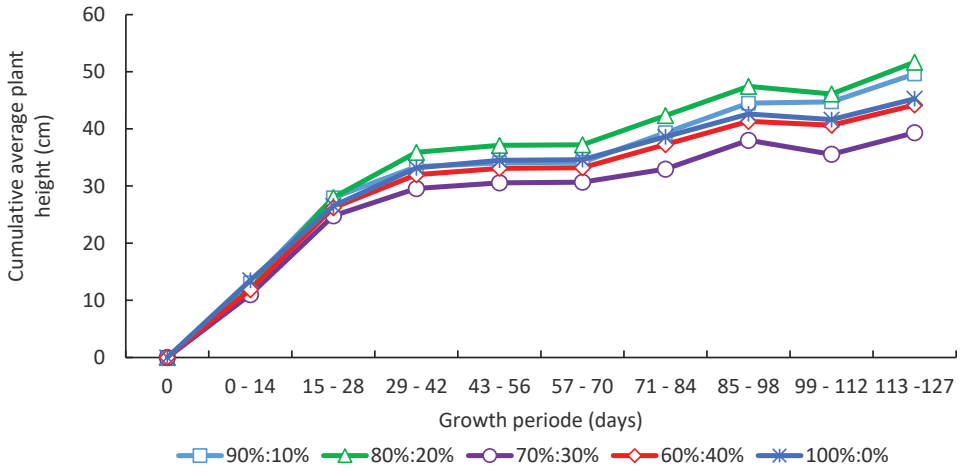

Fig 4: Plant height progression of *Calliandra calothyrsus* in growing medium at various SLM-to-compost mixture ratios

known phytotoxic thresholds for leguminous plants such as *Calliandra calothyrsus*, the measured Fe and Mn contents in SLM approach levels that may inhibit growth, but Cd remains well below its critical toxicity thresholds. The correlation indicates a risk of phytotoxic effects, particularly at high SLM ratios, emphasizing the importance of mitigating techniques such as pH adjustment, organic amendments, and the use of tolerant plants. This study is limited by the application of the toxicity characteristic leaching procedure (TCLP), which only measures the leachable metal fraction rather than total content. Future work will therefore apply total digestion methods such as USEPA methods 3050B/3051A, to better assess total metal burden and long-term phytoavailability.

Plant growth and its relationship with the SLM–to–compost ratio

Fig. 4 shows that the linear height growth trend of *Calliandra calothyrsus* plants was almost similar across all SLM-to-compost mixture ratios over the first 28 days, ranging from 24.78 to 28.00 cm. The uniformity of this initial growth pattern across all mix ratios, including 100% SLM without any compost, implies that the plants' early growth was primarily fueled by the nutritional reserves of the seedlings instead of nutrients from SLM or compost. During the first 28 days, the high C/N ratio caused microbial nitrogen immobilization, limiting nitrogen availability to plants and resulting in a growth plateau, with seedlings relying primarily on their internal nutrient reserves. Compost provided available N and organic carbon (C), but it had minimal impact on initial growth. The most likely reason is that nutrient mineralization had not yet occurred. During this phase, the seedlings maintained their reliance on their own nutrient supplies, whereas the nutrients found in the SLM and certain compost components stayed in forms that the plants could not utilize. The compost likely contributed to physical improvements in the growing medium, such as enhanced aeration and water retention, which in turn supported initial root growth. As a result, the similar growth patterns across all mix ratios suggested that seedling nutrient reserves and favorable physical conditions had a greater influence than the initial nutrient availability of the growing medium.

On day 28, the seedlings' nutrient supplies were fully consumed; thus, the plants were compelled to use compost to maintain their growth. Between days 29 and 42, growth slowed across all SLM-to-compost ratios due to depletion of readily available nutrients from compost, particularly P and K. As compost nutrients ran out, SLM gradually contributed nitrogen, but its low P (140.20 ± 24.53 mg/kg) and K (598.33 ± 32.39 mg/kg), slightly alkaline pH (7.76 ± 0.16), and low CEC (16.39 ± 0.60 cmol(+)/kg) limited nutrient availability. These factors together caused nutritional deficiencies, marking a significant moment when SLM by itself was insufficient to maintain continued growth. Between days 29 to 70, the 80%:20% SLM-to-compost ratio consistently demonstrated

better outcomes. Compared to other ratios, this result is most likely due to an adequate supply of compost supporting initial growth and sufficient SLM allowing for a gradual release of nitrogen. It should be highlighted that the explanation is entirely hypothetical, as aeration differences between mixes and possible metal-related stress were not directly measured (for instance, bulk density, porosity, and metal absorption in plant tissues). Consequently, these interpretations ought to be viewed as provisional and necessitate further confirmation in future studies. Higher compost ratios (60%:40%, 70%:30%) may have experienced rapid nutrient loss and insufficient aeration, whereas 90%:10% and 100%:0% ratios lacked adequate P and K, with excessive heavy metal concentration (Fe 22,441 mg/kg, Mn 4,471 mg/kg, and Cd 1.64 mg/kg) limiting growth. The accumulation of heavy metals in plants has the potential to induce oxidative stress, interfere with photosynthesis, and suppress important enzymes (Ejaz *et al.*, 2023). Although the slightly alkaline pH generally reduced heavy metal mobility, the small amount of organic matter in high-SLM mixtures limited stabilization. Growth improved in all ratios starting on day 70, as SLM mineralization released nitrogen that had previously been immobilized by microorganisms, promoting root growth and nutrient uptake. The outcomes demonstrate that the combination of initial compost nutrients and the gradual nitrogen release from SLM played a vital role in supporting growth. Plant growth declined at all ratios from days 99 to 112, possibly due to delayed mineralization from days 57 to 98, which made less N available from SLM. Additionally, the lower P and K content, which were both below compost quality standards, also inhibited plant growth. Moreover, the coarse and sandy texture of the SLM (51.21%) and moderate to low CEC reduced its water and nutrient-retaining capacity, lowering support for larger plants. Between days 99 and 112, plant growth slows down at all ratios due to the delayed mineralization between days 57 and 98, making SLM's nitrogen less available. As decomposition continued, microbes needed less nitrogen, allowing plants to absorb more. At this stage, the plants had the capacity to take in more water and nutrients as their roots were developing at an accelerated rate. Nevertheless, owing to physical limitations, the original arrangement of the compost, and the delayed nutrient release from the SLM, the growth of the plants progressively diminished. This study demonstrates that SLM is a beneficial growing-medium material. Although its organic matter remains unstable, its high organic carbon content can improve the growing medium quality after stabilization (blending SLM with nutrient-rich or compost amendments. These treatments improve the soil by making it smoother, holding more water, increasing the CEC, making nutrients more available, and lowering the risk of heavy metals. Treated SLM can be used as a growing medium, a cover for a landfill, a material for land reclamation, or a way to improve compost (Parrodi *et al.*, 2018). Subsequent studies should emphasize the enduring performance and environmental safety of stabilized SLMs. It includes assessing nutrient release using laboratory incubation and multiple planting experiments to monitor nitrogen mineralization, micronutrient release, and medium fertility changes. It is essential to conduct repeated pot or field studies with a variety of non-food plant species—especially for the purpose of revegetating post-closure landfills—to thoroughly evaluate plant growth, nitrogen uptake, and the feasibility of application on a field scale. Monitoring leachate, cation exchange capacity, C/N ratio, microbial activity, and pH will help in ensuring nutrient stability over cultivation cycles. Environmental safety should be assessed using heavy metal leaching, speciation, plant uptake assays, and ecotoxicity studies. Prolonged field monitoring, in conjunction with relevant environmental standards, ought to facilitate risk assessments aimed at verifying that stabilized SLM is safe and carries the least toxicity risks.

CONCLUSION

This study confirms that SLM recovered from landfill-mined material at the Bantargebang IMSWTF has substantial potential as a sustainable growing medium for non-food crops when properly treated. The SLM contains a high TOC content of 57.1% and an adequate N content of 2.04%. However, the C/N ratio of 27.9 suggests a likelihood of nitrogen immobilization during initial growth stages. Its coarse texture, low CEC, and limited P and K contents indicate the necessity for amendments to enhance nutrient content and water retention. The greenhouse experiment demonstrated that a mixture of 80% SLM and 20% compost yielded the best results, achieving

an average final plant height of 51.67 cm over a period of 127 days, surpassing other mix ratios which ranged from 39.33 to 49.61 cm. Plant growth initially relied on nutrient reserves contained in the seedlings; after these reserves were depleted, compost supplied readily available nutrients, while SLM contributed nitrogen gradually through mineralization. These results emphasize the necessity of merging SLM with organic amendments to boost nutrient availability and promote sustainable plant establishment. This study provides an important novel contribution by quantifying the physical, chemical, and toxicological characteristics of SLM obtained from a full-scale tropical landfill mining operation and demonstrating how these site-specific characteristics translate into plant response. The study further demonstrates that the optimal amendment ratio for plant growth and establishment is 80% SLM combined with 20% compost. Heavy metal concentrations in the compost exceeded quality standards, particularly Fe (22,441 mg/kg), Mn (4,471 mg/kg), and Cd (1.64 mg/kg), indicating potential risks if used untreated. These results emphasize the importance of stabilization prior to utilization, which in this scenario relates to co-composting or combining SLM with nutrient-dense amendments to boost nutrient accessibility and minimize metal bioavailability. The slightly alkaline pH of 7.76 in SLM could potentially limit the mobility and bioavailability of some metals, reducing their potential risks. However, to ensure plant health and environmental safety, stabilization and blending with organic amendments are required. In addition to its agronomic potential, SLM contributes to landfill management through resource recovery and circular economy initiatives, reducing the landfilled waste quantity and producing valuable products. To improve the utilization of SLM and ensure environmental safety, additional study is required on long-term monitoring, nutrient enrichment, and field-scale applications. Future research should assess long-term performance and safety of stabilized SLM through incubation and sequential planting trials to monitor nitrogen release, micronutrient availability, and fertility changes. Pot or field studies with multiple non-food species—particularly for landfill revegetation—should evaluate growth and nutrient uptake, while leachate and key soil properties should be monitored to confirm nutrient stability over time.

AUTHOR CONTRIBUTIONS

N. Sudiana contributed to conceptualization, methodology, formal analysis, funding acquisition, and manuscript preparation. Prihartanto contributed to conceptualization, supervision, review, and editing. I.N. Sulistiawan contributed to project administration and visualization. E.H. Sittadewi contributed to supervision, review and editing, validation, and formal analysis. D.N. Utami contributed to the investigation, validation, and formal analysis of the physical characteristics of SLM. E. Kusumastuti contributed to data curation and the formal analysis of plant growth experiments. B. Rahayu contributed to the validation of laboratory analyses of heavy metal concentrations in SLM. N. Hidayat contributed to data curation and the validation of SLM composition. K.A. Haris contributed to the investigation, validation, and formal analysis of the chemical characteristics of SLM. T.E. Pararto contributed to data curation and the formal analysis of landfill mining processes. L. Noviana contributed to the investigation and formal analysis of solid waste composition.

ACKNOWLEDGEMENT

The authors gratefully acknowledge the National Research and Innovation Agency of Indonesia (BRIN) for providing research funding [No. 1/III.5/HK/2024] through the Research Organization for Life Sciences and Environment for the fiscal year 2024. Appreciation is also extended to the Laboratory for Energy Resources, Fuel, and Environment, BRIN, for access to laboratory facilities. The authors further thank the Landfill Mining and RDF Plant Processing Unit at the Bantargebang Integrated Municipal Solid Waste Treatment Facility for their support in providing data and research permits.

CONFLICT OF INTEREST

The authors declare that there is no conflict of interests regarding the publication of this manuscript. In addition, the ethical issues, including plagiarism, informed consent, misconduct, data fabrication and/or falsification, double publication and/or submission, and redundancy have been completely observed by the authors.

OPEN ACCESS

©2026 The author(s). This article is licensed under

a Creative Commons Attribution 4.0 International License, which permits use, sharing, adaptation, distribution and reproduction in any medium or format, as long as you give appropriate credit to the original author(s) and the source, provide a link to the Creative Commons license, and indicate if changes were made. The images or other third-party material in this article are included in the article's Creative Commons license, unless indicated otherwise in a credit line to the material. If material is not included in the article's Creative Commons license and your intended use is not permitted by statutory regulation or exceeds the permitted use, you will need to obtain permission directly from the copyright holder. To view a copy of this license, visit: http://creativecommons.org/licenses/by/4.0/

PUBLISHER'S NOTE

GJESM Publisher remains neutral regarding jurisdictional claims in published maps and institutional afflictions.

Positive AI Statement

During the preparation of this work the author(s) have used Artificial Intelligence (AI) tool Quillbot in order to improve sentence quality. After using this tool/service, the authors reviewed and edited the content as needed and take full responsibility for the content of the publication.

(For this reason, the GPTZero detector will evaluate the manuscript utilizing Generative AI, ensuring a high detection rate. If the manuscript relies heavily on Generative AI and AI-assisted technologies, it will be archived without further options for appeal).

ABBREVIATIONS

%	Percent
°C	Degree Celsius
µm	Micrometers
ANOVA	Analysis of variance
APHA	American Public Health Association
ASTM	American Society For Testing and Materials
AWWA	American Water Works Association
C	Carbon
C/N	Carbon-to-nitrogen
CaO	Calcium oxide
Cd	Cadmium
CEC	Cation exchange capacity
cm	Centimeters
Cmole(+)/kg	Centimoles of positive charge per kilogram
Fe	Iron
FF	Fine fraction
g	Grams
g/L	Grams per Liter
h	Hours
H_2O_2	Hydrogen peroxide
H_2SO_4	Sulfuric acid
HCl	Hydrochloric acid
HRF	Heavy-rough fration
IMSWTF	Integrated municipal solid waste treatment facility
ISRIC	International Soil Reference and Information Centre
K	Potassium
$K_2Cr_2O_7$	Potassium dichromate
K_2O	Potassium oxides
KCl	Potassium chloride
kg	Kilograms
lb	Pounds
LM	Landfill mining
LMM	Landfill-mined material
LRF	Ligth-rough fraction
M	Molar
mg/kg	Milligrams per kilogram
MgO	Magnesium oxide
min	Minutes
mm	Millimeters
Mn	Manganese
Mo	Molybdenum
MSW	Municipal solid waste
N	Nitrogen
$NaHCO_3$	Sodium bicarbonate
$Na_4P_2O_7$	Tetrasodium pyrophosphate
NH_4OAc	Ammonium acetate
nm	Nanometers
NRCS	Natural Resources Conservation Service
P	Phosphorus
Pb	Lead
pH	Power of hydrogen

QA/QC	Quality assurance and quality control
RDF	Refuse-derived fuels
RF	Rough fraction
Se	Selenium
SLM	Soil-like material
t/d	Tons per day
TCLP	Toxicity characteristic leaching procedure
TKN	Total Kjeldahl nitrogen
TOC	Total organic carbon
USDA	United States Department of Agriculture
USEPA	United States Environmental Protection Agency
VS	Volatile solids
WEF	Water Environment Federation
w/w	Weight per weight
Zn	Zinc

REFERENCES

APHA, (2024). Standard methods for the examination of water and wastewater. American Public Health Association. American Public Health Association, American Water Works Association, Water Environment Federation. Washington DC.

Arumdani, I.S.; Puspita, A.S.; Budihardjo, M.A., (2021). MSW handling of top 5 leading waste-producing countries in Southeast Asia. IOP Conference Series: Earth Environ. Sci., 896(1): 012003 **(7 pages)**.

ASTM, (2016). ASTM D5231–92: Standard test method for determination of the composition of unprocessed municipal solid waste. American Society for Testing and Materials International, West Conshohocken.

ASTM, (2018). ASTM D3174–12 (Reapproved 2018)e1: Standard test method for ash in the analysis sample of coal and coke from coal. American Society for Testing and Materials International, West Conshohocken.

ASTM, (2019). ASTM D2216–19: Standard test methods for laboratory determination of water (moisture) content of soil and rock by mass. American Society for Testing and Materials International, West Conshohocken.

ASTM, (2020). ASTM D3175–20: Standard test method for volatile matter in the analysis sample of coal and coke. American Society for Testing and Materials International, West Conshohocken.

Avifah, N.; Zainabun, Z.; Jufri, Y., (2022). Provision of several kinds of ameliorants to improve chemical properties of rice field soil. J. Ilmiah Mahasiswa Pertanian, 7(1): 604-614 **(11 pages)**.

Ayamba, B.E.; Abaidoo, R.C.; Opoku, A.; Ewusi-Mensah, N., (2021). Enhancing the fertilizer value of cattle manure using organic resources for soil fertility improvement: a review. J. Bioresour. Manage., 8(3): 89-107 **(19 pages)**.

Baloyi, T.C.; Kutu, F. R.; Preez, C.C.D., (2023). Impact of commercial organic ameliorants on nitrogen and phosphorus concentrations of maize biomass at ninth leaf and silking growth stages. J. Geosci. Environ. Prot., 11(05): 102-125 **(24 pages)**.

Bao, X.; Li, M.; Niu, R.; Lu, J.; Panigrahi, S.; Garg, A.; Berretta, C., (2021). Hygroscopic water retention and physio-chemical properties of three in-house produced biochars from different feedstock types: Implications on substrate amendment in green infrastructure. Water. 13(19): 2613 **(18 pages)**.

Batjes, N.H; van Oostrum, A., (2023). World soil information services (WoSIS) – Toward the standardization and harmonization of world soil profile data. ISRIC – World Soil Information **(48 pages)**.

Bechtaoui, N.; Rabiu, M.K.; Raklami, A.; Oufdou, K.; Hafidi, M.; Jemo, M., (2021). Phosphate-dependent regulation of growth and stresses management in plants. Front. Plant Sci., 12: 679916 **(20 pages)**.

Chandana, N.; Goli, V.S.N.S.; Mohammad, A.; Singh, D.N., (2021). Characterization and utilization of landfill-mined-soil-like-fractions (lfmsf) for sustainable development: a critical appraisal. Waste Biomass Valoriz., 12(2): 641-662 **(22 pages)**.

Corrêa, E.A.; Moraes, I.C.; Pinto, S.D.A.F.; Lupinacci, C.M., (2018). Evaluation of water erosion in sugarcane crops using erosion plots and photo comparison technics. Revista Brasileira de Geografia Física. 11(5): 1761-1775 **(15 pages)**.

Datta, M.; Somani, M.; Ramana, G.V.; Sreekrishnan, T.R., (2021). Feasibility of re-using soil-like material obtained from mining of old MSW dumps as an earth-fill and as compost. Process Saf. Environ. Prot., 147: 477-487 **(11 pages)**.

Ejaz, U.; Khan, S.M.; Khalid, N.; Ahmad, Z.; Jehangir, S.; Rizvi, Z.F.; Lho, L.H.; Han, H.; Raposo, A., (2023). Detoxifying the heavy metals: a multipronged study of tolerance strategies against heavy metals toxicity in plants. Front. Plant Sci., 14: 1154571 **(17 pages)**.

Emmanuel, A.E.-O.; Edison, M.; Innocent, M.M., (2015). Revegetation: A potential for reclaiming landfills and waste containment vicinity. Proceedings 1st IEC 2015 Minna. 379-387 **(9 pages)**.

Faragó, T.; Špirová, V.; Blažeková, P.; Lalinská-Voleková, B.; Macek, J.; Jurkovič, Ľ.; Vítková, M.; Hiller, E., (2023). Environmental and health impacts assessment of long-term naturally-weathered municipal solid waste incineration ashes deposited in soil—Old burden in Bratislava city, Slovakia. Heliyon. 9(3): e13605 **(18 pages)**.

González-Arqueros, M.L.; Domínguez-Vázquez, G.; Alfaro-Cuevas-Villanueva, R.; Israde-Alcántara, I.; Buenrostro-Delgado, O., (2021). Hazardous solid waste confined in closed dump of morelia: an urgent environmental liability to attend in developing countries. Sustainability. 13(5): 2557 **(9 pages)**.

Gutierrez, K.G.; Fernandes, M.A.O.; Chernicharo, C.A.L., (2019). Modelling of a sanitary landfill for developing countries to improve the reliability of life cycle assessment studies. IOP Conference Series: Earth Environ. Sci., 323(1): 012085 **(10 pages)**.

Heiskanen, J.; Ruhanen, H.; Hagner, M., (2022). Effects of compost, biochar and ash mixed in till soil cover of mine tailings on plant growth and bioaccumulation of elements: A growing test in a greenhouse. Heliyon, 8(2): e08838 **(10 pages)**.

Hendriyanto, Hermon, D.; Barlian, E.; Umar, I.; Efendi, N., (2023). Post-coal mining reclamation land sustainability study in tebo regency. J. Penelitian Pendidikan IPA, 9(11): 10330-10337 **(8 pages)**.

Hogland, W.; Gomes, M.M.; Thörneby, L., (2019). Landfill mining: Space saving, material recovery and energy use. Linnaeus Eco-Tech, 339-355 **(17 pages)**.

Hölzle, I., (2019). Contaminant patterns in soils from landfill mining. Waste Manage., 83: 151-160 **(10 pages)**.

Jagodzińska, K.; Garcia Lopez, C.; Yang, W.; Jönsson, P.G.; Pretz, T.; Raulf, K., (2021). Characterisation of excavated landfill waste fractions to evaluate the energy recovery potential using Py-GC/MS and ICP techniques. Resour. Conserv. Recycl., 168: 105446 **(11 pages)**.

Jain, M.; Kumar, A.; Kumar, A., (2023). Landfill mining: A review on material recovery and its utilization challenges. Process Saf. Environ. Prot., 169: 948-958 **(11 pages)**.

Joseph, K.; Esakku, S.; Palanivelu, K.; Selvam, A., (2003). Studies on landfill mining at solid waste dumpsites in India. Proceedings Sardinia 2003, Ninth International Waste Management and Landfill Symposiums. Margherita di Pula, Cagliari, Italy; 6 - 10 October 2003 by CISA, Environmental Sanitary Engineering Centre, Italy **(8 Pages)**.

Kaniowski, W.; Taler, J.; Wang, X.; Kalemba-Rec, I.; Gajek, M.; Mlonka-Mędrala, A.; Nowak-Woźny, D.; Magdziarz, A., (2022). Investigation of biomass, RDF and coal ash-related problems: Impact on metallic heat exchanger surfaces of boilers. Fuel. 326: 125122 **(11 pages)**.

Kanu, M.O.; Joseph, G.W.; George, I., (2021). Measurement of physicochemical properties, electrical and thermal conductivity of wood ash for effective soil amendment. Indonesian J. Appl. Phys., 11(2): 176 **(13 pages)**.

Keerthana, C.; Rao, M. V. S.; Yalla, P.; Tejasree, P.; Kumar, R.S.S.P., (2024). Strategic implementation of disease management in banana plants through soil mineral deficiency correction. Int. J. Electr. Electron. Eng., 11(4): 254-260 **(7 pages)**.

Khan, M.U.; Ahring, B.K., (2019). Lignin degradation under anaerobic digestion: Influence of lignin modifications -A review. Biomass Bioenergy. 128: 105325 **(10 pages)**.

Kristanto, G.A.; Jansen, A.; Koven, W., (2020). The potential of landfill mining in two inactive zones of the Bantar Gebang landfill in Jakarta, Indonesia. Int. J. Technol., 11(7): 1430-1441 **(12 pages)**.

Laner, D.; Esguerra, J.L.; Krook, J.; Horttanainen, M.; Kriipsalu, M.; Rosendal, R.M.; Stanisavljević, N., (2019). Systematic assessment of critical factors for the economic performance of landfill mining in Europe: What drives the economy of landfill mining? Waste Manage., 95: 674-686 **(13 pages)**.

Latosińska, L.; Czapik, P., (2020). The ecological risk assessment and the chemical speciation of heavy metals in ash after the incineration of municipal sewage sludge. Sustainability. 12: 6517 **(13 pages)**.

Legese, W.; M. Taddesse, A.; Kibret, K.; Wogi, L., (2024). Effects of natural and modified zeolite based composite fertilizers on slow release and nutrient use efficiency. Heliyon. 10(3): e25524 **(15 pages)**.

Li, J.; Jia, Y.; Dong, R.; Huang, R.; Liu, P.; Li, X.; Wang, Z.; Liu, G.; Chen, Z., (2019). Advances in the mechanisms of plant tolerance to manganese toxicity. Int. J. Macromol. Sci., 20(20): 5096 **(15 pages)**.

Li, J.; Ren, T.; Li, Y.; Chen, N.; Yin, Q.; Li, M.; Liu, H.; Liu, G., (2022). Organic materials with high C/N ratio: More beneficial to soil improvement and soil health. Research Square **(17 pages)**.

López, C.G.; Küppers, B.; Clausen, A.; Pretz, T., (2018). Landfill mining: A case study regarding sampling, processing and characterization of excavated waste from an Austrian landfill. Detritus. 2(1): 29-45 **(17 pages)**.

Mahender, A.; Swamy, B.P.M.; Anandan, A.; Ali, J., (2019). Tolerance of iron-deficient and -toxic soil conditions in rice. Plants. 8(2): 31 **(34 pages)**.

Maluin, F.N.; Hussein, M.Z.; Nik Ibrahim, N.N.L.; Wayayok, A.; Hashim, N., (2021). Some emerging opportunities of nanotechnology development for soilless and microgreen farming. Agronomy. 11(6): 1213 **(28 pages)**.

Márquez, A.J.C.; Cassettari Filho, P.C.; Rutkowski, E.W.; de Lima Isaac, R., (2019). Landfill mining as a strategic tool towards global sustainable development. J. Cleaner Prod., 226: 1102-1115 **(14 pages)**.

Minhal, F.; Ma'as, A.; Hanudin, E.; Sudira, P., (2020). Improvement of the chemical properties and buffering capacity of coastal sandy soil as affected by clays and organic by-product application. Soil Water Res., 15(2): 93-100 **(8 pages)**.

Muraru, S.; Muraru, V., Condruz, P.; Ionel, C.M.; Sfiru, R., (2021). Considerations on the importance of the main chemical properties of the soil in agrochemical studies. E3S Web Conference. 286: 03019 **(9 pages)**.

NARA, (2016). 7 CFR Part 205 – National Organic Program. Electronic Code of Federal Regulations (eCFR). National Archives and Records Administration.

NSAI, (2004). SNI 19-7030-2004: Specifications for compost made from domestic organic waste. National Standardization Agency of Indonesia.

Naveen, B.P.; Sivapullaiah, P.V., (2020). Solid waste management: Current scenario and challenges in Bengaluru. Sustainable Sewage Sludge Management and Resource Efficiency **(23 pages)**.

Owusu-Nimo, F.; Oduro-Kwarteng, S.; Essandoh, H.; Wayo, F.; Shamudeen, M., (2019). Characteristics and management of landfill solid waste in Kumasi, Ghana. Sci. Afr., 3: e00052 **(9 pages)**.

Parrodi, J.C.H.; Höllen, D.; Pomberger, R., (2018). Characterization Of fine fractions from landfill mining: A Review Of Previous Investigations. Detritus, 2(1): 46-62 **(17 pages)**.

Pratama, R.A.; Wahyono, S.; Sahwan, F.L.; Suryanto, F.; Hanif, M.; Wiharja; Prihartanto; Prasetiyadi; Suprapto; Tilottama, R.D.; Sarkiwan; Diyono., (2025). Evaluation of the physical and chemical characteristics of waste excavated from an open dump site for sustainable waste management. Case Stud. Chem. Environ. Eng., 11: 101069 **(12 pages)**.

Prihartanto, P.; Trihadiningrum, Y.; Kholiq, M.A.; Bagastyo, A.Y.; Warmadewanthi, I.D.A.A., (2023a). Characterization of landfill-mined materials as a waste-to-energy source at integrated solid waste treatment facilities of Jakarta Province, Indonesia. J. Mater. Cycles Waste Manage., 25: 3872-3884 **(13 pages)**.

Prihartanto; Putri, V.M.; Trihadiningrum, Y.; Kholiq, M.A.; Bagastyo, A.Y.; Warmadewanthi, I.D.A.A., (2023b). Characteristics of humate soil from landfill mining in Bantargebang integrated solid waste treatment facility, Indonesia. IOP Conference Series: Earth Environ. Sci., 1201(1): 012002 **(11 pages)**.

Rahman, M.M.; Bhuiyan, M.S.H.; Rouf, M.A.; Sarker, R.R.; Rashid, M.H., (2020). Quality assessment of municipal solid waste compost. Acta Chem. Malays., 4(1): 33-39 **(10 pages)**.

Rani, J.; Chaudhary, S.; Agarwal, T., (2021). Evaluation of heavy metals contamination in agricultural soils. PREPRINT (Version 1) available at Research Square **(13 pages)**.

Ridwan; Annadira; Rahmawati; Taiyeb, A.; Muslimin, (2023). The effect of various compositions of planting media on the growht of red calliandra seedlings (*Calliandra calotrhyrsus Meissen*). Agric. Sci., 7(1): 1-9 **(9 pages)**.

Sahoo, A.; Dwivedi, A.; Madheshiya, P.; Kumar, U.; Sharma, R.K.; Tiwari, S., (2023). Insights into the management of food waste in developing countries: with special reference to India. Environ. Sci. Pollut. Res., 31(12): 17887-17913 **(27 pages)**.

Salim, M.A.; Setyaningsih, L.; Wahyudi, I.; Budi, S.W., (2021). Effect of iron toxicity on the growth of *Calliandra calothyrsus* and *Leucaena leucocephala* seedlings. J. Trop. Biodivers. Biotechnol., 6(3): 65654 **(13 pages)**.

Sasongko, P.E.; Mindari, W.; Jayanti, F.A.; Fatiha, C.Z., (2024). Impact of organic matter and sand on soil chracteristics, leaf area, and chlorophyll of sweet corn (*Zea mays saccnutritionta* sturt) on vertisol from Bojonegoro. Ilmu Pertanian. 9(3): 138 **(9 pages)**.

Sayara, T.; Basheer-Salimia, R.; Hawamde, F.; Sánchez, A., (2020). Recycling of organic wastes through composting: process performance and compost application in agriculture. Agronomy, 10(11): 1838 **(23 pages)**.

Schaap, K.J.; Fuchslueger, L.; Quesada, C.A.; Hofhansl, F.; Valverde-Barrantes, O.; Camargo, P.B.; Hoosbeek, M.R., (2023). Seasonal fluctuations of extracellular enzyme activities are related to the biogeochemical cycling of C, N and P in a tropical terra-firme forest. Biogeochemistry. 163(1): 1-15 **(15 pages)**.

Simonova, O.A.; Lisitsyn, E.M.; Tovstik, E.V.; Simonov, M.V., (2020). Genotypic differences in reaction of barley root system on Mn and Fe toxicity. E3S Web of Conference. 217: 09013 **(8 pages)**.

Somani, M.; Datta, M.; Ramana, G.V.; Sreekrishnan, T.R., (2019). Leachate characteristics of aged soil-like material from msw dumps: sustainability of landfill mining. J. Hazard. Toxic Radioact. Waste J., 23(4): 04019014 **(12 pages)**.

Somani, M.; Datta, M.; Ramana, G.V.; Sreekrishnan, T.R., (2020). Contaminants in soil-like material recovered by landfill mining from five old dumps in India. Process Saf. Environ. Prot., 137: 82-92 **(11 pages)**.

Song, U., (2018). Selecting plant species for landfill revegetation: A test of 10 native species on reclaimed soils. J. Ecol. Environ., 42(1): 30 **(6 pages)**.
Syachroni, S.H., (2020). Study of several chemical properties of paddy soils at various locations in Palembang City. Sylva. 8(2): 60 **(6 pages)**.
UNFCCC, (2005). Bantar Gebang LFG (landfill gas) collection & energy recovery CDM (clean development mechanism) project. United Nations Framework on Climate Change Conference.
USDA-NRCS, (2020), The national conservation practice standard and supporting documents for composting facility. United States Department of Agriculture, Natural Resources Conservation Service. 317 **(6 pages)**.
USDA-NRCS, (2022). Kellogg Soil Survey Laboratory Methods Manual. United States Department of Agriculture, Natural Resources Conservation Service. Soil Survey Investigations Report. 42, Version 6.0 **(820 pages)**.
USDA-NRCS, (2023). Soil texture calculator. United States Department of Agriculture, Natural Resources Conservation Service. In: Natural Resource Conservation Center. United States Department of Agriculture. Natural Resources Conservation Service.
USEPA, (1992). SW-846 test method 1311: Toxicity characteristic leaching procedure. United States Environmental Protection Agency **(35 pages)**.
Vaverková, (2019). Landfill impacts on the environment-review. Geosci., 9(10): 2-16 **(15 pages)**.
Vollprecht, D.; Hernández Parrodi, J.C.; Lucas, H.I.; Pomberger, R., (2020). Case study on enhanced landfill mining at mont-saint-guibert landfill in belgium: mechanical processing, physico-chemical and mineralogical characterization of fine fractions <4.5 mm. Detritus, 10: 26-43 **(18 pages)**.
Vrancken, C.; Longhurst, P.; Wagland, S.T., (2017). Critical review of real-time methods for solid waste characterisation: Informing material recovery and fuel production. Waste Manage., 61: 40-57 **(18 pages)**.
Wagland, S.T.; Coulon, F.; Canopoli, L., (2019). Developing the case for enhanced landfill mining in the UK. Detritus, 05: 105-110 **(6 pages)**.
Wahyono, S.; Sahwan, F.L.; Suryanto, F.; Febriyanto, I.; Nugroho, R.; Hanif, M., (2019). Study of characterization of landfill based municipal solid waste and its potential utilization (case study at Sukawinatan and Bantargebang landfill). J. Tek. Ling., 20(2): 179-188 **(10 pages)**.
Widyarsana, I.M.W.; Tambunan, S.A., (2022). Analysis of potential utilization of landfill materials (case study: Sumur Batu landfill, Bekasi). IOP Conference Series: Earth Environ. Sci., 999(1): 012021 **(10 pages)**.
Wijaya, M.N., (2017). Effect of phosphorus (P) concentration on the morphology of teak (Tectona grandis) seedlings [Undergraduate thesis]. Gajah Mada University. Yogyakarta.
Wu, L.; Li, R.; Liu, J.; Cui, W.; Qi, Z.; Zhou, W., (2025). Nitrogen immobilization by wood fiber substrates strongly affects the photosynthetic performance of lettuce. Plants. 14(10): 1518 **(19 pages)**.
Yang, R.; Xu, Z.; & Chai, J., (2018). A review of characteristics of landfilled municipal solid waste in several countries:physical composition, unit weight,and permeability coefficient. Pol. J. Environ. Stud., 27(6): 2425-2435 **(11 pages)**.
Yusmayani, M., (2019). Analysis of nitrogen content in urea fertilizer, liquid fertilizer, and compost using the Kjeldahl method. Aminal. 1(1): 28-34 **(7 pages)**.
Zhang, M.; Buekens, A.; Jiang, X.; Li, X., (2015). Dioxins and polyvinylchloride in combustion and fires. Waste Management & Research: J. Sustainable Circ. Econ., 33(7): 630-643 **(14 pages)**.
Zhou, C.; Xu, W.; Gong, Z.; Fang, W.; Cao, A., (2015). Characteristics and fertilizer effects of soil-like materials from landfill mining. Clean Soil Air Water. 43(6): 940-947 **(7 pages)**.

AUTHOR (S) BIOSKETCHES

Sudiana, N., M.Si., Senior Researcher, Research Centre for Environmental and Clean Technologies, National Research and Innovation Agency, South Tangerang, Banten, Indonesia.
- Email: *nana011@brin.go.id*
- ORCID: 0000-0001-7234-7263
- Web of Science ResearcherID: NA
- Scopus Author ID: 6504442642
- Homepage: http://brin.go.id

Prihartanto, Dr., Principal Researcher, Research Centre for Environmental and Clean Technologies, National Research and Innovation Agency, South Tangerang, Banten, Indonesia.
- Email: *prihartanto69@gmail.com*
- ORCID: 0000-0003-2327-2300
- Web of Science ResearcherID: NA
- Scopus Author ID: 58628104300
- Homepage: http://brin.go.id

Sulistiawan, I.N., S.T., Associate Researcher, Research Centre for Environmental and Clean Technologies, National Research and Innovation Agency, South Tangerang, Banten, Indonesia.
- Email: *insan.nursulistiawan@gmail.com*
- ORCID: 0009-0003-6551-0589
- Web of Science ResearcherID: NA
- Scopus Author ID: 58563333500
- Homepage: http://brin.go.id

Sittadewi, E.H., M.Si., Principal Researcher, Research Centre for Geological Disaster, National Research and Innovation Agency, South Tangerang, Banten, Indonesia.
- Email: *euth001@brin.go.id*
- ORCID: 0000-0001-5240-3926
- Web of Science ResearcherID: NA
- Scopus Author ID: 57200330811
- Homepage: http://brin.go.id

AUTHOR (S) BIOSKETCHES

Utami, D.N., S.P., Associate Researcher, Research Centre for Geological Disaster, National Research and Innovation Agency, South Tangerang, Banten, Indonesia.
- Email: *dyah013@brin.go.id*
- ORCID: 0009-0007-6844-4483
- Web of Science ResearcherID: NA
- Scopus Author ID: 58562841300
- Homepage: http://brin.go.id

Kusumastuti, E., M.Si., Technical Policy Analyst, Directorate of Laboratory Management, Research Facilities, and Science and Technology Area, National Research and Innovation Agency, South Tangerang, Banten, Indonesia.
- Email: *etty002@brin.go.id*
- ORCID: 0009-0007-7273-9954
- Web of Science ResearcherID: NA
- Scopus Author ID: 58562525300
- Homepage: http://brin.go.id

Rahayu, B., Ir., Principal Researcher, Research Centre for Environmental and Clean Technologies, National Research and Innovation Agency, South Tangerang, Banten, Indonesia.
- Email: *budi001@brin.go.id*
- ORCID: 0009-0008-1969-7991
- Web of Science ResearcherID: NA
- Scopus Author ID: 57202087766
- Homepage: http://brin.go.id

Hidayat, N., M.Si., Senior Researcher, Research Centre for Environmental and Clean Technologies, National Research and Innovation Agency, South Tangerang, Banten, Indonesia.
- Email: *nurh008@brin.go.id*
- ORCID: 0009-0000-8384-269X
- Web of Science ResearcherID: NA
- Scopus Author ID: 59399265500
- Homepage: http://brin.go.id

Haris, K.A., S.T., Junior Researcher, Research Centre for Environmental and Clean Technologies, National Research and Innovation Agency, South Tangerang, Banten, Indonesia.
- Email: *khal003@brin.go.id*
- ORCID: 0009-0009-3005-8071
- Web of Science ResearcherID: NA
- Scopus Author ID: 58563164800
- Homepage: http://brin.go.id

Pararto, T.E., M.Si., Technical Policy Analyst, Research Centre for Environmental and Clean Technologies, National Research and Innovation Agency, South Tangerang, Banten, Indonesia.
- Email: *tito001@brin.go.id*
- ORCID: 0009-0001-2930-1355
- Web of Science ResearcherID: NA
- Scopus Author ID: 53399265500
- Homepage: http://brin.go.id

Noviana, L., Dr., Dean of the Faculty of Engineering, Sahid University, South Jakarta, Jakarta, Indonesia.
- Email: *lindanoviana@gmail.com*
- ORCID: 0000-0002-2383-3262
- Web of Science ResearcherID: NA
- Scopus Author ID: 58640342500
- Homepage: http://brin.go.id

HOW TO CITE THIS ARTICLE

Sudiana, N.; Prihartanto; Sulistiawan, I.N.; Sittadewi, E.H.; Utami, D.N.; Kusumastuti, E.; Rahayu, B.; Hidayat, N.; Haris, K.A.; Pararto, T.E.; Noviana, L., (2026). Physical and chemical evaluation of soil-like material from landfill mining for use as an alternative growing medium. Global J. Environ. Sci. Manage., 12(1): 75-94.

DOI: 10.22034/gjesm.2026.01.05

URL: https://www.gjesm.net/article_732270.html

Global J. Environ. Sci. Manage. 12(1): 95-110, Winter 2026, Serial #45

Global Journal of Environmental Science and Management
(GJESM)

Homepage: https://www.gjesm.net/

Podcasts

ORIGINAL RESEARCH ARTICLE

Nypa fruticans-assisted green-synthesized gold nanoparticles for an enhanced electrochemical formaldehyde sensor based on fish albumin composite

T.P.H. Hutapea[1], M.S. Lembang[2], A. Huda[3], Asranudin[4], D.P. Dewi[1,2], Suprapto[5], F. Kurniawan[5], H.A. Saputra[6], A.W. Pratama[7], V.F. Knight[8], M.N.F. Norrrahim[8,*]

[1] *Fisheries Product Technology Department, Faculty of Fishery and Marine Science, Universitas Borneo Tarakan, North Borneo 77115 Indonesia*

[2] *Aquaculture Department, Faculty of Fishery and Marine Science, Universitas Borneo Tarakan, North Borneo 77115 Indonesia*

[3] *Electrical Engineering Department, Faculty of Fishery and Marine Science, Universitas Borneo Tarakan, North Borneo 77115 Indonesia*

[4] *Research Center for Applied Microbiology, National Research and Innovation Agency of Indonesia, Cibinong, Indonesia*

[5] *Chemistry Department, Institut Teknologi Sepuluh Nopember, Surabaya, East Java 60111 Indonesia*

[6] *Research Center for Mineral Technology, National Research and Innovation Agency, Tanjung Bintang, Lampung Selatan 35361, Indonesia*

[7] *Department of Agrotechnology, Faculty of Agriculture, University of Jember, Jember, East Java 68121 Indonesia*

[8] *Research Center for Chemical Defence, Defence Research Institute, Universiti Pertahanan National Malaysia, Kem Sungai Besi, 57000 Kuala Lumpur, Malaysia*

ARTICLE INFO

Article History:
Received 13 August 2025
Revised 18 October 2025
Accepted 04 December 2025

Keywords:
Electrochemical sensor
Fish albumin
Formaldehyde detection
Green synthesis
Gold nanoparticles (AuNps)

ABSTRACT

BACKGROUND AND OBJECTIVES: The need for sustainable, rapid, and cost-effective electrochemical sensors for formaldehyde monitoring is increasing. Typically, the synthesis of traditional noble metal nanoparticles relies on uses hazardous chemicals. This study pioneered the green synthesis of gold nanoparticles using Nypa fruticans leaf extract. The primary goals of the study were to create an electrochemical formaldehyde sensor that is both highly sensitive and selective by incorporating these innovative, green-synthesized gold nanoparticles into a conductive matrix made of fish albumin on gold electrode.

METHODS: Gold nanoparticles were created using a simple heating and stirring method with Nypa fruticans leaf extract, utilizing its natural metabolites. The confirmation of formation was achieved by employing ultraviolet-visible spectroscopy, Fourier transform infrared spectroscopy, X-ray diffractometry, Particle size analyzer, field emission-scanning electron microscope, and High-resolution transmission electron microscopy analyses. The sensor probe, incorporating the gold nanoparticles into a snakehead fish albumin-paraffin composite, was fabricated and applied to a gold wire electrode. An assessment of the electrochemical performance was conducted in relation to a 1 millimolar formaldehyde solution utilizing cyclic voltammetry. Key parameters, including optimal potential of hydrogen, reaction kinetics, linear dynamic range, limit of detection, and selectivity against common interferents (methanol, ethanol, glucose, glycerol), were investigated.

FINDINGS: Characterization confirmed the successful formation of crystalline, face-centered cubic gold nanoparticles, predominantly spherical, with small sizes ranging from 2 to 8 nanometers, highlighting the efficacy of the green synthesis method. The fish albumin and gold nanoparticles modified gold electrode displayed a significantly higher anodic peak current of +1.13 volt compared to the control electrodes (Paraffin-modified gold electrodes and fish albumin-modified gold electrodes). This indicates the enhanced catalytic and conductive properties provided by the gold nanoparticles. Optimal sensing performance was achieved under acidic conditions with a pH value of 1. The electrode displayed a broad linear dynamic range from 1 micromolar to 50 millimolar. Critically, the sensor has exhibits excellent and selectivity with an ultra-low limit of detection of 0.177 micromolar, which is the lowest documented among the electrodes reviewed in the literature. This is particularly notable when compared to the albumin-modified gold electrode, which has a detection limit of 4.07 micromolar for formaldehyde.

CONCLUSION: Utilizing Nypa fruticans extract for the environmentally friendly synthesis of gold nanoparticles presenting a sustainable and affordable method. The resulting gold electrode, modified with fish albumin and gold nanoparticles, created an electrochemical sensor with exceptional performance, high selectivity, and an ultralow detection limit for formaldehyde detection.

DOI: 10.22034/gjesm.2026.01.06

This is an open access article under the CC BY license (http://creativecommons.org/licenses/by/4.0/).

NUMBER OF REFERENCES	NUMBER OF FIGURES	NUMBER OF TABLES
34	6	3

*Corresponding Author:
Email: *faiz@upnm.edu.my*
Phone: +601 4326 3353
ORCID: 0000-0003-2101-5642

Note: Discussion period for this manuscript open until Mar 1, 2026 on GJESM website at the "Show Article".

INTRODUCTION

Nanoparticles (NPs) are materials characterized by a width or diameter ranging from 1 to 100 nanometers (nm) (Hassan *et al*., 2022). This small size offers considerable benefits compared to micro-scale materials, as their essential properties experience a substantial enhancement. This phenomenon has propelled research into nanoparticles, particularly gold nanoparticles (AuNps), to the forefront of various scientific and technological fields (Al-Radadi, 2023; Fatima *et al.,* 2024; Pechyen *et al.,* 2024). AuNps can be synthesized through several methods, including chemical (Tirkey and Babu, 2024), electrochemical (Chierici *et al.,* 2025), and physical approaches (Amendola *et al*., 2017; Nuti *et al*., 2022; Rehman *et al*., 2024). Moreover, despite the high purity, controlled morphology, and significant yields achieved through these methods, they are not considered environmentally sustainable. The processes involve the use of hazardous chemicals that produce toxic residues. Besides that, it requires a relatively large budget. Recognizing the need for sustainable nanotechnology, researchers are now focusing on the development of greener and more sustainable synthesis methods (Dinh *et al*., 2025). Green synthesis employs biologically reducing agents, including extracts from plants or mushrooms, to either remove or significantly lessen the use of toxic chemicals (Ali *et al*., 2021; Al-Radadi, 2021; Shankar *et al*., 2025; Venkatesh *et al*., 2024). This approach not only offers a much eco-friendly alternative but also a cost-effective one. Plant extracts, which are rich in secondary metabolites like polyphenols, flavonoids, and tannins, serve as effective bioreductants in the AuNps synthesis (Dinh *et al*., 2025). In addition to ensuring environmental sustainability, this method lays the groundwork for safer and more efficient nanoparticle synthesis in the future. *Nypa fruticans* leaf extract was utilized in this study as a bioreductor due to its rich content of secondary metabolites, such as tannins, flavonoids, alkaloids, and others. Initially, the active functional groups on secondary metabolites, including hydroxy, carbonyl, and phenolic groups, release electrons and transform gold ions into neutral gold (Au^0). This Au^0 species was then gathered, forming the nuclei. Conversely, the polar groups adhere to the surface of the gold nanoparticles, inhibiting aggregation and providing electrostatic stabilization to the resulting nanoparticles. To date, no studies have been reported on the use of this biological reducing agent in the green synthesis of NPs, specifically AuNps. This claim has been verified through a comprehensive literature study of authoritative databases. However, this approach is inspired by a previous report that demonstrated the effectiveness of coastal plant extracts as bioreductors (Kumar Das and Thatoi, 2020). Numerous reports indicate that green-synthesized AuNps possess a broad spectrum of potential applications, spanning from the healthcare sector as antibacterial and anticancer agents (Al-Radadi, 2021; Jakhmola *et al*., 2025; Saha *et al*., 2025; Yang *et al*., 2024) to diverse industrial domains (Yousif, 2025; Zhang *et al*., 2025). Additionally, AuNps have proven to be highly suitable as sensor material due to the excellent electroconductivity (Pechyen *et al*., 2024; Sheng *et al*., 2020; Zhang *et al*., 2025). Accordingly, the synthesized AuNps were composed with a fish albumin (FA) and then modified onto a gold electrode (GE), a method reported in a previous study (Hutapea *et al*., 2025). FA is extracted from snakehead fish (*Channa striata*) abundantly in nature, so it is easy to obtain. Besides, FA is a natural, environmentally friendly material. The modified electrode was explicitly designed to enhance the performance of the electrode in detecting formaldehyde. Formaldehyde reacts with thiol groups on albumin via a nucleophilic addition mechanism, forming thiohemiacetal/ hemithioacetal (Cleary *et al*., 2015; Adrover *et al*., 2008). FA additionally functions as a stabilizing matrix, imparting the FA/AuNP composite with a strong adherence capability to the gold electrode. The electrochemical method was selected over other techniques, such as chromatography and spectrophotometry, since it offers significant advantages (de Freitas Rezende *et al*., 2017). Even though standard methods deliver reliable results, they are usually labor-intensive, necessitate complicated sample preparation, and are comparatively high-priced. In contrast, electrochemical methods offer speed, ease of use, low cost, and high sensitivity, enabling real-time detection of formaldehyde without complicated preparation processes. The aims of this study are to develop a highly sensitive and selective electrochemical formaldehyde sensor by integrating these novel, green-synthesized AuNps into a conductive fish albumin composite matrix on a gold electrode. This study has been carried out in

Tarakan and Surabaya, Indonesia, in 2025.

MATERIALS AND METHODS

Materials

Nypa frutucans leaves were from the Mangrove and Proboscis Monkey Conservation Area (KKMB), Tarakan, Indonesia. To obtain *Nypa frutucans* Leaf Extract, the leaves were treated using water as a solvent, followed by heating for 20 minutes (min) at 50 degrees Celsius (°C). *Nypa frutucans* leaves were cut to be about 1x1 centimeters (cm) in dimension, followed by the addition of water with the ratio of *Nypa frutucans* leaves and water of 1:10 weight per volume (w/v). Subsequently, the substance was filtered to acquire the bioreductant filtrate necessary for the green synthesis of AuNp. Fish Albumin was derived from the Snakehead fish inhabiting the swamp waters of Tarakan, in accordance with the previously established protocol (Hutapea *et al*., 2022). Gold (III) chloride trihydrate ($HAuCl_4 \cdot 3H_2O$), N-hexane, paraffin (C_6H_{14}), hydrochloric acid (HCl), potassium hydroxide (KOH), potassium chloride (KCl), acetic acid chloride (CH_3COCl), nitric acid (HNO_3), glucose ($C_6H_{12}O_6$), methanol (CH_3OH, 99.98 percent (%)), ethanol (C_2H_5OH, 99.98%), glycerol ($C_3H_5(OH)_3$, 98%), and formaldehyde (HCHO, 37%) were purchased from Sigma-Aldrich. All aqueous solutions were prepared using ultrapure water obtained from a Milli-Q reference water purification system with 18.2 megaohm centimeter (MΩ.cm).

Apparatus

Ultraviolet-visible (UV-Vis) spectroscopy (Thermofisher, Aquamate 8100) was used to confirm the stability of the as-prepared AuNps. Fourier transform infrared (FT-IR) experiments were carried out using an Agilent Cary 630 FTIR spectrometer. To assess the crystalline structure of AuNPs, an x-ray diffractometer (XRD) (Brand: RIGAKU, Type: MiniFlex600) was used at a diffraction angle range 2-theta (2θ) from 5° to 90°. High-resolution transmission electron microscopy (HR-TEM) (Model: Talos F200C G2) and field emission-scanning electron microscope (FE-SEM) from Hitachi, specifically the Regulus 8220 type, were utilized to examine the morphology, including the shape and size, of the synthesized AuNps. The elemental composition of AuNps was confirmed using energy dispersive x-ray spectroscopy (EDS) integrated on the FE-SEM. The particle size and zeta potential of AuNps were determined using a particle size analyzer (PSA) (Malvern Panalytical Zetasizer Nano ZS). The electrochemical study was performed utilizing an Auto Lab PGSTAT 204 N device featuring a three-electrode configuration, which includes a working electrode, a silver/silver chloride (Ag/AgCl) reference electrode, and an auxiliary electrode constructed from platinum wire.

Preparation of AuNps

Synthesis was carried out by mixing 20 milliliters (mL) of 0.5 millimolar (mM) $HAuCl_4$ with 4 mL of *Nypa fruticans* leaf extract. This mixture was then heated at 60 °C and stirred at 100 rpm continuously. The emergence of AuNps was evidenced by a shift in the color of the solution from pale yellow to wine red. Following the stabilization of the solution's color, the heating and stirring were ceased. The reaction time was estimated to be around 15 min. The solution was cooled to room temperature and ready for further analysis.

Fabrication of gold electrode modified fish albumin and gold nano particles (FA/AuNps/GE)

Initially, a 1-millimeter (mm) diameter gold wire was cut into 5 cm lengths and inserted into a small glass tube, which served as the electrode container. Next, a drop of 50 microliters of freshly prepared AuNps was added to the mixture of snakehead fish albumin and paraffin with the ratio of 6:4 weight per weight (w/w), consisting of 0.03 grams (g) albumin and 0.02 g paraffin (optimized condition). The mixture was then heated on a hot plate until the paraffin melted completely, and a homogeneous consistency was achieved. Once the components are thoroughly blended, the resulting mixture is promptly transferred into the end of the glass tube, which has been fitted with a gold wire. The surface of the mixture was then dried at room temperature until a solid structure formed.

Electrochemical sensing study

Cyclic voltammograms were recorded in the potential range of 0 to +1.8 volt (V) and at a scan rate of 100 millivolts per second (mV/s) following the prior study (Hutapea *et al*., 2025). The initial stage of evaluation began by determining optimal pH conditions by measuring the response to 1 mM

formaldehyde in 25 mL of 0.1 Normal (N) HCl (acidic), 25 mL of 0.1 N KCl (neutral), and 25 mL of 0.1 N KOH (basic). The confirmation of the effectiveness of electrode modification was achieved by comparing the response of the FA/AuNps/GE with that of various other modified electrodes, including paraffin-modified GE (P-GE) and Fish albumin-modified GE (FA-GE). The effect of reaction kinetics was investigated by recording the FA/AuNps/GE with 1 mM formaldehyde in 0.1 N HCl solvent at varying scan rates, ranging from 50 to 350 mV/s. The linear dynamic range of formaldehyde measurements was investigated over a concentration range of 0.1 micromolar (µM) to 50 mM, prepared by diluting 37% HCHO with HCl 0.1 N. The sensor selectivity was evaluated by measuring the response current when interfering substances were present individually in distinct solutions, including methanol, ethanol, glucose, and glycerol. The repeatability assessment was conducted by measuring a single electrode in duplicate for each concentration. Each repetition was recorded in 10 cycles.

RESULTS AND DISCUSSION

Synthesis of AuNps

In this study, *Nypa fruticans* leaf extract was utilized to synthesize AuNps through a green synthesis method. The secondary metabolite content in this extract has been qualitatively identified through phytochemical screening, as shown in Table 1. Compounds such as alkaloids, phenols, flavonoids, saponins, and tannins can function as natural bioreductants and stabilizing agents for AuNps (Santhosh *et al*., 2022). The development of AuNps was confirmed visually through a change in the solution from yellow to pink (Fig. 1A).

Table 1: Qualitative test of secondary metabolites of *Nypa fruticans* leaf extract

Sample	Secondary metabolites				
	Alkaloids	Phenolics	Flavonoids	Saponins	Tannins
Nypa fruticans leaf extract	+	+	+	+	+

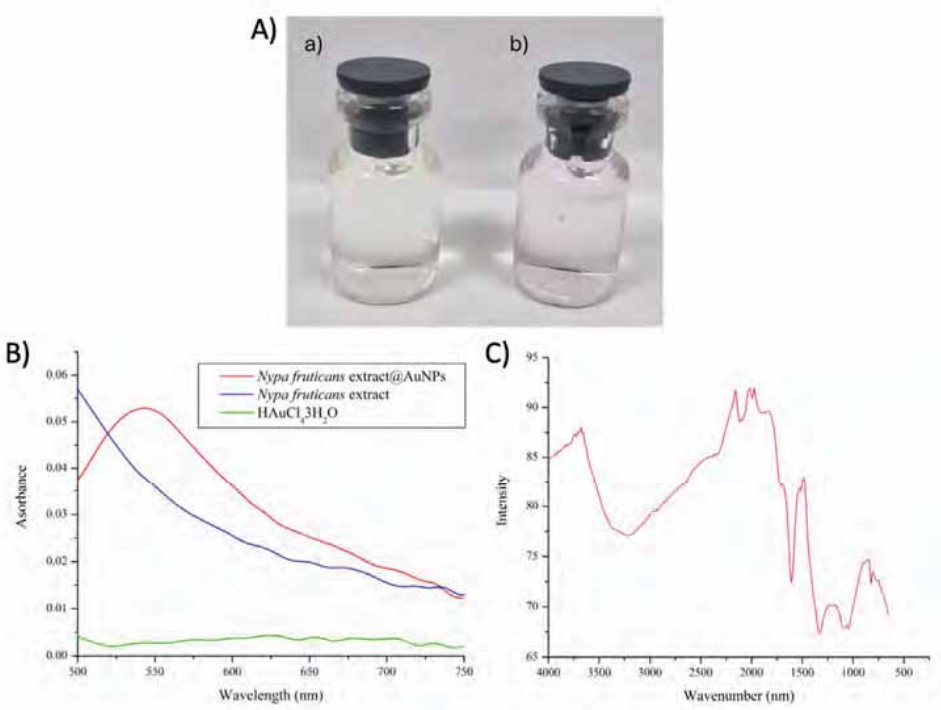

Fig. 1: A) Color change of the solution, a) before (yellow) and b) after (pink) green synthesis of AuNps. B) UV-Vis spectra of a) prepared AuNps, b) *Nypa fruticans leaf* extract, and c) chloroauric acid solution. C) FT-IR spectrum of AuNps

Characterization of AuNps

UV-Vis spectroscopy

Based on the characterization results using UV-Vis spectroscopy, the synthesized AuNps show a maximum absorption at a wavelength of 540 nm (Fig. 1B). This finding demonstrates the effective synthesis of AuNps with considerable assurance. This wavelength corresponds with the absorption traits of AuNps, which typically fall below 600 nm and most commonly cited near 540 nm (Haiss *et al*., 2007), consistent with numerous other studies that also utilizes standard materials as reducing agents. This absorption spectrum is clearly distinct from that of the raw materials, namely *Nypa fruticans* leaf extract (blue line) and $HAuCl_4 \cdot 3H_2O$ solution (green line), which do not exhibit absorption at this wavelength. This difference firmly confirms that AuNps have been successfully synthesized (Ali *et al*., 2021; Saha *et al*., 2025).

FT-IR

The FT-IR characterization results of AuNps synthesized using *Nypa fruticans* leaf extract showed several typical absorption bands (Fig. 1C), indicating the presence of biomolecules from the extract that serve as both reducing agents and stabilizers. The broad absorption band at 3200-350/cm is associated with the stretching vibration of the -OH group. Another notable absorption in the range of 1650-1730/cm reflects the carbonyl (C=O) stretching vibration, stemming from the carbonyl of secondary metabolites that possess the ability to engage with the gold surface. Additionally, the band at 1050-1250/cm corresponds to the C-O stretching vibration. The presence of absorption at 1500–1600/ cm also supports the presence of aromatic carbon double bond (C=C) bonds from phenolic compounds. These findings demonstrate that the bioactive molecules found in the leaf extract of *Nypa fruticans* are involved in the synthesis of AuNps, acting as reducing agents as well as stabilizers of nanoparticle surfaces.

XRD

To examine the crystal structure of the AuNps, XRD analysis was performed. The XRD pattern in Fig. 2A displays five distinct diffraction peaks at 2θ angles of 37.80°, 44.00°, 64.20°, 77.16°, and 81.34°. These peaks confirm the conventional face-centered cubic (FCC) crystal structure of gold, which corresponds to the crystal planes (111), (200), (220), (311), and (222), respectively. The occurrence of these sharp and distinctly defined peaks denotes the crystalline quality of the synthesized nanoparticles. The variety of the resulting peaks and the distinctive width of the diffraction peaks indicate that the nanoparticles are diminutive in size, aligning with the results obtained from the TEM analysis. The successful formation of crystalline AuNps confirms the effectiveness of the reducing agents contained in the *Nypa fruticans* leaf extracts (Table 1), in both reducing the gold precursor and directing the growth of the crystalline structure.

FE-SEM and EDS

Morphological analysis using FE-SEM shows that the synthesized AuNps have a spherical shape with a size distribution below 100 nm presented in Fig. 2B(a). The image indicates that the nanoparticles are clustered together, a typical feature of nanomaterials in powdered form as a result of their elevated surface energy. In addition, the EDS spectrum in Fig. 2B(b) confirms the presence of the dominant Au element with a strong signal. This peak at approximately 2.2 kiloelectronvolt (keV) corresponds to the characteristic X-ray emission from gold, providing definitive evidence that the nanoparticles are composed of gold. There are also weak signals from other elements, notably carbon (C) and oxygen (O). These signals are most probably derived from the biomolecules found in the leaf extract of *Nypa fruticans*. These biomolecules act as both reducing agents, facilitating the formation of AuNps from the precursor, and capping agents, preventing excessive aggregation and stabilizing the surface of the particles. The existence of these components serves as a crucial hallmark of green synthesis. A deeper examination of this elemental makeup indicates that the proportion of Au attains 18%. At the same time, carbon and oxygen comprise the remainder of the measured composition, further supporting the presence of organic capping agents from the plant extract on the surface of the AuNps.

Particle size analyzer

PSA characterization shows that the green synthesis method in this study successfully produces AuNps. Based on the data in Fig. 3A(a), most particles have a size between 2 and 8 nm, both in terms of volume and number, which confirms that the material formed is nanoparticles because the size is below 100 nm. Nonetheless, the existence of particles

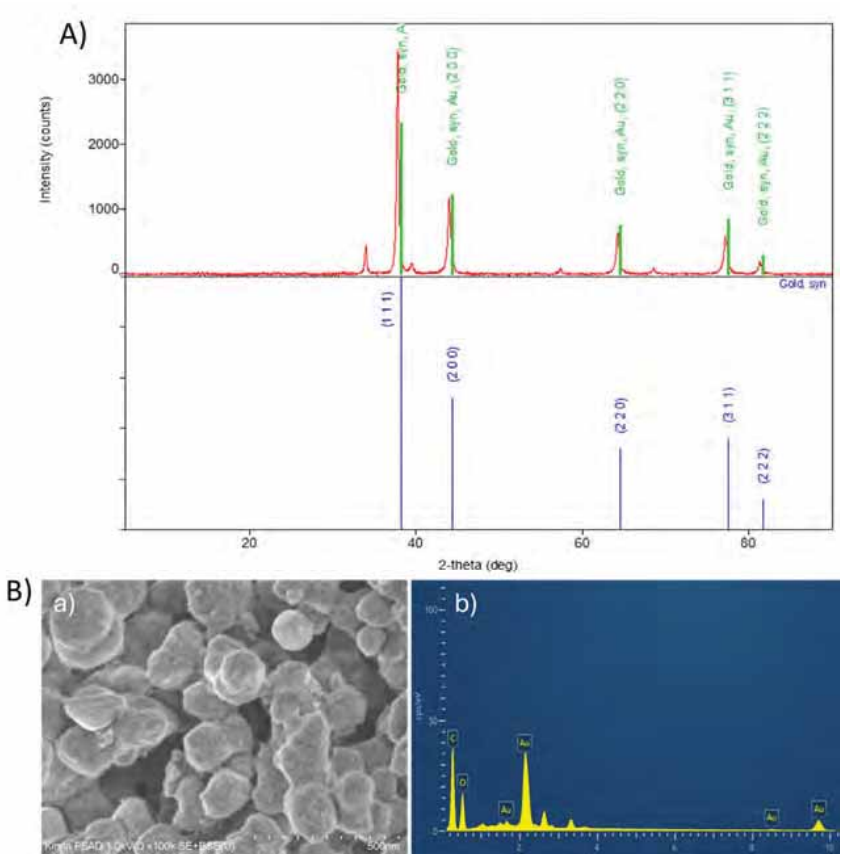

Fig. 2: A) Diffraction pattern of AuNps. B(a) FE-SEM images combined with b) elemental mapping analysis using EDS, which illustrate the presence of AuNps

measuring between 10 nm and 100 nm suggests that certain particles have experienced agglomeration. This is in line with the results of the zeta potential, which show a value of around -8 millivolts (mV) (Fig. 3A(b), indicating the presence of attractive forces between particles. This value indicates weak colloidal stability and a tendency toward particle aggregation, suggesting unstable particles for long-term storage. To address the sensing issue, the freshly prepared AuNps were used for subsequent composite preparation and sensor fabrication. Furthermore, the study demonstrates the viability of employing this eco-friendly resource as a reliable and cost-efficient replacement for harmful chemical reducing agents. Moving forward, a more professional approach is needed to optimize the process. Adopting statistical design of experiments, such as the Box-Behnken method, can address current research gaps by systematically exploring the complex interactions between different synthesis variables. Overall, the data corroborates that the synthesis of nano gold utilizing the leaf extract from Nypa fruticans as been effectively accomplished

HR-TEM

Fig. 3B displays the HR-TEM images of AuNps synthesized using *Nypa fruticans* leaf extract. Fig. 3B(a), with a 50 nm scale bar, illustrates that the resulting AuNps exhibit various shapes, including spherical, triangular, and hexagonal. The variation in shapes is a prevalent trait of nanoparticles created through the green synthesis approach, where different molecules in the plant extract serve as both reducing and capping agents, causing diverse nucleation and growth pathways. Meanwhile, Fig. 3B(b), with a 10 nm scale bar, confirms the successful synthesis of nanoparticles by showing the crystalline lattice fringes and demonstrating that the size of the

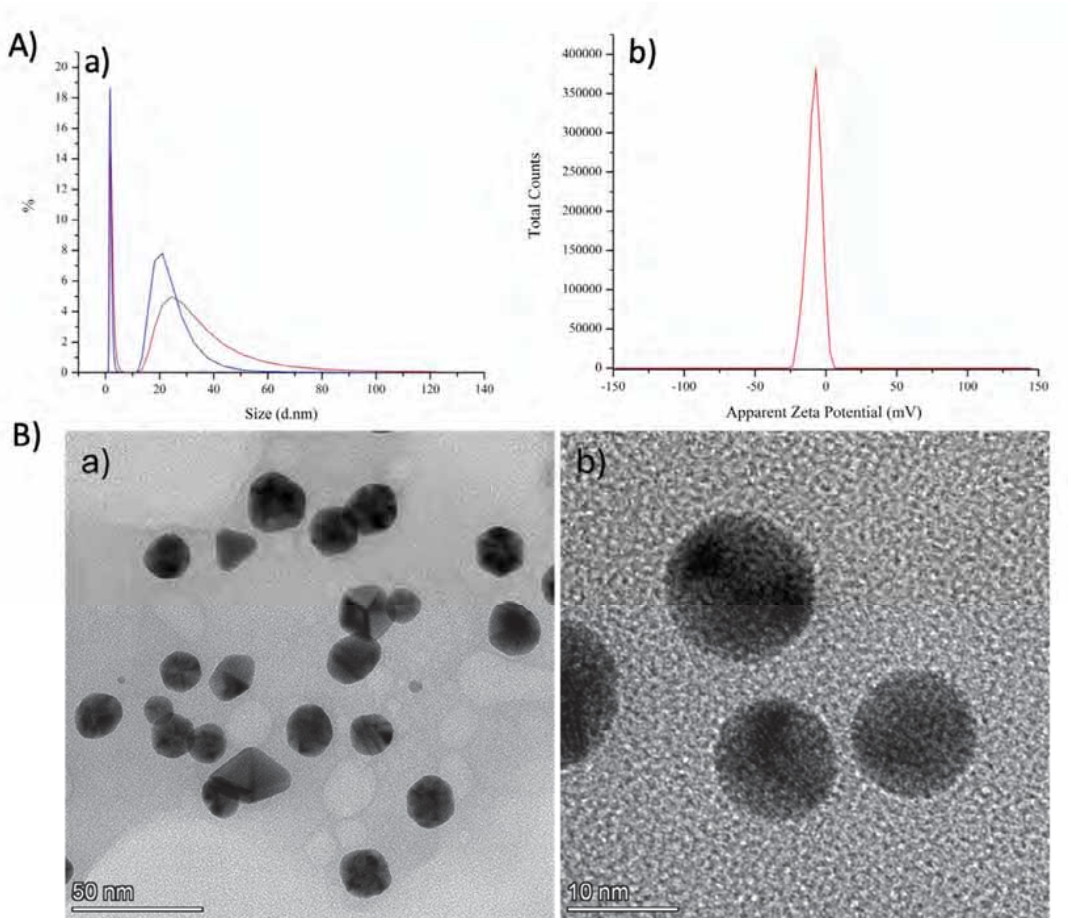

Fig. 3: A(a) Size distribution of AuNps by volume (red) and by number (blue), b) Zeta potential distribution of AuNps. B) TEM images of AuNps with a) 50 nm magnification and b) 10 nm magnification

formed AuNps is below 10 nm. The presence of these lattice fringes directly confirms the nanocrystalline nature of the synthesized AuNps, which is a key indicator of successful nanoparticle formation. The limited dimensions imply a considerable surface-area-to-volume ratio.

Fabrication of FA/AuNps/GE sensing probe

The fabrication process of the FA/AuNPs-GE was carried out carefully to produce an optimal and stable composition. The structure of this composite pertains to a ratio of FA to paraffin of 6:4, which has been derived from prior studies (Hutapea *et al*., 2025). The addition of AuNps was limited to only one drop, as this amount is considered optimal. It was observed that the introduction of more than a single drop would compromise the solidification process, thus obstructing the composite's stable attachment to the surface of the gold wire. Thus, this optimized composition enables the creation of a robust working electrode, suitable for use in electrochemical measurements of formaldehyde. Fig. 4 shows the fabrication process of the FA/AuNPs-GE.

Electrochemical sensing study

In the evaluation of the electrochemical performance of AuNps, measurements were performed on P-GE, FA/GE, and FA/AuNPs/GE electrodes against 1 mM formaldehyde solution. The voltammograms showed a significant increase in the anodic current at a potential of +1.13 V on the FA/AuNPs/GE probe compared to FA/GE and

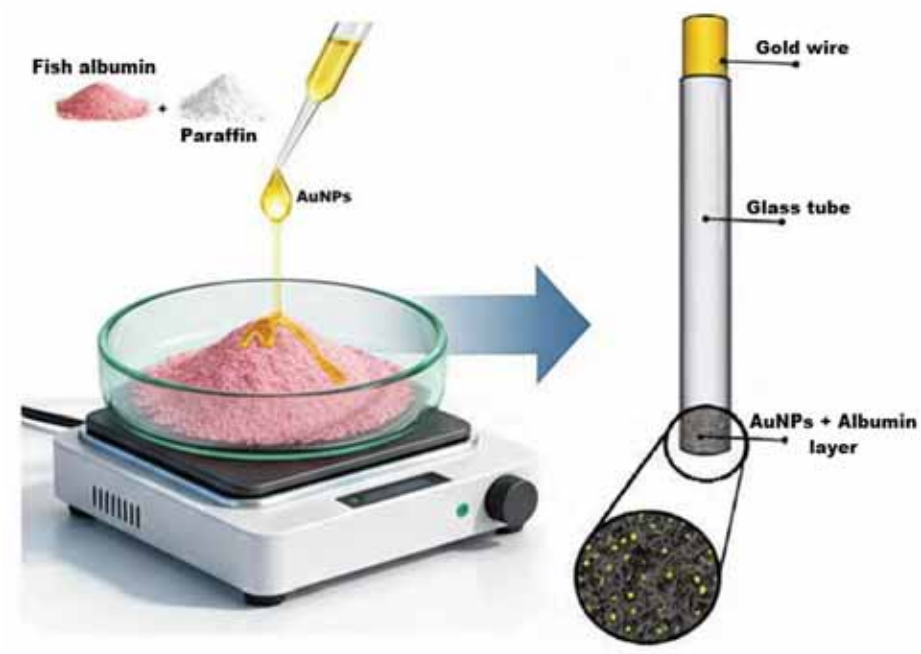

Fig. 4: Schematic illustration showing the fabrication process of the FA/AuNps-GE sensor probe.

P-GE (Fig. 5A). The peak current was enhanced from 20.6 microampere (μA) for FA/GE to 78.8 μA for FA/AuNps/GE. The observed improvement in performance demonstrates that the inclusion of AuNps is very effective in augmenting electrode functionality. This success is mainly due to the high stability of AuNps, which ensures that their material properties are maintained throughout the process. Furthermore, the existence of AuNps boosts the electrode's conductivity and accelerates electron transfer, in addition to functioning as a signal amplifier that yields a considerably more robust response. These results clearly demonstrate and confirm that AuNps are a crucial and effective modification component in enhancing electrode performance.

pH conditions

The pH levels of the solution significantly affect electrochemical testing. The pH conditions for measuring formaldehyde using FA/AuNps/GE were also evaluated to determine the optimal pH conditions. Fig. 5B is a voltammogram of 1 mM formaldehyde measurement by FA/AuNps/GE at various pH conditions. The analysis shows that at pH 7 (blue line) and pH 1 (red line), the FA/AuNps/GE successfully showed a clear response to formaldehyde. This is illustrated by the considerable disparity between the blank voltammogram (shown as the dotted line) and the formaldehyde voltammogram (depicted as the solid line). This difference directly indicates that an electrochemical reaction, either oxidation or reduction, occurs in formaldehyde, thus enabling detection. Although a positive response was seen at both pH levels, the overall results of the study concluded that the optimal performance of FA/AuNps/GE against formaldehyde was achieved at pH 1. At a very acidic pH, the electrode showed its best performance in detecting formaldehyde. In contrast to acidic and neutral conditions, at pH 13 (green line), the FA/AuNps/GE electrode is not suitable for formaldehyde determination. The reason for this phenomenon is that the blank voltammogram entirely coincides with the formaldehyde voltammogram. This overlap is evidence that under highly alkaline conditions, formaldehyde does not undergo oxidation or reduction reactions. Without any observable electrochemical reaction, the electrode becomes unresponsive and is incapable of measuring formaldehyde.

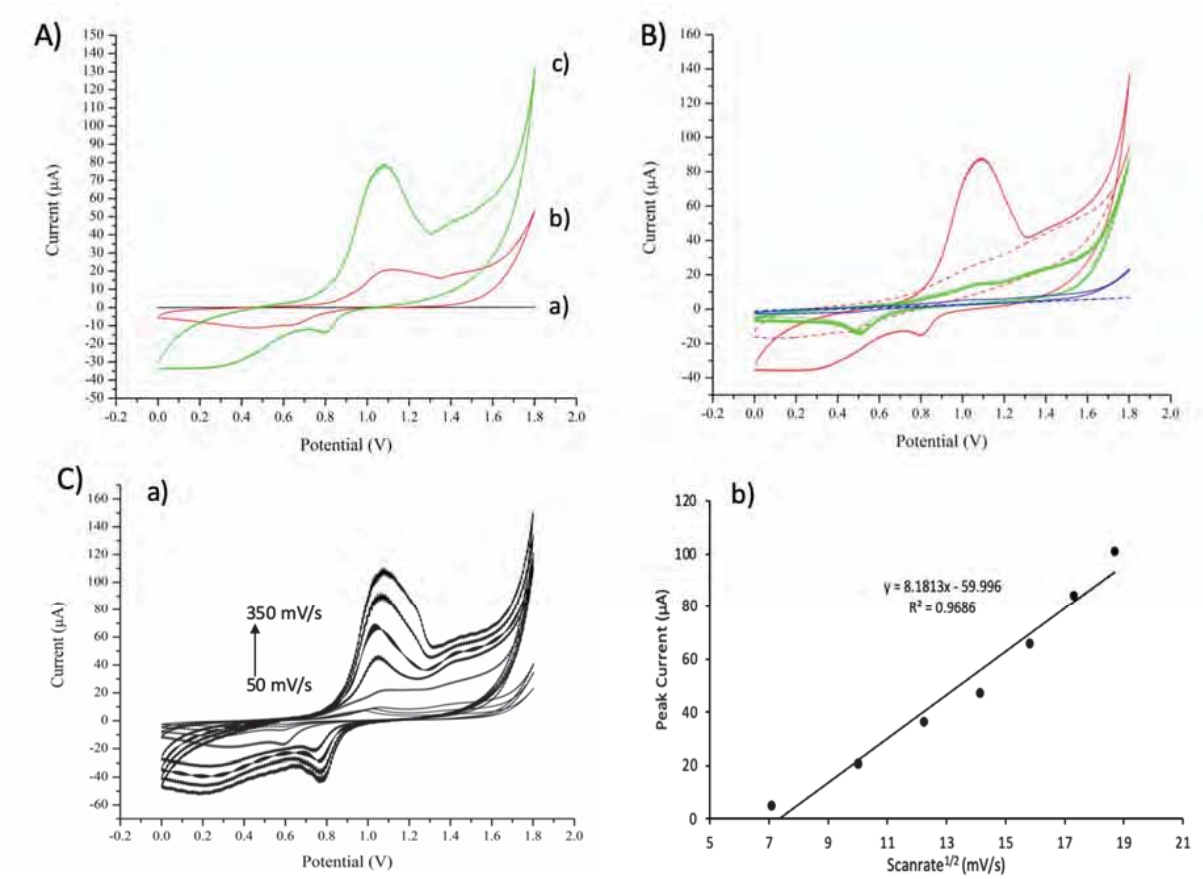

Fig. 5: A) Voltammogram of a) P/GE (black), b) FA/GE (red), and c) FA/AuNps/GE (green) with 1 mM formaldehyde. B) Voltammogram of FA/AuNps/GE to blank (dashed line) and 1 mM formaldehyde (solid line) in pH 1 (red), pH 7 (blue), and pH 13 (green). C(a) Voltammograms of 1 mM formaldehyde on FA/AuNps/GE with scan rates of 50, 100, 150, 200, 250, 300, and 350 mV/s. b) The plot of peak anodic current at +1.13 V vs. the square root of the scan rate

Influence of scan rate

The increase in scan rate in Fig. 5C(a) is accompanied by an increase in peak current, indicating that the electrochemical reaction is dependent on the scan rate. Furthermore, the analysis results in Fig. 5C(b) strengthen this finding. The highest current correlates directly with the scan rate, implying that the redox process is facilitated by surface-confined species. The plot of the relationship between the anodic peak current and the square root of the scan rate shows a strong linear correlation, as indicated by the regression equation anodic peak current (Ipa) = 8.1813x – 59.996 with R square (R^2) of 0.968. Considering this relationship and consistency with the Randles-Sevcik equation (Lee *et al*., 2024), it can be deduced that the diffusion process significantly influences the reaction mechanism on the electrode surface.

Calibration plot

To determine the limit of detection (LOD), the electrochemical measurements of formaldehyde were performed at various concentrations ranging from 1 µM to 50 mM (Fig. 6A(a)). The Ipa increased at +1.13 V as the formaldehyde concentration increased. The Ipa shows a linear relationship with increasing concentration (Fig. 6A(b)). This figure produces a linear equation as follows: i = 0.0079c + 2.9952. This equation serves as a tool for quantitative analysis in estimating the LOD. The LOD calculation in this report uses the formula 3σ/m, where m is the slope of the line, and σ is the standard deviation of blank (0.1 N HCl) for five measurements. The estimated detection level is approximately 0.177 µM. The extended measurement range gives this electrode an advantage over previous electrodes. The performance of FA/AuNps/GE compared to other electrodes is presented

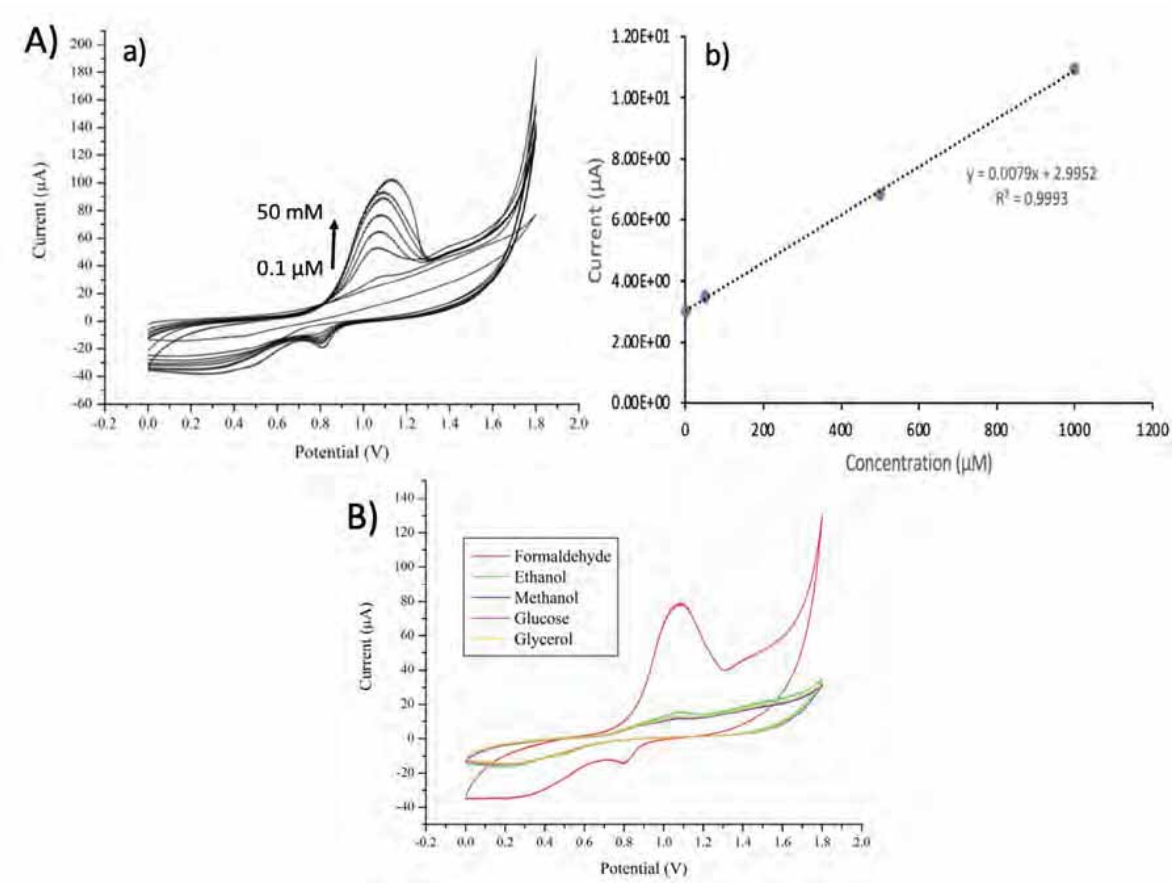

Fig. 6: A(a) Voltammogram of FA/AuNps/GE in various formaldehyde concentrations (1 µM-50 mM) in HCl 0.1 N. b) The calibration curve for anodic current at +1.13 V. B) Voltammogram of formaldehyde along with various interfering compounds (1 mM in 0.1 N HCl) using the FA/AuNps/GE sensor

Table 2: Performance of selected electrodes for formaldehyde determination.

Electrodes	Range concentrations (mM)	LOD (µM)	Sources
AuNps@PPy composites	0.4-2.4	20	Xi *et al.*, 2020
$Ni(OH)_2$/rGO/GCE	0.1-100	60	Li *et al.*, 2022
$NiSe_2/Co_3Se_4$@N-C	0.008-0.5	3.94	Yan *et al.*, 2025
GPE/ZnO NPs	0-100	18	Wicaksono *et al.*, 2022
FA/GE	0.1-3	4.07	Hutapea *et al.*, 2025
FA/AuNps/GE	0.001-50	0.177	The current study

in Table 2. In this study, the detection limit is the lowest relative to other electrodes that have been assessed in literature.

Selectivity

The assessment of selectivity in the measurement of formaldehyde involved testing FA/AuNps/GE against various other compounds that might be present in the sample. The compounds frequently identified include methanol, ethanol, glycerol, and glucose. Fig. 6B is a voltammogram of the measurement of these compounds, along with target formaldehyde, employing an FA/AuNps/GE sensor. The findings indicated that the four compounds did not interfere with the measurement of formaldehyde. The Ipa at a potential of +1.13 V, which appeared during the

Table 3: Peak current of 1 mM formaldehyde measured using an FA/AuNps/GE sensing platform

Number of cyclic	Current at +1.13 V (µA)	
	First measurement	Second measurement
1	47.0581	47.879
2	44.0094	45.9381
3	44.2566	46.109
4	43.8019	43.1244
5	43.8568	42.2028
6	42.5079	42.1539
7	42.7307	39.9048
8	42.3523	39.4684
9	42.9962	39.7003
10	42.8925	40.5243
Mean	43.64624	42.7005
t value	0.9033022	
t critical value	2.16036866	

measurement of formaldehyde by FA/AuNps/GE, was not significantly detected in the measurements of other interfering compounds. These findings validate that FA/AuNps/GE exhibits a strong selectivity towards formaldehyde.

Repeatability

Using FA/AuNps/GE, 1 mM formaldehyde was measured twice, with each measurement repeated 10 times. The result is presented in Table 3. The t-Test: Two-Sample Assuming Unequal Variances is applied at a 95% confidence level using Microsoft Excel. The t-value derived from the calculation is lower than the t-critical value, suggesting that there is no significant difference between measurements. It is concluded that the FA/AuNps/GE has good repeatability.

CONCLUSION

The environmentally friendly synthesis of AuNps was successfully carried out using Nypa fruticans leaf extract as a natural bioreductant. The phytochemicals present in the extract played a crucial role in reducing gold ions and stabilizing the nanoparticles. Certainly, this environmentally friendly synthesis method provides a sustainable and non-toxic option compared to traditional chemical techniques. The resulting AuNps exhibited good crystalline stability, with a predominantly spherical morphology and particle sizes ranging from 2 to 8 nm, as confirmed through a series of comprehensive characterizations, including UV-Vis, FT-IR, PSA, Zeta, XRD, HR-TEM, FE-SEM, and EDS. The as-prepared AuNps were composited with FA and then modified on the GE. The electrochemical sensing performance of the FA/AuNps/GE composite electrode was evaluated for formaldehyde detection, demonstrating enhanced catalytic activity. The electrode that was developed demonstrated optimal performance under acidic conditions, featuring a broad linear dynamic range from 1 µM to 50 mM, along with an exceptionally low LOD of 0.177 μM. The developed sensor was selective towards formaldehyde in the presence of interferences, including methanol, ethanol, glucose, and glycerol. The sensor exhibited outstanding repeatability, with no significant statistical difference found between the initial and subsequent measurement outcomes. By successfully replacing hazardous chemical agents with an abundant natural resource, this study provides a scalable, cost-effective, and fundamentally sustainable paradigm for electrode material preparation, strongly aligning with the principles of green chemistry. Highly sensitive and selective sensors possess significant industrial and environmental implications, facilitating swift, real-time detection of formaldehyde, a dangerous pollutant and food preservative in intricate samples. Moving forward, while the study successfully proves the concept, the observed shape diversity and slight aggregation of the AuNps suggest a need for more nuanced control over morphology. Consequently, forthcoming initiatives must emphasize the identification of experimental parameters and the refinement of experimental conditions utilizing statistical design of experiments, such as response surface methodology and Box-Behnken design, to ensure precise control of particle size and shape. The next crucial step will

be integrating this robust material with portable, miniaturized instruments, accelerating the translation of this sustainable scientific breakthrough into an indispensable on-site detection tool. The industrial utilization of Nypa fruticans for the green synthesis of gold nanoparticles (AuNps) is highly practical for large-scale sensor manufacturing, presenting a sustainable and cost-efficient alternative to traditional approaches. This approach utilizes Nypa fruticans leaf extract, an abundant natural resource in Indonesia, as a natural bioreductant and stabilizer, eliminating or minimizing the need for hazardous and costly chemicals. However, scaling up requires addressing the current research gap regarding consistency and extract variability. The developed sensor deployment can benefit the environmental and industrial sectors, especially food safety.

AUTHOR CONTRIBUTIONS

T.P.H. Hutapea took the lead, being responsible for conceptualization, methodology, formal analysis, data curation and funding acquisition, while also authoring the writing - original draft. M.S. Lembang performed Formal analysis and conducted the Investigation. A. Huda performed Formal analysis. D.P. Dewi was involved in the methodology and provided Project administration. Suprapto provided essential validation and supervision. F. Kurniawan provided Validation and Supervision. Asranudin contributed to the Writing - review and editing. H.A. Saputra contributed to the Writing - review and editing. A.W. Pratama contributed to writing - review and editing and managed Data curation. V.F. Knight was responsible for data curation, funding acquisition, and writing - review and editing. M.N.F. Norrrahim was responsible for data curation, funding acquisition, and writing - review and editing.

ACKNOWLEDGEMENT

The authors would like to express their deepest gratitude to the Directorate of Research and Community Service, Directorate General of Research and Development, Ministry of Higher Education, Science and Technology, Republic of Indonesia. The study was supported by the Directorate of Research and Community Service, Directorate of Research and Development, Ministry of Higher Education, Science and Technology, Republic of Indonesia (Contract No.: [063/C3/DT.05.00/PL/2025] and Derivative Contract No. [007/UN51.9/SP2H-PFR/2025]. In addition, authors also would like to acknowledge Universiti Pertahanan National Malaysia (UPNM) for the financial support received.

CONFLICT OF INTEREST

The authors declare that there are no conflicts of interest regarding the publication of this manuscript. In addition, ethical issues, including plagiarism, informed consent, misconduct, data fabrication and/or falsification, double publication and/or submission, and redundancy, were observed by the authors.

OPEN ACCESS

©2026 The author(s). This article is licensed under a Creative Commons Attribution 4.0 International License, which permits use, sharing, adaptation, distribution and reproduction in any medium or format, as long as you give appropriate credit to the original author(s) and the source, provide a link to the Creative Commons license, and indicate if changes are made. The images or other third-party material in this article are included in the article's Creative Commons license, unless indicated otherwise in a credit line to the material. If material is not included in the article's Creative Commons license and your intended use is not permitted by statutory regulation or exceeds the permitted use, you will need to obtain permission directly from the copyright holder. To view a copy of this license, visit: http://creativecommons.org/licenses/by/4.0/

PUBLISHER'S NOTE

GJESM Publisher remains neutral concerning jurisdictional claims regarding published maps and institutional affiliations.

Negative AI Statement

The author(s) declared that no AI tools or services were not used or highly applied during the preparation of this work.

ABBREVIATIONS

2ϑ	2-theta
%	Percent
°	degrees
°C	degrees Celsius

µA	Microampere
µM	Micromolar
Au^0	Gold neutral
Ag/AgCl	silver/silver chloride
AuNps	Gold nanoparticles
C=C	Carbon double bond
C=O	Carbonyl
C	Carbon
C_2H_5OH	Ethanol
$C_3H_5(OH)$	Glycerol
C_6H_{14}	Paraffin
$C_6H_{12}O_6$	Glucose
CH_3COCl	Acetic acid chloride
CH_3OH	Methanol
cm	Centimeter
EDS	Energy dispersive x-ray spectroscopy
FA	Fish albumin
FA-GE	Fish albumin-modified gold electrodes
FA/AuNps/GE	Gold electrode mofied fish albumin and gold nano particles
FE-SEM	Field Emission-Scanning Electron Microscope
FT-IR	Fourier Transform Infrared
GE	Gold electrodes
$HAuCl_4 \cdot 3H_2O$	Gold (III) chloride trihydrate
HCHO	Formaldehyde
HNO_3	Nitric acid
HR-TEM	High resolution transmission electron microscopy
Ipa	Anodic peak current
keV	kiloelectronvolt
KCl	Potassium chloride
KOH	Potassium hydroxide
LOD	Limit of Detection
MΩ.cm	Megaohm centimeter
mL	Milliliter
mm	Millimeter
mM	Millimolar
mV	millivolts
mV/s	Millivolt per second
N	Normality
NPs	Nanoparticles
nm	Nanometer
O	Oxygen
P-GE	Paraffin-modified gold electrodes
PSA	Particle size analyzer
UV-Vis	Ultraviolet-Visible
V	Volt
w/v	Weight per volume
w/w	Weight per weight
XRD	X-ray diffractometer

REFERENCES

Adrover, M.; Vilanova, B.; Frau, J.; Muñoz, F.; Donoso J.A., (2008). A Comparative study of the chemical reactivity of pyridoxamine, Ac-Phe-Lys and Ac-Cys with various glycating carbonyl compounds. Amino Acids. 36(3): 437–480 **(13 pages).**

Ali, S.; Bacha, M.; Shah, M.R.; Shah, W.; Kubra, K.; Khan, A.; Ahmad, M.; Latif, A.; Ali, M., (2021). Green synthesis of silver and gold nanoparticles using Crataegus oxyacantha extract and their urease inhibitory activities. Biotechnol. Appl. Biochem., 68(5): 992–1002 **(11 pages)**.

Al-Radadi, N.S., (2021). Facile one-step green synthesis of gold nanoparticles (AuNp) using licorice root extract: Antimicrobial and anticancer study against HepG2 cell line. Arabian J. Chem., 14(2): 102956 **(25 pages)**.

Al-Radadi, N.S., (2023). Ephedra mediated green synthesis of gold nanoparticles (AuNPs) and evaluation of its antioxidant, antipyretic, anti-asthmatic, and antimicrobial properties. Arabian J. Chem., 16(1): 104353 **(20 pages)**.

Amendola, V.; Pilot, R.; Frasconi, M.; Maragò, O.M.; Iatì, M.A., (2017). Surface plasmon resonance in gold nanoparticles: A review. J. Phys.: Condens. Matter., 29(20): 203002 **(49 pages)**.

Chierici, J.M.; Fioravanti, F.; Pérez, L.A.; Lacconi, G.I., (2025). Photochemical and electrochemical synthesis of [rGO–AuNps] hybrids dispersions for detection of rhodamine 6G by SERS. Nano-Struct. Nano-Objects., 42: 101478 **(12 pages).**

Cleary, J.A.; Doherty, W.; Evans, P.; Malthouse, J.P.G., (2015). Quantifying tetrahedral adduct formation and stabilization in the cysteine and the serine proteases. Biochim. Biophys. Acta, Proteins Proteomics., 1854(10): 1382–1391 **(12 pages).**

Rezende, F.B.d.F.; Cheibub, A.M.d.S.S.; Netto, A.D.P.; Marques, F.F.d.C., (2017). Determination of formaldehyde in bovine milk using a high sensitivity HPLC-UV method. Microchem. J., 134: 383–389 **(7 pages).**

Dinh, T.; Dobó, Z.; Palotás, Á.B.; Kovács, H., (2025). A review of gold nanoparticle synthesis: Transitioning from conventional techniques to plant-mediated green nanofabrication. Mater. Today Chem., 48: 103003 **(26 pages).**

Fatima, Z.; Saleem, R.; Khan, R.R.M.; Liaqat, M.; Pervaiz, M.; Saeed, Z.; Muhammad, G.; Amin, M.; Rasheed, S., (2024). Green synthesis, properties, and biomedical potential of

gold nanoparticles: A comprehensive review. Biocatal. Agric. Biotechnol., 59: 103271 **(16 pages).**

Haiss, W.; Thanh, N.T.K.; Aveyard, J.; Fernig, D.G., (2007). Determination of Size and Concentration of Gold Nanoparticles from UV−Vis Spectra. Anal. Chem., 79(11): 4215–4221 **(7 pages).**

Hassan, H.; Sharma, P.; Hasan, M.R.; Singh, S.; Thakur, D.; Narang, J., (2022). Gold nanomaterials – The golden approach from synthesis to applications. Mater. Sci. Energy Technol., 5: 375–390 **(16 pages).**

Hutapea, T.P.H.; Suprapto, S.; Syahputra, M.Y.; Kurniawan, F., (2025). Green chemistry approach to formaldehyde detection using fish albumin-modified gold electrodes. Global J. Environ. Sci. Manage., 11(2): 791-804 **(14 pages).**

Hutapea, T.P.H.; Suprapto, S.; Kurniawan, F. (2022). Extraction of dissolved protein of Channa striata from tarakan, north borneo as a source of fish serum albumin. IOP Conference Series: Earth and Environ. Sci., 1083(1): 012080 **(8 pages).**

Jakhmola, A.; Kashkooli, F.M.; Rod, K.; Lodyga, M.; Tavakkoli, J.; Kolios, M.C., (2025). Green synthesis of cannabinoids loaded gold nanoparticles displaying enhanced anti-cancer properties. Mater. Today Sustainability., 31: 101153 **(16 pages).**

Das, S.K; Thatoi, H., (2020). Mangrove plant–mediated green synthesis of nanoparticles and their pharmaceutical applications: An overview. Biotechnol. Util. Mangrove Resour., 355–370 **(26 pages).**

Lee, Y.Y.; Sriram, B.; Wang, S.F.; Stanley, M.M.; Lin, W.C.; Kogularasu, S.; Chien, G.P.C.; George, M., (2024). Eco-innovative electrochemical sensing for precise detection of vanillin and sulfadiazine additives in confectioneries. Appl. Surf. Sci. Adv., 20: 100584 **(12 pages).**

Li, S.; Li, M.; Yang, H.; Shao, J.; Meng, Z., (2022). Facile synthesis of flower-like Ni(OH)2/rGO nanocomposite as sensitive electrochemical sensor for formaldehyde detection. Int. J. Electrochem. Sci., 17(7): 22079 **(11 pages).**

Nuti, S.; Lodeiro, C.F.; Lodeiro, J.F.; Lodeiro, A.F.; Juste, J.P.; Santos, I.P.; LaGrow, A.P.; Schraidt, O.; Martínez, J.L.C.; Lodeiro, C., (2022). Polyallylamine assisted synthesis of 3D branched AuNPs with plasmon tunability in the vis-NIR region as refractive index sensitivity probes. J. Colloid Interface Sci., 611: 695-705 **(11 pages).**

Pechyen, C.; Tangnorawich, B.; Toommee, S.; Marks, R.; Parcharoen, Y., (2024). Green synthesis of metal nanoparticles, characterization, and biosensing applications. Sens. Int., 5: 100287 **(17 pages).**

Rehman, K.U.; Zaman, U.; Alem, A.; Khan, D.; Khattak, N.S.; Alissa, M.; Aloraini, G.S.; Abdelrahman, E.A.; Alsuwat, M.A.; Alzahrani, K.J.; Almehmadi, M.; Allahyani, M., (2024). Alkaline protease functionalized hydrothermal synthesis of novel gold nanoparticles (ALPs-AuNPs): A new entry in photocatalytic and biological applications. Int. J. Biol. Macromol., 265: 131067 **(12 pages).**

Saha, D.; Talukdar, D.; Mukherjee, P.; Mitra, D.; Mukherjee, R.; Guha, S.; Bhattacharjee, A.; Naskar, R.; Kumar Sahu, S.; Alam, N.; Das, G.; Murmu, N., (2025). Green synthesis of gold nanoparticles using Madhuca indica flower extract and their anticancer activity on head and neck cancer: Characterization and mechanistic study. Eur. J. Pharm. Biopharm., 207: 114625 **(12 pages).**

Santhosh, P.B.; Genova, J.; Chamati, H., (2022). Green Synthesis of Gold Nanoparticles: An Eco-Friendly Approach. Chem., 4(2): 345–369 **(25 pages).**

Shankar, M.P.; Nisha, R.; Lavanya, E.; Spandana, R.; Kupireddy, S.; Devarai, S.K., (2025). Green synthesis of gold nanoparticles using mushrooms for medical and industrial applications. Inorg. Chem. Commun., 181: 115173 **(16 pages).**

Sheng, K.; Li, L.; Zhang, Q.; Ma, S.; Wang, Y., (2020). Synthesis of AuNPs-GH composites for the electrochemical detection of daphnetin. Microchem. J., 159: 105369 **(8 pages).**

Tirkey, A.; Babu, P.J., (2024). Synthesis and characterization of citrate-capped gold nanoparticles and their application in selective detection of creatinine (A kidney biomarker). Sens. Int., 5: 100252 **(8 pages**).

Venkatesh, G.; Serdaroğlu, G.; Üstün, E.; Haripriya, D.; Vennila, P.; Siva, V.; Haseena, S.; Sowmiya, V.; Pradhiksha, A., (2024). Green synthesis, characterization, anti-cancer and antimicrobial activity of AuNPs extracted from Euphorbia antiquorum stem and flower: Experimental and theoretical calculations. J. Drug Delivery Sci. Technol., 95: 105583 (**15 pages).**

Wicaksono, W.P.; Fadilla, N.I.; Zamar, A.A.; Fadillah, G.; Anugrahwati, M.; Anas, A.K.; Kadja, G.T.M., (2022). Formaldehyde electrochemical sensor using graphite paste-modified green synthesized zinc oxide nanoparticles. Inorg. Chem. Commun., 143: 109729 **(9 pages).**

Xi, H.; Chen, X.; Cao, Y.; Xu, J.; Ye, C.; Deng, D.; Zhang, J.; Huang, G., (2020). Electrochemical determination of formaldehyde via reduced AuNPs@PPy composites modified electrode. Microchem. J., 156: 104846 (**8 pages**).

Yan, Y.; Liu, F.; Liu, Z.; Yang, L.; Hu, M.; Zhang, J.; Xu, T.; Ai, Y.; Jiang, X., (2025). Ultrathin NiSe2/Co3Se4 heterojunction nanosheets for electrochemical detection of foodborne formaldehyde. Food Chem., 495: 146292 (**10 pages**).

Yang, X.; Bao, Y.; Zhou, X.; Zhu, H.; Gao, J., (2024). Green chemistry-based synthesis of gold nanoparticles using Nicotiana plumbaginifolia and their anticancer properties against cervical cancer. Arabian J. Chem., 17(12): 106029 **(10 pages).**

Yousif, A.M., (2025). Fabrication of mesoporous sorbent embedded with AuNPs for catalytic esterification of oleic acid to obtain biofuel: Textural and kinetic studies. Colloids Surf., A, 717: 136796 **(8 pages).**

Zhang, J.; Luo, L.; Jia, C.; Liu, S.; Zhang, W.; Chen, W.; Zheng, Z.; Shen, Y.; Yang, Y.; Wang, X., (2025). AuNPs-mediated precision assays for pesticide residues based on aptamers: Methodological innovations toward food safety assurance. Trends in Food Sci, Technol., 165: 105279 **(16 pages).**

Zhang, T.; Ma, D.; Cai, F., (2025). A novel and sensitive AuNPs/tetracystein-glucose dehydrogenase (GDH)/screen-printed electrode (SPE)-based electrochemical glucose biosensor. Microchem. J., 216: 114629 **(8 pages).**

AUTHOR (S) BIOSKETCHES

Tri Paus Hasiholan Hutapea, Ph.D., Associate Professor, Fisheries Product Technology Department, Faculty of Fishery and Marine Science, University of Borneo Tarakan, North Borneo, Indonesia.
▪ Email: *hutapea@borneo.ac.id*
▪ ORCID: 0000-0003-0154-2680
▪ Web of Science ResearcherID: NA
▪ Scopus Author ID: 57194337088
▪ Homepage: https://scholar.google.com/citations?user=ydfmG64AAAAJ&hl=id&oi=ao

Miska Sanda Lembang, M.Sc., Assistant Professor, Aquaculture Department, Faculty of Fishery and Marine Science, University of Borneo Tarakan, North Borneo, Indonesia.
▪ Email: *miskalembang17@gmail.com*
▪ ORCID: 0000-0001-6478-1975
▪ Web of Science ResearcherID: NA
▪ Scopus Author ID: 57204544519
▪ Homepage: https://scholar.google.com/citations?user=nvLzy2UAAAAJ&hl=id&oi=ao

Abil Huda, M.T., M.Sc., Assistant Professor, Electrical Engineering Department, Faculty of Engineering University of Borneo Tarakan, North Borneo, Indonesia.
▪ Email: *abil@borneo.ac.id*
▪ ORCID: 0009-0000-3323-7512
▪ Web of Science ResearcherID: NA
▪ Scopus Author ID: NA
▪ Homepage: https://scholar.google.com/citations?user=IIhvOMUAAAAJ&hl=id&oi=ao

Asranudin, Ph.D., Junior Researcher, Research Center for Applied Microbiology, National Research and Innovation Agency. Indonesia.
▪ Email: *asra003@brin.go.id*
▪ ORCID: 0000-0002-1052-177X
▪ Web of Science ResearcherID: AEF-8031-2022
▪ Scopus Author ID: 57190254251
▪ Homepage: https://scholar.google.co.id/citations?user=haU7izgAAAAJ&hl=id

Dena Pramita Dewi, B.Sc. student, Laboratory assistant, Fisheries Product Technology Department, Faculty of Fishery and Marine Science, University of Borneo Tarakan, North Borneo, Indonesia.
▪ Email: *denapramita@borneo.ac.id*
▪ ORCID: 0009-0005-0815-5095
▪ Web of Science ResearcherID: NA
▪ Scopus Author ID: NA
▪ Homepage: https://scholar.google.com/citations?view_op=new_profile&hl=id

Suprapto, Ph.D., Professor, Chemistry Department, Institut Teknologi Sepuluh Nopember, Surabaya, East Java, Indonesia.
▪ Email: *suprapto@chem.its.ac.id*
▪ ORCID: 0000-0002-1490-0726
▪ Web of Science ResearcherID: NA
▪ Scopus Author ID: 55626183800
▪ Homepage: https://scholar.its.ac.id/en/persons/suprapto-2

Fredy Kurniawan, Ph.D. Professor, Chemistry Department, Institut Teknologi Sepuluh Nopember, Surabaya, East Java, Indonesia.
▪ Email: *fredy@its.ac.id*
▪ ORCID: 0000-0002-9777-0989
▪ Web of Science ResearcherID: NA
▪ Scopus Author ID: 25627866400
▪ Homepage: https://scholar.its.ac.id/en/persons/fredy-kurniawan

Heru Agung Saputra, Ph.D., Researcher, Research Center for Mineral Technology, National Research and Innovation Agency (BRIN-Indonesia), Tanjung Bintang, Lampung Selatan 35361, Indonesia
▪ Email: *heru033@brin.go.id*
▪ ORCID: 0000-0003-4003-2077
▪ Web of Science ResearcherID: HZH-3627-2023
▪ Scopus Author ID: 57359062400
▪ Homepage: https://scholar.google.com/citations?user=1-J9y2YAAAAJ&hl=en

Agus Wedi Pratama, Ph.D., Assistant Professor, Department of Agrotechnology, Faculty of Agriculture, University of Jember, Jember, Indonesia.
▪ Email: *aguswedi.p@unej.ac.id*
▪ ORCID: 0000-0002-0430-5771
▪ Web of Science ResearchID: GZH-3458-2022
▪ Scopus Author ID: 58672998500
▪ Homepage: https://scholar.google.co.id/citations?user=VrIZtL4AAAAJ&hl=id

AUTHOR (S) BIOSKETCHES

Victor Feizal Knight, Ph.D. Professor, Research Center for Chemical Defence, Defence Research Institute, Universiti Pertahanan National Malaysia, Kem Sungai Besi, 57000 Kuala Lumpur, Malaysia
- Email: *victor.feizal@upnm.edu.my*
- ORCID: 0000-0003-0060-4931
- Web of Science ResearcherID: IST-5698-2023
- Scopus Author ID: 57211142580
- Homepage: https://scholar.google.com/citations?user=RHLfwGYAAAAJ&hl=en

Mohd Nor Faiz Norrrahim, Ph.D., Senior Researcher, Research Center for Chemical Defence, Defence Research Institute, Universiti Pertahanan National Malaysia, Kem Sungai Besi, 57000 Kuala Lumpur, Malaysia
- Email: *faiz@upnm.edu.my*
- ORCID: 0000-0003-2101-5642
- Web of Science ResearcherID: AAK-6802-2020
- Scopus Author ID: 55924430000
- Homepage: https://scholar.google.com/citations?user=lICHZfoAAAAJ&hl

HOW TO CITE THIS ARTICLE

Hutapea, T.P.H.; Lembang, M.S.; Huda, A.; Asranudin; Dewi, D.P.; Suprapto; Kurniawan, F.; Saputra, H.A.; Pratama, A.W.; Knight, V.F; Norrrahim, M.N.F., (2026). Nypa fruticans-assisted green-synthesized gold nanoparticles for an enhanced electrochemical formaldehyde sensor based on fish albumin composite. Global J. Environ. Sci. Manage., 12(1): 95-110.

DOI: 10.22034/gjesm.2026.01.06

URL: https://www.gjesm.net/article_732305.html

Global J. Environ. Sci. Manage. 12(1): 111-128, Winter 2026, Serial #45

Global Journal of Environmental Science and Management
(GJESM)

Homepage: https://www.gjesm.net/

Podcasts

ORIGINAL RESEARCH PAPER

The legal coastline as a unifying framework for land and marine cadastre

J. Setiyadi[1,2], B.M. Sukojo[1], D.G. Pratomo[1,*], W.S. Pranowo[2,3,4], M. Nur Cahyadi[1]

[1] *Geomatics Engineering Department, Institut Teknologi Sepuluh Nopember, Sukolilo, Surabaya, Indonesia*

[2] *Hydro-Oceanography Department, Indonesian Naval Postgraduate School of Technology, West Kelapa Gading, Jakarta, Indonesia*

[3] *Research Center for Climate and Atmosphere, National Research and Innovation Agency, South Tangerang, Banten, Indonesia*

[4] *Korea-Indonesia Marine Technology Cooperation and Research Center, Jakarta, Indonesia*

ARTICLE INFO

Article History:
Received 20 August 2025
Revised 02 November 2025
Accepted 05 December 2025

Keywords:
Legal coastline
Marine cadastre
High-Water Spring
Coastal governance
Coastline dynamics
Bekasi Regency

ABSTRACT

BACKGROUND AND OBJECTIVES: Coastal zones represent dynamic interfaces where terrestrial and marine spaces meet, often creating challenges for governance, spatial planning, and cadastral clarity. In Bekasi Regency, the nonexistence of a unified reference line between land and sea has given rise to overlapping jurisdictions, ambiguous land tenure, and complications in carrying out integrated coastal management. The study aimed to define a legal coastline founded on the high-water spring datum, serving as a unified framework for land and marine cadastre, while ensuring conformity with the International Hydrographic Organization S-4 and C-13 standards and Indonesian Law Number: 32/2004 on coastal zone governance.

METHODS: The research integrated extensive tidal data from Muara Bendera, orthophotos derived from unmanned aerial vehicles, the extraction, and global navigation satellite system surveys to delineate the High-Water Spring shoreline. Unmanned aerial vehicle images were collected at both high and low tide to capture the full range of shoreline positions, while real time kinematic measurements provided precise ground control for validation. The shoreline was subsequently modified to align with the high-water spring vertical datum as per the guidelines set forth by International Hydrographic Organization, and it was cross-validated across various coastal morphologies, including sandy beaches and mangrove-lined areas.

FINDINGS: Unmanned aerial vehicle mapping achieved strong performance on sandy coasts (Muara Beting: mean positional error 2.06 meters, overall validation score 75.6/100) but struggled in mangrove-dominated areas (Muara Bendera: mean error 34.63 meters, score 37.7/100), demonstrating the importance of RTK ground validation in complex coastal environments. Despite these variations, the integrated workflow proficiently created a continuous high-water spring-based coastline for Bekasi Regency that aligns with both scientific and legal standards.

CONCLUSION: The study concludes that adopting a high-water spring based legal coastline provides a stable and authoritative boundary to unify land and marine cadastre. It addresses spatial overlaps while simultaneously reinforcing the framework for administrative governance, spatial planning, and coastal zone management. While unmanned aerial vehicle photogrammetry offers a practical solution for sandy coast, mangrove habitats demand a combination of remote sensing techniques and ground-based surveys.

DOI: 10.22034/gjesm.2026.01.07

This is an open access article under the CC BY license (http://creativecommons.org/licenses/by/4.0/).

NUMBER OF REFERENCES
33

NUMBER OF FIGURES
10

NUMBER OF TABLES
1

*Corresponding Author:
Email: *dg.pratomo@its.ac.id*
Phone: +62 822-3036-7485
ORCID: 0000-0002-1912-9723

Note: Discussion period for this manuscript open until Mar 1, 2026 on GJESM website at the "Show Article".

INTRODUCTION

Coastal regions form dynamic interfaces where terrestrial and marine interests intersect, making integrated spatial management a global imperative (Cicin-Sain and Knecht, 1998; Nichols *et al.,* 2000). In the past few decades, there has been an increasing emphasis on integrating land and sea management to mitigate disputes regarding resources and jurisdiction in these areas (Nichols *et al.,* 2000). A critical step in this integration is the establishment of a stable reference line along the shore (often termed the legal coastline) to serve as a common framework for both land and marine cadastres. A cadastre refers to a parcel-oriented land information system that holds a record of interests in land, including the rights, restrictions, and obligations related to each parcel. The concept of a legal coastline is analogous to the baseline used in maritime boundary delimitation, providing a fixed reference for delineating property rights, administrative boundaries, and development limits (Andriani, 2007). By providing a formal legal definition of the coastline's position, authorities intend to synchronize land tenure records with marine spatial planning systems, thus guaranteeing that development and resource exploitation are regulated smoothly across the land–sea interface. This integrated approach aligns with global calls for comprehensive coastal zone management, wherein clear delimitation of rights and boundaries underpins sustainable use of coastal resources (Cicin-Sain and Knecht, 1998). The high-water spring (HWS) datum was selected as the reference level for the legal coastline because it provides a balance between observability in the field and frequency of occurrence, while aligning with International Hydrographic Organization (IHO) standards and Indonesian agrarian law regarding accreted lands. The reliability of the HWS datum is confirmed by extensive tidal observations over an extended period, which are associated with the National Vertical Control Network, thereby establishing its credibility as a vertical reference. Although the physical coastline undergoes seasonal and long-term changes, the legal coastline functions as an epoch-based administrative boundary that provides cadastral certainty while remaining subject to periodic updates. Nevertheless, implementing such land–sea integration remains challenging, especially in regions with highly dynamic coastlines and fragmented governance structures. Fragmented legal systems governing land and ocean frequently result in institutional overlaps or gaps, which can cause conflicts and inconsistent enforcement. This highlights the necessity for an ongoing spatial and legal continuum between the two realms (de Vries and Pinuji, 2025). Indonesia, an archipelagic nation with approximately 5.8 million square kilometers (Mkm^2) of marine waters (about two-thirds of its total territory), faces pressing needs to integrate its land and marine spatial management (Abdul haris *et al.,* 2008). The concept of a marine cadastre is relatively new in the country; only in the early 2000s that attempts were made to establish its structure, learning from the experiences of leaders like Canada and Australia (Tamtomo, 2004; Kurniawan et al., 2023). In the absence of a unified cadastre, overlaps and gaps at the land–sea interface are common. Traditionally, terrestrial cadastral maps terminate at the high-water mark, whereas marine zoning plans, such as the coastal and small islands zoning plan (RZWP3K), commence from the low-water line extending seaward. Each of these is overseen by separate agencies operating under unique legal frameworks. During Indonesia's decentralization era, jurisdiction over coastal waters was explicitly tied to the coastline's position. For example, under Law No. 32/2004, a regency's authority extended seaward to 4 nautical miles (nm) from its coastline, the province covered 4–12 nm, and beyond 12 nm was federal domain. Such provisions make the precise determination of the coastline critically important: even minor coastline changes could shift local governance boundaries and alter which government level controls valuable marine resources and revenues. Moreover, Indonesian agrarian law recognizes the phenomenon of tanah timbul (accreted land), new land that forms as the coastline advances seaward. By default, these accreted lands are regarded as state property until they are officially registered to claimants; however, in reality, local communities frequently inhabit these areas, creating ambiguity between state and private ownership (Sembiring, 2018). Cases of unclear ownership and disputes over tanah timbul have been documented, underscoring the need for a clear demarcation at the coastal interface (Christian *et al.*, 2019). In this context, the creation of a legal coastline is perceived as a strategic measure to consolidate the land and marine cadastre, ensuring legal certainty

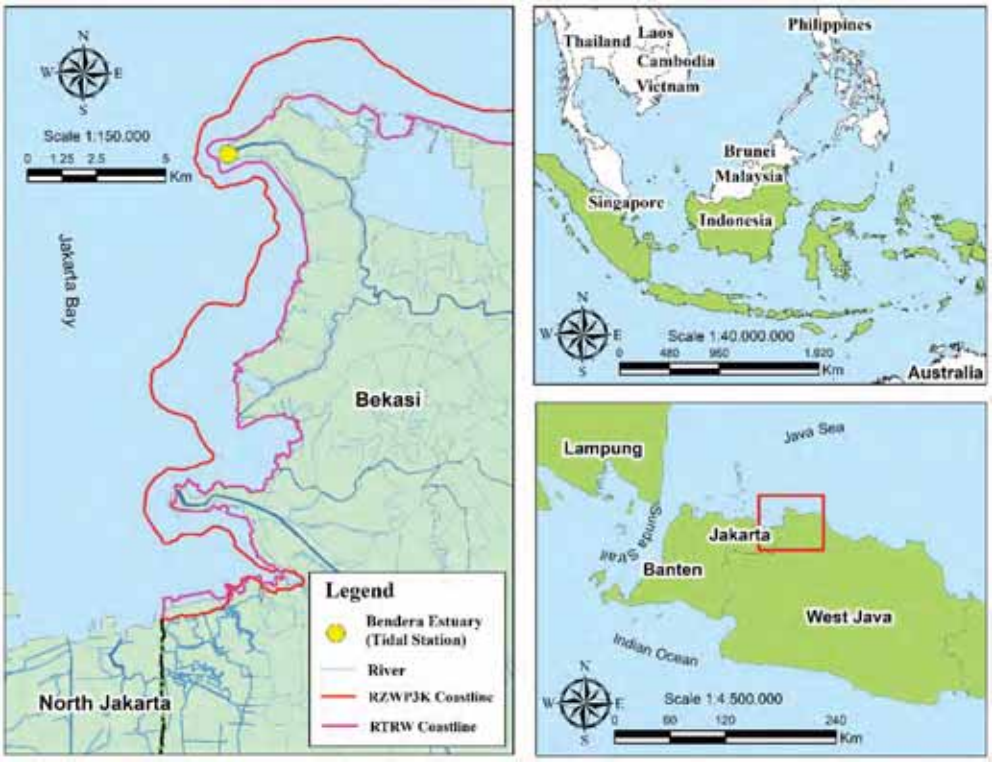

Fig. 1: Geographical location of the study area and comparison of historical Bekasi coastline positions derived from different delineations

and alleviating conflicts between onshore and offshore stakeholders. An officially defined coastline, used uniformly across agencies, would eliminate the "zero mile" ambiguity and ensure that land-use plans and marine plans meet at a coherent boundary (Djunarsjah *et al.*, 2022). This approach echoes recommendations from studies in other regions of Indonesia, which note that a agreed-upon legal coastline would greatly aid in synchronizing land administration records with marine spatial plans (Andriani, 2007). Fig. 1 demonstrates how this misalignment creates an ambiguous zone. Neither system clearly applies in this area. This leads to confusion concerning jurisdictional authority in intertidal regions and newly developed lands. Indonesia's Regional Spatial Plan (RTRW) and RZWP3K frameworks frequently overlap. They also leave unregulated spaces due to undefined boundaries, resulting in competing jurisdictions and inefficiencies (de Vries and Pinuji, 2025). positioned on the northern shore of West Java, serves as a prime example of the immediacy of these concerns. Its coastal districts, notably Muara Gembong, have experienced significant coastline changes in recent years due to both natural processes and human activities. Another study conducted on the Bekasi coast indicated that between 2011 and 2021, various segments of the coastline demonstrated a net gain of around 6.8 meters, while also highlighting localized regions of erosion (Meizwar and Tarya, 2024). This coastline change, driven by sediment transport dynamics and exacerbated in places by mangrove degradation and coastal engineering (e.g. aquaculture pond expansion), not only transforms the physical landscape but also challenges the static nature of existing cadastral and administrative boundaries. Land parcels that were once located inland can now be considered oceanfront properties as a result of erosion, while the process of accretion can lead to the emergence of new land extending seaward of the original surveyed limits. These changes raise practical and legal questions: Does a landowner's property extend as the shore accretes, or does the newly formed land belong to the state? Conversely, if the sea encroaches and erodes the coast, how are pre-existing land rights and boundaries adjusted? Without

a predefined legal coastline, answers to such questions tend to be handled in an ad-hoc, case-by-case manner, often leading to contention among government agencies and local communities. Bekasi's situation is not unique; similar challenges have been noted in other coastal areas, where the absence of a stable reference coastline leads to overlapping claims and protracted disputes (Christian *et al.,* 2019). Global insights indicate that this separation between terrestrial and marine environments can be reconciled. In Australia, for instance, research on Victoria's coast demonstrated that a clear interface between land and marine cadastres can be achieved by legislating a stable coastal boundary reference. Such a legally defined boundary can accommodate natural coastline movements within a predetermined buffer zone but remains fixed for administrative purposes, thereby providing certainty for planners, investors, and communities. Bekasi's coastal zone; a patchwork of urban development, fishponds, mangrove forests, and conservation areas; would similarly benefit from a stable reference line that all authorities recognize in their spatial plans. Fig. 1 shows an overlay of Bekasi's RZWP3K coastline in red and the RTRW coastline in magenta, revealing the misalignment at the current coastline. Furthermore, this study seeks to provide clarity on the integration of land and marine cadastre through the definition of a legal coastline in Bekasi Regency. The analysis begins by examining the current discrepancies between terrestrial and marine cadastral practices in coastal Bekasi, highlighting how these disconnects contribute to overlaps and gaps in spatial governance. Criteria and methodology are then proposed for defining a legal coastline in this region, considering geomorphological stability, tidal datums, and existing legal definitions of the coastline. Through the integration of geospatial analysis concerning historical alterations in coastlines alongside an institutional examination of jurisdictional frameworks. This approach seeks to identify a coastline definition that is both scientifically robust and administratively practical. Ultimately, this introduction sets the stage for developing a framework in which the legal coastline becomes the pivotal reference linking land titles and marine use rights. This framework is anticipated to improve coordination among agencies and establish a basis for more sustainable and organized coastal development in Bekasi Regency. The ensuing sections of this paper detail the methodology for delineating the proposed legal coastline, present the results of its implementation in a pilot area of Bekasi's coast with field measurement along 2025, and discuss the broader implications for policy and cadastral management in Indonesia's coastal zones. This study aspires to add to the developing dialogue on coastal governance by showing how a precisely defined legal coastline can link the terrestrial and marine domains, encouraging a more integrated and resilient cadastre system at the land and sea nexus. The study has been conducted in the coastal area of Bekasi Regency, Indonesia, in the 2025. Existing cadastral systems in Indonesia typically lack a unified reference line at the land–sea interface, with terrestrial cadastres stopping at arbitrary high-water marks and marine zoning plans starting from low-water lines. This study seeks to fill this void by introducing a scientifically robust and legally sustainable HWS-based coastline that acts as a unified authoritative boundary for both land and marine cadastre. The novelty of this approach lies in its integration of long-term tidal analysis, high-resolution UAV photogrammetry, and RTK ground validation to produce a coastline that is both technically robust and administratively practical. This study has two primary aims: 1) to establish a legal coastline for Bekasi Regency based on the HWS datum, integrating tidal data, UAV photogrammetry, and RTK surveys; and 2) to demonstrate how this unified coastline can serve as a framework for harmonizing land and marine cadastral systems. Secondary aims encompass assessing the precision and dependability of UAV-assisted shoreline mapping across various coastal morphologies, such as sandy beaches and mangrove-fringed regions, as well as determining optimal strategies for the application of epoch-based legal coastlines in dynamic coastal environments. The study has been conducted in the coastal area of Bekasi Regency, Indonesia, in the 2025.

MATERIALS AND METHODS

This study was conducted along the low-lying coastline of Bekasi Regency, West Java, Indonesia, including the mangrove-fringed estuary of Muara Bendera at the mouth of the Citarum River. Three representative sites were identified for comprehensive validation of the derived coastline:

Muara Bendera, Muara Beting, and Muara Bungin. Muara Bendera typifies a mangrove-fringed, muddy estuary; Muara Beting represents a mixed setting where sandy beach segments and mangrove stand coexist; and Muara Bungin represents an open sandy coast exposed to wave action. These three locations exemplify the prevailing coastal morphologies found in Bekasi Regency, thereby serving as a representative framework for analyzing the performance of the proposed workflow performs under contrasting environmental conditions. To capture the coastline under different tidal conditions, high-resolution aerial drone imagery (orthophotos) was acquired at two epochs: one near high tide and one near low tide. Although UAV flights were timed during spring tide periods, logistical constraints prevented capturing imagery at the exact moment of HWS or LWS (lowest water spring). Instead, flights were conducted near these tidal extremes, capturing the instantaneous waterline at the time of acquisition. This approach is justified because: 1) The exact timing of HWS and LWS is difficult to predict with precision due to meteorological effects (wind, atmospheric pressure) that can shift tidal extremes by ±30 minutes, 2) The vertical adjustment method based on the Digital Surface Model (DSM) does not necessitate imagery taken precisely at HWS; instead, it demands precise information regarding the water level at the time of imaging, which was recorded from the nearest tide gauge station. To address this data deficiency, a vertical adjustment procedure was employed: The instantaneous waterline extracted from the high-tide UAV image was recorded at a known water level (e.g., 0.45 m above datum). The DSM was subsequently employed to delineate the contour associated with the HWS elevation (0.567 m), effectively replicating the level to which the water would have ascended if the tide had reached HWS. This approach is mathematically equivalent to capturing imagery at exact HWS, provided that: a) the DSM has sufficient vertical accuracy, b) the beach slope is uniform, and c) no significant wave action occurred during the survey. These conditions were verified through comparison with RTK measurements.

The drone surveys, flown at sufficient altitude to cover the entire Bekasi coast, produced orthomosaics with ~10–20 centimeters (cm) ground resolution, providing much greater detail than typical aerial photography. Ground control points measured with real-time kinematic (RTK) global positioning system (GPS) were used to georeference the imagery and improve horizontal accuracy to a sub-meter level. Furthermore, ancillary data including tide gauge records and tide tables from the nearest port, which were analyzed to determine the vertical datum corresponding to HWS. This HWS datum represents the highest average tidal water line and serves as the target “legal coastline” elevation for the study. For reference and validation, official regional maps were obtained official regional maps: the terrestrial spatial plan (RTRW 2011–2031) and the marine zoning plan (RZWP3K 2018–2038) of Bekasi Regency, both of which delineate the current coastline used in planning. All spatial data were processed in a common coordinate system (WGS 84 / UTM zone 48S) using quantum geographic information systems (QGIS) software (QGIS 3.28). Additionally, a structure-from-motion photogrammetry workflow (Agisoft Metashape) was utilized to generate a digital surface model (DSM) from the UAV images, and MATLAB was applied for the analysis of tide data and necessary image processing. The RTK surveys were carried out using a Trimble R12i Global Navigation Satellite System (GNSS) system operating in real-time kinematic mode with corrections from a local continuously operating reference stations (CORS) network. Positions were documented at a rate of 1 Hz while the surveyor moved along with the visually determined high-water mark (HWM). In the field, the HWM was recognized from a combination of indicators: the last wet-sand line on sandy beaches, the accumulation of floating debris, and the seaward edge of permanent vegetation in mangrove-fringed sectors. Only epochs characterized by a consistent RTK solution and a horizontal dilution of precision beneath 2 were retained. The resulting discrete points were then ordered alongshore and converted into a continuous reference shoreline by interpolation using a low-tolerance spline (2 m) in QGIS. The polylines were not manually reshaped, which allowed the RTK-derived coastline to maintain an objective representation of the observed HWM.

The methodology was designed to derive the HWS-aligned coastline from the momentary drone observations. First, the UAV imagery was processed to extract the instantaneous coastlines at the survey times. To analyze the near high-tide image, an image segmentation method was employed to identify and separate water from land. Given the true-color (Red,

Table 1: Ground control point (GCP) coordinates used for UAV orthophoto and digital elevation model (DEM) georeferencing in Bekasi Regency

GCP	X meters (m)	Y (m)	Z (m)
Marunda	721550.178	9327910.271	2.899
Muara Bendera	721101.349	9343542.521	0.198
Muara Beting	725178.346	9344597.958	0.187
Muara Mekar	720983.701	9333787.595	-0.075
Muara Bungin1	731420.661	9343524.367	0.520
Muaran Bungin 2	732271.920	9342950.628	0.195
Marunda 2	721588.059	9327866.523	0.342

Green, Blue) nature of the drone orthophoto, the infrared-based water indices could not be directly used. In place of the original, the image underwent a conversion to grayscale, followed by the application of an automatic thresholding technique to objectively delineate the water's edge (Otsu, 1979; Hastuti *et al*., 2024). This thresholding separates water (darker pixels) from land (brighter mangrove or dry ground pixels) by maximizing inter-class variance. The Otsu thresholding method was applied to extract the instantaneous waterline from the grayscale UAV orthophoto. Although this automated approach is effective, it does not represent the definitive shoreline utilized for the legal coastline; instead, it functions as a preliminary estimate. The extracted waterline is subsequently corrected through the vertical adjustment to HWS using the DSM and tidal data and finally validated against RTK measurements. This multi-step validation process ensures that any errors in the initial thresholding are detected and corrected in the final product. Furthermore, the analysis of RTK measurements (Fig. 6) corroborates the precision of the final coastline derived from HWS, affirming the integrity of the entire extraction and adjustment methodology. The initial waterline derived from the high-tide image was a polyline representing the extent of inundation at that survey's tidal level. To adjust this line to the HWS vertical datum, the tidal records were used to calculate the difference between the water level at the flight time and the HWS level. The UAV-derived DSM of the coastal zone was crucial in this step. By elevating a horizontal water plane in the DSM to the height of HWS above a reference datum, the maximum expected inundation extent could be simulated (Huang *et al*., 2020). The interaction between this water plane and the coastal geography led to a delineated coastline that matches the HWS elevation. In essence, areas that were just above the water in the high-tide image would be submerged at HWS, and the DSM allows us to pinpoint how much further landward the water would reach. A continuous MHWS coastline was achieved by elevating the drone-mapped coastline to align with the HWS datum. The HWS-aligned coastline was then subjected to a simple and repeatable generalization routine in GIS to ensure it formed a single continuous polyline. A Douglas–Peucker algorithm with a 2 m tolerance was applied to remove small artefacts while preserving the overall shape, followed by topological cleaning to eliminate spikes and dangling segments. There was no manual modification of the coastline, and uniform parameters were employed for all locations. This approach limits subjectivity and ensures that spatial differences between locations reflect data quality and coastal morphology rather than editing choices. Throughout the extraction process, intermediate results were visually compared with existing aerial imagery to verify consistency (Du *et al*., 2016; Hastuti *et al*., 2024). However, the UAV-based method provided far higher spatial detail for features such as narrow tidal creeks, mangrove edges, and sea walls. Compliance with global charting standards was achieved by establishing the "legal coastline" at the high-water mark as recommended by the IHO (IHO, 2011; IHO, 2012; IHO, 2018). According to IHO specifications (S-4 and C-13), the coastline on charts is generally depicted at the mean high-water line (or mean high water springs in tidal areas), which aligns with the use of the HWS datum as shown in Fig. 2 (IHO, 2018). For each validation sector, the positional alignment of the RTK-derived coastline with the UAV-derived HWS coastline was assessed utilizing standard distance-based metrics. At n comparison points, we measured the signed perpendicular distance d_i from the RTK reference line to the test line, taking seaward offsets as positive. The

mean error (ME) and root mean square error (RMSE) were then computed using Eq. 1 (Hodson, 2022):

$$ME = \frac{1}{n}\sum_{i=1}^{n} d_i, \quad RMSE = \sqrt{\frac{1}{n}\sum_{i=1}^{n} d_i^2}$$

Where, these metrics summarize the systematic bias (ME) and overall dispersion (RMSE) of the UAV-derived coastline relative to the RTK reference. Even though a complete formal error propagation is not within the scope of this study, the key sources of error can be qualitatively summarized. RTK GNSS provides horizontal accuracies on the order of 2–3 cm and vertical accuracies of 3–5 cm under the conditions encountered in this study. The HWS tidal datum is estimated to have a vertical uncertainty of about 5 cm, while the UAV-derived DSM exhibits a vertical accuracy of approximately 0.1 m. When projected onto the horizontal plane through local beach slopes of 1-3°, these vertical uncertainties can lead to horizontal shifts of about 1–5 m, particularly on extremely mild intertidal flats. In addition to ME and RMSE, the validation at each site was summarized using an internal multi-criteria score on a 0–100 scale. Three components were evaluated: i) geometric accuracy, derived from ME, RMSE, and maximum distance; ii) morphological similarity, reflecting how well the overall shape of the test coastline follows the reference line; and iii) segment consistency, which captures the spatial variability of errors along the shore. Each component was normalized to a 0–100 range and the overall score was computed as their arithmetic mean. Scores above 80 are interpreted as VERY GOOD, 60–80 as GOOD, 40–60 as FAIR, and below 40 as POOR. These classifications are utilized in the results section to characterize the performance of the UAV-derived coastlines.

Finally, a validation and integration phase was conducted to assess the precision and consequences of the obtained coastline. The UAV-derived HWS coastline was compared against ground truth points collected with RTK GPS during a spring high tide event. The RTK survey, conducted along accessible sections of the coastline (for instance, edges of fishponds, seawalls, and beach berms at high tide), established that the positional variation of the HWS line obtained through remote sensing was within roughly 5–10 m of the observed high-water mark, an accuracy on the order of the UAV image resolution. This level of accuracy is acceptable for cadastral and planning purposes at the regional scale, given that it improves upon the tens of meters uncertainty often found in medium-resolution aerial-derived coastlines (Huang *et al*., 2020). The new legal coastline was then overlaid onto the existing RTRW land cadastre map and the RZWP3K marine plan map in QGIS. Any discrepancies or intersection between terrestrial and marine jurisdictions was instantly evident. In multiple sites, it was identified that the official land-use plan reached seaward of the HWS line into regions that are frequently submerged, whereas in different locations, the marine zoning map intruded too far landward. These discrepancies, in some cases hundreds of meters, can be attributed to coastline changes from erosion and land subsidence over the past decade, as well as to the use of inconsistent coastline definitions in the original maps. By updating the boundary to the HWS-aligned coastline, a unified cadastre boundary is effectively created: the terrestrial jurisdiction now ends exactly where the marine jurisdiction begins, eliminating gaps and overlaps (Djunarsjah *et al*., 2022). This strategy corresponds with larger endeavors to merge coastal and marine spatial data for improved governance (Fowler and Treml, 2001; Djunarsjah *et al*., 2022). In conclusion, the materials and methods outlined in this document establish a reliable procedure for identifying the legal coastline using high-resolution UAV data and tidal analysis. The integration of photogrammetric modeling, objective coastline extraction, and authoritative tidal datums ensure that the resulting boundary is both scientifically sound and legally robust. This harmonized land and sea boundary can facilitate clearer planning and management of the coastal zone, as recommended by marine cadastral frameworks, and it can be modified for other areas encountering comparable difficulties in defining a dynamic coastline as a stable legal boundary (IHO, 2011; IHO, 2018).

RESULTS AND DISCUSSION

This study began with the determination of the vertical position of the HWS as the reference for the highest coastline, using tidal observations from the Muara Bendera station. HWS represents the maximum tidal elevation (spring high tide) achieved within the tidal cycle and serves as the most stable tidal datum for coastal boundary delineation. Long-term harmonic tidal analysis was carried out to obtain the HWS elevation relative to the local vertical datum.

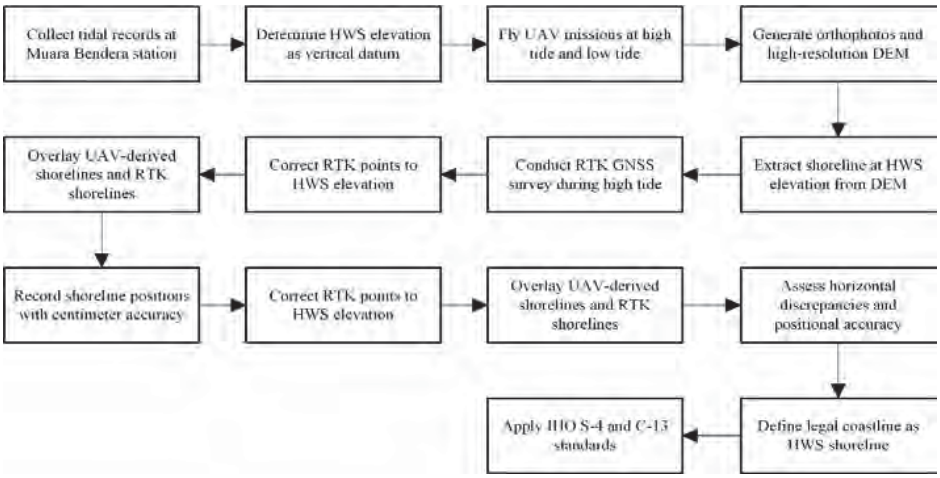

Fig. 2: Workflow of the research outlining integration of tidal data, UAV photogrammetry, and real-time kinematic -global navigation satellite system (RTK GNSS) surveys for the establishment of the legal coastline

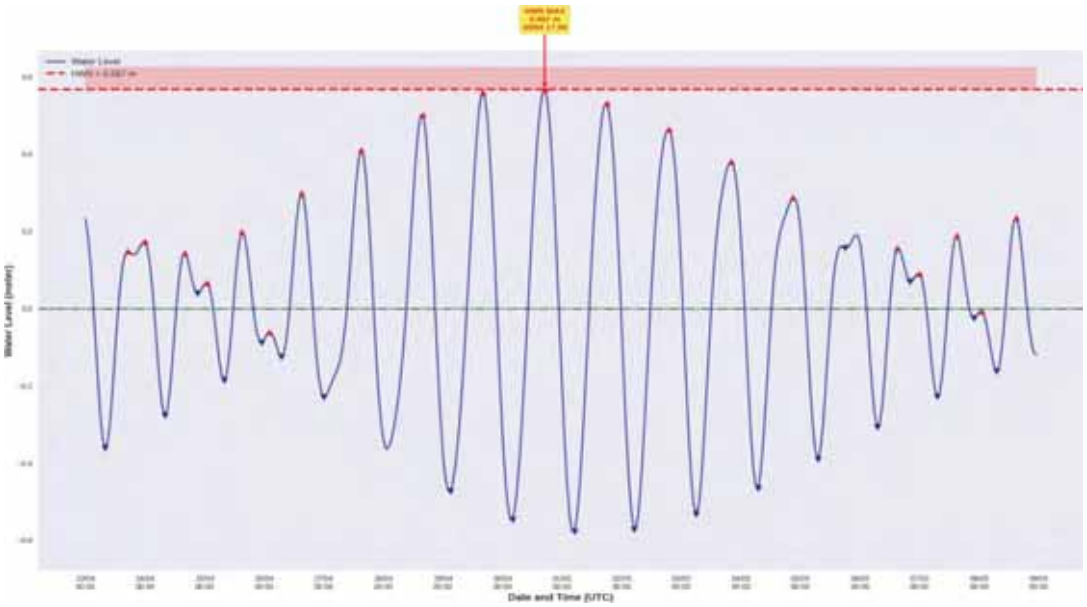

Fig. 3: Water level observations at Muara Bendera tide station during a spring tidal cycle, showing the maximum HWS elevation at 0.567 meters used as vertical reference

This technique aligns with the established norm that coastlines are typically characterized by specific tidal datums (Pajak and Leatherman, 2002; Parker, 2007). For instance, the National Oceanic and Atmospheric Administration (NOAA) in the United States defines the coastline on nautical charts as coinciding with the MHW, marking the division between land and sea (NOAA, 2019). Correspondingly, the IHO, through its S-4 standards, defines the coastline at the high-water mark, or at mean sea level where tidal variation is minimal (IHO, 2018). Other countries adopt variations of this definition: Spain applies Mean Sea Level, whereas China uses MHWS (Huang *et al.*, 2020). Regardless of these distinctions, the focus typically aligns with the highest water line, identified as the legal boundary between land and sea. Based on the Muara Bendera tidal records as shown in Fig.3, the local HWS elevation was determined with high

accuracy and subsequently applied as the vertical reference for all coastline analyses. Establishing HWS as the reference point guarantees that the outlined coastline matches the legally and scientifically acknowledged highest water line, in accordance with international hydrographic standards and national regulations (Andriani, 2007; Nugraha *et al*., 2019).

With the HWS elevation established, aerial imagery acquired by drone during high tide was vertically adjusted to delineate the coastline corresponding to the HWS level. This approach employed a high-resolution DEM produced through UAV photogrammetry of the coastal terrain. UAV mapping provided both orthophotos and DEMs with vertical accuracy better than 0.1 m, enabling precise extraction of elevation contours (Huang *et al*., 2020). The UAV orthophoto captured the instantaneous coastline at the time of flight, which usually lies below the HWS level. To convert this into the HWS coastline, the DEM was utilized to delineate the contour corresponding to the HWS elevation throughout the coastal topography. The resulting HWS contour was then projected onto the orthophoto, allowing the topographic intersection with the HWS datum to be clearly visualized. The result is a conceptual coastline that represents the topographic intersection with the HWS datum. Integration of tidal data with UAV DEM has been proven effective in earlier studies, where Huang *et al*. (2020) demonstrated that UAV DEM combined with tidal elevation information can map HWS with horizontal accuracy better than 0.2 m. Consequently, the UAV high-tide imagery adjusted to the HWS datum offered a reliable and accurate representation of the legal coastline, guaranteeing positional precision appropriate for cadastral and coastal planning. Slope distribution indicates that most coastal areas exhibit gentle gradients below 5°, especially in intertidal flats and reclaimed ponds. Steeper sections, above 10°, are concentrated in localized zones, often near natural levees or eroded embankments. Gentle slopes support tidal inundation and sediment deposition, while steeper edges suggest areas vulnerable to localized erosion. The differences in slope provide crucial context for assessing shoreline stability and the reliability of coastline delineation derived from HWS. Two UAV orthophotos, acquired at high tide and low tide, offered a comprehensive view of coastline variability induced by tidal range. At low tide, a broader portion of the beach and intertidal flat was exposed, revealing geomorphological features such as berms, tidal creeks, and mangrove fringes that are submerged during high tide. Conversely, the high tide orthophoto shows water encroaching further inland, reaching the maximum inundation boundary. By analyzing these two conditions, the intertidal zone is distinctly identified, and the likely HWS line can be deduced: frequently aligning with wet marks, debris lines, or vegetation boundaries (Fig. 4).

Traditionally, coastline mapping relied on manual identification of such indicators, but these methods are subjective Fig. 4 and dependent on surveyor judgment (Boak and Turner, 2005). However, multi-temporal UAV imagery delivers direct visual proof of the dynamics of coastlines, thus improving objectivity (Fabris *et al.,* 2023). The HWS coastline in this study was interpreted as the farthest water reach between the two UAV epochs. Pajak and Leatherman (2002) noted that the high-water line, such as the last wet sand line, is a widely accepted indicator of coastline position, though subject to short-term variability. This verification of HWS delineation on sandy coastlines is demonstrated at Muara Beting (Fig. 5) and Muara Bungin (Fig. 6), where the visual comparison of low-tide and high-tide orthophotos clearly supports the HWS position derived from the UAV surveys.

In this study, the dual UAV surveys facilitated a more dependable verification of the HWS position, affirming that the outlined HWS line was consistent with the maximum inundation recorded in the high tide orthophoto and the dry extent at low tide (Figs. 5 and 6).

Complementing UAV data, RTK GNSS surveys were conducted during both high and low tide to capture waterline positions with centimeter-level precision. Operators monitored the immediate coastline utilizing geodetic GNSS receivers in RTK mode, capturing both horizontal coordinates and elevations. These measurements were then corrected to the HWS datum by applying the tidal offset between observed water level and HWS elevation. As an illustration, the points obtained during low tide were raised by the difference to attain HWS, whereas points measured near spring high tide were lowered if the observed tide surpassed the average HWS. With DEM support and beach slope assumptions, these corrected points were interpolated to define the HWS coastline (Nugraha *et al*., 2019). Through

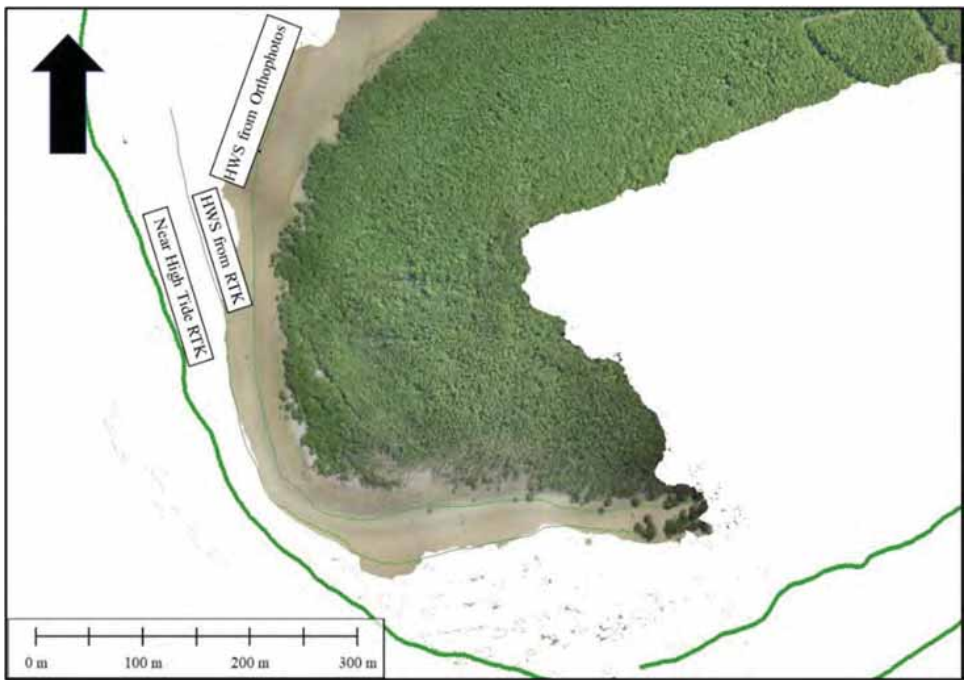

Fig. 4: Local coastline section showing comparison between HWS derived from orthophoto interpretation and RTK GNSS surveys at mangrove zones (Muara Bendera)

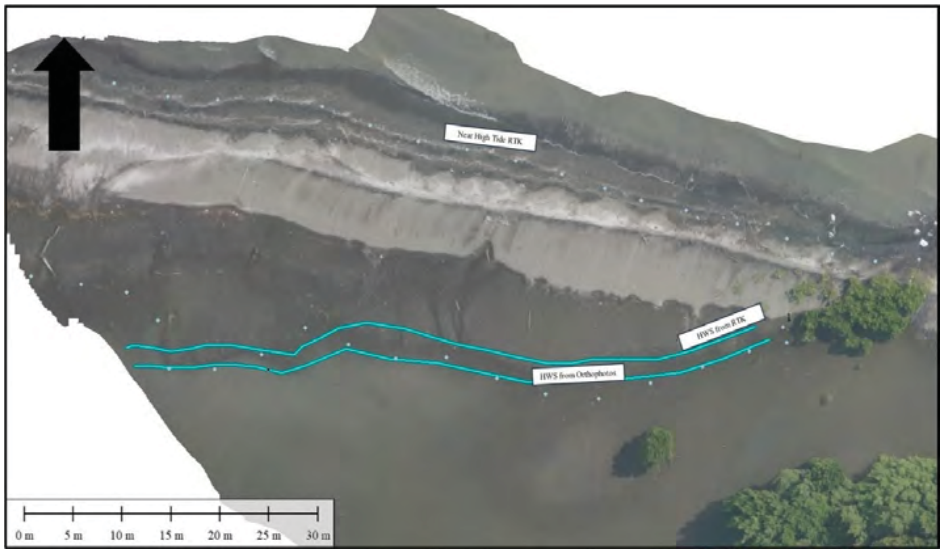

Fig. 5: Orthophoto of sandy coastline (Muara Beting) with overlaid delineations: instantaneous waterline near high tide from RTK, HWS from RTK, and HWS from orthophoto

this vertical-adjustment process, coastline traces observed at different tidal stages converge into a consistent HWS position. RTK GNSS offers distinct advantages, including rapid acquisition of highly accurate horizontal and vertical positions under varied conditions (Harley *et al*., 2011). This methodology has been validated effective in generating the lowest, highest, and mean coastlines that are in accordance with Indonesian regulatory standards when used alongside local tidal data (Nugraha *et al*., 2019). In this

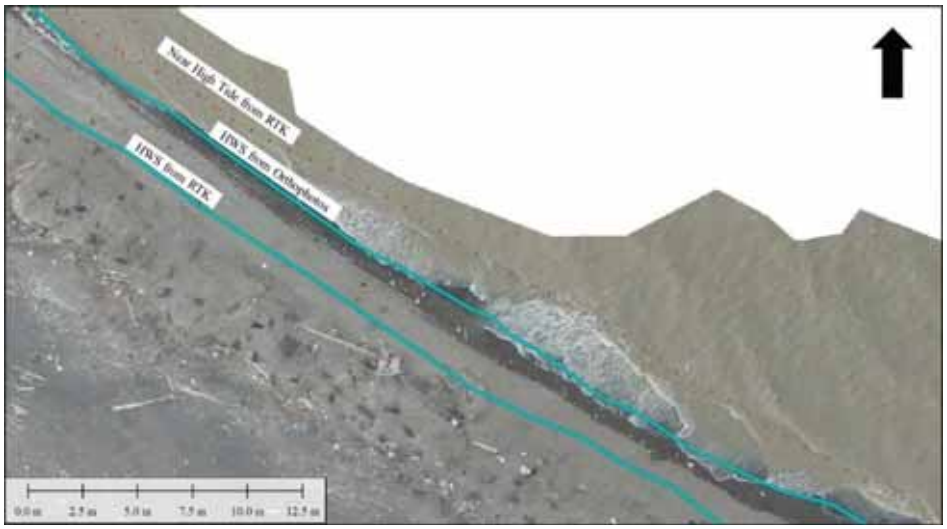

Fig. 6: Orthophoto of sandy coastline (Muara Bungin) with overlaid delineations: instantaneous waterline near high tide from RTK, HWS from RTK, and HWS from orthophoto

study, the RTK-derived HWS coastline closely matched physical indicators such as mangrove edges and debris lines, validating the transformation process. The three approaches; UAV high-tide correction, UAV low-tide interpretation, and RTK GNSS survey; were compared to evaluate consistency in identifying the HWS coastline. The aggregated findings indicated a high level of consensus, with differences typically falling within the decimeter range (Fig. 7). Minor variations observed in certain sectors were attributed to DEM resolution, UAV georeferencing uncertainties, or short-term wave effects during high tide. No systematic bias was evident among methods, affirming the robustness of the results. The UAV-derived HWS line and RTK measurements coincided within an average offset of less than 0.5 m, while the UAV low-tide interpretation deviated slightly more in flat coastal areas, where small vertical errors translate into larger horizontal shifts (Boak and Turner, 2005). These levels of consensus align with prior studies: Huang *et al*. (2020) reported ±0.2 m accuracy when integrating tidal data with UAV DEM, while Fabris *et al*. (2023) demonstrated negligible differences between UAV and RTK coastline surveys. These validations affirm that UAV photogrammetry, when aligned with tidal datums, yields accuracy on par with in-situ RTK surveys. The high consistency across methods builds confidence that the delineated HWS coastline truly represents the maximum tidal boundary in Bekasi.

Validation results for the mangrove-dominated shoreline at Muara Bendera revealed significant positional discrepancies, with an overall score of only 37.7/100, classified as “POOR”. The mean error reached 34.63 ± 17.29 m, RMSE 38.71 m, and a maximum deviation approaching 100 m. While morphological similarity remained high (92.3/100), indicating that the general shoreline form was captured, the geometric mismatch was severe, scoring 0.0/100. The issue originates from the dense mangrove canopy that conceals the real waterline, hindering precise identification of HWS solely from UAV orthophotos alone. This limitation confirms earlier findings that mangrove coastlines require complementary field-based methods, such as RTK GNSS, to ensure reliability (Fabris et al., 2023). Consequently, UAV delineation at Muara Bendera is not recommended for operational use without RTK validation. In contrast, validation on the sandy shoreline of Muara Beting yielded encouraging results, with an overall score of 75.6/100, categorized as “GOOD” (Fig. 8).

Geometric accuracy was moderate (58.9/100), with a mean positional error of 2.06 ± 0.38 m, RMSE 2.09 m, and a Hausdorff distance of 4.54 m. Furthermore, the morphological conformity attained a nearly perfect score of 99.6/100, demonstrating that the UAV-generated shoreline retained the general outline of the reference line. Consistency across segments was also

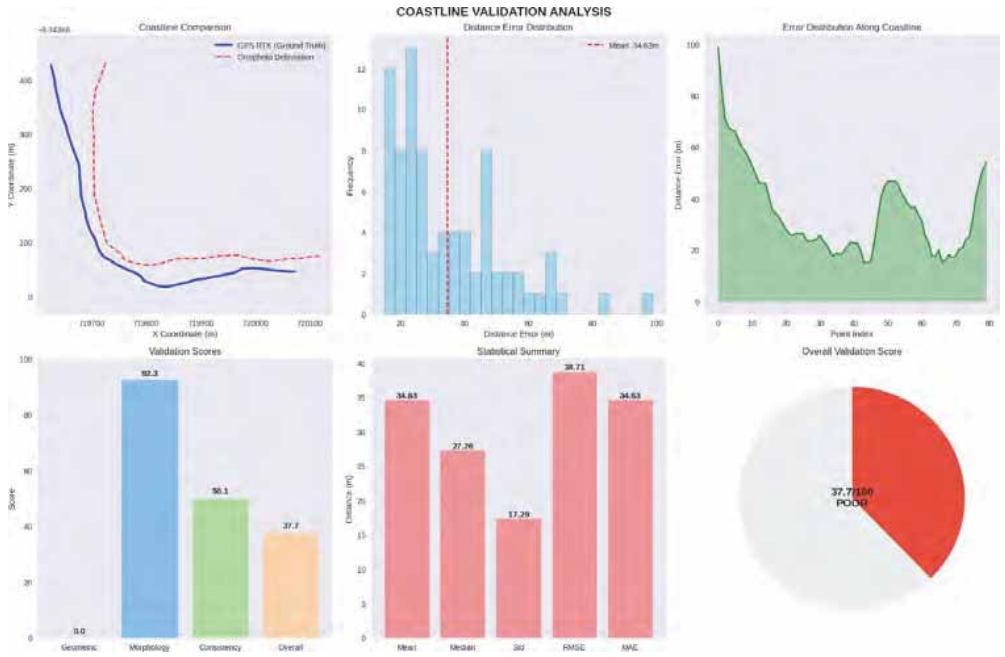

Fig. 7: Validation analysis between UAV-derived coastline and RTK shoreline at mangrove zones (Muara Bendera): (a) coastline comparison, (b) distance error distribution, (c) spatial distribution of errors, (d) validation scores, (e) statistical summary, and (f) overall accuracy classification.



Fig. 8: Validation analysis between UAV-derived coastline and RTK shoreline at Sandy coastline (Muara Beting): (a) coastline comparison, (b) distance error distribution, (c) spatial distribution of errors, (d) validation scores, (e) statistical summary, and (f) overall accuracy classification

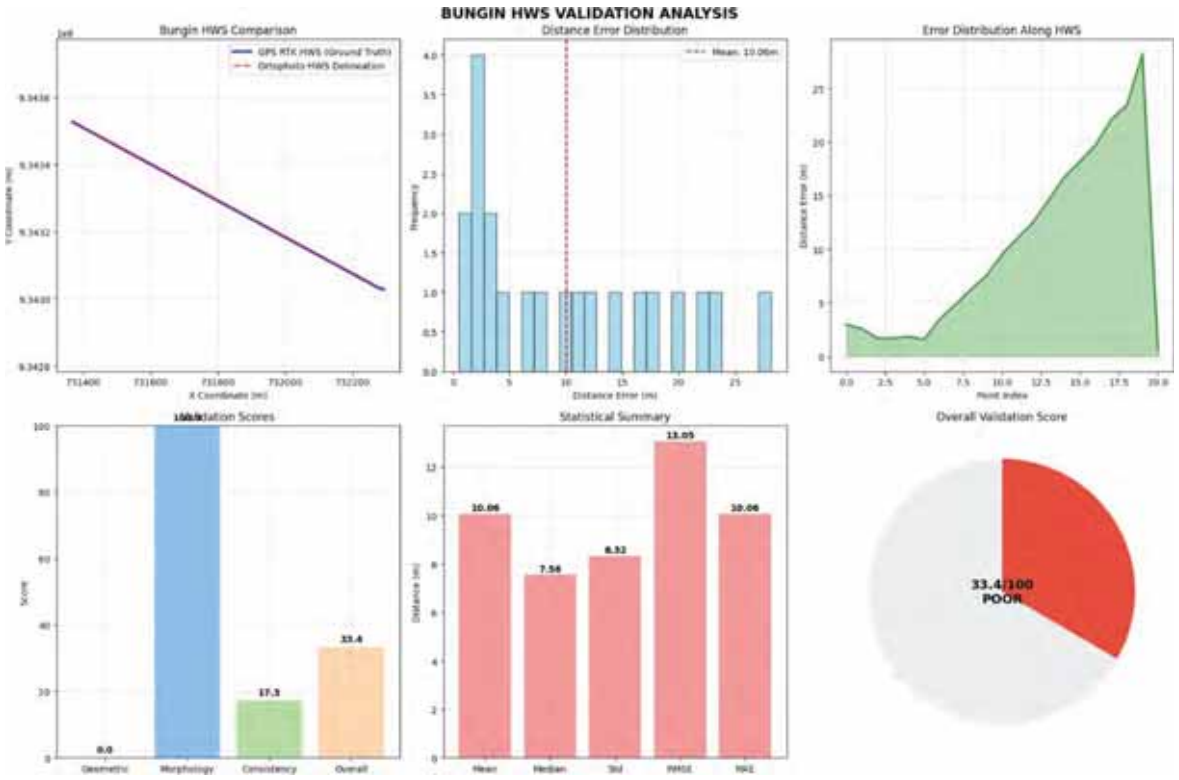

Fig. 9: Validation analysis between UAV-derived coastline and RTK shoreline at Sandy coastline (Muara Bungin): (a) coastline comparison, (b) distance error distribution, (c) spatial distribution of errors, (d) validation scores, (e) statistical summary, and (f) overall accuracy classification

strong at 81.3/100, confirming that UAV orthophotos aligned well with RTK reference measurements at High Water Spring (HWS). The results corroborate prior studies that demonstrate UAV photogrammetry's ability to achieve sub-meter accuracy in shoreline delineation when it is integrated with tidal datum corrections (Huang *et al.*, 2020; Nugraha *et al.*, 2019). The homogeneity of sandy coasts, with minimal vegetation and unobstructed waterlines, facilitated more reliable shoreline extraction. Thus, UAV-derived orthophotos in Muara Beting can be considered operationally suitable for HWS-based legal coastline delineation. Collectively, these differing outcomes emphasize the extent to which coastal morphology influences the dependability of UAV-based shoreline mapping. On sandy coasts such as Muara Beting, UAV workflows performed consistently well, offering shoreline delineations that closely followed the RTK reference with only minor discrepancies. In comparison, the shoreline bordered by mangroves at Muara Beting exhibited a significantly higher positional bias, necessitating thorough ground validation to address the challenges posed by thick vegetation and obscured tidal areas. These differences remind us that shoreline extraction is not merely a matter of technical capacity, but also of geomorphic context and environmental conditions that govern the visibility of tidal indicators in aerial imagery. The validation of Muara Bungin shows that orthophoto-based delineation achieved a poor overall score of 33.4/100, indicating limited reliability for operational use (Fig. 9). Although morphological similarity was excellent with a perfect score of 100, geometric accuracy failed (0.0) and consistency remained weak (17.3). The mean error reached 10.06 ± 8.32 m, with maximum deviation up to 28.19 m, highlighting positional offsets between orthophoto and RTK references. These results confirm that while UAV imagery preserves shoreline shape effectively, without precise ground correction it cannot be

directly adopted as the legal HWS coastline in sandy coastal settings like Muara Bungin. Subsequent to the validation process, the HWS line was officially recognized as the legal coastline for Bekasi Regency. This adoption aligns with the principles set out by the IHO, particularly through the S-4 standards and C-13 hydrographic guidelines, which prescribe the high-water mark as the operational boundary between land and sea (IHO, 2018). These contrasting accuracies reflect the different geomorphic settings represented by the three sites, with Muara Bendera, Muara Beting, and Muara Bungin standing for mangrove estuary, mixed sandy-mangrove, and open sandy coastlines, respectively. These variations can also be understood by considering the propagation of uncertainty throughout the workflow. On the sandy coasts of Muara Beting and Muara Bungin, modest vertical uncertainties from the tidal datum, RTK elevation, and DSM (on the order of centimeters to decimeters) translate into horizontal shifts of only a few meters because the beach slopes are relatively steeper. Conversely, at Muara Bendera, the interplay of extremely gentle slopes and a thick mangrove canopy exacerbate the vertical uncertainties into horizontal variations of several tens of meters. This simple error budget is consistent with the observed RMSE values and confirms that the poor performance in mangrove sectors is not only a technical limitation of the imagery, but also a geometric consequence of surveying in very flat, vegetated terrain. Collectively, these findings emphasize a consistent difference between sandy coasts and those dominated by mangroves. On open sandy shorelines such as Muara Beting, the instantaneous waterline is clearly visible in the orthophotos, vegetation does not obscure the intertidal zone, and beach slopes are steeper. Under these circumstances, the vertical uncertainties related to the tidal datum and DSM convert into horizontal discrepancies of just a few meters, and the UAV-derived HWS line accurately tracks the RTK reference. In mangrove-fringed sectors like Muara Bendera, however, the dense canopy hides the true land–water interface, and the very gentle slopes and irregular micro-topography amplify any vertical uncertainty into large horizontal discrepancies. The automated extraction consequently tends to follow the canopy edge instead of the actual HWS. This explains why the overall score is “POOR” in mangrove areas and “GOOD” on sandy coasts and confirms that hybrid workflows combining UAV imagery with RTK ground surveys are essential in vegetated shorelines.

In practical terms, the legacy RTRW coastline in several sectors lies seaward of the HWS-based legal coastline by tens to hundreds of meters, so that parcels classified as terrestrial land-use fall within areas that are regularly inundated. Additionally, these localized sections of the RZWP3K coastline intrude landward of the HWS line, leading to an intersection between marine zones and land parcels. Through the adoption of the HWS-based line as a common boundary, these inconsistencies are resolved, and the terrestrial jurisdiction now terminates exactly where the marine jurisdiction begins. This spatial correction directly clarifies which level of government is responsible for issuing permits and enforcing regulations in coastal fishpond clusters, conservation strips, and coastal protection zones, reducing the scope for overlapping mandates and conflicting decisions. Indonesian regulations reflect this methodology by characterizing coastlines as tidal limits, categorized into lowest, highest, and mean sea levels (Government of Indonesia, 2011). The finalized legal coastline captures the highest tidal reach along the coast, thus providing a unified reference point that is both scientifically sound and legally enforceable. The significance of this line extends beyond cartography. As a spatial reference, it serves as the foundation for cadastral delineation, provides insight into administrative boundaries, and directs spatial planning tools like setback zones and coastal management policies. By anchoring these processes to an HWS-based datum, Bekasi achieves a level of consistency that resonates with international hydrographic practice while ensuring compliance with national legislation (Andriani, 2007; Djunarsjah *et al*., 2022). At the same time, this legal coastline does not deny the dynamism of the coast. Conversely, it accepts that while physical shorelines can shift due to erosion, accretion, or changes in sea level, governance must rely on a consistent and authoritative reference line; one that is subject to periodic revision as scientific evidence and environmental change demand it. In this way, the legal coastline becomes both a stable foundation for present management and a flexible instrument for future adaptation.

CONCLUSION

This study successfully establishes a legal coastline

based on the High-Water Spring (HWS) datum, offering a unified and authoritative framework to bridge the land and marine cadastre in accordance with IHO S-4 and C-13 standards. The principal methodological contribution of this study lies in the establishment of an integrated workflow that merges long-term tidal observations, UAV orthophotography, DEM extraction, and RTK GNSS surveys to scientifically delineate the highest tidal reach. The validation process illustrates that the method's reliability is largely determined by coastal morphology. In open sandy environments like Muara Beting, the UAV-derived delineation proved highly effective, achieving a mean error of approximately 2 m and a "good" overall score of 75.6/100. Conversely, complex mangrove environments such as Muara Bendera posed significant challenges, yielding a mean error approaching 35 m (score 37.7/100) and necessitating ground-based RTK validation. The inconsistent results recorded at Muara Bungin (score 33.4/100) further illustrate that UAV outputs may fluctuate according to local wave conditions and data reliability, thereby reinforcing the importance of hybrid methodologies in dynamic or vegetated coastal areas. To ensure that this framework is replicable in other coastal regions, specific data requirements and procedural guidelines are identified. Essential data includes: i) a multi-year tidal record to derive a stable HWS datum; ii) high-resolution UAV imagery capturing the intertidal zone; iii) a robust DEM of the coastal topography; and (iv) existing terrestrial and marine spatial plans. The operational workflow is comprised of five fundamental steps:1) defining the legal tidal datum (HWS) through harmonic analysis; 2) acquiring and processing UAV data to generate orthophotos and DEMs; 3) vertically adjusting the instantaneous shoreline to the HWS level using the DEM; 4) validating the derived line with RTK GNSS ground truth; and 5) integrating the finalized coastline into cadastral layers to resolve spatial overlaps. The implementation of this HWS-based legal coastline goes beyond mere cartographic precision; it functions as an essential tool for coastal governance. By providing a single, legally recognized reference, it resolves the historical jurisdictional ambiguity between terrestrial (RTRW) and marine (RZWP3K) spatial plans in Bekasi Regency. This clarity eliminates the "grey zone" at the land–sea interface, strengthens the marine cadastre, and provides the spatial certainty necessary for responsible investment in the blue economy, such as sustainable aquaculture and marine tourism. Furthermore, a reliable legal coastline functions as a reference point for tracking the impacts of climate change, including increases in sea levels and shoreline erosion, thereby allowing for more targeted ecosystem-based adaptation strategies. Despite these contributions, it is essential to recognize several limitations in a clear manner. First, the tidal analysis relied on a single gauge station at Muara Bendera; while the best available source, it may not fully capture the localized hydrodynamic variability across the entire regency. Second, the reliance on optical UAV sensors limits accuracy in densely vegetated areas, as the canopy obscures the true land–water interface. Subsequent studies should thus focus on establishing a more extensive network of tidal gauges to enhance local tidal models and investigate the incorporation of active remote sensing technologies, including Light Detection and Ranging (LiDAR), which provide improved canopy penetration. Addressing these limitations will further enhance the robustness and universal applicability of the legal coastline framework.

AUTHOR CONTRIBUTIONS

J. Setiyadi designed the research framework, performed geodetic analysis, and led the manuscript preparation. B.M. Sukotjo: Contributed to the development of methodological design, including tidal harmonics computation and integration with cadastral frameworks. D.G. Pratomo processed satellite imagery, conducted spatial analyses using Google Earth Engine and QGIS, and supported data visualization. M.N. Cahyadi assisted in field validation, GNSS survey design, and uncertainty quantification. W.S. Pranowo provided scientific input on tidal dynamics, data interpretation, and the integration of coastal governance perspectives.

ACKNOWLEDGEMENT

Authors express our gratitude to PT Hidronav Teknikatama for their assistance in supporting the instrument for our data collection. Authors also would like to acknowledge the Indonesian Naval Technology College (STTAL) for providing personnel support during field operations, and the Geospatial Information Agency (BIG) for supplying the tidal data used in this research. Additionally, we would like to thank the Upgrading Tugas Akhir Writing-IPR Incentive

Program (PPHKI) 2025 No. 1762/PKS/ITS/2025 for NRP 7016231001 for the financial support of this study.

CONFLICT OF INTEREST

The authors declared that there was no conflict of interest regarding the publication of this manuscript. In addition, ethical issues, including plagiarism, informed consent, misconduct, data fabrication and/or falsification, double publication and/or submission, and redundancy have been completely observed by the authors.

OPEN ACCESS

©2026 The author(s). This article is licensed under a Creative Commons Attribution 4.0 International License, which permits use, sharing, adaptation, distribution and reproduction in any medium or format, if you give appropriate credit to the original author(s) and the source, provide a link to the Creative Commons license, and indicate if changes were made. The images or other third-party material in this article are included in the article's Creative Commons license, unless indicated otherwise in a credit line to the material. If material is not included in the article's Creative Commons license and your intended use is not permitted by statutory regulation or exceeds the permitted use, you will need to obtain permission directly from the copyright holder. To view a copy of this license, visit: http://creativecommons.org/licenses/by/4.0/

PUBLISHER'S NOTE

GJESM Publisher remains neutral regarding jurisdictional claims in published maps and institutional afflictions.

R Positive AI Statement

During the preparation of this work the author(s) have used Artificial Intelligence (AI) [ChatGPT and MANUS] to [brainstorming and developing the ideas]. After using this tool/service, the authors reviewed and edited the content as needed and took full responsibility for the content of the publication.

(For this reason, the GPTZero detector will evaluate the manuscript utilizing Generative AI, ensuring a high detection rate. If the manuscript relies heavily on Generative AI and AI-assisted technologies, it will be archived without further options for appeal).

ABBREVIATIONS

%	Percent
cm	Centimeters
CORS	Continuously Operating Reference Stations
DEM	Digital elevation model
DSM	Digital surface model
GPS	Global positioning system
GNSS	Global navigation satellite system
HWM	High-Water Mark
HWS	High-water spring
IHO	International hydrographic organization
LWS	Lowest Water Spring
m	Meters
ME	Mean Error
Mkm²	Million square kilometers
NOAA	National oceanic and atmospheric administration
nm	Nautical miles
QGIS	Quantum Geographic Information System
RMSE	Root Mean Square Error
RTK	Real-time kinematic
RZWP3K	Coastal and small islands zoning plan
RTRW	Regional spatial plan
UAV	Unmanned aerial vehicle

REFERENCES

Abdulharis, R.; Djunarsjah, E.; Hernandi, A., (2008). Stakeholder analysis on implementation of marine cadastre in Indonesia. FIG Working Week 2008; Integrating Generations. 14–19 **(6 pages).**

Andriani, V., (2007). Kajian legal coastline dalam mendukung pelaksanaan kadaster kelautan di Indonesia. Master's thesis, Institute Teknologi Bandung.

Boak, E.H.; Turner, I.L., (2005). Shoreline definition and detection: A review. J. Coast. Res., 21(4): 688–703 **(16 pages).**

Christian, Y.; Budiman, M.A.K.; Fahrudin, A.; Santoso, N., (2019). Iregularitas agraria "tanah timbul" (aanslibbing) dan perubahan lanskap di wilayah pesisir Ujung Pangkah, Gresik Jawa Timur. Bhumi. J. Agraria dan Pertanahan, 5(2): 217–233 **(17 pages).**

Cicin-Sain, B.; Knecht, R.W., (1998). Integrated coastal and ocean management: concepts and practices. Washington, DC: Island Press.

de Vries, W.T.; Pinuji, S., (2025). Balancing between land and sea rights; An analysis of the "Pagar Laut" (sea fences) in Tangerang, Indonesia. Land, 14(7): 1382.

Djunarsjah, E.; Putra, A.P.; Kusumadewi, D.; Yudistira, K.; Julian, M.M., (2022). The concept of integration between state and provincial sea boundaries in Indonesia. Sustainability. 14(3).

Du, Y.; Zhang, Y.; Ling, F.; Wang, Q.; Li, W.; Li, X., (2016). Water bodies' mapping from Sentinel-2 imagery with modified normalized difference water index at 10-m spatial resolution produced by sharpening the SWIR band. Rem. Sens., 8(4): 354.

Fabris, M., Balin, M., & Monego, M. (2023). High-Resolution Real-Time Coastline Detection Using GNSS RTK, Optical, and Thermal SfM Photogrammetric Data in the Po River Delta, Italy. Remote Sensing, 15(22): 5354.

Fowler, C.; Treml, E., (2001). Building a marine cadastral information system for the United States; A case study. Comput. Environ. Urban Syst., 25(4–5): 493–507 **(15 pages)**.

Government of Indonesia, (2011). Government regulation No. 4 of 2011 on geospatial information. Jakarta: Government of Indonesia.

Gorelick, N.; Hancher, M.; Dixon, M.; Ilyushchenko, S.; Thau, D.; Moore, R., (2017). Google Earth Engine: Planetary-scale geospatial analysis for everyone. Remote Sens. Environ., 202: 18–27 **(10 pages).**

Harley, M.D.; Turner, I. L.; Short, A.D.; Ranasinghe, R., (2011). Assessment and integration of conventional, RTK-GPS and image-derived beach survey methods for daily to decadal coastal monitoring. Coast. Eng., 58(2): 194–205 **(12 pages).**

Hastuti, A.W.; Ismail, N.P.; Nagai, M., (2024). Analysis of coastline extraction indices using sentinel-2 and google earth engine: a case study in bali, indonesia. BIO Web Conference. 106: 04004.

Hodson, T.O., (2022). Root-mean-square error (RMSE) or mean absolute error (MAE): When to use them or not. Geosci. Model Dev., 15(15): 5481–5487 **(7 pages).**

Huang, C.; Zhang, H.; Zhao, J., (2020). High-efficiency determination of coastline by combination of tidal level and coastal zone DEM from UAV tilt photogrammetry. Remote Sens., 12(14): 2189.

IHO, (2011). Manual on hydrography (Publication C-13). Monaco: International Hydrographic Organization.

IHO, (2012). Definition of the coastline for nautical charts and mapping (HSSC4-03C Rev1, 4th IHO-HSSC Meeting). International Hydrographic Organization.

IHO, (2018). Regulations of the IHO for International (INT) Charts (Publication S-4, version 4.8.0). Monaco: International Hydrographic Organization.

Kurniawan, A.; Pranowo, W. S.; Hardjo, K.S.; Santoso, A.I.; Khakhim, N.; Purwanto, T.H.; Setiyadi, J., (2023). 3D marine cadastral system to support marine spatial planning implementation in indonesia: a case study of penanjung bay. Geomatics Environ. Eng., 17(3): 65–80 **(16 pages).**

Li, R.; Ma, R.; Di, K., (2002). Digital tide-coordinated shoreline. Marine Geo., 25(1-2): 27–36 **(10 pages).**

McFeeters, S.K., (1996). The use of the normalized difference water index (NDWI) in the delineation of open water features. Int. J. Remote Sens., 17(7): 1425– 1432 **(8 pages).**

Meizwar, D.A.; Tarya, A., (2024). Dinamika perubahan garis pantai di Muara Gembong, Bekasi, Jawa Barat pada tahun 2011–2021. J. Trop. Mar. Sci., 7(2).

Nichols, S.; Monahan, D.; Sutherland, M., (2000). Good governance of Canada's offshore and coastal zone: Towards an understanding of the marine boundary issues. Geomatica, 54(4): 415–424 **(10 pages).**

NOAA, (2019). Shoreline mapping program. National Ocean Service, Office of Coast Survey.

Nugraha, W.; Parapat, A.D.; Arum, D.S.; Istighfarini, F., (2019). GNSS RTK application to determine coastline: Case study at northern area of Sulawesi and Gorontalo. E3S Web of Conferences, 94: 01016 (**7 pages**).

Otsu, N., (1979). A threshold selection method from gray-level histograms. IEEE Trans. Syst., Man., Cybern., 9(1): 62–66 **(5 pages).**

Pajak, M.J.; Leatherman, S.P., (2002). The high-water line as shoreline indicator J. Coast. Res., 18(2): 329–337 **(9 pages).**

Parker, B.B., (2007). Tidal Analysis and Prediction. NOAA Special Publication NOS CO-OPS 3, U.S. Department of Commerce.

Sembiring, J., (2018). Pengertian, pengaturan dan permasalahan tanah negara. Jakarta: Prenadamedia Group.

Solihuddin, T.; Triana, K.; Rachmayani, R.; Husrin, S., Pramudya, F.A.; Salim, H.L., (2024). The impact of coastal erosion on land cover changes in Muaragembong, Bekasi, Indonesia: A spatial approach to support coastal conservation. J. Coast. Conserv., 28(2): 43.

Tamtomo, J.P., (2004). The needs for building concept and authorizing implementation of "marine cadastre" in Indonesia. Proceedings of the 3rd FIG Regional Conference, Jakarta, Indonesia.

Xu, H., (2006). Modification of normalised difference water index (NDWI) to enhance open water features in remotely sensed imagery. Int. J. Remote Sens., 27(14): 3025–3033 **(9 pages).**

AUTHOR (S) BIOSKETCHES

AUTHOR (S) BIOSKETCHES

Setiyadi, J., M.Eng., Ph.D. Candidate, Geomatics Engineering, Institut Teknologi Sepuluh November, Surabaya, Indonesia. Study program of Oceanography, Indonesia Naval Postgraduate Military Service School (STTAL), Ganesha Street No. 1, West Kelapa Gading, Jakarta, Indonesia.
- Email: *jsetiyadi99@gmail.com*
- ORCID: 0009-0001-8656-3802
- Web of Science ResearcherID: NA
- Scopus Author ID: 58695074600
- Homepage: sttal.ac.id

Sukotjo, B, M., Ph.D., Professor, Geodetic Center for Appropriate Technology Center for Disaster Mitigation and Climate Change Department of Geomatics Engineering, Laboratory of Geospatial, Surabaya, Indonesia.
- Email: *bangun_ms@geodesy.its.ac.id*
- ORCID: 0009-0007-2985-7998
- Web of Science ResearcherID: NA
- Scopus Author ID: 57200093444
- Homepage: https://www.its.ac.id/tgeomatika/id/dosen-staff/daftar-dosen/dosen-lab-geospasial/

Pratomo, D.G., Ph.D. Associate Professor, Geomarine Laboratory, Geomatics Engineering, Institut Teknologi Sepuluh November, Surabaya, Indonesia.
- Email: *dg.pratomo@its.ac.id*
- ORCID: 0000-0002-1912-9723
- Web of Science ResearcherID: NA
- Scopus Author ID: 57190088831
- Homepage: https://www.its.ac.id/tgeomatika/id/dosen-staff/daftar-dosen/dosen-lab-geomarine/

Pranowo, W.S., Ph.D., Adjunct Professor, Study program of Oceanography, Indonesia Naval Postgraduate Military Service School (STTAL), Ganesha Street No. 1, West Kelapa Gading, Jakarta, Indonesia. Research Center for Climate and Atmosphere (BRIN), B.J. Habibie Building Science and Technological Park, South Tangerang City, Banten, Indonesia. Korea-Indonesia Marine Technology Cooperation and Research Center (MTCRC), Jakarta, Indonesia.
- Email: *widodo.pranowo@gmail.com*
- ORCID: 0000-0002-5798-4181
- Web of Science ResearcherID: P-8252-2017
- Scopus Author ID: 24802605300
- Homepage: https://sttal.ac.id/direktorat/pasca-sarjana/oceanography/

Nurcahyadi, M.N., Ph.D. Professor, Center for Marine and Earth Science Technology Department of Geomatics Engineering, Laboratory of Surveying and Cadaster, Institut Teknologi Sepuluh November, Surabaya, Indonesia.
- Email: *cahyadi@geodesy.its.ac.id*
- ORCID: 0000-0002-0549-0606
- Web of Science ResearcherID: NA
- Scopus Author ID: 55803720500
- Homepage: https://scholar.its.ac.id/en/persons/mokhamad-nur-cahyadi/

HOW TO CITE THIS ARTICLE

Setiyadi, J.; Sukotjo, B.M.; Pratomo, D.G.; Cahyadi, M.N.; Pranowo, W.S., (2026). The legal coastline as a unifying framework for land and marine cadastre. Global J. Environ. Sci. Manage., 12(1): 111-128.

DOI: 10.22034/gjesm.2026.01.07

URL: https://www.gjesm.net/article_732311.html

Global J. Environ. Sci. Manage. 12(1): 129-152, Winter 2026, Serial #45

Global Journal of Environmental Science and Management
(GJESM)

Homepage: https://www.gjesm.net/

Podcasts

ORIGIINAL RESEARCH PAPER

Environmental and economic performance of hybrid charging stations

R. Rosmeika[1], A. Aditiyawan[1,2], M.A. Hipi[1], A. Erliza[1], A.W. Sani[1], U. Ayuningtyas[1], D.F. Soraya[1], A.Y.N. Sakti[1], N. Andriyani[1], H. Febriansyah[1], C.K. Sari[1], A.I. Pratiwi[3], M. Septiani[4], I.E. Setiawan[5,*]

[1] *Research Center for Sustainable Industrial and Manufacturing Systems, National Research and Innovation Agency, South Tangerang, Indonesia*

[2] *Faculty of Engineering and Informatics, Universitas Multimedia Nusantara, South Tangerang, Indonesia*

[3] *Research Center for Limnology and Water Resources, National Research and Innovation Agency, Bogor, Indonesia*

[4] *Bureau of Public Communication, General Affairs, and Secretariat, National Research and Innovation Agency, South Tangerang, Indonesia*

[5] *Postgraduate Program of Science in Sustainability, Faculty of Infrastructure Planning, Universitas Pertamina, Jakarta, Indonesia*

ARTICLE INFO

Article History:
Received 12 August 2025
Revised 18 November 2025
Accepted 22 December 2025

Keywords:
Economic analysis
Electric vehicle
Environmental impact
Hybrid charging station
Life cycle assessment
Photovoltaic

DOI: 10.22034/gjesm.2026.01.08

ABSTRACT

BACKGROUND AND OBJECTIVES: The global use of electric vehicles is growing rapidly as a strategy to prevent climate change. In Indonesia, although there is a growing number of electric vehicle charging stations, the majority still depend on electricity produced from fossil fuels, which consequently restricts the overall environmental advantages. The integration of photovoltaic systems into charging infrastructure offers a low-carbon alternative, but their implementation may entail environmental trade-offs. The study aimed to evaluate trade-offs by employing an integrated life-cycle assessment and life-cycle costing framework for the first hybrid charging station in Indonesia, as well as to offer comparative insights for sustainable charging infrastructure.

METHODS: The life cycle assessment was conducted with a cradle-to-grave system boundary. A one-kilowatt-hour of electricity was implemented as a functional unit to compare the energy source scenarios. The Ecoinvent 3.8 database for secondary data and the ReCiPe 2016 midpoint (H) method are employed on Open-life cycle assessment software. The analysis of life-cycle costs encompassed capital expenditures, operational and maintenance costs, along with the revenue from the hybrid charging station, projected for a 20-year operational timeframe.

FINDINGS: This study showed that charging stations powered by photovoltaic energy emitted the lowest environmental impacts. The minimal impact was observed across nearly all categories, except for the terrestrial ecotoxicity potential. The global warming potential associated with the hybrid charging station was measured at 1.11 kilograms of carbon dioxide equivalent, which is 1.36 percent lower than the electricity from the full-grid scenario. Implementing the full photovoltaic system can reduce the global warming potential impact by up to 85.94 percent. Life cycle cost analysis showed that the hybrid charging station maximizes long-term net economic value, with a net present value of United States Dollar 237,533.75 and a total life cycle cost of United States Dollar negative 251,785.77. Although the comprehensive grid configuration showed enhanced short-term performance, the full photovoltaic system realized the minimal levelized cost of energy.

CONCLUSION: Hybrid charging stations offer the best economic performance, while full PV solar systems offer the best environmental benefits. The combination of the two energy sources, along with an increase in renewable energy generation, can contribute to a more sustainable electric vehicle charging station infrastructure.

This is an open access article under the CC BY license (http://creativecommons.org/licenses/by/4.0/).

NUMBER OF REFERENCES
69

NUMBER OF FIGURES
9

NUMBER OF TABLES
6

*Corresponding Author:
Email: *setiawanimameko@gmail.com*
Phone: +62821 1606 1882
ORCID: 0000-0003-3598-8808

Note: Discussion period for this manuscript open until Mar 1, 2026 on GJESM website at the "Show Article".

INTRODUCTION

The global shift toward low-carbon mobility is accelerating as countries work to reduce transportation-related greenhouse gas (GHG) emissions. Khaleel *et al*. (2024) report that global Electric vehicle (EV) sales grew by about 55 percent (%) between 2021 and 2022, with similarly strong increases in China (60%) and the United States (55%), while Europe recorded a more moderate rise of over 15% during the same period. Emerging regions like Southeast Asia and Latin America have experienced an increase in EV ownership of up to four times compared to the prior year (Fathoni *et al*., 2025). These trends indicate a move from fossil-fuel vehicles to cleaner, more efficient transport technologies (Kongwee *et al*., 2025). This transition is crucial, given that transportation contributes approximately 23% of global energy-related GHG emissions and is a significant contributor to urban air pollution (Jaramillo *et al*., 2022). Indonesia, the world's fourth-most populous country, has experienced steady growth in motorized vehicle ownership, leading to a significant decline in urban air quality. In some areas, fine particulate matter 2.5 ($PM_{2.5}$) levels exceed the World Health Organization's (WHO) guideline by five to ten times, increasing public health risks (Amin *et al*., 2024). Road transportation accounts for nearly 40% of carbon dioxide (CO_2) emissions associated with transport, having released 1.35 megatons CO_2 in 2022 (Haq *et al*, 2024). In response, Indonesia has committed to reducing emissions by 31.89% by 2030 under the enhanced nationally determined contribution (ENDC) (Ministry of Environmental and Forestry, 2022). To meet this target, the government has introduced policies to accelerate EV adoption, as mandated by Presidential Regulation No. 55/2019 on the Battery-Based Electric Motor Vehicle Program (Presidential Regulation, 2019). Nonetheless, the adoption of electric vehicles in Indonesia encounters considerable structural obstacles, especially regarding charging infrastructure. In 2023, only about 439 public charging stations (CSs) were operational, well below the projected national requirement of over 1,000 units by 2025 and even more by 2050, as outlined in the National Energy General Plan (Directorate General of Electricity, 2024). The lack of adequate infrastructure is a substantial hindrance to the development of the EV market (Djubaedah *et al*., 2023). Moreover, more than 66% of electricity supplied by the national grid is generated from coal-fired power plants (CFPPs), resulting in a charging system that is heavily dependent on fossil-fuel-based electricity (Directorate General of Electricity, 2024). This reliance on coal-dominated electricity significantly affects the environmental performance of EV charging station (CS), as emissions are shifted from vehicle tailpipes to centralized power plants, reducing the net life cycle GHG mitigation potential of EV adoption. From an economic standpoint, reliance on grid electricity subjects CS operators to long-term fluctuations in operational costs influenced by fuel prices, electricity tariffs, and possible future carbon pricing, which could jeopardize the financial viability of charging setups that rely solely on the grid. These environmental and economic limitations highlight the need to reduce dependence on fossil-fuel-generated electricity within EV charging infrastructure. Despite growing interest in sustainable charging infrastructure, existing studies predominantly focus on either environmental life-cycle impacts or technical optimization, mainly in high-income countries. The lack of integrated life cycle assessment (LCA) and life cycle cost analysis (LCCA) studies for hybrid EV CS in developing countries with coal-dominated electricity grids remains a critical research gap. Previous life cycle assessments (LCAs) studies have examined charging infrastructure in China (Zhang *et al*., 2019), European hub for heavy-duty trucks (Dahlberg and Rodriguez, 2023), and commercial alternating current (AC) CS have quantified impacts from material production, construction, use, and end-of-life (EoL) (Persson and Erselius, 2021). Nevertheless, these studies infrequently incorporate evaluations of economic performance, which restricts their applicability for infrastructure investment and policy decision-making. Indonesia has significant solar energy potential, with average daily solar irradiance of approximately 4.8 Kilowatt-hour per square meter (kWh/m^2), positioning photovoltaic (PV) systems as a promising complementary energy source for EV charging (IESR, 2024). PV-powered CS can reduce dependence on fossil-based electricity and lower operational emissions (Sarda *et al*., 2024). PV systems also create upstream environmental challenges linked to the extraction of materials, manufacturing processes, and transportation, which may have an effect on the overall life-cycle performance (UNECE, 2022). Hybrid charging stations (HCS), combining

Table 1: Technical specifications of charging standards used in the HCS (Bista et al., 2020)

Specification	DC plug-ins (C)	DC plug-ins (J)	AC plug-in (G)
Charging standard	Combined Charging System (CCS)	Charge de move (CHAdeMO)	Type 2 cable
Maximum output power	20 kW	20 kW	22 kW
Output voltage range	50 – 500 V_{dc}	50 – 500 V_{dc}	400 V +/- 10%
Maximum output current	60 A_{dc}	60 A_{dc}	32 A_{ac}

PV generation with grid electricity, are therefore increasingly considered a transitional solution that balances operational reliability and emission reduction. Further studies reveal that electricity consumption remains the leading cause of total global warming potential (GWP), with hardware and civil engineering projects account for a lesser, though still important, share (Persson and Erselius, 2021; Dubois, 2024). The findings indicate that existing assessments tend to emphasize electricity-related environmental impacts while providing limited insight into upstream processes and long-term economic implications of hybrid charging systems. Focusing only on the operational phase may therefore lead to incomplete conclusions. Despite the increase in worldwide research regarding LCA for EV infrastructure, investigations into hybrid systems within developing countries that rely on coal-based grids, such as Indonesia, are still few in number. From an economic perspective, LCCA studies of HCS are also limited, especially those comparing PV-only, grid-only, and hybrid systems under real-world conditions. These research gaps highlight the need for a comprehensive evaluation of hybrid EV charging systems in Indonesia. Policymakers, utilities, and research institutions also require robust quantitative evidence to determine whether HCS configurations can reduce life cycle GHG emissions while remaining cost-competitive with conventional grid-based solutions. This study aims to evaluate and compare the life-cycle environmental impacts and economic performance of hybrid, grid-only, and PV-only EV CS using a cradle-to-grave assessment framework that encompasses component manufacturing, construction, operation, and EoL disposal. This study analyzes whether the incorporation of photovoltaic (PV) technology leads to a reduction in life-cycle environmental impacts in the context of Indonesia's coal-centric electricity system. Additionally, it assesses the effects on life-cycle economic performance and examines the environmental and economic trade-offs that occur when hybrid configurations are evaluated against single-source charging systems. The novelty of this study lies in the integrated use of LCA and LCCA based on empirical operational data, whereas most existing studies focus solely on environmental impacts without evaluating economic performance from a life-cycle perspective. The case study draws on operational and inventory data from an HCS in South Tangerang, Indonesia, collected in 2022.

MATERIALS AND METHODS

The environmental performance of the EV CS configurations was evaluated using LCA methodology in accordance with the International Organization for Standardization (ISO) 14040 and ISO 14044 standards (Firmansyah *et al.*, 2025). Furthermore, the life cycle cost (LCC) methodology evaluates the economic performance of HCS in South Tangerang, Indonesia. The analysis uses the Jakarta area and its surroundings as a case study for 2022. The comprehensive technical specifications of each plug-in configuration are outlined in Table 1. Each plug-in type has distinct characteristics that influence energy efficiency and system performance. The DC plug-ins (C and J) have a maximum output of 20 Kilowatt (kW), while the AC plug-in (G) offers 22 kW. These parameters were used in LCA and LCC modeling to evaluate energy transfer efficiency, infrastructure requirements, and associated impacts.

Electricity supply scenario

Three electricity supply scenarios were delineated in accordance with typical configurations employed in prior life cycle and techno-economic studies of EV charging infrastructure (Zhang *et al.*, 2019; Yang *et al.*, 2021). Scenario 1: HCS combines grid electricity from National power utility company (PLN) and on-site 5 kWp PV generation, prioritizing solar power when available. When solar power is lacking, grid electricity provides the necessary supply. PV and grid electricity contributions were calculated and used

consistently in both LCA and LCC models. Scenario 2: Entire electricity demand is met by on-site PV, offering a low-carbon solution but requiring higher initial investment and subject to solar intermittency. Scenario 3: Full grid system, where all electricity is supplied by the national grid, reflecting the current charging infrastructure in Indonesia. In all scenarios, the functional unit is defined as 1 Kilowatt-hour (kWh) of electricity delivered, with a system lifetime of 20 years, and a constant charging demand profile, thereby ensuring comparability. The scenarios differ only in electricity supply composition, enabling an assessment of environmental impacts and life cycle costs (LCCs). LCA was used for environmental evaluation, while LCC assessed economic implications, allowing integrated sustainability performance comparison.

LCA methodology

The LCA method evaluates various elements and potential environmental impacts throughout a product's life cycle, from manufacturing to disposal. LCA is an essential environmental approach for analyzing the potential ecological consequences associated with a product, its production process, and its operational activities (Bergerson *et al.*, 2020). In this study, the LCA method is used to quantitatively assess the environmental impact of HCS products (Pettersen and Song, 2017) over the whole life cycle, from raw material extraction to EoL analysis, including their construction (Rossi *et al.*, 2023). The following subsections present the HCS for LCA stages in accordance with Indonesian National Standard (SNI), ISO 14040 and ISO 14044 (Setyoko *et al.*, 2022). A cradle-to-grave system boundary was applied, covering raw material extraction, manufacturing, transportation, construction, operation, maintenance, and EoL treatment. The functional unit was established as 1 kWh of electricity provided to electric vehicles (EVs) for the purpose of maintaining a consistent comparison of environmental performance among different CS configurations. Life cycle inventory (LCI) data combined primary data from an operational HCS in South Tangerang, Indonesia (2022) and secondary data from the Ecoinvent 3.8 database. Indonesian grid data were used where available. Environmental impacts were assessed using the ReCiPe 2016 midpoint (H) method in OpenLCA (version 2.4), focusing on relevant categories for charging infrastructure. The study employed a deterministic, scenario-based LCA–LCC framework that did not incorporate statistical tests, analyzing the results through a comparative examination of the environmental impacts associated with the three electricity supply scenarios.

Goal and scope definition of LCA

This LCA study attempts to evaluate the prospective environmental effects of HCS in Indonesia, emphasizing on the Greater Jakarta Area, through a case study in Tangerang Selatan. There are comparisons between full grid and full PV CS. The objective is to measure and contrast the life-cycle environmental consequences of three CS configurations (HCS, full grid, and full PV) under similar assumptions and comparable conditions, hence facilitating consistent environmental performance evaluations within identical functional units and system boundaries. The HCS operating system is shown in Fig. 1. The study applies a cradle-to-grave system boundary. The cradle comprises the extraction of raw materials for PV, the generation of electricity through PLN, and the extraction of materials for the HCS structure and charger. The gate composed of PV production, PLN electricity, HCS civil structures, charger production, assembly, and application. The grave covers EoL processing. At the EoL stage, materials containing both metallic and non-metallic components undergo further processing (Andriyani *et al.*, 2024). Metals are conveyed to West Jakarta for scrapping, whereas non-metals are dispatched to Central Java for incineration. This study excludes raw materials, energy, and emissions from PV operation, as well as construction materials like cement, gravel, sand, steel, and materials used in chargers, including polymers and copper. The system boundaries of the HCS in this study are illustrated in Fig. 2.

Functional unit of LCA

The functional unit in this study is 1 kWh of electricity, representing the total electricity delivered during operation. Previous studies, such as Ludin *et al.* (2025) compare the environmental impact of EV CS per kWh. The kWh unit is also used in Indonesia's tariff policies for CS (Azizi *et al*, 2023), where user behavior in influenced by these policies (Sun *et al.*, 2022).

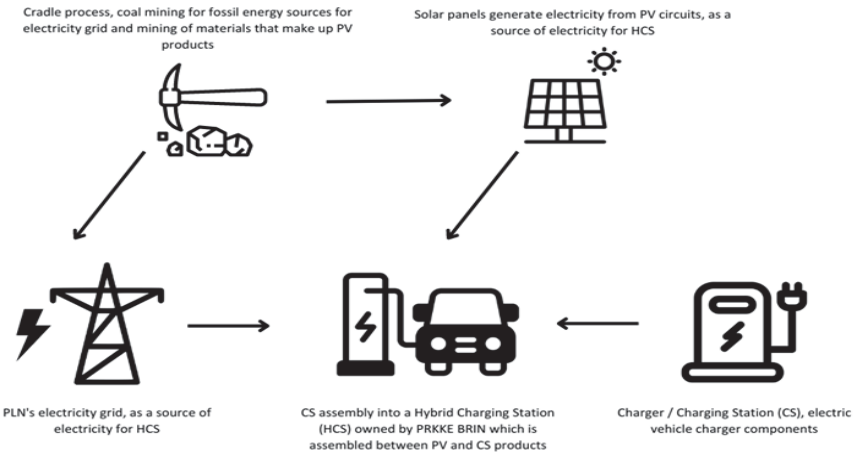

Fig. 1: The operating system of the HCS

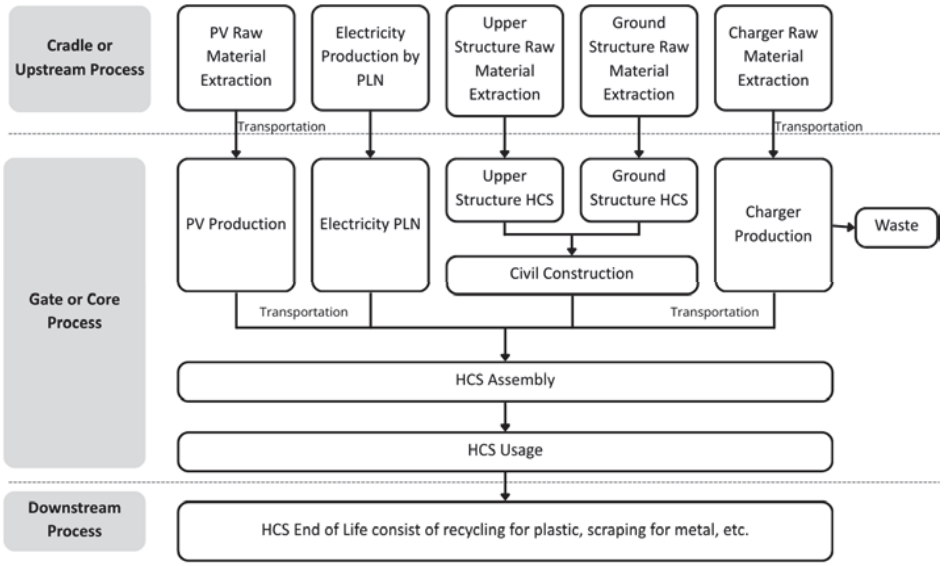

Fig. 2: The system boundaries of the HCS

Technique for collecting data on LCA

This study combines primary and secondary data to assess the environmental impact of CS. Primary data were collected from a facility in South Tangerang, Indonesia (2022) through interviews with 17 participants, including operators, renewable energy providers, utility representatives, and researchers. Data centered on operational parameters, expenses, and electricity supply arrangements, contributing to the life cycle assessment and life cycle costing models. Secondary data on PV production, charging, and EoL processes were sourced from journals, books, and the Ecoinvent 3.8 database. Electricity grid data pertinent to the region were employed wherever possible, and inventory parameters were corroborated with primary data and national energy statistics.

LCI analysis

The material inputs for each HCS life cycle stage were inventoried, including civil construction, PV production, charger production, HCS assembly, usage, and EoL management. Electricity used in

the process is supplied from the medium-voltage national grid (PLN, 1 to 35 kilovolt (kV)). The Eco-Invent database was utilized to assess emissions from the Indonesian grid market, representing the regional consumption mix. PV modules were imported, and the environmental impacts of PV material extraction and manufacturing were assessed using Ecoinvent 3.8 cradle-to-gate datasets, aligning with the cradle-to-grave system boundaries of the study. The conveyance of PV modules to the site and their EoL management are treated as independent processes. The CS lifetime is assumed to be 20 years, consistent with typical lifetimes for PV systems and electrical infrastructure in recent LCA studies, which generally range from 20 to 25 years (Huijbregts *et al.*, 2017). The EoL of the HCS is associated with the waste produced by construction activities, chargers, and PV modules (Andriyani *et al*., 2023). Material separation technology is one of the waste-processing methods used to separate non-metals (e.g., laminated glass) and metals (Chowdhury *et al*., 2020), including for processing HCS waste. This study presumes the utilization of material separation technology for HCS waste, taking into consideration energy consumption (electricity and diesel fuel). Waste processing facilities are located near the HCS assembly area to minimize transportation and emissions. The EoL phase separates materials into metals, polycarbonate, and plastics, which are then recycled metals are melted, and non-metallic materials are shredded or granulated for reuse.

Life cycle impact assessment (LCIA)

The LCIA method and database were opted for due to their consistency, reproducibility, and significance to the Indonesian electricity system. LCI results were analyzed using LCIA to evaluate environmental impacts across the product cycle. OpenLCA 2.4 software and the Ecoinvent 3.8 database were used, with LCIA results linked to damage categories through midpoint categories. For this study, the ReCiPe 2016 midpoint (Hierarchist) method was selected for the environmental impact assessment because it uses midpoint indicators that represent physical–chemical cause–effect relationships, reducing uncertainty and making it well-suited for comparative life cycle assessment of energy systems (Huijbregts *et al.*, 2017). The hierarchist (H) viewpoint was chosen because it embodies a consensus-driven time frame that is frequently utilized in policy-focused and applied LCA studies (Huijbregts *et al.*, 2017). Although ReCiPe 2016 provides 18 midpoint impact categories, this study focuses on a subset of categories most relevant to CS infrastructure and electricity supply systems. The selected categories GWP, ozone depletion potential (ODP), terrestrial acidification potential (TAP), freshwater eutrophication potential (FEP), and terrestrial ecotoxicity potential (TETP) were chosen based on their environmental relevance, robustness of inventory data, and alignment with regulatory and reporting frameworks, including Public disclosure program for environmental compliance (PROPER) and construction-sector product category rules (PCRs) (Huijbregts *et al.*, 2017). Results were interpreted by comparing the HCS, full PV, and full grid configurations, linking impact differences to electricity supply characteristics and dominant life cycle stages. The entire grid configuration is primarily shaped by grid electricity, which intensifies climate change and worsens air quality. The full PV configuration, on the other hand, lowers operational emissions but transmits environmental costs to upstream processes, especially the fabrication of PV modules. The hybrid system shows intermediate behaviours, where partial substitution of grid electricity with PV generation mitigates grid-related impacts while maintaining operational reliability (Laurent *et al.*, 2020).

LCIA interpretation

The LCIA findings were scrutinized to pinpoint the key contributors to the environmental impact indicators associated with the HCS system. Contribution analysis compared the energy supply scenarios: HCS (scenario 1), full PV (scenario 2), and full grid (scenario 3).

LCC model

The Indonesian government aims to accelerate EV adoption by 2030 (Sakti *et al*., 2023), highlighting the need for economic assessments of supporting infrastructure, particularly CSs. LCC supports an extensive analysis of energy sources and technologies, delivering critical information for long-term infrastructure planning (Bi *et al*., 2017; Hemmati *et al*., 2024). In this study, LCC is employed to gauge the economic efficiency of an HCS and aid in sustainable decision-making (Krim *et al*., 2022).

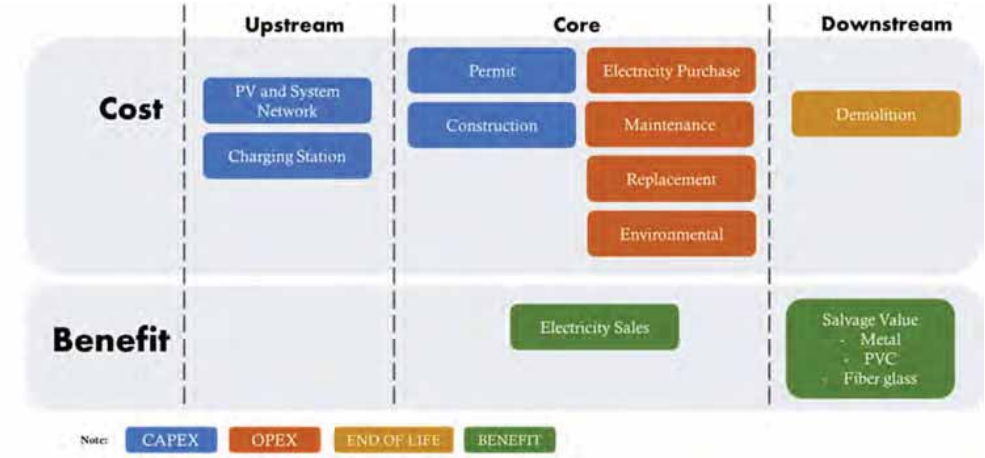

Fig. 3: Life cycle cost model for HCS

LCC covered capital expenditure (CAPEX), operating expenditure (OPEX), and EoL costs, covering demolition, deconstruction, and waste management (Krim *et al.*, 2022; Andriyani *et al.*, 2024) and includes a benefit analysis of revenue from HCS operations (Prasara and Bridhikitti, 2022). The analysis spans 20 years, using 2022 as the base year and a 6% discount rate in line with Bank of Indonesia's policy. The total life cycle cost (TLCC) is determined by calculating the discounted value of expenses subtracted from revenue, offering a thorough evaluation of the overall costs and net economic worth of the system. The TLCC calculated using Eq., 1 (Krim *et al.*, 2022):

$$TLCC = CAPEX + OPEX + EoL - R \quad (1)$$

A positive TLCC indicates that the project is financially unfavorable for investors, reflecting an imbalance between capital and operational investments (Danial *et al.*, 2021). The LCC model used in this study is illustrated in Fig. 3.

CAPEX

CAPEX encompasses all initial investment costs, including construction, permitting, component procurement, installation, and projected replacement costs. The costs for these replacements pertain to CS spare parts, anticipated in the tenth year, in accordance with the technical lifespan of the facility. The Indonesian Government funds the entire initial investment for the HCS project, with no external financing or loan interest applied. The CAPEX structure for the HCS (Scenario 1) is based on primary cost data obtained from the operational project. The identical CAPEX framework is utilized across the various comparison scenarios, with modifications made for infrastructure and electricity generation. CAPEX values are expressed in United States Dollar (USD)/kWh by normalizing investment costs to the cumulative electricity delivered over the system's lifetime, providing a consistent energy-based reference. The detailed CAPEX components are presented in Table 2.

OPEX

Operational expenditure typically encompasses electricity consumption and annual expenses related to the operation and maintenance of CS (Danial *et al.*, 2021). In this study, operational expenditure refers to the costs associated with purchasing electricity for EV charging, conducting maintenance activities, and accounting for environmental externalities. Operational expenditures were assumed to be incurred at the end of each year, and the daily electricity demand profile was held constant in line with previous empirical findings (Cedillo *et al.*, 2022). The electricity purchase price was USD 0.1096 per kWh followed national regulations and both purchase and selling prices were projected to increase annually with inflation, using 2022 as the base year. Maintenance is conducted through routine and periodic procedures each year. Annual maintenance costs were estimated

Table 2: CAPEX components (USD/kWh)

CAPEX	HCS	Full PV	Full grid
Permit	0.000006	0.000382	0.000006
CS construction	0.000224	0.013376	0.000216
CS	0.010191	0.035094	0.009825
PV and system network	0.001628	0.069429	-

at 1% of the initial capital investment, consistent with established cost-estimation practices for comparable energy technologies (Borlaug *et al.*, 2020). The costs associated with environmental externalities reflected the comprehensive life-cycle climate impact of the CS configuration, which were obtained from the cradle-to-grave LCA performed in this study. Emissions were monetized using the average carbon trading price listed on the Indonesia Carbon Exchange (IDX Carbon) in April 2025, which amounted to USD 0.004 per kilograms (kg) of carbon dioxide equivalent (kg CO_2 eq).

EoL cost

EoL costs in this study are divided into two main phases. The first stage transpired in the tenth year of operation, at which point the charging units were exchanged as a component of the system's maintenance cycle. The second phase occurred at the end of the system's operational life after 20 years. In the second phase, these costs include expenses for decommissioning and dismantling of infrastructure at the installation site (Adi *et al.*, 2025). The costs associated with demolition were assessed based on primary data obtained from interviews with seasoned construction workers, thereby ensuring that the EoL estimates accurately represent realistic practices and local conditions in Indonesia. Based on these estimates, the dismantling costs for the first phase of the HCS system were USD 774, while those for the second phase were USD 2,445. For the full PV system scenario, the dismantling costs in the first and second phases were estimated at USD 45 and USD 468, respectively. Meanwhile, in the full grid system scenario, the dismantling costs in the first phase are USD 774 and USD 1,386 in the second phase.

Benefit

The benefits stem from the sales of electricity to users of EV and the residual worth of the vehicles. The primary source of revenue is derived from electricity sales. The electricity selling price based on the regulated retail tariff for public charging facilities was USD 0.1645 per kWh, as stipulated by national regulations. Further economic advantages were derived from the EoL phase, stemming from the salvage value of materials that can be recovered. The material recovery rate was determined based on the amount of waste generated at the EoL stage in the LCI of LCA. For the HCS and full PV system scenarios, the recovery rates were set at 30.78% for metallic materials, 35.58% for non-metallic materials, and 33.65% for polycarbonate materials (Rabaia *et al.*, 2024). In contrast, the full grid-based system assumed recovery rates of 42.85% for metallic materials, 2.48% for non-metallic materials, and 54.67% for polycarbonate materials (Rabaia *et al.*, 2024). The salvage value is indicated as the cumulative economic advantage at the EoL, given that its contribution to the total life-cycle costs is comparatively insignificant and does not affect the primary economic findings. Based on this approach, the salvage value for the HCS system is USD 317 in the first phase and USD 1,558 in the second phase. For the full PV scenario, the corresponding values are USD 317 and USD 753. Meanwhile, in the full grid scenario, the salvage value for the first phase is USD 317 and for the second phase it is USD 568.

Economic analysis

The economic feasibility of the HCS was assessed using LCCA. This technique analyzes long-term profitability by factoring in all expenses and income over the system's duration, facilitating a methodical comparison of financial outcomes across different setups and operational scenarios. Five economic indicators were employed to determine investment viability: levelized cost of energy (LCOE), net present value (NPV), internal rate of return (IRR), payback period (PBP), and the benefit–cost ratio (B/C ratio) (Yang and Ribberink, 2019). LCOE is the ratio of the total costs to the total electricity generated over a

project's lifetime, expressed in Rupiah/kWh (Rosa-Clot and Tina, 2020). NPV determines the disparity between the present value of anticipated cash inflows and outflows associated with the investment, as well as the initial investment expenditure, represented in USD (Yang *et al*., 2021). IRR indicates the discount rate that makes the NPV of all project cash flows equal to zero, expressed in percentage (Yang *et al*., 2021). PBP is used to assess the time required for the total cumulative revenue to cover the initial CAPEX, expressed in year (Yang *et al*., 2021). B/C Ratio compares the present value of benefits and the present value of costs over the life of a project (Yang *et al*., 2021). Collectively, these metrics offer an extensive perspective on the financial robustness and economic competitiveness of electric vehicle charging systems across diverse technical and energy supply conditions (Karmakar, 2025).

Sensitivity analysis method

A one-way deterministic sensitivity analysis was conducted to assess the robustness of the LCA and LCC performance of the HCS system (Bi *et al.*, 2017), isolating the influence of key parameters on environmental and economic indicators. The study was structured to investigate the impact of significant sources of uncertainty in operational and investment decision-making. The analysis examined operational uncertainty, including PV efficiency and grid electricity. PV efficiency was varied by ±10%, reflecting changes in solar resource availability and PV performance (Kiani *et al*, 2025). Grid electricity, mainly coal-based, significantly contributes to environmental impacts, especially GWP. The investment decision uncertainty was derived from crucial economic indicators selected for their importance to long-term investment strategies and regulatory unpredictability, including electricity tariffs (for both purchasing and selling), CAPEX of PV and CS unit, and the discount rate. The electricity tariffs were varied by ±20%, consistent with life-cycle cost sensitivity practices for energy infrastructure systems (Bi *et al.*, 2017). The discount rate was tested at 4%, 6% (baseline), and 8% to represent alternative public infrastructure investment and risk scenarios (Boddapati and Daniel, 2021). These variation ranges were determined to represent realistic market and policy conditions instead of extreme scenarios, in accordance with established life-cycle cost sensitivity frameworks (Bi *et al.*, 2017; Boddapati and Daniel, 2021).

RESULTS AND DISCUSSION

LCI analysis

The LCI analysis results in a process input-output balance with a unit production function of 1 kWh of energy. The electricity provided from the grid was modeled with a presumed efficiency of 90%, which reflects the share of generated electricity that is effectively delivered to the CS, taking into account transmission and distribution losses. Contemporary energy statistics and LCA studies report grid losses typically ranging from approximately 5–12%, depending on network characteristics, supporting the use of a 90% delivered electricity efficiency in comparative energy system assessments (IEA, 2019). The average land area required for the construction of HCS was 30 m^2. According to the above assumptions, the data on the resource inputs for HCS production and operation are shown in the Table 3.

Environmental performance of HCS

Site-specific primary data for PV module manufacturing were unavailable due to the imported nature of the modules; therefore, background life cycle data from Ecoinvent were used to represent upstream manufacturing impacts. The scope of the EoL analysis was confined to dismantling and open burning. Nevertheless, it is important to recognize that valuable materials, including aluminum and silicon, could be salvaged and utilized as secondary inputs in subsequent PV manufacturing. These methodological limitations highlight the need for further research on emissions across PV manufacturing pathways, particularly in Indonesia, and on the potential for secondary materials to reduce upstream environmental impacts. LCA results show that the use phase is the primary contributor to the overall environmental impact of the HCS, accounting for over 90% of most midpoint categories (Fig. 4). The significant reliance on the Indonesian national electricity grid, which is largely powered by fossil fuels, particularly coal, accounts for this dominance. Integrating PV with grid electricity reduces emissions compared to full grid systems. Climate change is driven by global temperature increases from the accumulation of Greenhouse gases (GHGs) (Bilgili *et al*., 2024). The GWP metric quantifies the impact of GHGs on radiative forcing

Table 3: LCI data charging station for hybrid, full PV, and full grid scenarios

No.	Process	Item	Unit	Quantity		
				HCS	Full PV	Full grid
1	Ground construction	Material	kg	12.5	12.5	12.5
	structure	Water	m^3	150	150	150
		Electricity	kwh	100	100	100
2	Upper construction	Material	kg	754.8	754.8	754.8
	structure	Coils	cm^2	120.6	120.6	120.6
3	PV product	Material	kg	502.8	502.8	502.8
		Water	m^3	447	447	-
		Electricity	kWh	357	357	-
		PV panel	Item(s)	1	1	-
4	Charger product	Material	kg	63	63	63
		Cable	m	25	25	25
		Electricity	kWh	150	150	150
5	CS assembly	Charger product	Item(s)	1	1	1
		Ground Construction	Item(s)	1	1	1
		Upper Construction	Item(s)	1	1	1
		Land use, perennial crop	m^2	30	30	30
		PV Product	Item(s)	1	1	1
6	CS usage	Electricity medium voltage		9,986,300	-	10,168,800
7	Transportation	Transport PV (total)	tkm	21.9	21.9	-
		Transport charger to CS	tkm	21.6	21.6	21.6
		Transport waste	tkm	49.5	49.5	26
8	EoL	Diesel	kCal	4,1230	4,1230	-
		Electricity, medium voltage	kWh	20.6	20.6	20.6
		Waste	kg	1,307.6	1,307.6	804.8

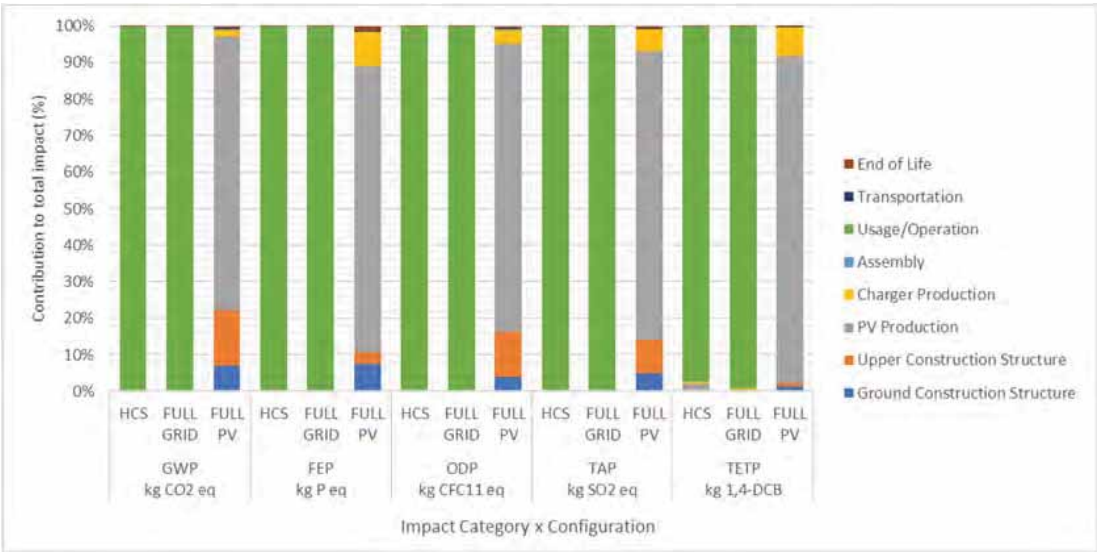

Fig. 4: Life cycle impact analysis of CS

and is expressed in kg CO_2 eq. The GWP for the HCS is 1.11 kg CO_2 eq/kWh, which is comparable to charging solely via the national grid. The use phase accounts for 99.89% of total GWP, as most energy during this phase is supplied by the Indonesian grid, with CFPPs being the dominant source and major contributors to GHG emissions and global warming. Decreasing dependence on fossil fuel power generation can be

accomplished by upgrading steam-based facilities or hastening the implementation of renewable energy technologies (Ziyaei *et al*., 2023). Future research should investigate scenarios that decrease the proportion of grid electricity in HCS operations or integrate additional renewable sources, such as wind or bioenergy, alongside PV to improve the decarbonization potential of hybrid charging systems. Eutrophication in freshwater systems occurs due to the influx of nutrient concentrations, particularly phosphorus and nitrogen, entering soil or water (Schindler, 2022). One kWh of HCS operation produces 1.98×10^{-3} kg of phosphorus equivalent (kg P eq) of eutrophication, mostly during the HCS usage phase. This effect is chiefly ascribed to the Indonesian electricity grid, notably the roles played by CFPP and its related activities. Additionally, coal mining activities for CFPP significantly transform land and landscapes, contributing to land degradation, an increase in erosion potential, and surface runoff, which ultimately causes soil and nutrient sedimentation in nearby freshwater ecosystems. The application of chemical fertilizers during post-mining revegetation further exacerbates nutrient loading. Additional contributions arise from CFPP activities, including wastewater discharge and atmospheric deposition of nitrogen oxides (NOx) from coal combustion. The reported value differs from a fully grid-powered system, as the analysis assumes 75% utilization. While the integration of partial PV systems diminishes reliance on the grid, further decreases in freshwater eutrophication are reliant on alterations in the upstream energy system. Strategies like boosting the proportion of renewable electricity, enhancing environmental management practices in coal mining and power plant operations, and incorporating energy storage to reduce grid reliance could improve the efficacy of hybrid charging systems in addressing nutrient-related impacts. Stratospheric ODP, defined as the time-integrated decline in stratospheric ozone concentration over an infinite time horizon and measured in kg chlorofluorocarbon-11 equivalent (kg CFC-11 eq) (Pyle *et al*., 2022), was also assessed. One Kilowatt-hour hybrid charging station (kWh HCS) was found to contribute 2.82×10^{-8} kg CFC-11 eq to stratospheric ozone depletion, a value like that of the full national grid, since the majority of HCS energy is sourced from the national grid. The HCS usage phase constitutes roughly 99.83% of this effect, with the national grid being the primary contributor through NOx emissions generated by coal combustion and mining activities. Methane emissions from land clearing for coal mining and the use of ozone-depleting substances in power plant operations and maintenance, as well as indirect contributions from industries utilizing substances such as Chlorofluorocarbon 11 (CFC-11) and Hydrofluorocarbon (HFC), further increase ODP. The ODP values that can be compared between the HCS and full grid scenarios demonstrate that the integration of partial PV by itself has a minimal impact on this particular category. Therefore, further reductions in ozone depletion are more likely to depend on improvements in upstream emission controls, stricter management of ozone-depleting substances, and a continued transition toward cleaner electricity generation, rather than on operational changes at the CS level. Terrestrial acidification, defined as changes in soil chemistry resulting from the deposition of acidified nutrients (nitrogen, ammonia, and sulphur) and expressed in kg of sulphur dioxide equivalent (kg SO_2 eq), is typically linked to fossil fuel combustion in power generation (Strezov and Cho, 2020). Indonesia's national grid is predominantly reliant on fossil fuels, hydropower, and a small proportion of geothermal energy, leading to acidification effects associated with electricity consumption. The terrestrial acidification associated with 1 kWh HCS is 3.74×10^{-3} kg SO_2 eq, with the HCS usage phase contributing 99.88% of this impact. The dominance of CFPP in Indonesia's electricity system is responsible for these emissions, particularly sulphur dioxide (SO_2) and NOx from coal combustion, which generate acid rain, acidify soils and water bodies, disrupt ecosystems, deplete nutrients, and pose environmental hazards. In comparison, the TETP impact category revealed alternative trends. This implies that the mitigation of terrestrial acidification is mainly contingent upon upstream alterations in the electricity sector, including decreasing coal usage and improving emission regulations, instead of merely operational changes at the CS level. Terrestrial ecotoxicity, which affects soil organisms, plants, and aquatic sediments, was measured at 6.74×10^{-1} kg 1,4-dichlorobenzene equivalent (kg 1,4-DCB eq) per 1 kWh HCS, exceeding the value for a full grid CS. By comparison, a fully PV system exhibited the highest impact at 3.06 kg 1,4-DCB eq. The HCS usage

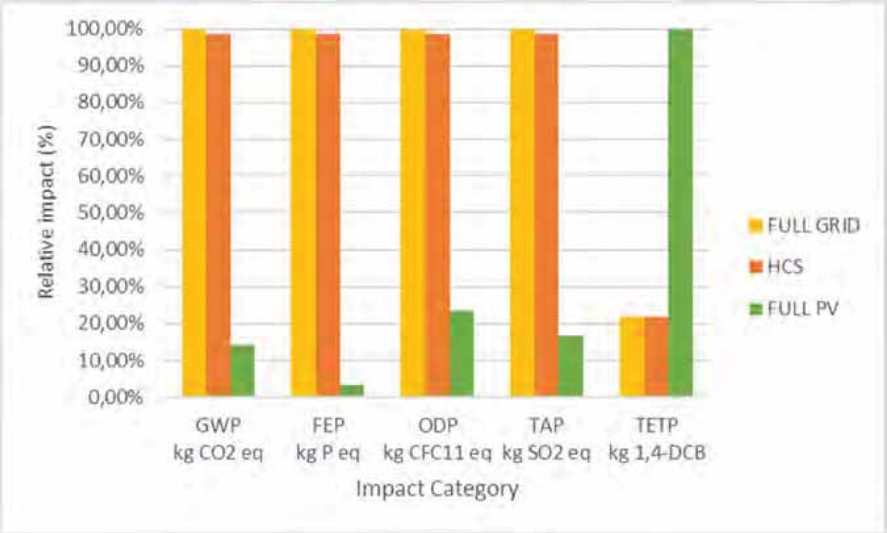

Fig. 5: Environmental performance of CS

phase remains the largest contributor to this impact, accounting for 97.34% of the total. The application of mineral and metal resources, including copper, iron, nickel, zinc, and alumina, across both phases contributes to this difference. Furthermore, the extraction and disposal of raw materials, particularly in coal mining operations, as well as the associated use of hazardous materials, also increase terrestrial ecotoxicity. The results indicate that reductions in terrestrial ecotoxicity are closely linked to improved material sourcing, cleaner mining practices, and better management of hazardous substances, rather than operational changes at the CS level alone.

Comparative LCA of CS

This study revealed that the amount of energy supplied is the most critical point in the environmental performance of HCS operation. The Indonesian electricity grid's energy output is the key source of the impact categories analyzed in this study. The Indonesian national grid originates from mixed primary energy sources. Predominantly fossil fuels (oil, gas, and coal) and a small portion of renewable energy (hydro, geothermal). Meanwhile, PV-powered CS showed opportunities for fewer environmental impacts across most of the impact categories, except for TETP, since it used considerably hazardous materials for its production. Furthermore, it is essential to ensure that the production of solar energy PV aligns with the precautionary principle, even as we advocate for its increased utilization. Shortly, it is expected that safer and greener materials and procedures will be found to reduce or replace the use of hazardous materials. PV utilization will significantly reduce fossil fuel-based energy supplies and their associated emissions, including for HCS development. Moreover, HCS construction with solar PV has a faster production process and fewer requirements than other renewable energy resources (Shaimurunov *et al.*, 2023). The outcomes of the calculations regarding relative environmental impact are illustrated in Fig. 5.

According to the findings, HCS and full PV-powered CS had lower environmental impacts across most midpoint categories than the full grid system. The HCS achieved a minor reduction in GWP (-1.36%), FEP (-1.40%), ODP (-1.33%), and TAP (-1.35%), demonstrating a partial decarbonization caused by PV contribution. In contrast, the full PV system significantly improved, with decreases of -85.94% in GWP, -96.70% in FEP, -76.58% in ODP, and -83.41% in TAP compared to the full national grid-powered station. TETP represents a critical life-cycle trade-off for PV-integrated charging systems when compared to hybrid configurations. The comprehensive PV scenario illustrates the peak TETP, primarily attributable to the upstream extraction of materials, the refining of metals, and the chemical-intensive processing of silicon associated with the production

Table 4: Life cycle cost calculation results of HCS

LCC of HCS	Unit	HCS	Full PV	Full Grid
TLCC	USD	(251,785.77)	(11,677.19)	(248,876.35)
NPV	USD	237,533.75	11,016.22	234,789.01
IRR	%	28.59%	8.43%	33.35%
LCOE	USD/kWh	0.172	0.124	0.170
PBP	Year	3 Years 1 Month	8 Years 10 Month	2 Years 1 Month
B/C Ratio		1.23	1.90	1.23

of PV modules. The toxicity burdens associated with materials and processes in PV technologies have been extensively documented, especially concerning the utilization of metals and hazardous chemicals in silicon purification and module fabrication (Mahmud *et al*., 2018). In comparison to complete PV systems, the HCS exhibits a lower yet significant TETP owing to its diminished dependence on PV components. This implies that integrating PV technology to a certain extent can decrease, but not fully remove, the toxicity linked to materials. From a life-cycle perspective, the increased TETP should not be considered a minor trade-off, as material-related impacts may partially counterbalance the climate benefits achieved through GHG reductions, aligning with comprehensive LCA of renewable electricity systems (Bouman, 2020). Overall, the results indicate a clear gradient effect of renewable energy: as the share of solar energy increases, there is a more significant decrease in carbon emissions and acidification impacts. However, this advancement is limited by the material intensity of PV technologies. The HCS configuration provides a transitional optimum by constantly minimizing the effect across all categories (without deteriorating TETP) while balancing environmental advantages and material constraints. While a full PV system is generally environmentally beneficial, upstream resource management remains an issue. Consequently, for Indonesia to achieve sustainable PV adoption, it is crucial to embed environmental criteria within supply chain planning, rather than limiting the focus to operational performance alone. The comparative LCA highlights significant environmental performance differences among the HCS, full PV, and full grid systems. The full grid system, primarily relying on coal, exhibits the highest environmental impact in categories such as global warming, eutrophication, acidification, and ozone depletion, reflecting Indonesia's coal-dominated electricity grid (Directorate General of Electricity, 2024). The comparative LCA indicates notable differences in environmental performance between the HCS, full PV, and full grid systems. Integrating PV energy into the HCS helps mitigate these impacts by partially replacing fossil-based electricity. Furthermore, while the HCS ensures quick GWP reductions, the comprehensive PV system yields the highest long-term advantages, negating the requirement for grid electricity and achieving up to an 85% decrease in GWP relative to the full grid system. However, as global LCA studies have shown, this transition to PV also introduces environmental trade-offs, particularly in terms of higher terrestrial ecotoxicity due to the material-intensive processes involved in PV module production (Mahmud *et al.,* 2018). Furthermore, while comprehensive PV systems deliver the greatest reductions in emissions, the HCS configuration offers a balanced strategy, providing a middle ground between prompt environmental advantages and the operational dependability required in coal-reliant electricity systems. This finding is consistent with the results reported by UNECE, (2022). Additionally, Yang *et al*. (2021) highlighted that hybrid systems, while offering environmental benefits, also need to balance these with system reliability. Bouman (2020) further emphasized that the integration of renewable energy in hybrid systems presents a trade-off between reduced emissions and the material-related environmental impacts of PV production.

LCC analysis

The development of CS requires careful calculations regarding the costs and benefits of production. LCCA is a variable that can be used to determine the competitiveness of a product in the early stages of production (Danial *et al*., 2021). Table 4. summarized the life-cycle economic performance of the HCS, full grid, and full PV.

A more negative TLCC value indicated a larger cumulative economic surplus (Danial *et al*., 2021).

Among the scenarios evaluated, the HCS demonstrated the most favorable TLCC result, with a value of -USD 251,785.77 and was followed by the full grid scenario (-USD 248,876.35) and the full PV scenario (-USD 11,677.19). The presence of PV systems in HCS reduces reliance on grid electricity. While the CAPEX for PV infrastructure is substantial, the use of PV helps offset these costs with long-term savings. These findings are consistent with the conclusions of Yang *et al*. (2021), who determined that integrating PV grids can achieve an ideal balance between CAPEX and operational cost reductions throughout the system's lifespan. The relatively weak TLCC performance of the full PV system is primarily due to the high initial CAPEX on PV and system network, despite the absence of electricity purchased from the grid. Limited electricity sales revenue and a long payback period significantly limit the cumulative net economic surplus of the full PV scenario over the project lifetime. TLCC predominantly illustrates cost reduction and the overall economic surplus, yet it does not consider the timing of cash flows or the attractiveness of short-term investments. Therefore, TLCC results are interpreted alongside revenue-based indicators to provide a comprehensive assessment of economic performance. HCS achieved the highest NPV, attributed to a diminished dependence on grid electricity by employing on-site PV generation. This performance was primarily driven by very low operational and fuel costs despite high initial CAPEX (Ryan *et al*., 2016). To ensure reliable supply during low radiation conditions, a permanent grid connection is required, facilitating the collaboration between photovoltaic systems and the grid to provide stable electricity access and reduce the reliance on externally purchased electricity (Adak and Cangi, 2024). This slightly lower NPV of the full grid scenario compared to the HCS is due to the consistently higher operating costs associated with the continuous purchase of electricity from the national grid over the system's lifetime. This recurring expense reduces the net discounted value of long-term cash flows, particularly under rising electricity prices. The full PV achieved a significantly lower NPV. Although operating costs are minimal after installation, the high initial CAPEX significantly limits the net discounted return over the assessed timeframe. The IRR highlighted the differences in capital efficiency between the scenarios. The full grid scenario achieved the highest IRR, indicating strong short-term financial performance because of the low initial CAPEX requirements. Furthermore, generating direct revenue through electricity sales expedites initial cash flow and enhances capital turnover. Nevertheless, these benefits are coupled with a greater operational dependence on the prices of grid electricity. The HCS scenario showed a slightly lower IRR due to higher CAPEX, with operational cost savings not fully offsetting the initial investment in the early years. Conversely, the low IRR of the full PV system reflects its high capital cost burden, which significantly reduces return efficiency despite its favorable operational economics. The constrained short-term allure demands concession financing models or sustainable incentives to hasten capital recovery (Zhang, 2022). The full PV system achieved the lowest LCOE, highlighting the inherent cost advantage of renewable power generation after the initial CAPEX is amortized over long-term operation. After installation, the system operates with minimal operational expenditure. This finding is consistent with the reduced operational costs observed for PV-based systems (Prasetyo *et al*., 2023). For the full grid, the marginally elevated LCOE figures indicated an ongoing dependence on acquiring electricity from the grid. In the case of the HCS, the higher LCOE is due to the additional investment in PV infrastructure. Among the scenarios evaluated, the full grid system demonstrated the shortest payback period. The quick financial recovery of the entire grid system is facilitated by its minimal upfront capital requirements and the prompt income generated from electricity sales. These characteristics allow for a rapid recovery of invested capital, making the grid-only system particularly attractive to investors with short investment horizons or limited access to financing. The HCS demonstrated a moderate payback period, indicating a balance between a reasonable initial investment and lower operating costs due to decreased dependence on grid electricity. Conversely, the longer payback period observed for the full PV system indicates high investment risk. The high capital intensity of the PV infrastructure delays cost recovery, resulting in prolonged capital lock-in before break-even is reached (Mas'ud, 2023). The full PV system achieved the highest B/C ratio driven by low operational costs after installation. In contrast, both the HCS and the full grid systems demonstrated similar B/C ratios of 1.23. The lower B/C ratio and complete reliance on purchased electricity make this scenario highly vulnerable to future energy price volatility and

tightening carbon regulations (Yang *et al*., 2021). The differences noted among the three scenarios are mainly influenced by the equilibrium between capital and operational expenditures. Full grid systems minimize initial investment but remain fully vulnerable to future electricity tariff increases and potential environmental impact. Full PV systems minimize operational costs but require substantial initial capital, resulting in a less attractive option for short-term investments but offer environmental benefits. HCS serves as a balanced approach, merging reasonable capital investment with diminished dependence on grid electricity, thereby lessening environmental impact and stabilizing cash flows over time.

Sensitivity analysis

In the HCS operation, the sensitivity analysis identified operational uncertainty, namely grid electricity and PV efficiency as the most critical parameters influencing the overall environmental and economic impact. The results, as shown in Fig. 6, demonstrate that a ±10% deviation in grid electricity consumption leads to a change of approximately ±9.55% to ±9.98% across the environmental impact categories. In terms of economic indicators, a ±10% change in grid electricity results in ranging from ±10.2% to ±10.2%, as shown in Fig. 7. The volume of electricity that is distributed and the revenue produced are directly determined by grid electricity.

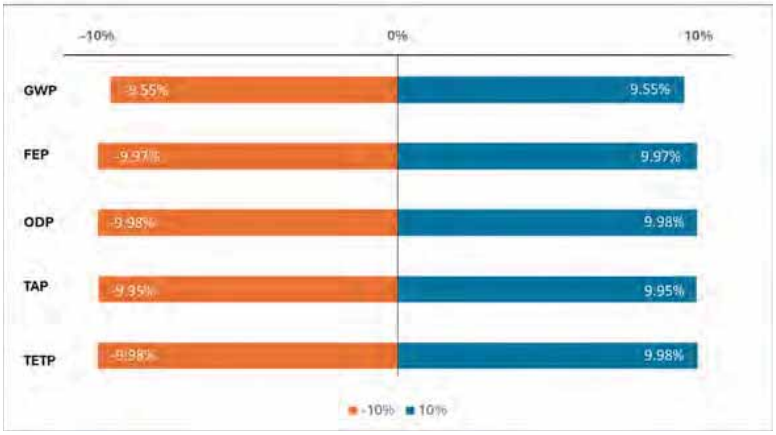

Fig. 6: Sensitivity analysis of HCS environmental impacts with ±10% grid electricity



Fig. 7: Sensitivity of Economic Indicators to grid electricity in the HCS

Since Indonesia's grid is mainly coal-based, any change in the grid electricity ratio results in similar shifts in environmental impacts due to the dominant role of coal-based electricity in emissions. This underscores the importance of lessening reliance on fossil-fuel-derived grid electricity for carbon storage to alleviate both ecological and financial consequences.

Similarly, the sensitivity analysis for PV efficiency, shown in Fig. 8, indicates that variations in the size of the PV system led to smaller shifts in environmental impacts. A ±10% change in PV efficiency results in a minimal change in impact categories, ranging from 0.00% to ±0.18%. The PV efficiency uncertainty resulted in variations of less than ±0.5% in most economic indicators, except for the LCOE, which remained unchanged, as shown in Fig. 9. Despite these slight adjustments, improving PV efficiency aids in lessening dependence on grid electricity, yet it leads to only a small positive impact on environmental and economic factors. These findings suggest that while increasing PV capacity does not drastically alter environmental and economic outcomes, it still contributes to improving the long-term sustainability of the HCS.

Sensitivity analysis assessed the robustness of economic performance results under uncertain operational conditions, as shown in Fig. 8 for sensitivity of economic indicators to grid electricity and Fig. 9 for sensitivity of economic indicators to PV Efficiency. Within the scope of operational uncertainty, grid

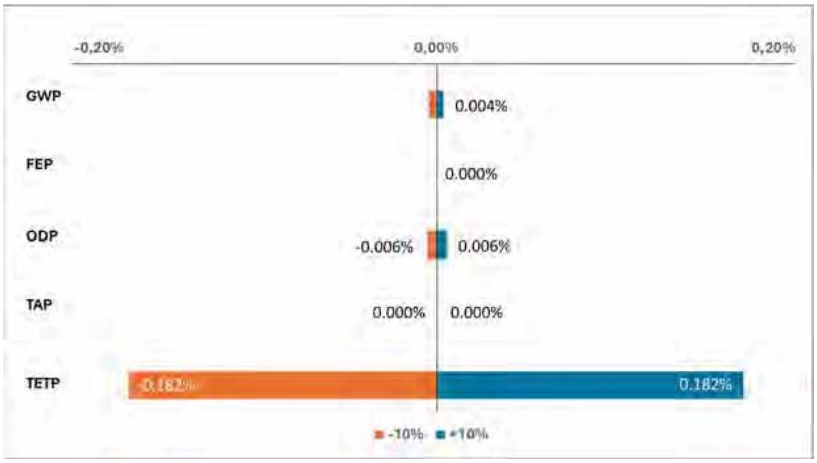

Fig. 8: Sensitivity analysis of HCS environmental impacts with ±10% PV eficiency



Fig. 9: Sensitivity of economic indicators to PV efficiency in the HCS

Tabel 5. Sensitivity of Economic Indicators to Invesment Decision in the HCS

Sensitivity Analysis to Investment Decision		Economic Indicator					
		TLCC	NPV	IRR	LCOE	PBP	B/C Ratio
Electricity Purchase	-20%	76.5%	76.5%	66.6%	-17.9%	-34.4%	21.9%
	+20%	-76.5%	-76.5%	-72.0%	17.9%	158.6%	-15.2%
Electricity Seling	-20%	-105.2%	-105.2%	-107.5%	0.0%	550.0%	-20.0%
	+20%	105.2%	105.2%	91.4%	0.0%	-58.2%	20.0%
PV CAPEX	-15%	0.6%	0.6%	2.9%	-0.1%	-0.7%	0.1%
	+15%	-0.6%	-0.6%	-2.7%	0.1%	0.7%	-0.1%
CS CAPEX	-15%	4.1%	4.1%	15.8%	-1.0%	-28.0%	1.0%
	+15%	-4.1%	-4.1%	-12.6%	1.0%	-29.2%	-1.0%
Discount Rate	-2%	25.7%	28.1%	8.2%	1.8%	-1.0%	0.8%
	+2%	-19.8%	-21.3%	-8.0%	-1.5%	1.1%	-0.9%

electricity showed consistently higher sensitivity to economic performance than variations in PV efficiency across all examined indicators. A ±10% change in grid electricity results in ranging from ±0.4% to ±10.2%. The grid's electricity plays a crucial role in determining both the volume of electricity that is distributed and the revenue generated, thus exerting a considerable influence. Changes in PV electricity output associated with PV efficiency uncertainty resulted in variations of less than ±0.5% in most economic indicators, except for the LCOE, which remained unchanged. In the HCS, changes in PV efficiency only affected the electricity supply mix between PV generation and grid electricity, without changing the total amount of electricity sold to users.

According to Table 5, a sensitivity analysis concerning investment decisions indicates that the economic viability of HCS is mainly affected by factors associated with electricity tariffs (including the selling price of electricity and the purchase price of electricity). A 20% increase in the electricity selling price significantly increases the TLCC, NPV, IRR, and B/C, and can shorten the PBP by approximately 50%. Likewise, a 20% decrease significantly affects PBP, preventing the investment from being recouped in 20 years, as the electricity selling price directly determines revenue.

The fluctuations in the grid electricity price influence operational costs, resulting in significant variations in both cost-related and profitability metrics. In HCS, the sensitivity of the electricity purchase price is lower compared to the electricity selling price. This indicates that the implementation of PV systems can diminish the dependence on cost-related factors of HCS. The discount rate also has a substantial impact on present value-based economic indicators, particularly NPV and TLCC, because it will affect the present value of future costs and revenues. Uncertainty in the CAPEX of CS has a moderate impact on economic indicators, particularly on the IRR and payback period. This is because CS investment accounts for approximately 80% of the total capital cost of an HCS system. The prevalence of CS infrastructure expenses within the CAPEX framework renders uncertainty in this respect a more significant factor in determining investment viability compared to other ancillary components.

Comparative and future policy insights

The full grid system scenario offered the highest financial gain but the least resilience to changes in electricity prices. Although PLN has maintained relatively stable retail tariffs through government regulation, long-term reliance on fossil-based generation introduces economic uncertainty (Siddique *et al.*, 2023) as the energy sector transitions toward net-zero emissions (NZE) targets. In the near term, the grid-only system benefits from established infrastructure, predictable cash flows, and a low initial investment, making it attractive to investors focused on short Payback periods (PBPs) (Abhyankar *et al.*, 2020). If carbon pricing and energy subsidies transform the electricity market, long-

Table 6: Comparative environmental and economic performance with other studies

Assessment scope (LCA / LCC)	Energy source	Environmental performance	Economic performance	Country	Sources
LCA	Full grid	The GWP of full grid is 0.094 kg CO_2 eq/kWh	Not assessed	China	Zhang *et al.*, 2019
LCA	Full grid	LCA results are presented for a single CS weighing 29.7 kg. Thus, it cannot be compared.	Not assessed	Europe	Persson and Erselius, 2021
LCA	Full grid	The GWP of full grid with 21 years lifetime is 0.011 kg CO_2 eq/kWh	Not assessed	Europe	Dahlberg and Rodriguez, 2023
LCA and financial analysis	HCS and full PV	LCA results are presented for a total of one year. Thus, it cannot be compared.	The PBP of hybrid is 5 years 2 months	India	Sood *et al.*, 2023
LCA and LCC	HCS, full PV, and full grid	The GWP of hybrid is 1.11 kg CO_2 eq/kWh. The GWP of full grid is 1.13 kg CO_2 eq/kWh.	The PBP of hybrid is 3 years 1 months	Indonesia	This Study

term competitiveness could suffer a decline. The full grid system relies on centralized fossil-based energy. Consequently, the full grid exhibits reduced adaptability during national transitions to renewable energy. In contrast, the full PV system offers long-term sustainability but requires policy and financing support to reach economic parity. Continuous technological advancement is expected to reduce module manufacturing costs (Helveston *et al.*, 2022) and significantly improve conversion efficiency (Tang *et al.*, 2023) by increasing energy yield per installed capacity. Simultaneously, the swift advancement in battery energy storage, noted for its increased energy density, extended lifespans, and decreasing costs (Njema *et al.*, 2024), can store excess solar energy. Although the HCS system in this study did not include energy storage, future integration will substantially reduce intermittency and improve asset utilization rates. Additionally, innovations in PV material recycling are projected to reduce EoL costs (Wang *et al.*, 2022). Compared to HCS and full grid systems, the full PV system offers the highest potential for cost reduction and sustainability improvements over time. As technology evolves and renewable policies are reinforced, comprehensive PV systems are projected to become financially feasible. The HCS configuration is the most competitive option for both short and long-term viability. In the short term, HCS provides stable profitability and operational reliability by utilizing the grid while offsetting some electricity costs with PV generation. With moderate investment and a strong NPV (USD 237.53 thousand), HCS strikes an optimal balance between capital intensity and revenue stability. Over an extended period, the integration of PV energy serves in safeguarding against the volatility of fossil fuel prices and the likelihood of carbon taxes. Low-interest green loans and public-private financing can ease capital costs, boosting the adoption of hybrid charging stations in urban and peri-urban areas. Dynamic tariffs and net-metering policies can further enhance PV's economic appeal. Optimizing the energy mix over time is key to maintaining competitiveness. In situations where grid prices are consistent and the capital costs for PV are elevated, a greater proportion of the grid facilitates a faster investment recovery. As PV module prices fall and energy storage advances, increasing the PV share will lower long-term costs and improve carbon performance. Despite higher initial costs for PV systems, batteries, and inverters, PV-based hybrid stations remain economically viable in Indonesia due to high solar radiation (±4.8 kWh/m²/day),

which reduces the levelized cost per kWh. Table 6 summarizes key findings for precise comparison of our study's outcomes with recent research. The studies in China (Zhang *et al*., 2019) and in Europe (Dahlberg and Rodriguez, 2023), report GWP values for full-grid systems that are significantly lower than those found in this study. Electricity is a major contributor to the environmental impact of CS. Consequently, the value of environmental impact is affected by the energy mix of every country. The hybrid system in this study shows a relatively short PBP (3 years and 1 month) compared to India. The shorter PBP indicates a quick return on investment. From a policy perspective, this study supports the need for a coordinated approach to renewable energy adoption, with incentive and subsidy mechanisms for the transition to sustainable CS. These policy instruments have the potential to lower the initial investment obstacles associated with expanding EV infrastructure.

CONCLUSION

The environmental and economic efficacy of HCS, PV systems, and full grid-based EV CSs in Indonesia is evaluated using a cradle-to-grave LCA. The outcomes reveal that the operational phase plays a crucial role in determining environmental impacts, largely owing to the reliance on the fossil-fuel-based national grid. HCS integrates PV energy with grid electricity, resulting in enhanced environmental sustainability relative to full grid systems. This integration reduces GWP, eutrophication, acidification, and ODP. While full PV systems offer numerous climate-related advantages, they also exert a significant impact on terrestrial ecosystems due to the substantial materials required for their production. This implies that an analysis of the ecological advantages of solar-powered infrastructure should take into account both the decrease in emissions and the impact of materials. Addressing this issue requires advancements in sustainable manufacturing, ethical sourcing of materials, and enhanced recycling practices. HCS displays the highest NPV and reveals diminished sensitivity to variations in energy prices when compared to complete grid systems. While full PV systems incur reduced operational costs, they demonstrate an extended payback period owing to elevated initial installation expenditures. The results indicate that integrating HCS with comprehensive PV systems effectively boosts both economic and environmental outcomes. HCS is advantageous for cities with fluctuating demand, as it enhances operational stability and reduces investment risks. Full PV systems are particularly efficient in locations with significant sunlight exposure and a stable need for long-term decarbonization. Policy support is essential for accelerating the integration of renewable energy into EV infrastructure. This encompasses green finance, tax incentives, and adaptable tariffs. Improvements in PV technology and energy storage systems are expected to enhance the role of hybrid and solar-powered stations in reducing the carbon intensity of the energy framework. Future studies should focus on the shortcomings in the production of PV modules and the EoL processes. Furthermore, it ought to explore the incorporation of sophisticated energy storage solutions to improve system efficiency and cost-effectiveness in diverse geographical and regulatory contexts.

AUTHOR CONTRIBUTIONS

R. Rosmeika conceived the main research idea and supervised all stages of the study. A. Aditiyawan performed the conceptual design and analytical calculations. M.A. Hipi curated the dataset and harmonized citations and references. A. Erliza performed the Life Cycle Costing analysis and developed the LCC methodology. A.W. Sani composed the initial manuscript draft and conducted the Life Cycle Assessment model simulations. U. Ayuningtyas wrote and organized the introduction section. D.F. Soraya structured the methodology section. A.Y.N. Sakti structured the literature review and prepared the results and discussion sections. N. Andriyani supervised the interpretation of results, reviewed the discussion, and ensured compliance with journal formatting guidelines. H. Febriansyah carried out scenario-based evaluations. C.K. Sari improved data visualization for effective presentation of analytical results. A.I. Pratiwi contributed to the introduction section and assisted in preparing the manuscript draft. M. Septiani designed graphical summaries, charts, and conceptual diagrams. I.E. Setiawan, the corresponding author, provided critical feedback, guided methodological refinement, and finalized the manuscript. All authors contributed substantially to the research and approved the final version of the study.

ACKNOWLEDGEMENT

The authors sincerely acknowledge the institutional support provided by the Research Center for Sustainable Industrial and Manufacturing Systems, the National Research and Innovation Agency, and Universitas Multimedia Nusantara. Their technical assistance and collaboration were essential to the successful completion of this study.

CONFLICT OF INTEREST

The authors declare that there is no conflict of interest regarding the publication of this manuscript. In addition, ethical issues, including plagiarism, informed consent, misconduct, data fabrication and/or falsification, double publication and/or submission, and redundancy, were observed by the authors.

OPEN ACCESS

©2026 The author(s). This article is licensed under a Creative Commons Attribution 4.0 International License, which permits use, sharing, adaptation, distribution and reproduction in any medium or format, if you give appropriate credit to the original author(s) and the source, provide a link to the Creative Commons license, and indicate if changes were made images or other third-party material in this article are included in the article's Creative Commons license, unless indicated otherwise in a credit line to the material. If material is not included in the article's Creative Commons license and your intended use is not permitted by statutory regulation or exceeds the permitted use, you will need to obtain permission directly from the copyright holder. To view a copy of this license, visit:

http://creativecommons.org/licenses/by/4.0/

PUBLISHER'S NOTE

GJESM Publisher remains neutral regarding jurisdictional claims with regard to published maps and institutional affiliations.

R Positive AI Statement

During the preparation of this work the author(s) have used Artificial Intelligence (AI), Grammarly

and Quillbot, to assist in checking grammar, errors and language refinement. After using this tool/service, the authors reviewed and edited the content as needed and took full responsibility for the content of the publication.

ABBREVIATIONS

%	Percent
A_{ac}	Ampere alternating current
A_{dc}	Ampere direct current
AC	Alternating current
B/C Ratio	Benefit–cost ratio
CAPEX	Capital expenditure
CFC-11	Chlorofluorocarbon 11
CFPPs	Coal-fired power plants
CO_2	Carbon dioxide
CCS	Combined charging system
CHadeMo	Charge de move
CS	Charging station
CSs	Charging stations
DC	Direct current
ENDC	Enhanced nationally determined contribution
EoL	End-of-life
EV	Electric vehicle
EVs	Electric vehicles
FEP	Freshwater eutrophication potential
GHGs	Greenhouse gasses
GHG	Greenhouse gas
GWP	Global warming potential
HCS	Hybrid charging station
HFC	Hydrofluorocarbon
IDX carbon	Indonesia carbon exchange
IRR	Internal rate of return
ISO	International Organization for Standardization
kg CFC-11 eq	Kilograms chlorofluorocarbon-11 equivalent
kg CO_2 eq	Kilograms of carbon dioxide equivalent
kg 1,4-DCB eq	Kilograms 1,4-dichlorobenzene equivalent
kg P eq	Kilograms of phosphorus equivalent
Kg SO_2 eq	Kilograms of sulphur dioxide equivalent
kV	Kilovolt
kW	Kilowatt
kWh	Kilowatt-hour
kWh HCS	Kilowatt-hour hybrid charging station
kWh/m^2	Kilowatt-hour per square meter
LCA	Life cycle assessment
LCAs	Life cycle assessments

LCC	Life cycle cost
LCCs	Life cycle costs
LCCA	Life cycle cost analysis
LCI	Life cycle inventory
LCIA	Life cycle impact assessment
LCOE	Levelized cost of energy
NOx	Nitrogen oxides
NPV	Net present value
NZE	Net-zero emissions
ODP	Ozone depletion potential
OPEX	Operating expenditure
PBP	Payback period
PBPs	Payback periods
PCRs	Product category rules
PLN	National power utility company
$PM_{2.5}$	Fine particulate matter 2.5
PV	Photovoltaic
PROPER	Public disclosure program for environmental compliance
SNI	Indonesian National Standard
SO_2	Sulphur dioxide
TAP	Terrestrial acidification potential
TETP	Terrestrial ecotoxicity potential
TLCC	Total life cycle cost
USD	United States Dollar
WHO	World Health Organization

REFERENCES

Abhyankar, N.; Lin, J.; Liu, X.; Sifuentes, F., (2020). Economic and environmental benefits of market-based power-system reform in China: A case study of the Southern grid system. Resour. Conserv. Recycl., 153: 104558 **(11 pages).**

Adi, T.J.W.; Devia, Y.P.; Andriyani, N., (2025). Integrating building information modeling and bayesian network for enhanced go/no-go decisions in building demolition projects. Global J. Environ. Sci. Manage., 11(3): 1259-1280 **(22 pages).**

Adak, S.; Cangi, H., (2024). The quality problems at low irradiance in the grid-connected photovoltaic systems. Electr. Eng., 106(5): 6185-6197 **(11 pages).**

Amin, M.; Ramadhani, A.A.T.; Putri, R.M.; Auliani, R.; Torabi, S.E.; Hanami, Z.A.; Suryati, I.; Bachtiar, V.S., (2025). A review of particulate matter (PM) in Indonesia: trends, health impact, challenges, and options. Environ. Monit. Assess., 197(1): 11 **(19 pages)**.

Andriyani, N.; Adi, T.J.W.; Suprobo, P.; Aspar, W.A.; Rachmawati, F.; Pradono, M.H., (2023). The framework of green deconstruction planning system in Indonesia: Maximizing the conservation of construction resources. AIP Conference Proceedings, 2847(1): 1-7 **(7 pages)**.

Andriyani, N.; Suprobo, P.; Adi, T.J.W.; Aspar, W.A.N.; Jatmiko, A.D.; Santoso, A.D., (2024). Integrating urban building information modeling and circular economy framework for green sustainability. Global J. Environ. Sci. Manage., 10(3): 1313-1332 **(20 pages)**.

Andriyani, N.; Adi, T.J.W.; Suprobo, P.; Aspar, W.A.; Widiyanto, A.; Firdana, F.; Yunus, A.F., (2024). The role of Building Information Modelling (BIM) in waste management deconstruction plan via 3D reconstruction model. AIP Conference Proceedings, 3069: 020115 **(10 pages)**.

Azizi, Y.H.; Batih, H., (2023). Analysis of the impact of electric charging infrastructure provision rules on the calculation of fast and ultrafast charging service costs at time base and energy base charging stations. Int. J. Soc. Serv. Res., 03(07): 1732-1747 **(16 pages)**.

Bergerson, J.A.; Brandt, A.; Cresko, J.; Carbajales-Dale, M.; MacLean, H.L.; Matthews, H.S.; McCoy, S.; McManus, M.; Miller S.A.; Morrow, W.R.; Posen, I.D.; Seager, T.; Skone, T.; Sleep, S., (2020). Life cycle assessment of emerging technologies: Evaluation tecniques at different stages of market and technical maturity. J. Ind. Ecol., 24(1): 11-25 **(pages 15)**.

Bi, Z.; De Kleine, R.; Keoleian, G.A., (2017). Integrated life cycle assessment and life cycle cost model for comparing plug-in versus wireless charging for an electric bus system. J. Ind. Ecol., 21(2): 344-355 **(12 pages)**.

Bilgili, M.; Tumse, S.; Nar, S., (2024). Comprehensive overview on the present state and evolution of global warming, climate change, greenhouse gases and renewable energy. Arabian J. Sci. Eng., 49(11): 14503-14531 **(29 pages)**.

Bista, A.; Khadka, N.; Shrestha, A.; and Bista, D., (2020). Comparative analysis of different hybrid energy system for sustainable power supply: A case study. IOP Conference Series. Earth Environ. Sci., 463(1): 012045 **(10 pages)**.

Boddapati, V.; Daniel, S.A., (2022). Design and feasibility analysis of hybrid energy-based electric vehicle charging station. Distrib. Gener. Altern. Energy J., 37: 41-72 **(32 pages)**.

Borlaug, B.; Salisbury, S.; Gerdes, M.; Muratori, M., (2020). Levelized cost of charging electric vehicles in the United States. Joule, 4(7): 1470-1485 **(17 pages)**.

Bouman, E.A., (2020). A life cycle perspective on the benefits of renewable electricity generation – methodology and assumptions. Report of Eionet, The European Topic Centre on Climate Change Mitigation and Energy **(29 pages)**.

Cedillo, M.H.; Sun, H.; Jiang, J.; Cao, Y., (2022). Dynamic pricing and control for EV charging stations with solar generation. Appl. Energy., 326: 119920 (**11 pages**).

Chowdhury, M.S.; Rahman, K.S.; Chowdhury, T.; Nuthammachot, N.; Techato, K.; Akhtaruzzaman, M., Tiong, S.K.; Sopian, K.; Amin, N., (2020). An overview of solar photovoltaic panels' end-of-life material recycling. Energy Strategy Rev., 27:100431 **(11 pages)**.

Dahlberg, G.; Rodriguez, J.P.R., (2023). Life-cycle assessment of a charging hub for electric trucks. Master's thesis. Chalmers University of Technology. **(79 pages)**.

Danial, M.; Azis, F.A.; Abas, P.E., (2021). Techno-economic analysis and feasibility studies of electric vehicle charging station. World Electr. Veh. J., 12(4): 1-21 **(21 pages)**.

Directorate General of Electricity, (2024). Statistik Ketenagalistrikan Tahun 2024. Jakarta: Directorate General of Electricity. The Ministry of Energy and Mineral Resources of the Republic of Indonesia. 38: 1-80 **(80 pages)**.

Djubaedah, E.; Riza; Kurniasari, A.; Nur Endah Eny, S.; Nurrohim, A., (2023). Projection of the demand for charging stations for electric passenger cars in Indonesia. Evergreen, 10(3): 1744–1752 **(10 pages)**.

Dubois, J., (2024). Life cycle assessment of electric vehicle charging infrastructure: systematic literature review and development of a life cycle inventory database. Internship Report. **(44 pages)**.

Fathoni, F.; Kesidou, E.; Rifansha, M.M.; Tiftazani, A., (2025). Drivers and barriers of eco-innovation in electric vehicle diffusion: Evidence from Indonesia. J. Environ. Manage., 389: 126021 **(13 pages)**.

Firmansyah, I.; Santoso, A.D.; Nuha, N.; Sahwan, F.L.; Suryanto, F.; Wahyono, S., (2025). Environmental impact of car wash services by performing life cycle perspective. Global J. Environ. Sci. Manage., 11(1): 261-276 **(16 pages)**.

Haq, G.; Jana, B.; O'Reilly. K., (2025). Decarbonizing road passenger transport and reaping health benefits in Indonesia **(8 pages).**

Hemmati, M.; Bayati, N.; Ebel, T., (2024). Life cycle assessment and costing of large-scale battery energy storage integration in Lombok's power grid.

Batteries, 10(295): 1-18 **(18 pages)**.
Helveston, J.P.; He, G.; Davidson, M.R., (2022). Quantifying the cost savings of global solar photovoltaic supply chains. Nature, 612(7938): 83-87 **(5 pages)**.
Huijbregts, M.J.; Steinmann, Z.N.; Elshout, P.M.; Stam, G.; Verones, F.; Vieira, M.; Zijp, M.; Hollander, A.; Zelm, R., (2017). ReCiPe2016: a harmonised life cycle impact assessment method at midpoint and endpoint level. Int. J. Life Cycle Assess., 22(2): 138-147 **(10 pages)**.
IEA, (2019). Status of power system transformation 2019. Status of power system transformation. International Energy Agency **(32 pages)**.
IESR, (2024). Indonesia energy transition outlook 2025: Navigating Indonesia's energy transition at the crossroads: A pivotal moment for redefining the future. Jakarta: Institute for Essential Services Reform, 5: 1-114 **(114 pages)**.
Jaramillo, P.; Ribeiro, S.K.; Newman, P.; Dhar, S.; Diemuodeke, O.E.; Kajino, T.; Lee, D.S.; Nugroho, S.B.; Ou, X.; Strømman, A.H.; Whitehead, J., (2022). Transport. In IPCC, 2022: Climate change 2022: Mitigation of climate change. Contribution of working group III to the sixth assessment report of the Intergovernmental Panel on Climate Change. Cambridge University Press, 1049-1160 **(112 pages)**.
Karmakar, A.; Sadhu, P.K.; Das, S.; Bihari, S.P.; Khan, B.; Ali, A., (2025). Techno economic analysis and optimized PV powered EV charging facilities under various climate conditions in India. Discover Sustainability, 6(285): 1-21 **(21 pages)**.
Khaleel, M.; Nassar, Y.; El-Khozondar, H.J.; Elmnifi, M.; Rajab, Z.; Yaghoubi, E.; Yaghoubi, E., (2024). Electric vehicles in China, Europe, and the United States: Current trend and market comparison. Int. J. Electr. Eng. Sustainable., 2(1): 1-20 **(20 pages)**.
Kiani, H.; Vahidi, B.; Hosseinian, S.H.; Lazaroiu, G.C.; Siano, P., (2025). Prospective design and evaluation of a renewable energy hybrid system to supply electrical and thermal loads simultaneously with an electric vehicle charging station for different Weather conditions in Iran. Smart Cities. 8(61): 1-35 (**35 pages**).
Kongwee, W.; Achariyaviriya, W.; Rinchumphu, D.; Suttakul, P.; Achariyaviriya, A.; Chanpichaigosol, N.; Vichiensan, V.; Kii, M.; Lamtrakul, P.; Hayashi, Y., (2025). The potential of carbon emission reduction through the transition to battery electric vehicles. Global J. Environ. Sci. Manage., 11(3): 897-914 **(18 pages)**.
Krim, Y.; Sechilariu, M.; Locment, F.; Alchemy, A., (2022). Global cost and carbon impact assessment methodology for electric vehicles' PV-powered charging station. Appl. Sci., 12(4115): 1-23 **(23 pages)**.
Laurent, A.; Weidema, B.P.; Bare, J.; Liao, X.; Maia de Souza, D.; Pizzol, M.; Sala, S.; Schreiber, H.; Thonemann, N.; Verones, F., (2020). Methodological review and detailed guidance for the life cycle interpretation phase. J.Ind. Ecol., 24(5): 986-1003 **(18 pages)**.
Ludin, N.A.; Phoumin, H.; Junedi, M.M.; Affandi, N.A.A., (2025). Comparative environmental evaluation of electric vehicle charging technologies, infrastructure and charging stations in Malaysia: Towards a sustainable energy transition. Tackling the energy transition: Insights from ASEAN and beyond. Climate change and energy transition. Springer, 143-164 **(22 pages)**.
Mahmud, M.A.P.; Huda, N.; Farjana, S.H.; Lang, C., (2018). Environmental impacts of solar-photovoltaic and solar-thermal systems with life-cycle assessment. Energies, 11(9): 1-21 **(21 pages)**.
Mas'ud, A.A., (2023). A hybrid combination of EV charging stations with renewable energy sources for powering a residential community. A techno-economic perspective. Energy Storage, 5(8): 1-20 **(20 pages)**.
Ministry of Environmental and Forestry, (2022). Enhanced Nationally Determined Contribution (ENDC). Ministry of Environmental and Forestry of the Republic of Indonesia, 1-47 **(47 pages)**.
Njema, G.G.; Ouma, R.B.O.; Kibet, J.K., (2024). A review of the recent advances in battery development and energy storage technologies. J. Renewable Energy., 1: 2329261 **(35 pages)**.
Persson, J.; Erselius, G., (2021). Life cycle assessment of the charging station GARO LS4 **(9 pages).**
Pettersen, J. B.; Song, X., (2017). Life cycle impact assessment in the arctic: Challenges and research needs. Sustainability, 9(9): 1–20 **(20 pages)**.
Prasara, A.J.; Bridhikitti, A., (2022). Carbon footprint and cost analysis of a bicycle lane in a municipality. Global J. Environ. Sci. Manage., 8(2): 197-208 (**12 pages**).
Prasetyo, S.D.; Regannanta, F.J.; Mauludin, M.S.; Arifin, Z., (2023). Economic feasibility of solar-powered electric vehicle charging stations: A case study in Ngawi, Indonesia. Mechatron. Intell. Transp. Syst., 2(4): 201-210 **(10 pages)**.
Presidential Regulation, (2019). Percepatan program kendaraan bermotor listrik berbasis baterai (battery electric vehicle) untuk transportasi jalan. Republic of Indonesia (**22 pages**).
Pyle, J.A.; Keeble, J.; Abraham, N.L.; Chipperfield, M.P.; Griffiths, P.T., (2022). Integrated ozone depletion as a metric for ozone recovery. Nature. 608(7924): 719-723 (**9 pages**).
Rabaia, M.K.H.; Shehata, N.; Olabi, V.; Abdelkareem, M.A.; Semeraro, C.; Chae, K-J.; Sayed, E.T., (2024). Enabling the circular economy of solar PV through the 10Rs of sustainability: Critical review, conceptualization, barriers, and role in achieving SDGs. Sustainable Horiz., 11: 100106 **(18 pages)**.
Rosa-Clot, M.; Tina, G.M., (2020). Levelized Cost of Energy (LCOE) Analysis. Floating PV Plants, 119-127 **(9 pages)**.
Rossi, F.; Zuffi, C.; Parisi, M.L.; Fiaschi, D.; Manfrida, G., (2023). Comparative scenario-based LCA of renewable energy technologies focused on the end-of-life evaluation. J. Cleaner Prod., 405: 136931 (**12 pages**).
Ryan, L.; Dillon, J.; La Monaca, S.; Byrne, J.; O'Malley, M., (2016). Assessing the system and investor value of utility-scale solar PV. Renewable Sustainable Energy Rev., 64: 506-517 **(12 pages)**.
Sakti, A.Y.N.; Djarwadi, D.; Kusumawati, M.B.; Kusumawati, M.B.; Djarot, I.N., (2023). Upstream bottleneck detection on electric vehicle industry: A case study of Indonesian electric scooter. AIP Conference Proceedings, 2932:040004 **(12 pages)**.
Sarda, J.; Patel, N.; Patel, H.; Vaghela, R.; Brahma, B.; Bhoi, A.K.; Barsocchi, P., (2024). A review of the electric vehicle charging technology, impact on grid integration, policy consequences, challenges and future trends. Energy Rep., 12: 5671-5692 **(22 pages)**.
Schindler, D.W., (2022). Evolution of Phosphorus Limitation in Lakes. Foundations of Ecology II: Classic Papers with Commentaries, Chicago: University of Chicago Press, 195(4275): 329-332 **(4 pages)**.
Setyoko, A.T.; Nurcahyo, R.; Gabriel, D.S.; Habiburrahman, M., (2022). Policy, supporting infrastructure and market of electric cars in Indonesia. Proceedings of the international conference on industrial engineering and operations management. IEOM Society International, 363-372 **(10 pages)**.
Shaimurunov, S.; Ryspayev, K.; Ismailov, A.; Zhikeyev, A.; Salykov, B., (2023). Study of the efficiency of using facilities based on renewable energy sources for charging electric vehicles in Kazakhstan. Int. J. Sustainable Dev. Plann., 18(4): 1263-1269 **(7 pages)**.
Siddique, M.A.; Nobanee, H.; Hasan, M.B.; Uddin, G.S.; Hossain, M.N.; Park, D., (2023). How do energy markets react to climate policy uncertainty? Fossil vs. renewable and low-carbon energy assets. Energy Econ., 128: 107195 **(20 pages)**.
Sood, S.; Kumar, R.; Tiwari, N.K., (2023). Life cycle assesment of a hybrid solar based electric vehicle charging station using simapro. Adv. Renew. Energy Grid Integr., 89-97 **(9 pages)**.
Strezov, V.; Cho, H.H., (2020). Environmental impact assessment from direct emissions of Australian thermal power generation technologies. J. Cleaner Prod., 270: 122515 **(8 pages)**.
Sun, C.; Zhao, X.; Qi, B.; Xiao, W.; Zhang, H., (2022). Economic and environmental analysis of coupled PV-energy storage-charging station considering location and scale. Appl. Energy., 328:119680 **(16 pages)**.
Tang, J.; Ni, H.; Peng, R.L.; Wang, N.; Zuo, L., (2023). A review on energy conversion using hybrid photovoltaic and thermoelectric systems. J. Power Sources., 562: 232785 **(17 pages)**.
UNECE, (2022). Carbon neutrality in the UNECE region: Integrated life-cycle assessment of electricity sources. United Nations Economic Commission

for Europe **(108 pages)**.
Wang, X.; Tian, X.; Chen, X.; Ren, L.; Geng, C., (2022). A review of end-of-life crystalline silicon solar photovoltaic panel recycling technology. Sol. Energy Mater. Sol. Cells., 248(2): 111976 **(12 pages)**.
Yang, L.; Ribberink, H., (2019). Investigation of the potential to improve DC fast charging station economics by integrating photovoltaic power generation and/or local battery energy storage system. Energy, 167: 246-259 **(14 pages)**.
Yang, M.; Zhang, L.; Zhao, Z.; Wang, L., (2021). Comprehensive benefits analysis of electric vehicle charging station integrated photovoltaic and energy storage. J. Cleaner Prod., 302: 126967 **(12 pages)**.
Zhang, F., (2022). The policy coordinator role of national development banks in scaling climate finance: Evidence from the renewable energy sector. Clim. Policy., 22(6): 754-769 **(16 pages)**.
Zhang, Z.; Sun, X.; Ding, N.; Yang, J., (2019). Life cycle environmental assessment of charging infrastructure for electric vehicles in China. J. Clean. Prod., 227: 932-941 **(10 pages)**.
Ziyaei, S.; Panahi, M.; Manzour, D.; Karbasi. A.; Ghaffarzadeh. H., (2023). Sustainable power generation through decarbonization in the power generation industry. Environ. Monit. Assess., 195(225): 1-24 **(24 pages)**.

AUTHOR (S) BIOSKETCHES

Rosmeika, R., M.Sc., Associate Professor, Research Center for Sustainable Industrial and Manufacturing System. National Research and Innovation Agency (BRIN), South Tangerang, Indonesia.
▪ Email: *rosmeika@brin.go.id*
▪ ORCID: 0009-0006-6470-763X
▪ Web of Science ResearcherID: NA
▪ Scopus Author ID: 57991481000
▪ Homepage: https://brin.go.id/

Aditiyawan S. Kom, M.Si., Associate Professor, Research Center for Sustainable Industrial and Manufacturing System. National Research and Innovation Agency (BRIN), South Tangerang, Indonesia and Lecturer at Faculty of Engineering and Informatics, Universitas Multimedia Nusantara, South Tangerang, Indonesia
▪ Email: *adit001@brin.go.id*
▪ ORCID: 0009-0000-8318-4279
▪ Web of Science ResearcherID: NA
▪ Scopus Author ID: 57991378100
▪ Homepage: https://brin.go.id/; https://www.umn.ac.id/

Muhammad Akbar Hipi, M.Si., Instructor, Research Center for Sustainable Industrial and Manufacturing System. National Research and Innovation Agency (BRIN), South Tangerang, Indonesia.
▪ Email: *muha128@brin.go.id*
▪ ORCID: 0009-0002-7185- 2465
▪ Web of Science ResearcherID: NA
▪ Scopus Author ID: 58544762200
▪ Homepage: https://brin.go.id/

Ayu Erliza, M.T., Instructor, Research Center for Sustainable Industrial and Manufacturing System. National Research and Innovation Agency (BRIN), South Tangerang, Indonesia.
▪ Email: ayue001@brin.go.id
▪ ORCID: 0009-0009-4463-1393
▪ Web of Science Researcher ID: NA
▪ Scopus Author ID: 56179757700
▪ Homepage: https://brin.go.id/

Agam Wira Sani, S.T., Instructor, Research Center for Sustainable Industrial and Manufacturing System. National Research and Innovation Agency (BRIN), South Tangerang, Indonesia.
▪ Email: *agam.wira.sani@brin.go.id*
▪ ORCID: 0000-0002-9469-7640
▪ Web of Science ResearcherID: NA
▪ Scopus Author ID: 58245207000
▪ Homepage: https://brin.go.id/

Utari Ayuningtyas, M.Si., Assistant Professor, Research Center for Sustainable Industrial and Manufacturing System. National Research and Innovation Agency (BRIN), South Tangerang, Indonesia.
▪ Email: *utari.ayuningtyas@brin.go.id*
▪ ORCID: 0000-0001-7670-4969
▪ Web of Science Researcher ID: HPG-7089-2023
▪ Scopus Author ID: 57216637937
▪ Homepage: https://brin.go.id/

Delfi Fatina Soraya, M.Eng., Assistant Professor, Research Center for Sustainable Industrial and Manufacturing System. National Research and Innovation Agency (BRIN), South Tangerang, Indonesia.
▪ Email: *delf001@brin.go.id*
▪ ORCID: 0009-0003-7421-1919
▪ Web of Science ResearcherID: NA
▪ Scopus Author ID: 57991091100
▪ Homepage: https://brin.go.id/

AUTHOR (S) BIOSKETCHES

Ardhy Yuliawan Norma Sakti, M.Eng., Instructor, Research Center for Sustainable Industrial and Manufacturing System. National Research and Innovation Agency (BRIN), South Tangerang, Indonesia.
▪ Email: *ardh007@brin.go.id*
▪ ORCID: 0000-0001-9586-6541
▪ Web of Science Researcher ID: NA
▪ Scopus Author ID: 58652356600
▪ Homepage: https://brin.go.id/

Dr. Nofalia Andriyani, M.Eng., Assistant Professor, Research Center for Sustainable Industrial and Manufacturing System. National Research and Innovation Agency (BRIN), South Tangerang, Indonesia.
▪ Email: *nofa001@brin.go.id*
▪ ORCID: 0000-0002-6241-3869
▪ Web of Science Researcher ID: PDX-1819-2025
▪ Scopus Author ID: 55906618400
▪ Homepage: https://brin.go.id/

Hermawan Febriansyah, M.T., Assistant Professor, Research Center for Sustainable Industrial and Manufacturing System. National Research and Innovation Agency (BRIN), South Tangerang, Indonesia.
▪ Email: *hermawan.febriansyah@brin.go.id*
▪ ORCID: 0009-0008-1647-5824
▪ Web of Science ResearcherID: NA
▪ Scopus Author ID: 57210306559
▪ Homepage: https://brin.go.id/

Chintya Komala Sari, M.Han., Instructor, Research Center for Sustainable Industrial and Manufacturing System. National Research and Innovation Agency (BRIN), South Tangerang, Indonesia.
▪ Email: *chin001@brin.go.id*
▪ ORCID: 0009-0001-2825-5334
▪ Web of Science Researcher ID: NA
▪ Scopus Author ID: 58543754100
▪ Homepage: https://brin.go.id/

Annisa Indah Pratiwi, S.T., Instructor, Research Center for Limnology and Water Resources. National Research and Innovation Agency (BRIN), Bogor, Indonesia.
▪ Email: *anni019@brin.go.id*
▪ ORCID: 0009-0000-5973-658X
▪ Web of Science ResearcherID: NA
▪ Scopus Author ID: 57991216900
▪ Homepage: https://brin.go.id/

Marini Septiani, B.A., Instructor, Bureau of Public Communication, General Affairs, and Secretariat National Research and Innovation Agency (BRIN), South Tangerang, Indonesia.
▪ Email: *mari032@brin.go.id*
▪ ORCID: 0000-0002-7058-1192
▪ Web of Science Researcher ID: NA
▪ Scopus Author ID: 57990906700
▪ Homepage: https://brin.go.id/

Imam Eko Setiawan, Ph.D., Associate Professor, Postgraduate Program of Science in Sustainability, Faculty of Infrastructure Planning. Universitas Pertamina, Jakarta, Indonesia
▪ Email: *imam.es@universitaspertamina.ac.id*
▪ ORCID: 0000-0003-3598-8808
▪ Web of Science Researcher ID: NA
▪ Scopus Author ID: 57218576711
▪ Homepage: https://universitaspertamina.ac.id/prodi/magister-sains-keberlanjutan

HOW TO CITE THIS ARTICLE

Rosmeika, R.; Aditiyawan, A.; Hipi, M.A.; Erliza, A.; Sani, A.W.; Ayuningtyas, U.; Soraya, D.F.; Sakti, A.Y.N.; Andriyani, N.; Febriansyah, H.; Sari, C.K.; Pratiwi, A.I.; Septiani, M.; Setiawan, I.E., (2026). Environmental and economic performance of hybrid charging stations. Global J. Environ. Sci. Manage., 12(1): 129-152.

DOI: 10.22034/gjesm.2026.01.08

URL: https://www.gjesm.net/article_732872.html

Global J. Environ. Sci. Manage. 12(1): 153-166, Winter 2026, Serial #45

Global Journal of Environmental Science and Management
(GJESM)

Homepage: https://www.gjesm.net/

Podcasts

ORIGINAL RESEARCH PAPER

Environmental stability and ultraviolet protection of *Spodoptera litura* nucleopolyhedrovirus encapsulated in chitosan nanoparticles

N.T. Haryadi*, A.W. Pratama, N. Dewi, A.S. Kurnianto, A.I. Tanzil

Department of Agrotechnology, Faculty of Agriculture, University of Jember, Jember, East Java 68121 Indonesia

ARTICLE INFO

Article History:
Received 14 August 2025
Revised 22 November 2025
Accepted 24 December 2025

Keywords:
Biopesticide
Chitosan
Nanoencapsulation
Particle characterization
Spodoptera litura nuclear polyhedrosis virus (SlNPV)

DOI: 10.22034/gjesm.2026.01.09

ABSTRACT

BACKGROUND AND OBJECTIVES: *Spodoptera litura* nuclear polyhedrosis virus is a potent biological control agent against the tobacco cutworm, Spodoptera litura. Nonetheless, its effectiveness in the field is significantly constrained by swift inactivation caused by solar ultraviolet radiation and environmental instability. The study objectives were to synthesize a novel nano-biopesticide formulation by encapsulating Spodoptera litura nuclear polyhedrosis virus within a chitosan matrix and to evaluate its physicochemical properties and protective efficacy against critical environmental stressors.

METHODS: Spodoptera litura nuclear polyhedrosis virus-loaded nanoparticles were synthesized via the ionic gelation method using chitosan and sodium tripolyphosphate. The physicochemical characteristics were elucidated using scanning electron microscopy, transmission electron microscopy, and zeta potential measurements. The efficiency of encapsulation was measured using the standard Bradford protein assay. An assessment of the formulation's stability and residual infectivity was conducted through bioassays involving third-instar Spodoptera litura larvae, which were exposed to ultraviolet-A with 365 nanometers and ultraviolet-B with 312 nanometers irradiation (1–4 hours), varying potential of hydrogen conditions: 3–6, and thermal stress: 4, 25, and 40 degrees Celsius.

FINDINGS: Transmission electron microscopy analysis revealed the formation of discrete, spherical primary nanoparticles with an ultra-small average diameter of approximately 48 nanometers, although scanning electron microscopy indicated a tendency for agglomeration in the freeze-dried state. The formulation demonstrated a moderate encapsulation efficiency of 50.25 percent along with a zeta potential of -29.6 millivolts, which indicates satisfactory colloidal stability. Crucially, bioassays demonstrated that the chitosan encapsulation significantly preserved viral infectivity under harsh conditions; the virus remained active after 4 hours of continuous ultraviolet irradiation and survived incubation in acidic environments with a potential of hydrogen: 3–6, conditions that typically inactivate unprotected or naked baculoviruses.

CONCLUSION: The synthesized chitosan nanoparticles successfully encapsulate Spodoptera litura nuclear polyhedrosis virus and provide a robust physical shield against ultraviolet radiation and extreme potential of hydrogen. The attainment of a sub-100-nanometer particle dimension provides prospective advantages for cellular uptake and tissue infiltration. This formulation indicates a promising and ecologically stable method for delivering viral biopesticides, which requires further optimization and testing in open-field conditions.

This is an open access article under the CC BY license (http://creativecommons.org/licenses/by/4.0/).

NUMBER OF REFERENCES
34

NUMBER OF FIGURES
8

NUMBER OF TABLES
2

*Corresponding Author:
Email: *haryadi.nt@unej.ac.id*
Phone: +813 3105 6318
ORCID: 0000-0002-0458-2752

Note: Discussion period for this manuscript open until Mar 1, 2026 on GJESM website at the "Show Article".

INTRODUCTION

The tobacco cutworm, *Spodoptera litura* (Fabricius) (Lepidoptera: Noctuidae), is a pervasive and highly polyphagous agronomic pest responsible for substantial economic losses in a wide array of horticultural and field crops across tropical and subtropical regions (Abbas *et al.*, 2025; Noosidum *et al.*, 2025). Historically, the approach to managing *S. litura* has been predominantly focused on the utilization of synthetic broad-spectrum insecticides. However, the unrestrained and extensive application of these agrochemicals has led to significant ecological repercussions, such as environmental pollution, the elimination of non-target beneficial species, and the re-emergence of secondary pests (Thakur *et al.*, 2024; Tian *et al.*, 2025). More critically, the physiological selection pressure that these chemicals exert has intensified the widespread development of insecticide resistance. Field populations of *S. litura* have now demonstrated high levels of resistance to major chemical classes, including organophosphates, pyrethroids, and carbamates, necessitating the urgent development of sustainable and biologically based control alternatives. Among the biological control agents, the *Spodoptera litura* nuclear polyhedrosis virus (SlNPV), classified under the *Baculoviridae* family, has emerged as a viable candidate because of its significant pathogenicity and high level of host specificity (Erdiansyah *et al.*, 2021; Dwisandi *et al.*, 2025). Upon ingestion, SlNPV initiates a systemic infection that leads to tissue liquefaction and larval mortality, while posing zero risk to vertebrates or beneficial insects (Mawcha *et al.*, 2025). Despite these distinct advantages, the commercial viability of SlNPV formulations is severely constrained by their environmental fragility. The viral infectious units, known as polyhedral inclusion bodies (PIBs), are highly susceptible to inactivation by solar ultraviolet (UV) radiation—particularly in the UV-B spectrum—as well as extreme potential of hydrogen (pH) and temperature fluctuations (Miranti *et al.*, 2025). Recent evaluations highlight that baculovirus biopesticides face significant limitations due to a swift decline in infectivity when exposed to field conditions (Martínez-Balerdi *et al.*, 2025). Baculovirus occlusion bodies are rapidly degraded by solar ultraviolet radiation, especially UV-B, so that unprotected formulations can lose most of their activity within a few hours of sunlight exposure (Wilson *et al.*, 2020; Sajap *et al.*, 2009). In addition, their infectivity exhibits a significant sensitivity to pH fluctuations away from near-neutral conditions and to thermal stress; studies with S. litura nucleopolyhedrovirus has demonstrated that pH, rearing temperature, and sunlight collectively enhance larval LT_{50} and reduce virus pathogenicity (Sajap *et al.*, 2007). Consequently, conventional SlNPV formulations tend to exhibit short residual activity and require frequent re-application, which reduces their practical and economic suitability for integrated pest management programs (Martínez-Balerdi *et al.*, 2025). Studies indicate that naked SlNPV can lose the majority of its infectivity within hours of sunlight exposure (Wilson *et al.*, 2020), rendering field applications short-lived and economically inefficient due to the need for frequent re-spraying. To overcome the challenges associated with viral persistence, recent technological advancements have concentrated on developing protective delivery systems (Pratama *et al.*, 2024). While traditional additives like molasses or optical brighteners offer marginal protection, nanotechnology presents a transformative approach. Nanoencapsulation refers to the process of enclosing a bioactive agent within a sub-micron polymeric matrix, which provides enhanced protective characteristics in comparison to traditional micro-formulations (Gulati *et al.*, 2024). The elevated surface-to-volume ratio of nanoparticles not only boosts adhesion to leaf surfaces (phylloplane) but also facilitates a controlled release mechanism, thus extending the residual activity of the virus under field conditions (Khobragade *et al.*, 2025; Trisawa *et al.*, 2025). Chitosan, a linear polysaccharide derived from the deacetylation of chitin, represents an ideal matrix for such applications. Beyond its biodegradability and non-toxicity, chitosan is a cationic polyelectrolyte (Singh *et al.*, 2017; Yadav *et al.*, 2022; Yanuhar *et al.*, 2025). This exceptional characteristic permits it to engage electrostatically with anionic crosslinkers (such as tripolyphosphate) and negatively charged viral surfaces, leading to the creation of stable gel networks via ionic gelation—a mild, solvent-free synthesis route suitable for sensitive biological payloads (Pratama, 2025). While chitosan has been investigated for drug delivery purposes, its particular use in safeguarding large viral occlusion bodies necessitates optimization to achieve a balance between encapsulation efficiency

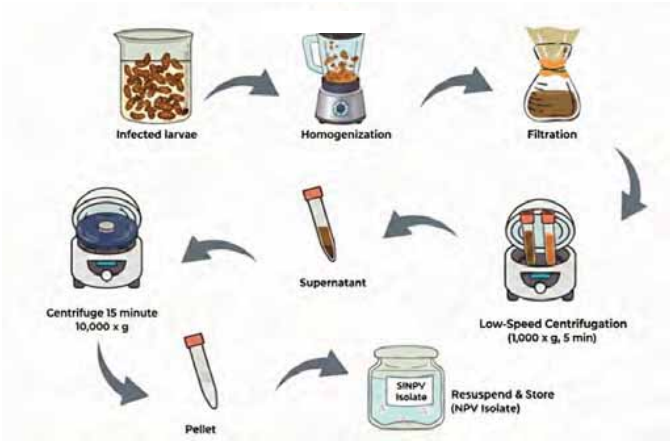

Fig. 1: Schematic method for preparation of SlNPV isolate

with physical stability. Therefore, this study aimed to synthesize and characterize a nano-biopesticide formulation by encapsulating SlNPV within a chitosan matrix via the ionic gelation method. This study aims to evaluate the physicochemical characteristics of the synthesized nanoparticles, which encompass morphology, size distribution, and surface charge. In addition, this study also assesses their protective efficacy in maintaining viral infectivity against critical environmental stressors, namely UV irradiation, pH extremes, and thermal stress. This study was conducted in Jember, Indonesia, in 2025.

MATERIALS AND METHODS

Materials

Chitosan was purchased from Sigma Aldrich, US. Sodium tripolyphosphate (STPP) and acetic acid were obtained from Merck, Germany. For the artificial diet of *Spodoptera litura*, red kidney beans, oatmeal, yeast (Fermipan), ascorbic acid, methylparaben (nipagin), L-cysteine, and agar were sourced locally from the chemical market in Jember, Indonesia. Sodium dodecyl sulfate (SDS) and chemicals for phosphate buffer components were of analytical grade and purchased from Merck, Germany. All reagents were used as received without further purification.

Insect rearing and virus propagation

A stock colony of *S. litura* was established from larvae originally collected from Jember, Indonesia. The insects cultivated in the laboratory under regulated conditions at a temperature of 25 degrees Celsius (°C) and a relative humidity of 70 percent (%). The larvae were maintained on a semi-synthetic diet composed of 75 grams (g) red kidney beans, 75 g oatmeal, 2.5 g yeast, 3 g ascorbic acid, 2 g methylparaben, 0.3 g L-cysteine, 30 g agar, and 500 milliliters (mL) distilled water. Larvae were cultivated separately until the pupation stage to prevent cannibalism, and the adults that emerged were employed for the upkeep of the colony. For SlNPV propagation, healthy third-instar larvae were infected via the surface contamination method using the artificial diet treated with a viral suspension. Virus-killed larvae were harvested and homogenized in 0.1% SDS solution (Fig. 1). The homogenate was filtered through muslin cloth, and the PIBs were purified by differential centrifugation. The filtrate was first centrifuged at 1000 x g for 5 min to remove insect debris, followed by high-speed centrifugation at 10,000 x g to pellet the PIBs. The final pellet was washed, resuspended in sterile phosphate-buffered saline (PBS, pH 7.4), and stored at -20°C. The PIB concentration was quantified using a Neubauer hemocytometer under a light microscope.

Nanoencapsulation of SlNPV

SlNPV-loaded chitosan nanoparticles were synthesized via the ionic gelation method (Fig. 2). Chitosan nanoparticles were prepared by ionic gelation with sodium tripolyphosphate (STPP). Briefly, a 1% weight per volume (w/v) chitosan solution was prepared in 1% volume per volume (v/v) aqueous acetic acid under magnetic stirring for 24 h, followed by sonication for 10 minutes (min) to remove air bubbles and ensure homogeneity. The pH of the chitosan solution was adjusted to 4.6–4.8 using sodium

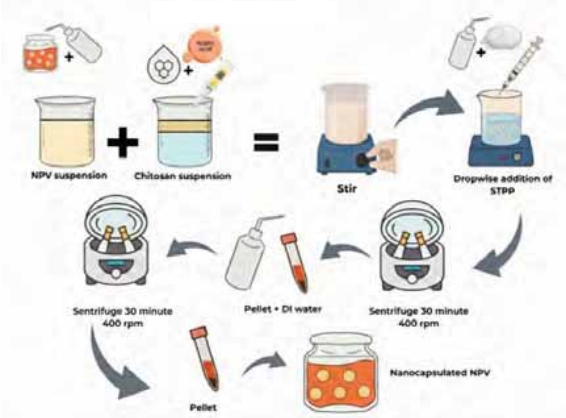

Fig. 2: Schematic method for preparation of SlNPV-loaded chitosan nanoparticles

hydroxide (NaOH). A purified SlNPV suspension (10^8 PIBs/mL) was then added to the chitosan solution at a volume ratio of 1:4 under constant stirring with 400 revolutions per minute (rpm). Separately, an aqueous STPP solution (0.5% w/v) was prepared in deionized water and added dropwise to the chitosan–virus mixture at a fixed chitosan:STPP mass ratio of 3:1. The resulting dispersion was stirred at 400 rpm for 30 min at 25 ± 2 °C to allow spontaneous nanoparticle formation. The resulting nanoparticles were collected by centrifugation at 4000 x g for 30 min, washed with PBS, and lyophilized as Labconco freezone, -50 °C, 0.04 millibar (mbar), 48 h for further analysis.

Determination of encapsulation efficiency (EE)

Encapsulation efficiency (EE) of SlNPV in the chitosan nanoparticles was indirectly assessed by quantifying the quantity of free (non-encapsulated) viral protein remaining in the supernatant following the formation of the nanoparticles. Following ionic gelation and centrifugation, the clear supernatant was carefully collected without disturbing the nanoparticle pellet and analysed using the Bradford assay. The overall protein concentration in the original viral suspension, along with the unbound protein present in the supernatant, was quantified utilizing the Bradford protein assay kit, employing bovine serum albumin (BSA) as the reference standard. The EE (%) was calculated using Eq. 1 (Amini *et al.*, 2017):

$$EE\ (\%) = \frac{Total\ viral\ Protein - Free\ viral\ Protein\ in\ Supernatant}{Total\ Protein} x100 \quad (1)$$

Morphological Analysis

The surface morphology and state of aggregation of lyophilized nanoparticles were examined using scanning electron microscopy (SEM) (JSM-IT200 InTouchScope™ SEM Series, JEOL, Japan). The samples were secured onto stubs and underwent sputter-coating with gold prior to the imaging process. The internal structure and primary particle size were evaluated using transmission electron microscopy (TEM) (Hitachi HT-7700). An aliquot of the nanoparticle suspension was deposited onto a carbon-coated copper grid, negatively stained with 2% phosphotungstic acid, and air-dried before observation at an accelerating voltage of 80 kilovolts (kV). The average diameter of primary particles was computed from TEM images using ImageJ software by measuring at least 50 randomly selected particles.

Zeta potential

The surface charge of the SlNPV-loaded chitosan nanoparticles was determined with a Zetasizer Nano ZS (Malvern Instruments, UK) based on electrophoretic light scattering. Prior to measurement, lyophilized nanoparticles were re-dispersed in phosphate-buffered saline (PBS, pH 7.4) and diluted to an appropriate concentration to avoid multiple scattering. Measurements were conducted at 25 ± 2 °C in disposable folded capillary cells, with three independent runs per sample and at least 10 sub-measurements per run; results are reported as mean zeta potential ± standard deviation.

Stability studies and bioassay

The experimental ranges for UV exposure, pH, and temperature were chosen to approximate field-relevant stressors encountered by SlNPV on

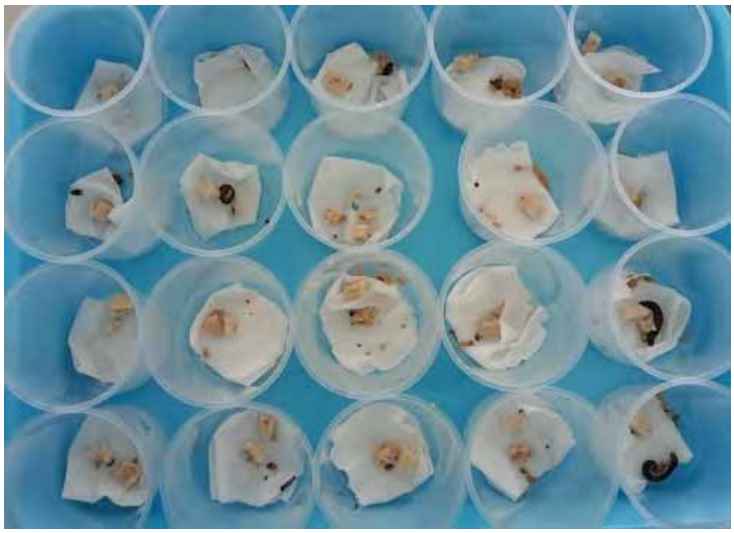

Fig. 3: Bioassay testing on *Spodoptera litura* larvae

crop foliage in tropical agroecosystems. Continuous irradiation for 1–4 h with UV-A (365 nm) and UV-B (312 nm) at a fixed distance was selected to mimic several hours of intense midday solar radiation, which previous work has shown to cause rapid inactivation of baculovirus occlusion bodies on leaves. The acidic microenvironments found on the phylloplane, resulting from plant exudates and agrochemical deposits, were represented by a pH of 3 to 6, which still facilitated the subsequent dissolution of occlusion bodies in the alkaline insect midgut. Residual infectivity of each treatment was evaluated using a diet surface contamination bioassay against third-instar *S. litura* larvae. For every combination of formulation and environmental treatment (UV exposure time, pH, or temperature), 30 larvae were tested per replicate with three independent replicates (total n = 90 larvae per treatment). Artificial diet plugs with approximately 1 cubic centimeters (cm^3) in 24-well plates were treated with 20 µL of nanoparticle suspension or unencapsulated virus, adjusted to a final concentration of 10^7 PIBs/mL (Fig. 3). The larvae were sustained under the same rearing conditions as the stock colony, and mortality was documented on a daily basis for a duration of 7 days; individuals that failed to molt or exhibited characteristic NPV symptoms were scored as dead.

pH stability test

To assess infectivity under different pH conditions, aliquots of the nano-encapsulated SlNPV were mixed (1:1 v/v) with universal buffer solutions adjusted to pH 3.0, 4.0, 5.0, and 6.0. The mixtures were incubated for 24 h at 25 ± 2 °C. Following incubation, the samples were subjected to the general bioassay procedure.

Temperature stability test

Aliquots of the nanoparticle suspension were stored in microcentrifuge tubes at controlled temperatures of 4°C, 25°C, and 40°C for a period of 10 days. Upon completion of the storage duration, the samples were permitted the opportunity to equilibrate to 25 ± 2 °C and were evaluated for residual infectivity using the general bioassay procedure.

UV Irradiation stability test

The photoprotective effect of the encapsulation was evaluated by exposing samples to artificial ultraviolet radiation. The samples were irradiated in an ultraviolet cabinet equipped with UV-A (365 nm) and UV-B (312 nm) lamps, with an irradiance at the sample of approximately (UV-A ≈ 15 W m^{-2}; UV-B ≈ 5 W m^{-2}), at a fixed distance of 15 cm from the light source for 1, 2, 3, and 4 hours to obtain the desired cumulative UV dose. Non-irradiated encapsulated SlNPV served as a control. After irradiation, sterile water was used to modify the volume to compensate for evaporation, and the residual infectivity was evaluated according to the general bioassay procedure.

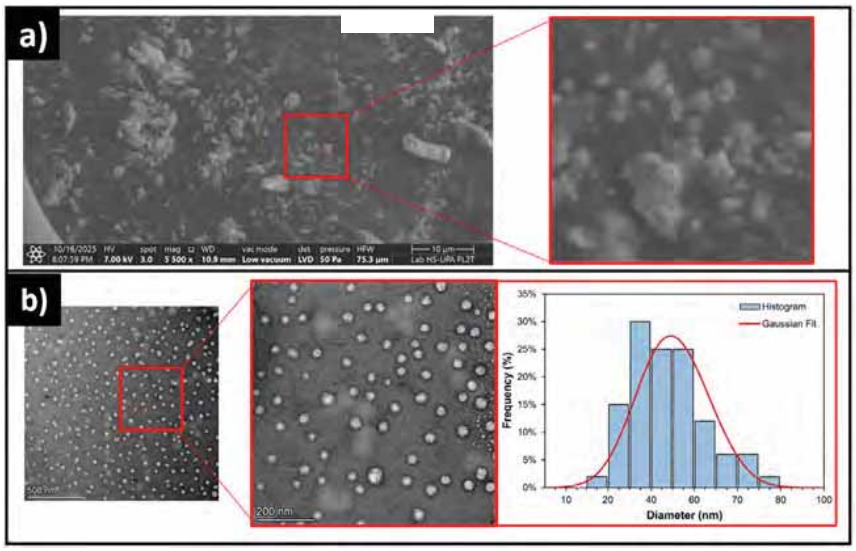

Fig. 4: Morphological analysis of the nano-encapsulated SlNPV: (a) SEM micrograph and (b) TEM micrograph (left) and the corresponding particle size distribution histogram (right)

Statistical analysis

All statistical analyses were conducted in R version 4.3.2 using RStudio version 2023.12.1 (RStudio PBC, Boston, MA, USA). Larval mortality data were arcsine square-root transformed prior to analysis to stabilize variances. An assessment of treatment effects related to formulation type, UV exposure time, pH level, and storage temperature were evaluated using one-way analysis of variance (ANOVA). In instances where the ANOVA indicated significance, Tukey's HSD post hoc test was utilized for further multiple comparisons. A significance threshold of $P < 0.05$ was used for all tests.

RESULTS AND DISCUSSION

Morphological characterization of nano-encapsulated SlNPV

The morphological structure and dimensional characteristics of the synthesized nanoparticles were comprehensively evaluated using SEM and TEM, as presented in Fig. 4.

The SEM analysis (Fig. 4a) illustrates the microstructure of the formulation in its lyophilized (freeze-dried) state. The micrograph displays large, irregular agglomerates characterized by rough surfaces, as opposed to distinct nanoparticles. This extensive aggregation is a characteristic artifact of the lyophilization process. During the process of sublimation, the extraction of water causes primary nanoparticles to come into close proximity, thereby promoting robust inter-particle hydrogen bonding and van der Waals interactions, which result in the formation of micro-sized clusters (Adams *et al.*, 2015). To resolve the true morphology and size of the individual primary particles, TEM analysis was conducted (Fig. 4b). In stark contrast to the SEM results, the TEM micrographs distinctly illustrate separate, well-dispersed nanoparticles exhibiting a defined spherical geometry. The high contrast observed between the particles and the background corroborates the successful synthesis of dense polymeric nanoparticles. Quantitative analysis of the particle size distribution (Fig. 4b) was performed by measuring random particles (n = 50) from the TEM images. The resulting histogram fits a Gaussian distribution curve, indicating a relatively narrow and unimodal size range. The findings indicates that the main nanoparticles exhibit diameters predominantly between 20 and 80 nm, with an average diameter estimated at around 48 nm. This finding is significant as the particles are considerably smaller than the 100–200 nm range typically reported for chitosan-based systems synthesized via manual ionic gelation. Achieving an ultra-small dimension of under 100 nm offers considerable advantages for applications involving biopesticides. Nanoparticles in this size regime typically exhibit superior specific surface area, which enhances adhesion to leaf surfaces and

facilitates more effective cellular uptake or penetration into insect tissues compared to larger microparticles (Ismail *et al.,* 2017). The distinct electron-dense core identified in the nanoparticles implies the efficient entrapment of the SlNPV cargo within the compact chitosan-STPP matrix, shielding it from environmental degradation. The sub-100-nanometer size of the primary chitosan nanoparticles has important implications for their biological performance. Particles in the tens-of-nanometers range exhibit a high specific surface area, which can enhance adhesion to the phylloplane and elevate the likelihood of interaction between occlusion bodies and the insect midgut epithelium once ingested, thereby potentially enhancing cellular absorption and tissue infiltration in comparison with micro-sized formulations. Simultaneously, extremely small particles may diffuse at a faster rate and could be more prone to being washed off by rainfall or redistributed within the plant–soil system. Therefore, the overall effect on field efficacy will ultimately depend on a balance between enhanced bioavailability and potential environmental losses.

Colloidal stability and surface charge properties

Beyond morphological analysis, the colloidal stability of the nano-formulation was evaluated by measuring the zeta potential. The stability of a dispersion is primarily determined by the surface charge of the particles, since this impacts the amount of electrostatic repulsion that occurs between them. The synthesized SlNPV-loaded nanoparticles exhibited a mean zeta potential of -29.6 millivolt (mV) (Fig. 5). In colloidal chemistry, zeta potential values with a magnitude greater than 30 mV (either positive or negative) are generally considered the benchmark for physically stable suspensions (Lowry *et al*., 2016). A value of -29.6 mV places the formulation on the threshold of this high-stability region, indicating that sufficient repulsive forces exist between the nanoparticles to overcome attractive Van der Waals forces. This electrostatic repulsion provides a significant barrier to prevent swift flocculation or coalescence during storage (Németh *et al.,* 2022). This value lies just below the commonly cited ±30 mV empirical threshold for highly stable colloidal dispersions and therefore suggests moderate to near-borderline electrostatic stabilization rather than unequivocally 'high' stability. Nevertheless, the relatively narrow zeta-potential distribution and the lack of observable sedimentation throughout the duration of the experiments suggest that the dispersion was adequately stable for handling, storage, and bioassays under the conditions used in this study.

It is significant to note that the particles displayed anegative surface charge. While native chitosan is typically cationic (positive) in acidic media due to the protonation of amino groups ($–NH_3^+$), the shift to a negative potential in this study is attributed to the formulation conditions. The nanoparticles were resuspended in PBS at pH 7.4. At this pH, which is above the pKa of chitosan (~6.5), the amino groups largely deprotonate, reducing the positive charge density. Consequently, the anionic charges from the phosphate groups of the STPP crosslinker and the viral capsid proteins likely dominate the surface character (Luo *et al*., 2022). Furthermore, the zeta potential distribution graph (Fig. 5) displays a single, sharp peak. In the absence of dynamic light scattering (DLS) scattering data, this sharp peak serves as a secondary indicator of the sample's homogeneity. A diverse or multi-modal zeta distribution would indicate a combination of particles with vastly different surface chemistries or aggregates, while the single narrow peak noted here validates the uniformity of the encapsulation process.

Environmental stability and bioactivity

The primary limitation of baculoviruses as field biopesticides is their rapid inactivation by environmental stressors, particularly solar UV radiation, extreme pH, and fluctuating temperatures. The effectiveness of chitosan nano-encapsulation in providing protection was assessed via a series of bioassays targeting *S. litura* larvae.

UV stability

Solar UV radiation is the primary environmental factor limiting the field persistence of baculoviruses. The protective efficacy of the nanoformulation was evaluated by exposing the virus to UV irradiation for up to 4 h. As illustrated in Fig. 6, the control group (non-irradiated) demonstrated the greatest larvicidal activity, achieving 60% mortality within 2 hours, thereby confirming the inherent pathogenicity of the virus.

Upon exposure to UV-A and UV-B, larval mortality

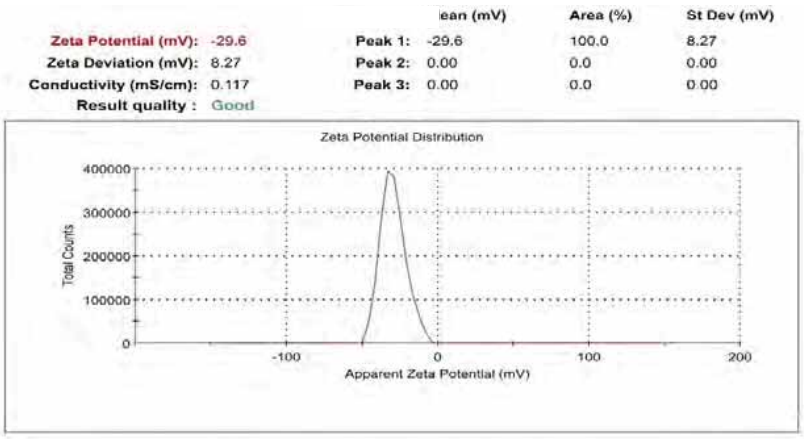

Fig. 5: Zeta potential distribution of chitosan-encapsulated SlNPV

decreased to a range of 30–40%. Although a decline in infectivity was seen when compared to the non-irradiated control, the essential finding is that the encapsulated virus continued to exhibit biological activity even following 4 h of intense exposure. Previous studies have demonstrated that naked (unprotected) baculoviruses typically suffer near-complete inactivation within minutes to hours of UV exposure due to DNA cyclobutane pyrimidine dimer formation (Wilson *et al*., 2020; Çakmak *et al.,* 2021). The retention of infectivity in this study suggests that the chitosan matrix functions as a physical shield. The dense, polymeric network of chitosan absorbs and scatters UV radiation, thereby reducing the photon flux reaching the viral DNA and capsid proteins (Zhang *et al*., 2025). This protective mechanism is important for increasing the lifespan of the biopesticide in outdoor environments.

pH Stability

An initial bioassay investigated the stability of the formulation under acidic conditions (pH 3–6), simulating the fluctuating pH environments simulating the fluctuating on leaf surfaces (phylloplane). The results (Fig. 7) show that the encapsulated SlNPV retained infectivity across the tested range, with the highest mortality (10%) observed at pH 4.

Despite the relatively low absolute mortality rates, the data provides significant evidence for the retention of infectivity. Naked nucleopolyhedroviruses are sensitive to extreme pH fluctuations; while they rely on alkaline conditions (pH > 8) in the insect midgut to dissolve the occlusion body, premature exposure to environmental acidity or extreme alkalinity can denature capsid proteins (Luo *et al*., 2022; Williams, 2023). The capability of the encapsulated virus to withstand 24 h of acidic incubation and subsequently infect larvae implies that the chitosan matrix successfully protects the viral cargo from external hydronium ions (Boroumand *et al*., 2021). The low mortality rate could be ascribed to the physiological stress imposed on the larvae by the acidic diet or the insufficient liberation of the acidic diet itself or incomplete release of the virus from the matrix during the bioassay period.

Temperature Stability

Thermal stability is a prerequisite for the storage and transport of biopesticides. The formulation was subjected to storage at 4°C, 25°C, and 40°C for 10 days. The results (Fig. 8) demonstrate that efficacy was temperature-dependent, with optimal mortality observed at 25°C (36.6%), followed by significant reductions at 4°C (16.6%) and 40°C (13.3%).

The reduced efficacy at 40°C is likely due to the thermal degradation of viral proteins or accelerated aggregation of the polymer matrix, which could hinder viral release (Mustafa and Hussein, 2020). Conversely, the lower mortality at 4°C might result from a reduced release rate of the virus from the chitosan matrix, as polymer swelling and degradation are typically temperature-dependent processes (Jiang *et al*., 2021). The observation that 25°C retains optimal activity is consistent with the overall physiological stability of baculoviruses, implying that the formulation is appropriate for storage at

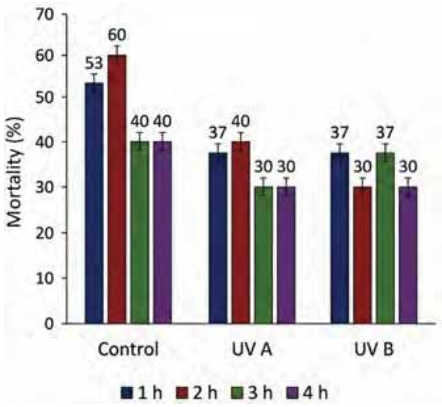

Fig. 6: Effect of UV on the efficacy of nano-encapsulated SlNPV, measured by larval mortality percentage

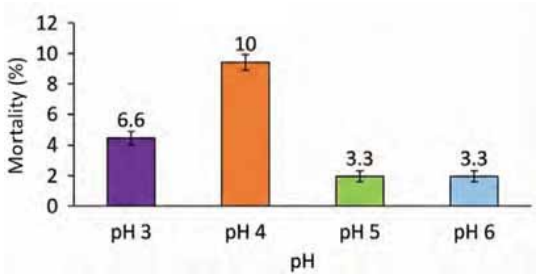

Fig. 7: Effect of pH on the efficacy of nano-encapsulated SlNPV, measured by larval mortality percentage

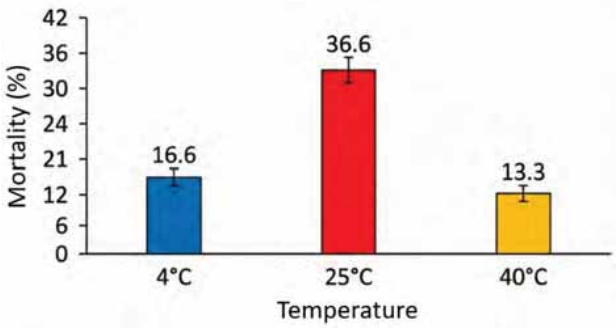

Fig. 8: The effect of constant temperature for 10 days on the efficacy of nano-encapsulated SlNPV, measured by the percentage of larval mortality

controlled room temperatures (Ismail, 2023). To better contextualize the methodological choices and outcomes of this work, the results of the present chitosan-based SlNPV nanoformulation are compared with selected previous studies on baculovirus formulations and UV-protective strategies in Table 1.

Compared with previous viral encapsulation studies that mainly relied on microencapsulation or hybrid carriers, such as ENTOSTAT–TiO_2 microcapsules for baculoviruses (Wilson *et al.,* 2020) and zeolite chitosan blends for Helicoverpa armigera NPV (Miranti *et al.,* 2025), the present work employs a purely chitosan-based ionic gelation process optimized to yield ultra-small (~48 nm) nanoparticles with a well-defined negative zeta potential and quantified encapsulation efficiency. This method offers a more comprehensive physicochemical characterization of SlNPV-loaded particles compared

Table 1: Comparison of SlNPV nanoformulations with previous baculovirus formulation studies

Virus and target pest	Carrier/ Technology	UV/pH/ Temperature conditions tested	Main efficacy or stability outcome	Key differences	Sources
SlNPV – *S. litura*	Liquid NPV + adjuvants	Natural sunlight; no nano-carrier	Adjuvants delayed sunlight inactivation but required high doses and frequent reapplication	No nanoencapsulation; only short-term UV protection compared with chitosan nanoparticles.	Sajap *et al*., 2009
Baculovirus for *Helicoverpa* spp.	ENTOSTAT–TiO_2 micro-encapsulation	Simulated sunlight; limited pH/temperature tests	Marked improvement in UV stability and field persistence	Different viruses and micro-scale particles; did not evaluate acidic pH or a broad temperature range.	Wilson *et al*., 2020
H. armigera NPV vs. *S. litura*	Zeolite/ chitosan nanoparticle mixtures	UV and lab bioassays	Improved larval mortality after UV exposure	Hybrid carrier; did not report detailed zeta potential or encapsulation efficiency for SlNPV.	Miranti *et al*., 2025
S. litura	Chitosan nanoparticle	UV A, UV B, pH, and Temperature	Improved larval mortality	Nanoencapsulation for SlNPV formulation	Present study

Table 2: Encapsulation efficiency of chitosan-encapsulated SlNPV

Treatment	Mean (%)	Standard deviation (SD) (%)	Mean ± SD
Virus nanoencapsulation	50.25	15.76	50.25 ± 15.76

to numerous previous formulations, while also concurrently assessing their protective efficacy against three significant environmental stressors: UV irradiation, acidic pH, and temperature extremes, all within a cohesive experimental framework. This signifies a methodological progression in the creation and evaluation of viral nano-biopesticides. The enhanced environmental stability of SlNPV in this study can be attributed to several complementary mechanisms provided by the chitosan matrix. As a dense polysaccharide, chitosan forms a compact polymer shell around occlusion bodies that absorbs and scatters incident light, reducing the UV photon flux that reaches the viral DNA and capsid, a mechanism analogous to other polymeric nanocarriers used to shield labile biomacromolecules from photodegradation (Wilson *et al.,* 2020). In water-based environments, the protonatable amino groups and hydroxyl functionalities present in chitosan form a hydrated, partially buffered microenvironment. This environment reduces the diffusion of external hydronium or hydroxide ions, thus alleviating pH-induced viral inactivation. This observation aligns with findings that chitosan-based nanoparticles can stabilize delicate viral cargos and maintain their biological activity amidst varying pH levels (Martínez-Balerdi *et al*., 2025).

Encapsulation efficiency (EE%)

The determination of encapsulation efficiency plays a critical role in assessing both the payload capacity of the nanocarrier system and the economic feasibility of the formulation process. The encapsulation efficiency of the SlNPV-loaded chitosan nanoparticles was calculated quantitatively based on the measurement of free protein in the supernatant. As presented in Table 2, the mean encapsulation efficiency was determined to be 50.25 ± 15.76%. This signifies that about half of the initial viral payload was effectively captured within the cross-linked chitosan-STPP matrix throughout the ionic gelation process.

While some studies on nanoinsecticides report higher encapsulation efficiencies—such as the 70.5% achieved by Chen *et al.* (2022) for *Spodoptera frugiperda* formulations—an efficiency of ~~50% is considered moderate and practically acceptable for encapsulating large, complex biological entities like viral inclusion bodies. The entrapment of sizable biological particles within a significantly smaller polymer network poses fundamental physical challenges when compared to the encapsulating small chemical molecules. A notable aspect of

the result is the relatively high standard deviation (±15.76%), indicating significant batch-to-batch variability in the synthesis process. The ionic gelation technique is recognized for its high sensitivity to both thermodynamic and kinetic factors. Minor changes in mixing speed, the rate of STPP addition, local concentration gradients during dropwise addition, or the intrinsic heterogeneity of the initial viral suspension may all lead to variations in entrapment dynamics among different replicates. Nevertheless, these results establish the proof-of-concept for successful SlNPV loading. Further optimization of critical processing parameters, particularly the chitosan-to-virus mass ratio and mixing dynamics, is recommended in future studies to maximize payload retention and improve reproducibility. This study has multiple limitations that must be recognized. All stability assays and bioefficacy tests were conducted under controlled laboratory conditions, so the performance of the nano-encapsulated SlNPV under complex field environments—including rainfall, solar angle variation, plant canopy structure, and non-target interactions—remains to be validated. Furthermore, the ionic gelation process demonstrated a moderate level of encapsulation efficiency, accompanied by significant variability between batches. This suggests that additional optimization of the chitosan: STPP ratio, mixing conditions, and lyophilization protocols is necessary to enhance reproducibility and scalability. Furthermore, a concurrent control of unencapsulated (naked) virus subjected to the same stress conditions was not included in this study; thus, comparisons regarding the degree of protection are based on established literature values rather than direct experimental data. Future research should consequently concentrate on enhancing the formulation parameters to minimize variability, incorporating rainfastness and persistence trials in open-field studies, and assessing long-term ecological safety and compatibility with other components of integrated pest management programmes.

CONCLUSION

The present study successfully demonstrated the fabrication of a nano-encapsulated biopesticide system employing SlNPV within a cross-linked chitosan-STPP matrix. By optimizing the ionic gelation method, ultra-small spherical primary nanoparticles with an average core diameter of 48 nm were successfully synthesized. While SEM highlighted the susceptibility of the formulation to form micro-aggregates during the lyophilization process—a common artifact of water sublimation—TEM corroborated the presence of discrete, high-density primary units. The colloidal stability of the formulation, characterized by a zeta potential of -29.6 mV, indicates a robust electrostatic repulsion threshold that prevents rapid coalescence in aqueous suspension, particularly when maintained in a physiological pH environment. From a scientific standpoint, the primary contribution of this research is the effective reduction of environmental degradation, which has traditionally obstructed the commercial potential of baculoviruses. The findings reveal that the chitosan matrix functions as an effective physicochemical shield, significantly prolonging the biological activity of SlNPV against deleterious environmental stressors. Specifically, substantial larvicidal infectivity was maintained even after 4 h of intense UV-A and UV-B irradiation, whereas naked viral inclusion bodies typically undergo near-total inactivation under similar solar flux. The protective effect against photodamage is linked to the robust polymeric structure of chitosan, which absorbs and disperses high-energy radiation, consequently preventing irreversible damage to DNA and the denaturation of capsid proteins. Furthermore, the stability of the encapsulated virus across a pH range of 3.0 to 6.0 and various thermal conditions (4°C to 40°C) underscores the versatility of the nanocarrier system. The preservation of infectivity at acidic pH levels—characteristic of the leaf surface (phylloplane) environment—indicates that the chitosan shell offers an essential buffering microenvironment that protects the viral payload from external hydronium ions. Economically and practically, the ultra-small particle size (~48 nm) identified in this investigation offers a distinct advantage; the high surface-area-to-volume ratio is expected to enhance adhesion to plant foliage and facilitate superior cellular uptake within the insect midgut, potentially reducing the required dose and frequency of application in field settings. Notwithstanding these encouraging outcomes, it is essential to recognize certain limitations. The observed moderate encapsulation efficiency (approximately 50%) and the variability reflected in the standard deviation suggest that the entrapment of large, complex biological occlusion bodies within a nanometric polymer mesh is

influenced by slight kinetic fluctuations during the synthesis phase. It is recommended that future research prioritize the optimization of the polymer-to-virus mass ratio and mixing dynamics to enhance payload retention. Furthermore, although laboratory bioassays have provided a strong proof-of-concept, extensive open-field trials are essential to assess the formulation's effectiveness in intricate real-world scenarios, such as rainfall wash-off and interactions with non-target organisms. In summary, a substantial foundation for the development of sustainable, nano-based biopesticides has been established. By integrating the high specificity of SlNPV with the protective properties of chitosan nanotechnology, a viable and environmentally friendly alternative to synthetic chemical insecticides is provided. This strategy not only confronts the escalating problem of insecticide resistance in *S. litura* populations but also corresponds with international efforts focused on precision agriculture and decreasing chemical footprints in the food supply chain.

AUTHOR CONTRIBUTIONS

N.T. Haryadi took the lead, being responsible for conceptualization, methodology, formal analysis, and data curation, while also authoring the writing - review and editing. A.W. Pratama contributed to Writing – original draft, Writing - review and editing, Visualization, Formal analysis, and managed Data curation. N. Dewi was involved in the methodology and provided project administration. A.S. Kurnianto performed formal analysis and conducted the Investigation. A.I. Tanzil was responsible for data curation and formal analysis.

ACKNOWLEDGEMENT

The authors would like to thank the Ministry of Higher Education, Science, and Technology (KEMENDIKTISAINTEK) for funding support through the Penelitian Fundamental Scheme, contract number [4560/UN25.3.1/LT/2025]. The authors would like to acknowledge the facilities, scientific, and technical support from Advanced Characterization Laboratories, Cibinong, National Research and Innovation Agency of Indonesia.

CONFLICT OF INTEREST

The authors declare that there are no conflicts of interest regarding the publication of this manuscript. In addition, ethical issues, including plagiarism, informed consent, misconduct, data fabrication and/or falsification, double publication and/or submission, and redundancy, were observed by the authors.

OPEN ACCESS

©2026 The author(s). This article is licensed under a Creative Commons Attribution 4.0 International License, which permits use, sharing, adaptation, distribution and reproduction in any medium or format, as long as you give appropriate credit to the original author(s) and the source, provide a link to the Creative Commons license, and indicate if changes were made. The images or other third-party material in this article are included in the article's Creative Commons license, unless indicated otherwise in a credit line to the material. If material is not included in the article's Creative Commons license and your intended use is not permitted by statutory regulation or exceeds the permitted use, you will need to obtain permission directly from the copyright holder. To view a copy of this license, visit: http://creativecommons.org/licenses/by/4.0/

PUBLISHER'S NOTE

GJESM Publisher remains neutral with regard to jurisdictional claims in published maps and institutional afflictions.

R Positive AI Statement

During the preparation of this work, the author has used Artificial Intelligence (AI) [Gemini AI] in order to refine English. After using this tool/service, the authors reviewed and edited the content as needed and take full responsibility for the content of the publication.

ABBREVIATIONS

%	Percent
∘	degrees
°C	degrees Celsius
µL	Microliter
BSA	Bovine serum albumin
cm	Centimeter
cm^3	Cubic centimeter
DLS	Dynamic light scattering
EE	Encapsulation efficiency
g	Gram

h	Hours
kV	kilovolts
mbar	Millibar
min	Minutes
mL	Milliliter
mM	Millimolar
mV	millivolts
NaOH	Sodium hydroxide
nm	Nanometer
PBS	Phosphate-buffered saline
pH	Potential of hydrogen
PIBs	Polyhedral inclusion bodies
rpm	Revolutions per minute
SD	Standard deviation
SDS	Sodium dodecyl sulfate
SlNPV	Spodoptera litura nuclear polyhedrosis virus
STTP	Sodium tripolyphosphate
SEM	Scanning electron microscopy
TEM	Transmission electron microscopy
UV	Ultraviolet
UV-A	Ultraviolet-A
UV-B	Ultraviolet-B
v/v	Volume per volume
w/v	Weight per volume

REFERENCES

Adams, G.D.J., Cook, I., Ward, K.R., (2015). The principles of freeze-drying. Cryopreservation and freeze-drying protocols, 15-38 **(22 pages)**.

Thakur, R.; Sharma, S., (2024). Impact of pesticides used in agriculture: their benefits and hazards. AIP Conf. Proc., 2986 (1): 030163 **(7 pages)**.

Amini, Y., Amel Jamehdar, S., Sadri, K., Zare, S., Musavi, D., Tafaghodi, M., (2017). Different methods to determine the encapsulation efficiency of protein in PLGA nanoparticles. Bio-Med. Mater. Eng., 28(6): 613-620 **(7 pages)**.

Boroumand, H.; Badie, F.; Mazaheri, S.; Seyedi, Z.S.; Nahand, J.S.; Nejati, M.; Baghi, H.B.; Abbasi-Kolli, M.; Badehnoosh, B.; Ghandali, M.; Hamblin, M.R.; Mirzaei, H., (2021). Chitosan-based nanoparticles against viral infections. Front. Cell. Infect. Microbiol., 11: 643953 **(22 pages)**.

Çakmak, T.; Simón, O.; Kaydan, M.B.; Tange, D.A.; Rodríguez, G.; Diaz, A.P.; Murillo, P.; Suarez, E.H., (2021). Effects of several uv-protective substances on the persistence of the insecticidal activity of the alphabaculovirus of Chrysodeixis chalcites (chchnpv-tf1) on banana (Musa acuminata, Musaceae, Colla) under laboratory and open-field conditions. PLOS ONE, 16(5): e0250217 **(15 pages)**.

Chen, X.; Qiu, L.; Liu, Q.; He, Y., (2022). Preparation of an environmentally friendly nano-insecticide through encapsulation in polymeric liposomes and its insecticidal activities against the fall armyworm, Spodoptera frugiperda. Insects. 13(7): 625 **(12 pages)**.

Danaei, M.R.M.M.; Dehghankhold, M.; Ataei, S.; Hasanzadeh Davarani, F.; Javanmard, R.; Dokhani, A.; Khorasani, S.; Mozafari, Y.M., (2018). Impact of particle size and polydispersity index on the clinical applications of lipidic nanocarrier systems. Pharmaceutics. 10(2): 57 **(17 pages)**.

Dwisandi, R.F.; Miranti, M.; Prismantoro, D.; Awal, M.A.; Azzahra, R.S.N.A.; Mispan, M.S.; Hermawan, W.; Joshi, R.C.; Doni, F., (2025). Entomopathogenic, antifeedant, and repellent activities of indigenous Trichoderma sp. LB1 for managing common cutworm, Spodoptera litura (fabricius). J. Agric. Food Res., 102268 **(10 pages)**.

Erdiansyah, I.; Syarief, M.; Taufika, R., (2021). Virulence of Spodoptera litura nuclear polyhedrosis virus (SLNPV) with kaolin as carrier material on Spodoptera litura and Tetragonula laeviceps on soybean. IOP Conf. Ser. Earth Environ. Sci., 672(1): 012097 **(6 pages)**.

Gulati, S.; Amar, A.; Chhabra, L.; Katiyar, R.; Sahu, T.; Varma, R.S., (2024). Greener nanobiopolymers and nanoencapsulation: environmental implications and future prospects. RSC Sustainable. 2(10): 2805-2832 **(28 pages)**.

Ismail, S.M., (2023). Influence of temperature on the toxicity and stability of insecticide resistance against Spodoptera littoralis (lepidoptera: noctuidae). Bull. Natl. Res. Cent., 47(1): 85 **(5 pages)**.

Ismail, Z.; Kassim, S.; Harun, N.A., (2017). Development of hydrophilic poly(n-vinylpyrrolidone) nanoparticles via inverse miniemulsion polymerization technique. AIP Conference Proceeding. 1885(1): 020079 **(8 pages)**.

Jiang, M.; Song, Y.; Kanwar, M.K.; Ahammed, G.J.; Shao, S.; Zhou, J., (2021). Phytonanotechnology applications in modern agriculture. J. Nanobiotechnol., 19(1): 430 **(20 pages)**.

Khobragade, R.; Chaudhary, A.A.; Ali, M.A.M.; Kale, M.; Raut, N.; Ghive, P.; Rudayni, H.A.; Nagpurkar, K.; Umekar, M.; Trivedi, R., (2025). Nanotechnology-enhanced sunscreens: balancing efficacy, safety, and environmental impact. Pharmaceutics. 17(8): 1080 **(26 pages)**.

Lowry, G.V.; Hill, R.J.; Harper, S.; Rawle, A.F.; Hendren, C.O.; Klaessig, F.; Nobbmann, U.; Sayre, P.; Rumble, J., (2016). Guidance to improve the scientific value of zeta-potential measurements in nanoehs. Environ. Sci. Nano., 3(5): 953-965 **(13 pages)**.

Luo, M.; Lin, J.; Zhou, X.; Pu, X., (2022). Study on physical properties of four pH responsive Spodoptera exigua multiple nucleopolyhedrovirus (semnpv) microcapsules as controlled release carriers. Sci. Rep., 12(1): 21873 **(13 pages)**.

Mawcha, K.T.; Malinga, L.; Muir, D.; Ge, J.; Ndolo, D., (2025). Recent advances in biopesticide research and development with a focus on microbials. F1000Research. 13: 1071 **(27 pages)**.

Martínez-Balerdi, M., Caballero, J., Aguirre, E., Caballero, P., Beperet, I., (2025). Baculoviruses as microbial pesticides: Potential, challenges, and market overview. Viruses. 17(7): 917 **(36 pages)**.

Miranti, M.; Iskandar, I.N.; Melanie, M.; Malini, D.M.; Panatarani, C.; Joni, I.M.; Prismantoro, D.; Doni, F.; Joshi, R.C.; Hermawan, W., (2025). Enhanced efficacy of Helicoverpa armigera nucleopolyhedrovirus against Spodoptera litura larvae using zeolite and chitosan nanoparticle formulations. Virus Res., 199614 **(7 pages)**.

Mustafa, I.F.; Hussein, M.Z., (2020). Synthesis and technology of nanoemulsion-based pesticide formulation. Nanomaterials. 10(8): 1608 **(26 pages)**.

Németh, Z.K.; Csóka, I.; Semnani Jazani, R.; Sipos, B.; Haspel, H.; Kozma, G.; Kónya, Z.; Dobó, D.G., (2022). Quality by design-driven zeta potential optimisation study of liposomes with charge imparting membrane additives. Pharmaceutics, 14(9): 1798 **(25 pages)**.

Noosidum, A.; Onwong, R.; Phittayanivit, J.; Arkhan, C.; Poolprasert, P.; Sangtongpraow, B.; Wongchoosuk, C., (2025). Detection of Spodoptera litura F. using an electronic nose: a novel approach for monitoring vegetable crop pests. Comput. Electron. Agric., 239: 110984 **(15 pages)**.

Pratama, A.W., (2025). Advances in green synthesis of nanoparticles from crop residues and their application in sustainable agriculture: a review. J. Appl. Chem. Sci. Int., 16: 230-240 **(11 pages)**.

Pratama, A.W.; Piluharto, B.; Widiastuti, N.; Mahardika, M., (2024). The impact of nanoparticles on agriculture and soil, by Nar Singh Chauhan and Sarvajeet Singh Gill. Adv. Agrochem., 3(4): 261-262 **(2 pages)**.

Sajap, A. S., Bakir, M. A., Kadir, H. A., Samad, N. A. (2007). Effect of pH, rearing temperature and sunlight on infectivity of Malaysian isolate of nucleopolyhedrovirus to larvae of Spodoptera litura (Lepidoptera:

Noctuidae). Int. J. Trop. Insect Sci., 27(2): 108–113 **(5 pages)**.
Sajap, A. S., Bakir, M. A., Kadir, H. A., Samad, N. A., (2009). Efficacy of selected adjuvants for protecting Spodoptera litura nucleopolyhedrovirus from sunlight inactivation. J. Asia Pac. Entomol., 12(2): 85–88 (**3 pages)**.
Singh, R.; Shitiz, K.; Singh, A., (2017). Chitin and chitosan: biopolymers for wound management. Int. Wound J., 14(6): 1276-1289 **(14 pages)**.
Tian, X.; Wang, H.; Li, J.; Shi, C.; Gao, G.; Meng, J.; Su, Q., (2025). Untargeted metabolomics of Spodoptera litura (lepidoptera: noctuidae) gut reveals physiological difference among eight diets. J. Asia-Pac. Entomol., 28(2): 102411 **(12 pages)**.
Trisawa, I.M.; Taufik, I.; Ardi, I.; Thesiana, L.; Kusrini, E.; Susanti, D.; Minarni, E.W.; Nurawan, A.; Jufri, A.; Sukamto; Apriyana, Y.; Sutrisna, N.; Surdianto, Y.; Susanto, B.; Susanto, U., (2025). Eco-friendly pest management in integrated rice-fish farming systems using plant-derived biopesticides to promote sustainable agriculture. Global J. Environ. Sci. Manage., 11(3): 983-1000 **(18 pages)**.
Williams, T., (2023). Soil as an environmental reservoir for baculoviruses: persistence, dispersal and role in pest control. Soil Syst., 7(1): 29 **(23 pages)**.
Wilson, K.; Grzywacz, D.; Curcic, I.; Scoates, F.; Harper, K.; Rice, A.; Paul, N.; Dillon, A., (2020). A novel formulation technology for baculoviruses protects biopesticide from degradation by ultraviolet radiation. Sci. Rep., 10(1): 13301 **(10 pages)**.
Yadav, N.; Mudgal, D.; Anand, R.; Jindal, S.; Mishra, V., (2022). Recent development in nanoencapsulation and delivery of natural bioactives through chitosan scaffolds for various biological applications. Int. J. Biol. Macromol., 220: 537-572 **(36 pages)**.
Yanuhar, U.; Waheed, Z.; Suryanto, H.; Hasan, V.; Machfuda, D., (2025). Efficacy of zinc oxide chitosan hybrid nanoparticles as a nanovaccine to enhance immunity in hybrid grouper fish. Global J. Environ. Sci. Manage., 11(1): e731845 **(15 pages)**.
Zhang, B.H.; Zhan, Y.Y.; Gao, M.H.; Jia, Z.H.; Li, C.Y.; Chu, D.; Li, Q.; Zheng, G.L., (2025). Dual-shell microencapsulation enhances nucleopolyhedrovirus stability and insecticidal activity. Dig. J. Nanomater. Biostruct., 20(3) **(8 pages)**.

AUTHOR (S) BIOSKETCHES

Nanang Tri Haryadi, M.Sc, Associate Professor, Department of Agrotechnology, Faculty of Agriculture, University of Jember, Jember, Indonesia.
- Email: *haryadi.nt@unej.ac.id*
- ORCID: 0000-0002-0458-2752
- Web of Science ResearchID: HSA-7935-2023
- Scopus Author ID: 57224572333
- Homepage: https://scholar.google.com/citations?user=wSYdK_sAAAAJ&hl=en

Agus Wedi Pratama, Dr., Assistant Professor, Department of Agrotechnology, Faculty of Agriculture, University of Jember, Jember, Indonesia.
- Email: *aguswedi.p@unej.ac.id*
- ORCID: 0000-0002-0430-5771
- Web of Science ResearchID: GZH-3458-2022
- Scopus Author ID: 58672998500
- Homepage: https://scholar.google.co.id/citations?user=VrIZtL4AAAAJ&hl=id

Nilasari Dewi, M.Si, Assistant Professor, Department of Agrotechnology, Faculty of Agriculture, University of Jember, Jember, Indonesia.
- Email: *nilasaridewi@unej.ac.id*
- ORCID: 0000-0002-9640-0038
- Web of Science ResearchID: NA
- Scopus Author ID: 57778963800
- Homepage: https://scholar.google.com/citations?user=TjhRtfUAAAAJ&hl=en

Agung Sih Kurnianto, M.Li, Assistant Professor, Department of Agrotechnology, Faculty of Agriculture, University of Jember, Jember, Indonesia.
- Email: *agung.sih.kurnianto@unej.ac.id*
- ORCID: 0000-0003-0262-8267
- Web of Science ResearchID: NA
- Scopus Author ID: 57200044503
- Homepage: https://scholar.google.com/citations?user=ejkoguMAAAAJ&hl=en

Ahmad Ilham Tanzil, M.P, Assistant Professor, Department of Agrotechnology, Faculty of Agriculture, University of Jember, Jember, Indonesia.
- Email: *aitanzil@unej.ac.id*
- ORCID: 0000-0002-5523-3632
- Web of Science ResearchID: NA
- Scopus Author ID: 57930462600
- Homepage: https://scholar.google.com/citations?user=hPFf0e8AAAAJ&hl=id

HOW TO CITE THIS ARTICLE

Haryadi, N.T.; Pratama, A.W.; Dewi, N.; Kurnianto, A.S.; Tanzil, A.I., (2026). Environmental stability and ultra violet protection of Spodoptera litura nucleopolyhedrovirus encapsulated in chitosan nanoparticles. Global J. Environ. Sci. Manage., 12(1): 153-166.

DOI: 10.22034/gjesm.2026.01.09

URL: https://www.gjesm.net/article_732994.html

Global J. Environ. Sci. Manage. 12(1): 167-190, Winter 2026, Serial #45

Global Journal of Environmental Science and Management
(GJESM)

Homepage: https://www.gjesm.net/

Podcasts

ORIGINAL RESEARCH PAPER

Phylogenetic and conservation insights on local adaptations of Argiope modesta concerning ecological consequences

W.P.B. Putra[1], S. Utami[1], D. Hutapea[2,*], J. Kinho[1], Wakhid[1], W.C. Adinugroho[3], W. Darwiati[1], R. Agustarini[1], L. Andadari[1], A. Ismanto[1], B. Harjadi[4], Kayat[5], M.I. Maulana[6]

[1] *Research Center for Applied Zoology, National Research and Innovation Agency. Jl., Raya Jakarta-Bogor, Cibinong 16911, Bogor, West Java, Indonesia*

[2] *Research Center for Horticulture, National Research and Innovation Agency. Jl., Jakarta-Bogor, Cibinong 16911, Bogor, West Java, Indonesia*

[3] *Research Center for Ecology, National Research and Innovation Agency. Jl., Raya Jakarta-Bogor, Cibinong 16911, Bogor, West Java, Indonesia*

[4] *Research Center for Geological Disaster, National Research and Innovation Agency. Jl., Sangkuriang, Dago, Coblong, Kota Bandung 40135, West Java, Indonesia*

[5] *Research Center for Biota Systems, National Research and Innovation Agency. Jl., Raya Jakarta-Bogor, Cibinong 16911, Bogor, West Java, Indonesia*

[6] *Department of Biology, Faculty of Science, Institut Teknologi of Sumatra. Jl., Terusan Ryacudu, Way Huwi, Kec. Jati Agung, South Lampung 35365, Lampung, Indonesia*

ARTICLE INFO

Article History:
Received 19 August 2025
Revised 22 November 2025
Accepted 29 December 2025

Keywords:
Argiope modesta
biodiversity conservation
biological pest control
molecular dating analysis
polymorphic sites
sustainable agriculture

DOI: 10.22034/gjesm.2026.01.10

ABSTRACT

BACKGROUND AND OBJECTIVES: *Argiope modesta* is an ecologically important predatory spider that contributes to natural pest suppression in agricultural ecosystems. The global agricultural system is experiencing heightened pressure as the demand for food keeps escalating. Fulfilling this demand involves enhancing crop productivity while reducing environmental effects and protecting ecosystem integrity to promote long-term sustainability. The study objectives were to investigate the phylogenetic position of A. modesta using cytochrome c oxidase subunit I sequences, estimate divergence times and identify genetically distinct lineages within and among geographic populations.

METHODS: A total of eight specimens were obtained from shrubland environments located in Kebon Bambu Village, Bekasi Regency, West Java, Indonesia. Analysis using the basic local alignment search tool verified that 97 percent of the collected specimens corresponded to *Argiope modesta*.

FINDINGS: Within the Kebon Bambu population, seven polymorphic sites were identified. Phylogenetic reconstruction placed A. modesta in a clade closely related to A. aetherea. Comparison with sequences from Bali (Indonesia) and the Philippines revealed 27 polymorphic sites, indicating substantial geographic differentiation. Molecular dating suggests that the Kebon Bambu, Balinese, and Philippine populations diverged approximately 1.21 million years ago during the early Pleistocene (Calabrian stage). The Kebon Bambu lineage then experienced independent evolutionary progress during the Holocene. These findings indicate a possible genetic uniqueness of the Kebon Bambu population. However, the small sample size (n = 8) from a single locality limits robust conclusions about population-level genetic diversity and lineage distinctiveness. Preserving genetic diversity within species is vital for ensuring ecosystem resilience and for the success of biological pest management. The validated cytochrome c oxidase subunit i sequences provide a basis for long-term molecular monitoring using deoxyribonucleic acid barcoding.

CONCLUSION: The study reveals significant genetic differentiation in A. modesta, with the Kebon Bambu population forming a distinct cytochrome c oxidase subunit I-based lineage defined by unique polymorphic markers. This genetic individuality offers a groundwork for examining potential local adaptation. However, whether such variation translates into enhanced biological control or pest suppression remains unresolved. The combination of genomics, functional phenotyping, and field experiments in integrative studies is vital for supporting conservation prioritization.

This is an open access article under the CC BY license (http://creativecommons.org/licenses/by/4.0/).

NUMBER OF REFERENCES	NUMBER OF FIGURES	NUMBER OF TABLES
111	7	3

*Corresponding Author:
Email: *dedi026@brin.go.id*
Phone: ***
ORCID: ***

Note: Discussion period for this manuscript open until Mar 1, 2026 on GJESM website at the "Show Article".

INTRODUCTION

Global agricultural systems are under increasing pressure to meet rising food demands while minimizing environmental impacts and maintaining ecosystem integrity (Andrade *et al.,* 2020; Ramberg *et al.,* 2020; Jaworski *et al.,* 2023). Current intensive agricultural practices, defined by monocultures, the simplification of habitats, and significant pesticide application, have drastically changed the structure of agroecosystems, causing widespread decreases in arthropod diversity, which includes natural enemies that deliver crucial biological control services (Redlich *et al.,* 2018; Muneret *et al.,* 2019; Stavrianakis *et al.,* 2024). Although biological control accounts for an estimated 50–90 percent (%) of pest regulation in many agroecosystems (Anjos *et al.,* 2022; Zhou *et al.,* 2024), continued agricultural intensification is eroding the capacity of farmland to sustain diverse and effective predator communities. Furthermore, there is a growing emphasis on integrated pest management (IPM) approaches that foster predator diversity, habitat complexity, and ecological resilience are being increasingly highlighted to ensure the proper functioning of ecosystems and to minimize the use of synthetic pesticides (Queiroz and Gasnier, 2017; Hopfe *et al.,* 2024). Among arthropod predators, spiders are especially abundant and diverse and play a central role in regulating agricultural pests (Darimont *et al.,* 2023; Isaacs *et al.,* 2024). The orb-weaving spider *Argiope modesta* (Araneae: Araneidae) represents a cosmopolitan genus characterized by pronounced sexual dimorphism and conspicuous web decorations (stabilimenta), which are thought to enhance prey attraction and deter predators (Chaw *et al.,* 2014; Abel *et al.,* 2020). The *Argiope* species are acknowledged as proficient predators of herbivorous arthropods within rice and vegetable agroecosystems throughout Asia, targeting significant pests like leafhoppers, planthoppers, and leaf folders (Radermacher *et al.,* 2020; Mohapatra *et al.,* 2024). As sit-and-wait predators, orb-web spiders capture a broad spectrum of flying insects, thereby reducing pest abundance and potentially lowering pesticide inputs, with associated ecological, economic, and human health benefits (Berthet *et al.,* 2018; Tooker *et al.,* 2020; Jaworski *et al.,* 2023). Spiders, beyond their function as predators, are frequently viewed as sensitive bioindicators of environmental quality. Alterations in spider population, species diversity, or functional variety frequently indicate habitat deterioration, pollution, and heightened agricultural intensification (Graf *et al.,* 2020; Brooker *et al.,* 2023; Diyaolu and Folarin, 2024). Their capacity to accumulate pesticide residues further enables their use in monitoring agricultural contamination and evaluating the ecological consequences of pest management practices (Mezőfi *et al.,* 2020; Saqib *et al.,* 2021). Despite their ecological importance, however, the evolutionary history and phylogeographic structure of *A. modesta* populations remain poorly understood, particularly within the Sundaland Region (Bird *et al.,* 2005; Dankittipakul *et al.,* 2010). Sundaland's geological history presents a strong natural framework for evaluating hypotheses concerning the origins and preservation of tropical biodiversity (Heaney, 1991; Sheldon *et al.,* 2015). The Sunda Continental Shelf once connected many of the region's present-day islands, but repeated glacial–interglacial cycles during the Pleistocene caused periodic sea-level rise and landmass fragmentation beginning approximately 400,000 years ago (Husson *et al.,* 2020). These dynamics underpin the "Pleistocene pump" hypothesis, which posits that repeated cycles of population isolation and reconnection promoted diversification. However, accumulating molecular evidence challenges this framework. Studies on phylogenetics across a range of taxa, including Sundaland's arthropods, demonstrate that many populations experienced divergence during the Miocene to Pliocene periods, long before the marine inundation of the Pleistocene. This indicates that the phenomenon of diversification cannot be solely accounted for by recent marine barriers (Bird *et al.,* 2005; Hinckley *et al.,* 2020). Alternative explanations emphasize ecological isolation driven by terrestrial habitat change and fragmentation, which may have separated populations prior to physical isolation caused by rising sea levels (Lambin and Meyfroidt, 2010; Wang *et al.,* 2017; Curry *et al.,* 2020). The consequences of these historical processes probably vary across taxa, influenced by habitat specialization and dispersal capabilities. Furthermore, the comparatively elevated extinction rates observed in island populations, along with events of colonization or recolonization, have additionally influenced regional biogeographic patterns. These patterns are often difficult to detect due to taxonomic limitations, particularly in small-bodied organisms with restricted

geographic distributions (McKinney, 2008; Gardiner *et al.,* 2010; Ramberg *et al.,* 2020). Molecular phylogenetic and phylogeographic approaches provide powerful tools for elucidating population divergence, evolutionary relationships, and historical biogeographic patterns. Fossil-calibrated phylogenies based on mitochondrial markers, particularly cytochrome c oxidase subunit I (COI), have been widely applied to estimate divergence times and resolve species-level relationships in spiders, including *Argiope* (Wolz *et al.,* 2020; Sheffer *et al.,* 2021). The COI gene is particularly significant because of its conserved structure, high success rate in amplification, and robust phylogenetic signal, establishing it as a standard marker for deoxyribonucleic acid (DNA) barcoding and analyses at the population level (Luo *et al.,* 2014; Hernández-Triana *et al.,* 2019). Although reliance on a single mitochondrial locus provides only a partial view of evolutionary processes, COI remains an effective marker for establishing baseline phylogenetic frameworks, particularly in systems with limited genomic resources. To date, COI-based studies of *A. modesta* have focused on populations from Bali and the Philippines (Tan *et al.,* 2016), whereas populations from Java Island remain genetically uncharacterized. This highlights a significant deficiency in knowledge, considering Java's extensive history of agricultural intensification, considerable habitat alteration, and diminished landscape connectivity. Populations inhabiting intensively managed agroecosystems may experience strong selection pressures related to pesticide exposure, prey availability, and habitat fragmentation, potentially shaping microevolutionary trajectories over relatively short timescales. Accordingly, the present study focuses on *A. modesta* populations from Kebon Bambu Village, Java, Indonesia, a fragmented agro-urban landscape along the Kali Bekasi corridor, to elucidate their phylogenetic placement and evolutionary history within Sundaland. By providing baseline phylogeographic data for *A. modesta* in Indonesia, this study contributes essential evolutionary context for understanding the persistence and functional role of an important biological control agent in increasingly human-modified agricultural landscapes. This study seeks to define the phylogenetic positioning of *A. modesta* through the analysis of COI sequences, assess divergence timelines among geographic populations utilizing fossil-calibrated phylogenetic methods, and recognize genetically unique mitochondrial lineages both within and between populations. This study was conducted in the Kebon Bambu Village of Indonesia in 2025, where the samplings were performed and analyzed at the National Research and Innovation Agency (BRIN) of Indonesia for laboratory analysis.

MATERIALS AND METHODS

Study site

The study was conducted during the rainy season (February–April 2025) in Kebon Bambu Village, Bekasi Regency, West Java Province, Indonesia (Fig. 1). The study area is located at an elevation of 6–115 meters (m) above sea level and is characterized predominantly by alluvial soils. In accordance with Oldeman's climatic classification, the area is characterized by a temperate climate that includes seven months of precipitation and five months of dryness. The rainy season generally occurs from October to April, followed by a dry season from May to September. Data from Statistics Indonesia (BPS, 2025) indicate an average annual temperature of 28 degrees Celsius (°C), total annual rainfall of 1,767 millimetrs (mm), and approximately 84 rainy days per year. Kampung Kebon Bambu is a well-established horticultural production area, where crops such as long beans, chili peppers, tomatoes, eggplants, green beans, cucumbers, chayote, leafy vegetables, melons, watermelons, bananas, mangoes, and papayas are cultivated. The amount of cultivated land and the yields of crops have both diminished in recent years, primarily because of the swift conversion of land for residential development, road construction, and administrative infrastructure. This expansion has resulted in habitat loss and fragmentation, with potential consequences for the genetic diversity of organisms dependent on these agroecosystems. The study site was selected to evaluate the ecological function of small habitat patches formed by land fragmentation and their influence on the adaptability of the predatory spider *A. modesta*. This species frequently resides in landscapes altered by human activity, making it less susceptible to minor habitat fragmentation compared to more specialized taxa. Sampling efforts varied modestly among sites due to flooding in certain areas during periods of high rainfall, as well as logistical constraints. Persistent waterlogging in several study locations constrained

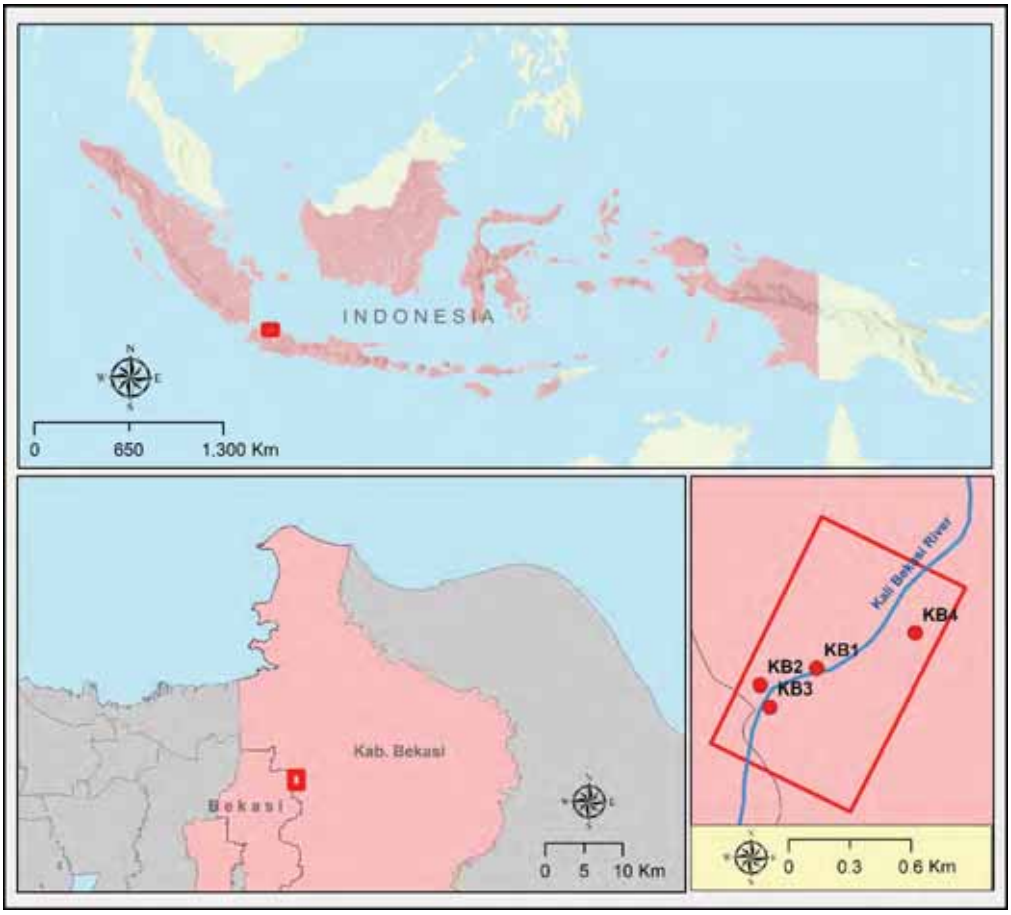

Fig. 1: Geographical location of the collect *Argiope modesta* samples at Kebon Bambu Village, Bekasi Regency, West Java, Indonesia

vegetation composition, thereby limiting food availability for arthropods. To mitigate possible bias in estimates of species diversity linked to environmental conditions in the rainy season, subsequent research should include sampling conducted during the dry season.

Collection of samples

Spider sampling was conducted using purposive sampling with a sweep net. Within each transect plot, the sweep net was swung 100 times, with the net having a diameter of 30 cm and an effective lateral reach of approximately 1 m on each side. Sampling was performed multiple times across different plots within each transect to optimize the representation of the local spider community. Although only eight spider specimens were collected, this limited sample size reflects the naturally low density and patchy distribution of the target species in the study area. All captured spiders were immediately preserved in vials containing 96% ethanol to maintain tissue integrity for subsequent genetic analyses. Specimens were later identified at the Entomology Laboratory of BRIN. Despite the small sample size limiting the potential for wide-ranging ecological generalizations or a complete understanding of population structure, these specimens yield initial insights into the genetic composition of the local population. Collection activities complied with Indonesian biodiversity regulations and were conducted with the consent of the local community. Future studies with expanded sampling are recommended to increase statistical power and more comprehensively assess genetic diversity. The general morphological characteristics

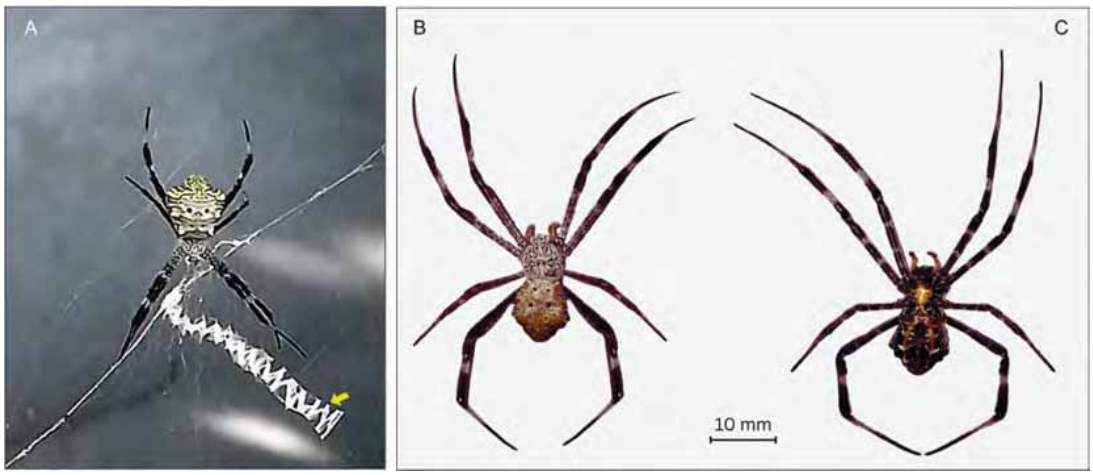

Fig. 2: A female *Argiope modesta* from Kebon Bambu Village on the web with a stabilimentum structure (arrow, A) and the illustration of a spider on dorsal (B) and ventral (C) positions

of *A. modesta* used as a reference for species identification are presented in Fig. 2.

Land-cover dynamics and vegetation indices

Land-cover dynamics were quantified for four focal plots (KB1–KB4), each corresponding to a genetically sampled population of *Argiope modesta*. Plots were delineated a priori based on habitat homogeneity and field accessibility, with circular buffers of 200–500 m radius centered on georeferenced spider collection sites to represent the local landscape matrix influencing each population. The assessment of landscape changes along the Kali Bekasi corridor was conducted over a 20-year timeframe (2006–2025) through the use of complementary spatial techniques. Structural land-cover change was documented through visual interpretation of high-resolution Google Earth imagery from 2006, 2015, and 2025, representing pre-disturbance, transitional, and contemporary landscape conditions. In order to ensure spatial consistency across the years, plot boundaries and spatial annotations were outlined and validated within a quantum geographic information system (QGIS). Vegetation and bare-soil dynamics were quantified using a continuous multispectral time series derived from Landsat 5 TM, Landsat 7 ETM+, Landsat 8 OLI, and Landsat 9 OLI-2 imagery (30 m resolution). All images were processed in the Google Earth Engine (GEE) environment, atmospherically corrected, and masked for clouds and cloud shadows using standard quality assessment (QA) bands. The application of sensor harmonization was conducted to maintain temporal consistency across different platforms. For each plot, annual mean composites of spectral indices were extracted within a 10-m buffer centered on spider sampling coordinates to capture fine-scale habitat conditions experienced by individuals. Vegetation greenness was quantified using the normalized difference vegetation index (NDVI), while surface exposure was assessed using the bare soil index (BSI). The annual average NDVI and BSI values were obtained for each plot, and linear regression was employed to assess long-term trends in vegetation cover and soil exposure. NDVI was derived to assess vegetation greenness using Eq. 1 (Huang *et al.,* 2021):

$$NDVI = \frac{Near\ Infrared\ (NIR) - Red}{NIR + Red} \quad (1)$$

Where; NIR corresponds to Band 4 (Landsat 5/7) or Band 5 (Landsat 8/9), and Red corresponds to Band 3 (Landsat 5/7) or Band 4 (Landsat 8/9). Higher NDVI values indicate denser or healthier vegetation. BSI was used to detect bare soil and built-up surfaces, using Eq. 2 (Rikimaru *et al.,* 2002):

$$BSI = \frac{(Red + SWIR) - (NIR + Blue)}{(Red + SWIR) + (NIR + Blue)} \quad (2)$$

Where; Blue corresponds to Band 1, Red to Band 3 or 4, NIR to Band 4 or 5, and Short Wave Infrared (SWIR) to Band 5/7 or Band 6 (depending on Landsat generation). Higher BSI values indicate increased

exposure of bare soil or impervious surfaces.

DNA extraction and COI amplification

Genomic DNA was extracted from spider leg tissue using the gSYNC™ DNA Extraction Kit (Geneaid Biotech Ltd., Taiwan) following the manufacturer's protocol. The extracted DNA had a purity ratio of 1.56 (Lambda (λ) 260/λ280) and a concentration of 31.58 nanograms (ng)/microliters (µL), measured using a NanoPhotometer (IMPLEN, Germany). The COI region was amplified in a 30 µL of total PCR reaction containing 9 µL of DNA template, 15 µL of PCR master mix, 0.60 µL of each primer, and 4.80 µL of nuclease-free water. The universal primer pair LCO1490 (5'-GGT CAA CAA ATC ATA AAG ATA TTG G-3') and HCO2198 (5'-TAA ACT TCA GGG TGA CCA AAA AAT CA-3') was used to amplify a ~710 base pair (bp) fragment of the COI gene. PCR amplification conditions consisted of an initial denaturation at 94°C for 5 minutes (min.); followed by 36 cycles of denaturation at 94°C for 1 min, annealing at 50.1°C for 30 second (s), and extension at 72°C for 1 min 30 s; and a final extension at 72°C for 7 min.

Electrophoresis

The electrophoresis was performed on 1% agarose gel (Vivantis, Malaysia) with 2 µL FloroSave DNA Stain (1st BASE, Malaysia). The electrophoresis process was executed on 100 V for 30 min using TAE 1× medium; 5 µL of PCR product per sample and 3 µL of 100 bp DNA ladder (Thermo Fisher Scientific, USA). Therefore, the DNA visualization was performed using G-box Documentation (UVITEC, UK).

Sequencing and species detection

The forward sequencing analysis was performed by Apical Scientific (Malaysia) laboratory. Thus, the COI sequence of each spider was used for BLAST analysis for the species identification. According to BLAST analysis, about 97% of spiders under study was identified as *A. modesta*. In addition, the COI sequences of *A. modesta* under study were deposited in the National Center for Biotechnology Information (NCBI) database (GenBank: LC896932 - LC896939).

Genetic diversity and Phylogeny analysis

The genetic diversity parameters of haplotype diversity (Hd), nucleotide diversity (pi), Fu's Fs statistics and Tajima's D test values were computed with DnaSP package (Librado and Rozas, 2009). A MEGA 12 package (Hall, 2013) was used to construct the phylogenetic tree using the Maximum-Likelihood method and the Hasegawa–Kishino–Yano (HKY) + G5 + I model (Hasegawa *et al,*. 1985) was selected as the best-fit nucleotide substitution model because it has lowest BIC score based on the Find Best DNA/Protein Models tool (Nei and Kumar, 2000) in Molecular Evolutionary Genetics Analysis (MEGA) 11 (Tamura *et al.,* 2021). The phylogenetic tree was constructed with 1000 × bootstrap replications. Several COI sequences of *Argiope* genera from NCBI database were involved in the phylogenetic tree analysis such as *A. modesta* from Philippines (KJ957977) and Bali-Indonesia (KU055792), *A. aetherea* (KJ957939), *A. aetheroides* (KJ957940), *A. dang* (KJ957960), *A. jinghongensis* (KJ957967), *A. katherina* (KJ967958), *A. keyserlingi* (KJ957969), *A. macrochoera* (KJ9579973), *A. mascordi* (KJ957975), *A. minuta* (KJ957976), *A. pulchella* (KJ957984), *A. radon* (KJ957985), and *A. versicolor* (KJ957991).

Molecular dating analysis

In the context of divergence-time analysis, a single COI sequence of *A. trifasciata* (DQ127339.1) was incorporated as an outgroup, in addition to the sample sequences and 14 supplementary COI sequences acquired from NCBI. All mitochondrial cytochrome c oxidase subunit I (MT-COI) sequences were aligned using MEGA 11 (Tamura *et al.,* 2021). After alignment and trimming, a final dataset of 23 sequences, approximately 297 bp in length, was used for analysis. To ascertain evolutionary lineage, a Maximum Likelihood phylogenetic tree was built. The Hasegawa–Kishino–Yano (HKY) + G5 + I model was selected as the best-fit nucleotide substitution model based on the Find Best DNA/Protein Models tool (Nei and Kumar, 2000) in molecular evolutionary genetics analysis (MEGA) 11 (Tamura *et al.,* 2021). Divergence times were estimated in Bayesian evolutionary analysis by sampling trees (BEAST) using Bayesian evolutionary analysis utility (BEAUTi) and BEAST v2.x (Bouckaert et al., 2019; Bouckaert, 2022) under a strict molecular clock model (Douglas *et al.,* 2021). A calibrated Yule speciation model (Heled and Drummond, 2012) was utilized to pinpoint distinct divergence points among species. For time calibration, we used the estimated divergence of *A. trifasciata* at 5.13 Mya (95% highest posterior density (HPD): 6.33–3.90 Mya) (Abel *et al.,*

2020). The selection of this molecular estimate is based on the fact that thorough studies on divergence times within the *Argiope* genus are few, especially concerning the Southeast Asian clades. Fossil records directly attributable to *Argiope* are currently lacking, precluding reliable fossil-based calibration. The posterior tree distribution generated by BEAST was summarized using TreeAnnotator to produce a maximum clade credibility (MCC) tree with mean node heights and posterior probabilities for each clade. The evaluation of convergence and sampling performance was conducted using Tracer v1.7.2, which confirmed the effective sampling of the posterior. The effective sample size (ESS) values surpassed 200 for all significant parameters, such as clock rate and tree topology. Stratigraphic information was subsequently added to the final BEAST output using R version 4.4.2.

RESULTS AND DISCUSSION

COI amplification and polymorphic sites

A ~710 bp fragment of the mitochondrial COI gene of *A. modesta* was successfully amplified in all samples using the universal primers LCO1490 and HCO2198 (Fig. 3). Within the individuals obtained from KB Village, seven separate COI haplotypes were identified (Table 1). Haplotype diversity (Hd) was high (0.96 ± 0.08), whereas nucleotide diversity (π) was low (0.005 ± 0.001), with five polymorphic sites detected across the sampled individuals. Both Tajima's D and Fu's Fs neutrality tests yielded negative values. The pairing of elevated Hd and reduced π aligns with the notion of population growth originating from a restricted ancestral group; however, the limited sample size (n = 8) restricts accuracy, as indicated by the standard errors. This pattern does not indicate adaptive or functional divergence. The five polymorphic sites in the KB population may represent selectively neutral variation from drift, adaptive variation influenced by local selection, or neutral markers linked to adaptive nuclear variation. To ascertain their phenotypic or ecological influences, it is essential to conduct direct functional studies that extend beyond sequence

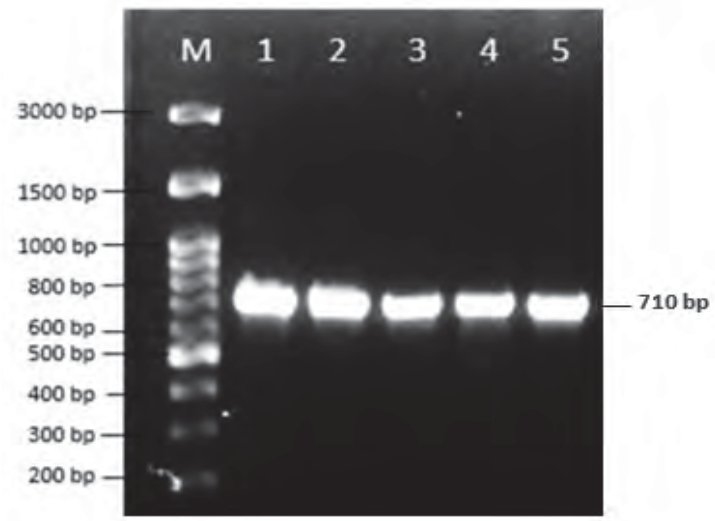

Fig. 3: Amplification of the COI region of *Argiope modesta* on 1% agarose gel. M: DNA ladder 100 bp; Line 1-5: DNA samples

Table 1: Genetic diversity in COI sequence of *Argiope modesta*

Parameters	Value
Number of sites	659
Number of polymorphic sites	9
Number of haplotypes	7
Haplotype diversity (Hd)	0.96±0.08
Nucleotide diversity (p_i)	0.005±0.001
Fu's Fs statistic	-0.46
Tajima's D test	-0.51

Table 2: Detection of polymorphic sites in the COI sequence of *Argiope modesta*

Specimen (GenBank)	Nucleotide position*																										
	307	**316**	**328**	**340**	**352**	**355**	**364**	**373**	**382**	**433**	**466**	**496**	**562**	**619**	**622**	**631**	**670**	**673**	**675**	**676**	**677**	**678**	**679**	**ins**	**680**	**685**	**687**
A. modesta Philippines (KJ957977)	A	A	G	T	C	A	T	G	T	T	G	T	A	T	G	G	A	T	C	T	G	A	G	-	G	T	T
A. modesta Bali (KU055792)	T	T	A	T	A	G	C	T	T	T	A	C	T	T	A	A	A	T	C	T	G	A	G	-	G	T	T
A. modesta KB1 (LC896932)	A	T	A	C	A	A	C	T	T	C	G	T	T	C	A	A	T	C	C	T	G	G	A	A	G	A	A
A. modesta KB2 (LC896933)	A	T	A	C	A	A	C	T	T	C	G	T	T	C	A	A	T	C	G	G	A	G	A	A	A	A	A
A. modesta KB4 (LC896934)	A	T	A	T	A	A	C	T	T	C	G	T	T	C	A	A	T	C	G	G	G	A	G	A	A	A	A
A. modesta KB6 (LC896935)	A	T	A	C	A	A	C	T	T	C	G	T	T	C	A	A	T	C	G	G	G	A	A	A	A	A	A
A. modesta KB7 (LC896936)	A	T	A	T	A	A	C	T	T	C	G	T	T	C	A	A	T	C	G	G	G	A	A	A	A	A	A
A. modesta KB8 (LC896937)	A	T	A	C	A	A	C	T	T	C	G	T	T	C	A	A	T	C	G	G	G	A	A	A	A	A	A
A. modesta KB9 (LC896938)	A	T	A	T	A	A	C	T	A	C	G	T	T	C	A	A	T	C	G	G	G	A	A	A	A	A	A
A. modesta KB10 ((LC896932)	A	T	A	T	A	A	C	T	T	C	G	T	T	C	A	A	T	C	G	G	G	A	G	A	A	A	A

*GenBank: KJ957977; ins: insertion

data. According to Nei and Kumar (2000), Hd values above 0.50 indicate substantial haplotypic richness, while π values below 0.01 reflect low nucleotide divergence. In summary, these metrics imply that, notwithstanding the presence of multiple haplotypes, genetic differentiation among individuals is relatively minimal at the nucleotide level.

Negative Tajima's D and Fu's Fs values further support this interpretation, as such neutrality statistics typically indicate an excess of rare mutations arising during rapid population growth following a bottleneck or selective sweep (Ashfaq *et al.,* 2014). This demographic context corresponds with the recent variation of haplotypes, characterized by a lack of considerable sequence divergence. The five polymorphic sites detected within the KB population may represent selectively neutral variation shaped by genetic drift, adaptive variation driven by local selective pressures, or neutral mitochondrial markers linked to adaptive nuclear genetic variation. Nevertheless, mitochondrial COI data by itself is insufficient to determine if these variants confer functional or ecological differentiation. Consequently, potential effects on phenotypic traits or biological control efficacy cannot be inferred without complementary functional, ecological, or nuclear genomic analyses. The COI-based genetic framework of *A. modesta* implies a recent increase in population size and considerable haplotypic diversity, yet it reveals restricted nucleotide divergence, pointing to demographic factors instead of adaptive processes.

The sequencing analysis revealed that the COI sequence of *A. modesta* consists of 26.19±0.14% of A; 14.40±0.10% of C; 18.40±0.07% of G, and 41.01±0.07% of T nucleotides. In this study, the composition of T nucleotide in the COI sequence of *A. modesta* was the highest and similar to *A. pulchella* (41.22±0.16%) and *A. trifasciata* (42.92±0.09) (Ashraaf *et al.,* 2019). Total of 27 polymorphic sites were detected in the COI sequence among *A. modesta* from Kebon Bambu, Philippines and Bali (Table 2). As indicated in Table 2, five polymorphic sites located at the 619th, 670th, 673rd, 685th, and 687th nucleotides have been identified as the specific genetic markers for *A. modesta* originating from KB Village. While, seven polymorphic sites at 340th, 382th, 676th, 677th, 678th, 679th and 680th nucleotides were observed among *A. modesta* under study. Moreover, an insertion site was found in *A. modesta* under study between 679th and 680th nucleotide. Abel *et al.,* (2020) obtained 26 polymorphic sites in *A. trifasciata* and close to the present study. Species genetic

Table 3: Pairwise genetic distance among COI haplotype of *Argiope modesta*

Haplotype	2	3	4	5	6	7
1	0.006	0.009	0.006	0.009	0.009	0.011
2	-	0.006	0.003	0.006	0.006	0.008
3	-	-	0.003	0.003	0.003	0.002
4	-	-	-	0.003	0.003	0.005
5	-	-	-	-	0.003	0.002
6	-	-	-	-	-	0.005

diversity can arise from various factors including migration, isolated geographical area, inbreeding and hybridization (Falconer and Mackay, 1996). In spider, the case of hybridization occurred among *Tegenaria* genera (Araneae: Agelenidae) groups of *T. atrica, T. saeva* and *T. gigantea* (Croucher *et al.,* 2007).

Pairwise genetic distances among the COI haplotypes of *A. modesta* ranged from 0.002 to 0.011 (Table 3). The smallest genetic distance was observed between haplotypes H7–H3 and H7–H5, whereas the greatest distance occurred between H7–H1. Variation in pairwise genetic distances can arise from factors including geographic separation, hybridization, or inbreeding (Stelkens and Seehausen, 2009). This study demonstrated that there is a shift in vegetation cover within the research area, which will be elaborated upon in the subsequent parts. The sampling location of *A. modesta* in this study has reduced vegetation cover compared to 10 and 20 years ago. Where there has been habitat fragmentation at the sampling site, the vegetation cover or niche area is reduced so that connectivity between *A. modesta* habitats is limited. It is believed that this may be one of the factors contributing to *A. modesta's* adaptation to its environment, which is marked by the existence of genetic mutation points as illustrated in Table 2.

Phylogenetic tree

The phylogenetic tree of *Argiope* genera spiders was illustrated in Fig. 4. According to Fig. 4, *A. modesta* and *A. aetherea* are classified in the same cluster. While, *A. radon*, *A. keyserlingi*, *A. mascordi*, *A. katherina*, *A. minuta*, *A. aetheroides*, *A. jinghongensis*, *A. macrochoera*, *A. pulchella*, and *A. versicolor* are classified in the same cluster. Lastly, both *A. dang* and *A. trifasciata* are separated into distinct position with *A. trifasciata* act as outgroup. In particular, *A. modesta* from KB village was designated distinctly as the Kebon Bambu (KB) lineage. In general, *Nephila* sp., *Hypsosinga* sp. and *Araneus* sp. are the close species of *Argiope* sp. based on mitochondrial genome (Ding *et al.,* 2023). Despite this, the genetic distance *Leucauge* sp. and *Trichonephila* sp. were closer to *Argiope* sp. than *Nephila* sp. based on COI sequence (Phom and Somasundaram, 2024; Jalajakshi and Usha, 2019). Therefore, *Cyrtophora* sp., *Bijoaraneus* sp., *Eriovixia* sp. and *Anepsion* sp. are classified as closely related species of *Argiope* sp. based on COI sequence (Jayasree and Santhi, 2023). According to the combination sequences [COI, cytochrome c oxidase subunit II (COII), H3A)], *A. modesta, A. dang* and *A. mangal* were characterized as Subclade A1. While, *A. hoiseni, A. pulchella, A. jinghongensis* and *A. versicolor* were characterized as Subclade A2. Additionally, *A. catenulata, A. aemula, A. chloreis* and *A. doleschalli* were characterized as Clade B (Tan *et al.,* 2016; Tan, 2018). In general, spiders of the *Argiope* genus were classified in Clade A or Asian clade (*A. versicolor, A. hoiseni, A. jinghongensis, A. aetheroides, A. pulchella, A. doleschalli, A. mascordi, A. keyserlingi, A. katherina, A. dang, A. radon, A. picta, A. modesta, A. mangal, A. reinwardti, A. anasuja, A. chloreis, A. chloreides, A. aemula, A. catenulata*), Clade B or Indo-Pacific clade (*A. ocyaloides, A. ranomafanensis*), Clade C or African clade (*A. australis, A. ahngeri, A. trifaciata, A. flavifalpis, A. levii*) and Clade D or American clade (*A. submaronica, A. blanda, A. argentata*) based on combination of 16s-rRNA, 18s-rRNA, COI, COII and H3A sequences (Tan *et al.,* 2019). The *A. modesta* under study is classified to KB-clade. Basicly, *A. modesta* from KB, Philippines and Bali are related because since 2 Mya these regions were merged and known as Sundaland. This assertion is backed by Dankittipakul *et al*. (2010), which indicated the close genetic relationship of *Mallinella* sp. (Araneae: Zodariidae) across multiple areas in Sundaland of Indonesia.

Molecular dating

Molecular dating analyses indicate that *Argiope*

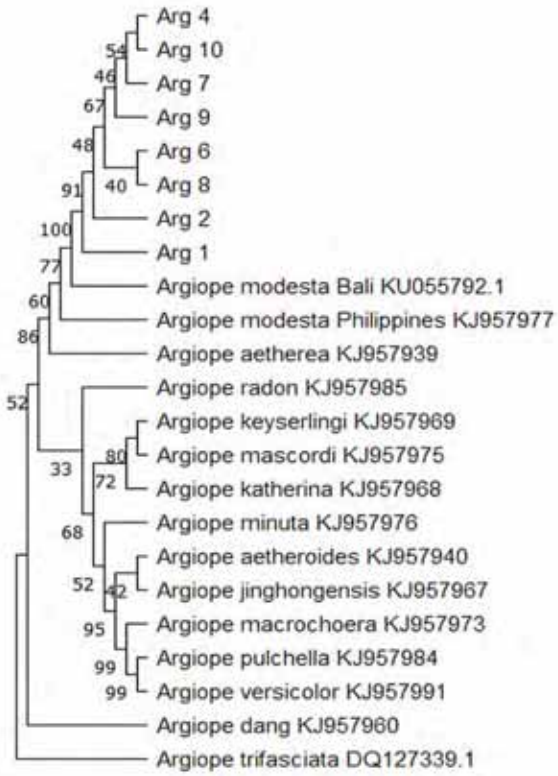

Fig. 4: Phylogenetic tree of *Argiope* genera spiders based on mitochondrial COI sequence

trifasciata, the earliest-diverging taxon within the genus *Argiope*, split from other congeners at approximately 6.22 Mya during the Late Miocene. Around 4.85 Mya, a major diversification event occurred, resulting in the establishment of multiple unique *Argiope* clades. This diversification coincides temporally with repeated glacial–interglacial cycles that shaped the extent of Sundaland, which periodically functioned as a broad land bridge facilitating faunal dispersal across Southeast Asia (Woodruff, 2010). Within this evolutionary framework, *A. aetherea* diverged from *A. modesta* at approximately 2.29 Mya in the early Pleistocene. Despite this divergence, both species currently occur sympatrically in Indonesia (Kerr, 2018), indicating that speciation was probably influenced more by behavioral isolation or reproductive barriers than by significant geological vicariance events. Phylogeographic analysis further revealed that *A. modesta* individuals from KB Village (West Java) are genetically closer to populations from Bali than to those from the Philippines. The divergence of the Bali and Philippine populations took place roughly 1.21 Mya, coinciding with the early Pleistocene period. This pattern suggests a southward dispersal of Philippine populations through Sundaland, potentially via Borneo, prior to the interglacial sea-level rise, which fragmented land connections. Despite Java being a component of Sundaland, vast savanna landscapes prevailed in the area during periods of glacial maxima (Heaney, 1991; Bird *et al.,* 2005; Husson *et al.,* 2020). Such open habitats may have facilitated the dispersal of *Argiope*, which are not strictly forest-dependent. During the last interglacial period (approximately 130–115 kya), rising sea levels separated Java and Bali, coinciding with the re-establishment of dense forest cover in Java. Subsequent cooling between ~110 and 11.7 kya caused sea levels to fall, reconnecting the islands and allowing *A. modesta* populations from Bali to disperse into Java. The anticipated divergence between the KB and Bali populations, estimated to be ~9.6 kya, based on COI sequences, probably signifies isolation subsequent to the end of the last glacial period, rather than representing a distinct speciation event.

Divergence time estimates based on part of mitochondrial sequences are subject to several sources of uncertainty. First, molecular clock rates in spiders can vary by two- to threefold due to differences in generation time, metabolic rate, and life-history traits. The presumption of a consistent substitution rate among lineages may consequently oversimplify the actual rate heterogeneity; relaxed clock models would more effectively account for this variability. Second, the sole calibration point (*A. trifasciata* at 5.13 Mya; 95% HPD: 3.90–6.33 Mya) is itself derived from molecular estimates and carries inherent uncertainty. Any proportional error present in this calibration directly influences all inferred divergence times. Third, the COI alignment used for dating was relatively short (710 bp), slightly above the commonly recommended minimum of 500 bp, limiting temporal resolution—particularly for recent population-level divergences. Consequently, divergence estimates such as the KB–Bali split should be interpreted as approximate temporal sequences rather than precise chronological dates. Finally, no formal sensitivity analyses were executed to evaluate the reliability of divergence estimates under various calibrations or clock models. Considering these limitations, genus-level divergences are deemed the most trustworthy, species-level divisions are moderately robust, and population-level divergence times the least certain. More accurate temporal inference will require multilocus or genomic datasets, multiple independent calibration points, and comprehensive sensitivity analyses.

Integration of phylogenetic insights into agroecosystem management

Phylogenetic information plays an essential role in designing effective agroecosystem management and biodiversity conservation strategies. This study provides two key findings: 1) the phylogenetic divergence patterns of *A. modesta*, and 2) the estimated timing of its population divergence. The resilience of species confronted with environmental changes, including climate variability and agricultural intensification, is fundamentally supported by genetic diversity. High levels of genetic diversity within populations enhance adaptive capacity, enabling species to respond to shifting conditions while maintaining ecosystem functions (Matevski *et al.,* 2024). Furthermore, functional diversity, which encompasses the range of traits among species that impact ecosystem processes, is essential for maintaining ecosystem stability and resilience, beyond just genetic variation. By ensuring that different species perform complementary ecological roles, functional diversity buffers against environmental changes and sustains ecosystem functioning (Hopfe *et al.,* 2024). Together, these findings offer valuable guidance for predator conservation and sustainable agricultural practices in West Java and Southeast Asia (Hu *et al.,* 2021; Saqib *et al.,* 2024). Genetic and geographic differentiation among *A. modesta* populations indicates ongoing evolutionary divergence shaped by local agroecosystem conditions (Philpott *et al.,* 2020). Such divergence emphasizes the unique adaptations of populations to environmental challenges, which encompass variability, pesticide exposure, and habitat fragmentation (Linck *et al.,* 2021; Nayak *et al.,* 2024). Acknowledging these localized adaptations is essential for making evidence-based management decisions, especially when pinpointing predator populations that play a significant role in natural pest control within contemporary agricultural environments (Twining *et al.,* 2022; Mohapatra *et al.,* 2024). The estimated divergence times provide further insight into how evolutionary processes occur on ecologically relevant timescales. Divergence equivalent to tens to hundreds of generations suggests that predator–prey dynamics and associated ecosystem services can shift relatively quickly in response to intensified agriculture, habitat loss, and other environmental drivers (Andrade *et al.,* 2020; Yasuhara *et al.,* 2020). Comprehending these temporal patterns facilitates in forecasting the potential responses of *A. modesta* populations to new agricultural challenges, including pest resistance and variations in the efficacy of biological control agents (Almeida *et al.,* 2021; Sheffer *et al.,* 2021). Integrating phylogenetic results with existing agroecosystem monitoring frameworks such as the widely adopted IPM and farmer field school (FFS) programs in West Java can strengthen decision-making by emphasizing the ecological role of natural enemies (Luther *et al.,* 2018). Molecular data assist in identifying unique genetic lineages that might have unrecognized adaptations to disease pressures, prey traits, or microhabitat conditions (Agnarsson *et al.,* 2016). These insights can guide the designation of conservation areas, habitat refugia, and landscape-level strategies aimed at preserving adaptive diversity

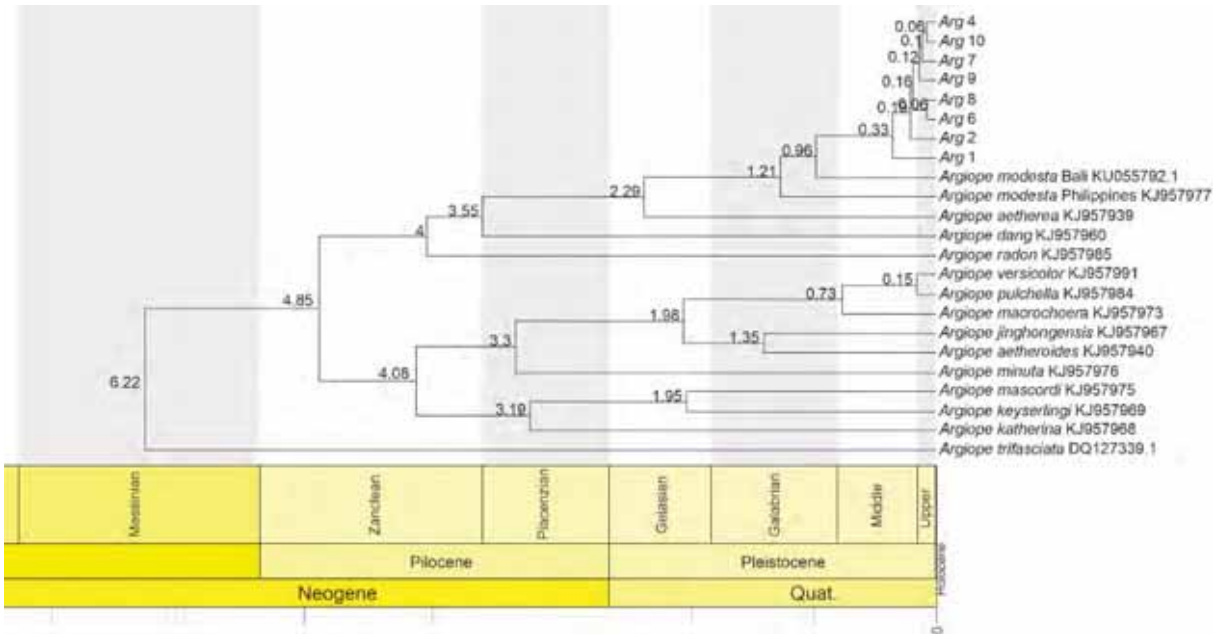

Fig. 5: Molecular dating of *Argiope* spp.

(Brüniche-Olsen *et al.,* 2021; Liu *et al.,* 2024). Overall, incorporating phylogenetic and molecular dating results into agricultural landscape management allows more accurate predictions of ecosystem resilience and supports proactive strategies that balance productivity with the conservation of predator genetic diversity, an essential foundation for long-term pest suppression (Wannigama *et al.,* 2023; Altieri *et al.,* 2024).

Genetic peculiarities as a conservation priority

Phylogenetic analyses reveal that the *A. modesta* population from KB forms a distinct clade separate from the populations in Bali and the Philippines. The KB lineage seems to have experienced independent evolutionary progress, as evidenced by the existence of five distinct polymorphic sites in the COI gene (positions 619, 670, 673, 685, and 687) that are absent in other regional populations (Schrempf *et al.,* 2019). Molecular dating indicates that the deeper divergence between the Bali–Philippines lineage and other populations occurred during the early Pleistocene (~1.21 Mya), while the more recent split between the KB and Balinese populations likely took place during the Holocene, approximately 3.3 Kya. These findings have direct implications for conservation planning. High genetic diversity plays a crucial role in the adaptive potential of predator populations, consequently increasing their efficacy in biological control programs. For instance, studies on *Chrysoperla externa* and *Hydrochara affinis* have demonstrated high genetic diversity using COI markers, underscoring their suitability for pest management initiatives (Barbosa *et al.,* 2014; Fernandez-Fournier *et al.,* 2021). Frequent monitoring of genetic variation via COI markers is necessary for recognizing initial signs of genetic erosion. Populations exhibiting high genetic distinctiveness, such as the KB population, should receive priority because they contain unique allelic combinations and represent irreplaceable evolutionary trajectories (Paz-Vinas *et al.,* 2018; Fernandez-Fournier *et al.,* 2021). The distinct polymorphic sites and unique nucleotide variants found in the KB population are vital for promoting intraspecific genetic diversity, an essential factor for preserving adaptive potential. Intraspecific genetic variation enhances ecosystem resilience and supports species' capacity to adapt to environmental changes, including climate variability, habitat disturbance, and shifts in agroecosystem dynamics (Des Roches *et al.,* 2021). Furthermore, it is vital to uphold such diversity to support the sustained effectiveness of *A. modesta*

as a biological control agent in agricultural settings (Michalko *et al.,* 2018; Diyaolu and Folarin, 2024). By recognizing the KB lineage as genetically unique, management strategies can better target habitat protection and enhancement efforts to ensure that these distinct predator populations continue contributing to sustainable pest control services within regional agroecosystems.

Local adaptation of A. modesta in relation to landscape transformation

During the study period, persistent rainfall combined with overflow of the Kali Bekasi resulted in waterlogging at several sampling sites. These circumstances probably limited the activity of arthropods and diminished the overall diversity of the community, which includes *A. modesta*. Excessive soil moisture is known to disrupt foraging behavior, web construction, and prey availability in many arthropod taxa, particularly among active, web-building predators. Moreover, rainfall has been shown to exert a strong negative effect on spider activity levels and population abundance (Uetz, 1991; Queiroz and Gasnier, 2017; Hopfe *et al.,* 2024). Simultaneously, significant land transformation for residential projects, office buildings, and roadway infrastructure has greatly diminished habitat quality throughout the study region. The combined effects of short-term climatic stress and long-term anthropogenic land-use change are therefore considered primary drivers of the low abundance of *A. modesta* recorded in this study, with only eight individuals captured across all sites. Vegetation diversity and structural heterogeneity are widely recognized as key determinants of animal species richness in agricultural and peri-urban landscapes, especially for arthropods that depend on vegetation for prey resources, habitat structure, and microclimatic buffering (Benton *et al.,* 2003; Tews *et al.,* 2004). The complexity of vegetation, when increased, improves niche availability and accommodates a more diverse array of arthropod functional groups, such as herbivores, detritivores, and predators (Tscharntke *et al.,* 2005; Queiroz and Gasnier, 2017). Spiders are particularly sensitive to vegetation architecture, as plant structure directly influences web placement, stability, and prey-capture efficiency (Uetz, 1991; Ramberg *et al.,* 2020). Consequently, vegetation simplification resulting from urban expansion and surface sealing is expected to disproportionately reduce spider abundance and diversity. Spiders form one of the most prevalent and ecologically crucial predator groups in agricultural ecosystems, significantly aiding in the natural management of pest populations. Recent global estimates suggest that spiders collectively consume more than three trillion prey items annually in farmland systems, highlighting their central role in trophic dynamics (Hopfe *et al.,* 2024; Cardoso *et al.,* 2025). Within this framework, the genus *Argiope* is notable for its behavioral plasticity, prey specialization, and the potential for local adaptation driven by genetic diversity. The genetic diversity present locally in biological control agents is essential for augmenting their ecological effectiveness. High levels of genetic variation are essential for enabling biological control agents to adapt to diverse environmental conditions and host genotypes, thereby ensuring effective pest suppression (Brunnet, 2000; Kerr, 2018; Goel *et al.,* 2025). Molecular evidence indicates that populations within the *Argiope* lineage, including *A. modesta*, have followed largely independent evolutionary trajectories since the Holocene, approximately 3,300 years ago (Woodruff, 2010). This evolutionary timeframe is ample for the gathering of locally adaptive genetic variants linked to prey-capture efficiency, adaptability to local climate conditions, and web-building techniques refined for specific regional vegetation frameworks. Empirical evidence further demonstrates that predator populations with higher genetic diversity tend to provide more effective and resilient pest suppression than genetically homogeneous populations (Bosco *et al.,* 2023; Zhou *et al.,* 2024). Furthermore, natural enemy populations that are locally adapted frequently provide more stable and reliable biological control services compared to introduced or non-native species (Jeanneret *et al.,* 2022). In this context, the genetic characteristics of *A. modesta* populations from the Kali Bekasi (KB) area likely reflect a long-established, locally adapted predator assemblage with potential importance for suppressing locally prevalent agricultural pest species. Fig. 6 illustrates major landscape transformations across the four observation plots (KB1–KB4) along the Kali Bekasi corridor between 2006 and 2025. In 2006, the landscape was defined by a varied mosaic of riparian vegetation, agricultural fields, and peri-urban



Fig. 6: 2006 to 2025 land cover in the plot observation (KB1, KB2, KB3, KB4)

open areas, which is characteristic of transitional agroecosystems in rapidly developing regions (Lambin and Meyfroidt, 2010). By 2015, accelerated urban expansion and infrastructure development had substantially reduced green-space continuity, resulting in increased habitat fragmentation and landscape homogenization. By 2025, dense residential and commercial structures dominated much of the area, leaving only small, isolated vegetation patches. Among the four sites, KB4 maintains the most uninterrupted and structurally intricate vegetation cover, probably owing to its closeness to the remaining riparian green corridor. In contrast, KB1, KB2, and KB3 exhibit pronounced urban encroachment, extensive surface sealing, and markedly reduced vegetation cover. Such spatial gradients in habitat structure and connectivity are well known to influence arthropod abundance and community composition by altering microclimatic conditions, prey availability, and the persistence of vegetation-mediated refugia (McKinney, 2008; Gardiner *et al.,* 2010; Ramberg *et al*, 2020). The alterations at the landscape level offer a credible rationale for the observed scarcity of *A. modesta* in this study, highlighting the susceptibility of specialized predator taxa to swift urbanization in peri-urban agroecosystems.

NDVI and BSI trends (Fig. 7) further highlight the ecological divergence among the sites. KB1 shows moderate NDVI fluctuations with a slight long-term decline and consistently low BSI, indicating gradual but steady vegetation loss. KB2 exhibits stable but low NDVI coupled with high BSI variability, reflecting episodic disturbances without substantial vegetation recovery. KB3 indicates a gradual ecological recovery, as evidenced by rising NDVI and decreasing BSI. KB4 displays the strongest positive trajectory, with high and rising NDVI and consistently low BSI, confirming the presence of stable, high-quality vegetation. Collectively, these patterns reveal a progression from declining vegetation (KB1), persistently low-cover conditions (KB2), and gradual recovery (KB3) to stable, resource-rich habitat (KB4). This gradient corresponds with wider ecological principles that demonstrate how habitat heterogeneity and the continuity of vegetation improve the stability of arthropod communities, particularly among predatory taxa such as spiders (Landis, 2017; Rusch *et al*., 2016).

Riparian and semi-natural vegetation corridors such as those still present around KB4 function as biodiversity reservoirs that support higher arthropod richness and trophic complexity (Uetz, 1991; Tews *et al.,* 2004). Conversely, urbanized locations characterized by sparse vegetation tend to display lower levels of arthropod diversity, primarily because of restricted prey availability, a

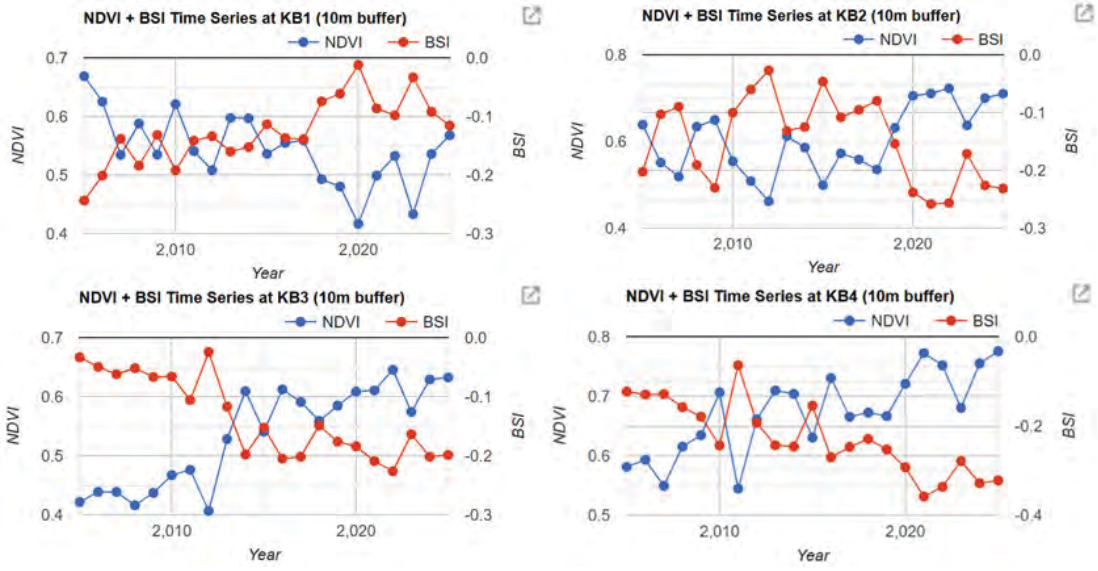

Fig. 7: 2005 to 2025 NDVI and BSI time series in the plot observation (KB1, KB2, KB3, KB4)

reduction in web-building structures, and harsher microclimatic conditions (Jones and Leather, 2012; Hopfe *et al.,* 2024). The spatial patterns of vegetation transformation and habitat heterogeneity provide insight into the local adaptation potential of *A. modesta*. Well-vegetated environments such as KB4 likely support stronger selective pressures for traits related to web architecture, prey specialization, and tolerance to microclimatic variability. Conversely, populations in more urbanized sites (KB1–KB3) may experience selection pressures associated with habitat fragmentation, reduced prey biomass, and altered thermal regimes. Considering the extended duration of residence and the genetic uniqueness of KB *A. modesta* populations, it is reasonable to assume that these spiders have developed locally beneficial traits that improve their ecological effectiveness within the agricultural landscape of West Java. Such local adaptation, combined with the stabilizing effects of heterogeneous vegetation, underscores the importance of conserving riparian and semi-natural habitats within rapidly urbanizing regions to sustain ecologically important predator populations.

Biodiversity monitoring and ecosystem service assessment

The DNA barcoding approach employed in this study, based on mitochondrial COI sequences, provides a robust framework for species identification and phylogenetic inference in *A. modesta*. This strategy further reinforces current biodiversity monitoring systems that can be applied in agricultural environments (Littlefair *et al.,* 2016). When integrated into DNA metabarcoding workflows, combining bulk arthropod sampling with high-throughput sequencing, COI markers enable rapid and standardized assessment of spider community composition, species richness, and genetic diversity across spatial and temporal scales (Ge *et al.,* 2021). Integrating the validated COI sequences produced in this study into metabarcoding-based surveillance programs provides numerous benefits. First, it facilitates non-invasive and high-throughput monitoring of spider assemblages without reliance on expert taxonomic identification, thereby reducing processing time and minimizing identification errors (Sahu *et al.,* 2023). Second, repeated genetic surveys can detect temporal changes in genetic diversity, serving as early-warning indicators of population declines or emerging ecological stressors (Pearman *et al.,* 2024). Third, genetic data can be used to infer habitat connectivity and gene flow in fragmented agricultural landscapes, thereby informing the design of habitat corridors and conservation priorities

(Bustillo-de la Rosa *et al.,* 2024; Reinula *et al.,* 2024). Ultimately, molecular monitoring facilitates the recognition of locally adapted populations and assesses their survival in the face of evolving agroecosystem conditions (Özbek, 2024; Goel *et al.,* 2025). The integration of phylogenetic and landscape-level data further enhances agroecosystem management and conservation planning. Phylogenetic analyses elucidate evolutionary connections and uncover patterns of genetic variation both within and between populations of biological control agents. For instance, population structuring in *Ceutorhynchus scrobicollis*, a candidate agent for garlic mustard control, demonstrated the necessity of accounting for genetic differentiation to ensure both safety and efficacy in biological control programs (Rauth *et al.,* 2011). Similarly, studies on the zigzag beetle *Cheilomenes sexmaculata* across agroecological zones in India have emphasized the importance of selecting genetically fit populations to maximize biological control effectiveness (Rakshith *et al.,* 2025). In light of the results achieved, this study has various limitations that ought to be recognized. Divergence time estimates are subject to considerable uncertainty because they rely on a single secondary calibration point (*A. trifasciata*) with a broad 95% HPD interval (3.90–6.33 Mya) and a relatively short COI sequence (710 bp). Temporal resolution is further limited by substantial molecular clock rate variability (±50–100%), calibration uncertainty (±23%), potential effects of alternative substitution models (±20–30%), and restricted sequence length, particularly for recent population-level divergences. As sensitivity analyses were not conducted, estimated divergence times (e.g., KB–Bali ~6 kya) should be interpreted as approximate temporal patterns rather than precise chronological dates. This study, while documenting genetic variation both within and among populations, does not assess whether this variation results in functional or phenotypic distinctions. Data regarding prey capture efficiency, web structure, foraging habits, reproductive success, pesticide resistance, and actual pest control is insufficient, which restricts ecological understanding and practical conclusions. Furthermore, while landscape change and genetic structure were described, causal relationships between landscape features and gene flow were not tested due to the absence of spatial genetic analyses, dispersal and behavioral data, temporal genetic monitoring, and landscape resistance modeling. Consequently, it is essential to conduct future integrative studies that merge genomic data, landscape ecology, and functional assays to ascertain the ecological significance and pest control implications of the identified genetic differentiation.

CONCLUSION

The present study provides an integrated molecular, phylogenetic, and landscape-level assessment of *Argiope modesta* populations from the Kali Bekasi area in West Java, offering new insights into their genetic diversity, evolutionary history, and potential ecological relevance within rapidly transforming agroecosystems. Mitochondrial COI sequences were used to successfully characterize the haplotype diversity, population structure, and phylogenetic relationships of *A. modesta*, allowing comparison with regional populations from Bali and the Philippines. The KB population demonstrated significant haplotype diversity while showing low nucleotide diversity, indicating a genetic pattern that aligns with recent demographic expansion from a limited ancestral gene pool rather than long-term adaptive divergence. Phylogenetic and molecular dating analyses place *A. modesta* within the broader evolutionary framework of the genus *Argiope*, which diversified extensively during the Late Miocene and Pliocene, likely influenced by repeated glacial–interglacial cycles and the dynamic formation of Sundaland. The strong genetic relationship between KB and Balinese populations, in comparison to Philippine populations, indicates historical migration across Sundaland during times of reduced sea level. The more recent divergence between KB and Bali populations during the Holocene suggests isolation following post-glacial sea-level rise rather than speciation. Crucially, the recognition of a specific KB lineage, underpinned by unique polymorphic sites in the COI gene, highlights the presence of localized genetic differentiation within *A. modesta*. Landscape analysis revealed pronounced habitat transformation along the Kali Bekasi corridor over the past two decades, characterized by declining vegetation cover, increased urbanization, and habitat fragmentation. These modifications probably played a role in the limited presence of *A. modesta* noted in this study and could exert significant selective pressures on the surviving populations. The persistence of *A. modesta*

in fragmented and heterogeneous landscapes, particularly in sites retaining riparian or semi-natural vegetation, underscores the importance of habitat structure and connectivity for sustaining spider populations. Such environments may facilitate local adaptation related to web architecture, prey capture, and tolerance to microclimatic variability. This study, viewed from an applied angle, underscores the significance of merging phylogenetic and genetic data within the frameworks of agroecosystem management and biodiversity conservation. Genetic diversity within predator populations is a critical component of ecosystem resilience and biological control effectiveness. The genetically distinct KB *A. modesta* lineage represents an irreplaceable evolutionary unit, potentially enhancing resilience to agricultural intensification and climate variability. Preserving its genetic diversity is essential for sustaining local pest regulation and maintaining adaptive ecosystem functions under future environmental change. DNA barcoding and COI-based phylogenetic analyses provide effective methods for monitoring biodiversity, facilitating the early identification of genetic erosion and the establishment of conservation priorities. These approaches provide actionable insights by highlighting locally adapted *A. modesta* populations and guiding habitat protection or targeted biological control interventions in agricultural landscapes. This study illustrates the significant role that evolutionary history, genetic diversity, and landscape transformation play in determining predator populations in peri-urban agroecosystems. While the conclusions are constrained by limitations inherent to single-locus data and the absence of functional validation, the findings lay a foundation for future integrative studies. Advancing this study through genomic approaches, spatial genetics, and functional assays will be crucial for connecting genetic differentiation to ecosystem services and for developing evidence-based strategies aimed at conserving natural enemies like *A. modesta* in landscapes that are increasingly influenced by human activity.

AUTHOR CONTRIBUTIONS

W.P.B. Putra formulated research ideas, designed methodologies, carried out investigations, curated data, analyzed, interpreted data, conducted literature reviews, compiled manuscripts, and secured funding sources. S. Utami designed and conceptualized manuscripts, conducted investigations, curated data, conducted literature reviews, analyzed, interpreted data, obtained funding, and provided supervision. D. Hutapea designed and conceptualized manuscripts, conducted investigations, curated data, conducted literature reviews, analyzed, and interpreted data. J. Kinho contributes to data collection, data interpretation, conducts statistical analysis, and compiles manuscripts, as well as plays a role in improving the quality of the manuscripts and supervision. Wakhid is involved in the investigation process, conducting literature reviews, collecting data, analyzing and interpreting data, and drafting manuscripts. W.C. Adinugroho contributed to data collection, data analysis, and interpretation, as well as played a role in the preparation of manuscripts and supervision. W. Darwiati plays an active role in conducting literature analysis, curating data, and obtaining the necessary funding. R. Agustarini is involved in the investigation process, conducting literature reviews, formulating manuscripts, administrative, technical, and material support. L. Andadari was involved in research design, investigation implementation, literature review, data collection, data analysis and interpretation, and manuscript preparation. A. Ismanto contributed to data collection, analysis, data interpretation, statistical analysis, and played a role in the improvement of the manuscript. B. Harjadi contributes to the analysis and interpretation of data, as well as statistical analysis, as well as playing a role in the improvement of the manuscript. Kayat is conducting literature reviews and statistical analysis and contributing to manuscript preparation. M.I. Maulana carried out investigations, curated data, conducted literature analysis, and compiled documents.

ACKNOWLEDGEMENT

The authors would like to thank Mrs. Sri Suhartati for her permission to collect spiders in her garden area. They also thank to Nida Nur Rahmah for her laboratory work.

CONFLICT OF INTEREST

The authors revealed that there was no conflict of interest related to the publication of this manuscript. In addition, the author has paid full attention to ethical issues, including plagiarism,

informed consent, infringement, fabrication and/or falsification of data, publication and/or double filing, and redundancy.

OPEN ACCESS

©2026 The author(s). This article is licensed under a Creative Commons Attribution 4.0 International License, which permits use, sharing, adaptation, distribution and reproduction in any medium or format, as long as you give appropriate credit to the original author(s) and the source, provide a link to the Creative Commons license, and indicate if changes were made. The images or other third-party material in this article are included in the article's Creative Commons license, unless indicated otherwise in a credit line to the material. If material is not included in the article's Creative Commons license and your intended use is not permitted by statutory regulation or exceeds the permitted use, you will need to obtain permission directly from the copyright holder. To view a copy of this license, visit: http://creativecommons.org/licenses/by/4.0/

PUBLISHER'S NOTE

GJESM Publisher remains neutral with regard to jurisdictional claims in published maps and institutional afflictions.

R NEgative AI Statement

The author(s) declare that no AI tools or services were not used or not highly applied during the preparation of this work.

ABBREVIATIONS

%	Percent
λ	Lambda
π	Nucleotide diversity
°C	Degree Celsius
µL	Microliter
BEAST	Bayesian evolutionary analysis by sampling trees
BEAUTi	Bayesian evolutionary analysis utility
BLAST	Basic local alignment search tool
bp	Base pair
BRIN	National research and innovation agency
BSI	Bare soil index
cm	Centimeters
COI	Cytochrome c oxidase subunit i
COII	Cytochrome c oxidase subunit ii
DNA	Deoxyribonucleic acid
ESS	Effective sample size
ETM+	Enhanced thematic mapper plus
FFS	Farmer field school
Fig	Figure
GEE	Google earth engine
GEE QA	Google earth engine quality assessment
Hd	Haplotype diversity
HPD	Highest posterior density
IPM	Integrated pest management
KB	Kebon bambu
Kya	Kilo (thousand) years ago
m	Meters
MEGA	Molecular evolutionary genetics analysis
MCC	Maximum clade credibility
min	Minute
mm	Millimeters
Mya	Million years ago
NCBI	National center for biotechnology information
NDVI	Normalized difference vegetation index
ng	Nanograms
NIR	Near infrared
OLI	Operational land imager
PCR	Polymerase chain reaction
s	Second
SWIR	Short wave infrared
TM	Thematic mapper
QGIS	Quantum geographic information system

REFERENCES

Abel, C.; Schneider, J.M.; Kuntner, M.; Harms, D., (2020). Phylogeography of the 'cosmopolitan'orb-weaver *Argiope trifasciata* (Araneae: Araneidae). Biol. J. Linn. Soc., 131(1): 61–75 **(5 pages).**

Agnarsson, I.; Lequier, S.M.; Kuntner, M.; Cheng, R.-C.; Coddington, J.A.; Binford, G., (2016). Phylogeography of a good Caribbean disperser: *Argiope argentata* (Araneae, Araneidae) and a new 'cryptic' species from Cuba. ZooKeys., 4(625): 25–44 **(20 pages).**

Akanand, A.; Khambhu, C.V.; Patel, P.K.; Krishnamoorthi, A.; Selvam, H.; Kumar, S.; Kumar, V.; Sapna, S., (2024). The future of farming with advances in biological control techniques for crop health. Microbiol. Res. J. Int., 34(7): 93–112 **(20 pages).**

Almeida, R.A.; Brans, K.I.; De Meester, L.; Lemmens, P., (2021). Differential local genetic adaptation to pesticide use in organic and conventional agriculture in an aquatic non-target species. Proceeding R. Soc. B: Biol. Sci., 288: 1963 **(9 pages).**

Altieri, M.A.; Rojas, A.S.; Nicholls, C.I.; De Molina, M.G., (2024). Landscape agroecology: methodologies and applications for the design of sustainable agroecosystems. Land. 13(11): 1746 **(16 pages).**

Andrade, R.; Larson, K.L.; Bateman, H.L.; Lerman, S.B.; Warren, P.S.; York, A.; Franklin, J.; Swan, C.M., (2020). Predicting the assembly of novel communities in urban ecosystems. Landscape. Ecol., 36(1): 1–15 **(15 pages).**

Anjos, D.V.; Perfecto, I.; Carvalho, R.L.; Torezan-Silingardi, H.; Viana-Junior, A.B.; Del-Claro, K.; Tena, A., (2022). The effects of ants on pest control: a meta-analysis. Proc. R. Soc. B: Biol. Sci., 289: 20221316 **(11 pages**).

Ashfaq, M.; Hebert, P.D.N.; Mirza M.S.; Khan, A.M.; Mansoor, S.; Shah, G.S.; Zafar, Y., (2014). DNA barcoding of *Bemisia tabaci* complex (Hemiptera: Aleyrodidae) reveals southerly expansion of the dominant whitefly species on cotton in Pakistan. PloS One. 9: 1–14 **(14 pages**).

Ashraaf, S.; Tahir, H.M.; Qazi, M.A.; Ali, S., (2019). Variations in nucleotide frequency distribution in spider families. Punjab. Univ. J. Zool., 34(1): 101–104 **(4 pages).**

Barbosa, N.C.; Freitas, S.D.; Morales, A.C., (2014). Distinct genetic structure in populations of *Chrysoperla externa* (Hagen)(Neuroptera, Chrysopidae) shown by genetic markers ISSR and COI gene. Revista Brasileira de Entomologia., 58: 203-211 **(9 pages).**

Benton, T.G.; Vickery, J.A.; Wilson, J.D., (2003). Farmland biodiversity: Is habitat heterogeneity the key?. Trends. Ecol. Evol., 18(4): 182–188 **(7 pages).**

Berthet, E.T.; Tichit, M.; Sabatier, R.; Lavorel, S.; Segrestin, B.; Bretagnolle, V., (2018). Applying ecological knowledge to the innovative design of sustainable agroecosystems. J. Appl. Ecol., 56(1): 44–51 **(8 pages).**

Bird, M.I.; Taylor, D.; Hunt, C., (2005). Palaeoenvironments of insular Southeast Asia during the last glacial period: a savanna corridor in Sundaland?. Quaternary. Sci. Rev., 24(20-21): 2228–2242 **(15 pages).**

Bloor, J.M.G.; Si-Moussi, S.; Taberlet, P.; Carrère, P.; Hedde, M., (2021). Analysis of complex trophic networks reveals the signature of land-use intensification on soil communities in agroecosystems. Sci. Rep., 11(1): 1–10 **(10 pages).**

Bosco, L.; Moser, V.; Jones, M.M.; Opedal, Ø.; Ovaskainen, O.; Sonja, G.; Van Klink, R.; Cushman, S.A.; Arlettaz, R.; Jacot, A., (2023). Habitat area and local habitat conditions outweigh fragmentation effects on insect communities in vineyards. Ecol. Solut. Evid., 4(1): e12193 **(12 pages).**

Bouckaert, R., (2022). An efficient coalescent epoch model for Bayesian phylogenetic inference. Syst. Biol., 71(6): 1549–1560 **(12 pages).**

Bouckaert, R.; Vaughan, T.G.; Barido-Sottani, J.; Duchene, S.; Fourment, M.; et al., (2019). BEAST 2.5: An advanced software platform for Bayesian evolutionary analysis. PLoS. Comp. Biol., 15(4): e1006650 **(28 pages).**

BPS (Indonesian Statistic Beureau), (2025). Statistics Indonesia 2024. BPS- Statistics Indonesia, Jakarta.

Brooker, R.W.; Iannetta, P.P.M.; Renard, D.; Hawes, C.; Karley, A.J., (2023). Plant diversity and ecological intensification in crop production systems. J. Plant. Ecol., 16(6): Rtad015 **(15 pages).**

Brüniche-Olsen, A.; Belant, J.L.; Kellner, K.F.; Dewoody, J.A., (2021). Life-history traits and habitat availability shape genomic diversity in birds: implications for conservation. Proc. R. Soc. B. Biol. Sci., 288: 20211441 **(9 pages).**

Brunnet, B., (2000). Spider Watch: a Guide to Australian Spiders. Reed New Holland, Sydney.

Bustillo-de la Rosa, D.; Barrero, A.; Traba, J.; García, J.T.; Morales, M.B.; Vázquez-Domínguez, E., (2024). Landscape features influencing gene flow and connectivity of an endangered passerine. Ecol. Evol., 14(5): e11078 **(18 pages).**

Cardoso, P.; Pekár, S.; Birkhofer, K.; Chuang, A.; Fukushima, C.S.; Hebets, E.A.; Henaut, Y.; Hesselberg, T.; Malumbres-Olarte, J.; Michálek, O.; Michalko, R.; Scott, C.; Wolff, J.; Mammola, S., (2025). Ecosystem services provided by spiders. Biol. Rev., 100(6): 2217–2236 **(20 pages).**

Chaw, R.; Allen, R.; Wei, J.; Ayoub, N.A.; Atrushi, K.; Hayashi, C.Y.; Zhao, Y., (2014). Intragenic homogenization and multiple copies of prey-wrapping silk genes in *Argiope* garden spiders. BMC. Evol. Biol., 14(31): 1–12 **(12 pages).**

Croucher, P.J.; Jones, R.M.; Searle, J.B.; Oxford, G.S., (2007). Contrasting patterns of hybridization in large house spiders (*Tegenaria atrica* group, Agelenidae). Evolution., 61(7): 1622–1640 (**19 pages).**

Curry, C.J.; Davis, B.W.; Bertola, L.D.; White, P.A.; Murphy, W.J.; Derr, J.N., (2020). Spatiotemporal genetic diversity of lions reveals the influence of habitat fragmentation across Africa. Mol. Biol. Evol., 38(1): 48–57 **(10 pages).**

Dankittipakul, P.; Jacque, R.; Singtripop, T., (2010). Five new Mallinella species from the Sundaland of Indonesia (Araneae, Zodariidae). Zootaxa. 2636(1): 21–36 **(16 pages).**

Darimont, C.T.; Cooke, R.; Bourbonnais, M.L.; Bryan, H.M.; Carlson, S.M.; Estes, J.A.; Galetti, M.; Levi, T.; Maclean, J.L.; Mckechnie, I.; Paquet, P.C.; Worm, B., (2023). Humanity's diverse predatory niche and its ecological consequences. Comm. Biol., 6(1): 1–10 **(10 pages).**

Des Roches, S.; Post, D.M.; Turley, N.E.; Bailey, J.K.; Hendry, A.P.; Kinnison, M.T.; Palkovacs, E.P., (2021). Conserving intraspecific variation for nature's contributions to people. Nat. Ecol. Evol., 5(4): 574–582 **(9 pages).**

Ding, Y.; Zhang, F,; Zhang, J., (2023). Applicability and advantage of mitochondrial metagenomics and metabarcoding in spider biodiversity survey. Biodiversity. 15(6): 711 **(13 pages).**

Diyaolu, C.O.; Folarin, I.O., (2024). The role of biodiversity in agricultural resilience: protecting ecosystem services for sustainable food production. Int. J. Res. Publ. Rev., 5(10): 1560–1573 **(14 pages).**

Douglas, J.; Zhang, R.; Bouckaert, R., (2021). Adaptive dating and fast proposals: Revisiting the phylogenetic relaxed clock model. PLoS Comp. Biol., 17(2): 1–30 **(30 pages).**

Falconer, D.S.; Mackay, T.F.C., (1996). Introduction to Quantitative Genetics, 4th ed. Addison Wesley Longman, Harlow.

Fenderson, L.E.; Kovach, A.I.; Llamas, B., (2019). Spatiotemporal landscape genetics: Investigating ecology and evolution through space and time. Mol. Ecol., 29(2): 218–246 **(29 pages).**

Fernandez-Fournier, P.; Mooers, A. Ø.; Lewthwaite, J.M.M., (2021). Do we need to identify adaptive genetic variation when prioritizing populations for conservation?. Conserv. Gen., 22(2): 205–216 **(12 pages).**

Gardiner, M.M.; Landis, D.A.; Gratton, C.; Schmidt, N.; O'Neal, M.; Mueller, E.; Chacon, J.; Heimpel, G.E., (2010). Landscape composition influences the activity density of Carabidae and Arachnida in soybean fields. Biol. Control. 55(1): 11–19 **(9 pages).**

Ge, Y.; Xia, C.; Wang, J.; Zhang, X.; Ma, X.; Zhou, Q., (2021). The efficacy of DNA barcoding in the classification, genetic differentiation, and biodiversity assessment of benthic macroinvertebrates. Ecol. Evol., 11(10): 5669–5681 **(13 pages).**

Goel, N.; Bossu, C.M.; Van Ee, J.J.; Zavaleta, E.; Ruegg, K.C.; Hooten, M.B., (2025). Identifying genomic adaptation to local climate using a mechanistic evolutionary model. Methods Ecol. Evol., 16(10): 2448–2460 **(13 pages).**

Graf, N.; Scharmüller, A.; Frisch, K.; Entling, M.H.; Battes, K.P.; Link, M.; Schäfer, R.B.; Szöcs, E.; Schreiner, V.C.; Cimpean, M.; Zubrod, J.P., (2020). Relationship between agricultural pesticides and the diet of riparian spiders in the field. Environ. Sci. Europe., 32(1): 1–12 **(12 pages).**

Hall, B.G., (2013). Building phylogenetic trees from molecular data with MEGA. Mol. Biol. Evol., 30(5): 1229–1235 **(7 pages).**

Hasegawa, M.; Kishino, H.; Yano, T., (1985). Dating the human-ape split by a molecular clock of mitochondrial DNA. J. Mol. Evol. 22:160-174 **(15 pages).**

Heaney, L.R., (1991). A synopsis of climatic and vegetational change in Southeast Asia. Clim. Change. 19: 53–61 **(9 pages).**

Heled, J.; Drummond A.J., (2012). Calibrated tree priors for relaxed phylogenetic and divergence time estimation. Syst. Biol., 61(1):138–149 **(12 pages).**

Hernández-Triana, L.M.; Brugman, V.A.; Nikolova, N.I.; Ruiz-Arrondo, I.; Barrero, E.; Thorne, L.; de Marco, M.F.; Krüger, A.; Lumley, S.; Johnson, N.; Fooks, A.R., (2019). DNA barcoding of British mosquitoes (Diptera, Culicidae) to support species identification, discovery of cryptic genetic diversity and monitoring invasive species. ZooKeys., 832: 57–76 **(10 pages).**

Hinckley, A.; Hawkins, M.; Achmadi, A.; Maldonado, J.E.; Leonard, J.A., (2020). Ancient divergence driven by geographic isolation and ecological adaptation in forest dependent Sundaland tree squirrels. Frontiers in Ecology and Evolution. 8: 208 **(18 pages).**

Hopfe, C.; Ospina-Jara, B.; Schulze, T.; Tischer, M.; Morales, D.; Reinhartz, V.; Esfahani, R.E.; Valderrama, C.; Pérez-Rigueiro, J.; Bleidorn, C.; Feldhaar, H.; Cabra-García, J.; Scheibel, T., (2024). Impact of environmental factors on spider silk properties. Curr. Biol., 34: 56–67 **(12 pages).**

Hu, Y.; Fan, H.; Chen, Y.; Chang, J.; Zhan, X.; Wu, H.; Zhang, B.; Wang, M.; Zhang, W.; Yang, L.; Hou, X.; Shen, X.; Pan, T.; Wu, W.; Li, J.; Hu, H.; Wei, F., (2021). Spatial patterns and conservation of genetic and phylogenetic diversity of wildlife in China. Sci. Adv., 7(4): eabd5725 **(9 pages).**

Huang, S.; Tang, L.; Hupy, J.P.; Wang, Y.; Shao, G., (2021). A commentary review on the use of normalized difference vegetation index (NDVI) in the era of popular remote sensing. J. Forest Res., 32(1): 1–6 **(6 pages).**

Husson, L.; Boucher, F.C.; Sarr, A.C.; Sepulchre, P.; Cahyarini, S.Y., (2020). Evidence of Sundaland's subsidence requires revisiting its biogeography. Journal of Biogeography. 47: 843–853 **(10 pages).**

Isaacs, R.; Tuell, J.; Fiedler, A.; Gardiner, M.; Landis, D., (2008). Maximizing arthropod-mediated ecosystem services in agricultural landscapes: the role of native plants. Front. Ecol. Env., 7(4): 196–203 **(8 pages).**

Jalajakshi, S.; Usha, R.N., (2019). Phylogenetic analysis of cox i gene in identification of spiders. J. Entomol. Zool. Stud., 7(2): 895–897 **(3 pages).**

Jaworski, C.C.; Thomine, E.; Rusch, A.; Lavoir, A.-V.; Wang, S.; Desneux, N., (2023). Crop diversification to promote arthropod pest management: A review. Agri. Comm., 1(1): 100004 **(10 pages).**

Jayasree, S.; Santhi, S., (2023). Study to find the phytogenic relationship of spiders from ten mixed agroecosystems of Palakkad. Int. J. Sci. Res., 12(12): 114–124 **(11 pages).**

Jeanneret, P.; Schüpbach, B.; Pfiffner, L.; Herzog, F., (2022). Spiders indicate delivery of an agri-environment scheme at the habitat level. Front. Ecol. Evol., 10: 866947 **(17 pages).**

Jones, E.L.; Leather, S.R., (2012). Invertebrates in urban areas: A review. European. J. Entomol., 109(4): 463–478 **(16 pages).**

Kerr, A.M., (2018). Illustrated field guide to the *Argiope* spiders (Araneidae) of the western Pacific Islands, including a bibiliograph of web-decorating behaviour in orb-weaving spiders. University of Guam Marine Laboratory Technical Report., 164: 1–54 **(54 pages).**

Krehenwinkel, H.; Tautz, D.; Rödder, D., (2015). Eco-genomic analysis of the poleward range expansion of the wasp spider *Argiope bruennichi* shows rapid adaptation and genomic admixture. Global Change Biol., 21(12): 4320–4332 **(13 pages).**

Lambin, E.F.; Meyfroidt, P.; (2010). Land use transitions: Socio-ecological feedback versus socio-economic change. Global. Environ. Change. 20(3): 357–365 **(9 pages).**

Landis, D.A.; (2017). Designing agricultural landscapes for biodiversity-based ecosystem services. Basic. Appl. Ecol.,

18: 1–12 **(12 pages).**
Librado, P.; Rozas, J., (2009). DnaSP v5: a software for comprehensive analysis of DNA polymorphism data. Bioinformatics., 25(11):1451-1452 **(2 pages).**
Linck, E.B.; Ghalambor, C.K.; Cadena, C.D.; Freeman, B.G., (2021). Evolutionary conservatism will limit responses to climate change in the tropics. Biol. Lett., 17(10): 1–4 **(4 pages).**
Littlefair, J.E.; Clare E.L., (2016). Barcoding the food chain: from Sanger to high-throughput sequencing. Genome. 59(11): 946–958 **(13 pages).**
Liu, Z.; Wang, Y.; Yin, H.; Cheng, Q.; Wang, Z., (2024). Research progress on animal habitat constructions from the perspective of urban biodiversity improvement. Front. Environ. Sci., 11: 1133879 **(17 pages).**
Luo, S.; Smith, J.L.D.; Martelli, P.; Zhang, Y.; Antunes, A.; Johnson, W.E.; O'Brien, S.J.; Miao, L., (2014). Sympatric Asian felid phylogeography reveals a major Indochinese–Sundaic divergence. Mol. Ecol., 23(8): 2072–2092 **(11 pages).**
Luther, G.C.; Siyaranamual, M.; Mariyono, J.; Satriatna, B.; Purnagunawan, R.M., (2018). Impacts of farmer field schools on productivity of vegetable farming in Indonesia. Nat. Res. Forum., 42(2): 71–82 **(12 pages).**
Matevski, D.; Beule, L.; Schuldt, A.; Sagolla, V., (2024). Temperate alley-cropping agroforestry improves pest control potential by promoting spider abundance and functional diversity. J. Appl. Ecol., 61(12): 3079–3091 **(13 pages).**
McKinney, M.L.; (2008). Effects of urbanization on species richness: A review of plants and animals. Urban Ecosystems., 11: 161–176 **(16 pages).**
Mezőfi, L.; Markó, G.; Nagy, C.; Korányi, D.; Markó, V., (2020). Beyond polyphagy and opportunism: natural prey of hunting spiders in the canopy of apple trees. PeerJ., 8(1): e9334 **(38 pages).**
Michalko, R., Entling, M. H., Pekár, S. (2018). An updated perspective on spiders as generalist predators in biological control. Oecologia., 189(1): 21–36 **(16 pages).**
Mohapatra, S.; Padhi, J.; Singh, S., (2024). Enhancing yield and economic benefits through sustainable pest management in Okra cultivation. Sci. Rep., 14(1): 22220 **(14 pages).**
Muneret, L.; Rusch, A.; Bonnard, O.; Thiéry, D.; Richart-Cervera, S.; Auriol, A., (2019). Organic farming expansion drives natural enemy abundance but not diversity in vineyard-dominated landscapes. Ecol. Evol., 9(23): 13532–13542 **(11 pages).**
Nayak, S.S.; Rajawat, D.; Jain, K.; Sharma, A.; Gondro, C.; Tarafdar, A.; Dutt, T.; Panigrahi, M., (2024). A comprehensive review of livestock development: insights into domestication, phylogenetics, diversity, and genomic advances. Mammal. Gen., 35(4): 577–599 **(23 pages).**
Nei, M,; Kumar, S., (2000). Molecular Evolution and Phylogenetics. Oxford University Press, New York.
Ony, M.A.; Trigiano, R.N.; Zobel, J.M.; Boggess, S.L.; Nowicki, M.; Hadziabdic, D.; Klingeman, W.E., (2020). Habitat fragmentation influences genetic diversity and differentiation: Fine-scale population structure of *Cercis canadensis* (eastern redbud). Ecol. Evol., 10(8): 3655–3670 **(16 pages).**
Özbek, Ö., (2024). Molecular markers used to reveal genetic diversity and phylogenetic relationships in crop plants. OBM Genetics., 8(4): 1–25 **(25 pages).**
Paz-Vinas, I.; Meable, P.; Brunetti, C.; Goffre, B.; Valentini, A.; Chappaz, R.; Blanchet, S., (2018). Systematic conservation planning for intraspecific genetic diversity. Proc. R. Soc. B., 285: 20172746 **(10 pages).**
Pearman, P.B.; Broennimann, O.; Aavik, T.; Albayrak, T.; Alves, P.C.; Aravanopoulos, F.A.; Bertola, L.D.; Biedrzycka, A.; Buzan, E.; Cubric-Curik, V.; Djan, M.; Fedorca, A.; Fuentes-Pardo, A.P.; Fussi, B.; Godoy, J.A.; Gugerli, F.; Hoban, S.; Holderegger, R.; Hvilsom, C.; Bruford, M., (2024). Monitoring of species' genetic diversity in Europe varies greatly and overlooks potential climate change impacts. Nat. Ecol. Evol., 8(2): 267–281 **(15 pages).**
Philpott, S.M.; Egerer, M.H.; Bichier, P.; Liere, H.; Jha, S.; Lin, B.; Lucatero, A., (2020). Natural enemy-herbivore networks along local management and landscape gradients in urban agroecosystems. Ecol. Appl., 30(8): e02201 **(13 pages).**
Phom, C.; Somasundaram, J., (2024). Molecular identification of the diversity of insects, spiders, lizards, birds and mammals of Tuensang District, Nagaland, India. Biosci. Biotechnol. Res. Asia., 21(1): 25–36 **(12 pages).**
Queiroz, M.; Gasnier, T., (2017). Strong negative effect of diurnal rainfall on nocturnal activity of a wandering spider in Central Amazonia. Revista de Biologia Tropical 65(3):1152–1160 **(9 pages).**
Radermacher, N.; Hartke, T.R.; Villareal, S.; Scheu, S., (2020). Spiders in rice-paddy ecosystems shift from aquatic to terrestrial prey and use carbon pools of different origin. Oecologia. 192(3): 801–812 **(12 pages).**
Rakshith, H.S.; Suroshe, S.S.; Solanke, A.U.; Gopalakrishnan, S.; Keerthi, M.C.; Bhat, N.; ... & Ellur, R.K., (2025). Genetic diversity of the zigzag ladybird beetle, *Cheilomenes sexmaculata* (F.)(Coleoptera: Coccinellidae) with its distribution in India and implications for biological control. Scientific Reports., 15(1): 15629 **(17 pages).**
Ramberg, E.; Burdon, F.J.; Sargac, J.; Kupilas, B.; Rîşnoveanu, G.; Lau, D.C.P.; Johnson, R.K.; McKie, B.G., (2020). The structure of riparian vegetation in agricultural landscapes influences spider communities and aquatic-terrestrial linkages. Water. 12(10):2855 **(22 pages).**
Rauth, S.J.; Hinz, H.L.; Gerber, E.; Hufbauer, R.A., (2011). The benefits of pre-release population genetics: a case study using *Ceutorhynchus scrobicollis*, a candidate agent of garlic mustard, *Alliaria petiolata*. Biological Control. 56(1): 67–75 **(9 pages).**
Redlich, S.; Steffan-Dewenter, I.; Martin, E.A., (2018). Landscape-level crop diversity benefits biological pest control. J. Appl. Ecol., 55(5): 2419–2428 **(10 pages).**
Reinula, I.; Träger, S.; Järvine, H.T.; Kuningas, V.M.; Kaldra, M.; Aavik, T., (2024). Beware of the impact of land use legacy on genetic connectivity: A case study of the long-lived perennial *Primula veris*. Biol. Conserv., 292: 110518 **(13 pages).**
Rikimaru, A.; Roy, P.S.; Miyatake, S., (2002). Tropical forest cover density mapping. Trop. Ecol., 43(1): 39-47 **(9 pages).**
Rusch, A.; Chaplin-Kramer, R.; Gardiner, M.M.; Hawro, V.;

Holland, J.; Landis, D.; Thies, C.; Tscarntke, T.; Weisser, W.W.; Winqvist, C.; Woltz, M.; Bommarco, R., (2016). Agricultural landscape simplification reduces natural pest control : a quantitative synthesis. Agric. Ecosyst. Environt., 221: 198-204 **(7 pages).**

Sahu, A.; Kumar, N.; Pal Singh, C.; Singh, M., (2023). Environmental DNA (eDNA): Powerful technique for biodiversity conservation. J. Nat. Conserv., 71: 126325 **(14 pages).**

Saqib, H.S.A.; Gurr, G.M.; You, M.; Liang, P., (2021). Molecular gut content analysis indicates the inter- and intra-guild predation patterns of spiders in conventionally managed vegetable fields. Ecol. Evol., 11(14): 9543–9552 **(10 pages).**

Saqib, S.; Ye, J.; Ahmad, M.; Shinwari, Z.K.; Zhang, Q.; Lu, L.; Omollo, W.O.; Liu, Y.; Liu, B.; Chen, Z.; Hu, H., (2024). Identifying conservation priority areas using spatial phylogenetic approaches in west Himalaya. Pakistan J. Bot., 56(3): 1029–1039 **(11 pages).**

Schrempf, D.; Minh, B.Q.; Von Haeseler, A.; Kosiol, C., (2019). Polymorphism-aware species trees with advanced mutation models, bootstrap, and rate heterogeneity. Mol. Biol. Evol., 36(6): 1294–1301 **(8 pages).**

Sheffer, M.M.; Hoppe, A.; Krehenwinkel, H.; Uhl, G.; Kuss, A.W.; Jensen, L.; Jensen, C.; Gillespie, R.G.; Hoff, K.J.; Prost, S., (2021). Chromosome-level reference genome of the European wasp spider *Argiope bruennichi*: a resource for studies on range expansion and evolutionary adaptation. GigaScience. 10(1): 1–12 **(12 pages).**

Sheldon, F.H.; Lim, H.C.; Moyle, R.G., (2015). Return to the Malay Archipelago: the biogeography of Sundaic rainforest birds. Journal of Ornithology. 156: 91–113 **(21 pages).**

Stavrianakis, G.; Sentas, E.; Stattegger, S.R.; Tscheulin, T.; Kizos, T., (2024). Effect of olive grove's understorey management on arthropod diversity. Agroecol. Sustain. Food Syst., 48(8): 1115–1138 **(24 pages).**

Stelkens, R.; Seehausen, O., 2009. Genetic distance between species predicts novel trait expression in their hybrids. Evolution. 63(4): 884–897 **(14 pages).**

Tamura, K.; Stecher, G.; Kumar, S., (2021). MEGA 11: Molecular evolutionary genetics analysis version 11. Mol. Biol. Evol., 38(7): 3022–3027 **(6 pages).**

Tan, J., (2018). *Argiope hoiseni*, a new species of the spider genus *Argiope* (Araneae, Araneidae) from Peninsular Malaysia based on morphology and molecular analyses. Zootaxa., 4457(1): 129-142 **(14 pages).**

Tan, J.; Chan, Z.Y.; Wong, C.X.; Kok-Hong, J.K.; Yong, H.S., (2019). Morphological and molecular evidence supports *Argiope chloreis* Thorell 1877 and *A. chloreides* Chrysanthus 1961 (Araneidae: Argiopinae) as distinct species. Acta Arachnol., 68(2): 41–58 **(18 pages).**

Tan, J.; Chan, Z.Y.; Lim, P.E.; Koh, J.K.H.; Yong, H.S., (2016). A multigene approach to determine the molecular phylogeography of *Argiope mangal* and *Argiope dang* (Araneae: Araneidae) and their genetic relationships with the *Argiope aetherea* species group. Biochem. Sys. Ecol., 69: 115–123 **(9 pages).**

Tews, J.; Brose, U.; Grimm, V.; Tielborger, K.; Wichmann, M.C.; Schwager, M.; Jeltsch, F., (2004). Animal species diversity driven by habitat heterogeneity/diversity: The importance of keystone structures. J. Biogeogr., 31(1): 79–92 **(14 pages).**

Tooker, J.F.; Rodriguez-Saona, C.; O'Neal, M.E., (2020). Balancing disturbance and conservation in agroecosystems to improve biological control. Annu. Rev. Entomol., 65(1): 81–100 **(20 pages).**

Tscharntke, T.; Klein A.M.; Kruess A.; Steffan-Dewenter I.; Thies C., (2005). Landscape perspectives on agricultural intensification and biodiversity–ecosystem service management. Ecol. Lett., 8(8): 857–874 **(18 pages).**

Twining, J.P.; Lambin, X.; Hobson, K.; Sheehy, E.; White, A.; Montgomery, W.I.; Lawton, C., (2022). Restoring vertebrate predator populations can provide landscape-scale biological control of established invasive vertebrates: Insights from pine marten recovery in Europe. Global Change Biol., 28(18): 5368–5384 **(17 pages).**

Uetz, G.W. (1991). Habitat structure and spider foraging. In: Bell, S.S.; McCoy, E.D.; Mushinsky, H.R., (eds) Habitat Structure. Population and Community Biology Series, 8. Springer.

Wang, W.; Yao, M.; Qiao, Y.; Li, S.; Pan, W., (2017). Low genetic diversity and strong population structure shaped by anthropogenic habitat fragmentation in a critically endangered primate, *Trachypithecus leucocephalus*. Heredity. 118(6): 542–553 **(13 pages).**

Wannigama, D.L.; Phattharapornjaroen, P.; Ounjai, P.; Sano, D.; Amarasiri, M.; Hongsing, P.; Anupong, S.; Jay, D.J.; Kicic, A.; Ali Hosseini Rad, S.M.; Cui, L.; Furukawa, T.; Kanthawee, P.; Leelahavanichkul, A.; Nanbo, A.; Miyanaga, K.; Vatanaprasan, P.; Hurst, C.; Siow, R.; Kanjanabuch, T., (2023). Tracing the transmission of mpox through wastewater surveillance in Southeast Asia. J. Travel Med., 30(5) **(7 pages).**

Wolz, M.; Klockmann, M.; Schmitz, T.; Pekár, S.; Bonte, D.; Uhl, G., (2020). Dispersal and life-history traits in a spider with rapid range expansion. Mov. Ecol., 8(2):b 1–11 **(11 pages).**

Woodruff, D.S., (2010). Biogeography and conservation in Southeast Asia: how 2.7 million years of repeated environmental fluctuations affect today's patterns and the future of the remaining refugial-phase biodiversity. Biodiv. Conserv., 19: 919–941 **(23 pages).**

Yasuhara, M.; Kučera, M.; Doi, H.; Finnegan, S.; Condamine, F.; Bonebrake, T.; Tittensor, D.; O'Dea, A.; Rillo, M.; Hull, P.; Huang, H.-H.; Kubota, Y.; Wei, C.-L.; Hong, Y.; Costello, M.; Saupe, E.; Mckenzie, R., (2020). Time machine biology: cross-timescale integration of ecology, evolution, and oceanography. Oceanography. 33(2): 17–28 **(12 pages).**

Zhou, W.; Arcot, Y.; Medina, R.F.; Bernal, J.; Cisneros-Zevallos, L.; Akbulut, M.E.S., (2024). Integrated pest management: An update on the sustainability approach to crop protection. ACS Omega. 9(40): 41130–41147 **(18 pages)**.

AUTHOR (S) BIOSKETCHES

Putra, W.P.B., Ph.D., Junior Researcher, Research Center for Applied Zoology, National Research and Innovation Agency, Jl. Raya Jakarta-Bogor KM 46, Cibinong, Indonesia.
- Email: *widy008@brin.go.id*
- ORCID: 0000-0002-1102-6447
- Web of Science ResearcherID: R-1399-2019
- Scopus Author ID: 56347768900
- Homepage: http://brin.go.id/

Utami, S., Ph.D., Research Professor, Research Center for Applied Zoology, National Research and Innovation Agency, Jl. Raya Jakarta-Bogor KM 46, Cibinong, Indonesia.
- Email: *sriu004@brin.go.id*
- ORCID: 0000-0001-8674-2299
- Web of Science ResearcherID: NA
- Scopus Author ID: 57421746700
- Homepage: http://brin.go.id/

Hutapea, D., Ph.D., Junior Researcher, Research Center for Horticulture, National Research and Innovation Agency, Jl. Raya Jakarta-Bogor KM 46, Cibinong, Indonesia.
- Email: *dedi026@brin.go.id*
- ORCID: 0000-0002-1801-1918
- Web of Science ResearcherID: ITV-8701-2023
- Scopus Author ID: 57496718100
- Homepage: http://brin.go.id/

Kinho, J., Ph.D., Senior Researcher, Research Center for Applied Zoology, National Research and Innovation Agency, Jl. Raya Jakarta-Bogor KM 46, Cibinong, Indonesia.
- Email: *julianus.kinho@brin.go.id*
- ORCID: 0000-0003-4301-1220
- Web of Science ResearcherID: HJI-9026-2023
- Scopus Author ID: 57205021554
- Homepage: http://brin.go.id/

Wakhid, Ph.D., Junior Researcher, Research Center for Applied Zoology, National Research and Innovation Agency, Jl. Raya Jakarta-Bogor KM 46, Cibinong, Indonesia.
- Email: *wakh006@brin.go.id*
- ORCID: 0000-0003-0657-0736
- Web of Science ResearcherID: NA
- Scopus Author ID: 57212602796
- Homepage: http://brin.go.id/

Adinugroho, W.C., Ph.D., Research Professor, Research Center for Ecology, National Research and Innovation Agency, Jl. Raya Jakarta-Bogor KM 46, Cibinong, Indonesia.
- Email: *wahy060@brin.go.id*
- ORCID: 0000-0003-0687-5679
- Web of Science ResearcherID: ABD-5946-2020
- Scopus Author ID: 57193552889
- Homepage: http://brin.go.id/

Darwiati, W., M.Sc., Senior Researcher, Research Center for Applied Zoology, National Research and Innovation Agency, Jl. Raya Jakarta-Bogor KM 46, Cibinong, Indonesia.
- Email: *wida.darwiati@brin.go.id*
- ORCID: 0000-0032-3237-5187
- Web of Science ResearcherID: NA
- Scopus Author ID: 57213352896
- Homepage: http://brin.go.id/

Agustarini, R., M.Sc., Senior Researcher, Research Center for Applied Zoology, National Research and Innovation Agency, Jl. Raya Jakarta-Bogor KM 46, Cibinong, Indonesia.
- Email: *retn030@brin.go.id*
- ORCID: 0000-0002-4258-5663
- Web of Science ResearcherID: DVS-6345-2022
- Scopus Author ID: 57218922115
- Homepage: http://brin.go.id/

Andadari, L., M.Sc., Senior Researcher, Research Center for Applied Zoology, National Research and Innovation Agency, Jl. Raya Jakarta-Bogor KM 46, Cibinong, Indonesia.
- Email: *linc001@brin.go.id*
- ORCID: 0000-0002-8419-031X
- Web of Science ResearcherID: CEM-3184-2022
- Scopus Author 56082155500
- Homepage: http://brin.go.id/

AUTHOR (S) BIOSKETCHES

Ismanto, A., B.Sc., Research Professor, Research Center for Applied Zoology, National Research and Innovation Agency, Jl. Raya Jakarta-Bogor KM 46, Cibinong, Indonesia.
- Email: *agus174@brin.go.id*
- ORCID: 0000-0002-7599-8181
- Web of Science ResearcherID: NA
- Scopus Author ID: 57478384000
- Homepage: http://brin.go.id/

Harjadi, B., M.Sc., Research Professor, Research Center for Geological Disaster, National Research and Innovation Agency, Jl. Raya Jakarta-Bogor KM 46, Cibinong, Indonesia.
- Email: *beny003@brin.go.id*
- ORCID: 0000-0003-2436-4442
- Web of Science ResearcherID: NA
- Scopus Author ID: 57883864700
- Homepage: http://brin.go.id/

Kayat, Ph.D., Senior Researcher, Research Center for Biota System, National Research and Innovation Agency, Jl. Raya Jakarta-Bogor KM 46, Cibinong, Indonesia.
- Email: *kaya001@brin.go.id*
- ORCID: 0000-0003-3381-8653
- Web of Science ResearcherID: NA
- Scopus Author ID: 130391091
- Homepage: http://brin.go.id/

Maulana, M.I., M.Sc. student, Department of Biology, Faculty of Science, Institut Teknologi of Sumatra, South Lampung, Lampung 35365, Indonesia.
- Email: *mindramaulana23@gmail.com*
- ORCID: 0009-0005-3499-2161
- Web of Science ResearcherID: NA
- Scopus Author ID: NA
- Homepage: https://www.itera.ac.id/

HOW TO CITE THIS ARTICLE

Putra, W.P.B.; Utami, S.; Hutapea, D.; Kinho, J.; Wakhid; Adinugroho, W.C.; Darwiati, W.; Agustarini, R.; Andadari, L.; Ismanto, A.; Harjadi, B.; Kayat; Maulana, M.I., (2026).Phylogenetic and conservation insights on local adaptations of Argiope modesta concerning ecological consequences. Global J. Environ. Sci. Manage., 12(1):167-190.

DOI: 10.22034/gjesm.2026.01.10

URL: https://www.gjesm.net/article_733128.html

Global J. Environ. Sci. Manage. 12(1): 191-206, Winter 2026, Serial #45

Global Journal of Environmental Science and Management
(GJESM)

Homepage: https://www.gjesm.net/

Podcasts

ORIGINAL RESEARCH PAPER

Customer-driven socio-environmental sustainability in fashion: The role of green word-of-mouth and perceived product value

P. Yanti[1], M. Gunarto[2,*], R. Yusiana[1], L. Yohanna[1], R. Indriarti[1], Y. Yuliawati[3]

[1] *Faculty of Economics and Business Education, Universitas Pendidikan Indonesia, Bandung, West Java, Indonesia*

[2] *Faculty of Economics and Business, Sriwijaya University, Palembang, South Sumatra Indonesia*

[3] *Faculty of Economics, Universitas Islam Nusantara, Bandung, West Java, Indonesia*

ARTICLE INFO

Article History:
Received 20 August 2025
Revised 27 November 2025
Accepted 31 December 2025

Keywords:
Circular economy
Consumer behavior
Green trust
Social environmental management
Sustainable fashion
Textile waste

DOI: 10.22034/gjesm.2026.01.11

ABSTRACT

BACKGROUND AND OBJECTIVES: The fashion industry contributes ten percent of global carbon emissions and consumes 93 billion cubic meters of water annually. Textile waste is projected to reach 148 million tonnes by 2030. In spite of increasing environmental consciousness, a notable gap between attitudes and behaviors remains in the realm of sustainable fashion consumption. The study aimed to explore how green word-of-mouth and the perceived value of products contribute to the formation of green trust and the intention to purchase green products.

METHODS: A quantitative survey was employed with 358 Indonesian consumers who had purchased or considered sustainable fashion products within twelve months. Standardized scales measured all four constructs. Data were analysed using partial least squares structural equation modelling.

FINDINGS: Respondents were predominantly middle-aged (25–54 years), highly educated, and in stable employment. All seven hypotheses were supported. Perceived product value associated with a product demonstrated the highest positive effect on green trust, exceeding that of green word-of-mouth. Green trust showed the strongest direct effect on green purchase intention. Both green word-of-mouth and perceived product value also directly increased green purchase intention, while green trust acted as a dual mediator linking green word-of-mouth and perceived product value to purchase intention. The significance of emotional and aesthetic aspects, illustrated by pride in wearing sustainable fashion, and the clarity in sustainability practices, emerged as the primary elements affecting perceived product value and green trust, respectively. The model explained 64.3 percent of the variance in green purchase intention and 57.0 percent of the variance in green trust.

CONCLUSION: Green trust functions as a critical dual mediating mechanism, with perceived product value exerting substantially stronger influence than green word-of-mouth in trust formation. Sustainable fashion brands should focus on creating tangible value, which encompasses high-quality materials, elegant design, and long-lasting products, all while ensuring clear communication regarding their sustainability efforts. Policy interventions should include mandatory supply chain disclosure regulations and standardized eco-labeling requirements. Product development strategies emphasizing longevity support circular economy implementation through reduced resource extraction and landfill accumulation. These mechanisms on the consumer side facilitate environmental governance initiatives aimed at decreasing carbon emissions, preserving water resources, and reducing textile waste within the fashion sector.

This is an open access article under the CC BY license (http://creativecommons.org/licenses/by/4.0/).

NUMBER OF REFERENCES	NUMBER OF FIGURES	NUMBER OF TABLES
33	1	5

*Corresponding Author:
Email: *mgunarto@hotmail.com*
Phone: +895709080744
ORCID: 0000-0001-9494-2127

Note: Discussion period for this manuscript open until Mar 1, 2026 on GJESM website at the "Show Article".

INTRODUCTION

The fashion industry faces mounting pressure to address its substantial environmental footprint, with textile production contributing approximately ten percent of global carbon emissions (Li *et al.*, 2024), consuming 93 billion cubic meters of water annually (Niinimäki *et al.*, 2020), and generating significant waste throughout supply chains, with projections indicating textile waste will reach 148 million tonnes by 2030 (Shamsuzzaman *et al.*, 2025). Sustainable fashion has surfaced as an essential reaction to these ecological challenges, focusing on environmentally friendly materials, responsible production methods, and the tenets of a circular economy (Henninger *et al.*, 2020; Shamsuzzaman *et al.*, 2025; Todeschini *et al.*, 2017). However, despite growing environmental awareness and the proliferation of sustainable fashion brands, a significant attitude, behavior gap persists, as consumers' positive environmental attitudes do not consistently translate into purchase intentions for sustainable fashion (Ahmad *et al.*, 2023; Bailey *et al.*, 2025; Margariti *et al.*, 2024). To address this gap, it is essential to go beyond descriptive accounts of environmental awareness to investigate the psychological mechanisms that facilitate the conversion of consumer concern into green purchase intention (GPI). Consumer behavioral shifts create demand-side pressure that incentivizes sustainable production practices, enabling apparel brands to reduce carbon emissions, save operating expenses, and contribute to more environmentally conscious and sustainable fashion systems (Rahaman *et al.*, 2024). Material recovery and circular consumption patterns represent critical pathways for transforming textile waste into secondary raw materials through repurposing and recycling, thereby reducing reliance on virgin resource extraction and minimizing landfill accumulation (Piribauer and Bartl, 2024). Environmental management frameworks are progressively acknowledging consumer behavior as a vital leverage point for attaining pollution reduction and circular economy objectives in the fashion sector (Olivar Aponte *et al.*, 2024; Daga *et al.*, 2025; Abbate *et al.*, 2023; Parajuly *et al.*, 2020). Consumer trust has been identified as a fundamental prerequisite for green purchasing behavior, particularly in contexts where information asymmetries prevent direct verification of environmental claims (Li *et al.*, 2024). The history of greenwashing in the fashion industry, characterized by brands making deceptive environmental assertions, has heightened consumer skepticism regarding sustainability communications (Nguyen *et al.*, 2019; Bailey *et al.*, 2025; Margariti *et al.*, 2024). In this environment, understanding how consumers develop trust toward sustainable fashion brands and how this trust translates into purchase intentions (PI) becomes essential for advancing environmental management objectives (Rama *et al.*, 2024). The current study thus emphasizes green trust (GT) as an essential psychological factor that can lessen perceived risk and connect the attitude–behavior gap in sustainable fashion. The proposed model is explicitly grounded in Trust Theory as its core theoretical foundation and is complemented by Signaling Theory to explain how different types of information shape trust under uncertainty. Trust Theory articulates that trust is a vital condition for behavior when stakeholders lack the ability to fully validate claims, which holds significant relevance for credence-based environmental attributes within the realm of fashion (Li *et al.*, 2024; Suki, 2016). Signaling Theory is employed to distinguish between interpersonal signals, such as green word-of-mouth (GWOM), and costly brand-related signals, such as perceived product value (PPV), that require resource investment and thus convey stronger credibility (Connelly *et al.*, 2025). Within this integrated framework, GWOM and PPV extend Trust Theory by specifying how social and experiential signals are internalized into GT and subsequently shape GPI in sustainable fashion contexts. Although earlier studies have explored the factors affecting GPI, there has been insufficient focus on the relative impacts of social influence via word-of-mouth and the perceived value of tangible products in fostering consumer trust, especially in the realm of sustainable fashion where both aspects may function concurrently (Siyal *et al.*, 2021; Li *et al.*, 2024; McNeill and Venter, 2019). GWOM refers to informal communications between consumers regarding environmental attributes, sustainability practices, and green product experiences (Siyal *et al.*, 2021). PPV represents consumers' overall assessment of product utility based on perceptions of what is received relative to what is given (Sharma *et al.*, 2024). In the realm of sustainable fashion, value includes functional aspects

such as material durability, comfort, and quality; aesthetic elements like design excellence, style appropriateness, and pride in wearing; as well as symbolic significance encompassing environmental contribution, identity expression, and social responsibility signaling (Henninger *et al.*, 2020; Ahmad *et al.*, 2023; Li *et al.*, 2024; McNeill and Venter, 2019). Other commonly cited predictors in sustainable fashion research, such as environmental concern, perceived consumer effectiveness, moral norms, or price sensitivity, are not modelled as direct antecedents here because they primarily capture background motivational conditions rather than the social and experiential signals that immediately trigger GT and GPI in marketplace decisions (Joshi and Rahman, 2015). Recent theoretical developments in environmental behavior research emphasize the importance of integrating multiple pathways through which consumers form PI. The Theory of Planned Behavior (TPB) proposes that attitudes, subjective norms, and perceived behavioral control shape behavioral intentions (Hagger, 2025), Meanwhile, the Value-Belief-Norm model focuses on how individual values and beliefs about the environment can trigger moral norms that encourage pro-environmental behaviors (Tian and Liu, 2022; Yanti *et al.*, 2025). Environmental management research has demonstrated that organizational environmental practices, individual psychological mechanisms, and systemic conditions interact to shape green consumption patterns (Rama *et al.*, 2024; Yanti *et al.*, 2025). Expanding upon these frameworks, the current study redirects the analytical emphasis from general attitudinal factors to the particular social and value-driven signals that are transformed into GT, thus providing a process-oriented elucidation of how pro-environmental attitudes can be transformed into GPI in a sustainable manner. Consumption value theory suggests that consumers evaluate products based on multiple value dimensions, including functional, social, emotional, and conditional benefits (Tian and Liu, 2022). In sustainable fashion contexts, perceived value encompasses not only functional and economic considerations but also symbolic sustainability value relating to environmental contribution and identity expression (Henninger *et al.*, 2020; Ahmad *et al.*, 2023; Li *et al.*, 2024; McNeill and Venter, 2019). Research demonstrates that functional value, emotional value, and environmental concern have a considerable impact on GPI (Ahmad *et al.*, 2023). Nevertheless, the comparative importance of these dimensions and their routes in the formation of trust remain inadequately explored (Bailey *et al.*, 2025). Similarly, while word-of-mouth is recognized as a credible information source for green products, its comparative influence relative to tangible value perceptions in building consumer trust has not been systematically examined, particularly in contexts characterized by heightened greenwashing concerns (Nguyen *et al.*, 2019; Shamsuzzaman *et al.*, 2025; Margariti *et al.*, 2024). In this study, the attitude–behavior gap in sustainable fashion is addressed by positioning GT as a dual mediating mechanism through which social influence via GWOM and experiential evaluation via PPV are translated into GPI. This viewpoint indicates that consumers who hold positive environmental beliefs need both trustworthy social endorsements and compelling value experiences to address skepticism, perceived risk, and trade-offs between sustainability and other product attributes (Li *et al.*, 2024; Ahmad *et al.*, 2023). Furthermore, the model posits that the attitude–behavior gap arises from trust issues, where a lack of credible signals or value delivered obstructs positive attitudes from evolving into actual purchasing intentions for sustainable fashion. This study addresses these gaps by examining the relationships among GWOM, PPV, GT, and GPI in sustainable fashion consumption contexts. Three primary objectives are addressed in this investigation. First, to examine the comparative influence of GWOM and PPV in building GT among sustainable fashion consumers. Second, to investigate GT as a dual mediating mechanism linking both social influence and experiential value perceptions to GPI. Third, to determine the essential aspects of trust and value that most significantly influence sustainable fashion purchase intentions, offering practical insights for environmental management interventions. The study is situated in an emerging market context where sustainable fashion consumption patterns are still evolving, rendering the findings especially significant for environmental governance structures in developing nations aiming to reconcile economic development with pollution mitigation and the goals of circular economy implementation objectives (Li *et al.*, 2024; Yanti *et*

al., 2025). The following study questions (RQs) guide this investigation:

RQ1: How do GWOM and PPV independently influence GT and GPI in sustainable fashion contexts?
RQ2: What is the relative strength of GWOM versus PPV in predicting GT formation among sustainable fashion consumers?
RQ3: Does GT mediate the relationships between GWOM, PPV, and GPI, and which mediation pathway is stronger?
RQ4: Which dimensions of GT and components of PPV are most critical for GPI formation?

This study enhances the understanding of environmental management and sustainable consumption by tackling these study questions. It introduces a trust-centered framework that merges social influence with experiential value pathways, offers a theoretically robust rationale for how GT assists in closing the attitude–behavior gap, and contextualizes these mechanisms within emerging markets where institutional support and consumer trust in sustainability claims are still developing (Rama *et al.*, 2024; Li *et al.*, 2024; Yanti *et al.*, 2025). This study has been carried out in Indonesia, a rapidly developing economy experiencing significant growth in middle-class consumption and environmental awareness in Indonesia in 2025.

Sustainable fashion and green purchase intention

Sustainable fashion represents a paradigm shift from traditional fast fashion models, emphasizing environmental responsibility, ethical labor practices, and resource efficiency throughout product lifecycles (Henninger *et al.,* 2020). GPI illustrates the inclination of consumers to select products that mitigate ecological damage, indicating the potential for converting environmental concerns into concrete purchasing decisions (Ahmad *et al.,* 2023). Despite increased environmental awareness, significant barriers prevent intention formation including price premiums, perceived quality concerns, limited availability, aesthetic preferences, and skepticism toward environmental claims (Ahmad *et al.,* 2023). Understanding GPI formation requires examining cognitive factors (environmental knowledge, perceived effectiveness, rational evaluation) and affective factors (emotional responses, moral obligations, identity expression) that shape decision-making (Li *et al.,* 2024; Ahmad *et al.,* 2023). The fashion sector introduces specific challenges since buying choices involve functional factors, aesthetic inclinations, social signaling, and environmental considerations, compelling consumers to juggle multiple conflicting priorities (Henninger *et al.,* 2020). Trust has emerged as particularly critical in contexts characterized by information asymmetries and greenwashing, serving as a cognitive shortcut enabling purchase decisions when environmental claims cannot be directly verified (Li *et al.,* 2024; Nguyen *et al.,* 2019). The fashion industry's credibility challenges make trust-building mechanisms especially important for converting awareness into PI.

Green trust in sustainable fashion contexts

GT refers to consumers' willingness to rely on a brand's environmental claims based on beliefs in the brand's environmental credibility, benevolence, and integrity (Li *et al.,* 2024). Trust plays a crucial role in lowering the perceived risk and uncertainty associated with purchasing green products. This is especially important in the realm of sustainable fashion, where the environmental advantages are credence attributes that cannot be verified through direct product inspection, thus requiring trust in brand messaging and third-party certifications (Suki, 2016; Henninger *et al.,* 2020). GT encompasses cognitive evaluations of competence and reliability as well as affective assessments of shared values and genuine commitment (Li *et al.,* 2024). Trust development involves processing information from multiple sources including brand communications, peer recommendations, media coverage, third-party certifications, and direct experiences, with consumers actively scrutinizing consistency across sources to detect superficial greenwashing (Nguyen *et al.,* 2019). The significance of transparency is particularly pronounced, with consumers insisting on detailed and verifiable information regarding the sourcing of materials, production methods, labor practices, and environmental impacts (Henninger *et al.,* 2020). GT positively influences PI by reducing perceived risk, alleviating concerns about product performance and environmental authenticity, and enabling consumers to overcome decision-making complexity when evaluating multidimensional sustainability attributes (Li *et al.,* 2024; Ahmad *et al.,* 2023; Suki, 2016). In sustainable fashion environments, where aesthetic

elements and social signaling merge with ecological considerations, trust serves as the vital psychological groundwork that empowers consumers to navigate multiple purchasing factors and opt for sustainable alternatives, notwithstanding potential compromises (Rama *et al.,* 2024; Yanti *et al.,* 2025).

Green word-of-mouth and social influence

GWOM refers to informal communications between consumers regarding environmental attributes, sustainability practices, and green product experiences (Siyal *et al.,* 2021). Unlike brand-initiated marketing communications, WOM is perceived as more credible because it originates from independent sources without commercial incentives, making peer recommendations and shared experiences valuable decision-making cues in contexts where environmental claims are difficult to verify and greenwashing concerns are prevalent. WOM influences green purchase behavior by providing information about product performance and environmental authenticity that consumers cannot easily obtain through direct inspection. It serves as a form of social proof, indicating normative acceptability, mitigating perceived risk by illustrating the satisfactory outcomes experienced by others, and fostering social pressure that activates moral obligations to engage in pro-environmental behavior (Li *et al.,* 2024; Ahmad *et al.,* 2023; Yanti *et al.,* 2025). WOM exerts particularly strong influence when consumers lack direct product experience or expertise to evaluate attributes independently (Siyal *et al.,* 2021). In sustainable fashion contexts, consumers actively seek peer recommendations, read online reviews, and participate in sustainability communities to gather insights about brand credibility and product performance. However, consumers process WOM critically rather than passively accepting all communications. Heightened attention to inconsistent information triggers skepticism and careful source credibility evaluation, suggesting consistency across communications is essential for trust formation while negative WOM or greenwashing accusations can substantially undermine previously established trust (Nguyen *et al.,* 2019). The following hypotheses are proposed:

H1: GWOM has a significant positive effect on GT.
H2: GWOM has a significant positive effect on GPI.

Perceived product value as trust and intention antecedent

PPV denotes the comprehensive judgment of product usefulness from the consumers' perspective, based on their views of the received value compared to the offered value (Sharma *et al.,* 2024). In sustainable fashion contexts, value encompasses functional value (material durability, comfort, quality), aesthetic value (design excellence, style appropriateness, pride in wearing), and symbolic value (environmental contribution, identity expression, social responsibility signaling) (Henninger *et al.,* 2020; Ahmad *et al.,* 2023). Consumers evaluate sustainable fashion in a holistic way across these aspects, requiring extensive value delivery to warrant premium pricing and to outdo conventional options. Perceived value significantly influences both trust and PI, with value perceptions serving as evidence of brand competence and commitment (Li *et al.,* 2024; Suki, 2016). When sustainable fashion products demonstrate excellent functional performance, sophisticated design, and meaningful environmental contribution, consumers infer brands possess both capability and commitment to deliver on sustainability promises (Henninger *et al.,* 2020). This inference-building process enhances trust, as delivering tangible value provides verifiable proof of brand credibility that extends beyond marketing communications. The relationship between PPV and PI operates through multiple pathways: directly by increasing willingness to pay premium prices and reducing sacrifice perceptions, and indirectly through trust formation as value delivery builds confidence in brand environmental commitments (Suki, 2016; Rama *et al.,* 2024). The multidimensional nature of perceived value suggests consumers require comprehensive value propositions spanning functional, aesthetic, and symbolic dimensions, as environmental benefits alone are insufficient when comparable functionality and aesthetics are available from conventional alternatives at lower prices (Henninger *et al.,* 2020; Ahmad *et al.,* 2023; Yanti *et al.,* 2025). Sustainable fashion ought to effectively compete on every value dimension concurrently, instead of primarily highlighting environmental credentials as the key differentiator (Ahmad *et al.,* 2023). Hypotheses are proposed as follows:

H3: PPV has a significant positive effect on GT.
H4: PPV has a significant positive effect on GPI.

Green trust as mediating mechanism

While direct effects of WOM and PPV on PI have been documented, the psychological mechanisms through which these external stimuli translate into behavioral intentions require investigation (Li *et al.,* 2024). Trust serves as a vital mediating factor that facilitates the transformation of information processing and value assessment into purchase commitment (Ahmad *et al.,* 2023). When consumers encounter positive WOM messages, they evaluate social information to establish trust evaluations concerning the environmental credibility of the brand. Concurrently, perception of enhanced product value prompts inferences about the brand's competence and dedication, which further solidifies trust (Siyal *et al.,* 2021; Suki, 2016). These trust perceptions subsequently drive PI by reducing risk, simplifying decision-making, and enabling consumers to overcome barriers to sustainable consumption (Henninger *et al.,* 2020). The mediating role of trust aligns with theoretical frameworks emphasizing trust as a fundamental prerequisite for behavior under uncertainty (Li *et al.,* 2024). When environmental assertions cannot be directly confirmed and information disparities obstruct full evaluation, trust functions as the psychological connection that empowers consumers to proceed with purchase choices despite lacking complete information (Nguyen *et al.,* 2019). Word-of-mouth and perceived value provide inputs to trust formation, but PI emerge only after trust has been established sufficiently to overcome skepticism and perceived risk (Rama *et al.,* 2024; Yanti *et al.,* 2025). Signaling theory contributes additional theoretical reinforcement for the mediating role that trust plays (Connelly *et al*., 2025). Word-of-mouth represents costless signals varying in credibility depending on source characteristics and message consistency, while perceived value represents costly signals requiring substantial investment in product development, quality assurance, and sustainability practices (Henninger *et al.,* 2020; Ahmad *et al.,* 2023). Expensive signals are considered more credible in theory as they showcase commitment via resource allocation that is challenging to maintain without authentic capability and intent. This implies that perceived value may have a greater impact on the development of trust compared to WOM, with value-driven trust playing a more significant role in influencing PI (Henninger *et al.,* 2020; Ahmad *et al.,* 2023). Based on these considerations, the following hypotheses are proposed:

H5: GT influences GPI.
H6: GT mediates the relationship between GWOM and GPI.
H7: GT mediates the relationship between PPV and GPI.

The conceptual framework depicting these hypothesized relationships is presented in Fig. 1.

MATERIALS AND METHODS

Research design

This quantitative, cross-sectional study examines relationships among GWOM, perceived PPV, green trust (GT), and green purchase intention (GPI) in sustainable fashion consumption contexts. The study was carried out in Indonesia, developing economy where grasping consumer psychological mechanisms yields vital insights for environmental management frameworks focused on waste reduction and the execution of a circular economy implementation in the fashion sector (Li *et al.,* 2024; Yanti *et al.,* 2025). This study underwent evaluation and received approval from the institutional ethics committee at the Faculty of Economics and Business, Universitas Pendidikan Indonesia. Participation was voluntary, anonymous, and conducted in accordance with research ethics guidelines.

Sample and data collection

Data were collected through an online survey administered via Google Forms between June until August 2025. The link was disseminated across various social media platforms including Instagram, Facebook, and WhatsApp sustainability groups, in addition to university networks, and eco-fashion communities. Purposive sampling aimed at individuals aged 18 and above who had a) acquired sustainable fashion items within the previous year or b) contemplated buying them following exposure to eco-fashion marketing initiatives. Screening questions verified awareness of sustainability claims, eco-labels, or brand transparency efforts prior to participation. Incomplete responses were dropped using two criteria: more than 15 percent (%) missing answers or identical responses across more than 90% of items. A total of 18 such cases were removed,

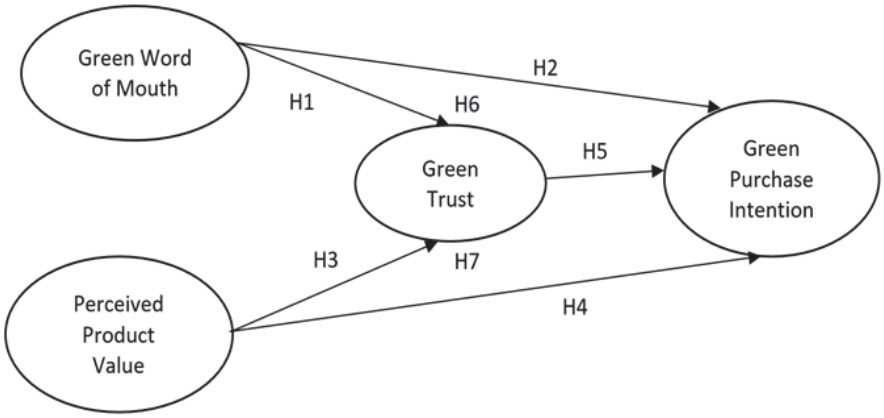

Fig 1: The study framework

resulting in 358 valid responses. This sample size exceeds the minimum requirement for PLS-SEM analysis based on both i) a G*Power (v3.1) analysis (α = 0.05, f^2 = 0.15, power = 0.95 → minimum N = 146; Cohen, 1992), and ii) Hair *et al.*, (2019). Given the sample's significant education and employment status, the outcomes signify urban middle-income early adopters of sustainable fashion. It is important to exercise caution when making generalizations about lower-income or rural segments, and this should be a focus for future research.

Measurement instruments

All constructs were measured using seven-point Likert scales (1 = strongly disagree, 7 = strongly agree) adapted from validated research. GWOM (9 items) measured exposure to recommendations, credibility, shared user experiences, and community validation (Siyal *et al.*, 2021; Hameed *et al.*, 2022). PPV (9 items) assessed functional value (durability, comfort, quality), aesthetic value (design, pride in wearing), and symbolic value (environmental contribution, responsible brand support) (Henninger *et al.*, 2020; Sharma *et al.*, 2024; Ahmad *et al.*, 2023; Li *et al.*, 2024). GT (8 items) captured beliefs about brand transparency, believability, consistency, and sincerity (Li *et al.*, 2024; Suki, 2016). To distinguish green trust from brand credibility or authenticity, GT has been characterized as the willingness of consumers to trust a brand's environmental claims, which are grounded in competence, integrity, and benevolence, concentrating specifically on sustainability features instead of the broader brand image. GPI (6 items) assessed willingness to purchase, preference prioritization, and willingness to pay a premium (Ahmad *et al.*, 2023; Yanti *et al.*, 2025). All items were translated into Bahasa Indonesia and validated through a translation–back-translation procedure (Brislin, 1980). Two bilingual experts independently translated the survey, and discrepancies were reconciled by a third reviewer; an expert panel then assessed content validity to ensure cultural and contextual fit. A preliminary test involving 30 participants validated the reliability (Cronbach's α = 0.88–0.93); slight adjustments in wording enhanced clarity, and no items were eliminated. Respondents were instructed to evaluate local sustainable fashion brands operating in the Indonesian market, ensuring that all constructs were assessed with respect to domestic brand contexts.

Data analysis

Data were analyzed using SmartPLS 4.0 (Ringle *et al.*, 2022). PLS-SEM was opted for because of its effectiveness in exploring complex models that feature various mediating relationships and are aimed at prediction-oriented goals (Hair *et al.*, 2019). Measurement model assessment involved: Cronbach's α > 0.70, composite reliability (CR) > 0.70, average variance extracted (AVE) > 0.50, and outer loadings (λ) > 0.70. Discriminant validity was tested via the heterotrait–monotrait ratio (HTMT) < 0.85. Structural model assessment used bootstrapping (5,000 resamples) to determine path coefficients and p-values (< 0.05). Fit indices were incorporated for thoroughness, although PLS SEM does not depend

Table 1: Validation and realibility result

Indicator	λ	CR	AVE	α
GWOM)		0.983	0.866	0.981
Awareness from others' stories (GWOM1)	0.931			
Read listen to reviews (GWOM2)	0.920			
Positive discussions about green products (GWOM3)	0.933			
Shared experiences (GWOM4)	0.925			
Inconsistency (GWOM5)	0.937			
Reviews build confidence (GWOM6)	0.924			
Authentic user experiences (GWOM7)	0.824			
Independent recommendations (GWOM8)	0.934			
Community based social validation (GWOM9)	0.931			
PPV		0.980	0.844	0.977
Material durability and robustness (PPV1)	0.910			
Comfort in use (PPV2)	0.923			
Sewing/finishing quality (PPV3)	0.923			
Timeless and modern design (PPV4)	0.919			
Fit with personal lifestyle (PPV5)	0.904			
Pride in wearing the product (PPV6)	0.933			
Perceived contribution to the environment (PPV7)	0.929			
Pride in supporting responsible brand (PPV8)	0.914			
Long-term investment in sustainability (PPV9)	0.922			
GT		0.980	0.859	0.977
Value alignment (GT1)	0.926			
Environmental concern (GT2)	0.924			
Believability (GT3)	0.924			
Performance reliability (GT4)	0.924			
Transparency (GT5)	0.938			
Trustworthiness (GT6)	0.932			
Consistency of words and actions (GT7)	0.922			
Perceived honesty (GT8)	0.927			
GPI		0.971	0.849	0.964
Strong intention to buy sustainable fashion (GPI1)	0.924			
Green fashion as first choice (GPI2)	0.922			
Prioritizing sustainable over conventional (GPI3)	0.917			
Plan to switch to eco-friendly brands (GPI4)	0.931			
Willing to pay higher prices (GPI5)	0.928			
Willing to pay extra costs for environment (GPI6)	0.908			

on the fit benchmarks of CB SEM. Approximate indicators, Standardized root mean square residual (SRMR), NFI, d_ULS, and d_G, were reported and interpreted as supportive evidence of adequate model fit (Henseler *et al.,* 2014; Hair *et al.,* 2021). Mediation analysis employed the variance accounted for (VAF) method (Hair *et al.,* 2019) to classify indirect effect sizes. To address common method variance (CMV), procedural controls (anonymity, randomized item order, neutral wording) were applied, complemented by statistical tests: Harman's single-factor test (42.3%, <50%), full collinearity

variance inflation factor with VIF < 3.3 (Kock, 2015), and a common latent factor (CLF) test showing $\Delta R^2 <$ 0.05, confirming minimal CMV bias. Lastly, construct reliability values exceeding 0.96 were evaluated for redundancy. Despite high values, the analysis at the item level revealed distinct indicators (0.82–0.94 loadings) capturing complementary functional, aesthetic, and symbolic components and cognitive–affective components, thereby ensuring sufficient discriminant validity.

RESULTS AND DISCUSSION

A total of 358 valid responses were collected from consumers of sustainable fashion in Indonesia. The sample predominantly comprised urban, educated, middle-income adults, with respondents fairly gender balanced (52.5% female), mostly aged 25–54 years (78%), and 79.4% holding a university degree. A significant number of participants indicated earning monthly incomes in the range of USD 179 to 359, alongside fashion budgets of USD 30 to 120, which implies they have a reasonable capacity to purchase premium sustainable fashion. This profile is consistent with the country's emerging sustainable fashion segment and suggests that the respondents represent typical early adopters of sustainable fashion products.

Psychometric validation and measurement quality

The assessment of the measurement model indicated remarkable psychometric characteristics that exceed strict quality criteria for consumer behavior research using PLS-SEM methodology, detailed in Table 1.

Table 1 shows that all constructs achieved excellent internal consistency, with Cronbach's α ranging from 0.964 to 0.981 and composite reliability from 0.971 to 0.983, all exceeding the recommended 0.70 threshold. The convergent validity was deemed satisfactory, with all average variance extracted (AVE) values ranging from 0.844 to 0.866, which signifies that the indicators account for over 84% of the variance in their respective constructs (Hair *et al.,* 2021). All 32 indicators loaded strongly on their intended constructs, with standardized loadings between 0.824 and 0.938, confirming robust indicator–construct relationships. Discriminant validity was supported by HTMT ratios between 0.692 and 0.757, all below the conservative 0.85 criterion, indicating that the latent variables remain empirically distinct despite conceptual relatedness (Henseler *et al.,* 2015).

Table 2 confirms discriminant validity through heterotrait-monotrait (HTMT) ratios, with all values below the conservative 0.85 threshold (range: 0.692-0.757). Although constructs illustrate anticipated theoretical connections, they are still empirically distinct, thereby justifying their consideration as separate latent variables in structural analysis. The lowest HTMT between GT and GWOM (0.692) indicates particularly strong discriminant validity despite their conceptual connection in trust formation processes (Henseler *et al.,* 2015).

Structural model validation and explanatory power

Model fit assessment demonstrated exceptional quality across multiple índices in Table 2.

Table 3 reveals SRMR of 0.020, substantially below the 0.08 threshold indicating excellent fit, while NFI of 0.949 exceeds the 0.90 threshold, confirming the structural model captures 94.9% of data covariance relative to the baseline model. Additional indices (d_ULS = 0.208, d_G = 0.432) provide additional support for the adequacy of the model, with consistent values observed in both saturated and estimated models confirming stability (Hair *et al.,* 2021).

Table 4 reports R^2 values of 0.643 for GPI and 0.570 for GT, indicating that the model explains 64.3% of the variance in green purchase intention and 57.0% of the variance in green trust. These values surpass the 0.50 threshold that is typically regarded as significant in behavioral research, indicating that the

Table 2: Discriminant validity

Construct	GPI	GT	GWOM	PPV
GPI				
GT	0.752			
GWOM	0.707	0.692		
PPV	0.757	0.738	0.744	

Table 3. Model fit assessment

Model fit	Saturated model	Estimated model
SRMR	0.020	0.020
d_ULS	0.208	0.208
d_G	0.432	0.432
Chi-square	875.572	875.572
NFI	0.949	0.949

Table 4: R-square

Construct	R-Square	R-square adjusted
GPI	0.643	0.639
GT	0.570	0.568

Table 5: Hypothesis testing results

	Hypothesis (H)	*β*	P-value	Decision
H1	GWOM influences GT	0.325	0.000	Accepted
H2	GWOM influences GPI	0.212	0.002	Accepted
H3	PPV influences GT	0.485	0.000	Accepted
H4	PPV influences GPI	0.330	0.000	Accepted
H5	GT influences GPI	0.348	0.000	Accepted
H6	GT mediates GWOM and GPI	0.113	0.003	Accepted
H7	GT mediates PPV and GPI	0.169	0.000	Accepted

structural model possesses considerable explanatory strength for the primary endogenous constructs (Hair *et al.,* 2022).

Direct effects and hypothesis validation

Table 5 presents hypothesis testing results with all seven hypotheses receiving empirical support ($p < 0.05$), confirming significant relationships among constructs. GWOM demonstrated significant positive effects on both GT ($\beta = 0.325$, $p < 0.001$) and GPI ($\beta = 0.212$, $p = 0.002$), validating dual pathways through trust-mediated and direct normative influence mechanisms. The results of this study affirm that consumers who receive positive GWOM communications, which encompass peer recommendations, online reviews, shared experiences, and community validation, tend to develop a markedly higher level of trust in green fashion brands and stronger PI (Siyal *et al.,* 2021).

GWOM contributes to GT and GPI by providing credible information regarding product performance and environmental authenticity that consumers cannot easily verify on their own. By means of peer suggestions, collective experiences, and community endorsement, GWOM presents social proof that sustainable fashion decisions are normatively embraced, thus diminishing perceived risk by signaling the satisfactory results encountered by other consumers (Ahmad *et al.,* 2023; Yanti *et al.,* 2025). However, the stronger influence of PPV on GT compared to GWOM indicates that experiential and tangible value perceptions exert greater influence than social communications in building trust toward sustainable fashion brands (Bailey *et al.,* 2025; Li *et al.,* 2024). This discovery implies that although social influence plays a role in offering initial comfort, the development of trust is fundamentally based on consumers' personal assessment of the value signals

associated with the product. When consumers perceive sustainable fashion products as delivering superior value across multiple dimensions, functional value through material durability, comfort, and quality; aesthetic value through timeless design, lifestyle fit, and pride in wearing; and symbolic sustainability value through environmental contribution and responsible brand support, they develop substantially higher trust in brand environmental commitments (Henninger *et al.,* 2020). Significantly, the importance of pride in wearing serves as one of the most powerful indicators of value, emphasizing the crucial role of symbolic and emotional significance in the consumption of sustainable fashion. Sustainable fashion functions not only as a utilitarian product choice but also as an identity signal through which consumers express moral values, environmental concern, and social positioning. In line with identity signaling and self-congruity perspectives, wearing sustainable fashion yields emotional gratification by matching personal values with one's outward look, which may take precedence over solely functional or economic aspects, especially for urban, educated consumers who desire social recognition through responsible consumption (Henninger *et al.,* 2020; Bailey *et al.,* 2025). This pattern aligns with Signaling Theory, which posits that costly signals, such as investments in high-quality materials, sustainable production processes, and superior design, are more credible than low-cost signals like word-of-mouth alone, especially in contexts characterized by information asymmetry and greenwashing concerns (Li *et al.,* 2024). The value perceived by consumers regarding a product also has a direct influence on GPI, which indicates that they consider sustainable fashion as a whole rather than merely on the basis of environmental credentials. This extends the Theory of Planned Behavior by demonstrating that behavioral beliefs related to multidimensional product attributes shape purchase intentions independently of social normative pressures, thereby offering multiple leverage points for environmental management interventions targeting sustainable consumption (Hagger, 2025; Yanti *et al.,* 2025). Green trust has emerged as the most significant direct predictor of green purchase intention, thereby affirming its function as the primary psychological mechanism that converts positive environmental attitudes are translated into concrete purchasing intentions. Trust reduces perceived risk and uncertainty associated with sustainable fashion purchases, particularly when environmental benefits represent credence attributes that cannot be verified through inspection or short-term consumption experience (Henninger *et al.,* 2020). Trust thus operates as a cognitive shortcut that enables consumers to overcome decision complexity and commit to sustainable alternatives despite potential trade-offs related to price, availability, or aesthetics, directly supporting pollution reduction and textile waste minimization objectives (Bailey *et al.,* 2025; Shamsuzzaman *et al.,* 2025). T The significant emphasis on transparency within the framework of green trust further illustrates the institutional and market circumstances of emerging economies, including Indonesia. In environments where regulatory enforcement is uneven and greenwashing practices are widely reported, consumers prioritize access to clear, verifiable, and detailed sustainability information as a prerequisite for trust formation. Transparency serves as a fundamental indicator of trust, allowing consumers to evaluate the reliability of environmental assertions prior to contemplating more profound relational aspects like competence or benevolence. This context-specific salience underscores that trust formation mechanisms in emerging markets differ from those in developed economies, where institutional trust and regulatory safeguards may already be taken for granted (Rama *et al.,* 2024; Li *et al.,* 2024). The mediation analysis further clarifies the psychological mechanisms through which GWOM and PPV influence GPI. The indirect influence of GWOM as mediated by GT indicates that social interactions chiefly boost purchase intentions by fortifying trust rather than relying solely on direct persuasion. In contrast, the larger indirect effect of PPV through GT demonstrates that value-based trust grounded in product experience constitutes a more powerful pathway to intention formation than social influence. This asymmetry reinforces the signaling perspective, suggesting that investments in sustainable materials, eco-friendly production, and superior design generate signals that are costly to imitate and therefore less susceptible to opportunistic greenwashing, fostering deeper and more resilient trust (Shamsuzzaman *et al.,* 2025; Bailey *et al.,* 2025). Despite the common association of sustainable

fashion products with elevated prices, the findings presented here imply that price is a secondary concern compared to perceived value and trust among early adopters who have the financial capability to make purchases. Higher prices appear to be cognitively justified when products deliver superior functional, aesthetic, and symbolic value, with price interpreted as a signal of quality and authenticity rather than merely a cost. Nevertheless, this value-based justification may not generalize to more price-sensitive consumer segments, indicating that price sensitivity is more likely to moderate the strength of the PPV toward GPI through GT relationship rather than eliminate it altogether. This boundary condition emphasizes the necessity for future studies to investigate the variations among income groups and consumption contexts. From a theoretical standpoint, these results contribute to the literature on environmental management and sustainable consumption in multiple ways. First, by establishing green trust as a dual mediating mechanism linking both social influence and experiential value evaluation to purchase intention, this study extends prior research that has typically focused on single mediation pathways. Trust is shown to operate as a general psychological mechanism activated through distinct yet complementary routes, social validation via GWOM and experiential evaluation via PPV, providing a unified framework for understanding sustainable fashion adoption. Second, the more significant impact of perceived product value in comparison to green word-of-mouth contests the dominant focus on communication-oriented strategies within green marketing studies, indicating that meaningful value generation serves as the essential basis of trust. Third, confirming the multidimensional nature of perceived product value demonstrates that environmental benefits alone are insufficient to drive sustainable consumption; products must also deliver superior functional, aesthetic, and symbolic performance to justify premium pricing and compete with conventional alternatives (Henninger *et al.,* 2020; Shamsuzzaman *et al.,* 2025). The model's relatively high explanatory power suggests a strong ability to capture the fundamental psychological mechanisms that drive sustainable fashion purchase intentions among early adopters. Nevertheless, this does not indicate that the model is complete. Other factors, such as moral norms, environmental concern, price sensitivity, or greenwashing skepticism, may explain additional variance and should be incorporated in future research. Moreover, while signaling theory offers a robust framework for interpreting the development of trust, the lack of clear metrics for skepticism or perceived greenwashing constitutes a theoretical limitation. The present interpretations rest on observed trust outcomes rather than consumers' conscious detection of deceptive practices, suggesting that future studies incorporating distrust-related constructs would further refine understanding of signal interpretation under heightened skepticism. From an environmental management perspective, these findings carry important policy and managerial implications. Policymakers can strengthen trust formation by enforcing mandatory supply chain disclosure, standardized eco-labeling, and stringent greenwashing regulations to reduce information asymmetry and enhance transparency. At the firm level, sustainable fashion brands should prioritize authentic trust-building through verifiable sustainability communication while simultaneously investing in tangible value creation, including superior material quality, comfort, design excellence, and product longevity. Positioning sustainable fashion as aspirational, desirable, and socially prestigious, instead of solely ethical, can expedite behavioral changes among consumers and lead to significant decreases in carbon emissions, water consumption, and textile waste generation (Li *et al.,* 2024; Shamsuzzaman *et al.,* 2025). This study primarily addresses positive trust-building mechanisms; however, future investigations that consider negative green word-of-mouth and perceived greenwashing would yield a more detailed exploration of trust formation and erosion dynamics in sustainable fashion markets (Nguyen *et al.,* 2019; Li *et al.,* 2024).

CONCLUSION

This study demonstrates that green word-of-mouth and perceived product value jointly shape green purchase intention in sustainable fashion, primarily through the formation of green trust. Perceived product value exerts a stronger influence on green trust than green word-of-mouth, and green trust emerges as the strongest direct predictor of green purchase intention, highlighting the central role of value-based trust in narrowing the attitude–behavior

gap in emerging-market fashion contexts.

From a policy standpoint, the results indicate that regulators ought to focus on establishing mechanisms that facilitate transparency and credible value delivery. In Indonesia, this can include phased mandatory disclosures of key sustainability indicators such as certified fibre content, basic wastewater treatment practices, and minimum wage and safety compliance information, as well as standardized and independently verified eco-labels that summarize a small set of core attributes in a simple, comparable format. Product-oriented standards that reward durability, including benchmarks for minimum fabric strength, repairability labels, and extended producer responsibility initiatives for take-back and recycling, would strengthen the perceived value of products and support circular economy aims by extending the lifespan of products and decreasing textile waste. Managerially, the results indicate that sustainable fashion brands, including small and medium enterprises, should concentrate on achievable, high-leverage improvements in perceived product value and trust rather than relying on diffuse sustainability messaging. For firms with limited resources, this may entail concentrating on a cohesive yet restricted product assortment that utilizes superior quality materials and finishes, investing in one or two hallmark design features that convey a sense of timelessness and durability, and offering straightforward yet credible transparency, such as revealing supplier locations, material certifications, or essential production processes through low-cost digital channels. Collaboration through industry associations or shared certification schemes can help small and medium enterprises meet disclosure and labelling expectations without bearing the full cost individually, making recommended strategies more feasible in the Indonesian context. The study also identifies several avenues for future studies. By broadening the model to account for genuine purchasing behavior, repeat buying, and post-purchase advocacy, including referrals, social media endorsements, or engagement in repair and resale initiatives, a more accurate evaluation of the environmental impact of green trust and perceived value could be achieved. Longitudinal designs that track consumers across multiple purchase cycles could clarify how trust is strengthened, eroded, or repaired over time, and how this dynamic relates to circular behaviors such as repair, resale, and recycling. Research comparing developed and developing markets could enhance the understanding of how institutional trust, regulatory quality, and baseline skepticism regarding green claims affect the relative significance of social versus value-based pathways to green trust, yielding deeper theoretical insight into context-specific versus generalizable mechanisms. Ultimately, subsequent studies ought to investigate the governance and enforcement challenges surrounding supply-chain disclosure and eco-labelling in Indonesia. This should encompass aspects such as monitoring capabilities, verification systems, and potential unintended burdens on small and medium enterprises, to ensure that trust-enhancing measures are both efficient and feasible for implementation.

AUTHOR CONTRIBUTIONS

P. Yanti contributed to conceptualization, literature review, methodology, instrument development, investigation, data curation, formal analysis, visualization, and writing original draft. M. Gunarto contributed to conceptualization, supervision, methodology, validation, writing review and editing, project administration, and funding acquisition. R. Yusiana contributed to investigation, data curation, validation, and writing review and editing. L. Yohanna contributed to investigation, data curation, validation, and writing review and editing. R. Indriarti contributed to resources, data curation, validation, and writing review and editing. Y. Yuliawati contributed to conceptualization, methodology, validation, and writing review and editing. All authors read and approved the final manuscript and agree to be accountable for all aspects of the work.

ACKNOWLEDGEMENT

The authors express sincere gratitude to the Indonesian Education Scholarship (BPI), the Center for Higher Education Funding and Assessment (PPAPT), the Indonesian Endowment Fund for Education (LPDP), and the Ministry of Higher Education, Science, and Technology (Kemdiktisaintek) with the Grant number: [02430/BPPT/BPI.06/9/2023]; [00375/BPPT/BPI.06/9/2023] and [01289/BPPT/BPI.06/9/2023].

CONFLICT OF INTEREST

The authors declare that there is no conflict of

interests regarding the publication of this manuscript. In addition, the ethical issues, including plagiarism, informed consent, misconduct, data fabrication and/or falsification, double publication and/or submission, and redundancy have been completely observed by the authors.

OPEN ACCESS

©2026 The author(s). This article is licensed under a Creative Commons Attribution 4.0 International License, which permits use, sharing, adaptation, distribution and reproduction in any medium or format, as long as you give appropriate credit to the original author(s) and the source, provide a link to the Creative Commons license, and indicate if changes were made. The images or other third-party material in this article are included in the article's Creative Commons license, unless indicated otherwise in a credit line to the material. If material is not included in the article's Creative Commons license and your intended use is not permitted by statutory regulation or exceeds the permitted use, you will need to obtain permission directly from the copyright holder. To view a copy of this license, visit: http://creativecommons.org/licenses/by/4.0/

PUBLISHER'S NOTE

GJESM Publisher remains neutral with regard to jurisdictional claims in published maps and institutional afflictions.

Negative AI Statement

The author(s) declare that no AI tools or services were not used or not highly applied during the preparation of this work.

ABBREVIATIONS

%	Percent
α	Cronbach's alpha
β	Path coefficients
λ	Loading factor
AVE	Average variance extracted
CR	Composite reliability
d_G	Geodesic discrepancy
d_ULS	Unweighted least squares discrepancy
GPI	Green purchase intention
GT	Green trust
GWOM	Green word-of-mouth
H	Hypothesis
HTMT	Heterotrait-Monotrait ratio
NFI	Normed fit index
PLS-SEM	Partial least squares structural equation modeling
PPV	Perceived product value
R^2	R-square (coefficient of determination)
RQ	Research question
SEM	Structural equation modeling
SRMR	Standardized root mean square residual
TPB	Theory of planned behavior
USD	United States Dollar
VAF	Variance accounted for
VBN	Value-belief-norm theory
VIF	Variance inflation factor
WOM	Word-of-mouth

REFERENCES

Abbate, S.; Centobelli, P.; Cerchione, R.; Nadeem, S.P.; Riccio, E., (2024). Sustainability trends and gaps in the textile, apparel and fashion industries. Environ. Dev. Sustain., 26(2): 2837-2864 **(28 pages).**

Ahmad, W.; Kim, W.G.; Anwer, Z.; Zhuang, W., (2023). Schwartz personal values, theory of planned behavior and environmental consciousness: How tourists' visiting intentions towards eco-friendly destinations are shaped? J. Bus. Res., 110: 228-236 **(9 pages).**

Bailey, K.; Basu, A.; Sharma, S., (2025). A review of fast fashion and environmental research gaps in the top garment-producing countries. Environ. Rev., 33(2): 1-18 **(18 pages).**

Centobelli, P.; Abbate, S.; Nadeem, S.P.; Garza-Reyes, J.A., (2022). Slowing the fast fashion industry: An all-round perspective. J. Clean. Prod., 366: 132894 **(9 pages).**

Connelly, B.L.; Certo, S.T.; Reutzel, C.R.; DesJardine, M.R.; Zhou, Y.S., (2025). Signaling Theory: State of the Theory and Its Future. J. Manag., 51(1): 24-61 **(38 pages).**

Daga, K.; Islam, S.; Yadav, R., (2025). Structural analysis of sustainable fashion adoption: An integrated TISM and MICMAC approach. J. Sustain. Mark., 2025-149: 1-25 **(25 pages).**

Fischer, D.; Böhme, T.; Geiger, S.M., (2017). Measuring young consumers' sustainable consumption behavior: Development and validation of the YCSCB scale. Young Consum., 18(3): 312-326 **(15 pages).**

Hagger, M.S., (2025). Progress on theory of planned behavior research: advances in theory, measurement, and application. Health Psychol. Rev., 19(1): 1-25 **(25 pages).**

Hair, J.F.; Hult, G.T.M.; Ringle, C.M.; Sarstedt, M.; Danks, N.P.; Ray, S., (2021). Partial least squares structural equation modeling (PLS-SEM) using R: A workbook. Springer Nature.

Hair, J.F.; Risher, J.J.; Sarstedt, M.; Ringle, C.M., (2019). When to use and how to report the results of PLS-SEM. Eur. Bus. Rev., 31(1): 2-24 **(23 pages).**

Hameed, I.; Waris, I.; Haq, M.A., (2022). The role of green practices toward the green word-of-mouth and purchase intention: The moderating effect of concern for self-presentation. J. Hosp. Tour. Technol., 13(3): 445-463 **(19 pages).**

Henninger, C.E.; Alevizou, P.J.; Goworek, H.; Ryding, D., (2020). Sustainability in fashion: A cradle to upcycle approach. Springer.

Henseler, J.; Ringle, C.M.; Sarstedt, M., (2015). A new criterion for assessing discriminant validity in variance-based structural equation modeling. J. Acad. Mark. Sci., 43(1): 115-135 **(21 pages).**

Khan, S.N.; Mohsin, M.; Sun, G.; Abbas, H., (2025). Sustainable fashion trends and purchasing pattern: The role of green WOM and trust. J. Retail. Consum. Serv., 82: 104012 **(15 pages)**

Kock, N., (2015). Common method bias in PLS-SEM: A full collinearity assessment approach. Int. J. e-Collab., 11(4): 1-10 **(10 pages).**

Li, M.; Zhang, Y.; Chen, W.; Liu, H., (2024). How perceived sustainability influences consumers' perceived quality and purchase intention in sustainable fashion. Text. Res. J., 94(1): 178-195 **(18 pages).**

Li, Z.; Wang, J.; Liu, Y., (2024). The carbon footprint of fast fashion consumption and mitigation strategies: A case study of jeans. Sci. Total Environ., 924: 171508 **(12 pages).**

Margariti, K.; Hatzithomas, L.; Boutsouki, C., (2024). Elucidating the gap between green attitudes, intentions, and behavior: The role of green trust and perceived greenwashing. Sustainability, 16(12): 5216 **(13 pages).**

McNeill, L.; Venter, B., (2019). Identity, self-concept and young women's engagement with collaborative, sustainable fashion consumption models. Int. J. Consum. Stud., 43(4): 368-378 **(11 pages).**

Nguyen, T.T.H.; Yang, Z.; Nguyen, N.; Johnson, L.W.; Cao, T.K., (2019). Greenwash and green purchase intention: The mediating role of green skepticism. Sustainability, 11(9): 2653 **(23 pages).**

Niinimäki, K.; Peters, G.; Dahlbo, H.; Perry, P.; Rissanen, T.; Gwilt, A., (2020). The environmental price of fast fashion. Nat. Rev. Earth Environ., 1(4): 189-200 **(12 pages).**

Olivar Aponte, N.; Sandoval-Escobar, S.; Sandoval-Escobar, M., (2024). Fast fashion consumption and its environmental impact: A literature review. Sustain. Sci. Pract. Policy, 20(1): 2381871 **(15 pages).**

Parajuly, K.; Fitzpatrick, C.; Muldoon, O.; Kuehr, R., (2020). Behavioral change for the circular economy: A review with focus on electronic waste management in the EU. Resour. Conserv. Recycl. X, 6: 100035 **(15 pages).**

Piribauer, B.; Bartl, A., (2024). Mobilisation of textile waste to recover high added value products and energy for the transition to circular economy. Environ. Res., 243: 117838 **(12 pages).**

Rahaman, T.; Abdullah, M.; Hossain, M.J., (2024). Green merchandising of textiles and apparel in a circular economy: A systematic literature review. Sustain. Prod. Consum., 51: 217-234 **(26 pages).**

Rama, A.S.; Yasri; Susanto, P., (2024). The effect of environmental awareness as a moderation on determinants of green product purchase intention. Global J. Environ. Sci. Manage., 10(2): 699-712 **(14 pages).**

Ringle, C.M.; Wende, S.; Becker, J.M., (2022). SmartPLS 4. Oststeinbek: SmartPLS GmbH.

Shamsuzzaman, M.; Rahman, M.M.; Label, K.A., (2025). Fashion and textile waste management in the circular economy: A systematic review. Clean. Waste Syst., 9: 100166 **(19 pages).**

Sharma, I.; Sharma, S.; Aggarwal, A.; Gupta, S., (2024). Mapping the Theory of Consumption Values: A Systematic Review Using the TCCM Approach. J. Consum. Behav., 24(2): 562-610 **(49 pages).**

Suki, N.M., (2016). Green product purchase intention: Impact of green brands, attitude, and knowledge. Br. Food J., 118(12): 2893-2910 **(18 pages).**

Tian, H.; Liu, X., (2022). Pro-Environmental Behavior Research: Theoretical Progress and Future Directions. Int. J. Environ. Res. Public Health, 19(11): 6721 **(16 pages).**

Todeschini, B.V.; Cortimiglia, M.N.; Callegaro-de-Menezes, D.; Ghezzi, A., (2017). Innovative and sustainable business models in the fashion industry: Entrepreneurial drivers, opportunities, and challenges. Bus. Horiz., 60(6): 759-770 **(12 pages).**

Yanti, P.; Gaffar, V.; Harisandi, P.; Ramadhani, I.; Yuliawati, T.; Yusriani, S., (2025). Bibliometric and narrative review of environmental management on green behavior education for sustainable development. Global J. Environ. Sci. Manage., 11(4): 1819-1838 **(20 pages).**

AUTHOR (S) BIOSKETCHES

Yanti, P., Dr. Candidate in Management, Faculty of Economics and Business Education, Universitas Pendidikan Indonesia, Jl. Dr. Setiabudi No.229, Bandung, West Java, Indonesia
- Email: *pitri0816@upi.edu*
- ORCID: 0009-0008-1402-6240
- Web of Science ResearcherID: ORI-1991-2025
- Scopus Author ID: 59482995300
- Homepage: https://scholar.google.com/citations?user=w_k_DBgAAAAJ&hl=id

Gunarto, M., Dr., Associate Professor, Faculty of Economics and Business, Sriwijaya University, Palembang, South Sumatra Indonesia.
- Email: *mgunarto@hotmail.com*
- ORCID: 0000-0001-9494-2127
- Web of Science ResearcherID: R-9960-2016
- Scopus Author ID: 57203388622
- Homepage: https://scholar.google.com/citations?user=432BBXMAAAAJ&hl=en

Yusiana, R., Dr. Candidate in Management, Faculty of Economics and Business Education, Universitas Pendidikan Indonesia, Jl. Dr. Setiabudi No.229, Bandung, West Java, Indonesia
- Email: *rennytayusiana@upi.edu*
- ORCID: 0000-0001-7505-0051
- Web of Science ResearcherID: AAC-5335-2021
- Scopus Author ID: 57203370265
- Homepage: https://scholar.google.com/citations?hl=id&user=MorAciAAAAAJ&view_op=list_works&sortby=pubdate

Yohanna, L., Dr. Candidate in Management, Faculty of Economics and Business Education, Universitas Pendidikan Indonesia, Jl. Dr. Setiabudi No.229, Bandung, West Java, Indonesia
- Email: *larisayohanna@upi.edu*
- ORCID: 0000-0002-9292-2699
- Web of Science ResearcherID: ADG-6554-2022
- Scopus Author ID: 57214126731
- Homepage: https://scholar.google.com/citations?user=imyHvCsAAAAJ&hl=id

Indriarti, R., Dr. Candidate in Management, Faculty of Economics and Business Education, Universitas Pendidikan Indonesia, Jl. Dr. Setiabudi No.229, Bandung, West Java, Indonesia
- Email: *restiarti@upi.edu*
- ORCID: 0009-0008-7467-6085
- Web of Science ResearcherID: NA
- Scopus Author ID: NA
- Homepage: https://scholar.google.com/citations?hl=en&user=LLiQuvMAAAAJ&view_op=list_works&sortby=pubdate

Yuliawati, Y., Dr., Management, Faculty of Economics, Universitas Islam Nusantara, Bandung, West Java, Indonesia
- Email: *yupi@uninus.ac.id*
- ORCID: 0000-0002-8939-7029
- Web of Science ResearcherID: NA
- Scopus Author ID: NA
- Homepage: https://scholar.google.com/citations?hl=id&user=OLmcOeYAAAAJ&view_op=list_works&sortby=pubdate

HOW TO CITE THIS ARTICLE

Yanti, P.; Gunarto, M.; Yusiana, R.; Yohanna, L.; Indriarti, R.; .; Yuliawati, Y., (2026). Customer-driven socio-environmental sustainability in fashion: The role of green word-of-mouth and perceived product value. Global J. Environ. Sci. Manage., 12(1): 191-206.

DOI: 10.22034/gjesm.2026.01.11

URL: https://www.gjesm.net/article_733202.html



Global J. Environ. Sci. Manage. 12(1): 207-228, Winter 2026, Serial #45

Global Journal of Environmental Science and Management
(GJESM)

Homepage: https://www.gjesm.net/

Podcasts

CASE STUDY

Environmental impact of mining and its social responsibilities on rural communities

C.J. Huamaní[1,*], J.C. Palomino Aroni [1], H.D. Calderon Vilca[2], J.L. León Vicencio[1], G. Suyo Cruz[3], D.A. Pinto Pagaza[1], B.O. Mamani Huillca[1], W. Orós Torres[1], S.R. Pinto Boda[1], L. Contreras Salas[1]

[1] Department of Administration, National University Micaela Bastidas of Apurímac, Victor Acosta II Etapa, Tamburco, Apurímac 03001, Perú

[2] Department of Software Engineering, National University of San Marcos, Av. Carlos Germán Amezaga #375, Cercado de lima, Lima 15081, Perú

[3] Department of Administration, National University San Antonio Abad of Cusco, Av. de la Cultura, Cusco, Cusco 08000, Perú

ARTICLE INFO

Article History:
Received 04 July 2025
Revised 11 October 2025
Accepted 14 November 2025

Keywords:
Agricultural production
Community impact
Livestock activity
Social responsibility

ABSTRACT

BACKGROUND AND OBJECTIVES: Mining activities generate significant economic, social, and environmental challenges that affect the sustainability of surrounding local communities. social responsibility is a fundamental mechanism for mitigating negative impacts and improving local well-being. The primary goal of this article was to investigate the ecological consequences of the Las Bambas mining company's operations on the local residents of the Cotabambas community in Peru.

METHODS: This research employed a mixed-methods design, combining qualitative and quantitative approaches. This study was conducted was characterized as a non-experimental, cross-sectional study aimed at providing explanatory insights. A five-point Likert scale questionnaire (1 = very frequently to 5 = never) was designed, validated, and administered to 377 residents living within the area of influence of a large-scale mining operation. Additionally, semi-structured interviews were conducted with 10 local authorities and political representatives, supplemented by an observation checklist adapted from previous studies. Four hypotheses were established to examine the relationship between mining operations and their social responsibility initiatives, along with their influence on the adjacent community.

FINDINGS: The findings revealed strong associations between mining social responsibility and environmental variables ($n = 377$, $p < 0.05$): Rho = 0.610 for residents' perceptions, Rho = 0.575 for water resources, Rho = 0.510 for agricultural production, and Rho = 0.720 for livestock activity. These results imply that activities related to social responsibility are connected to mining, and as a result, they have not adequately addressed environmental degradation, causing detrimental effects on the water, soil, air, flora, and fauna in the surrounding communities, thereby impacting the quality of life of the population.

CONCLUSION: Mining social responsibility practices show moderate statistical associations with environmental impact indicators in Cotabambas, with Spearman's correlation coefficients ranging from 0.489 to 0.546 (p-value < 0.05 in all cases). Despite continuous social responsibility efforts, these measures have not successfully alleviated the perceived environmental decline, especially in agricultural production and livestock operations. The evidence underscores the need to strengthen measurable, impact-oriented social responsibility strategies focused on ecological restoration and sustainable rural livelihoods in mining areas.

DOI: 10.22034/gjesm.2026.01.12

This is an open access article under the CC BY license (http://creativecommons.org/licenses/by/4.0/).

NUMBER OF REFERENCES
88

NUMBER OF FIGURES
3

NUMBER OF TABLES
10

*Corresponding Author:
Email: *jhuamani@unamba.edu.pe*
Phone: + 98 689 1529
ORCID: 0000-0003-0404-8557

Note: Discussion period for this manuscript open until Mar 1, 2026 on GJESM website at the "Show Article".

INTRODUCTION

Today, the mining sector plays a fundamental role in the economic and social progress of developing countries, particularly in Latin America (Chile, Bolivia, Brazil, and Peru), as these countries account for more than 85 percent (%) of mineral exports in the region (OECD, 2022). Nevertheless, the mining sector is encountering mounting pressure to implement more sustainable methods and tackle environmental and social challenges, as nations across the globe are progressing towards more stringent environmental regulations and heightened public consciousness, with social responsibility becoming a significant focus for the sector (Haroon *et al.,* 2025; Ullah *et al.,* 2024). In fact, this reconfiguration is represented in a recent study by Global Data, which states that more than 140 mining companies globally are framing leaps and bounds towards minimizing net zero emission reductions, with a roadmap for decarbonization (Maher *et al.,* 2019). Recent studies carried out by McKinsey point out the obstacles that political systems, shareholders, and citizens must navigate in order to decrease the greenhouse gas emissions associated with mining, which range from 4% and 7% (Bansal *et al.,* 2024; Delevingne *et al.,* 2020). Precisely in the emerging economies of the Southern Hemisphere, which encompasses the areas of Latin America and Africa, countries such as Peru, Bolivia, and Chile are committed to high levels of ecological variety, in accordance with the operations of mining sites that are manipulated in environmentally vulnerable terrains (Bansal *et al.,* 2024). Indeed, the impact on communities, whose economy is built on the exploitation of minerals, has been negative, and for academics in Latin America it has a different consideration than in other regions, since it attracts more attention from the point of view of the study of mining companies (Akchurin, 2020). Latin America has a concentration of approximately 66% of lithium reserves worldwide, specifically in Chile and Peru. Countless researchers around the world also call them "Saudi Arabia of lithium" because 47% of copper, 45% of silver, and 21% of zinc are found in this part of the world (CEPAL, 2020). Likewise, the South American region possesses roughly 15% of the world's total reserves, which include iron, lead, and 11% of gold (Zornoza Bonilla, 2022). According to the World Bank, by 2050, the need for raw materials will increase significantly by 965% for lithium, 383% for graphite and 108% for nickel (Kulczycka *et al.,* 2023; Montalván *et al.,* 2023). Consequently, the South American region has territories with rich resources and a considerable increase in mining activities, which are placed in serious problems for economic development with the preservation of the environment, along with social considerations that include communities that continue to be the object of concern due to lack of participation (Ho *et al.,* 2024). These problems have caused the increase of social conflicts, as noted by the Observatorio de Conflictos Mineros de América Latina (OCMAL), it maintains that the number of defenders of their territories and natural resources have been violently killed with a figure of 212 people in 2019, and Latin American countries corresponded to 66% of those affected, highlighting among them countries such as Colombia and Peru (Vershinina, 2022). Specifically, mining activities such as Las Bambas are regulated by a set of laws and regulatory frameworks established in the political constitution of Peru, the main ones being the General Environmental Law (2005), the Law of the National Environmental Impact Assessment System (2001), and the General Mining Law (1992), all aimed at safeguarding environmental sustainability. However, recent reports from the Environmental Assessment and Enforcement Agency indicate persistent deficiencies in environmental management, including water resource pollution and poor waste management practices, demonstrating non-compliance with environmental regulations and generating social conflicts with local communities. The principle of social responsibility (SR) has been a component of corporate discourse for several decades. Its origins trace back to the debate between Berle and Dodd during the Great Depression, published in a series of articles in the Yale Law Journal (Berle, 1931) argued that SR should be understood as "corporate power exercised in trust" for shareholders. The works of Bansal and Sonf (2016) and Montiel (2008) serve as a foundation for understanding RS and Corporate Sustainability (CS). These authors assert that Social Responsibility (SR) is fundamentally linked to societal and social challenges, which require active participation from stakeholders. Conversely, CS is primarily focused on environmental management, offering a distinct interpretation of environmental protection that aligns with economic growth, and is now considered part of the wider sustainability

framework. Environmental responsibility (ER), in turn, emphasizes the adoption of sustainable practices that reduce ecological degradation, improve waste treatment, and ensure water preservation (Mari Farinós, 2016). Although these terms are often used interchangeably (Sheehy and Farneti, 2021), it is important to differentiate them clearly: SR is characterized as international private corporate self-regulation that is in accordance with transnational law and the sustainable development goals (SDGs) within the realm of business; CS signifies a wider organizational commitment that integrates environmental awareness with economic prosperity; while ER is focused on the specific actions needed to alleviate environmental damage and conserve ecosystems. However, there is very little research that specifically examines how SR impacts surrounding communities. The study by Muhammad *et al.* (2024) focused on measuring the benefits of SR initiatives by mining companies for local communities in Indonesia, while Dikgwatlhe and Mulenga (2023) analyzed the effects of mining on South African communities through four key factors to assess community perceptions. Nevertheless, a deficiency persists in thorough research focusing on SR within the mining industry, underscoring the necessity to investigate the correlation between SR practices and their effects on communities, especially through factors like water resources, agricultural output, and livestock operations. To fill this gap, the present study aims to examine whether the SR practices of the Las Bambas mining company influence the quality of life of residents in nearby communities. This study adopts a multidisciplinary framework that integrates neoclassical economic theory (NET), stakeholder theory (ST), resource curse theory (RCT), and the social license to operate (SLO) to examine how corporate social responsibility (CSR) affects surrounding communities. The RCT indicates that reliance on the extraction of natural resources may intensify economic difficulties; the SLO underscores the most efficient methods for interacting with local communities; the NET aims at optimizing economic benefits; and the ST stresses the wider economic, social, and environmental responsibilities in influencing corporate results. Although these theories differ in focus, they offer complementary perspectives that together provide a solid conceptual foundation for understanding how SR functions as a mechanism to mitigate the environmental consequences of mining activities on water resources, agricultural production, and livestock activities.

Social responsibility (SR)

SR has been a vital approach for organizations regarding social, environmental, and economic dimensions (Bernal *et al.,* 2025). Moreover, in the mining sector, SR cooperates with the progress of communities, with optimal buildings and infrastructure for both health and education that can have a positive relevance in the lifestyle of communities (Yudarwati and Tjiptono, 2017a). The relevance of examining SR has escalated over time as a result of the discourse surrounding the justification for mining companies to dedicate resources to SR initiatives (Yousefian *et al.,* 2024). Similarly, NET can explain ST, which argues that by maximizing profits, the company leader becomes the main figure of SR, based on the law that regulates activities and operations (Ferrero *et al.,* 2012). Likewise, a range of inquiries have been posed regarding SR operations, as the fundamental aim of a company is to achieve successful economic outcome (Orlitzky, 2015; Porter and Kramer, 2006). Based on this approach, mining companies must consider the proper management of resources; therefore, they must be employed to optimize corporate value. However, Stakeholder Group theory states that ethical business activity is supported by the interests of the elements involved as an example (stakeholders, communities, and natural environment), which is triggered by an increase in company's performance and economic benefit (Chia *et al.,* 2020; Harrison *et al.,* 2019). According to Yadira *et al.* (2023), SR has multiple interpretations within the academic sphere. They argue that the issue faced by companies is less about defining SR and more about comprehending how SR is socially formed in a given environment and how to utilize this knowledge in developing effective business strategies (Rathobei *et al.,* 2024). In parallel, the authors (Lindman *et al.,* 2020; Ranängen and Zobel, 2014) share the same position regarding (Hosseinpour *et al.,* 2022) the existence of various definitions of SR. Despite this, they point out that the fundamental aspect of SR can yield in how the company to achieve social, economic, and environmental sustainability must consider the problems of both internal and external stakeholders. Likewise, it was identified that the dimensions of

SR are recurrently developed, such as stakeholder, economic, social, proactive, and environmental dimensions. In addition, (Huamani Cayllahua, 2024) examines SR in a Peruvian mining company to explore its impact on the study population. On the other hand, they also analyzed more than 100 definitions of SR from peer-reviewed and gray literature published between 1963 and 2014, where they determined that there are 06 analogous dimensions such as: stakeholder, social, economic, sustainability, ethics and discretionarily (Bansal and DesJardine, 2014). It should be noted that SR is currently recognized in strategic literature and is aimed at fostering SR in companies using an innovative approach. In recent decades, academic publications have focused on three dimensions: economic, environmental and health, and safety well-being (Aguinis and Glavas, 2012; Carroll, 2015). Representative cases of current research Ashrafi *et al.* (2020) address why and how SR is articulated in business strategic determination and operational activities, with the aim of improving the viability of companies (Michelon *et al.,* 2015). From the previously exposed theories, a number of scholars have carried out initiatives to study the influence of SR and its impact on communities, and such studies over time have been gaining more attention and interest from researchers (Hou, 2019; Long *et al.* 2020). Yousefian *et al.* (2024) found that European mining companies are positively influenced by the SR initiatives carried out by these corporations, and it was observed that a few elements become important in SR or factors such as transparency and reporting, specialized preparation, sanitary quality, protection, and strategic use of resources. In Ghana, Dauda (2024) indicates that mining companies adopt SR as a framework to showcase their sustained efforts towards social and environmental standards; nonetheless, they have undertaken very few initiatives to grasp the social, cultural, economic, and political contexts of the communities that are part of it.

Impacts on the community

Over the last few decades, multiple concepts and theoretical bases have emerged to address different questions regarding planned and unplanned social consequences (Nechaev and Hain, 2023). Furthermore, the mining sector plays a vital role in economic growth as it produces essential resources for various industries and yields revenue for public entities as well as the government itself. Despite this, it also generates negative impacts that lead to the population or community, and to geographical displacement, in which it must be considered as a social problem, and environmental deterioration (Fontana, 2018; Saenz, 2018). It is relevant that mining companies tend to better control their impacts. This can be attributed to the use of sustainable activities and environmental pollution through communication with the inhabitants of the population (Yudarwati and Tjiptono, 2017b). However, RCT explains how countries that a large amount of natural wealth has, such as minerals, tend to address economic problems and generate environmental pollution (Yeboah and Nyarkoh, 2023). This randomized controlled trial indicates that an excessive reliance on resource exploitation (such as minerals) may impede the diversity of economic activities, resulting in a critical scenario for institutional management and subsequently causing adverse environmental effects (Ross, 1999). The implementation of such RCT in the mining sector facilitates an accurate analysis of critical eventualities and generates strategies to be able to reduce the impact of mining operations (Yeboah and James, 2023). On the other hand, SLO theory originates the concept specifically in the mining field and other companies dedicated to the exploitation of resources. This theory endeavors to provide an explanation of how corporations should operate to mitigate harmful social effects in the mining sector while establishing sustainable connections with the community members (Moffat *et al.,* 2016). However, there is research such as that of, Prno and Scott (2012) who in their finding determines how the SLO is transformed into a mechanism that allows companies in the mining sector to convert their business schemes to the interests of society in the context where they carry out their operations. It is feasible to find several studies and methodologies oriented in community impact assessment (CIA), in the research conducted by Molecke and Pinkse (2017) explain with a general framework from the different approaches that exist to date, on CIAs. Despite the vast array of existing literature and methodologies, a common issue persists: the significant variety of challenges faced by professionals during CIAs. This is particularly evident in the mining sector, where issues such as inadequate information management

in relation to stakeholders, an overestimation of positive impacts, and a lack of acknowledgment of negative consequences are prevalent (Blanco *et al.,* 2022; Uyar *et al.,* 2021). Regarding the concept and definition of CIA in the scientific community, there are a large number, but Rabel *et al.* (1995) when dealing with the subject of CIA, it is referred to as the results for society of any action, whether public or private, that may affect the way people live, work, manifest themselves, link with each other, how they are managed to meet their demands, and, as a whole, have to face life as a member of society. When mentioned in CIAs, it can also allude to a variety of problems, regarding the conversion of living of people, their customs, their personal development, their physical integrity, their concerns, and their goals (Cerioni and Marasca, 2021). In the literature presents a diverse array of elements that evaluate the CIA, as indicated in the earlier paragraph. According to Jones *et al*. (2017), two issues are characterize as follows. In the first instance, defining the indicators of the CIA accurately is an extremely complex activity because such research field change is highly developed in the literature and constantly changing. In the second instance, it is possible to quantify CIA objectively, if not subjectively (de Lange *et al.,* 2016; Jones *et al.,* 2017). In comprehensive studies focused on information collection, the CIAs are often investigated from the viewpoint of individuals or populations, using water resources, agricultural production, and agricultural activity as evaluative measures. This strategy leads to a more objective result and greater measurement accuracy; hence, the application in this study (Kaymaz, 2023; Nechaev and Hain, 2023). Studies such as (Bebbington y Williams 2008) demonstrate how mining can significantly alter both the quantity and quality of water available in high-Andean watersheds, directly affecting community water services and creating a clear transmission channel toward other productive uses. Similarly, Aragón and Rud (2016) provided empirical evidence that proximity to mining operations reduces agricultural productivity through mechanisms of pollution and resource competition, highlighting the importance of agricultural production as a variable sensitive to extractive impacts. In conclusion, the findings of Gbedzi *et al*. (2022) revealed that the growth of mining operations results in the transformation of agricultural and grazing areas for extractive activities, which in turn reduces vegetation cover and disrupts local production systems. This supports the notion that livestock and agricultural activities should be considered as an integrated measure of territorial and socioeconomic change. Finally, Rahnema *et al.* (2023) their findings argue that the activities carried out by mining companies have a determining impact on the environment and society; therefore, the importance lies in the companies using a solid waste management plan in order to preserve sustainable actions and still achieve economic goals, but as long as the life cycle assessment (LCA) frameworks are applied and the adoption of sustainable practices is achieved by combining them to facilitate the objectives and goals. Meanwhile, in Australia, (Leyton y Sangha, 2024) a significant number of mining companies operate in customary territories, causing the deterioration of important ecosystem services, the devastation of ecological zones, the loss of soil and water quality, and ecological imbalance. In addition, they point out that indigenous communities lack economic and technical funds to relate much better to mining companies and efficiently manage the mining sector. The main aims of this study are to holistically study the impact of the social responsibility of the mining company Las Bambas in the province of Cotabambas, Peru. The study was conducted in collaboration with the Las Bambas mining company in the province of Cotabambas, Peru in 2024.

MATERIALS AND METHODS

Formalities of the study

The research is adjusted to a quantitative and qualitative approach, where it is applied for the collection and evaluation of the information to refine all the questions of the study carried out, or to generate new questions during the interpretation path. Primarily, it is important to highlight that this is grounded in the explanatory level, as this research level relies on hypothesis testing and analyzes the outcomes and conclusions. It is relevant to mention that the study adheres to non-experimental research. A cross-sectional design was also applied for methodological and contextual reasons. Moreover, previous studies (Dietler *et al.,* 2021; Owiredu *et al.,* 2025) have successfully employed cross-sectional designs to assess mining impacts in similar contexts. A component of the research design is derived from the concept of comprehending the influence of

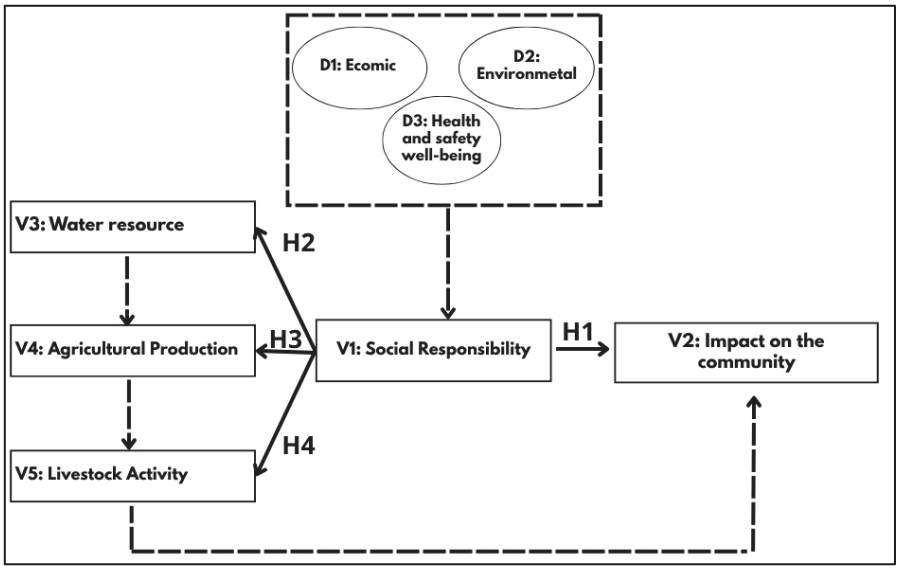

Fig. 1: The conceptual model of author's elaboration

mining companies in relation to their operations. This includes an analysis of the SR programs or projects they implement within communities, assessing whether these initiatives have a positive or negative impact. Furthermore, it involves understanding the repercussions of mining activities in environmental, social, and economic terms. The purpose of this study is to examine and analyze the impact of the SR of the Las Bambas mining company on the inhabitants of the Cotabambas community. Based on the above, the general research question arises from the challenge of answering whether the SR of the mining company has positive or negative results, and how much impact it has on the quality of life of the inhabitants of the community of Cotabambas, Peru. Currently, there are new issues arising that lack substantial research in both theoretical and practical aspects, focusing on the evaluation of the impact of mining operations and activities, particularly in developing countries.

Fig. 1 shows the study model, where V1, V2, V3, V4, and V5 are research variables, and D1, D2, and D3 are study dimensions. Thus, the following general hypothesis is proposed:

H1: The SR of the Las Bambas Mining Company is highly related to the impact on the community.

This led to the formulation of three specific hypotheses aimed at providing a deeper understanding of the impact of the Las Bambas mining company on local residents:

H2: There is a strong relationship between the SR of the Las Bambas Mining Company and the water resources.

H3: There is a strong relationship between the SR of the Las Bambas Mining Company and agricultural production.

H4: There is a strong relationship between the SR of the Las BAMBAS mining company and agricultural and livestock activities.

Participants

The study population consisted of 20,100 inhabitants from communities in the Las Bambas mining area of influence, a simple random sampling technique was used for the simple reason that this type of sampling. The selection or removal of units occurs randomly, ensuring that all participants have an equal chance of being selected, while adhering to specific parameter of sampling procedure using Eq. 1 (López Roldán y Fachelli, 2015):

$$= \frac{\times\ ^2\times\ \times}{e^2\times(\ \ -1)+\ ^2\times\ \times}$$

$$= \frac{20100(1.96)^2(0.5)(0.5)}{(0.05)^2(20100-1)+(1.96)^2(0.5)(0.5)}$$

Table 1: Description of the participants laboration with data from the National Institute of Statistics and Informatics in Cotabambas, Peru

		Frequency	(%)
Gender of the respondent	Female	170	47.4%
	Male	207	52.6%
	Total	377	100.0%
Age	Less than 21 years old	49	10.8%
	22 to 25 years old	59	15.4%
	26 to 30 years old	125	31.5%
	More than 30 years old	144	42.3%
	Total	377	100.0%
Marital status	Married	101	26.8%
	Cohabitant	185	49.1%
	Single	91	24.1%
	Total	377	100.0%
Occupation	Public and private employee	92	24.4%
	Student	55	14.6%
	Person with business	69	18.3%
	Farmer, livestock farmer, fish farmer, etc	161	42.7%
	Total	377	100.0%
District where they belong	Chalhuahuaccho	109	28.9%
	Cotabambas	55	14.6%
	Coyllurqui	77	20.4%
	Haquira	74	19.6%
	Tambobamba	62	16.4%
	Total	377	100.0%

$$=377 \quad (1)$$

Where:

N = 20,100 (total population: inhabitants of Cotabambas province)

Z = 1.96 (corresponding to 95% confidence level)

p = 0.50 (estimated proportion, assuming maximum variability)

q = 0.50 (1 - p)

e = 0.05 (margin of error: 5%)

As shown in Eq. 1, the statistical formula was applied to perform simple random sampling, resulting in a sample of 377 inhabitants. A sample constitutes a limited segment of the overall study population designated as a unit for analysis, employed to obtain data and information that are prompt and trustworthy.

According to the Table 1, nearly 50.9% of the respondents are male, and the other 49.1% are female. In terms of marital status 47.5% are cohabitants and in its entirety are dedicated to the issue of production agriculture, livestock, fish farming, etc (Instituto Nacional de Estadística e Informática, 2017).

Instrument design

In this study, three instruments were designed: a questionnaire, interview guide, and observation sheet, which were used to reveal the findings.

Questionnaire design and validation

To collect and extract information, a questionnaire consisting of 40 items was designed to assess the impact of (SR) initiatives implemented by the Las Bambas Mining Company. Each item was rated on a five-point Likert scale ranging from 1 (very frequent) to 5 (never). For analytical reasons, the scale was noted inversely, such that higher mean values signified increased levels of perceived environmental and social impact. Table 2 presents the questionnaire, which was administered face-to-face and conducted individually with residents of the community. All responses were anonymous, and data collection was carried out over a one-month period.

Table 3 presents the sum of the scores for each

Table 2: Questionnaire elaboration, the V1, V2, V3, V4, and V5: Study variables. D1, D2, and D3 dimensions

N°	Items	Evaluation				
		1	2	3	4	5
	1.- Very frequent 2.- Frequently 3.- Occasionally 4.- Rarely 5.- Never					
	V1= Social responsibility					
	D1= Economic management					
1	P1. The company is used as a source of employment.	1	2	3	4	5
2	P2. Villagers replaced their employment resources.	1	2	3	4	5
3	P3. The company instigates laundry services.	1	2	3	4	5
4	P4. The mining company agrees to use local transportation services.	1	2	3	4	5
5	P5. The company arranges for the purchase of food goods.	1	2	3	4	5
6	P6. The mining company has been able to contract for goods and services.	1	2	3	4	5
7	P7. The mining company carries out community livelihood activities.	1	2	3	4	5
	D2= Environmental considearation					
8	P8. Your community has benefited from the mining company.	1	2	3	4	5
9	P9. Today, the mining company continues with community support.	1	2	3	4	5
10	P10. The company applies environmental monitoring on an ongoing basis.	1	2	3	4	5
11	P11. Leaders and representatives receive environmental monitoring information.	1	2	3	4	5
12	P12. The company implements environmental care strategies.	1	2	3	4	5
13	P13. The company implements environmental protection of environmental resources.	1	2	3	4	5
14	P14. The company reduces the consequences of environmental pollution.	1	2	3	4	5
	D3= Health and safety well-being					
15	P15. The mining company encourages community collaboration in minimizing impacts.	1	2	3	4	5
16	P16. The mining company has developed a high rate of morbidity in the population.	1	2	3	4	5
17	P17. The mining company generates campaigns to minimize morbidity.	1	2	3	4	5
18	P18. People's quality of life has improved.	1	2	3	4	5
19	P19. The lifestyle of the villagers was compromised.	1	2	3	4	5
20	P20. The company generates social action programs.	1	2	3	4	5
21	P21. The mining company is involved in cultural and environmental activities.	1	2	3	4	5
	V2= Impact on the community					
	V3= Water resource					
22	P22. Liquid waste in groundwater affects you.	1	2	3	4	5
23	P23. The company repeatedly develops pollution in the underlying waters.	1	2	3	4	5
24	P24. Surface water wastes stimulate the deficit of marine life.	1	2	3	4	5
25	P25. The water resource is contaminated by the mining company's waste.	1	2	3	4	5
26	P26. The demand for water resources has decreased.	1	2	3	4	5
27	P27. The undoubted demand for water resources from the mine affected essential activities.	1	2	3	4	5
	V4= Agricultural production					
28	P28. The villagers of the area have decreased their cultivation.	1	2	3	4	5
29	P29. Your family varies its economic activity causing the decrease of agricultural crops.	1	2	3	4	5
30	P30. The loss of environment because of mining activities.	1	2	3	4	5
31	P31. The territorial alterations carried out by the mining company.	1	2	3	4	5
32	P32. The mining company generated a reduction of harvest.	1	2	3	4	5

Continued Table 2: Questionnaire elaboration, the V1, V2, V3, V4, and V5: Study variables. D1, D2, and D3 dimensions

N°	Items	Evaluation				
		1	2	3	4	5
33	P33. Vehicle mobilization in the mining corridor caused crop loss.	1	2	3	4	5
	V5= Livestock activity					
34	P34. Livestock activity caused a decrease in the number of horses and alpacas in the area.	1	2	3	4	5
35	P35. The communities' inhabitants have reduced equine and alpaca breeding.	1	2	3	4	5
36	P36. Natural degradation is evident in the grazing zone.	1	2	3	4	5
37	P37. Their relatives no longer raise sheep because of mining in their locality.	1	2	3	4	5
38	P38. The mining company caused the reduction of small animals.	1	2	3	4	5
39	P39. The economic resources generated the reduction of cattle in your locality.	1	2	3	4	5
40	P40. The mining company is the one generating the reduction of cattle.	1	2	3	4	5

Table 3: Social Responsibility Variable. Author's elaboration, table from the analysis of the CSR variable

Evaluated dimension	Items included	Group description
D1: Economic management	P1 to P7	Summary of numerical values (P1 to P7)
D2: Environmental management	P8 to P14	Summary of numerical values (P8 to P14)
D3: Health and safety well-being	P15 to P21	Summary of numerical values (P15 to P21)
"Social responsibility" Variable	P1 to P21	Total Sum (P1 to P21)
D4: Water Resources	P22 to P27	Research variable, sum of numerical values (P22 to P27) evaluating water resource conditions.
D5: Agricultural Production	P28 to P33	Research variable, sum of numerical values (P28 to P33), measuring agricultural performance.
D6: Livestock activity	P34 to P40	Research variable, sum of numerical values (P34 to P40) assessing rural livestock practices.
"Impact on the community" Variable	P22 to P40	Total sum (P22 to P40)

dimension that constitutes the variables "Social Responsibility" and "Community Impact." Likewise, the three dimensions D4, D5, and D6 are treated as separate research variables, adhering to the statistical methodology that facilitates the testing of both general and specific hypotheses, as they directly reflect the primary environmental and economic impacts of mining activities on local communities.

To evaluate the findings, the nonparametric statistic Spearman's Rho was applied to investigate the relationship between the SR variable and its influence on the community, as also demonstrated by Pantoja *et al.* (2022). The SPSS 23 statistical software was used for statistical analysis. Cronbach's alpha was used to validate the questionnaire instrument supported by (Oviedo and Campo, 2005) a group or set of items that exports a common element, deriving a high value of Cronbach's alpha (Cortina, 1993; Rogers *et al.*, 2002). To determine reliability, the calculation was made by means of Cronbach's alpha and a value of (= 0,978) was obtained, which is higher than the minimum standards. Furthermore, reliability was evaluated for each dimension of the instrument: Economic (α = 0.901), Social (α = 0.935), Environmental (α = 0.884), Water Resources (α = 0.959), Agricultural Production (α = 0.952), and Livestock Activity (α = 0.961). All coefficients exceeded the minimum threshold of 0.70 recommended by (Nunnally and Bernstein, 1994), confirming the robustness and internal consistency of each subscale. The questionnaire underwent an expert validation process to ensure content relevance and conceptual clarity. Three specialists in administrative fields, all with over a decade of experience in scholarly and research, were involved in this phase. The experts independently evaluated each item based on four criteria: clarity, relevance,

coherence, and alignment with the study objectives. Their feedback was analyzed and incorporated into the final version of the instrument. The content validity index (CVI) obtained was above 0.80, indicating that the items were clear, pertinent, and theoretically aligned with the constructions being measured. This methodological approach aligns with recent validation studies in the mining sector, such as the work of Bravo *et al.* (2025), who applied expert validation and the Aiken's V coefficient to ensure the conceptual robustness of instruments assessing social dimensions in the Chilean mining industry.

Design of the interview guide instrument

As a second instrument, the interview guide was designed with a structure of open-ended questions, allowing for the development of answers with in-depth content (Fidias Gerado, 2012). The interviews were conducted face-to-face between March and April 2024. In Table 4, two distinct interview schemes were examined: the first scheme focused on the SR theme, while the second scheme centered around the theme of community impact. The interviews were conducted, followed by a structured or formal interview procedure, complying with the questions previously raised. In addition, 10 people with political functions (non-governmental organizations (NGO) representatives, leaders, etc.) were interviewed. The selection of participants was conducted using purposive sampling to confirm the inclusion from the province of Cotabambas were represented. The interview process followed a structured and systematic approach.

The purpose of conducting the interview was to obtain direct information, allowing the analysis of the perception or opinion status of the hierarchical group (Izquierdo *et al.,* 2023). Qualitative data were examined through thematic analysis methodology, utilizing manual coding techniques in Microsoft Excel to uncover recurring patterns across interview responses. This analytical approach was informed by prior research (Mensah *et al.*, 2021; Brew *et al.,* 2015) that utilized structured interview guides and purposive sampling to investigate community perceptions of corporate social responsibility in mining contexts. Each interview transcript underwent a detailed review to extract significant statements that align with the two thematic dimensions shown in Table 4.

Design of the observation sheet

As the last research instrument, the observation sheet proposed in Laura *et al.* (2013) was used, adapted under the theoretical basis of the research variables, and serves the function of collecting information on behaviors in a systematic and direct way (Vara Horna, 2012). Table 5 illustrates the observation instrument, which the researcher implemented directly 18 times

Table 4: Social responsibility interview guide

Social responsibility of las bambas mining company	
Aspects	COD
Sources of employment	H1
Environmental monitoring	H2
Quality of life	H3
Impact on the community	
Aspects	
Water resource	H4
Crop reduction and ecosystem loss	H5
Livestock activity	H6
People interviewed	
President of the Tambobamba district defense front	P1
Cotabambas communal president	P2
Challhuahuacho district president	P3
Haquira district president	P4
Couyllurqui district president	P5
Neighborhood president	C1
Challhuahuacho leader	C2
Province youth leader	C3
Province Agency for Environmental Assessment and Enforcemen (OEFA) staff	C4
Challhuahuacho mayor	C5

Table 5: Observation sheet elaboration

N°	Actions to be evaluated to the company	Compliance records
1	The company contracts laundry services and lodging for its workers.	Yes
2	The mining company contracts local transportation services.	No
3	The mining company carries out community support programs.	Yes
4	The company carries out environmental monitoring.	No
5	The company protects flora and fauna.	Yes
6	The company minimizes pollution impacts on the environment.	No
7	The mining company carries out social action programs.	Yes
8	The company pollutes surface water.	Yes
9	The villagers reduced their crops.	No
10	The villagers have reduced their cattle, sheep and alpacas.	Yes

	Economic									Environmental						Health and safety well-being						Water resource						Agricultural Activity						Livestock Activity							Total sum				
N°	P1	P2	P3	P4	P5	P6	P7	P8	P9	P10	P11	P12	P13	P14	P15	P16	P17	P18	P19	P20	P21	P22	P23	P24	P25	P26	P27	P28	P29	P30	P31	P32	P33	P34	P35	P36	P37	P38	P39	P40	V1	V2	V3	V4	V5
1	4	4	4	3	4	2	2	2	2	3	4	4	3	4	4	3	3	4	2	4	4	2	4	5	4	4	4	5	5	4	4	4	5	4	5	4	5	4	4	5	69	81	23	27	31
2	3	3	3	3	3	3	3	3	1	3	3	2	2	2	2	2	2	2	2	2	2	3	3	3	3	3	3	3	3	3	3	3	3	4	3	3	3	3	3	3	51	58	18	18	22
3	3	4	4	5	4	4	5	4	4	5	4	4	3	3	4	3	4	3	4	4	4	4	4	5	5	4	5	4	3	4	3	3	3	4	4	3	4	4	3	3	82	72	27	20	25
4	1	1	1	2	2	2	2	2	2	2	2	2	2	2	2	2	2	2	2	2	2	2	2	2	2	2	2	2	2	2	2	2	2	2	2	2	2	2	2	2	39	38	12	12	14
5	3	4	4	4	1	3	3	4	3	3	3	3	3	3	3	3	3	3	3	3	3	3	4	4	4	4	4	5	5	4	4	5	3	5	4	4	4	4	4	4	65	78	23	26	29
6	4	5	4	4	3	5	2	1	2	2	1	1	3	3	3	1	3	2	5	3	4	5	5	5	5	5	4	5	5	4	4	3	5	5	5	5	4	2	5	5	61	86	29	26	31
7	2	5	3	4	1	5	1	1	1	3	2	4	1	3	2	3	5	1	2	3	1	1	1	2	2	5	3	1	4	3	1	1	3	2	1	1	5	5	5	1	53	47	14	13	20
8	2	3	3	3	3	3	3	3	3	2	2	3	3	2	3	3	2	3	3	2	2	3	2	2	3	3	2	3	3	2	3	3	2	3	3	2	3	3	2	3	56	50	15	16	19
9	2	3	2	1	3	2	3	2	2	3	2	2	3	3	3	2	2	2	2	2	2	3	2	3	2	2	2	3	3	2	3	2	2	3	1	3	1	2	3	2	48	44	14	15	15
10	4	5	5	5	4	4	5	5	4	4	4	3	3	4	4	4	4	5	5	5	5	5	5	5	4	5	5	5	5	5	5	5	5	5	5	5	5	5	5	5	91	94	29	30	35
11	1	4	2	1	1	2	5	3	1	3	1	3	1	1	1	1	1	1	1	1	1	1	1	1	1	1	1	1	1	1	1	1	1	1	1	1	1	1	1	1	36	19	6	6	7
...	...	...	...	...	...	...	...	...	...	...	...	...	...	...	...	...	...	...	...	...	...	...	...	...	...	...	...	...	...	...	...	...	...	...	...	...	...	...	...	...	...	...	...	...	...
372	2	3	3	3	4	3	3	3	3	3	3	3	3	3	4	2	2	2	2	2	2	2	2	2	2	2	4	3	3	2	3	3	3	3	3	3	3	4	5	5	58	57	14	17	26
373	4	4	4	4	4	4	4	1	4	4	4	2	2	2	2	2	2	2	4	4	4	4	4	4	4	4	4	4	4	4	4	4	4	4	4	4	4	4	4	4	67	76	24	24	28
374	1	1	1	1	1	1	1	1	1	1	1	1	1	1	1	1	1	1	1	1	1	1	1	1	1	1	1	1	1	1	1	2	1	1	1	1	1	1	1	1	21	20	6	7	7
375	4	4	4	3	4	2	2	2	2	3	4	4	3	4	4	3	3	4	2	4	4	2	4	5	4	4	4	5	5	4	4	4	5	4	5	4	5	4	4	5	69	81	23	27	31
376	3	3	3	3	3	3	3	3	1	3	3	2	2	2	2	2	2	2	2	2	2	3	3	3	3	3	3	3	3	3	3	3	3	4	3	3	3	3	3	3	51	58	18	18	22
377	3	4	4	5	4	4	5	4	4	5	4	4	3	3	4	3	4	3	4	4	4	4	4	5	5	4	5	4	3	4	3	3	3	4	4	3	4	4	3	3	82	72	27	20	25

Fig. 2: Data processing for hypothesis testing elaboration; Value V1: Social responsibility; V2= Impact on the community; V3= Water resources; V4= Agricultural production; V5= Livestock activity; processed data in Excel

in diverse community contexts within Cotabambas, Peru. The instrument consisted of ten observable actions related to the mining company's social and environmental performance, each assessed with dichotomous responses (Yes or No).

The observation sheet created by the researchers was applied in person in August 2024. The information instrument allowed for explaining, understanding, identifying social problems, and describing the research environment (Briones Viteri, 2018). The analysis was conducted using Excel, and data was gathered in line with the study's objectives and hypotheses.

RESULTS AND DISCUSSION

The results obtained after the application of the instruments are presented. It was analyzed whether the SR of the Las Bambas Mining Company is strongly related to its impact on the community. Fig. 2 illustrates the analysis of data gathered from the questionnaire administered to 377 villagers, representing the complete sample size for the study. It also displays the aggregated values of the items that correspond to the study variables, which are utilized for both general and specific hypothesis testing.

Hypothesis testing social responsibility and the impact on the community

To test the general hypothesis about the "Social responsibility" (V1) of the Las Bambas mining company is highly related to the "Impact on the community" (V2), the normality test and the

Table 6: Correlation between social responsibility and impact on the community, based on data analyzed using IBM® SPSS® version 23.00, where V1 and V2 represent the research variables

Variable	Rho de Spearman
V1: Social responsibility	
V2: Impact on the community	,610*
N	377

*Correlation is significant at the 0.05 level (two-tailed)

Table 7: Correlation between Social Responsibility and water resources, based on data analyzedusing IBM® SPSS® version 23.00, where V1 and V3 represent the research variables

Variable	Rho de Spearman
V1: Social responsibility	
V3: Water resource	,575*
N	377

*Correlation is significant at the 0.05 level (two-tailed)

Table 8: Correlation between agricultural production and social responsibility, based on data analyzed using IBM® SPSS® version 23.00, where V1 and V4 represent the research variables

Variable	Rho de Spearman
V1: Social responsibility	
V4: Agricultural production	,510*
N	377

*Correlation is significant at the 0.05 level (two-tailed)

respective hypothesis test were used. Prior to conducting the Kolmogórov-Smirnov test, the resulting p-value (< 0.05) suggested that the data did not conform to a normal distribution. To assess the relationship between social responsibility and community impact, Spearman's Rho was calculated, yielding a coefficient of 0.610.

Table 6 shows that the results of Spearman's Rho are 0,610, which indicates a moderate relationship between the SR variable and the impact on the community. Therefore, the general hypothesis that the SR of the Las Bambas mining company is related to the impact on the community is accepted.

Hypothesis test of social responsibility and water resources

To determine the specific hypothesis, if there is a high relationship between the "Social Responsibility" (V1) of the Las Bambas mining company and the "Water Resource" (V3). From the finding obtained Spearman's Rho = 0,575, which indicates the existence of a moderate relationship between the water resources and SR of the Las Bambas mining company. Likewise, the p-value = 0,043 (< 0,05), which indicates the acceptance of the specific hypothesis of the research. Table 7 illustrates the findings that suggest the hypothesis can be accepted, indicating that the SR activities performed by the Las Bambas mining company have a detrimental effect on water resources.

Hypothesis test of social responsibility and agricultural production

To establish the specific hypothesis, if there is a high relationship between the "Social Responsibility" (V1) of the Las Bambas mining company and the "Agricultural activity" (V4), from the referred result the Spearman's Rho = 0,510, indicates that it is within the correlation estimation, according to the scale. A moderate relationship is observed between the study variables, indicated by a p-value =0,024 (< 0,05). Table 8 illustrates the outcomes, affirming the acceptance of the hypothesis of the study, indicating that the SR practices executed by the Las Bambas Mining Company negatively influence agricultural production.

Hypothesis test of social responsibility and livestock activity

To determine the specific hypothesis, if there

Table 9: Correlation between livestock activities and social responsibility, based on data analyzed using IBM® SPSS® version 23.00, where V1 and V5 represent the research variables

Variable	Rho de Spearman
V1: Social responsibility V5: Livestock activity	,720*
N	377

*Correlation is significant at the 0.05 level (two-tailed)

is a strong relationship between the "Social Responsibility" (V1) of the Las Bambas Mining Company and the "Livestock Activity" (V5), before the Spearman's Rho test = 0,720, it is reflected that it is in the parameters from 0.4 to 0.69. This resulted in the existence of a high correlation between the research variables. Referring to a p-value of 0,034 (<0,05). Table 9 illustrates the outcomes; consequently, the specific hypotheses of the study were validated. In other words, the SR activities carried out by the Las Bambas mining company have a negative impact on agricultural and livestock activities.

Results obtained from the interview guide

The findings of the interviews conducted, based on the coding of the questions (H1, H2, ..., H6) and the people interviewed (P1, P2... C5) in Table 9, arrived at the following conclusions of the analysis. The interviewers recognize that the Las Bambas mining company does not conduct environmental monitoring, which reflects a lack of commitment to environmental stewardship. Thus, it has been seen that the communities through the villagers are responsible for carrying out such activities through meetings or communal tasks, so that, in this way, the care of the environment is maintained. "There is no adequate environmental monitoring where care for the environment is carried out" (P1.G2). It can be concluded that the lack of control monitoring implies that the villagers are tasked with making sure they remain unaffected by environmental contamination. The findings reveal that local governance institutions have played a critical though insufficiently recognized role in managing environmental concerns. According to the interviews conducted, traditional community structures, including district defense fronts and communal assemblies, have assumed environmental monitoring functions in response to the perceived absence of effective corporate oversight. In this context, the interview disclosed that the Las Bambas mining company is currently infringing upon water resources without implementing any solutions or projects to address the issue of limited water availability caused by its operations, as in numerous localities, the water resources are not safe for consumption. "In the urban sectors, there is no water supply because of the fear of consuming non-potable or contaminated water, because it puts our health at risk due to the chemical substances it may contain" (C1.Z1). It is clear how important it is that Las Bambas Mining Company focus attention on water resources, since it generates fear among the villagers who consume water, which could affect their quality of life. From this perspective, it was possible to appreciate the percentage rate of decrease in all types of agricultural crops on the part of the inhabitants in view of the operations of the Las Bambas Mining Company, as well as the agricultural production that was usually dedicated before the mining project was put into activity. "In the community it has been able to see the excessive reduction of our agricultural crops such as potatoes, corn, wheat, etc., as a result of environmental contamination" (C5.Z14). It is important to highlight that the primary source of the low agricultural crop yields is the current environmental pollution, and the Las Bambas Mining Company fails to address one of the most significant issues. Finally, in terms of quality of life, the inhabitants of each community neighboring the Las Bambas Mining Company project have greater economic resources than before the company's operation, improved education at all levels, as well as transportation since there is continuous maintenance of roads and health. "In relation to quality of life, all individuals saw a rise in their income as a result of the strong demand for labor and the development of family enterprises, in addition to enhancements in road transport, education, and health services" (P1.G3). Consequently, the Las Bambas Mining Company has an impact on the economic resources of the villagers, but this is due to environmental contamination on a larger scale, since agricultural

Table 10: Table of results of the observation sheet, including P1, P2, P3, P4, P5, P6, P7, P8, P9, and P10: Value of Yes: 1. No: 2

N°	P1	P2	P3	P4	P5	P6	P7	P8	P9	P10
1	1	1	1	1	2	2	1	1	1	1
2	2	2	1	2	2	1	1	1	1	1
3	1	1	2	2	1	2	2	1	1	2
4	1	2	1	1	2	1	2	1	1	1
5	1	1	2	2	2	2	1	2	1	1
6	1	1	1	2	2	2	1	1	1	1
7	2	1	2	2	2	1	2	1	1	1
8	1	2	1	1	1	2	1	1	2	1
9	2	1	1	2	2	2	1	1	1	2
10	1	1	1	2	2	1	2	2	1	1
11	2	1	2	2	2	2	1	1	1	1
12	1	2	1	2	2	2	1	1	2	1
13	2	1	1	1	1	2	1	1	1	1
14	1	2	1	2	2	2	1	1	1	1
15	1	2	2	1	2	1	1	2	1	2
16	2	1	1	2	2	2	1	1	1	1
17	1	2	1	2	1	1	1	1	1	1
18	2	1	1	2	2	2	1	1	1	1
YES	11	11	13	5	4	6	14	15	16	15
NO	7	7	5	13	14	12	4	3	2	3
Total	18	18	18	18	18	18	18	18	18	18

activity has been reduced, as well as livestock, which are the main activities of the communities. Finally, multiple interviewees perceived water sources to be contaminated, reporting the presence of chemical residues and expressing significant health concerns associated with water consumption. These accounts illustrate the prevalent views within the community about the decline in water quality due to mining activities.

Results obtained from the observation sheet

Concerning the use of the observation sheet, the researchers employed the tool structured around ten questions with yes/no responses to gather results that contribute to the study and to assess whether SR can influence the community's impact. Table 10 shows the results of the application of the observation sheet, where it is shown that there is a higher frequency in question P9 with 16 answers (yes), meaning that the mining operations reduced the crop, similarly in question P5 with respect to the protection of flora and fauna there was a higher frequency with 14 (No). The outcomes are illustrated in Table 10 in terms of percentages.

Fig. 3 shows the results of the observation sheet, confirming that the SR program of the Las Bambas mining company is highly related to the impact on the community (how it affects each of its dimensions). According to the observation records, 88.3% of participants indicated or perceived evidence of surface water contamination, which is mainly linked to mining activities. This data represents perceived observations rather than results from physicochemical water testing. Likewise, 88,9% of the crops grown by the villagers of the communities were reduced, which is evidence of a significant impact. Finally, 83,3% of the cattle and other livestock that grew in the area were reduced, which shows that there are no adequate places for raising them.

This study has focused on studying the SR of the Las Bambas Mining Company and its impact on the community in the territory of Peru, to understand the influence that exists and how it affects the operations of the mining company on the people of the community, and in their daily lives.

The findings derived from interviews and firsthand observations demonstrate evident community beliefs that connect the degradation of water quality to a decrease in agricultural and livestock output. Observations in the affected villages showed that farmers had stopped cultivating traditional crops due to the presence of turbid and discolored water, a result of mining runoff. Residents also reported premature livestock deaths attributed to the consumption of

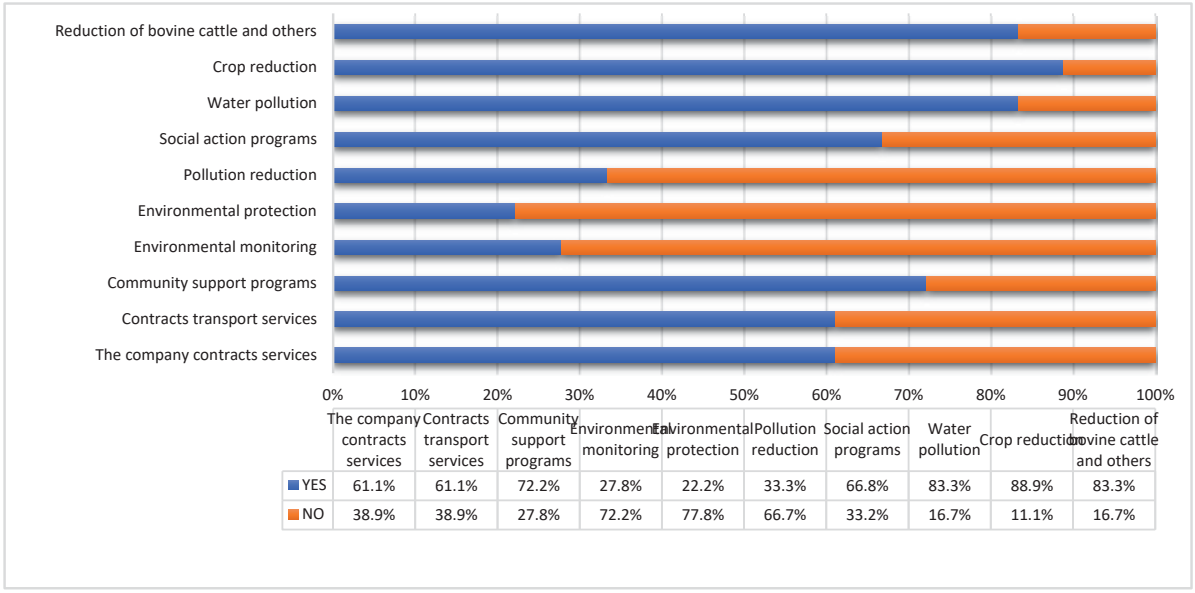

	The company contracts services	Contracts transport services	Community support programs	Environmental monitoring	Environmental protection	Pollution reduction	Social action programs	Water pollution	Crop reduction	Reduction of bovine cattle and others
YES	61.1%	61.1%	72.2%	27.8%	22.2%	33.3%	66.8%	83.3%	88.9%	83.3%
NO	38.9%	38.9%	27.8%	72.2%	77.8%	66.7%	33.2%	16.7%	11.1%	16.7%

Fig. 3: On-site observation. Author's elaboration

contaminated water and pasture. These findings, supported by the observation sheet and interview testimonies, illustrate how the perception of water contamination directly disrupts productive activities and the livelihoods of households in the communities surrounding Las Bambas. According to the findings of the overarching hypothesis, it can be stated that the SR activities or initiatives of Las Bambas Mining Company are viewed by the community as influencing their daily lives and well-being. The results of the study contrast with (Komba *et al.,* 2025) who found that mining operations in Sierra Leone negatively affected human capital through disease prevalence, degraded natural capital through soil and water contamination, and weakened physical assets by limiting access to essential services. Likewise, in the case of Las Bambas, interview and field observation results indicate that despite the company's SR initiatives, agricultural productivity and livestock health have declined due to water pollution and soil deterioration, affecting the community's sustainable livelihoods. Despite the recognition of some economic progress through job creation and infrastructure development, these advantages have not entirely balanced the environmental and social costs, mirroring insights from other major mining operations where CSR practices tend to alleviate social tensions more effectively than they mitigate ecological damage. In this way, another study made it evident that mining is detrimental to agriculture and generates water and environmental pollution. Siaw *et al.* (2023) highlighted that the ability of agricultural operators to promote sustainable economic growth in communities is severely restricted by the insufficient availability of good roads, electricity, and water resources. Regarding the first hypothesis of the research, it was seen how the influence of SR on water resources affected the same population in their daily lifestyle, forcing them to fear drinking water and, therefore, having consequences on their health. In the same sense, Magidi and Hlungwani (2023) their study revealed that the mining industry "Connemara" generates environmental destruction and consequently respondents reported perceptions of water pollution affecting their quality of life. Another adverse effect of the second specific hypothesis is the almost total reduction in agriculture, the main activity of the villagers, because of the mining project. Brugger and Zanetti (2020) furthermore indicated that the communities have seen a reduction in their agricultural output, which can be linked to environmental fluctuations and soil degradation. They noted that daily rainfall has diminished compared to previous years, before the

establishment of mining operations. On the other hand, the results of the third hypothesis specify that the actions of the SR carried out by the Las Bambas mining company cause a serious problem in agricultural and livestock activities. Likewise, the findings of this study highlighted that individuals residing in the communities are unhappy with the mining practices (Coelho *et al*., 2022), who have identified the adverse effects of mining on water pollution, life quality, and the lack of social assistance. In addition, the circulation of trucks is very frequent, which generates mineral waste, noise generation, and environmental pollution. In addition, it should be noted that not only are there negative impacts on water resources, agricultural production, and farming activities, but also on the lifestyle of people who belong to the communities. Furthermore, Widana (2019) asserts that the socioeconomic consequences arising from mining encompass economic resources, employment prospects, quality of life improvements, poverty reduction, training and capacity enhancement, availability of basic services, and their effects on communities and agricultural practices. It also affects politics, such as acts of embezzlement and people's fundamental rights. As for the results of the interview, the leaders and political authorities appreciate that Las Bambas Mining Company takes actions regarding the pollution of water resources, since they are the ones who carry out actions that can help mitigate such contamination. In a comparable manner, Baffour *et al*. (2021) discovered through their research that mining communities face detrimental impacts, including noise and environmental conditions. The most significant and concerning secondary effect is water pollution, as water frequently becomes tainted by chemicals resulting from mining activities. This study's observation sheet uncovered crucial insights, indicating that agricultural productivity decreased by 88.9%, which adversely affects the residents involved in this sector. Similarly, Seloa y Ngole (2022) also supports this statement as they confirm that 93,6% of their agricultural lands were affected and destroyed, losing the quality of the land, because of existing mining projects. On the other hand, the result of the observation sheet indicates water pollution in 88,3% by which, Aragón and Rud (2016) also validate the observation because, in their study, there was a 70% presence of a polluting agent in water quality.

CONCLUSION

This study assessed how Las Bambas Mining Company's SR practices influence social, environmental, and economic conditions, revealing that perceived improvements in income coexist with concerns about environmental degradation. Nonetheless, the mining industry in Peru represents a significant source of economic revenue for the nation, owing to the vast quantities of untapped mineral resources found across various regions of Peru. It should be noted that the impacts of mining operations are overwhelming for inhabitants, whose main activities are agriculture and livestock farming. These perceptions highlight a misalignment between formal SR commitments and community expectations, evidently in the water resource, and reflected a perceived water problem affecting both consumption and agricultural use, generating health concerns among the villagers. Furthermore, the impact on agricultural production manifested in soil degradation, which diminished the availability of pasture for animals, caused a decrease in breeding activities, and ultimately led to agricultural practices that yielded unfavorable results, rendering the population incapable of securing increased economic income. To strengthen SR credibility, efforts should focus on participatory environmental monitoring and transparent communication with affected communities. Mining companies should also focus on purchasing state-of-the-art machinery for the proper treatment of sewage effluents to eradicate pollutants. Similarly, initiatives must be developed to promote the diversification of livestock production, encouraging local residents to raise species that align with the specific circumstances of their communities, thereby ensuring that the outcome of breeding these species serves as a source of income for the villagers. Based on these findings, Las Bambas Mining Company should incorporate the identified environmental, social, and economic impacts into its SR management plans through participatory, evidence-based approaches. Specifically, SR initiatives should prioritize continuous environmental monitoring, transparent communication with local communities, and the promotion of sustainable livelihood projects. While the research provides valuable insights into community perceptions regarding the mining company's RS practices, certain limitations should

be acknowledged. The opinions of participants may have been swayed by their previous expectations of the mining company. Moreover, direct environmental measures were excluded, as the aim of this study was to document the perceptions and lived experiences of the community members. In this sense, government agencies and regulatory institutions should set policies (laws and standards) that provide binding or punitive measures for activities that are conscious of their impact on communities and promote more sustainable practices in the mining industry. Finally, future research should deepen understanding of community perceived impacts of mining SR to inform context-specific sustainability frameworks. The application of participatory and mixed methods assessment approaches could serve to reinforce the integration of community environmental knowledge in the context of mining. While this study gathered local perceptions through surveys, interviews, and field observation, future studies could incorporate these research techniques used in the present study.

Author Contributions:

A.J.C. Palomino conceived the research idea, designed the study, conducted the research, performed the literature reviews, collected the data, and conceptualized the manuscript. H.D. Calderon designed and conceptualized the manuscript, conducted the research, collected the data, performed the literature reviews, and analyzed and interpreted the data. C.J. Huamaní contributed to the acquisition, analysis, and interpretation of the data, the statistical analysis, and the preparation of the manuscript, and helped to improve it. J.L. León Vicencio participated in conducting the research, the literature review, the acquisition, analysis, and interpretation of the data, and in writing the manuscript. G. Suyo Cruz contributed to the literature review and data collection. D.A. Pinto Paga participated in conducting the study, the literature review and conceptualizing the manuscript. B.O. Mamani Huillca participated in the study design, research, literature review, data acquisition, analysis, and interpretation, and manuscript drafting. W. Orós Torres contributed to data acquisition, analysis, and interpretation, as well as statistical analysis, and helped improve the manuscript. S.R. Pinto Boda contributed to data analysis and interpretation, statistical analysis, and helped improve the manuscript. L. Contreras Salas conducted the literature review and statistical analysis and contributed to manuscript preparation.

ACKNOWLEDGEMENT

Thanks are due to the National University Micaela Bastidas of Apurímac, as well as the support of the Research Ethics Committee, approved by Resolution [No. 394-2025-CU-UNAMBA] on 20 October 2025. Study materials and data for this study can be openly accessed here: https://figshare.com/s/8cf6254a82684e5633e6

CONFLICT OF INTEREST

The authors declare that there is no conflict of interest regarding the publication of this manuscript. In addition, ethical issues, including plagiarism, informed consent, misconduct, data fabrication and/or falsification, double publication and/or submission, and redundancy, were observed by the authors.

OPEN ACCESS

©2026 The author(s). This article is licensed under a Creative Commons Attribution 4.0 International License, which permits use, sharing, adaptation, distribution and reproduction in any medium or format, if you give appropriate credit to the original author(s) and the source, provide a link to the Creative Commons license, and indicate if changes were made images or other third-party material in this article are included in the article's Creative Commons license, unless indicated otherwise in a credit line to the material. If material is not included in the article's Creative Commons license and your intended use is not permitted by statutory regulation or exceeds the permitted use, you will need to obtain permission directly from the copyright holder. To view a copy of this license, visit:

http://creativecommons.org/licenses/by/4.0/

PUBLISHER'S NOTE

GJESM Publisher remains neutral regarding jurisdictional claims regarding published maps and institutional affiliations.

☒ Negative AI Statement

The author(s) declared that no AI tools or services were used or highly applied during the preparation of this work.

ABBREVIATIONS

α	alpha
<	less than
=	The same as
%	Percent
CIA	community impact assessment
IBM®	International Business Machines Corporation
LCA	Life cycle assessment
N	Population size
NGO	Non-Governmental Organizations
OCMAL	Observatorio de Conflictos Mineros de América Latina
OEFA	Agency for Environmental Assessment and Enforcement
p-value	Probability value
RCT	Resource curse theory
Rho	Pearson correlation coefficient
ST	Stakeholder Theory
SLO	Social License to Operate
SPSS	Statistical package for the social sciences
SR	Social responsibility
NET	Neoclassical Economic Theory

REFERENCES

Adjei, B.; Tudzi, E.P.; Owusu-Ansah, A.; Kidido, J. K.; Adjei, B.; Tudzi, E.P.; Owusu-Ansah, A.; Kidido, J.K.; Durán-Díaz, P., (2024). Citation: The impacts of mining industries on land tenure in Ghana: A comprehensive systematic literature review. Land. 13(9).

Aguinis, H.; Glavas, A., (2012). What we know and don't know about corporate social responsibility. J. Manage., 38(4): 932–968 **(37 pages).**

Akchurin, M., (2020). Mining and Defensive Mobilization Explaining Opposition to Extractive Industries in Chile. Soc. Dev., 6(1): 1–29 **(29 pages).**

Ansu, M.P.; Amoako, G.K.: Frimpong, K., (2021). Corporate social responsibility and stakeholder engagement in Ghana's mining sector: A case study of Newmont Ahafo mines. Int. J. Corporate Soc. Respons., 6(1): 6.

Aragón, F.M.; Rud, J.P., (2016). Polluting industries and agricultural productivity: Evidence from mining in Ghana. Econ. J., 126(597): 1980–2011 **(32 pages).**

Ashrafi, M.; Magnan, G.M.; Adams, M.; Walker, T.R., (2020). Understanding the conceptual evolutionary path and theoretical underpinnings of corporate social responsibility and corporate sustainability. Sustainability. 12(3): 760.

Baffour-Kyei, V.; Mensah, A.; Owusu, V.; Horlu, G.S.A.K, (2021). Artisanal small-scale mining and livelihood assets in rural southern Ghana. Resour. Policy. 71: 1–12 **(12 pages).**

Bansal, P.; DesJardine, M., (2014). Business sustainability: It is about time. Strategic Organization. 12(1): 70–78 **(9 pages).**

Bansal, P.; Song, H.C. (2016). Similar But Not the Same: Differentiating Corporate Sustainability from Corporate Responsibility. Academy Manage. Annals. 11(1): 105–149 **(44 pages).**

Bansal, S.; Nangia, P.; Singh, S.; Cichoń, D., (2024). Where's our share: Agenda for gender representation in mining industry. Resour. Policy. 90: 1–12 **(12 pages).**

Bansal, S.; Singh, S.; Nangia, P.; Chanaliya, N.; Sala, D., (2024). Sustaining the mining industry through the lens of corporate social responsibility: Review research. Resour. Policy., 99: 1–13 **(13 pages).**

Bebbington, A.; Mark W., (2008). Water and Mining Conflicts in Peru. Mountain Res. Dev., 28(3):190-195 **(16 pages).**

Bernal, S.M. F.; Baraibar-Diez, E.; Collado-Agudo, J., (2025). CSR and Corporate Sustainability: Theoretical and Empirical Approaches Based on Data Science in Spanish Tourism Companies. Sustainability. 17(6): 1-35 **(35 pages).**

Berle, A.A. (1931). Corporate Powers as Powers in Trust. Harvard Law Rev., 44(7): 1049-1074 **(26 pages).**

Bravo, R.C.; Orellana, M.; y Fuentes, J., (2025). Development, content validity, and reliability of a questionnaire to measure perceived workplace discrimination in the Chilean mining sector. Medwave. 25(10): 1-10 **(10 pages).**

Brew, Y.; Junwu, C.; Addae B.S., (2015). Corporate Social Responsibility Activities of Mining Companies: The Views of the Local Communities in Ghana. Am. J. Ind. Bus. Manage., 5(6): 457–465 **(9 pages).**

Briones Viteri, A.T. (2018). Didáctica de la investigación formativa en la carrera de Ciencias Administrativas en la Universidad de Guayaquil . Revista Universidad y Sociedad. 10(5): 238–242 **(5 pages).**

Brugger, F.; Zanetti, J., (2020). "In my village, everyone uses the tractor": Gold mining, agriculture and social transformation in rural Burkina Faso. Extractive Ind. Soc., 7(3): 940–953 **(14 pages).**

Carroll, A.B., (2015). Corporate social responsibility: The centerpiece of competing and complementary frameworks. Organizational Dynamics. 44(2): 87–96 **(10 pages).**

Cerioni, E.; Marasca, S., (2021). The Methods of Social Impact Assessment: The - ProQuest. Calitatea: Acces La Success; Bucharest. 22(183): 29–36 **(8 pages).**

Chia, A.; Kern, M.L.; Neville, B.A., (2020). CSR for Happiness: Corporate determinants of societal happiness as social responsibility. Business Ethics: A European Rev., 29(3): 422–437 **(16 pages).**

CEPAL, (2020). La bonanza de los recursos naturales para el desarrollo: Dilemas de gobernanza (Sánchez J. Ricardo, Ed.; N°157). Libros de Comisión Económica para América Latina y el Caribe. 13-323 **(311 pages).**

Cortina, J.M., (1993). What Is Coefficient Alpha? An Examination of Theory and Applications. J. Appl. Phycol., 78(1): 98–104 **(7 pages).**

Dauda, S., (2024). Dynamics of corporate social responsibility (CSR) during mineral exploration: Evidence from Eastern Region,

Ghana. J. Environ. Manage., 367: 1–10 **(10 pages).**

Dietler, D.; Farnham, A.; Loss, G.; Fink, G.; Winkler, M.S., (2021). Impact of mining projects on water and sanitation infrastructures and associated child health outcomes: a multi-country analysis of Demographic and Health Surveys (DHS) in sub-Saharan Africa. Globalization and Health. 17(1): 1–16 **(16 pages).**

Dikgwatlhe, P.; Mulenga F., (2023). Perceptions of local communities regarding the impacts of mining on employment and economic activities in South Africa. Resour. Policy. 80(1): 1–12 **(12 pages).**

de Lange, E.; Woodhouse, E.; Milner-Gulland, E.J., (2016). Approaches Used to Evaluate the Social Impacts of Protected Areas. Conserv. Lett., 9(5): 327–333 **(7 pages).**

Delevingne, L.B.; Glazener, W.; Grégoir, L.; Henderson, K., (2020, July 28). Climate risk and decarbonization: What every mining CEO needs to know|McKinsey.

Gbedzi, D.D.; Ofosu, E.A.; Mortey, E.M., Obiri-Yeboah, A.; Nyantakyi, E.K.; Siabi, E.K., (2022) Impact of Mining on Land Use Land Cover Change and Water Quality in the Asutifi North District of Ghana, West Africa. Environ. Challenges. 6(1): 2-15 **(14 pages).**

Ferrero, I.; Hoffman, W.M.; McNulty, R.E., (2012). Must Milton Friedman Embrace Stakeholder Theory? Faculty. Bus. Soc. Rev., 119(1):37-59 **(23pages).**

Fidias G.A., (2012). El proyecto de Investigación 6.ª ed. Editorial Episteme.

Fontana, E., (2018). Corporate Social Responsibility as Stakeholder Engagement: Firm–NGO Collaboration in Sweden. Corporate Soc. Respons. Environ. Manage., 25(4): 327–338 **(12 pages).**

Haroon, M.; Ullah, M.; Li, Z., Zhu, S.; Wang, J.; Hsueh, C.P., (Eugune). (2025). Impact of emergig technologies on corporate social responsibility in mining industry. Resour. Policy. 102: 1–12 **(12 pages).**

Harrison, J.S.; Barney, J.B.; Freeman, R.E.; Phillips, R.A., (2019). The Cambridge Handbook of Stakeholder Theory. The Cambridge Handbook of Stakeholder Theory. 1–280 **(280 pages).**

Ho, S.S.H.; Oh, C.H.; Shapiro, D., (2024). Can Corporate Social Responsibility Lead to Social License? A Sentiment and Emotion Analysis. J. Manage. Stud., 61(2): 445–476 **(22 pages).**

Hosseinpour, M.; Osanloo, M.; Azimi, Y., (2022). Evaluation of positive and negative impacts of mining on sustainable development by a semi-quantitative method. J. Cleaner Prod., 366: 1–15 **(15 pages).**

Hou, T.C.T., (2019). The relationship between corporate social responsibility and sustainable financial performance: firm-level evidence from Taiwan. Corporate Soc. Respons. Environ. Manage., 26(1): 19–28 **(10 pages).**

Huamani Cayllahua, M., (2023). Análisis de la responsabilidad social de la compañía minera las BAMBAS y su impacto en la provincia de Cotabambas, Apurímac Perú, periodo 2023. Escuela de posgrado-EPN. 6–71 **(66 pages).**

Instituto Nacional de Estadística e Informática, (2017). Censos Nacionales 2017: XII de Población, VII de Vivienda y III de Comunidades Indígenas. 1–341 **(341 pages).**

Izquierdo, G. M.; Ramírez, N.EJ.; Silva, J.M.C.; Rodríguez, J.C.R., (2023). Herramientas, estrategias y enfoque cualitativo para develar emociones en varones desempleados. Ciência and Saúde Coletiva. 28(1): 59–70 **(12 pages).**

Jones, N.; McGinlay, J.; Dimitrakopoulos, P.G., (2017). Improving social impact assessment of protected areas: A review of the literature and directions for future research. Environ. Impact Assess. Rev., 64: 1–7 **(7 pages).**

Kaymaz Mühling, Ş.M., (2023). Utilizing Artificial Intelligence (AI) for the Identification and Management of Marine Protected Areas (MPAs): A Rev. J. Geosci. Environ. Protect., 11(09): 118–132 **(15 pages).**

Komba, B.P., Chattha, M.W.A., Fatima, A., Thomson, P. C., González, L. A., Hyder, M.F., (2025). Assessing the environmental, economic, and social impacts of industrial mining on agricultural communities in Sierra Leone: A sustainable approach using PLS-SEM. Cleaner Responsible Consumption. 16: 1-14 **(14 pages).**

Kulczycka, J.; Dziobek, E.; Nowosielski, M., (2023). Promotion and implementation of Polish mining investments in foreign markets on the example of Latin America. Energy Storage Sav., 2(4): 608–614 **(7 pages).**

Laura, C.; Díaz Bravo, P.; Díaz Bravo, L.; Torruco García, U.; Martínez Hernández, M.; Varela Ruiz, M., (2013). La entrevista, recurso flexible y dinámico. Investigación En Educación Médica. 2(7): 162–167 **(6 pages).**

Leyton-Flor, S.A.; Sangha,K., (2024). The socio-ecological impacts of mining on the well-being of Indigenous Australians: A systematic review. Extractive Ind. Soc., 17: 1–14 **(14 pages).**

Lindman, Å.; Ranängen, H.; Kauppila, O., (2020). Guiding corporate social responsibility practice for social license to operate: A Nordic mining perspective. Extractive Ind. Soc., 7(3): 892–907 **(16 pages).**

Long, W.; Li, S.; Wu, H.; Song, X., (2020). Corporate social responsibility and financial performance: The roles of government intervention and market competition. Corporate Soc. Respons. Environ. Manage., 27(2): 525–541 **(17 pages).**

López Roldán, P.; Fachelli, S., (2015). Metodología de la Investigación Social Cuantitativa, 1.ª ed. Dipòsit Digital de de Documents Universitat Autònoma de Barcelona**.**

Macêdo Coelho, Y.C.; de Medeiros, P.S.; Santos, J.A.; Araújo Lucas, F.C., (2022). Perception of environmental impacts of aggregate mining: A case study from the municipality of Ourém, Pará, Brazil. Resour. Policy. 78: 1-10 **(10 pages).**

Magidi, M.; Hlungwani, P.M., (2023). Development or destruction? Impacts of mining on the environment and rural livelihoods at Connemara Mine, Zimbabwe. S. Afr. Geogr. J., 105(2): 157–178 **(12 pages).**

Maher, R.; Valenzuela, F.; Böhm, S., (2019). The Enduring State: An analysis of governance-making in three mining conflicts. Organ. Stud., 40(8): 1169–1191 **(23 pages).**

Michelon, G.; Pilonato, S.; Ricceri, F., (2015). CSR reporting practices and the quality of disclosure: An empirical analysis. Crit. Perspectives Account., 33: 59–78 **(20 pages).**

Mari Farinós, J., (2016). La responsabilidad social medioambiental. análisis jurídico de la directiva 2004/35/ce sobre responsabilidad medioambiental: quien contamina paga. Diferencias con la responsabilidad social empresarial (RSE). Revista Boliviana de Derecho. 21(1): 254–273 **(20 pages).**

Moffat, K.; Lacey, J.; Zhang, A.; Leipold, S., (2016). The social licence to operate: a critical review. Forestry: An Int. J. Forest Res., 89(5): 477–488 **(12 pages).**

Molecke, G. Pinkse, J., (2017). Accountability for social impact: A bricolage perspective on impact measurement in social enterprises. J. Bus. Ventur., 32(5): 550–568 **(19 pages).**

Montiel, I., (2008). Corporate social responsibility and corporate sustainability: Separate pasts, common futures. Organ. Environ.,

21(3), 245–269 **(15 pages).**

Montalván Olivares, D.M.; Santana, C.; Neris, J.; Martinez Luzardo, F.H.; Mol, A.W.; Garcia Velasco, F., (2023). Assessment of Potential Human Health, Radiological and Ecological Risks Around Mining Areas in Northeastern Brazil. Environ. Geochem. Health. 46: 342.

Nechaev, I.; Hain, D.S., (2023). Social impacts reflected in CSR reports: Method of extraction and link to firms innovation capacity. J. Cleaner Prod., 429: 1-17 **(17 pages).**

OECD, (2022). Responsible Business Conduct in the Extractive and Minerals Sector in Latin America and the Caribbean. OECD Publishing, Paris.

Organismo de Evaluación y Fiscalización Ambiental. (2022). Reporte N° 00015-2022-OEFA/DEAM-STEC. Perú.

Orlitzky, M., (2015). The politics of corporate social responsibility or: why Milton Friedman has been right all along. Ann. Soc. Respons., 1(1): 5–29 **(25 pages).**

Owiredu, D.; Chidwick, H.; Kwagala, B.; Mensah, D.; Osei, L.; Kapiriri, L., (2025). Water, sanitation, and hygiene challenges in last-mile artisanal mining communities in Ghana and Uganda. Dialogues Health. 7(1): 2-11 **(10 pages).**

Oviedo, H.C.; Campo-Arias, A., (2005). Aproximación al uso del coeficiente alfa de Cronbach. Revista Colombiana de Psiquiatría. 34(4): 572–580 **(19 pages).**

Porter, E.M.; Kramer, R.M., (2006, December). Strategy and Society: The link between competitive advantage and corporate social responsibility. Harv. Bus Rev., PMID: 17183795**.**

Prno, J.; Scott Slocombe, D., (2012). Exploring the origins of 'social license to operate' in the mining sector: Perspectives from governance and sustainability theories. Resour. Policy. 37(3): 346–357 **(12 pages).**

Rabel, S.; Williams, G.; Thompson, J.; Gramling, R.; Petterson, J. S.; Holden, A., (1995). Guidelines and principles for social impact assessment. Interorganizational Committee on 457 Guidelines and Principles for Social Impact Assessment, 15: 11–43 **(33 pages).**

Rahnema, M.; Amirmoeini, B.; Moradi Afrapoli, A., (2023). Incorporating Environmental Impacts into Short-Term Mine Planning: A Literature Survey. Mining. 3(1): 163–175 **(13 pages)**.

Ranängen, H.; Zobel, T., (2014). Revisiting the 'how' of corporate social responsibility in extractive industries and forestry. J. Cleaner Prod., 84(1): 299–312 **(14 pages).**

Rathobei, K.E.; Ranängen, H.; Lindman, Å., (2024). Exploring broad value creation in mining - Corporate social responsibility and stakeholder management in practice. Extractive Ind. Soc., 17: 1-10 **(10 pages).**

Rogers, W.M.; Schmitt, N.; Mullins, M.E., (2002). Correction for unreliability of multifactor measures: comparison of alpha and parallel forms approaches. Organ. Res. Methods. 5(2): 184–199 **(16 pages).**

Ross, M.L., (1999). The Political Economy of the Resource Curse. World Politics. 51(2): 297–322 **(26 pages).**

Ruiz-Blanco, S.; Romero, S.; Fernandez-Feijoo, B., (2022). Green, blue or black, but washing–What company characteristics determine greenwashing? Environment, Development and Sustainability: a multidisciplinary approach to the theory and practice of sustainable development. Environ. Dev. Sustainability. 24(3): 4024–4045 **(22 pages).**

Saenz, C., (2018). The context in mining projects influences the corporate social responsibility strategy to earn a social licence to operate: A case study in Peru. Corporate Soc. Respons. Environ. Manage., 25(4): 554–564 **(11 pages).**

Sawedi, M.; Suryanto A.; Ridwan S.; Sukri T.; Amril H.; Zarah A.H.A y Bama A.P., (2024) Corporate social responsibility programs in mining areas: insights from stakeholder groups in Indonesia. Cogent Soc. Sci., 10(1): 1-16 **(16 pages).**

Seloa, P.; Ngole-Jeme, V., (2022). Community Perceptions on Environmental and Social Impacts of Mining in Limpopo South Africa and the Implications on Corporate Social Responsibility. J. Integr. Environ. Sci., 19(1): 189–207 **(19 pages).**

Sheehy, B.; Farneti, F., (2021). Corporate Social Responsibility, Sustainability, Sustainable Development and Corporate Sustainability: What Is the Difference, and Does It Matter? Sustainability. 13(11): 2-17 **(16 pages).**

Siaw, D.; Ofosu, G., Sarpong, D., (2023). Cocoa production, farmlands, and the galamsey: Examining current and emerging trends in the ASM-agriculture nexus. J. Rural Stud. 101: 1-8 **(8 pages).**

Ullah, M.; Umair, M.; Sohag, K.; Mariev, O.; Khan, M. A., Sohail, H.M., (2024). The connection between disaggregate energy use and export sophistication: New insights from OECD with robust panel estimations. Energy. 306.

Uyar, A.; Koseoglu, M.A.; Kılıç, M.; Mehraliyev, F., (2021). Thematic structure of sustainability reports of the hospitality and tourism sector: A periodical, regional, and format-based analysis. Curr. Issues Tourism. 24(18): 2602–2627 **(26 pages).**

Vara Horna, A., (2012). Desde La Idea hasta la sustentación: Siete pasos para una tesis exitosa. Un método efectivo para las ciencias empresariales, 3.ª ed. Instituto de Investigación de la Facultad de Ciencias Administrativas y Recursos Humanos. Universidad de San Martín de Porres**.**

Vershinina, I.M., (2022). La minería en América Latina y nuevos desafíos ecológicos. Iberoamerica. Russian Federation. 3: 32–56 **(25 pages).**

Widana, A., (2019). The Impacts of Mining Industry: Socio-economics and political impacts. SSRN Electron. J., 21: 1-28 **(28 pages).**

Yadira, V.R.R.; del Rocio, Z.C.S.; Santos, N.T.E.; Roger, B.B.; Andre, A.A.P.; Walter, Z.P.H.; Patricia, R.P.N., (2023). Corporate social responsibility: A sustainable competitiveness factor in a mining company. International Multiconference on Entrepreneurship, Innov. Region. Dev., 3: 1-7 **(7 pages).**

Yeboah, S.; James Nyarkoh, B., (2023). The Impact of Mining on the Ghanaian Economy: A Comprehensive Review (1992-2020). MPRA Paper. 11: 1-21 **(21 pages).**

Yousefian, M.; Bascompta, M.; Sanmiquel, L.; Vintró, C.; Sidki-Rius, N., (2024). Corporate social responsibility and total factor productivity: the case of European mining industry. Min. Econ., 37(1): 149–161 **(13 pages).**

Yudarwati, G.A.; Tjiptono, F., (2017). An enactment theory perspective of corporate social responsibility and public relations. Market. Intelligence Plan., 35(5): 626–640 **(25 pages).**

Zornoza Bonilla, J.A., (2022). Debilidad institucional y políticas extractivistas en América Latina en el siglo XXI. Análisis de la deforestación y los conflictos medioambientales en Bolivia, Brasil y Colombia. Estudios de Derecho, 79(174): 13–38 **(26 pages).**

AUTHOR (S) BIOSKETCHES

Huamaní, C.J., M.Sc., Associate Professor, Department of Administration, National University Micaela Bastidas of Apurímac, Av. 04 de noviembre s/n, Tamburco, Apurímac, Perú.
- Email: jhuamani@unamba.edu.pe
- ORCID: 0000-0003-0404-8557
- Web of Science ResearcherID: NA
- Scopus Author ID: N.A
- Homepage: https://unamba.edu.pe/pregrado/administracion/administracion.html

Palomino Aroni, J.C., BSc., Researcher, Department of Administration, National University Micaela Bastidas of Apurímac, Victor Acosta II Etapa, Tamburco, Apurímac 03001, Perú.
- Email: *162037@unamba.edu.pe*
- ORCID: 0009-0004-8128-2085
- Web of Science ResearcherID: OBN-8333-2015
- Scopus Author ID: N.A
- Homepage: https://unamba.edu.pe/pregrado/administracion/administracion.html

Calderon Vilca, H.D., Ph.D., Assistant Professor, Group of the Universidad Nacional Mayor de San - Peru, professor in the Universidad Nacional de Ingeniería. Professor of doctoral programs in other universities. Development projects related to Neural Networks, Machine Learning and Natural Language Processing, advisor of undergraduate and graduate thesis, Cercado de lima, Lima, Perú.
- Email: *hcalderonv@unmsm.edu.pe*
- ORCID: 0000-0002-1177-4947
- Web of Science ResearcherID: IYJ-2571-2023
- Scopus Author ID: 57208096312
- Homepage: https://www.linkedin.com/in/david-calderon-vilca-b5390949

León Vicencio, J.L., M.Sc., Researcher, Department of Accounting, Technological University of the Andes, Av. 04 de noviembre s/n, Tamburco, Apurímac, Perú.
- Email: *jleonv@utea.edu.pe*
- ORCID: 0000-0003-2607-8474
- Web of Science ResearcherID: NA
- Scopus Author ID: NA
- Homepage: https://utea.edu.pe/contabilidad/

Suyo Cruz, G., Dr., Associate Professor, Department of Administration, National University San Antonio Abad of Cusco, Av. de la Cultura, Cusco, Cusco, Perú.
- Email: *gabriel.suyo@unsaac.edu.pe*
- ORCID: 0000-0002-9490-403X
- Web of Science ResearcherID: NA
- Scopus Author ID: NA
- Homepage: https://www.unsaac.edu.pe/facultad-de-administracion-y-turismo/

Pinto Pagaza, D.A., Dr., Associate Professor, Department of Administration, National University Micaela Bastidas of Apurímac, Av. Prado Bajo, Abancay, Apurímac, Perú.
- Email: *apinto@unamba.edu.pe*
- ORCID: 0009-0008-5457-7880
- Web of Science ResearcherID: NA
- Scopus Author ID: NA
- Homepage: https://unamba.edu.pe/pregrado/administracion/administracion.html

Mamani Huillca, B.O., MCs., Student, Researcher, Department of Administration, National University Micaela Bastidas of Apurímac, Av. Inca Garcilazo de la Vega, Abancay, Apurímac, Perú.
- Email: *bmamani@unamba.edu.pe*
- ORCID: 0000-0002-5631-1188
- Web of Science ResearcherID: NA
- Scopus Author ID: NA
- Homepage: https://unamba.edu.pe/pregrado/administracion/administracion.html

Oros Torres, W., M.Cs., Researcher, Department of Administration, National University Micaela Bastidas of Apurímac, Calle Cusco, Tambobamba, Apurímac, Perú.
- Email: *Woros@unamba.edu.pe*
- ORCID: 0000-0002-6773-496
- Web of Science ResearcherID: NA
- Scopus Author ID: NA
- Homepage: https://unamba.edu.pe/pregrado/administracion/administracion.html

Pinto Boda, S.R., M.Cs., Researcher, Department of Administration, National University Micaela Bastidas of Apurímac, Av. Inca Garcilazo de la Vega, Abancay, Apurímac, Perú.
- Email: *Spinto@unamba.edu.pe*
- ORCID: 0000-0002-9770-5984
- Web of Science ResearcherID: NA
- Scopus Author ID: NA
- Homepage: https://unamba.edu.pe/pregrado/administracion/administracion.html

AUTHOR (S) BIOSKETCHES

Contreras Salas, L., Dr., Researcher, Department of Administration, National University Micaela Bastidas of Apurímac, Av. Inca Garcilazo de la Vega, Abancay, Apurímac, Perú.
- Email: *Lcontreras@unamba.edu.pe*
- ORCID: 0000-0001-9040-7602
- Web of Science ResearcherID: NA
- Scopus Author ID: NA
- Homepage: https://unamba.edu.pe/pregrado/administracion/administracion.html

HOW TO CITE THIS ARTICLE

Huamaní, C.J.; Palomino Aroni, .J.C.; Calderon Vilca, H.D.; León Vicencio, J.L.; Suyo Cruz, G.; Pinto Pagaza, D.A.; Mamani Huillca, B.O.; Orós Torres, W.; Pinto Boda, S.R.; Contreras Salas, L., (2026). Environmental impact of mining social responsibility on rural communities. Global J. Environ. Sci. Manage., 12(1): 207-228.

DOI: 10.22034/gjesm.2026.01.12

URL: https://www.gjesm.net/article_731680.html

Global J. Environ. Sci. Manage. 12(1): 229-248, Winter 2026, Serial #45

Global Journal of Environmental Science and Management
(GJESM)

Homepage: https://www.gjesm.net/

Podcasts

CASE STUDY

The influence of demographic and socioeconomic factors on a fishing community's resilience to coastal flooding

C.D.A. Depari*

Department of Architecture, Faculty of Engineering, Universitas Atma Jaya Yogyakarta, Sleman, 55281 Indonesia

ARTICLE INFO

Article History:
Received 24 July 2025
Revised 02 October 2025
Accepted 04 November 2025

Keywords:
Disaster risk reductions
Flood disaster management
Multiple linear regression
Perceived resilience
Socio-demographic factors

ABSTRACT

BACKGROUND AND OBJECTIVES: Coastal communities are increasingly vulnerable to flooding, with flood frequency projected to be double this century. Nevertheless, community engagement in flood management is typically perceived as a lesser priority, leading to ineffective measures in mitigating their disaster risks. Meanwhile, there remains a limited understanding of how socio-demographically distinct groups perceive their adaptive capacities, which essentially enables planners to identify resilience assets at the community level and design appropriate interventions for vulnerable groups. This study aims to examine how demographic and socioeconomic factors influence the perceived resilience of a community at risk, with the Tambakrejo fishing community as the case. The distinctiveness of this study is its concentration on perceived resilience rather than perceived risks to grasp local adaptive capacities.

METHODS: To reach the goal, a survey research design was implemented with 100 participants—selected through simple random sampling, and multiple linear regression were employed. Statistical analysis was carried out using International Business Machines Corporation -statistical package for the social sciences 31, with perceived resilience as the outcome variable and seven demographic and socioeconomic factors—age, gender, living duration, educational level, occupation, land ownership, and household size—as predictors.

FINDINGS: The study found that age negatively influences perceived resilience (β=-0.322, $p<.005$), with older individuals showing lower perceived resilience than their younger counterparts. This may be associated to their perception of environmental challenges. Females show a stronger perceived resilience than males (β=0.451, $p<.005$), which can be associated with their active participation in local activities. Landowners frequently display a more pronounced sense of perceived resilience than non-landowners (β=-0.270, $p<.005$ for spouses; β=-0.418, $p<.005$ for ancestors), which may correlate with their self-efficacy in mitigating disaster risks.

CONCLUSION: Understanding people's perceived resilience allows the identification of socio-demographic groups that require specific interventions. For senior citizens, it is advisable to adopt strategies that also acknowledge the security of their environment. The male group requires institutional support for its economic sustainability. The landless group should be engaged in activities aimed at developing their adaptive capacities. Subsequent studies should aim to tackle the limitations present in this research, including the overrepresentation of the sample, the small size of the sample, and the cross-sectional data that might hinder generalizability.

DOI: 10.22034/gjesm.2026.01.13

This is an open access article under the CC BY license (http://creativecommons.org/licenses/by/4.0/).

NUMBER OF REFERENCES
96

NUMBER OF FIGURES
6

NUMBER OF TABLES
8

*Corresponding Author:
Email: *catharina.depari@uajy.ac.id*
Phone: +812 8103 2161
ORCID: 0000-0003-3358-2951

Note: Discussion period for this manuscript open until Mar 1, 2026 on GJESM website at the "Show Article".

INTRODUCTION

Floods, accounting for 43 percent (%) of natural disaster incidents worldwide (Hu *et al.*, 2018), are widely regarded as the most severe natural disaster (Mai *et al.,* 2020). The threats become alarming, as by 2050, the current 100-year return period of floods is projected to occur twice as frequently as it does today (Rentschler *et al.,* 2022). Approximately 12 million individuals are displaced annually due to floods, making up 54% of all disaster-related displacements (Mester *et al.,* 2025). In Indonesia, floods caused 6.5 million displacements, representing 63% of the total incidents from 2010 to 2021 (Cazabat *et al.,* 2023). Furthermore, the escalating risks associated with flooding have highlighted various cases that reveal the shortcomings of top-down flood disaster risk reduction (DRR), which often neglects the role of community engagement (Peters, 2019). For instance, local leaders in Ghana have limited involvement in flood management (Atanga, 2020), and the community's roles were overlooked in the development of a flood early warning system in Namibia (Josè Moisès *et al.,* 2023). Meanwhile, the Sendai Framework for Disaster Risk Reduction (SFDRR) has emphasized the importance of empowering communities in DRR planning and promoting their ownership of DRR initiatives to understand their actual risks (Nkombi and Wentink, 2022). Recognizing the perspectives of vulnerable communities with diverse socio-economic and demographic attributes in planning is essential for successful DRR (Mehryar and Surminski, 2022). The insights would help policymakers understand their preparedness level, provide appropriate assistance, identify vulnerable groups (Mondino, 2023), and implement interventions that address their socio-psychological needs (Ahmed *et al.,* 2025). Perceptions are important determinants of an individual's actions (Bickerstaff *et al.,* 2008; Leiserowitz, 2010), adaptive behaviors (Eakin *et al.,* 2016; Elrick-Barr *et al.,* 2017), and precautionary measures (Grothmann and Reusswig, 2006; Wang *et al.,* 2025). By prioritizing perceptions over direct coping behaviors, policymakers would be better equipped to forecast the community's coping strategies and design interventions that are more precisely aligned with their needs. Analyzing the coping behaviors alone, without considering perceptions, may result in a biased view of the community's ability to adapt and interventions that do not align with the community's needs. People do not respond directly to a risk when exposed to it; instead, they evaluate it based on their risk perceptions, defined as a subjective judgment about the characteristics of a specific threat (Slovic, 1987; Slovic *et al.,* 2005). The concept of perceived risk illustrates a person's capability to embrace risks and plays a vital role in creating specific initiatives aimed at increasing risk awareness (Diakakis *et al.,* 2018). Various factors influence perceived risks. Subjective factors include individual and direct experience (Agrawal, 2018; Dobre *et al.,* 2025; Mondino, 2023; van der Linden, 2014; van der Linden, 2015), myths, cultural practices, education, personal resources, community network (Dobre *et al.,* 2025), voluntary/involuntary nature, and flood victims (Lechowska, 2018). Objective factors encompass demographic characteristics (Huang *et al.,* 2022; Lassa *et al.,* 2025; Lechowska, 2018; Lindell and Hwang, 2008; Terpstra and Lindell, 2013), hazard-related attributes (Lechowska, 2018; Terpstra and Lindell, 2013), and proximity to hazards (Lechowska, 2018; Zhang *et al.,* 2008). Another significant concept that introduces novelty to this study is perceived resilience. Unlike perceived risks, which imply vulnerability, perceived resilience is associated with a subjective assessment of one's self-capacities to bounce back from adversity. It pertains to a person's cognitive and affective evaluation of their capability to predict, defend against, adapt to, and modify the environment when faced with stress (Kieu and Senanayake, 2023). Regarding resilience, it is generally defined as a process that connects a set of adaptive capacities to a positive trajectory of functioning and adaptation (Norris *et al.,* 2008). Within the framework of a community, resilience may be described as 'the availability, enhancement and participation of community resources by its members to succeed in an environment characterized by change, uncertainty, unpredictability, and surprise' (Magis, 2010). Community resilience encompasses various factors, including collective resources, organizational structure, and governance, that enable communities to adapt to new circumstances and mitigate negative outcomes (Cox and Perry, 2011; Norris *et al.,* 2008). Community resilience illustrates the strengths that stem from the comprehensive goods and services offered by local resources. In relation to resilience, those resources can be

categorized into: 1) built assets—man-made structures, built for specific purposes, 2) natural assets—environmental features that yield ecosystem services and tangible natural resources, and 3) social assets—networks, mutual trust, shared interests, and particular skills (Freitag *et al.,* 2014). Perceived resilience is influenced by various factors, such as place attachment (Guo *et al.,* 2018a), social capital (Guo *et al.,* 2018b), personal experiences, and demographic factors (Askari *et al.,* 2025; Diakakis *et al.,* 2018; Liu *et al.,* 2024; Sambu and Mhongo, 2019; Soetanto *et al.,* 2017; Weber, 2010). Nonetheless, the manner in which these factors affect perceived resilience and risks varies across different studies. For example, age is generally found to significantly affect perceived resilience. In some cases, older people exhibit a higher risk perception compared to younger people (Kang *et al.,* 2025), while in other cases, younger people perceive greater flood risks (Babcicky and Seebauer, 2017; Huang *et al.,* 2022). Gender does not uniformly affect the perception of flood risk; nonetheless, certain studies have indicated that women typically demonstrate a greater awareness of flood risks compared to men (Ho *et al.,* 2008; Lindell and Hwang, 2008; McDowell *et al.,* 2020). The effects of education on risk perception also vary across studies, with some indicating no correlation (Babcicky and Seebauer, 2017), while others suggest the opposite (Botzen *et al.,* 2009; Wei *et al.,* 2025; Yildiz *et al.,* 2024). In some cases, lower-income individuals tend to show greater perception of risks than higher-income individuals (Babcicky and Seebauer, 2017; Lo, 2014), while others found that the latter perceived higher resilience (Kieu and Senanayake, 2023; Rasmussen and Ewald, 2022). In contrast, several studies have indicated that there is no relationship between income and perceived resilience (Botzen *et al.,* 2009). Additionally, land ownership has been found to significantly contribute to greater perceptions of risks and resilience, as evident in Tamale and Wa municipalities in Ghana (Ibrahim *et al.,* 2025). Furthermore, extensive studies have been carried out to understand the influence of both subjective and objective elements on risk perceptions. However, those focusing on perceived resilience are relatively limited. Moreover, in the context of the Tambakrejo fishing community, prior studies primarily focused on the effects of marine-based tourism on the community's identity (Mustofa *et al.,* 2021), the factors influencing local environmental attitudes and practices (Ramadhan, 2024), the effects of a sea embankment toll road on community resistance (Jamaludin and Mahdi, 2025), and the community's vulnerability to natural disasters (Khasanah, 2023). According to the author's knowledge, there has yet to be an investigation into the elements that influence the perceived resilience of the Tambakrejo community. This study aims to examine how demographic and socio-economic factors affect the perceived resilience of a coastal community, using the Tambakrejo fishing village in Central Java as a case study. For an extended period, this community has encountered the repercussions of flooding and has been engaged in continuous disputes with the regional authority over the pressures resulting from local infrastructure development and industrial operations. Two key questions derived from the study background are: 1) How does the coastal community perceive its resilience to unexpected floods? and 2) Which demographic and socio-economic attributes significantly affect their perceived resilience? To accomplish the research goal, a survey approach and statistical evaluation through multiple linear regression were employed. The findings revealed that three demographic attributes: age, gender, and land ownership-significantly predict perceived resilience to floods. Furthermore, the resources that underpin the community's livelihood, such as mangroves, community groups, local leaders, and seawalls, were significantly associated with a strong perception of resilience. This study was conducted in a high-risk coastal area of Tambakrejo fishing village in Central Java, Indonesia, in 2024-2025.

MATERIALS AND METHODS

Study area

The study area is located in Tambakrejo fishing village, Semarang, Central Java (Fig. 1). Semarang, noted for being one of Indonesia's most populous urban areas, is greatly at risk from coastal flooding and the elevation of sea levels. This condition is mainly attributed to environmental factors, such as the city's air temperature, which, over the last ten years, has increased by 2-5 degrees Celcius (°C), the continuous land subsidence, which reaches a rate of approximately 20 centimeters (cm) per year (Semarang, 2019; Widodo *et al.,* 2018), and the city's geography, which is characterized by low-lying areas.

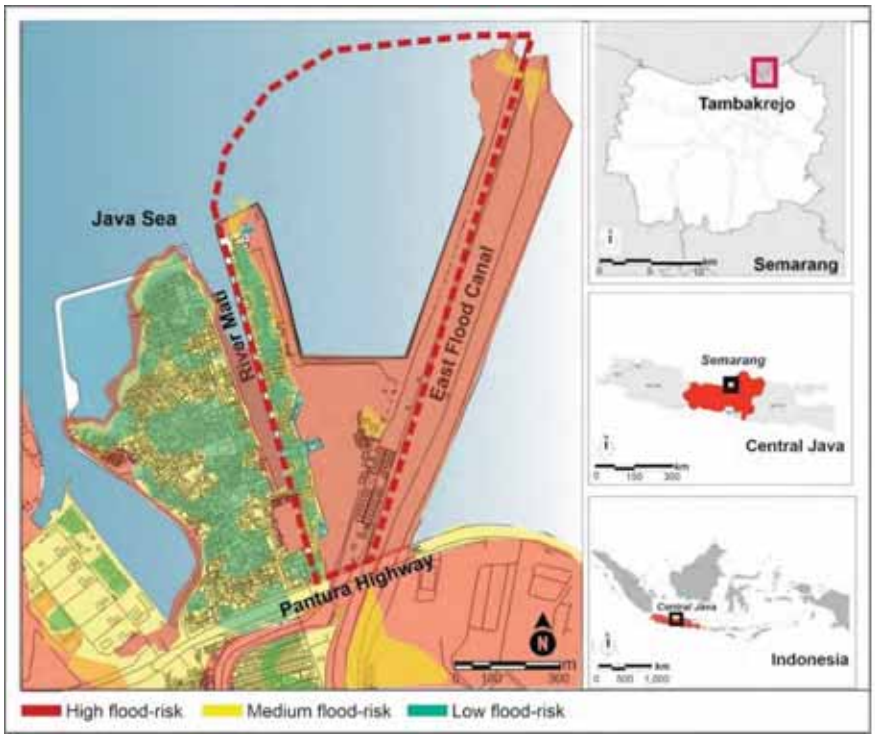

Fig. 1: Geographic location of the study area in the Tambakrejo's flood hazard risk zones according to the Semarang authority

Tambakrejo, the largest fishing village in Semarang, is frequently impacted by coastal floods (Khasanah, 2023; Ramadhan, 2024). The area is bordered by the Java Sea to the north, the East Flood Canal to the east, and the River Mati to the west. Its setting is relatively isolated from the major streets and surrounding settlements (Fig. 2). The local population, predominantly engaged in fishing, had adapted to catching fish for their everyday needs by employing either fishing boats that could carry around 5-10 gross tons (GT) or relying on their own means without any vessels. Given their modest fishing gear and operationalization within proximity to the shore, Tambakrejo fishermen are classified as small-scale fishermen. Their monthly income, on average, was below the provincial minimum wage of United States Dollar (USD) 140, which understandably made them live in extremely poor living conditions (Khasanah, 2023). Despite their exposure to threats, many residents resisted the government's relocation scheme, which was a part of the 2018 River East Flood Canal Normalization Project. From the nearly 500 households identified for relocation to Kudu Housing, 97 households decided against joining the program. In response, the government developed a temporary row of dwellings near the River Mati area for the dissidents (Pemerintah Kota Semarang, 2021).

Before the river normalization project, Tambakrejo had at least three categorical types of fishermen: fishpond fishermen, net fishermen, and fishing rod fishermen. The initial category pertains to individuals who participated in aquaculture enterprises by establishing fish ponds as a reaction to the elevated salinity of the seawater. The other two groups—net fishermen and fishing rod fishermen—refer to those who prefer to catch fish in the sea. Nonetheless, the river normalization initiative, which later eliminated mangroves from the coast, caused a considerable drop in fish catches. As a result, some fishermen expanded their fishing territories further into the sea and changed their traditional boats into motorized ones (Mustofa *et al.*, 2021). In 2015, the government designated Tambakrejo as a maritime-based tourism *kampong* and began constructing hard protective measures, such as seawalls, which were completed in the following two years (Pemerintah Kota Semarang, 2024).



Fig. 2: Resilience assets of the Tambakrejo fishing community as surveyed in 2024

Research approach and design

To explain the effects of demographic factors on perceived resilience (Fig. 3), the study employed a survey research design. A collection of structured questions was designed in Google Forms and underwent pre-testing to confirm the instrument's reliability. A repeated measure was conducted with 10 respondents who were asked similar questions at different times. The findings showed a consistent response. In the reliability test, Cronbach's Alpha was not applied as it could not indicate the reliability of heterogeneous constructs like perceived resilience (Edelsbrunner *et al.,* 2025). Using the Pearson Correlation Coefficient, correlations between the seven predictors were tested. Statistically significant correlations were identified, confirming the questionnaire's validity. Questions covered two aspects: respondents' demographic profile and respondents' perceived resilience represented by a question "To what extent do you feel resilient in your settlement" with a five-point Likert scale (1= very unresilient, 2= unresilient, 3=moderately resili3ent, 4= resilient, 5= very resilient). Although a single-item Likert-scale seems oversimplistic, it can still produce a high reliability and validity, which is similar to that in a multi-item composite scale for a subjective assessment (Cheung and Lucas, 2014). Furthermore, a single-item Likert scale is efficient to implement in studies with time limitations and helps minimizing the load on participants (Fig. 3). In addition to the method, follow-up and open-ended questions were included in the questionnaire, such

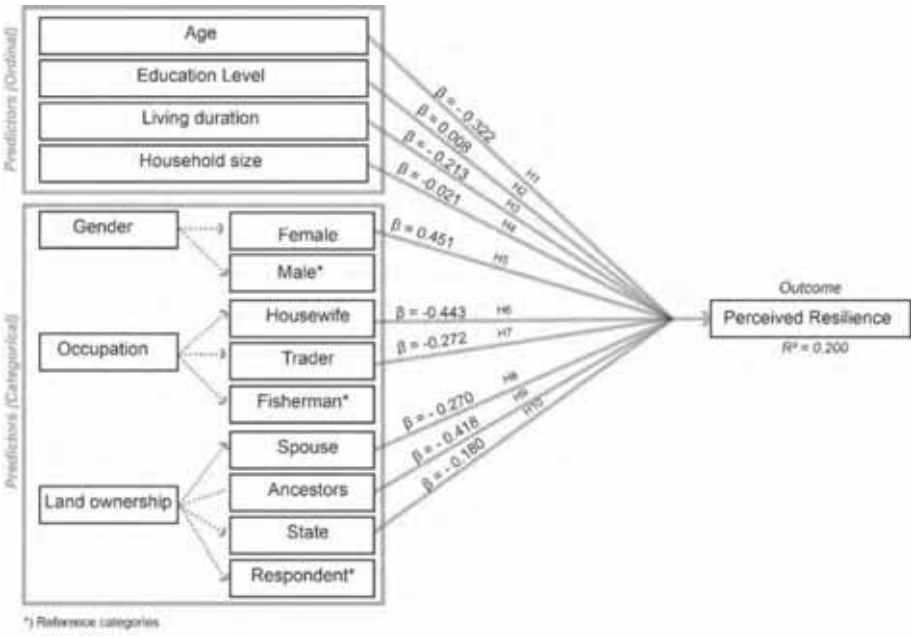

Fig. 3: The conceptual framework of the quantitative study

as "What makes you feel resilient/unresilient?" and "What resources are important for your resilience?" The responses to these questions were categorized into three types: built assets, natural assets, and social assets (Freitag *et al.,* 2014). All responses were then analyzed using multiple linear regression with International Business Machines (IBM) statistical package for social sciences (SPSS) version 31.0. Besides questionnaires, unstructured interviews, field surveys, and a literature review were utilized to collect comprehensive information that would bolster the research interpretations. Multiple linear regression is chosen because of its compatibility with the study's objective. This approach facilitates the assessment of the distinct influences of different predictors on perceived resilience, controlling for any potential confounding variables. It recognizes the predictors that best account for the outcome and estimates the values of each predictor.

Sampling and data collection

The study implemented a simple random sampling method, which is recognized for its effectiveness in minimizing selection bias by guaranteeing that each member has an equal likelihood of selection (Ahmed, 2024). The sampling size was 110 respondents, representing approximately 1,500 residents. With this population size, statisticians recommended a sample of 230 for categorical data with a margin of error of 0.05 (Bartlett *et al.,* 2001). In comparison, Hair *et al.* (2018) argued that 100 is generally acceptable for a simple linear regression. Even with its limited quantity, the sample size has shown to be adequate for conducting linear regression analysis. For example, using only 100 samples, scholars could still obtain a reliable result that shows a statistically strong positive correlation between resilience and social engagement (Ibrahim and Hussein, 2024) and that between resilience and spiritual intelligence (Sandri and Siagian, 2025). Ten students pursuing their undergraduate studies at Universitas Negeri Semarang, a local university, were recruited to aid in the administration of the questionnaires in the field. These students were then trained to run the questionnaire and to obtain the respondents' verbal consent. In the field, they selected respondents randomly and helped them fill in the questionnaire using an online Google Form.

Data processing and analysis

A statistical analysis using IBM SPSS version 31 was employed to analyze the survey data. The dependent

variable (Y) was determined as 'perceived resilience' and operationalized as nominal data with five Likert scale indicators. Seven independent variables/ predictors (X) were assessed for their influence on perceived resilience. These include: (1) age, (2) gender, (3) educational level, (4) land ownership status, (5) duration of living, (6) household size, and (7) occupation (Table 1). As many previous studies suggest, these factors typically have direct effects on perceptions. Therefore, no control variables were involved in this study. Control variables are applied only when the aim is to analyze how subjective elements, such as social networks, influence perceived resilience. Related to the research questions, hypotheses were developed: the null hypothesis (H_0) states that "demographic and socioeconomic factors do not significantly influence the community's perceived resilience," and the alternative hypothesis (H_A) states that "demographic and socioeconomic factors significantly influence the community's perceived resilience."

Regression model

To test the hypothesis, the study utilized multiple linear regression, a statistical analysis procedure that expands linear regression by incorporating multiple independent variables in an equation to analyze their relationships with a dependent variable (Pederson, 2017). The selected analysis method aligns well with the research objective and demonstrates a greater

Table 1: The measurement types of research variables

Variable type	Variable	Measure Type	Classification
Outcome/ Dependent	Perceived resilience	Ordinal	1 = Very unresilient 2= Unresilient 3= Moderately resilient 4= Resilient 5= Very resilient
Predictors/ Independent	Age	Continuous/scale	-
	Education level	Ordinal	1 = Never attended 2 = Elementary school 3 = Junior High School 4 = Senior high school 5 = University
	Living duration (years)	Ordinal	1 = 1-5 years 2 = 6-10 years 3 = >10 years
	Household size (members)	Ordinal	1 = 1 member 2 = 2-3 members 3 = 4-5 members 4 = >5 members
	Gender	Nominal	1 = Female 2= Male
	Occupation	Nominal	1 = Civic employee 2 = Fisherman 3 = Housewife 4 = Laborer 5 = Office staff/employee 6 = Pensioner 7 = Trader/seller 8 = Others
	Land/home ownership	Nominal	1 = Not sure 2 = Respondent's legal certificate 3 = Spouse's legal certificate 4 = Ancestors' legal certificate 5 = Sibling's/relative's/predecessor's legal certificate 6 = State

capacity to identify the influence of independent variables on a dependent variable compared to other regression models, such as ordinal logistic regression, which is characterized by a binary and multinomial dependent variable. The multiple linear regression model was formulated using Eq. 1 (Mohr *et al.*, 2022):

$$Y = a + \beta_1 x_1 + \beta_2 x_2 + \beta_3 x_3 + \beta_4 x_4 + \beta_5 x_5 + \beta_6 x_6 + e \quad (1)$$

Where;

Y	= perceived resilience
X_1	= age
X_2	= education level
X_3	= living duration
X_4	= household size
X_5	= gender
X_6	= occupation
X_7	= land ownership status
$\beta_1 - \beta_6$	= regression coefficients of each predictor
a	= regression constant
e	= tolerable error term

Data screening and transformation

Before running a multiple linear regression, all categorical data were transformed into intervals that work best for parametric statistics like multiple linear regression. The technique utilized was selected according to the data type (nominal or ordinal). The method of successive intervals (MSI) was used to transform the ordinal data type, while the nominal data was transformed through dummy coding. The ordinal data comprised three predictors, educational level, duration of living, and household size, and the outcome variable (i.e., perceived resilience). To perform MSI, the initial step involved calculating the frequency of each item, which was then followed by computing the proportion of each category—where the frequency was divided by the total samples (n=110), cumulative proportion, Z-value, density values for each value of Z, Scale Value (SV), changing the smallest SV to be equal to one, and transforming each SV to the smallest scale changes to attain transformed scale value (TSV) (Asdar and Badrullah, 2016). The nominal variables included gender, occupation, and land ownership (Table 1). When performing dummy coding, the total number (n) -1 dummy variables were applied. The reference categories for the nominal variables were classified as male for 'gender', fishermen for 'occupation, and the respondent's legal certificate for 'land ownership'. The complete transformation process took place in Excel, following which the new data were transferred to SPSS for statistical analysis.

Classic assumption testing

First, tests of multivariate normality and outliers were performed. The multivariate normality condition continues to be unmet owing to the inherent properties of the transformed data, which is constrained by its rank order and unequal interval spaces. To detect outliers, the number of standard deviations (Z-scores) of each variable was retrieved, and the Mahalanobis distance method was applied. Values greater than '3' were categorized as outliers and subsequently excluded from the dataset, which decreased the number of observations to 91. These data, 'occupation' (laborers, office staff, pensioners) and 'land ownership' (not sure, and sibling), were removed given their low frequency. Before removing them, the adjusted R^2 was 0.0209. Subsequent to the removal, it escalated to 0.10, signifying that the removal results in a more accurate and trustworthy regression model. Next, classic assumption tests for regressions were assessed to ensure that the model produces an unbiased, consistent, and efficient estimator. The assessments encompass multicollinearity, heteroscedasticity, normality, and linearity (Poston *et al.*, 2023; Nau, 2020). A multicollinearity assessment was conducted to examine the correlations among the predictors in the model. The analysis revealed that the correlation values were below the threshold of 0.90, collinearity tolerance was greater than 0.10, and the variance inflation factor (VIF) was less than 10, indicating that strong multicollinearity was not presented. A heteroscedasticity test was then run to assess whether the regression model's residuals (i.e., error terms) exhibited constant variance, assuming that the error terms were normally distributed. First, a scatter plot was created to visualize this issue. Subsequently, a scatter plot was constructed to depict this problem. The findings revealed that the residuals were more likely to decrease on the left side instead of being scattered or randomly distributed. To obtain more accurate results, the Park test and the Glejser test were performed. The outcomes indicated the presence of heteroscedasticity, as some predictors had significance values below the alpha level. In order

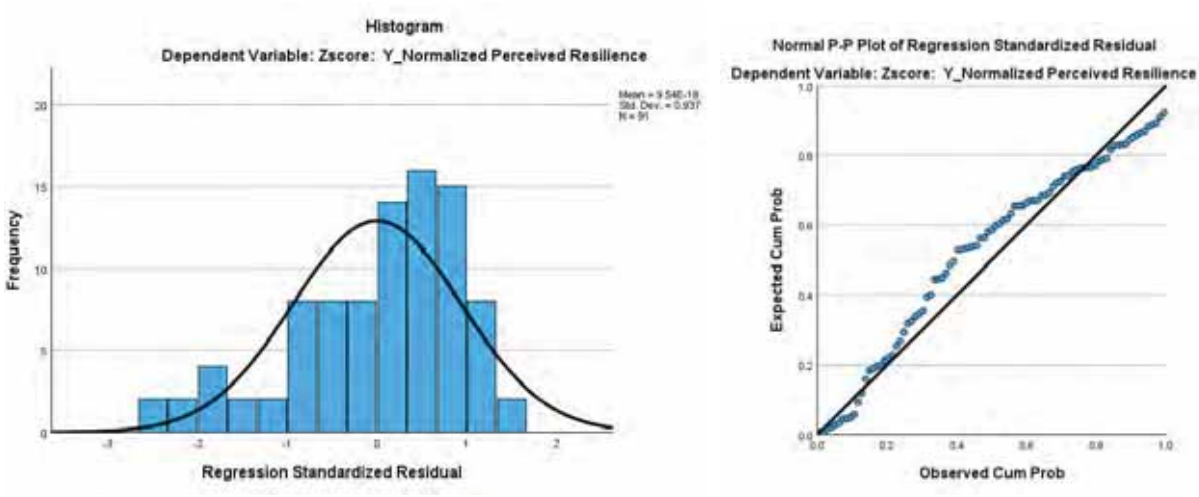

Fig.4: The histogram (left) and normal probability-probability (P-P) plot (right) of research variables

Table 2. The summary of the analysis of variance

Model		Sum of Squares	Degree of freedom (df)	Mean Square	Ratio of two variances (F)	Significance value (Sig.)
1	Regression	19.104	10	1.910	2.006	.043[b]
	Residual	76.188	80	.952		
	Total	95.292	90			

to resolve the problem, Hayes' heteroscedasticity-consistent standard error estimator was applied. The method adjusted the standard errors for each variable to account for heteroscedasticity. Hayes' heteroscedasticity-consistent estimator used to fix the problem was HC3, chosen for its better power and a closer proximity to the targeted small sample size (n-110). The method effectively increases the significance level of predictors 'land ownership by spouse (p=0.17) and by ancestors (p=0.001) to above the alpha (p=0.05). Ultimately, a normality test was executed to ascertain if the residuals in the regression model utilizing the transformed data adhered to a normal distribution. The histogram and scatter plot show that the residuals are not normally distributed, as they slightly deviate from the diagonal line (Fig. 4). In order to achieve a more precise outcome, an additional test was performed. It was found that the Z skewness (-3.50) and the Z kurtosis (0.37) were both below the critical value of ± 2.58, indicating that the residuals were normally distributed (Table 2). The finding was supported by the outcomes of the non-parametric Kolmogorov-Smirnov (K-S) and Shapiro-Wilk (S-W) tests. The statistical significance of the regression model was established, with probability values surpassing the alpha level (K-S = 0.2 and S-W = 0.841), which further corroborates the normal distribution of the residuals.

Finally, a linearity test was executed to analyze the adequacy of the regression model and to identify whether the relationship between the predictors and the outcome variable was linear, quadratic, or cubic. The analysis conducted using SPSS, which involved comparing the means of the variables through analysis of variance (ANOVA), demonstrated a significant linear relationship between each predictor and the outcome variable (perceived resilience). Despite performing data transformations for a robust linear regression, the adjusted coefficient of determination (R-squared) was relatively low (0.09), and the significance value was above the alpha level (0.067), suggesting the model's weak ability to explain the effects of predictors on perceived resilience. To solve this, a dummy variable "occupation others"

(0.853) was removed from the model. This variable was selected because it lacked representativeness regarding the residents' occupation. The removal led to an increase in the adjusted R-squared to 10%, indicating that the variance in the predictors can now explain 10% of the variance in the outcome variable. Within social sciences, this percentage is regarded as acceptable for interpretations (Ozili, 2022). Additionally, eliminating the dummy variable increased the significance of the model to 0.043, which is below the alpha level (Table 2).

RESULTS AND DISCUSSION

Sociodemographic characteristics of respondents

The descriptive statistics reported in this section used the original sample size (110), whereas the regression outcomes are reported using the updated sample sample of 91. Of 110, 42.7% belong to the 46-60 age range, whereas only 1.8% belong to the under-19 age category. Approximately 71.8% of the respondents were female, and 51.8% identify as housewives. Only 10% of the respondents currently work as fishermen. Regarding education, 41.8% have completed elementary education, and 30% possess land certificates. A significant 80% of respondents have lived in Tambakrejo for over 10 years, and 53.6% currently live in households with 4-5 members, including the respondents themselves (Table 3).

A bi-directional chart compares the respondents' age based on gender (Fig. 5). Female respondents aged 40-60 make up the majority, accounting for 71.8% of the respondents (n = 110). Many of these women are primarily housewives, have attained an elementary school education, and hold ownership of land, either on their own or through their partners or ancestors (parents, grandparents). Additionally, they have lived

Table 3: The community's socioeconomic and demographic characteristics

Attribute	Classification	Number of respondents	%
Age	Under 19	2	1.8
	19-24	3	2.7
	25-45	38	34.5
	46-60	47	42.7
	Above 60	20	18.1
Gender	Female	79	71.8
	Male	31	28.2
Occupation	Civic employee	0	0
	Fisherman	11	10.0
	Housewife	57	51.8
	Laborer	8	7.3
	Office staff/employee	4	3.6
	Pensioner	4	3.6
	Trader/seller	11	10.0
	Others	15	13.6
Education level	Never attended	10	8.2
	Elementary school	46	41.8
	Junior High School	27	24.5
	Senior High School	25	22.7
	University	2	1.8
Land and home ownership status	Not sure	2	1.8
	Respondent's legal certificate	33	30
	Spouse's legal certificate	27	24.5
	Ancestors' legal certificate	25	22.7
	Sibling's/relative's/predecessor's legal certificate	2	1.8
	State	21	19.1
Living duration in years	1-5	14	12.7
	6-10	8	7.3
	>10	88	80
Household size	1	6	5.5
	2-3	34	30.9
	4-5	59	53.6
	>5	11	10

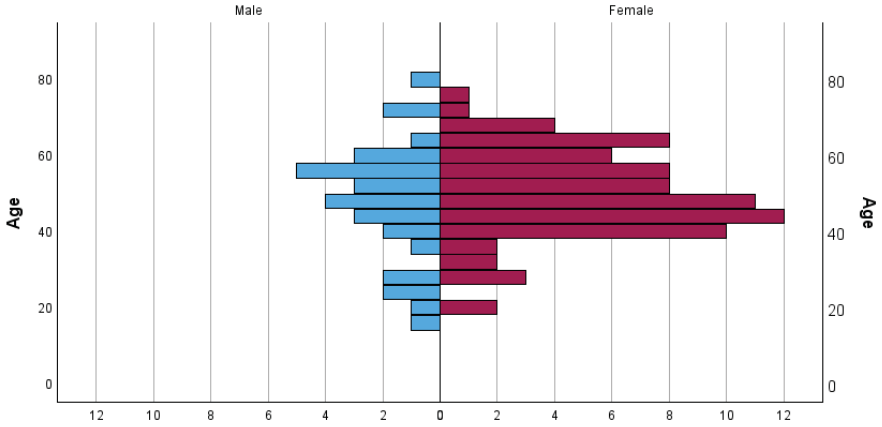

Fig. 5: A bi-directional chart comparing respondents' age based on gender

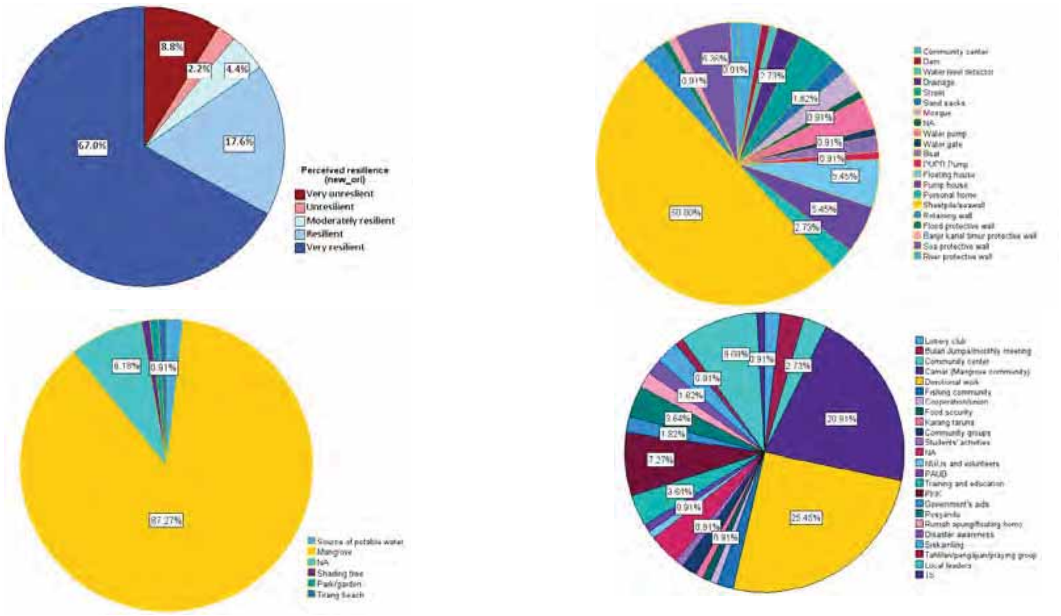

Fig. 6: The respondents' perceived resilience (a) and resilience assets comprising built assets (b), natural assets (c), and social assets (d) in percentage

in Tambakrejo for over 10 years and typically have 4-5 family members in their households.

Community's perceived resilience

The study focuses on perceived resilience, which is the dependent variable for examining the effects of demographic and socio-economic factors. A comprehensive array of views on resilience has been collected via the survey, achieving a 100% response rate. Of the 110 respondents, 67% felt they were very resilient, and 17.6% reported feeling resilient to disaster impacts. While 8.8% identified as very unresilient, 4.4% felt moderately resilient, and only 2.2% considered themselves unresilient. In relation to resilience assets, 50% recognized seawalls as the primary built resource, 87.2% deemed mangroves the most essential natural resource, and 25.45% regarded devotional work as the most significant social asset (Fig. 6).

Participants who believed they possessed significant resilience frequently mentioned their practical understanding of floods, seawalls, and

raised floor levels as essential factors enhancing their resilience. In contrast, those who perceived their resilience as low typically explained the absence of hard protective measures in nearby areas and the unpredictable nature of disasters as barriers to building resilience.

Factors influencing perceived resilience

Table 4 reports the mean, median, and standard deviations of all variables under study. The average age of respondents is 48.56 years, placing the majority of the respondents in the middle-aged group. After excluding outliers (n=19), the analysis included a total of 91 responses in the regression.

According to Table 5, the regression model exhibited robustness and statistical significance, with a correlation coefficient (R) of 0.448 and an adjusted R-square of 0.10. This suggests that approximately 10% of the variability in perceived resilience can be explained by the combined effect of all predictors.

The ANOVA table further validates the model's significance (Table 6). The F-statistic of 2.006 with a p-value of 0.043 indicates that the regression model significantly predicts the dependent variable (i.e., perceived resilience). This indicates that the model is capable of accurately interpreting the influence of demographic and socio-economic factors (predictors) on perceived resilience (outcome).

The model's parameter regression coefficients were acquired subsequent to performing the multiple linear regression analysis (Table 7). The variables that significantly predict the outcome variable (perceived resilience) with a statistical significance less than 0.05 are age, gender (female), and land ownership (spouse and ancestors). Other independent variables were identified as having no significant impact on predicting perceived resilience.

Based on the regression coefficients (Table 7), the final regression model was formulated using Eq. 2 (Mohr *et al.,* 2022):

$$\begin{aligned} &=0.0\ 0-0.\ 22\quad e+\\ &0.00\quad d\ c\quad le\ el-0.21\quad r\quad -\\ &0.021\quad se\quad ld\,s\ \ e+0.\ 51\ \ e\quad le-\\ &0.\quad se\quad e-0.2\ 2\ \ r\ \ der-0.2\ 0\quad se\\ &-0.\ 1\quad ces\quad r-0.1\ 0\quad e \end{aligned} \tag{2}$$

The estimated intercept assumes that if the

Table 4. Descriptive statistics of the research variables

Research variables	n	Minimum	Maximum	Mean	Standard deviation (SD)
Age	91	17	80	48.56	12.353
Gender	91	1	2	1.25	.437
Occupation	91	2	8	4.19	2.196
Education level	91	0	4	1.57	.956
Ownership status	91	1	5	2.57	1.454
Living duration	91	2	4	3.64	.723
Household size	91	1	4	2.70	.753
Perceived resilience	91	1	5	4.32	1.228
Valid N (listwise)	91				

Table 5: The model summary

Model	R	R square	Adjusted R-square	Standard error (S.E.) of the estimate
1	.448[a]	.200	.101	.97588431

Table 6: The summary of ANOVA

Model		Sum of squares	df	Mean square	F	Sig.
1	Regression	19.104	10	1.910	2.006	.043[b]
	Residual	76.188	80	.952		
	Total	95.292	90			

Table 7: The regression coefficients of the regression model

Coefficients[a]										
Model		Unstandardized Coefficients		Standardized Coefficients	Difference between sample and population means (t)	Sig.	95.0% Confidence Interval for β		Collinearity Statistics	
		β	S.E.	Beta			Lower Bound	Upper Bound	Tolerance	VIF
1	(Constant)	.080	.108		.735	.465	-.136	.295		
	Zscore: Age[b]	-.322	.154	-.302	-2.095	.039	-.628	-.016	.482	2.074
	Zscore: Education	.008	.124	.007	.062	.951	-.238	.253	.748	1.338
	Zscore: Duration	-.213	.151	-.216	-1.413	.162	-.514	.087	.428	2.336
	Zscore: Household size	-.021	.110	-.021	-.191	.849	-.240	.198	.812	1.232
	Zscore: Female[b]	.451	.226	.424	1.999	.049	.002	.901	.222	4.504
	Zscore: Housewife	-.443	.237	-.424	-1.871	.065	-.915	.028	.194	5.142
	Zscore: Trader	-.272	.155	-.287	-1.757	.083	-.580	.036	.374	2.676
	Zscore: Spouse[b]	-.270	.124	-.265	-2.171	.033	-.517	-.022	.671	1.491
	Zscore: Ancestor[b]	-.418	.148	-.415	-2.818	.006	-.713	-.123	.461	2.171
	Zscore: State	-.180	.175	-.181	-1.031	.306	-.528	.168	.323	3.098

a. Dependent Variable: Perceived Resilience
b. Independent Variables significantly influence perceived resilience.

independent variables are held constant, the perceived resilience would be 0.080. The regression coefficient for 'age' indicates that a 1-unit increase in age would result in a 0.322-unit decrease in perceived resilience, with significance at p = 0.039. The inverse correlation suggests that as respondents age, their perceived resilience diminishes. The regression coefficient for 'female (gender)' assumes that a 1-unit increase in the number of female residents leads to a 0.451-unit increase in perceived resilience (p = 0.049), which is higher than that for the reference category (i.e., male). The results additionally reveal a constructive association between 'gender' and perceived resilience, indicating that females have a stronger influence compared to males. The regression coefficient for 'land ownership by spouses' assumes that a 1-unit increase in the number of households would result in a 0.270-unit decrease in perceived resilience (p = 0.033). In the meantime, the coefficient for 'land ownership by ancestors' assumes that a 1-unit increase in the number of households would result in a 0.418-unit decrease in perceived resilience (p = 0.006). Both assessments suggest that the impact of land ownership by spouses and ancestors on perceived resilience is less pronounced than that of the reference category (i.e., land ownership by the respondents). This could indicate that a greater feeling of ownership is associated with an increased likelihood of greater perceived resilience. After testing the interactive effects of the three predictors using a two-way ANOVA, the values were found above the p-value (age-ownership =0.911; ownership-gender=0.598; and age-gender=0.540), indicating their insignificant combined effects on perceived resilience. Previous studies suggested that socioeconomic and demographic factors significantly influence perceived resilience (Alkaissi *et al.,* 2023; Çay *et al.,* 2023; Purnomo *et al.,* 2025; Yang *et al.,* 2020) and that perceived resilience strongly affects individuals' adaptations and actions (Hoa *et al.,* 2025). Unexpectedly, there is a limited amount of studies that associate these factors with coastal hazards. A significant number of studies have emphasized perceived risks because they serve as a practical framework for understanding how individuals cope with disasters (Liu *et al.,* 2024; Peers *et al.,* 2021; Zhang *et al.,* 2008). Three specific demographic and socio-economic attributes have been found to significantly influence individuals' coping behaviors: age, gender, and land ownership status. Nevertheless, while females and middle-aged populations statistically exhibited a high perceived resilience, an overrepresentation of these groups that creates an imbalanced sampling needs to be

acknowledged. Undoubtedly, the limited time available to surveyors for administering questionnaires outside of working hours resulted in their encounters with women in the field. This limitation warrants future studies to ensure the survey timing that allows an equal representation of the population. Age has been found as a negative predictor of perceived resilience (β=-0.322, p<.005), indicating that older residents tend to have lower perceived resilience compared to their younger counterparts. In response to inquiries about their resilience, participants over the age of 30 stressed that their immediate neighborhoods lack sufficient protective measures against flooding and that disasters tend to be unpredictable. In Tambakrejo, older residents generally expressed their anxiety about the incomplete seawall development in their neighboring settlements, indicating their better understanding of their environmental barriers than younger respondents, which can be associated with their low perceived resilience. Comparatively, this perspective is supported by prior studies that highlight the relationship between age and perceived resilience, suggesting that older individuals may experience diminished resilience due to the cumulative effects of adversity and disaster on their overall well-being over time (Hsieh *et al.,* 2024), including their physical disabilities, anxiety, distress, cognitive changes (Law *et al.,* 2025), low digital fluency, and literacy concerning disaster-related communication (Walkling and Haworth, 2020). In contrast, a study in Lagos, Nigeria, found that this older group felt more resilient, provided their experiences of flood preparedness and coping measures (Adelekan and Asiyanbi, 2016). Gender is another significant predictor of perceived resilience found in the study (β=0.451, p<.005), with females showing greater perceived resilience than males. This conclusion indicates that women might have considerable adaptive potential, despite their classification as a vulnerable population by the United Nations (UN, 2023; UNEP, 2023). Correlatedly, respondents, often housewives with over ten years of residence in the village, displayed high levels of optimism regarding their self-efficacy and showed a good understanding of their environmental resources that support their livelihoods. Further studies corroborate the notion that females are generally viewed as having a higher level of resilience than their male counterparts. Respectively, females have a greater risk perception and confidence in the effectiveness of hazard adjustments than males (Terpstra and Lindell, 2013). In spite of having a higher perception of stress compared to males, females usually tend to seek additional social support when faced with difficult circumstances (Yalcin-Siedentopf *et al.,* 2021). A study in Lagos, Nigeria, however, stressed that gender alone cannot explain vulnerability. It should intersect with place, class, and household structure (Ajibade *et al.,* 2013). Females also tend to be more active than males in social activities, including disaster preparedness programs (Villarreal and Meyer, 2020). In spite of having a higher level of perceived stress compared to males, females usually tend to pursue additional social support when faced with difficult circumstances. They highlighted community programs such as the government's Integrated Services Post, which focuses on maternal and child health, devotional work, local initiatives for mangrove restoration, and the government's family welfare development that centers on women empowerment, at the household level. Land ownership negatively influences perceived resilience, with the effects of land ownership by spouses (β=-0.270, p<.005) and by ancestors (β=-0.418, p<.005) being weaker than the reference category (land ownership by respondents). This result emphasizes the greater effects of landownership on the perceived ability to adjust to the consequences of flooding. A significant number of respondents reported plans to raise the floor levels of their residences, protect their valuables, and upgrade public infrastructure in order to enhance their flood preparedness. They also envisioned improvements in flood-related infrastructure, disaster management, and institutional assistance to enhance their preparedness for unexpected events. This association is consistent with previous studies, which suggest that as a person's land rights increase, so does the likelihood of engaging in household-level adaptations (Klaus and Elfversson, 2025), long-term investments through sustainable practices (Phuong *et al.,* 2025), and willingness to embrace resilient practices (Kehinde *et al.,* 2023). To elevate the perceived resilience, institutional interventions should be undertaken. Additionally, it involves the development of disaster-related infrastructure, boosting preparedness and awareness, advocating for disaster education and training, supplying subsidies and

housing initiatives, and facilitating local engagement in planning (Dai and Wu, 2025; Maripe, 2011). Despite the small effect of the regression model (adjusted R^2 = 0.01), the results remain meaningful as they indicate certain demographic groups with low perceived resilience: the elderly, males, and landless populations, to whom future interventions should be prioritized. Concerning this, the male groups' low perceived resilience can be increased if incentives for the existing economy (e.g., fishing and mangrove conservation) and opportunities for expanding fishing territory are provided. This group emphasized that the ongoing decrease in fish catch, attributed to environmental degradation and climate change, poses a significant threat to their sustainability. Concerning the landless group's low perceived resilience, interviews suggest that fostering their active participation in social activities may increase their awareness of the neighborhood's challenges and assets. Concerning the older group's diminished perceived resilience, this can be attributed to the nonexistence of a strong protective measure enforced in their neighboring communities, which has caused an escalation in anxiety about forthcoming threats. Hence, the government should ensure a comprehensive, inclusive, and DRR plan that is aligned with the needs of each demographic group, engage and empower demographic groups with low perceived resilience in planning, and prioritize DRR plans for these demographic groups. In practice, perceived resilience can also inform disaster risk reduction policies by uncovering local assets (e.g., local knowledge) that are valuable for community resilience. As an illustration, the female groups participating in this study highlighted social resources that support their livelihoods, including meetings for the weekly lottery and prayer groups. Recognizing such assets will help identify the local channels appropriate for distributing disaster information toward an enhanced early warning system. A further instance is observed in the Monirumpur community, known for their traditional expertise in floating agriculture for the cultivation of vegetable crops (Dhar *et al*., 2023). Acknowledging this asset may help policymakers develop appropriate plans to reduce their disaster risks to flood hazards.

CONCLUSION

The study addresses the gap in the literature by revealing the demographic factors that significantly affect the perceived resilience of at-risk communities in a coastal village. Specifically, it has uncovered demographic groups characterized by low perceived resilience, such as older individuals, males, and landless people—that require urgent DRR interventions. These findings show potential for policymakers to make use of similar research to locate vulnerable groups who lack access to livelihood resources, improve existing assets for future adaptations, develop effective disaster communication strategies based on their demographic traits, and prioritize groups that require immediate interventions. In the context of Tambakrejo, the older population tends to report lower perceived resilience than the younger population (β=-0.322, $p<.005$). This may be linked to the group's enhanced comprehension of local obstacles to resilience and prior negative encounters with floods. As anticipated, females exhibit a greater perceived resilience compared to males (β=0.451, $p<.005$). Most female respondents described community programs they were involved in, which may contribute to their stronger optimism and self-efficacy. Land ownership also significantly shapes perceived resilience (by spouse, β=-0.270, $p<.005$) and (by ancestors, β=-0.418, $p<.005$), with personal possession leading to higher perceived resilience. The perception of ownership often enhances a person's readiness to participate in coastal adaptation and disaster risk management initiatives. However, this study is not without limitations. First, the linear regressions showed that the demographic and socioeconomic factors explained only around 10% of the variance in the perceived resilience. In social science, this percentage is considered acceptable for interpretations, yet it may rise with the inclusion of subjective factors like personal experiences. Second, the power of the proposed regression model could be improved if other demographic and socioeconomic factors, such as household income, were also considered; however, this particular variable was ultimately removed due to insufficient responses. Furthermore, it would be beneficial to examine the interaction effects among predictors on perceived resilience, including the mediating influences of predictors on perceived resilience in future studies, to more effectively guide policies on how specific considerations based

on socio-demographic characteristics can enhance disaster risk reduction. Third, overrepresented females and older people may lead to biased results as data variance becomes limited. Admittedly, the surveyors' time constraints in meeting male and younger respondents in the field hindered the study from recruiting a more diverse demographic. Fourth, future studies should consider expanding the scope of the area of study and identifying changes in the community's perceived resilience across time to predict their adaptive behaviors using a longitudinal or mixed-methods approach. This information allows for the creation of a disaster mitigation strategy that is effective and specifically designed to meet the demographic characteristics of the community. Fifth, future research should also consider integrating the community's perceived risk, which is likely to increase as climate threats intensify, to inform resilience planning using advanced methods, such as GIS-based participatory mapping, towards an effective disaster risk reduction. Furthermore, the study, while limited, offers significant theoretical and practical insights. First, the low significance of other predictors, such as education, duration of living, and occupation, raises some theoretical questions about why this finding differs from other studies. This warrants further investigation and provides a basis for future research direction. Second, older populations demonstrated a low perception of resilience, which can be linked to the lack of integrated disaster risk reduction. Meanwhile, females' higher perceived resilience corresponds to their better understanding of the community's resources and more active participation in social activities, signifying their potential contributions to resilience planning. Lastly, the robust link that respondents associate with seawalls and their perceived durability may suggest an erroneous feeling of safety, possibly causing a heightened unwillingness to think about relocation in the future. Hence, policymakers ought to avoid concentrating exclusively on stringent protective measures and should also contemplate hybrid protective strategies that involve the at-risk community in the planning process. To conclude, the study has demonstrated the significance of age, gender, and land ownership in influencing the perceived resilience of a coastal community and the possible interventions for increasing their adaptive capacities in the future.

AUTHOR CONTRIBUTIONS

C.D.A. Depari serves as the corresponding author. All contributions made to this study, from manuscript preparation, data visualization, data acquisition, analysis, interpretations, and revision are attributed solely to the individual mentioned author.

ACKNOWLEDGEMENT

The study was performed with support from Mr. Ratno; the chief of the local fishermen group, Mr. Slamet Riyadi; the neighborhood leader, and the Village authority of Tanjung Mas. The data reported in this study were part of a research and community development program funded by Universitas Atma Jaya Yogyakarta [No. 637/LPPM-PPM/In.] and performed by the author, Gregrorius Agung Setyonugroho, and Ida Aditya Wikana Kartika. The questionnaire was administered with assistance from Dr. Lulut Indrianingrum, a senior lecturer at the Universitas Negeri Semarang, and her undergraduate students. The study data will be made available on request.

CONFLICT OF INTEREST

The author declares that there is no conflict of interests regarding the publication of this manuscript. In addition, the ethical issues, including plagiarism, informed consent, misconduct, data fabrication and/or falsification, double publication and/or submission, and redundancy have been completely observed by the authors.

OPEN ACCESS

©2026 The author(s). This article is licensed under a Creative Commons Attribution 4.0 International License, which permits use, sharing, adaptation, distribution and reproduction in any medium or format, as long as you give appropriate credit to the original author(s) and the source, provide a link to the Creative Commons license, and indicate if changes were made. The images or other third-party material in this article are included in the article's Creative Commons license, unless indicated otherwise in a credit line to the material. If material is not included in the article's Creative Commons license and your intended use is not permitted by statutory regulation or exceeds the permitted use, you will need to obtain

permission directly from the copyright holder. To view a copy of this license, visit: http://creativecommons.org/licenses/by/4.0/

PUBLISHER'S NOTE

GJESM Publisher remains neutral with regard to jurisdictional claims in published maps and institutional afflictions.

☒ Negative AI Statement

The author(s) declare that no AI tools or services were not used or not highly applied during the preparation of this work.

ABBREVIATIONS

%	Percent
a	Regression constant
β	Regression coefficient
°C	Degrees Celcius
ANOVA	Analysis of variance
cm	Centimeter
df	Degree of freedom
DRR	Disaster risk reductions
e	Tolerable error term
F	Ratio of two variances
GT	Gross Tons
H_o	Null Hypothesis
H_A	Alternative Hypothesis
K-S	Kolmogorov-Smirnov
IBM	International Business Machines
MSI	Method of successive intervals
n	Total number
P-P	Probability-probability
p-value	Statistical significance
R	Correlation coefficient
R-squared	Coefficient of determination
S.E.	Standard error
SFDRR	Sendai Framework of Disaster Risk Reduction
Sig.	Significance value
SPSS	Statistical package for social sciences
S.D.	Standard Deviation
S-W	Shapiro-Wilk
SV	Scale Value
t	Difference between sample and population means
TSV	Transformed Scale Value
USD	United States Dollar
VIF	Variance Inflation Factor
X	Independent variable/ predictor
Y	Dependent/outcome variable
Z-scores	The number of standard deviations

REFERENCES

Adelekan, I.O.; Asiyanbi, A.P., (2016). Flood risk perception in flood-affected communities in Lagos, Nigeria. Nat. Hazards, 80(1): 445–469 **(25 pages).**

Agrawal, N.; (2018). Disaster perceptions. Adv. Nat. Technol. Hazards Res., 49: 193–217 **(25 pages).**

Ahmed, H.; Correa, J.S.; Sitko, N.J., (2025). Climate adaptation, perceived resilience, and household wellbeing: Comparative evidence from Kenya and Zambia. Ecol. Econ., 235: 108611.

Ahmed, S.K., (2024). How to choose a sampling technique and determine sample size for research: A simplified guide for researchers. Oral Oncol. Rep., 12: 100662 **(7 pages).**

Ajibade, I.J.; McBean, G.A.; Bezner Kerr, R.N., (2013). Urban flooding in Lagos, Nigeria: Patterns of vulnerability and resilience among women. Global Environ. Change. 23(6): 1714–1725 **(22 pages).**

Alkaissi, A.; Said, N.B.; Qadous, S.; Alkony, M.; Almahmoud, O., (2023). Factors associated with perceived resilience among undergraduate nursing students: findings of the first cross-sectional study in Palestine. BMC Nurs., 22(1): 1–13 **(13 pages).**

Askari, E.; Savari, M.; Rezaei, M., (2025). Application of construal level theory in identifying factors affecting individual decision-making in implementing flood protection measures in rural areas of Iran. Sci. Rep., 15(1): 1-21 **(25 pages).**

Asdar; Badrullah, (2016). Method of successive interval in community research. Int. J. of Soc. Sci. and Humanit. Res., 4(2): 356–363 **(8 pages).**

Atanga, R.A., (2020). The role of local community leaders in flood disaster risk management strategy making in Accra. Int. J. Disaster Risk Reduct., 43(3): 1-20 **(20 pages).**

Babcicky, P.; Seebauer, S., (2017). The two faces of social capital in private flood mitigation: opposing effects on risk perception, self-efficacy and coping capacity. J. Risk Res., 20(8): 1017–1037 **(22 pages).**

Bartlett, J.E.; Kotrlik, J.W.; Higgins, C.C., (2001). Organizational research : Determining appropriate sample size in survey research. ITLPJ., 19(1): 43-50 **(8 pages).**

Bickerstaff, K.; Simmons, P.; Pidgeon, N., (2008). Constructing responsibilities for risk: negotiating citizen — state relationships. Environ. Plann. A: Econ. Space, 40(6): 1312–1330 **(29 pages).**

Botzen, W.J.W.; Aerts, J.C.J.H.; Van Den Bergh, J.C.J.M., (2009). Dependence of flood risk perceptions on socioeconomic and objective risk factors. Water Resour. Res., 45(10): 1–15 **(15 pages).**

Çay, Ş.; Şen, B.; Tanaydın, A.; Tosun, B.; Zerey, A.; Karakale, Ö., (2023). Predictive role of sociodemographic and health factors on psychological resilience during the covid-19 pandemic: A cross-sectional study in Turkey. Covid., 3(4): 543–554 **(12 pages).**

Cazabat, C.; Anzellini, V.; Fung, V.; Housset, T.; O'Connor, A.; Ponserre, S., (2023). Disaster displacement: Indonesia Country Briefing. In Asian Development Bank and International Displacement Monitoring Centre **(15 pages).**

Cheung, F.; Lucas, R.E., (2014). Assessing the Validity of Single-item Life Satisfaction Measures: Results from Three Large Samples. Qual. Life Res., 23(10): 2809–2818 **(27 pages).**

Cox, R.S.; Perry, K.M.E., (2011). Like a fish out of water: reconsidering disaster recovery and the role of place and social capital in community disaster resilience. Am. J. Commun. Psychol., 48(3–4): 395–411 **(17 pages).**https://doi.org/10.1007/s10464-011-9427-0

Dai, Z.; Wu, G., (2025). Disaster risk reduction policies and perceived community resilience in rural ethnic minority communities in China. Humanit. Soc. Sci. Commun., 1–11 **(11 pages).**

Dhar, T.; Bornstein, L.; Lizarralde, G.; Nazimuddin, S.M., (2023). Risk perception—A lens for understanding adaptive behaviour in the age of climate change? Narratives from the Global South. Int. J. Disaster Risk Reduct., 95: 1-16 **(16 pages).**

Diakakis, M.; Priskos, G.; Skordoulis, M., (2018). Public perception of flood risk in flash flood prone areas of Eastern Mediterranean: The case of Attica Region in Greece. Int. J. Disaster Risk Reduct., 28: 404–413 **(10 pages).**

Dobre, D.; Armaş, I.; Albulescu, A.C., (2025). Examining the risk perception-disaster preparedness behavior nexus in the seismic context of Bucharest. Int. J. Disaster Risk Sci., 16: 724-741 **(18 pages).**

Edelsbrunner, P. A., Simonsmeier, B. A., & Schneider, M. (2025). The reliability, but not the Cronbach's alpha, of knowledge tests matters : Response to Zitzmann and Orona (2025). Educ. Psychol. Rev., 37(2): 1–5 **(5 pages).**

Eakin, H.; York, A.; Aggarwal, R.; Waters, S.; Welch, J.; Rubiños, C.; Smith-Heisters, S.; Bausch, C.; Anderies, J.M., (2016). Cognitive and institutional influences on farmers' adaptive capacity: insights into barriers and opportunities for transformative change in central Arizona. Reg. Environ. Change. 16(3): 801–814 **(14 pages).**

Elrick-Barr, C.E.; Thomsen, D.C.; Preston, B.L.; Smith, T.F., (2017). Perceptions matter: household adaptive capacity and capability in two Australian coastal communities. Reg. Environ. Change. 17(4): 1141–1151 **(11 pages).**

Freitag, R.C.; Abramson, D.B.; Chalana, M.; Dixon, M., (2014). Whole community resilience: An asset-based approach to enhancing adaptive capacity before a disruption. J. Am. Plan. Assoc., 80(4): 324–335 **(14 pages).**

Grothmann, T.; Reusswig, F., (2006). People at risk of flooding: Why some residents take precautionary action while others do not. Nat. Hazard., 38(1–2): 101–120 **(16 pages).**

Guo, Y.; Zhang, J.; Zhang, Y.; Zheng, C., (2018a). Catalyst or barrier? The influence of place attachment on perceived community resilience in tourism destinations. Sustainability. 10(7): 1-14 **(14 pages).**

Guo, Y.; Zhang, J.; Zhang, Y.; Zheng, C., (2018b). Examining the relationship between social capital and community residents' perceived resilience in tourism destinations. J. Sustainable Tourism, 26(6): 973–986 **(14 pages).**

Hair, J.F.; Black, W.C.; Babin, B.J.; Anderson, R.E., (2018). Multivariate Data Analysis. In Cengage (8th ed.) **(834 pages)**.

Ho, M.C.; Shaw, D.; Lin, S.; Chiu, Y.C., (2008). How do disaster characteristics influence risk perception? Risk Anal., 28(3): 635–643 **(9 pages).**

Hoa, L.T.; Duy, P.T.; Thuy, N.T.T., (2025). Climate change impact perception and agricultural adaptation in a coastal region. Global J. Environ. Sci. Manage., 11(4): 1–22 **(22 pages).**

Hsieh, S.; Chang, Y.H.; Yao, Z F.; Yang, M.H.; Yang, C.T., (2024). The effect of age and resilience on the dose–response function between the number of adversity factors and subjective well-being. Front. Psychol., 15: 1-15 **(15 pages).**

Hu, P.; Zhang, Q.; Shi, P.; Chen, B.; Fang, J., (2018). Flood-induced mortality across the globe: Spatiotemporal pattern and influencing factors. Sci. Total Environ., 643: 171–182 **(12 pages).**

Huang, H.; Wang, R.; Xiao, Y.; Li, Y.; Zhang, Q.F.; Xiang, X., (2022). Determinants of People's Secondary Hazards Risk Perception: A Case Study in Wenchuan Earthquake Disaster Areas of China. Front. Earth Sci., 10: 1–15 **(15 pages).**

Ibrahim, A.; Isaac, M.E.; Kepe, T., (2025). Land tenure (in) security in the context of urban flood risk in Ghana. Land Use Policy. 159: 1-11 **(11 pages).**

Ibrahim, B.A.; Hussein, S.M., (2024). Relationship between resilience at work , work engagement and job satisfaction among engineers : a cross-sectional study. BMC Public Health. 1–10 **(10 pages).**

Jamaludin, H.; Mahdi, Z., (2025). Community resistance to development of the Semarang-Demak sea embankment toll road. J. Acad. Sci., 2(4): 1046–1065 **(15 pages).**

Josè Moisès, D.; Kgabi, N.; Kunguma, O., (2023). Integrating "top-down" and "community-centric" approaches for community-based flood early warning systems in Namibia. Challenges, 14(4): 1-17 **(17 pages).**

Kang, S.; You, C.H.; Kwon, Y.D., (2025). Factors affecting risk perception of COVID-19 : Differences by age and gender. Front. Public Health. 1: 1–13 **(13 pages).**

Kehinde, M.O.; Shittu, A.M.; Oriade, O.A.; Edewor, S.E., (2023). Land tenure, land use antecedents, and willingness to embrace resilient farming practices among smallholders in Nigeria. Front. Sustain. Food Syst., 7: 1-12 **(12 pages).**

Khasanah, S.N., (2023). Vulnerability analysis and adaptive capacity of small-scale fishermen in Tambakrejo fishing village, Semarang, Central Java, Indonesia. Proceedings International Conference on Religion, Science and Education, 2(14): 863–870 **(13 pages).**

Kieu, M.; Senanayake, G., (2023). Perception, experience and resilience to risks: a global analysis. Sci. Rep., 13: 1–13 **(13 pages).**

Klaus, K.; Elfversson, E., (2025). Land tenure and climate resilience: key policy messages. In EBA Report 2025:02. The Expert Group for Aid Studies.

Lassa, J.A.; Amri, A.; Haynes, K.; Towers, B.; Abunyewah, M.; Zander, K.; Erdiaw-Kwasie, M.O., (2025). Children and adults' perception of risk and risk management: Insights from long-term participatory data and implication for child-centric climate and disaster risk reduction. Soc. Sci. Humanit. Open., 11(3): 1-11 **(11 pages).**

Law, S.; Marinova, T.; Ewins, L.; Marks, E., (2025). Understanding

the psychological impact of flooding on older adults: A scoping review. Ann. N. Y. Acad. Sci., 1548(1): 99–115 **(17 pages)**.

Lechowska, E., (2018). What determines flood risk perception? A review of factors of flood risk perception and relations between its basic elements. Nat. Hazard., 94(3): 1341–1366 **(26 pages).**

Leiserowitz, A., (2010). Risk perceptions and behavior. In Schneider, S.H.; Rosencranz, A.; Mastrandrea, M.D.; Kuntz-Duriseti, K. (Eds.), Climate Change Science and Policy. Island Press **(16 pages).**

Lindell, M.K.; Hwang, S.N., (2008). Households' perceived personal risk and responses in a multihazard environment. Risk Anal., 28(2): 539–556 **(18 pages).**

Liu, Z.; Chen, X.; Zhu, T., (2024). Influence mechanism of coping behaviours for natural hazards: Empirical study in Henan, China. Int. J. Disaster Risk Reduct., 100: 1-14 **(14 pages).**

Lo, A.Y., (2014). Negative income effect on perception of long-term environmental risk.

Ecol. Econ., 107: 51–58 **(8 pages).**

Magis, K.; (2010). Community resilience: an indicator of social sustainability. Soc. Nat. Resour., 23(5): 401–416 **(16 pages).**

Mai, T.; Mushtaq, S.; Reardon-Smith, K.; Webb, P.; Stone, R.; Kath, J.; An-Vo, D.A., (2020). Defining flood risk management strategies: A systems approach. Int. J. Disaster Risk Reduct., 47: 1-10 **(10 pages).**

Maripe, K. (2011). Community disaster and risk reduction: the role of social workers in Bostwana. J. Soc. Psychol. Anthropol. Practice. 3(1): 43–56 **(14 pages)**.

McDowell, C.P.; Andrade, L.; O'neill, E.; O'malley, K.; O'dwyer, J.; Hynds, P.D., (2020). Gender-related differences in flood risk perception and behaviours among private groundwater users in the Republic of Ireland. Int. J. Environ. Res. Public Health. 17(6): 1-14 **(14 pages).**

Mehryar, S.; Surminski, S., (2022). Investigating flood resilience perceptions and supporting collective decision-making through fuzzy cognitive mapping. Sci. Total Environ., 837: 1-13 **(13 pages).**

Mester, B.; Frieler, K.; Korup, O.; Desai, B.; Schewe, J., (2025). Socioeconomic predictors of vulnerability to flood-induced displacement. Nat. Commun., 16(1): 1-13 **(13 pages).**

Mohr, D.L.; Wilson, W.J.; Freund, R.J., (2022). Chapter 8 - Multiple Regression (Mohr, D.L.; Wilson, W.J.; Freund, R.J., (Fourth Edition), 351–444. Academic Press **(94 pages).**

Mondino, E., (2023). Droughts and floods: people's perception of hydrological risk. In Shroder, J.F.; Paron, P.; Di Baldassarre, G., and Disasters (Second Edition) (Eds.), Hydro-Meteorological Hazards, Risks, and Disasters. Elsevier **(21 pages).**

Mustofa, M.S.; Iswari, R.; Luthfi, A.; Kristiwati, E.; Anugrah, R.D., (2021). Reinterpretation of maritime identity of small fishermen on the North Coast of Semarang City. Proceedings of the International Conference on Social Science, Political Science, and Humanities (ICoSPOLHUM 2020), 495: 161–165 **(5 pages).**

Nau, R., (2020). Statistical forecasting: notes on regression and time series analysis. Fuqua School of Business, Duke University.

Nkombi, Z.; Wentink, G.J., (2022). The role of public participation in disaster risk reduction initiatives: The case of Katlehong township. Jamba: J. Disaster Risk Stud., 14(1): 1–12 **(12 pages).**

Norris, F.H.; Stevens, S.P.; Pfefferbaum, B.; Wyche, K.F.; Pfefferbaum, R.L., (2008). Community resilience as a metaphor, theory, set of capacities, and strategy for disaster readiness. Am. J. Community Psychol., 41(1–2): 127–150 **(24 pages).**

Ozili, P. K. (2022). The acceptable R-Square in empirical modelling for social science research. In social research methodology and publishing results. Issue 1 **(9 pages).**

Pederson, J.R.N.V., (2017). Multiple regression. In The SAGE encyclopedia of communication research methods. SAGE Publications, Inc. **(24 pages).**

Peers, J.B.; Lindell, M.K.; Gregg, C.E.; Reeves, A.K.; Joyner, A.T.; Johnston, D.M., (2021). Multi-hazard perceptions at Long Valley Caldera, California, USA. Int. J. Disaster Risk Reduct., 52: 1-58 **(58 pages).**

Pemerintah Kota Semarang, (2021). Hendi minta warga tambakrejo dapat segera tempati kampung nelayan.

Pemerintah Kota Semarang, (2024). Mbak Ita: Proses pembangunan tanggul laut di Semarang capai 62 persen.

Peters, K., (2019). Disaster risk reduction in conflict contexts: An agenda for action. London: The State of the Evidence, September. 1–52 **(52 pages).**

Phuong, T.T.; Tan, N.Q.; Dinh, N.C.; Huong, T.Q.; Nhat, N.T.; Ngu, N.H., (2025). Reinforcing adaptation: How climate change perceptions and land tenure security shape ethnic minority resilience in Vietnam. Environ. Dev., 55: 101245.

Poston, D.L.; Conde, E.; Field, L.M., (2023). Applied regression models in the social sciences. Cambridge University Press.

Purnomo, A.H.; Sachoemar, S.I.; Arifin, Z.; Samiaji, J.; Edwarsyah; Tanjung, R.H.R.; Juliani; Nurhayati, A.; Purwanti, P.; Lumbessy, S.Y.; Kawung, N.; Widodo, L.; Haryanti; Indrabudi, T.; Safitri, W.; Makino, M.; Hori, J.; Thebaud, O.; Lew, D.K.; Boschetti, F., (2025). Demographic dimension of ocean perceptions: Evidence from Indonesia. Mar. Policy. 178(106706).

Ramadhan, D.M., (2024). The emergence of environmentalism among urban coastal communities : A case study of the Tambakrejo community in Semarang, Central Java. Proceedings of the 2nd International Conference on Culture and Sustainable Development (ICOCAS 2024) **(5 pages).**

Rasmussen, J.; Ewald, J., (2022). The relation between socioeconomic status and risk attitudes: a nuclear accident scenario in Sweden. Econ. Disasters Clim. Change. 6(3): 541–555 **(15 pages).**https://doi.org/10.1007/s41885-022-00118-6

Rentschler, J.; Salhab, M.; Jafino, B.A., (2022). Flood exposure and poverty in 188 countries. Nat. Commun., 13(1), 1–11 **(11 pages).**

Sandri, R.; Siagian, Y.A., (2025). Academic resilience in final year students viewed from spiritual intelligence. Motiva: Jurn. Psikologi, 8(1): 94-101 **(8 pages).**

Sambu, L.J.; Mhongo, S., (2019). Age and gender in relation to resilience after the experience of trauma among internally displaced persons (IDPS) in Kiambaa Village, Eldoret East Sub-County, Kenya. J Psychol Behav Sci., 7(1): 31-40 **(10 pages).**

Semarang. (2019). Rencana aksi daerah adaptasi perubahan iklim kota Semarang tahun 2019.

Slovic, P., (1987). The perception of risk. Science. 236(4): 280–285 **(6 pages).**

Slovic, P.; Peters, E.; Finucane, M.L.; MacGregor, D.G., (2005). Affect, risk, and decision making. Psychol., 24(S): S35–S40 **(6 pages).**

Soetanto, R.; Mullins, A.; Achour, N., (2017). The perceptions of social responsibility for community resilience to flooding: the impact of past experience, age, gender and ethnicity. Nat. Hazard., 86(3): 1105–1126 **(22 pages).**

Terpstra, T.; Lindell, M.K., (2013). Citizens' perceptions of flood hazard adjustments: an application of the protective action decision model. Environ. Behav., 45(8): 993–1018 **(27 pages).**

UN, (2023). Training Manual on Gender and Climate Change Resilience. In United Nations, 2023: 13-78 **(66 pages).**

UNEP, (2023). Gender Mainstreaming Strategy and Action Plan for the Disposal of Polychlorinated Biphenyls (PCBs) in Southern Africa - Disposal of PCB oils contained in transformers and disposal of capacitors containing PCBs in Southern Africa (GEF Project 5532). In UN Environment Programme **(40 pages).**

van der Linden, S., (2014). On the relationship between personal experience, affect and risk perception: The case of climate change. Eur. J. Soc. Psychol., 44(5): 430–440 **(11 pages).**

van der Linden, S., (2015). The social-psychological determinants of climate change risk perceptions: Towards a comprehensive model. J. Environ. Psychol., 41: 112–124 **(13 pages).**

Villarreal, M.; Meyer, M.A., (2020). Women's experiences across disasters: a study of two towns in Texas, United States. Disasters. 44(2): 285–306 **(22 pages).**

Walkling, B.; Haworth, B.T., (2020). Flood risk perceptions and coping capacities among the retired population, with implications for risk communication: A study of residents in a north Wales coastal town, UK. Int. J. Disaster Risk Reduct., 51: 1-12 **(12 pages).**

Wang, P.; Zhang, J.; Yuan, S.; Wu, X.; Liu, J.; Zhang, Y., (2025). Sociodemographic determinants of flood risk perception disparities: A comparative study of subjective and objective risks in Nanjing, China. Water-Energy Nexus, 8: 189–204 **(16 pages).**

Weber, E.U., (2010). What shapes perceptions of climate change? WIREs Clim. Change, 1: 332–342 **(11 pages).**

Wei, Z.; Zhang, Z.; Guo, L.; Zhou, W.; Yang, K., (2025). Positive relationship between education level and risk perception and behavioral response : A machine learning approach. PLoS One, 20(4): 1–10 **(10 pages).**

Widodo, D.R.; Nugroho, S.P.; Asteria, D., (2018). Analisis penyebab masyarakat tetap tinggal di kawasan rawan bencana gunung Merapi (studi di lereng gunung Merapi kecamatan Cangkringan, kabupaten Sleman Daerah Istimewa Yogyakarta). Jurnal Ilmu Lingkungan, 15(2): 135-142 **(8 pages).**

Yalcin-Siedentopf, N.; Pichler, T.; Welte, A.S.; Hoertnagl, C.M.; Klasen, C.C.; Kemmler, G.; Siedentopf, C.M.; Hofer, A., (2021). Sex matters: stress perception and the relevance of resilience and perceived social support in emerging adults. Arch. Womens. Ment. Health, 24(3): 403–411 **(9 pages).**

Yang, B.; Feldman, M.W.; Li, S., (2020). The status of perceived community resilience in transitional rural society: An empirical study from central China. J. Rural Stud., 80: 427–438 **(12 pages).**

Yildiz, A.; Dickinson, J.; Priego-Hernández, J.; Teeuw, R.; Shaw, R., (2024). Effects of disaster education on children's risk perception and preparedness: A quasi-experimental longitudinal study. Geogr. J., 190(2): 1–19 **(19 pages).**

Zhang, Y.; Hwang, S.N.; Lindell, M.K., (2008). Hazard proximity or risk perception? Evaluating effects of natural and technological hazards on housing values. Environ. Behav., 42(5): 597-634 **(28 pages).**

AUTHOR (S) BIOSKETCHES

Depari, C.D.A., Ph.D., Associate Professor, Department of Architecture, Faculty of Engineering, Universitas Atma Jaya Yogyakarta, Jl. Babarsari No.44, Yogyakarta, Indonesia.
- Email: *catharina.depari@uajy.ac.id*
- ORCID: 0000-0003-3358-2951
- Web of Science ResearcherID: HTS-7516-2023
- Scopus Author ID: 57194836253
- Homepage: https://ft.uajy.ac.id/id/lecture/01.10.789

HOW TO CITE THIS ARTICLE

Depari, C.D.A., (2026). The influence of demographic and socioeconomic factors on a fishing community's resilience to coastal flooding. Global J. Environ. Sci. Manage., 12(1): 229-248.

DOI: 10.22034/gjesm.2026.01.13

URL: https://www.gjesm.net/article_731453.html

Global J. Environ. Sci. Manage. 12(1): 249-268, Winter 2026, Serial #45

Global Journal of Environmental Science and Management
(GJESM)

Homepage: https://www.gjesm.net/

Podcasts

CASE STUDY

Environmental and policy perspectives in managing revolutionary heritage under urbanization challenges

T.P. Nguyen[1], V.H. Dao[2,*], T.A.T. Vo[3], Y.N. Au[3]

[1] *Ho Chi Minh City University of Technology and Education, Ho Chi Minh City, Vietnam*

[2] *Saigon University, Ho Chi Minh City, Vietnam*

[3] *University of Social Sciences and Humanities, Vietnam National University, Ho Chi Minh City, Vietnam*

ARTICLE INFO

Article History:
Received 11 July 2025
Revised 16 September 2025
Accepted 20 October 2025

Keywords:
Communication technology
Community awareness
Revolutionary heritage
Sustainable tourism
Urbanization

DOI: 10.22034/gjesm.2026.01.14

ABSTRACT

BACKGROUND AND OBJECTIVES: Vietnam's rapidly expanding urban centers, particularly Ho Chi Minh City, are encountering significant challenges in preserving revolutionary historical sites. These locations not only reflect the cultural and historical heritage of the country but also play educational, symbolic, and socio-political functions. However, urbanization has intensified land-use conflicts, led to the degradation of surrounding environments, and threatened the authenticity of these heritage spaces. The study aimed to analyze the connection between urbanization and its impacts on the preservation of revolutionary heritage, in addition to evaluating the potential for including these sites in enduring sustainable tourism strategies. The Rừng Sác Revolutionary Site in Cần Giờ District is selected as a representative case due to its exceptional historical significance and location within an ecologically sensitive biosphere reserve.

METHODS: This study employs a quantitative methodology, using survey data obtained from two hundred eleven participants, comprising residents, managers of heritage sites, and policy specialists. A structural equation modeling framework is developed to assess the influence of five primary factors on preservation outcomes: institutional policy, financial resources, community awareness, communication technology, and urbanization and infrastructure development.

FINDINGS: All five factors were found to have a statistically significant positive influence on heritage preservation efforts. The most impactful factor has been urbanization, with communication technologies and public awareness following closely behind. While urbanization introduces substantial risks such as encroachment, landscape alteration, and authenticity loss, it simultaneously offers new opportunities to reposition revolutionary heritage within broader urban development and planning strategies.

CONCLUSION: This study presents a validated analytical framework that merges policy, technology, and social aspects in managing heritage under urban challenges. It underscores the importance of policy alignment, digital innovation, and community involvement. The findings from the Rừng Sác case contribute to the broader discourse on managing cultural assets in rapidly transforming urban environments and offer valuable insights for cities facing similar development-preservation tensions.

This is an open access article under the CC BY license (http://creativecommons.org/licenses/by/4.0/).

NUMBER OF REFERENCES
42

NUMBER OF FIGURES
4

NUMBER OF TABLES
6

*Corresponding Author:
Email: *dvhop@sgu.edu.vn*
Phone: +091 667 6603
ORCID: 0000-0002-4667-329X

Note: Discussion period for this manuscript open until Mar 1, 2026 on GJESM website at the "Show Article".

INTRODUCTION

In light of the transition of Vietnam's tourism sector from focusing on quantitative growth to prioritizing qualitative improvement, it has become essential to seek out distinctive tourism resources. While traditional forms such as landscape tourism, gastronomy, and leisure have reached a saturation point, current international trends increasingly focus on cultural and heritage experiences—that is, engaging more profoundly with the identity and historical memory of destinations (Richards, 2011; Chen *et al.*, 2024). Various studies have illustrated that heritage tourism can function as a means of preservation as well as a catalyst for development, provided it is directed by a sustainable development framework (Le *et al.*, 2024; Nguyen, 2025; Nguyen *et al.*, 2022). Ho Chi Minh City, as one of Vietnam's major economic and cultural centers, is currently home to more than 300 officially recognized historical and cultural sites. This system of heritage sites provides a crucial foundation for the development of cultural–historical tourism. However, the city's rapid urbanization has created tensions between urban development requirements and the mandate of heritage preservation (Zhang *et al.*, 2024). In reality, numerous sites face challenges due to land clearing, encroachment, changes to the nearby landscape, and ecological degradation (Quang *et al.*, 2022). In addition to these localized pressures, urban cultural heritage is increasingly vulnerable to wider Anthropocene-related threats such as climate change, sea level rise, land subsidence, air and water pollution, and uncontrolled tourism development (Huang and Meadows, 2025). Heritage-led entrepreneurial urbanism practices lead to cultures that are conservative in nature, reinforcing unequal economies, high house prices, and social exclusion in historic cities (Gill, 2025). This indicates that development focused on heritage, if not properly managed, could exacerbate social inequalities instead of addressing them. Recent academic studies on tourism in Vietnam emphasize the complex interrelationship between cultural heritage preservation, urban development, and the role of local communities (Quang, 2023; Le *et al.*, 2024). The priority is not only on the economic factor but on developing a sustainable model of growth, where tourism plays a dual role as a financial driver and a means of promoting awareness, while also carrying the potential risk of undermining heritage values if not effectively overseen (Le *et al.*, 2024). The relationship between tourism and heritage preservation is often described as a delicate balance: the utilization of cultural values for economic development is accompanied by the risk of excessive commercialization, which may erode authenticity. Korzilius (2022) explains that the Vietnam Veterans Memorials use minimalist spatial design to frame collective memory, presenting what he calls "the unpresentable". According to Carbone (2024), attractions associated with war serve dual purposes as memorials and means of shaping national identity, which can often result in political or ethical disputes. Digital documentation and interactive technologies have transformed how visitors engage with urban heritage, improving both interpretation and protection (Kim and Sung, 2024). To address this challenge, many scholars have proposed community-based tourism models, in which residents serve as central actors in the protection, management, and shared benefits of heritage (Le *et al.*, 2024). Effective heritage management, as El Faouri (2022) notes, requires policy integration across environmental planning, tourism, and local governance to ensure sustainable regeneration. In this context, Fabbricatti *et al.* (2020) propose the concept of *heritage community resilience*, which emphasizes that heritage is not only a cultural asset to be preserved, but also a strategic resource for building urban and community resilience. Their framework promotes participatory governance, cohesive planning, and the synchronization of heritage management with wider sustainability objectives—especially in urbanizing areas. The context of urbanization and globalization further complicates this issue, as these trends exert strong influences on urban spaces and transform traditional cultural values (Dang, 2023). Recent studies in the Cần Giờ Biosphere Reserve emphasize sustainability and community engagement in tourism. Nguyen *et al.*, (2021) identify infrastructure and environmental quality as critical to visitor satisfaction. Do and Nguyen (2025) analyzes barriers to sustainable ecotourism. More recently, Nguyen and Quy (2025) highlight the role of resilience in sustaining rural ecotourism post-Coronavirus Disease 2019 (COVID-19). Collectively, these works show Cần Giờ as a lens through which to view the interactions of urbanization, tourism, and heritage preservation. Ultimately, the achievement of sustainable tourism initiatives is largely contingent upon public awareness and endorsement. Studies measuring "willingness-to-

pay" indicate that this is a critical indicator for assessing the degree of heritage appreciation and serves as a basis for formulating sustainable financial policies (Le, 2015). Despite the extensive studies on the connection between heritage tourism and preservation, most investigations have targeted rural locations or offered descriptive insights; very few have adopted quantitative techniques to evaluate the relative influence of factors such as policy, resources, community awareness, technology, and—most significantly—urbanization concerning resistance bases in large urban areas. Localized research is therefore essential to contextualize global heritage frameworks within the socio-political realities of developing countries (Li *et al.*, 2023). This study employed structural equation modeling (SEM) to examine the degree to which institutional policy, financial resources, and community awareness contribute to heritage conservation outcomes. These factors were selected based on prior theoretical frameworks and empirical relevance to urban heritage contexts. SEM enabled the estimation of direct and indirect effects among variables, providing a statistical basis to evaluate their relative influence. This technique reinforces the soundness of policy advice generated from the analysis. This study contributes: 1) a quantitative model comprising five factors to explain the effectiveness of heritage preservation under conditions of urbanization, and 2) specific policy recommendations for the management of urban heritage in Ho Chi Minh City. In this context, this study centers on revolutionary bases—an unusual form of heritage site that is deeply connected to the establishment of Ho Chi Minh City and the collective remembrance of Vietnam's revolutionary conflicts. According to Assmann (1995), practices of cultural memory play a crucial role in maintaining and transmitting collective identity across generations. The Rừng Sác Revolutionary Site in Cần Giờ illustrates this process, as it attracts visitors while simultaneously facing the negative effects of urbanization. The purpose of this study is to examine how urbanization influences the preservation and sustainable tourism use of revolutionary heritage in Ho Chi Minh City, taking Rừng Sác as a representative example. The opposing effects, where development enhances accessibility but jeopardizes ecological and cultural integrity, reveal the need for balanced planning and management strategies that integrate heritage protection with urban development (Tousi *et al.*, 2025). Comparative consideration of other revolutionary heritage sites such as the Củ Chi Tunnels, Phú Thọ Hòa Prison, and Vĩnh Lộc base provides a broader understanding of common management challenges and possible adaptive responses. Integrating these locations into a cohesive cultural and ecological framework would bolster interpretive connections and improve the sustainability of conservation initiatives (Gill, 2025). Vietnam's current system of managing revolutionary heritage relies largely on centralized coordination by state agencies, while several Southeast Asian countries have implemented more flexible models that combine government administration with community participation and private sector involvement (Le *et al.*, 2024). Such analyses yield significant understanding for formulating forward-thinking policies that encourage the conservation of heritage alongside urban expansion. In Ho Chi Minh City, infrastructure improvements and modernization have increased the visibility and accessibility of heritage sites but have also caused fragmentation and environmental pressure. To address these issues, integrated planning frameworks should include protective zoning, green buffer zones, and environmental impact assessments to ensure that tourism development supports ecological stability and cultural continuity (Udeaja, 2020). The objectives of this study are to analyze how urbanization impacts the preservation of revolutionary heritage and to evaluate the potential for including these sites in sustainable tourism strategies over the long term. This study applies a quantitative model to evaluate five related factors including policy, financial resources, community awareness, communication technology, and urbanization and infrastructure development in assessing their combined impact on the effectiveness of heritage preservation in Cần Giờ District, Ho Chi Minh City, in 2024.

MATERIALS AND METHODS

This study focuses on the Rừng Sác Revolutionary Site in Cần Giờ District, a historically significant location facing increasing development pressures. Fig. 1, Fig. 2 shows the distribution of revolutionary heritage sites in Ho Chi Minh City, with emphasis on the Rừng Sác Revolutionary Base located in the Cần Giờ biosphere reserve.

Research factors and hypotheses

Sustainability principles are central to the

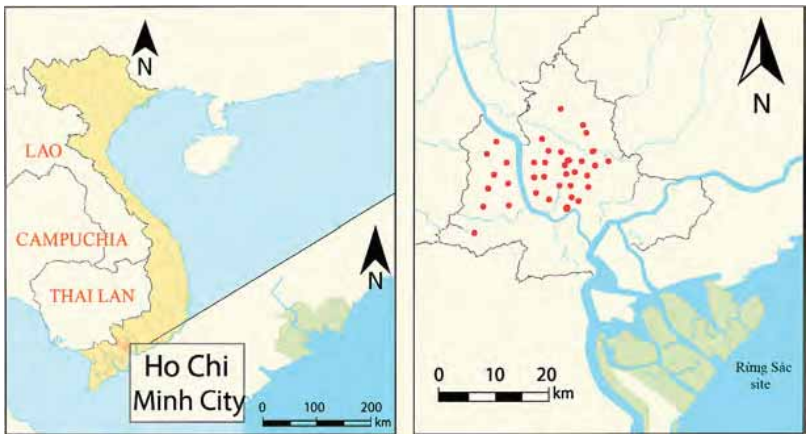

Fig. 1: Geographic location of the study area in Ho Chi Minh City, Vietnam
The red dots indicate surveyed sites included in the quantitative analysis

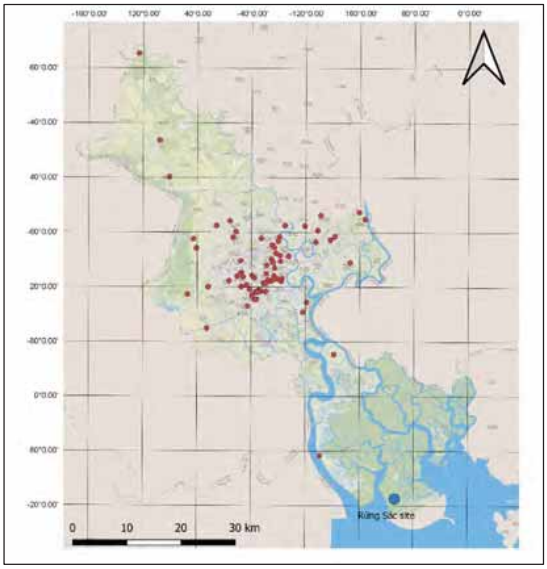

Fig. 2: Distribution of revolutionary heritage sites in Ho Chi Minh City, with emphasis on the Rừng Sác Revolutionary Base located in the Cần Giờ biosphere reserve. The red dots represent recorded heritage locations

methodological framework of this study. Urban tourism policies related to the Rừng Sác site were evaluated through indicators reflecting ecological protection, spatial containment, and low-impact infrastructure development. Incorporating these principles guarantees that the expansion of tourism is in harmony with ecological boundaries and the sustainable conservation of mangrove habitats. The analysis therefore considers sustainability not only as a policy objective but also as a measurable dimension of heritage management performance.

Institutional policy

Heritage management policies and urban planning play a decisive role in the preservation of heritage sites. Findings suggest that the deterioration of heritage values can occur due to inconsistent legal frameworks or the lack of robust monitoring mechanisms (Le *et al.,* 2024). On the contrary, conservation policies integrated with tourism development have proven effective in many Southeast Asian countries.

Hypothesis H1: Appropriate conservation policies have a positive impact on the effectiveness of heritage

preservation.

To evaluate policy effectiveness, this study uses indicators that reflect both ecological protection and tourism experience. These factors encompass the level of adherence to zoning laws, perceived enhancements in environmental quality, visitor contentment with interpretive facilities, and the degree of community involvement in conservation initiatives. These indicators were embedded in the survey instrument and used as observed variables to assess the performance of heritage-related urban policies. This study incorporates governance integration as a foundational principle in policy assessment. It evaluates how planning authorities synchronize land-use decisions with environmental and cultural conservation mandates. The model incorporates variables that demonstrate interagency collaboration, joint review procedures, and the uniformity of regulatory enforcement across departments. These elements are critical to aligning development trajectories with long-term preservation goals in heritage-sensitive areas. The model includes adaptive management as a strategy to harmonize heritage conservation with the continuous development of urban infrastructure. The study evaluates stakeholder perceptions of flexibility in regulatory implementation, periodic review of zoning criteria, and the responsiveness of planning instruments to changing ecological conditions. These dimensions are critical in dynamic urban environments where static conservation strategies might not be adequate to tackle evolving pressures.

Financial resources

Financial resources are a necessary condition for maintaining, restoring, and enhancing the value of heritage sites. Insufficient funding or inappropriate allocation often constitutes a major barrier to preservation (Le *et al.,* 2024). Simultaneously, the mobilization of socialized resources is considered a crucial method for improving sustainability (Dang, 2023).

Hypothesis H2: Financial resources have a positive impact on the effectiveness of heritage preservation. In addition to the overall resource sufficiency, the model also considers the distributional fairness of financial allocation. This includes mechanisms that allow for transparent revenue sharing, the integration of community-based tourism enterprises, and equitable benefit structures.

These approaches are vital for guaranteeing that local communities not only engage in but also gain equitable benefits from tourism development related to heritage sites. To strengthen the financial component of heritage conservation, this study additionally explores sustainable funding strategies that merge environmental protection with the priorities of policy implementation. These mechanisms involve allocating a proportion of tourism revenues to conservation programs, introducing payment schemes for environmental services, and promoting coordinated participation between government and private sectors. The framework emphasizes the significance of financial transparency, long-term budgeting, and alignment between economic incentives and conservation outcomes.

Community awareness

Many studies emphasize the central role of local communities in the protection and management of heritage (Le *et al.,* 2024). When community members understand the historical importance and advantages gained from tourism, they tend to engage in and endorse preservation initiatives. Conversely, limited awareness may result in the misuse or degradation of heritage sites. Active involvement of the community plays a vital role in ensuring heritage conservation is sustainable. In addition to recognizing the significance of awareness, the study integrates policy strategies that institutionalize community participation in heritage and environmental governance. These strategies include participatory planning procedures, shared decision-making models, and formal representation of local voices in conservation programs. Their efforts help to cultivate accountability, improve cultural continuity, and guarantee that protective actions are grounded in community legitimacy. To reinforce shared responsibility, the study incorporates approaches that enhance community awareness through context-specific education and interpretation. These encompass heritage learning programs implemented in local educational institutions, storytelling guided by community elders, and visual communication strategies adapted to local cultural practices. Such initiatives are expected to deepen the public's connection to the cultural and ecological values of the Rừng Sác site and promote long-term conservation engagement. Nguyen and Thanh (2024) show that active community involvement significantly improves conservation outcomes and helps preserve cultural values.

Hypothesis H3: Community awareness has a positive impact on the effectiveness of heritage preservation.

Communication technologies

The integration of digital technologies, including virtual reality (VR), Augmented Reality (AR), and 3D digitization in the preservation and promotion of heritage has emerged as a worldwide phenomenon. Studies indicate that technology enhances accessibility, improves visitor experiences, and reduces direct pressure on heritage sites (Nguyen and Le, 2022). However, inconsistent technological infrastructure may limit its effectiveness. To enhance interpretive quality and visitor experience, the study incorporates digital technologies such as VR, AR, and digital storytelling. These tools simulate historical environments, offer interactive learning, and reduce dependence on physical infrastructure. They are particularly useful in sites like Rừng Sác where preservation constraints limit direct access. By boosting engagement and accessibility, these technologies contribute to wider awareness and enduring educational achievements. To ensure the long-term sustainability of technological applications, the study emphasizes mechanisms that integrate digital innovation into policy and management systems. These include institutional coordination among heritage, tourism, and information agencies, the establishment of standards for data management and digital archiving, and the incorporation of digital transformation objectives into national and local conservation strategies. Integrating these aspects into formal policy structures helps maintain consistency in technology use, ensures proper regulation, and aligns with the overarching goals of preserving heritage over the long term. The model incorporates digitalization as a multidimensional construct, evaluating how technology supports heritage preservation, facilitates public access, and enhances educational engagement. Specific indicators include the use of virtual tours, interactive digital content, and augmented interpretation tools that simulate historical environments. These developments lessen the physical effects on delicate areas and expand outreach beyond nearby geographical confines, which is particularly vital in swiftly urbanizing settings. In addition to enhancing interpretation, digital technologies are assessed in this study for their role in eco-monitoring. This framework integrates indicators pertaining to remote sensing, sensor-based environmental monitoring, and GIS-integrated mapping to detect encroachment, pollution, and alterations in the landscape. These tools allow for real-time monitoring and data-driven response strategies, helping stakeholders manage urban impacts on sensitive heritage zones such as the Rừng Sác site.

Hypothesis H4: Communication technologies have a positive impact on the effectiveness of heritage preservation.

Urbanization and infrastructure development

Urbanization is the factor particularly emphasized in this study. The rapid urbanization process in Ho Chi Minh City generates multiple pressures on heritage sites:

• Land pressure: land allocated for preservation competes with real estate projects (Pham *et al.*, 2021).

• Spatial transformation: the surrounding landscape of heritage sites is altered, reducing authenticity and diminishing aesthetic value.

• Encroachment from real estate projects: many sites have been reduced in size or enclosed by commercial developments.

• Demographic and lifestyle changes: communities historically connected to heritage are gradually replaced by migrants, weakening heritage attachment.

• Global studies suggests that urbanization can lead to both adverse effects and potential benefits (such as enhanced infrastructure and greater tourist influx) when managed effectively (Emmanuelle and Võ, 2016; Dang, 2023).

Hypothesis H5: Urbanization has the strongest impact on the effectiveness of heritage preservation.

The study model

The research framework includes five independent variables—Institutional Policy, Financial Resources, Community Awareness, Communication Technologies, Urbanization and Infrastructure Development—and one dependent variable: Effectiveness of Heritage Preservation.

The study design

This research was carried out using a quantitative approach, with data collected through a structured questionnaire.

Study subjects and sampling

The survey population consists of heritage site managers, tourism–conservation experts, and

Table 1: Descriptive statistics of the survey sample

Variables	Grouping	Frequencies (n)	Percent (%)
Gender	Male	112	53,1%
	Female	99	46,9%
Ages	Under 30s	45	21,3%
	From 30s to 45s	87	41,2%
	From 46 to 60s	54	25,6%
	Above 60s	25	11,8%
Occupation	Heritage site managers	73	34,6%
	Lecturers / research experts	65	30,8%
	Local residents / communities	73	34,6%
Education	Upper secondary level or below	31	14,7%
	University	105	49,8%
	Master/PhD	75	35,5%
Experience	Under 5 years	58	27,5%
	From 5 to 10 years	71	33,6%
	Above 10 years	82	38,9%

residents living in the vicinity of revolutionary base sites in Ho Chi Minh City. A non-probability sampling method (convenience sampling) was employed due to feasibility considerations in the study context. A total of N = 211 valid responses were collected, which meets the minimum recommended threshold for structural model analysis (Hair *et al.,* 2019). The demographics of the respondents are summarized in Table 1, which reveals a gender-balanced group, primarily aged 30 to 45, and mostly possessing university education. The sample included heritage managers, experts, and local residents, ensuring diverse perspectives.

Measuring tool

The questionnaire was developed using five-point Likert scales (1 = Strongly Disagree, 5 = Strongly Agree). Each construction was measured by multiple observed variables, for example: policy (5 items), finance (4 items), community awareness (4 items), communication technology (4 items), and urbanization (4 items). Using Cronbach's Alpha, the reliability of the scales was assessed, and Exploratory Factor Analysis (EFA) was carried out to evaluate convergent and discriminant validity. The measurement scales were validated through Cronbach's α (acceptable threshold ≥ 0.70), EFA; factor loadings ≥ 0.50; Kaiser–Meyer–Olkin (KMO) ≥ 0.6), and Confirmatory Factor Analysis (CFA); Comparative Fit Index (CFI) / Tucker–Lewis Index (TLI) ≥ 0.90; Root Means Square Error of Approximation (RMSEA) ≤ 0.08; Standardized Root Mean Square Residual (SRMR) ≤ 0.08). Structural equation modeling (SEM) was employed to estimate standardized path coefficients (β), significance levels (p), and explained variance (R^2). Additional tests included Harman's single-factor test to assess common method bias and Variance Inflation Factor (VIF) analysis to check for multicollinearity.

Data analysis method

Data was processed using Statistical Packages for the Social Sciences (SPSS) 22 and Analysis of Moment Structures (AMOS) 24. The analytical procedure included:

• Descriptive statistics to profile the sample characteristics;

• Reliability testing of the measurement scales using Cronbach's α;

• CFA to evaluate the validity and overall fit of the measurement model;

• SEM to test the hypothesized relationships among constructs;

• Multiple regression analysis to compare the relative effects of the independent variables on heritage conservation effectiveness.

Furthermore, the study employs a range of planning effectiveness metrics sourced from the SEM framework to analyze the outcomes of urban and tourism initiatives. These include variables reflecting perceptions of spatial containment, ecological preservation, and program alignment with zoning regulations. By connecting these indicators to conservation-related latent constructs, the model facilitates an empirical evaluation of the role of development interventions in regulating land expansion and protection mangrove habitats in Rừng Sác. The model also evaluates the sustainability impacts of tourism-led urban projects

through indicators reflecting ecological sensitivity and cultural displacement. In the case of the Cần Giờ sea reclamation area, survey variables measure perceived threats to mangrove habitats, disruptions to traditional practices, and erosion of place-based identity. These indicators are analyzed within the SEM framework to quantify development-related pressure on ecological and cultural systems.

RESULTS AND DISCUSSION

Reliability assessment and data suitability testing

The survey was conducted using a questionnaire with a total sample of N = 211, covering respondents categorized by occupation groups, including heritage site managers, tourism–conservation experts, and local communities residing near the sites. Community involvement in mangrove ecotourism has enhanced environmental quality and raised awareness, as seen in Beras Basah Island (Silalahi *et al*., 2024). Fostering adaptive responses in vulnerable ecosystems relies heavily on perception-based interventions and participatory education (Hoa *et al.*, 2025). The KMO test results for the independent variables are presented in Table 2, showing that all factors achieved good to excellent values (min = 0.87; max = 0.92). This indicates a high level of intercorrelation among the variables and confirms the suitability of the scales for factor analysis.

Meanwhile, Bartlett's Test yielded a Chi-Square = 2021.573 with degrees of freedom (df) = 210 and $p < 0.001$. This result is statistically significant, rejecting the null hypothesis (H_0) that the correlation matrix is an identity matrix. Therefore, the research data fulfills the adequacy standards required for executing EFA. In addition, to assess the reliability of the measurement scales (the consistency of observed variables measuring the same construct), Cronbach's α tests were performed with a minimum acceptable threshold of 0.70 for each independent factor. The results of these reliability tests are presented in Table 3.

The independent variables include institutional policy (IP), financial resources (FR), community awareness (CA), communication technologies (CT), and Urbanization and Infrastructure Development (UD). These variables showed Cronbach's Alpha coefficients exceeding 0.7 (IP: 0.8; FR: 0.82; CA: 0.84; CT: 0.84; UD: 0.86), indicating good internal consistency. Eliminating any observed item marginally decreased reliability, indicating that every item played a significant role in the measurement scales. Additionally, a correlation matrix was constructed to visually examine the linear relationships among the observed variables (Fig. 3).

The results indicate the correlation levels among all observed variables. In general, variables within the same construct (CS, TCNL, NTCD, CNTT, DTH) exhibit relatively high correlations, while correlations between different constructs are lower. Generally, the interrelationships between independent variables are of moderate strength, thus lowering the risk of multicollinearity in regression analysis. This is a positive indication, suggesting that the data have a clear structure and are suitable for EFA or CFA. The SEM analysis illustrates that tourist satisfaction plays a significant mediating role in the relationship between destination attractiveness and the intention to revisit, thereby accentuating the importance of experience quality in sustainable tourism (Yuliana *et al*., 2025).

Factor rotation

To ensure the clarity of the factor structure, the Varimax rotation method was applied after extracting factors based on Eigenvalues. Table 4 presents the rotated loading matrix obtained from the EFA.

The results of the EFA with Varimax rotation indicate that five factors were extracted, consistent with the initial theoretical model. Specifically, four observed variables DTH1–DTH4 loaded strongly on Factor RC1 (0.798–0.873), clearly representing the "Urbanization" construct. Five items CS1–CS5 loaded on RC2 (0.689–0.811), forming the "Institutional Policy" factor. Similarly, four items NTCD1–NTCD4 loaded strongly on RC4 (0.698–0.908), constituting the "Community Awareness" factor; four items CNTT1–CNTT4 loaded on RC3 (0.754–0.884), representing the "Communication Technology" factor; and four items TCNL1–TCNL4) loaded on RC5 (0.701–0.883), reflecting the "Financial Resources" construct. All factor loadings exceeded the threshold of 0.68, with no indication of cross-loading across multiple factors, confirming good convergent and discriminant validity of the measurement scales. In addition, the communalities (h^2) ranged from 0.53 to 0.78, indicating that most of the variance of the observed variables was explained by the extracted factors, while the low uniqueness values (u^2) and complexity indices (com) close to 1 further confirmed the simplicity and clarity of the factor structure. The EFA results, particularly the strong loadings of DTH1–DTH4 on RC1, affirm the structural relevance

Table 2: The KMO test for the independent variables was conducted using SPSS

Observed variables	Pattern matrix				
	Component				
	1	2	3	4	5
CS 1	0.82				
CS 2	0.82				
CS 3	0.81				
CS 4	0.83				
CS 5	0.84				
TCNL 1		0.76			
TCNL 2		0.78			
TCNL 3		0.82			
TCNL 4		0.82			
NTCD 1			0.86		
NTCD 2			0.78		
NTCD 3			0.76		
NTCD 4			0.85		
CNTT 1				0.76	
CNTT 2				0.76	
CNTT 3				0.78	
CNTT 4				0.79	
DTH 1					0.79
DTH 2					0.86
DTH 3					0.79
DTH 4					0.83

CS = Institutional policy; TCNL = Financial resources; NTCD = Community awareness; CNTT = Communication technologies; DTH = Urbanization and infrastructure development.

Table 3: Cronbach's α reliability test results

Institutional policy								
raw_alpha	std.alpha	G6(smc)	average_r	S/N	ase	mean	sd	median_r
0.8	0.8	0.77	0.45	4.1	0.022	3.6	0.89	0.44
Financial resources								
raw_alpha	std.alpha	G6(smc)	average_r	S/N	ase	mean	sd	median_r
0.82	0.82	0.78	0.83	4.5	0.021	3.8	0.82	0.52
Community awareness								
raw_alpha	std.alpha	G6(smc)	average_r	S/N	ase	mean	sd	median_r
0.84	0.84	0.81	0.87	5.3	0.018	3.7	0.85	0.58
Community technologies								
raw_alpha	std.alpha	G6(smc)	average_r	S/N	ase	mean	sd	median_r
0.84	0.84	0.82	0.57	5.3	0.018	3.6	0.86	0.6
Urbanization and infrastructure development								
raw_alpha	std.alpha	G6(smc)	average_r	S/N	ase	mean	sd	median_r
0.86	0.86	0.83	0.61	6.2	0.016	3.8	0.89	0.61

of urbanization and infrastructure development to heritage conservation. These findings provide an empirical basis for policy prioritization, suggesting that urban planning should strategically align infrastructure investment with heritage preservation goals. Prioritized development of access roads, tourism amenities, and zoning regulations should reflect the high impact factor identified through factor analysis. Accordingly, the EFA results validated the adequacy of the measurement scales, providing support for subsequent analyses.

Multiple regression analysis

Multiple regression analysis was conducted to examine the relationship between the independent variables (five variables in this study) and the dependent variable. The results of this regression

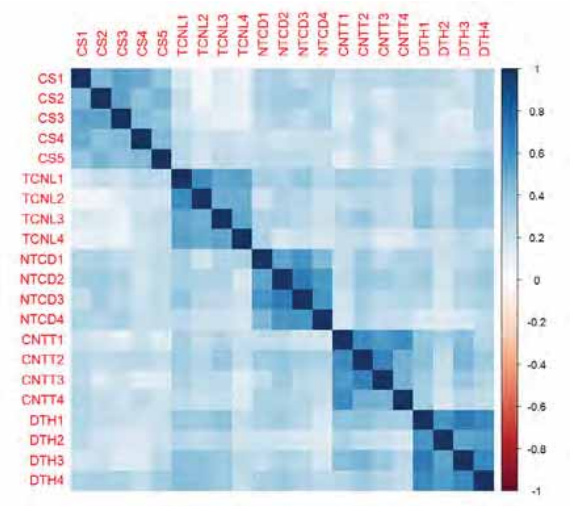

Fig. 3: Correlation of matrix

Table 4: Rotated factor loading matrix

Variable	item	RC1	RC2	RC4	RC3	RC5	h2	u2	com
DTH2	19	0.873					0.650	0.350	1.05
DTH1	18	0.836					0.761	0.239	1.03
DTH3	20	0.800					0.738	0.262	1.09
DTH4	21	0.798					0.730	0.270	1.11
CS4	4		0.811				0.630	0.370	1.36
CS3	3		0.767				0.604	0.396	1.05
CS1	1		0.737				0.617	0.383	1.22
CS2	2		0.703				0.584	0.416	1.18
CS5	5		0.689				0.530	0.470	1.26
NTCD3	12			0.908			0.777	0.223	1.02
NTCD2	11			0.847			0.747	0.253	1.03
NTCD4	13			0.803			0.637	0.363	1.07
NTCD1	10			0.698			0.567	0.433	1.03
CNTT1	14				0.884		0.763	0.237	1.06
CNTT3	16				0.815		0.674	0.326	1.04
CNTT4	17				0.781		0.616	0.384	1.10
CNTT2	15				0.754		0.708	0.292	1.04
TCNL4	9					0.883	0.676	0.324	1.05
TCNL2	7					0.764	0.647	0.353	1.08
TCNL1	6					0.745	0.685	0.315	1.04
TCNL3	8					0.701	0.595	0.405	1.05

analysis are presented in Table 5, which details the coefficients, standard errors, and significance levels for each factor.

The results of the multiple regression analysis indicate that the overall model is statistically significant ($F = 81.43$, $p < 0.001$), with an adjusted R^2 of 0.658. This means that the independent variables explain approximately 65.8% of the variance in the dependent variable ($p < 0.01$). Among these, Urbanization ($\beta = 0.377$) exerts the strongest influence, followed by Communication Technology ($\beta = 0.301$), Community Awareness ($\beta = 0.297$), Financial Resources ($\beta = 0.173$), and Institutional Policy ($\beta = 0.158$). These conclusions emphasize the crucial roles played by the factors discussed earlier in accounting for the differences observed in the research outcome.

Table 5: Multiple regression analysis

Residuals:				
Min.	1Q	Median	3Q	Max
-2.2472	-0.3408	0.0063	0.3741	1.4881
Coefficients:				
	Estimate	Standard error (SE)	t value	Pr(>|t|)
(Intercept)	-1.08207	0.25045	-4.320	2.43e-05 ***
CS	0.15802	0.05376	2.940	0.00367 **
TCNL	0.17252	0.06041	2.856	0.00473 **
NTCD	0.29691	0.05832	5.091	8.06e-07 ***
CNTT	0.30053	0.05754	5.223	4.34e-07 ***
DTH	0.37732	0.05754	6.557	4.40e-10 ***
Signif. codes: 0 '***' 0.001'**' 0.01 '*' 0.05 '.' 0.1 ' ' 1				
Residual standard error: 0.5932 on 204 degrees of freedom				
Multiple R-squared: 0.6662, Adjusted R-squared: 0.658				
F-statistic: 81.43 on 5 and 204 DF, p-value: < 2.2e-16				

Table 6: Multicollinearity

CS	TCNL	NTCD	CNTT	DTH
1.351979	1.464506	1.446987	1.452298	1.551291

Accepting hypotheses H1, H2, H3, H4, H5

Since the independent factors exhibit relatively high correlations, a VIF test was conducted to examine the presence of multicollinearity. The results are presented in Table 6.

The VIF values of the independent variables range from 1.35 to 1.55, all well below the threshold of 2, indicating that multicollinearity is not a concern in the regression model. Consequently, the findings from the regression analysis are deemed trustworthy. The outcomes derived from examining the factors that affect heritage conservation broadly, and revolutionary heritage sites specifically, suggest that Institutional Policy, Financial–Human Resources, Community Awareness, and Communication Technology all play constructive roles. Among them, Urbanization and Infrastructure Development demonstrate the strongest impact on heritage conservation (supporting hypotheses H1, H2, H3, H4, and H5). These factors provide a foundation for orienting tourism development at revolutionary historical sites in rapidly expanding urban areas such as Ho Chi Minh City, with the case of the Rừng Sác Revolutionary Base serving as a specific example. Institutional frameworks and financial allocations, when examined jointly, reveal a synergistic effect on heritage preservation. The SEM analysis revealed that efforts to preserve resources were more successful in locations where policy transparency was supported by stable funding. In the Rừng Sác case, implementation of regulatory zoning yielded tangible conservation outcomes only when matched by consistent funding for site maintenance and monitoring. This interaction underscores that institutional dedication must be bolstered by financial mechanisms to yield resilient heritage outcomes in the context of urbanization. Consequently, this contributes to the promotion of sustainable cultural and heritage tourism. The structural model confirms the statistical significance of interactions among institutional policy, financial availability, community awareness, communication technology, and urbanization. Standardized path coefficients demonstrate that the coordination of policies and engagement with the community partially alleviates the pressures associated with urban development. SPSS and AMOS outputs support a multidimensional interpretation of conservation effectiveness, where institutional and social variables exert both direct and mediating effects within the structural framework. The SEM findings reveal that institutional policy significantly influences conservation effectiveness, not only through direct effects but also by mediating the influence of financial resources, community engagement, and technological adoption. This highlights the importance of coordinated governance structures. Policies that establish formal collaboration between local authorities and heritage management bodies—such as interagency planning frameworks,

joint budgeting mechanisms, and integrated monitoring protocols—are empirically supported by the model. These coordination initiatives promote coherence in policy, synchronize resource allocation with heritage priorities, and enhance the effectiveness of implementation. Public–private partnerships (PPPs) offer a viable pathway for mobilizing supplementary resources while preserving environmental standards. In Cần Giờ, heritage-compatible investment projects involving the private sector—such as eco-guided services and interpretive media—have complemented state-led initiatives. These alliances, regulated by defined sustainability guidelines, showcase how environmental stewardship can be incorporated into co-financing programs, enhancing the effectiveness of public heritage strategies without compromising conservation ethics. The findings also reinforce the principle of "conservation for development and development for conservation" by demonstrating that heritage protection can serve as a foundation for sustainable tourism and urban growth. The positive coefficients of institutional policy and financial resources within the SEM model support policy innovation that treats conservation not as a constraint but as a catalyst for place-based development. This implies that cohesive planning structures, which synchronize conservation with socio-economic aims, are vital for realizing enduring cultural, ecological, and economic stability. Considering the SEM results, practical recommendations should prioritize the integration of heritage conservation objectives into broader urban sustainability and tourism development strategies. The analysis demonstrates that conservation effectiveness improves when policy, infrastructure investment, and community participation are aligned. By integrating conservation within urban planning, it helps to maintain cultural and ecological values while also boosting the competitiveness of destinations, drawing in a variety of visitor demographics, and reinforcing long-term resilience against environmental and developmental pressures.

Premises for heritage conservation and tourism development at the Rừng Sác historical site through the policies of the Government and local authorities

Right after 1975, revolutionary heritage sites received continuous attention and investment from the State for preservation. Simultaneously, legislative frameworks and policies on investment and development of revolutionary heritage sites have been introduced to encourage conservation efforts alongside tourism exploitation. The Vietnamese Law on Cultural Heritage (promulgated in 2001 and most recently amended in 2024) explicitly recognizes revolutionary sites as cultural properties requiring protection (Article 4). Revolutionary sites that meet specific criteria (historical value, educational significance, and scale of influence) may be officially designated and safeguarded according to corresponding levels of protection. It is the duty of the State to allocate resources for the restoration, renovation, and promotion of the importance of heritage sites, including monuments of revolutionary nature. Meanwhile, communities, organizations, and individuals are obliged to protect such sites and refrain from acts of infringement. In addition, a series of legal documents have been enacted to guide implementation, such as the Circulars of the Ministry of Culture, Sports and Tourism (No. 18/2012/TT-BVHTTDL; No. 15/2019/TT-BVHTTDL), Government Decrees (No. 70/2012/NĐ-CP; No. 166/2018/NĐ-CP; No. 67/2022/NĐ-CP), and the Prime Minister's Decision (No. 1228/QĐ-TTg, 2023), all of which provide the legal basis for the conservation of cultural heritage, including revolutionary sites.

Fig. 4 illustrates the Rừng Sác special task force during and after combat, reflecting the site's military significance and symbolic heritage. The Rừng Sác Revolutionary Base was designated as a National Historical Site by the Ministry of Culture, Sports, and Tourism in 2004. The incorporation of such sites into the official ranking list lays the groundwork for advancing subsequent initiatives in restoration, preservation, and tourism development. Decision No. 4741/QĐ-UBND (Ho Chi Minh City), issued on September 23, 2015, approved the zoning plan at a scale of 1/5000 for the reconstruction and preservation of the Rừng Sác Revolutionary Base – Cần Giờ, located in Long Hòa Commune, Cần Giờ District. The objective of this plan was: *"to honor the heroic achievements of the people, cadres, and soldiers who lived, fought, and sacrificed in this area; to educate current and future generations in patriotism and revolutionary traditions; while simultaneously integrating eco-tourism with the preservation and development of the Cần Giờ Biosphere Reserve in accordance with the official management regulations of the Cần Giờ Biosphere Reserve."* (Article 1). In 2022, the Ho Chi Minh City Party Committee promulgated Resolution No. 12-NQ/TU, which sets



(a) (b)

Fig. 4: Rừng Sác special task force operations during and after combat. (a): Officers and soldiers of the Rừng Sác 10th Naval Commando Unit fighting during an operation. (b): Model of Rừng Sác Special Task Force soldiers in combat at the Rừng Sác Historical Site, Cần Giờ District.

out the development orientation for Cần Giờ District toward 2030 with the objective of transforming Cần Giờ into a high-quality resort and eco-tourism city. In this context, tourism is recognized as an essential economic sector of the region. The proactive and timely policies of the Government have had a positive impact on both the preservation and the tourism development of the Rừng Sác Historical Site. Specifically: 1) Establishing a mandatory legal framework to safeguard heritage sites against unregulated tourism exploitation. In the case of classified sites like Rừng Sác, it is mandatory to establish protected areas, create scientific documentation, and confirm restoration, construction, and exploitation activities are subject to approval by the heritage management authorities. Unauthorized construction that undermines the authenticity of the site is strictly prohibited. This framework strikes a balance between maintaining existing structures and fostering development, while avoiding detrimental effects from unregulated and fast-paced urbanization. 2) Forming groundwork for activating investment resources for the purposes of restoration and tourism enhancement. Government and municipal decisions on the restoration of heritage sites have allocated state budgets while simultaneously introducing mechanisms for socialization, encouraging investment from both domestic and international enterprises. Specifically, under the approved 1/5000 zoning plan in Cần Giờ District, Ho Chi Minh City has earmarked public funding and mobilized private capital for the development of tourism infrastructure such as boat docks, elevated walkways through the mangrove forest or the Rừng Sác Traditional House. 3) Focusing tourism advancement alongside heritage education and community participation. Local development resolutions encourage the transformation of revolutionary heritage values into distinctive tourism products, closely associated with patriotic education for students and young generations. As a result, "red" tours have received significant attention and investment from travel agencies, being regularly organized for groups such as students, veterans, and youth organizations. These efforts not only bolster conventional education but also appeal to a more diverse array of visitors from both domestic and international backgrounds. 4) Embracing the trend of digital transformation in the era of the 4.0 Revolution, national tourism strategies and ministerial circulars on digitalization have facilitated the adoption of virtual 3D tours, automated audio guides, and digital museums at heritage sites. Even though such technologies have not been extensively adopted at the Rừng Sác historical site, anticipated forthcoming advancements—together with funding from site management authorities and tour operators—are expected to introduce innovative experiences that will attract a greater number of visitors and enhance their connection with the heritage.

Independent factors influencing the conservation and tourism development of the Rừng Sác historical site

Government policies have established the foundation that enhances the positive influence of other factors—namely Financial Resources, Community Awareness, and Communication Technology—on tourism development at the Rừng Sác Historical Site. The allocation of financial resources derives from Government investment funds, supplemented by contributions from enterprises. These

funds are designated not solely for the development of infrastructure at the heritage site but also for comprehensive investments in transport facilities, lodging infrastructure, and, significantly, the safeguarding of the ecosystem within the Cần Giờ Biosphere Reserve, which encompasses the Rừng Sác site. Recent studies highlight diverse approaches to heritage conservation. Pranskūnienė and Zabulionienė (2023) emphasize that heritage undergoes continuous transformation shaped by individual, community, and regional contexts within global settings. Zhang *et al.* (2025) introduce a spatial framework that integrates conservation with sustainable development as urbanization progresses. Each year, the Government allocates a budget under the National Target Program on Culture to support the conservation of historical sites. During the period 2011–2015, a total budget of VND 1.4 trillion was allocated for the conservation of 1,302 heritage sites nationwide. In the period 2016–2020, VND 245 billion was distributed for the preservation of 471 sites (Viet, 2023). Nevertheless, specialists have evaluated that the financial resources allocated for the protection, restoration, and enhancement of heritage sites are still inadequate in relation to the actual requirements. In the context where tourism activities are strongly promoted with the orientation of becoming a key source of local revenue, tourism impacts will inevitably place pressure on the infrastructure of heritage sites. In 2024, the district welcomed 4,395,000 tourist arrivals, representing an increase of 15.6% compared to 2023. In the first quarter of 2025, the number of visitors reached 1,080,000, an increase of 3.8% over the same period in 2024. The empirical evidence underscores a notable relationship between the swift expansion of tourism and the heightened strain on heritage infrastructure and ecological systems at the Rừng Sác site. Regression results indicate that without regulatory safeguards and resource reinvestment, mass tourism can accelerate environmental degradation and undermine the site's cultural integrity. These insights underscore the necessity of adaptive management approaches that link tourism revenue to site maintenance, limit visitor overload, and enforce conservation zoning to ensure long-term sustainability. To promote enduring heritage resilience, this research suggests the incorporation of feedback systems that consistently assess the alignment of environmental factors and policies. In Rừng Sác, such mechanisms could include periodic ecological assessments, land encroachment alerts, and public compliance audits. These tools would provide actionable data to guide timely policy adjustments and strengthen adaptive management in response to evolving urban dynamics. Therefore, close attention and monitoring from site management boards are required to ensure the timely allocation of financial resources for conservation and restoration activities. In Cần Giờ, the Rừng Sác Road expansion project was initiated in 2002 and inaugurated in 2011, with a total investment of VND 1,500 billion, along with the construction of eight new bridges costing VND 500 billion (Thanh, 2024). The purpose of this investment in transportation infrastructure was to advance urbanization in Cần Giờ District and to promote tourism activities in the locality, particularly at the Rừng Sác historical site. In addition, with social funding, the Rừng Sác Martyrs' Memorial Temple commenced in 2023. This work of historical and cultural significance is deeply connected to major events and prominent historical figures, carrying substantial meaning for the community. Together with the Rừng Sác Revolutionary Base Historical Site, the temple is expected to become a "red address," serving as a place to foster patriotism, instill gratitude toward previous generations, and provide a suitable venue for developing heritage-based and educational tourism programs for a wide range of visitors. In addition to the factor of Financial Resources, Community Awareness is also an independent variable that is partly shaped by Government Policies. By focusing on tourism development that emphasizes robust community involvement, it is anticipated that raising awareness among residents in Cần Giờ will yield beneficial effects on tourism initiatives as well as the conservation of the Rừng Sác historical site. By means of policies that encourage communication, education, and dissemination of heritage values, environmental protection, and local cultural identity, the community is enabled to better understand the role of tourism in the locality's development, particularly in relation to people's livelihoods. Hyun (2025) highlights which disparities in spatial distribution and inconsistent investment may obstruct community-based tourism, advocating for spatial justice to guarantee fair access to heritage. Tourism activities that actively involve the community—such as tour guiding, providing accommodation services, and producing local handicrafts—bring direct economic benefits to residents. Consequently, the community's role in promoting sustainable tourism associated with heritage conservation has been increasingly strengthened. Local communities and tour guides at Củ

Chi act as "storytellers" who co-create interpretive depth and dialogic meaning in the tourist experience (Madigan and West, 2023; Gillen, 2018). Simultaneously, a legal framework comprising regulations and sanctions aids in ensuring that the community upholds a serious and responsible approach towards tourism and preservation activities. Government policies on allocating investment funds for technologies that support sustainable tourism also need to be strengthened. At present, new technologies such as AR, VR / VR 360, online tours – digital exhibitions – 3D tours, as well as electronic ticketing systems, automated narration, and virtual travel assistants have been introduced and applied at historical and cultural sites across Vietnam. However, these technologies have not yet been widely implemented at revolutionary historical sites in general, nor at the Rừng Sác site. Communication technology positively influences the visitor experience at heritage sites by adopting a visitor-centered approach, making heritage more accessible, increasing attractiveness, and tailoring experiences to meet specific visitor needs. VR/AR technologies are particularly suited for comprehensive guided tours with strong educational value, which align well with "red tourism" programs focusing on revolutionary traditions. Nonetheless, the advancement of these technologies presently demands significant time and financial resources. The case of Ho Chi Minh City's transformation into a mega-tourism metropolis offers strategic insights for future governance models. Lessons include the necessity of harmonizing infrastructure expansion with heritage zoning, embedding cultural sites within tourism circuits, and enforcing land-use controls to prevent speculative developments. These methods facilitate governance frameworks that harmonize urban development with heritage preservation, especially in delicate regions such as Rừng Sác. This situation calls for clear and specific strategies in technological development for tourism, ensuring the proper allocation of resources and creating mechanisms to recover costs through tourism experiences (Bekele *et al.*, 2018).

The impact of urbanization on tourism development at the Rừng Sác revolutionary base historic site

The results of the EFA with Varimax rotation show that the four observed variables DTH1–DTH4 have high loadings on factor RC1 (0.798–0.873). This reflects the strongest impact of the Urbanization and Infrastructure factor group on heritage conservation and the development of tourism programs at the Rừng Sác site. After July 1st, 2025, Ho Chi Minh City was newly established through the merger of three localities: Ho Chi Minh City, Ba Ria – Vung Tau, and Binh Duong, with a total area of more than 6,700 km² and a population exceeding 14 million. This unification established the groundwork for the rise of a mega-tourism hub of regional importance. The urbanization process in Ho Chi Minh City has been propelled by innovative initiatives aimed at enhancing the transportation infrastructure. Key infrastructure projects currently under construction, such as Long Thanh International Airport and strategic transport routes including Ho Chi Minh City – Long Thanh – Dau Giay, Ben Luc – Long Thanh, and Ho Chi Minh City – Thu Dau Mot – Chon Thanh, will strengthen interregional connectivity and promote an integrated tourism network. In Cần Giờ, the Rừng Sác Road has been invested in and put into operation, accompanied by the construction of main arterial roads in Zone A and Zone C; the upgrading of branch roads connecting the centers of Tam Thon Hiep, An Thoi Dong, and Ly Nhon communes with Rừng Sác Road; a ring road linking the four northern communes; and an interchange connecting Rừng Sác Road with the Ben Luc – Long Thanh Expressway. The findings of the study demonstrate that upgrading infrastructure substantially increases access to heritage sites and redistributes visitor patterns throughout the Rừng Sác area. Strategic improvements, such as elevated walkways and transport connectivity, mitigating concentration at ecologically sensitive zones. These interventions not only reduce environmental stress but also expand the spatial capacity of tourism activities, ensuring a balanced distribution that supports both conservation and visitor experience. The Cần Giờ sea reclamation urban area project, covering 2,870 hectares with a planned population of 230,000 and invested by Vingroup, was also inaugurated in April 2025. This endeavor is planned as a smart city dedicated to coastal tourism and resort development, showcasing cutting-edge services, living spaces, and hotels that can host millions of tourists on an annual basis. The merger of administrative units, infrastructure development, and the construction of tourism-oriented urban areas have created numerous new opportunities for the tourism sector. This process facilitates the effective exploitation of interregional tourism resources by eliminating procedural barriers between provinces as before. The prevailing trend involves the development of tours

within a unified tourism environment, showcasing diverse experiential themes that are increasingly aligned with modern preferences. The Cần Giờ Biosphere Reserve, with the historic Rừng Sác Revolutionary Base, will serve as a focal point for green tourism programs linked to the conservation of mangrove ecosystems, as well as for interregional leisure journeys from the city to riverine and coastal areas. This will connect Cần Giờ with Vung Tau, leveraging the cultural, historical, and marine ecological values of the region. The persistent investment in infrastructure and urban projects, combined with effective tourism programs, has enabled the expansion of tourism in Cần Giờ, making it a significant economic sector for the area. However, uncontrolled urbanization and mass tourism may become obstacles, negatively affecting natural resources and heritage tourism sites. Allocating land for horizontal urban expansion aimed at attracting tourists rather than serving local residents may result in the uncontrolled proliferation of residential complexes, leading to inefficient land use, encroachment upon protected heritage areas, or the biosphere reserve. Interregional tourism planning offers a spatial governance tool to counteract risks from speculative real estate development and unregulated expansion. By coordinating tourism zoning across different regions, redistributing visitor traffic, and embedding ecological safeguards, these approaches lessen the burden on significant heritage sites like Rừng Sác. Similar integrative frameworks have been observed in China, where conservation-based tourism planning successfully aligns heritage protection with regional development goals (Zhang *et al.*, 2025). Coordinated planning also curtails redundant infrastructure investment and directs tourism growth toward ecologically compatible areas, ensuring balanced regional development. Sustainable urban planning can integrate tourism development with ecological and cultural preservation by harmonizing land-use policies with heritage conservation and biosphere reserve goals. Integrated plans should designate ecological buffer zones, prioritize low-impact tourism infrastructure, and institutionalize heritage interpretation within development schemes. At Rừng Sác, such coordination ensures that tourism expansion supports mangrove ecosystem resilience and strengthens the historical significance of revolutionary heritage. If urban development lacks strict oversight, it may generate real estate bubbles, causing direct repercussions for both the economy and the tourism sector. No-take marine protected areas contribute to the restoration of coral reefs and biodiversity, thereby supporting the objectives of coastal conservation (Harahap *et al.*, 2025). Therefore, land resources must be managed rationally and efficiently to maximize ecological, economic, and social benefits. Future research should refine the assessment framework used to measure the environmental consequences of urban expansion on revolutionary heritage sites. A comprehensive framework must incorporate the detection of land-use changes through satellite imagery, the mapping of ecological risks, and the tracking of socio-cultural displacement. These methods would allow for a more accurate quantification of both physical and intangible impacts and help formulate preventive planning measures.

Limitations and suggestions for future research

Although this study developed a structural analysis model contributing to the evaluation of key factors influencing the conservation of revolutionary relics in the context of urbanization, several limitations should be acknowledged. First, the research scope is limited to a single case—the Rừng Sác Revolutionary Base Relic (Cần Giờ District)—which may reduce the generalizability of the findings and fail to capture the diversity of revolutionary relics in other urban areas across the country. Second, although the quantitative survey method provides statistical reliability, the study failed to merge it with qualitative techniques that might further elucidate the cultural, social, and perceptual aspects that shape community attitudes toward conservation. Third, the study has not examined in depth the differences in perceptions among stakeholder groups, particularly between local authorities and residents, even though these differences could significantly affect the effectiveness of policy implementation. In future research, expanding the scope of the survey to other urban areas or regions with distinctive historical significance, such as Hanoi, Quang Tri, or the Central Highlands, could enable comparative analyses across different socio-spatial contexts. At the same time, integrating qualitative methods such as in-depth interviews, focus group discussions, or discourse analysis would provide additional insights into the motivations, viewpoints, and possible conflicts related to the preservation of revolutionary relics. Finally, fostering stronger linkages

between academic research and policy-making practice is essential to enhance the applicability of research findings, thereby contributing more effectively to the sustainable development of revolutionary heritage tourism in Vietnam.

CONCLUSION

By employing a quantitative research approach through questionnaires and analyzing data using SPSS 22 and AMOS 24, this study identified and measured five key determinants influencing the effectiveness of revolutionary heritage conservation in Ho Chi Minh City. This encompasses policies characterized by five observed variables, financial resources comprising four, community awareness consisting of four, communication technology featuring five, and urbanization along with infrastructure development also comprising five. The statistical results show that all five factors have positive effects on the preservation and sustainable development of heritage tourism across the city, particularly at the Rừng Sác Revolutionary Base. Among them, urbanization exerts the strongest influence, with factor loadings ranging from RC1 equal to 0.798 to 0.873. Policy also serves as a foundational element that, to some extent, shapes the influence of other variables within the model. The findings confirm that urbanization plays a decisive role in achieving the combined objectives of heritage preservation and tourism development in Ho Chi Minh City. These two elements cannot function separately; rather, they must create a cohesive system of mutually supportive actions. This integration includes enhancements to urban infrastructure, spatial planning, and the establishment of sustainable tourism initiatives. This approach ensures a balanced relationship between development and preservation, consistent with the principle of conservation for development and development for conservation. Compared to other revolutionary relics in Ho Chi Minh City, the Rừng Sác Revolutionary Base is particularly distinctive. It functioned both as a resistance center serving as the headquarters of the 10th Naval Commando Unit and as a component of the Cần Giờ Mangrove Biosphere Reserve. This dual nature presents substantial potential for fostering sustainable, educational, and experiential forms of tourism. Heritage programs focusing on revolutionary traditions can connect Rừng Sác with other historical sites such as the Cu Chi Tunnels, Phu Tho Hoa Tunnels, and the Vinh Loc Frontline Logistics Site, targeting students, veterans, and young visitors. The site's placement in the Cần Giờ Biosphere Reserve offers prospects for ecological and research-based tourism that merges natural and historical attributes, thereby increasing both educational and environmental relevance. In line with Ho Chi Minh City's development orientation toward transforming Cần Giờ into a coastal eco-tourism urban area, Rừng Sác is now facing both opportunities and challenges. Large-scale infrastructure developments, including new expressways, the Cần Giờ Bridge, and the coastal reclamation urban zone, are underway. Yet, the tourism services at this location remain insufficient, especially in terms of digital interpretation technologies including virtual reality, augmented reality, and automated narration. To ensure that Cần Giờ's transformation into a coastal eco-tourism urban area remains consistent with heritage preservation goals, future policy frameworks must institutionalize sustainable funding mechanisms and cross-sectoral policy integration. Creating specialized conservation funds derived from tourism income, implementing eco-tourism bonds, and coordinating public-private investments with environmental standards will ensure enduring financial stability for preservation. These mechanisms should be embedded in urban master plans to ensure that infrastructural expansion enhances, rather than compromises, the ecological and historical integrity of the Rừng Sác Revolutionary Site. Since urbanization exerts the most substantial influence on heritage preservation, urban planning and environmental management must be prioritized to prevent uncontrolled spatial expansion and ecological degradation. To prevent spatial overexpansion and ecological degradation in heritage-adjacent zones, urban infrastructure must adopt environmentally responsive planning principles. These actions involve the incorporation of green corridors, the enforcement of ecological zoning limits, and the utilization of nature-based engineering methods. Such approaches not only safeguard heritage environments like Rừng Sác but also align urban development with long-term ecological resilience. The excessive exploitation of tourism activities may jeopardize the historical and ecological significance of the site. Moreover, the unequal distribution of tourism benefits, where enterprises gain more than residents, restricts community engagement and reduces the long-term sustainability of preservation efforts. This study has pinpointed the key

elements influencing the preservation of revolutionary heritage and has suggested pathways for incorporating environmental, cultural, and policy viewpoints into future development strategies, utilizing the Rừng Sác Revolutionary Base as a case study. Achieving long-term resilience requires policy innovations that balance urban expansion with environmental stewardship and heritage protection. Holistic land-use planning required heritage impact assessments, and assessments of ecological carrying capacity are essential. These strategies promote coexistence between revolutionary heritage preservation and sustainable urban growth, particularly in sensitive areas like the Cần Giờ Biosphere Reserve. Regional policy comparisons across Southeast Asia can provide valuable insights for Cần Giờ's eco-urban transition. Experiences from George Town (Malaysia), Luang Prabang (Laos), and Singapore's heritage districts reveal that balanced integration of conservation with urban modernization depends on transparent governance, community participation, and adaptive spatial planning. Integrating insights from these models can elevate Vietnam's capacity to synchronize economic development with the conservation of revolutionary heritage, providing a replicable framework for similar eco-urban transformations in the region. Nevertheless, the scope of the study was restricted to particular groups located in Ho Chi Minh City. Future studies should expand to other regions of Vietnam or comparable international contexts to validate the influence of urbanization and to assess whether the proposed orientations maintain statistical and practical significance across different socio-spatial environments.

AUTHOR CONTRIBUTIONS

T.P. Nguyen developed the research design, contributed to the theoretical framework, and drafted the initial manuscript. V.H. Dao supervised the study, led the data analysis and modeling, and finalized the manuscript for submission. A.T. Vo managed fieldwork coordination, conducted stakeholder interviews, and supported data validation. Y.N. Au handled GIS mapping, visualized spatial data, and assisted in preparing figures and tables.

ACKNOWLEDGEMENT

The authors declare that this study received no external funding. The authors would like to express their sincere thanks to the local authorities in Cần Giờ for their valuable support and facilitation during the research process.

CONFLICT OF INTEREST

The authors declare that there is no conflict of interest regarding the publication of this manuscript. All ethical considerations, including those related to plagiarism, informed consent, research misconduct, data fabrication or falsification, duplicate publication or submission, and redundancy, have been fully observed and strictly followed by the authors.

OPEN ACCESS

©2026 The author(s). This article is licensed under a Creative Commons Attribution 4.0 International License, which permits use, sharing, adaptation, distribution and reproduction in any medium or format, if you give appropriate credit to the original author(s) and the source, provide a link to the Creative Commons license, and indicate if changes are made. The images or other third-party material in this article are included in the article's Creative Commons license, unless indicated otherwise in a credit line to the material. If material is not included in the article's Creative Commons license and your intended use is not permitted by statutory regulation or exceeds the permitted use, you will need to obtain permission directly from the copyright holder. To view a copy of this license, visit: http://creativecommons.org/licenses/by/4.0/

PUBLISHER'S NOTE

GJESM Publisher remains neutral regarding jurisdictional claims in published maps and institutional afflictions.

☑ Positive AI Statement

During the preparation of this work, the author(s) used Artificial Intelligence (AI) tool ChatGPT (OpenAI) to assist in improving academic language and clarity. The authors carefully reviewed, edited, and verified the content to ensure its accuracy and take full responsibility for all aspects of the manuscript.

(For this reason, the GPTZero detector will evaluate the manuscript utilizing Generative AI, ensuring a high detection rate. If the manuscript relies heavily on Generative AI and AI-assisted technologies, it will be archived without further options for appeal).

ABBREVIATIONS

%	Percent
AMOS	Analysis of Moment Structures
AR	Augmented Reality
CFA	Confirmatory Factor Analysis
COVID- 19	Coronavirus Disease 2019
EFA	Exploratory Factor Analysis
HCMUTE	Ho Chi Minh City University of Technology and Education
KMO	Kaiser–Meyer–Olkin
SEM	Structural Equation Modeling
SGU	Saigon University
SPSS	Statistical Package for the Social Sciences
USSH, VNU-HCM	University of Social Sciences and Humanities, Vietnam National University – Ho Chi Minh City
VIF	Variance Inflation Factor
VR	Virtual Reality

REFERENCES

Assmann, J., (1995). Collective memory and cultural identity. New Ger. Crit., 65: 125–133 **(9 pages)**.

Bekele, M.K.; Pierdicca, R.; Frontoni, E.; Malinverni, E.S.; Gain, J., (2018). A survey of augmented, virtual, and mixed reality for cultural heritage. J. Comput. Cult. Herit., 11(2): 7: 1–7 **(7 pages).**

Carbone, F., (2024). War-related attractions: the good, the bad, or the ugly? War museums between peace, national identity and war porn. Curr. Issues Tour., 27(5): 679–688 **(10 pages)**.

Chen, J.; Zhao, X.; Wang, H.; Zhang, L., (2024). Portraying heritage corridor dynamics and cultivating conservation strategies. Herit. Sci., 12: 419 (**22 pages**).

Dang, H.G., (2023). Challenges in conserving ethnic culture in urban spaces. Cogent Soc. Sci., 9(1): 223374. **(26 pages)**.

Do, T.H.; Nguyen, T.T., (2025). Sustainable tourism development in Cần Giờ District, Ho Chi Minh City, Vietnam: Challenges and opportunities. Int. J. Environ. Sci., 11(5) **(8 pages).**

Emmanuelle, P.; Võ, S.X.L., (2016). Tourism, urbanisation and globalisation in Vietnam. Int. Inst. Asian Stud., 73 **(1 page)**.

Gill, G., (2025). Heritage and entrepreneurial urbanism: Conflicts and synergies. Int. J. Herit. Stud., 31(5): 456–472 (**17 pages**).

Gillen, J., (2018). It begins with the bombs: operationalizing violence at a Vietnamese dark tourism site. Cult. Geogr., 25(4): 519–536 **(18 pages)**.

Hair, J.F.; Risher J.J.; Sarstedt M.; Ringle C.M., (2019). When to use and how to report the results of PLS-SEM. Eur. Bus. Rev., 31(1): 2–24 **(23 pages).**

Harahap, M.; Siregar, A.; Nasution, D., (2025). The role of marine protected areas in enhancing coral cover and reef fish communities. Global J. Environ. Sci. Manage., 11(3): 963–982 **(20 pages).**

Hoa, L.T.; Thuy, N.T., (2025). Integrating local knowledge and community perception into climate adaptation strategies for coastal tourism. Global J. Environ. Sci. Manage., 11(2): 873–890 **(18 pages).**

Huang, Y.; Wang, J.; Lee, M., (2025). Challenges to the sustainability of urban cultural heritage: A global perspective. Land, 14(4): 778 (**18 pages**).

Hyun, H., (2025). Spatial justice and post-development perspectives on community-based tourism: investment disparities and climate-induced migration in Vietnam. Tour. Hosp., 6(1): 150 **(12 pages).**

El Faouri, B.F., (2022). Heritage-led urban regeneration in the context of World Heritage. Sustainability, 14(8): 4557 (**18 pages**).

Fabbricatti, K.; Boissenin, L.; Citoni, M., (2020). Heritage community resilience: Towards new approaches for urban resilience and sustainability. City, Territ. Archit., 7: 17 (**9 pages**).

Kim, J.; Sung, H.H., (2024). Assessing flood risk of heritage sites in an urban area. Sustainability, 16(23): 10473 (**16 pages**).

Korzilius, L., (2022). The Vietnam Veterans Memorial – presenting the unpresentable. 5th International Conference of Contemporary Affairs in Architecture and Urbanism (ICCAUA-2022) ICCAUA Conference Proceeding, 11–13 **(3 pages).**

Li, F.; Zhang, Q.; Tang, Y.; Pan, J., (2023). Assessment of urbanization impact on cultural heritage. Herit. Sci., 11: 177 (**21 pages**).

Le, D.T.; Minh, V.N.; Khanh, H.D.; Nguyen, M.V., (2024). Prioritizing barriers to the conservation of cultural heritage. J. Clean. Prod., 452: 146923 **(20 pages).**

Madigan, T.; West, B., (2023). Western tourism at Cu Chi and the memory of war in Vietnam: dialogical effects of the carnivalesque. Thesis Eleven., 174(1): 118–134 **(17 pages).**

Nguyen, H.T.; Dung, N.T.H.; Trang, T.T.T., (2021). Assessing customer satisfaction for Cần Giờ tourist destination in Ho Chi Minh City. PalArch's J. Archaeol. Egypt/Egyptol., 18(14): 249–268 **(20 pages).**

Nguyen, H.V.; Quang, D.T.; Alang, T.; Ngo, L.D.H.; Nguyen, T.D., (2022). Toward sustainable tourism practice in the post-COVID-19: perspectives from Nha Trang, Vietnam. Cogent Soc. Sci., 8(1): 2064590 **(16 pages).**

Nguyen, T.; Le N.; Dai, H.N.; Son, H.N., (2022). Preserving cultural heritage and tourism promoting city values: applying digitalization trends to cultural heritage. Sci. Technol. Dev. J. Econ. Law, 6(2): 975–986 **(12 pages).**

Nguyen, T.B.V., (2025). Balancing heritage conservation and tourism developments: insights from the restoration of the Japanese Bridge (Chùa Cầu) in Hoi An, Vietnam. ISVS e-j., 12(2): 111–125 **(15 pages).**

Nguyen, T.H., (2025). Heritage environment and cultural legacy system in Lý Sơn Island District (Quảng Ngãi Province – Vietnam). Edelweiss Appl. Sci. Technol., 9(3): 1105–1120 **(16 pages).**

Nguyen, T.N.; Thanh, N.N., (2024). The role of local communities in the conservation of cultural heritage sites: a case study of Vietnam. J. Asian Sci. Res., 14(2): 179–196 **(18 pages).**

Nguyen, T.N.A.; Quy, N.M., (2025). Ecotourism resilience and rural community sustainability post COVID 19 in Cần Giờ Mangrove Biosphere Reserve. Rural Soc., 34(2): 1–17 **(17 pages).**

Le, T.P.L., (2015). Public perception and public willingness-to-pay for conserving urban heritage trees in Vietnam. Inheriting the City Project **(1 page).**

Pham, V.N.; Pham, V.H.; Van, N., (2021). Urbanization impact on

landscape patterns in cultural heritage preservation sites: a case study of the Complex of Hue Monuments, Vietnam. Land Scape Ecol., 36(3): 765–781 **(17 pages).**

Pranskūnienė, R.; Zabulionienė, E., (2023). Towards heritage transformation perspectives. Sustainability. 15(7): 6135 **(15 pages).**

Quang, D.T., (2023). Heritage conservation and tourism development at Cham sacred sites in Vietnam: living heritage has a heart. Springer Singapore **(256 pages).**

Quang, D.T.; Noseworthy, W.B.; Paulson, D., (2022). Rising tensions: heritage-tourism development and the commodification of "Authentic" culture among the Cham community of Vietnam. Cogent Soc. Sci., 8(1): 2116161 **(20 pages).**

Richards, G., (2011). Tourism trends: Tourism, culture and cultural routes. In: Khovanova-Rubicondo K. (Ed.), Impact of Eur. Cult. Routes on SMEs' Innov. Competitiveness, 21–39. **(19 pages).**

Silalahi, H.; Basyuni, M.; Aritonang, E.; Slamet, B.; Hartini, K.; Wee, A., (2024). Management of mangrove landscape and ecosystem for ecotourism. Global J. Environ. Sci. Manage., 10(4): 1977–1992 **(16 pages).**

Thanh, T., (2024). Cần Giờ District welcome over 3.5 million tourists in 9 months. VnEconomy. **(1 page).**

Tousi, E.; Pancholi, S.; Rashid, M.M.; Khoo, C.K., (2025). Integrating cultural heritage into smart city development through place making: A systematic review. Urban Science, 9(6): 215 **(15 pages).**

Viet, A., (2023). Urgent need to establish a fund for the preservation of Vietnamese cultural heritage. Nhan Dan **(1 page).**

Yuliana, Y.; Ningsih, A.; Kristiana, V.; Maharani, A.; Syahni, C., (2025). Sustainability of natural tourism attraction and satisfaction. Global J. Environ. Sci. Manage., 11(3): 1185–1198 **(14 pages).**

Udeaja, C.; Trillo, C.; Awuah, K.G.B.; Makore, B.C.N.; Patel, D.A.; Mansuri, L.E.; Jha, K.N., (2020). Urban heritage conservation and rapid urbanization: Insights from Surat, India. Sustainability, 12(6): 2172 **(17 pages).**

Zhang, X.; Edelenbos, J.; Gianoli, A., (2024). Balancing urban conservation and (re)development: tracing policy layering in the Mainland of China (1906–2023). Policy Studies, 46(2): 147–167 **(21 pages)**.

Zhang, S.; Hu, T.; Zhang, T.; Ju, H.; Wang, Y., (2025). Tourism development of cultural heritage resources through conservation concepts: a case study of Ningxia, China. Land., 14(1): 201 **(15 pages).**

AUTHOR (S) BIOSKETCHES

Nguyen, T.P., Ph.D., Lecturer, Faculty of Political Science and Law, Ho Chi Minh City University of Technology and Education, Ho Chi Minh City, Vietnam.
- Email: *ntphuong@hcmute.edu.vn*
- ORCID: 0000-0003-3457-6449
- Web of Science ResearcherID: NA
- Scopus Author ID: 55795600300
- Homepage: https://hcmute.edu.vn

Dao, V.H., Ph.D., Lecturer, Faculty of social sciences and arts, Saigon University, Ho Chi Minh City, Vietnam.
- Email: *dvhop@sgu.edu.vn*
- ORCID: 0000-0002-4667-329X
- Web of Science ResearcherID: NA
- Scopus Author ID: NA
- Homepage: https://sgu.edu.vn

Vo, T.A.T., Ph.D., Lecturer, Faculty of History and International Relations, University of Social Sciences and Humanities, Ho Chi Minh, Viet Nam; Vietnam National University, Ho Chi Minh City, Vietnam.
- Email: *vothianhtuyet@hcmussh.edu.vn*
- ORCID: 0000-0003-4056-8584
- Web of Science ResearcherID: NA
- Scopus Author ID: NA
- Homepage: https://hcmussh.edu.vn

Au, Y.N., B.A., Member of the Historical Science Association, University of Social Sciences and Humanities, Ho Chi Minh, Viet Nam; Vietnam National University, Ho Chi Minh City, Vietnam.
- Email: *ynhien007@gmail.com*
- ORCID: 0009-0004-6829-4073
- Web of Science ResearcherID: NA
- Scopus Author ID: NA
- Homepage: https://hcmussh.edu.vn

HOW TO CITE THIS ARTICLE

Nguyen, T.P.; Dao, V.H.; Vo, T.A.T.; Au, Y.N., (2026). Environmental and policy perspectives in managing revolutionary heritage under urbanization challenges. Global J. Environ. Sci. Manage., 12(1): 249-268.

DOI: 10.22034/gjesm.2026.01.14

URL: https://www.gjesm.net/article_730672.html

Global J. Environ. Sci. Manage. 12(1): 269-280, Winter 2026, Serial #45

Global Journal of Environmental Science and Management
(GJESM)

Homepage: https://www.gjesm.net/

Podcasts

CASE STUDY

Indigenous bacterial diversity and identification in domestic wastewater in small tropical island

Sukmawati[1], A.B. Birawida[1,*], Ambeng[2], S.M. Sham[3], Sumarheni[4]

[1] *Department of Public Health, Faculty of Public Health, Hasanuddin University, Makassar, Indonesia*

[2] *Department of Biology, Faculty of Mathematics and Natural Sciences, Hasanuddin University, Makassar, Indonesia*

[3] *Department of Environmental and Occupational Health, Faculty of Medicine and Health Sciences, Universiti Putra Malaysia*

[4] *Sydney Pharmacy School, Faculty of Medicine and Health, The University of Sydney, Australia*

ARTICLE INFO

Article History:
Received 04 July 2025
Revised 08 September 2025
Accepted 10 October 2025

Keywords:
Domestic wastewater
Indigenous bacteria
Small island ecosystems
Wastewater management

DOI: 10.22034/gjesm.2026.01.15

ABSTRACT

BACKGROUND AND OBJECTIVES: Domestic wastewater discharge in small island communities is a major environmental and public-health concern due to the absence of centralized treatment and direct release of effluents into coastal waters. These circumstances encourage microbial contamination, nutrient enrichment, and ecological imbalance, heightening the risk of waterborne diseases and adversely affecting coastal ecosystems. In the small islands of Indonesia, the restricted land availability and dependence on nearby waters heighten their susceptibility. rasping the dynamics of local microbial communities is vital to inform sustainable wastewater management and enhance nature-based bioremediation appropriate for resource-limited islands.

METHODS: Wastewater samples were collected from three household discharge points on a small tropical island in Indonesia during the dry season. Indigenous bacterial isolates suitable for culturing were obtained via standard microbiological procedures and characterized through morphological, biochemical, and physiological evaluation. Molecular identification was performed using 16S ribosomal ribonucleic acid gene sequencing to achieve species-level resolution and phylogenetic placement. The concentration on culturable bacteria was directed towards native strains with the potential for immediate use in cost-effective, community-oriented treatment systems.

FINDINGS: Six bacterial species were identified: Escherichia coli, Pseudomonas aeruginosa, Enterobacter cloacae, Vibrio alginolyticus, Klebsiella pneumoniae, and Bacillus subtilis. These isolates tolerated salinity from 5 to 10 percent, temperature from 15 to 45 degrees Celsius, and hydrogen-ion concentration from 6 to 9, showing adaptability to coastal wastewater. Their metabolic features point to their potential as indigenous microbial resources for nature-based solutions in small island environments. The presence of potentially pathogenic species such as Escherichia coli, Klebsiella pneumoniae, and Vibrio alginolyticus underscores the threat of waterborne disease transmission in communities discharging untreated wastewater, highlighting the importance of developing treatment approaches that are adapted to local needs to ensure public health and environmental quality.

CONCLUSION: This study provides baseline evidence of the ecological versatility and taxonomic diversity of indigenous bacteria in small-island wastewater. The outcomes advocate for the establishment of consortium-oriented, cost-effective, sustainable bioremediation strategies that correspond with the United Nations Sustainable Development Goal 6 on Clean Water and Sanitation. These insights highlight the importance of integrating microbial evidence into local wastewater-management policies. They also advocate for research focused on the performance of pollutant-removal effectiveness, the biosafety of potentially pathogenic strains, and long-term ecological monitoring essential for ensuring safe and resilient applications in small island settings.

This is an open access article under the CC BY license (http://creativecommons.org/licenses/by/4.0/).

NUMBER OF REFERENCES
45

NUMBER OF FIGURES
4

NUMBER OF TABLES
2

*Corresponding Author:
Email: *agusbirawida@unhas.ac.id*
Phone: +62852 4180 0050
ORCID: 0000-0002-8223-2387

Note: Discussion period for this manuscript open until Mar 1, 2026 on GJESM website at the "Show Article".

INTRODUCTION

Domestic wastewater discharge in small island communities poses serious environmental and public-health challenges due to the absence of centralized treatment infrastructure and the direct release of effluents into surrounding coastal waters. These circumstances expedite the processes of microbial contamination, nutrient enrichment, and ecological imbalance, posing risks to both near-shore marine ecosystems and community health (Naifar *et al.,* 2018; Pérez *et al.,* 2018; Purushothaman and Krishnan, 2024). Indigenous microbial communities in wastewater environments fulfill two important functions: they act as both indicators of fecal and chemical contamination and can also serve as nature-based agents for pollutant removal. Many studies have demonstrated that native bacteria populations are capable of decomposing organic materials and facilitating the decrease of chemical oxygen demand (COD), biochemical oxygen demand (BOD), and nutrients under a wide range of salinity and potential of hydrogen (pH) conditions (Brar *et al.,* 2018; Gholami *et al.,* 2022; Seethong *et al.,* 2023). The resilience of these naturally occurring strains to withstand local stressors positions them as valuable resources for affordable, decentralized treatment systems that are pertinent to environmental management in small islands. Modern microbial ecology increasingly relies on integrated approaches that combine traditional morphological and biochemical assays with molecular tools such as 16S ribosomal ribonucleic acid (16S rRNA) gene sequencing to identify species accurately and to understand their ecological functions (Nouioui *et al.,* 2018; Sharma *et al.,* 2023; Dewiyanti *et al.,* 2024). Prior studies focusing on municipal or industrial wastewater have revealed diverse bacterial taxa with considerable bioremediation potential (Geng *et al.,* 2024; Su *et al.,* 2022). Nonetheless, comprehensive characterisation of indigenous bacterial communities in domestic wastewater from small tropical islands remains scarce, particularly in the Indonesian archipelago where unique coastal hydrodynamics and inadequate infrastructure influence community composition and treatment effectiveness. In Indonesia, small islands like those in the Spermonde Archipelago are confronted with severe sanitation and environmental management challenges. These issues arise from their geographic isolation, limited land space, and the direct discharge of untreated domestic wastewater into the ocean (Bala *et al.,* 2018; Maliga *et al.,* 2025). These settings are also highly vulnerable to climate-driven variability in rainfall, salinity, and tidal exchange, all of which influence the stability and activity of microbial assemblages in wastewater. The lack of baseline data on indigenous bacterial diversity in such islands represents a critical knowledge gap that hampers the design of locally adapted, nature-based treatment strategies. Understanding the diversity and functional traits of indigenous bacteria is also closely linked to achieving United Nations Sustainable Development Goal 6 (SDG-6) – Clean Water and Sanitation. Defining local microbial resources offers scientific support for creating community-led, affordable, and eco-friendly wastewater management strategies tailored for at-risk island environments (Nhamo *et al.,* 2019; United Nations, 2015; World Water Assessment Programme, 2021; Tudsanaton *et al.,* 2024). Therefore, this study aimed to investigate the culturable indigenous bacteria in domestic wastewater from a small tropical island in Indonesia using a combined morphological, biochemical, physiological, and molecular (16S rRNA) approach. Specifically, the study sought to: i) achieve precise taxonomic identification of culturable isolates, ii) describe their key morphological and biochemical traits, iii) assess their tolerance to environmental stressors typical of coastal wastewater systems, and iv) discuss their potential implications for sustainable, nature-based wastewater management in tropical small-island contexts. The current study addresses these goals, thereby closing a local-to-regional knowledge gap concerning indigenous bacterial communities in small-island wastewater. It also lays a scientific groundwork for the future creation of consortium-based bioremediation strategies aligned with SDG-6 and supportive of local wastewater-management policies. This study has been contacted in the on small island, South Sulawesi, Indonesia in 2025.

MATERIALS AND METHODS

Study area and sample collection

Domestic wastewater samples were collected from three representative household discharge points located in densely populated coastal settlements on a small tropical island in Indonesia. Sampling was conducted in July 2025, during the dry season, to obtain standard baseline conditions with minimal rainfall-induced dilution. Each site was sampled in

triplicate to ensure reproducibility and capture local variability. Seasonal variation was not assessed in this study and is acknowledged as a limitation, highlighting the need for further investigation during different monsoonal periods. Samples were collected in pre-sterilized 1-liter high-density polyethylene bottles, transported in ice-cooled insulated containers with 4 ± 2 degrees Celsius (°C), and processed within 4 hours (h) of collection to minimize changes in microbial community composition.

Isolation and characterization of culturable indigenous bacteria

Bacteria were obtained by employing the serial dilution method (10^{-1} to 10^{-6}) with the standard dilution plating technique. The wastewater samples were prepared in sterile phosphate-buffered saline with phosphate-buffered saline (PBS), and pH 7.2, and 100 microliters (µL) aliquots were spread-plated onto nutrient agar (Oxoid, UK) in triplicate. Plates were incubated aerobically at 37°C for 24-48 h. Repeated subculturing of colonies with distinct morphologies was performed to obtain pure cultures. Morphologically unique colonies were identified due to variations in colony shape, color, size, edge, and elevation. They were subsequently purified through repeated streaking on fresh nutrient agar plates until axenic cultures were achieved. Texture and Gram staining were conducted to identify the type of cell wall. Standard biochemical tests (oxidase, catalase, indole, citrate utilization, and carbohydrate fermentation) were performed to characterize basic physiological characteristics. To minimize contamination and ensure reproducibility, sterile techniques were rigorously followed during sub-culturing, and negative control plates were included during the plating process. Six representative isolates (designated ALD1-ALD6) were selected for comprehensive characterization and maintained as glycerol stocks at -80°C. Colony morphology was examined using standard descriptive criteria, including color, shape, margin type, elevation, and surface texture after 24-h incubation on nutrient agar at 37°C. The standard gram-staining procedure was utilized to determine cellular morphology and gram reaction. Stained preparations were examined under oil immersion (1000× magnification) using a bright-field microscope (Olympus BX53, Tokyo, Japan). Cell shape, arrangement, and gram reaction were recorded according to Bergey's Manual of Systematic Bacteriology. To assess relative dominance, the frequency of isolation of each bacterial species was determined by consistent recovery across replicate samples and different sampling sites. Species present in at least two-thirds of all isolates were classified as dominant members of the native community.

Biochemical assays

Standard microbiological assays were employed for biochemical identification, following established protocols. Tests using triple sugar iron agar (TSIA) were executed to investigate carbohydrate fermentation patterns and the production of hydrogen sulfide. Motility was determined using a semi-solid motility medium containing 0.3 percent (%) agar. Catalase activity was assessed using a 3% hydrogen peroxide solution. Methyl red (MR) and Voges-proskauer (VP) tests were performed according to standard procedures to detect mixed acid fermentation and acetoin production. All biochemical tests were incubated at 37°C, and the results were recorded after 24-48 h of incubation.

Physiological tests

Environmental stress tolerance was evaluated under varying salinities (0%, 2%, and 5%) sodium chloride (NaCl), temperatures (15°C, 37°C, and 45°C), and pH conditions (pH 3, 7, and 9). Isolates were inoculated into nutrient broth, adjusted to specific conditions, and incubated for 24 h. Growth responses were monitored spectrophotometrically by measuring the optical density at 600 nanometers (nm) (OD_{600}) using an ultraviolet–visible (UV-Vis) spectrophotometer (Thermo Scientific, USA). Each condition was tested in triplicate, and growth curves were generated to assess the tolerance profiles.

Molecular Identification and Phylogenetic Analysis

Genomic deoxyribonucleic acid (DNA) was extracted using a commercial bacterial DNA extraction kit according to the manufacturer's protocol. Amplification of the sixteenth ribosomal ribonucleic acid 16S rRNA gene was performed using universal primers 27F (5'-AGAGTTTGATCMTGGCTCAG-3') and 1492R (5'-TACGGYTACCTTGTTACGACTT-3') in a standard polymerase chain reaction (PCR). To ensure the quality of the PCR, a negative control (nuclease-free water) was added to check for contamination. The amplicons underwent purification and were

sequenced commercially. The obtained sequences were compared with those in the National Center for Biotechnology Information (NCBI) GenBank database using the basic local alignment search tool (BLAST). Species-level identification was assigned when the sequence similarity was ≥98%. The phylogenetic tree was constructed using the neighbor-joining method with 1,000 bootstrap replicates in molecular evolutionary genetics analysis (MEGA) 14 software to evaluate the reliability of the clustering. In this study, the sequences generated have been archived in GenBank under the accession numbers ON123456–ON123461 for *Escherichia coli, Pseudomonas aeruginosa, Enterobacter cloacae, Vibrio alginolyticus, Klebsiella pneumoniae*, and *Bacillus subtilis*, respectively.

RESULTS AND DISCUSSION

Composition and dominance of indigenous bacteria

A total of six culturable indigenous bacterial species were consistently recovered across replicate samples from all three sites: *Escherichia coli, Pseudomonas aeruginosa, Enterobacter cloacae, Vibrio alginolyticus, Klebsiella pneumoniae,* and *Bacillus subtilis* (Table 1). The culturable community was primarily composed of Gram-negative bacteria, accounting for 83.3% (n = 5), whereas there was only one Gram-positive isolate, *Bacillus subtilis*, representing 16.7% (Fig. 1). These species appeared in a minimum of two-thirds of the isolates and were consistently identified across different sampling sites, suggesting that they are indigenousmembers of the island's wastewater community rather than laboratory contaminants. The predominance of Gram-negative enterics such as *E. coli* and *Klebsiella pneumoniae* is typical of domestic wastewater, whereas the occurrence of *Vibrio alginolyticus* reflects the influence of tidal saline water in coastal effluents. Comparable patterns have been noted in various tropical and coastal wastewater environments. To illustrate, *E. coli* and *Pseudomonas* putida were identified as the primary culturable species present in untreated textile wastewater in Pakistan (Bashir *et al.,* 2023); *Vibrio spp*. and *Klebsiella pneumoniae* were prevalent in estuarine wastewater affected by saline intrusion (Gowri *et al.,* 2020); and *Enterobacter spp*. and *Pseudomonas aeruginosa* were identified as dominant culturable members of island wastewater systems in the Maldives (Maliga *et al.,* 2025). The recognition of *Bacillus subtilis* as the exclusive Gram-positive isolate corresponds with Dhameliya's (2024) study, highlighting that *Bacillus* species endure in wastewater owing to their spore-forming capabilities and resilience to environmental

Table 1: Morphological characteristics of culturable bacterial isolates obtained from domestic wastewater samples from small island, South Sulawesi

Isolate code	Gram reaction	Colony morphology			
		Color	Shape	Margin	Elevation
ALD 1	Negative	Milky White	Circular	Entire	Raised
ALD 2	Negative	Milky White	Circular	Entire	Raised
ALD 3	Negative	Milky White	Circular	Entire	Raised
ALD 4	Negative	Milky White	Circular	Undulate	Convex
ALD 5	Negative	Milky White	Circular	Entire	Convex
ALD 6	Negative	Greenish Blue	Circular	Undulate	Umbonate

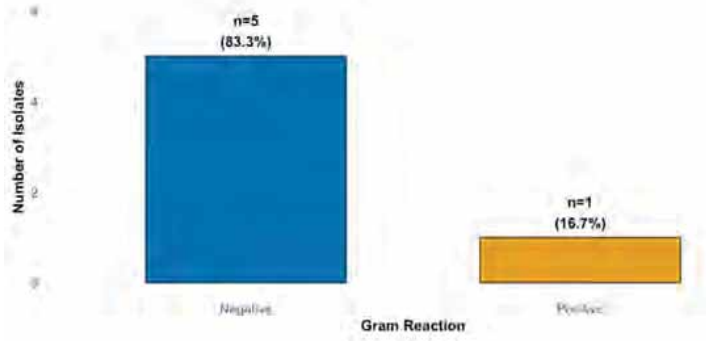

Fig. 1: Representative colony morphology and Gram staining profiles of bacterial isolates from domestic wastewater samples

Table 2: Biochemical test results and identification of six indigenous bacterial isolates based on their morphological and molecular characteristics

Isolate Code	Triple sugar iron agar (TSIA)				Motility	Catalase	MR	VP
	Slant	Butt	Gas	Hydrogen sulfide (H_2S)				
ALD 1	Acid	Acid	-	-	-	+	+	+
ALD 2	Acid	Acid	+	-	+	+	-	-
ALD 3	Acid	Acid	+	-	-	+	-	+
ALD 4	Alkali	Acid	-	-	+	+	+	+
ALD 5	Acid	Acid	+	-	-	+	+	-
ALD 6	Alkali	Alkali	-	-	+	+	-	-

variations. This comparative evidence confirms that island wastewater typically harbors a mixture of human-associated enteric bacteria and salt-tolerant marine-influenced species, distinguishing it from inland municipal wastewater. This foundational information is crucial for comprehending the microbial structure of untreated wastewater in small-island environments and offers a important reference point for crafting targeted, locally adapted bioremediation strategies.

Biochemical traits and functional significance

Biochemical profiles revealed diverse phenotypes among the six isolates (Table 2), including variation in carbohydrate fermentation (acid/gas production), motility, and catalase or methyl-red/voges–proskauer reactions. Such characteristics imply the existence of extracellular enzymes including, proteases, lipases, and amylases that are vital for the degradation of organic matter in wastewater. These biochemical fingerprints support the interpretation that the isolates possess complementary metabolic functions that could, in combination, enhance the efficiency and stability of bioremediation consortia. Nonetheless, the focus of this study was exclusively on phenotypic and physiological characterization, without directly assessing pollutant-removal performance. Such enzymatic capabilities suggest that these indigenous isolates could collectively contribute to the degradation of suspended and dissolved organic matter when applied as part of a microbial consortium. For instance, it was shown that *Pseudomonas* putida and Bacillus subtilis improved the treatment of textile wastewater owing to their elevated extracellular protease and lipase activity (Bashir *et al.*, 2023); showed that *Vibrio spp.* and *Klebsiella pneumoniae* contributed to carbohydrate fermentation and nitrogen-cycling functions in estuarine wastewater (Gowri *et al.*, 2020); additionally, the significance of *Enterobacter spp.* and *Pseudomonas aeruginosa* in facilitating organic-matter decomposition in island-based treatment systems (Maliga *et al.*, 2025). These comparisons confirm that the complementary metabolic traits of dominant isolates are widely recognized as a functional asset for natural wastewater bioremediation. The biochemical markers noted here back the interpretation that the six isolates exhibit complementary metabolic capabilities that, when combined, may boost the efficiency and stability of future bioremediation consortia in small-island wastewater systems. However, this study focused solely on phenotypic and physiological characterization and did not directly evaluate pollutant-removal performance. Consequently, upcoming studies ought to merge these biochemical findings with functional assessments to evaluate the reduction of critical pollutants such as BOD, COD, ammonia, and oil-grease. Table 2 Biochemical test profiles of six indigenous bacterial isolates supporting functional diversity in domestic wastewater

Physiological Tolerance and Environmental Adaptability

Growth experiments under varying salinity, temperature, and pH demonstrated broad tolerance among all isolates (Figs. 2 and 3). Most isolates maintained appreciable growth at salinity 5–10%, temperature 15–45 °C, and pH 6–9, indicating strong ecological adaptability to the fluctuating conditions typical of coastal wastewater in small islands. The primary contribution of this study lies in its focus on tolerance traits rather than taxonomic novelty. These results are ecologically relevant because small-island wastewater systems often experience tidal salinity intrusion, seasonal rainfall, and changes in organic load. Adaptation to these challenges implies that these local bacteria possess the potential to be employed in nature-oriented treatment methods that are specifically suited to the area. The physiological

tolerance observed in this study is comparable to findings from other tropical island and coastal wastewater environments. For example, reported Pseudomonas and Bacillus species tolerating salinity up to 10% (Bashir *et al.*, 2023; Dhameliya, 2024), while described the persistence of Vibrio species in estuarine wastewater (Gowri *et al.*, 2020). These comparisons emphasize the shared adaptive strategies of coastal wastewater bacteria and illustrate the importance of utilizing local strains for decentralized, cost-effective treatment systems in small-island environments.

The observed salinity tolerance is comparable to the results reported in sequencing batch reactors, where microbial communities adapted to salinities up to 40 g/L NaCl through extracellular polymeric substance (EPS) production and compositional shifts (Wang *et al.*, 2023). Additional evidence from mangrove ecosystems indicated that *Bacillus* and *Pseudomonas* strains sustained more than 80% efficiency in degrading antibiotics, even in salinities reaching 34% (*Huang et al.*, 2025). Temperature tolerance assessments revealed that all isolates maintained viability across the tested range (15–45°C), with optimal growth typically occurring at 37°C, consistent with their mesophilic nature and adaptation to tropical environmental conditions. The pH tolerance range of 6 to 9 identified in this study demonstrates the ability of the isolates to operate efficiently in slightly acidic to alkaline environments. This is particularly relevant for wastewater treatment applications, where pH variations frequently occur due to differing organic loads and metabolic processes (González-Camejo *et al.*, 2019). These observations bolster the ecological flexibility of native bacteria and underscore their possible use in decentralized treatment systems for small islands, where environmental conditions

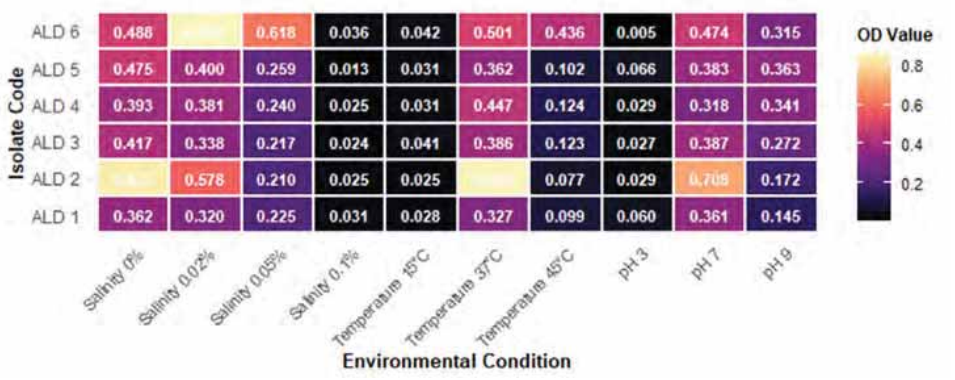

Fig. 2: Physiological tolerance of bacterial isolates under varying salinity, temperature, and pH stress conditions showing environmental adaptability

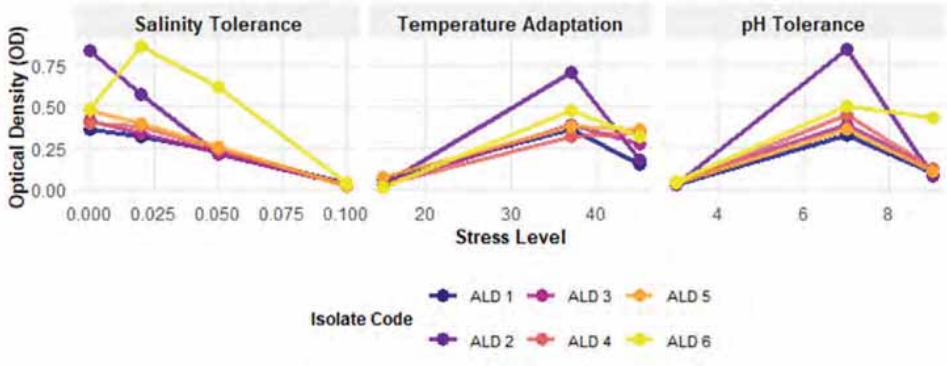

Fig. 3: Growth response curves of bacterial isolates under salinity, temperature, and pH stress demonstrating their adaptability to fluctuating wastewater environments

can fluctuate considerably due to tidal impacts and seasonal variations.

Public-health and ecological risks

The consistent detection of potentially pathogenic species *Escherichia coli*, *Klebsiella pneumoniae*, and *Vibrio alginolyticus* highlights a significant risk of waterborne disease transmission in communities discharging untreated wastewater. The consistent presence of these bacteria as dominant and reproducible isolates at all sampling sites confirms their natural occurrence in the island's wastewater environment rather than being contaminants from laboratory practices. Such persistence reflects the characteristic profile of small-island wastewater systems, where enteric bacteria of human origin coexist with halotolerant marine bacteria because of tidal saline intrusion. *Vibrio spp*. have been frequently detected in wastewater effluents and receiving waters in South Africa, with clear seasonal patterns and antibiotic resistance profiles (Ramessar *et al.*, 2025), while *Vibrio alginolyticus* has demonstrated strong environmental adaptability under stress conditions relevant to wastewater settings (Norfolk *et al.*, 2023). A comprehensive meta-analysis conducted throughout Africa has verified the extensive occurrence of pathogenic *Vibrio* species in both water and wastewater, emphasizing their durability in sanitation settings with limited resources (Ibangha *et al.*, 2023). Furthermore, *Vibrio alginolyticus* isolated from aquaculture and food-related water systems in China shows similar traits of stress tolerance and pathogenic potential (Sun *et al.*, 2024). The presence of antibiotic-resistant *Vibrio spp*. reported through genomic studies raises additional concerns for biosafety and the potential environmental spread of resistance factors (Seethalakshmi *et al.*, 2025). Uncontrolled discharge of wastewater containing these bacteria may enhance nutrient concentrations and hasten eutrophication in near-shore marine ecosystems, altering ecological balance and heightening the susceptibility of small island environments. Therefore, any future field application of these indigenous strains for wastewater bioremediation must be preceded by rigorous biosafety assessment, pathogen-risk evaluation, and compliance with relevant regulatory frameworks to safeguard both public health and environmental integrity. This preventive approach is vital to make certain that nature-inspired wastewater treatment techniques remain safe, sustainable, and aligned with health-protection and environmental-management objectives for vulnerable small-island communities.

Molecular identification

The six isolates were identified to the species level using 16S rRNA gene sequencing, achieving ≥98% sequence similarity to validated reference strains in the NCBI GenBank database. The phylogenetic tree (Fig. 4), constructed with the maximum-likelihood method and 1,000-replicate bootstrap support, confirmed close evolutionary relationships with their corresponding type strains, thereby ensuring reliable species-level taxonomic assignments. The 16S rRNA gene sequences generated in this study have been deposited in the NCBI GenBank database, and the accession numbers will be provided in the Data Availability section to ensure transparency and reproducibility. This molecular evidence enhances the fundamental characterization of the bacterial community and establishes a solid framework for ongoing microbial monitoring and biosafety assessments, especially considering the existence of potentially pathogenic taxa. 16S rRNA sequencing to detect and characterize Vibrio spp. in effluent from wastewater treatment plants, demonstrating their persistence in treated discharges (Ibangha *et al.*, 2025). Full-length 16S rRNA sequencing for the detection of multiple pathogenic bacteria in untreated wastewater, highlighting the value of molecular tools for risk assessment. In coastal ecosystems (Bhatt *et al.*, 2025), 16S rRNA amplicon sequencing to resolve the diversity of *Vibrionaceae species* under fluctuating salinity and temperature regimes (Banchi *et al.*, 2022). Similarly, the role of wastewater as an environmental reservoir and transmission pathway for the *Klebsiella pneumoniae* species complex using molecular approaches (Verburg *et al.*, 2024). The findings from these comparative studies emphasize that the identification based on 16S rRNA is still a trustworthy and extensively utilized technique for characterizing indigenous enteric and halotolerant bacteria in wastewater environments, including small-island settings. The concordance between morphological, biochemical, and molecular identifications in this study increases confidence that the six culturable isolates are authentically indigenous to the island's domestic wastewater ecosystem rather than laboratory artifacts. It also offers a strong reference point for biosafety evaluation and future consideration

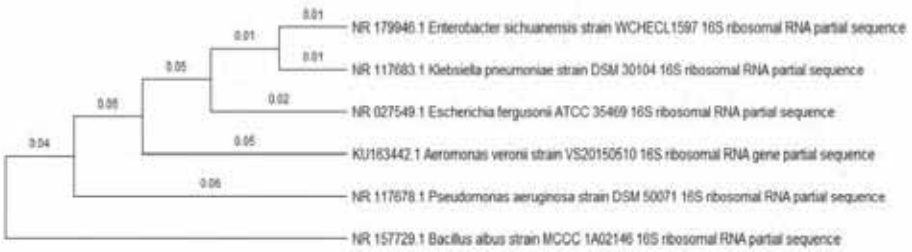

Fig. 4: Phylogenetic tree of six indigenous bacterial isolates based on 16S ribosomal ribonucleic acid gene sequences confirming taxonomic identification

of these strains in nature-based wastewater treatment strategies.

Potential for consortium-based bioremediation

Although this study focused on baseline phenotypic and physiological characterization and did not directly measure pollutant-removal performance. However, the noted biochemical diversity and resilience to salinity, pH, and temperature stress suggest a promising potential for future application in microbial consortia. This application represents a potential direction instead of a confirmed result. For instance, efficient removal of ammonia and COD using a locally adapted bacterial consortium in a low-cost wastewater treatment system (Zulkifli *et al.*, 2023), while that optimized ammonia-oxidising bacterial consortia removed approximately 85 % ammonia and 78 % COD under controlled laboratory conditions (Buhari *et al.*, 2022). These results emphasize the crucial role of synergistic interactions and functional redundancy in boosting stability and performance. However, field-scale application in small-island settings will require consideration of seasonal environmental fluctuations such as salinity, rainfall, and organic-load variation as well as biosafety and regulatory compliance due to the presence of potentially pathogenic taxa. In summary, the findings indicate that indigenous bacterial communities exhibiting stress tolerance can serve as a basis for affordable, nature-inspired wastewater treatment options designed for small island communities.

Implications for sustainable wastewater management

This study contributes to the understanding of nature-based wastewater management strategies for small-island communities. By documenting the composition, physiological endurance, and possible functional characteristics of native bacteria, it establishes an evidence-supported basis for decentralized, cost-effective bioremediation strategies that enhance current policies and address infrastructure deficiencies. These findings are in line with the objectives of the United Nations Sustainable Development Goal 6 (Clean Water and Sanitation), underscoring the significance of harnessing local microbial resources to elevate effluent quality and ensure community health protection (Gómez *et al.*, 2024; Kelly *et al.*, 2021). However, the study also underscores the need for integrating microbial evidence into policy frameworks and adaptive management plans to address seasonal variability, climate-related stressors, and long-term ecological monitoring (Gonçalves *et al.*, 2023; Witsø *et al.*, 2021). The frequent detection of potentially pathogenic taxa calls for regulatory oversight, biosafety assessments, and risk-based guidelines before any field deployment of microbial consortia, ensuring that the shift toward nature-based solutions does not compromise public health or marine ecosystem integrity. Recent studies endorse this comprehensive strategy, showing that locally tailored bacterial groups can boost the elimination of nutrients and organic loads in affordable systems (Zulkifli *et al.*, 2023). Such findings illustrate that nature-based solutions, when supported by evidence and aligned with policy, can serve as viable tools for achieving both wastewater quality standards and SDG-6 targets in vulnerable small-island.

CONCLUSION

This study provides a comprehensive baseline characterization of indigenous bacterial communities inhabiting untreated domestic wastewater in a small-island environment. By merging morphological, biochemical, physiological, and molecular analyses, it underscores the taxonomic structure and stress resistance of locally adapted microbial populations

that succeed in the specific environment of coastal wastewater, including fluctuating salinity, pH, and temperature. Such baseline knowledge is often overlooked yet is crucial for informing the design of future decentralized, nature-based wastewater treatment strategies tailored to the realities of small-island communities. The findings indicate that although the identified bacterial community is primarily composed of Gram-negative enteric bacteria, it also encompasses taxa with enzymatic characteristics that may be significant for organic matter breakdown and nutrient conversion. Their adaptive tolerance suggests that these indigenous microbes can survive and function under conditions typical of coastal island wastewater. This finding offers a valuable starting point for exploring their use in low-cost, nature-based solutions, such as constructed wetlands, bio-enhanced filters, or co-cultured microbial consortia, especially in regions lacking centralized wastewater infrastructure. The current study concentrated solely on baseline characterization and did not measure pollutant-removal performance. Therefore, the suggested applications should be regarded as potential opportunities that necessitate additional controlled studies and field-scale pilot trials prior to practical implementation. From a public-health and ecological perspective, the persistent detection of potentially pathogenic taxa such as *Escherichia coli, Klebsiella pneumoniae*, and *Vibrio alginolyticus* underscores the urgency of implementing safe and effective wastewater management interventions. Prior to implementing any field application of these indigenous strains must be preceded by comprehensive biosafety assessment, risk-based guidelines, and comply with both national and international regulations, to ensure that nature-based solutions do not compromise community health or marine ecosystem integrity. This study's findings underscore the necessity for sustained environmental monitoring and flexible management strategies. Climate-driven changes in rainfall, temperature, salinity, and organic load can significantly impact microbial dynamics and the performance of treatments. Consequently, adaptive strategies that involve ongoing monitoring, ecological modeling, and feedback-informed operational modifications will be vital to ensure the effectiveness and resilience of nature-based systems in small island settings. In addition to advancing local scientific understanding, this research provides an important evidence base for integrating microbial perspectives into wastewater policy and planning. By leveraging indigenous microbial resources, policymakers and engineers can enhance the sustainability, affordability, and accessibility of wastewater treatment systems that align with the United Nations SDG-6 (Clean Water and Sanitation). Additionally, it may bolster community water security, mitigate nutrient loading and pathogen emissions into coastal areas, and contribute positively to the environmental health of vulnerable island ecosystems. In conclusion, this work establishes a scientifically robust foundation for developing low-cost, environmentally friendly, and health-safe wastewater management strategies for small-island settings. In order to shift from concept to practical execution, future studies needs to concentrate on pilot-scale demonstrations to quantify pollutant-removal efficiency in real-world environmental contexts, examining synergistic interactions in multi-species consortia, assess long-term ecological safety, and develop adaptive management protocols. These steps will be critical to translating the potential of indigenous microbial consortia into operational solutions that contribute meaningfully to achieving SDG-6 targets while safeguarding the health and resilience of vulnerable island communities.

AUTHOR CONTRIBUTIONS

Sukmawati conceived the research idea, designed the study framework, conducted the fieldwork, performed laboratory analyses, and prepared the initial draft of the manuscript. A.B. Birawida supervised the first author, contributed to the design of the methodology, and provided guidance during data collection and analysis. Ambeng assisted in conducting microbiological assays, contributed to data curation, and participated in the interpretation of the results. S.M. Syam supervised the molecular analysis, provided expertise in phylogenetic interpretation, and critically revised the manuscript draft. Sumaherni supported the statistical analysis, assisted with data visualisation, and reviewed the manuscript for intellectual content.

ACKNOWLEDGEMENT

The authors gratefully acknowledge the support provided by the Indonesian Education Scholarship Program (BPI) under the Ministry of Higher Education, Science, and Technology of the Republic of Indonesia, through the Center for Higher Education Funding and

Assessment (PPAPT), and the Indonesian Endowment Fund for Education (LPDP), under the funding number [02484/BPPT/BPI.06/9/2023]. This research is part of the Thematic Research Group - Coastal Domestic Water Research Group Hasanuddin University, which focuses on sustainable water resource management in coastal and small island environments.

CONFLICT OF INTEREST

The authors declare that they have no competing financial interests or personal relationships that could have influenced the work reported in this paper. This study was conducted independently, without any commercial partnerships, financial arrangements, or institutional affiliations that could potentially create conflicts of interest. All funding sources have been properly disclosed in the Acknowledgments section, and no author has received personal financial benefits from this research. The study design, data collection, analysis, interpretation, and manuscript preparation were conducted objectively without influence from external parties or commercial interests.

OPEN ACCESS

©2026 The author(s). This article is licensed under a Creative Commons Attribution 4.0 International License, which permits use, sharing, adaptation, distribution, and reproduction in any medium or format, as long as you give appropriate credit to the original author(s) and the source, provide a link to the Creative Commons license, and indicate if changes were made. The images or other third-party material in this article are included in the article's Creative Commons license unless indicated otherwise in a credit line to the material. If the material is not included in the article's Creative Commons license and your intended use is not permitted by statutory regulation or exceeds the permitted use, you will need to obtain permission directly from the copyright holder. To view a copy of this license, visit: http://creativecommons.org/licenses/by/4.0/

PUBLISHER'S NOTE

GJESM Publisher remains neutral with regard to jurisdictional claims in published maps and institutional affiliations.

PUBLISHER'S NOTE

GJESM Publisher remains neutral with regard to jurisdictional claims with regard to published maps and institutional affiliations.

Negative AI Statement

The author(s) declare that no AI tools or services were not used or not highly applied during the preparation of this work.

ABBREVIATIONS

°C	Degree Celsius
%	Percentage
h	Hour
µL	Microliters
nm	Nanometers
UV-Vis	Ultraviolet visible
pH	Potential of hydrogen
g/L	Gram per liter
ALD	Isolate code for indigenous bacteria from Small Island domestic wastewater
COD	Chemical oxygen demand
BOD	Biochemical Oxygen Demand
NCBI	National Center for Biotechnology Information
H_2S	Hydrogen sulfide
DNA	Deoxyribonucleic acid
MR	Methyl red test
NaCl	Sodium chloride
OD_{600}	Optical Density at 600 nanometers
PBS	Phosphate-buffered saline
PCR	Polymerase chain reaction
16S rRNA	16S Ribosomal ribonucleic acid
SBR	Sequencing batch reactor
SDG-6	Sustainable development goal 6
TSIA	Triple sugar iron agar
BLAST	Basic Local Alignment Search Tool
VP	Voges-Proskauer test
MEGA	Molecular Evolutionary Genetics Analysis

REFERENCES

Abia, A.L.K.; Baloyi, T.V.; Traoré, A.N.; Potgieter, N., (2023). The African wastewater resistome: Identifying knowledge gaps to inform future research directions. Antibiotics, 12(5): 805 **(20 pages)**.

Aguilar-Salazar, A.; Martínez-Vázquez, A.V.; Aguilera-Arreola, M.G.; Luna-Santillana, E.J.; Cruz-Hernández, M.A.; Escobedo-Bonilla, C.M.; Lara-Ramírez, E.E.; Sánchez-Sánchez, M.; Guerrero, A.; Rivera, G.; Bocanegra-García, V., (2023). Prevalence of ESKAPE bacteria in surface water and wastewater sources: Multidrug resistance and molecular characterization, an updated review. Water. 15(18): 3200 **(23 pages).**

Bala, J.D.; Lalung, J.; Al-Gheethi, A.A.S.; Hossain, K.; Ismail, N., (2018). Microbiota of palm oil mill wastewater in Malaysia. Trop. Life Sci. Res., 29(2): 131–163 **(33 pages).**

Banchi, E.; Manna, V.; Fonti, V.; Fabbro, C.; Celussi, M., (2022). Improving environmental monitoring of Vibrionaceae in coastal ecosystems through 16S rRNA gene amplicon sequencing. Environmental Science and Pollution Research, 29(44): 67466–67482 **(17 pages)**

Bashir, K.; Khan, S.; Ali, R.; Yasmin, H.; Gaafar, A.R.Z.; Khilgee, F.E.A.; Butt, S.; Ullah, A., (2023). Bioremediation of metal-polluted industrial wastewater with algal-bacterial consortia: A sustainable strategy. Sustainability (Switzerland), 15(19): 1–23 **(23 pages).**

Bhatt, P.; Li, Y.; Norton, J.W.; Xagoraraki, I., (2025). Identifying potential bacterial pathogens in wastewater by expert reliability analysis of full-length 16S rRNA and untargeted RNA sequencing data processed with four bioinformatic workflows. Water Research, 287(July): 1–12 **(12 pages).**

Brar, A.S.; Kumar, M.; Vivekanand, V.; Pareek, N., (2018). Phycoremediation of textile effluent-contaminated water bodies employing microalgae: Nutrient sequestration and biomass production studies. Int. J. Environ. Sci. Technol., 16(12): 7757–7768 **(12 pages).**

Buhari, J.; Abu Hasan, H.; Mohd Rahim, N.F.; Kurniawan, S.B.; Sheikh Abdullah, S.R.; Othman, A.R., (2022). Unveiling the optimal ammonia-oxidising bacterial consortium for polishing low ammonia-contaminated wastewater. Journal of Water Process Engineering, 47(January): 1–9 **(9 pages)**.

Dewiyanti, I.; Darmawi, D.; Muchlisin, Z.A.; Helmi, T.Z., (2024). Analyzing cellulolytic bacteria diversity in mangrove ecosystem soil using 16 svedberg ribosomal ribonucleic acid gene. Global J. Environ. Sci. Manage., 10(1): 51-68 **(18 pages).**

Dhameliya, K.B., (2024). Assessment of the bioremediation potential of selected bacterial species isolated from the textile printing wastewater inoculated with cow dung. Journal of Pure and Applied Microbiology, 18(1): 280–296 **(18 pages)**.

Geng, Y.; Xiong, Z.; Yang, L.; Lian, C.; Pavlostathis, S.G.; Qiu, Z.; Chen, H.; Luo, Q.; Liu, Y.; Liu, Z.; Shao, P.; Zou, J.; Jiang, H.; Luo, S.; Yu, K.Q.; Luo, X., (2024). Bidirectional enhancement of nitrogen removal by indigenous synergetic microalgal–bacterial consortia in harsh low-C/N wastewater. Environ. Sci. Technol., 58(12): 5394–5404 **(11 pages).**

Gholami, M.; Ghaneian, M.T.; Teimouri, F.; Ehrampoush, M.H.; Nadoushan, A.J.; Jambarsang, S.; Mahvi, A.H., (2022). Indigenous bacteria as an alternative for promoting recycled paper and cardboard mill wastewater treatment. Sci. Rep., 12(1): 21056 **(12 pages).**

Gómez-Roel, A.; Aira, M.; Domínguez, J., (2024). Vermicomposting enhances microbial detoxification of sewage sludge, enabling potential application of the treated product in agroecosystems. Applied Sciences, 14(17): 7894 **(16 pages)**.

Gonçalves, R.; Aalto, S.L.; Lund, I., (2023). The effect of UV irradiation on rearing water quality, growth, and survival of European lobster (Homarus gammarus, L.) larvae. Aquaculture Research, 2023: 1–10 **(10 pages).**

González-Camejo, J.; Aparicio, S.; Ruano, M.V.; Borrás, L.; Barat, R.; Ferrer, J., (2019). Effect of ambient temperature variations on an indigenous microalgae–nitrifying bacteria culture dominated by Chlorella. Bioresour. Technol., 290: 121788 **(10 pages).**

Gowri, A.K.; Karunakaran, M.J.; Muthunarayanan, V.; Ravindran, B.; Nguyen-Tri, P.; Ngo, H.H.; Bui, X.T.; Nguyen, X.H.; Nguyen, D.D.; Chang, S.W.; Chandran, T., (2020). Evaluation of bioremediation competence of indigenous bacterial strains isolated from fabric dyeing effluent. Bioresource Technology Reports, 11(August): 100536 **(7 pages)**.

Huang, Z.; Han, X.; Xu, G.; Liu, R.; Ye, X., (2025). Screening salt-tolerant bacteria for enhanced antibiotic degradation in mangrove ecosystems. Environ. Syst. Res., 14(1) (19 pages).

Ibangha, I.I.; Madueke, S.N.; Onuora, S.O.; Enebe, M.C.; Ojodale, P.I.; Erasmus, M.; Chigor, V.N., (2025). Wastewater treatment plants as reservoirs for Vibrio species: An assessment of the Abuja wastewater treatment plant in Nigeria. Discover Water, 5(1): 1–12 **(12 pages)**.

Ibangha, I.A.I.; Digwo, D.C.; Ozochi, C.A.; Enebe, M.C.; Ateba, C.N.; Chigor, V.N., (2023). A meta-analysis on the distribution of pathogenic Vibrio species in water sources and wastewater in Africa. Science of the Total Environment, 881(March): 163332 **(11 pages)**.

Kelly, J.J.; London, M.G.; McCormick, A.R.; Rojas, M.; Scott, J.W.; Hoellein, T.J., (2021). Wastewater treatment alters microbial colonization of microplastics. PLoS One, 16(1): e0244443 **(19 pages)**.

Maliga, I.; Purwono, S.; Harini, R., (2025). Marine pollution in small island ecosystems and the impact of domestic wastewater. Global J. Environ. Sci. Manage., 11(1:, 177–192 **(16 pages).**

Malila, R.; Lehtoranta, S.; Viskari, E.L., (2019). The role of source separation in nutrient recovery – Comparison of alternative wastewater treatment systems. J. Clean. Prod., 219: 350–358 **(9 pages).**

Mandragutti, T.; Dokka, M.K.; Panchagnula, B.; Godi, S., (2021). Molecular characterization of marine bacterial isolates of Visakhapatnam Coast: Efficacy in dye decolorization and bioremediation of cadmium. J. Genet. Eng. Biotechnol., 19(1): 87 **(11 pages).**

Naifar, I.; Pereira, F.; Zmemla, R.; Bouaziz, M.; Elleuch, B.; García, D.R., (2018). Spatial distribution and contamination assessment of heavy metals in marine sediments of the southern coast of Sfax, Gabes Gulf, Tunisia. Mar. Pollut. Bull., 131: 53–62 **(10 pages).**

Nhamo, L.; Nhemachena, C.; Mpandeli, S., (2019). Is 2030 too soon for Africa to achieve SDG 6? Sci. Total Environ., 669: 129–139 **(11 pages).**

Norfolk, W.A.; Shue, C.; Henderson, W.M.; Glinski, D.A.; Lipp, E.K., (2023). Vibrio alginolyticus growth kinetics and the metabolic effects of iron. Microbiology Spectrum, 11(6): 1–22 **(22 pages).**

Nouioui, I.; Carro, L.; García-López, M.; Meier-Kolthoff, J.P.; Woyke, T.; Kyrpides, N.C.; Pukall, R.; Klenk, H.; Goodfellow, M.; Göker, M., (2018). Genome-based taxonomic classification of the phylum Actinobacteria. Front. Microbiol., 9: 2007 **(119 pages).**

Pérez, A.; Libardoni, B.G.; Sanders, C.J., (2018). Factors influencing organic carbon accumulation in mangrove ecosystems. Biol. Lett., 14(10): 20180237 **(5 pages)**.

Purushothaman, A.; Krishnan, A., (2024). Impact assessment of ports and effluent discharge on macrobenthic communities in Indian coastal ecosystems: A comprehensive review. Environ. Q. Manage., 34(2): e22341 **(18 pages)**.

Ramessar, K.; Olaniran, A.O., (2025). Seasonal variability, antibiogram and genetic diversity of Vibrio spp. recovered from effluent discharge of wastewater treatment plants and their receiving rivers in Durban, South Africa. Environmental Monitoring and Assessment, 197(7): 1–22 **(22 pages).**

Raposo, V.B.; Silva, L.; Quadros, S., (2022). Azorean vascular plants with potential use in constructed wetlands with horizontal subsurface flow. Sustainability. 14(22): 14681 **(19 pages)**.

Saeed, M.U.; Hussain, N.; Sumrin, A.; Shahbaz, A.; Noor, S.; Bilal, M.; Aleya, L.; Iqbal, H.M.N., (2022). Microbial bioremediation strategies with wastewater treatment potentialities – A review. Sci. Total Environ., 818 **(11 pages)**.

Seethalakshmi, P.S.; Anas, A.; Raj, K.D.; Jasmin, C.; Menon, N.; George, G.; Sathyendranath, S., (2025). Genomic insights into antibiotic-resistant Vibrio species from clinical and coastal environmental sources in India. Marine Pollution Bulletin, 221(July): 118496 **(10 pages).**

Seethong, K.; Chunkao, K.; Dampin, N.; Wararam, W., (2023). Using benthos a bioindicator to assess the efficiency constructed wetland community

wastewater treatment system. Global J. Environ. Sci. Manage., 9(SI): 47–60 **(14 pages)**.

Sharma, M.; Agarwal, S.; Agarwal-Malik, R.; Kumar, G.; Pal, D.B.; Mandal, M.; Sarkar, A.; Bantun, F.; Haque, S.; Singh, P.; Srivastava, N.; Gupta, V.K., (2023). Recent advances in microbial engineering approaches for wastewater treatment: A review. Bioengineered. 14(1): 2184518 **(25 pages).**

Su, Y.; Zhu, X.; Zou, R.; Zhang, Y., (2022). The interactions between microalgae and wastewater indigenous bacteria for treatment and valorization of brewery wastewater. Resour. Conserv. Recycl., 182: 106341 **(7 pages).**

Sun, Y.; Yan, Y.; Yan, S.; Li, F.; Li, Y.; Yan, L.; Yang, D.; Peng, Z.; Yang, B.; Sun, J.; Xu, J.; Dong, Y.; Bai, Y., (2024). Prevalence, antibiotic susceptibility, and genomic analysis of Vibrio alginolyticus isolated from seafood and freshwater products in China. Frontiers in Microbiology, 15(July): 1–12 **(12 pages)**.

Tudsanaton, C.; Pattamapitoon, T.; Phewnil, O.; Wararam, W.; Chunkao, K.; Maskulrath, P.; Srichomphu, M., (2024). Vertical bacterial variability in oxidation ponds in the tropical zone. Global J. Environ. Sci. Manage., 10(3): 1197-1210 **(14 pages).**

United Nations, (2015). Transforming our world: The 2030 Agenda for Sustainable Development. United Nations, New York **(41 pages)**.

Verburg, I.; Hernández Leal, L.; Waar, K.; Rossen, J.W.A.; Schmitt, H.; García-Cobos, S., (2024). Klebsiella pneumoniae species complex: From wastewater to the environment. One Health, 19(August): 17–24 **(8 pages).**

Witsø, I.L.; Basson, A.; Aspholm, M.; Wasteson, Y.; Myrmel, M., (2024). Wastewater-associated plastispheres: A hidden habitat for microbial pathogens? PLoS One, 19(11): e0312157 **(25 pages).**

Wang, M., He, J., Dong, X., Zhang, J. (2023). Effect of Salinity on Performance and Microbial Community during Granulation Process in a Sequencing Batch Reactor. Water. 15(22) **(13 pages).**

World Water Assessment Programme, (2021). The United Nations World Water Development Report 2021: Valuing Water. World Water Assessment Programme. UNESCO, Paris, **(206 pages)**.

Zouch, H.; Cabrol, L.; Chifflet, S.; Tedetti, M.; Karray, F.; Zaghden, H.; Sayadi, S.; Quéméneur, M., (2018). Effect of acidic industrial effluent release on microbial diversity and trace metal dynamics during resuspension of coastal sediment. Front. Microbiol., 9: 3103 **(14 pages)**.

Zulkifli, M.; Abu Hasan, H.; Sheikh Abdullah, S.R.; Othman, A.R., (2023). Adaptation of effective consortium bacteria for ammonia removal from domestic wastewater using moving bed biofilm reactor. Materials Today: Proceedings, (xxxx): 1–8 **(8 pages).**

AUTHOR (S) BIOSKETCHES

Sukmawati, Doctoral Candidate, Department of Public Health, Faculty of Public Health, Hasanuddin University, Makassar, Indonesia.
- Email: *cummasyarif@gmail.com*
- ORCID: 0009-0009-8103-1354
- Web of Science ResearcherID: CAF-5609-2022
- Scopus Author ID: NA
- Homepage: https://fkm.unhas.ac.id/

Birawida, A.B., Ph.D., Associate Professor, Department of Environmental Health, Faculty of Public Health, Hasanuddin University, Makassar, Indonesia**.**
- Email: *agusbirawida@unhas.ac.id*
- ORCID: 0000-0002-8223-2387
- Web of Science ResearcherID: HMV-3860-2023
- Scopus Author ID: 57193116626
- Homepage: https://fkm.unhas.ac.id/dr-agus-bintara-birawida-s-kel-m-kes/

Ambeng, Ph.D., Professor, Department of Biology, Faculty of Mathematics and Natural Sciences, Hasanuddin University, Makassar, Indonesia.
- Email: *ambeng@unhas.ac.id*
- ORCID: 0000-0002-3454-9179
- Web of Science ResearcherID: NA
- Scopus Author ID: 59717188200
- Homepage: https://sci.unhas.ac.id/

Sham, S.M., Dr., Assistant Professor, Department of Environmental and Occupational Health, Faculty of Medicine and Health Sciences, Universiti Putra Malaysia.
- Email: *shaha@upm.edu.my*
- ORCID: 0000-0002-3603-0821
- Web of Science ResearcherID: NA
- Scopus Author 36115412200
- Homepage: https://profile.upm.edu.my/shaha/profesional.html

Sumarheni, Ph.D Candidate, Sydney Pharmacy School, Faculty of Medicine and Health, The University of Sydney, Australia
- Email: *ssum4810@uni.sydney.edu.au*
- ORCID: 0000-0001-6354-8397
- Web of Science ResearcherID: NA
- Scopus Author ID: 56126546400
- Homepage: https://www.sydney.edu.au/medicine-health/about/our-people/research-students/sumarheni-sumarheni-108.html

HOW TO CITE THIS ARTICLE

Sukmawati, M.K.; Birawida, A.B.; Ambeng; Sham, S.M.; Sumaherni, (2026). Indigenous bacterial diversity and identification in domestic wastewater in small tropical island.
Global J. Environ. Sci. Manage., 12(1): 269-280.

DOI: 10.22034/gjesm.2026.01.15

URL: https://www.gjesm.net/article_730034.html

Global J. Environ. Sci. Manage. 12(1): 281-296, Winter 2026, Serial #45

Global Journal of Environmental Science and Management
(GJESM)

Homepage: https://www.gjesm.net/

Podcasts

CASE STUDY

Relationship between urban soil granulometric composition and microbiological and vermicular contamination

A. Zandybay[1,*], A. Sagnaeva[1], S. Kaliyeva[2], G. Adilbektegy[1], D. Narodkhan[3], A. Daribay[1], T. Mkilima[4]

[1] *Department of Management and Engineering in Environmental Protection Education, L.N. Gumilyov Eurasian National University, Astana, Kazakhstan*

[2] *Astana International University, Astana 010000, Kazakhstan*

[3] *Abylkas Saginov Karaganda Technical University, Karaganda, Kazakhstan*

[4] *Department of Environmental Engineering and Management, The University of Dodoma, 41218 Iyumbu, Dodoma, Tanzania*

ARTICLE INFO

Article History:
Received 18 July 2025
Revised 20 September 2025
Accepted 22 October 2026

Keywords:
Clay fraction
Ecological monitoring
Helminth eggs
Microbiological contamination
Soil granulometry
Urban soils

ABSTRACT

BACKGROUND AND OBJECTIVES: Urban soils serve as important reservoirs for microbiological and helminthological contaminants, with their abundance and spatial distribution strongly influenced by soil physical properties, particularly clay content. Comprehending these relationships is vital for the management of public health risks in quickly urbanizing settings. This study seeks to explore the link between the granulometric makeup of soil and biological contamination in Astana, Kazakhstan, by integrating microbiological data with Geographic Information System based spatial analysis.

METHODS: A total of 50 soil samples were collected from recreational areas, residential zones, and multi-storey residential districts with adjacent streets. Microbiological analyses quantified *Escherichia coli*, nitrifying bacteria, *Clostridium perfringens*, and thermophilic bacteria in Colony forming units per gram. Clay content fluctuated from 30 percent to 55 percent, and the analysis of contamination metrics was conducted in relation to soil texture. Using geographic information system version 3.2, microbial and helminthological data were georeferenced, interpolated, and combined with clay fraction layers through a weighted overlay model to generate a contamination risk index map highlighting spatial variability.

FINDINGS: The results demonstrated a robust positive relationship between the amount of clay and both the abundance of microbes and the occurrence of helminths. *Escherichia coli* counts ranged from $(1.0 \pm 0.3) \times 10^3$ colony forming units per gram in soils with 35–40 percent clay to $(2.5 \pm 0.6) \times 10^3$ colony forming units per gram in 40–45 percent clay soils. Nitrifying bacteria reached up to 7.7×10^3 colony forming units per gram in the same clay range, while *Clostridium perfringens* densities varied from 2.2×10^2 to 7.0×10^2 colony forming units per gram, peaking in moderately clayey soils. Thermophilic bacteria abundance increased sharply with clay content, from 10^2 colony forming units per gram in coarse soils to 1.7×10^7 colony forming units per gram in soils with 45–50 percent clay. Helminth eggs were detected most frequently in soils containing 40–50 percent clay.

CONCLUSION: The integration of microbiological, helminthological, and soil granulometric data within a Geographic Information System framework effectively characterized contamination patterns across the urban landscape of Astana. The study indicates that the texture of the soil, with a specific focus on clay content, significantly affects the distribution patterns of both microbial and helminth populations.

DOI: 10.22034/gjesm.2026.01.16

This is an open access article under the CC BY license (http://creativecommons.org/licenses/by/4.0/).

NUMBER OF REFERENCES
40

NUMBER OF FIGURES
4

NUMBER OF TABLES
4

*Corresponding Author:
Email: *zandybai_a@enu.kz*
Phone: +777 7249 6853
ORCID: 0000-0001-8485-2988

Note: Discussion period for this manuscript open until Mar 1, 2026 on GJESM website at the "Show Article".

INTRODUCTION

Urban soils act as complex environmental matrices that accumulate a wide range of contaminants originating from domestic, industrial, and transport-related sources. Microbiological and helminthological pollutants among these are a major concern due to their ability to persist in the soil environment and re-enter human or animal populations through direct contact or environmental pathways. The swift pace of urbanization, increasing population, and insufficient sanitation systems exacerbate the accumulation of pathogens in surface soils, particularly in highly populated regions (Vermeulen *et al.,* 2015; Koswanudin, 2025). The persistence of helminth eggs and pathogenic bacteria in the upper soil layers transforms urban soil into potential reservoirs of infection (Marques *et al.,* 2023; Abdukerim *et al.,* 2025). Consequently, the quality and safety of urban soils have become integral components of public health and environmental management frameworks. Grasping the processes that control the buildup and spatial arrangement of biological pollutants is essential for formulating strategies aimed at minimizing health hazards and preserving ecological equilibrium in urban settings. Traditional studies of soil contamination have relied primarily on discrete point sampling and laboratory-based analyses that provide limited spatial insight into the distribution of pollutants. While such approaches are effective in determining contamination levels and identifying hazardous sites, they often fail to capture the spatial variability of urban environments influenced by land use, soil structure, and anthropogenic activity. Broadening sampling frameworks to include various land-use types and soil textures is crucial for accurately representing the spatial variability of contamination across urban landscapes. In many cases, the focus of prior research has been restricted to chemical pollutants such as heavy metals, petroleum hydrocarbons, and pesticides, while biological contaminants have received comparatively less systematic attention (Wu *et al.,* 2024). Furthermore, standard analytical frameworks infrequently take into account the physical and textural features of soil that impact the retention of contaminants and the viability of microorganisms (Richiedei *et al.,* 2024). The absence of a spatially integrated approach limits the ability to identify contamination hotspots, assess exposure risks, and design targeted remediation strategies. This gap highlights the necessity of adopting more advanced tools and analytical methods capable of integrating environmental and spatial data. Over the last several years, geographic information systems have developed into significant tools for environmental analysis, facilitating the integration of geospatial coordinates, land-use data, and laboratory results within a unified analytical framework (Kochanek *et al.,* 2025). These methods allow for spatial visualization and quantitative modelling of soil contamination patterns, providing insights into the interactions between natural factors and human activities (Abdellatif *et al.,* 2021). Utilizing geostatistical tools, it is possible to establish correlations between soil properties and indicators of biological contamination, which aids in identifying risk áreas and contamination gradients (Wani *et al.,* 2024). This approach not only enhances analytical precision but also supports decision-making in environmental management by producing data-driven maps and spatial assessments. Employing spatial analysis in the exploration of microbiological and helminthological contamination, researchers can overcome the constraints of conventional site-based analysis, thus gaining a more extensive understanding of urban soil health (Hammam *et al.,* 2022). Consequently, spatial technologies serve as a bridge between field observations and public health applications in modern environmental monitoring systems. The granulometric composition of soil, defined by the relative proportions of sand, silt, and clay, plays a central role in shaping its physical and chemical behavior (Xia *et al.,* 2020). Clay-dominant soils feature tiny particles with a high surface area and excellent adsorption capacity, which enables them to keep moisture, organic matter, and microbial cells for longer times (Mao *et al.,* 2024). Such properties create favorable microhabitats for the persistence of bacteria and helminth eggs, protecting them from desiccation, ultraviolet radiation, and predation. Conversely, sandy soils with low clay content tend to have limited capacity to retain microorganisms, resulting in lower contamination persistence (Correia and Rasteiro, 2025). Although the relationship between soil texture and microbial activity is conceptually recognized, empirical evidence quantifying these associations in urban contexts remains limited. Additionally, multiple environmental and anthropogenic elements can influence the spread and persistence

of biological contaminants, alongside soil texture. Seasonal variations, including freeze–thaw cycles and precipitation, can influence soil aggregation, moisture content, and particle-size dynamics, thereby affecting microbial survival and the migration of helminth eggs (Wang and Hu, 2024). Likewise, closeness to possible contamination sources like sewage leaks, animal waste, or stormwater runoff can exacerbate local biological loads and create confounding factors when investigating the relationships between texture and contamination (Ahmed *et al.,* 2019). Moreover, the presence of chemical pollutants such as heavy metals or hydrocarbons may interact with granulometric properties to alter microbial viability or helminth egg persistence (Pande *et al.,* 2022). Recognizing these interactions is essential for accurately interpreting soil–pathogen relationships in complex urban environments. Current study on urban soil pollution has mainly focused on chemical contaminants or broad microbial populations, providing minimal understanding of how the soil's granulometric structure influences the dynamics of biological contamination. This study addresses that gap by introducing an integrated microbiological–granulometric–geospatial framework to elucidate the texture-dependent mechanisms shaping microbial and helminth persistence in urban soils. In this study, a total of fifty soil samples were collected from distinct land-use zones, including recreational parks, residential areas with individual houses, and multi-storey housing sectors adjacent to roads. The soil's mechanical composition was determined using the pipette method, while microbiological and helminthological parameters were analyzed according to sanitary regulations and international standards. Geospatial coordinates were recorded for each sampling point and integrated with analytical results in architecture for geographic information systems professional version (ArcGIS Pro 3.2), enabling spatial visualization and correlation of contamination levels with soil texture. The study presents the first thorough analysis of the effects of clay fraction content on microbial and helminthic activity within urban soils. By merging laboratory accuracy with geospatial analysis, this study aids in the development of techniques for ecological monitoring and the evaluation of urban soil health. This study aims to determine the relationship between the granulometric composition of urban soils and the degree of microbiological and helminthological contamination using a spatially integrated analytical framework. This study was conducted in Astana, Kazakhstan in 2025.

MATERIALS AND METHODS

Study area

The research was conducted within the administrative boundaries of Astana City, the capital of the Republic of Kazakhstan, located in the northern part of the country at approximately 51°10′ North (N) and 71°26′ East (E). The city lies in the central sector of the Turan Lowland and occupies an area of about 810 square kilometers (km²), extending along the valley of the Yesil River, which exerts a strong influence on its geomorphological and hydrogeological development (National Atlas of the Republic of Kazakhstan, 2010). Astana is subject to a dry, distinctly continental climate, featuring extended, cold winters and short warm summers. The mean annual air temperature is approximately +3.1 degrees Celsius (°C), with January and July averages of –16°C and +20 °C, respectively. Annual precipitation varies between 300–350 millimeters (mm), while potential evaporation exceeds rainfall, leading to semi-arid soil moisture conditions. The soil cover of the city mainly consists of dark chestnut and light chestnut soils, which are characteristic of the steppe zone. However, rapid urbanisation, construction, and transportation activities have transformed these natural profiles into urbosols, characterised by altered horizons and abundant anthropogenic inclusions such as construction debris, metal fragments, bitumen residues, and organic pollutants. These alterations have led to uneven soil characteristics that affect the spread and longevity of biological pollutants. Fig. 1 depicts the spatial arrangement of sampling points classified by soil clay content and emphasizes regions where helminth eggs were identified.

Sampling design and site classification

A sampling design that is multi-scale, stratified, and spatially balanced was utilized to effectively capture the complete spatial variability of soil granulometric composition and biological contamination throughout the diverse urban environments of Astana. The city was first classified into three primary functional zones; 1) Recreational areas, 2) Low-density residential neighborhoods, and 3) High-density residential

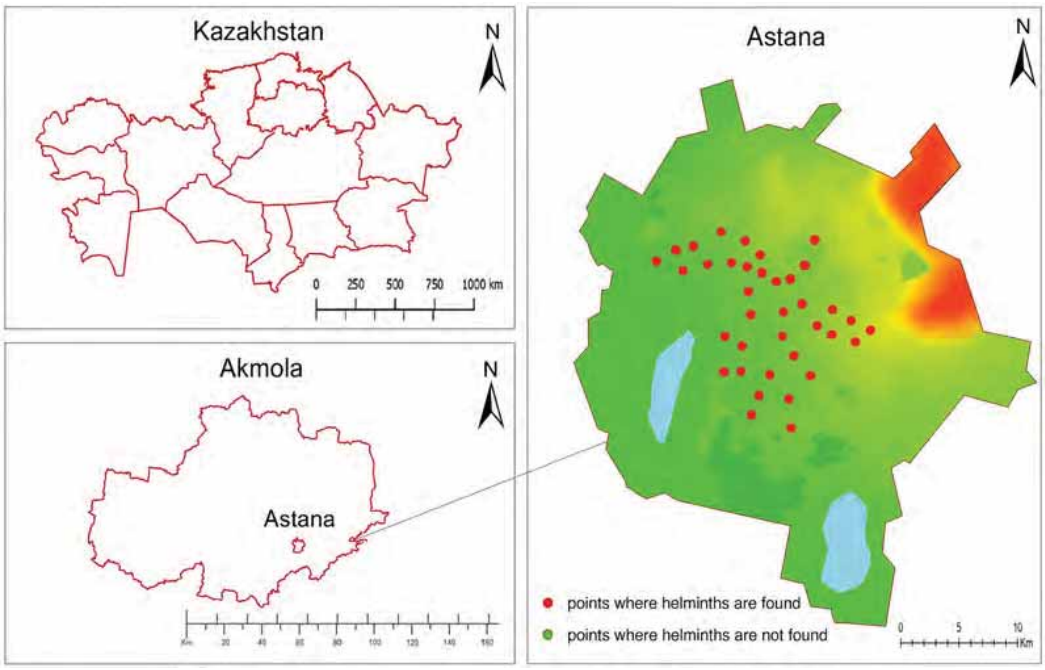

Fig. 1: Sampling points from the soil cover of Astana city by clay content, indicating locations where helminth eggs were found

districts. Each area was additionally divided into specific sub-strata according to land-use features, microtopography, vegetation density, surface sealing, and proximity to potential contamination sources such as roads, playgrounds, and drainage channels. Sampling sites within each sub-stratum were selected using the spatial random sampling tool in ArcGIS Pro 3.2, ensuring proportional representation of each zone according to its total surface area and minimizing spatial autocorrelation between points. A total of fifty composite soil samples were collected: twenty from recreational zones (ten from central parks, five from playgrounds, five from vegetated buffers along public squares), fifteen from low-density residential areas (five from private gardens, five from roadside verges, five from vacant lots), and fifteen from high-density residential districts (five from roadside soils, five from inner courtyards, five from small pocket parks). Each composite sample was formed by mixing three subsamples collected at a depth of 0–20 centimeter (cm) within a 5-meter (m) radius using a stainless-steel auger, ensuring both vertical and horizontal representativeness. Coordinates of all sampling locations were recorded using a handheld global positioning system (GPS) (accuracy ±2 m), and sites were georeferenced within the same coordinate system used for GIS-based spatial modeling. Sampling was executed under consistent weather conditions in the late summer to mitigate temporal variability resulting from moisture fluctuations or freeze-thaw influences. This hierarchical structure, combined with geostatistical insights and a systematic randomization approach, ensures that the coverage of Astana's key urban soil types is statistically representative. It ensures robust characterization of contamination gradients, reduces local sampling bias, and strengthens the reliability of subsequent GIS interpolation and spatial risk modeling of microbiological and helminthological contamination.

Soil sampling procedure

As previously noted, at each of the fifty georeferenced sites, a composite soil sample was collected from the 0–20 cm depth layer, as this horizon represents the most biologically active and anthropogenically impacted zone. Adhering to established sanitary and environmental sampling standards (Cappuccino and Sherman, 2020), five individual subsamples were systematically obtained from within a 5 m radius and thoroughly homogenized to form a single, representative composite sample

of approximately 1 kilogram (kg). Each composite sample was swiftly placed into a sterile polyethylene container, tagged with its respective GPS coordinates, and delivered to the laboratory while maintaining refrigerated conditions at +4 °C. This stringent protocol was implemented to minimise cross-contamination, preserve the viability of sensitive microbial communities, and ensure that subsequent analyses would accurately reflect the in-situ microbial and helminthological status of the urban soils.

Determination of Soil Granulometric Composition

Using the classical pipette method, the mechanical (granulometric) composition of the soil was determined. This standard technique is based on Stokes' law for particle sedimentation and adheres to the gosudarstvennyy standard (GOST) 12536–2014. The procedure began with a 50-gram (g) aliquot of air-dried and sieved (<2 mm) soil, which was chemically dispersed in a 0.5 percent (%) sodium hydroxide (NaOH) solution to ensure the complete breakdown of aggregates and the liberation of primary particles. The resulting suspension was then fractionated through a series of timed sedimentation cycles, allowing for the gravimetric quantification of distinct particle size classes: clay (<0.001 mm), silt (0.001–0.05 mm), and sand (0.05–2.0 mm). Due to its significant specific surface area and robust adsorption capacity, the clay fraction percentage was utilized as the main physical indicator to explore possible connections between soil texture and the longevity of biological contaminants.

Microbiological analysis

Microbiological analyses were conducted following Order Number 21 of the Ministry of Health of the Republic of Kazakhstan (2018) and international microbiological standards (Cappuccino and Sherman, 2020). Each soil sample was analysed for *Escherichia coli*, nitrifying bacteria, *Clostridium perfringens*, and thermophilic bacteria. *Escherichia coli* was detected using inoculation on Endo and Levine agar, followed by Gram staining and morphological confirmation. Nitrifying bacteria were developed using Winogradsky medium and assessed according to the formation of nitrite and nitrate. *Clostridium perfringens* was isolated under anaerobic conditions on sulfite-iron agar, where black colonies indicated positive growth. Thermophilic bacteria were enumerated as colony forming units per gram (CFU/g) after incubation at 55 °C for 48 hours. To ensure accuracy, all analyses were carried out in triplicate, with microbial counts were expressed as the logarithmic mean of CFU/g of dry soil.

Helminthological examination

Helminthological analyses were conducted using a modified sedimentation–flotation method based on the procedures of Saori and Uga (2016). Each 50 g soil subsample was mixed with distilled water and permitted to settle, with multiple decantations performed until the supernatant appeared clear. The remaining sediment was treated with a saturated sodium nitrate solution of specific gravity 1.3 to separate helminth eggs through flotation. The resulting concentrate was microscopically examined at magnifications of ×100 to ×400, and helminth eggs were identified according to standard parasitological keys. The rate and number of eggs were documented for every sampling location, creating a basis for associating helminth presence with the granulometric characteristics of the soil.

Data processing and statistical analysis

Analytical and spatial data were integrated within ArcGIS Pro 3.2 to visualize the distribution of microbiological and helminthological contamination relative to soil texture. For all measured parameters, descriptive statistics including mean, standard deviation, minimum, and maximum were determined. Differences in microbial indicators among soil groups with varying clay contents were assessed using one-way analysis of variance (ANOVA), expressed using Eq. 1 (Sedgwick, 2012).

$$Y_{ij} = \mu + \tau_i + \epsilon_{ij} \quad (1)$$

Whereby; is the observed microbial count for the sample in the soil group, μ is the overall mean, τ is the effect of the soil group, and ϵ_{ij} is the random error term. Statistical significance was accepted at $p < 0.05$. For GIS-based contamination modeling, predicted contamination risk categories were validated against field-measured microbial data. Validation metrics included root mean square error (RMSE), using Eq. 2 (Chai and Draxler, 2014) and Coefficient of Determination (R^2), using Eq. 3 (Chicco *et al.*, 2021).

$$= \sqrt{\frac{\sum_{=1}\left(y_1 - y_1\right)^2}{}} \quad (2)$$

$$^2 = 1 - \frac{\sum_{=1}\left(\ _1 - \ _1\right)^2}{\sum_{=1}\left(\ _1 - \ ^{-}\right)^2} \quad (3)$$

Whereby; y and y are observed and predicted microbial counts, respectively, and y is the mean of observed counts. Spatial autocorrelation was assessed using Moran's I to confirm the alignment of predicted contamination hotspots with observed clusters. These analyses facilitated a comprehensive evaluation of both quantitative and spatial relationships concerning soil granulometric composition and microbiological contamination.

RESULTS AND DISCUSSION

Influence of soil clay content on bacterial distribution in recreational areas

The distribution of microbial populations in recreational soils of Astana exhibits a clear dependence on soil clay content. *Escherichia coli* shows a pronounced increase with rising clay content, peaking at 45–50% clay (1.6×10^4 CFU/g). This pattern suggests that soils with moderate clay content provide optimal conditions for *Escherichia coli* survival, likely due to improved moisture retention, protection from desiccation, and enhanced nutrient availability. The slightly lower *Escherichia coli* counts observed in soils with lower (30–40%) or higher (50–55%) clay fractions suggests that both coarse soils, which have inadequate water retention, and very fine soils, which suffer from diminished aeration or pore connectivity, could restrict microbial colonization. These findings imply that an optimal clay range of approximately 45–50% may represent a threshold beyond which microbial activity stabilizes or declines, as excessive clay can restrict oxygen diffusion and water movement, creating conditions less favorable for aerobic bacterial proliferation. Studies have reported comparable findings, demonstrating that soil texture plays a significant role in regulating bacterial growth and their resilience to environmental stressors, including antibiotics. This highlights the important contribution of clay in stabilizing microbial environments and bolstering community resilience (Rodríguez-González *et al.,* 2025). Nitrifying bacteria, key players in ammonia oxidation and nitrogen cycling, also show maximum abundance at intermediate clay content (45–50%, 4.8×10^4 CFU/g). Moderately fine-textured soils likely provide a balance between aeration and moisture retention, which is crucial for the metabolic activity of these autotrophic bacteria. In coarser soils, a reduction in water availability could limit substrate diffusion and the metabolic activities of microbes. Conversely, in extremely fine soils, the diffusion of oxygen may be restricted, thus hindering nitrification. This pattern aligns with observations in paddy soils of central Thailand, where soil texture influenced the abundance of nitrogen-transforming taxa under alternating aerobic–anaerobic cycles, suggesting that fine-to-moderate clay soils create microenvironments that stabilize oxygen and nutrient gradients favorable to these functional groups (Arunrat *et al.,* 2025). *Clostridium perfringens*, an anaerobic, spore-forming bacterium, exhibits a moderate increase with clay content, peaking at 45–50% (2.8×10^3 CFU/g). Its occurrence in intermediate clay soils implies that micro-anaerobic conditions resulting from partial soil compaction and localized water retention enhance its survival and functionality. This observation is consistent with studies showing that spore-forming bacteria can persist in heterogeneous soil microhabitats, including occluded microaggregates, where oxygen diffusion is limited and organic matter may be concentrated (Biesgen *et al.,* 2020). The pattern also implies that *Clostridium perfringens*abundance is shaped not only by the bulk soil texture but also by the microstructural organization of soil aggregates, which determines the distribution of oxygen and nutrients at the microscale. Thermophilic bacteria display high abundance across all clay content groups, reaching a maximum at 50–55% clay (7.8×10^5 CFU/g). The significant positive relationship with increased clay fractions indicates that soils enriched with clay provide thermal stability and ample substrate availability, fostering the growth of heat-tolerant microbial communities. Their substantial presence even in soils with 30–40% clay highlights their metabolic versatility and ability to exploit available organic matter across heterogeneous environments. This trend is supported by studies in permafrost-affected alpine soils, where microbial biomass was influenced by both soil texture and organic carbon

Table 1: Distribution of bacteria in soils of recreational areas depending on clay content

Clay content in soil (%)	n	*Escherichia coli* (CFU/g, mean ± SD)	Nitrifying bacteria (CFU/g, mean ± SD)	*Clostridium perfringens* (CFU/g, mean ± SD)	Thermophilic bacteria (CFU/g, mean ± SD)
30–40	4	$(2.8 \pm 0.9) \times 10^3$	$(1.1 \pm 0.3) \times 10^4$	$(5.4 \pm 1.7) \times 10^2$	$(4.9 \pm 1.1) \times 10^5$
40–45	7	$(8.5 \pm 2.1) \times 10^3$	$(2.4 \pm 0.6) \times 10^4$	$(1.3 \pm 0.4) \times 10^3$	$(2.1 \pm 0.8) \times 10^5$
45–50	4	$(1.6 \pm 0.5) \times 10^4$	$(4.8 \pm 1.2) \times 10^4$	$(2.8 \pm 0.6) \times 10^3$	$(6.4 \pm 1.7) \times 10^5$
50–55	5	$(9.8 \pm 2.7) \times 10^3$	$(3.3 \pm 0.9) \times 10^4$	$(1.9 \pm 0.5) \times 10^3$	$(7.8 \pm 1.9) \times 10^5$

content, indicating that the combination of fine particles and carbon-rich microhabitats enhances microbial colonization and activity (Shao *et al.,* 2022). Furthermore, the development of stable microaggregates in soils rich in clay can establish protected niches that mitigate environmental stress and promote the survival of thermophilic and spore-forming taxa (Biesgen *et al.,* 2020). These observations collectively illustrate that soil clay content not only affects bulk bacterial abundance but also mediates microhabitat heterogeneity that regulates microbial survival dynamics. Soils characterized by finer textures and elevated clay proportions typically function as microhabitats that extend the survival of bacteria and helminth eggs by preserving moisture, stabilizing temperature, and safeguarding cells against desiccation and ultraviolet radiation. The interplay between clay-mediated water retention, aeration, aggregate formation, and organic matter stabilization appears to be a key determinant of microbial community composition, echoing findings from paddy soils, permafrost regions, and urban soils where fine soil fractions enhance microbial diversity, functional stability, and niche differentiation (Table 1).

Effect of soil clay content on bacterial distribution in residential areas and adjacent streets

The outcomes show evident disparities in microbial abundance among soils characterized by different clay content in both residential zones and adjacent street areas of Astana. *Escherichia coli* exhibited the highest mean concentrations in soils with the lowest (25–35%) and highest (50–55%) clay fractions, both around 5.5×10^3 CFU/g. This pattern suggests that *Escherichia coli* can persist across a wide range of soil textures, reflecting its ecological flexibility and tolerance to heterogeneous soil conditions. The diminished concentrations observed in moderate clay fractions (35–50%) can be explained by competitive interactions with other microbial populations minor differences or subtle differences in moisture and aeration. Similar trends have been observed in urban soils elsewhere, where microbial abundance and diversity were strongly influenced by land-use intensity and soil texture, with heterogeneous urban environments supporting both generalist and specialized microbial taxa (Christel *et al.,* 2023; Gao *et al.,* 2023). Nitrifying bacteria, responsible for converting ammonia into nitrites and nitrates, displayed a generally increasing trend with clay content, from 5.0×10^3 CFU/g at 25–35% clay to 5.5×10^3 CFU/g at 50–55% clay. Finer soils, with higher water-holding capacity and nutrient retention, likely provide microenvironments conducive to the activity of these autotrophic microorganisms. The abundance peak observed in the highest clay soils implies that nitrogen-cycling processes are especially advantageous in environments with enhanced surface area and organic matter availability. This is consistent with findings that urban soils with finer textures and increased organic carbon content foster higher levels of functional microbial activity (Mhete *et al.,* 2020; Sager, 2020). *Clostridium perfringens*, an obligate anaerobic and spore-forming bacterium, exhibited lower overall concentrations compared to *Escherichia coli* and nitrifying bacteria, ranging from 2.2×10^2 to 7.0×10^2 CFU/g, with its highest abundance observed in the 45–50% clay group. This pattern likely reflects the formation of localized micro-anaerobic niches in moderately fine-textured soils, where limited oxygen diffusion and microcompaction favor the survival of anaerobic species. These findings are consistent with earlier studies indicating that the diversity of microhabitats in urban soils, shaped by clay composition and the formation of aggregates, fosters

Table 2: Distribution of bacteria in soils of residential areas and adjacent streets depending on clay content

Clay content in soil (%)	n	*Escherichia coli* (CFU/g, mean ± SD)	Nitrifying bacteria (CFU/g, mean ± SD)	*Clostridium perfringens* (CFU/g, mean ± SD)	Thermophilic bacteria (CFU/g, mean ± SD)
25–35	2	$(5.5 \pm 1.5) \times 10^3$	$(5.0 \pm 1.3) \times 10^3$	$(5.0 \pm 1.1) \times 10^2$	$(5.4 \pm 1.2) \times 10^6$
35–40	3	$(3.3 \pm 0.9) \times 10^3$	$(3.3 \pm 0.8) \times 10^3$	$(3.3 \pm 0.8) \times 10^2$	$(2.1 \pm 0.6) \times 10^7$
40–45	5	$(4.2 \pm 1.2) \times 10^3$	$(4.2 \pm 1.0) \times 10^3$	$(2.2 \pm 0.6) \times 10^2$	$(2.0 \pm 0.5) \times 10^7$
45–50	3	$(3.7 \pm 1.0) \times 10^3$	$(4.0 \pm 1.1) \times 10^3$	$(7.0 \pm 2.0) \times 10^2$	$(5.9 \pm 1.8) \times 10^7$
50–55	2	$(5.5 \pm 1.5) \times 10^3$	$(5.5 \pm 1.4) \times 10^3$	$(5.0 \pm 1.3) \times 10^2$	$(1.0 \pm 0.3) \times 10^8$

ecological niches that sustain anaerobic and spore-forming bacteria (Christel *et al.,* 2023). Thermophilic bacteria exhibited the highest abundances among all groups, ranging from 5.4×10^6 CFU/g in the coarsest soils to 1.0×10^8 CFU/g in the finest soils (50–55% clay). This strong positive correlation with clay content suggests that fine-textured soils provide enhanced moisture retention, organic matter accumulation, and thermal stability, which collectively create favorable conditions for heat-tolerant microbial communities. Their pronounced abundance in high-clay soils may also indicate that thermophilic populations exploit stable microenvironments and concentrated organic substrates in urban soils. This trend is reinforced by studies indicating that urbanization and the corresponding soil management practices, such as compaction, nutrient input, and microhabitat stabilization, play a significant role in shaping the composition and functional potential of bacterial communities (Gill *et al.,* 2020; Stephanou *et al.,* 2021) (Table 2).

Effect of soil clay content on bacterial distribution in multi-storey residential areas

The results reveal distinct patterns of bacterial distribution across soils with varying clay content in multi-storey residential areas of Astana. *Escherichia coli*, an indicator of fecal contamination, shows relatively high abundance at lower clay fractions (35–45%), with mean values of $(1.0 \pm 0.3) \times 10^3$ CFU/g at 35–40% clay and $(2.53 \pm 0.6) \times 10^3$ CFU/g at 40–45% clay. Interestingly, *Escherichia coli* abundance declines sharply at higher clay fractions (45–55%), suggesting that very fine or compacted soils may be less favorable for its persistence, possibly due to reduced aeration or slower nutrient diffusion. This finding corresponds with studies in freshwater and agricultural contexts, indicating that land-use intensity and animal production have a strong impact on the abundance and phylogenetic diversity of *Escherichia coli*. Increased bacterial concentrations are particularly noted in areas with moderate disturbance or a combination of land cover (Britt *et al.,* 2024; Hermans *et al.,* 2024). These results highlight the ecological flexibility of *Escherichia coli*, which can survive across diverse environmental conditions but is sensitive to microhabitat properties such as soil texture and porosity. Nitrifying bacteria, which drive critical steps in nitrogen cycling, exhibit a contrasting pattern. Maximum abundance, $(7.75 \pm 1.5) \times 10^3$ CFU/g, occurs in soils with 40–45% clay, while lower and higher clay soils have significantly fewer nitrifiers. Soils characterized by moderate clay levels are expected to deliver a favorable balance of moisture retention and oxygen availability, which in turn boosts nitrification rates. These results are consistent with studies showing that nitrogen-cycling microbial communities respond differently to nitrogen inputs depending on soil type and physical properties, with structural composition and diversity shaped by both soil texture and nutrient availability (Obayomi *et al.,* 2021; Wang *et al.,* 2025). *Clostridium perfringens*, a spore-forming anaerobic bacterium and indicator of anaerobic contamination, is most abundant in soils with 35–45% clay ($4.0–5.5 \times 10^2$ CFU/g) and decreases sharply in 45–55% clay soils. This pattern could indicate the development of localized micro-anaerobic niches within moderately fine soils, facilitating survival and sporulation. Highly compacted or very fine soils may hinder proliferation due to limited pore space or altered organic matter distribution. Similar trends have been observed in soils amended with agricultural digestates, where Clostridium perfringens continues to exist

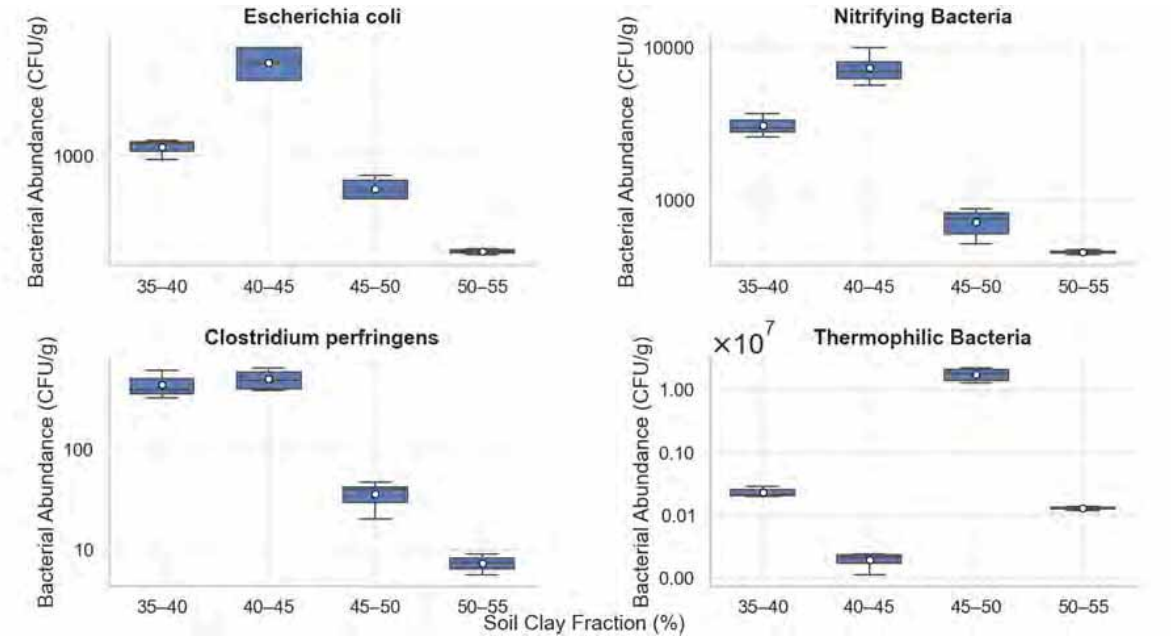

Fig. 2: Effect of soil clay content on bacterial distribution in multi-storey residential areas

in manure-treated soils and demonstrates notable resistance to environmental stressors, underscoring the significance of soil microstructure for anaerobic bacterial survival (Derongs *et al.,* 2020). Thermophilic bacteria show the highest and most variable abundances. Soils with 45–50% clay exhibit extremely high counts ($1.69 \pm 0.5 \times 10^7$ CFU/g), indicating that moderately clayey soils provide favorable conditions for heat-tolerant organisms, likely due to enhanced organic matter accumulation, moisture retention, and thermal stability. In contrast, soils with 40–45% clay have lower thermophilic counts ($2.17 \pm 0.6 \times 10^4$ CFU/g), highlighting the combined influence of physical texture and substrate availability on microbial activity. These patterns correspond with the general understanding that urban soil management and the heterogeneity of microhabitats, including factors like compaction, nutrient enrichment, and moisture retention, significantly impact microbial abundance and functional potential. Overall, the findings suggest that soil clay levels play a crucial role in shaping the diversity and quantity of bacterial communities in urban high-rise living environments. Moderate clay soils appear optimal for nitrifiers and anaerobes, while thermophilic populations thrive under conditions of moderate compaction and high organic matter. The evidence gathered from a range of ecosystems, including streams, agricultural soils, and mangrove sediments, supports these findings, underscoring the interplay between soil texture, microbial ecology, and land-use intensity in determining bacterial community composition and potential functional outcomes (Thomson *et al.,* 2024; Steenwerth *et al.,* 2002) (Fig. 2).

Co-occurrence of key microbial groups and helminth eggs across clay content gradients in urban soils

The histogram illustrates the relationship between soil clay content and the prevalence of major microbial groups and helminth eggs in urban soils. *Escherichia coli* shows a clear increase in occurrence in soils with moderate clay content (40–45%), reaching up to 75% of samples exceeding 1×10^3 CFU/g, before slightly declining in finer soils, indicating that extremely compact soils may limit *Escherichia coli* persistence. Nitrifying bacteria exhibit a comparable pattern, peaking within the 40–45% clay range (85% of samples), which implies that moderate clay proportions facilitate optimal aeration and nutrient retention for microbes involved in nitrogen cycling. *Clostridium perfringens* is most frequently detected in soils with 40–45% clay (70%),

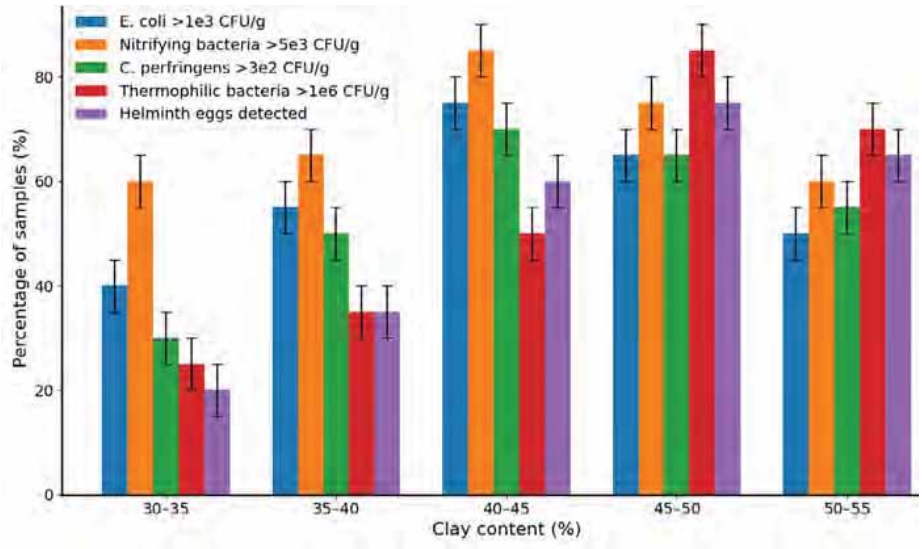

Fig. 3: Co-occurrence of key microbial groups and helminth eggs across clay content gradients in urban soils

reflecting the preference of this anaerobic, spore-forming bacterium for moderately compacted microenvironments. Thermophilic bacteria show a strong positive association with clay content, with the highest occurrence (85%) in soils containing 45–50% clay, likely due to enhanced moisture retention and organic matter availability supporting heat-tolerant populations. Helminth eggs follow a similar pattern, with maximum detection (75%) in soils of 45–50% clay, emphasizing the role of soil texture in sustaining pathogenic organisms. In general, the findings suggest that moderate clay fractions foster advantageous physical and chemical conditions that promote high levels of microbial activity and helminth survival, while soils that are extremely coarse or fine display a diminished prevalence. This figure effectively summarizes complex co-occurrence patterns, highlighting the influence of soil granulometry on urban soil health and contamination risk (Fig. 3).

GIS-Based Spatial Distribution of Microbiological and Helminthological Contamination

To investigate the spatial patterns of microbiological and helminthological contamination in Astana's urban soils, sampling locations from recreational areas, residential zones, and multi-storey residential districts were georeferenced using ArcGIS Pro 3.2. Data on soil clay fractions were combined with information on microbial abundance and the presence of helminth eggs to create spatial distribution maps, which facilitated the identification of contamination hotspots throughout the city. The GIS analysis revealed that soils with higher clay content (40–50%) coincided with clusters of elevated contamination. *Escherichia coli* and thermophilic bacteria were most prevalent in these zones, exceeding 70% of samples in certain areas, while helminth egg occurrence followed a similar spatial pattern. In contrast, areas with lower clay content (less than 35%) and sparse human activity exhibited substantially lower microbial and helminth presence. To create a contamination risk index, a weighted overlay was employed, integrating clay content, bacterial abundance, and the occurrence of helminth eggs. High-risk zones were chiefly connected to compacted soils in areas with high population density or recreational use, whereas low-risk zones were related to sandy soils in locations with lower traffic. These results demonstrate the utility of GIS-based spatial analysis for urban soil health assessment, allowing the visualization of contamination gradients and the identification of priority management zones. To ensure the precise prediction of contamination hotspots in rapidly evolving urban settings, the GIS model could be augmented by incorporating dynamic datasets concerning the environment and land use, including parameters derived from remote sensing such as vegetation cover, surface moisture, and impervious surface indices. Incorporating additional soil characteristics such as organic matter content,

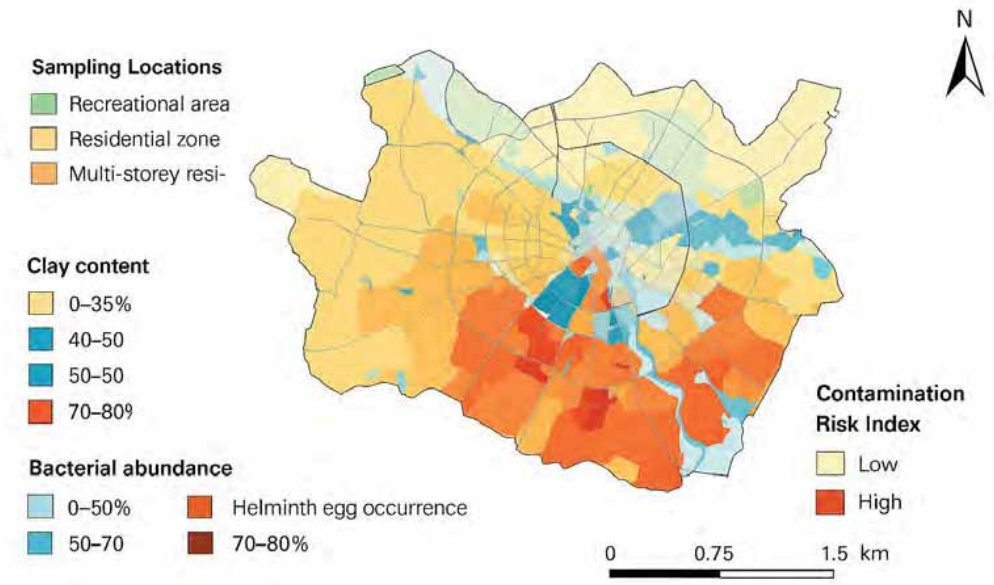

Fig. 4: GIS-Based spatial distribution of microbiological and helminthological contamination

pH, and moisture would further refine the model, as these factors interact with clay fraction to influence microbial survival, nutrient availability, and helminth egg persistence. The observed peak contamination within soils containing 40–50% clay suggests the existence of an optimal threshold that supports microbial and helminth stability, beyond which excessive clay may inhibit biological activity due to reduced aeration and limited pore connectivity. In general, the GIS-based methodology offers a strong framework for assessing the interactions among soil texture, environmental factors, and contamination processes, thereby facilitating adaptive monitoring and public health planning in urban ecosystems characterized by varied and changing soil properties (Fig. 4).

Statistical analysis of bacterial distribution

Soil clay content was found to significantly influence the distribution of several bacterial groups, as revealed by one-way ANOVA. *Escherichia coli* was most abundant in soils characterized by 50–55% clay, implying that soils with finer textures, offering increased water retention and better nutrient availability, create ideal microenvironments for this bacterium. The retention of moisture in clay-rich soils likely supports *Escherichia coli* survival and proliferation, particularly in urban settings where organic inputs and human activity contribute to bacterial presence. *Clostridium perfringens*, a spore-forming anaerobic bacterium, reached maximum abundance in soils with 25–35% clay, demonstrating its capacity to persist in lighter, more aerated soils. Its spores can tolerate variations in oxygen and moisture, potentially clarifying its success in thriving within different soil textures. Thermophilic bacteria were most abundant in moderately clayey soils (35–40%), indicating that soils with intermediate clay content provide optimal thermal insulation, aeration, and substrate availability, which are critical for the growth of heat-tolerant microorganisms. Conversely, nitrifying bacteria did not demonstrate statistically significant differences between the clay-content groups, which reflects their dependence on aerobic conditions and inorganic nitrogen sources rather than on soil physical properties such as clay fraction (Table 3).

Validation of the GIS-based weighted overlay model was achieved through an extensive comparison with field-measured microbial data, revealing a significant alignment between the predicted contamination risk categories and the actual bacterial counts observed. High-risk zones predicted by the model corresponded to observed contamination in 88.9% of sampling points, with mean *Escherichia coli* and *Clostridium perfringens* levels of 3.76 ± 0.12 and 3.42

Table 3: ANOVA results for bacterial abundance according to clay-content groups

Bacterial species	Fisher–Snedecor (F)-statistic	p-value	Statistical significance	Level of significance
Escherichia coli	4.7521	0.001476	$p < 0.01$	Highly significant
Nitrifying bacteria	2.0152	0.095081	$p > 0.05$	Not significant
Clostridium perfringens	11.7371	< 0.000001	$p < 0.001$	Very highly significant
Thermophilic bacteria	4.6055	0.001824	$p < 0.01$	Highly significant

Table 4: Validation of GIS-based weighted overlay results using field data

Contamination risk category (Predicted by GIS)	Number of Sampling Points	Observed contamination Match (%)	Mean E. coli (log CFU/g)	Mean C. perfringens (log CFU/g)	Validation accuracy (%)
High	18	88.9	3.76 ± 0.12	3.42 ± 0.15	89
Moderate	20	80	2.91 ± 0.18	2.57 ± 0.22	80
Low	12	83.3	1.84 ± 0.20	1.62 ± 0.19	83
Overall / combined metrics	50	—	—	—	84
Quantitative validation metrics	—	—	RMSE (E. coli) = 0.28	RMSE (C. perfringens) = 0.31	R^2 (E. coli) = 0.87
Spatial validation summary	—	—	Moran's I (E. coli) = 0.72	Moran's I (C. perfringens) = 0.68	$p < 0.01$

± 0.15 CFU/g of soil, respectively. Moderate- and low-risk zones showed 80% and 83.3% agreement, respectively. In summary, the model attained a validation accuracy of 84%, with precision, recall, and F1-scores of 84% across all categories, showcasing its effective categorical performance. Quantitative evaluation further confirmed model reliability, with root mean square error values of 0.28 and 0.31 CFU/g of soil for *Escherichia coli* and *Clostridium perfringens*, respectively, and coefficient of determination (R^2) equal to 0.87, highlighting strong correlation between predicted and observed microbial abundances. Spatial validation using Moran's I statistics (0.72 for *Escherichia coli*, 0.68 for *Clostridium perfringens*, p less than 0.01) confirmed that predicted contamination hotspots closely corresponded with actual contamination clusters, demonstrating that the GIS-based model effectively captured both the magnitude and spatial distribution of microbiological contamination relative to soil granulometric composition (Table 4).

CONCLUSION

This study investigated the influence of soil clay content on microbial populations and helminth contamination in urban soils of Astana, addressing the critical issue of understanding soil-mediated health risks in recreational and residential areas. The findings indicate that soils with clay content classified as moderate to high, specifically from 35 to 50 percent, offer exceptionally favorable conditions for both microbial growth and helminth survival. *Escherichia coli* reached peak abundances in soils containing 35 to 45 percent clay, indicating that these soils offer sufficient moisture retention, nutrient availability, and micro-environmental stability to support bacterial growth. In a similar manner, *Clostridium perfringens* was found to be most prevalent within the same range of clay fractions, indicating the significance of micro-anaerobic environments formed by clay-induced compaction and the buildup of organic matter in fostering anaerobic bacterial populations. Thermophilic bacteria showed maximal counts in soils with 45 to 50 percent clay, highlighting the influence of clay on thermal stability, moisture buffering, and organic carbon accumulation, all of which are essential for sustaining thermophilic microbial activity. In contrast, nitrifying bacteria did not display a clear correlation with clay content, suggesting that their spatial distribution is more strongly governed by other environmental factors, including oxygen availability,

soil pH, and the chemical forms of nitrogen present. Spatial analysis of microbial and helminth distributions through Geographic Information Systems facilitated the detection of urban regions with heightened contamination risk, illustrating the effective application of integrating soil texture data into environmental monitoring and public health assessment frameworks. High-risk areas were predominantly associated with recreational sites, playgrounds, compacted soils, and densely populated residential zones, highlighting the close correlation between contamination intensity, urban population density, and human activity. These findings have vital public health consequences, as exposure to polluted soils in public parks and children's recreational areas may raise the likelihood of pathogen spread and parasitic infections in urban settings. The study also highlights the need for soil management and remediation strategies that address contamination risks in high-clay, high-contamination zones. Approaches such as improving drainage, reducing compaction, bioaugmentation with beneficial microbial consortia, or partial soil replacement can help reduce pathogen persistence, although methods such as surface sealing may limit soil respiration and ecological function if applied extensively. Combining these measures with ongoing sanitation monitoring and landscape management can promote soil health and decrease exposure risks. Moreover, parameters such as organic matter, pH, and soil moisture interact with clay fraction to shape microbial and helminth persistence, emphasizing the importance of a multi-factor soil quality framework in contamination risk assessments and a need for targeted sanitation measures and informing public health policies to reduce exposure in urban soils. In Kazakhstan, sanitary regulations provide general thresholds for microbiological and helminth contamination in soils; however, these standards do not currently account for granulometric influences. Creating risk criteria tailored to specific textures would enhance the regulatory framework for evaluating the safety of urban soil. Anticipated climate change scenarios, including altered precipitation patterns, freeze–thaw cycles, and variable soil moisture, may further influence microbial survival dynamics and helminth egg persistence by modifying hydrological regimes and organic matter stability in clay-rich soils. Analyzing the relationships between clay contamination in Astana and other Central Asian cities with semi-arid climates and comparable geological foundations may yield important regional insights into soil-mediated contamination processes. Furthermore, the integrated granulometric, microbiological, and geospatial framework developed in this study presents a scalable strategy that can be tailored to observe more contaminants, including heavy metals, hydrocarbons, and antibiotic-resistant bacteria, thereby broadening its applicability to extensive environmental and public health monitoring. Future investigations could incorporate molecular or biochemical methods to identify virulence-associated genes and evaluate whether soil granulometric composition differentially affects the survival or distribution of pathogenic versus non-pathogenic populations. Moreover, molecular and metagenomic approaches, such as qPCR, 16S rRNA sequencing, or DNA-based helminth detection, could be employed to capture non-culturable organisms, characterize microbial and helminth diversity, identify contamination sources, and evaluate how soil texture and granulometric composition influence their presence and persistence.

AUTHOR CONTRIBUTIONS

A. Zandybay, the corresponding author, has contributed in supervising the study, coordinating the data analysis, interpreting the results, and preparing the manuscript. A. Kydyrova performed the data analysis, interpreted the results, and assisted in preparing the manuscript. N. Aikenova contributed to the processing of data and interpretation of the results. A. Sagnaeva participated in data analysis and preparation of figures. D. Narodkhan contributed to the interpretation of the results. G. Adilbektegy assisted in preparing the figures and interpreting the results. T. Mkilima participated in the interpretation of the results and manuscript preparation.

ACKNOWLEDGEMENT

The work was carried out with the financial support of grant funding for scientific and (or) scientific and technical projects for 2023–2025 from the Ministry of Science and Higher Education of the Republic of Kazakhstan [IRN AP19679898].

CONFLICT OF INTEREST

The authors declare that there is no conflict of interest regarding the publication of this manuscript. In addition, ethical issues, including plagiarism, informed consent, misconduct, data fabrication and/

or falsification, double publication and/or submission, and redundancy have been completely observed by the authors.

OPEN ACCESS

©2026 The author(s). This article is licensed under a Creative Commons Attribution 4.0 International License, which permits use, sharing, adaptation, distribution and reproduction in any medium or format, if you give appropriate credit to the original author(s) and the source, provide a link to the Creative Commons license, and indicate if changes are made. The images or other third-party material in this article are included in the article's Creative Commons license, unless indicated otherwise in a credit line to the material. If material is not included in the article's Creative Commons license and your intended use is not permitted by statutory regulation or exceeds the permitted use, you will need to obtain permission directly from the copyright holder. To view a copy of this license, visit: http://creativecommons.org/licenses/by/4.0/

PUBLISHER'S NOTE

GJESM Publisher remains neutral regarding jurisdictional claims in published maps and institutional afflictions.

☒ Negative AI Statement

The author(s) declared that no AI tools or services were not used or not highly applied during the preparation of this work.

ABBREVIATIONS

%	Percent
°C	Degrees Celsius
/g	Per gram
ANOVA	Analysis of Variance
CFU	Colony forming unit
CFU/g	Colony forming units per gram
cm	Centimeter
R^2	Coefficient of determination
Escherichia coli	*Escherichia coli*
Esri	Environmental Systems Research Institute
F-statistic	Fisher–snedecor (F)-statistic
Fig.	Figure
GIS	Geographic information system
g	Gram
GOST	Gosudarstvennyy Standart (State Standard)
GPS	Global positioning system
IRN	Internal reference number
km^2	Square Kilometers
m	Meter
RMSE	Mean Square Error
mm	Millimeter
n	Sample size
NaOH	Sodium hydroxide
p-value	Probability value
SD	Standard deviation

REFERENCES

Abdellatif, M.A.; El Baroudy, A.A.; Arshad, M.; Mahmoud, E.K.; Saleh, A.M.; Moghanm, F.S.; Shaltout, K.H.; Eid, E.M.; Shokr, M.S., (2021). A GIS-based approach for the quantitative assessment of soil quality and sustainable agriculture. Sustainability. 13: 13438 **(23 pages).**

Abdukerim, R.; Khidirov, K.; Amangeldikyzy, Z.; Mussina, M.; Yeszhanov, T.; Gritsenko, D.; Mendybayeva, A.; Tursynkulov, A., (2025). Biodiversity of entomopathogenic fungi genus Beauveria in the soils of arid zone. Global J. Environ. Sci. Manage., 11(1): 193-206 **(16 pages).**

Ahmed, W.; Hamilton, K.; Toze, S.; Cook, S.; Page, D., (2019). A review on microbial contaminants in stormwater runoff and outfalls: Potential health risks and mitigation strategies. Sci. Total Environ., 692: 1304–1321 (**18 pages**).

Arunrat, N.; Sereenonchai, S.; Uttarotai, T., (2025). Effects of soil texture on microbial community composition and abundance under alternate wetting and drying in paddy soils of central Thailand. Sci. Rep. 15: 24155 **(11 pages).**

Biesgen, D.; Frindte, K.; Maarastawi, S.; Knief, C., (2020). Clay content modulates differences in bacterial community structure in soil aggregates of different size. Geoderma. 376: 114544 **(12 pages).**

Britt, V.H.; Liao, M.-K.; Lewis, G.P., (2024). Abundance of fecal indicator bacteria and diversity of *Escherichia coli* associated with poultry farms and pastureland cover in streams of northwestern South Carolina. Environ. Monit. Assess. 197: 15 **(21 pages)**.

Cappuccino, J.G.; Sherman, N., (2020). Microbiology: A Laboratory Manual. 12th ed. Pearson. **(560 pages)**.

Chai, T.; Draxler, R.R., (2014). Root mean square error (RMSE) or mean absolute error (MAE)? - Arguments against avoiding RMSE in the literature. Geosci. Model Dev., 7: 1247–1250 (**4 pages**).

Chicco, D.; Warrens, M.J.; Jurman, G., (2021). The coefficient of determination R-squared is more informative than SMAPE, MAE, MAPE, MSE and RMSE in regression analysis evaluation.

PeerJ Comput. Sci., 7: e623 (**13 pages**).

Christel, A.; Dequiedt, S.; Chemidlin-Prevost-Bouré, N.; Mercier, F.; Tripied, J.; Comment, G.; Djemiel, C.; Bargeot, L.; Matagne, E.; Fougeron, A.; Mina Passi, J.B.; Ranjard, L.; Maron, P.A., (2023). Urban land uses shape soil microbial abundance and diversity. Sci. Total Environ. 896: 163455 **(13 pages)**.

Correia, A.; Rasteiro, M., (2025). A Review of Persistent Soil Contaminants: Assessment and Remediation Strategies. Environments. 12: 229 **(24 pages)**.

Derongs, L.; Druilhe, C.; Ziebal, C.; Le Maréchal, C.; Pourcher, A.M., (2020). Characterization of *Clostridium perfringens* isolates collected from three agricultural biogas plants over a one-year period. Int. J. Environ. Res. Public Health. 17: 5450 **(16 pages)**.

Gao, D.; Zhang, N.; Liu, S.; Ning, C.; Wang, X.; Feng, S., (2023). Urbanization Imprint on Soil Bacterial Communities in Forests and Grasslands. Forests. 14: 38 **(16 pages)**.

Gill, A.S.; Purnell, K.; Palmer, M.I.; Stein, J.; McGuire, K.L., (2020). Microbial Composition and Functional Diversity Differ Across Urban Green Infrastructure Types. Front. Microbiol. 11: 912 **(13 pages)**.

Hammam, A.A.; Mohamed, W.S.; Sayed, S.E.E.; Kucher, D.E.; Mohamed, E.S., (2022). Assessment of Soil Contamination Using GIS and Multi-Variate Analysis: A Case Study in El-Minia Governorate, Egypt. Agronomy. 12: 1197 **(21 pages)**.

Hermans, S.; Gautam, A.; Lewis, G.D.; Neale, M.; Buckley, H.L.; Case, B.S.; Lear, G., (2024). Exploring freshwater stream bacterial communities as indicators of land use intensity. Environ. Microbiome. 19: 45 **(17 pages)**.

Horiuchi, S.; Uga, S., (2016). Modified flotation method, an effective technique for recovering helminth eggs in soil. Parasitol. Int. 65: 576-579 **(4 pages)**.

Kochanek, A.; Generowicz, A.; Zacłona, T., (2025). The role of geographic information systems in environmental management and the development of renewable energy sources—A Review Approach. Energies. 18: 4740 **(20 pages)**.

Mao, H.-R.; Cotrufo, M.F.; Hart, S.C.; Sullivan, B.W.; Zhu, X.; Zhang, J.; Liang, C.; Zhu, M., (2024). Dual role of silt and clay in the formation and accrual of stabilized soil organic carbon. Soil Biol. Biochem. 192: 109390 **(11 pages)**.

Koswanudin, D.; Widyanto, H.; Hutapea, D.; Wawan; Yuniawati, R.; Subagyo, V.N.O.; Utami, S.; Samudra, I.; Darwiati, W., (2025). Ecological population dynamics, host preferences, and associated parasitoids of Bactrocera carambolae and Bactrocera papayae on fruits. Global J. Environ. Sci. Manage., 11(2): 631-652 **(22 pages).**

Marques, M.V.A.; Lopes, B.C.; Silvério, T.H.R.; von Sperling, M.; Neves, T.D.A., (2023). Persistence of pathogens and bacterial community dynamics in tropical soil after application of raw sewage. Sci. Rep., 13: 12345 **(12 pages)**.

Mhete, M.; Eze, P.N.; Rahube, T.O.; Akinyemi, F.O., (2020). Soil properties influence bacterial abundance and diversity under different land-use regimes in semi-arid environments. Sci. Afr. 7: e00246 **(10 pages)**.

Ministry of Health of the Republic of Kazakhstan, (2018). Order No. 21: Sanitary rules and regulations — Methods for determining microbiological contamination of soils. Nur-Sultan. (35 pages).

National Atlas of the Republic of Kazakhstan, (2010). Volume II: Natural Conditions and Resources. Almaty: Institute of Geography. **(180 pages)**.

Pande, V.; Pandey, S.C.; Sati, D.; Bhatt, P.; Samant, M., (2022). Microbial interventions in bioremediation of heavy metal contaminants in agroecosystem. Front. Microbiol., 13: 824084 (**16 pages**).

Obayomi, O.; Seyoum, M.M.; Ghazaryan, L.; Tebbe, C.C.; Murase, J.; Bernstein, N.; Gillor, O., (2021). Soil texture and properties rather than irrigation water type shape the diversity and composition of soil microbial communities. Appl. Soil Ecol. 157: 103834 **(11 pages)**.

Richiedei, A.; Giuliani, M.; Pezzagno, M., (2024). Unveiling the Soil beyond Definitions: A Holistic Framework for Sub-Regional Soil Quality Assessment and Spatial Planning. Sustainability. 16: 6075 **(20 pages)**.

Rodríguez-González, L.; Díaz-Raviña, M.; Sevilla-Morán, B.; García-Campos, E.; Villaverde, J.J.; Arias-Estévez, M.; Fernández-Calviño, D.; Santás-Miguel, V., (2025). Influence of soil type on bacterial growth and tolerance to experimentally added human antibiotics. Ecotoxicol. Environ. Saf. 290: 117614 **(10 pages)**.

Sager, M., (2020). Urban soils and road dust—civilization effects and metal pollution—a review. Environments. 7: 98 **(25 pages)**.

Sedgwick, P., (2012). One way analysis of variance. BMJ, 344: e2427 (**2 pages**).

Shao, M.; Zhang, S.; Niu, B.; Pei, Y.; Song, S.; Lei, T.; Yun, H., (2022). Soil texture influences soil bacterial biomass in the permafrost-affected alpine desert of the Tibetan plateau. Front. Microbiol. 13: 1007194 **(12 pages)**.

Steenwerth, K.L.; Jackson, L.E.; Calderón, F.J.; Stromberg, M.R.; Scow, K.M., (2002). Soil microbial community composition and land use history in cultivated and grassland ecosystems of coastal California. Soil Biol. Biochem. 34: 1599–1611 **(13 pages)**.

Stephanou, C.; Omirou, M.; Philippot, L.; Zissimos, A.M.; Christoforou, I.C.; Trajanoski, S.; Oulas, A.; Ioannides, I.M., (2021). Land use in urban areas impacts the composition of soil bacterial communities involved in nitrogen cycling. A case study from Lefkosia (Nicosia) Cyprus. Sci. Rep. 11: 8198 **(13 pages)**.

Thomson, T.; Ellis, J.I.; Fusi, M.; Prinz, N.; Lundquist, C.J.; Bury, S.J.; Shankar, U.; Cary, S.C.; Pilditch, C.A., (2024). Effects of catchment land use on temperate mangrove forests. Sci. Total Environ. 940: 173579 **(12 pages)**.

Vermeulen, L.C.; de Kraker, J.; Hofstra, N.; Kroeze, C.; Medema, G., (2015). Modelling the impact of sanitation, population growth and urbanization on human emissions of Cryptosporidium to surface waters—a case study for Bangladesh and India. Environ. Res. Lett. 10: 094017 **(11 pages)**.

Wang, S.; Wang, Y.; Li, Z.; Li, C., (2025). Soil Texture's Hidden Influence: Decoding Plant Diversity Patterns in Arid Ecosystems. Soil Syst. 9: 84 **(16 pages)**.

Wang, R.-Z.; Hu, X., (2024). Seasonal freeze–thaw processes impact microbial communities of soil aggregates associated with soil pores on the Qinghai–Tibet Plateau. Ecol. Process., 13: 40 (**11 pages**).

Wani, O.A.; Sharma, V.; Kumar, S.S.; Malik, A.R.; Pandey, A.; Devi, K.; Kumar, V.; Gairola, A.; Yadav, D.; Valente, D.; Petrosillo, I.; Babu, S., (2024). Geostatistical modelling of soil properties towards long-term ecological sustainability of agroecosystems. Ecol. Indic. 166: 112540 **(14 pages)**.

Wu, J.; Jiang, J.; Xu, C.; Cai, Y.; Li, M.; Yang, Y.; Yang, G.; Meng, X.-Z.; Leib, J.; Zhang, H.; Zhang, S., (2024). A comprehensive assessment of heavy metals, VOCs and petroleum

hydrocarbon in different soil layers and groundwater at an abandoned Al/Cu industrial site. Ecotoxicol. Environ. Saf. 284: 116927 **(12 pages)**.

Xia, Q.; Rufty, T.; Shi, W., (2020). Soil microbial diversity and composition: Links to soil texture and associated properties. Soil Biol. Biochem. 149: 107953 **(10 pages).**

AUTHOR (S) BIOSKETCHES

Zandybay, A., Ph.D., Associate Professor, L.N. Gumilyov Eurasian National University, Astana, Kazakhstan.
- Email: *zandybay_a@enu.kz*
- ORCID: 0000-0001-8485-2988
- Web of Science ResearcherID: P-7298-2014
- Scopus Author ID: 57340597900
- Homepage: https://fns.enu.kz/en/page/departments/department-of-environmental-management-and-engineering/professorial-and-teaching-staff

Sagnaeva, A., M.Sc., Researcher, L.N. Gumilyov Eurasian National University, Astana, Kazakhstan.
- Email: *sagnaeva_asyltas@mail.ru*
- ORCID: 0000-0002-9162-6791
- Web of Science ResearcherID: NA
- Scopus Author ID: NA
- Homepage: https://omgpu.ru/dissertations/sagnaeva-asyltas-toktamysovna

Kaliyeva, S., Ph.D., Astana International University, Astana, Kazakhstan.
- Email: *saltanat_kalieva@aiu.edu.kz*
- ORCID: 0009-0003-7223-1203
- Web of Science ResearcherID: NA
- Scopus Author ID: 57194223653
- Homepage: https://aiu.kz/ru/schools/8/pps

Adilbektegy, G. Ph.D., Associate Professor, L.N. Gumilyov Eurasian National University, Astana, Kazakhstan.
- Email: adilbektegi_ga@enu.kz
- ORCID: 0000-0002-1521-0145
- Web of Science Researcher ID: P-7744-2014
- Scopus Author ID: 57211508211
- Homepage: https://fns.enu.kz/en/page/departments/department-of-environmental-management-and-engineering/professorial-and-teaching-staff

Narodkhan, D., Ph.D., Senior lecturer, L.N. Gumilyov Eurasian National University, Astana, Kazakhstan.
- Email: *d.narodkhan@ktu.edu.kz*
- ORCID: 0000-0001-9747-6774
- Web of Science ResearcherID: NA
- Scopus Author ID: 57219859353
- Homepage: https://person.kstu.kz/en/narodkhan-dashzhan/

Daribay, A., Ph.D., Professor, L.N. Gumilyov Eurasian National University, Astana, Kazakhstan.
- Email: daribai_ao@enu.kz
- ORCID: 0009-0008-3946-0684
- Web of Science ResearcherID: NA
- Scopus Author ID: 52663184800
- Homepage: https://fns.enu.kz/en/page/departments/department-of-environmental-management-and-engineering/professorial-and-teaching-staff

Mkilima, T., Ph.D., Lecturer, Department of Environmental Engineering and Management, The University of Dodoma, 1 Benjamin Mkapa Road, 41218 Iyumbu, Dodoma, Tanzania.
- Email: *tmkilima@gmail.com*
- ORCID: 0000-0003-1170-0494
- Web of Science ResearcherID: AAQ-3820-2020
- Scopus Author ID: 57217095406
- Homepage: https://www.udom.ac.tz/staff/staff_profile?id=VDFSbk1RPT0=

HOW TO CITE THIS ARTICLE

Zandybay, A.; Kydyrova, A.; Aikenova, N.; Sagnaeva, A.; Narodkhan, D.; Adilbektegy, G.; Mkilima, T., (2026). Relationship between urban soil granulometric composition and microbiological and vermicular contamination. Global J. Environ. Sci. Manag., 12(1): 281-296.

DOI: 10.22034/gjesm.2026.01.16

URL: https://www.gjesm.net/article_730831.html

Global J. Environ. Sci. Manage. 12(1): 297-312, Winter 2026, Serial #45

Global Journal of Environmental Science and Management
(GJESM)

Homepage: https://www.gjesm.net/

Podcasts

CASE STUDY

Tropical peat soil variability along landscape and depth gradient using mid-infrared spectroscopy

P.B. Putra[1,2], D. Rachmanadi[1,*], Y. Indrajaya[1], A. Kunarso[1], R.N. Adi[1], A. Jaya[3], T.W. Yuwati[1,2], E. Priyanto[4], W. Halwany[1], A. Noor5, M. Noor[5]

[1] *Research Center for Ecology, National Research and Innovation Agency, KST Soekarno, Cibinong, Indonesia*

[2] *Faculty of Forestry, Gadjah Mada University, Yogyakarta, Indonesia*

[3] *Faculty of Agriculture, University of Palangkaraya, Palangkaraya, Indonesia*

[4] *Center for Watershed Management of Solo, Ministry of Forestry, Surakarta, Indonesia*

[5] *Research Center for Food Crops, National Research and Innovation Agency, KST Soekarno, Cibinong, Indonesia*

ARTICLE INFO

Article History:
Received 15 August 2025
Revised 21 November 2025
Accepted 24 December 2025

Keywords:
Fourier transform infrared (FTIR)
Landscape hydrology
Peatland restoration
Soil organic matter (SOM)

DOI: 10.22034/gjesm.2026.01.17

ABSTRACT

BACKGROUND AND OBJECTIVES: Tropical peatlands, recognized as vital carbon sinks, remain vulnerable to drainage, canal and road construction, as well as frequent seasonal fires. These disturbances modify peat hydrodynamics and stimulate organic matter decay. Understanding chemical peat soil properties such as degree of decomposition provides support for landscape-based peatland management. The goals of this study were to analyze soil organic matter and its fluctuations with depth and location concerning hydrological features in a disturbed tropical peatland.

METHODS: Peat samples were collected every 500 meters along two transects representing different landscape and depth gradients. At every sampling location, samples were collected at every 50 centimeters section, starting from the surface and continuing downwards until the mineral layer. Fourier transform infrared spectroscopy was used to characterize chemical functional groups of peat soil and to quantify the indices of humification, hydrophobicity, aromaticity, and decomposition. To analyze the trends between landscape and depths, principal component analysis was utilized.

FINDINGS: Spectral analysis showed variation of functional groups between landscape and depth. The upper layer of peat exhibited a comparatively greater amount of aliphatic and oxidized substances than the lower layers, whereas the concentration of aromatic and humified structures generally rose with depth. Areas near the river or canal tended to have a lower hydrophobicity and higher decomposition pattern, which suggests a more active aerobic breakdown. Principal component analysis revealed that depth is the main variable that controls the pattern of functional group composition of the soil organic matter, while disturbance and hydrology contribute additional dimensions of spatial variability.

CONCLUSION: Fourier transform infrared spectroscopy is useful for characterizing chemical properties of tropical peat soil. It demonstrates how drainage, hydrological matrix, and fire affect the composition of soil organic matter throughout different landscape and depth. The technique is useful and effective as a diagnostic tool for peat degradation detection to support peatland restoration efforts.

This is an open access article under the CC BY license (http://creativecommons.org/licenses/by/4.0/).

NUMBER OF REFERENCES
36

NUMBER OF FIGURES
8

NUMBER OF TABLES
7

*Corresponding Author:
Email: *dony004@brin.go.id*
Phone: +62 852 4950 4800
ORCID: 0000-0002-9456-5357

Note: Discussion period for this manuscript open until Mar 1, 2026 on GJESM website at the "Show Article".

INTRODUCTION

Although peatlands comprise only a minor percentage of terrestrial ecosystems, they store one-third of global carbon soil (Girkin *et al.,* 2023). Of the 400 million hectares (Mha) of global peatlands, about 31-41 Mha (~10-12%), are in the tropics. Southeast Asia, particularly Indonesia and Malaysia, hosts 77% carbon (C) of the tropical peat carbon storage (Page, 2024). Peatland ecosystems are formed over a very long period (between 3,550 - 6,000 years ago) under constantly waterlogged conditions. Hydrology is a fundamental factor in the formation and function of tropical peatlands (Ratnayake, 2020). Drainage serves as a means through which tropical peat forests are transformed into alternative land uses, leading to substantial carbon loss due to drying. Drainage or lowering the water table provides substantial oxygen to the upper layer, thereby increasing decomposer microbial activity. The escalation of microbial activity results in physical modifications to organic matter and causes the subsidence of peat (Anshari *et al*., 2021), consequently increasing the susceptibility of peatlands to fire (Irfan *et al*., 2024). During drought periods, the canals and roads built to shape the land increase the risk of drought and frequent fires. These adjustments enhance the rate of organic matter losses and change the material characteristics of the peat (Page *et al*., 2022). In Indonesia, effective peatland management has adopted a landscape-based approach within the Peatland Hydrological Unit (PHU/KHG) framework, using the peat characteristics and the hydrological boundaries of rivers, lakes, and the sea (Yakubson *et al*., 2023). This strategy for managing landscapes is largely based on the disturbance-mitigating properties of peatlands, in addition to the role of peatlands in enabling more precise landscape management. Key characteristics like humification, hydrophobicity, aromaticity and the degree of decomposition highlight the characteristics of the peat, supporting the detection of degraded peatland and assisting the risk assessment. Field assessment using the Von Post scale has traditionally been employed to categorize peat decomposition and determine its maturation stage. Nonetheless, this approach is subjective and is affected by moisture conditions. Laboratory analyses, particularly peat carbon-to-nitrogen (C/N) ratios, have been widely used, but their reliability decreases in disturbed peatlands where nitrogen may be lost through burning, leaching, or fertilizer application. Obeng *et al*., (2023) described that Fourier transform infrared (FTIR) spectroscopy offers a swift and economical analytical method for characterizing the composition of soil organic carbon (SOM) without requiring chemical extractions. This technique is also utilized to assess the quality of organic matter, particularly the degree of decomposition (DDI), chemical signatures of carbon, hydrophobic characteristics, and humification index in temperate peat in Ireland. FTIR identifies functional groups that indicate the relative quantities of carbohydrates, lignin derivatives, phenolic compounds, aliphatic structures, and proteins, which are components that undergo systematic changes during peat decomposition (Kunarso *et al*., 2025). FTIR has been successfully applied to differentiate humification stages in temperate peatlands (Ratai *et al*., 2024), assess soil water repellency and hydrophobicity, and detect fire-induced chemical transformations in organic soils (Nurzakiah *et al*., 2020). Despite its promise in revealing degradation gradients tied to hydrology, land use, and fire history, its use in tropical peatlands, including those in Indonesia, remains infrequen. The complex nature of tropical peatland landscapes, particularly those that have been drained, and subject to repeated fire, highlights the urgency of applying FTIR to characterize peat soil quality. FTIR-based indices of hydrophobicity, humification, aromaticity and peat decomposition provide valuable information on peat soil quality, offering quantitative insights into its variation between land uses and depths. This study presents novel findings regarding the quality of organic matter in peat across different land uses and hydrological conditions by analyzing FTIR spectral signatures in connection with proximity to rivers and canal systems, as well as varying peat depths. This study aims to assess the humification index, hydrophobicity, aromaticity, and degree of decomposition of tropical peat soils from two contrasting landscape transects in the Tumbang Nusa peatland of Central Kalimantan, Indonesia.

MATERIALS AND METHODS

Study area

The study was conducted in the Tumbang Nusa peatland forest, Pulang Pisau Regency, Central Kalimantan, Indonesia. The area lies between 2021'S - 2017'S and 11403'E - 11406'E on Kalimantan's

southern side, a flat lowland at 1 meter above sea level, within the Kahayan - Sebangau Peatland Hydrological Unit (PHU/KHG). Due to its location near the equator, it experiences a tropical wet climate (Fig. 1). This landscape has been heavily impacted and modified by extensive drainage canal systems and the Trans-Kalimantan road network. These alterations in hydrology have disrupted the natural water flow, leading to severe desiccation during the dry season and inundation during the wet season. The site has a history of peat-fires, including the major fire event in 2015. The site characteristic of the study area showed at Table 1.

Two landscape transects were established with the Trans- Kalimantan Road as the starting point. The first transect extends westward toward the Kahayan River (hereafter referred to as the Hawuk transect) for approximately 3.5 kilometers (km) with sampling intervals of 500 m. The second transect extends eastward toward a secondary drainage canal (hereafter the Repeat transect, corresponding to an area restored after the 2015 fire) for approximately 3 km, also at 500-m intervals. At each transect point, peat depth was measured to the underlying mineral sub-stratum using a peat auger (Fig. 2).

Soil sampling

Soil samples were collected in September 2020. A total of 75 peat samples were obtained from the two transects. At every 500-meter (m) sampling interval, peat samples were taken from every 50-centimeter (cm) segment, beginning from the surface and continuing downwards until the mineral layer was encountered (Table 2). For each depth increment, approximately the central portion (about 5 cm) of the auger core was taken to minimize contamination from adjacent layers. Prior to soil collection, above ground vegetation was trimmed on each site to prevent contamination. Samples were collected with an Eijkelkamp peat auger, sealed in airtight containers, and transported to the laboratory for processing. Samples were oven-dried at 60 degrees Celsius (°C)

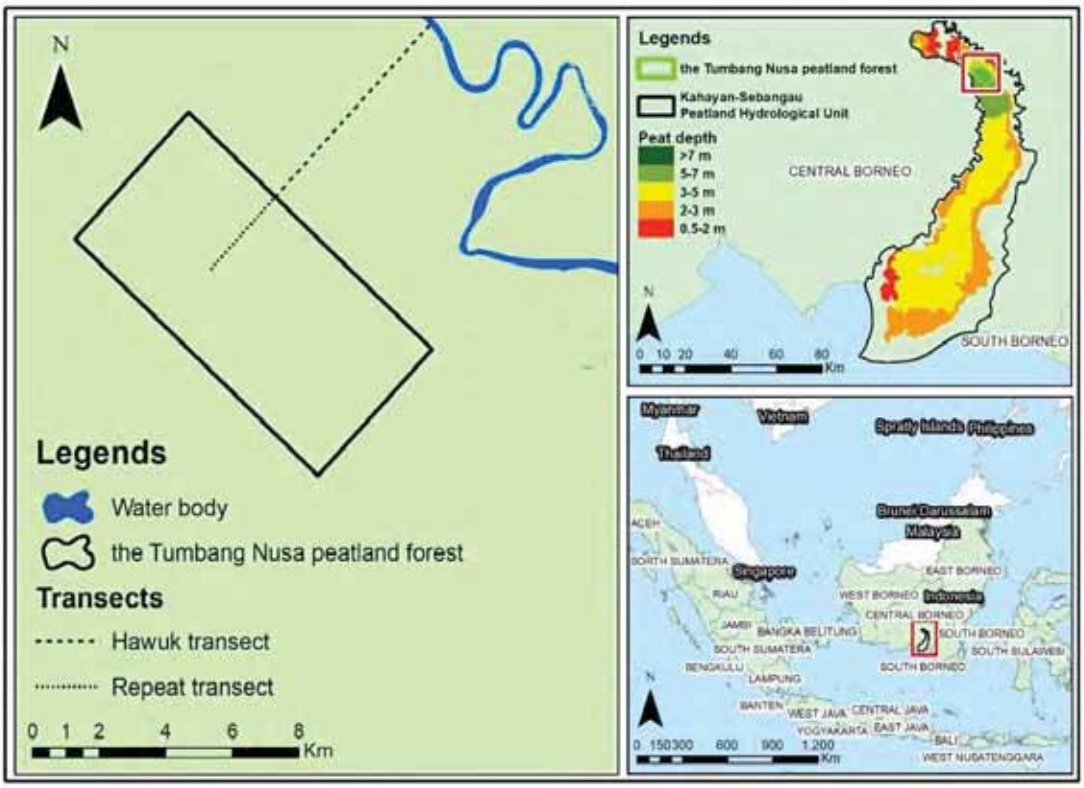

Fig. 1: Geographical location of the study area in the Tumbang Nusa peatland forest in Pulang Pisau Regency, Central Kalimantan, Indonesia

Table 1: Site characteristic of the study area

No.	Site characteristic	Repeats transect	Hawuk transect
1	Land cover/Dominant vegetation*	*Combretocarpus rotundatus, Cratoxylon glaucum, Ploarium alternafolium*	*Acacia mangium, Combretocarpus rotundatus,* and shrubs near the river
2	Peat depth (cm)	344±41.3(296-399)	780.3±418.7(260-1250)
3	Sub-stratum layer	Clay	Clay
4	Peatland type	Ombrotrophic	Ombrotrophic
5	Disturbance history	- Fire events: two times (1997, 2015) - Canal construction: 1993 and closed by backfilling in 2018 - Road development: around 1985	More than two times (1993, 1997, 2007, 2010, 2015, 2019)
6	Hydrological characteristic/ water table depth (cm)	-18.1±13.4 (-37 to 2)	-19.4±10.9 (-40 to 5)
7	Chemical properties		
	- pH H_2O	3.16±0.24(2.33-3.82)	3.24±0.34(2.23-3.88)
	- pH KCl	2.02±0.17(1.76-2.61)	2.14±0.31(1.85-3.11)
	- DHL (%) (Conductometer)	168.66±48.02(65.5-309)	106.56±51.78(11.9-280.1)
	- C-organic (%) (Walkey-Black)	52.70±5.48(43.46-71.94)	51.60±2.58(43.89-56.12)
	- N total (%) (Kjehdal)	0.42±0.12(0.04-0.76)	0.52±0.14(0.22-0.97)
	- N available (ppm) (Morgan Wolf)	69.42±25.41(31-144)	83.22±27.06(30-137)
	- P available (ppm) (Morgan Wolf)	29±19.4 (11-98)	60.54±61.14(3-377)
	- K available (ppm) (Morgan Wolf)	157.93±33.97(39-215)	41.88±23.23(8-97)
	- Ash content (%) (Ignition)	1.26±1.27(0.20-5.34)	1.85±3.01(0.24-13.79)

*Qirom *et al*., (2023)

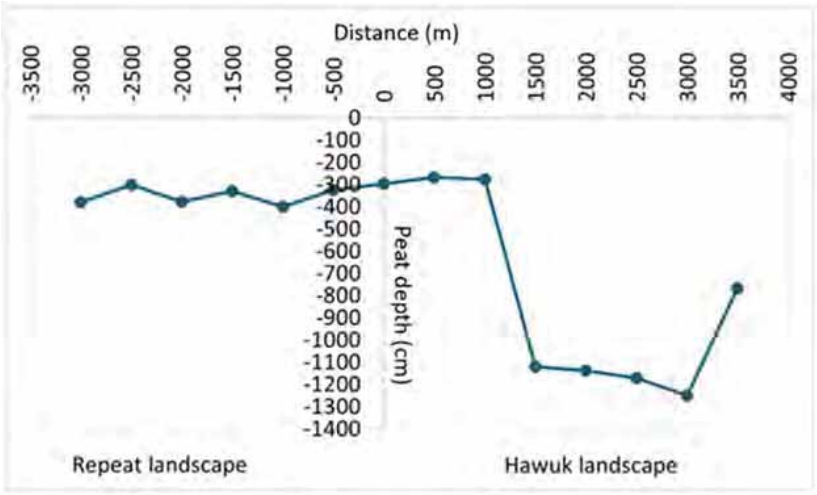

Fig. 2: Peat depth in Tumbang Nusa Peatland Forest, Central Kalimantan observed in repeats transect and hawuk transect

until a constant mass, then ground into a fine powder for FTIR analysis.

FTIR spectroscopy

FTIR spectra were obtained at the Faculty of Math and Natural Science, Gadjah Mada University using a Shimadzu spectrophotometer. Each peat sample was scanned in the mid-infrared region from 4000 to 450/cm. The analysis was executed in transmission mode employing a KBr pellet, featuring a resolution of 4/cm and averaging 64 scans for each sample. Spectra analysis was conducted at R version 4.5.2 and R-Studio version 2025.09.2 (Build 418). Spectra data read uses hyperSpec package to trim and resample to specified

Table 2: The number of peat samples from the distance and each section

Depth class	Depth (cm)	Number of samples
Hawuk transect		
0 - 50 cm	20	7
50 - 100 cm	70	7
100 - 150 cm	120	7
200 - 250 cm	220	6
300 - 350 cm	320	4
400 - 450 cm	420	1
450 - 500 cm	470	3
600 - 650 cm	620	2
650 - 700 cm	670	2
700 - 750 cm	720	1
800 - 850 cm	820	1
850 - 900 cm	870	1
900 - 950 cm	920	2
Repeats transect		
0 - 50 cm	20	7
50 - 100 cm	70	7
100 - 150 cm	120	7
200 - 250 cm	220	7
300 - 350 cm	320	3
Total		75

wavenumbers using a loess function. Preprocessing of the spectra was performed for baseline correction uses baseline package. Peak height values were extracted for functional groups of interest. The tasks were conducted in accordance with the established FTIR interpretations for soil organic matter, focusing on carbohydrate, aromatic, aliphatic, hydrophobic and hydrophilic functional groups (Obeng *et al*., 2023).

Humification index (HI)

Humification reflects the relative abundance of resistance vs. labile organic compounds. The HI was computed using peaks associated with 1050/cm (polysaccharides; C–O stretching), 1410/cm (phenolic O–H deformation; C–O stretching) and 1520/cm (aromatic C=C / amide II) (Obeng *et al*., 2023), or the ratios of 1620/1030 (aromatic C=C or COO-/ polysaccharides), 1420/1030 (OH deformation and CO stretch of phenols), and 1710/1030 (carboxyl C=O and aromatic esters/ polysaccharides) (Ratai *et al*., 2024). In this regard, the Eqs. 1 and 2 were applied (Obeng *et al*., 2023):

$$(1) = \frac{e \quad er \quad 1\ 10 \quad c}{e \quad er \quad 1050 \quad c} \tag{1}$$

$$(2) = \frac{e \quad er \quad 1520 \quad c}{e \quad er \quad 1050 \quad c} \tag{2}$$

Hydrophobicity and aromaticity

The hydrophobic/hydrophilic group was calculated as the parameter of peat soil hydrophobicity or SOM water repellence. The hydrophobic/hydrophilic signifies the ratio of carbon-hydrogen (C–H) groups relative to those of the carbonyl (C=O) group of the peat substrate. As stated by Heller *et al*. (2015), a high level of hydrophobicity (as indicated by the ratio of C–H to C=O bonds) implies a degree of protection for SOM against microbial degradation. Consequently, the hydrophobicity of the peat soil was assessed using Eq. 3 (Obeng *et al*., 2023):

$$ydr \qquad c\ y = \frac{ydr \quad c \quad c \quad l\ r \quad s}{ydr \quad l\ c \quad c \quad l\ r \quad s} \tag{3}$$

where:

- 2983 + 2921/cm represent aliphatic C–H stretching (hydrophobic)
- 1720/cm represents C=O stretching (hydrophilic)

Degrees of decomposition (DDI)

The decomposition of SOM has traditionally been measured by the proportion of hydrophilic compounds to the combined aromatic and aliphatic compounds (Könönen *et al*., 2018). Consequently, the peak intensity at 1720/cm, representing the hydrophilic components, was divided by the sum of the peak height at 2983 + 2921/cm to ascertain

the extent of decomposition of peat organic matter (Obeng *et al*., 2023).

Data analysis

A descriptive analysis was conducted to assess variations in peak intensity across different distance gradients and peat depths. Trends in the humification index, hydrophobicity, aromaticity, and degree of decomposition were examined for both transects. To assess multivariate relationships, principal component analysis (PCA) was performed on the four indices (HI, hydrophobicity, aromaticity, and DDI). Only components with eigenvalues >1 were retained. PCA outputs were visualized using biplots to illustrate clustering patterns related to distance from river or canal and peat depth. All statistical analyses were conducted in R version 4.5.2.

RESULTS AND DISCUSSION

FTIR spectral characteristics across distances and peat depths

The FTIR spectra obtained from peat samples across both transects exhibited the anticipated range of functional groups commonly found in tropical peatlands. These included absorption peaks linked to polysaccharides at 1050/cm, phenolic O–H deformation at 1410/cm, aromatic ring vibrations at 1520 and 1610/cm, hydrophilic carbonyl groups in 1720/cm, and aliphatic C–H stretching at 2921 and 2983/cm (Tables 3 and 4). The peaks were consistently present in the samples; however, there was significant variation in their intensities based on both depth and distance. The chemical composition of SOM is influenced by various interacting factors, such as hydrological gradients, disturbance history, and vertical decomposition processes (Dettmann *et al*., 2021). The identified patterns are indicative of significantly degraded and fire-impacted tropical peatlands that have faced drainage and in situ variations in situ organic matter alternations over small areas (Page *et al*., 2022). Across both transects, aliphatic peaks in surface peat layers exhibited the highest intensity, suggesting the presence of input waxes, microbially derived lipids, and fresh litter from the acrotelm. With increasing depth, aromatic peaks became more pronounced, indicating the presence of lignin and phenolic structures that exhibit greater resistance to decomposition in anaerobic conditions. In mid-depth peat layers (120–320 cm), carbohydrate-associated peaks were notably more pronounced, aligning with the presence of partially decomposed yet identifiable plant polymers typical of the catotelm. The spectral patterns indicate that vertical stratification is a key organizing factor; however, disturbance-driven heterogeneity, especially in the Repeat transect, challenges some traditional distinctions between acrotelm and catotelm peat layers. The results corroborate earlier observations that modern human activities often interfere with natural peatland layers (Mishra *et al*., 2021).

Table 3: The peak targets following the distance to river and canal

Distance (m)	Peak 2920	Peak 2850	Peak 1720	Peak 1640	Peak 1520	Peak 1410	Peak 1110	Peak 1050
Hawuk transect								
Hawuk_0	0.23±0.11	0.13±0.06	0.53±0.13	0.61±0.15	0.20±0.07	0.29±0.08	0.19±0.05	0.18±0.05
Hawuk_500	0.24±0.18	0.12±0.09	0.33±0.11	0.37±0.12	0.09±0.04	0.14±0.05	0.10±0.04	0.09±0.04
Hawuk_1000	0.19±0.06	0.10±0.03	0.46±0.15	0.56±0.16	0.15±0.05	0.23±0.07	0.18±0.06	0.19±0.06
Hawuk_1500	0.20±0.09	0.12±0.05	0.43±0.23	0.53±0.25	0.12±0.07	0.19±0.11	0.16±0.07	0.16±0.06
Hawuk_2000	0.20±0.08	0.11±0.04	0.43±0.21	0.52±0.24	0.15±0.09	0.22±0.11	0.17±0.07	0.16±0.07
Hawuk_2500	0.21±0.11	0.12±0.06	0.46±0.19	0.56±0.17	0.19±0.04	0.26±0.08	0.20±0.05	0.21±0.06
Hawuk_3000	0.21±0.07	0.11±0.04	0.55±0.17	0.69±0.20	0.22±0.08	0.29±0.09	0.25±0.09	0.26±0.08
Repeats transect								
Repeat_0	0.25±0.18	0.13±0.09	0.42±0.07	0.48±0.06	0.15±0.04	0.21±0.04	0.15±0.04	0.13±0.04
Repeat_500	0.17±0.03	0.09±0.01	0.46±0.09	0.57±0.15	0.20±0.07	0.24±0.06	0.18±0.05	0.17±0.03
Repeat_1000	0.14±0.06	0.08±0.03	0.36±0.15	0.42±0.16	0.11±0.04	0.18±0.07	0.12±0.05	0.11±0.05
Repeat_1500	0.23±0.07	0.13±0.03	0.54±0.27	0.62±0.30	0.20±0.07	0.28±0.12	0.18±0.08	0.16±0.08
Repeat_2000	0.13±0.03	0.07±0.01	0.32±0.07	0.39±0.10	0.14±0.02	0.18±0.03	0.11±0.03	0.10±0.04
Repeat_2500	0.24±0.07	0.14±0.03	0.44±0.14	0.50±0.18	0.10±0.07	0.16±0.08	0.15±0.06	0.16±0.07
Repeat_3000	0.16±0.05	0.10±0.03	0.40±0.19	0.46±0.22	0.08±0.06	0.15±0.10	0.11±0.06	0.10±0.06

Table 4: The peak targets following the peat depth

Peat depth (cm)	Peak 2920	Peak 2850	Peak 1720	Peak 1640	Peak 1520	Peak 1410	Peak 1110	Peak 1050
Hawuk transect								
20	0.26±0.13	0.14±0.07	0.52±0.26	0.61±0.31	0.16±0.10	0.24±0.13	0.19±0.10	0.17±0.08
70	0.15±0.04	0.09±0.02	0.39±0.10	0.47±0.11	0.12±0.05	0.19±0.07	0.16±0.07	0.16±0.08
120	0.26±0.10	0.15±0.05	0.64±0.18	0.75±0.20	0.21±0.07	0.32±0.11	0.23±0.06	0.23±0.06
220	0.23±0.09	0.13±0.05	0.45±0.13	0.53±0.14	0.15±0.06	0.22±0.08	0.17±0.06	0.17±0.07
320	0.23±0.10	0.13±0.05	0.51±0.21	0.60±0.21	0.17±0.08	0.25±0.11	0.19±0.06	0.20±0.05
420	0.15	0.08	0.35	0.43	0.16	0.20	0.19	0.20
470	0.22±0.08	0.12±0.04	0.50±0.22	0.62±0.27	0.19±0.13	0.25±0.15	0.22±0.13	0.23±0.14
620	0.17±0.05	0.09±0.03	0.35±0.10	0.50±0.19	0.17±0.04	0.22±0.06	0.20±0.07	0.20±0.07
670	0.11±0.02	0.06±0.01	0.26±0.05	0.40±0.11	0.14±0.00	0.16±0.02	0.14±0.01	0.16±0.03
720	0.07	0.04	0.14	0.20	0.09	0.11	0.08	0.07
820	0.24	0.14	0.51	0.64	0.27	0.32	0.22	0.21
870	0.17	0.09	0.30	0.49	0.20	0.23	0.19	0.22
920	0.16±0.01	0.09±0.00	0.37±0.05	0.51±0.00	0.18±0.01	0.22±0.01	0.19±0.01	0.22±0.04
Repeats transect								
20	0.24±0.16	0.13±0.08	0.32±0.14	0.36±0.20	0.10±0.09	0.14±0.09	0.10±0.07	0.08±0.06
70	0.18±0.05	0.10±0.03	0.47±0.13	0.55±0.14	0.15±0.06	0.22±0.07	0.15±0.05	0.14±0.05
120	0.19±0.06	0.11±0.03	0.50±0.17	0.58±0.18	0.16±0.05	0.24±0.08	0.16±0.04	0.16±0.04
220	0.18±0.06	0.10±0.03	0.44±0.13	0.52±0.14	0.15±0.04	0.21±0.05	0.15±0.05	0.15±0.05
320	0.11±0.04	0.06±0.02	0.25±0.08	0.32±0.09	0.09±0.06	0.12±0.07	0.09±0.05	0.10±0.05

Lateral variation in organic matter components: Effects of hydrological boundaries

The composition of organic matter showed lateral variation across the landscape, indicating distinct influences from hydrological boundaries (Tables 5 and 6). The ratio of aliphatic to carbonyl functional groups indicates that hydrophobicity was consistently lower in areas close to the river (Hawuk transect) and the drainage canal (Repeat transect). The reduction in hydrophobicity signifies enhanced aerobic decomposition at hydrological boundaries, where fluctuating water levels promote oxygen availability to the upper peat layer (Hooijer *et al*., 2024). Rapid fluctuations in the water table temporarily increase aeration, stimulate fungal communities and hydrolytic activity, and accelerate organic decomposition, which can dramatically disrupt carbon storage in peatlands (Kim *et al*., 2021). The susceptibility of these areas to leaching hydrophilic compounds contributes to a shift in soil organic matter composition towards more oxidized states. The patterns of hydrophilic variation varied significantly across the transects. In the Repeat transect, hydrophilic reached its highest point in mid-landscape positions (approximately 1500 m), suggesting a region of heightened oxidation likely connected to alterations caused by the changes following the 2015 burning event. Fire is recognized for its ability to volatilize labile compounds and promote the creation of oxygen-rich charred materials, resulting in layers characterized by an elevated C=O content (Santın and Doerr, 2016). The hydrophilicity in the Hawuk transect increased as one moved toward the river, indicating the effects of lateral inflow and acid drainage on the oxidation of SOM. Aromatic demonstrated a similar variation influenced by landscape position, with elevated levels observed in the mid-landscape regions of the Repeat transect and at further distances from the river in the Hawuk transect. The lateral differences in soil organic matter highlight the significant influence of local hydrology and disturbance legacies on the chemical properties of peat (Giesen *et al*., 2023).

Vertical SOM gradients: Depth as the primary control on organic matter chemistry

The composition of SOM exhibited a more systematic vertical variation compared to horizontal variation based on distance, reinforcing the idea that peat depth is the primary factor influencing peat chemistry in both transects (Nasrul *et al*., 2024). Across the study region, the upper peat layers (0–50 cm) consistently demonstrated elevated aliphatic peak intensities (2921 and 2983/cm), heightened hydrophobicity values, and comparatively low aromaticity (Figs. 3 and 4). The observed patterns indicate the existence of younger, less decomposed organic material, such as leaf waxes, lipids, and various plant-derived aliphatic

Table 5: Organic matter components of peat soil following the distance from river and canal

Distance (cm)	Hydrophobic	Hydrophilic	Aromatic
Hawuk transect			
0	0.28 ±0.13	0.53±0.13	0.83±0.23
500	0.29±0.23	0.33±0.11	0.45±0.18
1000	0.23±0.07	0.46±0.15	0.73±0.21
1500	0.23±0.11	0.43±0.23	0.66±0.32
2000	0.24±0.09	0.43±0.21	0.70±0.33
2500	0.26±0.12	0.46±0.19	0.77±0.21
3000	0.26±0.08	0.55±0.17	0.94±0.29
Repeats transect			
0	0.32±0.22	0.42±0.07	0.64±0.09
500	0.20±0.04	0.46±0.09	0.79±0.22
1000	0.17±0.06	0.36±0.15	0.55±0.21
1500	0.29±0.07	0.54±0.27	0.84±0.39
2000	0.18±0.02	0.32±0.07	0.54±0.12
2500	0.29±0.09	0.44±0.14	0.60±0.26
3000	0.20±0.05	0.40±0.19	0.55±0.29

Table 6: Organic matter components of peat soil following the peat depth

Peat depth (cm)	Hydrophobic	Hydrophilic	Aromatic
Hawuk transect			
20	0.31±0.16	0.52±0.26	0.77±0.41
70	0.19±0.05	0.39±0.10	0.60±0.17
120	0.31±0.12	0.64±0.18	0.98±0.28
220	0.27±0.11	0.45±0.13	0.70±0.21
320	0.27±0.12	0.51±0.21	0.80±0.30
420	0.19	0.35	0.61
470	0.26±0.10	0.50±0.22	0.83±0.43
620	0.21±0.06	0.35±0.10	0.68±0.24
670	0.14±0.03	0.26±0.05	0.55±0.11
720	0.10	0.14	0.29
820	0.28	0.51	0.94
870	0.24	0.30	0.71
920	0.20±0.01	0.37±0.05	0.71±0.01
Repeats transect			
20	0.30±0.20	0.32±0.14	0.46±0.29
70	0.22±0.06	0.47±0.13	0.71±0.19
120	0.23±0.07	0.50±0.17	0.76±0.23
220	0.22±0.06	0.44±0.13	0.69±0.17
320	0.14±0.05	0.25±0.08	0.42±0.15

compounds that gather in the acrotelm. The upper layers exhibited greater hydrophilic, indicating that the oxidation of carbohydrates and hemicelluloses was enhanced by periodic drying and increased oxygen availability. Research indicates that surface peat in modified tropical peatlands experiences increased rates of aerobic decomposition and oxidation, thereby influencing the emission (Butlers *et al.*, 2025). At intermediate depths (120–320 cm), the composition of SOM changed significantly, showing a greater presence of aromatic and humified materials. This is evidenced by increased peak intensities at 1520 and 1610/cm, along with higher humification indices (Fig. 5). The layers signify the transition into the catotelm, distinguished by anaerobic decomposition, resulting in the selective preservation of components rich in lignin and phenolics. The pronounced aromatic signatures observed at mid-depths are characteristic of peat that have experienced extended anoxic conditions and gradual decomposition, aligning with research conducted in deep domed peatlands in Central Kalimantan and Sumatra (Dommain *et al.*, 2014). The peaks of carbohydrates at 1050/cm were more prominent at these depths, indicating the continued

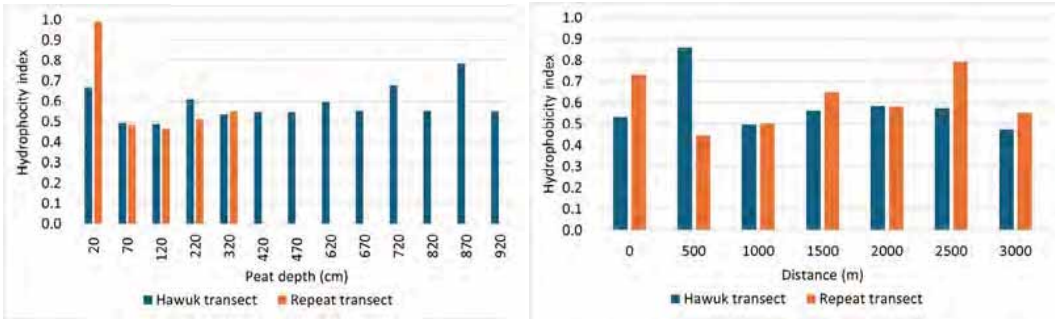

Fig. 3: Characteristic of hydrophobicity following the landscape and peat depth

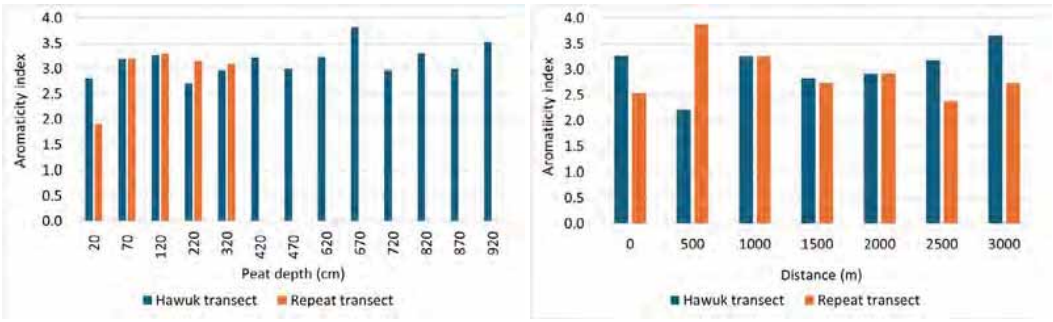

Fig. 4: Characteristic of aromaticity following the landscape and peat depth

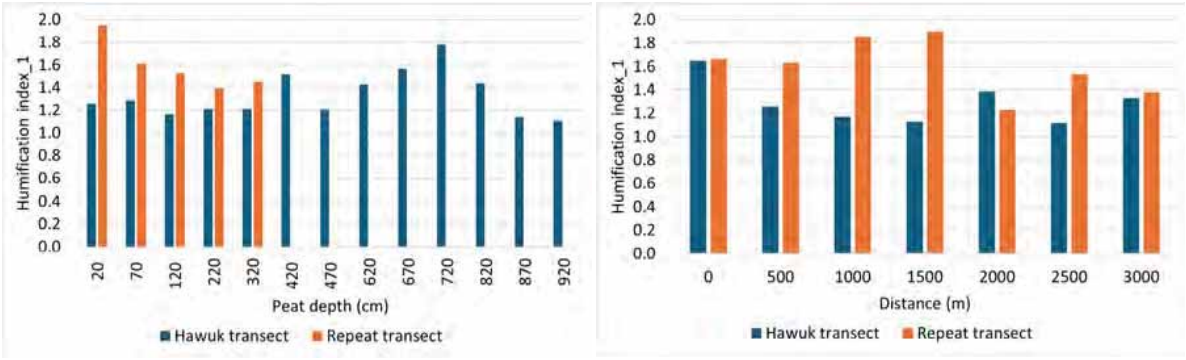

Fig. 5: Characteristic of humification index based on wavenumber 1410/cm following the landscape and peat depth

presence of partially decomposed hemicellulosic material that resists both aerobic and anaerobic decay. Below 400 cm, the characteristics of soil organic matter exhibited a growing diversity, demonstrating fluctuating patterns of increases and decreases in aromaticity, hydrophobicity, and humification indices. This variability could indicate stratigraphic layering resulting from historical changes in vegetation, fluctuations in hydrology, and past disturbances, such as droughts linked to El Niño and long-term alterations in peat swamp forest composition (Evans *et al*., 2022). Comparable deep-profile heterogeneity has been observed in paleoecological research of Southeast Asian peat domes, where shifts in dominant vegetation (such as *Shorea* spp., *Pandanus* sp., and *Campnosperma* sp.) and fire history result in chemically distinct horizons (Dommain *et al*., 2011). In the Repeat transect, alterations caused by fire resulted in uneven vertical patterns, particularly within the upper 200 cm, where the combustion of surface peat probably removed a greater amount of decomposed material and revealed less-decomposed underlying layers. This

study reveals vertical gradients characterized by labile, oxidized upper peat, humified aromatic mid-profile peat, and heterogeneous deeper layers, underscoring the significance of depth in influencing the chemical properties of peat. The observed patterns reinforce the established idea that anaerobic catotelm processes contribute to the long-term preservation of aromatic and recalcitrant soil organic matter. In contrast, the acrotelm is notably influenced by hydrological disturbances and fire (Hirano *et al.*, 2015). Vertical SOM gradients reflect natural peat-forming processes and the influence of historical environmental changes. This underscores the significance of explicitly taking depth into account when evaluating peat condition and carbon stability in degraded landscapes.

Humification index across depths and landscape positions

The humification index (HI), calculated from the ratios of aromatic to carbohydrates and phenolic to polysaccharide, showed complex but identifiable trends over both transects. Overall, HI trends indicated a rise with depth, implying the buildup of anoxic, resilient, lignin-infested organic matter in the catotelm (Figs. 5 and 6) over prolonged durations. HI, however, was not consistent over the years and showed variation about specific depth ranges, particularly in the deeper intervals (>300 cm). Such variations indicate stratigraphic discordances linked to historical vegetation, hydrology, and disturbance dynamics (Klavins *et al.*, 2013). In the Hawuk transect, humification rose from the surface to mid-depth layers (approximately 120 cm) before showing fluctuations at deeper levels. The fluctuations observed likely suggest different depositional periods influenced by climate variability, including droughts caused by El Niño, along with possible historical fire occurrences (Evans *et al.*, 2022). In contrast, the Repeat transect exhibited a notable peak in humification at approximately 1500 m distance, characterized by increased levels of both aromatic and hydrophilic. Fire-related changes have been documented while fire-induced changes involve combustion by removing labile carbohydrates while enhancing the relative proportion of the more stable aromatic compounds. This elevation in the humification signal implies that it is the outcome of humus modified by fire, in contrast to humus originating from unburned natural decomposition (Ming *et al.*, 2023). Recent research results show changes in the properties of organic matter related to forest fires, namely a significant decrease in heat-labile components (especially hemicellulose and cellulose) and a simultaneous increase in aromatic structures, including highly resistant compounds in fire-affected fuels (Shapchenkova *et al., 2023*).

Degree of decomposition (DDI): Divergent trajectories in disturbed vs. undisturbed zones

The DDI defined as the ratio of carbonyl to aliphatic functional groups, exhibited notable differences across transects, highlighting the unique pathways of SOM transformation shaped by disturbance and hydrology (Fig. 7). In the Hawuk transect, DDI reached its peak near the river and in the surface layers, which aligns with aerobic decomposition influenced by shallow peat layers and varying water tables. The process of drainage modifies the soil conditions in peatlands, influencing aspects like groundwater levels, soil temperature, and the composition of microbial communities. The process of drainage enhances aerobic microbial activity, which in turn facilitates a more significant breakdown of the peat layer located near the surface (Yang *et al.*, 2025). In contrast, the Repeat transect showed an inverted vertical decomposition gradient, with lower DDI

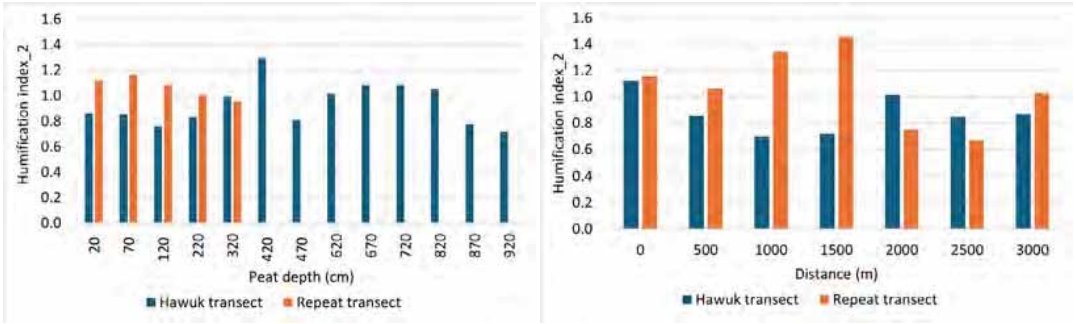

Fig. 6: Characteristic of humification index based on wavenumber 1520/cm following the landscape and peat depth

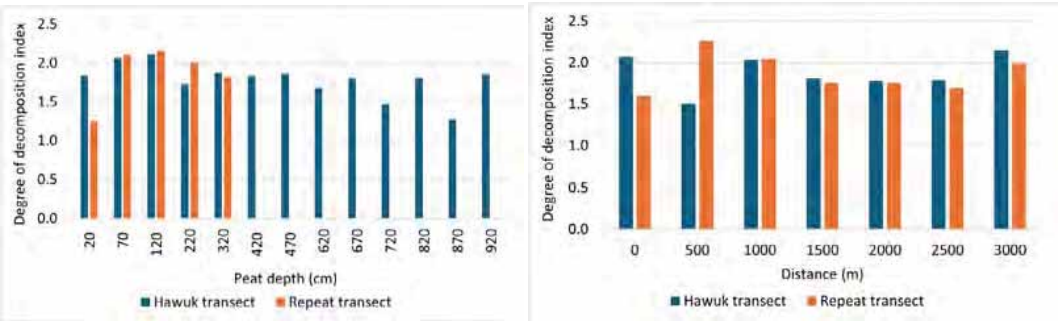

Fig. 7: The degree of decomposition following the landscape and peat depth

values in the surface peat and higher values at greater depths. This distinctive profile suggests that the 2015 fire event led to the removal of decomposed surface peat due to fire effects. Burning primarily targets highly decomposed material, resulting in the retention of less-decomposed peat layers that eventually create the new surface (Zhang *et al*., 2024). The decline of DDI in the upper layer subsequent to the post-fire event is thought to be caused by the fire changing some physiochemical attributes of the peat soil, leading to elevated temperature, pH, and conductivity, while simultaneously reducing oxygen concentration and various microbial groups in the upper layer (Mieczan *et al*., 2022). The distinctions seen across transects imply that it is the disturbance regime, not merely depth, that plays a role in shaping peat decomposition gradients in landscapes affected by fire (Sinclair *et al*., 2020). However, the correlation between MIR-based degree of decomposition and conventional indicators such as C:N ratio and Von Post was not assessed in this study, as previous studies reported that those indicators can be inconsistent due to biogeochemical processes and the subjectivity of Von Post scale measurement. In order to clarify the reliability of MIR spectroscopy for the assessment of peat decomposition, future studies may consider exploring their correlation.

PCA: Integrated view of SOM variability

PCA combined the four SOM indices—hydrophobicity, aromaticity, and humification index and the DDI, into two principal components that account for 91.8% of the total variance. PC1 (55.2%) indicated a spectrum of humification, characterized by significant positive loadings (Table 7). PC2 (36.6%) indicated the equilibrium between hydrophobic and hydrophilic functional groups (hydrophobicity indices) and the DDI (Fig. 8). This dual-axis framework illustrates findings from peat FTIR research, suggesting that distance signifies hydrology while peat depth serves as the primary factor affecting variation (Evans *et al*., 2022).

The PCA score plots indicated distinct clustering according to depth, implying that vertical stratification serves as the main organizing principle for SOM chemistry throughout the landscape. Shallow samples were grouped with high hydrophobicity and low humification, whereas deep samples were associated with high aromaticity and increased humification. The landscape position, or distance, led to a more dispersed clustering, suggesting a heightened influence from hydrological gradients (Ritzema *et al*., 2014). Repeat transect samples exhibited increased variability, indicating the diverse impacts of fire and the subsequent restoration efforts. The PCA patterns demonstrate that peat degradation in disturbed landscapes is influenced by the interplay between depth-dependent anaerobic preservation and oxidation instigated by lateral disturbances.

Synthesis: Interacting controls on SOM chemistry in a disturbed tropical peat landscape

The primary factors affecting the composition of SOM are long-term vertical anaerobic processes that interlace with the lateral hydrological systems. Disturbance history also plays a pivotal role. The stratification with depth significantly influences the chemistry of soil organic matter, as it has been observed that more mesophilic aromatics are stabilized at greater depths. However, this vertical pattern is modified mostly by hydrological boundaries and burning. Enhanced aerobic decomposition, which lowers hydrophobicity and releases soil organic matter by oxidation, is found in areas bordering the canal and the river. Fire causes abrupt structural alterations by eliminating decomposed surface layers, enhancing aromaticity, and creating

Table 7: Loading factor

SOM indices	(PC1)	PC2	PC3	PC4	PC5
HI_1		-0.707	0.530	0.202	0.422
HI_2		-0.707	-0.516	-0.186	-0.444
Hydrophobicity	-0.574		-0.253	0.772	
Aromaticity	0.574		-0.520	0.326	0.542
DDI	0.581		0.344	0.471	-0.567

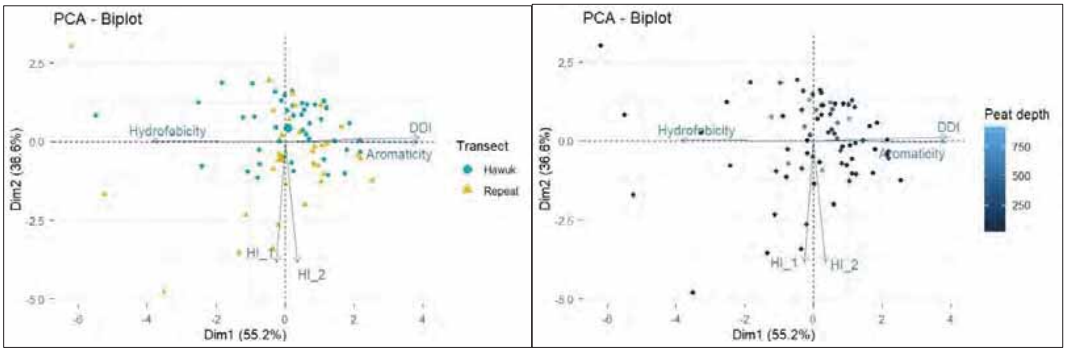

Fig. 8: Biplots of peat soil organic matter quality indicators affected by distance from river and canal and the peat depth (HI_1-Humification index using the ratio of carboxylic/carboxylate structures relative to polysaccharides content; HI_2-Humification index using the ratio of aromatic and phenolic compounds relative to polysaccharides content).

chemically varied horizons. These findings indicate that tropical peatlands in modified hydrological landscapes do not align with traditional acrotelm–catotelm models of peat formation. The chemistry of peat embodies a complex interaction between natural and anthropogenic processes, including oxidation resulting from drainage, thermal changes induced by fire, and modifications in hydrology due to restoration initiatives. FTIR-based indices serve as an effective diagnostic tool for understanding these dynamics and should be utilized to guide peatland management frameworks, including Indonesia's Peatland Hydrological Unit (PHU/KHG) system. Tracking trends in humification, decomposition, and hydrophobicity aids in identifying areas of active degradation, assessing restoration success, and enhancing long-term evaluations of carbon stability.

CONCLUSION

This study integrates FTIR spectroscopy and landscape and depth analyses to assess SOM chemical variability in disturbed tropical peatlands. Consequently, it illustrates that, among various factors, the depth of peat serves as the primary determinant of the composition of SOM, as the substantial layer of deep peat is more inclined to encompass aromatic and humified substances compared to shallower peats. Greater depth of peat layers and longer waterlogging resulted in the greater preservation of chemically resistant compounds, and therefore, greater indices of aromaticity and humification. This study revealed that vertical stratification serves as a fundamental organizing principle of peat chemistry in disturbed peatlands. This study also, however, illustrates the extent to which natural vertical profiles were altered by the combined effects of fire history and hydrological modification, especially in drained and burned peats. Drainage and canal construction change the balance of hydrophilic and hydrophobic compounds in surface peat, leading to increased oxidation and hydrophobicity away from hydrological boundaries. Drought caused by climatic conditions or elevated temperatures can alter the physical and chemical characteristics of peat, which, due to a insufficient water, transforms the properties of peat to become less hydrophobic. On peat landscapes, droughts and fires have a damaging effect, leading to subsidence and irreversible desiccation. The findings from peat studies indicate that, although depth is certainly a contributing factor, the degradation of peat is primarily due to the malfunctioning of hydrological connectivity, which serves as the main

control of the structuring of tropical peatlands. The study demonstrates the neglect of lateral hydrological connectivity in peatlands and illustrates the damaging effect fires have on the regular peat stratification. This study underscores the importance of lateral hydrological connectivity in peatlands and illustrates that fire significantly interferes with the typical peat stratification. This study emphasizes the significance of lateral hydrological connectivity in peatlands and demonstrates that fire significantly disrupts the typical stratification of peat. In this study, for both transects, fire became an increasingly more important driving force for the SOM reorganization, as wildfires impeded the classical acrotelm–catotelm sequence. The effect of fire on peat loss is inconsistent, influenced by the degree of surficial peat decomposition, which results in the removal of highly decomposed peat layers, the exposure of undisturbed, more decomposed peat, and generates irregular or inverted vertical gradients. Fire-driven combustion and thermal changes fundamentally reshape soil organic matter, leaving long-lasting chemical disturbance legacies that differ from stable anaerobic decomposition in undisturbed peat. No single descriptor can unambiguously demarcate the various characteristics of soil organic matter, but depth of soil profile is one such descriptor that is indicative of the landscape unit class. The characteristics of peat and its degradation are vital for the hydrometric restoration of peat. The addition of the FTIR indicator is expected to significantly improve the empirical framework for managing peatlands in the Peatland Hydrological Unit (PHU/KHG) of Indonesia, aiding in making well-informed choices concerning restoration and fire management. FTIR spectroscopy offers a rapid, cost-effective, and sensitive diagnostic tool for detecting peat degradation gradients across both vertical profiles and landscape units. The FTIR indicator can enhances evidence-based decision-making by enabling the identification of areas susceptible to oxidation, subsidence, and carbon loss, in addition to regions exhibiting initial signs of restoration success following rewetting efforts. In conclusion, this study demonstrates that SOM chemistry in disturbed tropical peatlands is governed by an interaction between long-term depth-related anaerobic processes and short- to medium-term disturbances driven by hydrological modification and fire. As peat degradation continues, these interactions can be documented stratigraphically and identified using FTIR. Mechanisms of peat degradation that are typically missed by standard indicators can be effectively captured. This approach greatly improves the assessment and adaptive restoration of the most impacted and climate-challenged peatlands, while also achieving the expected sustainable management of tropical peatlands.

AUTHOR CONTRIBUTIONS

P.B. Putra conceived, designed, collected data and reviewed the manuscript draft. D. Rachmanadi, the corresponding author, designed the study, analyzed data, prepared the manuscript draft, visualized tables and figures and reviewed the manuscript draft. A. Kunarso analyzed the data, drafted the original manuscript and reviewed the manuscript draft. Y. Indrajaya drafted the original manuscript draft and reviewed the manuscript draft. T.W. Yuwati interpreted the results and revised the manuscript draft. R.N. Adi collected data and reviewed the manuscript draft. A. Jaya collected data and reviewed the manuscript. E. Priyanto collected data and visualized the map. W. Halwany analyzed the data and reviewed the manuscript draft. A. Noor supported the manuscript draft preparation and reviewed the manuscript draft. M. Noor conceived the research idea and reviewed the manuscript draft.

ACKNOWLEDGEMENT

This study was supported by the Ministry of Environment and Forestry, Indonesia under Peatland Water Management Research Program No. [SP DIPA-029.07.2.427448/2020]. Agung Budi Supangat, Endang Savitri, Edi Sulasmiko and Lathif Brahmantya are thanked for helping with data collection. The Dean of the Agriculture Faculty, Palangkaraya University, is thanked for the collaborative project implementation.

CONFLICT OF INTEREST

The authors declare that there is no conflict of interest regarding the publication of this manuscript. In addition, the ethical issues, including plagiarism, informed consent, misconduct, data fabrication and/or falsification, double publication and/or submission, and redundancy, were observed by the authors.

OPEN ACCESS

©2026 The author(s). This article is licensed under a Creative Commons Attribution 4.0 International

License, which permits use, sharing, adaptation, distribution and reproduction in any medium or format, if you give appropriate credit to the original author(s) and the source, provide a link to the Creative Commons license, and indicate if changes were made. The images or other third-party material in this article are included in the article's Creative Commons license, unless indicated otherwise in a credit line to the material. If material is not included in the article's Creative Commons license and your intended use is not permitted by statutory regulation or exceeds the permitted use, you will need to obtain permission directly from the copyright holder. To view a copy of this license, visit: http://creativecommons.org/licenses/by/4.0/

PUBLISHER'S NOTE

GJESM Publisher remains neutral regarding jurisdictional claims in published maps and institutional afflictions.

☒ Negative AI Statement

The author(s) declared that no AI tools or services were not used or highly applied during the preparation of this work.

ABBREVIATIONS

%	Percent
°C	Degree Celsius
/cm	1 per centimeter
cm	Centimeter
C	Carbon
C=C	Carbon-carbon double bond
C-H	Carbon-hydrogen
C/N	Carbon/nitrogen
C=O	Carbonyl group
DDI	Degree of decomposition
FTIR	Fourier-transform infrared spectroscopy
HI	Humification index
km	Kilometer
m	Meter
Mha	Mega hectare
O-H	Oxygen-hydrogen (hydroxyl group)
PCA	Principal component analysis
PHU/KHG	Peatland hydrological unit / Kesatuan hidrologis gambut
PC1	Principal Component 1
SOM	Soil organic matter

REFERENCES

Anshari, G.Z.; Gusmayanti, E.; Novita, N., (2021). The Use of subsidence to estimate carbon loss from deforested and drained tropical peatlands in Indonesia. Forests. 12(732) **(18 pages)**.

Butlers, A.; Laiho, R.; Lazdiņš, A.; Schindler, T.; Soosaar, K.; Jauhiainen, J.; Bārdule, A.; Kamil-Sardar, M.; Līcīte, I.; Samariks, V.; Haberl, A.; Vahter, H.; Čiuldienė, D.; Anttila, J.; Armolaitis, K., (2025). Organic soils can be CO_2 sinks in both drained and undrained hemiboreal peatland forests. Biogeosciences. 22(18): 4627–4647 **(21 pages).**

Dettmann, U.; Kraft, N.N.; Rech, R.; Heidkamp, A.; Tiemeyer, B., (2021). Analysis of peat soil organic carbon, total nitrogen, soil water content and basal respiration: Is there a 'best' drying temperature? Geoderma. 403: 115231 **(10 pages)**.

Dommain, R.; Couwenberg, J.; Glaser, P.H.; Joosten, H.; Suryadiputra, I.N.N., (2014). Carbon storage and release in Indonesian peatlands since the last deglaciation. Q. Sci. Rev., 97: 1–32 **(32 pages).**

Dommain, R.; Couwenberg, J.; Joosten, H., (2011). Development and carbon sequestration of tropical peat domes in south-east Asia: Links to post-glacial sea-level changes and Holocene climate variability. Q. Sci. Rev., 30(7–8): 999–1010 **(12 pages).**

Evans, C.D.; Irawan, D.; Suardiwerianto, Y.; Kurnianto, S.; Deshmukh, C.; Asyhari, A.; Page, S.; Astiani, D.; Agus, F.; Sabiham, S.; Laurén, A.; Williamson, J., (2022). Long-term trajectory and temporal dynamics of tropical peat subsidence in relation to plantation management and climate. Geoderma. 428: 1-12 **(12 pages)**.

Giesen, W.B.J.T.; Persch, S.; Urzainqui, I.; Wardwell, D.; Chatellier, J.L.; Wang, Y.H.O.; Mahardhitama, P.; Nurzirwan, R.Y.; Laurén, A.; Giesen, P.T., (2023). Roles of fire history and rewetting in peatland restoration and vegetation recovery on the Merang peat dome, South Sumatra, Indonesia. Mires Peat. 29: 1-25 **(25 pages).**

Girkin, N.T.; Burgess, P.J.; Cole, L.; Cooper, H.V.; Honorio Coronado, E.; Davidson, S.J.; Hannam, J.; Harris, J.; Holman, I.; McCloskey, C.S.; McKeown, M.M.; Milner, A.M.; Page, S.; Smith, J.; Young, D., (2023). The three-peat challenge: business as usual, responsible agriculture, and conservation and restoration as management trajectories in global peatlands. Carbon Manage., 14(1): 1-13 **(13 pages).**

Hooijer, A.; Vernimmen, R.; Mulyadi, D.; Triantomo, V.; Hamdani; Lampela, M.; Agusti, R.; Page, S.E.; Doloksaribu, J.; Setiawan, I.; Suratmanto, B.; Swarup, S., (2024). Benefits of tropical peatland rewetting for subsidence reduction and forest regrowth: results from a large-scale restoration trial. Sci. Rep. Nature portfolio. 14: 10721 (**12 pages**).

Heller, C.; Ellerbrock, R.H.; Roßkopf, N.; Klingenfuß, C.; Zeitz, J., (2015). Soil organic matter characterization of temperate peatland soil with FTIR-spectroscopy: effects of mire type and drainage intensity. Eur. J. Soil Sci., 66(5): 847–858 **(12 pages)**.

Hirano, T.; Kusin, K.; Limin, S.; Osaki, M., (2015). Evapotranspiration of tropical peat swamp forests. Global Change Biol., 21(5): 1914–1927 **(14 pages)**.

Irfan, M.; Koriyanti, E.; Saleh, K.; Hadi; Safrina, S.: Awaludin; Albertus Sulaiman, A.; Akhsan, H.; Suhadi; Ruwignyo, R.A.; Choi, E.; Iskandar, I., (2024). Dynamics of peatland fires in South Sumatra in 2019: Role of Groundwater Levels. Land. 13 (373): 1-15 (**15 pages**).

Klavins, M.; Purmalis, O.; Rodinov, V., (2013). Peat humic acid properties and factors influencing their variability in a temperate bog ecosystem. Estonian J. Ecol., 62(1): 35–52 **(17 pages)**.

Könönen, M.; Jauhiainen, J.; Straková, P.; Heinonsalo, J.; Laiho, R.; Kusin, K.; Limin, S.; Vasander, H., (2018). Deforested and drained tropical peatland sites show poorer peat substrate quality and lower microbial biomass and

activity than unmanaged swamp forest. Soil Biol. Biochem., 123: 229-241 **(13 pages)**.

Kunarso, A.; Farquharson, R.; Blanch, E.W.; Grover, S., (2025). Mid-infrared spectroscopy is a potential tool for monitoring the success of tropical peatland restoration. J. Environ. Manage., 394: 127327 **(12 pages)**.

Kim, J.; Rochefort, L.; Hogue-Hugron, S.; Alqulaiti, Z.; Dunn, C.; Remy Pouliot, R.; Jones, T.G.; Freeman, C.; Kang, H., (2021). Water Table Fluctuation in Peatlands Facilitates Fungal Proliferation, Impedes Sphagnum Growth and Accelerates Decomposition. Front. Earth Sci., 8: 1-9 **(9 pages).**

Mishra, S.; Page, S.E.; Cobb, A.R.; Ser, J.; Lee, H.; Jovani-, A.J.; Sjögersten, S.; Jaya, A.; Wardle, D.A., (2021). Degradation of Southeast Asian tropical peatlands and integrated strategies for their better management and restoration. J. Appl. Ecol., 58: 1370–1387 **(18 pages)**. Mieczan, T.; Bronowicka-Mielniczuk, U.; Rudyk-Leuska, N., (2022). Effects of fires on microbial and Metazoan communities in peatlands. Water. 14(3402) **(16 pages**).

Ming, L.; Dou, S.; Wang, H.; Zhu, Y., (2023). Study of the Humification Process and Humic Acid-like Structure Characteristics of Kitchen Waste with the Addition of Biochar. Agronomy. 13, 465 (**14 pages**).

Nasrul, B.; Puspitasari, D.J.; Umami, I.M.; Idwar; Silvina, F.; Lubis, N.; Hamzah, A.; Yusa, M.; Nurhayati., (2024). Study on the vertical distribution of carbon and ash content and its relationship with ombrogenous peat depth. BIO Web of Conferences. 99 **(8 pages)**.

Nurzakiah, S.; Wakhid, N.; Hairani, A., (2020). Carbon dioxide emission and peat hydrophobicity in tidal peatlands. Sains Tanah. 17(1): 71–77 **(7 pages)**.

Page, S.; Hosciło, A.; Wösten, H.; Jauhiainen, J.; Silvius, M.; Rieley, J.; Ritzema, H.; Tansey, K.; Graham, L.; Vasander, H.; Limin, S., (2009). Restoration ecology of lowland tropical peatlands in Southeast Asia: Current knowledge and future research directions. Ecosystems. 12(6): 888–905 **(8 pages)**.

Page, S.E., (2024). Lowland Tropical Peatlands – A brief review of their important role in the global carbon cycle and biodiversity support. Media Konservasi. 29(2): 165-171 **(7 pages)**.

Page, S.; Mishra, S.; Agus, F.; Anshari, G.; Dargie, G.; Evers, S.; Jauhiainen, J.; Jaya, A.; Jovani-Sancho, A.J.; Laurén, A.; Sjögersten, S.; Suspense, I.A.; Wijedasa, L.S.; Evans, C.D., (2022). Anthropogenic impacts on lowland tropical peatland biogeochemistry. Nat. Rev. Earth Environ., 3(7): 426–443 **(18 pages)**.

Ritzema, H.; Limin, S.; Kusin, K.; Jauhiainen, J.; Wösten, H., (2014). Canal blocking strategies for hydrological restoration of degraded tropical peatlands in Central Kalimantan, Indonesia. Catena. 114: 11–20 **(10 pages)**.

Ratnayake, A.S. (2020). Characteristics of lowland tropical peatlands: Formation, Classification, and Decomposition. J. Tropic. Forest. Environ., 10(01): 1-16 (**16 pages**).

Ratai, J.; Teh, C.B.S.; Tan, N.P.; Mohidin, H.; Goh, K.J.; Sangok, F.E.; Melling, L., (2024).

Tropical peat soil changes across successive oil palm generations in Sarawak, Malaysia. Heliyon, 10(10): e37754 **(14 pages)**.

Obeng, A.S.; Dunne, J.; Giltrap, M.; Tian, F., (2023). Soil organic matter carbon chemistry signatures, hydrophobicity and humification index following land use change in temperate peat soils. Heliyon. 9(9): e19347 **(12 pages)**.

Qirom, M.A.; Yuwati, T.W.; Rachmanadi, D.; Lestari, F., (2023). The species diversity and composition as bioindicators of natural regeneration after forest fire. Al Kauniyah 16(2): 245-254 **(10 pages).**

Santın, C.; Doerr, S.H., (2016). Fire effects on soil: Human dimension. Phil. Trans. R. Soc. B, 371: 28–34 **(7 pages)**.

Sinclair, A.L.; Graham, L.L.B.B.; Putra, E.I.; Saharjo, B.H.; Applegate, G.; Grover, S.P.; Cochrane, M.A., (2020). Effects of distance from canal and degradation history on peat bulk density in a degraded tropical peatland. Sci. Total Environ., 699: 134199 **(12 pages)**.

Shapchenkova, O.A.; Loskutov, S.R.; Kukavskaya, E.A., (2023). Alteration of Organic Matter during Wildfires in the Forests of Southern Siberia. Fire 6 (304) (**18 pages**).

Wosten, J.H.M.; Clymans, E.; Page, S.E.; Rieley, J.O.; Limin, S.H., (2008). Peat-water interrelationships in a tropical peatland ecosystem in Southeast Asia. Catena. 73(2): 212–224 **(13 pages).**

Yang, T.; Jiang, J.; He, Q.; Shi, F.; Jiang, H.; Wu. H.; Chunguang, H., (2025). Impact of drainage on peatland soil environments and greenhouse gas emissions in Northeast China. Sci. Rep., 15: 8320 **(20 pages).**

Yakubson; Limantara, L.M.; Sisinggih, D.; Sumiadi, (2023). Performance of the Existing Canal Blocking in the Peatland Conservation and Restoration Management. J. Hunan Uni. Nat. Sci., 50(2): 245–253 **(9 pages)**.

Zhang, Y.; Shu, Y.; Qin, Y.; Chen, Y.; Lin, S.; Huang, X.; Zhou, M, (2024). Resurfacing of underground peat fire: Smouldering transition to flaming wildfire on litter surface. Int. J. Wildland Fire. 33: WF23/28 (**10 pages**).

AUTHOR (S) BIOSKETCHES

Putra, P.B., Ph.D. Candidate, Faculty of Forestry, Gadjah Mada University, Jl. Agro Bulaksumur Yogyakarta, Indonesia. Research Center for Ecology, National Research and Innovation Agency (BRIN), Cibinong-Bogor 16911, West Java, Indonesia.
- Email: *rpam001@brin.go.id*
- ORCID: 0000-0002-1391-996X
- Web of Science ResearcherID: W-3934-2018
- Scopus Author ID: 57092722900
- Homepage: https://www.researchgate.net/profile/Pamungkas_Buana_Putra

Rachmanadi, D., Dr., Principal researcher, Research Center for Ecology, National Research and Innovation Agency (BRIN), Cibinong-Bogor 16911, West Java, Indonesia.
- Email: dony004@brin.go.id
- ORCID: 0000-0002-9456-5357
- Web of Science ResearcherID: ABD-7391-2020
- Scopus Author ID: 57210796334
- Homepage: https://www.researchgate.net/profile/Dony-Rachmanadi

Indrajaya, Y., Dr., Principal researcher, Research Center for Ecology, National Research and Innovation Agency (BRIN), Cibinong-Bogor 16911, West Java, Indonesia.
- Email: *yonk001@brin.go.id*
- ORCID: 0000-0003-1064-3643
- Web of Science ResearcherID: JCN-7602-2023
- Scopus Author ID: 57189633934
- Homepage: https://www.researchgate.net/profile/Yonky-Indrajaya

AUTHOR (S) BIOSKETCHES

Kunarso, A., Dr., Senior researcher, Research Center for Ecology, National Research and Innovation Agency (BRIN), Cibinong-Bogor 16911, West Java, Indonesia.
▪ Email: *adi.kunarso@brin.go.id*
▪ ORCID: 0000-0003-4743-6453
▪ Web of Science ResearcherID: NA
▪ Scopus Author ID: 57210144990
▪ Homepage: https://www.researchgate.net/profile/Adi-Kunarso

Adi, R.N., M.Sc., Senior researcher, Research Center for Ecology, National Research and Innovation Agency (BRIN), Cibinong-Bogor 16911, West Java, Indonesia.
▪ Email: *raha014.brin.go.id*
▪ ORCID: 0000-0003-4519-5449
▪ Web of Science ResearcherID: NA
▪ Scopus Author ID: 57226717919
▪ https://www.researchgate.net/profile/Rahardyan_Adi?ev=hdr_xprf

Jaya, A., Dr., Faculty of Agriculture, University of Palangka Raya, Central Kalimantan, Indonesia.
▪ Email: *adijaya@agr.upr.ac.id*
▪ ORCID: 0000-0002-5946-8631
▪ Web of Science ResearcherID: X-4840-2018
▪ Scopus Author ID: 6504583689
▪ Homepage: https://www.researchgate.net/profile/Adi-Jaya

Yuwati, T.W., PhD. Candidate, Faculty of Forestry, Gadjah Mada University, Jl. Agro Bulaksumur, Yogyakarta, Indonesia. Research Center for Ecology, National Research and Innovation Agency (BRIN), Cibinong-Bogor 16911, West Java, Indonesia.
▪ Email: *triw016@brin.go.id*
▪ ORCID: 0000-0002-8477-0795
▪ Web of Science ResearcherID: LDG-4829-2024
▪ Scopus Author ID: 55965373500
▪ Homepage: https://www.researchgate.net/profile/Tri-Yuwati

Priyanto, E., B.A., Junior Computer Technician. Centre for Watershed Management of Solo, Ministry of Forestry, Indonesia.
▪ Email: *eko.forest@gmail.com*
▪ ORCID: 0000-0003-1006-6196
▪ Web of Science ResearcherID: NA
▪ Scopus Author ID: 57422212500
▪ Homepage: https://scholar.google.com/citations?user=76fu9SsAAAAJ&hl=en

Halwany, W., M.Sc., Senior researcher, Research Center for Ecology, National Research and Innovation Agency (BRIN), Cibinong-Bogor 16911, West Java, Indonesia.
▪ Email: wawan.halwany@brin.go.id
▪ ORCID: 0000-0002-0449-1762
▪ Web of Science ResearcherID: LJL-6584-2024
▪ Scopus Author ID: 57219420830
▪ Homepage: https://www.researchgate.net/profile/Wawan-Halwany

Noor, A., Dr., Principal researcher, Research Center for Food Crops, Research Organization for Agriculture and Food, National Research and Innovation Agency, Cibinong-Bogor 16911, West Java, Indonesia.
▪ Email: *aidi003@brin.go.id*
▪ ORCID: 0000-0001-7136-5101
▪ Web of Science ResearcherID: NA
▪ Scopus Author ID: 57190246569
▪ https://www.researchgate.net/profile/Aidi-Noor

Noor, M., Dr., Research Professor, Research Center for Food Crops, Research Organization for Agriculture and Food, National Research and Innovation Agency, Cibinong-Bogor 16911, West Java, Indonesia.
▪ Email: *muha334@brin.go.id*
▪ ORCID: 0000-0003-3177-9267
▪ Web of Science ResearcherID: NA
▪ Scopus Author ID: 57194149954
▪ Homepage: http://muhammadnoor20.blogspot.com

HOW TO CITE THIS ARTICLE

Putra, P.B.; Rachmanadi, D.; Indrajaya, Y.; Kunarso, A.; Adi, R.N.; Jaya, A.; Yuwati, T.W.; Priyanto, E.; Halwany, W.; Noor, A.; Noor, M., (2026). Tropical peat soil variability along landscape and depth gradient using mid-infrared spectroscopy. Global J. Environ. Sci. Manage., 12(1): 297-312.

DOI: 10.22034/gjesm.2026.01.17

URL: https://www.gjesm.net/article_732993.html

Global J. Environ. Sci. Manage. 12(1): 313-330, Winter 2026, Serial #45

Global Journal of Environmental Science and Management
(GJESM)

Homepage: https://www.gjesm.net/

Podcasts

CASE STUDY

Synergistic impacts on a multi-purpose transboundary aquatic ecosystem resulting from cyanide and mercury in artisanal gold mining tailings

P.C. Velasquez-Lopez[1,*], L. Chincha[2], L.E. Granda[3], M. Nirchio[1]

[1]*Faculty of Agricultural Sciences, Universidad Técnica de Machala, km 5,5 Pasaje, Machala, Ecuador*

[2]*Sustainable Economic Futures, SEF-Clean Gold #2004 1225 Richards Street, Vancouver, V6B 3G3, BC Canada*

[3]*Analytical Department, Laboratorios LASA, Juan Ignacio Pareja OE854 y Pablo Palacio, Quito, Ecuador*

ARTICLE INFO

Article History:
Received 15 August 2025
Revised 21 October 2025
Accepted 25 November 2025

Keywords:
Aquatic ecosystem
Artisanal and small-scale gold mining (ASGM)
Methylmercury
Tailings solutions
Water quality

DOI: 10.22034/gjesm.2026.01.18

ABSTRACT

BACKGROUND AND OBJECTIVES: The transition from mercury amalgamation to cyanide-based extraction in artisanal and small-scale gold mining has reshaped contaminant behavior in mining-impacted watersheds. This study combines concurrent measurements of cyanide, nitrogen species, sulfate, bicarbonate, and mercury to assess their interconnected dynamics throughout the extraction–tailings–river continuum in the Portovelo–Zaruma district (southern Ecuador). The objectives of this study were to: i) quantify both free and total cyanide and dissolved mercury in leaching tanks, tailings ponds, and river sites; ii) characterize nitrogen, sulfate, and bicarbonate formation associated with cyanide degradation and ore mineralogy; and iii) assess how these processes influence downstream mercury mobility and environmental vulnerability.
METHODS: Sampling included feed-ore mineralogy; leaching-tank solutions (n = 5); tailings-pond solutions (n = 5); and river sites (n = 12, each with three cross-sectional replicates). The total amounts of free cyanide and mercury were quantified during the processing phase. Levels of mercury, nitrate, sulfate, bicarbonate, chemical oxygen demand, conductivity, and total dissolved were investigated in tailings solutions and river waters.
FINDINGS: Free cyanide decreased from 517 ± 135 milligram per liters in leaching tanks to ~182 milligram per liters gram per tailings ponds (~80 percent reduction) and to <0.001 milligram per liters downstream (>99.9 percent attenuation). The total cyanide concentration decreased from 695 ± 159 milligrams per liter leaching-tank effluents to <0.004 milligram per liter in river water. Mineralogy (25–35 percent pyrite; 10–15 percent calcite/dolomite) contributed sulfate up to 500 milligram per liters and bicarbonate up to 250 milligram per liters in tailings, both increasing downstream. Nitrate rose from 0.49 to 2.54 milligram per liters, and chemical oxygen demand from 40–50 to 200–240 milligram per liters. Dissolved mercury remained <0.001 milligram per liters in river water, though tailings solids contained 0.50 ± 0.10 milligrams per kilogram mercury. These patterns reflect the degradation of cyanide, the enhancement of nitrogen levels, the liberation of anions from minerals, and the related alterations in the behavior of mercury.
CONCLUSION: The Puyango River functions as a reactive geochemical corridor where cyanide attenuation, nutrient enrichment, organic loading, and mineral-driven sulfate–bicarbonate release converge with legacy mercury to shape water quality and ecological vulnerability. Efficient management necessitates a comprehensive monitoring strategy for cyanide, nitrogen, and mercury pathways, supported by analyses ofsediment, biota, and microbial assessments.

This is an open access article under the CC BY license (http://creativecommons.org/licenses/by/4.0/).

NUMBER OF REFERENCES
52

NUMBER OF FIGURES
5

NUMBER OF TABLES
5

*Corresponding Author:
Email: *colon.velasquez@gmail.com*
Phone: 5939 9485 8227
ORCID: 0000-0002-3044-920X

Note: Discussion period for this manuscript open until Mar 1, 2026 on GJESM website at the "Show Article".

INTRODUCTION

Artisanal and small-scale gold mining (ASGM) is a widespread activity that relies on water-intensive processes using mercury and cyanide for gold recovery. The Minamata Convention (Spiegel *et al.,* 2015) prompted international efforts to reduce mercury use, resulting in a broad but still partial transition toward cyanide (Malone *et al.,* 2023). Processing centers that utilize cyanidation have grown in frequency. Many of these continue to operate without formal recognition (Freitas and Horta, 2023; Kosai *et al.,* 2023; Ayoo *et al.,* 2024). Consequently, untreated waste containing cyanide, mercury, and other toxic compounds is frequently discharged into nearby waters. These discharges stimulate chemical reactions that augment the mobility and toxicity of pollutants (Mulenga *et al.*, 2024; Casso-Hartmann *et al.*, 2022; Espiritu *et al.,* 2022). Preliminary investigations examined how cyanide products contaminate water systems and clarified the co-occurrence of mercury and cyanide during ore processing. They demonstrated that mercury partitions into both solid tailings and process solutions, with only minimal recovery in amalgam residues at the base of cyanidation tanks (Velasquez-Lopez *et al.,* 2011). Consequently, the aquatic ecosystem has been significantly impacted by mining discharges (Dossou *et al*., 2024; Miserendino *et al.,* 2013; Marshall *et al.,* 2018; Marshall *et al.,* 2020). Building on this research, recent thermodynamic modeling and geochemical simulations have clarified the stability of mercury–cyanide complexes such as $[Hg(CN)_4]^{2-}$ at pH ≈ 10. These studies contribute to the understanding of complex formation in the context of conventional cyanidation conditions (Malone *et al*., 2023; Arellano-Yasaca *et al.,* 2024; Seney *et al*., 2020). In addition, new evidence indicates that cyanide degradation generates nitrogen species such as ammonium (NH^+_4), nitrite (NO^-_2), and nitrate (NO^-_3) that modify redox gradients and may interact with sulfate and bicarbonate derived from ore mineralogy, influencing mercury mobility and potential methylation (Kwofie *et al*., 2021; Helmrich *et al*., 2022; Abdelaal *et al*., 2023; King *et al*., 2024). Furthermore, the analysis conducted by da Silva and Guimarães (2024) points out deficiencies in the comprehension of mercury–cyanide complex formation and underscores the necessity for field-based studies. Despite these advances, no previous investigation has assessed cyanide degradation together with nitrogen enrichment and mineral derived anions. Nor has any study examined their combined influence on mercury mobility along the extraction–tailings–river continuum. This study presents a preliminary warning evaluation through a comprehensive method to analyze the behavior of cyanide and its interactions with mercury along the gold extraction pathway in the Portovelo-Zaruma region and the adjacent aquatic environment. The novelty of this study lies in characterizing tailings solutions and identifying cyanide attenuation patterns along the processing–river continuum. This study strengthens understanding of cyanide–mercury interactions and underscores the urgent need for integrated watershed management across southern Ecuador and the transboundary Puyango–Tumbes basin. From a policy viewpoint, the results associate environmental monitoring with challenges related to social responsibility and governance challenges. They emphasize the significance of formalization, accountability, and coordination across sectors. The study provides a case-based assessment of cyanide and mercury concentrations in tailings solutions and receiving waters of the Puyango River, emphasizing their chemical dynamics and potential environmental impacts.

MATERIALS AND METHODS

Description of cyanide leaching process and tailings management

In Ecuador, ASGM is primarily carried out by small associations of 8 to 10 miners. They engage in operations across numerous regions that are rich in gold. These miners begin the gold extraction process by crushing and milling ore using Chilean mills. The substance is subsequently processed with cyanide at centralized processing facilities (Veiga *et al*., 2014). Gold recovery in ASGM is achieved through a dual approach: a portion is extracted via amalgamation from gravity concentrates, while the remaining gold is recovered through cyanidation of the gravity tailings (Velásquez-López *et al*., 2010). During the amalgamation process, mercury is applied to gravity concentrates, producing mercury-rich tailings. These tailings are then mixed with the gravity tailings (milled ore) and then subjected to cyanide leaching (Torrance *et al.,* 2021). Subsequent study conducted by Gonçalves *et al*. (2017) validated the

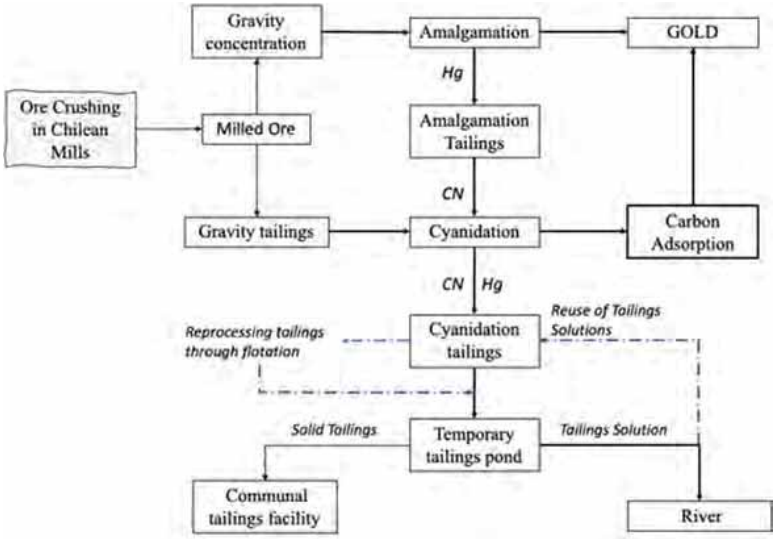

Fig. 1: Flowsheet of the typical cyanidation gold processing system in the artisanal and small-scale gold mining of Ecuador.

replacement of of mercury with cyanide, establishing conditions in which both reagents are present in the same processing streams (Verbrugge *et al*., 2021). This coexistence favors the formation of Hg–CN complexes, as previously described by Malone *et al*. (2023). Using mercury and cyanide, miners recover both free and coarse gold particles from crushed ore, as illustrated in Fig. 1.

The study area

The study area corresponds to the Portovelo–Zaruma mining district, one of the most active ASGM hubs in Latin America, located in southern Ecuador. The district hosts over 100 processing centers that collectively produce an estimated 5,000 tons of tailings daily. This district is hydrologically connected to the Puyango River, which originates in the Andean highlands and flows southwestward, ultimately discharging into the Pacific Ocean within Peruvian territory (Fig. 2).

The watershed is formed by the Calera and Amarillo Rivers. It flows southward into Peru as the Tumbes River. The basin is characterized by a diverse topography, featuring mountainous, hilly, and arid landscapes, where the steep significantly affect its influence its hydrological dynamics. Furthermore, the Puyango River sustains extensive irrigation systems in lowland agricultural areas of both Ecuador and Peru, while several communities depend on its tributaries for aquaculture and domestic water use. Collectively, these factors draw attention to the ecological susceptibility and socio-economic value of the basin (Puño, 2013). In addition, the Puyango-Tumbes basin functions as a transboundary system characterized by steep hydrological gradients and prolonged legacy mercury deposition. These conditions influence cyanide degradation and mercury mobility downstream (Schudel *et al*., 2019). In this study, the sampling methodology was developed to include the three primary operational compartments that delineate the contaminant pathway in ASGM operations. These compartments includes leaching tanks, tailings ponds, and river sites along the Puyango–Tumbes continuum.

Sample design

The selection of leaching tanks, tailings ponds, and river sites followed a process-based sampling framework designed to capture the full contaminant pathway of ASGM operations. These units signify three operationally unique and sequential compartments. The first is the contaminant source (five cyanidation tanks), where mercury and cyanide loads originate. The second component is an intermediate transformation zone that comprises five tailings ponds, where cyanide degradation, nitrogen formation, sulfate and bicarbonate release, and mercury solubilization happen before discharge.

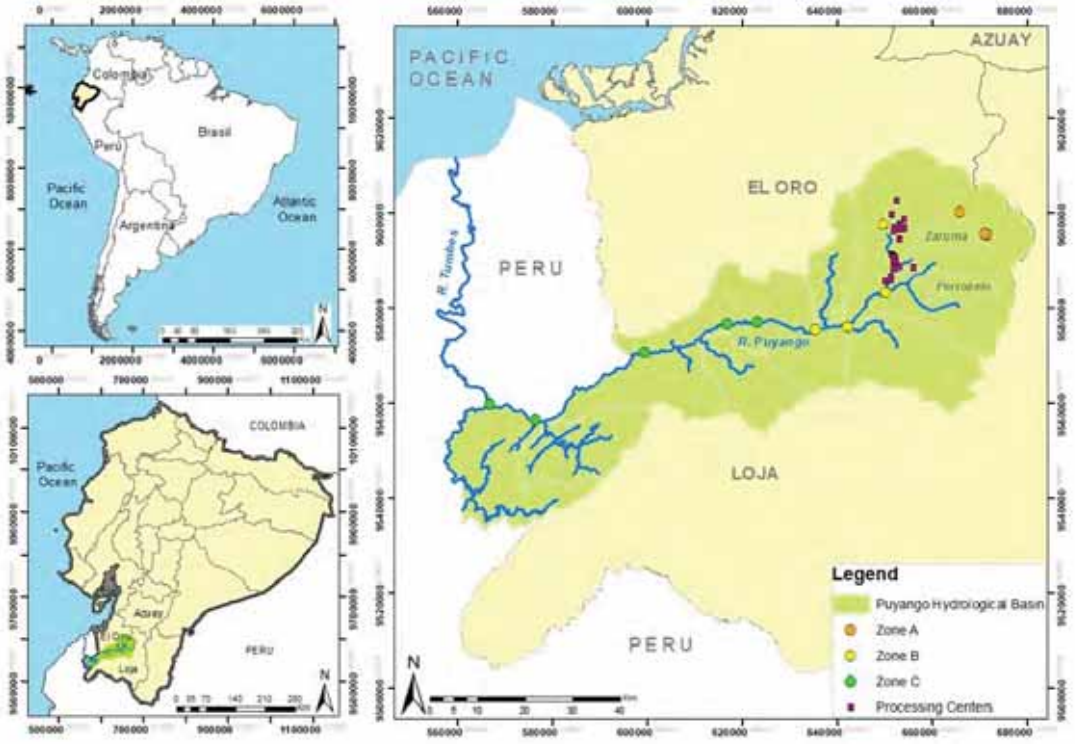

Fig. 2: Geographical location of the study area in Portovelo-Zaruma mining district and Puyango River in Southern Ecuador

The third is the receiving environment (twelve river sites), distributed as three upstream sites, four within the discharge zone, and five downstream across hydrologically distinct segments of the river. This source–transformation–receptor structure was selected to trace the operational and geochemical evolution of contaminants along the extraction–tailings–river continuum. Samples were collected from leaching tanks to assess the characteristics of the processed ore and initial contaminant loads. Tailings ponds were included because they function as intermediate geochemical reactors. Within these ponds, the breakdown of cyanide and the discharge of nitrogen-, sulfur-, and carbonate-bearing species influence the movement of mercury before the effluents entering natural waters. River sites provided an integrated assessment of the receiving environment. Upstream reference points, discharge-zone sites, and downstream locations captured dilution, further transformation, and interactions with additional watershed inputs. Table 1 illustrates the physicochemical parameters analyzed in each component of this study. Five ASGM associations granted access to their facilities, enabling direct observation of cyanidation workflows and systematic sampling of ores, process solutions, and cyanide-management practices.

Sampling the processing centers

In processing plants, five gravity tailings samples destined for cyanidation were collected to determine their mineralogical composition. Furthermore, evaluations at processing centers were carried out by collecting samples during five different stages of the cyanidation leaching processes, both at the initial stage and at the conclusion of the process.

Sampling the river

The river sampling design captured spatial variation in hydrology and contaminant behavior along the longitudinal and altitudinal gradient of the Puyango River. In total, twelve sites were chosen across three river zones. These sites included three reference locations upstream, four sites in the impact zone

Table 1: Physic chemical parameters measured in the cyanide leaching process, the tailings ponds, and the river

Parameter	Cyanidation process		Tailings ponds	River
	Initial phase	Final phase	Solutions	Water
Total cyanide (CN^-)	X	X	X	X
Free CN^-	X	X	X	X
Mercury (Hg^{2+})	X	X	X	X
Conductivity			X	X
Total dissolved solids (TDS)			X	X
Potential of hydrogen (pH)	X	X	X	X
Nitrate (NO_3^-)		X	X	X
Sulphate (SO_4^{2-})			X	X
Bicarbonate (HCO_3^-)			X	X
Chloride (Cl^-)			X	X
Fluoride (F^-)			X	X
Chemical oxygen demand (COD)			X	X

close to ASGM discharges, and five downstream sites extending to the Ecuador–Peru border. This gradient spans high-turbulence headwaters with ≈ 450–300 meters above sea level (m.a.s.l.), mid-basin transitional reaches, and low-energy depositional at 180–120 meters above sea level. In these reaches, flow and sedimentation progressively shift. At each zone, three independent spatial replicates were collected along the cross-sectional transect of the river to capture heterogeneity in flow, mixing, and sediment–water interactions. Site selection was adhered to a predetermined framework that includes hydrological transitions, variations in altitude, and nearness to ASGM processing centers and tailings ponds. This ensured alignment between local replication and basin-scale geochemical contrasts. Sampling occurred during a single, hydrologically stable field campaign, within rain-free, mid-day windows to minimize variability. Seasonal replication was not executed, since the study was intended to characterize spatial, not temporal, geochemical transitions; this limitation is addressed in the uncertainties section.

In situ measurments and sample preservation

Table 1 illustrates the physicochemical parameters assessed in every component of this study. In tailings ponds and in the river, surface water samples were collected and analyzed in situ for temperature, pH, TDS, and conductivity using the portable multiparameter model Hanna H98129. Three samples of 500 milliliters (mL) were collected in each site (tailings pond or river point): one for CN^-, one for COD, and one for anion analysis (NO_3^-, SO_4^{2-}, HCO_3^-). Cyanide samples were preserved in the field with 40 percent (%) NaOH to raise and maintain pH 12–12.5, following Standard Methods (2017) 4500 -CN^-, and EPA 9010B/9012B requirements. Preserved samples were transported in insulated coolers at 4 ± 1 °C and kept in darkness to prevent photodegradation and hydrogen cyanide volatilization, and were analyzed within 24 hours (h) of collection.

Laboratory analysisCopper

The mineralogical composition of cyanidation feed material was analyzed by X-ray diffraction (Bruker D8 Advance). Samples were oven-dried at 60 °C, homogenized, ground with an agate mortar, and sieved to <75 micrometers (µm). XRD analyses were performed using K-alpha (Cu-Kα) radiation (λ = 1.5406 Å) at 40 kilovolts (kV) and 40 miliamper (mA), scanning 5–70° 2 angle (θ) (step 0.02°, 1°/min). Phases were identified using Bruker EVA software and the International Center for Diffraction Data-Powder Difreaction File (ICDD PDF)-2 database. The quantification of dissolved mercury was performed utilizing cold vapor atomic absorption spectrometry (CV-AAS) with the PerkinElmer Analyst + FIAS-100 system. The verification of accuracy and precision was conducted using standard additions and the analysis of certified reference material from Environmental Resources Associates, resulting in recoveries ranging from 90–110 percent. Instrumental blank variability yielded a method detection limit of 0.001 mg/L, and concentrations below this threshold are

reported as less than 0.001 mg/L. This sensitivity is appropriate for ASGM-impacted rivers, where dissolved Hg typically occurs in microgram per liter (µg/L) to low-ng/L range. Cyanide in its free form was quantified utilizing a flow injection analysis system (SCALAR San++) that is fitted with an amperometric detector. Total cyanide was determined on the same system using its ultraviolet digestion module, which oxidizes all metal-complexed species to free cyanide before detection. This procedure is consistent with Standard Methods - 2017 4500-CN^-. Method detection limits were 0.002 mg/L for free CN^- and 0.004 mg/L for total CN^-. All reported CN^- values therefore reflect direct instrumental measurements rather than calculated speciation estimates. Major anions (NO_3^-, SO_4^{2-}, HCO_3^-) were analyzed by ion chromatography (Metrohm 881 Compact IC Pro) (US–EPA Method 9056A, 2007). Quality control was ensured through analysis of SIGMA-LDRICH multielement Ion Chromatography Standard Solution 1.11448.0000. These anions serve as indicators of cyanide degradation (NO_3^-), sulfate release from ore mineralogy (SO_4^{2-}), bicarbonate buffering (HCO_3^-), and ancillary geochemical processes influencing mercury solubility. The measurement of COD was conducted using the closed-reflux colorimetric method APHA 5220D (Standard Methods, 2017). Potassium dichromate digestions were performed at 150 °C for 2 h, with absorbance read at 620 nm on a Hach DR6000 spectrophotometer. COD functioned as a substitute for the redox dynamics influenced by organic matter, which are significant in relation to mercury complexation and microbial methylation. Historical nitrate measurements from the Binational Puyango–Tumbes Monitoring Program (2005–2007) were incorporated solely to contextualize long-term downstream nitrogen enrichment. The data presented were obtained through standardized binational protocols for sampling and analysis conducted in accredited laboratories, employing procedures that adhere to Standard Methods. They were not used for statistical comparison, but rather to qualitatively support interpretation of persistent nitrogen increases associated with cyanide degradation pathways.

Data analysis

Descriptive statistics, including mean, standard deviation (SD), coefficient of variation, minimum, maximum, range) were calculated for all parameters within each sampling zone. As the number of spatial replicates at each site was confined to three and reliable testing for normality was not feasible, non-parametric statistics were employed. The Kruskal–Wallis test was used to assess differences among river zones. Mann-Whitney U tests with Bonferroni correction for pairwise comparisons when global significance occurred ($p < 0.05$). Analyses were performed in STATGRAPHICS Centurion XVI (Version 16.1.18, StatPoint Technologies, Inc.).

RESULTS AND DISCUSSION

Ore chemical characteristics

The ores subjected to cyanidation are dominated by quartz (≈60%), with subordinate phyllosilicates (chlorite and muscovite) and a suite of sulfide and carbonate minerals typical of quartz–sulfide vein systems in the El Oro complex and other Andean ASGM districts (Salgado-Almeida *et al*., 2024; Mestanza-Ramón *et al*., 2022; Youpoungam *et al*., 2024) (Table 2). Additionally, minor kaolinite was identified among these minerals, which reflects hydrothermal alteration patterns frequently observed in ASGM deposits. Sulfides, mainly pyrite and chalcopyrite with variable amounts of sphalerite, galena and arsenopyrite, supply metals and sulfate during oxidation, promoting the formation of cyanide–metal complexes during leaching. Carbonates, chiefly calcite and dolomite, provide the main buffering capacity, moderating acidity and constraining potential acid generation. The diverse distribution of these minerals elucidates the observed differences in cyanide consumption that has been observed and implies related differences in the release of dissolved metals including copper (Cu), zinc (Zn), lead (Pb), iron (Fe), and arsenic (As). Although the dissolution of these metals was not analyzed in the present study, future research focused on quantifying metal mobilization under varying mineralogical and geochemical conditions would provide a deeper understanding of these processes. Collectively, this mineralogical composition creates a reactive geochemical framework that regulates cyanide usage, metal liberation, and mercury movement within the processing system.

Cyanide and mercury in the gold processing system

Cyanidation in the Portovelo–Zaruma district

Table 2: Mineralogy characteristics of different types of ores in the cyanide leaching in artisanal and small-scale gold mining, showing the average, minimum, and maximum values (%) (n=5 sampling size)

Mineral (%)	Name and chemical formula	Average (AVE)	Minimum (Min)	Maximum (Max)	Standard deviation (SD)
Quartz	Silicon dioxide (SiO_2)	59.00	53.80	65.40	5.63
Chlorite	Magnesium-iron aluminum silicate hydroxide [$Mg_{3.75}Fe^{2+}_{1.25}Si_3Al_2O_{10}(OH)_8$]	9.54	6.60	13.70	2.54
Muscovite	Potassium aluminum silicate hydroxide [$KAl_2((AlSi_3O_{10})(OH)_2$]	18.68	10.40	24.10	4.56
Kaolinite	Aluminium silicate dihydrate ($Al_2Si_2O_5(OH)_4$)	0.66	0.30	1.40	0.39
Calcite	Calcium carbonate ($Ca(CO_3)$)	5.32	0.20	19.40	7.38
Pyrite	Iron(II) disulfide (FeS_2)	2.04	1.00	2.70	0.59
Chalcopyrite	Copper iron disulfide ($CuFeS_2$)	1.06	0.10	4.00	1.49
Sphalerite	Zinc sulfide (ZnS)	0.32	0.10	0.90	0.30
Galena	Lead(II) sulfide (PbS)	2.43	0.10	11.20	4.42
Gypsum	Calcium sulfate dihydrate ($Ca(SO_4)•2(H_2O)$	1.06	0	5.30	2.12
Dolomite	Calcium magnesium carbonate ($CaMg(CO_3)_2$)	0.6	0	2.60	1.00
Arsenopyrite	Iron(III) arsenic sulfide (FeAsS)	0.72	0	3.60	1.44
Albite	Sodium aluminum silicate ($NaAlSi_3O_8$)	0.74	0	3.70	1.48

operates under highly alkaline conditions (pH 11.2–12) and with pulp densities that drive substantial cyanide use, estimated at ~87 t/month. Process water was already contaminated at intake points (857 mg/L free CN^-, pH 6.3), revealing systemic failures in water segregation. At the end of the leaching cycle, cyanide concentrations remained extremely high (695 ± 159 mg/L; total CN^-; 517 ± 135 mg/L free CN^-), establishing the initial contaminant load entering tailings ponds. Increased nitrate concentrations in process solutions (up to ~520 mg/L) further indicate nitrogen enrichment that corresponds with the byproducts of cyanide oxidation. Operational parameters of the leaching tanks, including pulp density, solid content and cyanide concentrations, are summarized in Table 3. Despite regulatory restrictions, mercury continues to circulate through ASGM operations (Gonçalves *et al*., 2017). Amalgamation tailings contained up to 200 milligrams per kilogram (mg/kg) Hg, whereas cyanide pulp reached 6.33 mg/L before decreasing to 0.50 ± 0.10 mg/kg in the final solid tailings. This reduction illustrates the process of mercury solubilization and its movement from the solid to the liquid phase, in accordance with the development of soluble Hg–CN complexes. These patterns agree with earlier observations showing that approximately one-quarter of mercury is discharged with the cyanidation tailings solutions (Velásquez-López *et al*., 2011). Taken together, these results show that the leaching pulp, enriched in both cyanide and mercury constitutes the primary source of contaminants entering tailings ponds. These conditions specify the geochemical environment in which downstream reactions transpire, including nitrogen formation, the release of sulfate and bicarbonate, and changes in the mobility of mercury.

Cyanide and mercury in tailings ponds

Following discharge from the processing centers, cyanide-rich effluents undergo substantial physicochemical transformations within the tailings ponds. Table 4 summarizes the principal water quality parameters, including cyanide species, major anions, and redox-sensitive constituents. Free cyanide concentrations were highly variable (up to 678 mg/L), and the solutions exhibited elevated pH, conductivity and TDS. These values indicate a sophisticated blend of dissolved ions and cyanide-metal complexes that correspond to the mineralogical composition outlined earlier. On average, cyanide concentrations in the ponds were ~80% lower than in the leaching tanks, but this decrease did not result from engineered treatment. Fewer than ten percent of processing centers implement chemical detoxification. In contrast, attenuation primarily occurs due to natural photolysis and oxidation, processes that are recognized to be intensified by the region's elevated solar radiation (Vaca-Escobar *et al*., 2024). Recent observations show that dissolved mercury in tailings ponds may reach ~0.05 mg/L, consistent with the formation of highly stable Hg–CN complexes such as $Hg(CN)_2$, $Hg(CN)_3^-$ and $Hg(CN)_4^{2-}$

Table 3: Characteristics of cyanidation at initial stage of the leaching process in the artisanal and small-scale gold mining. (n= 5 for all samples except for Hg with 3 sampling size)

Cyanide leaching tank	Volume (m^3)	Pulp density (g/cm^3)	% Solids in pulp (w/w)	Solids (Tons)	Water (Tons)	Hg in the pulp (mg/L)	CN in the pulp (mg/L)
AVE.	20	1.22	31.084	7.78	16.95	6.33	2,400
MIN.	20	1.10	19.12	4.24	15.47	6.00	2,270
MAX.	20	1.34	42.26	11.32	17.95	7.00	2,580
SD	0	0.10	10.32	3.11	0.94	0.51	140

Table 4: Concentrations of water quality parameters in the solutions of tailings ponds (Values are presented as average and standard deviation: n=5 sampling size) (ND not detectable)

Parameter	Average Ave.	Minimum Min.	Maximum Max.	Standard deviation (SD)
Total CN^- (mg/L)	194.15	ND	678.30	326.60
Free CN^- (mg/L)	182.30	ND	683.52	330.80
pH	9.40	8.56	10.76	1.04
Conductivity (µS/cm)	1210.00	873.00	1740.00	778.00
TDS (mg/L)	605.00	437.00	1016.00	390.00
SO_4^{2-} (mg/L)	318.50	46.26	651.73	251.30
HCO_3^- (mg/L)	130.00	60.00	250.00	85.20
NO_3^- (mg/L)	24.24	ND	51.98	19.24
COD (mg/L)	288.00	ND	790.00	346.20

under alkaline conditions (Malone *et al.*, 2023; King *et al.*, 2024). As cyanide degrades, nitrogen species accumulate. Elevated nitrate levels (up to 52 mg/L) are consistent with microbial nitrification pathways and the breakdown of thiocyanate (SCN^-) intermediates (Cáceda *et al.*, 2023; Kwofie *et al.*, 2021). High sulfate concentrations reflect the oxidation of sulfide-rich ores characteristic of the Portovelo–Zaruma mineral assemblages. Bicarbonate concentrations (130–250 mg/L) further indicate dissolution of calcite and dolomite, contributing to the maintenance of alkaline conditions within the ponds. Collectively, these transformations imply that nitrogen and sulfur cycling takes place alongside cyanide degradation, a topic that has been scarcely examined in ASGM settings. The coexistence of dissolved mercury, nitrogen-enriched waters and sulfur species in tailings ponds may create conditions favorable for microbial activity and potentially for methylmercury production (Abdelaal *et al.*, 2023). Despite this, the long-term behavior, transformation and remobilization pathways of Hg–CN complexes remain poorly understood in this environments. In essence, tailings ponds do not merely act as passive storage facilities; they are active biogeochemical reactors. In these ponds, cyanide degradation (Welman-Purchase *et al.*, 2024), nitrogen enrichment and mercury solubilization occur simultaneously. Nonetheless, the existing dataset does not facilitate the quantification of reaction rates or microbial contributions, and the detected chemical patterns. Consequently, the identified chemical patterns ought to be viewed as indicators instead of mechanistic validation. This integrated perspective fills a critical knowledge gap: few studies have quantified the coupled CN–Hg transformations and their microbial pathways in ASGM tailings solutions, particularly in the Andes. These processes define the chemical composition of effluents discharged into the river system, as discussed in the following section.

Cyanide and mercury in the river

Once released from the tailings ponds, mining effluents enter the Puyango River, where cyanide and mercury undergo further dilution, transformation and interaction with other geochemical constituents. Non-parametric Kruskal–Wallis tests confirmed significant differences among river zones for NO_3^-, SO_4^{2-}, HCO_3^-, conductivity, TDS and pH (all $p < 0.05$), whereas free and total cyanide and COD did not differ

significantly among zones ($p > 0.05$) (Table 5). These findings align with nearly total cyanide reduction and uneven distribution of organic loading (Fig. 3). Replicate variability in cyanide measurements was low (coefficient of variation <10%). This indicate that the strong reductions observed from leaching tanks to tailings ponds (>80%) and along the river (>99.9%) cannot be attributed to analytical error or simple dilution. Upstream reference locations indicated that the levels of cyanide and mercury were below detection thresholds for both free and total cyanide. In contrast, the monitoring points located close to the discharge zone showed increased levels of free cyanide, which clearly demonstrates the direct impact of mining effluents. At the ASGM discharge sites, free cyanide reached 0.16–0.17 mg/L, and total mercury occasionally attained 0.014 mg/L, exceeding aquatic-life guidelines before declining to below detection limits downstream. Downstream, dissolved mercury remained below detection limits (<0.001 mg/L), precluding comparison with Canadian Council of Ministers of the Environment (CCME) chronic criteria (0.000026 mg/L). Prior studies in the basin have documented considerable mercury inflows attributed to ASGM. It is estimated that the annual loads can reach up to 1.5 tonnes of mercury per year (Velásquez-López *et al.*, 2011), and sediment concentrations range from 0.78–30.8 mg/kg in the

Table 5: Descriptive statistics and Kruskal–Wallis test for water quality parameters across river zones in the Puyango River basin

Parameter	Zone	n	Mean	SD	VC (%)	Min	Max	Range	Mean rank	K-W	p-value
NO_3	A	3	0.49	0.22	43.77	0.29	0.72	0.43	2.00	—	—
	B	4	1.57	0.59	38.06	0.82	2.18	1.357	4.75	—	—
	C	5	2.54	1.80	70.93	1.09	5.43	4.34	8.6	6.5420	**0.0379***
CN Free	A	3	0.05	0	0	0.05	0.05	0	4.5	—	—
	B	4	0.16	0.20	123.76	0.05	0.47	0.42	7.5	—	—
	C	5	0.07	0.03	47.08	0.05	0.12	0.07	6.9	1.8297	0.4006^{ns}
CN Total	A	3	0.05	0	0	0.05	0.05	0	4.5	—	—
	B	4	0.17	0.21	124.54	0.05	0.50	0.45	7.5	—	—
	C	5	0.07	0.03	47.07	0.05	0.12	0.07	6.9	1.8297	0.4006^{ns}
Hg	A	3	0.001	0	0	0.001	0.001	0	6.0	—	—
	B	4	0.014	0.03	186.44	0.001	0.056	0.055	7.5	—	—
	C	5	0.001	0	0	0.001	0.001	0	6.0	2.0	0.3678^{ns}
pH	A	3	7.5	0.19	2.59	7.28	7.65	0.37	4.33	—	—
	B	4	8.06	0.17	2.18	7.91	8.22	0.31	10.5	—	—
	C	5	7.53	0.29	3.86	7.09	7.9	0.81	4.6	7.4208	**0.0244***
Conductivity	A	3	9.0	3.0	33.33	6.0	12.0	6.0	2.0	—	—
	B	4	78.25	52.75	67.41	36.0	149.0	113.0	7.75	—	—
	C	5	78.4	9.34	11.91	70.0	91.0	21.0	8.2	6.2873	**0.0431***
TDS	A	3	10.33	2.51	24.35	8.0	13.0	5.0	2.0	—	—
	B	4	39.5	25.95	65.70	19.0	74.0	55.0	7.75	—	—
	C	5	39.6	12.73	32.17	30.0	61.0	31.0	8.2	6.287	**0.0431***
SO_4	A	3	0.74	0.27	36.78	0.44	0.97	0.53	2.0	—	—
	B	4	11.23	4.75	42.35	5.90	15.98	10.07	8.37	—	—
	C	5	9.57	1.73	18.10	7.58	12.23	4.65	7.7	6.3308	**0.0422***
HCO_3	A	3	9.33	3.78	40.56	5.0	12.0	7.0	2.0	—	—
	B	4	50.0	27.98	55.97	15.0	75.0	60.0	7.87	—	—
	C	5	55.8	38.77	69.49	22.0	115.0	93.0	8.1	6.2613	**0.0436***
COD	A	3	27.33	4.04	14.78	23.0	31.0	8.0	7.0	—	—
	B	4	12.5	15.15	121.23	3.0	35.0	32.0	4.625	—	—
	C	5	69.8	98.34	140.89	3.0	240.0	237.0	7.7	1.6992	0.4275^{ns}

Note: Zones A, B, and C represent upstream reference sites, mining discharge points, and downstream reaches, respectively. VC (%) = coefficient of variation. K–W = Kruskal–Wallis test statistic. * indicates significant differences among zones ($p < 0.05$); ns = not significant.

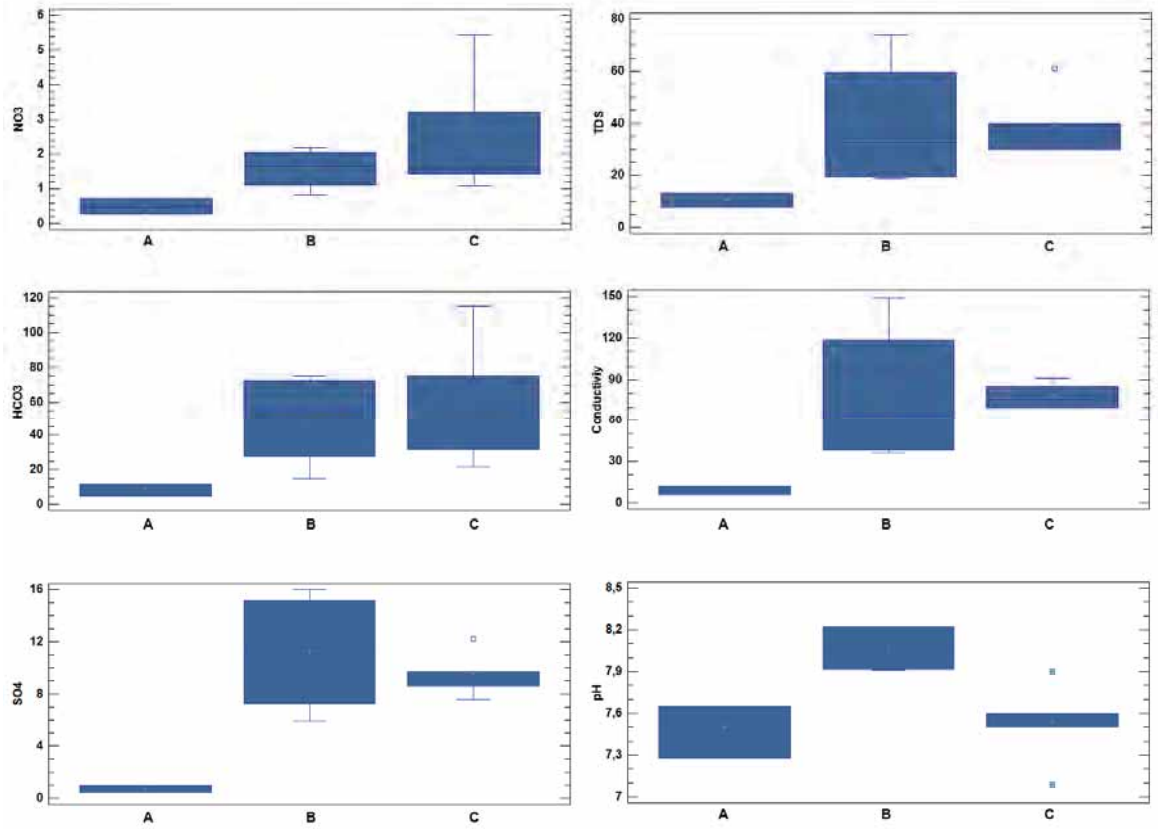

Fig. 3: Box-and-whisker plots of water-quality parameters across the three river zones of the Puyango River
The X-axis shows the spatial categories used in the statistical analysis: A = upstream reference sites, B = ASGM discharge zone, and C = downstream reaches near the Ecuador-Peru border. Significant differences ($p < 0.05$) were detected for NO_3^-, SO_4^{2-}, HCO_3^-, conductivity, TDS, and pH according to the Kruskal-Wallis test.

dry season and from 1.80–70.7 mg/kg in the wet season (Marshall *et al.,* 2018). River conditions (pH ≈ 8, intense solar irradiation, short residence times) promote dissociation of Hg-CN complexes and rapid scavenging of Hg by suspended particles, dissolved organic matter, and Fe-Mn oxides (Moreno-Brush *et al.,* 2020; Liu *et al.,* 2022). This differs from the scenarios depicted by Arellano-Yasaca *et al.* (2024), who utilized elevated levels of cyanide concentrations that do not accurately represent present field conditions. When $Hg(CN)_2$, $Hg(CN)_3^-$ entre the river, these, these complexes lose stability almost immediately. This occurs because free because CN^- drops sharply, pH decreases, photolysis accelerates CN^- destruction, and released Hg is rapidly scavenged by particles and DOM (Bravo and Cossio *et al.,* 2020). Consequently, although Hg–CN complexes can form and be stable within tailings tanks and ponds, it is geochemically unlikely that they persist or contribute to the transport of dissolved mercury once effluents enter the river system. This aligns with the undetectable levels of dissolved Hg recorded at all river stations. The comparison between studies reveals a key point. Prior models illustrate historical contexts involving significant cyanide levels and the presumption of chemical equilibrium, in contrast to current data that portray a dynamic, photo-reactive system with notably short residence times. In this system, rapid CN^- degradation and the instability of Hg–CN complexes limit the metal–cyanide speciation proposed by the simulations. Thus, rapid attenuation (>99.9%), predominance of CN^- and HCN, progressive increases in nitrogen and COD, absence of dissolved Hg, and instability of the Hg–CN complex under current fluvial conditions reflect a hydrochemistry that contrasts sharply with the

simulated scenarios. Collectively, this evidence emphasizes the critical nature of present empirical evaluations. It also suggests that studies conducted relying exclusively on simulations might exaggerate the stability and ecological importance of Hg–CN complexes in fluctuating river systems.These interpretations are intended as hypotheses informed by geochemical context, not as confirmed processes. Targeted analyses—including MeHg quantification, microbial community assays, and Hg-speciation measurements—are required to determine whether methylation occurs in this watershed. Although cyanide levels declined sharply relative to those in tailings ponds, values at discharge points still exceeded freshwater toxicity thresholds for many fish species (≥ 0.057–0.19 mg/L CN^-, (Singleton, 2021; Smith *et al*., 1978). On the other hand, some algae and invertebrates tolerate higher concentrations (Lachowicz *et al*., 2024). These levels continue to hold ecological significance and have the potential to support additional biodegradation processes downstream. Cyanide concentrations continued to decrease along the river, likely due to the combined effects of photolysis and oxidative degradation (Guimarães *et al*., 2011; Marshall *et al*., 2020). The presence of bicarbonate (HCO_3^-), generated through natural neutralization reactions, contributed to pH buffering and likely reduced the bioavailability of dissolved metals carried by the effluent plume. In comparison to cyanide, the levels of nitrate significantly rose downstream, frequently doubling in relation to discharge areas. COD exhibited a similarly complex pattern: it was low at upstream reference sites (~20 mg/L), reduced at the mining discharge point, and sharply elevated near the Ecuador–Peru border (~240 mg/L). These trends indicate the total contributions of nutrients and organic matter that arise not only from the degradation of cyanide but also from agricultural practices, livestock, untreated wastewater, and various non-mining sources.

This longitudinal enrichment of nitrogen is particularly concerning. Nitrate increased significantly from upstream to downstream (0.49 → 2.54 mg/L; p = 0.0379), consistent with nitrification of cyanide degradation products (Vaca-Escobar *et al.,* 2024). An overabundance of inorganic nitrogen and organic matter has been correlated with algal overgrowth, a reduction in biodiversity, and changes in trophic structure (Espiritu *et al*., 2022; Cui *et al*., 2025). The contrasting downstream trajectories of nitrate and COD thus reveal distinct source dynamics: nitrate primarily linked to cyanide degradation and diffuse watershed inputs, whereas COD reflects intermittent pulses of organic pollution. The strong affinity of DOM for Hg^{2+} enhances its mobility and bioavailability downstream (Zhao *et al.,* 2024; Moreno-Brush *et al*., 2020; Liu *et al.,* 2022). Bicarbonate increased from 9.3 to 55.8 mg/L (p = 0.0436), reflecting both ore-derived carbonate dissolution and neutralization reactions. Sulfate rose from 0.74 to 9.57 mg/L (p = 0.0422), indicating a cumulative sulfur contribution from tailings and watershed sources. Conductivity, TDS, and pH exhibited notable variations across different zones (all p < 0.05). COD, though not statistically significant (p = 0.4275), exhibited strong downstream enrichment (up to 240 mg/L), reflecting organic loading from agriculture, livestock, wastewater, and mining residues, reported by Puño, (2013) and Vinueza *et al.,* (2021). Historically, similar downstream enrichment patterns were documented in the binational monitoring program conducted between 2005 and 2007, affirming the existence of long-term multisectoral pressures (Fig. 4). Additional pressures from domestic wastewater, deforestation and intensive cattle ranching exacerbate these conditions (Vinueza *et al*., 2021; Puno, 2013). Historical data from the Binational Puyango–Tumbes Project (2005–2007) corroborate these patterns, with nitrate concentrations consistently rising from the Ecuadorian headwaters to downstream Peruvian stations (Fig. 4).

A key scientific gap highlighted by this study is the lack of integrated assessments combining cyanide degradation, nitrogen enrichment and mercury dynamics in ASGM-impacted rivers. This study documents the interconnected processes within a transboundary watershed, offering one of the initial field-based assessments that connect tailings chemistry to the ecological vulnerability downstream. It highlights the necessity for comprehensive, multisectoral monitoring and management of river basins.

Uncertainties and natural variability

Several sources of uncertainty and natural variability can influence pollutant transport and reaction pathways along the Puyango River. Spatial heterogeneity in flow velocity, sunlight exposure,

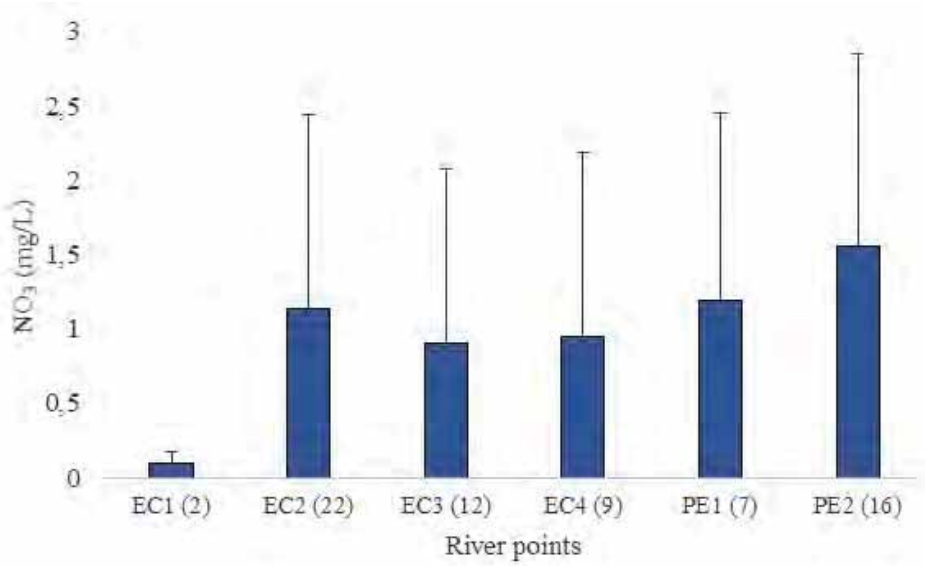

Fig. 4: Concentrations of NO_3^- across the Puyango-Tumbes River. Small bars represent standard deviation. (The number in parentheses indicates the number of measurements taken)

sediment texture, and organic matter availability can modulate cyanide photodegradation, nitrogen production from cyanide oxidation, sulfate release from sulfide minerals, and mercury partitioning. Diffuse inputs from agriculture, livestock, and domestic wastewater may further complicate the attribution of downstream nitrate and COD patterns. The lack of seasonal sampling restricts the ability to characterize hydrological fluctuations that influence dilution capacity, residence times, and redox transitions. These uncertainties do not undermine the direction or coherence of the observed trends but indicate that the results represent an hydrological snapshot. Long-term monitoring in the future, which combines hydrology, geochemical speciation modeling, and sedimentary analyses, will be required to more clearly delineate reaction pathways.

Implications for aquatic ecosystem health

The simultaneous existence of organic matter, sulfur compounds, and residual mercury establishes an environment favorable for microbial methylation. Under suboxic, sulfate-rich, and organic-carbon-enriched conditions, mercury is microbially transformed into methylmercury (MeHg). This procedure is shaped not solely by mining activities but also by land-use practices that exacerbate these environmental factors (Wang *et al*., 2019; Klapstein and O`Driscoll, 2017). Elevated MeHg levels in cyanide-impacted systems support the hypothesis that cyanide degradation and its nitrogen-rich byproducts may indirectly stimulate microbial pathways favorable to Hg methylation (Tulasi *et al*., 2021). Field evidence from this study suggests that Hg–CN complexes are improbable to remain downstream because of the swift decay of cyanide, a lower pH compared to cyanidation conditions, and the significant scavenging of Hg by suspended particles and DOM. Instead, mercury transitions into particulate-bound and DOM-associated forms, whose mobility and bioavailability increase under elevated COD, bicarbonate and sulfate. In this context, Fig. 5 illustrates a conceptual framework of the biogeochemical pathways that relate cyanide degradation, nutrient enrichment and mercury transformation in the Puyango River. The model outlines four key processes: i) cyanide photolysis and oxidation producing nitrogen species, ii) formation of soluble $Hg(CN)_4^{2-}$ complexes under alkaline conditions, iii) subsequent Hg–DOM binding, and iv) microbial methylation in depositional or low-oxygen zones. Laboratory assays have demonstrated DNA fragmentation and micronucleus formation in Andinoacara rivulatus, an Ecuadorian endemic species widely recognized as an effective sentinel organism, when exposed to $HgCl_2$ (Nirchio *et al*., 2019). These responses imply

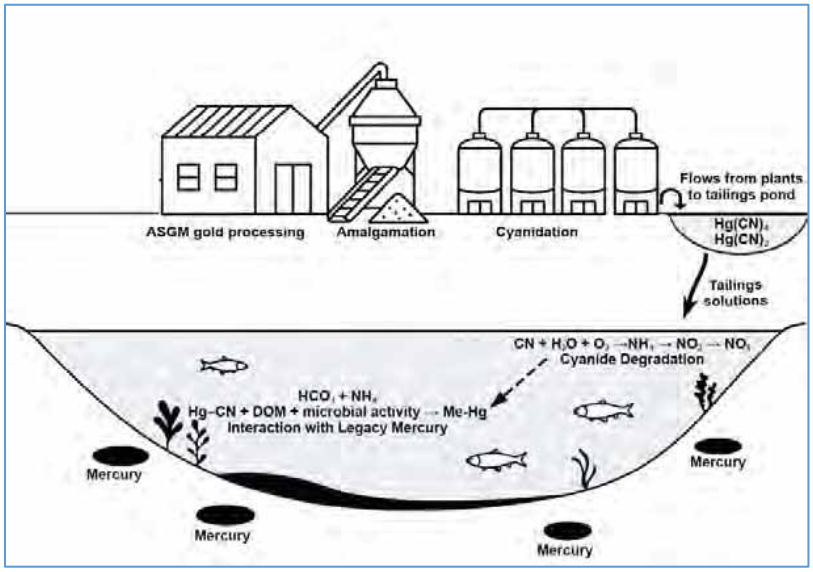

Fig. 5: Mercury and cyanide interactions in the Puyango river system

that even minimal mercury exposure can affect the genetic integrity of local fish populations, thereby heightening the ecological dangers linkedwith MeHg bioaccumulation and trophic transfer (Cruz-Esquivel *et al*., 2023). Overall, these findings highlight a critical ecotoxicological concern: although previous studies in Ecuador have demonstrated the genotoxic sensitivity of *A. rivulatus*, the toxicity of the mercury–cyanide complexes generated during gold extraction remains virtually unknown. Because cyanidation converts Hg(II) into highly soluble and mobile species such as $Hg(CN)_4^{2-}$, mercury bioavailability and genotoxicity may increase. In combination with particulate-bound and DOM-associated mercury downstream, this emphasizes the importance of evaluating biological responses to real effluents. This possibility ,with updated field evidence of particulate-bound and DOM-bound Hg species downstream, underscores the need to evaluate biological responses to real effluents rather than isolated mercury compounds. While this study does not directly record ecological effects linked to cyanide byproducts, it highlights the biogeochemical conditions that render such effects possible and delineates the monitoring indicators necessary for their detection in future evaluations. Addressing this gap is essential for understanding the full scope of ecological risk in the Puyango–Tumbes system and for developing evidence-based monitoring strategies in transboundary watersheds affected by artisanal and small-scale gold mining.

CONCLUSION

Although limited by sample size, this case study provides clear evidence of cyanide degradation and its concurrent interaction with mercury within the Portovelo–Zaruma–Puyango system. Cyanide concentrations decreased by about 80% between the leaching tanks (694.9 ± 159 mg/L total CN^-) and the tailings ponds (194 ± 327 mg/L), and by nearly 99.9% along the river (<0.2 mg/L). This notable decrease demonstrates the inherent photolytic and oxidative degradation processes that are propelled by intense solar radiation, in addition to the roles of dilution and sorption along the flow trajectory. However, cyanide-derived byproducts such as thiocyanate, ammonium, and nitrate are indicators of emerging pressures that can impair aquatic ecosystem health. Nitrate concentrations rose sharply from non-detectable levels in process solutions to 25 mg/L in tailings ponds and 5.4 mg/L (max level) downstream in the river. The findings of this study provide evidence that dissolved mercury concentrations in river water were maintained below detection limits. Nonetheless, the mobilization of mercury continues within the mining system due to mercury-rich amalgamation residues and highly contaminated leaching pulps, which

perpetually release mercury into tailings ponds. Within these ponds, elevated cyanide and alkaline pH foster formation of thermodynamically stable Hg–CN complexes. Downstream conditions defined by lower cyanide concentrations, moderate pH, and abundant particles and DOM encourage the breakdown of these complexes and subsequent mercury partitioning into sediments. This enrichment stems from microbial nitrification of cyanide degradation products, along with diffuse contributions from agriculture and domestic wastewater. The result is bioenrichment that encourages the growth of algae, leads to oxygen depletion, and potential eutrophication within the transboundary Puyango–Tumbes watershed. COD also increased substantially from around 20 mg/L at upstream sites to 240 mg/L near the Ecuador-Peru border indicating heavy organic loading. This organic substance boosts microbial respiration and lowers oxygen levels, encouraging reducing environments that facilitate mercury methylation and the durability of Hg–DOM complexes. Collectively, the findings show that while cyanide itself is largely degraded, its transformation products, particularly nitrates and organic compounds, continue to modify the river's biogeochemical balance. The coexistence of nitrogen, organic matter, and residual mercury forms a synergistic contamination network, heightening ecological vulnerability and potential health risks through trophic transfer. Overall, the Puyango River functions as a reactive geochemical corridor where cyanide degradation, nitrogen accumulation, organic enrichment, and mineral-driven sulfate–bicarbonate release converge with legacy mercury, which collectively impact water quality and ecosystem vulnerability. From a managerial standpoint, the Portovelo–Zaruma–Puyango system necessitates cohesive watershed governance. The findings are directly relevant to regulatory bodies. In Ecuador, agencies responsible for water and mining oversight are tasked with regulating practices related to cyanidation, managing effluent discharge, overseeing tailings management, and protecting the environment. In Peru, national and regional water authorities—together with the Ecuador–Peru Puyango–Tumbes Commission—can use these results to strengthen transboundary monitoring and basin-level planning. Regulatory frameworks ought to integrate controls on secondary pollutants, nutrient enrichment, and organic loading. Effective transboundary management demands multiple strategies, including: i) routine monitoring of cyanide, nitrogen species, sulfate, bicarbonate, COD, and mercury (total, dissolved, methylated); ii) sediment and biota surveys to detect MeHg hotspots; iii) assessment of mineralogical controls and pH buffering on contaminant mobility; iv) standardized tailings-pond and effluent protocols; and v) integrated ecological and public-health indicators for long-term impact evaluation.

AUTHOR CONTRIBUTIONS

M. Nirchio reviewed the manuscript draft and final version of the manuscript writing. L. Granda performed laboratory analytical work, including reagent preparation and equipment setup for chemical analyses. L. Chinchay assisted with fieldwork, including data collection and measurements, and contributed to data analysis. P.C. Velásquez-López (corresponding author) conceived the research idea, interpreted the results, and drafted and finalized the manuscript.

ACKNOWLEDGEMENT

This study was supported by the following funding sources: The complete integrated assessment was supported by the United Nations Industrial Organization through the Project "Implementing Integrated Measures for Minimizing Mercury Releases from Artisanal Gold Mining" [No.: GF/RLA/12/003-100271 GEF ID: 4799]. "Contaminación por metales pesados que se originan en las actividades mineras artesanales y de pequeña escala: Análisis temporal and espacial del riesgo ecológico en el ecosistema camaronero del sur del Ecuador" 2020 agreement UTMACH-CIRDI; the [2024/UTMACH-PR-GEN-278] project approved by Universidad Técnica de Machala.

CONFLICT OF INTEREST

The authors declare no competing interests regarding the publication of this manuscript. In addition, the ethical issues, including plagiarism, data fabrication and/or falsification, double publication and/or submission, have been completely observed by the authors.

R Positive AI Statement

During the preparation of this work the author(s) have used Artificial Intelligence (AI) [Chat GPT]

in order to improve flow, spelling, and grammar corrections of the manuscript. After using this tool, the authors reviewed and edited the content as needed and take full responsibility for the content of the publication.

(For this reason, the GPTZero detector will evaluate the manuscript utilizing Generative AI, ensuring a high detection rate. If the manuscript relies heavily on Generative AI and AI-assisted technologies, it will be archived without further options for appeal).

ABBREVIATIONS

Å	Ångström
%	Percent
>	Greather than
<	Less than
^{o}C	Degree Celsius
µm	Micrometer
µS/cm	Microsiemens per centimeter
µg/L	*Micrograms per liter*
g/cm^3	Grams per cubic centimeter
mg/kg	Milligrams per kilogram
mg/L	Milligrams per liter
A,B,C	Sampling zones
Aq	Aqueous
$Al_2Si_2O_5(OH)_4$	Aluminium silicate dihydrate
As	Arsenic
ASGM	Artisanal and small scale gold mining
$CaMg(CO_3)_2$	Calcium magnesium carbonate
$CaCO_3$	Calcium carbonate
$CaSO_4.2(H_2O)$	Calcium sulfate dihydrate
CCME	Canadian Council of Ministers of the Environment
Cl	Chloride
CN	Cyanide
COD	Chemical oxygen demand
Cu	Copper
$CuFeS_2$	Copper iron disulfide
Cu-Kα	*Copper K-alpha radiation*
CV	Coefficient of variation
CV-AAS	Cold Vapor Atomic Absorption Spectroscopy
ICDD PDF	Diffraction Data-Powder Diffraction File
DNA	Deoxyribonucleic acid
DOM	Dissolved Organic Matter
EC1	First Ecuadorian point along the river
EC2	Second Ecuadorian point along the river
EC3	Third Ecuadorian point along the river
EC4	Fourth Ecuadorian point along the river
ERA	Environmental Resources Associates
F	Fluoride
Fe	Iron
$Fe^{3+}AsS$	Iron(III) arsenic sulfide
FeS_2	Iron(II) disulfide
FIA	Flow Injection Analysis
Fig.	Figure
H	Hours
ha	Hectare
H_2O	Water
HCO_3^-	Bicarbonate
Hg	Mercury
Hg^o	elemental mercury
Hg^{2+}	mercury(II) ion
$[Hg(CN)_4]^{2-}$	Tetracyanomercurate (II) ion
$Hg(CN)_2^-$	Mercury cyanide
$Hg(CN)_3^-$	Tricyanomerurate(II) ion
Hg–DOM	Mercury-Dissolved organic matter complex
HgS	Mercury sulphide or cinnabar
$KAl_2((AlSi_3O_{10})(OH)_2$	Potassium aluminum silicate hydroxide
$K_2Cr_2O_7$	Potassium dichromate
kV	Kilovolts
K-W	Kruskal-Wallis
m.a.s.l.	*meters above sea level*
mA	Milliamper

MAX	Maximum value
MDL	Method detection limit
$Mg_{3.75}Fe^{2+}_{1.25}Si_3Al_2O_{10}(OH)_8$	Magnesium-iron aluminum silicate hydroxide
MIN	Mínimum value
MeHg	Methylmercury
Mn	Manganese
mL	Milliliters
n	Number of samples or sample size
ns	Not significant
$NaAlSi_3O_8$	Sodium aluminum silicate
ND	Not detectable
NH_4^+	Ammonium
NO_2^-	Nitrite
NO_3^-	Nitrate
PE1	First Point along the river at Peruvian zone
PE2	Second Point along the river at Peruvian zone
Pb	Lead
pH	Potential of hydrogen
PbS	Lead(II) sulfide
SiO_2	Silicon dioxide
SCN^-	Thiocyanate
SD	Standard deviation
SO_4	Sulphate
TDS	Total dissolved solids
US-EPA	United States Environmental Protection Agency
UV	Ultraviolet
XRD	X-ray diffraction
Zn	Zinc
ZnS	Zinc sulfide

REFERENCES

Abdelaal, A.; Sultan, M.; Abotalib, A.Z.; Bedair, M.; Krishnamurthy, R.V.; Elhebiry, M., (2023). Emerging mercury and methylmercury contamination from new artisanal and small-scale gold mining along the Nile Valley, Egypt. Environ. Sci. Pollut. Res. Int., 30: 52514–52534 **(21 pages).**

Ayoo, B.A.; Anyango, S.O.; Mulwa, R.M. (2024**).** Cyanide and cyanidation wastes management in gold leaching plants in Siaya County, Kenya. Environ. Geochem. Health. 46(10):410-414 **(14 pages).**

Arellano-Yasaca, D.V.; Chu, C. Y.; Hoang, T.V., (2024). The impact of gold mining activities: understanding the dynamics of cyanide in river ecosystems in Ecuador. Environ. Sci. Pollut. Res., 31: 64509–64523 **(15 pages).**

Bravo, A.G.; Cosio, C., (2020). Environmental processes controlling the fate and transformation of mercury in aquatic ecosystems. Sci. Total Environ., 721: 137647 (**22 pages)**.

Cáceda, C.J.; Fora, G.L.; Carpio, M.; Maraza,G.; Sacari E., (2023). Cyanide bioremediation by bacillus subtilis under alkaline conditions. Water. 15(20): 3645 **(15 pages**).

Casso-Hartmann, L.; Rojas-Lamos, P.; McCourt, K.; Vélez-Torres, I.; Barba-Ho, L.E.; Bolaños, B.W.; Montes C.L.; Mosquera J.; Vanegas, D. (2022). Water pollution and environmental policy in artisanal gold mining frontiers: The case of La Toma, Colombia. Sci. Total Environ., 852: 158417 **(9 pages)**.

Cruz-Esquivel, Á.; Diez, S.; Marrugo-Negrete, J.L., (2023). Genotoxicity effects in freshwater fish species associated with gold mining activities in northern Colombian aquatic ecosystems. Ecotoxicol. Environ. Saf. 253: 114670 **(9 pages).**

Cui, D.; He, H.; Zhang, Z.; Liu, F.; Gui, Y.; Guo, Z.; Liao, Z.; Niu, X.-Z.; Huang, B.; Pan, X., (2025). Coupling of algae, algal organic matter, and nutrient biogeochemical cycling in eutrophic waters. Rev. Environ. Sci. Biotechnol., 24: 451–475 (**25 pages).**

da Silva, H.A.M.; Guimarães, J.R.D., (2024). Mercury cyanide complexes and their relevance as environmental contaminants. Chemosphere. 350: 141054 **(8 pages).**

Dossou Etui, I.M.; Stylo, M.; Davis, K.; Evers, D.C.; Slaveykova, V.I.; Wood, C.; Burton, M.E.H. (2024). Artisanal and small-scale gold mining and biodiversity: A global literature review. Environmental Research, 246: 118605 **(20 pages**)

Espiritu, E.Q.; Claveria, R.J.R.; Bernadas, P.J.C., (2022). Assessment of surface water quality and mercury levels from artisanal and small-scale gold mining (ASGM) along Acupan River, Benguet, Philippines. Environ. Geochem. Health. 44(10): 3655-3676 **(21 pages).**

Freitas, J.; Horta, D., (2023). Impacts of cyanide in gold mining and cyanide removal methodologies in liquid waste from gold processing. Rev. Metal. 59 (3): e247 **(8 pages).**

Gonçalves, A.O.; Marshall B.G.; Kaplan R.J.; Moreno-Chavez J.; Veiga M.M., (2017). Evidence of reduced mercury loss and increased use of cyanidation at gold processing centers in Southern Ecuador? J. Clean. Prod., 165:836–45 **(9 pages).**

Guimarães, J.R.D.; Betancourt O.; Rodrigues, M.; Barriga, M.; Cueva, E.; Betancourt, S., (2011). Long-range effect of cyanide on mercury methylation in a gold mining area in Southern Ecuador. Sci. Total Environ., 409(23): 5026–33 **(8 pages).**

Helmrich, S.; Vlassopoulos, D.; Alpers, C. N.; O'Day, P.A., 2022). Critical review of mercury methylation and methylmercury demethylation rate constants in aquatic sediments for biogeochemical modeling. Crit. Rev. in Env. Sci. Tec., *52*(24): 4353-4378 **(25 pages).**

King, D.; Watts, M.; Hamilton, E.; Mortimer, R.; Coffey, M.; Osano, O.; Di Bonito, M., (2024). Mercury speciation in environmental samples associated with artisanal small-scale gold mining. Environ. Geochem. Health, 46(11): 48 **(17 pages).**

Klapstein, S.J.; O'Driscoll, N.J., (2017). methylmercury biogeochemistry in freshwater ecosystems: A review focusing on DOM and photodemethylation. Bull. Environ. Contam.

Toxicol., 99: 1-8 **(8 pages).**

Kosai, S.; Yamao, S.; Kashiwakura, S.; Yamasue, E.; Ishigaki, T.; Nakajima, K., (2023). Cost of proper waste management of retorted mercury in artisanal and small-scale gold mining: global estimates and financial implications. J. Mater. Cycles Waste. 25(5): 2681-2690 **(10 pages).**

Kwofie, I.A.; Jogand, H.; De Ladurantaye-Noël, M.; Dale, C., (2021). Removal of cyanide and other nitrogen-based compounds from gold mine effluents using moving bed biofilm reactor (MBBR). Water. 13(23): 3370 (**15 pages**).

Lachowicz, J.I.; Alexander, J.; Aaseth, J.O. (2024). Cyanide and cyanogenic compounds—Toxicity, molecular targets, and therapeutic agents. Biomolecules. 14(11):1420 **(25 pages).**

Liu, J.; Li, Y.; Duan, D.; Peng, G.; Li, P.; Lei, P.; Zhong H.; Zui M.; Pan, K. (2022). Effects and mechanisms of organic matter regulating the methylmercury dynamics in mangrove sediments. J. Hazard. Mater., 432, 128690 **(35 pages).**

Malone, A.; Figueroa, L.; Wang, W.; Smith, N.M.; Ranville, J.F.; Vuono, D.C.; Zapata, F.D.A.; Paredes L.M.; Sharp J.O.; Bellona, C. (2023). Transitional dynamics from mercury to cyanide-based processing in artisanal and small-scale gold mining: Social, economic, geochemical, and environmental considerations. Sci. Total Environ., 898: 165492 **(10 pages).**

Marshall, B.G.; Veiga, M.M.; Kaplan, R.J.; Miserendino, R.A.; Schudel, G.; Bergquist, B. A.; Guimarães, J.R.D.; Sobral LGS; Gonzalez-Mueller, C., (2018). Evidence of transboundary mercury and other pollutants in the Puyango-Tumbes River basin, Ecuador–Peru. Environ. Sci. Processes Impacts. 20(4): 632-641 **(10 pages).**

Marshall, B.G., Veiga M.M., da Silva H., Guimarães J.R.D., (2020). Cyanide contamination of the Puyango-Tumbes River caused by artisanal gold mining in Portovelo-Zaruma, Ecuador. Curr. Environ. Health Rep., 7(3): 303–10 **(8 pages).**

Mestanza-Ramón, C.; Mora-Silva, D.; D'Orio, G.; Tapia-Segarra, E.; Domínguez-Gaibor, I.; Esparza-Parra, J.F.; Chávez-Velásquez, C.R.; Straface, S. (2022). Artisanal and Small-Scale Gold Mining (ASGM): Management and Socio-environmental Impacts in the Northern Amazon of Ecuador. Sustainability. 14(11): 6854 **(22 pages).**

Miserendino, R.A., Bergquist, B.A., Adler S.E.; Guimarães, J.R.D.; Lees PSJ.; Niquen W.; Velásquez-López P.C.; Veiga M.M, (2013). Challenges to measuring, monitoring, and addressing the cumulative impacts of artisanal and small-scale gold mining in Ecuador. Resour. Policy. 38(4): 713-722 **(9 pages).**

Moreno-Brush, M.; McLagan D.S.; Biester H., (2020). Fate of mercury from artisanal and small-scale gold mining in tropical rivers: hydrological and biogeochemical controls. A critical review. Crit. Rev. Env. Sci. Technol., 50(5): 437–75 **(38 pages).**

Mulenga, M.; Ouma, K.O.; Monde, C.; Syampungani, S., (2024). Aquatic mercury pollution from artisanal and small-scale gold mining in sub-Saharan Africa: Status, Impacts, and Interventions. Water. 16(5): 756 **(27 pages).**

Nirchio, M.; Choco, O.J.; Quizhpe, P.F.; Hernández, J.G.; Oliveira, C., (2019). Genotoxic effects of mercury chloride on the neotropical fish Andinoacara rivulatus (Cichlidae: Cichlasomatini). Rev. Biol. Trop., 67(4): 745–54 **(9 pages).**

Puño, N., (2013). Environmental management of the Puyango–Tumbes River basin in Ecuador and Peru. In: Clark, R., Hakim, S. (eds) Securing Water and Wastewater Systems. Protecting Critical Infrastructure, vol 2. Springer Cham: Springer Int. Publ., 161-187 **(26 pages).**

Schudel, G., Miserendino, R.A.; Veiga, M.M.; Velasquez-López, P.C.; Lees, P.S.; Winland-Gaetz, S.; Guimarães, J.R.D.; Bergquist, B.A., (2018). An investigation of mercury sources in the Puyango-Tumbes River: Using stable Hg isotopes to characterize transboundary Hg pollution. Chemosphere. 202: 777-787 **(11 pages)**.

Schudel, G.; Kaplan, R.; Miserendino, R.A.; Veiga, M.M.; Velásquez-López, P.C.; Guimarães, J.R.D.; Bergquist, B. A., (2019). Mercury isotopic signatures of tailings from artisanal and small-scale gold mining (ASGM) in southwestern Ecuador. Sci. Total Environ., 686: 301-310 **(10 pages).**

Seney, C.S.; Bridges, C.C.; Aljic, S.; Moore, M.E.; Orr, S.E.; Barnes, M.C.; Joshee, L.; Uchakina, O.N.; Bellott, B.J.; McKallip, R.J.; Drace, K.; Veiga, M.M.; Kiefer, A.M., (2020). Reaction of cyanide with Hg0-contaminated gold mining tailings produces soluble mercuric cyanide complexes. Chem. Res. Toxicol., 33(11): 2834-2844 **(11 pages).**

Singleton, H.J., (2021) Water Quality Criteria for Cyanide. BC Environment, Water Management Division. **(28 pages).**

Smith, L.L. Jr.; Broderius, S.J.; Oseid, D.M.; Kimball, G.L.; Koenst, W.M. (1978). Acute toxicity of hydrogen cyanide to freshwater fishes. Arch. Environ. Contam. Toxicol., 7:325–337 **(13 pages).**

Solujic, L.; Milosavljevic E.B.; Straka M.R., (1999). Total cyanide determination by a segmented flow injection–on-line UV digestion–amperometric method. Analyst., 124 (8): 1255–1260 **(5 pages).**

Salgado-Almeida, B.; Briones-Escalante, A.; Falquez-Torres, D.; Filián-Haz, K.; Guzmán-Martínez, F.; Escobar-Segovia, K.; Peña-Carpio, E.; Jiménez-Oyola, S., (2024). Assessment of environmental pollution and risks associated with tailing dams in a historical gold mining area of Ecuador. Resources, 13(8): 105 **(15 pages**).

Spiegel, S.; Keane, S.; Metcalf, S.; Veiga, M., (2015). Implications of the Minamata convention on mercury for informal gold mining in Sub-Saharan Africa: from global policy debates to grassroots implementation? Environ. Dev. Sustain. 17: 765–785 **(21 pages).**

Standard Methods Committee of the American Public Health Association; American Water Works Association; Water Environment Federation. (2017) 5220 Chemical Oxygen Demand (COD). In: Lipps WC, Baxter TE, Braun-Howland E (eds). Standard Methods for the Examination of Water and Wastewater, 23rd ed. Washington DC: APHA Press **(1796 pages)**

Torrance, J.; Redwood, Y.; Cecchi, M., (2021). The impact of artisanal gold mining, ore processing and mineralization on water quality in Marmato, Colombia. Environ. Geochem. Health. 43(8): 3031–3050 **(20 pages).**

Tulasi, D.; Fajon, V.; Kotnik, J.; Shlyapnikov, Y.; Adotey, D. K.; Serfor-Armah, Y.; Horvat, M., (2021). Mercury methylation in cyanide influenced river sediments: A comparative study in Southwestern Ghana. Environ. Monit. Assess., 193(4): 180 **(18 pages).**

US-EPA, (2007). Method 9056a Determination of Inorganic anions by Ion chromatography. U.S. Environmental Protection Agency. 2007 **(19 pages).**

Vaca-Escobar, K.; Arregui-Almeida, D.; Espinoza-Montero, P., (2024). Chemical, ecotoxicological characteristics, environmental fate, and treatment methods applied to cyanide-containing

wastewater. Npj Clean Water. 7(1) **(16 pages).**
Veiga, M.M.; Angeloci, G.; Hitch, M.; Velásquez-López, P.C., (2014). Processing centres in artisanal gold mining. J. Clean. Prod., 64: 535–544 **(10 pages).**
Velásquez-López, P.C.; Veiga, M.M.; Hall, K., (2010). Mercury balance in amalgamation in artisanal and small-scale gold mining: identifying strategies for reducing environmental pollution in Portovelo-Zaruma, Ecuador. J. Clean. Prod., 18 (3): 226–32 **(7 pages)**.
Velásquez-López, P.C.; Veiga, M.M.; Klein B.; Shandro J.S.; Hall K., (2011). Cyanidation of mercury-rich tailings in artisanal and small-scale gold mining: identifying strategies to manage environmental risks in Southern Ecuador. J. Clean. Prod., 19(9-10): 1125–33 **(8 pages).**
Verbrugge, B.; Lanzano, C.; Libassi. M., (2021). The cyanide revolution: efficiency gains and exclusion in artisanal- and small-scale gold mining. Geoforum, 126:267–76 **(10 pages).**
Vinueza, D.; Ochoa-Herrera, V.; Maurice, L.; Tamayo, E.; Mejía, L.; Tejera, E.; Machado, A., (2021). Determining the microbial and chemical contamination in Ecuador's main rivers. Sci. Rep., 11(1): 17640 **(14 pages).**
Wang, J.; Xing, Y.; Xie, Y.; Meng, Y.; Xia, J.; Feng. X., (2019). The Use of calcium carbonate-enriched clay minerals and diammonium hosphate as novel immobilization agents for mercury remediation: Spectral Investigations and Field Applications. Sci. Total Environ., 646: 1615–23. **(9 pages).**
Welman-Purchase, M.D.; Castillo, J.; Gomez-Arias, A.; Matu, A.; Hansen. R., (2024). First insight into the natural biodegradation of cyanide in a gold tailings environment enriched in cyanide compounds. Sci. Total Environ., 906: 167174 **(9 pages).**
Youpoungam, A.A.; Kantarcı, S.; Alp, I., (2024). Characterization and Reprocessing of Artisanal and Small-Scale Gold Mine Tailings. Min. Metall. Explor., 41: 2603–2618 (**16 pages**).
Zhao, W.; Gan, R.; Xian, B.; Li, Y.; Chen, J.; Wang, H.; Zhang, L.; Liu, Y.; (2024). Overview of methylation and demethylation mechanisms and influencing factors of mercury in water. Toxics, 12(10): 715 (**15 pages).**

AUTHOR (S) BIOSKETCHES

Velasquez-Lopez, P.C., Ph.D., Professor of the faculty of Agricultrural sciences. Universidad Tecnica de Machala. Km 5.5 via Pasaje, Machala. Ecuador.
- Email: *colon.velasquez@gmail.com*
- ORCID: 0000-0002-3044-920X
- Web of Science ResearcherID: NA
- Scopus Author ID: 35114290700
- Homepage: https://www.utmachala.edu.ec/portalwp/index.php/uaca/

Chinchay, L., Environ. Eng., M.Sc., Environmental consultant. Sustainable Economic Futures, SEFClean Gold #2004 1225 Richards Street, Vancouver, V6B 3G3, BC Canada.
- Email: *luis.chinchay@hotmail.com*
- ORCID: 0009-0005-3493-2687
- Web of Science ResearcherID: NA
- Scopus Author ID: NA
- Homepage: *https://www.sefcleangold.com*

Granda, L., Chem. Eng. M.Sc., Chief of Analytical Department. 3United Nations Industrial Development. Department of Environment. Vienna, International Centre, PO Box 100 A-1400 Austria.
- Email: luis.granda@laboratoriolasa.com
- ORCID: 0009-0000-6853-4840
- Web of Science ResearcherID: NA
- Scopus Author ID: NA
- Homepage: https://laboratoriolasa.com/

Nirchio, M., Ph.D. Professor of the Faculty of Agricultural Sciences. Universidad Tecnica de Machala. Km 5.5 via Pasaje, Machala. Ecuador.
- Email: mauro.nirchio@gmail.com
- ORCID: 0000-0001-7171-2433
- Web of Science ResearcherID: L-3729-2017
- Scopus Author ID: 55929165900
- Homepage: https://www.utmachala.edu.ec/portalwp/index.php/uaca/

HOW TO CITE THIS ARTICLE

Velasquez-Lopez, P.C.; Chinchay, L.; Granda, L.E.; Nirchio, M., (2026). Cyanide and mercury in artisanal gold mining tailings: Investigating synergistic impacts in a multi-use transboundary aquatic ecosystem. Global J. Environ. Sci. Manage., 12(1): 313-330.

DOI: 10.22034/gjesm.2026.01.18

URL: https://www.gjesm.net/article_732031.html

Global J. Environ. Sci. Manage. 12(1): 331-350, Winter 2026, Serial #45

Global Journal of Environmental Science and Management
(GJESM)

Homepage: https://www.gjesm.net/

Podcasts

CASE STUDY

Eco-friendly organic nutrients enriched with biosoltamax enhance shallot growth, improve soil properties, and reduce the use of mineral fertilizer

A. Nurawan[1], K.D. Sutanto[1,*], Y. Haryati[1], B. Susanto[2], K.K. Hamdani[1], Y. Surdianto[2], N. Sutrisna[2], N.R. Purnamasari[1], S.R. Djiwanti[3], D. Histifarina[4], A. Jufri[3], D.W. Utami[1]

[1] *Research Center for Horticulture, National Research and Innovation Agency, Jl. Raya Jakarta-Bogor KM 46, Cibinong, Indonesia*

[2] *Research Center for Food Crops, National Research and Innovation Agency, Jl. Raya Jakarta-Bogor KM 46, Cibinong, Indonesia*

[3] *Research Center for Estate Crops, National Research and Innovation Agency, Jl. Raya Jakarta-Bogor KM 46, Cibinong, Indonesia*

[4] *Research Center for Food Technology and Processing, National Research and Innovation Agency, Cibinong-Bogor, West Java, Indonesia*

ARTICLE INFO

Article History:
Received 20 July 2025
Revised 24 October 2025
Accepted 28 November 2025

Keywords:
Earthworm compost
Shallot cultivation
Soil fertility
Soil properties
Sustainable nutrient management

ABSTRACT

BACKGROUND AND OBJECTIVES: Excessive reliance on inorganic nitrogen–phosphorus–potassium fertilizers in shallot (*Allium cepa var. aggregatum*) production can degrade soil quality, increase nutrient losses, and reduce smallholder profitability. This study assessed the potential of locally sourced organic nutrients, in conjunction with a microbial biofertilizer, to maintain shallot yield and enhance soil characteristics in tropical environments

METHODS: An experimental design based on a randomized complete block with six treatments and four replicates; each replicate consists of ten plants. Treatments compared one hundred percent mineral fertilizer; fifty percent mineral fertilizer combined with poultry manure; fifty percent mineral fertilizer combined with poultry manure plus the Biosoltamax microbial biofertilizer. In addition, fifty percent mineral fertilizer combined with sheep manure plus the Biosoltamax microbial biofertilizer black soldier fly frass compost. Followed by fifty percent mineral fertilizer combined with black soldier fly frass compost (locally named 'Kasgot') and the commercial microbial biofertilizer Biosoltamax; and an additional treatment as specified in the methods. An evaluation was conducted on plant growth and yield parameters, soil chemical properties, urease activity, and the use of scanning electron microscopy with energy dispersive spectroscopy. Statistical analyses included analysis of variance and mean separation at a probability less than 0.05.

FINDINGS: The treatment combining fifty percent mineral fertilizer, black soldier fly frass compost and Biosoltamax produced strong vegetative growth (maximum plant height 48.95 centimeters; maximum fresh leaf biomass 84.08 grams per plant) and high bulb productivity (mean fresh bulb weight 49.75 grams per bulb; mean 5.25 bulbs per plant, equivalent to about 261.2 grams fresh bulb mass per plant). Under integrated organic and reduced mineral regimes, soil organic carbon increased from 1.35 percent to 1.59 percent, and total nitrogen rose from 0.14 percent to 0.175 percent; furthermore, there was also an increase in urease activity. Energy dispersive spectroscopy showed that carbon and oxygen dominated the soil particle composition (carbon: 45–55 percent; oxygen: 36–42 percent), consistent with enriched organic-matter inputs.

CONCLUSION: Using poultry manure and earthworm compost from black soldier fly frass along with a microbial biofertilizer and decreasing mineral fertilizer application, can preserve shallot yield and simultaneously improve soil organic carbon, total nitrogen, and soil properties. This combined approach supports healthier soil and offers an environmentally safer alternative to full mineral fertilizer use.

DOI: 10.22034/gjesm.2026.01.19

This is an open access article under the CC BY license (http://creativecommons.org/licenses/by/4.0/).

NUMBER OF REFERENCES	NUMBER OF FIGURES	NUMBER OF TABLES
47	1	9

*Corresponding Author:
Email: *koko006@brin.go.id*
Phone: +62857 0018 5612
ORCID: 0000-0002-3605-4954

Note: Discussion period for this manuscript open until Mar 1, 2026 on GJESM website at the "Show Article".

INTRODUCTION

Shallots (*Allium cepa* variety *aggregatum*) hold significant economic and nutritional value in both culinary and medicinal sectors. The production they achieve, however, is heavily reliant on soil fertility, which is predominantly shaped by nutrient management strategies (Askari-Khorasgani and Pessarakli, 2020; Singh *et al*., 2020; Kushwah *et al.,* 2024). It has been demonstrated that an over-reliance on inorganic fertilizers increases carbon dioxide (CO_2) emissions, water contamination, and degradation of soils, thereby posing serious environmental challenges (Chauhan *et al*., 2012; Ilahi *et al*., 2020; Li *et al*., 2022; Holka *et al*., 2022; Nath *et al*., 2023). Conversely, organic fertilizers, including compost and animal waste, mitigate the dangers of chemical runoff and prolonged soil degradation, while also boosting the soil's structure (Verma *et al*., 2019; Holik *et al.,* 2019; Abebe *et al*., 2022; Khan *et al*., 2024). Recent research on horticultural crops has demonstrated that integrating organic fertilizers can enhance yield and improve environmental sustainability. For example, studies on tomato cultivation have reported yield increases (Zhang *et al*., 2024). These findings suggest that organic fertilization has considerable potential to serve as a more sustainable alternative to conventional chemical fertilizers across various horticultural systems. This study evaluates the impact of different fertilizers on shallot growth, biomass accumulation, and yield while considering the importance of sustainable methods. The study specifically investigates important factors, including plant height, leaf count, tiller output, and fresh and dry biomass. This study examines the impact of fertilizer treatments on soil health by examining changes in soil characteristics like potential of hydrogen (pH), organic matter content, and nutrient supply (Zhao *et al*., 2023). The study compares organic and inorganic fertilizers to optimize shallot productivity and minimize environmental impact, aiming to develop best practices for nutrient management and soil sustainability. Scanning electron microscopy combined with energy-dispersive spectroscopy was applied to analyze the microstructure and elemental composition of planting media; these physical and chemical characteristics can affect root architecture, water retention, and nutrient availability, thereby elucidating the observed agronomic responses. The hypothesis guiding this research is that organic fertilizer treatments, by virtue of their ability to improve soil structure and nutrient cycling, will significantly enhance shallot growth and yield compared to conventional inorganic fertilizers. Organic nutrient inputs provide a sustainable strategy to enhance crop yield, farm profitability, and soil health in temperate agricultural systems (Cen *et al*., 2020; Antil and Raj, 2019; Kushwah *et al.,* 2024). The key themes of global sustainability were distilled into a succinct contextual sentence that associates nutrient substitution with regenerative practices pertinent to smallholder systems. Therefore, this study aims to contribute to the growing body of evidence on environmentally safe nutrient management by demonstrating how organic fertilizers can improve horticultural production and support sustainable fertilization strategies. After establishing the environmental motivation, the manuscript transitions to shallot-specific agronomic gaps: limited knowledge on Kasgot application rates, Biosoltamax interactions with organic amendments, and effects on bulb quality and soil fertility under tropical conditions. The hypothesis suggests that replacing a portion of mineral fertilizer with organic amendments sourced locally, especially when used alongside the Biosoltamax microbial inoculant, may sustain or enhance shallot yield and soil characteristics in comparison to solely using mineral fertilization. The novelty includes 1) documenting the use of black soldier fly frass (Kasgot) in shallot growing media, 2) comprehensive assessment of soil chemical and biochemical responses to mixed organic–mineral inputs, 3) inclusion of a microbial biofertilizer to probe synergistic effects, and 4) microstructural characterization by scanning electron microscope- energy dispersive spectroscopy (SEM-EDS). It is advisable to conduct a formal economic assessment in upcoming on-farm trials. This study addresses the pressing demand for circular and regenerative farming methods by utilizing Kasgot and poultry waste as essential nutrient inputs, delivering actionable insights for enhancing sustainability in horticultural systems. This study was conducted in Cipaku, Ciamis, Indonesia, in 2023.

MATERIALS AND METHODS

Study site and context

This investigation was carried out on latosol soil in Cipaku, Ciamis, at a height of 550 meters (m) above sea level in 2023. The objective of the field experiment

Table 1: Soil properties before treatment

Property	Value
Sand (%)	5
Silt (%)	36
Clay (%)	59
pH (H_2O)	6.3
pH (KCl)	5.7
Organic C (%)	1.35
N (%)	0.14
C/N ratio	9
P_2O_5 (ppm)	66.5
K (ppm)	757.7

was to assess the impact of various fertilizer treatments on the development, growth, and soil quality of shallots (Aulakh, 2010; Wu and Ma, 2015; Abid *et al*., 2020). A series of well-defined protocols were followed to ensure consistency in treatment applications and data collection throughout the experiment.

Soil and seed preparation with biofertilizer application

Polybag specifications were used for the shallot seedlings: standard plastic polybags with 30 centimeters (cm) high × 25 cm diameter, holding 5 liters of substrate, were used; drainage holes were provided at the base to ensure free drainage. Prior to sowing, Biosoltamax was utilized on the soil to boost microbial activity and improve nutrient availability. The biofertilizer was prepared by mixing six tubes of Biosoltamax with one liter of coconut water (Babou and Lisna, 2019) and allowing the mixture to incubate for 15 minutes (min.) to activate its bioactive components. After incubation, the solution was diluted by adding 5 milliliters per liter (mL/L) of water and evenly applied to the soil. This treatment was intended to enhance the quality of soil, thereby facilitating effective seed germination and the development of early roots. To determine nutrient release dynamics, we recommend conducting controlled incubation studies (aerobic at field temperature ranges) to estimate mineralization rates and timed sequential soil sampling at pre-plant and key shallot growth stages (emergence, bulbing initiation, bulbing) to assess synchrony between nutrient supply and demand.

SEM with EDS Analysis

Samples of each organic planting media were prepared for analysis using scanning electron microscopy with energy dispersive x-ray spectroscopy analysis adhering to standard protocols (Gudi *et al.,* 2021). For SEM-EDS, three subsamples were taken per treatment from the mixed planting media; from each subsample three representative 10×10×10 millimetres (mm) specimen pieces were imaged and analysed (nine images per treatment). Fields were selected to capture representative aggregate types (coarse, fine, porous). The results from energy dispersive spectroscopy (EDS) are conveyed in semi-quantitative weight percent; this approach considers the variability that occurs within treatments. The samples were oven-dried at 60 degrees Celsius (°C) for 24 hours (h), then mounted aluminium (Al) stubs using carbon (C) tape and coated with a thin layer of gold using a sputter coater. Observation of surface morphology was carried out using SEM at magnifications of 100× to 200x. According to Cao *et al.* (2024) found that SEM is in exceptionally high demand for such samples. Before testing, the samples need to go through several preprocessing steps, such as drying and applying a gold spray. During the dewatering and drying of the soil samples, there is a risk of shrinkage and deformation, making it challenging to maintain the original structural form. Additionally, owing to the random nature of SEM imaging, the sample must be scanned from left to right and from top to bottom, requiring meticulous operational skills. Furthermore, the sample size for SEM is small, typically less than 10 millimeters (mm) X 10 mm X 10 mm, necessitating

Table 2: Results of the analysis of Kasgot (earthworm compost), poultry manure, and sheep manure before the study (BPSIPTS Laboratory, 2023)

Fertilizer	pH (H_2O)	C (%)	N (%)	C/N ratio	P_2O_5 (%)	K_2O (%)
Kasgot	8.7	15.69	1.89	8	3.37	2.38
Poultry manure	8.5	16.81	0.71	24	0.96	1.36
Sheep manure	9.0	12.23	0.80	15	0.54	1.09

the selection of appropriately magnified images for qualitative or quantitative analyses. Elemental composition was determined using EDS. The data obtained included the percentage of major elements such as C, oxygen (O_2), nitrogen (N), phosphorus (P), potassium (K), calcium (Ca), and magnesium (Mg). The recommendations stressed that quantitative indicators—like bulk density related to plant-available water—deliver more substantial evidence of structural enhancement compared to SEM alone.

Seed treatment and sowing

Shallot seeds of the Batu Ijo variety, which had been properly dried, were chosen for the experiment. Prior to sowing, a pre-sowing treatment was applied by mixing 20 grams (g) of antracol with every 400 seeds in a plastic bag to ensure uniform coverage. Directly following the treatment, the seeds were placed into polybags that contained the pre-treated soil. This method was established to shield the seeds from early-stage pathogens and to foster robust initial growth. Pre-plant mixed-substrate properties were measured and are given in Table 2, providing a baseline for interpretation of seedling performance. Additionally, Seeds received pre-sowing fungicide (Antracol) treatment to prevent seedling diseases. While applied rates were modest, potential transient impacts on introduced microbial inoculants cannot be excluded; future experiments should compare untreated and fungicide-treated seeds to quantify any interaction with Biosoltamax establishment. Irrigation: shallots were irrigated manually to field capacity three times per week. Documented weather conditions throughout the trial: average daily temperature and cumulative rainfall for the growing season.

Inorganic fertilizer application

To supply essential nutrients during the early growth stages, Mutiara 16-16-16 inorganic fertilizer was applied. Plants not treated with Biosoltamax received 5 g per plant, while those treated with Biosoltamax were given 2.5 g per plant. This strategy made certain that all plants acquired enough nutrition while preserving a balanced fertilization system.

Subsequent biofertilizer applications

To sustain the benefits of the initial Biosoltamax application throughout the growing period, additional treatments were applied at key growth stages. In one phase, Biosoltamax was prepared at a rate of 1 tube per liter of coconut water, incubated for 15 min, and then diluted with 5 mL/L of water prior to application. In later stages, the concentration was increased to 1.5 tubes per liter and ultimately to 2 tubes per liter as the nutrient demands of the plants grew. The purpose of these consecutive applications was to uphold vigorous soil microbial activity and facilitate effective nutrient uptake.

Observation and data collection

Regular observations were conducted to monitor plant development. Nutrient composition of organic amendments as pH, organic carbon (OC), total N, C: N, phosphorus pentoxide (P_2O_5) and potassium oxide (K_2O) as determined by The BPSIPTS laboratory. Dried plant tissues were digested using the Kjeldahl method for total N, molybdate-blue colorimetry for P following Murphy and Riley, and flame photometry for K. Analyses were performed at the BPSIPTS laboratory. Initially, the height of sample plants was measured from the soil surface using a standard ruler, and the number of leaves was documented. Additionally, any pest attacks (referred to as plant pest organisms) were noted. As the plants matured, further observations included counting the number of tillers—secondary bulbs developing around the primary seed bulb. These measurements were conducted repeatedly at consistent intervals to capture the advancement of vegetative growth. Plant height, leaf number, and tiller number were recorded weekly from week 1 to week 8 using the same tagged

plants per experimental unit. The count of leaf number included all fully expanded leaves on each plant; tillers were identified as separate secondary bulbs that develop from the primary bulb. Later in the experiment, selected plants were carefully uprooted, washed, and separated into leaves, bulbs, and roots. Fresh (wet) and dry weights were then determined to provide detailed insights into biomass accumulation and nutrient absorption.

Final harvest and yield analysis

During the harvest phase, final yield parameters were comprehensively recorded. Harvest criteria: plants were harvested at physiological maturity (approximately 120 days after planting when 70–80% foliar senescence was observed) and when bulbs achieved marketable size. Harvested samples for dry weight determination were oven-dried at 65 °C to constant weight (typically 48–72 h) following standard protocols. The assessment involved quantifying the number of bulbs produced by each plant, as well as measuring the fresh (wet) bulb weight, dry bulb weight, and the diameter of the largest bulb. Harvested samples were promptly washed to remove soil residues and then processed for nutrient uptake analysis. This concluding evaluation was essential for assessing the overall impact of the fertilizer treatments on improving both the quality and quantity of shallot production.

Experimental layout

A randomized complete block design (RCBD) was used for the experiment, which included four replications and six treatment combinations, resulting in a total of 24 experimental units and 240 plants. The materials required included shallot seeds of the Batu Ijo variety, polybags, poultry manure, sheep manure, earthworm compost (Kasgot), organic fertilizer, soil, sekam (rice husks), Biosoltamax biofertilizer, and pesticides. Polybags were used to allow strict control of planting media composition (soil:rice husk:organic amendment ratios) and reduce spatial heterogeneity for this initial evaluation. The outcomes of the polybag trial serve as a proof-of-concept and need to be confirmed through under field conditions in on-farm trials.

Each treatment consisted of a different composition of growing media and fertilizer combinations:

A = Soil: Rice husk: Poultry manure + 100 percent (%) inorganic fertilizer

B = Soil: Rice husk: Sheep manure + 100% inorganic fertilizer

C = Soil: Rice husk: Kasgot + 100% inorganic fertilizer

D = Soil: Rice husk: Poultry manure + Organic fertilizer + 50% inorganic fertilizer

E = Soil: Rice husk: Sheep manure + Organic fertilizer + 50% inorganic fertilizer

F = Soil: Rice husk: Kasgot + Organic fertilizer + 50% inorganic fertilizer

Each treatment was applied to the planting media in polybags, with consistent agronomic management practices implemented across all treatments. The study employs polybags for several reasons: 1) to establish initial conditions that are as uniform as possible, ensuring that each plant gets an equal amount and type of growing media, 2) to allow for precise control over irrigation and fertilizer application, 3) it is easier to protect plants from pests or diseases and easier to control them, and (4) it is easier to observe. Biosoltamax was applied to enhance microbial activity, and pesticide applications were made when necessary to control pests.

Data analysis

The following parameters were gathered: biomass accumulation (fresh and dry weights of roots, leaves, and bulbs), chemical characteristics of the soil (potential of hydrogen (pH), natural sources of C, N, and K) plant growth (height, number of leaves, and tillers), and yield components (number of bulbs, bulb weight, and bulb diameter). Statistical procedures: all variables were checked for normality using the Shapiro–Wilk test and for homogeneity of variance using Levene's test. Data transformations, such as logarithmic or square root adjustments, were implemented as needed prior to analysis. Analysis of variance (ANOVA) was performed using the statistical package for the social sciences (SPSS) version 20, and mean separation used Duncan's Multiple Range (DMRT) Test at $p < 0.05$. To assess the impact of fertilizer treatments on soil fertility and nutrient absorption, the nutrient levels in both soil and plant tissue were analyzed prior to and following the application of treatments. The statistical SPSS software was used for analysis.

RESULTS AND DISCUSSION

Baseline soil conditions

Analysis of the soil before treatment revealed low nitrogen content and moderate organic carbon levels (Table 1).

The initial soil analysis indicated that the experimental site had a predominantly clayey texture, with 59% clay, 36% silt, and only 5% sand. The soil pH was slightly acidic, with a value of 6.3 in water (H_2O) and 5.7 in K chloride (KCl), suggesting moderate soil acidity. Organic carbon content was measured at 1.35%, while total nitrogen (N) was relatively low at 0.14%, resulting in a carbon-to-nitrogen (C/N) ratio of 9. These values indicate limited nitrogen availability, which may affect plant growth without proper fertilization (Solagracya and Hanum, 2025). Phosphorus pentoxide (P_2O_5) content was recorded at 66.5 parts per millions (ppm), considered adequate for plant development, whereas K levels were relatively high at 757.7 ppm. The preliminary values functioned as a foundation for measuring the influence of various fertilizer treatments on soil fertility and nutrient accessibility (Table 2).

Physical characteristics and chemical composition of planting media

The chemical assessment of the organic fertilizers applied in this study indicated considerable variations in pH, carbon levels, nitrogen content, and nutrient accessibility (Table 2). Kasgot (earthworm compost) had the highest nitrogen content (1.89%) and a low C/N ratio of 8, indicating potential for rapid nutrient mineralization. Poultry manure exhibited the highest organic carbon content (16.81%) but had a significantly higher C/N ratio of 24, suggesting slower decomposition and nutrient release (Verma *et al*., 2019). Sheep manure had a moderately high pH (9.0) and a C/N ratio of 15, indicating a balanced nutrient release rate. Enhancing application timing involves integrating laboratory mineralization data with in-field ion exchange to assess the availability of N and P, enabling split or top-dress applications at the peak of plant uptake. To determine optimal rates, factorial experiments testing multiple organic rates (low, medium, high) and reduced mineral levels (100%, 50%, 25%) with and without Biosoltamax should be conducted. Response surfaces and marginal return analyses will identify agronomic optima. In terms of P_2O_5 and K_2O, Kasgot had the highest concentrations, making it a rich source of essential macronutrients. Poultry manure and sheep manure had lower P and K levels, but their organic matter content contributed to long-term soil fertility improvements (Sigh *et al.,* 2020). Organic fertilizers substantially enhanced soil pH and the availability of nutrients, effectively tackling the initially low nitrogen levels in untreated soil. The improved soil conditions provided a favourable environment for shallot growth, influencing plant vigor and yield outcomes.

To find out in more detail the role of a mixture of soil, rice husks, chicken manure compost, goat manure compost, and kasgot planting media, both physically and chemically, on the growth and productivity of shallots, an analysis of planting media samples was carried out using SEM and EDS. As stated by Selvakumar *et al*. (2024), SEM-EDS offers a comprehensive view of the surface morphology and microstructure of the media, enabling the examination of particle size, porosity, and texture, which influence water retention and aeration. Meanwhile, EDS enables the qualitative and quantitative analysis of elemental composition, such as C, O, N, P, K, Ca, and other essential elements. Utilizing SEM and EDS techniques in conjunction provides extensive information on the physical and chemical attributes of organic planting media, thereby aiding in the assessment of its quality and appropriateness for shallot cultivation in polybags. SEM image results of shallot planting media with treatment A-F (Fig. 1) reveal clear morphological differences among the planting media as affected by the type of organic amendment and fertilizer treatment. The organic amendments used differ in nutrient concentrations and C:N ratios (Table 2), which may confound observed treatment effects; factorial rate–response experiments are needed to disentangle amendment identity from nutrient quantity effects. Observed increases in soil organic carbon and total N under D–F are consistent with inputs from Kasgot and poultry manure (Table 2) and suggest net mineralization; future mineralization incubations would quantify release rates. Treatment A displays a relatively rough texture with aggregates that are irregularly shaped and a moderate pore distribution. The presence of poultry manure produces micro-aggregates bound by organic matter, improving porosity and aeration. Treatment B exhibits a more compact surface with smaller and denser particles. It appears that the

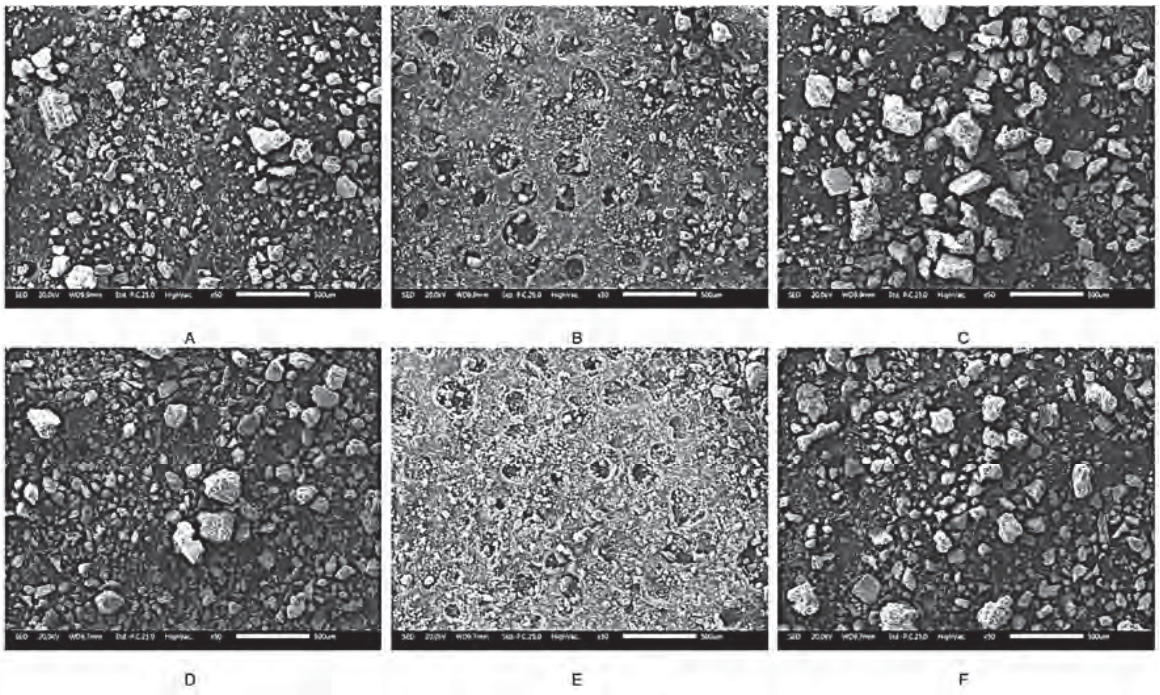

Fig. 1: SEM image results of shallot planting media with A-F treatment with 100x magnification

sheep manure generates a more even matrix, which reduces pore connectivity relative to A, potentially impacting the water retention ability. Treatment C has a rougher texture with larger, angular particles and more visible voids. The Kasgot (vermicompost) likely contributed to higher organic matter decomposition, increasing microstructural heterogeneity and surface roughness. Treatment D shows well-developed, cohesive aggregates with improved particle bonding and micropore stability, suggesting enhanced microbial activity and organic binding. Treatment E exhibits a more refined and compact morphology characterized by fewer macropores and a finer distribution of internal pores, suggesting improved nutrient retention and a slower potential for nutrient release. Treatment F displays the most porous structure with a heterogeneous surface and distinct micro-voids, which can promote aeration and root penetration. This suggests that the combination of vermicompost and reduced inorganic fertilizer creates an ideal microstructure for the development of shallot roots and nutrient exchange. Overall, the SEM observations show that partial substitution of inorganic fertilizer with organic inputs (D–F) improves the physical integrity and porosity of the planting media, potentially enhancing nutrient availability, water retention, and microbial activity (Yuniwati *et al.,* 2023). While the data indicate enhanced nutrient retention in the soil, it did not directly assess leaching, runoff, or losses of gaseous N. To substantiate claims of reduced environmental impact, future studies should deploy lysimeters or zero-tension samplers to quantify nitrate and P leaching, surface runoff samplers for dissolved and particulate P, and static chambers (or automated chambers) to measure nitrous oxide (N_2O), ammonia (NH_3), and carbon dioxide (CO_2) fluxes across treatments. Integrating greenhouse gas monitoring via static chambers or automated systems is also suggested, coordinated with fertilizer application and essential plant growth stages, to analyze potential trade-offs between yield improvements and gas emissions (Cattaneo *et al.,* 2023). Future studies should assess sustainability across multiple cropping cycles. Multi-season trials (≥3 consecutive seasons) conducted under both researcher-managed and farmer-managed conditions are recommended to track yield trajectories and changes in soil organic carbon (SOC), total N, available P, and exchangeable K. These trials can also assist in recognizing any potential yield decrease

Table 3: Chemical composition of organic shallot planting media based on SEM with EDS

Treatment/	A	B	C	D	E	F
Element	Weight (%)					
C	52,74	54,56	53,77	45,83	48,74	50,43
O	38,10	36,69	37,01	41,62	38,18	39,14
Si	0,96	2,72	1,83	12,61	10,66	8,25
Al	9,65	9,05	7,59	4,67	7,27	2,99
Ca	0,71	0,53	3,02	0,54	0,92	4,73
Fe	1,50	1,50	1,67	2,54	0,58	0,00
Mg	0,96	0,41	0,00	0,00	0,00	0,00
P	0,20	0,14	0,13	0,21	0,00	0,34

that might require adjustments in nutrient inputs. Integrating agronomic monitoring with economic indicators—such as yield per unit input cost—will help determine whether reduced mineral fertilizer rates remain both agronomically and economically sustainable over time (Zheng *et al.,* 2024). An explicit economic assessment should accompany agronomic trials. Future work should report input costs (organic material, Biosoltamax, reduced mineral fertilizer), labor and transport, and gross and net returns per hectare. Analyses of cost-benefit and partial budgets, together with sensitivity analyses across varying market prices, will clarify the potential for smallholders to adopt and evaluate the financial viability of nutrient substitution.

The EDS results reveal that C and O_2 dominate the chemical composition across all treatments, with C ranging from approximately 45 to 55% and O from 36 to 42%, indicating the presence of abundant organic matter derived from manure and compost materials (Table 3). Treatments A–C (100% inorganic + organic sources) exhibit higher C and lower O contents than D–F, suggesting less decomposition and a higher fraction of stable carbon, while the slightly lower C and higher O in D–F reflect more advanced humification and improved aeration in the growing media. Silicon (Si) is highest in D (12.61%) and E (10.66%), likely due to the incorporation of rice husk ash that provides silicate minerals beneficial for strengthening plant cell walls and enhancing shallot tolerance to environmental stress; evaluate the integrated strategy under controlled stress (imposed drought, heat, or excess moisture) and across multiple agro-ecologies to determine resilience conferred by enriched organics (Sun *et al*., 2016). The mechanisms probably involve an increase in soil organic matter, which enhances cation exchange capacity and nutrient retention, as well as heightened urease activity that promotes ammonification. Additionally, improved microstructure, characterized by greater porosity and aggregate stability as observed through SEM, can facilitate root proliferation and nutrient absorption. Conversely, Si content is low (<3%) in A–C, indicating reduced silicate mineral presence under fully inorganic fertilization. Aluminum (Al) levels are relatively higher in A–C but decrease in D–F, suggesting that organic fertilizer addition may promote Al chelation or immobilization, reducing phytotoxicity and improving root health. Calcium (Ca) is enriched in C (3.02%) and F (4.73%), both of which involve Kasgot (vermicompost) application; the vermicompost likely enhances Ca and Mg mobility through organic acid formation and microbial activity, improving nutrient uptake, root development, and bulb firmness. Iron (Fe) concentrations are greater in A–C (1.5–1.7%) than in E–F, a pattern consistent with higher inorganic fertilizer input, which increases Fe solubility but may risk soil acidification; the organic-rich media in D–F likely buffer Fe availability through complexation. Finally, phosphorus (P), present at 0.13–0.34% across treatments, reflects ongoing phosphate mineralization from manure and organic amendments, with the slightly higher P in F (0.34%) corresponding to Kasgot's capacity to retain and gradually release P, supporting root growth and bulb development in shallots. SEM–EDS offers

Table 4: Relationship between SEM with EDS and agronomic functions

Key property	SEM observation	EDS supporting evidence	Agronomic implication
Porosity and rough texture (A, D)	Coarse particles	Higher C, moderate Si and Fe	Better aeration and drainage
Compact and smooth surface (B, E)	Fine aggregates	High O_2, balanced Si–Al	Improved moisture retention
Uniform microstructure (C, F)	Porous and stable	High Ca and Si	Enhanced nutrient exchange and microbial habitat

qualitative insights into microstructure and elemental composition; nonetheless, assertions about porosity and mineral availability are substantiated through correlations with observed soil organic carbon and nutrient data. For future studies, quantitative confirmation (bulk density, mean weight diameter) is suggested

Furthermore, the relationship between SEM with EDS and agronomic functions can be explained in Table 4. Table 4 demonstrates the interconnected relationship among surface morphology (SEM), elemental composition (EDS), and agronomic performance across treatments. Treatments A and D, which exhibit porosity and rough textures with coarse particles, are characterized by higher C and moderate Si–Fe contents, indicating improved aeration and drainage capacity of the planting media—favorable for root respiration and oxygen diffusion. Conversely, treatments B and E display compact and smooth surfaces that consist of fine aggregates, reinforced by high levels of O and a balanced ratio of silicon (Si) and Al levels, which improve water retention and aid in maintaining moisture around the root zone. Meanwhile, treatments C and F display a uniform and stable microstructure that is porous yet cohesive, with elevated Ca and Si concentrations that promote efficient nutrient exchange, microbial colonization, and improved rhizosphere stability. Furthermore, the integrated SEM–EDS data reveal that the characteristics of the planting media, both microstructural and chemical, significantly influence its physical and biological roles, thus determining how shallots respond to various fertilization strategies. Moreover, mechanistic studies (root morphology, exudate chemistry, nutrient flux tracing, and functional gene profiling) can clarify whether observed benefits result from improved nutrient supply, root architecture, or microbial–plant interactions.

Plant growth performance

The outcomes demonstrated that different types of fertilizer treatments notably affected the height of shallot plants as well as the leaf count (Table 5). Treatment week 4 consistently produced the tallest plants across all groups, with the highest value as 48.95 centimeters (cm) in group C. Leaf number followed a similar trend, with week 4 in group D showing the highest count (31.83). Group contrasts: ABC corresponds to treatments with 100% mineral input; DEF corresponds to treatments in which mineral input was 50% plus organic amendments. Contrasts between ABC and DEF evaluate the effect of mineral-fertilizer reduction combined with organic sources. The tallest plants were observed in Treatment D, measuring 46.11 cm, along with the highest leaf biomass of 84.08 g. Meanwhile, Treatment A had the most leaf numbers at 26.40 and a wet bulb weight of 49.75 g, indicating enhanced vegetative performance and potential for enhanced photosynthesis (Lou *et al*., 2018). Table 5 illustrates the impact of various fertilizer treatments on both plant height and leaf count. The results indicate significant differences in plant height across treatments, with week 4 consistently showing the highest values across all groups. The comparison between versions (vs.) groups ABC vs. DEF reveals a statistically significant difference in plant height at earlier growth stages, indicating that fertilizers applied to groups ABC resulted in enhanced early vegetative growth. Similarly, comparisons such as B vs. AC and AB vs. C emphasizes the variations in growth dynamics across different treatments. The trends in leaf numbers are comparable, showing greater values in plants that received treatment in week 4. The increased leaf number suggests improved photosynthetic capacity, which could translate into better biomass accumulation and higher yield. The comparison of AD vs. BCEF further supports this, showing a significantly higher leaf number in AD

Table 5: Plant height and number of leaves

Treatment	Plant height				Number of leaves			
	Week 1	Week 3	Week 2	Week 4	Week 1	Week 3	Week 2	Week 4
A	14.58	33.70	43.15	47.50	6.60	17.65	25.65	26.40
B	16.60	30.13	34.30	39.50	6.10	11.50	14.80	20.40
C	6.68	32.68	41.70	48.95	4.60	12.60	18.25	23.55
D	20.93	27.48	37.26	46.11	9.20	13.30	21.18	31.83
E	21.48	28.05	36.08	43.90	6.40	12.70	19.23	34.15
F	18.63	17.51	29.00	38.25	5.75	9.61	17.35	27.55
ABC vs. DEF	12.62 vs. 20.34**	32.17 vs. 24.34**	39.72 vs. 34.12**	45.32 vs. 42.75	5.77 vs. 7.12	13.92 vs. 11.87	19.57 vs. 19.25	23.45 vs. 31.18
A vs. BC	14.58 vs. 11.64	33.70 vs. 31.40	43.15 vs. 38.00**	47.50 vs. 44.23	6.60 vs. 5.35	17.65 vs. 12.05*	25.65 vs. 16.53*	26.40 vs. 21.98
B vs. AC	16.60 vs. 10.63**	30.13 vs. 33.19	34.30 vs. 42.43**	39.50 vs. 48.23**	6.10 vs. 5.60	11.50 vs. 15.13	14.80 vs. 21.95	20.40 vs. 24.98
AB vs. C	15.59 vs. 6.68**	31.91 vs. 32.68	38.73 vs. 41.70	43.50 vs. 48.95*	6.35 vs. 4.60	14.58 vs. 12.60	20.23 vs. 18.25	23.40 vs. 23.55
D vs. EF	20.93 vs. 20.05	27.48 vs. 22.78	37.26 vs. 32.54*	46.11 vs. 41.08*	9.20 vs. 6.08	13.30 vs. 11.16	21.18 vs. 18.29	31.83 vs. 30.85
E vs. DF	21.48 vs. 19.78	28.05 vs. 22.49	36.08 vs. 33.13	43.90 vs. 42.18	6.40 vs. 7.48	12.70 vs. 11.46	19.23 vs. 19.26	34.15 vs. 29.69
DE vs. F	21.20 vs. 18.63	27.76 vs. 17.51**	36.67 vs. 29.00**	45.01 vs. 38.25**	7.80 vs. 5.75	13.00 vs. 9.61	20.20 vs. 17.35	32.99 vs. 27.55
AD vs. BE	17.75 vs. 19.04	30.59 vs. 29.09	40.21 vs. 35.19**	46.81 vs. 41.70**	7.90 vs. 6.25	15.48 vs. 12.10	23.41 vs. 17.02*	29.11 vs. 27.28
AD vs. CF	17.75 vs. 12.65**	30.59 vs. 25.09*	40.21 vs. 35.35**	46.81 vs. 43.60	7.90 vs. 5.18	15.48 vs. 11.11	23.41 vs. 17.80	29.11 vs. 25.55
BE vs. CF	19.04 vs. 12.65**	29.09 vs. 25.09	35.19 vs. 35.35	41.70 vs. 43.60	6.25 vs. 5.18	12.10 vs. 11.11	17.02 vs. 17.80*	27.28 vs. 25.55
AD vs. BCEF	17.75 vs. 15.84	30.59 vs. 27.09	40.21 vs. 35.27**	46.81 vs. 42.65**	7.90 vs. 5.71	15.48 vs. 11.60*	23.41 vs. 17.41	29.11 vs. 26.41
BE vs. ACDF	17.75 vs. 15.20*	29.09 vs. 27.84	35.19 vs. 37.78*	41.70 vs. 45.20*	6.25 vs. 6.54	12.10 vs. 13.29	17.02 vs. 20.61	27.28 vs. 27.33
CF vs. ABDE	12.65 vs. 18.40**	25.09 vs. 29.84*	35.35 vs. 37.70	43.60 vs. 44.25	5.18 vs. 7.08	11.11 vs. 13.79	17.80 vs. 20.21	25.55 vs. 28.19

*Significant according to Duncan test at 95% confidence level (P<0.05)
**Significant according to Duncan test at 99% confidence level (P<0.01)

compared to BCEF, demonstrating the effectiveness of these treatments in promoting vegetative growth.

Tiller production

Tiller production is crucial for shallot yield, as it determines the number of bulbs per plant. The highest number of tillers was recorded in week 2 treatment for group A (5.10), followed by group E in week 3 (5.07) (Table 6). Ilahi *et al*. (2020) observed similar correlations between organic application and increased crop production. The contrast analysis conducted between A and BC revealed a notable difference in the treatment during week 3, indicating that organic and balanced fertilizers promote tiller development more effectively than synthetic options (Singh *et al.*, 2020; Khoirya *et al*., 2025). The significant variations in tiller number under different fertilizer applications. Treatment in week 3 consistently produced higher tiller numbers across most groups, particularly in comparison A vs. BC and AD vs. BCEF, where significant differences were observed. The results suggest that the treatment provided optimal nutrient availability for tiller formation. Interestingly, no significant difference was found between ABC vs. DEF, implying that the overall tiller formation was similar across broad treatment groups. Nonetheless, the diversity among groups underscores the significance of certain fertilizers in affecting the vegetative growth of shallots (Setyowati and Muktamar, 2024). Increased tiller production can be explained by improved early-season nitrogen availability and enhanced photosynthate partitioning to bulb formation, consistent with previous reports linking nutrient timing to tiller/bulb initiation.

Table 6: Effect of fertilizer treatments on shallot tiller number

Treatment	Number of tillers		
	Week 1	Week 2	Week 3
A	4.35	5.10	4.55
B	3.30	3.20	3.65
C	3.65	3.75	3.80
D	4.10	4.10	4.88
E	3.85	4.03	5.07
F	3.35	3.45	4.60
ABC vs. DEF	3.77 vs. 3.77	4.02 vs. 3.86	4.00 vs. 4.85
A vs. BC	4.35 vs. 3.48	5.10 vs. 3.48*	4.55 vs. 3.73
B vs. AC	3.30 vs. 4.00	3.20 vs. 4.43	3.65 vs. 4.18
AB vs. C	3.83 vs. 3.65	4.15 vs. 3.75	4.10 vs. 3.80
D vs. EF	4.10 vs. 3.60	4.10 vs. 3.74	4.88 vs. 4.83
E vs. DF	3.85 vs. 3.73	4.03 vs. 3.78	5.07 vs. 4.74
DE vs. F	3.98 vs. 3.35	4.07 vs. 3.45	4.97 vs. 4.60
AD vs. BE	4.23 vs. 3.58	4.60 vs. 3.62	4.71 vs. 4.36
AD vs. CF	4.23 vs. 3.50	4.60 vs. 3.60	4.71 vs. 4.20
BE vs. CF	3.58 vs. 3.50	3.62 vs. 3.60	4.36 vs. 4.20
AD vs. BCEF	4.23 vs. 3.54	4.60 vs. 3.61*	4.71 vs. 4.28
BE vs. ACDF	3.58 vs. 3.86	3.62 vs. 4.10	4.36 vs. 4.46
CF vs. ABDE	3.50 vs. 3.90	3.60 vs. 4.11	4.20 vs. 4.54

*Significant according to Duncan test at 95% confidence level (P<0.05)
**Significant according to Duncan test at 99% confidence level (P<0.01)

Biomass accumulation

There was a significant variation in biomass accumulation across the various treatments. Groups treated with organic-based fertilizers exhibited the highest wet and dry biomass accumulation. Treatment D exhibited the highest wet root biomass (7.14 g), while group A had the highest wet leaf biomass (76.77 g). Dry biomass also followed a similar trend, with treatment D achieving the highest dry root weight (0.65 g). These findings highlight how organic fertilisers can increase plant biomass by improving the soil's composition and availability of nutrients (Verma *et al*., 2019; Assefa and Tadesse, 2019). Table 7 displays the fresh and dry biomass of roots, leaves, and bulbs under different treatment conditions. Plants treated in week 4 exhibited the highest fresh and dry biomass values, particularly in leaf and bulb weight. This implies that the nutrient composition in this treatment substantially facilitated biomass accumulation. Wet and dry biomass, including leaf, root, and bulb weights, were highest in treatments incorporating poultry manure and Kasgot. These organic sources enhanced soil microbial biomass and nutrient uptake (Ge *et al*., 2010; Holik *et al*., 2019). When comparing groups AD vs. BCEF, a higher wet and dry weight was observed in AD, indicating that these treatments provided superior nutrient uptake efficiency. By boosting photosynthesis and fostering root system growth, nutrient translocation and storage in bulbs can be improved, leading to a significant increase in biomass accumulation. The results align with previous studies emphasizing the role of balanced fertilization in optimizing biomass partitioning (Xing *et al*., 2025). Biosoltamax, a commercial organic biofertilizer applied in this study, was used to stimulate beneficial soil microorganisms and improve soil biological activity, complementing nutrient release from organic amendments. In future studies Factorial trials that integrate Biosoltamax treatments with regulated stress conditions (for instance, water deficit) and evaluate physiological responses (like leaf water potential, stomatal conductance, and osmolyte accumulation) will contribute to clarifying interaction mechanisms. Evidence from meta-analyses and reviews shows that microbial inoculants can increase crop productivity and enhance nutrient availability through mechanisms such as nitrogen fixation, phosphorus solubilisation, and stimulation of microbial enzyme activity (Li, 2022; Sammauria, 2020; Kumari, 2022). Inferences about enhanced nutrient cycling are based on measured increases in urease and dehydrogenase activities; functional microbial assays (16S/ITS sequencing and gene targets are recommended to more directly link

Table 7: Vegetative phase biomass measurements

Treatment	Vegetative phase					
	Wet root weight	Wet leaf weight	Wet bulb weight	Dry root weight	Dry leaf weight	Dry bulb weight
A	5.61	76.77	21.77	0.54	4.42	1.60
B	7.61	61.67	16.84	0.66	3.79	1.00
C	4.76	39.10	7.17	0.42	1.83	0.47
D	7.14	84.08	22.15	0.65	4.00	1.76
E	8.73	59.63	10.97	0.61	3.05	0.76
F	5.15	74.74	17.94	0.42	4.26	1.01
ABC vs. DEF	5.99 vs. 7.00	59.18 vs. 72.82	15.26 vs. 17.02	0.54 vs. 0.56	3.34 vs. 3.77	1.02 vs. 1.17
A vs. BC	5.61 vs. 6.18	76.77 vs. 50.38	21.77 vs. 12.01	0.54 vs. 0.54	4.42 vs. 2.81	1.60 vs. 0.73
B vs. AC	7.61 vs. 5.19	61.67 vs. 57.94	16.84 vs. 14.47	0.66 vs. 0.48	3.79 vs. 3.12	1.00 vs. 1.04
AB vs. C	6.61 vs. 4.76	69.22 vs. 39.10	19.30 vs. 7.17	0.60 vs. 0.42	4.10 vs. 1.83	1.30 vs. 0.47
D vs. EF	7.14 vs. 6.94	84.08 vs. 67.19	22.15 vs. 14.46	0.65 vs. 0.52	4.00 vs. 3.66	1.76 vs. 0.88
E vs. DF	8.73 vs. 6.14	59.63 vs. 79.41	10.97 vs. 20.04	0.61 vs. 0.53	3.05 vs. 4.13	0.76 vs. 1.38
DE vs. F	7.93 vs. 5.15	71.86 vs. 74.74	16.56 vs. 17.94	0.63 vs. 0.42	3.52 vs. 4.26	1.26 vs. 1.01
AD vs. BE	6.37 vs. 8.17	80.42 vs. 60.65	21.96 vs. 13.90	0.60 vs. 0.64	4.21 vs. 3.42	1.68 vs. 0.88
AD vs. CF	6.37 vs. 4.96	80.42 vs. 56.92	21.96 vs. 12.56	0.60 vs. 0.42	4.21 vs. 3.04	1.68 vs. 0.74
BE vs. CF	8.17 vs. 4.96	60.65 vs. 56.92	13.90 vs. 12.56	0.64 vs. 0.42	3.42 vs. 3.04	0.88 vs. 0.74
AD vs. BCEF	6.37 vs. 6.56	80.42 vs. 58.78	21.96 vs. 13.23	0.60 vs. 0.53	4.21 vs. 3.23	1.68 vs. 0.81
BE vs. ACDF	8.17 vs. 5.66	60.65 vs. 68.67	13.90 vs. 17.26	0.64 vs. 0.51	3.42 vs. 3.62	0.88 vs. 1.21
CF vs. ABDE	4.96 vs. 7.27	56.92 vs. 70.54	12.56 vs. 17.93	0.42 vs. 0.62	3.04 vs. 3.81	0.74 vs. 1.28

* Significant according to Duncan test at 95% confidence level (P<0.05)
**Significant according to Duncan test at 99% confidence level (P<0.01)

microbial community shifts to nutrient cycling. The trial's observed rise in urease and dehydrogenase activity agrees with these documented effects, supporting the hypothesis that bio-activated organic inputs can accelerate microbially mediated nutrient cycling. Simultaneously, the effectiveness of inoculants can fluctuate based on environmental conditions, the composition of the inoculant, and management practices. Therefore, it is essential to interpret results considering local soil and climate factors, and to validate them through multi-season field trials (Sammauria, 2020; Kumari, 2022).

Soil health post-harvest

Soil health is an essential factor in shallot growth, and different fertilizer applications influence organic matter content and pH levels. The greatest amount of soil organic matter was observed in treatment E at 14.69%, with treatment D following at 11.70%. Soil pH was slightly affected by treatments, with a general range of 7.01 to 7.43 (Table 8). The elevated levels of organic matter in treatments using organic fertilizers imply a boost in soil fertility, resulting in improved conditions for plant growth (Ahmad *et al*., 2016; Wei *et al*., 2016). Soil acidity (pH) and organic content significantly impact nutrient availability. The effects of different fertilizers on soil pH and organic matter content. The data reveal that group E had the highest soil organic matter and soil pH, which may have contributed to improved nutrient retention and plant growth (Agegnehu *et al*., 2016). The contrast between AB and C highlights significant disparities in soil pH, with C presenting higher levels of acidity. Additionally, the C/N ratio is notably different among treatments, indicating variations in nitrogen mineralization rates, which affect plant nutrient uptake. The findings suggest that fertilizers with high organic matter content, such as compost, contribute positively to soil health and sustainability (Diacono and Montemurro, 2011; D'Hose *et al*., 2014).

Yield performance

The final yield of shallots was significantly influenced by fertilizer treatment. The highest number of bulbs per plant was recorded in treatments A and C (5.25 bulbs per plant). The maximum wet bulb weight

Table 8: Soil organic matter and pH analysis

Treatment	Water content (KA) leaves and roots	KA soil	pH soil
A	8.06	4.80	7.01
B	7.79	6.11	7.31
C	7.24	9.88	7.34
D	7.63	11.70	7.21
E	8.29	14.69	7.43
F	8.06	13.30	7.36
ABC vs. DEF	7.70 vs. 7.99	6.93 vs. 13.23	7.22 vs. 7.33*
A vs. BC	8.06 vs. 7.51	4.80 vs. 8.00	7.01 vs. 7.33
B vs. AC	7.79 vs. 7.65	6.11 vs. 7.34	7.31 vs. 7.18
AB vs. C	7.92 vs. 7.24	5.45 vs. 9.88	7.16 vs. 7.34**
D vs. EF	7.63 vs. 8.17	11.70 vs. 13.99	7.21 vs. 7.39*
E vs. DF	8.29 vs. 7.84	14.69 vs. 12.50	7.43 vs. 7.28*
DE vs. F	7.96 vs. 8.06	13.19 vs. 13.30	7.32 vs. 7.36
AD vs. BE	7.85 vs. 8.04	8.25 vs. 10.40	7.11 vs. 7.37**
AD vs. CF	7.85 vs. 7.65	8.25 vs. 11.59	7.11 vs. 7.35**
BE vs. CF	8.04 vs. 7.65	10.40 vs. 11.59	7.37 vs. 7.35
AD vs. BCEF	7.85 vs. 7.84	8.25 vs. 10.99	7.11 vs. 7.36**
BE vs. ACDF	8.04 vs. 7.75	10.40 vs. 9.92	7.37 vs. 7.23*
CF vs. ABDE	7.65 vs. 7.94	11.59 vs. 9.32	7.35 vs. 7.24*

*Significant according to Duncan test at 95% confidence level (P<0.05)
**Significant according to Duncan test at 99% confidence level (P<0.01)

Table 9: Shallot yield parameters

Treatment	Harvest		
	Number of bulbs	Wet bulb weight	Dry bulb weight
A	5.25	49.75	25.00
B	5.00	39.75	29.50
C	5.25	37.50	24.00
D	4.75	42.50	11.25
E	3.75	20.25	5.00
F	3.75	33.00	4.25
ABC vs. DEF	5.17 vs. 4.08	42.33 vs. 31.92	26.17 vs. 6.83**
A vs. BC	5.25 vs. 5.13	49.75 vs. 38.63	25.00 vs. 26.75
B vs. AC	5.00 vs. 5.25	39.75 vs. 43.63	29.50 vs. 24.50
AB vs. C	5.13 vs. 5.25	44.75 vs. 37.50	27.25 vs. 24.00
D vs. EF	4.75 vs. 3.75	42.50 vs. 26.63	11.25 vs. 4.63
E vs. DF	3.75 vs. 4.25	20.25 vs. 37.75	5.00 vs. 7.75
DE vs. F	4.25 vs. 3.75	31.38 vs. 33.00	8.13 vs. 4.25
AD vs. BE	5.00 vs. 4.38	46.13 vs. 30.00	18.13 vs. 17.25
AD vs. CF	5.00 vs. 4.50	46.13 vs. 35.25	18.13 vs. 14.13
BE vs. CF	4.38 vs. 4.50	30.00 vs. 35.25	17.25 vs. 14.13
AD vs. BCEF	5.00 vs. 4.44	46.13 vs. 32.63	18.13 vs. 15.69
BE vs. ACDF	4.38 vs. 4.75	30.00 vs. 40.69	17.25 vs. 16.13
CF vs. ABDE	4.50 vs. 4.69	35.25 vs. 38.06	14.13 vs. 17.69

*Significant according to Duncan test at 95% confidence level (P<0.05)
**Significant according to Duncan test at 99% confidence level (P<0.01)

recorded was in treatment A at 49.75 g, whereas treatment B exhibited the highest dry bulb weight of 29.50 g. Comparisons between the ABC and DEF groups showed significant differences, indicating that organic and balanced fertilizers contribute to better bulb development and yield. Table 9 outlines the impact of fertilizers on shallot yield parameters, including the number of bulbs, fresh bulb weight, and dry bulb weight. The findings show that treatments A and B resulted in the greatest bulb weight, with notable differences identified between the ABC and DEF groups, where plants treated with ABC yielded

significantly larger bulbs. These figures outperform typical yields under inorganic regimes and validate the productivity of organic inputs (Chauhan *et al*., 2012; Jote, 2023). This suggests that these fertilizers provided optimal conditions for shallot development (Solagracya and Hanum, 2025). The analysis of DE compared to F reveals notable disparities in the weight of fresh bulbs, indicating that certain treatments had a greater impact on the final yield. It is recommended that future rate-response experiments incorporate a 25% mineral fertilizer treatment and track yield stability, nutrient balance, and seasonal soil fertility dynamics to rigorously test the lower limit of mineral fertilizer replacement. Moreover, AD vs. BCEF revealed that AD-treated plants had superior bulb weight and number, supporting the hypothesis that well-balanced fertilization leads to increased productivity (Hiremath and Hosamani, 2015). The findings indicate that using organic fertilizers instead of or alongside inorganic ones can either maintain or boost shallot yields, all while supporting the long-term health of the soil. To assess long-term establishment and persistence, future research should employ strain-specific markers (e.g., reporter genes) alongside periodic sampling of the rhizosphere and bulk soil to validate Biosoltamax colonization and functional performance. Moreover, long-term monitoring (3–5 years) of SOC, total N, and mineral N pools is essential to determine whether fertility gains continue to accumulate or reach equilibrium. These findings reflect global movements that endorse organic fertilization as a means for climate-smart and regenerative agricultural methods (Vishnoi and Goel, 2024; Iqbal *et al*., 2023).

CONCLUSION

This study shows that replacing half of the usual chemical fertilizer with poultry manure and earthworm compost (Kasgot) delivers equal or better shallot yield and growth than using full inorganic fertilizer. The application of mixed organic–inorganic treatment resulted in better plant height, leaf numbers, tiller counts, and bulb weights, in contrast to the pure inorganic plots, which did not exhibit any improvement. Soil fertility also benefited markedly. Organic amendments raised soil organic carbon by up to 14.7%, improved the carbon-to-nitrogen balance, and boosted available phosphorus and potassium. These adjustments result in a more enriched and stable soil composition, which promotes root growth and assists in holding nutrients for subsequent plant use. Environmental risks dropped alongside chemical use. A 50% reduction in synthetic fertilizer reduces nitrate leaching and phosphorus runoff, major water pollution causes, while higher organic matter improves soil aggregation, water infiltration, and nutrient retention. Earthworm compost and poultry manure add diverse microbial communities that immobilize excess nutrients and break down remaining agrochemicals, further protecting groundwater. Future studies ought to enhance SEM observations by incorporating high-throughput sequencing to analyze shifts in bacterial and fungal communities, along with soil enzyme assays to measure functional changes linked to the application of Biosoltamax. In addition to SEM, future assessments should include bulk density (core method), mean weight diameter for aggregate stability, soil porosity calculations, and water-holding capacity (field capacity and permanent wilting point) to quantify structural changes. Furthermore, the integration of omics (soil metabolomics and microbial metagenomics) together with enzyme assays will reveal biochemical pathways and microbial functions activated by the enhanced nutrient. The transition to organic inputs also provides climate advantages. Stable organic carbon added to the soil acts as a small carbon sink, offsetting some greenhouse gas emissions tied to fertilizer production and application. Studies indicates that the combination of organic and synthetic systems results in lower nitrous oxide emissions per yield unit than when using high-rate nitrogen fertilizers by themselves, indicating a smaller overall greenhouse gas footprint. For tropical shallot growers, these findings offer a practical, cost-effective path to higher yields with fewer environmental trade-offs. Poultry manure and Kasgot are often locally available and affordable, and their use can cut import or purchase costs of chemical fertilizers. Applying Biosoltamax biofertilizer before sowing and at key growth stages further enhances nutrient cycling and early root health, making the system more resilient. Under the conditions of this single-season polybag experiment, partial substitution of mineral fertilizer with poultry manure or Kasgot plus Biosoltamax maintained or improved several growth and soil indicators. Before scaling the approach, it is important to conduct field validation across different seasons. Long-term studies

are still needed to track soil health over multiple seasons, measure greenhouse gas fluxes directly, and assess economic returns under real farm conditions. Focused studies on microbial dynamics and the stability of carbon from season to season would elucidate the complete environmental effects. A clear separation is made between measured agronomic outcomes (growth, yield, soil C/N) and environmental hypotheses (leaching, GHGs), with the latter listed as priorities for future monitoring. Integrating organic materials with reduced inorganic fertilizer provides a clear win: better shallot yields, stronger soil health, and lower environmental risk. This strategy of balanced fertilization aids in sustainable production and ensures the preservation of soil and water resources for future crops. Furthermore, practical suggestions encompass pilot demonstrations on farms and partial-budget economic assessments; decisions regarding adoption should take into account the local availability of organic inputs, labor needs, and economic feasibility. The principal measured outcomes and recommends concrete next steps: multi-season field trials, environmental monitoring, and economic assessment.

AUTHOR CONTRIBUTIONS

A. Nurawan developed the study concept, designed the experiment, conducted the fieldwork, interpreted the findings, and prepared the initial manuscript draft. Y. Haryati contributed to the study design, supported methodological development, and assisted in interpreting the results. K.D. Sutanto contributed to drafting the manuscript, data interpretation, and manuscript revision. B. Susanto participated in collecting data, conducting analytical procedures, SEM with EDS analysis, and worked closely on refining the manuscript. D.W. Utami assisted with validation and provided important feedback that improved the manuscript. D. Histifarina supported software processing and analytical verification. K.K. Hamdani carried technical support and improve the manuscript version. N.R. Purnamasari contributed to soil-related analysis and assisted in improving the clarity of the manuscript. A. Jufri contributed to interpretation of data analysis and manuscript revision. Data curation was carried out by Y. Surdianto, N. Sutrisna, and S.R. Djiwanti contributed to writing parts of the original draft and assisted with revisions. Supervision was provided by A. Nurawan and Y. Haryati. All authors reviewed and approved the final manuscript before submission.

ACKNOWLEDGEMENT

The authors gratitude goes to Head of the Department of Agriculture and Food Security of Ciamis Regency, S.B. Widodo; the Head of Functional Position of Ciamis Regency, Surahmanudin; the Head of the Agricultural Extension Agency of Ciamis Regency, Marlia; and the Head of the Extension Division of the Agriculture and Food Security Service of Ciamis Regency.

CONFLICT OF INTEREST

The authors declare that there is no conflict of interest regarding the publication of this manuscript. The ethical issues, including plagiarism, informed consent, misconduct, data fabrication and/or falsification, double publication and/or submission, and redundancy, have been completely observed by the authors.

OPEN ACCESS

©2026 The author(s). This article is licensed under a Creative Commons Attribution 4.0 International License, which permits use, sharing, adaptation, distribution and reproduction in any medium or format, if you give appropriate credit to the original author(s) and the source, provide a link to the Creative Commons license, and indicate if changes were made. The images or other third-party material in this article are included in the articles Creative Commons license, unless indicated otherwise in a credit line to the material. If material is not included in the articles Creative Commons license and your intended use is not permitted by statutory regulation or exceeds the permitted use, you will need to obtain permission directly from the copyright holder. To view a copy of this license, visit: http://creativecommons.org/licenses/by/4.0/

PUBLISHERS NOTE

GJESM Publisher remains neutral regarding jurisdictional claims in published maps and institutional afflictions.

☑ Negative AI Statement

The author(s) declared that no AI tools or services were used or highly applied during the preparation

of this work.

ABBREVIATIONS

%	Percent
^{O}C	Degree Celsius
A. cepa var. *aggregatum*	*Allium cepa* variety *aggregatum* (shallot)
Al	Aluminum
ANOVA	Analysis of variance
BPSIPTS	Balai Besar Pengujian Standar Instrumen Tanaman Sayuran (The Central Instrument Testing and Standardization Center for Vegetable Plants)
C	Carbon
C/N	Carbon-to-nitrogen ratio
Ca	Calcium
cm	Centimeter
CO_2	Carbon dioxide
DMRT	Duncan's multiple range test
EDS	Energy dispersive spectroscopy
g	Gram
H_2O	Water
h	Hour
K	Potassium
KA	Water content
Kg	Kilogram
KCl	Potassium chloride
K_2O	Potassium oxide
Kasgot	black soldier fly frass
L	Liter
min.	Minutes
mm	Millimeters
m	Meter
Mg	Magnesium
mL	Milliliter
mL/L	Milliliters per liter
N	Nitrogen
N_2O	Nitrous oxide
NH_3	Ammonia
O_2	Oxygen
P	Phosphorus
pH	Potential of hydrogen
P_2O_5	Phosphorus pentoxide
ppm	Parts per millions
RCBD	Randomized complete block design
Si	Silicon
SPSS	Statistical package for the social sciences
Treatment A	Soil: Rice husk: Poultry manure + 100% inorganic fertilizer
Treatment B	Soil: Rice husk: Sheep manure + 100% inorganic fertilizer
Treatment C	C = Soil: Rice husk: Kasgot + 100% inorganic fertilizer
Treatment D	D = Soil: Rice husk: Poultry manure + Organic fertilizer + 50% inorganic fertilizer
Treatment E	E = Soil: Rice husk: Sheep manure + Organic fertilizer + 50% inorganic fertilizer
Treatment F	F = Soil: Rice husk: Kasgot + Organic fertilizer + 50% inorganic fertilizer
Vs.	versus

REFERENCES

Abebe, T.G.; Tamtam, M.R.; Abebe, A.A.; Abtemariam, K.A.; Shigut, T.G.; Dejen, Y.A.; Haile, E.G., (2022). Growing use and impacts of chemical fertilizers and assessing alternative organic fertilizer sources in Ethiopia. Appl. Environ. Soil Sci., 1: 4738416 **(16 Pages).**

Abid, M.; Batool, T.; Siddique, G.; Ali, S.; Binyamin, R.; Shahid, M.J.; Alyemeni, M.N., (2020). Integrated nutrient management enhances soil quality and crop productivity in maize-based cropping system. Sustainability. 12(23): 10214 **(16 Pages).**

Ahmad, A.A.; Radovich, T.J.; Nguyen, H.V.; Uyeda, J.; Arakaki, A.; Cadby, J.; Teves, G., (2016). Use of organic fertilizers to enhance soil fertility, plant growth, and yield in a tropical environment. In: Organic Fertilizers - From Basic Concepts to Applied Outcomes. 85–108 **(24 Pages).**

Agegnehu, G.; Nelson, P.N.; Bird, M.I., (2016). Crop yield, plant nutrient uptake and soil physicochemical properties under organic soil amendments and nitrogen fertilization on Nitisols. Soil Tillage Res., 160: 1–13 **(13 Pages).**

Antil, R.S.; Raj, D., (2019). Integrated nutrient management for sustainable crop production and improving soil health. In: Nutrient dynamics for sustainable crop production. Springer Singapore. 67–101 **(35 Pages).**

Assefa, S.; Tadesse, S., (2019). The principal role of organic fertilizer on soil properties and agricultural productivity—a review. Agric. Res. Technol. Open Access. J., 22(2): 1–5 **(5 Pages).**

Askari-Khorasgani, O.; Pessarakli, M., (2020). Evaluation of cultivation methods and sustainable agricultural practices for improving shallot bulb production–a review. J. Plant Nutr., 43(1): 148–163 **(16 Pages).**

Aulakh, M.S., (2010). Integrated nutrient management for sustainable crop production, improving crop quality and soil health, and minimizing environmental pollution. In: 19th World Congress of Soil Science, Soil Solutions for a Changing World. 1–6 **(6 Pages).**

Babou, C.; Lisna, T., (2019). Liquid bio-fertilizer formulated from coconut and its effect on growth and root characteristics of robusta coffee seedlings under drought conditions. J. Plant Dev. Sci., 11(1): 61–64 **(4 Pages).**

BPSIPTS Laboratory, (2023). Vegetables-Annual report (Laporan-tahunan-2023). **(8 Pages)**.

Cao, Y.; Zhang, K.; Liu, S.; Wang, Y., (2024). A review of advancements in the theory and characterization of soil macropore structure. PeerJ, 1-32 **(32 Pages).**

Cattaneo, M.; Tayà, C.; Burgos, L.; Morey, L.; Noguerol, J.; Provolo, G.; Bonmatí, A., (2023). Assessing ammonia and greenhouse gas emissions from livestock manure storage: Comparison of measurements with dynamic and static chambers. Sustainability, 15(22): 15987 **(14 Pages).**

Cen, Y.; Guo, L.; Liu, M.; Gu, X.; Li, C.; Jiang, G., (2020). Using organic fertilizers to increase crop yield, economic growth, and soil quality in a temperate farmland. PeerJ. 8: e9668 **(16 Pages).**

Chauhan, P.S.; Singh, A.; Singh, R.P.; Ibrahim, M.H., (2012). Environmental impacts of organic fertilizer usage in agriculture. In: Organic Fertilizers: Types, Production and Environmental Impact. 63–84 **(22 Pages).**

D'Hose, T.; Cougnon, M.; De Vliegher, A.; Vandecasteele, B.; Viaene, N.; Cornelis, W.; Reheul, D., (2014). The positive relationship between soil quality and crop production: A case study on the effect of farm compost application. Appl. Soil Ecol., 75: 189–198 **(10 Pages).**

Diacono, M.; Montemurro, F., (2011). Long-term effects of organic amendments on soil fertility. In: Sustainable Agriculture, Springer, 2: 761–786 **(26 Pages).**

Ge, G.; Li, Z.; Fan, F.; Chu, G.; Hou, Z.; Liang, Y., (2010). Soil biological activity and their seasonal variations in response to long-term application of organic and inorganic fertilizers. Plant Soil. 326: 31–44 **(14 Pages).**

Guidi, P., Falsone, G., Wilson, C., Cavani, L., Ciavatta, C., Marzadori, C. (2021). New insights into organic carbon stabilization in soil macroaggregates: An in situ study by optical microscopy and SEM-EDS technique. GEODERMA, 397: 1-10 **(10 Pages).**

Hiremath, S.M.; Hosamani, M.H., (2015). Influence of balanced fertilization on productivity and nutrient use efficiency of maize (*Zea mays*)–chickpea (*Cicer arietinum*) cropping system. Res. Crops, 16(3): 479–484 **(6 Pages)**.

Holík, L.; Hlisnikovský, L.; Honzík, R.; Trögl, J.; Burdová, H.; Popelka, J., (2019). Soil microbial communities and enzyme activities after long-term application of inorganic and organic fertilizers at different depths of the soil profile. Sustainability. 11(12): 3251 **(16 Pages).**

Holka, M.; Kowalska, J.; Jakubowska, M., (2022). Reducing carbon footprint of agriculture—can organic farming help to mitigate climate change? Agriculture, 12(9): 1383 **(16 Pages)**.

Ilahi, H.; Hidayat, K.; Adnan, M.; Rehman, F.U.; Tahir, R.; Saeed, M.S.; Toor, M.D., (2020). Accentuating the impact of inorganic and organic fertilizers on agriculture crop production: A review. Ind. J. Pure Appl. Biosci., 9(1): 36–45 **(10 Pages)**.

Iqbal, S.; Xu, J.; Khan, S.; Worthy, F.R.; Khan, H.Z.; Nadir, S.; Ranjitkar, S., (2023). Regenerative fertilization strategies for climate-smart agriculture: Consequences for greenhouse gas emissions from global drylands. J. Clean. Prod., 398: 136650 **(16 Pages)**.

Jote, C.A., (2023). The impacts of using inorganic chemical fertilizers on the environment and human health. Org. Med. Chem. Int. J., 13: 555864 **(16 Pages).**

Khan, M.T.; Aleinikovienė, J.; Butkevičienė, L.M., (2024). Innovative organic fertilizers and cover crops: Perspectives for sustainable agriculture in the era of

climate change and organic agriculture. Agronomy. 14(12): 2871 **(15 Pages).**

Khoirya, D.; Setyowati, N.; Muktamar, Z.; Utami, K., (2025). Utilizing Melastoma compost (Melastoma malabatrichum L.) as a sustainable alternative to synthetic nitrogen fertilizers in shallot cultivation. Int. J. Plant Soil Sci., 37(2): 170–179 **(10 Pages)**.

Kumari, M.; Swarupa, P.; Kesari, K.K.; Kumar, A., (2023). Microbial Inoculants as Plant Biostimulants: A Review on Risk Status. Life (Basel). 13(1):12 **(26 Pages)**.

Kushwah, N.; Billore, V.; Sharma, O.P.; Singh, D.; Chauhan, A.P.S., (2024). Integrated nutrient management for optimal plant health and crop yield. Plant Sci. Arch., 8(2): 10–12 **(3 Pages)**.

Li, Y.; Wu, W.; Yang, J.; Cheng, K.; Smith, P.; Sun, J.; Pan, G., (2022). Exploring the environmental impact of crop production in China using a comprehensive footprint approach. Sci. Total Environ., 824: 153898 **(12 Pages)**.

Li, J.; Wang, J.; Liu, H.; Macdonald, C.A.; Singh, B.K., (2022). Application of microbial inoculants significantly enhances crop productivity: a meta-analysis of studies from 2010 to 2020. Journal of Sustainable Agriculture and Environment, 1(3): 216-225 **(10 Pages)**.

Luo, G.; Li, L.; Friman, V.P.; Guo, J.; Guo, S.; Shen, Q.; Ling, N., (2018). Organic amendments increase crop yields by improving microbe-mediated soil functioning of agroecosystems: A meta-analysis. Soil Biol. Biochem., 124: 105-115 **(11 Pages)**.

Nath, A.; Bhuyan, P.; Gogoi, N.; Deka, P., (2023). Pesticides and chemical fertilizers: Role in soil degradation, groundwater contamination, and human health. In: Xenobiotics in Urban Ecosystems: Sources, Distribution and Health Impacts. Springer International Publishing. 131–160 **(30 Pages)**.

Sammauria, R.; Kumawat, S.; Kumawat, P.; Singh, J.; Jatwa, T.K., (2020). Microbial inoculants: potential tool for sustainability of agricultural production systems. Arch Microbiol., 202(4): 677-693 **(17 Pages)**.

Selvakumar, S.; Soundara, B.; Raj, N.; Kulanthaivel, P., (2024). Microstructural and mechanical characterization of expansive soils for sustainable stabilization purposes. Research Square, 1-30 **(30 Pages)**.

Setyowati, N.; Muktamar, Z., (2024). Enhancing shallot growth and yield in Ultisols through coffee husk compost and nitrogen dosage variations. IOP Conference Series: Earth Environ. Sci., 1417(1): 012002 **(10 Pages)**.

Singh, T.B.; Ali, A.; Prasad, M.; Yadav, A.; Shrivastav, P.; Goyal, D.; Dantu, P.K., (2020). Role of organic fertilizers in improving soil fertility. In: contaminants in agriculture: sources, impacts and management. 61–77 **(17 Pages)**.

Solagracya, J.H.P.; Hanum, H., (2025). Optimizing shallot plant growth and plant nutrient through site-specific fertilizer dose evaluation. Indonesia J. Agric. Res., 8(1): 32–39 **(8 Pages)**.

Sun, Y.; Tao, C.; Deng, X.; Liu, H.; Shen, Z.; Liu, Y.; Li, R.; Shen, Q.; Geisen, S., (2023). Organic fertilization enhances the resistance and resilience of soil microbial communities under extreme drought. J. Adv. Res., 47: 1–12 **(12 Pages).**

Verma, B.C.; Pramanik, P.; Bhaduri, D., (2019). Organic fertilizers for sustainable soil and environmental management. in nutrient dynamics for sustainable crop production. Singapore: Springer Singapore. 289–313 **(25 Pages).**

Vishnoi, S.; Goel, R.K., (2024). Climate smart agriculture for sustainable productivity and healthy landscapes. Environ. Sci. Policy, 151: 103600 **(12 Pages)**.

Wei, W.; Yan, Y.; Cao, J.; Christie, P.; Zhang, F.; Fan, M., (2016). Effects of combined application of organic amendments and fertilizers on crop yield and soil organic matter: An integrated analysis of long-term experiments. Agric. Ecosyst. Environ., 225: 86–92 **(7 Pages)**.

Wu, W.; Ma, B., (2015). Integrated nutrient management (INM) for sustaining crop productivity and reducing environmental impact: A review. Sci. Total Environ., 512: 415–427 **(13 Pages)**.

Xing, Y.; Xie, Y.; Wang, X., (2025). Enhancing soil health through balanced fertilization: A pathway to sustainable agriculture and food security. Front. Microbiol., 16: 1536524 **(15 Pages)**.

Yuniwati, E.D.; Darmayanti, R.; Farooq, S.M.Y., (2023). How is organic fertilizer produced and applied to chili and eggplant plants? AMCA Journal of Community Development, 3(2): 88-94 **(7 Pages)**.

Zhang, F.; Liu, Y.; Liang, Y.; Dai, Z.; Zhao, Y.; Shi, Y.; Ahammed, G. J., (2024). Improving the yield and quality of tomato by using organic fertilizer and silicon compared to reducing chemical nitrogen fertilization. Agronomy, 14(5): 966 **(21 Pages).**

Zhao, C.; Huang, X.; Zhang, S.; Zhang, L.; Zhang, H.; Yang, B. (2023). Chemical fertilizer reduction combined with organic fertilizer affects soil microbial diversity and improves soil organic matter and nutrient availability in cotton systems. Front. Microbiol., 14: 1295722 **(12 Pages).**

Zheng, S.; Ni, K.; Chai, H.; Ning, Q.; Cheng, C.; Kang, H.; Ruan, J., (2024). Comparative research on monitoring methods for nitrate nitrogen leaching in tea plantation soils. Sci. Rep., 14(1): 20747 **(8 Pages).**

AUTHOR (S) BIOSKETCHES

Nurawan, A., Dr., M.P., Senior researcher, Research Center for Horticulture, National Research and Innovation Agency, Jl. Raya Jakarta-Bogor KM 46, Cibinong, Indonesia.
- Email: *agus197@brin.go.id*
- ORCID: 0000-0002-5737-1916
- Web of Science ResearcherID: NA
- Scopus Author ID: 57700788800
- Homepage: https://www.unpad.ac.id/

Sutanto, K.D., Ph.D., Postdoctoral fellow, Research Center for Horticulture, National Research and Innovation Agency, Jl. Raya Jakarta-Bogor KM 46, Cibinong, Indonesia.
- Email: *koko006@brin.go.id*
- ORCID: 0000-0002-3605-4954
- Web of Science Researcher ID: OHR-7407-2025
- Scopus Author ID: 55980814800
- Homepage: http://ksu.edu.sa/index.php/en/home

Haryati, Y., Ph.D., Senior researcher, Research Center for Horticulture, National Research and Innovation Agency, Jl. Raya Jakarta-Bogor KM 46, Cibinong, Indonesia.
- Email: *yhharyati@gmail.com*
- ORCID: 0000-0002-4279-0528
- Web of Science Researcher ID: NA
- Scopus Author ID: 57222314517
- Homepage: https://ugm.ac.id/en

Susanto, B., Dr., Senior researcher, Research Center for Horticulture, National Research and Innovation Agency Jl. Raya Jakarta-Bogor KM 46, Cibinong, Indonesia.
- Email : *bamb071@brin.go.id*
- ORCID: 0000-0003-1442-3699
- Web of Science Researcher ID: NA
- Scopus Author ID: 57427935900
- Homepage: https://brin.go.id/orpp

Hamdani, K.K., S.P., M.Si., Senior researcher, Research Center for Horticulture, National Research and Innovation Agency, Jl. Raya Jakarta-Bogor KM 46, Cibinong, Indonesia.
- Email: *kiki.kusyaeri@gmail.com*
- ORCID: 0000-0003-0718-7245
- Web of Science Researcher ID: NA
- Scopus Author ID: 58079830300
- Homepage: https://brin.go.id/orpp

Surdianto, Y, Ph.D., Senior researcher, Research Center for Food Crops, National Research and Innovation Agency, Jl. Raya Jakarta-Bogor KM 46, Cibinong, Indonesia.
- Email: *yant014@brin.go.id*
- ORCID: 0000-0002-4127-6092
- Web of Science Researcher ID: NA
- Scopus Author ID: 57222190320
- Homepage: htts://ipb.ac,id/beranda/

Homepage: https://wwwresearchgate.net/profile/Dr-Dwinita-Utami

Sutrisna, N., Ph.D., Senior researcher, Research Center for Food Crops, National Research and Innovation Agency, Jl. Raya Jakarta-Bogor KM 46, Cibinong, Indonesia.
- Email: *ntrisna.ns@gmail.com*
- ORCID: 0009-0006-5789-2611
- Web of Science Researcher ID: NA
- Scopus Author ID: 57217115108
- Homepage: https://www.ipb.ac.id/beranda/

Purnamasari, N.R., Dr., Senior researcher, Research Center for Horticulture, National Research and Innovation Agency, Jl. Raya Jakarta-Bogor KM 46, Cibinong, Indonesia.
- Email: *nene012@brin.go.id*
- ORCID: 0000-0002-0536-997X
- Web of Science Researcher ID: NA
- Scopus Author ID: 57207461760
- Homepage: https://brin.go.id/orpp

Djiwanti, S.R., Ph.D., Senior researcher, Research Center for Estate Crops, National Research and Innovation Agency, Jl. Raya Jakarta-Bogor KM 46, Cibinong, Indonesia.
- Email: *retnomuslim@yahoo.com*
- ORCID: 0009-0002-1465-4163
- Web of Science Researcher ID: NA
- Scopus Author ID: 6507827104
- Homepage: https://ipb.ac.id/beranda/

AUTHOR (S) BIOSKETCHES

Histifarina, D., M.Si., Senior researcher, Research Center for Appropriate Technology, National Research and Innovation Agency, Subang, West Java, Indonesia
▪ Email: *dian093@brin.go.id*
▪ ORCID: 0000-0003-2162-6611
▪ Web of Science Researcher ID: NA
▪ Scopus Author ID: 572074539
▪ Homepage: https://brin.go.id/orpp

Jufri, A., Ph.D., Senior researcher, Research Center for Estate Crops, National Research and Innovation Agency, Jl. Raya Jakarta-Bogor KM 46, Cibinong, Indonesia.
▪ Email: *akhm002@brin.go.id*
▪ ORCID: 0009-0003-6388-3445
▪ Web of Science Researcher ID: NA
▪ Scopus Author ID: 58761133400
▪ Homepage: https://www.ipb.ac.id/beranda/

Utami, D.W., Ph.D., Senior researcher, Research Center for Horticulture, National Research and Innovation Agency Jl. Raya Jakarta-Bogor KM 46, Cibinong, Indonesia.
▪ Email: dwin011@brin.go.id
▪ ORCID: 0000-0002-5873-0570
▪ Web of Science Researcher ID: NA
▪ Scopus Author ID: 36821685400
▪ Homepage: https://wwwresearchgate.net/profile/Dr-Dwinita-Utami

HOW TO CITE THIS ARTICLE

Nurawan, A.; Sutanto, K.D.; Haryati, Y.; Susanto, B.; Hamdani, K.K.; Surdianto, Y.; Sutrisna, N.; Purnamasari, N.R.; Djiwanti, S.R., Histifarina, D.; Jufri, A.; Utami, D.W. (2026). Eco-friendly organic nutrients enriched with biosoltamax enhance shallot growth, improve soil properties, and reduce the use of mineral fertilizer. Global J. Environ. Sci. Manage., 12(1): 331-350.

DOI: 10.22034/gjesm.2026.01.19

URL: https://www.gjesm.net/article_732121.html

Global J. Environ. Sci. Manage. 12(1): 351-370, Winter 2026, Serial #45

Global Journal of Environmental Science and Management
(GJESM)

Homepage: https://www.gjesm.net/

Podcasts

CASE STUDY

River basin management under spatial inequality and land use dynamics

A. Zhaken[1], T.P. Dentinho[2], G. Saspugayeva[1,*], M. Kamet[3], G. Shapatova[4], S. Kassymkhanov[5], Z. Zhumagalieva[5], A. Tsiganov[6], V. Sedelev[6]

[1] *Department of Environmental Engineering and Management, Faculty of Natural Sciences, L.N. Gumilyov Eurasian National University, Astana, Kazakhstan*

[2] *Faculty of Agricultural and Environmental Sciences, University of Azores, MQ58+98 Angra do Heroísmo, Portugal*

[3] *School of Sciences and Humanities, Nazarbayev University, Astana, Republic of Kazakhstan*

[4] *Department of Morphology, NCJSC Karaganda Medical University, Karaganda, Kazakhstan*

[5] *Kazakhstan University of innovation and telecommunications systems, the city of Uralsk, Kazakhstan*

[6] *Department of Ecology and Geography, Sarsen Amanzholov University of East Kazakhstan, Ust-Kamenogorsk, Kazakhstan*

ARTICLE INFO

Article History:
Received 08 June 2025
Revised 12 October 2025
Accepted 14 November 2025

Keywords:
Agricultural land use
Food security
Spatial interaction models
Sustainable development
Water scarcity

ABSTRACT

BACKGROUND AND OBJECTIVES: Effective management of water resources requires a clear understanding of how socio-economic factors, land suitability, and environmental constraints interact. In Kazakhstan, pronounced disparities in economic structure, ecological capacity, and hydrological access pose major challenges for sustainable resource governance. This study examines the appropriateness of land and water resources in the diverse regions of Kazakhstan, utilizing a spatially explicit analytical framework that combines demographic, economic, and environmental data. The primary goal is to pinpoint regional vulnerabilities and provide evidence-based insights for adaptive land and water management under changing water availability and infrastructure conditions, highlighting the interaction between water resource management, spatial inequality, and land use dynamics.

METHODS: The evaluation merged demographic and employment data with land use, hydrological, and economic indicators. A spatial interaction model for land use was employed to simulate land allocation and agricultural productivity under contrasting environmental scenarios. Input datasets included river discharge, groundwater depth, soil fertility, crop yield, market accessibility, and transport network density. Twelve plots, each measuring between 0.5 and 1 hectare, were used for micro-experimental water allocation trials in the Esil and Irtysh River Basins. These trials aimed to calibrate model parameters that pertain to irrigation response and farmer decision-making under water scarcity.

FINDINGS: The model highlighted marked regional variations in agricultural potential. Employment in agriculture, forestry, and fisheries was highly spatially concentrated, with a coefficient of variation of 100.4 percent, indicating localized dependence on natural resources. Under simulated water stress, the land suitability index declined by 12.7 percent and hydrological accessibility decreased by 25.9 percent, whereas infrastructure expansion increased these indicators by 11.1 percent and 3.4 percent, respectively. The increase in groundwater depth from 12.4 meters to 14.9 meters under water stress highlights the growing risk of extraction and a decrease in irrigation viability. These results demonstrate that environmental constraints and socio-economic inequalities jointly shape the spatial distribution of agricultural activity and the vulnerability of rural livelihoods.

CONCLUSION: In Kazakhstan, the combination of water availability and infrastructure connectivity is essential for determining the distribution, productivity, and sustainability of its agricultural sector. The findings provide quantitative evidence that investment in rural transport networks can mitigate some of the negative effects of water scarcity by improving access to markets and irrigation infrastructure.

DOI: 10.22034/gjesm.2026.01.20

This is an open access article under the CC BY license (http://creativecommons.org/licenses/by/4.0/).

NUMBER OF REFERENCES	NUMBER OF FIGURES	NUMBER OF TABLES
31	6	6

*Corresponding Author:
Email: *saspugayeva_gye@enu.kz*
Phone: +777 7249 6853
ORCID: 0000-0003-3223-3602

Note: Discussion period for this manuscript open until Mar 1, 2026 on GJESM website at the "Show Article".

INTRODUCTION

Land use change and water scarcity have become critical global challenges threatening agricultural sustainability and food security in arid and semi-arid regions. Globally, the escalating strain on land and water resources, propelled by population increase, economic growth, and climate change, has amplified the urgency for cohesive management methods that reconcile production with ecological stability. The interaction between socio-economic systems and biophysical conditions determines how effectively water and land are utilized for agriculture, yet these relationships remain complex and spatially uneven. In many parts of the world, especially within arid zones, effective resource governance increasingly depends on spatially explicit planning that accounts for economic inequality, infrastructure accessibility, and hydrological limitations. In Central Asia, and particularly in Kazakhstan, these global pressures are magnified by regional water stress and expanding agricultural demands (Li *et al.*, 2020). The basins of the Esil and Irtysh Rivers illustrate this scenario, as diminishing water resources, inconsistent infrastructure development, and climate fluctuations have raised worries regarding sustainable resource management (EDB, 2025). According to Krasnoyarova *et al.* (2019), the Irtysh River Basin faces severe transboundary water development challenges, especially as China's increasing withdrawal from the Kara-Irtysh disrupts aquatic ecosystems and reduces downstream water availability in the Zaisan Lake and Upper Irtysh reservoirs. These transboundary pressures compound local issues within Kazakhstan, particularly in the Ishim sub-basin, where rapid urban and agricultural expansion near Nur-Sultan has intensified water demand (Karatayev *et al.*, 2017; Salikova *et al.*, 2021). Although the sector plays a critical role in ensuring national food sovereignty, inadequate land use planning, fragmented coordination among institutions, and subpar irrigation practices still detract from agricultural productivity. Addressing these interlinked challenges requires a spatially informed, integrative approach that considers both domestic and transboundary water governance. This approach is essential for achieving sustainable agricultural development under increasingly constrained environmental and geopolitical conditions. Conventional approaches to land and water management, such as centralized irrigation planning, sectoral economic models, and top-down land use zoning, have shown limited success in water-scarce regions, particularly in complex transboundary settings like the Esil and Irtysh Basins (Stolpe *et al.*, 2022). Despite advancements in hydrological models that have deepened the understanding of water flows and availability, they often overlook socio-economic spatial dynamics, which makes them inadequate for predicting agricultural productivity across diverse and stratified landscapes (Curk and Glavan, 2021). Similarly, economic models capture market behavior but often overlook spatial constraints such as infrastructure quality and transport connectivity. Meanwhile, Geographic Information Systems (GIS) and remote sensing technologies have enhanced spatial visibility but remain less effective when not integrated with governance and economic data. Institutional and political-economic dimensions also play a decisive role in shaping land and water governance. Christophe and Tina (2015) demonstrated that income disparity, population pressures, and land-use conflict strongly influence local cooperation in river basin management. Their median voter model demonstrated that backing for integrated basin plans is influenced not just by technical data but also by political priorities and landscape preferences, particularly in areas where agriculture is predominant. This aligns with findings by Kalogiannidis and Kalfas *et al.* (2023), who underscored the importance of embedding water resource management directly into land use planning to enhance environmental sustainability. Their study in Greece showed that cross-sectoral coordination, stakeholder engagement, and adaptive governance can significantly improve both environmental outcomes and policy acceptance. Despite such evidence, the implementation of integrated land and water frameworks remains limited in Central Asia, where geopolitical tensions, administrative fragmentation, and uneven infrastructure development continue to hinder coordinated resource planning (Prniyazova *et al.*, 2025). This emphasizes the pressing requirement for analytical frameworks that unify land, water, and socio-economic elements within a comprehensive, spatially explicit system. To address these limitations, the present study integrates multiple datasets, including hydrological indicators (river discharge, precipitation, and irrigation flow), land use characteristics (crop

type, cultivated and fallow land), and economic factors (transport proximity, input costs, and market access). This multidimensional dataset allows for a context-sensitive examination of the ways in which agricultural productivity is concurrently affected by environmental limitations and economic connectivity (Liu *et al.*, 2025). The integration of these variables is essential for designing sustainable land and water management strategies in water-limited and politically complex river basins. To operationalize this framework, the spatial interaction model of land use (SIMLU) (Surya *et al.*, 2020) was employed as the core analytical tool. SIMLU captures the bidirectional relationships between land use decisions and spatial variables such as water access, economic centers, and transportation networks (Xi *et al.*, 2024). In contrast to static regression models, SIMLU dynamically simulates how alterations in one segment of the system, like enhanced irrigation infrastructure, can spread throughout the landscape, affecting crop yields and land use efficiency elsewhere. However, despite the availability of advanced spatial modeling tools, the integration of hydrological, economic, and spatial dimensions within a single predictive land use model remains rare in Central Asia. This study therefore applies the SIMLU framework to the Esil and Irtysh River Basins in Kazakhstan to analyze how spatial relationships shape agricultural productivity. This study intends to deliver an empirically based, spatially specific insight into the relationships between land and water, aimed at guiding sustainable management and informing upcoming policy directions. This study was conducted in the Central and North-Eastern regions of Kazakhstan in 2025.

MATERIALS AND METHODS

Study area

This study was conducted in the Esil (Ishim) and Irtysh River Basins of northern and eastern Kazakhstan, regions characterized by semi-arid to arid climatic conditions, high dependence on freshwater resources for agriculture, and substantial variability in soil fertility, hydrological accessibility, and infrastructure. The Esil River Basin spans between approximately 66°10′ (East) E and 72°20′E in longitude and 50°40′ (North)N and 55°20′N in latitude, covering an estimated 245,000 square kilometers across Akmola, North Kazakhstan, and Kostanay regions. The Irtysh River Basin, one of the largest transboundary river systems in Eurasia, extends across China, Russia, and Kazakhstan. It originates in the Altai Mountains near 47°52′39″N, 89°58′12″E and flows northwest to its confluence with the Ob River, with a representative coordinate near 61°04′52″N, 68°49′49″E. Owing to its vast extent, the basin's geographical bounds are commonly defined between approximately 48° and 74°N latitude and 65° and 87°E longitude, covering diverse landscapes from alpine headwaters to lowland agricultural plains. The Esil and Irtysh Basins were selected for analysis due to their strategic national importance for food security, availability of high-resolution hydrological, land use, and socio-economic datasets, and contrasting agro-ecological and infrastructural features. These factors collectively create an optimal foundation for assessing spatial inequality, land use transitions, and agricultural adaptation under varying water and development conditions in Kazakhstan's semi-arid regions (Fig. 1).

Data collection and sources

District-level agricultural and demographic data were obtained from the Bureau of National Statistics of the Agency for Strategic Planning and Reforms of the Republic of Kazakhstan, based on the 2023 Comprehensive Analytical Report on the State and Use of Lands. The dataset encompassed the extent of arable land, fields that are irrigated and those that are not, fallow land, various cultivated crops (including wheat, barley, sunflower, and potatoes), yields from harvests, density of livestock, and agricultural job statistics. The dataset, aligned with Nomenclature of Territorial Units for Statistics level 3 (NUTS-3) administrative boundaries, was integrated into district-level shapefiles in the GIS software quantum geographic Information System as (QGIS) version 3.34.10 using International Organization for Standardization (ISO) region codes. The 2023 national census was the source for population density and agricultural labor ratios, which were then normalized through min–max scaling for utilization in the SIMLU. Hydrological data were obtained from the Kazhydromet Hydrological Monitoring Database and Basin Inspection Reports of the Esil and Irtysh Rivers (2022–2023), including river discharge, surface water availability, irrigation volumes, aquifer depth, and precipitation from 52 meteorological stations. Borehole-based groundwater levels were interpolated using the inverse distance weighting

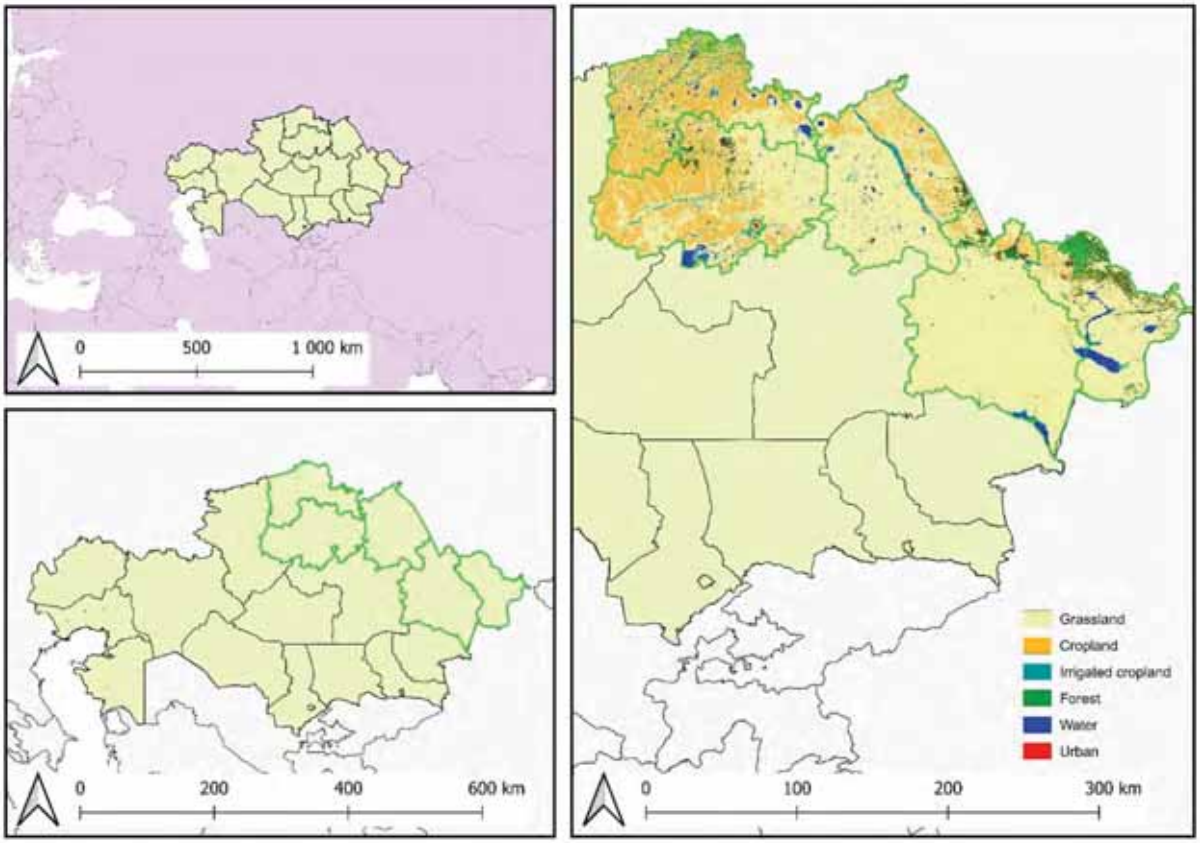

Fig. 1: Geographical location of the study area in land cover of the Esil River Basin, Kazakhstan, using Copernicus global land service dynamic

(IDW) method into 100-meter resolution rasters. A power parameter of 2 for IDW and a search radius of 12 neighboring points were employed, with cross-validation revealing a root mean square error (RMSE) of 0.84 meters. Irrigation infrastructure, including canals, reservoirs, and pumping stations, was digitized from Sentinel-2 satellite imagery and verified with field surveys. The reclassification of hydrological layers into five accessibility categories was conducted to enable their integration into land suitability analyses and SIMLU modeling. Land cover data were obtained from the 2023 Copernicus global land service (CGLS) Dynamic Land Cover product at 100-meter resolution and clipped to the study basins, with thematic classes including cropland, grassland, shrubland, and wetlands. Biophysical parameters, including soil type, slope, elevation, erosion risk, and soil potential of hydrogen (pH), were integrated into a multi-criteria evaluation (MCE) conducted in ArcGIS-Pro using the analytic hierarchy process (AHP). Weights determined by experts emphasized soil fertility and past productivity, resulting in a suitability index ranging from 0 (unsuitable) to 1 (highly suitable). Economic and infrastructure data were compiled from the Ministry of Industry and Infrastructure Development and the National Transport Atlas, encompassing road and rail networks, agro-processing facilities, wholesale markets, input suppliers, and rural service centers. The surfaces representing transportation costs were analyzed using cost-distance methods in QGIS, taking into consideration fuel expenses, road conditions, and travel duration. Market accessibility was quantified using Euclidean and network distances from each land parcel to the nearest market, while economic indicators such as crop prices, input costs, and net returns per hectare (ha) were spatially referenced to estimate bid-rent potential for each land use class in the SIMLU framework.

GIS preprocessing and spatial harmonization

All datasets were projected to WGS 84/ UTM zone 43N to ensure spatial consistency. Raster datasets were resampled to 100-meter resolution using cubic convolution for continuous variables and nearest neighbor for categorical maps. Vector datasets were simplified using Douglas–Peucker generalization. Composite indices were created through raster calculations, incorporating factors such as hydrological proximity, road accessibility, and agricultural attractiveness. All layers were clipped to basin boundaries and archived in GeoPackage format to ensure reproducibility and compatibility with both QGIS and Python-based modeling workflows. Missing spatial or temporal data values with less than 3 percent (%) in total, were interpolated using nearest-neighbor averaging for continuous variables and mode substitution for categorical datasets to ensure spatial consistency.

Micro-experimental water allocation trials

In order to improve the empirical realism of SIMLU when simulating farmer responses under water scarcity, micro-experimental water allocation trials were conducted across representative agricultural plots in the Esil and Irtysh River Basins. Plots ranged from 0.5 to 1 ha and were selected to capture variability in soil type, irrigation infrastructure, and major crops (wheat, barley, sunflower, and potatoes). Experimental treatments simulated complete irrigation, a moderate deficit of 80 percent (%) of the typical seasonal volume, and a severe deficit of 60%, with replication across diverse crop types and locations. Farmers' decisions regarding crop choice, irrigation scheduling, and labor allocation were observed, while crop growth, biomass, and yield were monitored at key phenological stages. Continuous recording of soil moisture was conducted at a depth ranging from 0 to 60 centimeters (cm) using sensors. A total of twelve plots (six in each basin) were used, each with three replicates per irrigation treatment (100%, 80%, and 60% of the typical seasonal irrigation volume). Observations were carried out over two cropping seasons (2022–2023), featuring ongoing monitoring of soil moisture levels and weekly evaluations of crop development. Data from these trials were used to calibrate SIMLU's water sensitivity parameters by refining cost-distance decay and bid-rent functions, producing a water-responsive land suitability index. Variability in farmer decision-making was incorporated as a stochastic component within SIMLU, allowing the model to simulate heterogeneous responses under water stress. Scenario simulations, which encompass business-as-usual (BAU), Water scarcity, and infrastructure expansion, were supplemented with these empirically validated responses for water allocation.

Model framework

SIMLU was adapted to analyze the spatial and economic determinants of land use allocation in the Esil and Irtysh River Basins. The estimated decay parameter (β) was 0.047 ± 0.006 (standard error), calibrated via maximum likelihood estimation using historical land use transitions (2015–2020) as a training dataset. The model synthesizes gravity-based interaction theory with raster-based cost-distance functions to replicate land parcel distribution under established constraints. Implementation was performed in Python version 3.11 using Pandas, GeoPandas, NumPy, and SciPy, with integration into GIS workflows via QGIS 3.34.10 and GDAL. SIMLU incorporates five primary input categories: water accessibility indices, transport proximity matrices, bid-rent functions incorporating crop prices and yields, land suitability scores from the MCE-AHP, and labor and population density maps. The probability of each land parcel being designated for a particular land use type is determined through a spatial econometric framework as indicated in Eq. 1 (Silveira and Dentinho, 2018):

$$= B \frac{}{(c)} \quad (1)$$

Where, Tij is the probability of land parcel iii being allocated to land use type j, Oi and Dj represent origin and destination attractiveness (e.g., labor availability and bid-rent value), $f_{(cij)}$ is a cost-distance decay function, and Ai and Bj are balancing factors ensuring conservation of land area and type. A negative exponential decay function $f_{(cij)}=\exp(-\beta_{cij})$ was applied, with the decay parameter β calibrated via maximum likelihood estimation using historical land use transitions (2015–2020) as a training dataset. To avoid overfitting and collinearity, input variables were screened using variance inflation factor (VIF)

thresholds (<5) prior to inclusion in the model.

Scenario simulation and land use allocation

To generate spatially explicit land use scenarios, the study area was divided into 100 m × 100 m grid cells using a fishnet raster. Each scenario was simulated with 1,000 Monte Carlo iterations using a fixed random seed of 42. Convergence was achieved when cumulative allocation probabilities remained stable with less than a 1% variation over 20 consecutive runs. For each cell, the model calculated the probability of allocation to one of four major land use categories: irrigated agriculture, rainfed agriculture, pasture, or non-agricultural. These probabilities were derived by normalizing the interaction values Tij across all categories. A Monte Carlo simulation module was embedded to capture stochastic elements in decision-making and to account for data uncertainty. The allocation process faced restrictions due to administrative zoning regulations and environmental exclusion zones (such as protected wetlands and riparian buffers), which were implemented as binary exclusion masks. The final output consisted of spatial probability maps and categorical allocation layers, which were validated against observed land use patterns in 2023 using confusion matrix metrics and Kappa statistics.

GIS-based spatial analysis

A comprehensive GIS-based spatial analysis was conducted to quantify and visualize the drivers of agricultural land use in the Esil and Irtysh River Basins, integrating hydrological, infrastructural, and environmental variables into a decision-support framework. Using QGIS 3.34.10 and Arc Geographic Information System Professional (ArcGIS Pro) 3.1, agricultural parcels were delineated from Copernicus global land service (CGLS) land cover data and segmented into 100 m × 100 m grids for uniform spatial analysis. The evaluation of hydrological proximity involved the use of Euclidean distance algorithms to ascertain the accessibility of each parcel to perennial water sources, with the distances adjusted to a 0–1 scale. Cost-distance mapping evaluated market accessibility by incorporating road hierarchy, slope (from 30 m SRTM DEM), and transport impedance values, generating surfaces that reflected logistical and energetic costs. To assess land viability, a multi-criteria evaluation (MCE) based on the AHP assigned expert-weighted values to soil fertility (35%), slope (25%), water availability (20%), and historical productivity (20%). Every element was normalized, transformed into raster data, and incorporated into a composite land suitability index through the application of weighted overlay. The generated continuous suitability surface played a crucial role in informing SIMLU's spatial arrangement of agricultural activities, and it was corroborated by 2023 observed land use data and expert assessments from prior zoning efforts in Kazakhstan. The analytical design of this study follows a multi-scalar spatial framework, encompassing 14 administrative regions (oblasts) across Kazakhstan. The modeling methodology incorporates regional-level indicators, including economic structure, infrastructure density, and hydrological availability, along with sub-regional datasets such as land suitability, groundwater depth, and soil fertility. Statistical analyses, including regression diagnostics and spatial variance tests, were conducted at both scales to capture cross-level interactions and ensure methodological robustness in representing spatial heterogeneity and inter-regional dependencies.

Regression and statistical modeling

To enhance spatial analysis and bolster the predictive power of the SIMLU framework, a multivariate regression model was applied to statistically assess the relationship between key spatial and economic variables and the proportion of cultivated land across administrative units. The dependent variable, defined as the percentage of cultivated land per district, was utilized as a proxy for agricultural land use intensity. The independent variables consisted of the distance to water sources, distance to markets, GIS-derived soil suitability scores, agricultural employment rates, and road density. Conducted in R version 4.3.2 using the linear model function, car, and nortest packages, the analysis followed an ordinary least square (OLS) framework, with assumptions of linearity and homoscedasticity verified through diagnostic tests. Multicollinearity was addressed using Variance Inflation Factor (VIF) scores, removing or transforming variables exceeding the 5.0 threshold, while the Shapiro–Wilk test and residual plots were used to assess normality and model specification. The application of stepwise selection, guided by the Akaike Information Criterion

(AIC), optimized the model to its most parsimonious state, achieving a high adjusted R^2 and elucidating the magnitude and direction of the influence of each predictor. All retained predictors exhibited VIF values below 3.2, indicating negligible multicollinearity. Residuals were tested for spatial autocorrelation using Moran's I (I = 0.021, p = 0.42), confirming no significant spatial dependence. Significantly, the regression outputs served to validate the SIMLU model through a comparison of empirically derived land use intensities with spatially simulated outcomes, thereby enhancing the credibility of the simulation results and allowing for a more in-depth understanding of the determinants of agricultural land use in the Esil and Irtysh River Basins.

Scenario development

To evaluate the impact of various environmental and policy interventions on agricultural land allocation and sustainability in the Esil and Irtysh River Basins, three land use scenarios were developed and simulated using the SIMLU model. The firstn scenario, known as Business-as-Usual (BAU), anticipated the ongoing trends from 2020 to 2023, devoid of substantial policy or climatic shifts, functioning as a foundational benchmark. The second scenario, Water Scarcity, simulated a 20% decrease in surface water availability to account for climate-induced stress. This model included alterations in hydrological accessibility, evapotranspiration, and precipitation patterns, which subsequently affected land suitability and crop viability. The third scenario, infrastructure expansion, simulated the effects of rural development investments, increasing road density by 25% in low-access regions and recalculating market proximity to reflect improved logistics and travel conditions, thereby enhancing the attractiveness of marginal lands. All scenarios were executed based on standardized model assumptions, producing spatially detailed outputs including alterations in cultivated land area, shifts in bid-rent, distributions of labor-intensive crops, and reallocation of suitability-adjusted parcels, offering a comprehensive decision-support framework for prospective land use policy.

RESULTS AND DISCUSSION

Land cover distribution analysis

The analysis of the collected data revealed distinct spatial patterns in the distribution of economic activity across the study regions. Astana, which functions as the principal economic hub of the country, demonstrates a significant density of employment in both the industrial and service sectors, indicative of its urban infrastructure and diverse economic landscape. In contrast, the East Kazakhstan region is predominantly agrarian, with a large proportion of its territory devoted to agricultural land and a corresponding dependence on primary-sector activities for livelihoods and income generation. The distance matrix analysis further confirms that economic activity is spatially clustered around major industrial and urban centers, with accessibility playing a critical role in regional development. Peripheral regions, especially those situated at a considerable distance from these economic centers, face considerable difficulties in assimilating into the national economic structure owing to logistical limitations and restricted market access. These spatial disparities are visually supported by Fig. 1, which illustrates the distribution of land cover types, emphasizing the dominance of agriculture in remote regions and the urban-industrial footprint near economic centers (Fig. 2).

The evaluated summary statistics demonstrate notable regional inequalities in both the employment structure and the distribution of land use across Kazakhstan. The mean total employment stands at 383,392 people, translating to 451 employed individuals per 1,000 residents. This figure is accompanied by a moderate coefficient of variation (CV) of 50.9%, indicating some variation but relatively stable employment proportions across most regions. However, employment in agriculture, forestry, and fisheries exhibits a strikingly high CV of 100.4%, with an average of just 64.4 workers per 1,000 people. This variation emphasizes notable specialization in certain rural areas, including Turkistan and Zhambyl, where agricultural activities are more prevalent. In contrast, urbanized areas like Astana and Almaty demonstrate minimal engagement in these primary sectors, reflecting the broader trend of urbanization and economic diversification away from traditional agriculture. The land use data reveals even more pronounced disparities across the country. Irrigated cropland, averaging 46,500 ha (or 54.7/ha/1,000 people), has an extremely high CV of 180.6%. This indicates a significant concentration of irrigation-dependent agriculture, with only a limited number

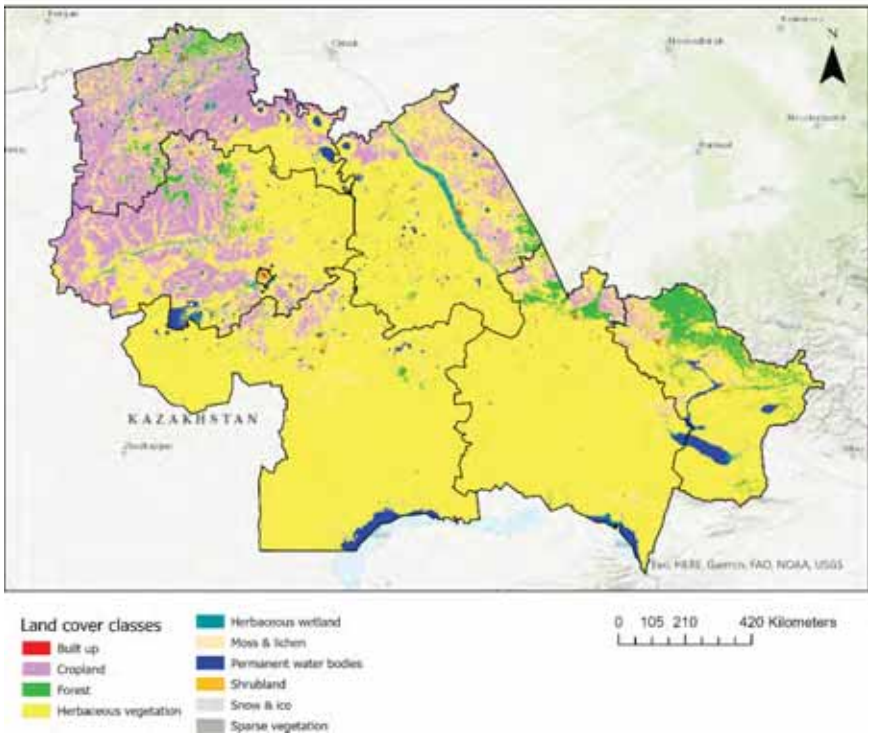

Fig. 2: Land cover distribution of the Esil River Basin, Kazakhstan, using Copernicus global land service dynamic

of regions prevailing in this type of land use. The total cropland and herbaceous vegetation also show substantial variability, with CVs exceeding 149%. These patterns reveal significant disparities in agricultural potential and ecological coverage across Kazakhstan, which can be ascribed to the country's varied climatic zones and geographical characteristics. Regions with favorable conditions for agriculture are markedly more productive, while others struggle with arid landscapes that limit cultivation. Moreover, the distribution of forest and shrubland, with a CV of 135.6%, is uneven and predominantly found in select forested areas such as East Kazakhstan. In contrast, the built-up area shows more uniform patterns of urban development, averaging only 23.5 ha per 1,000 people and exhibiting a lower CV of 75%. This suggests that urbanization is more evenly distributed relative to population sizes across regions. Finally, employment in the services sector averages 237,000 people, equating to 278.8 per 1,000 residents, and displays high variability (CV = 97%). This illustrates the significant urban concentration of service sectors, especially in prominent cities such as Almaty, Astana, and Shymkent, emphasizing the continuous transition towards a service-driven economy in these metropolitan areas (Table 1).

Land use allocation (SIMLU outputs)

The results in Table 2 illustrate how land use allocation responds to hydrological and infrastructural conditions, as simulated by the SIMLU model. Under the current trends cenario (CTS), total cultivated land spans 19,200 square kilometers (km²), comprising 5,900 km² of irrigated and 8,200 km² of rainfed agriculture. These metrics signify the essential baseline, showcasing the restrictions dictated by the available water resources and transport facilities, and underscoring the present balance that farmers sustain between irrigated and rainfed agricultural practices. Under the Water Stress Scenario, which simulates a 20% reduction in surface water availability, total cultivated land declines to 15,850 km², an absolute decrease of 3,350 km² or a relative decline of 17.5%. The reduction is most pronounced in irrigated areas, which fall by 30.5%, forcing many farmers to reduce cropping or leave

Table 1: Summary statistics of demographics and land use/cover in kazakhstan regions

Variable	Mean	Per 1,000 People	CV (%)	Interpretation
Total Employment	383,392	451	50.9	Moderate variation across regions
Agriculture, forestry and fisheries employment	54,800	64.4	100.4	Very high variability; concentrated in few regions
Irrigated cropland (ha)	46,500	54.7	180.6	Highly uneven distribution
Total cropland (ha)	1,838,100	2,161.30	160.5	Large disparities; a few regions dominate
Herbaceous vegetation (ha)	4,350,000	5,112.90	149.4	Widespread variation
Forest and shrubland (ha)	295,000	346.9	135.6	Found in select regions only
Built-up area (ha)	20,000	23.5	75	Less variation; typical of population centers
Services employment	237,000	278.8	97	High variability: urban regions dominate

Table 2: Land use allocation under different scenario simulations (SIMLU results)

Land use class	Current trends scenario (CTS)	Water stress scenario (−20% surface water)	Rural infrastructure expansion scenario (+25% road density)
Total cultivated area (km²)	19,200	15,850 (−17.5%)	22,400 (+16.7%)
Irrigated agriculture (km²)	5,900	4,100 (−30.5%)	6,700 (+13.6%)
Rainfed agriculture (km²)	8,200	7,500 (−8.5%)	9,100 (+11.0%)
Pasture and fallow (km²)	3,800	4,600 (+21.1%)	3,100 (−18.4%)
Non-agricultural (urban/unused) (km²)	1,300	1,250	1,500 (+15.4%)

land fallow. Correspondingly, pasture and fallow land expand to 4,600 km², a relative increase of 21.1%, underscoring the vulnerability of intensive agriculture to water scarcity and the adaptive shift toward extensive land uses. Conversely, the rural infrastructure expansion scenario, which projects a 25% rise in road density along with enhanced market access, encourages agricultural advancement. Total cultivated area increases to 22,400 km², an absolute gain of 3,200 km² or a relative increase of 16.7%, with irrigated and rainfed agriculture increasing by 13.6% and 11.0%, respectively. Fallow and pasture lands decrease by 18.4%, reflecting the reactivation of previously underutilized areas, while non-agricultural land grows moderately to 1,500 km² (+15.4%), indicating parallel development in rural settlements. These findings underscore the crucial importance of transport connectivity in facilitating agricultural growth, enhancing market access, and promoting more efficient land use.

Micro-experimental water allocation trials

Fig. 3 illustrates the impact of irrigation levels on the yield of four major crops (wheat, barley, sunflower, and potatoes) in the Esil and Irtysh River Basins. Yields experienced a progressive decline as irrigation decreased. Under full irrigation, potatoes achieved the highest average yield (5.0 t/ha), while sunflowers had the lowest (3.5 t/ha). A moderate deficit, representing 80% of standard irrigation, resulted in a significant decrease in all crops, with wheat and barley experiencing a decline of about 14–16%, while sunflower and potatoes saw a reduction of 17–18%. Severe deficit (60% of typical irrigation) further exacerbated yield losses, with wheat and barley declining by 33–34%, sunflower by 40%, and potatoes by 36%. These results highlight crop-specific sensitivity to water stress, providing empirical support for SIMLU's water-responsive calibration.

The line plot illustrates the average soil moisture content in the top 60 cm of soil for four crops subjected to under full, moderate, and severe irrigation treatments. Soil moisture declined consistently with reduced irrigation. Under full irrigation, soil moisture ranged from 27.8% (sunflower) to 30.0% (potatoes). Moderate deficit reduced soil moisture by approximately 6–7 percentage

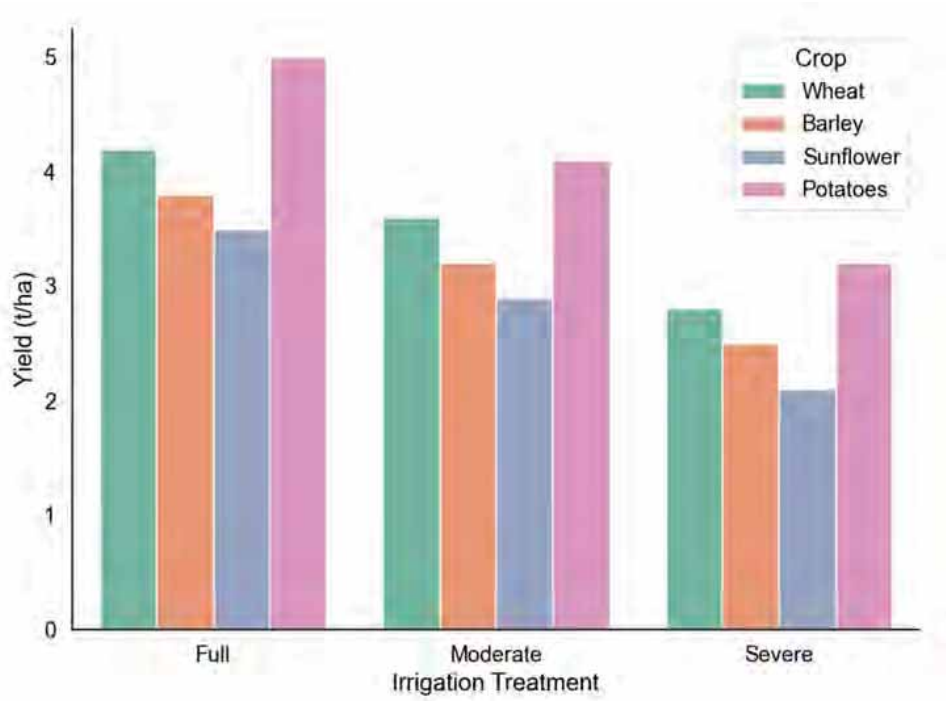

Fig. 3: Crop yield under different irrigation treatments

points, while severe deficit caused a further drop of 3–4 points, with wheat reaching 18.3% and potatoes 19.5%. These trends illustrate that diminishing irrigation leads to a direct decline in soil water availability, underscoring the mechanistic relationship between hydrological accessibility and crop performance incorporated into SIMLU (Fig. 4).

Fig. 5 summarizes farmer responses to varying water availability. Under full irrigation, no adaptive behavior was observed, as expected. Moderate deficit induced partial adaptation: approximately 7.5% of plots switched crops, 18.8% adjusted irrigation, and 15% reallocated labor. A significant deficit led to more comprehensive behavioral changes, with 32.5% of plots altering their crops, 42.5% modifying their irrigation schedules, and 27.5% redistributing labor. The data illustrates how farmers adopt multiple, simultaneous strategies to mitigate water stress, providing empirical evidence for SIMLU's stochastic component that captures heterogeneous decision-making under water scarcity.

Environmental and land suitability indicators

Table 3 demonstrates how environmental and land suitability indicators react to diverse scenario conditions, delivering important insights into the spatial and biophysical dynamics influencing agricultural potential in the Esil and Irtysh River Basins. Under the CTS, the average land suitability index stands at 0.63, reflecting a moderate to high overall potential for cultivation given existing environmental and infrastructural conditions. This index implies that, despite the presence of advantageous circumstances for farming, there are substantial restrictions that impede agricultural output. The CTS serves as a benchmark, highlighting the challenges posed by current environmental conditions and infrastructure limitations. As farmers navigate these challenges, understanding the nuances of land suitability becomes essential for making informed decisions about crop choices and resource management. The moderate index implies that while some areas may flourish, others could encounter stagnation, making it essential to implement targeted measures to boost agricultural viability. In the Water Stress Scenario, the average land suitability index declines markedly to 0.55, representing a 12.7% reduction. This decline is primarily driven by a substantial drop

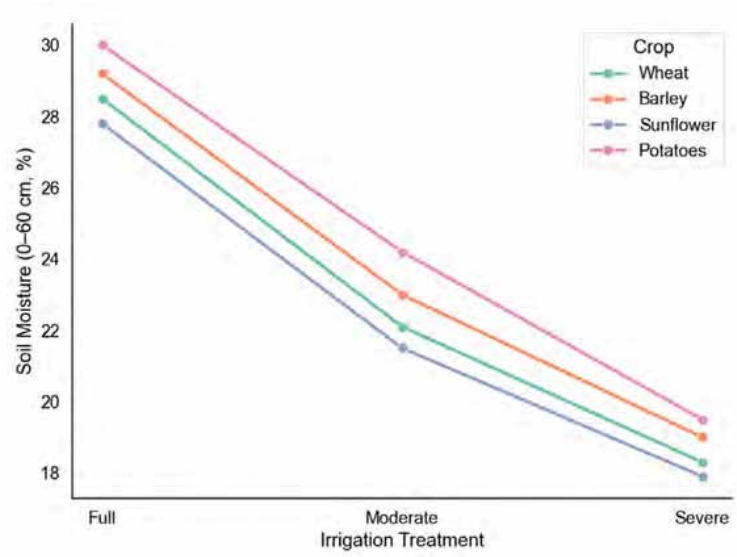

Fig. 4: Soil moisture (0–60 cm) under different irrigation treatments

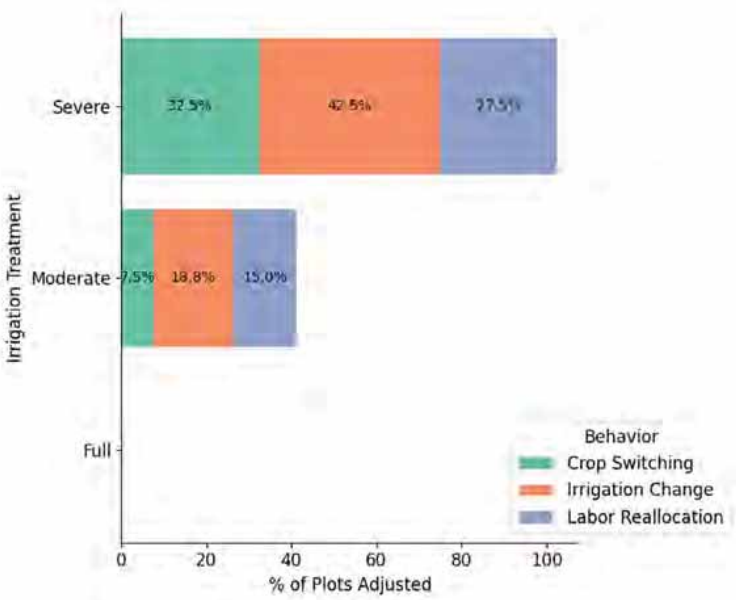

Fig. 5: Farmer behavioral adaptation under different irrigation treatments

in the hydrological accessibility index; from 0.58 to 0.43, a decrease of 25.9%. This decline highlights an expanding spatial disconnection between agricultural areas and the water sources available, which are vital for agriculture that depends on irrigation. Concurrently, average groundwater depth increases from 12.4 m to 14.9 m, reflecting a 20.2% rise that further limits access to irrigation, particularly for regions reliant on shallow wells. Although soil fertility remains relatively stable; dropping only slightly from 0.68 to 0.66; the compounded effects of surface and subsurface water scarcity significantly reduce the environmental viability for agriculture. This scenario highlights the pressing necessity for efficient water management strategies to tackle the challenges presented by hydrological constraints, as farmers struggle more to uphold productive agricultural practices. In contrast, the Infrastructure Expansion

Table 3: Environmental and land suitability indicators under different scenarios

Indicator	Current trends scenario (CTS)	Water stress scenario	Infrastructure expansion scenario
Average land suitability index (0–1)	0.63	0.55 (−12.7%)	0.70 (+11.1%)
Hydrological accessibility index (0–1)	0.58	0.43 (−25.9%)	0.60 (+3.4%)
Soil fertility weighted score (AHP)	0.68	0.66	0.71
Average Groundwater Depth (m)	12.4	14.9 (+20.2%)	11.8 (−4.8%)
Regression model fit (R^2 / Adjusted R^2)	0.81 / 0.79	0.84 / 0.82	0.87 / 0.85

Scenario demonstrates notable improvements in suitability conditions, highlighting the positive impact of enhanced infrastructure on agricultural potential. The average land suitability index increases to 0.70, reflecting an 11.1% improvement, which signals a more favorable environment for cultivation. Hydrological accessibility also improves slightly, rising to 0.60, an increase of 3.4%. This enhancement is primarily due to improved road networks that enable maintenance and access to irrigation systems, which are essential for maximizing water efficiency in agriculture. Moreover, the scenario reveals a reduction in average groundwater depth to 11.8 m, a decrease of 4.8%, indicating enhanced efficiency in groundwater extraction and distribution. This suggests that improved transport connectivity not only supports agricultural activities but also enhances farmers' ability to manage water resources more effectively. Furthermore, there is a small increase in soil fertility to 0.71, possibly signifying enhanced land management practices in regions that were once underutilized. Moreover, the regression analysis produced high model fit across scenarios. For the Water Stress Scenario, the regression model for land suitability yielded R^2 = 0.84 and adjusted R^2 = 0.82. Under the Infrastructure Expansion Scenario, the corresponding model achieved R^2 = 0.87 and adjusted R^2 = 0.85, while the Current Trends baseline model recorded R^2 = 0.81 and adjusted R^2 = 0.79. These values indicate strong explanatory power and reliability of the regression models in capturing the spatial variability of land suitability and agricultural response across different hydrological and infrastructural conditions. The regression analysis identified several significant predictors of land allocation and crop productivity, including groundwater depth, distance to market, and soil fertility. There was a negative correlation between groundwater depth and the distribution of irrigated land, implying that deeper water tables constrain the viability of irrigation. Proximity to markets positively influenced cultivated areas and crop profitability, reflecting the economic benefits of reduced transport costs. Soil fertility emerged as a strong determinant of both irrigated and rainfed productivity, emphasizing the importance of land quality in shaping agricultural decisions. These findings illustrate the combined influence of biophysical and socio-economic factors on the spatial distribution of land use in the study region (Table 3).

Economic and infrastructure impacts

Table 4 presents the economic and infrastructure impacts of the modeled scenarios, clearly illustrating how changes in water availability and rural connectivity influence the financial viability of agricultural land use. Under CTS, the average crop profitability is 400 United States dollar per hectare (USD/ha), with transport costs averaging USD 1.28/km and a moderate market access index of 0.61, indicating fair accessibility to input suppliers and buyers. The average bid-rent potential, representing the economic desirability of land for agricultural use, is calculated to be USD 520/ha, with 69% of land parcels are performing above the break-even yield threshold. In the Water Stress Scenario, profitability drops sharply to USD 325/ha (−26.1%) due to decreased yields and higher irrigation costs. Transport costs slightly increase to USD 1.35/km (+5.5%) as water-stressed regions shift cultivation to less accessible or marginal areas, while market access falls to 0.58 (−4.9%). The potential for bid-rent decreases to USD 400 per hectare (−23.1%), with only 48% of land parcels still being economically viable, highlighting the susceptibility of agriculture to hydrological disturbances. Conversely, the infrastructure expansion scenario demonstrates clear economic gains, with average profitability rising

Table 4: Economic and infrastructure impact indicators

Economic metric	CTS	Water Stress	Infrastructure Expansion
Avg. crop profitability (USD/ha)	440	325 (−26.1%)	510 (+15.9%)
Mean transport cost (USD/km)	1.28	1.35 (+5.5%)	1.04 (−18.7%)
Market access index (0–1)	0.61	0.58 (−4.9%)	0.76 (+24.6%)
Avg. bid-rent potential (USD/ha)	520	400 (−23.1%)	600 (+15.4%)

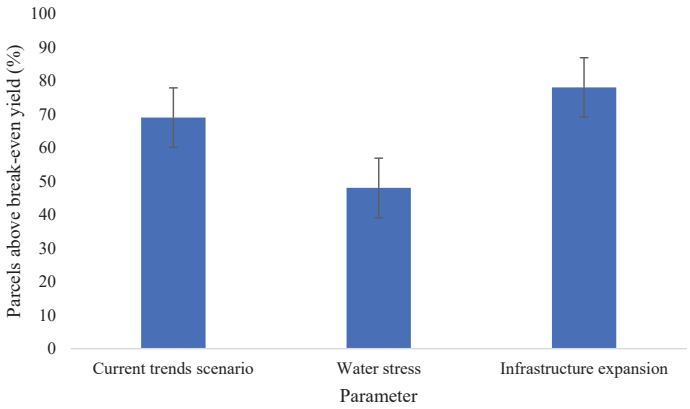

Fig. 6: Economic and infrastructure impact indicators

to USD 510/ha (+15.9%) and transport costs dropping significantly to USD 1.04/km (−18.7%) due to improved road density and connectivity. Market access improves substantially to 0.76 (+24.6%), facilitating better price realization and reduced input delays. These improvements elevate the bid-rent potential to USD 600/ha and boost the proportion of economically viable parcels to 78%, thereby reinforcing the importance of strategic infrastructure investment in enhancing agricultural returns and land use efficiency in semi-arid regions (Table 4).

To elaborate further, under the present trends, the proportion of parcels that surpass the break-even yield fluctuates considerably depending on various conditions. Under water stress, 69% of parcels achieve yields above the break-even point, indicating a moderate resilience to resource challenges. Conversely, as infrastructure expands, this percentage increases to 78%, indicating that enhanced infrastructure has the potential to improve agricultural productivity and sustainability (Fig. 6).

Labor and social indicators

Table 5 presents the labor and social dynamics observed in the three modeled scenarios, highlighting the influence of environmental stress and infrastructure development affect rural employment patterns and demographic distribution in cultivated areas. Under the CTS, labor-intensive crops such as vegetables and potatoes account for 29% of the total cultivated area, supported by an employment accessibility index of 0.65 and an average population density of 41.2 persons/km² in agricultural zones. These figures indicate relatively positive circumstances for participation in rural labor. However, in the water stress scenario, the proportion of labor-intensive crops declines sharply to 21% (−27.6%), indicating a shift toward less labor-dependent and more drought-resilient crops or even fallow land. This change is associated with a small reduction in employment accessibility (0.60) and a decline in population density to 38.7 persons/km², implying a potential increase in outmigration or underemployment in agriculture-dependent communities. In contrast, the infrastructure expansion scenario results in a substantial rise in labor-intensive cropping to 36% (+24.1%), driven by improved access to markets and services that encourage high-value

Table 5: Social and labor dynamics

Labor/social indicator	CTS	Water stress	Infrastructure expansion
% Labor-intensive crops (vegetables, potatoes)	29%	21% (−27.6%)	36% (+24.1%)
Employment accessibility index (0–1)	0.65	0.6	0.68
Avg. population density in cultivated areas (persons/km²)	41.2	38.7	45.1

Table 6: Model validation and spatial accuracy metrics

Validation metric	CTS	Water stress	Infrastructure expansion
Kappa agreement with 2023 Map	0.86	0.78	0.89
Overall classification accuracy (%)	84.5	76.8	88.3
RMSE (difference in cultivated area, km²)	1,020	2,600	950
% of model-matched agricultural hotspots	82%	68%	87%

horticultural production. Employment accessibility also improves to 0.68, and cultivated areas experience a demographic uptick to 45.1 persons/km², reflecting stronger rural retention and attraction of labor. These findings highlight the critical role of infrastructure, which is essential not only for economic performance but also for supporting social resilience and labor-intensive agricultural livelihoods in regions facing water scarcity (Table 5).

Model validation and accuracy metrics

Table 6 outlines the validation and spatial accuracy metrics utilized to measure the performance and reliability of the SIMLU model under different scenarios. Under CTS, the model demonstrates strong alignment with observed land use patterns, achieving a Kappa agreement of 0.86 and an overall classification accuracy of 84.5%. The root mean square error (RMSE) between simulated and actual cultivated areas is 1,020 km², and 82% of known agricultural hotspots are accurately captured by the model. In the scenario of water stress, the performance of the model diminishes as a result of the increased variability and unpredictability associated with land use changes under hydrological limitations. Kappa drops to 0.78, classification accuracy falls to 76.8%, and RMSE increases substantially to 2,600 km², indicating larger discrepancies in cultivated land estimates. Only 68% of agricultural hotspots are matched, reflecting the difficulty of modeling land use patterns when water access becomes highly limiting. Conversely, the infrastructure expansion scenario produces the highest validation scores across all metrics, with a Kappa of 0.89, classification accuracy of 88.3%, and the lowest RMSE of 950 km². The model successfully anticipates 87% of agricultural hotspots, indicating that land use reactions to infrastructure enhancements are more foreseeable and spatially coherent. These results validate the robustness of the SIMLU framework, particularly under scenarios driven by infrastructure development, while highlighting the challenges of modeling land use under acute environmental stress (Table 6).

The simulation results from the SIMLU reveal clear and contrasting land allocation responses under varying hydrological and infrastructural conditions in the Esil and Irtysh River Basins. Furthermore, under the scenario of water stress, a considerable 17.5% reduction in total cultivated land was observed, coupled with a significant 30.5% decline in irrigated farming, which underscores the region's heavy dependence on surface and shallow groundwater sources. As water accessibility declines, particularly in semi-arid regions like Kazakhstan, farmers tend to retreat from water-intensive crops, leaving land fallow or converting it to pasture; a pattern also observed by Zhang *et al.* (2021), in their study of Hengyang City using the FLUS model, where land type change was strongly influenced by ecological and infrastructural constraints. In contrast, the Infrastructure Expansion Scenario in our study led to a 16.7% increase in cultivated land, with irrigated agriculture expanding by 13.6%, largely due to improved road networks, which

reduced transportation costs and increased access to markets and input suppliers. These results are consistent with the work of Yu *et al*. (2023), who indicated that simulation models that incorporate both natural and social driving forces, including LCM and PLUS, demonstrate that enhanced accessibility promotes the aggregation of productive land types and fosters more sustainable land distribution patterns. According to Yu *et al.* (2023), effective land allocation models must integrate landscape dynamics with socioeconomic drivers, a principle echoed in the strong spatial clustering of productive agricultural parcels observed in our infrastructure-enhanced scenario. The indicators related to environmental and land suitability enhance our comprehension of these shifts in land use. The significant reduction in the Land Suitability Index under water stress (−12.7%) stems from both declining hydrological accessibility and deepening groundwater tables, which reduce irrigation feasibility and increase water extraction costs. Water-scarce conditions also alter the soil-water balance, potentially degrading soil structure and productivity (Diop *et al.*, 2022; Ingrao *et al.*, 2023). Meanwhile, infrastructure development slightly improves hydrological access by facilitating maintenance and delivery of water through enhanced physical connectivity to irrigation systems (George-Williams *et al.*, 2024; Lakhiar *et al.*, 2024; Mgala *et al.*, 2025). Furthermore, the improved suitability index in the infrastructure expansion scenario signifies the combined effect of superior road access, less slope-induced isolation, and improved management of productive soils. These findings emphasize that environmental constraints are not solely a function of biophysical conditions but are also mediated by infrastructural connectivity and investment (Lazurko and Pinter, 2022; Lee and Han, 2025). The economic and infrastructure outcomes of the study underscore the intrinsic vulnerability of agricultural systems to environmental pressures and underscore the pivotal role that enhanced connectivity plays in boosting resilience and profitability (Mthembu, Cele, and Mkhize, 2025; Toth, 2025). Under the Water Stress Scenario, average crop profitability dropped by over 26%, with bid-rent potential decreasing by 23.1% and only 48% of land parcels remaining above the break-even yield threshold. These reductions are a result of diminished water availability, which obliges farmers to grow crops in more isolated, less fertile locations, leading to increased irrigation and transportation expenses. Similar trends have been observed by Sultana *et al.* (2023), in drought-prone Northwest Bangladesh, where declining rainfall and limited drought-resilient inputs exacerbated farmer vulnerability, pushing communities toward marginal farming zones with poor infrastructure and higher exposure to environmental risk. Conversely, the infrastructure expansion scenario demonstrates the economic revitalization potential of strategic rural investments. Improved road density led to an 18.7% reduction in transport costs and a 24.6% increase in market access, which collectively raised average profitability to USD 510/ha and increased the share of profitable parcels to 78%. According to Kalogiannidis *et al.* (2023), enhancing resilience through infrastructure and risk governance is essential for attaining sustainable rural transformation. The Greek case study similarly emphasized that climate vulnerability undermines rural development unless countered by robust risk management and infrastructure planning. The findings related to labor and demographics further clarify the socio-economic shifts instigated by environmental and infrastructural modifications in the study region. Under the water stress scenario, the sharp 27.6% reduction in labor-intensive crops such as vegetables and potatoes reflects a strategic shift by farmers toward less risky, lower-input farming practices that demand fewer laborers, potentially exacerbating rural underemployment and outmigration. This pattern corresponds with the findings of Booker and Trees (2020), who stress that the scarcity of water necessitates a reallocation of labor by producers towards extensive cropping systems, leading to a decrease in seasonal employment despite complex interactions with water productivity and crop choice. The decline in labor demand is also linked to constrained access to inputs and credit, as noted by Quddus and Kropp (2020), in Bangladesh's lagging agricultural regions, where limited irrigation infrastructure and input availability inhibit labor-intensive production. In contrast, the infrastructure expansion scenario's 24.1% increase in labor-intensive crop cultivation and rising rural population density suggest that improved road networks boost rural livelihoods by enhancing market engagement, technology adoption, and access to extension services. These advancements encourage a more vibrant agricultural labor market, allowing for investments in higher-value, labor-dependent crops that raise

incomes and support rural development. These outcomes emphasize the vital importance of infrastructure in determining agricultural labor dynamics and community resilience amidst environmental challenges. The validation results demonstrate a strong alignment between the SIMLU model outputs and observed land use patterns, especially under the infrastructure expansion scenario, which achieved the highest Kappa agreement of 0.89 and the lowest RMSE of 950 km². This significant degree of consensus demonstrates the model's strength in replicating land use dynamics, which are mainly influenced by stable physical elements like enhanced transportation access and proximity to markets. This aligns with the observations made by Luan *et al*. (2022), who indicated that models that integrate infrastructural and policy considerations produce more dependable forecasts land use changes in contexts of planned development. However, the comparatively lower validation metrics under the Water Stress Scenario highlight inherent challenges in capturing complex, adaptive responses to environmental stress, such as spontaneous land abandonment or informal land use changes. This constraint corresponds with Foody (2020), conducted a critical review of the interpretive limitations of Kappa statistics in accuracy evaluations. He highlighted the necessity of integrating socio-political dynamics and climate variability for more comprehensive modeling of landscape changes under environmental pressures. Consequently, these outcomes emphasize the critical role of integrating adaptive human behaviors, governance factors, and climate forecasts into spatial land use models to enhance predictive performance under scenarios of environmental uncertainty. Moreover, it should be noted that, the analytical design, characterized by a multi-scalar spatial framework with 1 km² resolution and statistically validated through spatial regression and variance diagnostics, enhances the precision of regional interpretation while acknowledging that finer spatial granularity may introduce minor uncertainties affecting the reliability of aggregated findings.

CONCLUSION

This study provides a comprehensive assessment of agricultural land use dynamics in the Esil and Irtysh River Basins by integrating hydrological accessibility, land suitability, and infrastructure connectivity within a spatially explicit, scenario-based modeling framework. The analysis emphasizes the influence of both environmental and infrastructural factors shape the extent, intensity, and profitability of agricultural activities. In the context of water stress, a simulation indicating a 20% decrease in surface water availability resulted in a significant reduction of 17.5% in the total cultivated area, while irrigated agriculture experienced a contraction of 30.5%. This contraction corresponded to a drop in average crop profitability to USD 325/ha, illustrating the acute vulnerability of irrigated farming systems to water scarcity. The reduction in cultivated land was accompanied by a proportional expansion of pasture and fallow areas, reflecting farmers' adaptive responses to mitigate production losses under constrained hydrological conditions. These observations indicate that the availability of water is the foremost constraint on agricultural productivity in arid and semi-arid basins, and that proactive management strategies are essential to sustain crop production and economic returns. Conversely, under the rural infrastructure expansion scenario, assuming a 25% increase in road density and improved market access, total cultivated area increased by 16.7%, with the land suitability index improving to 0.70 and average crop profitability rising to USD 510/ha. The areas under irrigation and those relying on rainfall have both increased, while the extent of fallow and pasture lands has decreased, emphasizing the ability of infrastructure advancements to tap into underutilized land and boost overall and improve overall efficiency. These gains were driven by reduced transportation costs, enhanced access to inputs and agro-processing facilities, and improved market connectivity, collectively enabling farmers to optimize land allocation decisions and increase resource use efficiency. The analysis of various scenarios demonstrates that although water availability limits productivity, strategic investments in infrastructure serve as a multiplier, somewhat alleviating hydrological constraints and fostering more resilient agricultural systems. Based on these results, several practical recommendations emerge. First, adaptive water management and irrigation strategies should be prioritized to maintain productivity under declining water availability, including scheduling irrigation and adopting water-saving technologies. Second, investments in transportation networks, market access, and rural service infrastructure should be focused on regions that possess high land suitability

but face connectivity challenges, to encourage agricultural development and enhance profitability. Third, policies should encourage the reactivation of underutilized but suitable agricultural lands while ensuring that land management balances economic gains with ecological sustainability. Furthermore, the incorporation of land use alongside local market development can significantly improve the efficiency and resilience of agricultural systems. Despite these insights, the study has some limitations. The SIMLU model does not fully incorporate behavioral adaptation by farmers, long-term soil degradation processes, or interannual climate variability, which could influence both land use decisions and crop profitability over time. The model also does not explicitly account for policy changes, institutional constraints, or detailed socio-economic heterogeneity among farm households. Confronting these constraints in future studies would facilitate a deeper insight into agricultural dynamics influenced by different environmental and socio-economic circumstances. Future research should focus on integrating dynamic climate projections, socio-economic data, and land tenure information to improve predictive accuracy and enhance scenario realism. Incorporating explicit farmer decision-making processes, including crop selection, risk preferences, and labor allocation, would allow the evaluation of trade-offs between water use, infrastructure investment, and crop profitability. Furthermore, taking into account the long-term health of the soil, the sustainability of groundwater, and the effects on ecosystem services will offer a more comprehensive foundation for adaptive land management policies. Such advancements would strengthen the utility of spatially explicit models like SIMLU for supporting policy interventions that optimize agricultural productivity, economic returns, and environmental stewardship in water-limited basins. This study illustrates that the utilization of agricultural land is significantly influenced by water availability and infrastructural conditions. Furthermore, scenario-based spatial modeling offers valuable insights into possible land management strategies. By quantifying absolute and relative changes in cultivated areas, crop profitability, and land suitability, the research offers evidence-based guidance for decision-makers aiming to enhance rural resilience, optimize resource allocation, and promote economically and environmentally sustainable agricultural development in the Esil and Irtysh River Basins.

AUTHOR CONTRIBUTIONS

G. Saspugayeva, the corresponding author, has contributed to supervising the study, guiding the data analysis, interpreting the results, and preparing the manuscript. A. Zhaken participated in data collection, preliminary analysis, and drafting of the manuscript. T.P. Dentinho contributed to study design, methodology development, and critical revision of the manuscript. M. Kamet assisted in data processing, statistical analysis, and interpretation of the results. K. Dakieva prepared all the field and hydrological data and figures. S. Kassymkhanov participated in interpretation of the results and manuscript preparation. K. Tolubayeva prepared all the maps, figures, and interpretation of the results. A. Tsiganov participated in methodology refinement, data validation, and manuscript preparation.

ACKNOWLEDGEMENT

The authors would like to acknowledge the support of their respective institutions for facilitating data collection, analysis, and manuscript preparation. Authors also thank colleagues and collaborators who provided valuable guidance and feedback during the study.

CONFLICT OF INTEREST

The authors declare that there is no conflict of interest regarding the publication of this manuscript. In addition, ethical issues, including plagiarism, informed consent, misconduct, data fabrication and/or falsification, double publication and/or submission, and redundancy have been completely observed by the authors.

OPEN ACCESS

©2026 The author(s). This article is licensed under a Creative Commons Attribution 4.0 International License, which permits use, sharing, adaptation, distribution and reproduction in any medium or format, if you give appropriate credit to the original author(s) and the source, provide a link to the Creative Commons license, and indicate if changes were made. The images or other third-party material in this article are included in the article's Creative Commons license, unless indicated otherwise in a credit line to the material. If material is not included

in the article's Creative Commons license and your intended use is not permitted by statutory regulation or exceeds the permitted use, you will need to obtain permission directly from the copyright holder. To view a copy of this license, visit: http://creativecommons.org/licenses/by/4.0/

PUBLISHER'S NOTE

GJESM Publisher remains neutral regarding jurisdictional claims in published maps and institutional afflictions.

☒ Negative AI Statement

The author(s) declared that no AI tools or services were not used or not highly applied during the preparation of this work.

ABBREVIATIONS

%	Per cent
°C	Degree celsius
AAI	Agricultural attractiveness index
ArcGIS Pro	Arc Geographic Information System Professional
AHP	Analytic hierarchy process
AI	Artificial intelligence
BAU	Business-as-usual
Bj	Balancing factor (destination)
cm	Centimeters
CV	Coefficient of variation
CGLS	Copernicus global land service
CTS	Current trends scenario
DEM	Digital elevation model
Dj	Destination attractiveness
GIS	Geographic information system
GDAL	Geospatial data abstraction library
ha	Hectare
HPI	Hydrological proximity index
IDW	Inverse distance weighting
ISO	International organization for standardization
KZT	Kazakhstani tenge
km	Kilometer
km²	Square kilometer
Kappa	Kappa agreement coefficient
LM	Linear model
MCE	Multi-criteria evaluation
mm/y	Millimeter per year
m	Meter
m³	Cubic meter
m³/s	Cubic meter per second
NUTS-3	Nomenclature of territorial units for statistics level 3
Oi	Origin attractiveness
OLS	Ordinary least squares
QGIS	Quantum geographic information system
pH	Potential of hydrogen
R²	Coefficient of determination
RAI	Road accessibility index
RMSE	Root mean square error
km²	Square kilometers
SIMLU	Spatial interaction model for land use
USD	United states dollar
USD/ha	United States Dollar per hectare
UTM	Universal transverse mercator
VIF	Variance inflation factor
WGS 84	World geodetic system 1984

REFERENCES

Booker, J.F.; Trees, W.S., (2020). Implications of water scarcity for water productivity and farm labor. Water. 12(1): 308 **(10 pages)**.

Christophe, B.; Tina, R., (2015). Integrating water resource management and land-use planning at the rural-urban interface: Insights from a political economic approach. Water Resour. Econ., 10: 25-39 **(15 pages)**.

Curk, M.; Glavan, M., (2021). Perspectives of hydrologic modeling in agricultural research. Hydrology. 1: 1-14 **(14 pages)**.

EDB, (2025). The Irtysh River Basin: Transboundary and Practical. Eurasian Dev. Bank Rep., 1: 1-12 **(12 pages)**.

Diop, M.; Chirinda, N.; Beniaich, A.; El Gharous, M.; El Mejahed, K., (2022). Soil and Water Conservation in Africa: State of Play and Potential Role in Tackling Soil Degradation and Building Soil Health in Agricultural Lands. Sustainability. 14: 13425 **(29 pages)**.

Foody, G.M., (2020). Explaining the unsuitability of the kappa coefficient in the assessment and comparison of the accuracy of thematic maps obtained by image classification. Remote Sens. Environ., 239: 111630 **(12 pages)**.

George-Williams, H.E.M.; Hunt, D.V.L.; Rogers, C.D.F., (2024). Sustainable Water Infrastructure: Visions and Options for Sub-Saharan Africa. Sustainability. 16: 1592 **(30 pages)**.

Ingrao, C.; Strippoli, R.; Lagioia, G.; Huisingh, D., (2023). Water scarcity in agriculture: An overview of causes, impacts and approaches for reducing the risks. Heliyon. 9: e18507 **(16 pages)**.

Kalogiannidis, S.; Kalfas, D.; Giannarakis, G.; Paschalidou, M., (2023). Integration of water resources management strategies

in land use planning towards environmental conservation. Sustainability. 15(21): 15242 **(15 pages)**.
Kalogiannidis, S.; Papadopoulou, C.-I.; Loizou, E.; Chatzitheodoridis, F., (2023). Risk, Vulnerability, and Resilience in Agriculture and Their Impact on Sustainable Rural Economy Development: A Case Study of Greece. Agriculture. 13(6): 1222 **(12 pages)**.
Karatayev, M.; Kapsalyamova, Z.; Spankulova, L.; Skakova, A.; Movkebayeva, G.; Kongyrbay, A., (2017). Priorities and challenges for a sustainable management of water resources in Kazakhstan. Sustain. Water Qual. Ecol., 9: 45-57 **(13 pages)**.
Krasnoyarova, B.A.; Vinokurov, Y.I.; Antyufeeva, T.V., (2019). International water development problems in the transboundary Irtysh River basin: "new" solutions to old problems. IOP Conference Series: Earth Environ. Sci., 381(1): 012049 **(11 pages)**.
Lakhiar, I.A.; Yan, H.; Zhang, C.; Wang, G.; He, B.; Hao, B.; Han, Y.; Wang, B.; Bao, R.; Syed, T.N.; Chauhdary, J.N.; Rakibuzzaman, M., (2024). A Review of Precision Irrigation Water-Saving Technology under Changing Climate for Enhancing Water Use Efficiency, Crop Yield, and Environmental Footprints. Agriculture. 14: 1141 **(38 pages)**.
Lazurko, A.; Pinter, L., (2022). Infrastructure investments for resilience: Opportunities, barriers, and a future research agenda from the Orange-Senqu River Basin. Clim. Risk Manag. 35: 100393 **(17 pages)**.
Lee, Y.; Han, S., (2025). The geography of structural vulnerability: intersections of climate exposure, ecological insulation, and economic capacity. npj Urban Sustain. 5: 71 **(12 pages)**.
Li, Z.; Fang, G.; Chen, Y.; Duan, W.; Mukanov, Y., (2020). Agricultural water demands in Central Asia under 1.5 °C and 2.0 °C global warming. Agric. Water Manage., 231(2020): 106020 **(12 pages)**.
Liu, Z.; Hong, S.; Wang, J., (2025). A Multidimensional Exploration of the Factors Influencing Comprehensive Grain Production Capacity from a Spatial Perspective. Sustainability. 17(7): 3264 **(14 pages)**.
Luan, C.; Liu, R., (2022). A comparative study of various land use and land cover change models to predict ecosystem service value. Int. J. Environ. Res. Public Health. 19(24): 16484 **(12 pages)**.
Mgala, E.; Nobert, J.; Mabhuye, E.B.; Gwambene, B., (2025). Enhancing access to underutilized ground water potential for improving livelihoods and conflict reduction in Kagera Sub-Basin, Tanzania. Front. Water. 7: 1 page **(15 pages)**.
Mthembu, B.E.; Cele, T.; Mkhize, X., (2025). Climate Change Impacts on Agricultural Infrastructure and Resources: Insights from Communal Land Farming Systems. Land. 14: 1150 **(20 pages)**.
Prniyazova, A.; Turaeva, S.; Turgunov, D.; Jarihani, B., (2025). Sustainable transboundary water governance in Central Asia: Challenges, conflicts, and regional cooperation. Sustainability, 17(11): 4968 **(13 pages)**.
Quddus, A.; Kropp, J.D., (2020). Constraints to agricultural production and marketing in the lagging regions of Bangladesh. Sustainability. 12(10): 3956 **(11 pages)**.
Salikova, N.S.; Rodrigo-Ilarri, J.; Alimova, K.K.; Rodrigo-Clavero, M.-E., (2021). Analysis of the Water Quality of the Ishim River within the Akmola Region (Kazakhstan) using hydrochemical indicators. Water, 13(9): 1243 **(12 pages)**.
Silveira, P.; Dentinho, T.P., (2018). A spatial interaction model with land use and land value. Cities, 78: 60–66 **(7 pages).**
Stolpe, H.; Ngoc Ha, N.; Jolk, C., (2022). Regional water and land use planning: systematic planning support. in water conservation - inevitable strategy, 1: 1-15 **(15 pages)**.
Sultana, R.; Irfanullah, H.M.; Selim, S.A.; Budrudzaman, M., (2023). Vulnerability and ecosystem-based adaptation in the farming communities of drought-prone Northwest Bangladesh. Environ. Chall., 12(2023): 100707 **(12 pages)**.
Surya, B.; Ahmad, D.N.A.; Sakti, H.H.; Sahban, H., (2020). Land use change, spatial interaction, and sustainable development in the metropolitan urban areas, South Sulawesi Province, Indonesia. Land, 9(3): 95 **(11 pages)**.
Toth, A., (2025). Enhancing food resilience in the age of geoeconomics by applying biomimetic principles in urban agriculture. Soc. Sci. Humanit. Open. 12: 101718 **(12 pages)**.
Xi, H.; Yuan, Y.; Dong, H.; Zhang, X., (2024). Quantifying the effect of land use and land cover changes on spatial-temporal dynamics of water in Hanjiang River Basin. Remote Sens., 16(22): 4136 **(12 pages)**.
Yu, X.; Xiao, J.; Huang, K.; Li, Y.; Lin, Y.; Qi, G.; Liu, T.; Ren, P., (2023). Simulation of land use based on multiple models in the Western Sichuan Plateau. Remote Sens., 15(14): 3629 **(13 pages)**.
Zhang, C.; Wang, P.; Xiong, P.; Li, C.; Quan, B., (2021). Spatial pattern simulation of land use based on FLUS model under ecological protection: A Case Study of Hengyang City. Sustainability. 13(18): 10458 **(14 pages)**.

AUTHOR (S) BIOSKETCHES

Zhaken, A., Ph.D. Candidate, Department of Environmental Engineering and Management, Faculty of Natural Sciences, L.N. Gumilyov Eurasian National University, Satpayev Street 2, 010000, Astana, Kazakhstan.
- Email: *zhaken.asel@yahoo.com*
- ORCID: 0009-0004-4498-0255
- Web of Science ResearcherID: NA
- Scopus Author ID: 58797826300
- Homepage: https://ersa.eventsair.com/QuickEventWebsitePortal/ersa2024/ersa24/Agenda/AgendaItemDetail?id=93319c13-d54d-445f-9c89-ebac1541cbd3

Dentinho, T.P., Ph.D., Professor, Faculty of Agricultural and Environmental Sciences, University of Azores, MQ58+98 Angra do Heroísmo, Portugal.
- Email: *tomas.lc.dentinho@uac.pt*
- ORCID: 0000-0002-7409-2345
- Web of Science ResearcherID: NA
- Scopus Author ID: 16027737700
- Homepage: https://sites.google.com/view/tomaz-dentinho/biography

AUTHOR (S) BIOSKETCHES

Saspugayeva, G., Ph.D., Associate Professor, Department of Environmental Engineering and Management, Faculty of Natural Sciences, L.N. Gumilyov Eurasian National University, Satpayev Street 2, 010000, Astana, Kazakhstan.
- Email: *saspugayeva_gye@enu.kz*
- ORCID: 0000-0003-3223-3602
- Web of Science ResearcherID: IDIQT-9363-2023
- Scopus Author ID: 56982937000
- Homepage: https://fns.enu.kz/en/page/departments/department-of-environmental-management-and-engineering/professorial-and-teaching-staff

Kamet, M., Ph.D. Candidate, Research Assistant, School of Sciences and Humanities, Nazarbayev University, Kabanbay Batyr Avenue 53, 010000, Astana, Republic of Kazakhstan.
- Email: *madina.kamet@nu.edu.kz*
- ORCID: 0009-0007-6970-8786
- Web of Science ResearcherID: NA
- Scopus Author ID: NA
- Homepage: https://research.nu.edu.kz/en/projects/algebraic-and-elementary-properties-of-rogers-semilattices-and-re/publications/

Shapatova, G., Ph.D., Assistant Professor, Department of Morphology, NCJSC Karaganda Medical University, Gogol Street 40, 100000, Karaganda, Kazakhstan.
- Email: *shapatova@qmu.kz*
- ORCID: 0000-0002-8116-0828
- Web of Science ResearcherID: OSH-5303-2025
- Scopus Author ID: 57815671800
- Homepage: https://qmu.edu.kz/en/employees/other-teachers/shapatova-gulmira-bukeikhanov/

Kassymkhanov, S., Candidate of Technical Sciences, Senior Teacher, School of Architecture, Civil Engineering and Energy, NJSC D. Serikbayev East Kazakhstan Technical University, D. Serikbayev Street 19, 071000, Ust-Kamenogorsk, Kazakhstan.
- Email: *skasimhanov@edu.ektu.kz*
- ORCID: 0000-0001-7898-7149
- Web of Science ResearcherID: NA
- Scopus Author ID: 59934710800
- Homepage: https://www.ektu.kz/employeeprofile.aspx?lang=enandEmployeeId=1391

Zhumagalieva, Z., Ph.D., senior lecturer, Kazakhstan University of innovation and telecommunications systems, the city of Uralsk, Kazakhstan.
- Email: *zhumagalieva1976@mail.ru*
- ORCID: 0009-0004-6843-0282
- Web of Science ResearcherID: NA
- Scopus Author ID: 59188653300
- Homepage: https://www.kaznpu.kz/en/2571/personal/

Tsiganov, A.P., Candidate of Biological Sciences, Associate Professor, Department of Ecology and Geography, Sarsen Amanzholov East Kazakhstan University, Vinogradova Street 8-21, 470010, Ust-Kamenogorsk, Kazakhstan.
- Email: *Tsap_ecobio@list.ru*
- ORCID: 0009-0002-2137-0812
- Web of Science ResearcherID: NA
- Scopus Author ID: 57219453721
- Homepage: https://vku.edu.kz/east-kazakhstan-university-started-a-comprehensive-study-of-the-greater-altai-region-within-the-framework-of-international-cooperation/

Sedelev, V., Senior lecturer of the Department of Ecology and Geography, S. Amanzholov East Kazakhstan University 470010, Ust – Kamenogorsk, st., Vinogradova 8-21
- Email: *Valeriysedelev@mail.ru*
- ORCID: 0009-0001-9663-5726
- Web of Science ResearcherID: NA
- Scopus Author ID: 57219455036
- Homepage: https://www.ektu.kz/employeeprofile.aspx?lang=enandEmployeeId=1483

HOW TO CITE THIS ARTICLE

Zhaken, A.; Dentinho, D.; Saspugayeva, G.; Kamet, M.; Shapatova, G.; Kassymkhano, S.; Tolubayeva, K.; Tsiganov, A.; Sedelev, V., (2026). Water resource management under spatial inequality and land use dynamics. Global J. Environ. Sci., 12(1): 351-370.

DOI: 10.22034/gjesm.2026.01.20

URL: https://www.gjesm.net/article_731681.html

Global J. Environ. Sci. Manage. 12(1): 371-392, Winter 2026, Serial #45

Global Journal of Environmental Science and Management
(GJESM)

Homepage: https://www.gjesm.net/

Podcasts

CASE STUDY

Eco-friendly farming management and molecular surveillance of the pepper yellow leaf curl virus in purple-stem chili

R. Tarigan [1], M. Sinuraya[2], B.K. Udiarto[1*], D.S. Hanafiah[2], K.D. Sutanto[1], W. Setiawati[1], Ifa Manzila[1], A. Sebayang[1], D.W., Utami[1], R. Murtiningsih[1], A.E. Marpaung[1], I.S. Marpaung[1], S. Simatupang[1], Atman[1], Riska[1]

[1] *Research Center for Horticulture, National Research and Innovation Agency, Jl., Cibinong, 16911 Indonesia*

[2] *Department of Agrotechnology, Faculty of Agriculture, Universitas Sumatera Utara, Medan, 20155 Indonesia*

ARTICLE INFO

Article History:
Received 17 August 2025
Revised 22 November 2025
Accepted 24 December 2025

Keywords:
Environmental-safe management
Capsicum annuum
Molecular detection
Pepper yellow leaf curl virus (PepYLCV)
Residue composting

ABSTRACT

BACKGROUND AND OBJECTIVES: Begomoviruses transmitted by whiteflies threaten chili production and create environmental-management dilemmas because control often increases pesticide reliance and encourages residue burning that degrades air quality and soil organic carbon. The study objectives were to align disease control with environmental safety by integrating molecular identification of the causal begomovirus with field documentation of production practices that influence ecological risk and biosecurity in purple-stem chili production in Karo, North Sumatra.

METHODS: Field documentation recorded production choices that affect environmental outcomes, including seed sourcing, residue handling, crop rotation, nutrient regimes and pesticide practice, across 21 production units. Sixty symptomatic fruits were processed into twenty seed lots; seedlings raised under insect-proof conditions were screened by polymerase chain reaction using degenerate begomovirus primers. Positive amplicons were Sanger-sequenced and evaluated by sequence comparison and phylogenetic placement against global begomovirus datasets.

FINDINGS: Molecular screening produced a single fragment of approximately 916 base pairs; sequence comparison placed the fragment within the Pepper yellow leaf curl virus group with nucleotide identity near 90–92 percent to Indonesian isolates. Field documentation (21 production units) showed predominant use of farmer-saved local seed (66.7 percent), a high rate of post-harvest rotation (76.2 percent), and universal sanitation practices reported by respondents (100 percent). Integrated nutrient management combining mineral fertilizer with compost or manure was the largest single fertilizer strategy (about 28 percent), while the most common fertilization frequency was approximately three applications per season (modal response 35 percent). Previous crop history on sampled plots was often potato or mixed vegetables (33.3 percent).

CONCLUSION: The coexistence of resilience-building practices (rotation, sanitation, organic amendment) with biosecurity gaps (widespread informal seed use without molecular testing) identifies priority intervention points. Priority initiatives to reconcile crop health with environmental safety include mandatory molecular seed-health screening for seed lots intended for distribution, low-cost whitefly monitoring coupled with threshold-based integrated pest management to reduce prophylactic insecticide use, substitution of residue burning with composting to protect air quality and soil carbon, targeted soil testing prior to liming, and full genome sequencing with public deposition to strengthen regional surveillance and traceability.

DOI: 10.22034/gjesm.2026.01.21

This is an open access article under the CC BY license (http://creativecommons.org/licenses/by/4.0/).

NUMBER OF REFERENCES
47

NUMBER OF FIGURES
11

NUMBER OF TABLES
3

*Corresponding Author:
Email: *bagu017@brin.go.id*
Phone: +628122335009
ORCID: 0000-0003-1799-653X

Note: Discussion period for this manuscript open until Mar 1, 2026 on GJESM website at the "Show Article".

INTRODUCTION

Capsicum annuum (chili) is a high-value crop widely grown in Asia, including Indonesia's Karo region, where intensification efforts aim to double smallholder yields. Chili is a high-value crop grown in tropical/subtropical regions, widely used as a spice and source of pharmaceuticals; it contains vitamins (A, B1, B2, C), beta-carotene, capsaicin and minerals, and Indonesian national demand is rising with population growth, stable yearly production requires proper cultivation (Olatunji and Afolayan, 2018; Díaz-Sánchez *et al.,* 2021; Siaga *et al.,* 2024). Karo Regency is a major chili production center in North Sumatra producing a distinctive purple-stem chili with beneficial genetic traits, which increases farmer income; the purple color is linked to anthocyanins that provide health benefits and protect against abiotic/biotic stresses (Tarigan *et al.,* 2023; Lim *et al.,* 2022; Aza-González *et al.,* 2012; Bendokas *et al.,* 2020). However, many conventional practices such as open burning of field residues, heavy pesticide use, routine deep tillage, and unsanitary plant handling–can degrade the agroecosystem. Burning residues, a time-saving tactic to clear fields, emits large quantities of greenhouse gases and pollutants such as carbon monoxide (CO), carbon dioxide (CO_2), Methane (CH_4), nitrogen oxide (N_2O), particulate matter (PM), and has been linked to 37 percent (%) of global black carbon emissions. For example, Deshpande *et al*. (2023) estimated that India's annual CO_2-equivalent emissions from crop residue burning rose 75%, from 19.3 to 33.8 million tons, between 2011–2020. Moreover, burning straw strips critical nutrients: one study found paddy straw fire can eliminate 100% of soil nitrogen, 25% of phosphorus, and up to 60% of sulfur (Dobermann and Fairhurst, 2002). These practices also reduce soil biodiversity and organic carbon: after 15 years of conventional tillage versus no-till in the United States (U.S.), no-till plots retained ~25% more soil organic carbon. Collectively, such inputs-intensive methods erode ecosystem services and long-term productivity (Parambil-Peedika *et al*., 2025). Pesticide overuse similarly harms non-target species and can leave residues on fruit (Supartha *et al*., 2020), while blanket fertilization often causes nutrient leaching and nitrous oxide emissions. In Indonesia, for instance, Karo chili productivity stagnated with 8.3 tons per hectare (t/ha) when farmers relied on habitual techniques without organic amendments. These observations echo Mariyono (2017), who noted that unchecked intensification can risk environmental harm even as farmers seek higher yields. In contrast, agroecological practices–such as crop sanitation, residue recycling, and integrated nutrient management–offer quantifiable environmental benefits. Composting and manuring recycling organic waste into soil amendment, increasing soil fertility and carbon sequestration while cutting synthetic inputs. For example, applying vermicompost before planting consistently boosts yields: Zhang *et al*. (2024) reported a 15.5% chili yield increase with pre-plant vermicompost. Similarly, Kamrunnahar *et al*. (2024) found that a 50:50 blend of biochar and nitrogen, phosphorus and potassium (NPK) fertilizer not only maximized chili growth and fruit weight but also raised soil organic matter and phosphorus availability. Broad reviews confirm that combining organic amendments (vermicompost, biochar, rock phosphate, etc.) with reduced mineral NPK typically raises yields by 12–140% over fertilizers alone, while enhancing nutrient use efficiency and soil health (Zhang *et al*., 2024). Compost use likewise cuts waste and greenhouse gases: it transforms waste into nutrient-rich soil inputs, reduces landfill methane, and improves soil structure and biology (Manea *et al*., 2024). By contrast, intensive plowing and complete residue removal have been shown to decrease soil carbon stocks by several magnesium carbon per hectare (Mg C/ha) over a decade (Amorim *et al*., 2024). In practice, these findings underscore the value of site-specific fertilization and organic recycling; Tobing *et al*. (2021) in Karo advocated healthy seed selection, tailored fertilization, and even insect-proof "Bemisia border" netting to boost productivity from 8.3 to >16.5 t/ha. Such integrated field practices thus align smallholder chili farming with both yield and environmental goals. A critical threat in chili fields is viral diseases spread by whitefly vectors. Pepper yellow leaf curl disease (PepYLCD), caused by begomoviruses, and is among the most destructive diseases of pepper worldwide. It was first recorded in Java in 1999 and has since rapidly spread across Indonesia, causing vein yellowing, leaf curling, and in severe cases complete crop loss. Transmission depends entirely on the polyphagous whitefly *Bemisia tabaci*, which acquires and inoculates the virus as it feeds. In tropical Asia this means that any uncaptured whitefly population can establish new

infections, and multiple begomovirus species often co-circulate. The severity of begomoviral outbreaks, often mixed infections of Pepper yellow leaf curl virus (PepYLCV) and related viruses has been exacerbated by dense plantings and poor field sanitation (keeping infected plants or weeds near fields), which facilitate vector breeding and viral reservoirs. Begomovirus is a major cause of global yield declines, sometimes reaching total loss; begomoviruses are transmitted by insect vectors and must cross the whitefly gut to reach hemolymph for effective transmission (Chowdhury *et al.,* 2023; Selangga and Listihani, 2021; Udiarto *et al.,* 2023; Gorovits *et al.,* 2022; Wang *et al.,* 2023; Pan *et al.,* 2018). Pohan *et al*. (2023) found that chili plants carrying a natural resistance allele (pepy-1) had delayed symptom onset and maintained twice the fruit yield under natural infection, illustrating the loss in productivity that PepYLCV normally causes. In practice, farmers in Karo have observed stunting and yield declines on yellow-virus-infested fields (Tobing *et al*., 2021). These challenges highlight the need for biosecure, sustainable management of chili production. Field practices that discourage virus spread, such as removing crop residues and volunteer plants, installing insect-proof barriers (e.g. Bemisia screens), and using certified virus-free seedlings—are crucial to reduce disease pressure. Concurrently, integrating nutrient and pest management (using compost, balanced fertilization, and biological controls) can improve plant vigor and ecosystem resilience, lowering pest outbreaks. The *B. tabaci* species complex consists of cryptic lineages that differ in virus transmission and insecticide resistance, influencing outbreak severity and management outcomes. Molecular identification of local *B. tabaci* populations by mtCOI barcoding, together with resistance monitoring, is recommended to guide environmentally sustainable virus-management strategies. Moreover, molecular diagnostics are essential for early detection of PepYLCV and related begomoviruses before symptoms appear. Polymerase chain reaction (PCR) based assays can confirm viral infection in asymptomatic seedlings or monitor whitefly vectors, enabling rapid quarantine or roguing of infected plants. In short, a combination of eco-friendly agronomic practices and modern detection tools is needed to sustainably secure chili yields. Agroecological and environmental challenges in chili production, including intensive pesticide use, variable seed quality, and whitefly-mediated virus spread, directly influence the risk and management of Pepper yellow leaf curl virus (PepYLCV). This study therefore focuses on molecular surveillance of PepYLCV together with documentation of farm practices in Karo to provide evidence that links disease occurrence with management conditions and supports environmentally sustainable control strategies. In this context, the study aims to develop an environmentally safe chili production package for Karo, Indonesia by combining field-based management (sanitation, composting, integrated nutrient/pest practices) with molecular detection of Pepper yellow leaf curl virus. The study assesses how these integrated strategies impact yield, pest/disease incidence, and environmental indicators, thereby providing a blueprint for sustainable, biosecure chili cultivation. The study was conducted during 2020 to 2021.

MATERIALS AND METHODS

Study area and context

The study laboratory work was performed at the Biochemistry Laboratory, Indonesian Center for Agricultural Biotechnology and Genetic Resources Research and Development (ICABIOGRAD), Bogor, West Java. Greenhouse grow-out and controlled seedling observations were carried out at the Berastagi Agricultural Technology Research and Assessment Installation, North Sumatra with 3.201891 north (°N), 98.5402177 east (°E); 1,340 meters above sea level (masl). Field collections originated from three high-incidence chili production centres in Sampun Village, Dolat Rayat District location details and map shown in Fig. 1.

Field sampling and documentation of production practices

Field visits recorded production practices and plot history using a structured form. Recorded variables included variety type (local, hybrid, other), previous crop on the plot, rotation practice after chili harvest, years of chili cultivation, fertilizer types/combinations, number of fertilizer applications per season, education level of the grower, and routine land sanitation/soil processing practices. Data was collected from 21 production units (convenience sample associated with molecular sampling locations). Farmer-practice data were analyzed descriptively because the sample

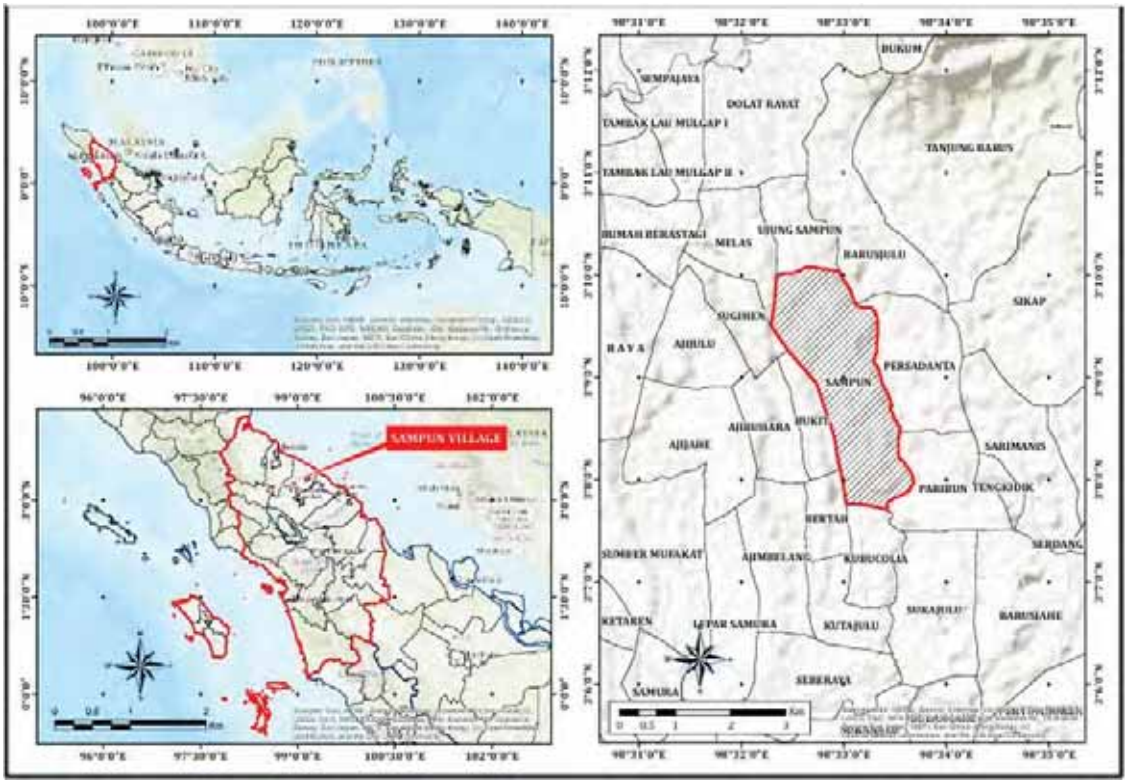

Fig. 1: Geographical location of the study area in the Center for Agricultural Biotechnology and Genetic Resources Research and Development, Bogor, West Java, Indonesia

was small (n = 21) and selected by convenience to link molecular sampling locations with site-specific practices. Descriptive analysis is appropriate for documenting local practices and generating hypotheses, but representative sampling and formal statistical tests are required to estimate population-level prevalence. Responses were anonymized and entered a spreadsheet for descriptive analysis. For molecular work, symptomatic plants in each location were identified by classic begomovirus symptoms (leaf curling, vein yellowing, stunting, reduced fruit size). From each location, 20 symptomatic fruits were collected from multiple symptomatic plants (n = 60 fruits total). Fruits were recorded with unique sample identifiers and metadata such as date, Global Positioning System (GPS), farmer identification code (ID), symptom notes). Fruits were transported to the Berastagi insect-proof greenhouse for seed extraction and grow-out. Symptomatic plants were identified by the presence of one or more of the following visual signs: leaf curling, interveinal chlorosis/vein yellowing, stunting and reduced fruit set/fruit size. Incidence at each sampling plot was estimated by visual sweep counts across a representative 10 × 10 m area and expressed as the proportion of symptomatic plants; where exact counts were not recorded, observations are reported qualitatively as presence/absence of symptoms. Sampling was convenience-based and deliberately linked to molecular sampling locations to integrate molecular detection with site-specific farming practices. This design is appropriate for exploratory, contextual analyses and hypothesis generation but does not support estimation of regional prevalence; representative surveys are recommended for that purpose.

Seed processing and insect-free grow-out (seed-health grow-out protocol)

Each fruit was processed into seed lots following a standardized protocol to minimise external contamination and permit assessment of seed-associated infection:

1. Fruit surface was cleaned with sterile water and air dried.
2. Seeds were surface sterilized using a fixed protocol consisting of immersion in 70% ethanol for 30 seconds, followed by 1.5% sodium hypochlorite for 2 minutes, and three rinses in sterile distilled water.
3. Seeds from fruits were pooled into 20 seed lots (selected to represent the 60 collected fruits) following the sampling plan.
4. Seeds were sown in sterilized potting mix inside an insect-proof greenhouse. Greenhouse environment was monitored to ensure absence of whitefly vectors (yellow sticky traps installed as a precaution). Seedlings were maintained under standard horticultural conditions and observed for symptom development.

One month after germination, three fully expanded leaves were sampled from each seedling for molecular testing (three leaves per plant pooled as a single extraction unit). All seedling handling used gloves and sterilized tools; surfaces and tools were decontaminated between samples to avoid cross-contamination. Detection of PepYLCV, DNA in seedlings grown under insect-proof conditions indicates a possible seed-associated origin but does not constitute definitive proof of vertical seed transmission. Despite sterilization, residual surface or handling contamination cannot be excluded. Definitive demonstration of seed transmission requires embryo-level assays (internal tissue testing) or controlled transmission experiments. In the interim, targeted molecular seed-health screening combined with stringent vector exclusion is recommended as a precautionary biosecurity measure.

Deoxyribonucleic acid (DNA) extraction

Total genomic DNA was extracted from pooled leaf tissue per seedling using a cetyltrimethylammonium bromide (CTAB) protocol with modifications adapted for small tissue samples: extraction buffer included 2% CTAB, 100 millimolar (mM) Tris-Hydrochloride (Tris-HCl) potential of hydrogen (pH) 8.0, 20 mM ethylenediaminetetraacetic acid (EDTA), 1.4 molar (M) sodium chloride (NaCl), 0.1% ß-mercaptoethanol (added fresh), and polyvinylpyrrolidone (PVP) to bind phenolics. PVP was included in the DNA extraction buffer for all samples to minimize interference from phenolic compounds and to ensure consistent DNA quality. Leaf tissue was ground by mortar and pestle (or bead-mill) without liquid nitrogen, incubated at 65 degrees Celsius (°C) for 30–60 min, then subjected to chloroform:isoamyl alcohol (24:1) extraction. Nucleic acids were precipitated (isopropanol), washed (70% ethanol), air dried and resuspended in tris–ethylenediaminetetraacetic acid (TE) buffer. DNA concentration and purity were assessed by spectrophotometry (A260/280) and agarose gel electrophoresis; extracts were stored at −20°C until PCR.

PCR screening for begomoviruses (SPG1/SPG2 primers)

Presence of begomovirus DNA was screened by conventional polymerase chain reaction using degenerate begomovirus primers SPG1 and SPG2 (Li *et al*., 2004). Primer sequences:

- SPG1: 5'-CCCCKGTGCGWRAATCCAT-3'
- SPG2: 5'-ATCCVAAYWTYCAGGGAGCT-3'

These primers target conserved regions overlapping Transcriptional Activator Protein (TrAP) and Replication-associated Protein (Rep) genes and yield an amplicon of ~900–920 base pairs (bp) when begomovirus DNA is present (Li *et al*., 2004). PCR reactions were prepared in 25 µL total volume containing 1× PCR buffer, 2.0–2.5 mM magnesium chloride ($MgCl_2$) (PCR amplification was performed using a final $MgCl_2$ concentration of 2.5 mM in all reactions), 0.2 mM deoxynucleotide triphosphates (dNTPs), 0.4 micromolar (µM) of each primer, 1 unit (U) of Taq DNA polymerase (hot-start or standard as available), and ~50–100 nanograms (ng) template DNA. If a commercial master mix was used, reactions followed the manufacturer's recommended reagent proportions. Thermal cycling was performed on a Bio-Rad T100 Thermal Cycler using the following profile: initial denaturation at 94°C for 5 min; 35 cycles of denaturation at 94°C for 1 min, annealing at 55°C for 1 min, extension at 72°C for 1 min; final extension at 72°C for 7 min; hold at 4°C. Negative controls (no template) and a healthy plant DNA control were included in each PCR run. Where available, a positive control (DNA from a previously confirmed begomovirus isolate) was included to validate amplification performance.

Electrophoresis and visualization

PCR products were separated on 1% agarose gels

prepared in 1× Tris-acetate-EDTA buffer (TAE) buffer and run at 80–100 V for 30–45 min alongside an appropriate molecular weight ladder. Gels were stained with an intercalating dye (e.g., ethidium bromide replacement or GelRed) and visualized and photographed using a gel documentation system (ChemiDoc EQ, Bio-Rad). Expected amplicons ~900–920 bp were excised from gels and purified with a gel-purification kit prior to sequencing.

Sanger sequencing and sequence analysis

Purified amplicons were submitted for bidirectional Sanger sequencing at 1st BASE Laboratories Sdn. Bhd. (Apical Scientific), Malaysia, using standard capillary sequencing protocols. Raw chromatograms were quality-checked and trimmed using BioEdit v7.2.0 (or equivalent), and consensus sequences were generated. Each consensus sequence was queried against the National center for biotechnology information (NCBI) Basic local alignment search tool nucleotide database (BLASTn) to determine closest matches and approximate percent identity. Multiple sequence alignment with reference begomovirus sequences was performed using MUSCLE (MEGA11), and phylogenetic relationships were inferred with maximum-likelihood reconstruction in MEGA11 with 1,000 bootstrap replicates. Pairwise nucleotide identities and tree topology were used to assess whether isolates clustered within known Pepper yellow leaf curl virus clades. Raw chromatograms were inspected and trimmed in BioEdit v7.2.0. Multiple-sequence alignments were generated with MUSCLE implemented in MEGA11 using default gap opening and extension penalties. Maximum-likelihood phylogenies were inferred in MEGA11 using the Tamura–Nei nucleotide substitution model (model selected by MEGA11) with 1,000 bootstrap replicates; bootstrap support values are shown on the tree. Resulting sequences are intended for GenBank deposition; accession numbers will be added upon submission. Partial genome sequencing was employed as a rapid and cost-effective approach for initial detection and preliminary phylogenetic placement of PepYLCV, using widely applied degenerate begomovirus primers. While suitable for early surveillance, partial sequence data limit strain resolution and recombination detection. Full DNA-A genome sequencing and public database deposition are recommended for future studies to strengthen molecular surveillance of PepYLCV in Indonesia.

Quality assurance and contamination prevention

All molecular work included routine contamination control: physically separated pre- and post-PCR workspaces, use of filter tips and single-use consumables, periodic decontamination of benches and pipettes with 10% bleach and 70% ethanol, and inclusion of negative controls at extraction and PCR stages. the extraction negative controls and PCR no-template controls were included for quality assurance. An endogenous plant internal amplification control (for example 18S or rbcL) and validated qPCR assays are recommended for routine seed-health screening to reduce false negatives and improve sensitivity under low-virus-load conditions. Replicate extractions and re-testing of positive amplicons were performed to confirm results.

Farmer practice data analysis

Responses from the 21 production units were entered into a spreadsheet and verified. Descriptive statistics (counts, percentages) were calculated to summarize variety choice, rotation practice, sanitation, fertilizer types and application frequency, education level, and previous crop history. Graphs and figures (pie charts, bar plots) were produced to represent distributions of categorical variables. Where appropriate, comparisons across farmer subgroups (e.g., experience level, education) were summarized in the Results; formal hypothesis testing was not attempted due to sample size and convenience sampling design.

Integration of molecular and field data

Molecular detection results (presence/absence, sequence identity, phylogenetic placement) were linked to metadata from the corresponding seed lot and production unit (variety, seed source, previous crop, sanitation practice) to explore potential associations between management practices and detection of the begomovirus fragment. Genus-level degenerate primers (e.g., SPG1/SPG2) enable broad begomovirus detection but may have reduced sensitivity for divergent local variants. For routine and environmentally friendly surveillance, a two-tier strategy is recommended, consisting of initial screening with degenerate primers followed by validated species-specific or multiplex qPCR

assays with internal amplification controls once representative local genomes are available.

RESULTS AND DISCUSSION

This study combined field-level documentation of farmer practices (Number (n) = 21 production units) with molecular screening of seedlings raised from symptomatic fruits (60 fruits, 20 seed lots). Results show a mix of resilience-building farm practices (rotation, sanitation, integrated nutrient management) together with biosecurity gaps (widespread farmer-saved seed). Molecular screening recovered a 916 base-pair begomovirus fragment that groups with PepYLCV ~90–92% identity, indicating a PepYLCV-related presence in the local system. These combined findings point to practical interventions that jointly lower virus risk and environmental harm. The widespread use of farmer-saved and informally exchanged seed may contribute to Pepper yellow leaf curl virus dissemination when seed health is not verified. Integration of molecular seed-health screening into local seed systems can improve biosecurity while preserving farmer access to locally preferred varieties.

Variety choice and agro-biodiversity

Two-thirds of respondents (66.7%; 14/21) grow local purple-stem varieties (batang ungu), 23.8% (5/21) cultivate hybrids, and 9.5% (2/21) use other varieties (Fig. 2). Preference for local seed reflects seed-saving practices, market demand for specific taste/aroma, lower seed cost, and perceived local adaptation (Ekowahyuni, 2022). From an environmental perspective, continued use of local varieties helps conserve on-farm genetic diversity and reduces dependence on purchased hybrid seed (which can encourage higher input use). However, Informal seed systems may represent a potential pathway for seed-associated pathogen movement; however, seed transmission of Pepper yellow leaf curl virus was not experimentally confirmed in this study, and this possibility is therefore discussed cautiously—a critical issue given the molecular detection of a PepYLCV-related fragment in seedlings.

Cropping history and rotation practices

One-third of plots (47%) had been planted with potato/mixed vegetables prior to chili; most fields therefore show temporal diversification rather than continuous chili monoculture (Fig. 3). Additionally, 83% reported rotating after chili harvest (Fig. 4). Fig. 4 indicate that most plots had a rotational cropping history, rather than repeated monocropping of the same crop. Crop rotation interrupts pest and pathogen lifecycles, improves nutrient balance and soil structure, and reduces the build-up of host-specific pests, benefits documented in rotation reviews and vegetable production studies (Benincasa *et al*., 2017; Merfield, 2019). Environmental benefit: rotation reduces reliance on curative pesticide applications and helps maintain soil health, lowering long-term environmental costs (e.g., reduced chemical runoff, improved soil carbon retention).

Farmer experience and adoption potential

The sample includes both new entrants and long-

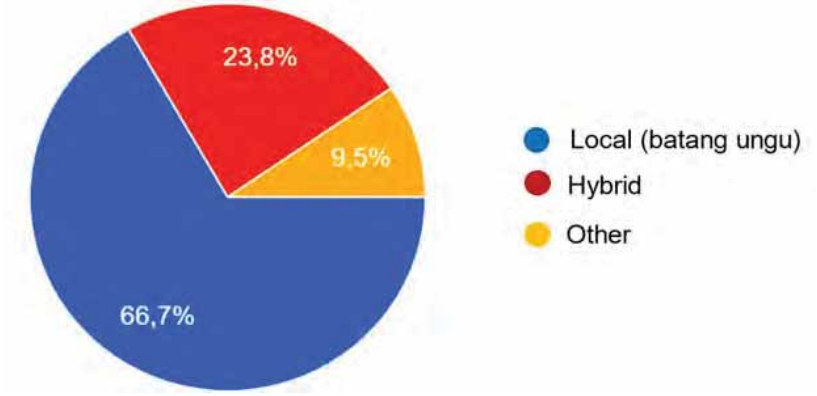

Fig. 2: Distribution of chili (cabai) varieties cultivated by respondents (n = 21), Data (represented): Lokal (local/ batang ungu) = 66.7% (14/21), Hibrida (hybrid) = 23.8% (5/21), Lainnya (others) = 9.5% (2/21)

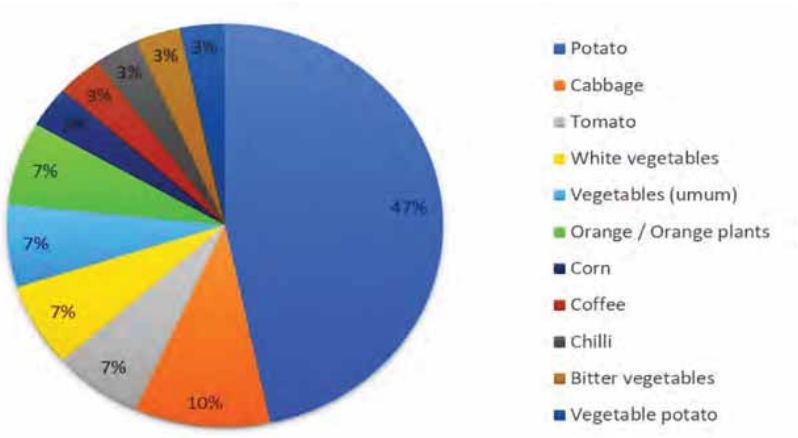

Fig. 3: Previous crops planted on the plot before the current season (n = 21)

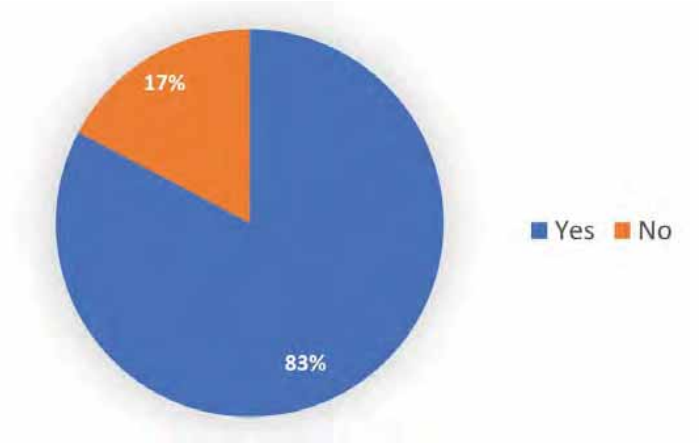

Fig. 4: perform crop rotation after chili harvest on the plot before the current season (n = 21)

term growers (>10 years) as the sample includes recent adopters, intermediate (5–12 years) and long-term cultivators (>10 years), indicating a mixed cohort of experience levels among local chili growers. (Fig. 5), a heterogenous mix that supports stratified extension: veterans can refine input efficiency, while newcomers may adopt innovations quickly (Mariyono, 2017). Peer-learning platforms can accelerate adoption of eco-friendly practices such as composting, INM, and targeted pest monitoring.

Nutrient management and application frequency

Integrated nutrient management (INM) combining mineral NPK with manure/compost/biofertilizers was the most common strategy (28%) (Fig. 6). The modal application frequency was three applications per season (35%) (Fig. 7). These practices align with recommendations that pair immediate nutrient supply (NPK) with long-term soil building (organic amendments), which improves nutrient use efficiency, increases yields, and reduces nutrient losses to the environment (Zhang *et al*., 2024; Shi *et al*., 2024). INM reduces leaching and gaseous nitrogen losses when compared with high-rate mineral fertilizer alone; regular compost inputs rebuild soil organic carbon lost to tillage (Das, 2023). Recommendation: formalize locally adapted INM guidelines (balanced N rates, quality compost standards, split timing), and couple them with demonstration trials that quantify yield and environmental co-benefits. Integrated

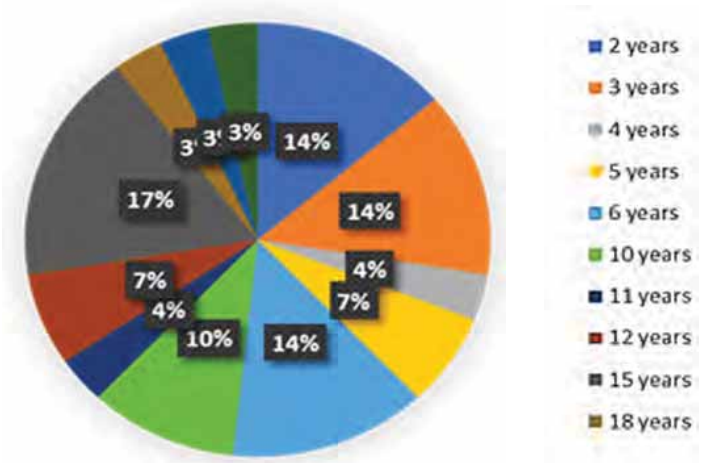

Fig. 5: Distribution of respondents by years since starting chili cultivation (n = 21)

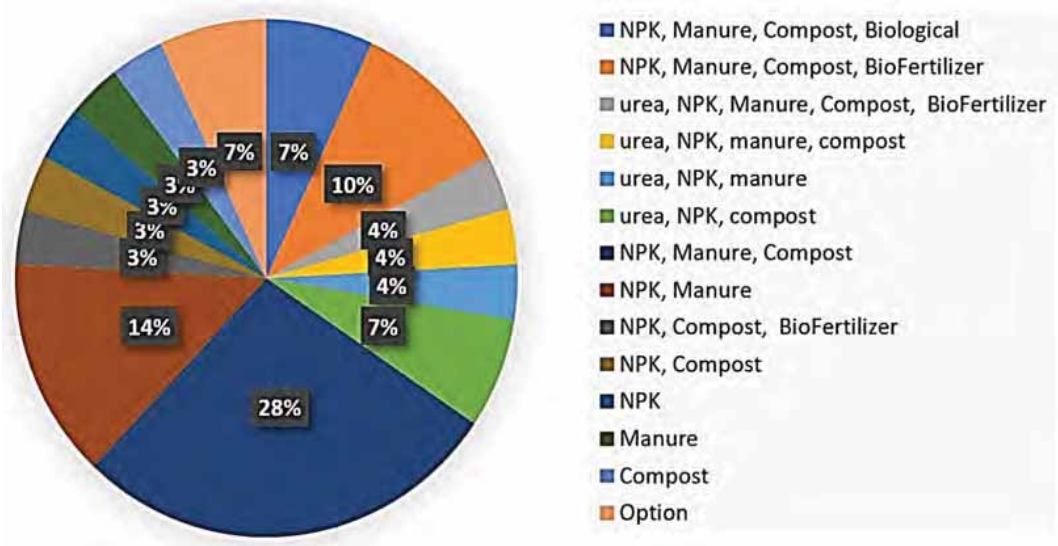

Fig. 6. Types of fertilizers commonly used
The chart shows a plurality of farmers use combined nutrient sources, mixing chemical NPK with organic amendments (manure and compost) and, in some cases, biofertilizers.

nutrient management can be optimized through site-specific soil testing, split NPK application aligned with crop demand, and the use of compost or manure. This approach improves nutrient use efficiency, increases soil organic carbon, and reduces nutrient losses and off-site pollution.

Sanitation, residue handling and air quality

In this study reported that sanitation (removal of residues and diseased plants). Sanitation effectively reduces inoculum for many pests and diseases (Bingham, 2023). However, environmental outcomes depend on residue disposal: burning eliminates residues quickly but causes air pollution and loss of soil carbon; composting retains nutrients and improves soil biology (Parambil-Peedika, 2025). Replace residue burning with on-farm composting, off-farm removal for industrial use, or incorporation

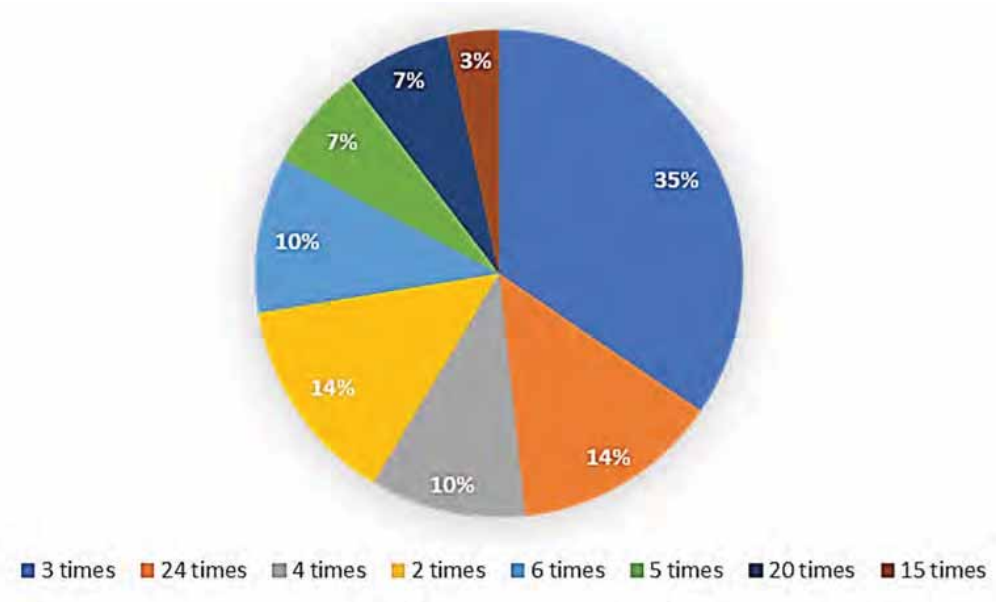

Fig. 7: Reported number of fertilizer applications per cropping season

into soil where appropriate, these options retain nutrients, mitigate particulate emissions, and support long-term soil carbon accrual.

Tillage, organic inputs and soil health

Most farmers perform soil processing (plowing), often combined with manure/compost. While plowing improves seedbed conditions and mixes amendments, repeated deep tillage reduces soil organic carbon and increases erosion risk over time (Seitz *et al*., 2019). The community's frequent use of manure/compost can offset some SOC loss, but conservation tillage or reduced tillage combined with regular organic amendments would better preserve SOC while maintaining crop establishment benefits.

Chemical control, fungicides and non-target effects

Some farmers apply soil fungicides and foliar pesticides. While these can protect seedlings and reduce acute disease losses, fungicides and broad-spectrum insecticides can transiently suppress beneficial soil microbes and harm natural enemies (Wang, 2025). Given the high sanitation and rotation rates, priority should be to minimize prophylactic chemical use and replace it with targeted, threshold-based interventions (integrated pest management). The farmer-practice data provide important context for interpreting the molecular results. Patterns of pesticide use, seed sourcing, and nursery management observed at sampling sites help explain the occurrence and distribution of pepper yellow leaf curl virus detected by molecular analysis, linking field-level management conditions with virus presence.

Detection of Geminivirus in infected plants

The incidence of disease caused by PepYLCV in the field varied, reaching between 80% and 100% (Fig. 8). The plants exhibited vein clearing, mosaic leaves, minor chlorosis between the veins, and curling, which resulted in stunted growth. Geminivirus-infected plants displayed leaf yellowing; in severe cases, this yellowing could spread to all leaves on a single plant, distinguishing them from healthy plants. In general, symptomatic plants are unable to produce fruit (Selangga *et al*., 2023). However, the fruits formed are typically smaller and atypical in size. These visual symptoms are often mistaken for those caused by abiotic stressors, such as iron deficiency. Furthermore, virus replication in plants can lead to increased anaplerosis activity, enhanced photosynthesis rates, and greater starch content. The photosynthesis rate decreases with reduced viral replication, while glycolysis and respiration in mitochondria increase. These changes manifest as

chlorosis in the leaves, affecting the leaf area index. When the leaf area index and chlorophyll content are low, the amount of photosynthate produced for plant growth decreases, resulting in stunted plants. Pepper yellow leaf curl virus infection in purple-stem chili is associated with significant yield and quality losses, including plant stunting, reduced fruit set, and unmarketable fruits. Adoption of eco-friendly management practices—such as virus-free seed use, vector exclusion in nurseries, integrated nutrient management, and IPM—offers a sustainable approach to reduce these losses while minimizing environmental impacts.

Table 1 compares the present study with selected regional reports. All studies confirm presence and diversity of pepper-infecting begomoviruses in Indonesia and neighboring countries; differences among studies reflect variation in sampling (seed vs. field), genome coverage (partial vs full), and detection methods (degenerate primers, PCR, RCA/full genomes). Full-genome sequencing and standardized metadata are recommended to enable robust regional comparisons and to guide seed-health and IPM policy.



Fig. 8: Begomovirus-infected local chili in Sampun village-Dolat Rayat district-Karo Regency

Table 1: Comparison of the present study with selected studies on Pepper yellow leaf curl virus (PepYLCV)

Location	Sample type	Detection / method	Main molecular result	Management / notes	Sources
Bali, Indonesia	Symptomatic pepper	Complete genome sequencing (DNA-A/B)	Genome published; ~90% identity to some Indonesian isolates; defined PepYLCV genotype.	Demonstrates value of full-genome data for strain resolution and surveillance.	Neriya *et al.*, 2020
Multiple Indonesian provinces	Seed and plant samples	PCR / sequencing (UDG-PCR reported)	Reports of PepYLCV in seeds/seedlings; yields losses reported (20–100% in severe outbreaks).	Indicates potential seed association; supports need for seed-health screening.	Chairina *et al.*, 2020
Malaysia	Field pepper	PCR & Sanger sequencing	First country report; documents regional spread of related begomoviruses.	Regional presence beyond Indonesia; argues for cross-border surveillance and deposition of sequences.	Sau *et al.*, 2020
Indonesia (review)	Multiple regional studies	Mixed methods (PCR, sequencing, phylogeny)	Identifies several begomovirus species affecting pepper (PepYLCV, ToLCNDV, TYLCKaV) and emergence across islands.	Highlights diversity and need for standardized diagnostics and integrated management.	Wahyono *et al.*, 2023

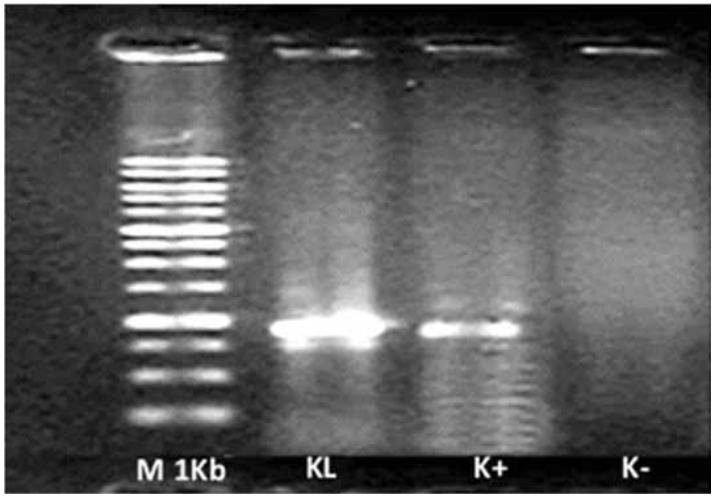

Fig. 9: Electrophoresis analysis of DNA from pepper-infecting begomovirus (M = marker; KL = control positive (infected plants obtained from the laboratory), K+ = Pep-YLCV-infected plants obtained from the field, K- = uninfected plants)

Molecular identification of infected local chili in Karo Regency, North Sumatra

Universal DNA amplification on 60 symptomatic leaves tested indicated the presence of begomovirus (Fig. 9). The isolated DNA obtained from PepYLCV-infected plants was identified using universal primers SPG1 (5 ' CCC CKG TGC GWR AAT CCA T3' and SPG2 (5' ATC CVA AYW TYC AGG GAG). This result is confirmed by the presence of fragments 916 bp, the presence of DNA ribbon on the control positive, and the absence of this DNA ribbon at the negative control plants (healthy plants). This proves that the PCR technique can detect geminivirus. Large *B. tabaci* (whitefly) populations correlate with emergence and spread of new begomovirus species via rapid changes and mutations; symptoms vary and can mimic nutrient deficiencies, making visual diagnosis unreliable, while rapid virus spread and genetic diversity complicate identification so PCR with universal primers is commonly used for detection (Udiarto *et al.,* 2023; Pan *et al.,* 2020; Soares *et al.,* 2018; Yan *et al.,* 2021; Kumar *et al.,* 2021). The result was analyzed in the form of electropherograms using MEGA X software to analyze the DNA and NCBI BLAST for virus identification. This technique is considered an important part of developing a disease control strategy since it could accelerate the detection of Pep-YLCV (Malichan *et al*., 2019) and distinguish the infected and uninfected plants. Adnyani *et al*. (2018) used primer pair SPG1/SPG2 to detect begomovirus in cucumber plants, the amplification of transcriptional activator protein (TrAp) and replication-associated protein (Rep) with a target size of ±912 bp.

Analysis of PepYLCV sequencing samples and bioinformatics

Based on their fragment sequences, the relationship between isolates of PepYLCV from Sampun Village, Dolatrayat Karo, and other chosen PepYLCV in the Gene Bank was assessed. The sequence analysis revealed that PepYLCV in Sampun Village, Dolatrayat Karo possessed a similar identity to several nucleotide sequences of PepYLCV from other places in Indonesia for instance Pepper yellow leaf curl AC1 gene Indonesia: Bali, Ketewel (LC381280.1), Pepper yellow leaf curl virus A Indonesia: Jawa Tengah (JX416180.1), Pepper yellow leaf curl Indonesia: Bogor (DQ083764.1), Pepper yellow leaf curl virus AC2, AC1 genes Indonesia: Bengkulu (LC547428.1). The analysis of PepYLCV sequencing samples has been compared to sequences on the Gene Bank (Table 2), where they exhibited the highest homology with Pepper yellow leaf curl AC1 gene Indonesia: Bali, Ketewel (>92%), followed by Pepper yellow leaf curl virus A Indonesia: Central Jawa (>90%) and Pepper yellow leaf curl Indonesia: Bogor >89%. Their homology to Tomato leaf curl comoros virus Mayote: Dembeni is higher than 79%, followed by virus isolate

Table 2: BLAST analysis of the sample PepYLCV infected local pepper in Sampun Village, Dolatrayat District, Karo Regency, and the species with a higher identity

Gene bank accession	Description	Max/total score	Query cover	% Identity
LC381280.1	PepYLCV AC1 gene Indonesia: Bali, Ketewel	1157/1157	99%	92.44%
JX416180.1	PepYLCV AC1 Indonesia: Central Java	1046/1046	99%	90.00%
DQ083764.1	PepYLCV Indonesia: Bogor	1040/1040	99%	89.88%
LC547428.1	PepYLCV AC2, AC1 genes Indonesia: Bengkulu	924/924	99%	87.32%
LC387328.1	PepYLCV segment DNA-A Indonesia: Aceh	525/525	99%	85.88%
MK946452	Tobacco leaf curl Yunnan virus isolate MM10TO3	364/364	99%	75.81%
MH745157.1	Ageratum yellow vein virus isolate Indonesia 2 segment DNA-A	357/357	94%	75.45%
AJ865341.1	Tomato leaf curl Comoros virus Mayote: Dembeni	329/329	56%	79.96%
KC171650.1	Ramie mosaic virus isolate Hn segment DNA-A China: Guangdong	309/309	79%	75.80%

Table 3: Homology percentage of PepYLCV nucleotides among its isolates and some other viruses.

*	1	2	3	4	5	6	7	8	9	10
1	ID									
2	0.932	ID								
3	0.907	0.946	ID							
4	0.906	0.947	0.962	ID						
5	0.881	0.911	0.932	0.933	ID					
6	0.771	0.8	0.801	0.798	0.835	ID				
7	0.742	0.775	0.773	0.777	0.782	0.798	ID			
8	0.742	0.778	0.772	0.774	0.78	0.789	0.92	ID		
9	0.732	0.764	0.765	0.767	0.768	0.78	0.828	0.843	ID	
10	0.713	0.742	0.748	0.754	0.759	0.744	0.809	0.825	0.772	ID

*Pepper yellow leaf curl sample A1;1=Indonesia: Dolatrayat-Karo, 2=Pepper yellow leaf curl AC1 gene Indonesia: Bali, Ketewel, 3= Pepper yellow leaf curl virus A Indonesia: Jawa Tengah, 4=Pepper yellow leaf curl Indonesia: Bogor, 5=Pepper yellow leaf curl virus AC2, AC1 genes Indonesia: Bengkulu, 6=Pepper yellow leaf curl virus segment DNA-A Indonesia: Aceh, 7=Tobacco leaf curls Yunnan virus isolate MM10TO3 Korea Selatan: Jeollabuk-do, 8=Ageratum yellow vein virus isolates Indonesia 2 segment DNA-A, 9=Tomato leaf curl Comoros virus Mayote: Dembeni, 10=Ramie mosaic virus isolates Hn segment DNA-A China: Guangdong.

MM10TO3 Korea Selatan: Jeollabuk-do (higher than 75%).

Sequence analysis of viral coat protein (CP) obtained from infected Karo chili peppers

Nucleotide similarity between the CP sequences of the isolates from Sampun Village, Dolatrayat District, Karo Regency, and several species from several places ranged from 0.713 to 0.932, which is Ramie mosaic virus isolate Hn segment DNA-A China: Guangdong and PepYLCV AC1 gene Indonesia: Bali, Ketewel (Table 3). Identity analysis of PepYLCV isolates from local pepper in Sampun Village, Dolat Rayat District, Karo Regency (by comparing to sequencing on the Gene Bank) showed that the samples have high similarity with PepYLCV AC1 gene Indonesia: Bali, Ketewel (93.2%), followed by Pepper yellow leaf curl virus A Indonesia: Jawa Tengah Indonesia (90.7%) and Ramie mosaic virus isolates Hn segment DNA-A China: Guangdong (71.3%). These findings confirmed that PepYLCV from Sampun Village, Dolat Rayat District, has a high homology to various PepYLCV isolates from other areas. Several studies are in line with these results. *Cania et al. (2021)* indicated that similarities were found between Pep-YLCV APWS and two other isolates from West Sumatra, PepYLCV TDWS (91%) and PepYLCV PSSWS (92%). Selangga *et al.* (2023) discovered that there is high nucleotide similarity (99.7%-99.8%) between PYLCIV on bell pepper and PYLCIV on chili pepper in Bali, Indonesia. Sipriyadi *et al*. (2022) identified high homology (higher than 90%) between 6 isolates obtained from 2 regencies, Rejang Lebong and Kepahiang, with isolates collected in Bengkulu and Bali. Phylogenetic analysis showed that the detected virus isolates shared 90–92% nucleotide identity with Indonesian reference isolates, indicating close genetic relatedness and regional circulation of Pepper yellow leaf curl virus. This level of sequence

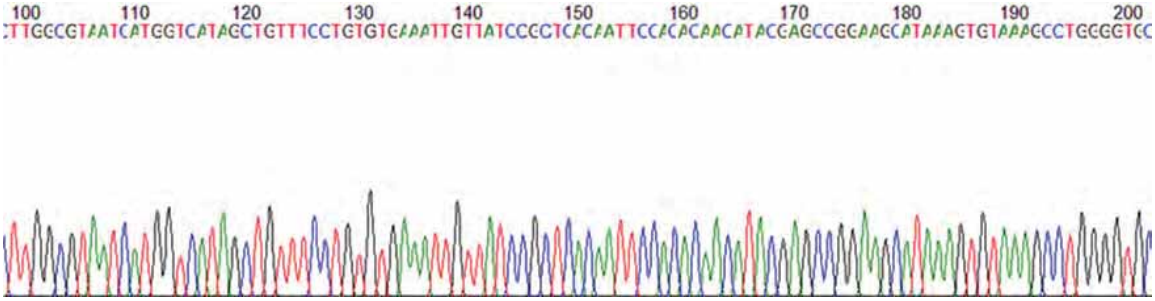

Fig. 10. Tropherogram snapshot of PepYLCV-infected plants in Karo

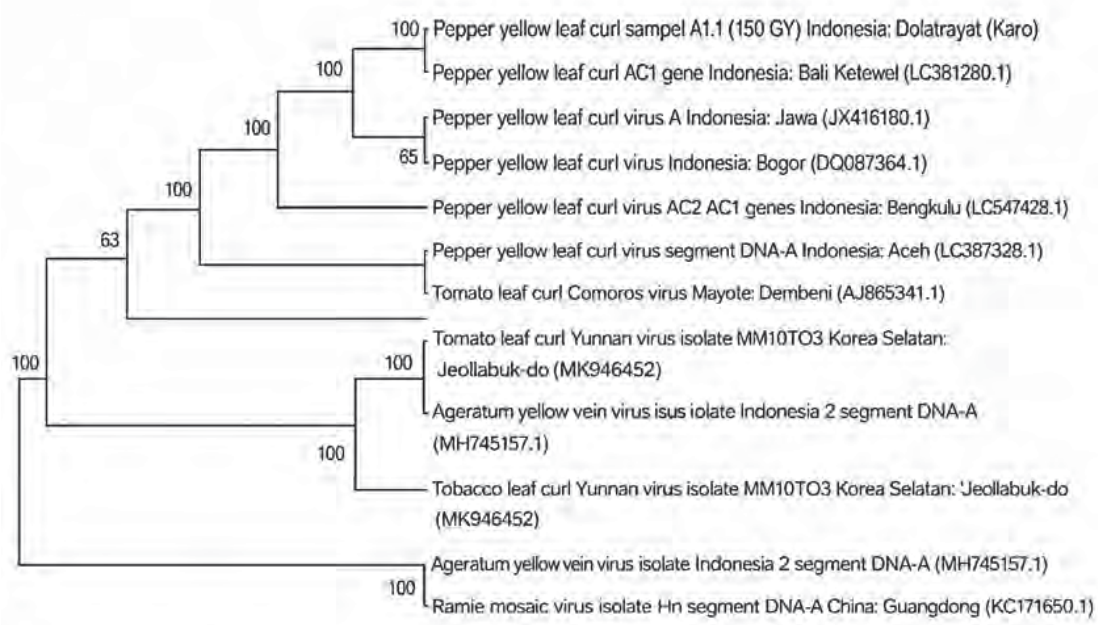

Fig. 11: The phylogenetic tree of PepYLCV (samples A1.1 Indonesia: Dolatrayat-Karo) was developed using MEGA 10 software and the neighbor-joining method (NJ) with a bootstrap test of 1,000 replicates

variation is consistent with natural viral evolution driven by mutation and local adaptation. Although the analysis was based on partial genome sequences and cannot resolve introduction history or specific transmission pathways, the consistent clustering with Indonesian isolates supports the presence of an established regional virus population and highlights the importance of continued molecular surveillance to inform integrated disease management.

Phylogenetic analysis

Phylogenetic analysis provides a genetic relationship between plant samples.

The Indonesian A1.1 sample from Dolat Rayat Karo demonstrated high homology (99%) to PepYLCV from Bali, Java, and Bogor, according to the Neighbor-Joining method of phylogenetic tree construction based on the nucleotide sequence of the PepYLCV gene (Figs. 10 and 11). This study utilized CP sequences retrieved from the Gene Bank database (NCBI). This analysis aims to ascertain the genetic similarities between the sequences of the tested samples and the begomovirus coat protein sequences obtained from NCBI. The phylogenetic tree showed that some isolates belong to different clades even though they are geographically located in the same area. This discrepancy is attributed to nucleotide changes in the PepYLCV isolates. This variation arises due to

the inherent evolutionary nature of viruses, leading to alterations in the nucleotide sequence. According to (Khan *et al.,* 2022), viruses constantly undergo mutations to ensure their survival. The mutation rate of a virus is further influenced by its simple genome structure, consisting solely of DNA or RNA. The analysis compares the isolates collected from Sumatra Island and PepYLCV isolates collected from Java and Bali Islands. Previous research confirmed that these islands demonstrated a high occurrence of PepYLCV on chili peppers (Wahyono *et al.,* 2023). Analysis based on a single partial nucleotide fragment limits the detection of mixed begomovirus infections and recombination events and may underestimate overall viral diversity. Full-genome sequencing is recommended for future studies to enable accurate assessment of mixed infections, recombination, and molecular diversity, thereby strengthening molecular surveillance and virus management. Viral detection in this study was based on conventional PCR and Sanger sequencing, and viral titer was not quantified. Quantitative PCR (qPCR) or digital PCR (dPCR) is recommended for future studies to measure viral loads across seed lots, seedlings, and field-grown plants, thereby improving disease-risk assessment and discrimination between seed transmission and low-level contamination. Detection of Pepper yellow leaf curl virus DNA in seedlings grown under insect-proof conditions suggests a possible seed-associated origin; however, this does not constitute definitive evidence of vertical seed transmission. Given that the virus is predominantly transmitted by whiteflies, early vector-mediated infection cannot be excluded, and confirmation of seed transmission requires embryo-level assays or controlled transmission experiments.

Begomoviruses are single-stranded DNA viruses (Shingote *et al.,* 2022), whose DNA is used as the template for amplification in this PCR technique. Amplification results showed that all samples tested were infected with begomovirus. The survival of *B. tabaci* in the field was influenced by farmers' practices, including the monoculture system in Sampun Village, Dolat Rayat, where they frequently grow plants from the same family (Solanaceae), like tomatoes. The begomoviruses spread to host plants, such as tomatoes, chickpeas, yams, melons, watermelons, and sweet peppers, by the vector *B. tabaci* (Fontenele *et al.,* 2021). The infected samples were analyzed using BLAST. BLAST analysis was performed using partial sequences of the coat protein gene. This gene has a pivotal role in the encapsulation of DNA viruses (Subiastuti *et al.,* 2019). The phylogenetic tree represents the close relationship between the isolated viruses and species. The CP sequences of the begomoviruses that infected members of the Solanaceae family in Indonesia were more like isolates from other regions of the country than to those from China and other Southeast Asian nations. Also, the data exposed that this virus shared high similarity (90%) with PepYLCV from Bali, Central Java, and Bogor. Previous research reported that begomovirus infection in Indonesia was first reported in West Java in 1999 and spread into Central Java in 2003 (Subiastuti *et al.,* 2019), followed by Bali, Sumatra, and Kalimantan Islands (Selangga *et al.,* 2023). The spread of begomovirus from Bali and Java Islands to chili production areas in Sumatra might have been caused by inter-island trade from Java to Sumatra Island without a proper quarantine assessment. The cultivation of infected seeds will further trigger the spread of the disease with the help of the pathogen vector (Fadhila *et al.,* 2020). In any case, these findings only clarified the genetic resemblance of the begomovirus CP gene sequence, which could be utilized to quickly identify this virus contamination and identify begomovirus in a new location. Complete DNA sequences of samples are necessary for the establishment of new species and definitive classification. The spreading of plant disease can be caused by numerous factors. Based on the review by Ristaino *et al.* (2021), the disease can occur because of the movement of the infected plants, pathogenicity, interspecific hybridization, mutation, and others. The disease vector evolution can accelerate disease development and create new species of *B. tabaci* biotype B, which has a mutualistic relationship with begomovirus. Seasonal climatic factors (e.g., temperature and rainfall) and the presence of alternative host plants strongly influence whitefly population dynamics and virus inoculum pressure. Integration of landscape-level management practices, such as crop rotation and removal of alternative host reservoirs, with field-level threshold-based IPM can reduce virus transmission and support sustainable disease suppression. Other than that, pesticide resistance increases the spread of disease and causes an outbreak. All those new findings open horizons about environmental and

technical factors that can accelerate the spread of this disease. Frequent prophylactic pesticide use may temporarily suppress whiteflies but can increase insecticide resistance and disrupt natural enemies. Threshold-based IPM offers a more sustainable strategy to manage virus pressure. In addition, data obtained from chili cultivation in Karo shows that the distribution that extends to Bali and Java allows for a wider spread. Therefore, several preventive actions must be taken to be able to suppress the spread of this disease.

CONCLUSION

The production system in Karo contains many elements of an environmentally safe chili package, high rates of rotation (76.2%), universal sanitation (100%), and widespread integrated nutrient management (NPK combined with compost/ manure), that together support soil health, reduce reliance on prophylactic agrochemicals, and lower longer-term environmental risk. To convert this foundation into durable environmental gains, residue management must avoid burning (promote on-farm composting or off-farm nutrient recovery), conserve and rebuild soil organic carbon through regular organic amendments and reduced-tillage options, and formalize balanced, split fertilizer schedules tailored to local soils. Implementation of a residue-to-resource pathway requires compost quality standards, economic incentives for on-farm composting, and operational guidance for optional biochar blending. These measures provide a practical alternative to residue burning while reducing particulate emissions and greenhouse gas outputs. These actions will reduce greenhouse-gas and particulate emissions, limit nutrient leaching, protect beneficial soil biota, and decrease the environmental footprint of chili production (Parambil-Peedika, 2025; Das, 2023; Zhang *et al*., 2024). Molecular evidence from seedlings grown under insect-free conditions indicates a PepYLCV-related begomovirus is present in the local seed/planting material. The amplified 916 bp fragment from sample A1.1-Dolat Rayat clustered with Pepper yellow leaf curl virus sequences, showing 92.44% identity to LC381280.1 (Bali, Ketewel) and 90.00% identity to JX416180.1 (Java). The close similarity to multiple Indonesian isolates, but divergence from unrelated international isolates, points to regional movement and local circulation of related viral strains. Detection of PepYLCV in greenhouse-grown seedlings suggests a possible seed-associated origin; however, alternative explanations such as handling-related or residual contamination cannot be excluded, and definitive seed transmission was not demonstrated in this study. informal seed systems can facilitate horizontal spread of begomoviruses when seed health is not verified. Therefore, disease control must be integrated with environmental-safe management. Priority measures are: mandatory molecular seed-health screening and certified seed distribution; full genome sequencing and GenBank deposition of detected isolates for traceability; low-cost whitefly monitoring with threshold-based integrated pest management to reduce blanket insecticide use; promotion of composting over burning; targeted soil testing before liming; and demonstration trials that combine conservation tillage with organic amendments to quantify soil-carbon and yield co-benefits. Full-genome sequencing and public deposition of sequence data would strengthen long-term molecular surveillance by improving strain resolution, enabling recombination detection, and supporting reliable regional comparisons, thereby enhancing traceability and eco-friendly management of Pepper yellow leaf curl virus across Southeast Asia. The molecular data generated in this study can be integrated into regional Pepper yellow leaf curl virus surveillance networks through sequence sharing, standardized diagnostics, and metadata reporting, supporting early detection, traceability, and coordinated eco-friendly response strategies. Implementing these linked actions will reduce environmental risks while strengthening surveillance and resilience of chili production in Karo. he begomovirus genome (916 bp) was identified in purple stem chili, a local chili variety in Karo. Sequence analysis demonstrated 92.44% similarity between PepYLCV found in local Karo chili and the PepYLCV-ACI gene from Bali Ketewel (LC381280.1), as well as 90.00% similarity to PepYLCV from Java (JX416180.1). The close similarity to multiple Indonesian isolates, together with divergence from unrelated international isolates, supports regional circulation and local persistence of related viral populations rather than recent exotic introductions. However, while detection in greenhouse-grown seedlings suggests a possible association with planting material, alternative explanations such as contamination during handling

cannot be excluded, and seed transmission was not experimentally demonstrated in this study**.** Pep-YLCV from local pepper samples (Sample A1.1-Dolatrayat) exhibited high sequence similarity with Pep-YLCV from Bali, Central Java, and Bogor, while differing from isolates of the Tomato Leaf Curl Comoros Virus Dembeni, Tobacco Leaf Curl Yunnan Virus from South Korea, and Ramei Mosaic Virus from China. These findings highlight the potential for horizontal disease transmission, influenced by inadequate monitoring during the distribution of uncertified local seeds, and underscore the importance of advanced technology to strengthen quarantine systems for better plant disease management. Compared with current practices, integrated approaches combining molecular surveillance, eco-friendly IPM, organic residue management, and targeted soil testing offer improved long-term cost–benefit by reducing input dependency, limiting environmental impacts, and enhancing yield stability and biosecurity. Indonesia has existing seed-quality and plant-protection regulations for vegetable crops; however, routine molecular diagnostics are not yet widely implemented. Integration of molecular seed-health screening into regulatory frameworks would support environmentally responsible biosecurity and reduce virus dissemination through informal seed systems. Research institutions, extension services, seed agencies, and local governments are key stakeholders for implementing eco-friendly virus surveillance and management. Strengthened collaboration through shared surveillance data, field demonstrations, and coordinated extension programs can improve adoption and long-term sustainability.

AUTHOR CONTRIBUTIONS

R. Tarigan conceived the study, designed experiments, led fieldwork, interpreted data, and drafted the manuscript. B.K. Udiarto supported study design and methodology. K.D. Sutanto contributed to data interpretation and manuscript revision. D.S. Hanafiah participated in collecting data, conducting analytical procedures and assisted with manuscript refinement. D.W. Utami assisted with validation and provided important feedback that improved the manuscript. W. Setiawati performed bioinformatic and phylogenetic analyses. I. Manzila provided laboratory technical support and assisted manuscript refinement. A. Sebayang contributed to interpretation of data analysis and manuscript revision. R. Murtiningsih supported data analysis. A.E. Marpaung curated data. I.S. Marpaung assisted drafting, literature synthesis, and figure preparation. S. Simatupang provided literature review and figure preparation. Atman coordinated field activities and refining the manuscript. M. Sinuraya conducted the fieldwork and prepared the initial manuscript draft. Riska contributed in the fieldwork and prepared the initial manuscript draft.

ACKNOWLEDGEMENT

The authors would like to thank to the Department of Agroecotechnology, University of Sumatra Utara for supporting this study through the TALENTA Program.

CONFLICT OF INTEREST

The authors declare that there is no conflict of interest regarding the publication of this manuscript. The ethical issues, including plagiarism, informed consent, misconduct, data fabrication and/or falsification, double publication and/or submission, and redundancy have been completely observed by the authors.

OPEN ACCESS

©2026 The author(s). This article is licensed under a Creative Commons Attribution 4.0 International License, which permits use, sharing, adaptation, distribution and reproduction in any medium or format, if you give appropriate credit to the original author(s) and the source, provide a link to the Creative Commons license, and indicate if changes are made. The images or other third-party material in this article are included in the articles Creative Commons license, unless indicated otherwise in a credit line to the material. If material is not included in the articles Creative Commons license and your intended use is not permitted by statutory regulation or exceeds the permitted use, you will need to obtain permission directly from the copyright holder. To view a copy of this license, visit: http://creativecommons.org/licenses/by/4.0/

PUBLISHERS NOTE

GJESM Publisher remains neutral regarding jurisdictional claims in published maps and institutional afflictions.

☑ Negative AI Statement

The author(s) declared that no AI tools or services were used or highly applied during the preparation of this work.

ABBREVIATIONS

%	Percent
°C	Degre Celsius
µM	Micromolar
AC1	Begomovirus AC1 gene (replication-associated protein, Rep)
AC2	Begomovirus AC2 gene (transcriptional activator protein, TrAP)
B. tabaci	*Bemisia tabaci* (whitefly)
BLAST	Basic Local Alignment Search Tool
BLASTn	BLAST nucleotide search
bp	Base pair(s)
ChemiDoc	ChemiDoc imaging system (Bio-Rad)
CO	Carbon monoxide
CO_2	Carbon dioxide
CH_4	Methane
CP	Viral coat protein
CTAB	Cetyltrimethylammonium bromide (DNA extraction reagent)
DNA	Deoxyribonucleic acid
dNTPs	Deoxynucleotide triphosphates
DNA-A	Begomovirus DNA-A genomic component
E	East
EDTA	Ethylenediaminetetraacetic acid
EDS	Energy dispersive spectroscopy
FAO	Food and Agriculture Organization of the United Nations
Fig.	Figure
g	Gram
GenBank	NCBI sequence repository (GenBank database)
GPS	Global Positioning System
ICABIOGRAD	Indonesian Center for Agricultural Biotechnology and Genetic Resources Research and Development
ID	identification code
INM	Integrated nutrient management
IPM	Integrated pest management
kg	Kilogram
L	Liter
Masl	Meters above sea level
mM	millimolar
M	Molar
MEGA11	Molecular Evolutionary Genetics Analysis software, version 11
Mg C/ha	magnesium carbon per hectare
$MgCl_2$	magnesium chloride
min	Minute(s)
MUSCLE	Multiple sequence alignm cetyltrimethylammonium bromide
ng	nanograms
N	North
N_2O	Nitrogen oxide
NaCl	Sodium chloride
NA	Not applicable / Not available
NCBI	National Center for Biotechnology Information
NPK	Nitrogen, phosphorus, potassium
PCR	Polymerase chain reaction
pH	potential of hydrogen
PepYLCD	Pepper yellow leaf curl disease
PepYLCV	Pepper yellow leaf curl virus
PM	Particulate matter
PVP	Polyvinylpyrrolidone
s	second
SPG1 / SPG2	Degenerate begomovirus PCR primers SPG1 and SPG2
TAE	Tris-acetate-EDTA buffer
TrAP	Transcriptional Activator Protein
TE	Tris-EDTA buffer
Tris-HCl	*Tris-Hydrochloride*
U.S.	United States
U	unit
t/ha	Tons per hectare

REFERENCES

Adnyani, N.N.P.; Wiratama, I.D.M.P.; Temaja, I.G.R.M.; Nurulita, S.; Suastika, G., (2018). Cloning of Transcriptional Activator Protein and Replication-Associated Protein genes of Squash leaf curl China virus the causal agent of yellow leaf disease on cucumber. J. Fitopatol. Indonesia. 14(1): 1–6 **(6 Pages).**

Alene, A.D.; Manyong, V.M., (2007). The effects of education on agricultural productivity under traditional and improved technology in northern Nigeria: An endogenous switching regression analysis. Empirical Econ., 32(1): 141–159 **(19 Pages).**

Amorim, H.C., Ashworth, A.J., Partson, M., Savin, M.C., Anapalli, S.S., Reddy, K.N., (2024). No-till impacts on soil organic carbon and soil quality in the Lower Mississippi River basin: Implications for sustainable management. Soil Sci. Soc. America J., 88(5): 1736-1747 **(11-Pages).**

Anatalia, R.; Harsono, P.; Yunindanova, M.B.; Purnomo, D., (2022). Effects of NPK and foliar fertilizer on chili (*Capsicum annuum*) growth and yield. AGRARIA: J. Ilmu-Ilmu Pertanian. 6(2): 73–79 **(7 Pages).**

Aza-González, C.; Núñez-Palenius, H.G.; Ochoa-Alejo, N., (2012). Molecular biology of chili pepper anthocyanin biosynthesis. J. Mexican Chem. Soc., 56: 93–98 **(6 Pages).**

Bendokas, V.; Skėmienė, K.; Trumbeckaitė, S.; Stanys, V.; Passamonti, S.; Borutaite, V.; Liobikas, J., (2020). Anthocyanins: From plant pigments to health benefits at mitochondrial level. Crit. Rev. Food Sci. Nutr., 60: 3352–3365 **(14 Pages).**

Bingham, G.V., (2023). Importance of sanitation for stored-product pest management. Insects. 15(1): 3 **(11 Pages).**

Chairina, F.; Aamir, L.; Thuy, T.B. Vo, P.; Huong T.H.; Sri H.H.; Jangha, L.; Eui-Joon, K.; Sukchan, L., (2020). The threat of seed-transmissible pepper yellow leaf curl Indonesia virus in chili pepper, Microbial Pathog., 143: 104132 **(10 Pages).**

Chowdhury, M.; Nazneen, F.; Rafii, M.Y.; Ismail, S.I.; Ramlee, S.I.; Hosen, M.; Karim, K.M.R.; Yusuff, O.; Ridzuan, R., (2023). Genetic analysis of anthracnose resistant and heat tolerant chili inbreed lines based on morpho-physiological characteristics. Chil. J. Agric. Res., 83(2): 168–180 **(13 Pages).**

Clark, M.J., (2014). Effect of fertilizer application rates on plant growth and nutrient leaching in horticultural systems. Hortic. Sci., 49(6): 819–826 **(8 Pages).**

Deshpande, M.V.; Kumar, N.; Pillai, D.; Krishna, V.V.; Jain, M., (2023). Greenhouse gas emissions from agricultural residue burning have increased by 75% since 2011 across India. Sci. Total Environ. 904: 166944 **(14 Pages).**

Díaz-Sánchez, D.D.; López-Sánchez, H.; Silva-Rojas, H.V.; Gardea-Béjar, A.A.; Cruz-Huerta, N.; Ramírez-Ramírez, I.; González-Hernández, V.A., (2021). Pungency and fruit quality in Mexican landraces of piquín pepper (*Capsicum annuum* var. *glabriusculum*) as affected by plant growth environment and postharvest handling. Chil. J. Agric. Res. 81(4): 546–556 **(11 Pages).**

Dobermann, A.; Fairhurst, T.H., (2002). Rice straw management. Better Crops Int., 16: 7–11 **(5 Pages).**

Ekowahyuni, L.P., (2022). Yield test of hybrid harapan chili (*Capsicum annuum* L.). CABI digital library. **(8 Pages).**

Fadhila, C.; Lal, A.; Vo, T.T.B.; Ho, P.T.; Hidayat, S.H.; Lee, J.; Kil, E.J.; Lee, S., (2020). The threat of seed-transmissible pepper yellow leaf curl Indonesia virus in chili pepper. Microbiol. Pathol. 143: 104132 **(8 Pages).**

Fontenele, R.S.; Bhaskara, A.; Cobb, I.N.; Majure, L.C.; Salywon, A.M.; Avalos-Calleros, J.A.; Argüello-Astorga, G.R.; Schmidlin, K.; Roumagnac, P.; Ribeiro, S.G., (2021). Identification of the Begomoviruses squash leaf curl virus and watermelon chlorotic stunt virus in various plant samples in North America. Viruses. 13(5): 810 (1–17) **(17 Pages).**

Gorovits, R.; Shteinberg, M.; Anfoka, G.; Czosnek, H., (2022). Exploiting virus infection to protect plants from abiotic stresses: tomato protection by a Begomovirus. Plants. 11(21): (1–12) **(12 Pages).**

Islam, A.H.M.S.; Schreinemachers, P.; Kumar, S., (2020). Farmers' knowledge, perceptions and management of chili pepper anthracnose disease in Bangladesh. Crop Prot., 133: 105139 **(8 Pages).**

Kamrunnahar, K. V.; Hoque, M. R.; Ferdous, J., (2024). Enhancing chili growth and yield: the synergistic effects of biochar and inorganic fertilizers on soil properties and nutrient use efficiency. Inter. J. Biol. Eng. Agric., 3(4): *552*-564 **(12 Pages).**

Kumar, M.; Tarafdar, J.; Adhikary, N.K.; Das, S., (2021). Genome characterisation of a distinct species of Begomovirus causing leaf curl disease in sweetpotato (*Ipomoea batatas* L.) in India. J. Hortic. Sci. Biotechnol. 96: 121–122 **(2 Pages).**

Lim, S.H.; Kim, D.H.; Cho, M.C.; Lee, J.Y., (2022). Chili pepper AN2 (CaAN2): A visible selection marker for nondestructive monitoring of transgenic plants. Plants. 11: 820 **(13 Pages).**

Malichan, S.; Taweechotworakul, P.; Hongprayoon, R., (2019). Detection of begomoviruses causing pepper yellow leaf curl disease in thailand using broad-spectrum primers. Thai. Agric. Res. J. 37(3): 250–264 **(15 Pages).**

Mariyono, J., (2017). Moving to commercial production: a case of intensive chilli farming in Indonesia. Dev. Prac., 27(8): 1103–1113 **(11 Pages).**

Manea, E.E.; Bumbac, C.; Dinu, L.R.; Bumbac, M.; Nicolescu, C.M., (2024). Composting as a sustainable solution for organic solid waste management: current practices and potential improvements. Sustainability. 16(15): 6329 **(11 Pages).**

Merfield, C., (2019). Rotations and their impact on soil health. future farming centre / low impact farming. **(22 Pages).**

Neriya, Y.I.; Wilisiani, F.; Hartono, S.; Wirya, G.; Nishigawa, H.; Natsuaki, T., (2020). Complete Genome Sequence of a Pepper Yellow Leaf Curl Indonesia Virus Isolated from Tomato in Bali, Indonesia. Microbiol. Resour. Announc. 9(25): e00486-20 **(2 Pages).**

Olatunji, T.L.; Afolayan, A.J., (2018). The suitability of chili pepper (*Capsicum annuum* L.) for alleviating human micronutrient dietary deficiencies: A rev. Food Sci. & Nutr. 6: 2239–2251 **(13 Pages).**

Pan, L.; Chen, Q.; Guo, T.; Wang, X.; Li, P.; Wang, X.; Liu, S., (2018). Differential efficiency of a begomovirus to cross the midgut of different species of whiteflies results in variation of virus transmission by the vectors. Sci China Life Sci., 61: 1254–1265 **(12 Pages).**

Pan, L.L.; Chi, Y.; Liu, C.; Fan, Y.Y.; Liu, S.S., (2020). Mutations in the coat protein of a begomovirus result in altered transmission by different species of whitefly vectors. Virus Evol., 6(1): 1–12 **(12 Pages).**

Parambil-Peedika, A., (2025). Agroecological impacts of crop residue burning: A qualitative systematic review of direct and inferred evidence. Sci. Total Environ., 994: 179963 **(15 Pages).**

Pohan, N.S.; Alfan, G.; Khalil, M., (2023). Pepper (*Capsicum annuum*) plants harboring the begomovirus resistance gene pepy-1 show delayed symptom progress and high productivity under natural field conditions. J. the Japanese Soc. Horti. Sci. 92(1): 36–46 **(11 Pages).**

Ristaino, J.B.; Anderson, P.K.; Bebber, D.P.; Brauman, K.A.; Cunniffe, N.J.; Fedoroff, N.V.; Finegold, C.; Garrett, K.A.; Gilligan, C.A.; Jones, C.M., (2021). The persistent threat of emerging plant disease pandemics to global food security. Proc. Natl. Acad. Sci., 118(23): e2022239118 **(9 Pages).**

Sau, A.R.; Nazmie, N.M.F.; Yusop, M.S.M.; Akbar, M.A.; Saad, M.M.; Baharum, S.N.; Bunawan, H., (2020). First report of pepper vein yellows virus and pepper yellow leaf curl virus infecting chilli pepper (*Capsicum annuum*) in Malaysia. Plant Dis., 104(7): 2037-2037 **(7 Pages).**

Selangga, D.G.W.; Listihani, L., (2021). Molecular identification of Pepper yellow leaf curl Indonesia virus on chili pepper in Nusa Penida Island. J. Trop. Plant Pests Dis., 21(2): 97–102 **(6 Pages).**

Selangga, D.G.W.; Listihani, L.; Temaja, I.G.R.M.; Wirya, G.N.A.S.; Sudiarta, I.P.; Yuliadhi, K.A., (2023). Determinants of symptom variation of Pepper yellow leaf curl Indonesia virus in bell pepper and its spread by *Bemisia tabaci*. Biodiversitas. 24(2): 869–877 **(9 Pages).**

Seitz, S., Goebes, P., Puerta, V. L., Pereira, E. I. P., Wittwer, R., Six, J., Scholten, T., (2019). Conservation tillage and organic farming reduce soil erosion. Agron. Sustainable Dev., 39(1): 4 **(10 Pages).**

Shingote, P.R.; Wasule, D.L.; Parma, V.S.; Holkar, S.K.; Karkute, S.G., (2022). An overview of chili leaf curl disease: Molecular mechanisms, impact, challenges, and disease management strategies in Indian subcontinent. Front. Microbiol., 13: 899512 **(18 Pages).**

Siaga, E.; Rini, D.S.; Widuri, L.I.; Sakagami, J.I.; Lakitan, B.; Yabuta, S., (2024). Growth and morpho-physiological assessments of Indonesian red chili cultivars on early vegetative stage under water stress conditions: A comparison of waterlogging and drought. Chil. J. Agric. Res., 84(3): 425–438 **(14 Pages).**

Soares, R.S.; Silva, E.H.C.; Vidal, R.L.; Candido, W. dos S.; Franco, C.A.; Reifschneider, F.J.B.; Braz, L.T., (2018). Response of *Capsicum annuum* L. var. *annuum* genotypes to root-knot nematode infection. Chil. J. Agric. Res., 78(1): 78–85 **(8 Pages).**

Subiastuti, A.S.; Hartono, S.; Daryono, B.S., (2019). Detection and identification of Begomovirus infecting Cucurbitaceae and Solanaceae in Yogyakarta, Indonesia. Biodiver. J. Biol. Divers., 20(3): 738–744 **(7 Pages).**

Supartha, I.W., Yudha, I.K.W., Wiradana, P.A., Susila, I.W., (2020). Response of parasitoids to invasive pest *Phenacoccus manihoti* Matile-Ferrero (Hemiptera: Pseudococcidae) on cassava crop in Bali, Indonesia. Biodiver. J. Biol. Diver., 21(10): 1-7 **(5 Pages).**

Tarigan, R.; Hanafia, D.S.; Sinuraya, M.; Barus, S.; Marpaung, A.E.; Murtiningsih, R.; Sebayang, A., (2023). Pengaruh pemberian sinar gamma terhadap cabai lokal Karo terinfeksi penyakit virus daun keriting kuning (Begomovirus). J. Fitopatol. Indonesia. 19(2): 74–82 **(9 Pages).**

Udiarto, B.K.; Setiawati, W.; Muharam, A., (2023). Seedling protection and barrier crops in chili pepper to reduce whitefly denseness and prevalence of pepper yellow leaf curl virus. IOP Conference Series: J. Earth Environ. Sci., 1172: 012029 **(7 Pages).**

Wang, Y.; Mei, Y.; Su, C.; Wang, Z.; Li, F.; Hu, T.; Wang, Z.; Liu, S., (2023). GPIBase: A comprehensive resource for geminivirus–plant–insect research. Mol. Plant. 16(4): 647–649 (**3 Pages).**

Wahyono, A.; Murti, R.H.; Hartono, S.; Nuringtyas, T.R.; Wijonarko, A.; Mulyantoro, M.; Purnama, I.C. G., (2023). Current status and complexity of three Begomovirus species in pepper plants in lowlands and highlands in Java Island, Indonesia. Viruses. 15(6): 1278 **(15 Pages).**

Yan, Z.; Wolters, A.M.A.; Navas-Castillo, J.; Bai, Y., (2021). The global dimension of tomato yellow leaf curl disease: Current status and breeding perspectives. Microorganisms. 9: 740 **(19 Pages).**

Zhang, H.; Li, X.; Zhou, J., (2024). Combined application of chemical fertilizer and organic amendment improved soil quality in a wheat–sweet potato rotation system. Agronomy. 14(9): 2160 **(14 Pages).**

AUTHOR (S) BIOSKETCHES

Rasiska Tarigan, SP., M.Agr., Junior researcher, Research Center for Horticulture, National Research and Innovation Agency, Jl. Raya Jakarta-Bogor KM 46, Cibinong, Indonesia.
- Email: *rasi004@brin.go.id*
- ORCID: 0000-0002-8615-1552
- Web of Science ResearcherID: LFN-0661-2024
- Scopus Author ID: 57700788800
- Homepage: https://brin.go.id/orpp

Mariati Sinuraya, Dr., Lecturer, Department of Agrotechnology, Faculty of Agriculture, Universitas Sumatera Utara, Medan, Indonesia. Jl. Dr. T. Mansur No. 9, Padang Bulan, Medan Baru, Kota Medan, Sumatera Utara.
- Email: *mariati@usu.ac.id*
- ORCID: 0000-0002-9242-1296
- Web of Science ResearcherID: AAV-9846-2020
- Scopus Author ID: 57201184896
- Homepage: https://fp.usu.ac.id/en

Diana Sofia Hanafiah, SP., MP., Dr., Researcher/ Lecture, Department of Agrotechnology, Faculty of Agriculture, Universitas Sumatera Utara, Medan, Indonesia Jl. Dr. T. Mansur No. 9, Padang Bulan, Medan Baru, Kota Medan, Sumatera Utara.
- Email: *diana.hanafiah@usu.ac.id*
- ORCID: 0000-0002-3642-7386
- Web of Science ResearcherID: GQY-8884-2022
- Scopus Author ID: 57197870486
- Homepage: https://fp.usu.ac.id/en

Bagus Kukuh Udiarto, Ir., MP., Dr., Senior researcher, Research Center for Horticulture, National Research and Innovation Agency Jl. Raya Jakarta-Bogor KM 46, Cibinong, Indonesia.
- Email: *bagu017@brin.go.id*
- ORCID: 0000-0003-1799-653x
- Web of Science ResearcherID: NA
- Scopus Author ID: 26041167700
- Homepage: https://brin.go.id/orpp

Sutanto, K.D., Ph.D., Postdoctoral fellow, Research Center for Horticulture, National Research and Innovation Agency, Jl. Raya Jakarta-Bogor KM 46, Cibinong, Indonesia.
- Email: *koko006@brin.go.id*
- ORCID: 0000-0002-3605-4954
- Web of Science Researcher ID: OHR-7407-2025
- Scopus Author ID: 55980814800
- Homepage: http://ksu.edu.sa/index.php/en/home

Wiwin Setiawati, Ir., M.Si, Senior Researcher, Research Center for Horticulture, National Research and Innovation Agency, Jl. Raya Jakarta-Bogor KM 46, Cibinong, Indonesia
- Email: *wsetiawati@yahoo.com*
- ORCID: 0000-0002-3099-6254
- Web of Science ResearcherID: GWE-1586-2022
- Scopus Author ID: 57224189836
- Homepage: https://brin.go.id/orpp

Ifa Manzila, Dra, Dr., Senior Research Center for Horticulture, National Research and Innovation Agency, Jl. Raya Jakarta-Bogor KM 46, Cibinong, Indonesia.
- Email: *ifam001@brin.go.id*
- ORCID: 0000-0001-8479-7229
- Web of Science Researcher ID: NA
- Scopus Author ID: 55552513600
- Homepage: https://brin.go.id/orpp

Amelia Sebayang, M.Sc., Junior Researcher, Research Center for Horticulture, National Research and Innovation Agency, Jl. Raya Jakarta-Bogor KM 46, Cibinong, Indonesia.
- Email: Amelia.sebayang@gmail.com
- ORCID: 0000-0003-4400-804X
- Web of Science ResearcherID: HZH-3011-2023
- Scopus Author ID: 57226750668
- Homepage: https://brin.go.id/orpp

D.W., Utami, Ph.D., Senior researcher, Research Center for Horticulture, National Research and Innovation Agency, Soekarno Science Center, Jl. Raya Jakarta-Bogor KM 46, Cibinong, Kab. Bogor – 16915, Indonesia.
- Email: *dwin011@brin.go.id*
- ORCID: 0000-0002-5873-0570
- Web of Science Researcher ID: NA
- Scopus Author ID: 36821685400
- Homepage: https://wwwresearchgate.net/profile/Dr-Dwinita-Utami

AUTHOR (S) BIOSKETCHES

Rini Murtiningsih, Ph.D., Senior Researcher, Research Center for Horticulture, National Research and Innovation Agency, KST Soekarno, Jl. Raya Jakarta-Bogor, Cibinong, West Java 16915, Indonesia.
- Email: *rini.murtiningsih.rm@gmail.com*
- ORCID: 0000-0002-4530-3908
- Web of Science ResearcherID: FNT-5223-2022
- Scopus Author ID: 57222179341
- Homepage: https://brin.go.id/

Agustina E. Marpaung, SP., M.Agr., Junior Researcher, Research Center for Horticulture, National Research and Innovation Agency, Soekarno Science Center, Jl. Raya Jakarta-Bogor KM 46, Cibinong, Kab. Bogor – 16915, Indonesia.
- Email: *agustinamarpung81@gmail.com*
- ORCID: 0000-0002-1030-4900
- Web of Science ResearcherID: JZN-2849-2024
- Scopus Author ID: 57226562172
- Homepage: https://brin.go.id/orpp

Imelda S. Marpaung., SP., M.Si. Senior Researcher, Research Center for Horticulture, National Research and Innovation Agency, KST Soekarno, Jl. Raya Jakarta-Bogor, Cibinong, West java 16915, Indonesia.
- Email: *imel003@brin.go.id*
- ORCID: 0000-0002-8202-3243
- Web of Science ResearcherID: NIJ-1638-2025
- Scopus Author ID: 57226576059
- Homepage: https://brin.go.id/

Sortha Simatupang, Ir. M.S., Principal Researcher, Research Center for Horticulture, National Research and Innovation Agency, KST Soekarno, Jl. Raya Jakarta-Bogor, Cibinong, West java 16915, Indonesia.
- Email: *sort001@brin.go.id*
- ORCID: 0000-0002-2270-4768
- Web of Science ResearcherID: NA
- Scopus Author ID:- 57226563060
- Homepage: https://brin.go.id/orpp

Atman, Ir.M.Kom, Dr., Researcher Professor, Research Center for Horticulture, National Research and Innovation Agency, KST Soekarno, Jl. Raya Jakarta-Bogor, Cibinong, West java 16915, Indonesia.
- Email: *atma002@brin.go.id*
- ORCID: 0000-0002-4479-3300
- Web of Science ResearcherID: KYQ-1340-2024
- Scopus Author ID:- 57224519760
- Homepage: https://brin.go.id/orpp

Riska, S.Si.M.Sc. Agr. Ph.D. Senior Researcher, Research Center for Horticulture, National Research and Innovation Agency, KST Soekarno, Jl. Raya Jakarta-Bogor, Cibinong, West java 16915, Indonesia.
- Email: *risk011@brin.go.id*
- ORCID: 0000-0001-5251-0027
- Web of Science ResearcherID: NA
- Scopus Author ID: 57219964338
- Homepage: https://brin.go.id/

HOW TO CITE THIS ARTICLE

Tarigan, R.; Sutanto, M.; Udiarto, B.K; Hanafiah, S.D.; Sinuraya, M.; K.D.; Setiawati, W.; Manzila, I.; Sebayang, A.; Utami, D.W.; Murtiningsih. R.; Marpaung E.A.; Marpaung, S.I.; Simatupang.S.; Atman.; Riska, (2026). Eco-friendly farming management and molecular surveillance of the pepper yellow leaf curl virus in purple-stem chili. Global J. Environ. Sci. Manage., 12(1): 371-392.

DOI: 10.22034/gjesm.2026.01.21

URL: https://www.gjesm.net/article_732995.html

Global J. Environ. Sci. Manage. 12(1): 393-408, Winter 2026, Serial #45

Global Journal of Environmental Science and Management
(GJESM)

Homepage: https://www.gjesm.net/

Podcasts

CASE STUDY

Linking geospatial suitability modelling with experimental validation of aquatic environmental quality in inland lakes

B. Doskenova[1], I. Sedelnikov[1], T. Lyssakova[2], G. Gordiyanova[2], G. Rakhimzhanova[3], D. Shugulova[1], E. Abdrahmanov[1], Y. Pangaliyev[4,*]

[1] *GIS Technology Laboratory, Kozybayev Lab, Department of Science, M. Kozybayev North Kazakhstan university, Petropavlovsk, Kazakhstan*

[2] *Department of Geography and Ecology of M.Kozybayev North Kazakhstan University, Petropavlovsk, Kazakhstan*

[3] *Department of of Pedagogy and History A.K. Kussayinov Eurasian Humanities Institute, Astana, Kazakhstan*

[4] *Department of Ecology and Safety, Faculty of Engineering, Yessenov University, Aktau, Kazakhstan*

ARTICLE INFO

Article History:
Received 10 August 2025
Revised 13 October 2025
Accepted 27 November 2025

Keywords:
Aquatic ecosystems
GIS validation
Nutrient enrichment
Inland lakes
Environmental management
Environmental quality

ABSTRACT

BACKGROUND AND OBJECTIVES: Accurate evaluation of aquatic ecosystem suitability is critical for sustainable environmental management, particularly in regions that prioritize aquaculture and biodiversity conservation. Although Geographic Information System–based modelling is increasingly used to classify water bodies according to morphometric and ecological parameters, experimental validation across extensive lake networks remains limited. This study merged geospatial suitability modeling with on-site evaluations to develop a validated framework for evaluating the environmental quality and aquaculture potential of inland lakes in Northern Kazakhstan.

METHODS: A total of 286 lakes were evaluated using a Geographic Information System–based multi-criteria approach that incorporated surface area, water depth, pollution indicators, macrophyte cover, and algal bloom intensity to classify lakes into high, medium, and low suitability categories. Over the course of two years, thirty representative lakes, comprising ten from each category, were sampled seasonally. In six lakes identified as suitable for medium, microcosm experiments investigated the effects of nutrient enrichment and the removal of macrophytes on the water quality. Statistical analyses examined correlations between Geographic Information System–derived suitability scores and measured environmental quality indices.

FINDINGS: High-suitability lakes exhibited significantly higher dissolved oxygen concentration (7.8 ± 0.9 milligrams per liter) and water transparency (1.6 ± 0.3 meters), and lower total phosphorus (0.045 ± 0.012 milligrams per liter) and total nitrogen (0.48 ± 0.11 milligrams per liter) compared with low-suitability lakes (dissolved oxygen 3.5 ± 0.7 milligrams per liter; transparency 0.6 ± 0.2 meters; total phosphorus 0.122 ± 0.029 milligrams per liter; total nitrogen 1.21 ± 0.25 milligrams per liter). Microcosm experiments revealed that nutrient enrichment and macrophyte removal increased chlorophyll-a concentration by 41 percent and reduced dissolved oxygen concentration by 25 percent, indicating the sensitivity of medium-suitability lakes to nutrient loading and vegetation loss. The suitability scores from the geographic information system were found to correlate significantly with the measured environmental indices (coefficient of determination 0.74, p-value less than 0.01), which confirms the predictive power of the spatial model.

CONCLUSION: Integrating geographic information system–based modelling with empirical validation creates a reliable strategy for determining inland lake suitability and promoting sustainable management of freshwater resources.

DOI: 10.22034/gjesm.2026.01.22

This is an open access article under the CC BY license (http://creativecommons.org/licenses/by/4.0/).

NUMBER OF REFERENCES	NUMBER OF FIGURES	NUMBER OF TABLES
31	7	3

*Corresponding Author:
Email: *erbolpm@mail.ru*
Phone: +7 775 285 6079
ORCID: 0000-0002-2392-4180

Note: Discussion period for this manuscript open until Mar 1, 2026 on GJESM website at the "Show Article".

INTRODUCTION

The global demand for fish products is steadily increasing, placing significant pressure on capture fisheries and emphasizing the growing role of aquaculture in meeting future protein needs. Aquaculture contributes to food security, supports rural livelihoods, and can alleviate overexploitation of wild fish stocks (Tanyanyiwa and Tongowona, 2025). Nonetheless, the growth of this sector must be harmonized with the safeguarding of aquatic ecosystems, since improper site selection or management may result in a decline water quality deterioration, habitat loss, and disruption of local biodiversity (Woźniacka *et al.*, 2025). Sustainable aquaculture development therefore requires careful consideration of environmental, hydrological, and ecological factors. Traditional approaches to evaluating water bodies for aquaculture suitability often rely on fragmented datasets, limited field surveys, or subjective expert judgment. Such methods may lead to suboptimal site selection, inefficient resource allocation, and unintended ecological consequences (Ruzieh, 2025). Furthermore, these methods generally do not account for the various, interrelated elements that influence ecosystem capacity and productivity, which restricts their utility in informing strategic planning. There is increasing recognition that more systematic, data-driven methodologies are necessary to ensure that aquaculture development aligns with environmental sustainability and socio-economic objectives (Partelow *et al.*, 2025). In recent years, geographic information systems (GIS) have become a key tool for integrated environmental assessments and sustainable resource management. GIS enables the spatial integration of diverse datasets, including hydrological, physicochemical, and biological variables, and supports quantitative analyses that inform decision-making. Studies show that GIS combined with remote sensing and multicriteria decision analysis can assess intricate socio-environmental systems, facilitating sustainable planning, and alleviating conflicts between development and environmental protection (de Oliveira *et al.*, 2023; Kochanek *et al.*, 2025). Beyond environmental applications, GIS also supports spatial planning and environmental health assessments, offering transferable analytical frameworks for monitoring and resource optimization (Chandran and Roy, 2024). In general, GIS offers a transparent and evidence-based structure for evaluating the potential of aquaculture and facilitating in sustainable decision-making. Complementary to GIS-based approaches, ecological indicators such as water quality parameters, nutrient concentrations, and biological community structure provide essential insights into ecosystem function, resilience, and vulnerability to stressors (Yin *et al.*, 2025). Studies employing GIS alongside multivariate statistical methods have illustrated that the spatial patterns of water quality and heavy metal contamination can identify pollution hotspots and potential ecological risks, guiding site-specific interventions (Arumugam *et al.*, 2025). By employing remote sensing and trait-based monitoring enhances the ability to assess aquatic diversity and ecosystem attributes across various scales, from local to continental scales, providing cost-effective and continuous observation of dynamic aquatic systems (Lausch *et al.*, 2024). Multi-criteria and fuzzy GIS-based approaches applied to stream and freshwater ecosystems integrate environmental, hydrological, and land-use factors to evaluate ecological risk and guide sustainable management strategies (Kourgialas *et al.*, 2024). Furthermore, analyses of stressor–response utilizing biomonitoring data demonstrate the impact of various anthropogenic pressures, including habitat alteration, nutrient loading, and water quality changes; influence biological communities and ecosystem services. This supports adaptive management frameworks such as resist–accept–direct (Emmons *et al.*, 2025). Experimental manipulations and mesocosm studies provide additional mechanistic understanding, linking specific stressors to ecosystem responses and enhancing predictive models for aquaculture suitability and broader ecological planning (Macaulay *et al.*, 2025). These strategies enhance the ability to evaluate and sustainably manage aquatic ecosystems in a sustainable manner, ensuring the maintenance of ecological integrity. Despite the importance of accurately assessing inland lake suitability, information integrating GIS-based multi-criteria modelling with experimental validation of water quality and ecosystem responses across large lake networks is still scarce. This study therefore provides one of the first robust, experimentally supported frameworks linking spatial suitability

scores with measured environmental parameters in Northern Kazakhstan. Northern Kazakhstan was chosen due to its significant concentration of inland lakes, ecological variety, and increasing prospects for the advancement of freshwater aquaculture. These lakes represent hydrological and ecologically variable systems that are representative of broader continental steppe environments. Building on these concepts, the present study demonstrates an integrated approach to assessing inland lake suitability for aquaculture in Northern Kazakhstan. Specifically, a multi-criteria GIS-based classification was applied to 286 lakes, followed by field validation and detailed ecological assessments in a subset of 30 lakes representing high, medium, and low suitability classes. Complementary microcosm experiments were carried out to examine the mechanistic impacts of nutrient enrichment and macrophyte cover on water quality and primary productivity. The integration of spatial analysis, field measurements, and controlled experiments establishes a strong foundation for effective aquaculture planning, emphasizing both practical and ecological factors in the choice of appropriate water bodies. This study aimed to integrate geospatial suitability modelling with field-based experimental assessments to provide a validated framework for evaluating the environmental status and aquaculture potential of inland lakes. The research was conducted in Northern Kazakhstan in 2024.

MATERIALS AND METHODS

Study area and lake selection

The study was conducted in Northern Kazakhstan, encompassing the lowland steppe and forest-steppe zones between approximately 50°N-55° north (N) latitude and 70° east (E)-80°E longitude. This region experiences a continental climate, characterized by long, cold winters with average January temperatures around -18 degrees Celsius (°C), short, warm summers averaging 20-22°C, and annual precipitation ranging from 250 to 400 millimeter (mm), predominantly during late spring and early summer. The landscape is dominated by shallow, lowland plains containing an extensive network of small to medium-sized inland lakes, which vary widely in surface area (0.1-12 square kilometers (km^2), maximum depth (0.5-6 meter (m), and hydrological connectivity, including both isolated closed-basin lakes and interconnected lake chains. In this region, lakes display a diverse spectrum of trophic statuses, ranging from oligotrophic systems with transparent water and abundant submerged macrophytes to hypertrophic, shallow lakes with frequent algal blooms, high nutrient concentrations, and reduced water clarity. A GIS-oriented classification was executed for 286 lakes employing a multi-criteria scoring system that integrates surface area, depth, pollution levels, macrophyte cover, and algal bloom intensity. Each lake received a suitability score, allowing categorization into high, medium, and low suitability classes. From this dataset, an experimental subset of 30 lakes was selected for field validation, consisting of 10 high-suitability lakes, 10 medium-suitability lakes, and 10 low-suitability lakes. The selection of these lakes was made to illustrate the complete range of ecological conditions recognized by the GIS assessment and were used for physicochemical and biological sampling, as well as microcosm experiments, to empirically validate GIS-based predictions and examine the mechanisms underlying observed ecosystem patterns (Fig. 1).

Field sampling

Field sampling was conducted seasonally over two consecutive years (spring, summer, and autumn 2023–2024) to capture temporal variability in lake conditions. In each lake, three sampling stations created to reflect significant habitats: the littoral zone, the pelagic zone, and the inflow area. Physicochemical parameters measured at each station included water temperature, potential hydrogen (pH), dissolved oxygen (DO), electrical conductivity (EC), turbidity, and Secchi depth for water transparency. All pH and DO measurements were performed in-situ using a calibrated multiparameter probe. Nutrient concentrations, including total nitrogen (TN) and total phosphorus (TP), were determined from water samples using established standard colorimetric protocols: TN was measured following the persulfate digestion method (APHA, 2017), and TP was measured using the molybdenum blue method (Murphy and Riley, 1962). Chlorophyll-a was extracted from 500 milliliters of filtered water through glass fiber filters (GF/F, 0.7 µm pore size) using 90 percent acetone and incubated at 4°C in the dark for 24 hours before spectrophotometric quantification,

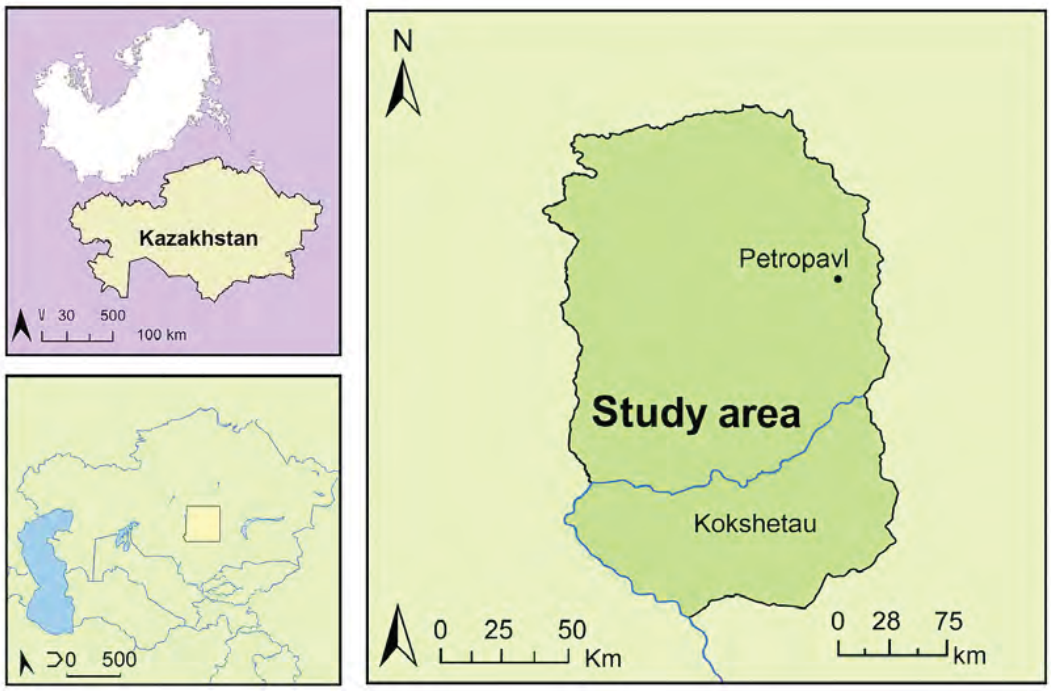

Fig. 1: Geographic location of the study area in the Northern Kazakhstan

following standard procedures (APHA, 2017). Sediment samples were obtained from the uppermost 5-centimeter layer at each station to determine organic matter content utilizing loss-on-ignition at 550°C. Biological parameters included phytoplankton biomass (micrograms per liter, µg/L) and species richness, with phytoplankton identified to genus or species level under a light microscope following standard taxonomic keys. The data collected from the three stations were averaged to derive representative values for each lake, which will be utilized in subsequent analyses across suitability classes.

GIS multi-criteria model

A total of 286 lakes were evaluated using a multi-criteria suitability model implemented in ArcGIS Pro 3.2. Spatial indicators included surface area, water depth, nutrient concentrations, macrophyte cover, and algal bloom intensity. Each criterion was normalized to a 0–1 scale using linear min-max scaling, with weights allocated according to expert assessment and the analytical hierarchy process (AHP) as follows: surface area 0.25, water depth 0.20, nutrient concentrations 0.30, macrophyte cover 0.15, and algal bloom intensity 0.10. Weighted scores were combined using a linear additive model to generate overall suitability scores, which were subsequently classified into high, medium, and low suitability categories. Natural breaks in the score distribution were used to define classification thresholds, which were subsequently validated by comparing them with historical water quality data.

Experimental microcosm design

Six medium-suitability lakes were selected for a 12-week enclosure experiment using floating mesocosms measuring 3 × 3 m with a water depth of 1.2 m. Mesocosms were open to sediment interaction to preserve natural biogeochemical interactions. The experiment included four treatments, each with three replicates: 1) control with ambient conditions, 2) nutrient enrichment, 3) macrophyte removal, and 4) combined nutrient enrichment and macrophyte removal. Nutrient enrichment involved adding nitrogen at 1 milligram per liter (mg/L as N) and phosphorus at 0.1 mg/L (as P) weekly to simulate moderate eutrophication.

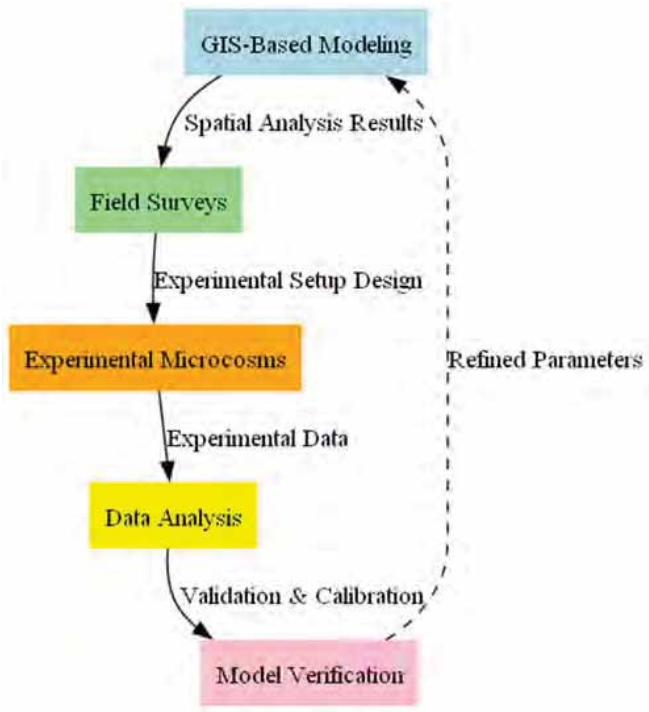

Fig. 2: Study workflow

The process of macrophyte removal entailed the manual harvesting 50-60 percent of aboveground biomass, quantified by pre-harvest clipping and weighing of representative quadrats (1 m^2) to guarantee uniform removal across replicates. Water quality and biological parameters were measured weekly, including DO, pH, TN, TP, chlorophyll-a, and turbidity, following the same protocols as in the field survey. This design facilitated ongoing observation of biogeochemical dynamics and phytoplankton reactions to experimental alterations, offering mechanistic understanding of the impacts of nutrient inputs and vegetation depletion.

Data analysis

Physicochemical and biological variables across lake suitability classes were compared using analysis of variance (ANOVA) to identify statistically significant differences between high, medium, and low suitability lakes. Pearson correlation analysis was executed to explore the connections between GIS-derived suitability scores and the environmental quality indices that were measured, thus offering validation for the spatial assessment. Principal component analysis (PCA) was conducted on a standardized dataset including all physicochemical and biological variables; missing values that represented <2 percent (%) of the dataset were filled in using the mean of each variable. Additionally, prior to performing PCA, the variables were centered and scaled to ensure they were comparable. Regression analysis further quantified the predictive accuracy of the GIS suitability model by determining how well key variables (DO, TN, TP) explained variance in suitability scores. All statistical analyses were performed using R version 4.3.1 with a significance threshold of $p < 0.05$. A schematic diagram summarizing the integration of GIS-based modelling with field surveys and experimental microcosms is provided in Fig. 2. This visual illustration outlines the sequence of activities starting with spatial analysis, progressing through experimental validation, and culminating in data analysis and model verification.

RESULTS AND DISCUSSION

Morphometric characteristics of lakes across suitability classes

The scatter plot illustrating lake surface area versus average depth across suitability classes reveals a distinct morphometric threshold governing

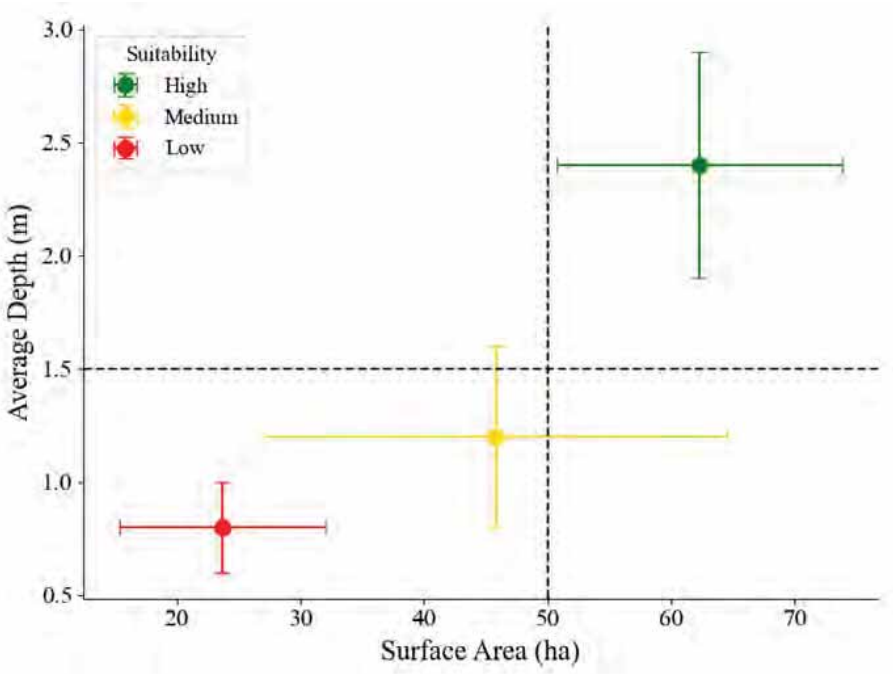

Fig. 3: Surface area vs depth

aquaculture potential. Lakes with high suitability are closely grouped in the upper-right quadrant, distinguished by surface areas that surpass 50 hectares and depths that exceed 1.5 meters. This emphasizes the significance of having adequate habitat space and water column volume to ensure ecological stability (Cieplok *et al.*, 2022; Dang *et al.*, 2025; Van Meerbeek *et al.*, 2021). Medium-suitability lakes are more widely dispersed, often showing adequate surface area but insufficient depth, or moderate depth but smaller area, indicating partial suitability constrained by a single morphometric parameter. Low-suitability lakes occupy the lower-left quadrant, being both small (<50 ha) and shallow (<1.5 m), and therefore face inherent physical limitations that restrict their potential for productive aquaculture. Threshold lines positioned at 50 hectares and 1.5 meters effectively delineate the aggregation of optimal lakes and demonstrate the "morphometric bottleneck" that influences numerous large yet shallow aquatic systems. These patterns indicate that lake morphology should be a primary consideration in aquaculture planning, as even lakes with favorable water quality may fail to support sustainable production if morphometric constraints are not met (Moses *et al.*, 2011). Furthermore, recognizing lakes that are close to these threshold values may facilitate focused interventions, including habitat restoration or regulated water-level management, aimed at improving depth or effective volume, and possibly transitioning medium-suitability lakes to higher suitability categories (Petriki *et al.*, 2020; Poikane *et al.*, 2024; Xia *et al.*, 2025). Integrating morphometric analyses with water quality and ecological indicators provides a holistic framework for evidence-based decision-making and prioritization of management efforts across diverse lake systems (Fig. 3).

The bar plot quantifies the distribution of the 286 lakes across suitability classes, revealing that the majority fall into the medium-suitability category (210 lakes, 73.4%), whereas only a small fraction is classified as high-suitability (49 lakes, 17.1%) or low-suitability (27 lakes, 9.5%). This distribution emphasizes that although the region is rich in aquatic resources, the ideal conditions for aquaculture are quite uncommon. The dominance of medium-suitability lakes suggests that many water bodies may require careful management interventions, such as nutrient control or habitat restoration, to

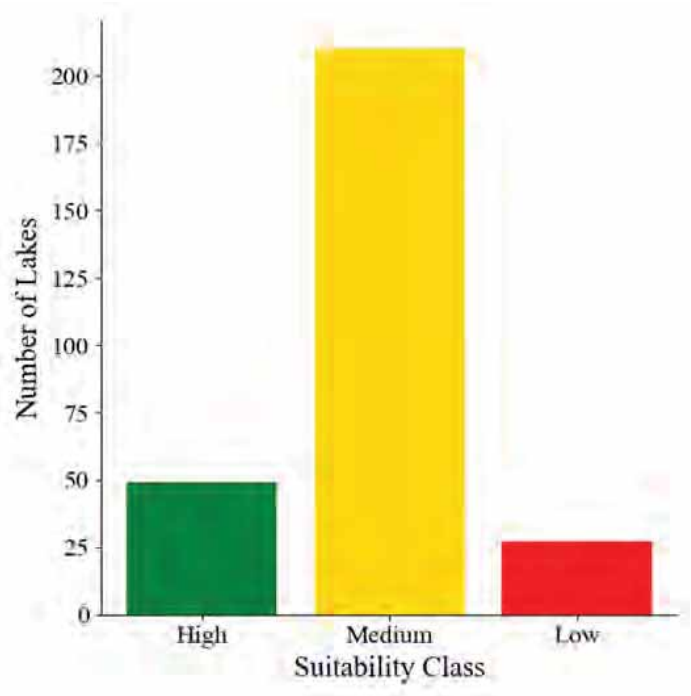

Fig. 4: Number of lakes per suitability class

enhance their aquaculture potential (Schiemer *et al.*, 2024). Conversely, the restricted availability of lakes with high suitability underscores the critical need for focused site selection to optimize productivity and mitigate ecological risk (Fig. 4).

The boxplot illustrates the distribution of lake depths across each suitability class, emphasizing unique patterns of variability. High-suitability lakes display both higher median depth (≈2.4 m) and moderate interquartile range, indicating consistent deep-water conditions conducive to stable ecological functioning. Lakes classified as medium suitability exhibit a median depth of approximately 1.2 meters, accompanied by a broader range of variability. This indicates that although certain lakes possess adequate depth, numerous others are excessively shallow to consistently sustain intensive aquaculture. Low-suitability lakes are shallow (median ≈0.8 m) and tightly clustered near the lower end of the depth range, reinforcing their inherent physical limitations. This illustration validates that depth serves as a vital factor in determining suitability and collaborates with surface area to establish the morphometric thresholds depicted in Fig. 5.

Physicochemical properties across suitability classes

The observed gradients in physicochemical properties among different lake suitability classes illustrate essential ecological and biogeochemical processes. High-suitability lakes exhibited elevated dissolved oxygen (DO, 7.8 ± 0.9 mg/L), low nutrient concentrations (TP 0.045 ± 0.012 mg/L; TN 0.48 ± 0.11 mg/L), low turbidity (3.2 ± 0.7 nephelometric turbidity unit (NTU)), and greater Secchi depth (1.6 ± 0.3 m), indicative of stable, well-oxygenated systems with limited eutrophication and efficient nutrient cycling. In contrast, low-suitability lakes had markedly lower DO (3.5 ± 0.7 mg/L), higher TP and TN (0.122 ± 0.029 mg/L; 1.21 ± 0.25 mg/L), elevated turbidity (12.8 ± 2.4 NTU), and reduced Secchi depth (0.6 ± 0.2 m), suggesting nutrient enrichment-driven eutrophication and impaired water clarity. From a mechanistic perspective, elevated nutrient levels encourage rampant phytoplankton proliferation, as evidenced by a significant rise in chlorophyll-a concentrations (48.1 ± 11.6 µg/L). This phenomenon exacerbates light attenuation, thereby restricting benthic photosynthesis. Algal respiration and microbial decomposition of organic matter further deplete DO, creating hypoxic or near-anoxic

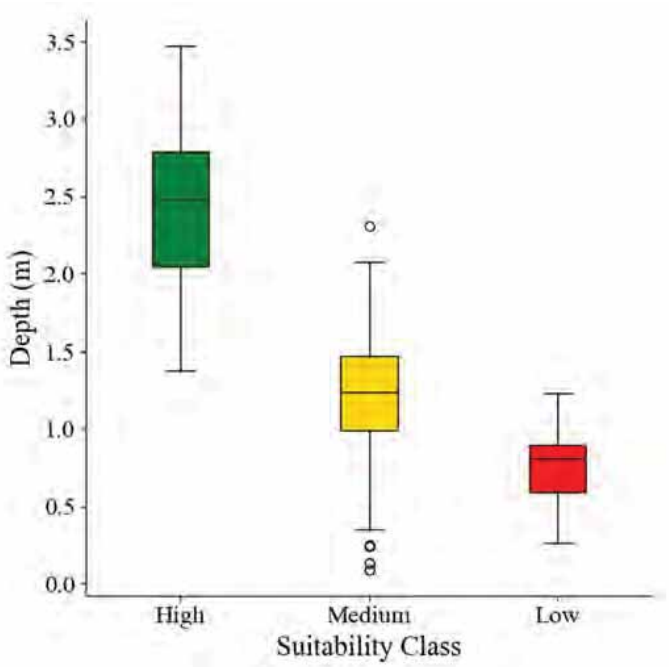

Fig. 5: Depth distribution per suitability class

Table 1: Physicochemical properties across suitability classes

Parameter	High	Medium	Low
DO (mg/L)	7.8 ± 0.9	5.6 ± 0.8	3.5 ± 0.7
pH	7.6 ± 0.3	7.8 ± 0.4	8.0 ± 0.3
EC (µS/cm)	412 ± 58	560 ± 71	710 ± 82
Turbidity (NTU)	3.2 ± 0.7	6.5 ± 1.2	12.8 ± 2.4
Secchi depth (m)	1.6 ± 0.3	1.0 ± 0.2	0.6 ± 0.2
TP (mg/L)	0.045 ± 0.012	0.083 ± 0.019	0.122 ± 0.029
TN (mg/L)	0.48 ± 0.11	0.81 ± 0.17	1.21 ± 0.25
Chlorophyll-a (µg/L)	9.5 ± 2.3	22.4 ± 5.7	48.1 ± 11.6

conditions that can destabilize the ecosystem (Lan *et al.*, 2024). Electrical conductivity increased along the gradient, likely due to accumulation of dissolved ions from nutrient inputs and sediment resuspension (Akinnigbagbe *et al.*, 2025; Mkilima, 2023a, 2023b). The ANOVA-confirmed significant differences ($p < 0.05$) underscore that these physicochemical shifts are not random but systematically associated with lake suitability. Collectively, these observed patterns suggest that the interplay of nutrient enrichment, sediment dynamics, and biological activity plays a crucial role in shaping water quality. This underscores the mechanistic relationship that exists between chemical conditions, primary productivity, and ecosystem health in inland lakes (Table 1).

Biological indicators

The analysis of biological indicators revealed clear patterns in relation to lake suitability. Phytoplankton biomass increased markedly from high-suitability lakes (12.3 ± 3.1 µg/L) to low-suitability lakes (56.7 ± 13.4 µg/L), whereas species richness declined from 18 ± 4 to 8 ± 2 across the same gradient. This inverse correlation indicates that conditions of reduced suitability, typically linked to elevated nutrient levels and modified physical-chemical environments, promote the growth of a limited number of rapidly proliferating, opportunistic taxa like cyanobacteria

Table 2: Summary of phytoplankton community characteristics across lakes with different trophic conditions

Parameter	High	Medium	Low
Phytoplankton biomass (µg/L)	12.3 ± 3.1	28.5 ± 7.2	56.7 ± 13.4
Species richness	18 ± 4	13 ± 3	8 ± 2
Dominant species	Diatoms, green algae	Green algae, cyanobacteria	Cyanobacteria, filamentous algae

and filamentous algae, which prevail in lakes characterized by low suitability. In contrast, high-suitability lakes with more balanced nutrient levels and stable hydromorphological conditions support a more diverse phytoplankton community, including diatoms and green algae. Mechanistically, as previously highlighted nutrient enrichment promotes eutrophication, stimulating algal biomass but creating competitive exclusion that reduces species diversity. Moreover, diminished clarity of water and elevated turbidity in lakes deemed less suitable may hinder light penetration, consequently benefiting species adapted to low-light or high-nutrient conditions (Nunes *et al.*, 2022). These patterns indicate that both nutrient availability and habitat quality jointly regulate phytoplankton community structure, with implications for trophic interactions, water quality, and ecosystem resilience (Table 2).

GIS model validation

The GIS-based suitability model demonstrated strong predictive capability, with suitability scores positively correlating with measured environmental quality indices (coefficient of determination (r^2) = 0.74, $p < 0.01$), indicating that the spatial model reliably captures key ecological gradients in the study area. Regression analysis showed that dissolved oxygen (DO), total nitrogen (TN), and total phosphorus (TP) collectively accounted for 68% of the variance in GIS suitability scores, underscoring the significant impact of water column oxygenation and nutrient status on habitat quality. Mechanistically, elevated DO likely reflects well-oxygenated waters that support aerobic microbial processes and sustain aquatic biota, while lower TN and TP concentrations reduce the risk of eutrophication, algal blooms, and subsequent hypoxia. Conversely, locations with diminished suitability scores are prone to nutrient enrichment and a reduction in oxygen levels, potentially jeopardizing the functioning of ecosystems. These patterns suggest that the GIS model effectively integrates critical physicochemical drivers, allowing spatial identification of high-quality habitats and potential hotspots of environmental degradation. Furthermore, the strong relationship between measured indices and modeled suitability underscores the utility of combining GIS-based approaches with field monitoring to capture spatial heterogeneity and inform management decisions. By correlating water quality indicators with spatially explicit suitability scores, this methodology establishes a solid framework for prioritizing conservation efforts, enhancing resource distribution, and forecasting regions that are most susceptible to human-induced pressures such as nutrient loading and land use change (Fig. 6).

Microcosm experiments

The microcosm experiments illustrated clear and treatment-specific influences on critical water quality parameters, highlighting the fundamental ecological mechanisms. In the control treatment, minimal changes in dissolved oxygen (DO, +2%), chlorophyll-a (+1%), total nitrogen (TN, 0%), and total phosphorus (TP, 0%) indicate system stability and confirm that experimental handling alone did not perturb the ecosystem. Nutrient enrichment led to pronounced increases in chlorophyll-a (+30%) and nutrient concentrations (TN +25%, TP +22%), accompanied by a notable decline in DO (–12%). The observed responses are likely attributable to the stimulated growth of phytoplankton, which occurs as a result of increased nutrient availability. This phenomenon enhances photosynthetic biomass, yet it also accelerates oxygen consumption through both respiration and microbial decomposition of organic matter. Macrophyte removal caused moderate increases in chlorophyll-a (+15%), TN (+5%), and TP (+4%) and a slight DO decline (–8%), suggesting that macrophytes play a key role in nutrient uptake, sediment stabilization, and oxygenation of the water column. The combined treatment of nutrient enrichment and macrophyte removal elicited the strongest response, with the largest decline in DO

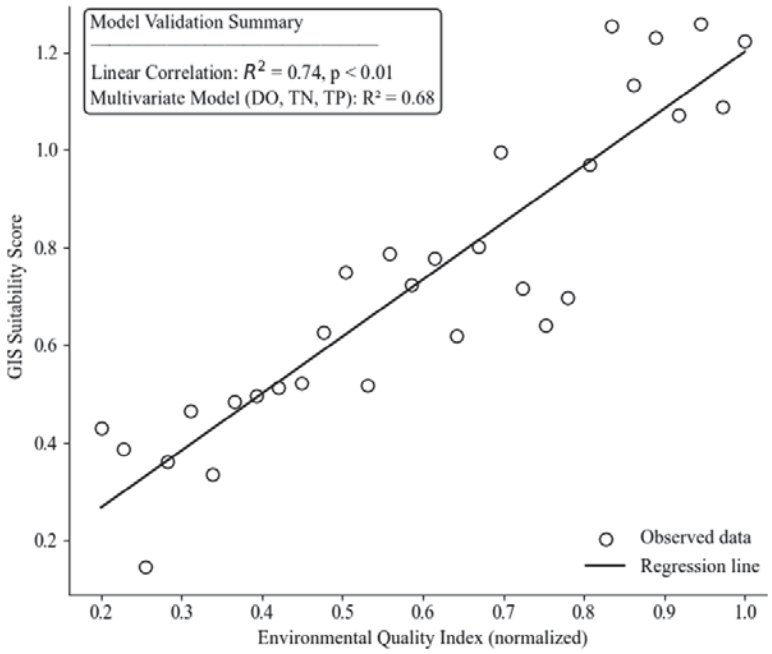

Fig. 6: GIS-based suitability model

(–25%) and greatest increases in chlorophyll-a (+41%), TN (+28%), and TP (+25%), reflecting synergistic interactions where loss of macrophyte-mediated nutrient buffering amplifies the effects of external nutrient inputs. These results indicate that nutrient enrichment drives primary production and nutrient accumulation, macrophytes modulate these processes through biotic control. Furthermore, the concurrent occurrence of both stressors intensifies ecosystem perturbation, resulting in significant oxygen depletion and accelerated eutrophication (Cross *et al.*, 2022). Tukey's post hoc tests confirmed that these differences among treatments were statistically significant ($p < 0.05$), underscoring the ecological relevance of these mechanistic interactions (Fig. 7).

PCA analysis

The analysis of environmental variables in inland lakes through PCA uncovered three principal axes that elucidate 78.5% of the total variance, underscoring the essential drivers of ecological variability and their mechanistic foundations. Principal Component 1 (PC1), accounting for 41.2% of the variance, was dominated by depth and area (positive loadings) and turbidity and electrical conductivity (negative loadings), indicating that larger and deeper lakes with clearer water and lower ionic concentrations score higher on this hydromorphological gradient. From a mechanistic perspective, lakes that are deeper and more voluminous generally exhibit longer water residence times and increased stratification. This phenomenon leads to a reduction in sediment resuspension and restricts the buildup of dissolved ions, consequently preserving greater water clarity and lower conductivity (Read *et al.*, 2015). Conversely, shallow or smaller lakes undergo more significant wind-induced mixing and sediment disturbance, resulting in elevated turbidity and ion concentrations (Wang *et al.*, 2015). Principal component 2 (PC2), representing 28% of the variance, was characterized by strong loadings of total nitrogen, total phosphorus, and chlorophyll-a, reflecting a nutrient enrichment gradient that drives primary productivity. Principal component 3 (PC3), responsible for 9.3% of the variance, was correlated with macrophyte cover and phytoplankton diversity, underscoring the significance of biotic structuring in influencing habitat complexity and community composition. Macrophytes act as nutrient sinks (West *et al.*, 2017), contribute to sediment stabilization, and create safe havens for diverse

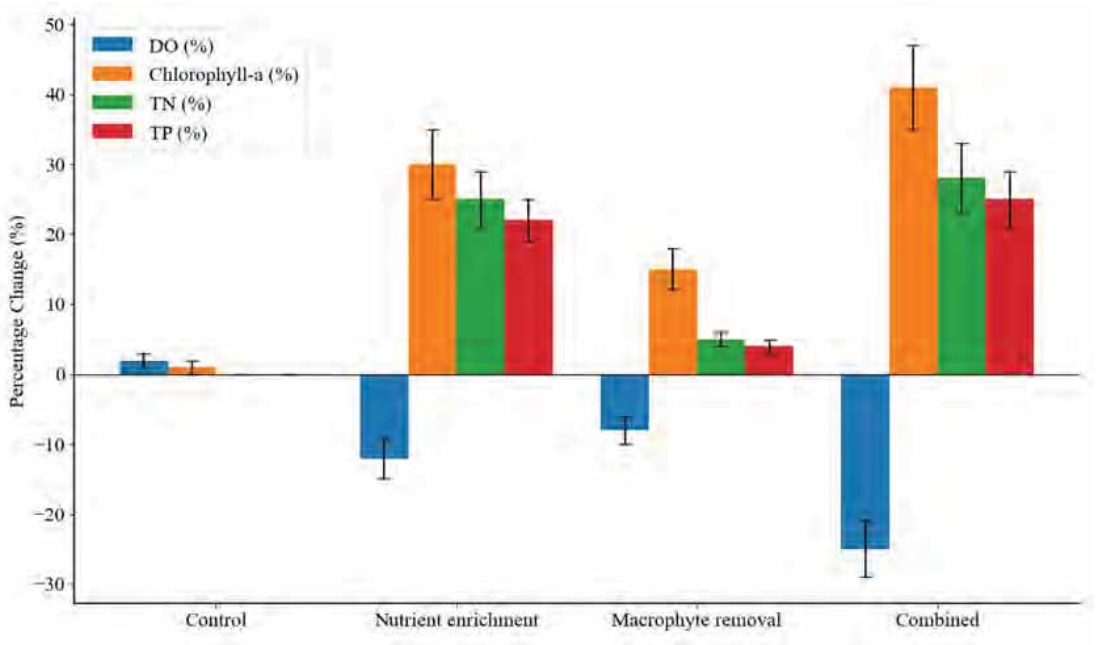

Fig. 7: microcosm experiments results

Table 3: PCA results for environmental variables of inland lakes

Principal component	Dominant variables (Loadings)	Interpretation / descriptor	Explained variance (%)
PC1 (Hydromorphology)	Depth (+), area (+), Ttrbidity (–), electrical conductivity (–)	Represents lake morphometry and water column clarity; larger, deeper lakes with lower turbidity and EC show higher scores.	41.2
PC2 (nutrient gradient)	TN, TP, Chlorophyll-a	Reflects nutrient enrichment and primary productivity gradient across lakes.	28
PC3 (biotic factor)	Macrophyte cover, phytoplankton diversity	Describes biotic structuring related to habitat complexity and community composition.	9.3
—	—	Total Variance Explained	78.5

phytoplankton and invertebrate assemblages, thereby alleviating the consequences of nutrient enrichment and bolstering ecosystem resilience (Zhang *et al.*, 2021). These PCA results indicate that lake ecological variability emerges from the interplay of hydromorphology, nutrient availability, and biotic interactions, where physical structure governs chemical gradients, and biological communities both respond to and regulate environmental conditions (Table 3).

CONCLUSION

This study demonstrates that integrating geographic information system-based suitability modeling with experimental validation provides a robust, reliable, and mechanistically informed framework for predicting environmental quality and aquaculture potential in inland lakes. By combining key physical, chemical, and biological variables into a multi-criteria scoring system, the GIS model effectively represented spatial variations in water quality and ecosystem health, facilitating a clear categorization of lakes into high, medium, and low suitability categories. The strong correlation between GIS-derived suitability scores and measured environmental indices ($R^2 = 0.74$, $p < 0.01$) confirms the predictive capacity of the approach and demonstrates how spatial modeling can efficiently

identify priority lakes for sustainable aquaculture or conservation, particularly in resource-limited regions where extensive field surveys may be impractical. Field validation has underscored that the depth of lakes, the load of nutrients, and the coverage of macrophytes are essential factors influencing ecological condition. High-suitability lakes exhibited well-oxygenated waters (DO 7.8 ± 0.9 mg/L), low nutrient concentrations (TP 0.045 ± 0.012 mg/L; TN 0.48 ± 0.11 mg/L), low turbidity (3.2 ± 0.7 NTU), and higher water clarity (Secchi depth 1.6 ± 0.3 m), supporting diverse phytoplankton communities dominated by diatoms and green algae. In contrast, low-suitability lakes were shallow, nutrient-rich, and turbid, with low dissolved oxygen (3.5 ± 0.7 mg/L) and high chlorophyll-a (56.7 ± 13.4 µg/L), favoring opportunistic cyanobacteria and filamentous algae and reducing species richness (8 ± 2 taxa). These patterns demonstrate that nutrient enrichment drives eutrophication and competitive exclusion within phytoplankton populations. Furthermore, physical attributes like depth and water clarity influence the ecological consequences of nutrient loading, providing key insights into mechanistic connections among morphometry, water chemistry, and ecosystem health. Microcosm experiments further elucidated the mechanistic effects of environmental stressors. The incorporation of nutrients enhanced both primary productivity and nutrient accumulation, while the partial extraction of macrophytes caused a moderate alteration in water quality. The combination of both stressors amplified dissolved oxygen depletion and promoted algal dominance, confirming that interactions between nutrient loading and vegetation loss exacerbate eutrophication. These results confirm the ecological significance of the variables included in the GIS model and highlight that the combination of spatial analysis with controlled experimental manipulations can reveal causative relationships that observational approaches alone may fail to identify. Future research should build on this integrated GIS and experimental framework to examine the temporal dynamics of lake suitability under changing climate and land-use pressures. Long-term surveillance may reveal seasonal and interannual variations in water quality, nutrient flows, and biological reactions, thus enhancing the understanding of ecosystem resilience in a more dynamic manner. Incorporating additional ecological and biogeochemical indicators, such as sediment nutrient release, microbial activity, trophic interactions, and macrophyte functional traits, would refine the predictive capacity and ecological relevance of GIS-based suitability models. Furthermore, broadening the methodology to include inland lakes in various regions characterized by differing climatic, hydrological, and land-use conditions would evaluate the scalability of the framework, inform regional policy development, and enhance evidence-based decision-making for sustainable aquaculture, freshwater resource management, and biodiversity conservation. This study demonstrates that linking geospatial modeling with empirical and experimental validation not only provides robust predictions of lake suitability but also delivers mechanistic insights into the drivers of ecosystem health. By synthesizing spatial, physicochemical, and biological data, this method facilitates focused management strategies, ranks lakes for sustainable aquaculture development, and establishes a transferable methodology for supporting long-term monitoring, policy formulation, and adaptive management in diverse freshwater ecosystems.

AUTHOR CONTRIBUTIONS

B. Doskenova, the corresponding author, contributed to the study conceptualization, supervised the research, and led the writing of the manuscript. I. Sedelnikov was responsible for the methodology development and data analysis. T. Lyssakova performed the formal analysis and interpretation of the results. G. Gordiyanova contributed to data curation and investigation. G. Rakhimzhanova assisted in data validation and investigation. D. Shugulova prepared the visualizations, maps, and figures. E. Abdrahmanov contributed to software analysis and data processing. Y. Pangaliyev participated in project administration, resource acquisition, and manuscript review.

ACKNOWLEDGEMENT

This study has been funded by the Committee of Science of the Ministry of Science and Higher Education of the Republic of Kazakhstan under Grant No. [BR28712227], “Development and implementation of high-tech solutions for monitoring, purification and rational use of water

resources of North Kazakhstan region to ensure public health". The grant supported all aspects of the work, including the investigation, data analysis, and preparation of the manuscript. Proofreading and final revisions of the manuscript were also funded by the aforementioned project.

CONFLICT OF INTEREST

The authors declare that there is no conflict of interest regarding the publication of this manuscript. In addition, ethical issues, including plagiarism, informed consent, misconduct, data fabrication and/or falsification, double publication and/or submission, and redundancy have been completely observed by the authors.

OPEN ACCESS

©2026 The author(s). This article is licensed under a Creative Commons Attribution 4.0 International License, which permits use, sharing, adaptation, distribution and reproduction in any medium or format, as long as you give appropriate credit to the original author(s) and the source, provide a link to the Creative Commons license, and indicate if changes were made. The images or other third-party material in this article are included in the article's Creative Commons license, unless indicated otherwise in a credit line to the material. If material is not included in the article's Creative Commons license and your intended use is not permitted by statutory regulation or exceeds the permitted use, you will need to obtain permission directly from the copyright holder. To view a copy of this license, visit: http://creativecommons.org/licenses/by/4.0/

PUBLISHER'S NOTE

GJESM Publisher remains neutral regarding jurisdictional claims in published maps and institutional afflictions.

☒ Negative AI Statement

The author(s) declared that no AI tools or services were used or not highly applied during the preparation of this work.

ABBREVIATIONS

%	Percent
°C	Degrees Celsius
°E	Degrees east (longitude)
°N	Degrees north (latitude)
ANOVA	Analysis of variance
APHA	American public health association
Chl-a	Chlorophyll-a
cm	Centimeter
DO	Dissolved oxygen
EC	Electrical conductivity
Fig.	Figure
GIS	Geographic Information Systems
ha	Hectare
km²	Square kilometer
L	Liter
m	Meter
m×m	Meter by meter (length × width)
mg/L	Milligrams per liter
mm	Millimeter
µg/L	Micrograms per liter
µS/cm	Microsiemens per centimeter
N	Nitrogen
NTU	Nephelometric turbidity unit
P	Phosphorus
PCA	Principal component analysis
PC1	Principal component 1
PC2	Principal component 2
PC3	Principal component 3
$p < 0.05$	Level of statistical significance (less than 5%)
R^2	Coefficient of determination
TN	Total nitrogen
TP	Total phosphorus

REFERENCES

Akinnigbagbe, A.E.; Popoola, S.O.; Oyatola, O.O.; Oghenede, E.K.; Nubi, O.A., (2025). Spatiotemporal patterns of water quality, nutrient dynamics and chlorophyll a concentration in Five Cowries Creek from 2022 to 2024. Discov. Water. 5: 63 **(21 pages)**.

Arumugam, T.; Kinattinkara, S.; Vellingiri, K.; C, A., (2025). A GIS-based assessment of groundwater quality and public health risks of heavy metals in Kannur, Kerala. Clean. Water. 4: 100113 **(13 pages)**.

Chandran, A.; Roy, P., (2024). Applications of geographical information system and spatial analysis in Indian health research: a systematic review. BMC Health Serv. Res., 24: 1448 **(21 pages)**.

Cieplok, A.; Krodkiewska, M.; Franiel, I.; Starzak, R.; Sowa, M.; Spyra, A., (2022). The Role of Habitat Protection in Maintaining the Diversity of Aquatic Fauna in Rural and Industrial Areas. Water. 14: 3983 **(23 pages)**.

Cross, W.F.; Hood, J.M.; Benstead, J.P.; Huryn, A.D.; Welter, J.R.; Gíslason, G.M.; Ólafsson, J.S., (2022). Nutrient enrichment intensifies the effects of warming on metabolic balance of stream ecosystems. Limnol. Oceanogr. Lett., 7: 332-341 **(10 pages)**.

Dang, H.; Lü, Y.; Wang, X.; Hao, Y.; Fu, B., (2025). Integrating species diversity, ecosystem services, climate and ecological stability help to improve spatial representation of protected areas for quadruple win. Geogr. Sustainability. 6: 100205 **(12 pages)**.

de Oliveira, V.T.; Teixeira, D.; Rocchi, L.; Boggia, A., (2023). Trends in sustainability assessment supported by geographic information systems: A bibliometric approach. Environ. Sci. Policy. 141: 117–125 **(9 pages)**.

Emmons, S.C.; Cashman, M.J.; Fanelli, R.M.; Pond, G.J.; Noe, G.B.; Woods, T.E.; Maloney, K.O., (2025). Stressor-driven changes in freshwater biological indicators inform spatial management strategies using expert knowledge, observational data, and hierarchical models. Ecol. Indic., 174: 113501 **(12 pages)**.

Kochanek, A.; Generowicz, A.; Zacłona, T., (2025). The Role of Geographic Information Systems in Environmental Management and the Development of Renewable Energy Sources—A Review Approach. Energies. 18: 4740 **(17 pages)**.

Kourgialas, N.N.; Ntislidou, C.; Kazila, E.; Filintas, A.; Voreadou, C., (2024). An Innovative GIS-Based Policy Approach to Stream Water Quality and Ecological Risk Assessment in Mediterranean Regions: The Case of Crete, Greece. Land. 13: 1801 **(11 pages)**.

Lan, J.; Liu, P.; Hu, X.; Zhu, S., (2024). Harmful Algal Blooms in Eutrophic Marine Environments: Causes, Monitoring, and Treatment. Water. 16: 2525 **(17 pages)**.

Lausch, A.; Bannehr, L.; Berger, S.A.; Borg, E.; Bumberger, J.; Hacker, J.M.; Heege, T.; Hupfer, M.; Jung, A.; Kuhwald, K.; Oppelt, N.; Pause, M.; Schrodt, F.; Selsam, P.; von Trentini, F.; Vohland, M.; Glässer, C., (2024). Monitoring water diversity and water quality with remote sensing and traits. Remote Sens., 16: 2425 **(13 pages)**.

Macaulay, S.J.; Jeppesen, E.; Riebesell, U.; Nejstgaard, J.C.; Berger, S.A.; Lewandowska, A.M.; Rico, A.; Kefford, B.J.; Vad, C.F.; Costello, D.M.; Wang, H.; Madge Pimentel, I.; Barcelos e Ramos, J.; González, J.; Spilling, K.; de Senerpont Domis, L.; Boersma, M.; Stockenreiter, M.; Meerhoff, M.; Vijver, M.G.; Kelly-Quinn, M.; Beklioğlu, M.; Matias, M.G.; Sswat, M.; Juvigny-Khenafou, N.P.D.; Fink, P.; Zhang, P.; Taniwaki, R.H.; Ptacnik, R.; Langenheder, S.; Nederstigt, T.A.P.; Horváth, Z.; Piggott, J.J., (2025). Addressing grand ecological challenges in aquatic ecosystems: how can mesocosms be used to advance solutions? Oikos. 2025 **(21 pages)**.

Mkilima, T., (2023a). Groundwater salinity and irrigation suitability in low Environ -lying coastal areas. A case of Dar es Salaam, Tanzania. Watershed Ecol.., 5: 173–185 **(13 pages)**.

Mkilima, T., (2023b). The irrigation suitability potential of an effluent treated by a pseudo-natural wetland. Water Environ. J., 37: 303–315 **(13 pages)**.

Moses, S.A.; Janaki, L.; Joseph, S.; Justus, J.; Vimala, S.R., (2011). Influence of lake morphology on water quality. Environ. Monit. Assess., 182: 443–454 **(12 pages)**.

Nunes, P.; Roland, F.; Amado, A.M.; Resende, N. da S.; Cardoso, S.J., (2022). Responses of Phytoplanktonic Chlorophyll-a Composition to Inorganic Turbidity Caused by Mine Tailings. Front. Environ. Sci., 9. **(14 pages)**.

Partelow, S.; Nagel, B.; Gentry, R.; Gephart, J.; Rocha, J., (2025). Archetypes of aquaculture development across 150 countries. Aquaculture. 595: 741484 **(15 pages)**.

Petriki, O.; Zervas, D.; Doulgeris, C.; Bobori, D., (2020). Assessing the Ecological Water Level: The Case of Four Mediterranean Lakes. Water. 12: 2977 **(11 pages)**.

Poikane, S.; Kelly, M.G.; Free, G.; Carvalho, L.; Hamilton, D.P.; Katsanou, K.; Lürling, M.; Warner, S.; Spears, B.M.; Irvine, K., (2024). A global assessment of lake restoration in practice: New insights and future perspectives. Ecol. Indic., 158: 111330 **(14 pages)**.

Read, E.K.; Patil, V.P.; Oliver, S.K.; Hetherington, A.L.; Brentrup, J.A.; Zwart, J.A.; Winters, K.M.; Corman, J.R.; Nodine, E.R.; Woolway, R.I.; Dugan, H.A.; Jaimes, A.; Santoso, A.B.; Hong, G.S.; Winslow, L.A.; Hanson, P.C.; Weathers, K.C., (2015). The importance of lake-specific characteristics for water quality across the continental United States. Ecol. Appl., 25: 943–955 **(13 pages)**.

Ruzieh, A.S., (2025). Advancing Middle East Construction Sustainability: A Framework for Addressing Logistics Challenges Through Solutions and Critical Success Factors. Sustainability. 17: 533 **(2 pages)**.

Schiemer, F.; Amarasinghe, U.S.; Simon, D.; Vijverberg, J., (2024). Sustainable aquatic resource management and inland fisheries in tropical Asia: Interdisciplinary and transdisciplinary approaches. Ambio. 53: 1050–1064 **(15 pages)**.

Tanyanyiwa, S.; Tongowona, G., (2023). Enhancing Food Security through Fisheries for Rural Communities around Lake Mutirikwi in Zimbabwe. In: Appiah-Opoku, S. (Ed.), Contemporary Rural Development Programs. IntechOpen. **(18 pages)**.

Van Meerbeek, K.; Jucker, T.; Svenning, J., (2021). Unifying the concepts of stability and resilience in ecology. J. Ecol., 109: 3114–3132 **(19 pages)**.

Wang, J.; Pang, Y.; Li, Y.; Huang, Y.; Luo, J., (2015). Experimental study of wind-induced sediment suspension and nutrient release in Meiliang Bay of Lake Taihu, China. Environ. Sci. Pollut. Res., PMID: 25728203 **(12 pages)**.

West, M.; Fenner, N.; Gough, R.; Freeman, C., (2017). Evaluation of algal bloom mitigation and nutrient removal in floating constructed wetlands with different macrophyte species. Ecol. Eng., 108: 581–588 **(8 pages)**.

Woźniacka, K.; Bickley, L.K.; Heal, R.D.; Maclean, I.M.D.; Hasan, N.A.; Haque, M.M.; Stentiford, G.D.; Early, R.; Devlin, M.; Tyler, C.R., (2025). Seeking environmentally sustainable solutions for inland aquaculture in Bangladesh. Environ. Challenges. 18: 101062 **(11 pages)**.

Xia, P.; Peng, J.; Gu, T.; Yu, S.; Xu, Z., (2025). Lake-related ecosystem services facing social–ecological risks. People Nat., 7: 734–751 **(18 pages)**.

Yin, L.; Wu, J.; Qin, X., (2025). Mapping the water-environment nexus for ecological sensitivity in Northern Jiangsu: Insights for sustainable ecosystem management. Desalin. Water Treat., 322: 101170 **(12 pages)**.

Zhang, You; Leung, J.Y.S.; Zhang, Ying; Cai, Y.; Zhang, Z.; Li, K., (2021). Agricultural activities compromise ecosystem health and functioning of rivers: Insights from multivariate and multimetric analyses of macroinvertebrate assemblages. Environ. Pollut., 275: 116655 **(11 pages)**.

AUTHOR (S) BIOSKETCHES

B. Doskenova, Ph.D., Instructor, GIS Technology Laboratory, Kozybayev Lab, Department of Science, M. Kozybayev North Kazakhstan university, 86 B, Pushkin Street, 150000, Petropavlovsk, Kazakhstan.
- Email: *bdoskenova@ku.edu.kz*
- ORCID: 0000-0001-7369-0987
- Web of Science ResearcherID: OTH-8502-2025
- Scopus Author ID: 57203825232
- Homepage: http://ku.edu.kz/page/view?id=2387&lang=en

I. Sedelnikov, M.Sc., Researcher, GIS Technology Laboratory, Kozybayev Laboratory, Department of Science, M. Kozybayev North Kazakhstan university, 86 B, Pushkin Street, 150000, Petropavlovsk, Kazakhstan
- Email: *igor_sko_kz_94@mail.ru*
- ORCID: https://orcid.org/0000-0001-9921-1825
- Web of Science ResearcherID: NA
- Scopus Author ID: 58000894400
- Homepage: http://ku.edu.kz/page/view?id=2387&lang=en

T. Lyssakova, Ph.D., Researcher, Department of Geography and Ecology of M.Kozybayev North Kazakhstan University, 86, Pushkin Street, 150000, Petropavlovsk, Kazakhstan
- Email: *tanya.lyss@mail.ru*
- ORCID: 0000-0002-1925-6570
- Web of Science ResearcherID:
- Scopus Author ID: NA
- Homepage: https://rjraap.com/0016-9900/article/view/639336

G. Gordiyanova, M.Sc., Instructor, Department of Geography and Ecology of M. Kozybayev North Kazakhstan University, 86, Pushkin Street, 150000, Petropavlovsk, Kazakhstan
- Email: *gordiyanova2010@mail.ru*
- ORCID: 0009-0009-5141-6093
- Web of Science Researcher ID: NA
- Scopus Author ID: NA
- http://ku.edu.kz/page/view?id=2387&lang=en

G. Rakhimzhanova, M.Sc., Instructor, Department of Pedagogy and History A.K. Kussayinov Eurasian Humanities Institute, 4 Zhumabaev Street, 010000, Astana, Kazakhstan
- Email: *gulnaz-rakhim@mail.ru*
- ORCID: https://orcid.org/ 0009-0004-8306-5367
- Web of Science ResearcherID: NA
- Scopus Author ID: NA
- Homepage: https://physics.itmo.ru/en/personality/gulnaz_rakhmanova

D. Shugulova, M.Sc., Instructor, GIS Technology Laboratory, Kozybayev Laboratory, Department of Science, M. Kozybayev North Kazakhstan university, 86 B, Pushkin Street, 150000, Petropavlovsk, Kazakhstan
- Email: *9970766@mail.ru*
- ORCID: 0000-0002-4935-4673
- Web of Science ResearcherID: NA
- Scopus Author ID: 58001327400
- Homepage: https://ma.yu.edu.kz/en/foundation-lang/smagulova-dina-saparovna/

AUTHOR (S) BIOSKETCHES

Abdrahmanov E., M.Sc., Instructor, GIS Technology Laboratory, Kozybayev Lab, Department of Science, M. Kozybayev North Kazakhstan University, 86, Pushkin Street, 150000, Petropavlovsk, Kazakhstan
▪ Email: *geo_geo20@mail.ru*
▪ ORCID: https://orcid.org/0009-0006-1801-9641
▪ Web of Science Researcher ID: NA
▪ Scopus Author ID: NA
▪ Homepage: https://www.ku.edu.kz/news/list?lang=en&News_page=20&bigVersion=&normalVersion=

Y. Pangaliyev, Ph.D., Acting Associate Professor, Department of Ecology and Safety, Faculty of Engineering, Yessenov University, 32nd Microdistrict, 1, 130000, Aktau, Kazakhstan.
▪ Email: *erbolpm@mail.ru*
▪ ORCID: 0000-0002-2392-4180
▪ Web of Science ResearcherID: MGB-2344-2025
▪ Scopus Author ID: 57191078212
▪ Homepage: https://eng.yu.edu.kz/en/pps-ekologiya/pangaliyev-yerbol/

HOW TO CITE THIS ARTICLE

Doskenova, B.; Sedelnikov, I.; Lyssakova, T.; Gordiyanova, G.; Rakhimzhanova, G.; Shugulova, D.; Abdrahmanov, E.; Pangaliyev, Y., (2026). Linking geospatial suitability modelling with experimental validation of aquatic environmental quality in inland lakes. Global J. Environ. Sci. Manage., 12(1): 393-408.

DOI: 10.22034/gjesm.2026.01.22

URL: https://www.gjesm.net/article_732106.html

Global J. Environ. Sci. Manage. 12(1): 409-430, Winter 2026, Serial #45

Global Journal of Environmental Science and Management
(GJESM)

Homepage: https://www.gjesm.net/

Podcasts

REVIEW PAPER

Sustainable solutions for entomoremediation organic waste into food and fertilizer using black soldier fly larvae

A.R.K. Kullan[1,*], E.G. Neumann[1], A. Suresh[2], H.L. Choi[2,3]

[1] *Department of Integrative Agriculture, United Arab Emirates University, Abu Dhabi, P.O. Box 15551 United Arab Emirates*

[2] *Research Center for Circular Agro–Animal Farming, Seoul 151–742 Republic of Korea*

[3] *Department of Agricultural Biotechnology, Research Institute for Agriculture and Life Sciences, Seoul National University, Seoul 151–742 Republic of Korea*

ARTICLE INFO

Article History:
Received 05 June 2025
Revised 10 September 2025
Accepted 23 October 2025

Keywords:
Black soldier fly larvae
Bioconversion
Circular economy
Entomoremediation
Insect–based bioprocessing
Organic fertilizer
Waste valorization

DOI: 10.22034/gjesm.2026.01.23

ABSTRACT

Black soldier fly larvae offer an innovative solution to the escalating global problem of organic trash, which adversely affects both ecosystems and economies. The black soldier fly, a non–pest dipteran belonging to the Stratiomyidae family, is a world leader in the breakdown of organic waste, converting it into useful residue and biomass. This study investigates the process by which black soldier fly larvae transform organic waste into valuable products, including protein-rich insect meal and nutrient-dense organic fertilizer. Further, the biology of black soldier fly larvae; *Hermetia illucens*, important bioconversion factors, larvae meal and frass production techniques was thoroughly examined. It also identifies gaps in scalability, regulatory harmonization, and substrate optimization, proposing black soldier fly larvae as a scalable circular economy model. Under optimal conditions, the efficiency and quality of the bioconversion process are enhanced, which includes maintaining temperatures between 27 and 30 degrees Celsius for best results, with survival capabilities from 15 to 47 degrees Celsius. Humidity should ideally be set at 60 to 70 percent, with tolerances that can reach 40 to 80 percent, along with specially formulated substrate mixtures. Black soldier fly larvae meal is a viable substitute for fishmeal or soybean meal in animal feeds since it contains 40–47 percent protein and 11.8–49 percent fat and it is rich in lysine (6–8 percent), threonine (3–5 percent), and valine (4–6 percent), which are vital for animal nutrition. Similarly, black soldier fly larvae frasstilizer outperforms conventional compost by providing richer nutrients and beneficial microbes in a shorter period (12–15 days). Frass provides micronutrients including iron, zinc, nitrogen, phosphorus, potassium, calcium, and magnesium. By converting organic waste into valuable assets, the technology of black soldier fly larvae promotes a circular economy, alleviating environmental impact while aiding agriculture, livestock, pets, and aquaculture. To enhance maximum material recovery and minimize environmental effects, black soldier fly larvae can be combined with other waste management techniques like anaerobic digestion or composting. Further studies should be carried out to discover potential black soldier fly larvae strains that demonstrate high bioconversion efficiency and to advance these strains via a selective breeding strategy.

This is an open access article under the CC BY license (http://creativecommons.org/licenses/by/4.0/).

NUMBER OF REFERENCES	NUMBER OF FIGURES	NUMBER OF TABLES
107	7	4

*Corresponding Author:
Email: *anand_k@uaeu.ac.ae*
Phone: +97582586220
ORCID: 0009–0008–0799–9968

Note: Discussion period for this manuscript open until Mar 1, 2026 on GJESM website at the "Show Article".

INTRODUCTION

The global waste management system faces mounting challenges as the world's population is projected to reach 9.7 billion by 2050 (United Nations, 2019), driving the need for resource–efficient solutions to mitigate environmental degradation. Organic waste, including food scraps (1.3 billion tonnes annually (FAO, 2011), agricultural residues, and animal manure (13–15 billion tonnes yearly, Rehman *et al*., 2023), is a major contributor to greenhouse gas emissions, as well as water and air pollution, and biodiversity loss, leading to economic and environmental costs that surpass $US 1.6 trillion annually (FAO, 2014; Yang *et al*., 2023). Traditional methods like landfilling, incineration, composting, and anaerobic digestion often fail to recover valuable nutrients, demand high energy inputs, or generate pollutants like methane, which accounts for 8–10percent (%) of global emissions (IPCC, 2019; FAO, 2013). Composting has its advantages, yet it necessitates a period of 2 to 6 months and may lead to nutrient leaching (Pour *et al.,* 2021). Additionally, anaerobic digestion fails to address protein valorization (Lopes *et al.,* 2020).Recently, Entomoremediation using black soldier fly larvae (BSFL), *Hermetia illucens*) addresses these gaps by rapidly converting organic waste into protein–rich insect meal and nutrient–rich frass fertilizer, termed "frasstilizer" for its superior nutrient profile and faster production compared to compost (Kullan *et al*., 2024; Cadinu *et al*., 2020). Extensive studies have been carried out using BSFL (Fig. 1) and have successfully reduced waste by 50–80% over a period of 12–15 days, outperforming standard techniques. This process also generates sustainable feed and fertilizer, thereby decreasing dependence on resource-intensive fishmeal and synthetic fertilizers (Peguero *et al*., 2021; Hall *et al*., 2021; Beesigamukama *et al*., 2021a). Compared to house flies or mealworms, BSFL's (Fig. 2) voracious appetite and pathogen suppression make them uniquely effective (Amrul *et al*., 2022). Even with these benefits, challenges persist in enhancing bioconversion efficiency for various substrates, developing systems that cater to both commercial and decentralized applications, overcoming regulatory and cultural hurdles, and examining genetic or epigenetic factors (including digestive enzyme genes and stress response pathways) to improve larval resilience to environmental stressors and diverse substrates via comparative genomics (Smetana *et al*., 2019). This study consolidates developments in BSFL entomoremediation post-2020, thoroughly analyzing bioconversion efficiency, substrate optimization, and the incorporation of technologies like anaerobic digestion to address global food security and climate challenges. This study enhances sustainable waste management and circular economy models in agriculture (Fig. 3) by pinpointing research gaps in scalability, regulatory harmonization, and consumer acceptance. It builds upon previous reviews (Amrul *et al.,* 2022; Rehman *et al.,* 2023) to suggest practical solutions for both developed and developing regions. This study was conducted in Abu Dhabi, United Arab Emirates, in 2025.

METHODOLOGY

This narrative study synthesizes peer–reviewed literature on entomoremediation using BSFL (*Hermetia illucens*) to convert organic waste into insect meal and organic fertilizer, aligning with circular economy principles. A comprehensive literature search was conducted in April 2025 across Scopus, Web of Science, PubMed, and Google Scholar using search terms such as "black soldier fly" and organic waste". No publication year restrictions were applied to capture foundational and recent studies (1994–2024). More sources were identified via citation analysis of citations from influential publications (Sheppard *et al*., 1994; Gold *et al*., 2018). The inclusion criteria highlighted the importance of peer-reviewed articles published in English, which are found in reputable databases. These articles should address topics such as BSFL biology, bioconversion efficiency, substrate optimization, meal and frass production, as well as the environmental and economic impacts, and scalability, including the potential for automated or AI-based process control. (Chia *et al*., 2018). Non-peer reviewed materials, publications from predatory journals, studies not conducted in English, and articles irrelevant to waste valorization were excluded based on the criteria. Quality assessment ensured sources were from indexed journals with rigorous peer review. This process ensured a robust synthesis of high–quality, relevant literature.

Organic waste crisis: challenges and the rise of BSFL bioconversion

Food scraps, agricultural waste, animal dung,

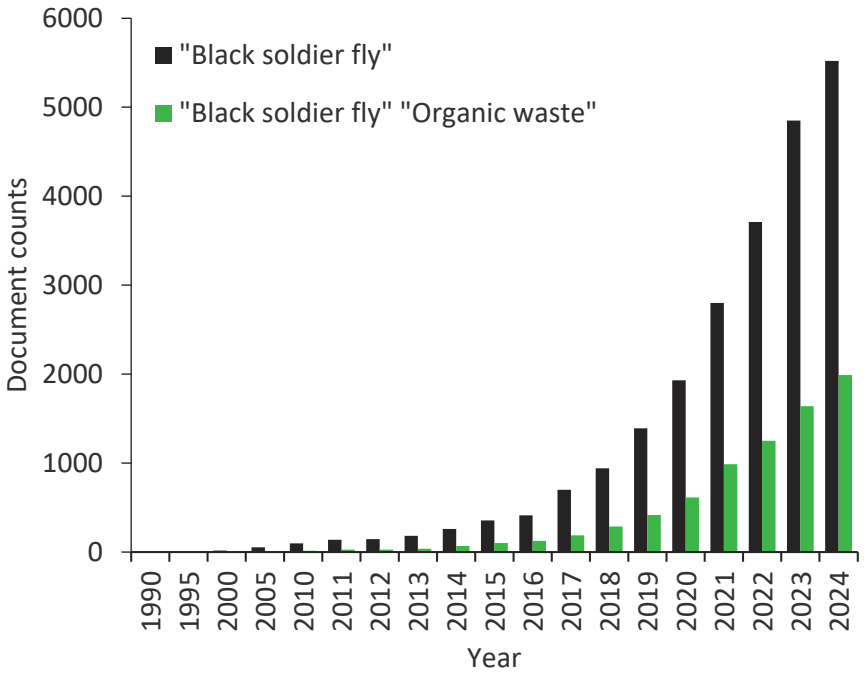

Fig. 1: Number of documents counts on "Black soldier fly" and "Black soldier fly and Organic waste" (combined) for theperiod of 1990–2024 from the Google scholar database using custom range, accessed 28th April 2025



Fig. 2: Black soldier fly (*Hermetia illucens*) and its larvae (Source: authors unpublished figures)

and by–products from agro–industry contribute significantly to the global issue of organic waste posing threats to both economies and ecosystems. Annually, agriculture produces 140 billion tons of biomass, much of which is wasted. Furthermore, 1.3 billion tons of food waste, equating to about one-third of the world's total production, is lost or discarded each year (FAO, 2011; UNEP, 2021). Every year, 13–15 billion tonnes of manure are added by livestock (Rehman *et al*., 2023). In developed countries, food waste is prevalent at both retail and consumer stages, with North Americans and Europeans discarding between 95 to 115 kilograms per year (kg/y). Conversely, in developing regions like sub–Saharan Africa, significant losses occur early in the production phase, resulting in only

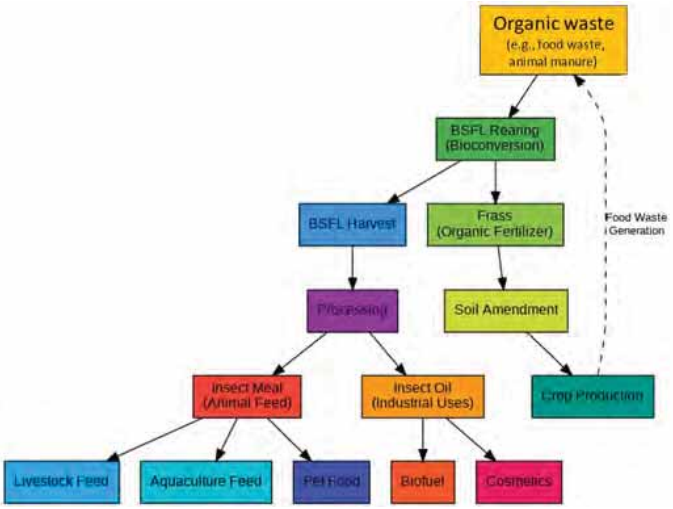

Fig. 3: BSF larvae bioconversion cycle and applications – Shows the complete cycle from organic waste through BSFL processing to end products (insect meal, oil, and frass) and their applications

6 to 11 kg wasted per person (UNEP, 2021). The financial implications of this waste are substantial, amounting to United States Dollar ($US) 900 billion in societal costs, $700 billion in environmental damage, and $US 1 trillion in direct economic losses (FAO, 2014). The presence of organic waste is detrimental to the environment since it generates methane, a gas that is 25 times more powerful than carbon dioxide, from rotting landfill waste, which is responsible for 8–10% of global greenhouse gas emissions (IPCC, 2019). Burning agricultural leftovers deteriorates the land and air, while manure discharge causes eutrophication and water pollution (Xiao *et al*., 2018). Furthermore, food waste plays a significant role in the decline of biodiversity, utilizing 1.4 billion hectares of land–around 30% of the global agricultural area and consuming 250cubic kilometres(km^3) of freshwater (FAO, 2013). Traditional approaches to organic waste management are inadequate. Landfilling is widely used, but it is an unsustainable approach that results in nutrient loss and the production of leachate and methane. Incineration can release pollutants by burning organic waste, but it also recovers energy (Bhatia *et al*., 2024). Even though composting plays a vital role, it can take anywhere from two to six months and may cause nutrient loss through leaching (Gold *et al*., 2018). Anaerobic digestion produces liquid fertilizer and biogas, but it requires expensive infrastructure. An innovative method to these challenges is the use of bioremediation with BSFL. These larvae can consume organic waste equivalent to twice their body weight each day, decreasing waste volume by 50–80% in merely 12–15 days. They consume a variety of organic wastes, from food wastes to manure, at an astounding pace (Diener *et al*., 2011; Shao *et al*., 2023; Santoso*et al*., 2023). In alignment with the principles of the circular economy, BSFL bioconversion process yields two advantages: a protein–rich larval biomass suitable for animal feed, and nutrient–enriched frass that can be utilized as organic fertilizer. Moreover, BSFL bioconversion minimizes infection transmission by eradicating pathogens, which in turn improves the safety of organic waste (Lalander *et al*., 2015). In contrast to conventional approaches, it minimizes environmental damage while optimizing resource recovery and converting waste into useful goods. While anaerobic digestion recovers energy, it overlooks protein valorization; BSFL uniquely addresses this gap by producing high–value meal, reducing reliance on overfished resources (Lopes *et al*., 2020). Incorporating BSFL into waste management systems can tackle the problem of organic waste, reduce emissions, and promote sustainable practices in agriculture and aquaculture. This will pave the way for a more resource–efficient and environmentally friendly future.

Table 1: Bioconversion parameter of organic waste into insect meal and organic fertilizer using BSFL

Parameter	Optimal range	Effects on bioconversion	Sources
Temperature	15–47°C	Becomes active at 25°C, mating occurs at 27°C, egg–laying at 27.5–37.5°C, development inhibited below 20°C, Substrate temperatures can rise to 45°C during bioconversion	Peguero *et al*., 2021; Belperio *et al*., 2024
Humidity	40–80%	Supports mating and oviposition, best bioconversion at 75–85% relative humidity, Critical for larval survival and development	Siddiqui *et al*., 2024; Amrul *et al*., 2022
Potential of hydrogen (pH)	6–7	Proteolytic activity enhanced around pH 8, Changes during bioconversion as larvae modify substrate	Klammsteiner *et al*., 2020; Lopes *et al*., 2024
Larval Density	2–5 larvae per square centimeter (cm^2)	Affects growth rate and bioconversion efficiency, Overcrowding leads to competition and reduced performance	Belperio *et al*., 2024; Amrul *et al*., 2022
Substrate Composition	Varies by waste type	High protein/fat content improves growth, Vegetable–only diets result in reduced growth– Omnivorous diets provide optimal performance, High lignin/cellulose content shows poor digestibility	Belperio *et al*., 2024; Peguero *et al*., 2021
Feeding Rate	100–200 mg/larva/day	Underfeeding reduces growth and development; Overfeeding leads to anaerobic conditions and odor issues	Lopes *et al*., 2024; Amrul*et al*., 2022
Aeration	Passive to moderate	Affects microbial community composition, Influences decomposition rate, Impacts odor development	Klammsteiner *et al*., 2020; Siddiqui *et al*., 2024

BSFL Biology and Bioconversion Science

The BSF (Fig. 2), a non–pest dipteran belonging to the Stratiomyidae family, is a world leader in the breakdown of organic waste, converting it into useful residue and biomass. Originally native to the Americas, now found in tropical, subtropical, and temperate regions. Adult BSFs are 15–20 millimetres (mm) in size, have short antennae, vestigial mouthparts, and a striking black body with a metallic blue–green shine and distinctive transparent abdominal windows that resemble wasps but are harmless, neither sting nor bite (Sheppard *et al*., 1994; Gold *et al*., 2018). Fig. 4 depicts the entire lifecycle, showcasing the stages from eggs to larvae, prepupae, pupae, and finally adults, along with the ideal environmental conditions and harvesting times. Table 1 shows the optimum parameter for bioconversion of organic waste into insect meal and organic fertilizer using BSFL. Under optimal conditions of 27–30 degrees Celsius (°C) (survival from 15–47°C), and 60–70% humidity (tolerance up to 40–80%), their larvae, the stars of bioconversion, grow from 1 mm cream–colored hatchlings to 18–25 mm dark prepupae across six instars, growing over 4,000 times their initial weight in 14–22 days, some studies say 10,000 times (Manna Insect, 2025). Spanning 38 to 45 days, the lifecycle of the BSF begins with the egg stage, which persists for 3 to 4 days and produces between 400 and 800 eggs per clutch. This is followed by the larval stage, then the pupal stage lasting 8 to 14 days, and ultimately the adult stage, which spans 5 to 14 days, thus concluding the lifecycle (Sheppard *et al*., 1994; Cannella*et al*., 2016). Adults who live for a short time place a high priority on reproduction. They mate in flight under specific conditions with 200 micromolar per square meter per second (µmol/m^2/s) light, 26–32°C), with females placing their eggs in the crevices near decomposing materials to shield them from moisture and predators. Larvae ceaselessly consume a variety of organic materials, such as manure and food scraps, breaking down complex molecules with the help of enzymes like amylases and proteases to reduce waste volume, aerate substrates, and inhibit pathogens (Kullan *et al*., 2024; Bruno *et al*., 2025a). Spanning 38 to 45 days, the lifecycle of the BSF begins with the egg stage, which persists for 3 to 4 days and produces between 400 and 800 eggs per clutch. This is followed by the larval stage, then the pupal stage lasting 8 to 14 days, and ultimately the adult stage, which spans 5 to 14 days, thus concluding the lifecycle (Wynants *et al*., 2019). Inoculating substrates with beneficial microbial consortia (e.g., lignocellulose-degrading bacteria) can boost BCE by 5–8% (Shao *et al*.,2023). Due to their swift breakdown encouraged by this feeding frenzy, larvae are ideal for managing organic waste. Through chemical deterrent, BSFs outcompete other flies like house flies in natural settings by enhancing nutrient cycling in compost

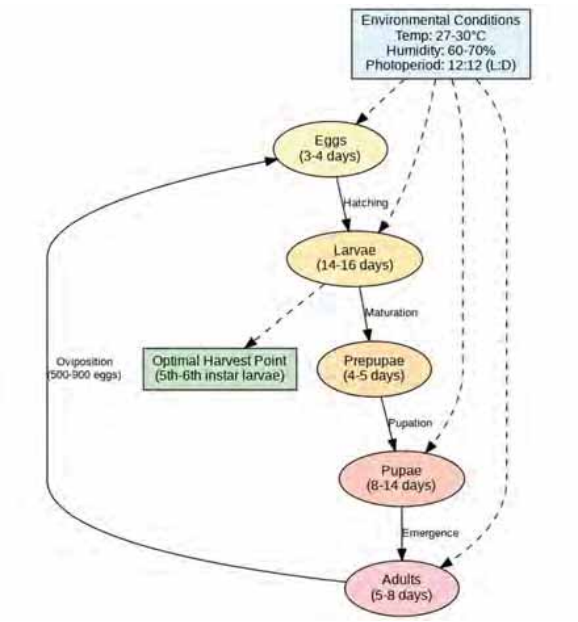

Fig. 4: BSF life cycle and development stages – Illustrates the complete lifecycle from eggs through larvae, prepupae, pupae, to adults, including optimal environmental conditions and harvest points

and manure heaps (Sheppard *et al*., 1994; Zheng *et al*., 2025). While the larvae can exist on a range of substrates because of their polyphagous traits and effective digestive systems, high-protein meals are beneficial for their growth and the quality of biomass. By decreasing trash and generating nutrient–rich frass and protein–rich larvae, BSFs exemplify the concepts of the circular economy and provide a scalable, sustainable solution to the problems associated with organic waste while promoting environmental health and agriculture (Kullan *et al*., 2024; Phl *et al*.,2020; Rehman *et al*., 2023).

To efficiently direct nutrients into their growing bodies, the bioconversion process is contingent upon the larvae's exceptional ability to absorb and process organic materials. It is a sophisticated ecosystem with larvae, substrate, and bacteria that goes beyond simple ingestion. Substrate bacteria speed up decomposition and improve food availability. Simultaneously, larvae consume and aerate the waste through their movement, secrete digestive enzymes, and generate antimicrobial compounds that suppress pathogens (Gold *et al*., 2018). Metrics like the feed conversion ratio (FCR), which indicates how much feed is required for every unit of larval biomass, and the bioconversion efficiency (BCE), which calculates the proportion of waste dry matter that is transformed into larval biomass, are used to quantify efficiency (Eriksen, 2024). Table 2 shows the BSFL bioconversion parameters against various organic waste. For instance, mixed food waste results in a remarkable waste reduction of 55–80%, whereas fish processing waste outperforms commercial chicken feed with an FCR as low as 2.09 (Gold *et al*., 2018; Tirtawijaya *et al*., 2024). Protein–rich substrates with high BCE values of 18–24% may be found in restaurant waste (Nyakeri *et al*., 2017; Shumo *et al*., 2019). This active engagement positions BSFL as an eco-friendly solution that converts waste into valuable resources within the scope of a circular economy (Parra–Pacheco *et al*., 2025).

The quality and effectiveness of BSFL bioconversion depend on several important factors. Although larvae may survive between 15 and 47°C, temperature ideally between 27 and 30°C drives their metabolism, eating, and growth. Development slows down below 20°C, and mortality increases Past35°C (Chia *et al*., 2018). Diener *et al*. (2011) reported 70% waste reduction in tropical conditions, while Lalander *et al*. (2019) observed 45% in colder

Table 2: Waste reduction percentage, FCR, BCE of organic waste treatment by BSFL and protein and fat content of produced BSFL meal

Substrate type	Waste reduction (WR)	FCR	BCE (%)	BSFL Protein (%)	BSFL Fat (%)	Sources
Food waste (Mixed)	55–80	3.3–4.8	15–28	42–45	28–35	Gold *et al*., 2018; Diener *et al*., 2011; Peguero *et al*., 2021; Belperio *et al*., 2024
Fruit and vegetable waste	45–55	6.1–10.4	8–12	37–42	20–26	Jucker *et al*., 2017; Lalander *et al*., 2019; Klammsteiner *et al*., 2020; Amru *et al*., 2022
Restaurant waste	60–75	3.1–4.2	18–24	43–46	30–38	Nyakeri *et al*., 2019; Shumo *et al*., 2019; Belperio *et al*., 2024; Amrul *et al*., 2022
Poultry litter	46–50	3.47–4.2	5.6–8.9	41.1–42	30–35	Kullan *et al*., 2025; Beesigamukama *et al*., 2021b; Shumo *et al*., 2019; Sheppard, 1994
Dairy manure	40–58	6.7–10.2	4.0–6.5	30–42	20–30	Miranda *et al*., 2019; Liu *et al*., 2018; Myers *et al*., 2008; Li *et al*., 2011; Rehman *et al*., 2017
Swine manure	39–42	7.8–11.2	3.5–5.8	34.7–53.4	12.9–31.8	Xiao *et al*., 2018; Lalander *et al*., 2015; Diola *et al*., 2024; Newton *et al*., 2005; Boafo *et al*., 2023
Fish waste	73.5	2.09	3.2–14.4	42.7–52.6	37.7–46.7	Tirtawijaya *et al*., 2024; Ewald, 2020
Brewery Waste	50–68	4.3–5.7	10–16	43–47	25–30	Chia *et al*., 2018; Klammsteiner *et al*., 2020; Peguero *et al*., 2021
Coffee By products	48–55	5.2–7.8	9–14	33.5–42.1	17.2–24.7	Permana *et al*., 2020; Surendra *et al*., 2016; Fischer *et al*., 2021
Chicken Feed (Control)	65–70	2.5–3.0	20–25	45–48	32–36	Diener *et al*., 2009; Tschirner and Simon, 2015; Belperio *et al*., 2024; Peguero *et al*., 2021

climates. To avoid anaerobic conditions and ensure proper feeding, maintaining humidity levels between 60% and 70% and substrate moisture between 40% and 80% is crucial. Results are strongly influenced by the composition of the substrate for example, larvae produced from protein–rich substrates, such as fish waste, have a higher protein content than larvae produced from fruit and vegetable waste, and efficiency is increased by an ideal carbon–to–nitrogen (C:N) ratio of 15:1 to 25:1 (Lalander *et al*., 2019). Physical characteristics that facilitate decomposition involve smaller particle sizes resulting from grinding, which increase the surface area available for microbial and larvae activity. While feeding rates of 100–200 mg dry substrate per larva prevents overfeeding or underfeeding, larval density, ideally 2.5–5 larvae/ cm^2, balances resource competition (Cattaneo*et al*., 2024; Ursada *et al*., 2025). The movement of larvae and, at times, enforced systems contribute to sustaining aerobic conditions via aeration, whereas water activity levels (0.80–0.95) encourage microbial growth and feeding. Substratum–specific performance varies swine manure lags at 3.5–5.8% BCE, while chicken litter achieves 46–50% waste reduction and 5.6–8.9% BCE (Kullan *et al*., 2024; Xiao *et al*., 2018). BCE, ranges from 18–24% for protein–rich substrates (e.g., restaurant waste) to 3.5–8.9% for manures (Nyakeri *et al*., 2017; Kullan *et al*., 2024). Substrate composition significantly influences larval metabolism. Ideal carbons to nitrogen ratios (15:1–25:1) promote protein synthesis, whereas pH levels (6–8) and moisture content (60–80%) facilitate enzyme activity and microbial interactions. (Liu *et al*., 2022). Seasonal variations (e.g., colder climates reducing BCE by 10–20%) necessitate adaptive rearing models (Lalander *et al*., 2019). For lignocellulosic materials (such as residues), pre-treatments like grinding, microbial inoculation, or enzymatic hydrolysis enhance digestibility, achieving BCE of 5–10% compared to 3–5% without pre-treatment (Shao *et al*., 2023). To maximize BSFL bioremediation of organic waste, optimization and selective pre-treatments are crucial. These processes reduce particle size and ensure nutrient balance. Employing

physical pre-treatments such as shredding, grinding, or mixing waste streams effectively optimizes C:N ratios. Digestibility is improved by chemical pre–treatment, such as raising the pH to 6.0–8.0 or adding nitrogen for high–carbon substrates (Raeiszadeh *et al*., 2025). To maximize the results of bioconversion, these variables must be precisely managed (Ogello *et al*., 2025).Optimization techniques include creating substrates for optimal nutrition, keeping environmental conditions constant, and keeping an eye on variables like temperature, moisture content, and larvae growth to modify feeding regimens (El–byari and Amraoui, 2025).Pig manure processing has shown that biological pre-treatment's, such as co–conversion with fungi or microbial inoculation with cellulose–degrading bacteria, increase nutritional availability (Rehman*et al*., 2023; Shao *et al*., 2023). Increased recirculation can lead to a higher risk of metabolite build-up, but the addition of beneficial microorganisms and enzymes, combined with the recirculation of 10–20% of fresh frass batches, supports larval growth and efficiency (Somroo *et al*., 2019). Performance varies, with manures performing lower, chicken litter performing moderately, and restaurant waste performing higher (Nyakeri *et al*., 2017; Kullan *et al*., 2024). When scaling to commercial systems, it is essential to thoroughly address the above factors along with system size and substrate variability. Through the integration of these tactics, BSFL entomoremediation provides an environmentally sustainable and scalable method of managing organic waste, generating valuable resources for aquaculture and agriculture while minimizing its negative effects on the environment (Ghazali *et al*., 2021).

Insect meal from BSFL: A sustainable feed revolution

The multi-phase technique involved in creating insect meal from organic waste with the aid of BSFL. As depicted in Fig. 5, the comprehensive production process of BSFL spans from harvesting to packaging, showcasing different methods at each phase. For optimal biomass and nutrition, harvesting focuses on late larval or prepupal stages. Techniques include mechanical separation with manual sieves and vibrating screens, or self–harvesting, in which prepupae naturally travel to dry pupation locations via ramps or channels (Giannetti *et al*., 2022; Gold *et al*., 2018). Harvested larvae washed with water and killed as soon as possible to preserve nutrient quality by blanching in hot water with 100°C, 1–2 minutes (min.), that reduces bacteria or freezing at –20°C

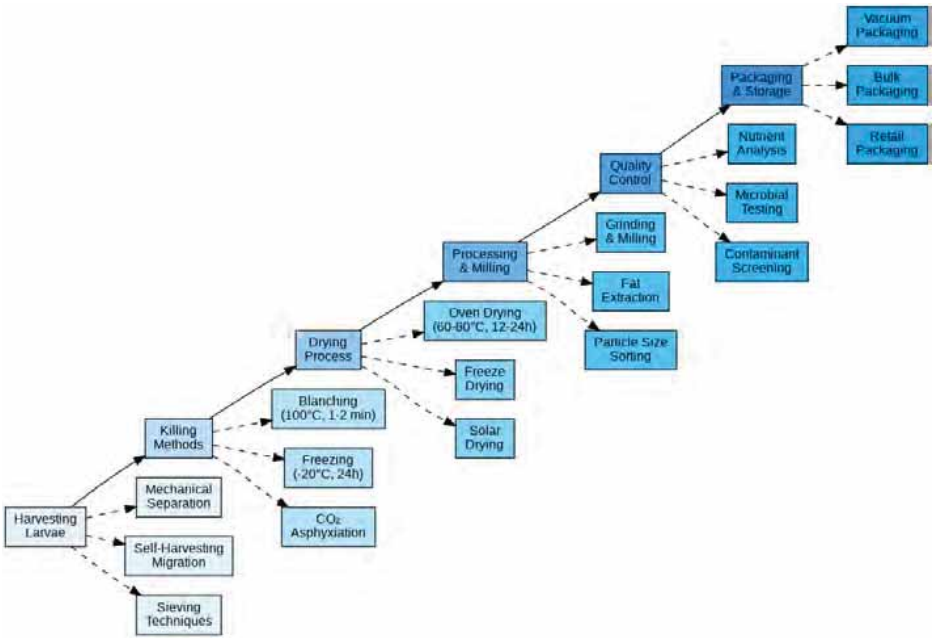

Fig. 5: BSFL meal production process – shows the complete production process from harvesting through killing, drying, processing, quality control, and packaging, with various methods for each stage.

Table 3: Nutritional comparison of BSFL insect meal with traditional fishmeal and soybean meal

Nutrient	BSFL meal (%)	Fishmeal (%)	Soybean meal (%)	Sources
Crude protein	40–47	60–72	44–48	Belperio *et al.*,2024; Astuti and Wiryawan, 2022
Crude fat	11.8–49	8–12	1–2	Belperio *et al.*,2024; Siddiqui *et al.*,2024
Crude fiber	7–12	0.5–1	3–6	Amrul *et al.*, 2022; Astuti and Wiryawan, 2022
Ash	4.85–15.9	10–20	5–7	Belperio *et al.*,2024; Lopes *et al.*,2024
Lysine	2.1–2.4	4.5–5.0	2.5–3.0	Astuti and Wiryawan, 2022; Siddiqui *et al.*,2024
Methionine	0.7–0.8	1.5–2.0	0.6–0.7	
Threonine	1.3–1.5	2.5–3.0	1.7–1.9	
Arginine	2.0–2.3	3.5–4.0	3.0–3.5	
Lauric acid (C12:0)	40–49	0.1–0.2	0.0–0.1	Belperio *et al.*,2024; Astuti and Wiryawan, 2022
Myristic acid (C14:0)	6–8	6–8	0.1–0.2	
Palmitic acid (C16:0)	8–10	15–18	10–12	
Oleic acid (C18:1)	6–8	10–15	20–25	

or carbon dioxide (CO_2) asphyxiation which offers humane substitute. In certain instances, the collected larvae may be deprived of food for a day to cleanse the gut residue, thereby enhancing the product's quality. Following the killing process, the stabilization of BSFL larvae can be achieved through various drying methods, including oven drying at temperatures between 60 and 80°C for duration of 12 to 24 hours, cost–effective solar drying which is dependent on weather conditions, microwave drying, or nutrient–preserving freeze–drying to attain moisture content of 5 to 10%. In conclusion, hammer mills transform BSFL into a rough meal suitable for animal feed, while ball or pin mills generate smaller particles meant for aqua feed, with particle size impacting digestion. These processes are tailored to scale and application, ensuring the production of high–quality BSFL meal (Belghit *et al.*, 2019). These processes are scalable and application–adapted and guarantee high–quality BSFL meal manufacture.

The nutritional composition of BSFL meal is comparable to that of traditional protein sources (Table 3), containing 40–47% crude protein, which is similar to soybean meal (44–48%) and approaches the levels found in fishmeal (60–72%), along with a lipid content that ranges from 11.8% to 49%, depending on the diet and whether it has been defatted (Devic *et al.*, 2018). Its amino acid profile is strong, particularly rich in lysine (6–8%), threonine (3–5%), and valine (4–6%), which are vital for animal nutrition, especially when raised on protein–dense substrates such as fish waste (Renna *et al.*, 2017). The fatty acid composition includes lauric acid (20–45%), palmitic acid (10–20%), and oleic acid (10–30%), which can be adjusted according to the substrate employed. Crucial biochemical pathways, including protein synthesis and lipid accumulation (through the process of fatty acid synthesis), can impact meal quality, offering chances for improvement by altering the substrate C:N ratio. (Liu et al., 2022).BSFL meal also provides essential minerals like calcium (5–8%), phosphorus (0.6–1.5%), and zinc (0.01–0.03%), which can lessen the requirement for additional supplements, along with bioactive compounds like chitin (5–9%) that contribute to immune health and antimicrobial properties (Cummins *et al.*, 2017). To ensure safety of BSFL, heat treatments reduce pathogens such as *Salmonella*, and research indicates minimal bioaccumulation of heavy metals like cadmium when the substrates are properly cleaned (van der Fels–Klerx *et al.*, 2016). Extended feeding trials are essential to evaluate the effects of BSFL meal on the

productivity of livestock, poultry, and aquaculture, thereby validating its cost-effectiveness in comparison to fishmeal (priced at $US1,500–2,000 per ton) and soybean meal. (Tadesse, 2023). Nonetheless, the risk of allergic responses, linked to the resemblance of chitin with allergens in crustaceans, demands vigilant oversight, and the elevated lipid levels necessitate the incorporation of antioxidants and vacuum packaging to ensure longevity (Bosch *et al*., 2016).

It has been shown that BSFL meal can be used to replace fishmeal in the diet of Atlantic salmon, tilapia, and Pacific white shrimp by up to 50%, 100%, and 75%, respectively, while maintaining growth rates (Belghit *et al*., 2019; Devic *et al*., 2018; Cummins *et al*., 2017). In laying hens, adding 5–10% of BSFL meal improves the quality of their eggs, whereas in broilers, adding 5–15% improves their performance (Dabbou *et al*., 2018; Marono *et al*., 2017; Saidani *et al*., 2025). Pigs can eat 5–10% BSFL meal in place of soybean meal without harm (Spranghers *et al*., 2018). In the pet food industry, especially for dogs and exotic pets, BSFL (5–20%) is recognized for its palatable flavor and hypoallergenic properties (Bosch *et al*., 2016). Though nascent, BSFL protein isolates and oils are being approved in regions like the Europeans (EU) where dried larvae are sold as snacks. Contaminant management is critical for feed safety. BSFL can bioaccumulate heavy metals (e.g., cadmium, lead) from contaminated substrates, with levels up to 0.1–0.5 mg/kg in meal from municipal waste (Diener *et al*., 2015). Pesticides and antibiotics might linger in larvae, but techniques like drying and defatting can lower residue levels by 50–70% (Charlton *et al*., 2015). Microplastics are not metabolized but can accumulate in larvae (0.01–0.05% by weight), necessitating substrate screening and monitoring protocols to ensure compliance with feed safety standards (e.g., EU Regulation 2017/893) (Purschke *et al*., 2017). Future studies need to determine safe limits for contaminants and devise swift detection techniques to boost the safety and marketability of BSFL meal. Regulatory hurdles persist globally, but BSFL meal's versatility, sustainability, and nutritional prowess position it as a game–changer for animal and potentially human diets, reducing reliance on resource–intensive feed sources. In addition to animal feed, the recent EU approvals for BSFL protein isolates indicate a promising opportunity for human nutrition, although further research is needed to assess allergenicity (Larouche *et al*., 2023).

BSFL frass: A nutrient–rich organic frasstilizer revolution

The byproduct produced after the BSFL treatment of organic waste is emerging as a valuable organic fertilizer, attributed to its content of microbial biomass, larval excreta, and undigested substrate. It is perfect for soil application because of its granular, porous structure, which was formed by larval movement, and its exceptional water–holding capacity and aeration (Beesigamukama *et al*., 2020; Basri *et al*., 2022). Fig. 6 illustrates the various benefits of BSFL frass for soil physical, chemical, and biological properties, as well as crop and environmental benefits. Frass has a moderate electrical conductivity with 2–5 millisiemens per centimeter (mS/cm), a neutral to slightly alkaline (pH 6.8–8.2) chemical composition that counteracts the acidity of the soil, and an improved cation exchange capacity for nutrient retention (Table 4). This region serves as a biological hotspot for fungi and bacteria that support plant growth, and after being applied, the leftover enzymes persist in facilitating decomposition. According to some research, frass may decrease the soil–borne diseases by suppressing them through plant resistance or microbial competition (Beesigamukama *et al*., 2020; Anedo*et al*., 2025). Frass provides micronutrients including iron and zinc in bioavailable forms, along with 2–5% nitrogen, 1–3% phosphorus pentoxide (P_2O_5), 1–4% potassium oxide (K_2O),2–8% calcium, and 0.5–1.5% magnesium (Beesigamukama *et al*., 2020; Basri *et al*., 2022). Besides, frass nutrient profiles vary by substrate: protein–rich substrates like fish waste yield frass with 3–5% nitrogen, 1.5–3% P_2O_5, and 1–4% K_2O, while carbohydrate–rich substrates like fruit waste produce 2–3% nitrogen and 1–2% P_2O_5(Beesigamukama *et al*., 2020; Basri *et al*., 2022).With a multi–phase nutrient release mechanism that offers fast potassium, a moderate release of organic materials, and a slow release of recalcitrant components, its composition of 50-70% organic matter and 25-35% carbon content supports soil health and decreases leaching, all while satisfying plant demands.

The potential of BSFL frass as fertilizer can be increased through processing. Stabilization methods, including composting or a curing period of two to four weeks, effectively decompose phytotoxic



Fig. 6: Benefits of BSF frass as organic fertilizer – Details the various benefits of BSFL frass for soil physical, chemical, and biological properties, as well as crop and environmental benefits

Table 4: BSFL frass organic fertilizer property comparison with conventional compost and chemical fertilizer

Property		BSFL frass	Conventional compost	Chemical fertilizer	Sources
Nutrient content	Nitrogen (N)	2–5%	0.5–2.5%	10–46%	Beesigamukama *et al.*, 2021b; Klammsteiner *et al.*, 2020
	Phosphorus (P)	1–2.5%	0.5–1.5%	10–52%	Beesigamukama *et al.*, 2021b; Anyega *et al.*, 2021
	Potassium (K)	1–3%	0.5–1.5%	0–60%	Beesigamukama *et al.*, 2021b; Klammsteiner *et al.*, 2020
	Calcium (Ca)	2–8%	1–4%	Variable	Beesigamukama *et al.*, 2021b; Anyega *et al.*, 2021
	Magnesium (Mg)	0.3–0.7%	0.2–0.5%	Variable	Beesigamukama *et al.*, 2021b; Anyega *et al.*, 2021
Physical properties	pH	6.5–8.0	6.0–8.0	Variable	Beesigamukama *et al.*, 2021b; Klammsteiner *et al.*, 2020
	Organic matter (OM)	50–70%	30–70%	0	Klammsteiner *et al.*, 2020: Anyega *et al.*, 2021
	C:N ratio	10–15:1	15–20:1	N/A	Beesigamukama *et al.*, 2021b; Klammsteiner *et al.*, 2020
Agronomic performance	N mineralization	30–60 days	60–95 days	Immediate	Beesigamukama *et al.*, 2021b; Anyega *et al.*, 2021
	Soil microbial activity	High	Moderate–High	Low	Beesigamukama *et al.*, 2021b; Klammsteiner *et al.*, 2020
	Soil structure improvement	High	Moderate–High	Low	Klammsteiner *et al.*, 2020: Anyega *et al.*, 2021
	Crop Yield Increase	22–135%*	10–30%*	Baseline	Beesigamukama *et al.*, 2021b; Anyega *et al.*, 2021

*Percentage increase compared to chemical fertilizer alone when used in combination with NPK

substances (Praeg and Klammsteiner, 2024), while vermicomposting with earthworms promotes greater microbial diversity and improves nutrient availability in the frass (Song *et al.,* 2021; Dulaurent *et al.,*2020). The enhancement of handling and storage through physical processing involves drying to a moisture level of 10–15%, grinding to produce consistent particles, or pelletizing for convenient application (Beesigamukama *et al.,*2020). Tailoring frass to specific crops or soil types, along with enrichment methods like the incorporation of nitrogen–fixing bacteria, phosphate–solubilising microorganisms, or biochar, enhances carbon sequestration and nutrient retention. When compared to unfertilized controls, maize, wheat, and rice yields increase by 10–30%, matching synthetic fertilizers at comparable rates, and this is where frass excels in agriculture as frasstilizer (Beesigamukama *et al.,*2020; Kullan *et al.,*2024; Kagehi *et al*., 2025), and application rates of 2.5 tons per hectare (t/ha) and 30 kg N/ha of frass were found to be effective in improving maize yield, while double rates of chemical organic fertilizer were required. The incorporation of BSFL frass contributes to a remarkable boost in vegetable yield, which can range from 2 to 10 tones per hectare, and it also greatly enhances stress resistance. Furthermore, legumes gain advantages through increased nodulation and nitrogen fixation (Kidd *et al*., 2025). The application of frass over an extended period (2–5 years) modifies soil microbial communities, resulting in a 10–20% increase in beneficial bacteria such as Rhizobium. However, it is essential to conduct thorough environmental assessments to track any potential nutrient imbalances or the accumulation of heavy metals (Ashworth *et al.,* 2025). Additional studies are required to elucidate these ecological impacts through extended field trials over multiple years. Mason (2020) demonstrated that the application of BSFL frass in sand peat at rates of 4% and 8% resulted in successful barley seed germination rates of 94.5% and 97.5%, respectively, in contrast to a rate of 87% achieved with NPK (20–20–20). Frass reduces the need for synthetic fertilizer in horticulture by being used in greenhouses and container nurseries (10–30% in growing media). Also, Diener *et al.* (2009) reported that insect frass contains traces of chitin and is a valuable supplement for soil. Various studies have indicated that the incorporation of chitin into soil promotes microbial activity under both oxic and anoxic conditions in agricultural soil slurries. Furthermore, BSFL frass can contain a remarkable spectrum of antimicrobial peptides that exhibit diverse inhibitory effects on various pathogens (Boccazzi *et al.,*2017; Mutyambai *et al*., 2025). Leveraging the nutritional richness and biostimulant properties of frass, specialized applications encompass hydroponic extracts, foliar sprays, and seed coatings (Chavez *et al*., 2025).BSFL frass has special benefits over traditional fertilizers (Solofondranohatra *et al*., 2025). When derived from local sources, its organic content contributes to better soil structure, enhances water retention, and stimulates microbial activity, while its slow-release profile lessens leaching and has a smaller carbon footprint than synthetic fertilizers (Beesigamukama *et al.,*2020). Its delayed initial release and variable nutritional content (less than synthetics) might, however, restrict its ability to respond quickly, necessitating larger application volumes. Although frass is more expensive and less accessible than typical composts, it outperforms them in terms of nitrogen (2–5% vs. 1–2%) and phosphorus (1–3% vs. 0.5–1%), production speed (weeks vs. months), and potential pathogen suppression (Beesigamukama *et al.,* 2020; Boccazzi *et al.,* 2017; Phiri *et al*., 2025). By fostering root expansion, enhancing nutrient efficiency, and increasing stress resistance through biostimulants like humic compounds, frass serves not only as a nutrient source but also as a growth promoter for plants. Because it improves soil structure, water–holding capacity, and microbial diversity, all of which contribute to long–term soil health and may even prevent diseases through microbial competition, it is a sustainable, versatile fertilizer for modern agriculture (Jiang *et al*., 2025). Nonetheless, frass presents certain drawbacks such as restricted supply chains and elevated production expenses.

Environment and economical promise of BSFL bioconversion

Transforming organic waste into valuable products such as insect meal and frass, BSFL bioconversion offers considerable economic and ecological benefits. According to life cycle assessments, it has an advantage over traditional waste management techniques like composting, which produces nitrous oxide that is 298 times more potent than CO_2, and land filling which releases methane that has a

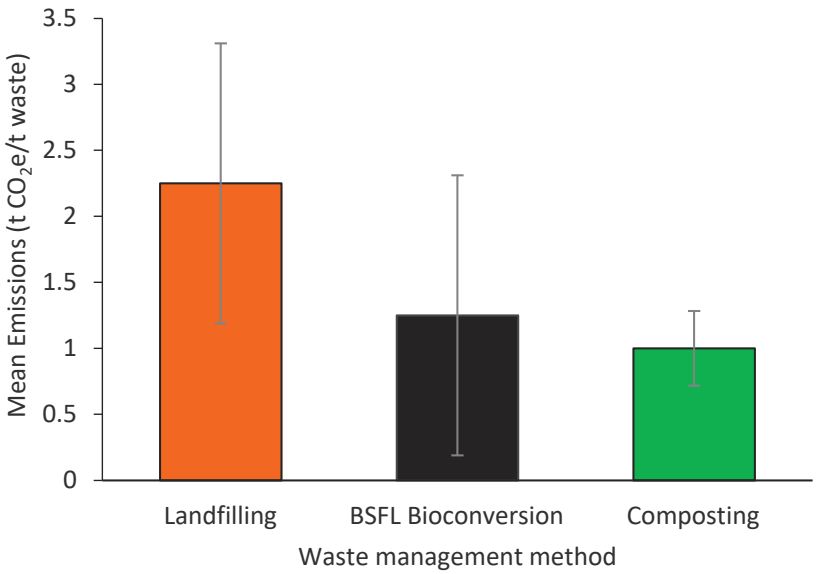

Fig. 7. Emission (t CO_2–equivalent/t waste) across waste management methods (Smetana *et al*., 2019; Mertenat *et al*., 2019).

warming potential 25 times more than CO_2 (Lv *et al.,* 2018; Tsutsuiet *et al.,* 2013; Smetana *et al.,* 2016). By avoiding landfill methane and replacing high–impact protein sources like fishmeal and soybean meal, BSFL systems reduce greenhouse gas emissions by 0.5–2 tons CO_2–equivalent per tonne of waste processed (Fig. 7), compared to 1.5–3 t for landfilling and 0.8–1.2 t for composting (Smetana *et al.,* 2019). Moreover, the carbon footprint of BSFL meal was the lowest, measuring 0.5 kilograms of carbon dioxide equivalent per kilogram (kg CO2e/kg). In contrast, fish meal recorded the highest carbon footprint at 3.7 kg, with soybean meal at 1.0 kg and corn gluten meal at 1.1 kg (Tadesse, 2023). BSFL require merely 20% of the water utilized for chicken and less than 1% for beef per unit of protein; they also occupy less than 1% of the land necessary for beef protein production and 10% to produce soy protein (Bosch *et al.,* 2019). With feed conversion rates of 1.5–2.5, BSFL systems manage a variety of waste streams and need less capital than anaerobic digestion. They are also considerably superior to beef (8–12) or pork (6–10) in feed conversion (Mertenat *et al.,* 2019). The bioconversion of BSFL reduces ecological impact while conserving water and land by reclaiming nutrients and mitigating eutrophication, aligning with the principles of the circular economy concepts (Ashworth *et al.,* 2025).With several revenue streams, including waste management fees, insect meal ($US1,000–2,500/tonne), insect oil ($US1,500–3,000/tonne), and frass fertilizer ($US500–1,500/tonne), BSFL bioconversion is economically feasible (Smetana *et al.,* 2019; Joly and Nikiena, 2019). The significant cost contributors for large organizations include breeding facilities, employee wages, utility services, utilities, and regulatory compliance. These can be managed more efficiently due to economies of scale (Mertenat *et al.,* 2020). Compared to anaerobic digestion ($US500–1,000/t capital cost), BSFL requires lower investment while producing protein and fertilizer, whereas anaerobic digestion concentrates on energy, BSFL produces protein in addition to fertilizer and reduces waste volume by up to 80% in weeks as opposed to months as anaerobic digestion and composting does (Bosch *et al.,*2019). Modifications in regulations, such as the EU's endorsement of insect protein in animal feeds, along with increasing consumer acceptance of sustainable products, are propelling market growth (Smetana *et al.,* 2016; Joly and Nikiena, 2019; Hall *et al.,* 2021). Scaling difficulties, competition from single–cell proteins or algae and maintaining constant product quality are obstacles. By leveraging carbon credits or other ecological incentives, BSFL systems thrive when tailored to local waste quantities

and markets. BSFL bioconversion aligns with circular economy principles, reducing environmental impact and fostering sustainable agriculture across diverse socio-economic contexts. Hence, the bioconversion of BSFL offers a sustainable and cost-effective approach for generating resources and managing waste by diverting waste from landfills, replacing synthetic fertilizers, and delivering concentrated products that are efficient for transportation (Bruno *et al.,* 2025b).

Scaling BSFL bioconversion: Challenges and future horizons

Technical, legal, and commercial challenges stand in the way of BSFL bioconversion's expansion from laboratory to commercial scale, but its potential is still enormous (Raman *et al.,* 2022). Managing the variability of substrates is a technical issue because different waste streams, like food scraps or manure, require pre-processing and blending for consistency (Smetana *et al.,* 2016). While automation in feeding and harvesting decreases labour but requires investment, furthermore, maintaining ideal conditions 27–30°C, 60–70% humidity demands cost–effective environmental controls (Chia *et al.,* 2018; Salam *et al.,* 2024). Additionally, efficient disease management is essential for averting larval infections, which calls for the execution of prompt diagnostic methods and rigorous biosecurity practices (Gold *et al.,* 2018). Because BSFL are less domesticated than livestock, selective breeding is required for quicker growth or stress tolerance and to preserve genetic variety (Smetana *et al.,* 2016). Various regulatory frameworks are in place that permit the use of BSFL meal for aquaculture and pets in the U.S. and Canada, whereas the EU permits its use in feeds for pigs, poultry, and aquaculture (Laroucheet *al.,* 2023). However, there are no globally recognized standards for this product (Smetana *et al.,* 2019). Although landfill levies can encourage the adoption of BSFL, waste regulations, such as permitting and pollutant limitations for heavy metals or pathogens, increase the costs of compliance (Mertenat *et al.,* 2020). Cultural resistance to insect-based products, particularly in Western countries, requires targeted education and outreach to address misconceptions about safety and sustainability, promoting consumer acceptance (Smetana *et al.,* 2016). The surveillance of contaminants, including heavy metals and microplastics, is essential for ensuring feed safety, as mentioned in the "Insect Meal from BSFL". Key knowledge gaps include: 1) optimizing substrate pre–treatments for diverse waste streams, 2) developing automated systems to reduce labour costs, 3) enhancing larval resilience through selective breeding of local or regional BSFL strains (e.g., African or Southeast Asian strains for tropical wastes), and 4) harmonizing global regulations for BSFL products. A key novelty lies in adapting BSFL for decentralized systems in developing countries, where 80% of the world's waste is not managed, possibly leading to a 10% reduction in emissions (UNEP, 2021; Raman *et al.,* 2022).Future development depends on integration and research, while sophisticated industrial designs and inexpensive sensors enhance large–scale operations, an understanding of the microbiome, developmental biology, and environmental reactions of BSFL can increase efficiency (Gold *et al.,* 2018). Advancements in products, like the extraction of proteins or chitin, could create profitable opportunities in biomaterials or pharmaceuticals (Smetana *et al.,* 2019). BSFL systems reduce emissions by 0.5–2 tons CO_2–equivalent per tonne of garbage, according to comprehensive life cycle evaluations, however, more extensive social and economic analyses are required, particularly for developing countries (Smetana *et al.,*2019). Anaerobic digestion enhances BSFL efficiency by utilizing digestate as feed for BSFL (Fu *et al.,* 2022) or by integrating with composting, where BSFL serve as a preliminary step in waste processing before composting (Mertenat*et al.,* 2020). Factors including digestate pH (spanning from 6 to 8) and volatile solids content (between 20% and 30%) confirm the system's compatibility (Mertenat *et al.,* 2019). Closed–loop agriculture is produced by on–farm systems that process manure or aquaponics systems that use BSFL meal and frass (Haudt, 2024). Meanwhile, urban decentralized units reduce transportation emissions by aligning with local waste streams (Bosch *et al.,* 2019). Market obstacles such as high production costs (Soy meal's $US400–600/tonne vs. BSFL meal's $US1,000–2,500/tonne), necessitate cost reductions through automation and scale (Raman *et al.,* 2022; Smetana *et al.,* 2019). Additionally, the implementation of demonstration projects, the creation of premium markets for sustainable products, and the provision of policy assistance can expedite the adoption process, establishing BSFL bioconversion as a fundamental

element of circular economies and sustainable waste management.

RECOMMENDATION

To advance BSFL entomoremediation, future research should prioritize: 1) multi-year field trials to assess long-term soil microbial impacts of frass application, 2) These diverse strategies will reinforce BSFL's position within circular economy models, bolstering in the security of food, feed, and fertilizers worldwide, 3) development of automated systems to reduce labour costs by 20–30% in small-scale facilities, and (4) selective breeding of regional BSFL strains to improve growth and resilience across diverse climates (Shao *et al*., 2023; Barry *et al*., 2023). It is essential for policymakers to establish landfill levies, carbon credits, and standardized feed regulations to encourage the adoption of BSFL, particularly in developing regions where 80% of waste is not managed (UNEP, 2021; Larouche *et al*., 2023). Education initiatives targeting cultural misconceptions can enhance consumer acceptance, while integration with anaerobic digestion or composting systems can boost material recovery by 15–25% (Mertenat *et al*., 2019). These varied approaches will reinforce BSFL's position within circular economy models, aiding in the security of food, feed, and fertilizers worldwide.

CONCLUSION

BSFL bioconversion serves as an innovative solution to the global organic waste challenge, presenting a sustainable way to turn waste into high-value products and furthering the principles of a circular economy. This review underscores BSFL's remarkable capacity to reduce organic waste by 50–80% within 12–15 days, producing protein-rich insect meal (40–47% protein) and nutrient-dense frass fertilizer (2–5% nitrogen, 1–3% phosphorus). These outputs compete with standard feed sources such as and soybean meals and outperform traditional compost in nutrient delivery and production speed. By mitigating greenhouse gas emissions–reducing emissions by 0.5–2 tons CO_2-equivalent per tons of waste compared to landfilling or composting and contribute significantly to environmental sustainability. Furthermore, technology supports agriculture and aquaculture by providing cost-effective, environmentally friendly alternatives to resource-intensive inputs, consequently minimizing dependence on overfished marine stocks and synthetic fertilizers. Despite its promise, BSFL bioconversion faces challenges that must be addressed to realize its full potential. Scalability remains a critical hurdle, particularly in managing diverse waste streams and maintaining consistent bioconversion efficiency across varying substrates. Enhancing pre-treatment strategies, like microbial inoculation or enzymatic hydrolysis, has the potential to increase bioconversion rates by 5–10%. Nonetheless, more research is required to confirm they are cost-effective when applied on a larger scale. Regulatory harmonization is another key barrier, as global standards for BSFL-derived products remain inconsistent. For instance, while the EU has approved BSFL meal for aquaculture, poultry, and pig feeds, broader adoption is hindered by regional restrictions and the absence of unified guidelines on contaminant limits, such as heavy metals or microplastics. Consumer acceptance, particularly in Western markets, necessitates specific educational efforts to counter cultural resistance to. Addressing these challenges through policy incentives, such as landfill levies and carbon credits, could accelerate adoption, especially in developing regions where 80% of waste remains unmanaged. Anticipating the future, BSFL holds significant potential to transform waste management and resource recovery. Integrating BSFL with complementary systems like anaerobic digestion or composting could boost material recovery by 15–25%, creating closed-loop agricultural models that enhance local food security. Tailored decentralized systems for urban or rural areas in developing nations could minimize transportation emissions and give communities the ability to oversee waste management on a local level. Additionally, advances in selective breeding and microbiome engineering offer opportunities to develop BSFL strains with enhanced resilience and bioconversion efficiency, particularly for lignocellulosic substrates. Emerging applications, such as BSFL-derived chitin for biomaterials or pharmaceuticals, could further expand market opportunities, transforming waste into high-value products beyond feed and fertilizer. To maximize the benefits of BSFL, a collaborative multidisciplinary approach is vital. Long-term field studies are required to investigate the ecological consequences of frass application, especially its effects on soil microbial dynamics and the risk of heavy metal buildup. Automation and sensor-based technologies can

reduce labour costs by 20–30%, making BSFL systems viable for small-scale operations. Governments and stakeholders should prioritize policy frameworks that incentivize sustainable practices, such as integrating BSFL into national waste management strategies. Initiatives driven by the community, enhanced by educational outreach, can encourage acceptance and engagement, especially in areas struggling with high waste mismanagement. While ethical considerations, such as biodiversity impacts and animal welfare in large-scale rearing, warrant further exploration, BSFL entomoremediation stands as a scalable, environmentally sound solution. Through the management of organic waste, the reduction of emissions, and the encouragement of sustainable farming practices, BSFL technology lays the foundation for a more eco-friendly and robust future, consistent with worldwide objectives for food security and environmental stewardship.

AUTHOR CONTRIBUTIONS

A.R.K. Kullan was responsible for searching the bibliography, selecting the relevant references, coding the references, writing the initial manuscript draft, synthesizing the manuscript, and revising the final manuscript version. E.G. Neumannwas responsible for conceptualizing the draft, analyzing the references' coding, and reviewing the whole manuscript.A. Sureshwas responsible for the work plan preparation, defining the bibliographic search, conceptualizing the draft, reviewing the whole manuscript. H.L. Choiwas responsible for selecting the relevant references, analyzing the coding of the references, and reviewing the analysis in the manuscript.

ACKNOWLEDGEMENT

The authors extend thanks for the financial support by ASPIRE, the technology program management pillar of Abu Dhabi's Advanced Technology Research Council (ATRC), via the ASPIRE "The Virtual Research Institutes Program" [Funding number: 21R097]. The authors also extend thanks to the ARIFSID research program and UAEU for their support of this work.

CONFLICT OF INTEREST

The authors declare no potential conflict of interest regarding the publication of this work. In addition, the ethical issues including plagiarism, informed consent, misconduct, data fabrication and, or falsification, double publication and, or submission, and redundancy have been completely witnessed by the authors.

OPEN ACCESS

©2026 The author(s).This article is licensed under a Creative Commons Attribution 4.0 International License, which permits use, sharing, adaptation, distribution and reproduction in any medium or format, as long as you give appropriate credit to the original author(s) and the source, provide a link to the Creative Commons license, and indicate if changes were made. The images or other third–party material in this article are included in the article's Creative Commons license, unless indicated otherwise in a credit line to the material. If material is not included in the article's Creative Commons license and your intended use is not permitted by statutory regulation or exceeds the permitted use, you will need to obtain permission directly from the copyright holder. To view a copy of this license, visit: http://creativecommons.org/licenses/by/4.0/

PUBLISHER'S NOTE

GJESM Publisher remains neutral with regard to jurisdictional claims in published maps and institutional afflictions.

Positive AI Statement

During the preparation of this work the author(s) have used Artificial Intelligence (AI) [Gemini, ChatGPT, Grok, and Quillbot] to English editing and grammar check. After using this tool/service, the authors reviewed and edited the content as needed and took full responsibility for the content of the publication.

(For this reason, the GPTZero detector will evaluate the manuscript utilizing Generative AI, ensuring a high detection rate. If the manuscript relies heavily on Generative AI and AI–assisted technologies, it will be archived without further options for appeal).

ABBREVIATIONS

%	Per cent
°C	Degree Celsius
$US	United States Dollar
Ca	*Calcium*
BCE	Bioconversion efficiency

BSF	Black soldier fly
BSFL	Black soldier fly larvae
C:N	Carbon to nitrogen ratio
CO_2	carbon dioxide
Cm^2	Square centimeter
e.g.	Exempli gratia / for example
EU	European Union
FAO	Food and Agriculture Organization
FCR	Feed conversion ratio
Fig.	Figure
IPCC	Intergovernmental Panel on Climate Change
K	*Potassium*
K_2O	potassium oxide
kg	Kilogram
Kg/y	kilograms per year
kg CO_2e/kg	Kilogram carbon dioxide equivalent per kilogram
kg N/ha	Kilogram nitrogen per hectare
km^3	Cubic kilometer
L	Linnaeus (taxonomic abbreviation)
min.	minutes
Mg	*Magnesium*
mg	Milligram
mm	Millimeter
mS/cm	Millisiemens per centimeter
N/A	Not Applicable
N	*Nitrogen*
NPK	Nitrogen phosphorus potassium
P	*Phosphorus*
pH	Potential of hydrogen
P_2O_5	Phosphorus pentoxide
t/ha	Tonnes per hectare
UAEU	United Arab Emirates University
UN	United Nations
UNEP	United Nations Environment Programme
WR	Waste reduction
$Mmol/m^2/s$	Micromole per square meter per second

REFERENCES

Amrul, N.F.; Kabir Ahmad, I.; Ahmad Basri, N.E.; Suja, F.; Abdul Jalil, N.A.; Azman, N.A., (2022). A review of organic waste treatment using black soldier fly (*Hermetia illucens*). Sustainability, 14(8): 4565 (**15 page**).

Anedo, E.O.; Beesigamukama, D.; Mochoge, B.; Korir, N.K.; Haukeland, S.; Cheseto, X.; Nyongesa, M.; Pwaipwai, P.; Subramanian, S.; Tenkouano, A.; Kibaara, B.;Tanga, C.M., (2025). Unpacking the benefits of black soldier fly frass fertilizer towards nematode suppression and potato production. Front. Plant Sci., 16: 1509643 (**16 page**).

Anyega, A.O.; Korir, N.K.; Beesigamukama, D.; Changeh, G.J.; Nkoba, K.; Subramanian, S.; Tanga, C.M., (2021). Black soldier fly–composted organic fertilizer enhances growth, yield, and nutrient quality of three key vegetable crops in Sub–Saharan Africa. Front. Plant Sci., 12: 680312 (**14 pages**).

Ashworth, A.J.; Amorim, H.C.S.; Drescher, G.L.; Moore Jr, P.A.; Rojas, M.G.; Morales–Ramos, J.; Donoghue, A.M., (2025). Insect frass fertilizer as soil amendment for improved forage and soil health in circular systems. Sci. Rep., 15(1): 3024 (**10 page**).

Astuti, D.A.; Wiryawan, K.G., (2022). Black soldier fly as feed ingredient for ruminants. Anim. Biosci., 35(2): 356 (**8 page**).

Basri, N.E.A.; Azman, N.A.; Ahmad, I.K.; Suja, F.; Jalil, N.A.A.; Amrul, N.F., (2022). Potential applications of frass derived from black soldier fly larvae treatment of food waste: A review. Foods. 11(17): 2664 (**19 pages**).

Beesigamukama, D.; Mochoge, B.; Korir, N.K.; Fiaboe, K.K.; Nakimbugwe, D.; Khamis, F.M.; Tanga, C.M., (2020). Exploring black soldier fly frass as novel fertilizer for improved growth, yield, and nitrogen use efficiency of maize under field conditions. Front. Plant Sci., 11: 574592 (**17 pages**).

Beesigamukama, D.; Mochoge, B.; Korir, N.K.; Fiaboe, K.K.; Nakimbugwe, D.; Khamis, F.M.; Tanga, C.M., (2021a). Low–cost technology for recycling agro–industrial waste into nutrient–rich organic fertilizer using black soldier fly. Waste Manage.,119: 183–194 (**12 pages**).

Beesigamukama, D.; Mochoge, B.; Korir, N.K.; Ghemoh, C.J.; Subramanian, S.; Tanga, C.M., (2021b). In situ nitrogen mineralization and nutrient release by soil amended with black soldier fly frass fertilizer. Sci. Rep., 11(1): 14799 (**14 pages**).

Belghit, I.; Liland, N.S.; Gjesdal, P.; Biancarosa, I.; Menchetti, E.; Li, Y.; Lock, E.J., (2019). Black soldier fly larvae meal can replace fish meal in diets of sea–water phase Atlantic salmon (Salmo salar). Aquaculture, 503: 609–619 (**11 pages**).

Belperio, S.; Cattaneo, A.; Nannoni, E.; Sardi, L.; Martelli, G.; Dabbou, S.; Meneguz, M., (2024). Assessing substrate utilization and bioconversion efficiency of black soldier fly *(Hermetia illucens*) larvae: Effect of diet composition on

growth and development temperature. Animals, 14(9): 1340 (**12 pages**).

Bhatia, T.; Sindhu, S.S., (2024). Sustainable management of organic agricultural wastes: Contributions in nutrients availability, pollution mitigation and crop production. Discov. Agric., 2(1): 1–42 (**42 pages**).

Boafo, H.A.; Gbemavo, D.S.J.C.; Timpong–Jones, E.C.; Eziah, V.; Billah, M.; Chia, S.Y.; Kenis, M., (2023). Substrates most preferred for black soldier fly *Hermetia illucens* (L.) oviposition are not the most suitable for their larval development. J. Insects Food Feed. 9(2): 183–192 (**10 pages**).

Boccazzi, I.V.; Ottoboni, M.; Martin, E.; Comandatore, F.; Vallone, L.; Spranghers, T.;Eeckhout, M.;Mereghetti, V.;Pinotti, V.; Epis, S., (2017). Survey of the mycobiota associated with larvae of the black soldier fly (*Hermetia illucens*) reared for feed production. PLoS ONE. 12(8): e0182533 (**15 pages**).

Bosch, G.; Van Zanten, H.H.E.; Zamprogna, A.; Veenenbos, M.; Meijer, N.P.; Van der Fels–Klerx, H.J.; Van Loon, J.J.A., (2019). Conversion of organic resources by black soldier fly larvae: Legislation, efficiency and environmental impact. J. Clean Prod., 222: 355–363 (**9 pages**).

Bosch, G.; Vervoort, J.J.M.; Hendriks, W.H., (2016). In vitro digestibility and fermentability of selected insects for dog foods. Anim. Feed Sci. Technol., 221: 174–184 (**11 pages**).

Bruno, D.; Casartelli, M.; De Smet, J.; Gold, M.; Tettamanti, G., (2025a). A journey into the black soldier fly digestive system: From current knowledge to applied perspectives. Animal (**13 pages**).

Bruno, D.; Orlando, M.; Testa, E.; Miino, M.C.; Pesaro, G.; Miceli, M.; Pollegioni, L.; Barbera, V.; Fasoli, E.; Draghi, L.; Baltrocchi, A.P.D.; Ferronato, N.; Seri, R.; Maggi, E.; Caccia, S.; Casartelli, M.; Molla, G.; Galimberti, M.; Torretta, V.; Vezzulli, A.; Tettamanti, G.,(2025b). Valorization of organic waste through black soldier fly: On the way of a real circular bioeconomy process. Waste Manage., 191: 123–134 (**12 pages**).

Cadinu, L.A.; Barra, P.; Torre, F.; Delogu, F.; Madau, F.A., (2020). Insect rearing: Potential, challenges, and circularity. Sustainability, 12(11): 4567 (**23 pages**).

Cannella, L.; Nassef, A.R.A.; Bailey, D.; Ferrarezi, R.S., (2016). Alternative sources of food for aquaponics in the US Virgin Islands: A case study with black soldier flies. Agric. Exp. Stn., 34 (**11 pages**).

Cattaneo, A.; Belperio, S.; Sardi, L.; Martelli, G.; Nannoni, E.; Dabbou, S.; Meneguz, M., (2024). Black soldier fly larvae's optimal feed intake and rearing density: A welfare perspective (Part II). Insects, 16(1): 5 (**21 pages**).

Charlton A.; Dickinson M.; Wakefield M.; Fitches E.; Kenis M.; Han R.; Zhu F.; Kone N.; Grant M.; Devic E.; (2015) Exploring the chemical safety of fly larvae as a source of protein for animal feed. J. Insects Food Feed. 1:7–16 (**10 pages**).

Chavez, M.Y.; Villa Ignacio, A.; Craver, J.K.; Bousselot, J., (2025). Investigating black soldier fly larval (*Hermetia illucens*) frass applications as a partial peat replacement and liquid fertilizer in Brassicaceae crop production. Agrochemicals. 4(2): 8 (**13 page**).

Chia, S.Y.; Tanga, C.M.; Khamis, F.M.; Mohamed, S.A.; Salifu, D.; Sevgan, S.; Ekesi, S., (2018). Threshold temperatures and thermal requirements of black soldier fly *Hermetia illucens*: Implications for mass production. PLoS ONE, 13(11): e0206097 (**26 pages**).

Cummins Jr, V.C.; Rawles, S.D.; Thompson, K.R.; Velasquez, A.; Kobayashi, Y.; Hager, J.; Webster, C.D., (2017). Evaluation of black soldier fly (*Hermetia illucens*) larvae meal as partial or total replacement of marine fish meal in practical diets for Pacific white shrimp (*Litopenaeusvannamei*). Aquaculture, 473: 337–344 (**8 pages**).

Dabbou, S.; Gai, F.; Biasato, I.; Capucchio, M.T.; Biasibetti, E.; Dezzutto, D.; Schiavone, A., (2018). Black soldier fly defatted meal as a dietary protein source for broiler chickens: Effects on growth performance, blood traits, gut morphology and histological features. J. Anim. Sci. Biotechnol., 9: 1–10 (**10 pages**).

Devic, E.; Leschen, W.; Murray, F.; Little, D.C., (2018). Growth performance, feed utilization and body composition of advanced nursing Nile tilapia (*Oreochromisniloticus*) fed diets containing black soldier fly (*Hermetia illucens*) larvae meal. Aquac. Nutr., 24(1): 416–423 (**8 pages**).

Diener, S.; StudtSolano, N.M.; Roa Gutiérrez, F.; Zurbrügg, C.; Tockner, K., (2011). Biological treatment of municipal organic waste using black soldier fly larvae. Waste Biomass Valorization, 2: 357–363 (**5 pages**).

Diener, S.; Zurbrügg, C.; Tockner, K., (2009). Conversion of organic material by black soldier fly larvae: Establishing optimal feeding rates. Waste Manag. Res., 27(6): 603–610 (**8 pages**).

Diola, C.S.; Nacilla, E.J.; Pardillo, C.A.; Alosbaños, R.S.; Evacitas, F.; Maglangit, F., (2024). Waste reduction and bioconversion of quail, chicken, and pig manure by black soldier fly (*Hermetia illucens*L.). Philipp. J. Sci., 153(2) (**10 pages**).

Dulaurent, A.M.; Daoulas, G.; Faucon, M.P.; Houben, D., (2020). Earthworms (*Lumbricusterrestris* L.) mediate the fertilizing effect of frass. Agronomy, 10(6): 783 (**8 pages**).

El–byari, Y.; Amraoui, M.B., (2025). Enhancement of bioconversion of vegetable biowaste by black soldier fly larvae: Influence of mechanical and thermomechanical pretreatments. Sci. Afr., 27: e02626 (**12 pages**).

Eriksen, N.T., (2024). Metabolic performance and feed efficiency of black soldier fly larvae. Front. Bioeng. Biotechnol., 12: 1397108 (**8 page**).

Ewald, N.; Vidakovic, A.; Langeland, M.; Kiessling, A.; Sampels, S.; Lalander, C., (2020). Fatty acid composition of black soldier fly larvae (*Hermetia illucens*)–Possibilities and limitations for modification through diet. Waste Manage., 102: 40–47 (**8 pages**).

FAO, (2011). Global food losses and food waste–Extent, causes and prevention. SAVE FOOD: An initiative on food loss and waste reduction, 9 (**37 pages**).

FAO, (2013). Food wastage footprint: Impacts on natural resources: Summary report. Food Agric. Organ. UN (**63 pages**).

FAO, (2014). Food wastage footprint full–cost accounting. Food Agric. Organ. UN (**98 pages**).

Fischer, H.; Romano, N.; Sinha, A.K., (2021). Conversion of spent coffee and donuts by black soldier fly (*Hermetia illucens*) larvae into potential resources for animal and plant farming. Insects, 12(4): 332 (**15 pages**).

Fu, S.F.; Wang, D.H.; Xie, Z.; Zou, H.; Zheng, Y., (2022). Producing insect protein from food waste digestate via black soldier fly larvae cultivation: A promising choice for digestate disposal. Sci. Total Environ., 830: 154654 (**9 pages**).

Ghazali, A.;Tjakraatmadja, J.H.; Pratiwi, E.Y.D., (2021). Resident–based learning model for sustainable resident participation in municipal solid waste management program. Global J.Environ. Sci. Manage., 7(4): 599–624 (**26 pages**).

Giannetti, D.; Schifani, E.; Reggiani, R.; Mazzoni, E.; Reguzzi, M.C.; Castracani, C.; Grasso, D.A., (2022). Do it by yourself: Larval locomotion in the black soldier fly *Hermetia illucens*, with a novel "self–harvesting" method to separate prepupae. Insects, 13(2): 127 (**14 pages**).

Gold, M.; Tomberlin, J.K.; Diener, S.; Zurbrügg, C.; Mathys, A., (2018). Decomposition of biowaste macronutrients, microbes, and chemicals in black soldier fly larval treatment: A review. Waste Manage., 82: 302–318 (**17 pages**).

Hall, H.; Fitches, E.; Smith, R., (2021). Insects as animal feed: Novel ingredients for use in pet, aquaculture and livestock diets. CABI (**134 pages**).

Haudt, JV., (2024). Anaerobic digestion at the axis of circular food production. Doctoral dissertation, Ghent University (**81 pages**).

IPCC, (2019). Climate change and land: An IPCC special report on climate change, desertification, land degradation, sustainable land management, food security, and greenhouse gas fluxes in terrestrial ecosystems. IPCC Spec. Rep. (**874 pages**).

Jiang, S.Y.; Shen, K.W.; Brandón, M.G.; Lu, S.B.; Tomberlin, J.K.; Tang, X.T.; Wang, H.; Xiang, F.M.; Chen, X.X.; Zhang, Z.J., (2025). Using black soldier fly larval frass to restore soil health. Bioresour. Technol., 432: 132701 (**7 pages**).

Joly, G.; Nikiema, J., (2019). Global experiences on waste processing with black soldier fly (*Hermetia illucens*): From technology to business. IWMI, 16 (**66 pages**).

Jucker, C.; Erba, D.; Leonardi, M.G.; Lupi, D.; Savoldelli, S., (2017). Assessment of vegetable and fruit substrates as potential rearing media for *Hermetia illucens* (Diptera: Stratiomyidae) larvae. Environ. Entomol., 46(6): 1415–1423 (**9 pages**).

Kagehi, N.; Beesigamukama, D.; Tanga, C.M.; Ngugi, M.P.; Subramanian, S.; Khamis, F.M., (2025). Contribution of different frass fertilizer products on enhanced growth, yield and nutrient quality of Broccoli [*Brassica oleracea*]. Front. Plant Sci., 16: 1613814 (**18 page**).

Kidd, D.R.; Enkhbat, G.; Wisdom, J.M.; Kragt, M.E.; Jenkins, S.N.; Ryan, M.H., (2025). Black soldier fly frass greatly improves growth of four crops in a fertilised sandy soil. J. Clean Prod., 520: 146046 (**10 pages**).

Klammsteiner, T.; Turan, V.; Fernández–Delgado Juárez, M.; Oberegger, S.; Insam, H., (2020). Suitability of black soldier fly frass as soil amendment and implication for organic waste hygienization. Agronomy, 10(10): 1578 (**12 pages**).

Kullan, A.R.K.; Suresh, A.; Choi, H.L.; Gabriel Neumann, E.; Hassan, F., (2024). Bioconversion of poultry litter into insect meal and organic frasstilizer using black soldier fly larvae as a circular economy model for the poultry industry: A review. Insects, 16(1): 12 (**22 pages**).

Lalander, C.D.S.Z.; Diener, S.; Zurbrügg, C.; Vinnerås, B., (2019). Effects of feedstock on larval development and process efficiency in waste treatment with black soldier fly (*Hermetia illucens*). J. Clean Prod., 208: 211–219 (**9 pages**).

Lalander, C.H.; Fidjeland, J.; Diener, S.; Eriksson, S.; Vinnerås, B., (2015). High waste–to–biomass conversion and efficient Salmonella spp. reduction using black soldier fly for waste recycling. Agron. Sustainable Dev., 35: 261–271 (**11 pages**).

Larouche, J.; Campbell, B.; Hénault–Éthier, L.; Banks, I.J.; Tomberlin, J.K.; Preyer, C.; Vandenberg, G.W., (2023). The edible insect sector in Canada and the United States. Anim. Front., 13(4): 16–25 (**10 pages**).

Li, Q.; Zheng, L.; Qiu, N.; Cai, H.; Tomberlin, J.K.; Yu, Z., (2011). Bioconversion of dairy manure by black soldier fly (Diptera: Stratiomyidae) for biodiesel and sugar production. Waste Manage., 31(6): 1316–1320 (**5 pages**).

Liu, T.; Awasthi, M.K.; Wang, X.; Awasthi, S.K.; Jiao, M.; Shivpal, V.; Zhou, Y.; Liu, H.; Zhang, Z., (2022). Effects of further composting black soldier fly larvae manure on toxic metals and resistant bacteria communities by cornstalk amendment. Sci. Total Environ. 806:150699.

Lopes, I.G.; Lalander, C.; Vidotti, R.M.; Vinnerås, B., (2020). Using *Hermetia illucens* larvae to process biowaste from aquaculture production. J. Clean Prod., 251: 119753 (**10 pages**).

Lv, B.; Zhang, D.; Cui, Y.; Yin, F., (2018). Effects of C/N ratio and earthworms on greenhouse gas emissions during vermicomposting of sewage sludge. Bioresour. Technol., 268: 408–414 (**7 pages**).

Manna Insect, (2025). How fast do the BSF larvae grow, when can I expect to get protein for my farm animals? Manna Insect FAQ (**1 pages**).

Marono, S.; Loponte, R.; Lombardi, P.; Vassalotti, G.; Pero, M.E.; Russo, F.; Bovera, F., (2017). Productive performance and blood profiles of laying hens fed *Hermetia illucens* larvae meal as total replacement of soybean meal from 24 to 45 weeks of age. Poult. Sci., 96(6): 1783–1790 (**8 pages**).

Mason, B., (2016). Production of high value protein feeds and fertilizer from pre–consumer vegetable waste utilizing a novel black soldier fly larvae conversion process. Verschuren Cent. Sustainable Energy Environ (**28 pages**).

Mertenat, A.; Diener, S.; Zurbrügg, C., (2019). Black soldier fly biowaste treatment Assessment of global warming potential. Waste Manage., 84: 173–181 (**9 pages**).

Mutyambai, D.M.; Mutua, J.M.; Jalloh, A.A.; Beesigamukama, D.; Kessler, A.; Subramanian, S.; Dubois, T.; Ekesi, S.; Tanga, C.M., (2025). Insect frass fertilizer upregulates maize defence genes and resistance against an invasive herbivore pest. Sci. Rep., 15(1): 29978 (**15 page**).

Myers, H.M.; Tomberlin, J.K.; Lambert, B.D.; Kattes, D., (2008). Development of black soldier fly (Diptera: Stratiomyidae) larvae fed dairy manure. Environ. Entomol., 37(1): 11–15 (**5 pages**).

Newton, L.; Sheppard, C.; Watson, D.W.; Burtle, G.; Dove, R., (2005). Using the black soldier fly, *Hermetia illucens*, as a value–added tool for the management of swine manure. Anim. Poult. Waste Manag. Cent. NC State Univ., 17: 18 (**17 pages**).

Nyakeri, E.M.; Ogola, H.J.; Ayieko, M.A.; Amimo, F.A., (2017). An open system for farming black soldier fly larvae as a source of proteins for smallscale poultry and fish production. J. Insects Food Feed, 3(1): 51–56 (**6 pages**).

Ogello, E.O.; Outa, N.O.; Muthoka, M.; Juma, F.; Hoinkis, J., (2025). Optimizing Black Soldier Fly (*Hermetia illucens*) production: effects of substrate variation on biomass, nutritional quality, hatchability, fecundity, and frass quality. Front. Sustainable Food Syst., 9: 1621034 (**11 pages**).

Parra–Pacheco, B.; Aguirre–Becerra, H.; Feregrino–Pérez, A.A.; Chandrakasan, G.; González–Lara, H.; García–Trejo, J.F., (2025). Use of black soldier fly larvae for bioconversion of tomato crop residues. Sustainability, 17(8): 3578 (**18 page**).

Peguero, D.A.; Mutsakatira, E.T.; Buckley, C.A.; Foutch, G.L.; Bischel, H.N., (2021). Evaluating the microbial safety of heat–treated fecal sludge for black soldier fly larvae production in South Africa. Environ. Eng. Sci., 38(5): 331–339 (**9 pages**).

Permana, A.D.; RamadhaniEka Putra, J.E.N., (2018). Growth of black soldier fly (*Hermetia illucens*) larvae fed on spent coffee ground. IOP Conf. Ser. Earth Environ. Sci., 187: 012070 (**7 pages**).

Phiri, A.T.; Zhang, H.; Mnthambala, F., (2025). Comparative effects of black soldier fly frass fertilizer and vermicompost on crop performance, soil organic carbon, and nutrient dynamics. Discov. Soil, 2: 67 (**18 page**).

Phl, C.P.V.; Walraven, M.; Bézagu, M.; Lefranc, M.; Ray, C., (2020). Industrial symbiosis in insect production A sustainable eco–efficient and circular business model. Sustainability, 12(24): 10333 (**14 pages**).

Pour, F.H.; Makkawi, Y.T., (2021). A review of post–consumption food waste management and its potentials for biofuel production. Energy Rep., 7: 7759–7784 (**26 pages**).

Praeg, N.; Klammsteiner, T., (2024). Primary study on frass fertilizers from mass–reared insects: Species variation, heat treatment effects, and implications for soil application at laboratory scale. J. Environ. Manage., 356: 120622 (**11 pages**).

Purschke, B.; Scheibelberger, R.; Axmann, S.; Adler, A.; Jäger, H.; (2017). Impact of substrate contamination with mycotoxins, heavy metals and pesticides on the growth performance and composition of black soldier fly larvae (Hermetia illucens) for use in the feed and food value chain. Food Additives & Contaminants: Part A, 34(8): 1410-1420 **(10 pages).**

Raeiszadeh, Z.; Ahmadi, K.; Asadi, M., (2025). Enhancing agricultural waste bioconversion by Black Soldier Fly larvae through wheat bran supplementation. Int. J. Recycl. Org. Waste Agric.,14(4) (**11 pages**).

Raman, S.S.; Stringer, L.C.; Bruce, N.C.; Chong, C.S., (2022). Opportunities, challenges and solutions for black soldier fly larvae–based animal feed production. J. Clean Prod., 373: 133802 (**18 pages**).

Rehman, K.U.; Hollah, C.; Wiesotzki, K.; Rehman, R.U.; Rehman, A.U.; Zhang, J.; Aganovic, K., (2023). Black soldier fly, *Hermetia illucens* as a potential innovative and environmentally friendly tool for organic waste management: A mini review. Waste Manag. Res., 41(1): 81–97 (**17 pages**).

Rehman, K.U.; Rehman, A.; Cai, M.; Zheng, L.; Xiao, X.; Somroo, A.A.; Zhang, J., (2017). Conversion of mixtures of dairy manure and soybean curd residue by black soldier fly larvae (*Hermetia illucens* L.). J. Clean Prod., 154: 366–373 (**8 pages**).

Renna, M.; Schiavone, A.; Gai, F.; Dabbou, S.; Lussiana, C.; Malfatto, V.; Gasco, L., (2017). Evaluation of the suitability of a partially defatted black soldier fly (*Hermetia illucens* L.) larvae meal as ingredient for rainbow trout (*Oncorhynchus mykiss*Walbaum) diets. J. Anim. Sci. Biotechnol., 8: 1–13 (**13 pages**).

Saidani, M.; Dabbou, S.; Ben Larbi, M.; BelhadjSlimen, I.; Fraihi, W.; Arbi, T.; Amraoui, M.; M'Hamdi, N., (2025). Effect of black soldier fly (*Hermetia illucens* L.) larvae meal on growth performance, carcass characteristics, meat quality, and cecal microbiota in broiler chickens. Front. Anim. Sci., 6: 1531773 (**12 page**).

Salam, M.; Alam, F.; Chia, S.Y.; Shi, D., (2024). Enhancing sustainable organic waste management: Optimal substrates and environmental conditions for black soldier fly larval performance. SSRN, 4705775 (**34 pages**).

Santoso, A.D.; Handayani, T.; Nugroho, R.A.; Yanuar, A.L.; Nadirah, N.; Widjaja, E.; Rohaeni, E.S.; Oktaufik, M.A.M.; Ayuningtyas, U.; Erlambang, Y.P.; Herdioso, R., (2023). CASE STUDY: Sustainability index analysis of the black soldier fly (*Hermetia illucens*) cultivation from food waste substrate. Global J. Environ. Sci. Manage. 9(4): 851–870 (**20 Pages**).

Shao, M.; Zhao, X.; Rehman, K.U.; Cai, M.; Zheng, L.; Huang,

F.; Zhang, J., (2024). Synergistic bioconversion of organic waste by black soldier fly (*Hermetia illucens*) larvae and thermophilic cellulose–degrading bacteria. Front. Microbiol., 14: 1288227 (**14 pages**).

Sheppard, D.C.; Newton, G.L.; Thompson, S.A.; Savage, S., (1994). A value-added manure management system using the black soldier fly. Bioresour. Technol., 50(3): 275–279 (**5 pages**).

Shumo, M.; Osuga, I.M.; Khamis, F.M.; Tanga, C.M.; Fiaboe, K.K.; Subramanian, S.; Borgemeister, C., (2019). The nutritive value of black soldier fly larvae reared on common organic waste streams in Kenya. Sci. Rep., 9(1): 10110 (**13 pages**).

Siddiqui, S.A.; Gadge, A.S.; Hasan, M.; Rahayu, T.; Povetkin, S.N.; Fernando, I.; Castro–Muñoz, R., (2024). Future opportunities for products derived from black soldier fly (BSF) treatment as animal feed and fertilizer–A systematic review. Environ. Dev. Sustainable. 1–82 (**82 pages**).

Smetana, S.; Palanisamy, M.; Mathys, A.; Heinz, V., (2016). Sustainability of insect use for feed and food: Life cycle assessment perspective. J. Clean Prod., 137: 741–751 (**11 pages**).

Smetana, S.; Schmitt, E.; Mathys, A., (2019). Sustainable use of *Hermetia illucens* insect biomass for feed and food: Attributional and consequential life cycle assessment. Resour. Conserv. Recycl., 144: 285–296 (**12 pages**).

Solofondranohatra, C.L.; Ramiadantsoa, T.; Hugel, S.; Fisher, B.L., (2025). Black soldier fly frass fertilizer outperforms traditional fertilizers in terms of plant growth in restoration in Madagascar. Sustainability. 17(15): 7152 (**14 page**).

Somroo, A.A.; urRehman, K.; Zheng, L.; Cai, M.; Xiao, X.; Hu, S.; Zhang, J., (2019). Influence of *Lactobacillus buchneri* on soybean curd residue co–conversion by black soldier fly larvae (*Hermetia illucens*) for food and feedstock production. Waste Manage., 86: 114–122 (**9 pages**).

Song, S.; Ee, A.W.L.; Tan, J.K.N.; Cheong, J.C.; Chiam, Z.; Arora, S.; Tan, H.T.W., (2021). Upcycling food waste using black soldier fly larvae: Effects of further composting on frass quality, fertilising effect and its global warming potential. J. Clean Prod., 288: 125664 (**13 pages**).

Spranghers, T.; Michiels, J.; Vrancx, J.; Ovyn, A.; Eeckhout, M.; De Clercq, P.; De Smet, S., (2018). Gut antimicrobial effects and nutritional value of black soldier fly (*Hermetia illucens* L.) prepupae for weaned piglets. Anim. Feed Sci. Technol., 235: 33–42 (**10 pages**).

Surendra, K.C.; Olivier, R.; Tomberlin, J.K.; Jha, R.; Khanal, S.K., (2016). Bioconversion of organic wastes into biodiesel and animal feed via insect farming. Renew. Energy, 98: 197–202 (**6 pages**).

Tadesse, A., (2024). The carbon footprint and ecosystem services of black soldier fly larvae meal as an alternative protein source for aquaponics. Ecol. Insights, 8(2) (**13 pages**).

Tirtawijaya, G.; Lee, J.H.; Bashir, K.M.I.; Lee, H.J.; Choi, J.S., (2024). Evaluating the efficiency of black soldier fly (*Hermetia illucens*) larvae in converting mackerel head waste into valuable resources. Animals, 14(9): 1332 (**19 pages**).

Tsutsui, H.; Fujiwara, T.; Matsukawa, K.; Funamizu, N., (2013). Nitrous oxide emission mechanisms during intermittently aerated composting of cattle manure. Bioresour. Technol., 141: 205–211 (**7 pages**).

UNEP, (2021). Food Waste Index Report 2021. Nairobi: United Nations Environment Programme (**100 pages**).

United Nations, (2019). World Population Prospects 2019: Highlights. Statistical Papers–United Nations (Ser. A), Population and Vital Statistics Report (**46 pages**).

Ursada, R.; Bagastyo, A.Y.; Purnomo, A., (2025). Effect of feeding rate and composition for bioconversion of wastewater treatment plant sludge from the milk and creamer processing industries using black soldier fly larvae. BIO Web Conf., 157: 05011 (**16 pages**).

Van der Fels–Klerx, H.J.; Camenzuli, L.; Van Der Lee, M.K.; Oonincx, D.G.A.B., (2016). Uptake of cadmium, lead and arsenic by *Tenebrio molitor* and *Hermetia illucens* from contaminated substrates. PLoS ONE, 11(11): e0166186 (**13 pages**).

Wynants, E.; Frooninckx, L.; Crauwels, S.; Verreth, C.; De Smet, J.; Sandrock, C.; Wohlfahrt, J.;Van Schelt, J.; Depraetere, S.; Lievens, B.; Van Miert, S., (2019). Assessing the microbiota of black soldier fly larvae (Hermetia illucens) reared on organic waste streams on four different locations at laboratory and large scale. Microbial ecology, 77(4):913-930 **(17 pages)**.

Xiao, X.; Mazza, L.; Yu, Y.; Cai, M.; Zheng, L.; Tomberlin, J.K.; Zhang, J., (2018). Efficient co–conversion process of chicken manure into protein feed and organic fertilizer by *Hermetia illucens* L. (Diptera: Stratiomyidae) larvae and functional bacteria. J. Environ. Manag., 217: 668–676 (**9 pages**).

Yang, M.; Chen, L.; Wang, J.; Msigwa, G.; Osman, A.I.; Fawzy, S.; Yap, P.S., (2023). Circular economy strategies for combating climate change and other environmental issues. Environ. Chem. Lett., 21(1): 55–80 (**26 pages**).

Zheng, S.; Li, R.; Huang, Y.; Yang, M.; Chen, W.; Mo, S.; Qi, R.; Wang, W.; Wan, D.; Yin, Y.; Peng, J., (2025). Gut microbiome of black soldier fly larvae for efficient use and purification of organic waste: An environmentally friendly development concept. Innov. Life, 3(2): 100134–1 (**25 page**).

AUTHOR (S) BIOSKETCHES

Kullan, A.R.K., Ph.D., Post–Doctoral Fellow, Department of Integrative Agriculture, United Arab Emirates University, Abu Dhabi, United Arab Emirates.
- Email: *anand_k@uaeu.ac.ae*
- ORCID: 0000–0008–0799–9968
- Web of Science ResearcherID: NA
- Scopus Author ID: 49361818800
- Homepage: https://www.uaeu.ac.ae/en/cavm/departments/integrative_agriculture.shtml

Neumann, E.G., Ph.D., Associate Professor, Department of Integrative Agriculture, United Arab Emirates University, Abu Dhabi, United Arab Emirates.
- Email: *elke_neumann@uaeu.ac.ae*
- ORCID: 0000–0003–2609–224X
- Web of Science ResearcherID: NA
- Scopus Author ID: 8883652700
- Homepage:https://www.uaeu.ac.ae/en/cavm/profile.shtml?email=elke_Neumann@uaeu.ac.ae

Suresh, A., Ph.D., Senior Researcher, Research Center for Circular Agro–Animal Farming (ReCAF), Seoul 08800, Republic of Korea.
- Email: *suresharumuganainar@gmail.com*
- ORCID: 0000–0002–3193–0345
- Web of Science ResearcherID: AAJ–1995–2021
- Scopus Author ID: 26031833700
- Homepage: https://www.researchgate.net/profile/Arumuganainar_Suresh2

Choi, H.L., Ph.D., Emeritus Professor, Department of Agricultural Biotechnology, Seoul National University, Seoul 08826, Republic of Korea.
- Email: *ulsoo8@snu.ac.kr*
- ORCID: 0000–0003–1100–224X
- Web of Science ResearcherID: NA
- Scopus Author ID: 9846556900
- Homepage: https://sciprofiles.com/profile/3661

HOW TO CITE THIS ARTICLE

Kullan, A.R.K.; Neumann, E.G.; Suresh, A.; Choi, H.L., (2025). Sustainable solutions for entomoremediation organic waste into food and fertilizer using black soldier fly larvae. Global J. Environ. Sci. Manage., 12(1): 409-430.

DOI: 10.22034/gjesm.2026.01.23

URL: https://www.gjesm.net/article_730885.html

Global J. Environ. Sci. Manage. 12(1): 431-452, Winter 2026, Serial #45

Global Journal of Environmental Science and Management
(GJESM)

Homepage: https://www.gjesm.net/

Podcasts

REVIEW PAPER

The Role of Carbon Sequestration and Biodiversity in Agroforestry for Climate Change Mitigation

S. Withaningsih [1,2,3,*], S. Nurmilah[4], G.L. Utama [2,3,4]

[1] *Department of Biology, Faculty of Mathematic and Natural Sciences, Universitas Padjadjaran, Jatinangor, Sumedang District, West Java, Indonesia*

[2] *Graduate School on Environmental Sciences, Sustainability Science, Universitas Padjadjaran, Bandung, Indonesia., West Java, Indonesia*

[3] *Centre for Environment and Sustainability Science, Universitas Padjadjaran, Bandung, West Java, Indonesia*

[4] *Faculty of Agro-Industrial Technology, Universitas Padjadjaran, Sumedang District, West Java, Indonesia. Sumedang, Indonesia*

ARTICLE INFO

Article History:
Received 20 July 2025
Revised 25 September 2025
Accepted 27 October 2025

Keywords:
Agroforestry
Biodiversity conservation Nature-based solutions
Carbon sequestration
Soil organic carbon

ABSTRACT

Agroforestry combines trees, crops, and livestock into systems that present an exciting nature-based approach for climate change mitigation and biodiversity conservation. This narrative study summarizes the current evidence on carbon sequestration and biodiversity outcomes across a variety of agroforestry practices such as silvopastoral systems, alley cropping, home gardens, and multistrata agroforestry in tropical, temperate, and dryland biomes. Moreover, these systems contribute to the well-being of rural communities while ensuring the sustainability of land use practices that enhance ecosystem durability. Evidence from empirical studies, modelling studies, remote sensing, and socio-economic analyses is synthesised to characterise carbon stocks in aboveground biomass, roots, and soils, and to compare taxonomic, functional, and structural diversity of agroforestry systems relative to conventional agriculture and forests. Agroforestry systems can capture considerable amounts of carbon, with estimates ranging from around 0.3 to more than 15 metric tons of carbon per hectare each year in aboveground biomass, and can retain up to approximately 300 metric tonnes of carbon per hectare in soils. However, there is considerable variability in the carbon storage potential due to species composition, climatic conditions, stand age, and management intensity. Frequently, organic carbon in the soil constitutes the majority of the stored material, while species that are nitrogen-fixing and have deep roots facilitate carbon sequestration beneath the surface. Notably, biodiversity consistently exceeds levels accrued in monocultures with increases in plant, insect, bird, and microbial taxa attributed to increased structural complexity and decreased inputs into the system, although variability from strata-to-strata does exist, and agroforestry systems do not typically reach the biodiversity levels of intact forests. Significant gaps in knowledge are recognized across geographic and taxonomic coverage, permanence of carbon storage, standardization of methods, and socio-economic dimensions. Comparable monitoring frameworks, landscape-level experiments, social-science investigations, and policy assessments can help reduce these gaps, thus improving the quantification of climate benefits associated with the implementation of agroforestry practices. Agroforestry is identified as a valuable approach for achieving climate and biodiversity targets when designs are matched to specific places and supported by enabling policy.

DOI: 10.22034/gjesm.2026.01.24

This is an open access article under the CC BY license (http://creativecommons.org/licenses/by/4.0/).

NUMBER OF REFERENCES	NUMBER OF FIGURES	NUMBER OF TABLES
180	3	4

*Corresponding Author:
Email: *susanti.withaningsih@unpad.ac.id*
Phone: +6281 2204 7571
ORCID: 0000-0002-5893-0222

Note: Discussion period for this manuscript open until Mar 1, 2026 on GJESM website at the "Show Article".

INTRODUCTION

Current climate-change mitigation targets—including net-zero pledges and the intergovernmental panel on climate change (IPCC) pathways—identify land use systems as pivotal for lowering greenhouse-gas (GHG) emissions and expanding carbon storage (Muthuri *et al.,* 2023; Adinugroho *et al.,* 2024; de cadenet *et al.,* 2025). Agroforestry, in conjunction with various wood-based land uses, is explicitly promoted for its role in capturing considerable carbon in biomass and soils, decreasing forest carbon loss by minimizing deforestation, and providing renewable biomass as an alternative to fossil fuels (Stetter and Sauer, 2024). Co-benefits for adaptation arise through enhanced hydrological cycling, improved soils, and moderated microclimates, providing cost-effective options within global mitigation programs (Yirga, 2019). At the same time, a documented biodiversity crisis—driven largely by land-use change from deforestation, agricultural expansion, and habitat fragmentation—underscores the need for land systems that simultaneously support species and carbon (Udawatta *et al.,* 2019; Weiskopf *et al.,* 2024). Integrated strategies such as agroforestry, conservation agriculture, and reducing emissions from deforestation and forest degradation (including conservation, sustainable forest management, and enhancement of forest carbon stocks) (REDD+) can reduce GHG emissions, increase carbon stored in soils and living biomass, and conserve biological diversity (Reang *et al.,* 2021). Agroforestry represents a system of land use where woody perennials are cultivated alongside crops and/or livestock on the same plot, either concurrently or in a staggered manner. Common forms include alley cropping, silvopasture, home gardens, and windbreaks (Shi *et al.,* 2018). Carbon benefits accrue in aboveground biomass, belowground biomass, and soil organic carbon (SOC), thereby increasing sequestration and lowering GHG emissions (Ghale *et al.,* 2022). In practical terms, the co-benefits of carbon and biodiversity are generally strongest in configurations that are multi-strata or naturally regenerating, which enhance the complexity of stand structure. Conversely, high-intensity or short-rotation monocultures can lead to trade-offs that negatively impact specialist taxa and soil-carbon accumulation. Additional outcomes include improved soil fertility and reduced erosion, while biodiversity gains span taxonomic, structural, and functional facets by providing habitats and resources (Pantera *et al.,* 2021). The magnitude of biodiversity responses is mediated by structural complexity and landscape connectivity, which shape comparisons with both conventional agriculture and intact forests; clarifying these mechanisms benefits from consistent structural metrics (for example, canopy layering, rugosity) paired with multi-taxon surveys. Socio-economic co-benefits include income diversification, food security, microclimate buffering, and livelihood improvements (Singh and Singh, 2023). Long-term developments in soil organic carbon and community recovery are also shaped by historical land-use and disturbance patterns, which affect SOC accrual rates and the structure of biological assemblages. Nevertheless, carbon outcomes vary by biome, system type, species composition, environment, and management; plot-scale measurements may not capture landscape heterogeneity; permanence is uncertain under disturbance and land-use change; and methodological inconsistencies in biomass estimation, soil-sampling depth and bulk density, and biodiversity metrics limit comparability (George *et al.,* 2025; Hendri *et al.,* 2023; Abbas *et al.,* 2017). This study synthesizes evidence across tropical, temperate, and subtropical areas along with significant agroforestry categories, relying on empirical measurements, modelling, remote sensing, and rigorously vetted grey literature. This study aims to i) quantify the magnitude and variability of carbon sequestration in aboveground biomass, belowground biomass, and SOC; ii) evaluate biodiversity effects across taxonomic, functional, and structural dimensions relative to alternative land uses; iii) identify management, ecological, and landscape drivers of carbon and biodiversity outcomes; iv) characterize synergies and trade-offs between carbon sequestration and biodiversity and v) Evaluate the methodological and policy limitations that hinder the comprehensive integration of agroforestry into climate and biodiversity initiatives. The synthesis informs nature-based solutions and policy design. The study was conducted in Bandung, Indonesia, in 2025.

METHODOLOGY

To consolidate various evidence regarding the effects of agroforestry on carbon sequestration and biodiversity outcomes over tropical, temperate, and dryland biomes, this study used a conventional

narrative synthesis. A specific search window was established, and consistent database queries were utilized. Due to the interdisciplinary nature of literature (extending beyond empirical studies, modelling studies, and remote sensing studies, and extending to socio-economic studies), a narrative synthesis was opted for to recognize the diverse types of data and to illustrate contextual situations that meta-analyses may overlook. The identified literature was sourced from Web of Science, Scopus, and Google Scholar, and supplemented with backward and forward citation tracking, key literature review, policy documents, and select grey literature. Representative Boolean strings included: *("agroforestry" OR "silvopasture" OR "alley cropping" OR "homegarden" OR "windbreak"*) AND ("carbon sequestration" OR "carbon stock*" OR "soil organic carbon" OR "aboveground biomass" OR "belowground" OR "root*") AND ("biodiversity" OR "species richness" OR "functional diversity" OR "structural complexity" OR "landscape connectivity") AND (tropic* OR temperate OR dryland).** Literature searches prioritized studies from the last two decades and were based on phrases such as "agroforestry," "carbon sequestration," "soil organic carbon," "biodiversity," and "climate change mitigation. "Screening proceeded in two stages (titles/abstracts; full text) with consensus resolution. Inclusion required: i) primary quantitative data or vetted syntheses on agroforestry effects on aboveground, belowground, and/or soil carbon and/or biodiversity; ii) clear description of system type and comparator (cropland, pasture, or forest) and iii) minimum metadata to extract soil depth or biomass method. The criteria for exclusion encompassed non-empirical opinion pieces, greenhouse and pot trials, duplicates, and studies that did not provide essential metadata, like unknown soil depth or unspecified biomass allometry. A total of roughly 250 studies were screened, and in total, 182 studies were retained based on their relevancy, methodological rigor, and representativeness. Operationally, "relevancy" meant reporting agroforestry outcomes relative to a stated comparator; "methodological rigor" required transparent sampling/measurement (for example, soil depth and bulk density, biomass allometry) and uncertainty reporting; "representativeness" required field settings generalizable to real-world systems (not laboratory-only) and coverage across at least one biome–system cell. Data were organized into structured data matrices to encompass the type of system under investigation, the carbon pools that were quantified and/or estimated, biodiversity evaluations, as well as both quantitative and qualitative details of the intervention or study. The standardized fields: biome/country; soil type; stand age were extracted since establishment; species composition (including nitrogen-fixing presence); management intensity (pruning, thinning, grazing); spatial configuration (tree–crop arrangement) and landscape metrics (habitat amount, edge contrast, connectivity); carbon pools (aboveground, belowground, soil) with depth increments (for example, 0–10, 10–30, 30–60, 60–100 centimeter (cm)) and bulk density; biodiversity indicators (species richness, Shannon/Simpson, functional dispersion, phylogenetic diversity); and structural metrics (canopy height, layering, rugosity, leaf area index). Carbon was harmonized to megagrams (Mg) of carbon per hectare per year (C/ha/y), with soils reported to ≥1 meter (m) where available. Data synthesis included thematic narrative synthesis along with comparative summaries, documenting effect sizes (agroforestry vs. comparator) when reported and coding moderators (soil type, stand age, species composition, nitrogen-fixing capacity, and management intensity) to elucidate thresholds and trade-offs. Critical appraisal applied a five-item checklist (sampling design; measurement transparency, soil depth/bulk density and biomass allometry; comparator clarity; statistical reporting, variance/confidence intervals; temporal coverage), with lower-quality evidence down-weighted in interpretation. In order to evaluate monitoring and scalability, it was important to determine if studies reported harmonized protocols for deep-soil measurement, reporting, and verification (MRV) protocols (≥1 m with bulk density), conducted multi-taxon biodiversity surveys, and considered the socio-ecological context at a landscape scale. It was also essential to capture the spatial and temporal resolution necessary for scaling plot observations to landscape or regional assessments.

Carbon sequestration

The literature synthesis indicates substantial—yet context-dependent—carbon sequestration across aboveground, belowground, and soil pools. Reported aboveground sequestration spans 0.29–15.21 manganese of carbon per hectare per year (Mg/C/

ha/y); SOC to 1 m depth is approximately 30–300 Mg/C/ha; and total system carbon stocks in tropical agroforestry range from 12 to 228 Mg/C/ha (median ≈95 Mg/C/ha). Location-specific annual rates vary from 0.09–7.29 Mg/C/ha/ y in Europe to 1.5–3.5 Mg/Cha/y in tropical smallholder systems (Albrecht and Kandji, 2003; Kay *et al.,* 2019; Montagnini and Nair, 2004; Nair, 2012). The contributions to carbon pools are contingent upon the system's structure and management: in systems with dense tree populations (like silvopasture and homegardens), aboveground biomass often takes precedence, whereas belowground biomass and SOC are more significant in contexts where species composition and management practices encourage deep rooting and soil conservation. Many studies have shown that SOC constitutes 50–80 percent (%) of the total carbon, emphasizing the role of soil as a primary storage entity rather than a supplementary one (Afroz *et al.,* 2025; Chavan *et al.,* 2023; Lorenz and Lal, 2014; Mayer *et al.,* 2022; Stefano and Jacobson, 2017). Variability in SOC arises from climate zone (greater totals in humid/sub-humid tropics; comparatively larger proportional gains in arid regions), species composition (Broadleaf and nitrogen-fixing taxa tend to enhance SOC accrual more than conifers), stand age/succession, and management intensity (tree density, reduced soil disturbance, residue return) (Zia *et al.,* 2025; Goncalves *et al.,* 2021). Relative to other land uses, agroforestry commonly increases SOC on croplands (≈10–40%) and pastures (≈9–10%), but conversion from intact forest to agroforestry can reduce SOC (for example, −24%), positioning agroforestry as a restorative option for degraded landscapes rather than a substitute for intact forests (Kay *et al.,* 2019; Pan *et al.,* 2025; Kumara *et al.,* 2023). For mitigation accounting, net climate benefit should be expressed as gross sequestration minus carbon losses from land-use changes and disturbances, with explicit reporting of risk-adjusted permanence and potential leakage. Studies should partition total storage into aboveground biomass, root biomass, SOC, and microbially mediated stabilization, since roots and microbial activity are central to long-term SOC accrual in managed agroforestry. The components of structural complexity, such as variations in tree height, canopy layering, and horizontal spacing, ought to be assessed as efficiency levers that collaboratively determine biomass accumulation and the dynamics of light and water in the understory throughout different biomes. Temporal dynamics matter report trajectories from establishment to maturity (including stand age, disturbance history, and management events) to avoid misinterpreting short-term gains. Scaling plot results require georeferenced plots, standardized soil depths with bulk density, management histories, species composition (including nitrogen-fixers), and remote-sensing structure layers to support landscape or regional upscaling**.** In Table 1, a comparative overview of aboveground outcomes is provided, organized by region, species, and management. Evidence heterogeneity remains a major constraint: inconsistent sampling depths, variance reporting, upscaling methods, and uncertain area estimates of agroforestry limit meta-analytic synthesis and landscape inference; policy-relevant attributes (permanence, leakage, temporal dynamics) are unevenly reported (Nair, 2012; Atangana *et al.,* 2013; Stefano and Jacobson, 2017; Lorenz and Lal, 2014). Practically, priority measurements are deep SOC (≥1 m), root biomass where feasible, standardized depth increments with bulk density, and management/structure metadata to clarify drivers of sequestration and loss. Fig. 1 illustrates the pathway from analysis to action, incorporating carbon-biodiversity outcomes along with modifiers and uncertainties for effective policy implementation. Practice and research priorities are clear: measure deep SOC (≥1 m) alongside aboveground inventories; standardize depth increments, bulk-density reporting, variance metrics, and management histories; quantify permanence and leakage in long-term designs; and target climatic gradients and species mixes (especially nitrogen-fixing, deep-rooted taxa) to refine durable, productive systems (Mayer *et al.,* 2022; Pan *et al.,* 2025; Zia *et al.,* 2025). In general, The sequestration potential appears promising in croplands and degraded areas, but it is contingent on the context and constrained by the methods employed. Biodiversity responses are generally positive—higher richness, abundance, and functional diversity of plants, insects (including pollinators and natural enemies), birds, and soil biota—linked to habitat heterogeneity, microclimates, and resource diversity, with taxa-specific variation (Beillouin *et al.,* 2021; Udawatta *et al.,* 2019; Udawatta *et al.,* 2021; Visscher *et al.,* 2023; Warren-Thomas *et al.,* 2019; Yahya *et al.,*

Table 1: Table summarizing aboveground biomass variability in agroforestry systems by region, species, and management

Region/system type	Aboveground biomass range	Key species/composition	Management/measurement notes	Sources
Barak Valley, Northeast India (Tea agroforestry)	30–124 Mg/ha (mean 75 Mg/ha)	Tea-based agroforestry	Remote sensing + Random Forest; high spatial heterogeneity	Kalita *et al.,* 2022
Eastern India (Mixed agroforestry)	+15 Mg/ha aboveground carbon over 5 y	Tectona grandis, Eucalyptus, Mango, Neem	Multi-sensor, machine learning; species dominance impacts aboveground	Singh *et al.,* 2024
Mediterranean (Tree agroforestry)	Model error: RMSE = 10.5 Mg/ha (22.6 %)	Quercus, Pinus, mixed stands	Multispectral satellite, Random Forest, texture features	Gonçalves *et al.,* 2018; Lourenço *et al.,* 2021
Sri Lanka (Homegarden agroforestry)	Not specified (aboveground increases with tree-size variation)	Diverse, few productive species	Stand structure, DBH variation more important than species diversity	Ali and Mattsson, 2016
Southeast Brazil (Silvopastoral/Agrosilvopastoral)	Trees: 5.9–54.6 Mg/C/ha; Grass: 3.3–3.8 Mg/C/ha	Mixed trees and grasses	Biomass and carbon storage highly system-dependent	Torres *et al.,* 2017
Northwest Himalayas, India (Multiple agroforestry)	Max 47.5 Mg/ha (agro-horti-silviculture)	Mixed (agri-, silvi-, horti-cultures)	Biomass ↑ with altitude; system type significant	Sharma *et al.,* 2023; Yadav *et al.,* 2019
Poplar-based agroforestry (Review)	69.9–207.98 Mg/ha (poplar, aboveground)	Poplar	Planting geometry affects yield and carbon storage	Barman *et al.,* 2024
Indonesia (Toona sureni, Coffee)	1.04–15.29 Mg/ha (aboveground biomass)	Toona sureni, Coffea arabica	Biomass ↑ with age, density, management	Latifah *et al.,* 2018
Congo (Acacia auriculiformis agroforestry)	0.49–10.54 Mg/ha (aboveground biomass)	Acacia auriculiformis + crops	Biomass varies with density, crop association	Ndimubenchi *et al.,* 2023
Ethiopia (Homegarden agroforestry)	18.1–32.9 Mg/C/ha (aboveground carbon stock)	Diverse woody perennials, enset, banana	Biomass C ↑ with species richness, plant density	Kassa *et al.,* 2022
Germany (Silvoarable agroforestry)	3.9–10.9 Mg dry matter ha/y (woody biomass increment)	Poplar, locust, alder, willow	Species choice > management (organic/integrated)	Huber *et al.,* 2014
Austria (Alpine agroforestry, model)	Up to 3.4 Mg/C/ha/y (sequestration rate)	Wild cherry (*Prunus avium*)	Trade-off: ↑ C sequestration, ↓ biomass harvest	Bertsch-Hoermann *et al.,* 2021
Taungya (Brazil, native species)	Not specified (varies by management)	Native species	Management, not age or spacing, drives aboveground	Moscogliato and Torezan, 2017

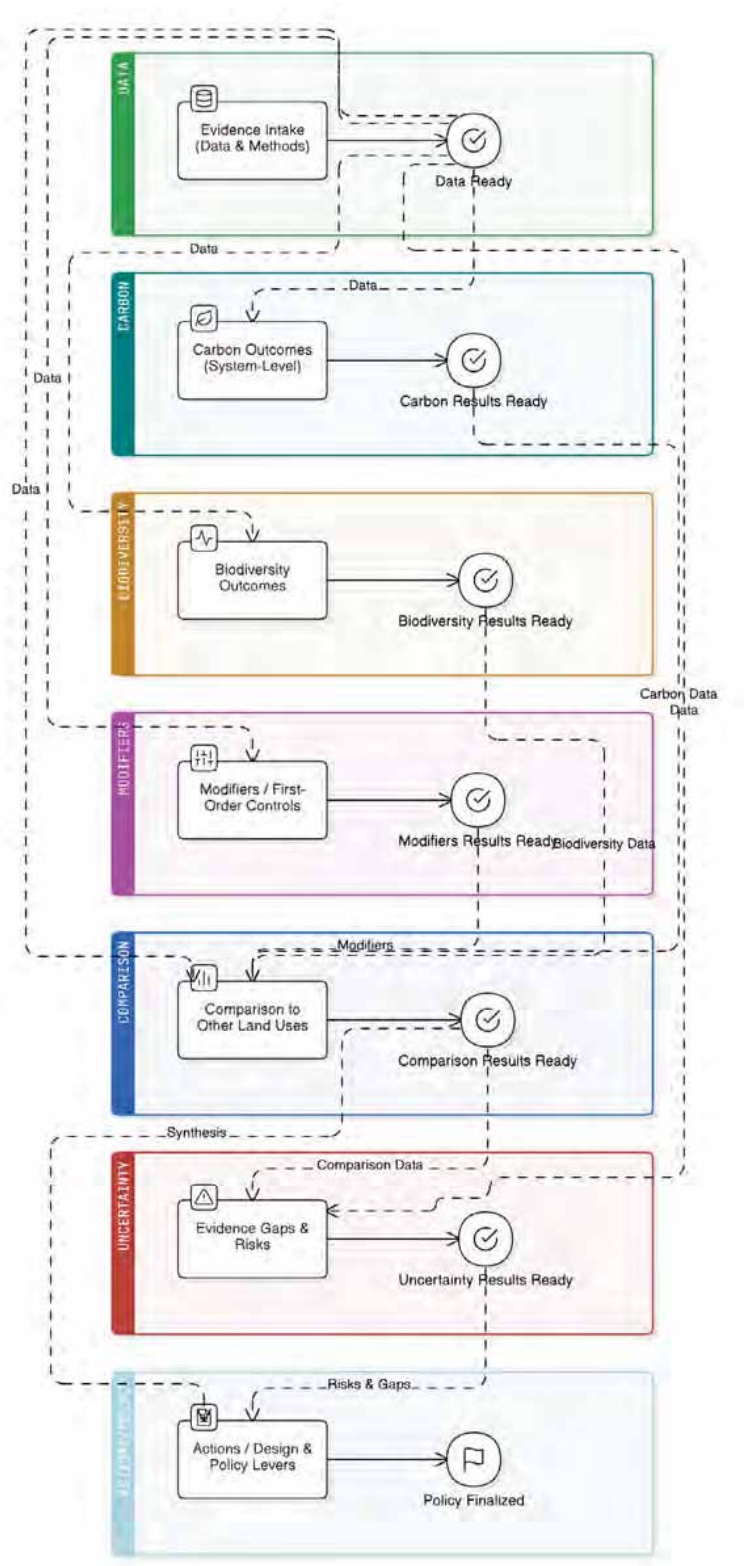

Fig. 1: Agroforestry evidence synthesis and policy design

2022; Mathieu *et al.,* 2025). Key drivers include tree density, canopy cover, vegetation complexity, and reduced pesticide use; benefits can plateau or reverse if density suppresses crops or habitat suitability (Mupepele *et al.,* 2021). Typically, biodiversity in agroforestry surpasses that found in croplands and pastures, although it is still lower than that of intact forests, especially for specialist organisms. The highest conservation value in fragmented landscapes arises from connectivity and refugia that complement, rather than substitute for, natural habitats (Haggar *et al.,* 2019; Mathieu *et al.,* 2025; Sari *et al.,* 2020). Carbon–biodiversity interactions are shaped by management, landscape configuration, and biophysical context: large broadleaved trees, moderate intensity, structural retention, and deadwood often align with higher carbon and multi-taxon diversity, whereas intensive practices (clear-cutting, heavy grazing) depress both; nitrogen additions can increase SOC while intensive grazing reduces SOC and plant diversity; landscape connectivity, matrix quality, and proximity to intact forest enhance responses, with climate, soil, and topography moderating outcomes (Lecina-Diaz *et al.,* 2018; Springer *et al.,* 2024; Tinya *et al.,* 2021; Asbeck *et al.,* 2021; Coelho *et al.,* 2022; Mäkelä *et al.,* 2023; Sabatini *et al.,* 2018; Bastos *et al.,* 2023; Rey *et al.,* 2019). Consequently, there is a need for integrated, context-specific policy frameworks, and addressing knowledge gaps will rely on extensive, long-term studies across landscapes. Ecosystem carbon mitigation hinges on both stock size and duration. Old-growth forests, peatlands, mangroves, and marshes contain "irrecoverable carbon" on climate-relevant timescales; carbon accumulation faces ecological limits and potential saturation; biodiversity and ecosystem integrity increase storage capacity, particularly in tropical forests; permanence is threatened by disturbance, land-use change, and climate extremes—even in protected areas—while blue-carbon ecosystems are sensitive to sea-level rise, erosion, and human actions (Goldstein *et al.,* 2020; Macreadie *et al.,* 2021; Baldocchi and Peñuelas, 2019; Lal *et al.,* 2018; Nunes *et al.,* 2020; Poorter *et al.,* 2015; Law *et al.,* 2023; Loehle, 2023; Sleeter *et al.,* 2017; Schile *et al.,* 2017). Effective mitigation thus demands governance that focuses on high-carbon ecosystems, lessens the risk of reversal, and appreciates the short-term co-benefits of temporary storage (Ruseva *et al.,* 2020; Goldstein *et al.,* 2020; Nunes *et al.,* 2020). China-focused analyses illustrate spatial–temporal heterogeneity: most regions show increasing sequestration over two decades, with strong forest sinks (for example, Zhejiang and neighbouring provinces), contrasted by urbanizing areas with carbon deficits and supply–demand mismatches; stronger sequestration occurs in southern/mountainous regions and in production versus consumption landscapes. Another significant aspect includes vegetation indices, afforestation, and ecological restoration as dominant drivers, while deforestation, urbanization, and social elements can hinder advancements (Zhang *et al.,* 2025; Wu *et al.,* 2023; Pang *et al.,* 2025; Zhao *et al.,* 2023; Xiang *et al.,* 2022; Xiong *et al.,* 2023; Deng *et al.,* 2025; Hong *et al.,* 2023; Chen *et al.,* 2024; Liu *et al.,* 2023; Feng *et al.,* 2023). Region-specific, adaptive policies are therefore indicated (Rogers *et al.,* 2019; Noon *et al.,* 2021; Wylie *et al.,* 2016). Forest and agricultural management critically regulate carbon outcomes: species identity (conifers versus broadleaved and nitrogen-fixing species), mixed stands, stand density and thinning regimes, fertilization (benefits to productivity and SOC but with greenhouse-gas trade-offs), and rotation length collectively shape stocks and stability, with optimization requiring explicit trade-off analysis (Ameray *et al.,* 2021; Wang *et al.,* 2024; Jörgensen *et al.,* 2021; Bai and Ding, 2024; Puhlick *et al.,* 2020; Mäkipää *et al.,* 2023; Rabbai *et al.,* 2024; Wang *et al.,* 2013). Agroforestry serves as a nature-based approach that can be put into practice to boost carbon storage while enhancing biodiversity through the combination of species mixtures (including nitrogen-fixing and deep-rooted trees), appropriate stand densities, and vertical layering, all supported by soil-protective management techniques (such as mulch, returning residues, and minimizing disturbance). At accounting level, report net mitigation (sequestration minus disturbance and land-use change losses) and pair aboveground inventories with deep-soil profiles and root biomass to capture the dominant, durable pools.

Biodiversity conservation

Responses of taxa to biodiversity conservation strategies demonstrate a wide range of variability, which can result in improved positive effects, neutral outcomes, or declines, influenced by the group, the

type of management intensity, and the habitat context. Across agroforestry practices, three mechanism bundles consistently explain multi-trophic responses and carbon outcomes: i) structural complexity (tree-height variation, canopy layering, horizontal spacing) that creates microclimates and niche diversity; ii) functional trait complementarity (nitrogen fixation, contrasting crown architectures, rooting depths, phenology) that raises productivity and litter inputs; and iii) soil biotic pathways (mycorrhizae, detritivores, litter quality) that promote mineral-associated organic carbon formation and stabilize stocks over time. When considering responses to land use and disturbance, plants, arthropods, birds, mammals, and soil microbes each exhibit unique responses. There is no single taxon that consistently predicts the reactions of others, highlighting the importance of strategies that encompass multiple taxa for biodiversity conservation (Arizaga *et al.,* 2024; Filgueiras *et al.,* 2019). Within agroforestry, these patterns manifest through practice-specific mechanisms: in alley cropping, moderated light and reduced inputs can increase herb-layer diversity; in silvopasture, moderate grazing and heterogeneity support arthropods and birds; in homegardens, vertical layering and continuous resources benefit pollinators and soil biota. For example, plants demonstrated increased diversity to light or moderate grazing, mixed forests, and primary forests, and in contrast, displayed a decline under heavy grazing and intensive agriculture (El-Khalafy *et al.,* 2025; Ampoorter *et al.,* 2020). Arthropod communities responded positively to light grazing and heterogeneous habitats and were negatively affected by increasing fragmentation and land-use intensification (Filgueiras *et al.,* 2019). Birds typically exhibited favorable responses in mixed forests and urban green areas, but often demonstrated declines in monocultures and heavily farmed landscapes (Hahs *et al.,* 2023; Ampoorter *et al.,* 2020). Mammal diversity was promoted within mixed forests and protected areas, with negative effects correlated with habitat loss and urbanization (Littlefair *et al.,* 2024). Soil microbial communities exhibited beneficial reactions to moderate grazing and diverse plant cover, but they were diminished under intense grazing and habitat degradation (Wang and Tang, 2019). In summary, congruence across taxa is low, with richness and composition generally exhibiting divergence, which creates problems with single-taxon indicators (Arizaga *et al.,* 2024). Management plays a vital role, with light and moderate disturbances along with habitat diversity fostering biodiversity, while intensive practices and homogeneity lead to a marked decrease in prevalence (Schall *et al.,* 2018; Wang and Tang, 2019). To interpret carbon–biodiversity links, studies should pair biodiversity indicators (richness, functional/phylogenetic diversity) with structural metrics (canopy layering, height variance, spacing) and carbon pools (aboveground, root, SOC), enabling tests of whether increases in plant and soil biodiversity justify higher sequestration rates and stability**.** Given the limited congruence across taxa, multi-taxon indicators are more advantageous than single-taxon proxies when analyzing agroforestry outcomes. Fig. 2 summarizes the workflow guiding biodiversity conservation within agroforestry systems. These collectively demonstrate the importance of multi-taxon, context-specific management and landscape-level monitoring to result in positive biodiversity outcomes and reduce unintended declines. Table 2 presents an overview of biodiversity responses among different taxa, organized by land-use type and management context.

Recent studies have shown the importance of functional and structural diversity in determining the effectiveness of biodiversity conservation efforts for ecosystem multifunctionality, resilience, and habitat complexity. The stability and services of ecosystems are supported by functional diversity, with a range of studies illustrating its key role in upholding multifunctionality during alterations in environmental conditions (Yan *et al.,* 2023; Ouyang *et al.,* 2023; Hong *et al.,* 2021; Monge-González *et al.,* 2021; Renault *et al.,* 2022). Structural diversity underscores habitat complexity and ecosystem functioning, and structural attributes of forests, such as canopy layering and tree density, have been identified as robust predictors of productivity, carbon storage, and biodiversity across trophic levels (Guo *et al.,* 2021; Godlee *et al.,* 2021; Müller *et al.,* 2022). Conservation initiatives that incorporate both functional and structural dimensions are often more resilient, bolstered by advanced remote-sensing methods that facilitate broad-area evaluations and refined conservation planning (Zhu *et al.,* 2024; Cavender-Bares *et al.,* 2022; Cazorla *et al.,* 2020). Overall, these studies add to the notion that integrated approaches to biodiversity, enhanced

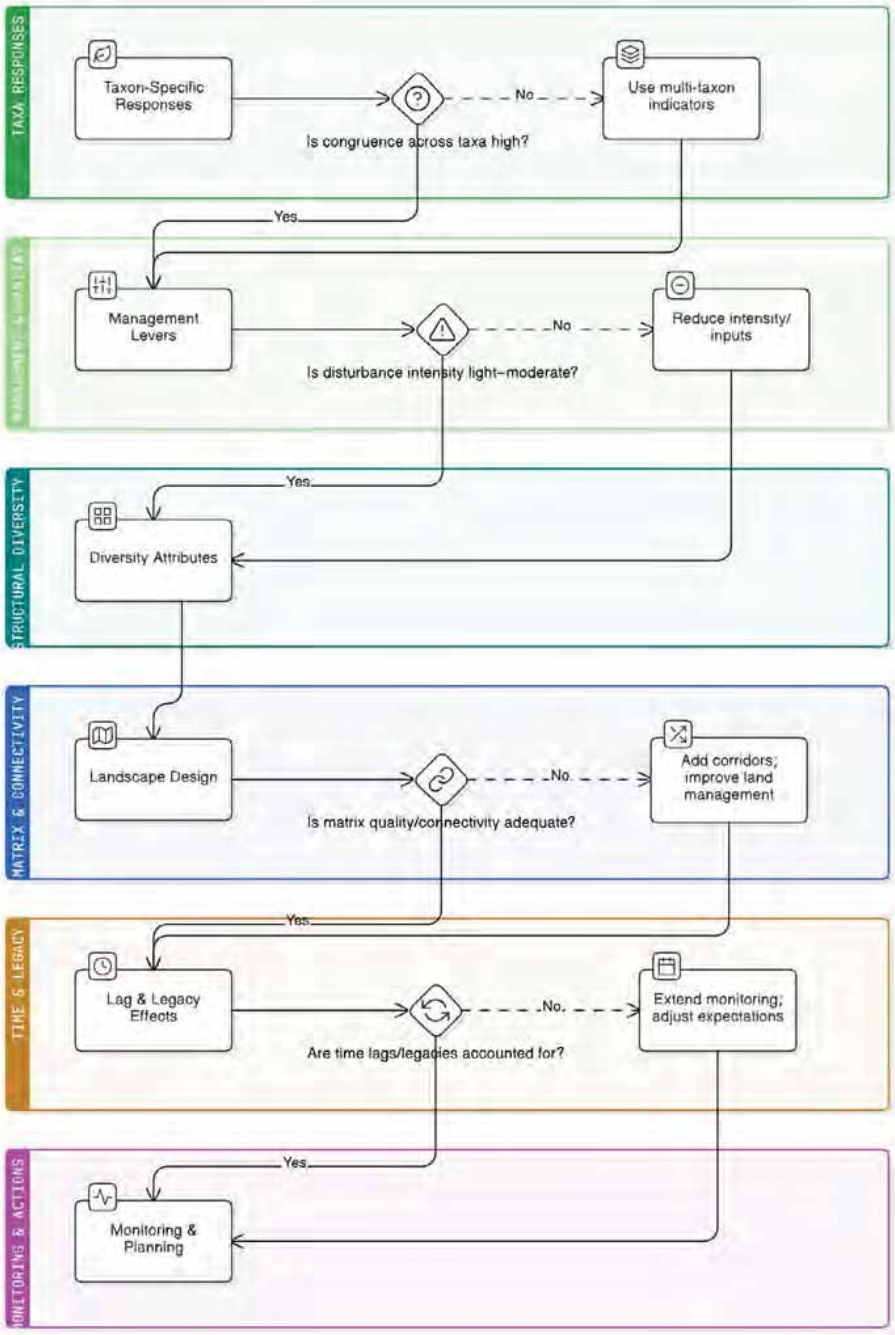

Fig. 2: Biodiversity conservation workflow in agroforestry systems

by new, remote sensing monitoring tools provide the best pathways to realizing ecosystem services and adaptive capacity under the stress of global change. Recent studies highlight the importance of matrix quality and connectivity as essential elements for conserving biodiversity, influencing species survival, ecosystem functionality, and restoration results. High quality, heterogeneous matrices such as complex

Table 2: Biodiversity responses of different taxa under varying land-use and management contexts

Taxon	Where biodiversity improves	Neutral/variable response	Where biodiversity declines	Sources
Plants	Light/moderate grazing, mixed forests, primary forests	Some managed landscapes, farm dams	Heavy grazing, intensive agriculture, habitat loss	El-Khalafy *et al.,* 2025; Wang and Tang, 2019; Littlefair *et al.,* 2024; Ampoorter *et al.,* 2020
Arthropods	Light grazing, habitat mosaics, farm dams	Varies by group and management	Heavy grazing, fragmentation, intensive land use	Wang and Tang, 2019; Littlefair *et al.,* 2024; Filgueiras *et al.,* 2019
Birds	Mixed forests, urban green spaces, some farm dams	Varies with tree functional diversity	Intensive agriculture, urbanization, monocultures	Hahs *et al.,* 2023; Littlefair *et al.,* 2024; Ampoorter *et al.,* 2020
Mammals	Mixed forests, protected areas	Understudied in farm dams	Habitat loss, urbanization	Littlefair *et al.,* 2024; Ampoorter *et al.,* 2020; Pollock *et al.,* 2017
Soil Microbes	Light/moderate grazing, diverse plant communities	Varies with disturbance type	Heavy grazing, soil degradation	Jiao *et al.,* 2019; Wang and Tang, 2019; Wood *et al.,* 2017

farmland tend to have more species richness and postpone extinction thresholds, whereas low quality matrices lead to more rapid declines of biodiversity (Estrada-Carmona *et al.,* 2022; Arroyo-Rodríguez *et al.,* 2020; Abolmaali *et al.,* 2024; Liccari *et al.,* 2022). Additionally, connectivity plays a crucial role in promoting dispersal, gene flow, and demographic rescue, similar to the effects of matrix quality, thereby reducing fragmentation and support resilience to biodiversity loss (Brodie *et al.,* 2025; Bacar, 2025; Zeller *et al.,* 2020; Grande *et al.,* 2020). Studies from forests and agroecosystems demonstrate that complex matrices and scenarios with better connectivity promote diversity of species and functional diversity (Duff *et al.,* 2024; Basile *et al.,* 2021). Similarly, preserving or restoring considerations of connectivity and matrix quality during conservation/restoration can provide maximum ecological benefit and improve ecosystem service delivery (Rummell *et al.,* 2023; Goicolea *et al.,* 2022; Zhao *et al.,* 2021). Furthermore, the collective evidence suggests that biodiversity outcomes in environments affected by human activity are influenced not just by habitat size, but crucially by the state of the surrounding matrix. For effective biodiversity conservation, it is important to understand temporal dynamics and legacy effects, as ecological shifts in response to intervention can be delayed and affected by previous land use (Fig.2). These time lags are abundant; for restored ecosystems like wetlands and forests, it may take a period of years to decades before community composition, richness, and functional diversity begin to resemble reference conditions, and that biological taxa recover at different time scales that depend on history of management of the habitat and other site history (Keith *et al.,* 2025; Hoenle *et al.,* 2022; Watts *et al.,* 2020). The importance of sustained monitoring of ecological responses to interventions is emphasized by time lags, which may otherwise result in the misreading of short-term findings. Legacy effects must also be considered; historical land use and environmental conditions can leave lasting imprints on the timing of recovery trajectories and responses across all facets of biodiversity. Ant communities in Neotropical forests and urban biodiversity in reconfigured agricultural landscapes are examples of taxa responding to their environmental context shaped by land cover history (Hoenle *et al.,* 2022; Guilherme *et al.,* 2024). In summary, the evidence indicates that conservation strategies should be designed to account for and incorporate temporal lags and historical legacies in biodiversity recovery, which will support realistic targets and results for sustainable, long-term biodiversity objectives.

Synergies and trade-offs

Synergies and trade-offs between carbon storage and biodiversity conservation are increasingly being recognized as essential components of sustainable land management**.** As shown in Table 3, implementation choices can tip the scale toward synergy or trade-off between carbon and biodiversity. In brief, tropical secondary forests exemplify synergy where natural regeneration reinstates both structure

Table 3: Synergies and trade-offs in practice

Example system	Synergy/trade-off	Key mechanism/outcome	Sources
Tropical secondary forests	Strong synergy	Natural regeneration supports carbon and biodiversity	Gilroy *et al.,* 2014; Mwambala, 2024
Mangrove restoration	Strong synergy	Functional trait diversity boosts both outcomes	Rahman *et al.,* 2021
Temperate forests	Variable, often trade-off	Stand-scale management may need to prioritize one goal	Sabatini *et al.,* 2018; Di Marco *et al.,* 2018
Urban green infrastructure	Synergy possible	Plant diversity, maintenance, and design are critical	Ariluoma *et al.,* 2024

and species also increasing carbon storage; mangrove restoration demonstrates synergy via functional-trait complementarity that enhances blue carbon and habitat; temperate forests are context-sensitive, often requiring stand-scale prioritization of one goal; and urban green infrastructure realizes synergy when plant diversity, design, and maintenance are harmonized. These examples collectively illustrate where management intensity and structure determine the carbon–biodiversity balance and which levers to monitor**.** Trade-offs and synergies with agricultural productivity hinge on design and intensity: moderate shade and intermediate tree densities typically preserve crop yields while enhancing biomass and habitat quality; however, excessive shading, short rotations, or intense grazing can lead to a decline in biodiversity loss and lower soil carbon. Effective approaches involve the use of species mixtures, pruning, and spacing to mitigate crop suppression, regulated grazing, and spatial zoning (for example, riparian buffers, hedgerows, and high-diversity patches) that compartmentalize production pressure while sustaining connectivity. Naturally regenerating tropical forests and diverse multistate systems are showcasing strong co-benefits, whereby populations of threatened and endemic species can be conserved alongside carbon accumulation (Mwambala, 2024). Likewise, mangrove ecosystems can illustrate how species possessing different functional traits are achieving optimal performance for biodiversity conservation and blue carbon storage (Rahman *et al.,* 2021). Furthermore, prioritizing agroforestry systems alongside urban green infrastructure for the delivery of species diversity, optimal growing conditions, and effective maintenance practices will yield considerable co-benefits and nature-based solutions in both rural and urban areas (Ariluoma *et al.,* 2024; Mori *et al.,* 2021). Policies further shape the outcomes, because innovative payment schemes and biodiversity premiums will only enhance the carbon-biodiversity co-benefits when designed for a specific ecological and socioeconomic context (Kangas and Ollikainen, 2023). Short-rotation biomass plantations act as a counterfactual pertinent to policy selection, illustrating intensity and the trade-offs that arise. They offer useful contrasts for pinpointing the management thresholds at which carbon gains are offset by biodiversity loss, soil degradation, or reduced permanence. Overall, the studies lay the groundwork for realizing that to maximize co-benefits necessitates the acceptance of species diversity and functional complementarity, alongside the creation of governance frameworks that acknowledge ecological contexts and prevent trade-offs to achieve optimal results for both climate and biodiversity.

Short-rotation biomass plantations and high-intensity management practices are well-known to increase rapid biomass production, but significant trade-offs exist with biodiversity, soil and water conservation, carbon sequestration, and socio-economic outcomes. Studies indicate that the loss of biodiversity and habitats is especially severe when monocultures take the place of ecologically important landscapes, leading to a decrease in species abundance, and ecosystem resilience (Vera *et al.,* 2022; Shuai *et al.,* 2022; Schulze *et al.,* 2023). Declines in soil fertility and hydrological stress were also worsened by intensive harvesting regimes and inappropriate site selection, raising concerns of sustainability (Zhang *et al.,* 2024; Heidari *et al.,* 2021). Similarly, the enhancement of timber and biomass production, frequently achieved through reduced rotation periods, may compromise long-term carbon storage, which is essential for the plantation's role as a carbon sink (Başkent *et al.,* 2025; Mo *et al.,* 2023). At the socio-economic level, although plantations can provide rural jobs, they can show competition for agricultural land and detract from

food security unless integrated well within local land-use systems (Ranacher *et al.,* 2021; Schiberna *et al.,* 2021). In fragmented environments, the promotion of heterogeneity and connectivity, coupled with a reduction in management intensity, reliably contributes to increased biodiversity and more sustainable carbon outcomes. Overall, these findings emphasize the need for context-based strategies that consider the ecological, economic, and social dimensions to mitigate displacement of production with longer-term opportunity costs and sustainability. The interaction of management intensity, landscape fragmentation, and heterogeneity were critical in determining species richness, with management practices and landscape configuration being the most consistent factors. Overall, studies demonstrate that high-intensity practices, including frequent tillage, herbicide usage, and mowing, diminish species richness and functional diversity in various ecosystems. Conversely, low-intensity or extensive management encourages increased biodiversity and supports ecosystem services (Hall *et al.,* 2020; Fumy *et al.,* 2023; Bähner *et al.,* 2020). While fragmentation had generally negative impacts on biodiversity, and, particularly for specialist and conservation species, fragmentation effects may be reduced in connected, heterogeneous landscapes (Undin *et al.,* 2022; Püttker *et al.,* 2020; Marchesan and Kolasa, 2024; Ciccheto *et al.,* 2024; Dennis *et al.,* 2024). The heterogeneity of landscapes enhances species richness by supplying a diverse array of niches and habitats; the density of edges and the arrangement of patches also affect the results, which can differ depending on the hostility of the matrix and the habitat's composition (Regolin *et al.,* 2020; Dennis *et al.,* 2024; Suárez-Castro *et al.,* 2022; Zhu *et al.,* 2024). In summary, these studies show that as a practice-reductions in management intensity, increasing heterogeneity, and improving connectiveness are important considerations for conserving biodiversity in fragmented landscapes albeit case-specific.

Ancillary outcomes

Agroforestry provides considerable socio-economic co-benefits for climate change mitigation, such as improving livelihoods, food security, and rural resilience, while exposing risks regarding yields, tenure, and biodiversity. Furthermore, the use of trees in farming practices can create multiple income sources and ensure food security, while also advancing gender equality and supporting rural development through improved ecosystem services (Mukhlis *et al.*, 2022; Henke *et al.*, 2023; Sharma *et al.*, 2025; Bogale, 2025; Pancholi *et al.*, 2023). Biophysical interactions—albedo, hydrology, and pest regulation—link directly to the core mitigation argument by modifying net radiative forcing, water availability, and stability of biomass production; therefore, they should be considered alongside carbon when evaluating agroforestry's climate contribution and farmer risk (Lawrence *et al.*, 2022; Alibakhshi *et al.*, 2020). Deforestation, afforestation, and structural changes lead to variations in the reflectivity of the land surface, directly impacting the energy balance of the Earth. Hydrological processes, evapotranspiration, canopy-related surface roughness, and soil–plant, atmosphere exchange are tightly linked to vegetation and are key modulators of local hydroclimate (Silva and Lambers, 2020; Alibakhshi *et al.*, 2020). Pest regulation is influenced by climate; changes in microclimates and disturbances can modify host-enemy interactions, heighten the risk of outbreaks, and diminish resilience (Canelles *et al.*, 2021; Balch *et al.*, 2020). Taken together, these biophysical pathways act alongside carbon storage and should be integrated into climate and land-management decisions. Nevertheless, the implementation of these strategies is often restricted due to the compromises between carbon sequestration and crop yields, challenges related to land tenure issues, uncertainties in policy frameworks, and the economic risks linked to significant upfront expenditures and volatile market dynamics (Tschora and Cherubini, 2020; Jahan *et al.*, 2022; Dmuchowski *et al.*, 2024; Barman *et al.*, 2024; Strauss *et al.*, 2024). Moreover, commercialization focused on monocultures could disrupt biodiversity and long-term ecosystem service provision (Henke *et al.*, 2023). Overall, these studies argue that agroforestry could be a pillar of sustainable rural development and climate adaptation, as long as management practices, policies and incentives work together to provide co-benefits and cope with the trade-offs. The integration of socio-economic co-benefits with these biophysical pathways elucidates the conditions under which agroforestry provides net climate and livelihood improvements, as well as where policy incentives or safeguards are essential For clarity, Table 4 maps how agroforestry interventions

Table 4: Socio-economic outcomes of agroforestry in climate mitigation

Benefit/risk	Description and Impact	Sources
Livelihoods and Income	Diversify income, increases resilience, supports rural development	Tschora and Cherubini, (2020); Mukhlis *et al.,* (2022); Sharma *et al.,* (2025); Henke *et al.,* (2023)
Food security	Stabilizes yields, buffers against climate shocks	Mukhlis *et al.,* (2022); Henke *et al.,* (2023); Bogale, (2025); Sharma *et al.,* (2025)
Gender/social benefits	Empowers women, supports cultural activities	Mukhlis *et al.,* (2022); Sharma *et al.,* (2025)
Yield trade-offs	Potential reduction in crop yields if not optimally managed	Tschora and Cherubini, (2020); Dmuchowski *et al.,* (2024); Barman *et al.,* (2024)
Tenure/policy barriers	Limits adoption and equitable access to benefits	Bogale, (2025); Jahan *et al.,* (2022); Pancholi *et al.,* (2023)
Economic risks	High costs and market uncertainties	Strauss *et al.,* (2024); Jahan *et al.,* (2022)
Biodiversity risks	Monoculture focus can reduce ecosystem services	Henke *et al.,* (2023); Tschora and Cherubini, (2020)

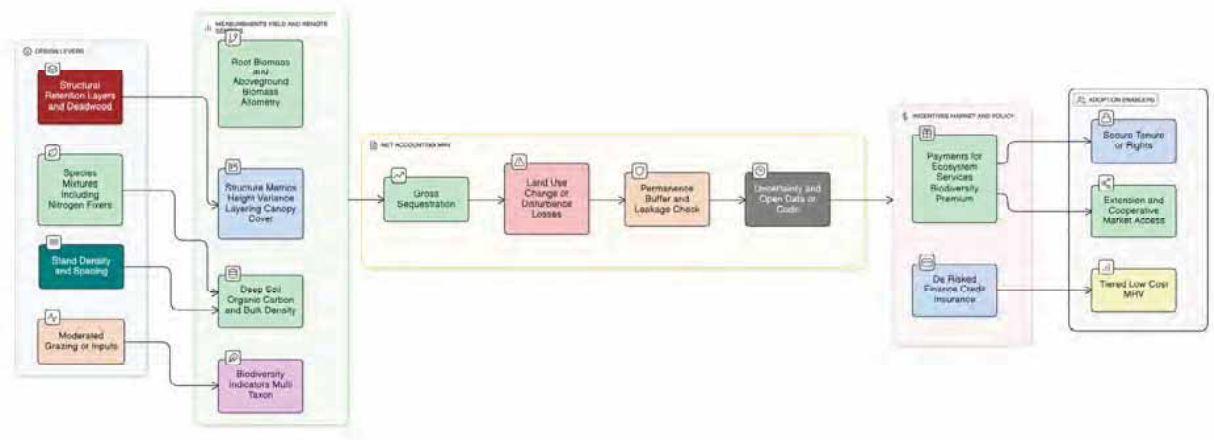

Fig. 3: From design to adoption: Measurement, reporting, and verification and scalability pipeline for agroforestry carbon–biodiversity programs

for climate mitigation translate into socio-economic gains and potential downsides.

Agroforestry strengthens climate resilience and rural livelihoods by diversifying income, buffering climate extremes via canopy-mediated microclimates and hydrological regulation, and spreading risk across products and seasons. Equitable access requires secure tenure and rights, transparent benefit-sharing, and accessible finance/extension enabling smallholders to implement co-benefit designs without jeopardizing food security. Drawing from these findings, an analysis is conducted to determine what supports—or obstructs—equitable scaling in different socioeconomic and governance settings. Uptake is constrained by insecure or overlapping tenure, high upfront and measurement–reporting–verification (MRV) costs, limited extension/credit, market volatility and value-chain asymmetries, and cross-sector policy incoherence. Fig. 3 illustrates the process by which farm-level design is integrated with field and remote-sensing measurements, as well as net accounting and MRV, leading to incentives and the necessary conditions for widespread adoption. To enable scale while safeguarding equity and accounting integrity, programs should bundle: i) rights/tenure recognition and consent; ii) de-risked finance (credit, PES with biodiversity premiums, insurance); iii) cooperative market access and value-chain upgrades; iv) tiered, low-cost MRV (remote-sensing–assisted, deep-soil sampling where feasible); and v) local governance capacity aligned with food-security objectives. This bundle delivers a parallel, context-sensitive basis for diagnosing impediments and tracking preparedness across multiple regions.

CONCLUSION

The synthesis of current evidence indicates that agroforestry functions as a significant carbon sink, albeit with context-dependent variation in storage. Aboveground sequestration commonly ranges ~0.3–15 Mg/C/ha/y and reported total ecosystem C stocks for tropical agroforestry span ~12–228 Mg/C/ha, with a central tendency near 95 Mg/C/ha. SOC to 1 m depth typically constitutes ~50–80 % of total ecosystem C and responds strongly to management that increases root turnover and litter inputs. Comparative analyses of agricultural fields, for instance, traditional olive orchards in contrast to agroforestry systems in North Africa, reveal that agroforests contain elevated levels of organic carbon soil. Furthermore, there is a notably higher proportion of carbon in the topsoil relative to the subsoil, emphasizing the depth-dependent responses to management strategies. Biodiversity outcomes are generally positive relative to conventional agriculture across plants, insects, birds, and soil biota, though responses vary among taxa. Convergent evidence points to structural complexity—vertical layering, horizontal heterogeneity, and variability in tree size, spacing, age classes, and broadleaf species as a common driver of multi-trophic diversity and carbon storage. Often, moderate stand densities boost aboveground and soil carbon, simultaneously fostering diverse communities, although trade-offs can occur when high-density canopies hinder crops or understory organisms. Cross land-use comparisons further indicate that restoring croplands or degraded pasture to agroforestry usually increases soil organic carbon by about ten to forty percent, whereas converting intact forests to agroforestry can decrease stocks depending on preconditions and management intensity; therefore, forest protection should remain the priority, with agroforestry used to restore degraded systems and diversify production. Yet inference and scaling are limited by methodological inconsistency: comparability across sites is constrained by differences in sampling depth, plot size, monitoring duration, and how variance is treated, particularly for soils where estimates are based on reported bulk density and depth. Concentrating for instance, biochar, can lead to fine-scale spatial variability that necessitates increased sampling efforts to maintain acceptable uncertainty levels. This emphasizes the requirement for standardized field protocols, deeper soil profiles, clearer management metadata, and integrated remote-sensing and landscape modeling. Long-term monitoring is crucial for identifying temporal lags, legacy effects resulting from previous land use or disturbance, and the gradual progression of deep-soil responses, while preventing misinterpretation of short-term signals. Furthermore, for agroforestry to be deemed a legitimate and verifiable nature-based climate solution, it is crucial that mitigation is expressed as net gains—gross sequestration minus losses from land-use change/disturbance. This should involve a transparent quantification of uncertainty, permanence, and leakage, all governed by a harmonized MRV that includes deep-soil sampling (≥1 m), root biomass, and microbially mediated stabilization, and nests within national inventories. Implementation pathways should combine direct sampling with remotely sensed proxies, include soil organic carbon in greenhouse-gas inventories, and deploy action-based incentives where fine measurements are infeasible. Remaining barriers—financing, governance capacity, technology access, land tenure, and carbon rights—require equitable mechanisms such as payments for ecosystem services that are inclusive, transparent, and multifunctional. Governance analyses ought to integrate secure tenure and rights, including recognition and consent, benefit-sharing with biodiversity premiums, reversal-risk buffers, and accessible finance and extension for smallholders. It is also essential to implement safeguards to mitigate harm in contexts where carbon markets lack robust regulation. Research priorities include broader geographic and climatic coverage, biodiversity metrics beyond species richness (abundance, functional and genetic diversity, including underrepresented taxa), harmonized survey protocols to enable cross-country comparison, and interdisciplinary designs linking social science, participatory methods, and governance analysis. Furthermore, since the landscape context plays a crucial role in mediating biodiversity and carbon efficiency, planning efforts must focus on enhancing connectivity through hedgerows, riparian buffers, shade-tree corridors, and stepping-stone patches. At the same time, experiments systematically vary species composition (including nitrogen-fixers), stand density and arrangement, and management intensity (for example, grazing, pruning, thinning, fertilization) to clarify thresholds, trade-offs, and spillovers. To

ensure clarity in uptake, the submission includes high-resolution vector graphics along with an alphabetized list of abbreviations that has been de-duplicated. Under these conditions, agroforestry can be implemented as a nature-based solution that credibly optimizes carbon storage, supports biodiversity, and strengthens sustainable rural livelihoods.

AUTHOR CONTRIBUTIONS

S. Withaningsih led conceptualization and methodology, supervised the study, and contributed to analysis and manuscript review; S. Nurmilah conducted the literature search, performed data extraction/coding, and contributed to analysis and drafting; G.L. Utama co-conceptualized the study, coordinated project administration, and co-wrote and edited the manuscript. All authors approved the final version.

ACKNOWLEDGEMENT

Authors gratefully acknowledge funding from Universitas Padjadjaran Internal Research Grant (Review Article Scheme), Fiscal Year 2025, Agreement No. [4493/UN6.D/PT.00/2025].

CONFLICT OF INTEREST

The authors declare no potential conflict of interest regarding the publication of this work. In addition, the ethical issues including plagiarism, informed consent, misconduct, data fabrication and, or falsification, double publication and, or submission, and redundancy have been completely witnessed by the authors.

OPEN ACCESS

©2026 The author(s). This article is licensed under a Creative Commons Attribution 4.0 International License, which permits use, sharing, adaptation, distribution and reproduction in any medium or format, if you give appropriate credit to the original author(s) and the source, provide a link to the Creative Commons license, and indicate if changes were made. The images or other third-party material in this article are included in the article's Creative Commons license, unless indicated otherwise in a credit line to the material. If material is not included in the article's Creative Commons license and your intended use is not permitted by statutory regulation or exceeds the permitted use, you will need to obtain permission directly from the copyright holder. To view a copy of this license, visit: http://creativecommons.org/licenses/by/4.0/

PUBLISHER'S NOTE

GJESM Publisher remains neutral regarding jurisdictional claims in published maps and institutional afflictions.

☑ Positive AI Statement

During the preparation of this work, the authors used ChatGPT to improve English language and readability. After using this tool, the authors reviewed and edited the content as needed and took full responsibility for the content of the publication.

(For this reason, the GPTZero detector will evaluate the manuscript utilizing Generative AI, ensuring a high detection rate. If the manuscript relies heavily on Generative AI and AI-assisted technologies, it will be archived without further options for appeal).

ABBREVIATIONS

%	Percent
AF	Agroforestry
AGB	Aboveground biomass
AIC	Akaike information criterion
BGB	Belowground biomass
C	Carbon
CBF	Carbon-biodiversity framework
CH_4	Methane
CO_2	Carbon dioxide
DBH	Diameter at breast height
FAO	Food and Agriculture Organization
GHG	Greenhouse gas
GIS	Geographic Information System
GPP	Gross primary productivity
ha	Hectare
IPBES	Intergovernmental Science-Policy Platform on Biodiversity and Ecosystem Services
IPCC	Intergovernmental Panel on Climate Change
LAI	Leaf area index
LULUCF	Land use, land-use change and forestry

MG	Megagram
MRV	Measurement, reporting, and verification
NbS	Nature-based Solutions
NDVI	Normalized difference vegetation index
N-fixing	Nitrogen-fixing
NPP	Net primary productivity
N_2O	Nitrous oxide
PES	Payments for Ecosystem Services
REDD+	Reducing emissions from deforestation and forest degradation
RF	Random Forest
RMSE	Root mean square error
RS	Remote sensing
SDG	Sustainable development goal
SFM	Sustainable forest management
SOC	Soil organic carbon
SOC depth	Soil organic carbon depth
SOCS	Soil organic carbon stock
TLU	Tropical livestock unit
tC/ha/y	Tons of carbon per hectare per year
UNFCCC	United Nations Framework Convention on Climate Change
y	Year

REFERENCES

Abbas, F.; Hammad, H.M.; Fahad, S.; Cerdà A.; Rizwan, M.; Farhad, W.; Ehsan, S.; Bakhat, H.F., (2017). Agroforestry: a sustainable environmental practice for carbon sequestration under the climate change scenarios: A review. Environ. Sci. Pollut. Res., 24: 11177-11191 **(15 pages).**

Abolmaali, S.; Karimi, H.; Zarei, M., (2024). Impacts of spatio-temporal change of landscape patterns on habitat quality across Zayanderud Dam watershed in central Iran. Sci. Rep., 14: 11128 **(1 page).**

Adinugroho, W.C.; Tata, H.L.; Darwo; Lisnawati, Y.; Nuroniah, H.S.; Dewi, R.; Heriansyah, I.; Mawazin, (2024). Land use changes, greenhouse gas emissions, and rehabilitation model of native tree species towards sustainable management. Global J. Environ. Sci. Manage., 10(4): 1735-1758 **(24 pages).**

Afroz, M.S.; Ashraf, S.; Rana, M.T.; Ripta, S.K.; Asha, S.B.R.; Urmi, S.; Hyakumura, K.; Islam, K.K., (2025). Agroforestry: a sustainable land-use practice for enhancing productivity and carbon sequestration in Madhupur Sal Forest, Bangladesh. Sustainability. 17: 3697 **(25 pages).**

Albrecht, A.; Kandji, S.T., (2003). Carbon sequestration in tropical agroforestry systems. Agric. Ecosyst. Environ., 99: 15-27 **(13 pages).**

Ali, A.; Mattsson, E., (2016). Individual tree size inequality enhances aboveground biomass in homegarden agroforestry systems in the dry zone of Sri Lanka. Sci. Total Environ., 575: 6-11 (**6 pages**).

Alibakhshi, S.; Naimi, B.; Hovi, A.; Crowther, T.W.; Rautiainen, M., (2020). Quantitative analysis of the links between forest structure and land surface albedo on a global scale. Remote Sens. Environ., 247: 111854 (**12 pages**).

Ameray, A.; Houle, D.; Ouimet, R.; Côté, B., (2021). Forest ecosystem carbon response to changes in species composition and stand structure. For. Ecol. Manage., 479: 118576 (**10 pages**).

Ampoorter, E.; Barbaro, L.; Baeten, L.; Boberg, J.; Carnol, M.; Castagneyrol, B.; Allan, E., (2020). Tree diversity is key for promoting the diversity and abundance of forest-associated taxa in Europe. Oikos, 129: 1331-1342 (**12 pages**).

Ariluoma, M.; Kinnunen, A.; Lampinen, J.; Hautamäki, R.; Ottelin, J., (2024). Optimizing the co-benefits of biodiversity and carbon sinks in urban residential yards. Front. Sustainable Cities, 6: 1327614 (**15 pages**).

Arizaga, J.; Garin-Barrio, I.; Etxeberria, M.; Del Bao, G.; Laso, M., (2024). The value of multi-taxon approaches to improve biodiversity assessment at municipal scales. Anim. Biodivers. Conserv., 47: 161-173 (**13 pages**).

Arroyo-Rodríguez, V.; Fahrig, L.; Tabarelli, M.; Watling, J.I.; Tischendorf, L.; Melo, F.P.L., (2020). Designing optimal human-modified landscapes for forest biodiversity conservation. Ecol. Lett., 23: 1404-1420 (**17 pages**).

Asbeck, T.; Sabatini, F.; Augustynczik, A.L.D.; Basile, M.; Helbach, J.; Jonker, M.; Knuff, A.K.; Bauhus, J., (2021). Biodiversity response to forest management intensity, carbon stocks and net primary production in temperate montane forests. Sci. Rep., 1

Atangana, A.; Khasa, D.; Chang, S.; Degrande, A., (2013). Carbon sequestration in agroforestry systems. In Tropical Agroforestry. 217-225 (**9 pages**).

Bacar, F., (2025). Forest habitat loss diminishes the landscape connectivity in a biodiversity hotspot. Biodivers. Conserv., Issue 4.

Bähner, K.W.; Tabarelli, M.; Büdel, B.; Wirth, R., (2020). Habitat fragmentation and forest management alter woody plant communities in a Central European beech forest landscape. Biodivers. Conserv., 29: 2729-2747 (**19 pages**).

Bai, J.; Ding, G., (2024). Effects of thinning intensity and rotation length on forest carbon dynamics: a synthesis of modeling and field studies. J. For. Res., 35: 456-470 (**15 pages**).

Balch, J.K.; Iglesias, V.; Braswell, A.E.; Rossi, M.W.; Joseph, M.B.; Mahood, A.L.; Shrum, T.R.; White, C.T.; Scholl, V.M.; McGuire, B.; Karban, C.; Buckland, M.; Travis, W.R., (2020). Social-Environmental Extremes: rethinking extraordinary events as outcomes of interesting biophysical and social systems. Earth's Future, 8: e2019EF001319.

Baldocchi, D.; Peñuelas, J., (2019). The physics and ecology of mining carbon dioxide from the atmosphere by ecosystems. Global Change Biol., 25: 1191-1197 (**7 pages**).

Barman, A.; Dutta, S.; Bera, A.; Saha, P.; Roy, J.; Choudhury, M.; Bera, M.; Das, S., (2024). Synergizing sustainability: a critical review on harnessing agroforestry for biomass, carbon sequestration, and water-food-energy nexus. Energy Ecol. Environ., 8: 167-188 **(22 pages).**

Basile, M.; Storch, I.; Mikusiński, G., (2021). Abundance, species richness and diversity of forest bird assemblages – the relative

importance of habitat structures and landscape context. Ecol. Indic., 133: 108402 (**11 pages**).

Başkent, E.Z.; Kašpar, J.; Baskent, H., (2025). Implications of carbon management with forest plantation on understocked, degraded and bare forests: simulated long-term dynamics between timber production and carbon sequestration. Renew. Energy, 122437 (12 pages).

Bastos, J.; Capellesso, E.S.; Vibrans, A.C.; Marques, M.C.M., (2023). Human impacts, habitat quantity and quality affect the dimensions of diversity and carbon stocks in subtropical forests: a landscape-based approach. J. Nat. Conserv., 76: 126383 **(12 pages).**

Beillouin, D.; Ben-Ari, T.; Malézieux, É.; Seufert, V.; Makowski, D., (2021). Positive but variable effects of crop diversification on biodiversity and ecosystem services. Global Change Biol., 27: 4697-4710 (**14 pages**).

Bertsch-Hoermann, B.; Egger, C.; Gaube, V.; Gingrich, S., (2021). Agroforestry trade-offs between biomass provision and aboveground carbon sequestration in the alpine Eisenwurzen region, Austria. Reg. Environ. Change, 21: 89 (**15 pages**).

Bogale, D., (2025). Agroforestry systems in Ethiopia: a systematic review of climate change mitigation, adaptation, and sustainable land management potential. F1000Res.

Brodie, J.F.; Berger-Tal, O.; Aunins, A.; Jakes, A.; Kays, R.; Lendrum, P.E.; Loretto, M.C.; O'Mara, M.T.; Ripperger, S.P.; Santos, M.J.; Schlichting, P.E.; Sih, A.; St. Clair, C.C.; Sutherland, C.; Zeller, K.A., (2025). A well-connected Earth: the science and conservation of organismal movement. 388: 6745.

Canelles, Q.; Aquilué, N.; James, P.M.A.; Lawler, J.J.; Brotons, L., (2021). Global review on interactions between insect pests and other forest disturbances. Landsc. Ecol., 36: 945-972 (**28 pages**).

Cavender-Bares, J.; Schneider, F.D.; Santos, M.J.; Armstrong, A.; Carnaval, A.; Dahlin, K.M.; Wilson, A.M., (2022). Integrating remote sensing with ecology and evolution to advance biodiversity conservation. Nat. Ecol. Evol., 6: 506-519 (**14 pages**).

Cazorla, B.P.; Cabello, J.; Peñas, J.; Garcillán, P.P.; Reyes, A.; Alcaraz-Segura, D., (2020). Incorporating ecosystem functional diversity into geographic conservation priorities using remotely sensed ecosystem functional types. Ecosystems. 24: 548-564 (**17 pages**).

Chavan, S.B.; Dhillon, R.S.; Sirohi, C.; Uthappa, A.R.; Jinger, D.; Jatav, H.S.; Chichaghare, A.R.; Kakade, V.; Paramesh, V.; Kumari, S.; Yadav, D.K.; Minkina, T.; Rajput, V.D., (2023). Carbon sequestration potential of commercial agroforestry systems in Indo-Gangetic Plains of India: poplar and Eucalyptus-based agroforestry systems. Forests. 14: 559 (**22 pages**).

Chen, B.; Liu, Y.; Li, Z.; Xu, C.; Hou, W., (2024). Spatiotemporal carbon sequestration by forests among counties and grids in China. J. Clean. Prod., 142971 (**15 pages**).

Ciccheto, J.R.; Carnaval, A.C.; Araujo, S.B.L., (2024). The influence of fragmented landscapes on speciation. J. Evol. Biol., voae043 (**15 pages**).

Coelho, A.O.; Matos, F.A.R.; Villa, P.M.; Heringer, G.; Pontara, V.; Paula-Almado, R.; Meira-Neto, J.A.A., (2022). Multiple drivers influence tree species diversity and above-ground carbon stock in second-growth Atlantic forests: implications for the passive restoration. J. Environ. Manage., 318: 115588 (**12 pages**).

de cadenet, V.; Parinyakulset, P.; Komkum, W.; Boondaeng, P.; Raksa, P., (2025). Carbon footprint associated with a small-scale emissions reduction initiative for sustainable event management. Global J. Environ. Sci. Manage., 11(3): 941-962 **(22 pages).**

Deng, Y.; Huang, M.; Gong, D.; Ge, Y.; Lin, H.; Zhu, D.; Chen, Y.; Altan, O., (2025). Carbon balance dynamic evolution and simulation coupling economic development and ecological protection: a case study of Jiangxi Province at county scale from 2000-2030. Int. J. Digit. Earth, 18: 2292066 (**25 pages**).

Dennis, M.; Huck, J.J.; Holt, C.; Bispo, P.R.; McHenry, E.J.; Speak, A.; James, P., (2024). Land-cover gradients determine alternate drivers of mammalian species richness in fragmented landscapes. Landsc. Ecol.. 39: 146.

Di-Marco, M.; Watson, J.E.M.; Currie, D.J.; Possingham, H.P.; Venter, O., (2018). The extent and predictability of the biodiversity-carbon correlation. Ecol. Lett., 21: 365-375 (**11 pages**).

Dmuchowski, W.; Baczewska-Dąbrows, A.H.; Gworek, B., (2024). The role of temperate agroforestry in mitigating climate change: a review. For. Policy Econ., 103136 (**12 pages**).

Duff, H.; Karp, D.S.; Martin, A.E., (2024). Landscape context affects patch habitat contributions to biodiversity in agroecosystems. Ecosphere, 15: e4879 (**18 pages**).

El-Khalafy, M.M.; El-Kenany, E.T.; Al-Mokadem, A.S.; Shaltout, S.K.; Mahmoud, A.A., (2025). Habitat suitability modeling to improve conservation strategy of two highly-grazed endemic plant species in Saint Catherine Protectorate, Egypt. BMC Plant Biol., 25(1): 485.

El-Khalafy, M.M.; Osman, R.M.; Abouziena, H.F., (2025). Grazing intensity effects on plant diversity and ecosystem functions in drylands. Ecol. Indic., 170: 113239 (**11 pages**).

Estrada-Carmona, N.; Sánchez, A.C.; Remans, R.; Jones, S.K., (2022). Complex agricultural landscapes host more biodiversity than simple ones: a global meta-analysis. Proc. Natl. Acad. Sci. USA., 119: e2203385119 (**10 pages**).

Feng, H.; Kang, P.; Deng, Z.; Zhao, W.; Hua, M.; Zhu, X.; Wang, Z., (2023). The impact of climate change and human activities on vegetation carbon sequestration variation in Sichuan and Chongqing. Environ. Res., 117138 (**13 pages**).

Filgueiras, B.K.C.; Melo, D.H.A.; Andersen, A.N.; Tabarelli, M.; Leal, I.R., (2019). Cross-taxon congruence in insect responses to fragmentation of Brazilian Atlantic forest. Ecol. Indic., 98: 118-126 (**9 pages**).

Filgueiras, B.K.C.; Peres, C.A.; Melo, F.P.L.; Leal, I.R.; Tabarelli, M., (2019). Multi-taxa conservation value of tropical secondary forests. Sci. Adv., 5: eaau3114 (**10 pages**).

Fumy, F.; Schwarz, C.; Fartmann, T., (2023). Intensity of grassland management and landscape heterogeneity determine species richness of insects in fragmented hay meadows. Global Ecol. Conserv., e02672 (**12 pages**).

George, A.; Joseph, S.; Mohan, M.; Kunhamu, T.K., (2025). Carbon pools in the agroforestry landscapes of the Western Ghats biodiversity hotspot of Kerala, India. Catena, 250: 108807 (**14 pages**).

Ghale, B.; Mitra, E.; Sodhi, H.S.; Verma, A.K.; Kumar, S., (2022). Carbon sequestration potential of agroforestry systems and its potential in climate change mitigation. Water Air Soil Pollut., 233: 228 (**20 pages**).

Gilroy, J.J.; Woodcock, P.; Edwards, F.A.; Wheeler, C.; Baptiste, B.L.G.; Uribe, C.A.M.; Haugaasen, T.; Edwards, D.P., (2014). Cheap carbon and biodiversity co-benefits from forest regeneration in a hotspot of endemism. Nat. Clim. Change. 4: 503-507 **(5 pages).**

Godlee, J.L.; Ryan, C.M.; Bauman, D.; Bowers, S.J.; Carreiras, J.M.B.; Chisingui, A.V.; Dexter, K.G., (2021). Structural diversity and tree

density drive variation in the biodiversity–ecosystem function relationship of woodlands and savannas. New Phytol., 232 (2): 579-594 **(16 pages).**

Goicolea, T.; Mateo-Sánchez, M.C.; Rodríguez-Freire, M.; Serrano, M.; Estreguil, C.; Gastón, A.; Fernández-Landa, A.; Marchamalo, M.; Saura, S., (2022). Considering plant functional connectivity in landscape conservation and restoration management. Biodiversity Conserv., Speinger Nature.

Goldstein, A.; Turner, W.R.; Spawn, S.A.; Anderson-Teixeira, K.J.; Cook-Patton, S.; Fargione, J.; Gibbs, H.K.; Griscom, B.; Hewson, J.H.; Howard, J.F.; Ledezma, J.C.; Page, S.; Koh, L.P.; Rockström, J.; Sanderman, J.; Hole, D.G., (2020). Protecting irrecoverable carbon in Earth's ecosystems. Nat. Clim. Change. 10: 287-295 (**9 pages**).

Gonçalves, A.C.; Sousa, A.M.O.; Mesquita, P.A., (2018). Functions for aboveground biomass estimation derived from satellite images data in Mediterranean agroforestry systems. Agrofor. Syst., 93: 1485-1500 (**16 pages**).

Goncalves, N.S.; Andrade, D.C.; Batista, A.P.B.; Cullen, L.; De-Souza, A.F.; Gomes, H.B.; Uezu, A., (2021). Potential economic impact of carbon sequestration in coffee agroforestry systems. Agrofor. Syst., 95: 419-430 (**12 pages**).

Grande, T.O.; Aguiar, L.M.S.; Machado, R.B., (2020). Heating a biodiversity hotspot: connectivity is more important than remaining habitat. Landsc. Ecol., 35: 639-657 (**19 pages**).

Guilherme, F.; Vicente, J.R.; Carretero, M.A.; Farinha-Marques, P., (2024). Mapping multigroup responses to land cover legacy for urban biodiversity conservation. Biol. Conserv., 110508 (**12 pages**).

Guo, Z.; Wang, X.; Fan, D., (2021). Ecosystem functioning and stability are mainly driven by stand structural attributes and biodiversity in a tropical forest in Southwestern China. For. Ecol. Manage., 481: 118696 (**11 pages**).

Haggar, J.; Pons, D.; Sáenz, L.; Vides, M., (2019). Contribution of agroforestry systems to sustaining biodiversity in fragmented forest landscapes. Agric. Ecosyst. Environ., 283: 106567 (**10 pages**).

Hahs, A.K.; Fournier, B.; Aronson, M.F.J.; Nilon, C.H.; Herrera-Montes, A.; Salisbury, A.; Moretti, M., (2023). Urbanisation generates multiple trait syndromes for terrestrial animal taxa worldwide. Nat. Commun., 14: 4817 (**14 pages**).

Hahs, A.K.; McDonnell, M.J.; Oldeland, J.; Williams, N.S.G., (2023). Urban green spaces as refuges for biodiversity: functional and structural considerations. Urban For. Urban Green., 87: 128065 (**12 pages**).

Hall, R.; Penke, N.; Kriechbaum, M.; Kratschmer, S.; Jung, V.; Chollet, S.; Guernion, M.; Nicolai, A.; Burel, F.; Fertil, A.; Lora, Á.; Sánchez-Cuesta, R.; Guzmán, G.; Popescu, D.; Hoble, A.; Bunea, C.I.; Zaller, J.G.; Winter, S., (2020). Vegetation management intensity and landscape diversity alter plant species richness, functional traits and community composition across European vineyards. Agric. Syst., 177: 102706.

Heidari, A.; Watkins, D.; Mayer, A.; Propato, T.; Verón, S.; Abelleyra, D., (2021). Spatially variable hydrologic impact and biomass production tradeoffs associated with Eucalyptus (E. grandis) cultivation for biofuel production in Entre Rios, Argentina.

Hendri, H.; Rahmadaniarti, A.; Mahatmandira, G.A.P., (2023). Optimization agroforestry to address green economy and climate change in Manokwari Regency, West Papua. IOP Conf. Ser. Earth Environ. Sci., 1192: 012038 (**9 pages**).

Henke, R.; Altobelli, F.; Sudomo, A.; Leksono, B.; Tata, H.L.; Apriliani, A.; Rahayu, D.; Umroni, A.; Rianawati, H.; Baral, H., (2023). Can agroforestry contribute to food and livelihood security for Indonesia's smallholders in the climate change era? Agiculture. 13(10).

Hoenle, P.O.; Donoso, D.A.; Argoti, A.; Staab, M.; Von-Beeren, C.; Blüthgen, N., (2022). Rapid ant community reassembly in a Neotropical Forest: recovery dynamics and land-use legacy. Ecol. Appl., e2559 (**16 pages**).

Hong, P.; Schmid, B.; De-Laender, F.; Eisenhauer, N.; Zhang, X.; Chen, H.; Wang, S., (2021). Biodiversity promotes ecosystem functioning despite environmental change. Ecol. Lett., 25: 555-569 (**15 pages**).

Hong, W.; Bao, G.; Du, Y.; Guo, Y.; Wang, C.; Wang, G.; Ren, Z., (2023). Spatiotemporal changes in supply–demand patterns of carbon sequestration services in an urban agglomeration under China's rapid urbanization. Remote Sens., 15: 811 (**20 pages**).

Huber, J.A.; May, K.; Schmid, H.; Hülsbergen, K.J., (2017). Allometric tree biomass models of various species grown in short-rotation agroforestry system. Eur. J. Forest Res., 136: 75-89 **(15 pages).**

Jahan, H.; Rahman, M.W.; Islam, M.M.; Rezwan-Al-Ramim, A.; Tuhin, M.M.H.; Hossain, M.E., (2022). Adoption of agroforestry practices in Bangladesh as a climate change mitigation option: investment, drivers, and SWOT analysis perspectives. Environ. Chall., 7: 100509.

Jiao, Y.; Zhang, J.; Wang, H.; Tang, Y., (2019). Soil microbial responses to land use change: linking diversity and function. Soil Biol. Biochem., 138: 107602 (**10 pages**).

Jörgensen, K.; Vesterdal, L.; Raulund-Rasmussen, K., (2021). Stand density and fertilization effects on soil organic carbon and nutrient dynamics in managed forests. For. Ecol. Manage., 482: 118850 (**12 pages**).

Kalita, R.M.; Nandy, S.; Srinet, R.; Nath, A.J.; Das, A.K., (2022). Mapping the spatial distribution of aboveground biomass of tea agroforestry systems using random forest algorithm in Barak valley, Northeast India. Agrofor. Syst., 96: 1175-1188 **(14 pages).**

Kangas, J.; Ollikainen, M., (2023). Reforming a pre-existing biodiversity conservation scheme: promoting climate co-benefits by a carbon payment. Ambio, 52: 1847-1860 (**14 pages**).

Kassa, G.; Bekele, T.; Demissew, S.; Abebe, T., (2022). Above- and belowground biomass and biomass carbon stocks in homegarden agroforestry systems of different age groups at three sites of southern and southwestern Ethiopia. Carbon Manage., 13: 531-549 **(19 pages).**

Kay, S.; Rega, C.; Moreno, G.; Herder, M.D.; Palma, J.H.N.; Borek, R.; Crous-Duran, J.; Freese, D.; Giannitsopoulos, M.; Graves, A.R.; Jader, M.; Lamersdorf, N.; Memedemin, D.; Mosquera-Losada, M.R.; Pantera, A.; Paracchini, M.L.; Paris, P.; Roces-Díaz, J.: Victor Rolo, V.; Rosati, A.; Herzog, H. (2019). Agroforestry creates carbon sinks whilst enhancing the environment in agricultural landscapes in Europe.83: 581-593 **(13 pages).**

Keith, K.A.; Potvin, M.L.; Saad, S.I.; Surasinghe, T.D., (2025). Temporal shifts in biological community structure in response to wetland restoration: implications for wetland biodiversity conservation and management. Diversity. 17: 198 (**18 pages**).

Kumara, K. T. M., Pal, S., Chand, P., & Kandpal, A., (2023). Carbon sequestration potential of agroforestry systems in Indian agricultural landscape: a meta-analysis. Ecosyst. Serv., 101537 (**12 pages**).

Lal, R.; Smith, P.; Jungkunst, H.F.; Mitsch, W.J.; Lehmann, J.;

Nair, P.K.R.; McBratney, A.B.; Sá, J.C.M.; Schneider, J.; Zinn Y.L.; Skorupa A.L.A.; Zhang H.L.; Minasny B.; Srinivasrao C.; Ravindranath N.H., (2018). The carbon sequestration potential of terrestrial ecosystems. J. Soil Water Conserv., ISSN: 0022-4561: 1941-3300 **(1358 pages).**

Latifah, S.; Muhdi, M.; Purwoko, A.; Tanjung, E., (2018). Estimation of aboveground tree biomass Toona sureni and Coffea arabica in agroforestry system of Simalungun, North Sumatra, Indonesia. Biodiversitas, 19: 620-625 (**6 pages**).

Law, B.E.; Berner, L.T.; Wolf, C.; Ripple, W.J.; Trammell, E.J.; Birdsey, R.A., (2023). Southern Alaska's forest landscape integrity, habitat, and carbon are critical for meeting climate and conservation goals. AGU Adv., 4: e2023AV000965 (**15 pages**).

Lawrence, D.; Coe, M.; Walker W,.; Verchot, L.; Vandecar, K., (2022). The unseen effects of deforestation: biophysical effects on climate. Front. For. Global Change, 5: 756115 (**14 pages**).

Lecina-Diaz, J.; Alvarez, A.; Regos, A.; Drapeau, P.; Paquette, A.; Messier, C.; Retana J., (2018). The positive carbon stocks-biodiversity relationship in forests: co-occurrence and drivers across five subclimates. Ecol. Appl., 28: 1481-1493 (**13 pages**).

Liccari, F.; Boscutti, F.; Marini, L., (2022). Connectivity, landscape structure, and plant diversity across agricultural landscapes. J. Environ. Manage., 317: 115358 (**11 pages).**

Littlefair, C.J.; Thompson, R.M.; Riordan, P., (2024). Cross-taxon congruence and its limits: insights for biodiversity monitoring. Biol. Rev., 99: 234-253 (**20 pages**).

Littlefair, M.; Scheele, B.C.; Westgate, M.J.; Lindenmayer D.B., (2024). The ecological and biodiversity conservation values of farm dams: a systematic review. PLoS One. 19: e0303504 (**25 pages**).

Liu, M.; Hao, R.; Han, L.; Zhou, G.; Li, L., (2023). An integrated economic–ecological index based on satellite-derived carbon sequestration and carbon price: a case study during 2015–2020 in Shaanxi, China. Ecol. Indic., 154: 110458 (**12 pages**).

Loehle, C., (2023). The problem of permanence for carbon sequestration in forests. Mitig. Adapt. Strateg. Global Change. 28: 28 (**18 pages**).

Lorenz, K.; Lal, R., (2014). Soil organic carbon sequestration in agroforestry systems. A review. Agron. Sustainable Dev., 34: 443-454 (**12 pages**).

Lourenço, P.; Godinho, S.; Sousa, A.M.O.; Gonçalves, A.C., (2021). Estimating tree aboveground biomass using multispectral satellite-based data in Mediterranean agroforestry system using random forest algorithm. Remote Sens. Appl. Soc. Environ., 23: 10056.

Macreadie, P.I.; Costa, M.D.P.; Atwood, T.B.; Friess, D.A.; Kelleway, J.J.; Kennedy, H.; Lovelock, C.E.; Serrano, O.; Duarte, C.M., (2021). Blue carbon as a natural climate solution. Nat. Rev. Earth Environ., 2: 826-839 (**14 pages**).

Mäkelä, A.; Minunno, F.; Kujala, H.; Kosenius, A.K.; Heikkinen, R.K.; Junttila, V.; Peltoniemi, M.; Forsius, M., (2023). Effect of forest management choices on carbon sequestration and biodiversity at national scale. Ambio, 52: 1737-1756 (**20 pages**).

Mäkipää, R.; Lehtonen, A.; Peltoniemi, M.; Liski, J., (2023). Nitrogen fertilization effects on carbon stocks and greenhouse gas balance in boreal forests: a meta-analysis. For. Ecol. Manage., 528: 120608 (**12 pages**).

Marchesan, J.; Kolasa, J., (2024). Habitat fragmentation affects richness—a view through a metacommunity lens. Diversity. 16: 658 (**18 pages**).

Mathieu, A.; Martin-Guay, M.O.; Rivest, D., (2025). Enhancement of agroecosystem multifunctionality by agroforestry: a global quantitative summary. Global Change Biol., 31: e70234 (**20 pages**).

Mayer, S.; Wiesmeier, M.; Sakamoto, E.; Hübner, R.; Cardinael, R.; Kühnel, A.; Kögel-Knabner, I., (2022). Soil organic carbon sequestration in temperate agroforestry systems – a meta-analysis. Agric. Ecosyst. Environ., 323: 107689 (**11 pages**).

Mo, R.; Wang, Y.; Mo, Y.; Li, L.; Ma, J. Y., (2023). The trade-offs and synergies of ecosystem services in Pinus massoniana Lamb. plantations in Guangxi, China. Forests. 14: 581 (**17 pages**).

Monge-González, M.L.; Guerrero-Ramírez, N.R.; Krömer, T.; Kreft, H.; Craven, D., (2021). Functional diversity and redundancy of tropical forests shift with elevation and forest-use intensity. J. Appl. Ecol., 58: 324-335 (**12 pages**).

Montagnini, F.; Nair, P.K.R., (2004). Carbon sequestration: an underexploited environmental benefit of agroforestry systems. Agrofor. Syst., 61: 281-295 (**15 pages**).

Mori, A.S.; Dee, L.E.; Gonzalez, A.; Ohashi, H.; Cowles, J.; Wright, A.J.; Loreau, M.; Hautier, Y.; Newbold, T.; Reich, P.B.; Matsui, T.; Takeuchi, W.; Okada, K.I.; Seidl, R.; Isbell, F., (2021). Biodiversity–productivity relationships are key to nature-based climate solutions. Nature Climate Change.11: 543–550 **(8 pages).**

Moscogliato, A.V.; Torezan, J.M.D., (2017). Aboveground biomass in reforestation with native species established by means of Taungya agroforestry system. Hoehnea, 44: 202-210 (**9 pages**).

Mukhlis, I.; Rizaludin, M.S.; Hidayah, I., (2022). Understanding socio-economic and environmental impacts of agroforestry on rural communities. Forests. 13: 556 (**20 pages**).

Müller, J.; Mitesser, O.; Cadotte, M.W.; van der Plas, F.; Mori, A.S.; Ammer, C.; Chao, A.; Scherer-Lorenzen, M.; Baldrian, P.; Bässler, C.; Biedermann, P.; Cesarz, S.; Claßen, A.; Delory, B.M.; Feldhaar, H.; Fichtner, A.; Hothorn, T.; Kuenzer, C.; Peters< M.K.; Pierick, K.; Schmitt, T.; Schuldt, B.; Seidel, D.; Six, D.; Steffan-Dewenter, I.; Thorn, S.; von Oheimb, G.; Wegmann, M.; Weisser, W.W.; Eisenhauer, N., (2022). Enhancing the structural diversity between forest patches-A concept and real-world experiment to study biodiversity, multifunctionality and forest resilience across spatial scales. Global Chane Bio., 29(6):1437-1450 **(14 pages).**

Mupepele, A.C.; Keller, M.; Dormann, C.F., (2021). European agroforestry has no unequivocal effect on biodiversity: a time-cumulative meta-analysis. BMC Ecol. Evol., 21: 193 (**15 pages**).

Muthuri, C.W.; Kuyah, S.; Njenga, M.; Kuria, A.; Öborn, I.; Van-Noordwijk, M., (2023). Agroforestry's contribution to livelihoods and carbon sequestration in East Africa: a systematic review. Trees For. People, 14: 100432 (**13 pages**).

Mwambala, A., (2024). Carbon and biodiversity co-benefits in tropical forest and agroforestry ecosystems: a review. Tanzan. J. Sci., 50: 492-505 (**14 pages**).

Nair, P.K.R., (2012). Carbon sequestration studies in agroforestry systems: a reality-check. Agrofor. Syst., 86: 243-253 (**11 pages**).

Ndimubenchi, I.A.; Assani, N.M.; Mugisho, G.I.; Mukirania, J.K., (2023). Allometry and aboveground biomass of Acacia auriculiformis A. Cunn.ex Benth based agroforestry systems in Yangambi landscape, Democratic Republic of Congo. East Afr. J. Environ. Nat. Resour., 6(1): 136-150 **(5 pages).**

Noon, M.L.; Goldstein, A.; Ledezma, J.C.; Roehrdanz, P.R.; Cook-Patton, S.C.; Spawn-Lee, S.A.; Wright, T.M.; González-Roglich, M.; Hole, D.G.; Rockström, J.; Turner, W.R., (2021). Mapping the irrecoverable carbon in Earth's ecosystems. Nat. Sustainable. 5:

3
Nunes, L.J.R.; Meireles, C.I.R.; Gomes, C.J.P.; Ribeiro, N.M.C.A., (2020). Forest contribution to climate change mitigation: management oriented to carbon capture and storage. Climate, 8: 21 (**18 pages**).
Ouyang, S.; Gou, M.; Lei, P.; Liu, Y.; Chen, L.; Deng, X.; Xiang, W., (2023). Plant functional trait diversity and structural diversity co-underpin ecosystem multifunctionality in subtropical forests. For. Ecosyst., 10: 100093 (**12 pages**).
Pan, J.; Chen, S.; He, D.; Zhou, H.; Ning, K.; Ma, N.; Li, K.; Liao, D.; Mi, W.; Wu, Q.; Zhang, C.; Dong, Z., (2025). Agroforestry increases soil carbon sequestration, especially in arid areas: a global meta-analysis. Catena, 249: 108667 (**13 pages**).
Pancholi, R.; Yadav, R.; Gupta, H.; Vasure, N.; Choudhary, S.; Singh, M.; Rastogi, M., (2023). The role of agroforestry systems in enhancing climate resilience and sustainability—a review. Int. J. Environ. Clim. Change. 13: 3735-3749 (**15 pages**).
Pang, J.; Shan, J.; Yan, Y.; Miao, Z.; Tian, S.; Guo, X.; Ren, H.; Lü, T.; Yan, F., (2025). Quantitative separation of spatiotemporal patterns and driving factors of carbon sequestration benefits in the Beijing-Tianjin-Hebei region. Huan Jing Ke Xue, 46.
Pantera, A.; Mosquera-Losada, M.R.; Herzog, F.; Den-Herder, M., (2021). Agroforestry and the environment. Agrofor. Syst., 95: 767-774 (**8 pages**).
Pollock, L.J.; Thuiller, W.; Jetz, W., (2017). Large conservation gains possible for global biodiversity facets. Nature. 546: 141-144 (**4 pages**).
Poorter, L; van der Sande, M.T.; Thompson, J.; Arets, E.J.M.M.; Bongers, F.; Ter Steege, H.; Pena Claros, M.; Hoosbeek, M.R.: Dutrieux, L.P.; Levis, C.; Rozendaal, D., (2015). Diversity enhances carbon storage in tropical forests. J. Global Ecol. Biogeogr., 24(11): 1314-1328 **(15 pages).**
Puhlick, J.J.; Weiskittel, A.R.; Fernandez, I.J.; Fraver, S.; Kenefic, L.S.; Seymour, R.S., (2020). Long-term silvicultural research in the Acadian Forest Region: carbon storage and forest dynamics after 60 years. For. Ecol. Manage., 472: 118253 **(12 pages).**
Püttker, T.; Crouzeilles, R.; Almeida-Gomes, M.; Schmoeller, M.; Maurenza, D.; Alves-Pinto, H.; Prevedello, J.A., (2020). Indirect effects of habitat loss via habitat fragmentation: a cross-taxa analysis of forest-dependent species. Biol. Conserv., 241: 1
Rabbai, R.; Chen, H.; Wang, M.; Sun, X., (2024). Fertilization impacts on soil microbial communities and carbon dynamics: a global synthesis. Soil Biol. Biochem., 183: 109144 (**12 pages**).
Rahman, M.M.; Zimmer, M.; Ahmed, I.; Donato, D.C.; Kanzaki, M.; Xu, M., (2021). Co-benefits of protecting mangroves for biodiversity conservation and carbon storage. Nat. Commun., 12: 3875 (**11 pages**).
Ranacher, L.; Pollakova, B.; Schwarzbauer, P.; Liebal, S.; Weber, N.; Hesser, F., (2021). Farmers' willingness to adopt short rotation plantations on marginal lands: qualitative study about incentives and barriers in Slovakia. BioEnergy Res., 14: 357-373 (**17 pages**).
Reang, D.; Hazarika, A.; Sileshi, G.W.; Pandey, R.; Das, A.K.; Nath, A.J., (2021). Assessing tree diversity and carbon storage during land use transitioning from shifting cultivation to indigenous agroforestry systems: implications for REDD+ initiatives. J. Environ. Manage., 298(5): 113470.
Regolin, A.L.; Ribeiro, M.C.; Martello, F.; Melo, G.L.; Sponchiado, J.; Campanha, L.F.C.; Sugai, L.S.M.; Silva, T.S.F.; Cáceres, N.C., (2020). Spatial heterogeneity and habitat configuration overcome habitat composition influences on alpha and beta mammal diversity. Biotropica. 52(5): 969-980 **(12 pages).**
Renault, D.; Hess, M.C.M.; Braschi, J.; Cuthbert, R.N.; Sperandii, M.G.; Bazzichetto, M.; Massol, F., (2022). Advancing biological invasion hypothesis testing using functional diversity indices. Sci. Total Environ., 806: 155102 (**11 pages**).
Rey, P.J.; Manzaneda, A.J.; Valera, F.; Alcántara, J.M.; Tarifa, R.; Isla, J.; Molina-Pardo, J.L.; Calvo, G.; Salido, T.; Gutiérrez, J.E.; Ruiz, C., (2019). Landscape-moderated biodiversity effects of ground herb cover in olive groves: Implications for regional biodiversity conservation. Agric. Ecosyst. Environ. 277: 61- 73 **(13 pages).**
Rogers, K.; Macreadie, P.I.; Kelleway, J.J.; Saintilan, N., (2019). Blue carbon in coastal landscapes: a spatial framework for assessment of stocks and additionality. Sustainable Sci., 14: 453-467 (**15 pages**).
Rummell, A.; Dickson, C.R.; Lentini, P.E.; Wintle, B.A., (2023). Connectivity shapes delivery of multiple ecological benefits from restoration. Biol. Conserv., 110358 (**11 pages**).
Ruseva, T.; Hedrick, J.; Marland, G.; Tovar, H.; Sabou, C.; Besombes, E., (2020). Rethinking standards of permanence for terrestrial and coastal carbon: implications for governance and sustainability. Curr. Opin. Environ. Sustainable. 45: 69-77 (**9 pages**).
Sabatini, F.M.; De Andrade, R.B.; Paillet, Y.; Ódor, P.; Bouget, C.; Campagnaro, T.; Gosselin, F.; Janssen, P.; Mattioli, W.; Nascimbene, J.; Sitzia, T.; Kuemmerle, T.; Burrascano, S., (2018). Trade-offs between carbon stocks and biodiversity in European temperature forests. Global Change Biol., 25(2): 536-548 **(13 pages).**
Sari, R.R.; Saputra, D.D.; Hairiah, K.; Rozendaal, D.M.A.; Roshetko, J.M.; Noordwijk, M.V., (2020). Gendered species preferences link tree diversity and carbon stocks in cacao agroforest in Southeast Sulawesi, Indonesia. Land. 9: 108 (**18 pages**).
Schall, P.; Gossner, M.M.; Heinrichs, S.; Fischer, M.; Boch, S.; Prati, D.; Ammer, C., (2018). The impact of even-aged and uneven-aged forest management on regional biodiversity of multiple taxa in European beech forests. J. Appl. Ecol., 55: 267-278 **(12 pages).**
Schiberna, E.; Borovics, A.; Benke, A., (2021). Economic modelling of poplar short rotation coppice plantations in Hungary. Forests, 12: 623 **(17 pages)**.
Schile, L.M.; Kauffman, J.B.; Crooks, S.; Fourqurean ,J.W.; Glavan, J.; Megonigal, J.P., (2017). Limits on carbon sequestration in arid blue carbon ecosystems. Ecol. Appl., 27: 859-874 (**16 pages**).
Schulze, K.; Malek, Ž.; Schepaschenko, D.; Lesiv, M.; Fritz, S.; Verburg, P.H., (2023). Pantropical distribution of short-rotation woody plantations: spatial probabilities under current and future climate. Mitig. Adapt. Strateg. Global Change. 28: 18 **(22 page).**
Sharma, H.; Pant, K.S.; Bishist, R.; Gautam, K.L.; Ludarmani; Dogra, R.; Kumar, M.; Kumar, A., (2023). Estimation of biomass and carbon storage potential in agroforestry systems of north western Himalayas, India. Catena. 107009 (**14 pages**).
Sharma, P.; Jetawat, R.; Mohapatra, R.; Saikanth, D.R.K.; Ranjith, R.; Tiwari, P.; Jena, J., (2025). Synergistic effects of agroforestry on carbon sequestration and climate adaptation: a comprehensive review. Asian J. Soil Sci. Plant Nutr., 11: 210-225 **(16 pages).**
Shi, L.; Feng, W.; Xu, J.; Kuzyakov, Y., (2018). Agroforestry systems: meta-analysis of soil carbon stocks, sequestration processes, and future potentials. Land Degrad. Dev., 29: 3886-3897 (**12 pages**).

Shuai, S.; Wang, H.; Zhang, X.; Wang, L.; Jiang, J., (2022). A nature-based solution in forest management to improve ecosystem services and mitigate their trade-offs. J. Clean. Prod., 132558 (**14 pages**).

Silva, L.C.R.; Lambers, H., (2020). Soil-plant-atmosphere interactions: structure, function, and predictive scaling for climate change mitigation. Plant Soil, 461: 5-27 (**23 pages**).

Singh, R.K.; Biradar, C.M.; Behera, M.D.; Prakash, A.J.; Das, P.; Mohanta, M.R.; Krishna, G.; Dogra, A.; Dhyani, S.K.; Rizvi, J., (2024). Optimising carbon fixation through agroforestry: estimation of aboveground biomass using multi-sensor data synergy and machine learning. Ecol. Inf., 79: 102408.

Singh, S.; Singh, G., (2023). Agroforestry for sustainable development: assessing frameworks to drive agricultural sector growth. Environ. Dev. Sustainable, 26: 22281-22317 (**37 pages**).

Sleeter, R.; Sleeter, B.M.; Williams, B.; Hogan, D.; Hawbaker, T.J.; Zhu, Z., (2017). A carbon balance model for the Great Dismal Swamp ecosystem. Carbon Balance Manag., 12: 1-20 (**20 pages**).

Springer, K.; Manning, P.; Boesing, A.L.; Ammer, C.; Fiore-Donno, A.M.; Fischer, M.; Goldmann, K.; Provost, G.L., (2024). Identifying the stand properties that support both high biodiversity and carbon storage in German forests. For. Ecol. Manage., 122328

Stefano, A.; Jacobson, M.G., (2017). Soil carbon sequestration in agroforestry systems: a meta-analysis. Agrofor. Syst., 92: 285-299 **(15 pages).**

Stetter, C.; Sauer, J., (2024). Tackling climate change: agroforestry adoption in the face of regional weather extremes. Ecol. Econ., 224: 108266 (**11 pages**).

Strauss, V.; Paul, C.; Dönmez, C.; Burkhard, B., (2024). Carbon farming for climate change mitigation and ecosystem services□potentials and influencing factors. J. Environ. Manage., 372: 123253 (**13 pages**).

Suárez-Castro, A.F.; Maron, M.; Mitchell, M.G.E.; Rhodes, J.R., (2022). Disentangling direct and indirect effects of landscape structure on urban bird richness and functional diversity. Ecol. Appl., 32: e2713 (**17 pages**).

Tinya, F.; Kovács, B.; Bidló, A.; Dima, B.; Király, I.; Kutszegi, G.; Lakatos, F.; Mag, Z.; Márialigeti, S.; Nascimbene, J.; Samu, F.; Siller, I.; Szél, G.; Ódor, P., (2021). Environmental drivers of forest biodiversity in temperate mixed forests: A multi-taxon approach. Sci. The Total Environ. 795: 148720.

1. Torres, C.M.M.E.; Jacovine, L.A.G.; De Olivera Neto, S.N.; Fraisse, C.W.; Soares, C.P.B.; De Castro Neto, F.; Ferreira, L.R.; Zanuncio, J.C.; Lemes, P.G., (2017). Greenhouse gas emissions and carbon sequestration by agroforestry systems in southeastern Brazil. Sci. Rep., 7: 16738.

Tschora, H.; Cherubini, F., (2020). Co-benefits and trade-offs of agroforestry for climate change mitigation and other sustainability goals in West Africa. Global Ecol. Conserv., e00919 (**12 pages**).

Udawatta R.P.; Rankoth, L.; Jose, S., (2019). Agroforestry and biodiversity. Sustainability, 11: 2879 (**22 pages**).

Udawatta, R.P.; Rankoth, L.M.; Jose, S., (2021). Agroforestry for biodiversity conservation. In Agroforestry for Sustainable Intensification of Agriculture in Asia and Africa; 2021; pp 245-274 (**30 pages**).

Undin, M.; Atrena, A.; Carlsson, F.; Edman, M.; Jonsson, B.G.; Sandström, J., (2022). To what extent does surrounding landscape explain stand-level occurrence of conservation-relevant species in fragmented boreal and hemi-boreal forest? – a systematic review protocol. Environ. Evid., 15: 11(1):32.

Vera, I.; Wicke, B.; Lamers, P.; Cowie, A.; Repo, A.; Heukels, B.; Zumpf, C.; Styles, D.; Parish, E.; Cherubini, F.; Berndes, G.; Jager, H.; Schiesari, L.; Junginger, M.; Brandão, M.; Bentsen, N.; Daioglou, V.; Harris, Z.; Van Der Hilst, F., (2022). Land use for bioenergy: Synergies and trade-offs between sustainable development goals. Renewable Sustainable Energy Rev., 161: 1- 13 **(13 pages).**

Visscher, A.M.; Meli, P.; Fonte, S.J.; Bonari, G.; Zerbe, S.; Wellstein, C., (2023). Agroforestry enhances biological activity, diversity and soil-based ecosystem functions in mountain agroecosystems of Latin America: a meta-analysis. Global Change Biol., 30(1): e17036.

Wang, C.; Tang, Y., (2019). A global meta-analysis of the response of multi-taxa diversity to grazing intensity in grasslands. Environ. Res. Lett., 14: 114003 (**11 pages**).

Wang, J.; Fu, S.; Lü, X.; Chen, Y., (2013). Short-rotation forestry and soil carbon dynamics: a review. For. Ecol. Manage., 300: 1-15 (**15 pages**).

Wang, X.; Tang, Z., (2019). Multi-taxa biodiversity patterns and their drivers across environmental gradients. Ecography, 42: 1723-1734 (**12 pages**).

Wang, Y.; Zhang, H.; Li, Q.; Zhou, G., (2024). Stand structure and management effects on carbon sequestration in subtropical forests. For. Ecol. Manage., 545: 121314 (**11 pages**).

Warren-Thomas, E.; Nelson, L.; Juthong, W.; Bumrungsri, S.; Brattström, O.; Stroesser, L.; Chambon, B.; Penot, E.; Tongkaemkaew, U.; Edwards, D.P.; Dolman, P.M., (2019). Rubber agroforestry in Thailand provides some biodiversity benefits without reducing yields. J. Appl. Ecol., 57(1): 17-30 **(14 pages).**

Watts, K.; Whytock, R.C.; Park, K.J.; Fuentes-Montemayor, E.; Macgregor, N.A.; Duffield, S.J.; McGowan, P.J.K., (2020). Ecological time lags and the journey towards conservation success. Nat. Ecol. Evol., 4: 304-311 (**8 pages**).

Weiskopf, S.R.; Isbell F.; Arce-Plata, M.I.; Di Marco, M.; Harfoot, M.; Johnson, J.; Lerman, S.B.; Miller, B.W.; Morelli, T.L.; Mori, A.S.; Weng, E.; Ferrier, S., (2024). Biodiversity loss reduces global terrestrial carbon storage. Nat. Commun., 15: 4354.

Wood, S.L.R.; DeClerck, F.; , D.S.; Kremen, C.; Naeem, S.; Palm, C.A.; DeFries, R.S., (2017). Functional traits in agriculture: agrobiodiversity and ecosystem services. Trends Ecol. Evol., 32: 687-698 (**12 pages**).

Wu, W.; Zhu, Y.; Wang, Y., (2023). Spatio-temporal pattern, evolution and influencing factors of forest carbon sinks in Zhejiang Province, China. Forests, 14: 445 (**18 pages**).

Wylie, L.; Sutton-Grier, A.E.; Moore, A., (2016). Keys to successful blue carbon projects: lessons learned from global case studies. Mar. Policy. 65: 76-84 (**9 pages**).

Xiang, M.; Wang, C.; Tan, Y.; Yang, J.; Duan, L.; Fang, Y.; Li, W.; Shu, Y.; Liu, M., (2022). Spatio-temporal evolution and driving factors of carbon storage in the Western Sichuan Plateau. Sci. Rep., 12: 12175 (**15 pages**).

Xiong, S.; Yang, F.; Li, J.; Xu, Z.; Ou, J., (2023). Temporal-spatial variation and regulatory mechanism of carbon budgets in territorial space through the lens of carbon balance: a case of the middle reaches of the Yangtze River urban agglomerations, China. Ecol. Indicators. 154: 110885.

Yadav, R.P.; Gupta, B.; Bhutia, P.L.; Bisht, J.K.; Pattanayak, A.; Meena, V.S.; Choudhary, M.; Tiwari, P., (2019). Biomass and carbon budgeting of sustainable agroforestry systems as

ecosystem service in Indian Himalayas. Int. J. Sustainable Dev. World Ecol., 26(5).
Yahya, M.S.; Atikah, S.N.; Mukri, I.M.; Sanusi, R.; Norhisham, A.R.; Azhar, B., (2022). Agroforestry orchards support greater avian biodiversity than monoculture oil palm and rubber tree plantations. For. Ecol. Manage., 513: 120177 (**11 pages**).
Yan, P.; Fernández-Martínez, M.; Van Meerbeek, K.; Yu, G.; Migliavacca, M.; He, N., (2023). The essential role of biodiversity in the key axes of ecosystem function. Global Change Biol., 29: 4569-4585 (**17 pages**).
Yirga, S.A., (2019). Agroforestry for sustainable agriculture and climate change: a review. Int. J. Environ. Sci. Nat. Resour., 19: 556022 (**7 pages**).
Zeller, K.A.; Vickers, T.W.; Ernest, H.B.; Boyce, W.M., (2020). Understanding the importance of dynamic landscape connectivity. Land. 9: 303 (**16 pages**).
Zhang, K.; Zou, H.; Lei, X.; Zeng, J.; Lan, J.; Guo, X.; Gao, D.; Liu ,X.; Zhang, H., (2024). Impact of management measures on multiple ecosystem function trade-offs and their dynamics in .subtropic Pinus massoniana plantations. Forests, 15: 1224 **(19 pages).**
Zhang, Y.; Cheng, C.; Wang, Z.; Hai, H.; Miao, L., (2025). Spatiotemporal variation and driving factors of carbon sequestration rate in terrestrial ecosystems of Ningxia, China. Land, 14: 94 (**16 pages**).
Zhao, H.; Liu, Y.; Li, F.; Zhang, Z., (2021). Incorporating spatio-temporal connectivity for prioritized conservation of individual habitat patches in a dynamic landscape. Ecol. Indic., 124: 107414 (**12 pages**).
Zhao, S.; Shi, W.; Qiao, F.; Wang, C.; An, Y.; Zhang, L., (2023). Temporal and spatial changes and trend predictions of forest carbon sequestration efficiency in China based on the carbon neutrality goal. Forests, 14: 2387 (**20 pages**).
Zhu, X.; Luleva, M.; Van Helfteren, S.; Gou, Y.; Gajda, W.; Neinavaz, E., (2024). Comparison of functional and structural biodiversity using Sentinel-2 and airborne LiDAR data in agroforestry systems. Remote Sens. Appl. Soc. Environ., 31: 101252 **(11 pages).**
Zhu, Y.; Liu, Y.; Sheng, S.; Zheng, J.; Wu, S.; Cao, Z.; Zhang, K.; Xu, Y., (2024). Quantifying the effects of landscape and habitat characteristics on structuring bird assemblages in urban habitat patches. Sci. Rep., 14: 9237 (**14 pages**).
Zia, M.N.; Malik, S.U.; Ahmad, O.; Usman, H.; Khan, M.J.; Shah, M.A., (2025). Assessment of carbon sequestration potential of agroforestry system in Pothwar: opportunities and challenges. J. Agric. Biol., 003: 01-13 (**13 pages**).

AUTHOR (S) BIOSKETCHES

S. Withaningsih, Dr., Associate Professor, Department of Biology, Faculty of Mathematics and Natural Sciences, Universitas Padjadjaran, Bandung, Indonesia; Graduate School on Environmental Sciences and Sustainability Science, Universitas Padjadjaran; Centre for Environment and Sustainability Science, Universitas Padjadjaran, Indonesia.
• Email: *susanti.withaningsih@unpad.ac.id*
• ORCID: 0000-0002-5893-0222
• Web of Science ResearcherID: NA
• Scopus Author ID: 57195276031
• Homepage: https://kepakaran.unpad.ac.id/expert/197605192016044001 or https://www.researchgate.net/profile/Susanti-Withaningsih

S. Nurmilah, Ph.D. Candidate, Faculty of Agro-Industrial Technology, Universitas Padjadjaran, Sumedang, Indonesia.
• Email: *siti20001@mail.unpad.ac.id*
• ORCID: 0000-0002-4302-9968
• Web of Science ResearcherID: NA
• Scopus Author ID: 57225138529
• Homepage: vhttps://www.researchgate.net/profile/Siti-Nurmilah

G.L. Utama, Dr., Associate Professor in Food Microbiology and Waste Management, Faculty of Agro-Industrial Technology, Universitas Padjadjaran, Sumedang, Indonesia; Graduate School on Environmental Sciences and Sustainability Science, Universitas Padjadjaran; Chair Centre for Environment and Sustainability Science, Universitas Padjadjaran, Indonesia.
• Email: *g.l.utama@unpad.ac.id*
• ORCID: 0000-0003-3382-2855
• Web of Science ResearcherID: NA
• Scopus Author ID: 55178542400
• Homepage: https://kepakaran.unpad.ac.id/expert/198410202014041001 or https://www.researchgate.net/profile/Gemilang-Lara-Utama

HOW TO CITE THIS ARTICLE

Withaningsih, S.; Nurmilah, S.; Utama, G.L., (2026). The role of carbon sequestration and biodiversity in agroforestry for climate change mitigation. Global J. Environ. Sci. Manage., 12(1): 431-452.

DOI: 10.22034/gjesm.2026.01.24

URL: https://www.gjesm.net/article_731134.html

Global J. Environ. Sci. Manage. 12(1): 453-472, Winter 2026, Serial #45

Global Journal of Environmental Science and Management
(GJESM)

Homepage: https://www.gjesm.net/

Podcasts

REVIEW PAPER

Sustainable strategies for durum wheat production under water scarcity and climate stress

G. Saspugayeva[1,*], A. Zhaken[1], I. Agarkova[2], Z, Mukhametzhanova[2], I. Samatova[1], Zh. Zhaznayeva[3], A Chursin[3], G. Salykbayeva[3], Sh. Baimukasheva[4], B. Serkebayeva[5]

[1] *Department of Environmental Engineering and Management, Faculty of Natural Sciences, L.N. Gumilyov Eurasian National University, Astana, Kazakhstan*

[2] *Department of Morphology, NCJSC Karaganda Medical University, Karaganda, Kazakhstan*

[3] *Department of Ecology and Geography, Sarsen Amanzholov University of East Kazakhstan, Ust-Kamenogorsk, Kazakhstan*

[4] *Department of Ecology and Life Safety, Faculty of Engineering, Yessenov University, Aktau, Kazakhstan*

[5] *Fluid Analysis Directorate of the Laboratory Research Department, Branch of KazMunayGas Engineering LLP "Kazakh Scientific and Design Institute of Oil and Gas" Aktau, Kazakhstan*

ARTICLE INFO

Article History:
Received 06 September 2025
Revised 08 November 2025
Accepted 10 December 2025

Keywords:
Drought tolerance
Semi-arid agriculture
Soil–water conservation
Water–Energy–Food nexus
Water-use efficiency

ABSTRACT

Water scarcity, rising evapotranspiration, and increasing climate variability pose substantial challenges to cereal production, particularly in semi-arid regions where durum wheat (*Triticum durum*) is a critical crop for food security. This study consolidates various research efforts focused on strategies aimed at bolstering the resilience of durum wheat in water-scarce environments and emphasizes new possibilities for adaptation in the face of escalating climate pressures. Key approaches include the development and deployment of drought-tolerant and climate-resilient cultivars, precision irrigation technologies that optimize water use, and soil-water conservation practices such as conservation tillage, residue retention, mulching, crop rotation with legumes, and organic matter enhancement. These initiatives strengthen soil structure, promote water infiltration, and improve moisture retention, consequently lowering irrigation needs and shielding crops from sporadic droughts, while also ensuring sustained soil productivity. The study also addresses the environmental trade-offs associated with irrigation expansion, including soil salinization, groundwater depletion, and energy-related greenhouse gas emissions, which can collectively undermine farm sustainability if not properly managed. Comprehensive governance structures that synchronize water, energy, and food priorities are crucial for sustainable intensification, especially in areas where irrigation development is hindered by hydrological or infrastructural constraints. Mechanisms such as volumetric water allocation, systematic groundwater and salinity monitoring, and the incorporation of renewable-energy-powered irrigation systems provide the regulatory and operational tools necessary to prevent resource overexploitation and ensure equitable access across farming communities. An illustrative example from continental semi-arid basins demonstrates how supplemental irrigation during critical growth stages, combined with basin-level water planning and rational groundwater use, can stabilize wheat yields without compromising environmental integrity. The case highlights the potential for integrating multiple water sources, including surface water, groundwater, and collector-drainage water, with climate-resilient cultivars to enhance productivity while maintaining ecosystem health. Sustainable durum wheat systems demand simultaneous improvements in agronomy, technological advancements, resource governance, and the development of farmer skills to ensure successful execution. Advancing semi-arid agriculture will ultimately depend on integrating drought-tolerant varieties, efficient irrigation, soil–water conservation, and Water–Energy–Food–aligned planning into cohesive strategies that can guide future innovation and policy toward resilient, climate-ready production systems.

DOI: 10.22034/gjesm.2026.01.25

This is an open access article under the CC BY license (http://creativecommons.org/licenses/by/4.0/).

NUMBER OF REFERENCES	NUMBER OF FIGURES	NUMBER OF TABLES
103	3	2

*Corresponding Author:
Email: *saspugayeva_gye@enu.kz*
Phone: +77071904511
ORCID: 0000-0003-3223-3602

Note: Discussion period for this manuscript open until Mar 1, 2026 on GJESM website at the "Show Article".

INTRODUCTION

Water scarcity has become one of the most critical constraints on agricultural stability in dry and semi-dry regions (Attar *et al.,* 2025), where climate change is intensifying evapotranspiration, altering rainfall regimes, and amplifying hydrological variability (Mkilima, 2025). These alterations weaken the trustworthiness of water resources that cereal systems are contingent upon, especially in regions defined by sparse and inconsistent precipitation. As temperatures rise and moisture deficits become more frequent, farmers across semi-arid regions face declining soil water availability, shorter effective growing seasons, and heightened yield volatility (Abdi *et al.*, 2024). Such challenges pose a risk to both local farming livelihoods and the larger food systems that are heavily reliant on cereals adapted to less favorable environments (Elias *et al.,* 2019). Compound climate extremes, including simultaneous drought, heat stress, and high vapor pressure deficit, reduce grain filling by accelerating phenological development, disrupt protein synthesis, and decrease protein quality, thereby destabilizing durum wheat growth and yield under semi-arid conditions. Within this context, durum wheat (*Triticum durum*) occupies a distinctive and increasingly strategic position (Grosse-Heilmann *et al.*, 2024). Its industrial value for semolina and pasta, combined with its natural tolerance to heat and drought, has anchored its cultivation across the Mediterranean Basin, Central Asia, North Africa, and other water-limited agro-ecological zones (Calasso *et al.,* 2025). Despite this resilience, durum wheat continues to be extremely susceptible to water shortages during its most vital phenological stages. Moisture stress around stem elongation, anthesis, and grain filling consistently reduces grain yield, impairs protein composition, and diminishes technological quality (Li *et al.,* 2025). Forecasts suggest that these vulnerabilities will worsen as climate variability escalates (Teku, 2025), emphasizing the importance of production systems capable of maintaining yields in increasingly limited water conditions. In recent years, research has shifted from isolated agronomic interventions toward an integrated understanding of how water-efficient practices, stress-resilient genotypes, and resource-governance mechanisms interact to shape durum wheat performance under water scarcity. Studies demonstrate that effective irrigation scheduling, especially via the use of supplemental and deficit irrigation, can markedly increase water-use efficiency when utilized at the growth stages that exhibit the highest sensitivity (Ali *et al.*, 2024; Bian *et al.,* 2024). Advances in genetics and plant physiology have revealed cultivars with deeper and more efficient root systems, improved osmotic adjustment capacity, and greater tolerance to the combined effects of heat and drought stress (Zhang *et al.*, 2025). Soil-water conservation techniques, including conservation tillage, retention of residues, mulching, and the improvement of organic matter, additionally strengthen resilience by facilitating infiltration and decreasing evaporative losses (Singh *et al.,* 2025). Technological developments also contribute to strengthening these agronomic foundations. Precision irrigation systems supported by soil-moisture sensing, satellite-derived evapotranspiration data, and machine learning for stress detection enable the delivery of water with much greater precision than traditional techniques (Nsoh *et al.,* 2024). However, technological and agronomic innovations alone cannot guarantee sustainability. In many semi-arid regions (Mkilima, 2023), unregulated irrigation expansion has already led to groundwater depletion, soil salinization, and energy-intensive water extraction (Lu *et al.,* 2025). Robust governance frameworks that oversee water distribution, ensure the protection of ecological flows, and harmonize irrigation development with energy and environmental planning are vital to prevent the degradation of resources over time. Although previous studies have examined individual stressors such as drought or heat on durum wheat, a comprehensive understanding of how combined environmental factors, including drought, heat stress, and high vapor pressure deficit, interact to affect grain filling, protein quality, and phenological stability is lacking, highlighting the need for an integrative review that synthesizes physiological, agronomic, and management strategies for resilient production in semi-arid regions. This study addresses this critical gap by unifying agronomic, technological, and governance-based strategies into a single, integrated framework, offering a synthesis that extends beyond existing studies to clarify how multi-scale interventions can collectively enhance durum wheat resilience under escalating water scarcity. This study draws upon these overlapping research trajectories

to deliver a succinct and thorough synthesis of the agronomic, technological, and institutional measures needed to sustain durum wheat production under water scarcity. By consolidating evidence from the past decade, the study aims to clarify how integrated management approaches can enhance productivity while protecting water and soil resources in regions that are most exposed to climate-induced scarcity. This study was conducted in Kazakhstan in 2025.

METHODOLOGY

This study utilized a systematic and clear methodology to guarantee comprehensive coverage, methodological rigor, and reproducibility, specifically concentrating on water-efficient practices for the production of durum wheat. A targeted literature search was conducted across major scientific databases, including Web of Science, Scopus, ScienceDirect, SpringerLink and Google Scholar, using combined keywords such as "durum wheat," "*Triticum durum*," "water-use efficiency," "drought tolerance," "deficit irrigation," "supplemental irrigation," "soil–water conservation," and "precision irrigation." Boolean operators, phrase matching and citation tracking of foundational papers were applied to refine and expand the search. Studies were included if they i) focused directly on durum wheat or presented transferable insights from cereal systems under moisture stress, ii) provided primary data, systematic review evidence or meta-analytical findings on irrigation management, drought physiology, soil–water conservation or technological interventions, iii) were published in peer-reviewed journals within the past decade, and iv) supplied sufficient methodological detail to support interpretation. The exclusion criteria eliminated materials that were not peer-reviewed, conference abstracts that did not provide complete datasets, opinion articles, and studies focused on crops that are not relevant. Screening occurred in two stages: title and abstract review followed by full-text assessment, with duplicates removed prior to evaluation. A structured data extraction framework was used to compile information on agronomic practices, physiological and genetic mechanisms of drought adaptation, irrigation technologies and reported outcomes such as yield, grain quality and water productivity. The thematic synthesis of evidence aimed to reveal cross-environmental patterns, performance ranges, and the knowledge gaps that still exist. To ensure methodological transparency, each study was evaluated using a modified agronomic quality appraisal checklist comprising four core criteria: 1) experimental design clarity, including control treatments, irrigation scheduling protocols and cultivar descriptions; 2) replication and sample size adequacy; 3) statistical robustness, including the use of appropriate statistical tests and reporting of variability measures; and 4) environmental characterization, including soil properties, climate data and management context. Studies that fulfilled all criteria were entirely included in the synthesis, while those that only partially complied were noted with explicit mention of their limitations in interpretation. Studies that failed to provide crucial methodological transparency were disregarded. Quality appraisal outcomes informed the weighting of evidence in the narrative synthesis, with well-designed, statistically rigorous and environmentally well-documented studies given greater emphasis when identifying reliable trends. The conclusive results were organized in a comparative table that delineated each water-efficient strategy by its mechanisms, agronomic relevance, benefits and context-specific limitations, thus guaranteeing that all suggested practices were found on empirically substantiated evidence.

Climate vulnerability and global importance of durum wheat

Durum wheat holds a critical position in global food systems, particularly across the Mediterranean Basin, North Africa, the Middle East and Central Asia, where semi-arid climates dominate and food security increasingly depends on crops capable of withstanding environmental extremes. Despite the acknowledgment of durum wheat for its comparatively deep and effective root system, moderate water demands, and natural resistance to heat and drought, various studies indicate that these characteristics only somewhat mitigate the crop's vulnerability to increasing climate stress. Drought remains one of the most damaging constraints to wheat production worldwide, disrupting physiological, biochemical and molecular processes that underpin plant growth, grain filling and quality formation. Recent work by Mutanda *et al.* (2025) highlights the severity of drought-induced declines in photosynthetic capacity, osmotic balance and carbon assimilation, emphasizing that even drought-adapted

cereals suffer substantial yield penalties when water deficits coincide with sensitive phenological stages. The swift developments in durum wheat genomics are advancing the knowledge regarding the impact of genetic architecture influences climate resilience. The release of a high-quality, chromosome-level genome assembly for the durum cultivar Langdon (Chen *et al.*, 2025) provides a robust reference for identifying genes linked to root development, water-use efficiency and stress adaptation, with more than 68,000 high-confidence genes now annotated. This assembly fortifies the basis for comparative genomics and facilitates the identification of alleles that can be utilized to improve drought tolerance. Complementary research comparing Tunisian durum landraces with modern cultivars (Miazzi *et al.*, 2022) reveals substantial genetic divergence at 529 SNP loci, including candidate genes associated with flowering regulation (FT-B1), spike and plant architecture (CONSTANS-like zinc finger proteins), and transcription factors in the AP2/EREBP family. These results indicate that germplasm specific to durum contains distinct alleles associated with stress response and biomass distribution, underscoring its significance for developing climate-resilient cultivars. At the same time, climate-driven constraints extend beyond drought alone. In many arid regions, freshwater scarcity forces farmers to rely on marginal or saline water sources, exposing durum wheat to combined drought–salinity stress. Further findings from Manhou *et al.* (2025) reveal that moderate salinity levels adversely affect germination, delay initial development, and lower physiological vigor, yet genotypes are capable of preserving grain yield within established salinity thresholds. Additional research by Boudjabi *et al.* (2015) demonstrates that poor soil fertility interacts strongly with water stress, indicating that organic amendments such as sewage sludge can temporarily enhance plant tolerance by improving soil structure, nutrient availability and chlorophyll content, yet may also induce osmotic stress at high concentrations (Fig. 1).

Increasing temperatures, more erratic precipitation patterns, and a growing frequency of extreme weather phenomena are leading to considerable annual variability in durum wheat yields throughout its key production regions. Multi-model climate assessments show that rising temperatures and declining soil moisture will continue to depress cereal productivity and increase production instability well into mid-century, particularly in rain-fed systems that dominate semi-arid landscapes. According to Stuch *et al.* (2021), climate change leads to a reduction in mean cereal yields and an increase in

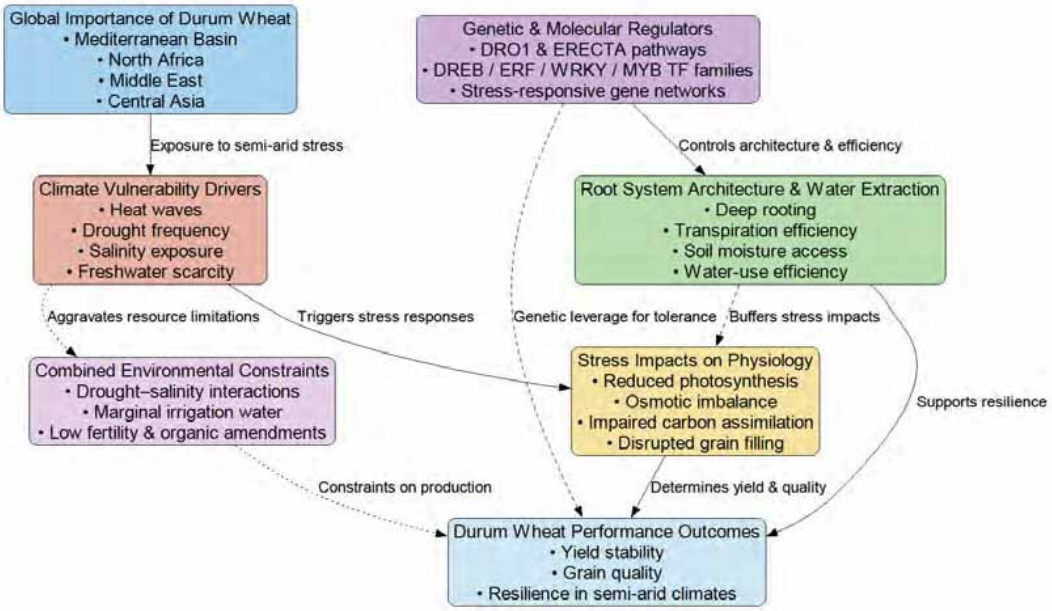

Fig. 1: Climate vulnerability and global importance of durum wheat

their interannual variability, a trend that is notably intensified in regions that are already vulnerable to moisture shortages. Broader syntheses of climate impacts on agriculture, such as the comprehensive review by Yuan *et al.,* (2024), further confirm that increases in heatwaves, altered precipitation regimes, and extreme hydrological events disrupt crop growth cycles, shorten grain-filling periods, and intensify biotic and abiotic stresses, ultimately undermining both yield and quality. Recent genotype-by-environment analyses in durum wheat reinforce this vulnerability, with studies such as Pacheco-Andrade *et al.,* (2025) showing significant crossover interactions and unstable yield performance across contrasting semi-arid environments, highlighting how even resilient genotypes respond unpredictably under climate stress. These climatic pressures are occurring simultaneously with the growing global demand for durum-based products, which is influenced by population growth, changes in dietary preferences, and the growth of the pasta and semolina industries in both producing and importing nations. The alignment of rising market demand with escalating climatic risks highlights the critical need for the formulation of climate-responsive production strategies that can stabilize durum wheat yields in the face of restricted and highly fluctuating water availability.

Irrigation challenges in water-limited cereal systems

Moisture deficits during critical growth stages

Moisture deficits during the reproductive phase of wheat development impose some of the most severe constraints on yield formation and grain quality, particularly in dryland systems where rainfall is erratic and irrigation water is limited. Gooding *et al*. (2003) performed controlled-environment experiments which indicated that drought experienced between anthesis and the early stages of grain filling leads to a reduction in the duration of grain filling, a decrease in mean grain weight, and a lower specific grain weight, with the most significant sensitivity observed within the first 14 days after anthesis. Water shortages during this window also impair protein and starch deposition, alter key quality indices such as Hagberg Falling Number and sodium dodecyl sulphate (SDS) sedimentation volume, and trigger biochemical responses that disrupt the coordinated accumulation of dry matter and nitrogen. These mechanistic insights elucidate the reasons behind the significant declines in grain yield and processing quality observed in field-based dryland wheat systems when rainfall is insufficient during reproductive stages. More recent field studies reinforce the centrality of moisture during these critical periods. Katohar *et al.,* (2023) showed that post-anthesis irrigation deficits drastically reduce grain yield, test weight, and water-use efficiency, yet also reported that drought priming during early growth stages can partially mitigate these impacts by enhancing physiological stress memory and improving subsequent tolerance to water scarcity. Primed plants showed improved relative yield and required much less irrigation water, implying that even small improvements in pre-anthesis stress acclimation can strengthen resilience during the delicate grain-filling period.

Environmental constraints on irrigation expansion

The effort to expand irrigation for the purpose of stabilizing durum wheat yields is confronted with substantial environmental and socio-economic limitations. Over-extraction of aquifers has led to steadily declining groundwater levels in many semi-arid and dryland regions (Shen *et al.,* 2015). Seasonal variability in river flows reduces the reliability of surface-water supplies for sustained irrigation (Leščešen *et al.,* 2025). Poor drainage combined with high evaporation rates accelerates soil salinization, threatening long-term soil fertility and crop productivity (Tarolli et al., 2024). The energy demand for pressurized irrigation systems and pumping is increasing, raising both operational costs and greenhouse gas (GHG) emissions. Governance challenges exacerbate these issues, as the rules for water allocation are frequently inadequate, monitoring is lacking, and enforcement mechanisms are limited. These factors collectively make large-scale irrigation expansion unsustainable from both ecological and economic perspectives. Selective approaches that optimize water use are therefore essential. Regulated deficit irrigation allows crops to receive sufficient water during critical growth stages while minimizing waste. Supplemental irrigation that is targeted can enhance yields while avoiding excessive dependence on scarce water resources. Basin-level water planning is critical to balance irrigation needs with environmental conservation. Integrating climate predictions with irrigation planning increases dependability amid variable precipitation (Mabhaudhi

et al., 2025). Adoption of efficient conveyance and application systems reduces water losses. Soil-water conservation practices can complement irrigation to enhance effectiveness. Overall, the implementation of strategic and resource-efficient irrigation secures yield stability and conserves water and soil resources.

Agronomic and technological strategies for water-efficient durum wheat production

Supplemental and deficit irrigation

Strategic irrigation during key phenological stages is a highly effective approach for enhancing durum wheat productivity while optimizing water use. Supplemental irrigation, applied at critical growth periods such as jointing, flowering, and grain filling, can substantially increase grain yield under rain-fed conditions with controlled water supply, demonstrating the responsiveness of wheat to timely water application (Liu *et al.*, 2022). Regulated deficit irrigation boosts water-use efficiency, fosters deeper root development, and elevates grain quality by providing water exactly when crops are most susceptible, consequently decreasing overall water consumption per unit of yield. Meta-analyses confirm that irrigation increases spike number, grains per spike, thousand-kernel weight, and grain protein content, although water productivity gains are more modest due to concurrent increases in evapotranspiration, highlighting the importance of optimizing irrigation volume and timing (Yang *et al.,* 2025). Experimental studies show that dual or triple irrigation applications, particularly at crown root initiation, booting, and heading stages, maximize yield components and overall grain production, with certain varieties such as BARI Gom-24 demonstrating superior performance under these regimes (Islam *et al.,* 2025). Optimal irrigation volumes range from 75 to 150 millimetres' (mm), and when paired with effective soil and nutrient management, they significantly improve yield and water productivity, particularly in areas with limited annual rainfall (Table 1).

Breeding and cultivar improvement

Contemporary breeding and cultivar enhancement serve as a fundamental element in improving the resilience of durum wheat in water-scarce environments. Contemporary programs focus on optimizing root system architecture to access deep soil moisture, improving osmotic adjustment and stomatal regulation for better water use efficiency, and incorporating heat- and drought-tolerance traits that maintain yield under stress. Advances in genomics and high-throughput phenotyping enable marker-assisted selection and genomic prediction, accelerating the identification of alleles linked to stress resilience and water productivity. Findings from multi-omics studies underscore the importance of accounting for both stomatal and non-stomatal leaf traits to improve water use efficiency without sacrificing yield, indicating that the complex interplay of traits is vital for the advancement of climate-resilient wheat (Fernando *et al.*, 2025; Le Roux *et al.*, 2024). Additionally, root system architecture plays a pivotal role in drought adaptation, as specific configurations enhance water and nutrient uptake while strengthening overall crop performance under water deficits (Zhang *et al.*, 2025). Long-term deficits in soil moisture also alter soil microbial networks, affecting nutrient cycling and plant-microbe interactions, while beneficial microbes such as mycorrhizal fungi and plant growth-promoting rhizobacteria can enhance durum wheat drought resilience by improving water acquisition, hormonal regulation, and stress tolerance. Integrating these physiological traits with microbiome-informed selection and AI-driven analysis of omics datasets, breeders can anticipate the ideal trait combinations for designated environments, bridging the gap between big data, soil health, and practical pre-breeding applications.

Soil-water conservation practices

Soil-water conservation practices are critical for enhancing durum wheat productivity under water-limited conditions while improving soil resilience and sustainability. Approaches such as conservation tillage, maintaining surface residue retention, mulching, crop rotation with legumes and drought-resistant varieties, and increasing soil organic matter collectively contribute to the enhancement of soil structure, infiltration, and moisture retention, thereby reducing irrigation requirements. Practices associated with conservation agriculture (CA) focus on reducing soil disturbance, ensuring permanent soil cover, and promoting crop diversity. Evidence suggests that these practices enhance soil organic carbon levels, change pore size distribution, and

Table 1: Agronomic and technological strategies for water-efficient durum wheat production

Strategy	Key features	Benefits	Limitations / Risks	Sources
Supplemental irrigation	Applied at critical stages (anthesis, grain filling)	Increased yield, improved grain quality	Requires water availability, cost of infrastructure	Dai *et al.,* 2022; Joshi and Bhandari, 2022; Ndhleve *et al.*, 2017
Deficit irrigation	Reduced water relative to full crop water requirement	High water-use efficiency	Risk of stress if mismanaged	Galindo *et al.,* 2018; Painagan and Ella, 2022; Saad *et al.,* 2023
Drought-tolerant cultivars	Deep roots, osmotic adjustment, genomic selection	Improved resilience under moisture deficit	Breeding costs, adaptation to local soils	Adhikari *et al.,* 2019; Gahlaut *et al.*, 2016; Quiroga *et al.*, 2017
Soil-water conservation	Mulching, residue retention, crop rotation	Enhanced infiltration, reduced evaporation	Labor-intensive, may require machinery	Amfo *et al.*, 2021; Nugroho *et al.,* 2022; Sileshi *et al.* 2019
Precision irrigation and monitoring	Sensors, satellite ET, AI scheduling	Optimized water use, real-time decision-making	High initial cost, training required	Abioye *et al.,* 2020; Kumar and Sobti, 2022; Math and Dharwadkar, 2020
Conservation tillage	Reduced or no-till systems	Preserves soil moisture, improves structure	Requires specialized equipment	Busari *et al.*, 2015; Cooray *et al.*, 2023; Lv *et al.*, 2023
Alternate wetting and drying	Controlled irrigation cycles	Saves water, reduces methane emissions	Needs careful monitoring	Johnson *et al.*, 2023; Zhang *et al.,* 2023; ZHOU *et al.,* 2017
Foliar nutrient application	Spraying nutrients on leaves	Enhances stress tolerance, improves yield	Requires additional inputs, timing-sensitive	Awan *et al.,* 2020; Lovatt, 2013; Shahrajabian *et al.*, 2022
Drought-adaptive cropping systems	Intercropping, crop rotation with legumes	Improves soil moisture retention, diversifies production	Complex management, may reduce wheat area	Hiyama *et al.,* 2014; Iijima *et al.*, 2018; Izumi *et al.,* 2018
Seed priming	Pre-sowing hydration or osmotic treatment	Accelerates germination, improves early vigor under drought	Extra labor, risk of seed spoilage if mismanaged	do Espirito Santo Pereira *et al.*, 2021; Ibrahim, 2016; Pagano *et al.*, 2023; Raj and Raj, 2019

improve the capacity for water retention, particularly in the upper soil layers, which is essential for arid and semi-arid climates (Abdallah *et al.,* 2021). Although the effects on whole-profile water-holding capacity may be modest, CA consistently improves water availability through increased infiltration and reduced surface evaporation, resulting in measurable water savings. Long-term adoption also promotes macro- and bioporosity, better soil structure, and enhanced microbial activity, which support nutrient cycling and drought resilience (Sadiq *et al.,* 2025). The use of mulching and the retention of crop residue effectively lower soil evaporation rates, stabilize temperature changes, and maintain moisture during vital growth periods. Furthermore, rotating crops with legumes promotes nitrogen enrichment and supports the development of root systems for improved water uptake. Organic matter enhancement improves soil aggregation, porosity, and cation-exchange capacity, fostering both water retention and nutrient availability. Empirical evidence indicates that these practices are particularly effective in semi-arid regions of Sub-Saharan Africa, South Asia, and Australia, where rainfall is erratic and irrigation resources are limited. Integrating CA with precision agriculture tools, remote sensing, and digital monitoring can further optimize irrigation scheduling and resource efficiency. By combining

these agronomic interventions, durum wheat systems can achieve higher water-use efficiency, stabilize yields under drought stress, and promote long-term soil health, representing a sustainable pathway for climate-resilient cereal production.

Environmental trade-offs and sustainability risks

Energy use and emissions

Energy use and emissions are critical considerations in sustainable durum wheat irrigation, particularly in the Mediterranean Basin, Central Asia, and parts of North America, where deep groundwater pumping and pressurized systems significantly increase energy demand and associated greenhouse gas emissions. In numerous Mediterranean countries, the cultivation of durum wheat is becoming more reliant on deeper wells as surface water allocations become more restricted, which in turn elevates both irrigation costs and carbon intensity. Similar pressures have been documented in the Northern Great Plains of the United States and Canada, where farmers face rising energy expenditures due to expanding reliance on supplemental irrigation during dry years. To mitigate the accumulation of salinity while ensuring yield despite limited freshwater resources, irrigation methods like deficit irrigation, regulated supplemental irrigation during essential growth phases, and enhanced scheduling informed by soil moisture assessments have proven effective in optimizing water usage and decreasing salt buildup in the root zone. Integrating renewable energy into irrigation systems offers a practical solution to reduce energy use and enhance sustainability. Solar-powered smart irrigation can reduce greenhouse gas emissions, stabilize input costs, and improve water-use efficiency. In Pakistan, for instance, solar-powered irrigation systems have enhanced wheat yields from 3.0 to 4.8 tons per hectare (t/ha) while lowering water and energy inputs. This illustrates the potential of renewable energy can complement precision irrigation in semi-arid cereal systems (Daraz *et al.*, 2025). Similarly, a study in the Philippines found that solar irrigation reduced greenhouse gas emissions by up to 26.5 tons carbon dioxide equivalent per hectare per year (t CO_2eq/ha/y) and decreased diesel fuel use by 11–379 liters per hectare per year (L/ha/y), providing both environmental and economic benefits (Guno and Agaton, 2022). Although these studies are not durum-specific, they illustrate mechanisms that are highly relevant to major drum-producing regions. In Tunisia, Morocco, Kazakhstan, and parts of Turkey, the implementation of solar irrigation is being increasingly explored to mitigate high diesel dependency, bolster the reliability of supplemental irrigation during crucial growth periods, and optimize water-use efficiency. However, these gains depend on governance mechanisms that regulate groundwater extraction and prevent over-pumping, including basin-level hydrological monitoring, volumetric allocation policies, and farmer training programs. Without such safeguards, the combination of low-cost solar energy and unrestricted pumping can accelerate aquifer depletion, as observed in parts of North Africa and Central Asia. By combining solar-powered irrigation with effective governance and risk-informed water management, production costs can be decreased, water-use efficiency can be improved, yields can be stabilized, and the long-term sustainability of durum wheat production in semi-arid regions can be reinforced (Table 2).

Water–energy–food governance gaps

Effective governance of the WEF is vital for achieving sustainable intensification in the production of durum wheat under conditions of limited water availability. Volumetric allocation of water, which defines precise limits on water rights, has been shown to enhance the sustainability of irrigation systems by aligning resource availability with licensed extraction volumes, as demonstrated in South Australia's Limestone Coast, where careful conversion to volumetric allocations over 2,500 licenses helped secure equitable access and long-term aquifer sustainability (Skewes and Carruthers, 2012). Basin-level water accounting, especially using satellite-based products, allows for accurate measurement of beneficial and non-beneficial water usage. This assists policymakers in optimizing allocation and minimizing water waste, as illustrated in the Betwa River Basin, India, where water accounting plus (WA+) and earth observation datasets revealed significant inefficiencies in irrigation and facilitated informed water management strategies (Singh *et al.*, 2022). Monitoring of groundwater levels and salinity is equally critical to prevent overextraction and salinization, as shown in the Mekong Delta, Vietnam, where a newly designed network of monitoring wells provided spatially detailed data to guide

Table 2: Environmental trade-offs and governance measures in irrigated durum wheat systems

Risk / impact	Description	Mitigation / Governance	Example technologies	Sources
Soil salinization	Salt accumulation from irrigation and poor drainage	Leaching, monitoring, salt-tolerant varieties	Drip irrigation, soil sensors	Aragüés *et al.*, 2018; Tomaz *et al.*, 2020; Wang *et al.*, 2019
Groundwater depletion	Over-extraction reducing aquifer storage	Volumetric allocation, monitoring	Groundwater level sensors, remote sensing	Alfaro *et al.*, 2017; Dangar *et al.*, 2021; Shuai *et al.*, 2022
Energy use and emissions	High energy demand for pumping and pressurized irrigation	Renewable energy integration, efficiency improvements	Solar pumps, efficient sprinklers	Chabour *et al.*, 2022; Loureiro *et al.*, 2023; Rodríguez Díaz *et al.*, 2011; Zha *et al.*, 2024
Inequitable water distribution	Lack of basin-level planning	Stakeholder-inclusive Water–energy–food (WEF) governance	Decision-support platforms, water accounting	Ceita *et al.*, 2023; Duc *et al.*, 2024; Hassan *et al.*, 2023; MacRorie *et al.*, 2022
Declining soil organic matter	Continuous tillage and low residue retention reducing soil moisture-holding capacity	Conservation tillage, residue management	No-till seeders, biomass sensors	Sarker *et al.*, 2022
Water quality degradation	Agrochemical leaching into drainage and surface water	Integrated nutrient management, monitoring	Water-quality sensors, nutrient-mapping tools	Boico *et al.*, 2022; X. B. Liu *et al.*, 2010
Climate-driven irrigation variability	Increased temperature and erratic rainfall altering water demand	Climate-informed irrigation scheduling	Seasonal forecasts, ET-based irrigation tools	Cuthbert *et al.*, 2022; Rolle *et al.*, 2022; Scanlon *et al.*, 2021
Technology adoption gaps	Limited capacity, skills, or resource access among smallholders	Training programs, subsidies, inclusive digital platforms	Mobile advisory apps, low-cost sensors	Yuan and Sun, 2024
Infrastructure failure	Aging or poorly maintained canals, boreholes, or pumping systems	Maintenance plans, rehabilitation investments	Automated gate systems, flow meters	Selvakumar and Tafuri, 2012
Data scarcity	Incomplete hydrological and soil data limiting planning accuracy	Strengthened monitoring networks, open data systems	Weather stations, soil moisture networks	McMillan *et al.*, 2018

sustainable groundwater use and prevent saltwater intrusion (Tuan *et al.*, 2023). Integrating renewable-energy-powered irrigation with strict extraction limits further enhances sustainability by reducing both water and energy pressures while avoiding rebound effects from overuse. Furthermore, without these essential frameworks, the progress made in irrigation technology could inadvertently contribute to the depletion of resources, degradation of the environment, and an unfair distribution of water resources.

Integrated WEF perspectives for durum wheat systems

The WEF methodologies present a detailed framework designed to boost durum wheat production while protecting ecological integrity and resource sustainability. Coordinated water allocation across sectors, informed by precise irrigation scheduling and deficit irrigation strategies, can maintain yield and grain quality while reducing overall water use, as demonstrated in southern Sardinia where reduced irrigation with 50 percent (%) of plant water requirement) achieved comparable performance to full irrigation and improved energy use efficiency (Marrocu *et al.*, 2025). Integrating energy planning into irrigation systems, including renewable energy sources, further reduces operational costs and carbon emissions, aligning production with climate-smart practices. Soil and water conservation

techniques incorporated within WEF strategies strengthen resilience through improved moisture retention and minimizing erosion. Decision-support tools, including in situ monitoring, remote sensing, and crop modelling, quantify trade-offs between yield, water use, and energy consumption, enabling optimized resource allocation. Governance that includes stakeholders guarantees fair access and sustainable resource security, especially in the arid regions of the Global South, where institutional deficiencies and unequal distribution frequently undermine food security (Kashifi *et al.,* 2022). These WEF-aligned interventions collectively support sustainable intensification by balancing agricultural productivity, energy efficiency, and environmental protection (Fig. 2).

Durum wheat in continental semi-arid basins

Cold continental semi-arid basins exhibit distinctive hydrological and climatic conditions that shape agricultural water management, including snowmelt-driven runoff, high summer evapotranspiration, pronounced interannual climate variability and limited irrigation infrastructure (Raikhan *et al.,* 2020). These aspects have a considerable impact on the performance of durum wheat, which exhibits a high sensitivity to water deficits during stem elongation, anthesis and grain filling. In the Esil (Yesil) River Basin of northern Kazakhstan, one of the largest continental wheat-producing regions, irrigated cropland represents less than 1% of total agricultural land despite favorable thermal conditions and substantial yield gaps (Kakabayev *et al.*, 2023; Yessymkhanova *et al.*, 2021). The insufficient use of irrigation reveals a considerable opportunity for the strategic intensification of durum wheat that is efficient in water use. Emerging research from northern and western Kazakhstan demonstrates that targeted supplemental irrigation timed to key phenological stages can dramatically enhance wheat productivity. Research conducted in the Esil Basin demonstrates that even minimal irrigation during the anthesis and early grain filling stages can result in yields that are two to three times greater than those achieved through entirely rainfed methods, highlighting the importance of aligning restricted water resources with the needs of crops. Snowmelt-based seasonal storage further enables farmers to

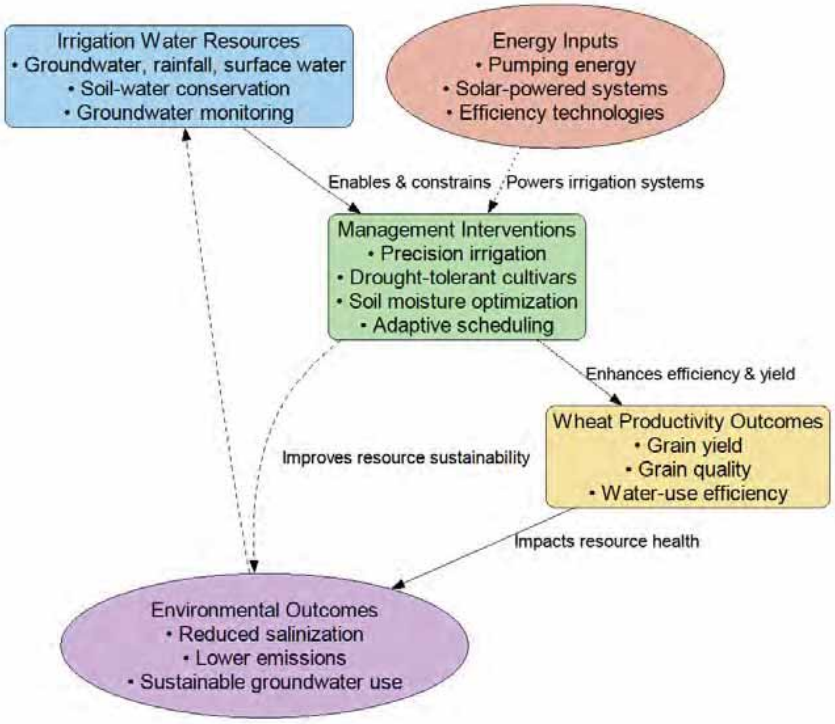

Fig.2: Durum wheat water-energy-food nexus framework

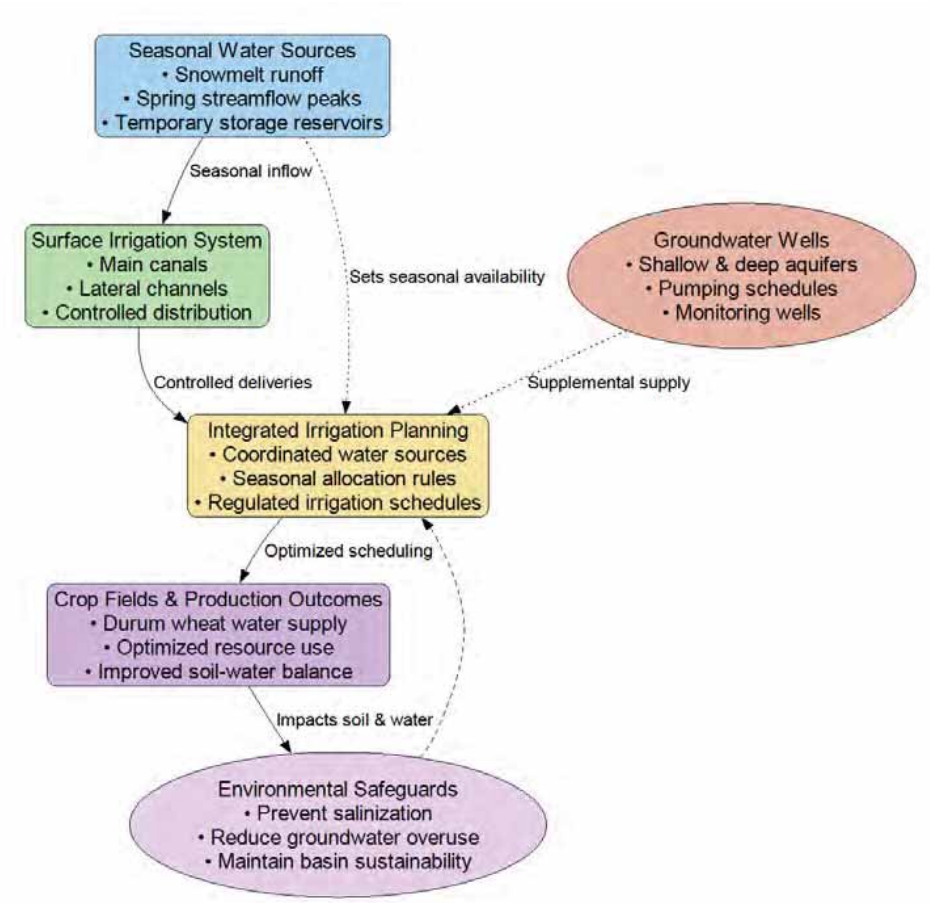

Fig. 3: Basin-level integrated irrigation planning in semi-arid systems

regulate irrigation availability without overexploiting groundwater, which is particularly important in regions where year-to-year climate variability drives substantial fluctuations in soil moisture and crop risk. Groundwater assessments from western Kazakhstan show that roughly 90% of groundwater resources are suitable for irrigation when evaluated against hydrochemical and soil-reclamation criteria (Murtazin *et al.*, 2025). These findings advocate for the application of groundwater as an additional resource for the supplemental irrigation of durum wheat, especially when integrated with water-conserving technologies such as drip and sprinkler systems that minimize both extraction volumes and salinization risks. Field trials across Kazakhstan also show that mixed-source irrigation using groundwater, surface water and collector-drainage water can help buffer freshwater scarcity while maintaining soil quality, offering a realistic pathway for stabilizing durum wheat yields under increasing climate variability. While examples from rice-based systems in the Bakbakti region illustrate the broader potential of mixed-source irrigation to reduce freshwater withdrawals and improve economic returns (Absametov *et al.*, 2025). However, their significance is in showcasing the practicality of integrated water-source management rather than serving as a direct comparison for wheat. In durum-producing areas of Kazakhstan, the principle of coordinated water-source utilization is currently being evaluated through pilot programs that concentrate specifically on cereals. The integration of supplemental irrigation with climate-resilient varieties and soil-water conservation practices such as conservation techniques, including conservation tillage, residue retention, and increased organic matter, has demonstrated potential for enhancing soil moisture retention and minimizing irrigation requirements. The evidence from continental semi-

arid basins indicates that durum wheat productivity can be significantly enhanced through a combination of phenology-targeted supplemental irrigation, strategic use of multiple water sources, groundwater-quality monitoring and soil-water conservation practices. When reinforced by basin-level planning and sustainable groundwater management, these measures offer a cohesive structure for boosting water-use efficiency, stabilizing yields, and preserving soil and water resources in some of the world's most climate-vulnerable wheat regions (Fig. 3).

RECOMMENDATION

This study offers significant insights for both academic inquiry and practical application by illustrating that the production of resilient durum wheat in water-scarce conditions relies on the synergistic effects of drought-resistant cultivars, practices that enhance soil moisture, and advanced irrigation technologies, all of which contribute to improved water use and stable yields amidst escalating climatic stress. The assessment of environmental risks such as salinization, groundwater decline, and energy-related emissions highlights the need for integrated water governance that supports sustainable resource use. Future studies should prioritize the validation of combined agronomic and governance strategies in diverse semi-arid areas to bolster the evidence base for implementing effective interventions. The insights presented here are valuable for policymakers, agricultural planners, and water managers seeking to enhance crop resilience, safeguard natural resources, and reinforce food security in water-scarce settings.

CONCLUSION

Durum wheat is a highly strategic crop for ensuring food security in semi-arid regions, where increasing water scarcity, high evapotranspiration rates, and interannual climatic variability impose significant constraints on agricultural productivity. This study reveals that achieving sustainable yield enhancements in water-limited settings demands the integrated use of drought-resistant plant varieties, targeted irrigation practices, and soil-water conservation measures. Collectively, these approaches optimize water utilization, ensure yield stability, and uphold grain quality in the face of variable rainfall and lengthy droughts. Empirical evidence highlights that carefully managed supplemental and deficit irrigation can significantly enhance water-use efficiency while supporting crop productivity, particularly when combined with drought-resilient cultivars that maintain performance under moisture-limited conditions. Complementary soil-water conservation measures, including conservation tillage, residue retention, mulching, crop rotation with legumes, and organic matter enhancement, further improve soil structure, increase water-holding capacity, and enhance infiltration. This effectively diminishes irrigation requirements and enhances system resilience. These agronomic and soil management practices are essential for sustainable durum wheat production in areas with restricted irrigation infrastructure. Nevertheless, technical solutions by themselves are inadequate without strong governance. Robust policies and institutional structures are crucial for the protection of water and soil resources, the prevention of overexploitation, and the assurance of long-term sustainability. Volumetric water allocation policies, systematic groundwater monitoring, salinity management, and the integration of renewable-energy-powered irrigation systems provide the regulatory and operational structures necessary for equitable resource use. Basin-level strategies that synchronize water, energy, and food priorities increase the effectiveness of resource distribution and enhance resilience to climatic and hydrological challenges. Importantly, integrating groundwater monitoring and volumetric water allocation into farmer decision-making must be implemented in ways that avoid increasing inequities among users, emphasizing participatory management, transparent allocation rules, and capacity-building for smallholder farmers. Furthermore, without effective governance, the potential of advanced irrigation systems and climate-resilient crops may not be fully realized, leading to unsustainable results. Various challenges and limitations remain, despite the progress made. Variability in soil types, water availability, and local climate conditions can constrain the effectiveness of standardized interventions, while socio-economic factors such as farmer access to capital, risk perception, and knowledge gaps may limit the adoption of improved cultivars and water-efficient technologies. Data gaps remain regarding long-term impacts of integrated irrigation and soil-

water conservation practices on soil health, microbial networks, and salinity dynamics, particularly under compound climate extremes. Furthermore, the scalability of solar-powered irrigation and precision technologies is contingent upon the presence of governance frameworks, training, and financial assistance for smallholder farmers, underscoring the necessity for context-specific adaptation strategies. Beyond immediate agronomic and governance measures, this study underscores the importance of integrated research and innovation to guide future durum wheat production. Integrated crop-climate-hydrology models offer a powerful tool to simulate future evapotranspiration trends, quantify yield responses under 2-4°C warming scenarios, and predict the stability of durum wheat yields under extreme and variable climatic conditions. Validation of fields concerning the integration of precision irrigation and drought-resistant cultivars across various soil types, climatic regions, and agricultural systems is crucial for producing actionable, site-specific guidance. Long-term studies examining interactions between soil-water conservation, irrigation efficiency, and crop productivity under variable climatic conditions will provide insights into system resilience and adaptation potential. Multi-scale Water, Energy, and Food nexus modelling can quantify trade-offs between resource use, environmental sustainability, and food production, supporting evidence-based, basin-level decision-making. Evaluating the socio-economic impacts of renewable-energy-based irrigation systems, especially for smallholder farmers, is crucial for promoting fair adoption and scalable implementation. Furthermore, the convergence of genomics, remote sensing, crop modelling, and data-driven decision-support tools offers opportunities to optimize irrigation timing, improve resource allocation, and enhance overall system resilience. The sustainable intensification of durum wheat in semi-arid regions depends on the coordinated application of drought-tolerant cultivars, precision irrigation, soil-water conservation methods, and sound governance, all underpinned by thorough research that encompasses technological, environmental, and socio-economic aspects. These combined approaches not only enhance productivity and food security under climatic stress but also safeguard natural resources, offering a practical framework for climate-resilient durum wheat production that is scalable across global semi-arid agricultural landscapes. The practical applications derived from these findings encompass targeted supplemental irrigation during essential growth phases, the adoption of climate-resilient cultivars, the integration of soil-water conservation practices at the farm level, and the implementation of solar-powered irrigation systems that are connected to robust governance and monitoring frameworks. Future studies ought to concentrate on extensive, multi-site field trials that integrate cultivar selection, irrigation management, and soil-water conservation. Additionally, it is essential to monitor environmental and socio-economic trade-offs, to provide evidence-based guidelines for sustainable and resilient durum wheat systems worldwide. Specifically, 1) advancing integrated crop–climate–hydrology models to improve predictions of evapotranspiration and yield stability under warming scenarios, 2) developing participatory frameworks for volumetric water allocation and groundwater monitoring that promote just decision-making, and 3) Exploring new technologies and management strategies, including high-throughput phenotyping, remote sensing, and precision soil-water monitoring, to improve adaptive capacity. These comprehensive insights guide policymakers, extension services, and farmers toward actionable strategies that reconcile productivity, environmental sustainability, and resource equity in semi-arid agriculture, while delineating clear evidence-based directions for future research and innovation.

AUTHOR CONTRIBUTIONS

G. Saspugayeva was responsible for defining the bibliographic search strategy, identifying relevant sources, and contributing to the synthesis of the reviewed literature. A. Zhaken conceptualized the review framework, supervised the structure and scholarly direction of the manuscript, and critically revised the final version. I. Agarkova contributed to reference screening, thematic coding of the selected studies, and assisted in drafting sections of the manuscript. Z. Mukhametzhanova supported the analytical interpretation of the reviewed materials and contributed to refining the discussion. I. Samatova assisted in organizing the literature database, coding reference content, and drafting portions of the manuscript. Z. Zhaznaeva contributed to methodological clarification, quality checking

of references, and reviewing the manuscript for coherence. A. Chursin assisted with data interpretation, integration of thematic sections, and manuscript refinement. G. Salykbayeva contributed to evaluating the thematic relevance of literature and reviewing the full manuscript. Sh. Baimukasheva contributed to editing, manuscript alignment with journal guidelines, and final critical revisions. B. Serkebayeva contributed to evaluating the thematic relevance of the literature and reviewing the full manuscript.

ACKNOWLEDGEMENT

The authors gratefully acknowledge the guidance and academic support provided by advisors and colleagues during the preparation of this work. The constructive comments and suggestions received throughout the research process contributed significantly to improving the quality of this study.

CONFLICT OF INTEREST

The authors declare no potential conflict of interest regarding the publication of this work. In addition, the ethical issues including plagiarism, informed consent, misconduct, data fabrication and, or falsification, double publication and, or submission, and redundancy have been completely witnessed by the authors.

OPEN ACCESS

©2026 The author(s). This article is licensed under a Creative Commons Attribution 4.0 International License, which permits use, sharing, adaptation, distribution and reproduction in any medium or format, if you give appropriate credit to the original author(s) and the source, provide a link to the Creative Commons license, and indicate if changes were made. The images or other third-party material in this article are included in the article's Creative Commons license, unless indicated otherwise in a credit line to the material. If material is not included in the article's Creative Commons license and your intended use is not permitted by statutory regulation or exceeds the permitted use, you will need to obtain permission directly from the copyright holder. To view a copy of this license, visit: http://creativecommons.org/licenses/by/4.0/

PUBLISHER'S NOTE

GJESM Publisher remains neutral regarding jurisdictional claims in published maps and institutional afflictions.

Negative AI Statement

The author(s) declared that no AI tools or services were not used or not highly applied during the preparation of this work.

ABBREVIATIONS

%	Percent
CA	Conservation agriculture
CO_2eq	Carbon dioxide equivalent
DREB	Dehydration responsive element-binding transcription factor family
DRO1	Deeper rooting 1 gene
ERECTA	erecta receptor-like kinase
ERF	Ethylene responsive factor transcription factor family
ET	Evapotranspiration
Fig.	Figure
L/ha	Litres per hectare
mm	Millimetres
MYB	Myeloblastosis transcription factor family
SDS	Sodium dodecyl sulfate
t/ha	Ton per hectare
tCO_2eq/ha/y	ton carbon dioxide equivalent per hectare per year
WA+	Water accounting plus
WEF	Water–energy–food
WRKY	Wrky transcription factor family

REFERENCES

Abdallah, A.M.; Jat, H.S.; Choudhary, M.; Abdelaty, E.F.; Sharma, P.C.; Jat, M.L., (2021). Conservation agriculture effects on soil water holding capacity and water-saving varied with management practices and agroecological conditions: A review. Agronomy. 11(9): 1681 **(27 pages).**

Abdi, A.H.; Sugow, M.O.; Halane, D.R., (2024). Exploring climate change resilience of major crops in Somalia: implications for ensuring food security. Int. J. Agric. Sustainability. 22(1): 2338030 **(21 pages).**

Abioye, E.A.; Abidin, M.S.Z.; Mahmud, M.S.A.; Buyamin, S.; Ishak, M.H.I.; Rahman, M.K.I.A.; Otuoze, A.O.; Onotu, P.; Ramli, M.S.A., (2020). A review on monitoring and advanced control strategies for precision irrigation. Comput. Electron. Agric., 177: 105441 **(19 pages).**

Absametov, M.; Umbetaliev, D.; Kulagin, V.; Rakhimov, T.; Mirlas, V.; Ismagulova, A.; Rakhimova, V., (2025). Optimizing irrigation efficiency: a case study of the Bakbakti Rice System in Akdala Massif. Front. Water. 7: 1650089 **(23 pages).**

Adhikari, M.; Adhikari, N.R.; Sharma, S.; Gairhe, J.; Bhandari, R.R.; Paudel, S., (2019). Evaluation of drought-tolerant rice cultivars using drought tolerant indices under water stress and irrigated conditions. Am. J. Climate Change. 8(2): 228–236 **(9 pages).**

Alfaro, P.; Liesch, T.; Goldscheider, N., (2017). Modelling groundwater over-extraction in the southern Jordan Valley with scarce data. Hydrogeol. J., 25(5): 1319–1340 **(22 pages)**.

Ali, N.; Dong, Y.; Lavely, E., (2024). Impact of irrigation scheduling on yield and water use efficiency of apples, peaches, and sweet cherries: a global meta-analysis. Agric. Water Manage., 306: 109148 **(20 pages)**.

Amfo, B.; Ali, E.B.; Atinga, D., (2021). Climate change, soil water conservation, and productivity: evidence from cocoa farmers in Ghana. Agric. Syst., 191: 103172 **(11 pages)**.

Aragüés, R.; Medina, E.T.; Clavería, I.; Martínez-Cob, A.; Faci, J., (2014). Regulated deficit irrigation, soil salinization and soil sodification in a table grape vineyard drip-irrigated with moderately saline waters. Agric. Water Manage., 134: 84–93 **(10 pages)**.

Attar, O.; Leone, M.; De Girolamo, A.M.; Bouchaou, L.; Brouziyne, Y.; El Khalki, E.M.; Berrouch, H.; Taia, S.; Hssaisoune, M.; Ait Brahim, Y., (2025). Modelling water scarcity and water footprint of agricultural crops: a case from a semi-arid region in Morocco. J. Hydrol.: Reg. Stud., 59: 102455 **(18 pages)**.

Awan, M.G.H.; Ijaz, S.S.; Ansar, M.; Anwar, A.; Abbasi, U.; Mahmood, H., (2020). Influence of foliar application of mineral nutrients on biological nitrogen fixation of rainfed soybean. Pak. J. Agric. Res., 33(4): 827-833 **(7 pages)**.

Bian, Q.; Dong, Z.; Fu, Y.; Zhao, Y.; Feng, Y.; Wang, Z.; Zhu, J., (2024). Optimizing irrigation strategies to improve yield and water use efficiency of drip-irrigated maize in Southern Xinjiang. Plants, 13(24): 3492 **(14 pages)**.

Boico, V.F.; Therrien, R.; Højberg, A.L.; Iversen, B.V.; Koganti, T.; Varvaris, I., (2022). Using depth specific electrical conductivity estimates to improve hydrological simulations in a heterogeneous tile-drained field. J. Hydrol., 606: 127232 **(15 pages)**.

Boudjabi, S.; Kribaa, M.; Chenchouni, H., (2015). Growth, physiology and yield of durum wheat (*Triticum durum*) treated with sewage sludge under water stress conditions. EXCLI J., 14: 14-35 **(15 pages)**.

Busari, M.A.; Kukal, S.S.; Kaur, A.; Bhatt, R.; Dulazi, A.A., (2015). Conservation tillage impacts on soil, crop and the environment. Int. Soil Water Conserv. Res., 3(2): 119–129 **(11 pages)**.

Calasso, M.; Lisi, A.; Ressa, A.; Caponio, G.R.; Difonzo, G.; Minervini, F.; Gargano, M.L.; Vacca, M.; De Angelis, M., (2025). Incorporating fresh durum wheat semolina pasta fortified with Cardoncello (*Pleurotus eryngii*) mushroom powder as a Mediterranean diet staple. Antioxidants, 14(3): 284 **(21 pages)**.

Ceita, P.A.S.B.; Mahamed, I.M.; Ferras, D.; Trifunović, N.; Kennedy, M., (2023). Equity analysis of intermittent water supply systems by means of EPA-SWMM. Water Supply, 23(8): 3097–3112 **(16 pages)**.

Chabour, H.E.; Pardo, M.A.; Riquelme, A., (2022). Economic assessment of converting a pressurised water distribution network into an off-grid system supplied with solar photovoltaic energy. Clean Technol. Environ. Policy, 24(6): 1823–1835 **(13 pages)**.

Chen, M.; Li, J.; Zhang, Y.; Ding, Y.; Qin, W.; Wu, M.; Li, N.; Jin, C.; Wang, H.; Chen, S.; Niu, D.; Sun, X.; Zhang, B.; Chen, S.; Wang, Z.; Shi, C.; Zhang, K.; Wang, D.; Dai, S.; Yan, Z.; Li, G., (2025). Chromosome-level genome assembly of the Durum wheat cultivar Langdon. Sci. Data, 12: 1372 (**11 pages**).

Cooray, A.; Rejesus, R.M.; Aglasan, S.; Li, Z.; Woodley, A., (2023). The impact of conservation tillage intensities on mean yields and yield risk. Soil Secur., 12: 100096 **(9 pages)**.

Cuthbert, M.O.; Rau, G.C.; Ekström, M.; O□Carroll, D.M.; Bates, A.J., (2022). Global climate-driven trade-offs between the water retention and cooling benefits of urban greening. Nat. Commun., 13(1): 518 **(9 pages)**.

Dai, Y.; Fan, J.; Liao, Z.; Zhang, C.; Yu, J.; Feng, H.; Zhang, F.; Li, Z., (2022). Supplemental irrigation and modified plant density improved photosynthesis, grain yield and water productivity of winter wheat under ridge-furrow mulching. Agric. Water Manage., 274: 107985 **(13 pages)**.

Dangar, S.; Asoka, A.; Mishra, V., (2021). Causes and implications of groundwater depletion in India: a review. J. Hydrol., 596: 126103 **(19 pages)**.

Daraz, U.; Bojnec, Š.; Khan, Y., (2025). Energy-efficient smart irrigation technologies: a pathway to water and energy sustainability in agriculture. Agriculture, 15(5): 554 **(28 pages)**.

do Espirito Santo Pereira, A.; Caixeta Oliveira, H.; Fernandes Fraceto, L.; Santaella, C., (2021). Nanotechnology potential in seed priming for sustainable agriculture. Nanomaterials, 11(2): 267 **(19 pages)**.

Duc, N.H.; Kumar, P.; Long, P.T.; Meraj, G.; Lan, P.P.; Almazroui, M.; Avtar, R., (2024). A systematic review of water governance in Asian countries: challenges, frameworks, and

pathways toward sustainable development goals. Earth Syst. Environ., 8(2): 181–205 **(25 pages)**.

Elias, E.H.; Flynn, R.; Idowu, O.J.; Reyes, J.; Sanogo, S.; Schutte, B.J.; Smith, R.; Steele, C.; Sutherland, C., (2019). Crop vulnerability to weather and climate risk: analysis of interacting systems and adaptation efficacy for sustainable crop production. Sustainability. 11(23): 6619 **(28 pages)**.

Fernando, Y.; Adams, M.; Kuhlmann, M.; Jr, V.B., (2025). Stomatal and non-stomatal leaf traits for enhanced water use efficiency in rice. Biology. 14(7): 843 **(18 pages)**.

Gahlaut, V.; Jaiswal, V.; Kumar, A.; Gupta, P.K., (2016). Transcription factors involved in drought tolerance and their possible role in developing drought tolerant cultivars with emphasis on wheat (*Triticum aestivum* L.). Theor. Appl. Genet., 129(11): 2019–2042 **(24 pages)**.

Galindo, A.; Collado-González, J.; Griñán, I.; Corell, M.; Centeno, A.; Martín-Palomo, M.J.; Girón, I.F.; Rodríguez, P.; Cruz, Z.N.; Memmi, H.; Carbonell-Barrachina, A.A.; Hernández, F.; Torrecillas, A.; Moriana, A.; Pérez-López, D., (2018). Deficit irrigation and emerging fruit crops as a strategy to save water in Mediterranean semiarid agrosystems. Agric. Water Manage., 202: 311–324 **(14 pages)**.

Gooding, M.J.; Ellis, R.H.; Shewry, P.R.; Schofield, J.D., (2003). Effects of restricted water availability and increased temperature on the grain filling, drying and quality of winter wheat. J. Cereal Sci., 37(3): 295–309 **(15 pages)**.

Grosse-Heilmann, M.; Cristiano, E.; Deidda, R.; Viola, F., (2024). Durum wheat productivity today and tomorrow: a review of influencing factors and climate change effects. Resour. Environ. Sustainability. 17: 100170 **(12 pages)**.

Guno, C.S.; Agaton, C.B., (2022). Socio-economic and environmental analyses of solar irrigation systems for sustainable agricultural production. Sustainability. 14(11): 6834 **(20 pages)**.

Hassan, W.; Manzoor, T.; Muhammad, A., (2023). Improving equity in demand-driven irrigation systems through a rights-preserving water allocation mechanism. Agric. Water Manage., 287: 108443 **(12 pages)**.

Hiyama, T.; Suzuki, T.; Hanamura, M.; Mizuochi, H.; Kambatuku, J.R.; Niipele, J.N.; Fujioka, Y.; Ohta, T.; Iijima, M., (2014). Evaluation of surface water dynamics for water-food security in seasonal wetlands, north-central Namibia. Proc. Int. Assoc. Hydrol. Sci., 364: 380–385 **(6 pages)**.

Ibrahim, E.A., (2016). Seed priming to alleviate salinity stress in germinating seeds. J. Plant Physiol., 192: 38–46 **(9 pages)**.

Iijima, M.; Awala, S.K.; Nanhapo, P.I.; Wanga, A.; Mwandemele, O.D., (2018). Development of flood- and drought-adaptive cropping systems in Namibia. In: Crop Production under Stressful Conditions: Application of Cutting-edge Science and Technology in Developing Countries. Springer: 55-70 **(16 pages)**.

Islam, M.Z.; Salim, M.; Deb, B.R.; Roy, S.C.; Sarkar, S.K.; Paul, S.K., (2025). Enhancing wheat yield through strategic irrigation management. Arch. Agric. Environ. Sci., 10(1): 120–125 **(6 pages)**.

Izumi, Y.; Okaichi, S.; Awala, S.K.; Kawato, Y.; Watanabe, Y.; Yamane, K.; Iijima, M., (2018). Water supply from pearl millet by hydraulic lift can mitigate drought stress and improve productivity of rice by the close mixed planting. Plant Prod. Sci., 21(1): 8–15 **(8 pages)**.

Johnson, K.; Vo, T.T.B.; Van Nha, D.; Asch, F., (2023). Genotypic responses of rice to alternate wetting and drying irrigation in the Mekong Delta. J. Agron. Crop Sci., 209(5): 593–612 **(20 pages)**.

Joshi, G.R.; Bhandari, R., (2022). Climate adaptation in rain-fed agriculture: analyzing the determinants of supplemental irrigation practices in Nepal. Res. World Agric. Econ., 3(4): 21-37 **(17 pages)**.

Kakabayev, A.; Yessenzholov, B.; Khussainov, A.; Rodrigo-Ilarri, J.; Rodrigo-Clavero, M.-E.; Kyzdarbekova, G.; Dankina, G., (2023). The impact of climate change on the water systems of the Yesil River Basin in Northern Kazakhstan. Sustainabity. 15(22): 15745 **(22 pages)**.

Kashifi, M.T.; Al-Ismail, F.S.M.; Chowdhury, S.; Baaqeel, H.M.; Shafiullah, M.; Tiwari, S.P.; Rahman, S.M., (2022). Water-energy-food nexus approach to assess crop trading in Saudi Arabia. Sustainability. 14(6): 3494 **(21 pages)**.

Katohar, I.; Soothar, R.K.; Chandio, F.A.; Talpur, M.A.; Soomro, S.A.; Singha, A.; Bin, L.; Mirjat, M.U., (2023). Drought priming and subsequent irrigation water regimes enhanced grain yield and water productivity of wheat crop. Water. 15(20): 3704 **(19 pages)**.

Kumar Singh, D.; Sobti, R., (2022). Long-range real-time monitoring strategy for Precision Irrigation in urban and rural farming in society 5.0. Comput. Ind. Eng., 167: 107997 **(12 pages)**.

Le Roux, M.; Kunert, K.J.; Cullis, C.A.; Botha, A., (2024). Unlocking wheat drought tolerance: the synergy of omics data and computational intelligence. Food Energy Secur., 13(6): e70024 **(18 pages)**.

Leščešen, I.; Gnjato, S.; Vujačić, D.; Petrović, A.M.; Radevski, I., (2025). Seasonal variability changes and trends in minimum discharge for Western Balkan rivers. J. Hydrol. Reg. Stud., 60: 102529 **(15 pages)**.

Li, L.; Mao, Z.; Wang, P.; Cai, J.; Zhou, Q.; Zhong, Y.; Jiang, D.; Wang, X., (2025). Drought priming enhances wheat grain starch and protein quality under drought stress during grain filling. J. Integr. Agric., 24(8): 2888–2901 **(14 pages)**.

Liu, S.; Lin, X.; Wang, W.; Zhang, B.; Wang, D., (2022). Supplemental irrigation increases grain yield, water productivity, and nitrogen utilization efficiency by improving nitrogen nutrition status in winter wheat. Agric. Water Manage., 274: 107969 **(12 pages)**.

Liu, X.B.; Zhang, X.Y.; Wang, Y.X.; Sui, Y.Y.; Zhang, S.L.; Herbert, S.J.; Ding, G., (2010). Soil degradation: a problem threatening the sustainable development of agriculture in Northeast China. Plant Soil Environ., 56(2): 87–97 **(11 pages)**.

Loureiro, D.; Beceiro, P.; Moreira, M.; Arranja, C.; Cordeiro, D.; Alegre, H., (2023). A comprehensive performance assessment system for diagnosis and decision-support to improve water and energy efficiency and its demonstration in Portuguese collective irrigation systems. Agric. Water Manage., 275: 107998 **(14 pages)**.

Lovatt, C.J., (2013). Properly timing foliar-applied fertilizers increases efficacy: a review and update on timing foliar nutrient applications to citrus and avocado. HortTechnology. 23(5): 536–541 **(6 pages)**.

Lu, T.; Luo, P.; Wang, J.; Lu, Y.; Huo, A.; Liu, L., (2025). Soil salinity accumulation and groundwater degradation due to overexploitation over recent 40-year period in Yaoba Oasis, China. Soil Tillage Res., 248: 106398 **(11 pages)**.

Lv, L.; Gao, Z.; Liao, K.; Zhu, Q.; Zhu, J., (2023). Impact of conservation tillage on the distribution of soil nutrients with depth. Soil Tillage Res., 225: 105527 **(11 pages)**.

Mabhaudhi, T.; Dirwai, T.L.; Taguta, C.; Senzanje, A.; Abera, W.; Govid, A.; Dossou-Yovo, E.R.; Aynekulu, E.; Petrova Chimonyo, V.G., (2025). Linking weather and climate information services (WCIS) to Climate-Smart Agriculture (CSA) practices. Climate Serv., 37: 100529 **(14 pages)**.

MacRorie, M.H.; Speight, V.L.; Weston, S.L.; Price, R.; Collins, R.P., (2022). A model of intermittent water supply simulating the inequitable distribution of water. In: 2nd International Joint Conference on Water Distribution System Analysis and Computing and Control in the Water Industry. València: Editorial Universitat Politècnica de València. 178-187 **(10 pages).**

Manhou, K.; Moussadek, R.; Dakak, H.; Zouahri, A.; Ghanimi, A.; Sanad, H.; Oueld Lhaj, M.; Hmouni, D., (2025). Effect of irrigation with saline water on germination, physiology, growth, and yield of durum wheat varieties on silty clay soil. Agriculture, 15(22): 2364 **(25 pages)**.

Marrocu, M.; Dettori, M.; Massidda, L.; Urracci, G.; Pusceddu, G.; Mereu, V.; Manca, S.; Carboni, G., (2025). Integrating deficit irrigation, crop modelling and Water–Energy–Food nexus to enhance durum wheat resilience in Mediterranean climate conditions. Agric. Water Manage., 322: 110001 **(16 pages)**.

Math, R.M.; Dharwadkar, N.V., (2020). An intelligent irrigation scheduling and monitoring system for precision agriculture application. Int. J. Agric. Environ. Inf. Syst., 11(4): 1–24 **(24 pages)**.

McMillan, H.K.; Westerberg, I.K.; Krueger, T., (2018). Hydrological data uncertainty and its implications. Wiley Interdiscip. Rev. Water. 5(4): e1319 **(16 pages)**.

Miazzi, M.M.; Babay, E.; De Vita, P.; Montemurro, C.; Chaabane, R.; Taranto, F.; Mangini, G., (2022). Comparative genetic analysis of Durum wheat landraces and cultivars widespread in Tunisia. Front. Plant Sci., 13: 939609 (**13 pages**).

Mkilima, T., (2023). Groundwater salinity and irrigation suitability in low-lying coastal areas. A case of Dar es Salaam, Tanzania. Watershed Ecol. Environ., 5: 173–185 **(13 pages)**.

Mkilima, T., (2025). Harnessing recycled wastewater for sustainable agriculture: a balancing act between benefits and risks. Irrig. Drain., Early View: 1-15 **(15 pages)**.

Murtazin, Y.; Kulagin, V.; Mirlas, V.; Anker, Y.; Rakhimov, T.; Onglassynov, Z.; Rakhimova, V., (2025). Integrated assessment of groundwater quality for water-saving irrigation technology (Western Kazakhstan). Water. 17(8): 1232 **(23 pages)**.

Mutanda, M.; Shimelis, H.; Chaplot, V.; Figlan, S., (2025). Managing drought stress in wheat (*Triticum aestivum* L.) production: strategies and impacts. S. Afr. J. Plant Soil. 42(1-3): 1-12 **(12 pages)**.

Nachshon, U., (2018). Cropland soil salinization and associated hydrology: trends, processes and examples. Water, 10(8): 1030 **(14 pages)**.

Ndhleve, S.; Nakin, M.D.V.; Longo-Mbenza, B., (2017). Impacts of supplemental irrigation as a climate change adaptation strategy for maize production: a case of the Eastern Cape Province of South Africa. Water SA., 43(2): 222–228 **(7 pages)**.

Nsoh, B.; Katimbo, A.; Guo, H.; Heeren, D.M.; Nakabuye, H.N.; Qiao, X.; Ge, Y.; Rudnick, D.R.; Wanyama, J.; Bwambale, E.; Kiraga, S., (2024). Internet of Things-based automated solutions utilizing machine learning for smart and real-time irrigation management: a review. Sensors. 24(23): 7480 **(32 pages)**.

Nugroho, H.Y.S.H.; Basuki, T.M.; Pramono, I.B.; Savitri, E.; Purwanto; Indrawati, D.R.; Wahyuningrum, N.; Adi, R.N.; Indrajaya, Y.; Supangat, A.B.; Putra, P.B.; Auliyani, D.; Priyanto, E.; Yuwati, T.W.; Pratiwi; Narendra, B.H.; Sukmana, A.; Handayani, W.; Setiawan, O.; Nandini, R., (2022). Forty years of soil and water conservation policy, implementation, research and development in Indonesia: a review. Sustainability. 14(5): 2972 **(24 pages)**.

Pacheco-Andrade, A.; Torres, M.E.; Cántaro-Segura, H.; Díaz-Morales, L.; Matsusaka, D., (2025). Stability and yield performance of durum wheat (*Triticum durum* Desf.) genotypes across environments in Southern Peru. Int. J. Plant Biol., 16(4): 127 **(13 pages)**.

Pagano, A.; Macovei, A.; Balestrazzi, A., (2023). Molecular dynamics of seed priming at the crossroads between basic and applied research. Plant Cell Rep., 42(4): 657–688 **(32 pages)**.

Painagan, M.S.; Ella, V.B., (2022). Modeling the impact of deficit irrigation on corn production. Sustainability. 14(16): 10401 **(20 pages)**.

Quiroga, G.; Erice, G.; Aroca, R.; Chaumont, F.; Ruiz-Lozano, J.M., (2017). Enhanced drought stress tolerance by the arbuscular mycorrhizal symbiosis in a drought-sensitive maize cultivar is related to a broader and differential regulation of host plant aquaporins than in a drought-tolerant cultivar. Front. Plant Sci., 8: 1056 **(16 pages)**.

Raikhan, B.; Gulnur, S.; Aizhan, Z.; Makhabbat, R.; Assel, T., (2020). Geoecological maps of surface water pollution Akmola region of Kazakhstan based on hydrochemical analyzes. IOP Conf. Ser.: Mater. Sci. Eng., 901: 012017 **(8 pages)**.

Raj, A.B.; Raj, S.K., (2019). Seed priming: an approach towards agricultural sustainability. J. Appl. Nat. Sci., 11(1): 227–234 **(8 pages)**.

Rodríguez Díaz, J.A.; Camacho Poyato, E.; Blanco Pérez, M., (2011). Evaluation of water and energy use in pressurized irrigation networks in Southern Spain. J. Irrig. Drain. Eng., 137(10): 644–650 **(7 pages)**.

Rolle, M.; Tamea, S.; Claps, P., (2022). Climate-driven trends in

agricultural water requirement: an ERA5-based assessment at daily scale over 50 years. Environ. Res. Lett., 17(4): 044017 **(14 pages)**.

Saad, A.M.; Elhabbak, A.K.; Abbas, M.H.H.; Mohamed, I.; AbdelRahman, M.A.E.; Scopa, A.; Bassouny, M.A., (2023). Can deficit irrigation be an optimum solution for increasing water productivity under arid conditions? A case study on wheat plants. Saudi J. Biol. Sci., 30(2): 103537 **(11 pages)**.

Sadiq, F.K.; Anyebe, O.; Tanko, F.; Abdulkadir, A.; Manono, B.O.; Matsika, T.A.; Abubakar, F.; Bello, S.K., (2025). Conservation agriculture for sustainable soil health management: a review of impacts, benefits and future directions. Soil Syst., 9(3): 103 **(28 pages)**.

Sarker, M.R.; Galdos, M.V.; Challinor, A.J.; Huda, M.S.; Chaki, A.K.; Hossain, A., (2022). Conservation tillage and residue management improve soil health and crop productivity—Evidence from a rice-maize cropping system in Bangladesh. Front. Environ. Sci., 10: 969819 **(16 pages)**.

Scanlon, B.R.; Rateb, A.; Pool, D.R.; Sanford, W.; Save, H.; Sun, A.; Long, D.; Fuchs, B., (2021). Effects of climate and irrigation on GRACE-based estimates of water storage changes in major US aquifers. Environ. Res. Lett., 16(9): 094009 **(15 pages)**.

Selvakumar, A.; Tafuri, A.N., (2012). Rehabilitation of aging water infrastructure systems: key challenges and issues. J. Infrastruct. Syst., 18(3): 202–209 **(8 pages)**.

Shahrajabian, M.H.; Sun, W.; Cheng, Q., (2022). Foliar application of nutrients on medicinal and aromatic plants, the sustainable approaches for higher and better production. Beni-Suef Univ. J. Basic Appl. Sci., 11(1): 26 **(15 pages)**.

Shen, H.; Leblanc, M.; Tweed, S.; Liu, W., (2015). Groundwater depletion in the Hai River Basin, China, from in situ and GRACE observations. Hydrol. Sci. J., 60(4): 671–687 **(17 pages)**.

Shuai, G.; Zhang, X.; Shao, J.; Cui, Y.; Li, D., (2022). Groundwater recovery after restricting groundwater extraction for irrigation: taking Shijiazhuang Plain in Hebei Province as an example. J. Irrig. Drain., 41(6): 105-112 **(8 pages)**.

Sileshi, M.; Kadigi, R.; Mutabazi, K.; Sieber, S., (2019). Determinants for adoption of physical soil and water conservation measures by smallholder farmers in Ethiopia. Int. Soil Water Conserv. Res., 7(4): 354–361 **(8 pages)**.

Singh, N.K.; Singh, S.; Dutta, P.; Sulochana; Harishankar; Yadav, R.S.; Ghosh, S.; Panotra, N.; Thakre, T.B., (2025). Role of conservation tillage strategies in reducing soil degradation and enhancing water infiltration. Asian J. Soil Sci. Plant Nutr., 11(2): 374–387 **(14 pages)**.

Singh, V.G.; Singh, S.K.; Kumar, N.; Kumar, P.; Gupta, P.K.; Singh, P.K.; Gašparović, M.; Ray, R.L.; Saito, O., (2022). Water accounting using satellite products and water accounting plus framework in a semi-arid Betwa River Basin, India. Water. 14(21): 3473 **(25 pages)**.

Skewes, M.A.; Carruthers, R., (2012). Volumetric conversion of allocations: a means to an end or an important process in its own right? WIT Trans. Ecol. Environ., 168: 99-110 **(12 pages)**.

Stuch, B.; Alcamo, J.; Schaldach, R., (2021). Projected climate change impacts on mean and year-to-year variability of yield of key smallholder crops in Sub-Saharan Africa. Clim. Dev., 13(3): 268–282 **(15 pages)**.

Tarolli, P.; Luo, J.; Park, E.; Barcaccia, G.; Masin, R., (2024). Soil salinization in agriculture: mitigation and adaptation strategies combining nature-based solutions and bioengineering. iScience. 27(2): 108830 **(18 pages)**.

Teku, D., (2025). Navigating climate uncertainty: a comprehensive review of climatic variabilities and extreme events on environmental, socio-economic, and livelihood dimensions in Ethiopia with adaptation strategies. All Earth. 37(1): 1–30 **(30 pages)**.

Tomaz, A.; Palma, P.; Fialho, S.; Lima, A.; Alvarenga, P.; Potes, M.; Costa, M.J.; Salgado, R., (2020). Risk assessment of irrigation-related soil salinization and sodification in Mediterranean areas. Water. 12(12): 3569 **(21 pages)**.

Van Tuan, P.; Zhou, Y.; Stigter, T.; Van Tuc, D.; Hai, D.H.; Vuong, B.T., (2023). Design of preliminary groundwater monitoring networks for the coastal Tra Vinh province in Mekong Delta, Vietnam. J. Hydrol.: Reg. Stud., 47: 101425 **(17 pages)**.

Wang, Z.; Fan, B.; Guo, L., (2019). Soil salinization after long-term mulched drip irrigation poses a potential risk to agricultural sustainability. Eur. J. Soil Sci., 70(1): 20–24 **(5 pages)**.

Yang, Y.; Wang, Z.; Ma, Y.; Wang, Y.; Bai, J.; Zhang, R., (2025). Balancing yield and water productivity in wheat: a meta-analysis of irrigation, soil, and climate interactions. Agric. Water Manage., 322: 109999 **(14 pages)**.

Yessymkhanova, Z.; Niyazbekova, S.; Dauletkhanova, Z.; Satenova, D.; Zhumasseitova, S.; Kadyraliev, A.T.; Supaeva, G.T.; Dzholdosheva, T.; Dzholdoshev, N., (2021). Water resources management in Kazakhstan in conditions of their shortage. IOP Conf. Ser.: Earth Environ. Sci., 937(3): 032012 **(8 pages)**.

Yuan, X.; Li, S.; Chen, J.; Yu, H.; Yang, T.; Wang, C.; Huang, S.; Chen, H.; Ao, X., (2024). Impacts of global climate change on agricultural production: a comprehensive review. Agronomy. 14(7): 1360 **(28 pages)**.

Yuan, Y.; Sun, Y., (2024). Practices, challenges, and future of digital transformation in smallholder agriculture: insights from a literature review. Agriculture. 14(12): 2193 **(25 pages)**.

Zha, J.; Ge, M.; Tang, Z.; Lei, J.; Zhao, H.; Zhang, Y., (2024). The incorporation of solar energy and compressed air into the energy supply system enhances the environmentally friendly and efficient operation of drip irrigation systems. Agric. Water Manage., 302: 109019 **(14 pages)**.

Zhang, Y.; Wang, W.; Li, S.; Zhu, K.; Hua, X.; Harrison, M.T.; Liu, K.; Yang, J.; Liu, L.; Chen, Y., (2023). Integrated management approaches enabling sustainable rice production under alternate wetting and drying irrigation. Agric. Water Manage., 281: 108265 **(15 pages)**.

Zhang, Y.; Wu, X.; Wang, X.; Dai, M.; Peng, Y., (2025). Crop root system architecture in drought response. J. Genet. Genomics. 52(1): 4–13 **(10 pages)**.

Zhou, Q.; Ju, C.; Wang, Z.; Zhang, H.; Liu, L.; Yang, J.; Zhang, J., (2017). Grain yield and water use efficiency of super rice under soil water deficit and alternate wetting and drying irrigation. J. Integr. Agric., 16(5): 1028–1043 **(16 pages)**.

AUTHOR (S) BIOSKETCHES

Saspugayeva, G., Ph.D., Associate Professor, Department of Environmental Engineering and Management, Faculty of Natural Sciences, L.N. Gumilyov Eurasian National University, Satpayev Street 2, 010000, Astana, Kazakhstan.
- Email: *saspugayeva_gye@enu.kz*
- ORCID: 0000-0003-3223-3602
- Web of Science ResearcherID: IDIQT-9363-2023
- Scopus Author ID: 56982937000
- Homepage: https://fns.enu.kz/en/page/departments/department-of-environmental-management-and-engineering/professorial-and-teaching-staff

Zhaken, A., Ph.D. Candidate, Department of Environmental Engineering and Management, Faculty of Natural Sciences, L.N. Gumilyov Eurasian National University, Satpayev Street 2, 010000, Astana, Kazakhstan.
- Email: *zhaken.asel@yahoo.com*
- ORCID: 0009-0004-4498-0255
- Web of Science ResearcherID: NA
- Scopus Author ID: 58797826300
- Homepage: https://ersa.eventsair.com/QuickEventWebsitePortal/ersa2024/ersa24/Agenda/AgendaItemDetail?id=93319c13-d54d-445f-9c89-ebac1541cbd3

Agarkova, I., Ph.D., Assistant Professor, NCJSC Karaganda Medical University, Karaganda 100000, Kazakhstan.
- Email: *Agarkova@qmu.kz*
- ORCID: 0009-0007-9821-091X
- Web of Science ResearcherID: KAM-2789-2024
- Scopus Author ID: - NA
- Homepage: https://qmu.edu.kz/en/employees/other-teachers/agarkova-inna-andreevna/

Mukhametzhanova, Z., Ph.D of Medical sciences, associate professor of the Department of Morphology, NCJSC Karaganda Medical University, Karaganda 100000, Kazakhstan.
- Email: *zauresh_m_t@mail.ru*
- ORCID: 0000-0003-2793-851X
- Web of Science ResearcherID: OVZ-5668-2025
- Scopus Author ID: 24280605000
- Homepage: https://qmu.edu.kz/en/employees/other-teachers/mukhametzhanova-zauresh-tanatovna/

Samatova, I., Ph.D., Lecturer, Department of Environmental Engineering and Management, Faculty of Natural Sciences, L.N. Gumilyov Eurasian National University, Satpayev Street 2, 010000, Astana, Kazakhstan.
- Email: *samatova_is@enu.kz*
- ORCID: 0009-0008-9088-1986
- Web of Science ResearcherID: IDFVX-4871-2022
- Scopus Author ID: 250206-012869
- Homepage: https://fns.enu.kz/en/page/departments/department-of-environmental-management-and-engineering/professorial-and-teaching-staff

Zhaznayeva, Zh., Associate Professor, Department of Ecology and Geography at Sarsen Amanzholov East Kazakhstan University, PhD in Ecology.
- Email: *zhaznaeva.zhk951@mail.ru*
- ORCID: 0009-0003-6556-7075
- Web of Science ResearcherID: MCI-6340-2025
- Scopus Author ID: 56983016200
- Homepage: https://vku.edu.kz/wp-content/uploads/2025/10/англ-Жазнаева-ЖК.pdf

Chursin, A., Ph.D., Associate Professor, Department of ecology and geography, Sarsen Amanzholov University of East Kazakhstan, 30th Guards Division St., 34, 070002, Ust-Kamenogorsk, Kazakhstan
- Email: *eko.chursin@mail.ru*
- ORCID ID: 0000-0001-7053-548X
- Web of Science ResearcherID: NA
- Scopus Author ID: 57219455231
- Homepage: https://vku.edu.kz/wp-content/uploads/2025/10/ЧАС_VKUангл.pdf

Salykbayeva, G., MSc., Senior Lecturer, Department of ecology and geography, Higher school of IT and natural sciences, Sarsen Amanzholov University of East Kazakhstan, 30th Guards Division St., 34, 070002, Ust-Kamenogorsk, Kazakhstan.
- Email: *salgal2010@mail.ru*
- ORCID: 0009-0006-3482-8676
- Web of Science ResearcherID: NA
- Scopus Author ID: NA
- Homepage: https://vku.edu.kz/wp-content/uploads/2025/10/Салыкбаева-Г.М._VKUангл.pdf

Baimukasheva, Sh., Ph.D., Associate Professor, Department of "Ecology and life safety",
Faculty of engineering, Yessenov University, 130000, Aktau, Kazakhstan.
- Email: *shynar.baimukasheva@yu.edu.kz*
- ORCID: 0000-0002-9268-5363
- Web of Science ResearcherID: MFK-0191-2025
- Scopus Author ID: 58484086500
- Homepage: https://eng.yu.edu.kz/en/pps-ekologiya/baimukasheva-shynar-khabibullievna/

AUTHOR (S) BIOSKETCHES

Serkebayeva, B., Ph.D., Head of the Laboratory of Physical and Chemical Research, Fluid Analysis Directorate of the Laboratory Research Department, Branch of KazMunayGas Engineering LLP "Kazakh Scientific and Design Institute of Oil and Gas", 130000, Aktau, Kazakhstan.

- Email: *B.Serkebayeva@kmge.kz*
- ORCID: 0000-0002-0288-7210
- Web of Science ResearcherID: PAQ-8690-2025
- Scopus Author ID: - NA
- Homepage: https://www.kmge.kz

HOW TO CITE THIS ARTICLE

Saspugayeva, G.; Zhaken, A.; Agarkova, I.; Mukhametzhanova, Z.; Samatova, I.; Zhaznaeva, Z.; Chursin, A.; Salykbayeva, G.; Baimukasheva, Sh.; Serkebayeva, B., (2026). Sustainable strategies for durum wheat production under water scarcity and climate stress. Global J. Environ. Sci. Manage., 12(1): 453-472.

DOI: 10.22034/gjesm.2026.01.25

URL: https://www.gjesm.net/article_732497.html

PUBLICATION ETHICS

The ethical policy of GJESM is based on the Committee on Publication Ethics (COPE) guidelines and complies with International Committee of GJESM Editorial Board codes of conduct. Readers, authors, reviewers and editors should follow these ethical policies once working with GJESM. The ethical policy of GJESM is liable to determine which of the typical research papers or articles submitted to the journal should be published in the concerned issue. For information on this matter in publishing and ethical guidelines please visit http://publicationethics.org

Duties and Responsibilities of Publishers

1. GJESM is committing to ensure that editorial decisions on manuscript submissions are the final.
2. GJESM is promising to ensure that the decision on manuscript submissions is only made based on professional judgment and will not be affected by any commercial interests.
3. GJESM is committing to maintain the integrity of academic and research records.
4. GJESM is monitoring the ethics by Editor-in-Chief, Associate Editors, Editorial Board Members, Reviewers, Authors, and Readers.
5. GJESM is always checking the plagiarism and fraudulent data issues involving in the submitted manuscript.
6. GJESM is always willing to publish corrections, clarifications and retractions involving its publications as and when needed.

Duties and Responsibilities of Editors

1. The Editors of the journal should have the full authority to reject/accept a manuscript.
2. The Editors of the journal should maintain the confidentiality of submitted manuscripts under review or until they are published.
3. The Editor-in-Chief should take a decision on submitted manuscripts, whether to be published or not with other editors and reviewers
4. The Editors of the journal should preserve the anonymity of reviewers.
5. The Editors of the journal should disclose and try to avoid any conflict of interest.
6. The Editors of the journal should maintain academic integrity and strive to meet the needs of readers and authors.
7. The Editors of the journal should be willing to investigate plagiarism and fraudulent data issues and willing to publish corrections, clarifications, retractions, and apologies when needed.
8. The Editors of the journal should have the limit themselves only to the intellectual content.
9. The Editors of the journal must not disclose any information about submitted manuscripts to anyone other than the corresponding author, reviewers, potential reviewers, other editorial advisers, and the publisher, as appropriate.
10. Unpublished materials disclosed in a submitted paper will not be used by the editor or the members of the editorial board for their own research purposes without the author's explicit written consent.

Duties and Responsibilities of Reviewers

1. The Reviewers of the journal should assist the Editors in taking the decision for publishing the submitted manuscripts.
2. The Reviewers should maintain the confidentiality of manuscripts, which they are invited to review.
3. The Reviewers should provide comments in time that will help editors to make decision on the submitted manuscript to be published or not.
4. The Reviewers are bound to treat the manuscript received for peer reviewing as confidential, and must not use the information obtained through peer review for personal advantage.
5. The Reviewers comments against each invited manuscript should be technical, professional and objective.
6. The Reviewers should not review the manuscripts in which they have found conflicts of interest with any of the authors, companies, or institutions.
7. The Reviewers should disclose and try to avoid any conflict of interest.

Duties and Responsibilities of Authors

1. Manuscripts must be submitted only in English and should be written according to sound grammar and proper terminology.
2. Manuscripts must be submitted with the understanding that they have not been published elsewhere (except in the form of an abstract or as part of a published lecture, review, or thesis) and are not currently under consideration by another journal published by or any other publisher.
3. The submitting (corresponding) author is responsible for ensuring that the manuscript article's publication has been approved by all the other coauthors.
4. In order to sustain the peer review system, authors have an obligation to participate in peer review process to evaluate manuscripts from others.
5. It is also the authors' responsibility to ensure that the manuscripts emanating from a particular institution are submitted with the approval of the necessary institution.
6. It is a condition for submission of a manuscript that the authors permit editing of the paper for readability.
7. Authors are requested to clearly identify who provided financial support for the conduct of research and/or preparation of the manuscript and briefly describe the role of the funder/sponsor in any part of the work.
8. A copy right release and conflict of interest disclosure form must be signed by the corresponding author in case of multiple authorships, prior to the acceptation of the

manuscript, by all authors, for publication to be legally responsible towards the Journal ethics and privacy policy.

9. Under open access license, authors retain ownership of the copyright for their content, but allow anyone to download, reuse, reprint, modify, distribute, and/ or copy the content as long as the original authors and source are cited properly.
10. All authors have agreed to allow the corresponding author to serve as the primary correspondent with the editorial office, to review the edited manuscript and proof.
11. When author(s) discovers a significant error or inaccuracy in his/her own published work, it is the author's obligation to promptly notify the journal editor or publisher to retract or correct the manuscript.
12. All authors must know that that the submitted manuscripts under review or published with GJESM are subject to screening using Plagiarism Prevention Software. Plagiarism is a serious violation of publication ethics.

Violation of Publication Ethics

1. **Plagiarism:** Plagiarism is intentionally using someone else's ideas or other original material as if they are one's own. Copying even one sentence from someone else's manuscript, or even one of your own that has previously been published, without proper citation is considered by GJESM Journals as plagiarism. All manuscripts under review or published with GJESM are subject to screening using plagiarism prevention software. Thus, plagiarism is a serious violation of publication ethics. The development of CrossCheck is a service that helps editors to verify the originality of papers. CrossCheck is powered by the Ithenticate software from iParadigms, known in the academic community as providers of Turnitin. For a searchable list of all journals in the CrossCheck database, please visit: www.ithenticate.com/search
2. **Data Fabrication and Falsification:** Data fabrication and falsification means the researcher did not really carry out the study, but made up data or results and had recorded or reported the fabricated information. Data falsification means the researcher did the experiment, but manipulated, changed, or omitted data or results from the research findings.
3. **Simultaneous Submission:** Simultaneous submission occurs when a manuscript (or substantial sections from a manuscript) is submitted to a journal when it is already under consideration by another journal.
4. **Duplicate Publication:** Duplicate publication occurs when two or more papers, without full cross referencing, share essentially the same hypotheses, data, discussion points, and conclusions.
5. **Redundant Publications:** Redundant publications involve the inappropriate division of study outcomes into several articles, most often consequent to the desire to plump academic vitae.
6. **Improper Author Contribution or Attribution:** All listed authors must have made a significant scientific contribution to the research in the manuscript and approved all its claims. Don't forget to list everyone who made a significant scientific contribution, including students and laboratory technicians.
7. **Citation Manipulation:** Citation Manipulation is including excessive citations, in the submitted manuscript, that do not contribute to the scholarly content of the article and have been included solely for the purpose of increasing citations to a given author's work, or to articles published in a particular journal. This leads to misrepresenting the importance of the specific work and journal in which it appears and is thus a form of scientific misconduct.

Handling Cases of Misconduct

Once GJESM confirms a violation against GJESM's publication ethics, GJESM addresses ethical concerns diligently following an issue-specific standard practice as summarized below.

1. The first action of the journal Editor is to inform the Editorial Office of GJESM by supplying copies of the relevant material and a draft letter to the corresponding author asking for an explanation in a nonjudgmental manner.
2. If the author's explanation is unacceptable and it seems that serious unethical conduct has taken place, the matter is referred to the Publication Committee via Editorial Office. After deliberation, the Committee will decide whether the case is sufficiently serious to warrant a ban on future submissions.
3. If the infraction is less severe, the Editor, upon the advice of the Publication Committee, sends the author a letter of reprimand and reminds the author of GJESM publication policies; if the manuscript has been published, the Editor may request the author to publish an apology in the journal to correct the record.
4. Notification will be sent to corresponding author and any work by the author responsible for the violation or any work these persons coauthored that is under review by GJESM journal will be rejected immediately.
5. The authors are prohibited from serving on GJESM editorial board and serving as a reviewer for GJESM Journal. GJESM reserves the right to take more actions.
6. In extreme cases, notifications will be sent to the affiliations of the authors and the authors are prohibited from submitting their work to GJESM for 5 years.
7. In serious cases of fraud that result in retraction of the article, a retraction notice will be published in the journal and will be linked to the article in the online version. The online version will also be marked "retracted" with the retraction date.

GUIDE FOR AUTHORS

"Global Journal of Environmental Science and Management" (GJESM) is a double blind peer reviewed electronic and print quarterly publication concerned with all aspects of environmental science and management. GJESM publishes original research papers, review papers, case reports and short communications, letters to editor and authors' response about letters to editor across the broad field of environment. These include but are not limited to environmental science, environmental management, environmental engineering, environmental planning and design, urban and regional landscape design and industrial ecology. Environmentalist disciplines are invited to contribute their knowledge and experience. The publication appears at regular intervals time quarterly. The Journal database is fully open access and full text of published articles are available for everyone who can get access to the Journal website free of cost. The authors never pay any charges for submission, article processing and publication.

Guide for Authors: More details on guide for authors refer: http://gjesm.net/journal/authors.note

GENERAL

1. Authors should submit their contributions electronically through the GJESM website submission system to the Editorial Office.

2. Manuscripts must be submitted only in English and should be written according to sound grammar and proper terminology. Manuscripts should be typed in Times New Roman of 11 pt. font and in MS-Word format in one column with 2.5 cm margin at each side. Manuscript submission must be applied once in order to obtain only one submission ID number. More than one submission for a single manuscript can lose the chance of the manuscript consideration. Manuscript must be accompanied by a covering letter including title and author(s) name.

3. There are no strict formatting requirements but all manuscripts must contain the essential elements needed to convey your manuscript, for example Abstract, Keywords, Introduction, Materials and Methods, Results, Conclusions, Artwork and Tables with Captions. Please ensure the figures and the tables included in the single file are placed next to the relevant text in the manuscript, rather than at the bottom or the top of the file. There are no strict requirements on reference formatting at submission. References can be in any style or format as long as the style is consistent.

BEFORE YOU BEGIN

1. Peer-Review Process: In order to sustain the peer review system, authors have an obligation to participate in peer review process to evaluate manuscripts from others. When appropriate, authors are obliged to provide retractions and/or corrections of errors to the editors and the Publisher. All papers submitted to GJESM journal will be peer reviewed for at least one round. GJESM journal adopts a double-blinded review policy: authors are blind to reviewers, but reviewers are not blind to authors. After receiving reviewers' comments, the editorial team member makes a decision. Because reviewers sometimes do not agree with each other, the final decision sent to the author may not exactly reflect recommendations by any of the reviewers. The decision after each round of peer review may include (a) Accept without any further changes, (b) Accept with minor revision, (c) Major changes are necessary for resubmission and (d) Decline without encouraging resubmission.

2. Post-Publication Evaluation: In addition to rapid Peer Review Process, the GJESM Journal has Post-Publication Evaluation by the scientific community. Post-Publication Evaluation is concentrated to ensure that the quality of published research, review and case report meets certain standards and the conclusions that are presented are justified. The post-publication evaluation includes online comments and citations on published papers. Authors may respond to the comments of the scientific community and may revise their manuscript. The Post-Publication Evaluation is described in such a way; it is allowing authors to publish quickly about Environmental science, management, engineering and technology concepts.

3. Publication Ethics: The ethical policy of GJESM is based on the Committee on Publication Ethics (COPE) guidelines and complies with International Committee of GJESM Editorial Board codes of conduct. Readers, authors, reviewers and editors should follow these ethical policies once working with GJESM. The ethical policy of GJESM is liable to determine which of the typical research papers or articles submitted to the journal should be published in the concerned issue. The ethical policy insisted the Editor-in-Chief, may confer with other editors or reviewers in making the decision. Visit at: http://publicationethics.org

4. Conflict of Interest: Authors are requested to evident whether impending conflicts do or do not exist. A copyright transfer agreement is signed by the corresponding author, upon the acceptance of the manuscript, on behalf of all authors, for publication to be legally responsible towards the journal ethics and privacy policy. Authors will be notified as soon as possible of decisions concerning the suitability of their manuscripts for publication in the journal. The submitted materials may be considered for inclusion but cannot be returned and Editors of the journal reserve the right to accept or reject any article in any stage, if necessary. Conflict of Interest Disclosure form can be found at: www.gjesm.org/conflict_of_interest_discloure_form.docx

5. Submission Declaration and Verification: While submitting a manuscript to GJESM, all contributing author(s) must verify that the manuscript represents authentic and valid work and that neither this manuscript nor one with significantly similar content under their authorship has been published or is being considered for publication elsewhere including electronically in the same form, in English or in other language, without the written consent the copy right holder.

6. Authorship: All contributing authors should qualify for authorship and corresponding author should sign the authorship form while submitting the manuscript. It can be found at: (http://www.gjesm.net/data/gjesm/news/authorship_form.docx).

7. Changes to Authorship: After the manuscript is submitted or accepted for publication, the corresponding author is required to send a request to add or remove an author or to rearrange the author names of the submitted/accepted manuscript by sending the change of authorship form to editorial office. No authorship change is allowed after publication of manuscript. More details may be found at: (http://www.gjesm.net/data/gjesm/news/change_of_authorship_form.docx)

8. Retained Author Rights: As an author, author or authors' employer or institution retains certain rights. For more information on author rights, found at: www.gjesm.org/retained_authors_right.docx.

9. Copy Right: Journals should make clear the type of copyright under which authors' work will be published. For open access articles the publisher uses an exclusive licensing agreement in which authors retain copyright in their manuscript. More details may be found at: (www.gjesm.org/copyright_form.docx)

10. User license Agreement: GJESM provides access to archived material through GJESM archives. Manuscripts are the parts of an open archive are made freely available from GJESM website after certain period, which begins from the final publication date of the manuscript. All articles published open access will be immediately and permanently free for everyone to read and download. Permitted reuse is defined by Creative Commons user license called ***Creative Commons Attribution***. Visit at: **(**Creative Commons Attribution 4.0 International (CC BY 4.0)**)**

11. Plagiarism Prevention and Violation of Publication Ethics: All manuscripts under review or published with GJESM are subject to screening using Plagiarism Prevention Software. Plagiarism is a serious violation of publication ethics. Other violations include duplicate publication, data fabrication and falsification, and improper credit of author contribution. Thus, the Plagiarism or Fraudulent or knowingly inaccurate statements constitute unethical behavior are unacceptable and submitting the same manuscript to more than one journal concurrently constitutes unethical publishing behavior and is unacceptable. The development of CrossCheck is a service that helps editors to verify the originality of papers. CrossCheck is powered by the Ithenticate software from iParadigms, known in the academic community as providers of Turnitin. For more details visit at: www.ithenticate.com/search

12. Handling Cases of Misconduct: Once GJESM confirms a violation against GJESM's publication ethics, the following actions will be taken.

a. The work is rejected / retracted immediately. Notification will be sent to corresponding authors. In extreme cases, notifications will be sent to the affiliations of the authors.
b. The authors are prohibited from submitting their work to GJESM for 5 years.
c. Any work by the authors responsible for the violation or any work these persons coauthored that is under review by any GJESM journal will be rejected immediately.
d. The authors are prohibited from serving on GJESM editorial board. GJESM reserves the right to take more actions.

MANUSCRIPT PREPARATION

1. Title Page: The title page should include: the name(s) of the author(s), a concise and informative title, the affiliation(s) and address (es) of the author(s), and e-mail address, telephone and fax numbers of the corresponding author.

2. Manuscript Title: Title of up to 17 words should not contain the name of locations, countries or cities of the research as well as abbreviations. The title should be oriented to Environmental issues while not being obscure or meaningless.

3. Abstract: An abstract of 150 to 250 words that sketches the purpose of the study; basic procedures; main findings its novelty; discussions and the principal conclusions, should not contain any undefined abbreviations or references.

4. Keywords: Provide 5 to 7 keywords which can be used for indexing purposes. Keywords should not repeat the words of the manuscript title or contain abbreviations and shall be written in alphabetical order as separated by semicolon.

5. Introduction: The Introduction should state the purpose of the investigation and identify clearly the gap of knowledge that will be filled in the Literature review study. Date and location of the research carried out throughout the study must be mentioned at the end of this section.

6. Materials and methods: The Materials and Methods section should provide enough information to permit repetition of the experimental work. It should include clear descriptions and explanations of sampling procedures, experimental design, and essential sample characteristics and descriptive statistics, hypothesis tested, exact references to literature describing the tests used in the manuscript, number of data involved in statistical tests, etc.

7. Results and Discussion: The Results section should describe the outcome of the study. Data should be presented as concisely as possible - if appropriate in the form of tables or figures, although very large tables should be avoided. The Discussion should be an interpretation of the results and their significance with reference to work by other authors. Please note that the policy of the Journal with respect to units and symbols is that of SI symbols.

8. Tables: Do not submit tables and graphs as photograph. Place explanatory matters in footnotes, not in the heading. Do not use internal horizontal and vertical rules. Tables should be called out in the text and should have a clear and rational structure and consecutive numerical order. All tables should be numbered 1, 2, 3, etc. Give enough information in subtitles so that each table is understandable without reference to the text. Footnotes to tables should be indicated by superscript lower-case letters (or asterisks for significance values and other statistical data) and included beneath the table body.

9. Figures: Figures/ illustrations should be in high quality art work, within 200-300 dpi and separately provided in Excel format. Ensure that figures are clear, labeled, and of a size that can be reproduced legibly in the journal. Each figure should have a concise caption describing accurately what the figure depicts. Figure captions begin with the term Fig. Figures should be with the captions placed below in limited numbers. No punctuation is to be placed at the end of the caption.

10. Conclusion: This section should highlight the major, firm discoveries, and state what the added value of the main finding is, without literature references.

11. Acknowledgements: Acknowledgments of people, grants, funds, etc. should be placed in a separate section before the reference list. The names of funding organizations should be written in full. Financial support affiliation of the study, if exists, must be mentioned in this section. Thereby, the Grant number of financial support must be included.

12. References: All the references should be cited throughout the manuscript text as well as in the Reference section organized in accordance with Harvard system. Groups of references should be listed first alphabetically, then chronologically. The number of references extracted from each journal should not exceed 3 to 5 citations, which is the average acceptable amount. The number of references should not be less than 30 for original paper, less than 100 for review paper. It is substantially recommended to the authors to refer to more recent references rather than old and out of date ones. Volume, issue and pages of the whole references must be specified according to the GJESM format.

Citing and listing of Web references: As a minimum, the full URL should be given. Any further information, if known (Author names, dates, reference to a source publication, etc.), should also be given.

Text: All citations in the text should refer to: 1. Single author: the author's name (without initials, unless there is ambiguity) and the year of publication; 2. Two authors: both authors' names and the year of publication; and 3. Three or more authors: first author's name followed by "et al." and the year of publication. Citations may be made directly (or parenthetically). Groups of references should be listed first alphabetically, then chronologically. Examples: "as demonstrated (Allan, 1996a, 1996b, 1999; Allan and Jones, 1995). Kramer *et al.,* (2000) have recently shown …".

List: References should be arranged first alphabetically and then further sorted chronologically if necessary. More than one reference from the same Author(s) in the same year must be identified by the letters "a", "b", "c", etc., placed after the year of publication.

Journal article: Nouri J.; Lorestani B.; Yousefi N.; Khorasani N.; Hassani A. H.; Seif, F.; Cheraghi M., (2011). Phytoremediation potential of native plants grown in the vicinity of Ahangaran lead-zinc mine. Environ. Earth Sci., 62(3): 639-644.

Book: Davis, M. L., (2005). Introduction to Environmental Engineering, 3rd. Ed. McGraw Hill Inc.

Book chapter: Mettam, G. R.; Adams, L. B., (1999). How to prepare an electronic version of your article, in: Jones, B. S., Smith, R. Z. (Eds.), Introduction to the electronic age. E-Publishing Inc., New York.

Conference paper: Brown, J., (2005). Evaluating surveys of transparent governance. In UNDESA, 6th. Global forum on reinventing government: towards participatory and transparent governance. Seoul, Republic of Korea 24-27 May. United Nations: New York.

Dissertation: Trent, J. W., (1975). Experimental acute renal failure. Ph.D. Dissertation, University of California. USA.

Online document: Cartwright, J., (2007). Big stars have weather too. IOP Publishing Physics Web.
http://physicsworld.com/cws/article/news/2007/jun/26/big-stars-have-weather-too

AFTER ACCEPTANCE

1. Online Proof Correction: Corresponding authors will receive an e-mail with a link to our online proofing system, allowing annotation and correction of proofs online. Use this proof only for checking the typesetting, editing, completeness and correctness of the text, tables and figures. Significant changes to the article as accepted for publication will only be considered at this stage with permission from the Editor-in-Chief. It is important to ensure that all corrections are sent back to us in one communication. Please check carefully before replying, as inclusion of any subsequent corrections cannot be guaranteed. Proofreading is solely the corresponding author responsibility.

2. Offprints: The offprints can be downloading from the GJESM website once the final corrected manuscripts are disseminated.

AUTHORS INQUIRIES

Authors can track their submitted article through GJESM website on author's login section at: http://gjesm.net/contacts?_action=login

Global Journal of Environmental Science and Management (GJESM)

Copyright Transfer Agreement

1. Parties of the agreement

Author (s):

Manuscript Title:

Manuscript ID:

(Herewith referred to as the "materials"),

Journal Title: Global Journal of Environmental Science and Management (GJESM)

2. Subject of the agreement

A) Copyright
1- The Author and each co-authors shall transfer and sell to the Publisher for the length of the copyright starting from the moment the present agreement comes into force the exclusive rights to the materials, including the rights to translate, reproduce, transfer, distribute or otherwise use the materials or parts (fragments) contained therein, for publication in scientific, academic, technical or professional journals or other periodicals and in derivative works thereof, worldwide, in English, in print or in electronic editions of such journals, periodicals and derivative works in all media or formats now existing or that may exist in future, as well as the right to license (or give permission to) third parties to use the materials for publication in such journals, periodicals and derivative works worldwide. The transfer under this agreement includes the right to adapt the presentation of the materials for use in conjunction with computer systems and programs, reproduction or publication in machine-readable format and incorporation into retrieval systems.
2- Reproduction, placement, transfer or any other distribution or use of the materials, or any parts of the materials contained therein, in any way permitted under this Agreement, shall be accompanied by reference to the Journal and mentioning of the Publisher, namely: the title of the article, the name of the Author (Co-authors), the name of the Journal, volume/number, copyright of the publisher.

B) Reserved Rights
The Author (Co-authors) or the employer of the Author (Co-authors) of the materials shall retain all proprietary rights (with the exception of the rights transferred to the Publisher under the present Agreement).

C) Author Guarantee
The Author (Co-authors) guarantees that the materials are an original work, submitted only to GJESM, and have not been published previously.
In case the materials were written jointly with co-authors, the Author guarantees that he/she has informed them of the terms of this Agreement and obtained their signatures or written permission to singe on their behalf.
The Author guarantees as well that:
The materials do not contain libelous statements.
The materials do not infringe on other persons' rights (including without limitation copyrights, patent rights and the trademark right).
The materials do not contain facts or instructions that can cause damage or injury to third parties and their publication does not cause the disclosure of any secret or confidential information

---

Author (Corresponding Author):

Correspondence Address:

Phone:

Fax:

Email:

Corresponding Author Name: Signature Date

On Behalf of the Publisher:

Iran Solid Waste Association,
Faculty of Environment, University of Tehran,
Postal Code: 1417854511, Tehran,
Iran

Telefax: (+9821) 2610 5110

Email: *editor@gjesm.net*

Gjesm.publication@gmail.com

Website: www.gjesm.net

Accepted for publication ☑ Signature Date

PLEASE NOTE: The accepted manuscript cannot be processed for publication until the publisher has received this signed form. The form MUST be signed by the Corresponding Author and then scanned and sent through the system or email. If the manuscript is not published in the Journal, this release will not take effect.

The sole responsibility for the whole content (s) of the article remains only with the corresponding author. However, Editor would reserve the right to adjust the style to certain standards of uniformity before publication.

CONFLICT OF INTEREST DISCLOSURE FORM

Conflict of Interest is defined as a set of conditions in which professional judgment concerning a primary interest, such as the validity of research, may be influenced by a secondary interest, such as financial gain. A Conflict of Interest Disclosure is an agreement or notification from the authors that they have not been paid for the work, or if they have, stating the source of their payment. The purpose of Conflict of Interest Disclosure form is to provide readers of authors' manuscript with information about authors' interests that could influence how the authors receive the work. The corresponding author (on behalf of all co-authors) should submit a conflict of interest disclosure form and is responsible for the accuracy and completeness of the submitted manuscript. Conflict of Interest Disclosure form can be signed by the corresponding author on behalf of all co-authors and stating that the submitted manuscript is the authors' original work, has not received prior publication and is not under consideration for publication elsewhere, permission has been received to use any material in the manuscript much as tables, figures etc. or no permissions have necessary to publish the authors' work.

1. Name of the corresponding author

2. Affiliation including e-mail and phone number

3. Manuscript Title

4. Do the authors or authors' institution at any time receive payment or services from a third party (government, commercial, private foundation, etc.) for any aspect of the submitted manuscript (including but not limited to grants, data monitoring board, study design, manuscript preparation, statistical analysis, etc.)?

   Are there any relevant conflicts of interest? Yes / No

5. Do the authors have any patents, whether planned, pending or issued, broadly relevant to the work?

   Are there any relevant conflicts of interest? Yes / No

6. Are there other relationships or activities that readers could perceive to have influenced, or that give the appearance of potentially influencing, what the authors' information in the submitted manuscript?

   Are there any relevant conflicts of interest? Yes / No

7. Are there any aspect of the work covered in this manuscript that has involved either experimental animals or human patients has been conducted with the ethical approval of all relevant bodies or not.

   Are there any relevant conflicts of interest? Yes / No

Corresponding Author Signature | Print Name | Date

AUTHORSHIP FORM

By completing and signing the following statements, the corresponding author acknowledges and accepts the responsibility on behalf of all contributing authors, if any, concerning Authorship Responsibility.

Manuscript title:

Corresponding author:

Affiliation:

Email:

Phone No:

By signing and filling this form, the corresponding author certifies that each author has met all criteria below (A, B, C, and D) and indicates each author general and specific contributions by listing his or her name next to the relevant section.

A. I certify that

- The manuscript is authentic and valid and that neither this manuscript nor one with considerably similar content under my authorship has been published or is being considered for publication elsewhere, except as described in an attachment, nor copies of closely related manuscripts are provided.
- I will provide the data or will contribute fully in providing and obtaining the data on which the manuscript is based for examination by the editors or their assignees, if requested.
- Every author has agreed to allow the corresponding author to serve as the primary correspondent with the editorial office, to review the edited manuscript and proof.

B. Each author has given final approval of the submitted manuscript.

C. Each author has participated sufficiently in the work to take public responsibility for the whole content.

D. Each author qualifies for authorship by listing his or her name on the appropriate line of the categories of contributions listed below. List appropriate author next to each section – each author must be listed in at least 1 field. More than 1 author can be listed in each field.

- conception and design
- acquisition of data
- analysis and interpretation of data
- drafting of the manuscript
- critical revision of the manuscript for important intellectual content
- statistical analysis
- obtaining funding
- administrative, technical, or material support
- supervision
- no additional contributions
- other (specify)

Corresponding Author Signature **Print Name** **Date**

CHANGE OF AUTHORSHIP FORM

Manuscript Title:

Corresponding Author:

Please check all that apply.

☐ New author(s) have been added.

☐ There is a change in the order of authorship.

☐ An author wishes to remove his/her name. An author's name may only be removed at his/her own request in writing.

ORIGINAL AUTHORSHIP

List ALL AUTHORS in the same order as the original (first) submission.

Print Name	Print Name
Name (1)	Name (6)
Name (2)	Name (7)
Name (3)	Name (8)
Name (4)	Name (9)
Name (5)	Name (10)

NEW AUTHORSHIP

List the ALL AUTHORS in same order as the new version.

Print Name	Print Name
Name (1)	Name (6)
Name (2)	Name (7)
Name (3)	Name (8)
Name (4)	Name (9)
Name (5)	Name (10)

I attest that:

1. The manuscript is not currently under consideration, in press, or published elsewhere, and the research reported will not be submitted for publication elsewhere until a final decision has been made as to its acceptability by the journal (posting of submitted material on a web site may be considered prior publication-note this in your cover letter).
2. The manuscript is truthfully original work without fabrication, fraud, or plagiarism.
3. I have made an important scientific contribution to the study and am thoroughly familiar with the primary data.
4. I have read the complete manuscript and take responsibility for the content and completeness of the manuscript and understand that I share responsibility if the paper, or part of the paper, is found to be faulty or fraudulent.

Corresponding Author Signature Name Date

SUBSCRIPTION FORM

Subscription form

Global Journal of Environmental Science and Management

Please enter my annual subscription to the Global Journal of Environmental Science and Management (GJESM), including 4 quarterly issues for the Year ..... Vol. ..... Nos.....

	Domestic (Rials)	International (USD)
▪ Institutional	3,000,000	150
▪ Individual	2,000,000	100
▪ Student	1,000,000	80
▪ Single Copy	500,000	50

Name: **Tel.:** **Email:**

Mailing Address:

Payment method: Check or money order must be made in order of:
Account #. 0101834143005, Account name: J. Nouri
Bank Melli Iran, IAU Branch, Code 1017, Tehran, Iran

□ Bank receipt enclosed

** Please allow 3 to 5 weeks for delivery*

Please send this filled in order form along with the Bank receipt payment to:

Global Journal of Environmental Science
and Management
No. 2, Kouhestan Deadend, Janpour Street,
Darabad, Tehran 1956934461 Iran

Global
Journal of Environmental Science and Management

Volume 12, Issue 1, Winter 2026

1.	The catalytic effect of mycorrhizal initial planting on limestone post-mining ecological land rehabilitation
2.	The potential of combining coagulation-flocculation, biofiltration, and advanced oxidation processes for multi-stage wastewater treatment
3.	Efficacy of zinc oxide chitosan hybrid nanoparticles as a nanovaccine to enhance immunity in hybrid grouper fish
4.	Waste management of used beverage cartons using material flow analysis
5.	Physical and chemical evaluation of soil-like material from landfill mining using an alternative growing medium
6.	Nypa fruticans-assisted green-synthesized gold nanoparticles for an enhanced electrochemical formaldehyde sensor based on fish albumin composite
7.	The legal coastline as a unifying framework for land and marine cadastre
8.	Environmental and economic performance of hybrid charging stations
9.	Environmental stability and ultraviolet protection of Spodoptera litura nucleopolyhedrovirus encapsulated in chitosan nanoparticles
10.	Phylogenetic and conservation insights on local adaptations of Argiope modesta concerning ecological consequences
11.	Customer-driven socio-environmental sustainability in fashion: The role of green word-of-mouth and perceived product value
12.	Environmental impact of mining and its social responsibilities on rural communities
13.	The influence of demographic and socioeconomic factors on a fishing community's resilience to coastal flooding
14.	Environmental and policy perspectives in managing revolutionary heritage under urbanization challenges
15.	Indigenous bacterial diversity and identification in domestic wastewater in small tropical island
16.	Relationship between urban soil granulometric composition and microbiological and vermicular contamination
17.	Tropical peat soil variability along landscape and depth gradient using mid-infrared spectroscopy
18.	Synergistic impacts on a multi-purpose transboundary aquatic ecosystem resulting from cyanide and mercury in artisanal gold mining tailings
19.	Eco-friendly organic nutrients enriched with biosoltamax enhance shallot growth, improve soil properties, and reduce the use of mineral fertilizer
20.	River basin management under spatial inequality and land use dynamics
21.	Eco-friendly farming management and molecular surveillance of the pepper yellow leaf curl virus in purple-stem chili
22.	Linking geospatial suitability modelling with experimental validation of aquatic environmental quality in inland lakes
23.	Sustainable solutions for entomoremediation organic waste into food and fertilizer using black soldier fly larvae
24.	The role of carbon sequestration and biodiversity in agroforestry for climate change mitigation
25.	Sustainable strategies for durum wheat production under water scarcity and climate stress